PHOTOBIOLOGY

The Science of Life and Light

Second Edition

LARS OLOF BJÖRN

Editor

Springer

Photobiology

Second Edition

Photobiology

The Science of Life and Light

Second Edition

Edited by

Lars Olof Björn

Lund University
Lund, Sweden

Lars Olof Björn
Department of Plant Physiology
Lund University
Sölvegatan 35
SE-223 62 Lund
Sweden
Lars_Olof.Bjorn@cob.lu.se

(Drawing by Per Nilsson)

Photobiology

I am lying on my back beneath the tree,
dozing, looking up into the canopy,
thinking: what a wonder!—I can see!

But in the greenery above my face,
an even greater miracle is taking place:
Leaves catch photons from the sun
and molecules from air around.
Quanta and carbon atoms become bound.
Life, for them, has just begun.

The sun not only creates life, it also takes away
mostly by deranging DNA.
Damage can be, in part, undone
by enzymes using photons from the sun.

Summer nears its end, already 'cross the sky
southward aiming birds are flying by.
Other birds for travel choose the night

relying on the stars for guiding light.

Imprinted in their little heads are Gemini,
Orion, Dipper, other features of the sky.
There is room for clocks that measure
day and night,
Correct for movement of the sky
and tell the time for flight

Deep into oceans, into caves
the sun cannot directly send its waves.
But through intricacies of foodweb's maze,
oxygen from chloroplasts, luciferin, luciferase,
at times, in place,
where night and darkness seem to reign,
solar quanta emerge as photons
once again.

L.O. Björn 2002

Preface

I started my first photobiological research project almost exactly 50 years ago, in the spring of 1957. My scientific interest ever since has been focused on photobiology in its many aspects. Because I have been employed as a botanist, my own research has dealt with the photobiology of plants, but throughout this time I have been interested in other aspects, such as vision, the photobiology of skin, and bioluminescence. A first edition of the present book was published in 2002, but this second edition is much expanded and completely updated. Several new authors have been recruited among my eminent colleagues.

It has not been possible to cover all aspects of photobiology in one volume, but I feel that we have managed to catch a fair and well-balanced cross section. Many colleagues promised to help, but not all lived up to their promises. To those who did, and who are coauthors to this volume, I direct my thanks; I think that they have done an excellent job.

Living creatures use light for two purposes: for obtaining useful energy and as information carrier. In the latter case organisms use light mainly to collect information but also (e.g., by coloration and bioluminescence) for sending information, including misleading information, to other organisms of their own or other species. Collection of free energy through photosynthesis and collection of information through vision or other photobiological processes may seem to be very different concepts. However, on a deep level they are of the same kind. They use the difference in temperature between the sun and our planet to evade equilibrium, i.e., to maintain and develop order and structure.

Obviously, all of photobiology cannot be condensed into a single volume. My idea has been to first provide the basic knowledge that can be of use to all photobiologists, and then give some examples of special topics. I have had to limit myself, and one of the interesting topics that had to be left out is the thermodynamics of processes in which light is involved.

Thus, this book is intended as a start, not as the final word. There are several journals dealing with photobiology in general, and an even greater number dealing with special topics such as vision, photodermatology, or photosynthesis. There are several photobiology societies arranging meetings and other activities. And last but not least, up-to-date information can be found on the Internet. The most important site, apart from the Web of Science and other scientific databases, is Photobiology Online, a site maintained jointly by the American and European Societies for Photobiology (ASP and ESP, respectively),

at http://169.147.169.1/POL.index.html or http://www.pol-europe.net/, where details about photobiology journals and books can be obtained.

The subtitle of this book may be somewhat misleading. There is only one science. But I wanted to point out that the various disciplines dealing with light and life have more in common than perhaps generally realized. I hope that the reader will find that the same principles apply to seemingly different areas of photobiology. For instance, we have transfer of excitation energy between chromophores active in photosynthesis, in photorepair of DNA, and in bioluminescence. Cryptochromes, first discovered as components in light-sensing systems in plants, are involved in the human biological clock, and probably in the magnetic sense of birds and other animals, and they have evolved from proteins active in DNA photorepair. The study of the photomagnetic sense of birds has, in turn, led to new discoveries about how plants react to a combination of light and magnetic fields.

Many colleagues have been helpful in the production of this book. Two of my coauthors—Professors Helen Ghiradella and Anders Johnsson—who are also close friends, have earned special thanks, because they have helped with more chapters than those who bear their names. Helen has also helped to change my Scandinavian English into the American twist of the islanders' tounge, but we have not changed the dialect of those who are native English speakers. Professor Govindjee has contributed not only with his knowledge of photobiology, but also with his great experience in editing. Drs. Margareta Johnsson and Helena Björn van Praagh have helped with improvements and corrections, and Professor Allan Rasmusson at our department in Lund has been very helpful when I and my computer have had disagreements. I have enjoyed the friendliness and help of other colleagues in the department. The staff of our biology library has been very helpful and service-minded.

Many others have also helped, but special thanks go to my wife and beloved photobiologist Gunvor, who has supported me during the work and put up with paper and books covering the floor in our common home; to her I dedicate those chapters of the book that bear my name.

Lars Olof Björn
Lund, Sweden
March 2007

Contents

Contributors

Lars Olof Björn
Lund University, Department of Cell and Organism Biology, Sölvegatan 35, SE-223 62 Lund, Sweden
Lars_Olof.Bjorn@cob.lu.se

Wolfgang Engelmann
Schlossgartenstr. 22, D-72070 Tübingen (Germany), Tel.: int+49-7071-68325
engelmann@uni-tuebingen.de

Helen Ghiradella
University at Albany, Department of Biology, Albany, New York 12222, USA
hghff@albany.edu

Govindjee
Prof.Em., Biochemistry, Biophysics and Plant Biology, Department of Plant Biology, University of Illinois, 265 Morrill Hall, MC-116, 505 South Goodwin Avenue, Urbana, IL 61801–3707, USA, Fax: int+01-217-244-7246
gov@life.uiuc.edu

Pirjo Huovinen
Centro de Investigación y Desarrollo de Recursos y, Ambientes Costeros (i~mar), Universidad de Los Lagos, Camino a, Chinquihue Km 6, Casilla 557, Puerto Montt, Chile
phuovinen@ulagos.cl

Anders Johnsson
Norwegian University of Science and Technology (NTNU), Department of Physics, NO-7491 Trondheim, Norway
anders.johnsson@phys.ntnu.no

Theresa Jurkowitsch
Medical University of Vienna, Wahringerguertel 18–20, A-1090 Vienna, Austria
theresa.dani@meduniwien.ac.at

Richard E. Kendrick
Department of Plant Science, Wageningen University, The Netherlands

Robert Knobler
Div. of Special and Environmental Dermatology, Medical University of Vienna, Wahringerguertel 18–20, A-1090 Vienna, Austria
robert.knobler@meduniwien.ac.at

Richard L. McKenzie
National Institute of Water and Atmospheric Research, (NIWA), Lauder, PB 50061 Omakau, Central Otago 9352, New Zealand
r.mckenzie@niwa.co.nz

Curtis D. Mobley
Sequoia Scientific, Inc., 2700 Richards Rd. Suite 107, Bellevue, WA 98005
curtis.mobley@sequoiasci.com

Rachel Muheim
Virginia Polytechnic Institute and State University, Department of Biological Sciences, Derring Hall, Blacksburg, VA 24061–0406, USA
muheimr@vt.edu

Mary Norval
University of Edinburgh Medical School, Biomedical Sciences
m.norval@ed.ac.uk

David Saunders
21, Leadervale Road, Edinburgh EH16 6PB, Scotland U.K.
d.s.saunders@btopenworld.com

Raymond C. Smith
Geography Department and ICESS, University of California, Santa Barbara, Santa Barbara, CA 93106
ray@icess.ucsb.edu

Villy Sundström
Department of Chemical Physics, Lund University, Box 124, SE-22100 Lund, Sweden

James L. Weller
School of Plant Science, University of Tasmania, Private Bag 55, Hobart, Tasmania 7001, Australia
jim.weller@utas.edu.au

1
The Nature of Light and Its Interaction with Matter

Lars Olof Björn

Abstract: This chapter provides a physical background to the following ones. It describes the particle and wave properties of light, and the diffraction, polarization, refraction, reflection, and absorption of light, statistics of photon emission and absorption. Planck's law of heat radiation is described in various mathematical and graphical ways. One section is devoted to a simplified description of the propagation of light in absorbing and scattering media. The final sections are devoted to interactions between light and matter: spectra of and energy levels in atoms and molecules, the relation between absorption and emission spectra, the molecular geometry of absorption and emission, and the transfer of electronic excitation energy between molecules, including the Förster mechanism, triplet states, and the photobiologically important properties of the dioxygen molecule.

1.1. Introduction

The behavior of light when it travels through space and when it interacts with matter plays a central role in the two main paradigms of twentieth-century physics: relativity and quantum physics. As we shall see throughout this book, it is also important for an understanding of the behavior and functioning of organisms.

1.2. Particle and Wave Properties of Light

The strange particle and wave properties of light are well demonstrated by a modification of Young's double slit experiment. In Young's original experiment (1801), a beam of light impinged on an opaque screen with two parallel, narrow slits. Light passing through the slits was allowed to hit a second screen. Young did not obtain two light strips (corresponding to the two slits) on the second screen, but instead a complicated pattern of several light and dark strips. The pattern

obtained can be quantitatively explained by assuming that the light behaves as waves during its passage through the system.

It is easy to calculate where the maxima and minima in illumination of the last screen will occur. We can get some idea of the phenomenon of *interference* by just overlaying two sets of semicircular waves spreading from the two slits (Fig. 1.1), but this does not give a completely correct picture.

For the experiment to work, it is necessary for the incident light waves to be in step, i.e., the light must be spatially coherent. One way of achieving this is to let the light from a well-illuminated small hole (in one more screen) hit the screen with the slits. The pattern produced (Fig. 1.2) is a so-called interference pattern or, to be more exact, a pattern produced by a combination of *diffraction* (see the next section) in each slit and *interference* between the lights from the two slits. It is difficult to see it if white light is used, since each wavelength component produces a different pattern. Therefore, at least a colored filter should be used to limit the light to a narrower waveband. The easiest way today (which Young could not enjoy) is to use a laser (a simple laser pointer works well), giving at the same time very parallel and very monochromatic light, which is also sufficiently strong to be seen well.

In a direction forming the angle α with the normal to the slitted screen (i.e., to the original direction of the light), waves from the two slits will enhance each other maximally if the difference in distance to the two slits is an integer multiple of the wavelength, i.e., d.sin α = n.λ, where d is the distance between the slits, λ the wavelength, and n a positive integer (0, 1, 2, …). The waves will cancel each other completely when the difference in distance is half a wavelength, i.e., d.sin α = (n + 1/2).λ. To compute the pattern is somewhat more tedious, and we need not go through the details. The outcome depends on the width of each slit, the distance between the slits, and the wavelength of light. An example of a result is shown in Fig. 1.2.

So far so good—light behaves as waves when it travels. But we also know that it behaves as particles when it leaves or arrives (see later). The most direct demonstration of this is that we can count the photons reaching a sensitive photocell (photomultiplier).

But the exciting and puzzling properties of light stand out most clearly when we combine the original version of Young's experiment with the photon counter. Instead of the visible diffraction pattern of light on the screen, we could dim the light and trace out the pattern as a varying frequency of counts (or, if we so wish, as a varying frequency of clicks as in a classical Geiger counter) as we move the photon counter along the projection screen (Fig. 1.3a). Since we count single photons, we can dim the light considerably and still be able to register the light. In fact, we can dim the light so much that it is very, very unlikely that more than *one photon at a time* will be in flight between our light source and the photon counter. This type of experiment has actually been performed, and it has been found that a diffraction pattern is still formed under these conditions. We can do the experiment also with an image forming device such as a photographic film or a charge coupled diode (CCD) array as the receiver and get a picture of where
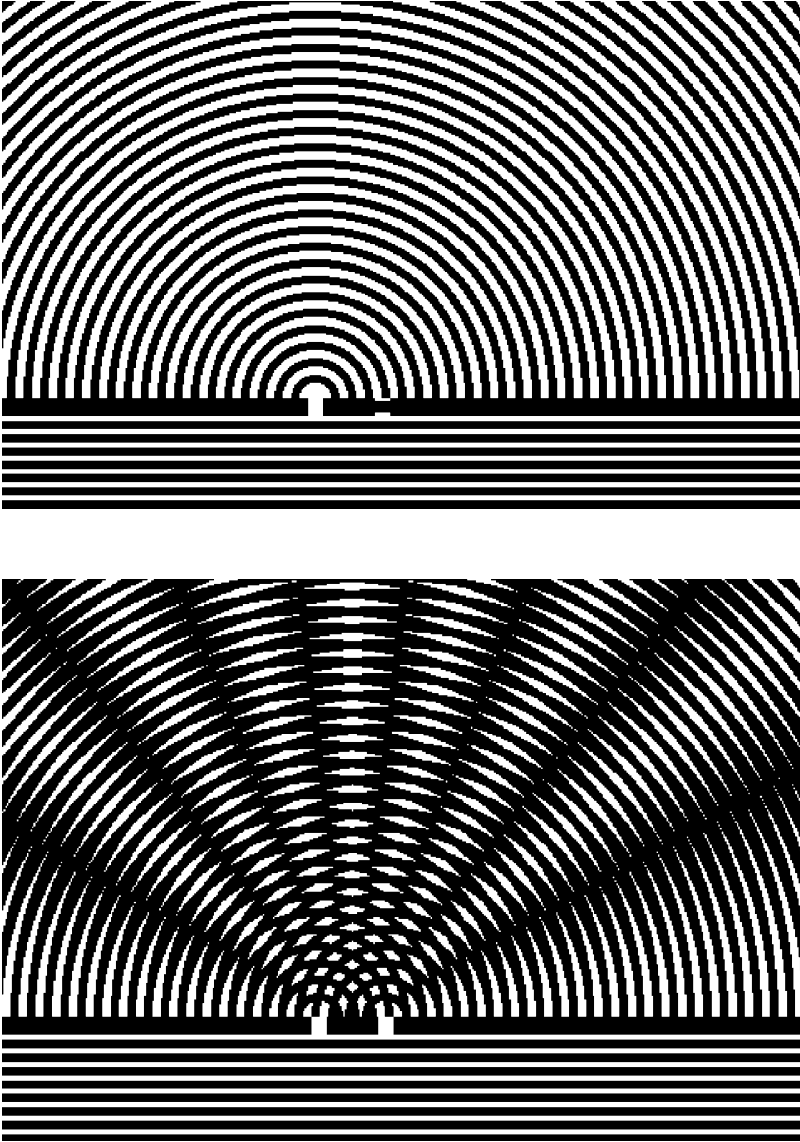
FIGURE 1.1. (**Top**) Light waves impinge from below on a barrier with only one slit open and spread from this in concentric rings. (**Bottom**) Light waves impinge from below on a barrier with two slits open. The two wave systems spreading on the other side interfere and in some sectors enhance, in others extinguish one another. The picture is intended only to simplify the understanding of the interference phenomenon and does not give a true description of the distribution of light.
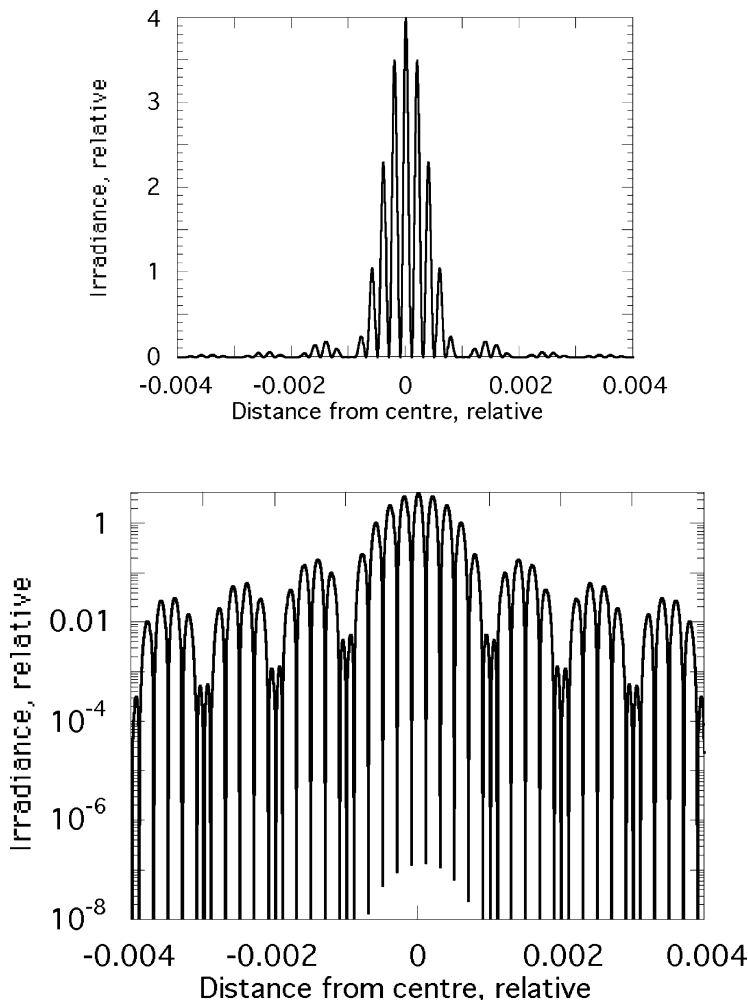
FIGURE 1.2. Interference pattern produced in Young's double slit experiment (computer simulation). The width of each slit is 1 mm, the distance between slit centers 4 mm, and the wavelength 0.001 mm (1 μm). The distance from the center of the screen is along the horizontal axis and the irradiance ("light intensity") along the vertical axis, both in relative units. Note that the vertical scale is linear in the upper diagram, logarithmic in the lower one.

the photons hit. A computer simulation of the outcome of such an experiment is shown in Fig. 1.3b.

If you think a little about what this means, you will be very puzzled indeed. For the diffraction pattern to be formed we need *two* slits. But we can produce the pattern by using only one photon at a time. There can be no interaction between two or more photons, which have traveled different paths, e.g., one
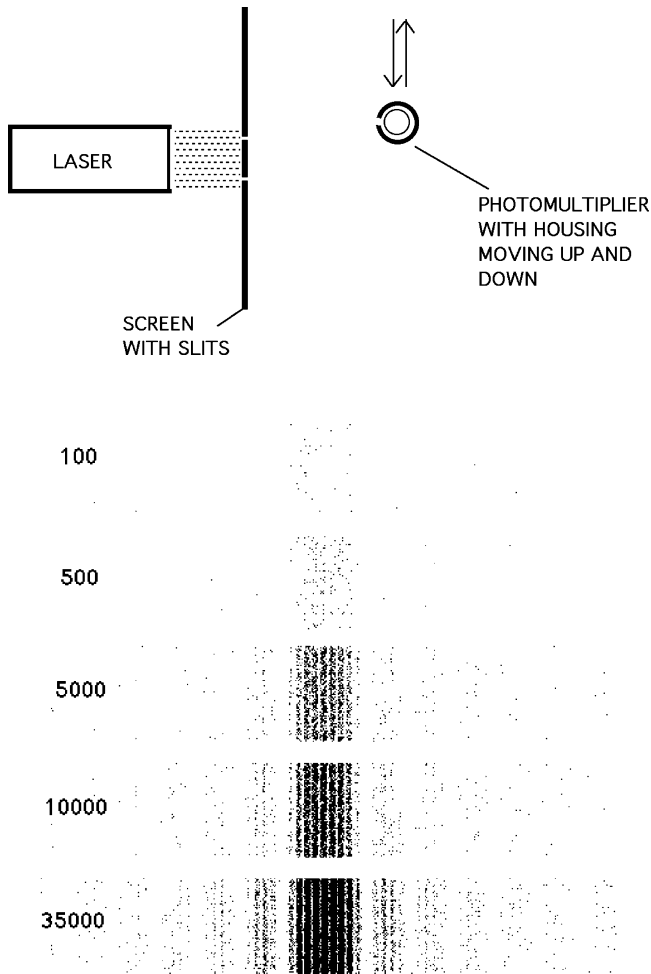
FIGURE 1.3. **(Top)** Double slit experiment set up to count single photons. The sketch is not to scale. In a real experiment the distance of the photomultiplier from the screen with slits would be greater, and the opening in the photomultiplier housing smaller. **(Bottom)** Simulation of the pattern of photon hits on a screen behind a double slit arranged in the same way as in Fig. 1.2. The number of photons is indicated for each experiment. Although the photon hits take place randomly and cannot be predicted, the interference pattern emerges more and more clearly with increasing number of photons.

photon through one slit and another photon through the other slit. The experiment shows that each photon "must be aware" of both slits, or, in other words, must have traveled through both slits. I know of no other physics experiment that demonstrates more clearly than this one that light is not waves or particles. The wave and the particle are both *models*, incomplete pictures or imaginations of the nature of light. The limitations of our senses and our brain prevent

us from getting closer to reality than this, simply because it has not made sense during our evolution to get closer to reality. This limitation does not prevent us from using our models very successfully as long as we use them in a correct way.

Let us take one more example to make clear how "weird" (i.e., counterintuitive) the scientific description of the behavior of light is. When I was younger I used to watch the Andromeda galaxy using my naked eyes (now it is difficult, not only because my vision has worsened, but because there is so much electric light around where I live). I could see the galaxy because atoms in it had emitted light about 2 million years earlier. The photons, after having traveled through empty space, interacted with rhodopsin molecules in my eyes. But no photon started on its course following a straight line towards the earth. It traveled as an expanding wave. Just before interacting with the rhodopsin molecule in my eye, the photon was *everywhere* on a wavefront with a radius of 2 million light years. The energy of the photon was not localized until it came into contact with my eye.

1.3. Light as Particles and Light as Waves, and Some Definitions

When we are dealing with light as waves, we assign a wavelength to each wave. Visible light has wavelengths in a vacuum in the range 400–700 nm (1 nm equals 10^{-9} m), while ultraviolet radiation has shorter and infrared radiation longer waves.

Photobiologists divide the ultraviolet part of the spectrum into ultraviolet A (UV-A) with 315–400 nm wavelength, UV-B with 280–315 nm wavelength, and UV-C with < 315 nm wavelength. You may see other limits for these regions in some publications, but these are supported by the Comité Internationale de l'Eclairage (CIE), which introduced the concepts. Just as everybody should use the same internationally agreed-upon length of the meter, everybody should honor the definitions of UV-A, UV-B, and UV-C; otherwise there is a risk for chaos in the scientific literature. Plant photobiologists, for whom the spectral region 700–750 nm is especially important, call this radiation "far-red light." They also call the region 400–700 nm "photosynthetically active radiation," or PAR, rather than visible light. Just as radiation outside this band is perfectly visible for some organisms such as some insects, birds, and fish (and some light in the range 400–700 nm invisible to many animals), so radiation with wavelengths shorter or longer than "photosynthetically active radiation" is photosynthetically active to many organisms.

Natural light never has a single wavelength, but can rather be regarded as a mixture of waves with different wavelengths.

When we characterize light by its wavelength, we usually mean the wavelength in a vacuum. When it travels through a vacuum, the velocity of light is always *exactly* 299792.4562 km/s, irrespective of wavelength and the movement of the

radiation source in relation to the observer. The reason that this value is exact is that the velocity of light in a vacuum links our definitions of the meter and the second. This velocity is usually designated c, and wavelength λ (the Greek letter lambda). A third property of light which we should keep track of is its frequency, i.e., how many times per time unit the wave (the electric field) goes from one maximum (in one direction) to another maximum (in the same direction). Frequency is traditionally designated ν (Greek letter nu), and in a vacuum we have the following relation between the three quantities just introduced: $c = \lambda \cdot \nu$, or $\lambda = c/\nu$, or $\nu = c/\lambda$. When light passes through matter (such as air or water or our eyes), the velocity and wavelength decrease in proportion, and frequency remains unchanged. Sometimes the wavenumber, i.e., $1/\lambda$, is used for the characterization of light. It is usually symbolized by ν with a line (bar) over it, and a common unit is cm^{-1}.

When we think of light as particles (photons), we assign an amount of energy (E) to each photon. This energy is linked to the wave properties of the light by the relations $E = h \cdot \nu$, where h is Planck's constant, 6.62617636 J·s (joule-seconds). It also follows from the preceding that $E = h \cdot c/\lambda$. We can never know the exact wavelength, frequency, or energy of a single photon.

1.4. Diffraction

We usually think of light traveling in straight lines if there is nothing in its way. We have seen in Young's double slit experiment that it does not always do that. In fact, the great physicist Richard Feynman has shown that its behavior is best understood if we think of it as always traveling every possible way at the same time and components traveling those different ways interfering with one another at every possible point.

We do not have to have two slits to show how the light "bends" near edges. This "bending" is called diffraction in scientific terminology. It is very important to take diffraction into account to understand some biological phenomena, such as the vision of insects (see Chapter 9). Light is diffracted in any small opening and also near any edge. To compute the diffraction pattern we can make use of something called Huygens' principle (sometimes the Huygens-Fresnel principle). It states that we can think of propagating light as a sum of semispherical waves emanating from a wavefront. If the wavefront is flat, the semispherical waves emanating from it add up to a new flat wavefront. But if something stops some of the semispherical waves, the new wavefront is no longer flat. In Fig. 1.1 (Top) we illustrate this in one plane. Flat waves impinge from below on a screen with an opening. Many semicircular waves start out from the opening. Along a line from the middle of the opening the resulting wavefront is flat, but at the edges the semicircular waves produce a bent pattern. We have calculated this pattern more exactly in Fig. 1.4.
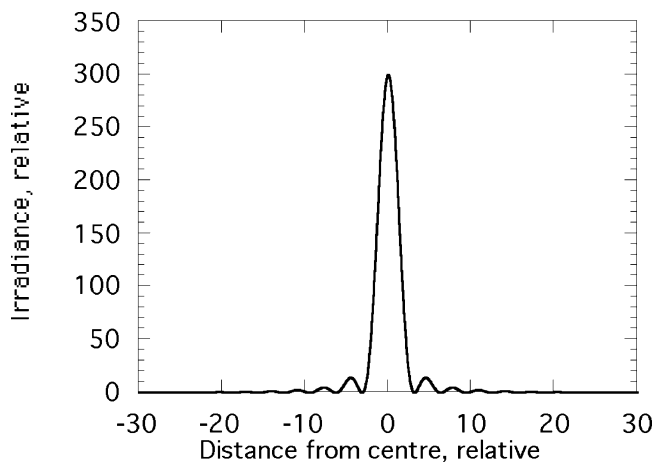
FIGURE 1.4. Diffraction pattern in a single slit (the pattern from a round hole looks similar in one dimension, but is slightly different). The horisontal axis shows the sine of the deviation angle in units of the ratio beween wavelength and slit width.

1.5. Polarization

Light waves are *transverse*, i.e., the oscillation is perpendicular to the direction of wave propagation, the direction of the light (this is in contrast to sound waves, in which particles vibrate in the line of wave propagation). In the case of light, there are no vibrating particles, but a variation in electric and magnetic fields. The electric and magnetic fields are both perpendicular to the direction of propagation, but also perpendicular to one another. When the electric fields of all the components of a light beam are parallel, the beam is said to be *plane-polarized.* The *plane of polarization* is the plane that contains both the electrical field direction and the line of propagation.

If we add two beams which travel in the same direction and are both plane-polarized and have the same *phase* (i.e., the waves are in step) but different planes of polarization, the resulting light is also plane-polarized with its plane of polarization at an intermediate angle.

Light can also be circularly polarized, in which case the electrical field direction spirals along the line of propagation. Since such a spiral can be left- or right-handed, there are two kinds of circular polarization, left-handed and right-handed (Fig. 1.5).

Circularly polarized light can be regarded as the sum of two equally strong plane-polarized components with right angles between the planes of polarizations, and a 90 degree *phase difference* between the components. On the other hand, plane-polarized light can be regarded as a sum of equally strong left- and right-handed components of circularly polarized light.

Natural light, such as direct sunlight, is often almost unpolarized, i.e., a random mixture of all possible polarizations. After reflection in a water surface
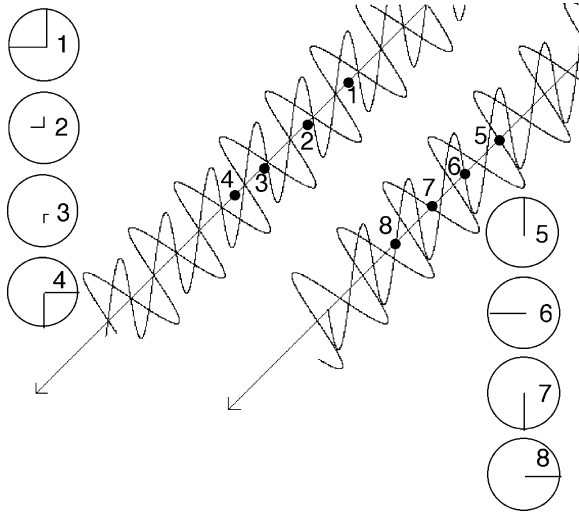
FIGURE 1.5. In the upper left part of the figure a plane-polarized light beam, composed of one vertically and one horisontally polarized component, is depicted in perspective and also "head on" at different points (or at one point at different moments). Numbered points in the perspective drawing correspond to the numbers on the "head-on" drawings. Only the electric components of the electromagnetic fields are shown (wavy lines in the perspective drawing, straight lines in the "head-on" drawings). In the lower right part of the drawing the same is shown for a circularly polarized beam.

the light becomes partially plane-polarized. Skylight is a mixture of circularly and plane-polarized light, which we call elliptically polarized light. We cannot directly perceive the polarization of the light we see. Insects do, and often use the polarization of skylight as an aid in their orientation. Plants in many cases react differently to plane-polarized light depending on its plane of polarization. This holds for chloroplast orientation in seed plants, mosses, and green algae and also for growth of fern gametophytes. A good treatise on the subject (in German) is provided by W. Haupt (1977).

1.6. Statistics of Photon Emission and Absorption

Usually the members of a population of excited molecules can be expected to emit photons independently of one another, i.e., the time of emission of one photon does not depend on the time of emission of another photon. One exception to this rule occurs when stimulated emission becomes significant, as happens in a laser. Another exception is when there is cooperation between different parts of a cell (e.g., when a dinoflagellate flashes), between different cells in an organism (e.g., when a firefly flashes), or between different individuals in a population (e.g., when fireflies in a tree send out synchronized flashes). The examples in

the last sentence are very obvious. However, careful study of the statistics of photon emission offers a very sensitive way of detecting cooperation between different parts of a biological system, and we shall therefore dwell a little on this subject, which also has a bearing on the reliability of measurement of weak radiation in general.

When photons are emitted independently of one another, the distribution of emission events in time is a Poisson distribution, just as in the case of radioactive decay. This means that if the mean number of events in time Δt is x, then the probability of getting exactly n events in the time Δt is $p = e^{-x} \cdot x^n / n!$ In this formula, n! stands for factorial n, i.e., $1 \cdot 2 \cdot 3 \cdot 4 \ldots \cdot n$. Thus $1! = 1$, $2! = 2$, $3! = 6$, $4! = 24$, and so on. By definition $0! = 1$.

We are familiar with the Poisson distribution of events from listening to a Geiger-Müller counter. That events are Poisson-distributed in time means that they are completely randomly distributed in time. When one event takes place does not depend on when a previous event occurred. One might think that there cannot be much useful information to be extracted from such a random process, but such a guess is wrong. The reader is probably already familiar with some of the useful things we can learn from the random decay of atomic nuclei. We can, in fact, use our knowledge of how Poisson statistics work for determining the number of photons required to trigger a certain photobiological process. The remarkable thing is that we can do this even without determining the number of photons we shine on the organism that we study.

The principle was first used by Hecht et al. (1942) to determine how many photons must be absorbed in the rods of an eye to give a visual impression. Their ingenious experiment was a bit complicated by the fact that our nervous system is wired in such a way that several rods have to be triggered within a short time for a signal to be transmitted to the brain (thereby avoiding false signaling due to thermal conversion of rhodopsin). We shall demonstrate the principle with a simpler example, an experiment on the unicellular flagellate *Chlamydomonas* (Hegemann and Marwan 1988). This organism swims around with two flagella, and it reacts to light by either stopping ("stop response") or by changing swimming direction ("turning response").

All one has to do is to take a sample of either light-adapted or dark-adapted *Chlamydomonas* cells, subject them to a flash of light, and note which fraction of the cells either stop or turn. The experiment is then repeated several times, with the flash intensity varied between experiments. The absolute fluence in each flash need not be determined, only a relative value. If one possesses a number of calibrated filters no light measurement at all need be performed. Then the fraction of reacting cells for each flash is plotted against the logarithm of the relative flash intensity. It turns out that (for dark-adapted cells) the curve so obtained, if plotted on a comparable scale, has the same shape as the curve labeled n = 1 in Fig. 1.6. This holds for both stop response and for turning response, and it means that both responses can be triggered by a single photon. If the experiment is carried out within 20 minutes of removing the cells from
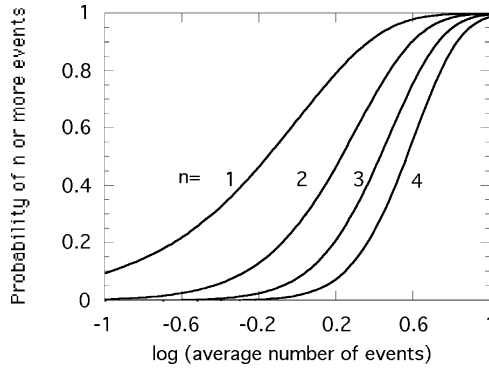
FIGURE 1.6. The probability that at least a certain number (n) of absorption events will occur during a sampling time plotted against the logarithm of the average number of events that would occur during a large number of similar samplings. It is seen that the shape of the curves depends on the value of n. If at least n absorption events are necessary for inducing a process, one can determine the number n by plotting the frequency of successful inductions against the logarithm of fluence and compare the shape of the curve obtained with the above diagram.

strong light, the stop-response curve has a shape similar to the curve labeled n = 2 in Fig. 1.6, meaning that in this case two photons are required.

The curves in Fig. 1.6 have been computed in the following way (let, as before, x be the average number of events recorded in a large number of trials): the curve for n = 1 is the probability (p) of absorption of at least one photon, which is one minus the probability for absorption of no photon, or $p = 1 - e^{-x} \cdot x^1/1! = x/e^x$. The curve for n = 2 follows the formula $p = 1 - e^{-x} \cdot x^1/1! - e^{-x} \cdot x^2/2!$, the curve for n = 3 follows the formula $p = 1 - e^{-x} \cdot x^1/1! - e^{-x} \cdot x^2/2! - e^{-x} \cdot x^3/3!$, etc.

1.7. Heat Radiation

The term heat radiation is sometimes (erroneously) used synonymously with infrared radiation. We shall use it here as the energy emitted when the energy of the random heat movement of the particles in condensed matter (solids, liquids, or compressed gases) is converted to radiation. It is easiest to think of heat radiation as the glow of a hot body (lamp filament, or the sun), but our own bodies also emit heat radiation, as does, in fact, a lump of ice or even a drop of liquid nitrogen. A body that is cooler than its environment absorbs more radiation than it emits, but still it radiates according to Planck's radiation law, to be described below. Heat radiation may be infrared, visible, or ultraviolet and, if we go to exotic objects in the cosmos, even outside this spectral range.

The starting point of the quantum theory was the attempt to explain the spectrum of the radiation emitted by a glowing body. To derive a function that matched the observed spectrum, Planck had to assume that the radiation

is emitted in packets (quanta or photons) of energy h·ν, where ν stands for frequency (which is also the velocity of light divided by the wavelength) and h is a constant, Planck's constant = $6.62620 \cdot 10^{-34}$ J·s. Planck's radiation law was derived for an ideal black body, best approximated by a hollow body with a small hole in it. With modifications it can be used for other bodies as well. The sun radiates almost as a black body.

Planck's formula can be written in different ways, depending on whether we consider radiation per frequency interval or per wavelength interval and whether we express the radiation as power (energy per time) or number of photons (per time). Furthermore, we may be interested in the radiation density inside a hollow body (mostly for theoretical purposes) or the radiation flux leaving a body (for most applications).

$$\text{Energy density per frequency interval} = (8\pi h/c^3) \cdot \nu^3 / (e^{h\nu/kT} - 1)$$

$$\text{Photon density per frequency interval} = (8\pi/c^3) \cdot \nu^2 / (e^{h\nu/kT} - 1)$$

$$\text{Energy density per wavelength interval} = 8\pi hc \cdot \lambda^{-5} / (e^{h\nu/kT} - 1)$$

$$\text{Photon density per wavelength interval} = 8\pi \lambda^{-4} / (e^{h\nu/kT} - 1)$$

These functions are mostly plotted with ν or λ as the independent variable and T as a parameter. It should be noted that even for the same T the functions all have maxima at different values of ν or λ (see Fig. 1.7, which shows the plots of energy per wavelength interval and photons per wavelength interval for 5000 K).

These examples are shown merely as an illustration of the fact that the maxima occur at different locations depending on which principle you use for plotting the spectra. This is not only true for heat radiation; it holds for all emission spectra,
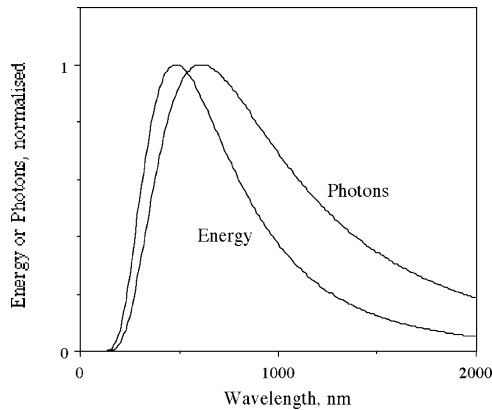
FIGURE 1.7. Blackbody radiation (5000 K) plotted as photons per wavelength interval and as energy per wavelength interval.

also for fluorescence emission spectra for instance. The most common sin of people publishing about fluorescence is that they do not understand this. They write "fluorescence, relative" on their vertical axis without further specification and do not realize that not even the shape of their spectrum, nor the positions of maxima, will be defined in such graphs. The second most common way of sinning is to spell fluorescence incorrectly.

You can see from Fig. 1.8 that the maxima occur at longer wavelengths when the temperature is lower and also that the total radiation is less in that case. In fact, the wavelength of the maximum is inversely proportional to absolute temperature (Wien's law), while the total photon emission is proportional to the third power of the absolute temperature (i.e., to T^3) and the total energy emission to the fourth power (T^4, Stefan-Boltzmann's law). Wien´s and Stefan-Boltzmann's laws can both be derived from Planck's radiation formula, but were found experimentally before Planck did his theoretical derivation.

The formulas shown above refer to radiation density in a closed cavity with radiating walls. The *fluence rate*, or amount of radiation per unit of time and unit of *cross-sectional* area falling from all directions on a sphere in this cavity, is obtained by multiplying the radiation density by the velocity of light. (Do not worry if you have some difficulty with this here. We shall return later to the concept of fluence rate, which is quite important in photobiology and often misunderstood.) Suppose that the sphere in the cavity is ideally black (absorbing all the radiation falling on it) and has the same temperature as the walls. The second law of thermodynamics states that (assuming that no heat energy is generated or consumed in the sphere) the sphere must stay at the same temperature as the walls, and it must radiate the same amount of radiation
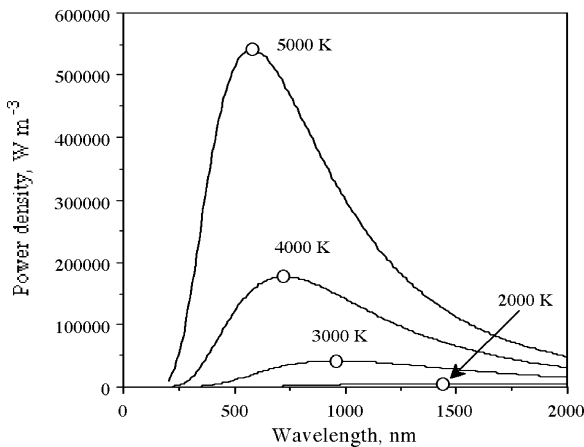
FIGURE 1.8. Blackbody radiation plotted as power per wavelength interval for different temperatures. Note that since the graphs show power (i.e., energy per time) per area and per wavelength interval, the dimension is power per volume and the unit W/m^3. The maximum of each curve is indicated by a circle.

(distributed in the same way across the spectrum) as it receives. Therefore its *excitance* (radiation given off per unit of time and unit of *surface* area) is the energy density given by the formulas above multiplied by the velocity of light and divided by 4 (since the *surface* area of the sphere is 4 times the *cross-sectional* area).

To obtain the excitance of a non–black body (such as a glowing tungsten filament in a light bulb, or your own body), the excitance computed for a black body should be multiplied by the *emissivity*. The emissivity varies quite a lot with wavelength, so the multiplication must be carried out separately for each wavelength value in which you are interested. The emissivity also varies somewhat with temperature. The *absorptivity*, or the ability to absorb radiation, is identical to the emissivity; otherwise the second law of thermodynamics would be violated.

It may seem that this is a little too much physics for a biology book, but an understanding of the basic physical principles is very helpful when it comes to the experimental work in photobiology. What has just been described can be used for calibrating measuring equipment in the photobiology laboratory.

1.8. Refraction of Light

From school you should be familiar with Snell´s law. This describes how light is refracted at an interface between two media with different indices of refraction (refractive indices), say n_1 and n_2. Figure 1.9, in which we assume $n_1 < n_2$, will serve as a reminder. If you need further explanation you will have to look in other books.

The refractive index can be regarded as the inverse of the relative velocity of light in the medium in question, i.e., it is the velocity in a vacuum divided by that in the medium. It can be shown that Snell´s law is equivalent to the statement that the light takes the fastest path possible between any two points on the rays shown. Compared to a straight line (dashed in Fig. 1.9) between point A on

$$n_1 \sin\alpha = n_2 \sin\beta$$
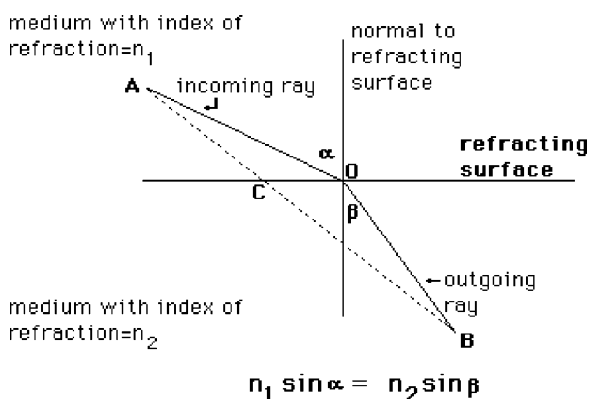
FIGURE 1.9. Refraction of light in a plane interface between transparent materials.

the upper ray and point B on the lower ray, you can see that the light goes a longer distance (solid line) in the medium with refractive index n_1 (lower index, higher velocity) than in the medium with refractive index n_2 (higher index, lower velocity), i.e., AO > AC and OB < CB. The refractive index is a pure number (no unit, as it is the ratio of two velocities). As we have used it here it is a real number (the usual type of number we use in most calculations, represented as a decimal number). In more advanced optical theory the refractive index is a complex ("two-dimensional") number.

As for the values of α and β in relation to one another, the figure looks the same if the light direction is reversed. However, this does not hold any longer when reflection is taken into account or when we consider the amount of light in the beams.

Throughout most of the spectrum the refractive index decreases with wavelength, but there are spectral regions (where absorption bands occur) where it increases steeply with wavelength; this phenomenon is, for historical reasons, called *anomalous dispersion*, although it is quite normal. In general, the change in refractive index with wavelength is called *dispersion*.

In some crystals and many biological materials the refractive index is different depending on direction and plane of polarization of the light. Such a medium is termed *birefringent*. Birefringence occurs in plant cell walls and other structures where elongated molecules are arranged in a certain direction. Measurement of birefringence has been an important method in elucidating the arrangement of molecules in such cases. Media that are originally *isotropic* (with the same properties in different directions, and thus not birefringent) may become birefringent by stretching or squeezing, application of electric fields, or other treatments.

When light passes through a birefringent medium of suitable thickness it becomes circularly or elliptically polarized because of the phase difference that develops between the components of different plane polarization.

1.9. Reflection of Light

Reflection may be *specular* (from a shiny, smooth surface or interface) or *diffuse* (from a more or less rough surface or interface). Diffuse reflection is very important in biology, but we shall limit ourselves here to specular reflection at interfaces between dielectric (nonmetallic) media.

The angle of incidence is always equal to the angle of reflection, but the amount of light reflected (as opposed to refracted) depends on the polarization of the light. The plane in which both the incident and the reflected rays (and the normal to the reflecting surface) lie is called the *plane of incidence*. The component of the light with an electric field parallel to this plane is designated by //, that with an electric field perpendicular to the plane of incidence by +. The fractions, R// and R+, of the irradiance of these components that are reflected are given by Fresnel´s equations, in which α is the angle of incidence (equal to

the angle of reflection) and β the angle of transmission (see Fig. 1.1. 9 in the section on refraction):

$$R// = [\tan(\alpha - \beta)/\tan(\alpha + \beta)]^2$$
$$R+ = [\sin(\alpha - \beta)/\sin(\alpha + \beta)]^2$$

The reflected fraction of unpolarized light is the mean of the two ratios. For normal incidence ($\alpha = \beta = 90°$) another set of equations has to be used, since with the equations above, divisions by zero would occur. In this case there is no distinction between R// and R+:

$$R = [(n_1 - n_2)/(n_1 + n_2)]^2$$

As an example of use of the last equation, let us consider the reflection in a glass plate ($n_2 = 1.5$) in air ($n_1 = 1$). When light strikes the glass plate (perpendicularly), $R = [(1–1.5)/(1+1.5)]^2 = [–0.5/2.5]^2 = 0.04 = 4\%$. When the light strikes the second interface (from glass to air) the value of R comes out the same again, because since the expression is squared, it does not matter in this case which of the indices you subtract from the other one. Thus 96% of the 96% of the original beam, or 92.16%, will be transmitted in this "first pass." It can be shown that after an infinite number of passes between the two surfaces the reflected fraction will be $R[1+(1–R)/(1+R)] = 2.0.04/(1+0.04) = 7.69\%$ and the transmitted fraction 92.31%. For most practical purposes we may estimate a reflection loss at normal incidence of about 8% in a clean glass plate or glass filter, but if the refractive index is exceptional this value may not hold. If the glass is not clean, it certainly does not.

The multiple internal reflection is not of much effect in a single glass plate, but I wanted to mention it here, because the effect is taken advantage of in so-called interference filters to be described in a later section.

Going back to the case of $\alpha < 90°$, we find by division, member by member, of the equations above, that R// divided by R+ is $[\cos(\alpha–\beta)/(\cos(\alpha+\beta)]^2$. This ratio will always be > 1, so R// > R+, or, in other words, the component of light with the electric field perpendicular to the plane of incidence and parallel to the interface will be more easily reflected than the other component. The interface can act as a polarizing device. It can be shown that the reflected beam becomes completely polarized when $\tan \alpha = n_2/n_1$, because none of the light polarized parallel to the plane of incidence is reflected (Fig. 1.10). The angle $\alpha = \arctan(n_2/n_1)$ is called the *Brewster* angle.

If a beam strikes a flat interface obliquely from the side where the refractive index is highest, the outgoing beam will have a greater angle to the normal than the ingoing (according to Snell's law). If the angle of incidence is increased more and more, an angle will eventually be reached when the outgoing beam is parallel to the interface. At greater angles of incidence there will be total
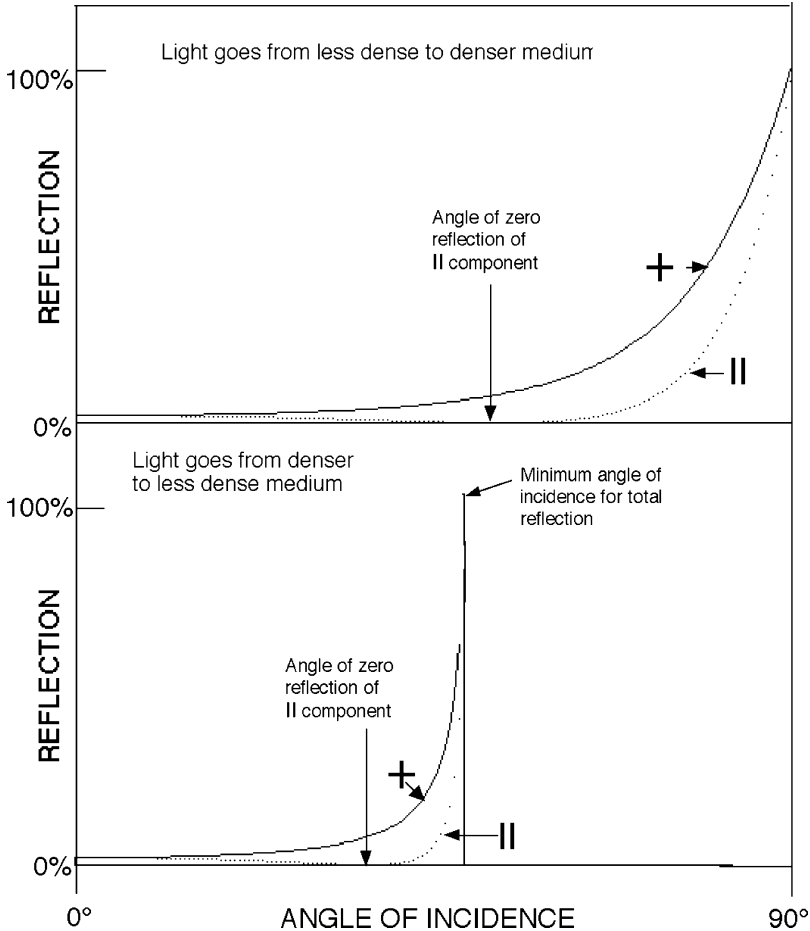
FIGURE 1.10. Percent of light reflected for different angles of incidence for light going from air ($n = 1$) to water ($n = 1.33$, top) and from water to air (bottom), and for light polarized with the electric vector in the plane of incidence (II) or perpendicular to the plane of incidence (+). For II-polarized light no light is reflected for a certain angle of incidence (the Brewster angle). For light going from the denser medium (water) to the less dense medium, total reflection occurs for angles of incidence larger than the critical angle.

reflection, i.e., all light will be reflected, and none transmitted. The smallest angle of incidence at which total reflection occurs is called the *critical angle*.

  If an object with higher refractive index immersed in the medium with lower refraction index comes very close to the reflecting interface (at a distance less than a wavelength), then light energy can "tunnel" through and interact with that object. It is a principle exploited for, e.g., fingerprint readers and some special kinds of microscopy (see Chapter 5).

1.10. Scattering of Light

Although, strictly speaking, reflection and refraction are also a result of scattering (absorption and reemission of electromagnetic energy by material oscillators), we do, in practice, use the term scattering in a more restricted sense for processes that tend to change the propagation of light from an ordered way to a random one. We can distinguish three types of scattering named after three distinguished scientists: Mie scattering, Rayleigh scattering, and Raman scattering.

Mie scattering is caused by particles larger than the wavelength of the light and having a refractive index different from that of the continuous phase in which they are suspended. Typical examples are water droplets (clouds, fog) or dust in the atmosphere, or the result of mixing a solution of fat in acetone with water. Almost any animal or plant tissue is a strong Mie scatterer due to the boundaries between cells and between different parts of the cells and, in the case of plant tissue, between cells and intercellularies. Mie scattering is nothing other than repeated reflection and refraction at numerous interfaces. As we have seen, light of different wavelengths is not reflected or refracted in exactly the same way, but most of these differences cancel out in Mie scattering, and there is no strong wavelength dependence of this phenomenon.

Rayleigh scattering is caused by the interaction of light with particles smaller than the wavelength of the light. The particles may even be individual molecules or atoms. In this case there are no interfaces at which reflection or refraction can take place. However, the closer the wavelength of the light is to an absorption band of the scattering substance (i.e., the closer the frequency of the light is to a natural oscillating frequency in the matter), the more strongly the electrons in the matter "feel" the light and the greater is the probability that the electromagnetic field is disturbed when it sweeps by. Most substances have their strongest absorption bands in the far ultraviolet. Therefore, in the infrared, visible, and near ultraviolet regions, Rayleigh scattering increases very steeply towards shorter wavelength. Ultraviolet is scattered more strongly than blue, which in turn is scattered more strongly than red. The blue color of the sky is due to more blue than red light being scattered out of the direction of the direct sunlight. To be more precise, Rayleigh scattering is inversely proportional to the fourth power of the wavelength, i.e., proportional to $1/\lambda^4$.

In Rayleigh scattering the direction of the electrical field is not changed. If, for instance, a horizontal beam, vertically polarized (i.e., with the electric field vertical), is scattered, the electric field remains vertical. But light can never propagate in the direction of its electric field (remember, it is a transverse wave). This means that the light is not scattered up or down, only in horizontal directions. If, on the other hand, the incident light is not polarized, it is scattered in all directions, but with different polarizations.

In both Mie and Rayleigh scattering the wavelength of the light remains unchanged. In Raman scattering, on the contrary, either part of the photon energy is given off to the scattering particles (which in this case are molecules) or some extra energy is taken up from the particles. The amount of energy taken up or

given off corresponds to energy differences between vibrational levels in the molecule. Raman scattering can be used as an analysis method and is also a source of error in fluorescence analysis, but we do not need to consider it in photobiological phenomena, since it is always very weak.

1.11. Propagation of Light in Absorbing and Scattering Media

We shall consider here first the simplest case: a light beam (irradiance I_o) that perpendicularly strikes the flat front surface of a homogeneous nonscattering but absorbing object. The most common objects of this kind that we deal with in the laboratory are spectrophotometer cuvettes and glass filters. A small fraction of the incident light is specularly reflected at the surface according to Fresnel's equation (see Section 1.9). For simplicity we disregard this in the present section. In spectrophotometry, reflection is taken care of by comparing a sample with a reference cuvette having approximately the same reflectivity as the sample cuvette.

At depth x within the object, the irradiance (see Chapter 2 for definitions of irradiance and other terms) will be $I_x = I_o \cdot e^{-Kx}$, where K is the linear absorption coefficient. The relationship is known as Lambert's law and follows mathematically from the conditions that (1) the light is propagated in a straight line and (2) the probability of a photon being absorbed is the same everywhere in the sample.

In spectrophotometry we also make use of Beer's law, which states that, under certain conditions, K is a product of the molar concentration of the absorbing substance and its molar absorption coefficient (or, in the case of several absorbing substances, the sum of several such products).

However, we are concerned now not with spectrophotometry, but with the propagation of light in living matter. Almost invariably we will be facing complications caused by intense scattering. A general quantitative treatment of scattering is so complicated as to be useless for the photobiologist. All it would lead to would be a system of equations with mostly unknown quantities.

A simplified theory, which has been found very useful as a first approximation is the Kubelka-Munk theory (Kubelka and Munk 1931). It should be observed that this theory is valid only for "macro-homogeneous" objects, i.e., those that on a macroscopic scale are uniform and isotropic, with absorption and scattering coefficients that can be determined. Seyfried and Fukshansky (1983) have shown how the theory can be modified for an object consisting of several macro-homogeneous layers. Specular reflection at the surfaces has to be dealt with separately. Uncertainty in the specular reflection leads to uncertainties in the absorption and scattering coefficients if they, as proposed by Seyfried and Fukshansky, are determined from overall reflection and transmission by the object. In any case the method is good enought to demonstrate here the general features of light propagation in media that both absorb and scatter light.

Suppose that we can determine, with sufficient confidence, the reflectance R (except for specular reflectance) and transmittance T of our sample. The linear absorption coefficient K and the linear scattering coefficient S, as well as the fluence rate at any point inside the sample, can then, with some effort, be computed from the system of equations:

$$R = 1/[a + b \cdot \coth(bSd)]$$

$$T = b/[a \cdot \sinh(bSd) + b \cdot \cosh(bSd)]$$

$$a = (S+K)/S$$

$$b = \sqrt{(a^2 - 1)}$$

$$I_x = I_o \cdot T \cdot [\{(a+1)/b\} \cdot \sinh\{bS \cdot (d-x)\} + \cosh\{bS \cdot (d-x)\}]$$

Here I_o is the fluence rate incident from one side and I_x the fluence rate at depth x of a sample of overall thickness d. The so-called hyperbolic operators sinh, cosh, and coth are defined by the following relationships: $\sinh(y) = (e^y - e^{-y})/2$; $\cosh(y) = (e^y + e^{-y})/2$; $\coth(y) = \cosh(y)/\sinh(y)$. If light is incident from both sides, the last equation has to be modified.

To demonstrate, without too much computation, the effect of scattering, we shall assume that we have determined K and S. For any sample thickness, d, we can then compute I_x as a function of x.

Note the following features in the examples of computer outputs (Figs. 1.11 and 1.12):
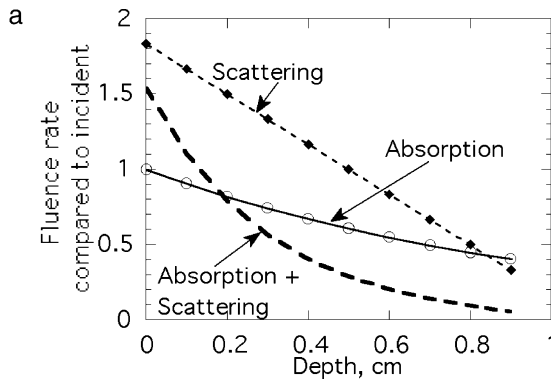
FIGURE 1.11. (a) Decrease of fluence rate with depth. The decrease of fluence rate with depth of penetration in a 1-cm-thick slab of a medium with absorption only (linear absorption coefficient 1 cm^{-1}), scattering only (linear scattering coefficient 5 cm^{-1}), and one with both absorption (1 cm^{-1}) and scattering (5 cm^{-1}). The values were computed using the Kubelka-Munk theory and assuming isotropic incident light. In the upper frame the fluence rate scale is linear, in the lower one logarithmic. Note that in a scattering medium fluence rate can exceed the fluence rate of the incident light. (Fig. 1.11a is a linear plot; Fig. 1.11b on the next page has a logarithmic vertical scale.)
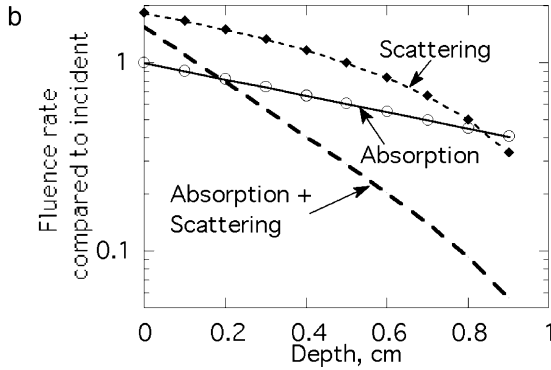
FIGURE 1.11. (b)

1. When S is given a low value (0.01), the Kubelka-Munk curve coincides with the Lambert curve (and is therefore invisible).
2. When S has a value similar to or higher than K, i.e., when scattering is appreciable compared to absorption, the fluence rate in the sample near the illuminated side is higher than the incident fluence rate. This is no violation of the law of energy conservation; the sample does not create any new light. However, the concentration of photons is increased by their bouncing back and forth.

The expediency with which the Kubelka-Munk equations can be evaluated using a computer must not cause us to forget the limitations of the Kubelka-Munk theory. One severe restriction is that only diffuse incident light is considered. We need only enter three constants, K, S, and thickness of the scattering medium, to describe the scattering object. A more complete description would give more
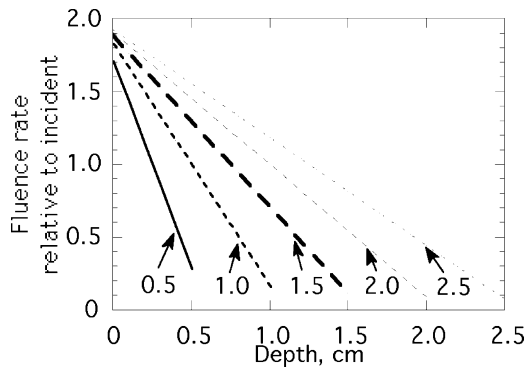
FIGURE 1.12. Decrease of fluence rate in layers of the indicated thickness (in cm) of a purely scattering medium (no absorption); the linear scattering coefficient is 5 cm^{-1} in all cases. Note that the fluence rate decreases more quickly in a thin scatterer because there is less backscatter of light.

realistic results, but apart from the difficulty in choosing the correct constants, the equations and algorithms would rise in complexity very fast. More complete theories are described by Star et al. (1988) and Keijzer et al. (1988).

1.12. Spectra of Isolated Atoms

We shall deal in this section with isolated atoms (which are not part of di- or polyatomic molecules and also not close to one another for other reasons, such as high pressure). They can increase their internal energy by absorbing photons and also give off energy by emitting photons. They can absorb or emit only very particular photons, whose energy corresponds very exactly to differences between energy levels in the atom. The simplest case is the hydrogen atom, and it has been found that its energy levels are inversely proportional to $1/n^2$, where n represents positive integers (1, 2, 3, …). The possible energy jumps are then proportional to the energy differences $1/n^2$-$1/m^2$, where n = 1, 2, 3, …and m = n+1, n+2, etc. Since, according to the relationships $E = h\nu$ and $\lambda = c\nu$, the energy (E) of a photon is inversely proportional to wavelength (λ), the wavelengths of light which can be absorbed or emitted by a hydrogen atom are given by $1/\lambda = R \cdot (1/n^2$-$1/m^2)$ (see Fig. 1.13). The proportionality constant is called the reduced Rydberg constant. It is slightly dependent on the mass of the atom's nucleus, and for ordinary hydrogen it amounts to 0.0109677581 nm^{-1}.

In ordinary hydrogen gas the atoms are combined in pairs. However, when an electric current runs through the gas, the pairs are split and photon emission from energized (excited) free hydrogen atoms takes place. In the laboratory we use lamps containing heavy hydrogen (deuterium), for instance, in the spectrophotometer. We use the continuous part of the spectrum in the ultraviolet (as well as continuous emission in the ultraviolet arising from molecular deuterium) for measuring ultraviolet absorption of samples. We can use the two first lines of the Balmer series, for which n = 2, (H_α at 656 nm and H_β at 486 nm) for wavelength calibration. In the program on which Fig. 1.13 is based, an approximate Rydberg constant in between that for light and heavy hydrogen was used. In Nature the H_α, H_β, and some other hydrogen lines appear in the spectrum from the sun as absorption lines (Fraunhofer lines), because of the presence of nonexcited hydrogen atoms in the atmosphere of the sun outside the glowing photosphere. Light of these particular wavelengths is therefore almost absent in the daylight spectrum. The absence of H_α light from daylight should make
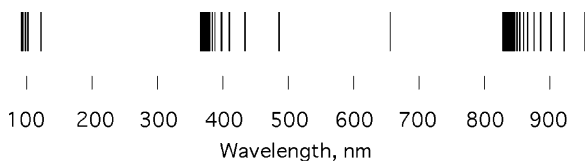
FIGURE 1.13. Spectrum of atomic hydrogen (computer simulation).

it possible to measure other light (e.g., fluorescence) at this wavelength in full daylight. However, the chlorophyll fluorescence from plants is weak at such a short wavelength.

One other case where the photobiologist is concerned with the spectrum of isolated atoms is when he or she uses low-pressure mercury lamps. We shall return to this in Chapters 3 and 25.

1.13. Energy Levels in Diatomic and Polyatomic Molecules

The energy relations immediately become much more complex when we proceed from single atoms to molecules consisting of two atoms each, i.e., diatomic molecules. The simplest example of such a molecule (if we disregard the hydrogen molecular ion H_2^+) is the hydrogen molecule, H_2.

In the molecule we have, in addition to the electronic energy described for the atom, vibrational and rotational energy. In diatomic molecules the bond between the atoms, mediated by the electrons, can be regarded as an elastic string or spring, which stretches and contracts. At one instant the nuclei of the two atoms move towards one another. When the positively charged nuclei come close enough, their mutual electric repulsion becomes strong enough to reverse the motion, and the distance between the nuclei starts to increase. The nuclei move apart until the attractive force from the negatively charged electrons becomes strong enough to reverse the motion again.

This oscillating movement of the nuclei has some resemblance to that of a pendulum, but one difference is that it is asymmetrical. The force on the nuclei is not proportional to the distance from a symmetry point, and therefore the molecule is an inharmonic oscillator rather than a harmonic one.

The changes in energy due to changes in oscillating movement are smaller than (the largest) energy jumps due to electronic transitions (changes in electronic energy).

In molecules consisting of more than two atoms each there are also oscillations due to the bending of bonds, but we shall disregard this in the following.

The molecule can also absorb or emit energy by changing its state of rotation. In diatomic molecules only rotation around an axis perpendicular to the bond contributes to the rotational energy, but in more complicated molecules we must consider three axes of rotation, all perpendicular to one another.

All these energy changes are quantized, i.e., only certain energy changes are possible. However, because the vibrational and rotational energy amounts are much smaller than the electronic energy amounts and are combined with them, the molecules have apparently continuous absorption and emission bands rather than lines. At equilibrium, the number of molecules (N_x, N_y) "occupying various energy states" as the jargon goes, i.e., having various amounts of energy (E_x, E_y), is related to the energy differences between the states by the formula $N_x/N_y = e^{(E_y - E_x)/(kT)}$.

We shall now restrict the discussion to the stretching vibrations and their interaction with the electronic energy transitions. At one point in the stretching oscillation the force acting on the nuclei is zero (the repulsive and attractive forces compensate one another exactly). All the vibrational energy is then kinetic (translational) energy. In contrast, when the distance between the nuclei is either minimal or maximal, i.e., at the inner and outer turning points, the velocity is zero, and therefore the kinetic energy is zero. All the vibrational energy is then potential (positional) energy. In between, the kinetic and potential parts of the energy change in such a way that their sum is constant.

In Fig. 1.14 the distance between the atomic nuclei is plotted in the horizontal direction (lowest values to the left) and the energy of the molecule in the vertical direction (lowest values at the bottom). The curved lines show the potential energy for various distances and for two different electronic states of the molecule. The various horizontal lines within the curved lines show the total energy for various vibrational states and for the two electronic states. The turning point in the oscillating movement of the nuclei is where these horizontal lines reach the curves. For these interatomic distances the kinetic energy is zero.
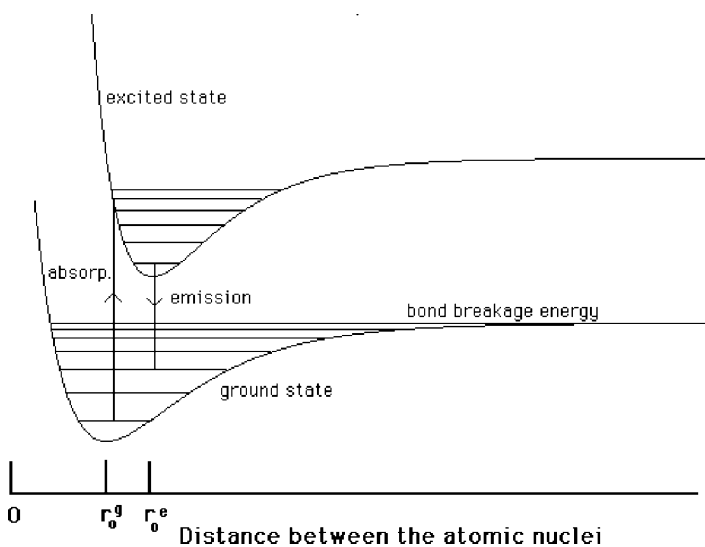
FIGURE 1.14. The potential energies (vertical coordinate) of the electronic ground state and the first excited state are shown by the curves as functions of the distance between the atomic nuclei in a diatomic molecule (horizontal coordinate). The equilibrium distances (lowest potential energy) for the ground and excited states are denoted by r_o^g and r_o^e, respectively. At this distance the potential energy is minimal, and the kinetic energy (distance between curves and horizontal lines) is maximal. However, the molecule never comes to rest at this position. Even at zero absolute temperature the vibrations continue (lowest horizontal lines on the curves).

Looking at Fig. 1.14 and the lengths of the vertical lines in it, we get some understanding of why absorption maxima occur at shorter wavelengths (higher photon energy) than emission maxima (this difference is referred to as the "Stoke's shift"). The maxima, which we can determine experimentally, of course correspond to the wavelengths and photon energies of the most likely transitions. Later we will see how one can look at the same phenomenon from quite a different point of view.

A macroscopic pendulum moves most slowly near the turning points. If it were possible to get snapshots of the molecule at random times, one would therefore expect most of the snapshots to show the atoms near the turning points. However, the quantum physics is more complicated than that. For the lowest vibrational state, the zero state, it is quite the opposite, and the probability is greatest that the molecule will be near the state of zero potential energy and maximum kinetic energy. Thus, when for some reason a molecule changes electronic state, in most cases the transition will occur from near the midpoint of the line for the lowest vibrational state. The vertical line to the left in Fig. 1.14 shows a likely transition from the lower electronic state to the higher electronic state, and the line to the right shows a likely transition from the higher electronic state to the lower one. The upward transition could be associated with absorption of photons, and the downward one by emission of photons.

In order to illustrate the various energy levels and transitions between them, it has become customary to use a kind of diagram named after Aleksander Jabłonski (pronounced Jabwonski). In such a diagram (see Fig. 1.15) the electronic energy levels (energy states of the molecule) are indicated by thick horizontal lines, the overlayered vibrational states by thinner horizontal lines, and state transitions by arrows.

Note that the downward pointing solid arrows (light emission) are generally shorter than the upward pointing ones (light absorption), corresponding to the fact that light emission is generally of longer wavelength (lower photon energy) than light absorption. This is, however, a matter of statistical distribution, and in stimulated emission the wavelength is the same for absorbed and emitted light.

Stimulated emission is a phenomenon theoretically stipulated by Einstein, but observed much later. According to Einstein, a molecule can be transformed by light absorption in two ways: either from a lower to a higher energy state, as we have described before, or from a higher to a lower state. In the latter case two photons are emitted (stimulated emission) for each one absorbed, and all three photons are of the same wavelength. The reason that it took a long time for stimulated emission to be observed is that the concentration of molecules in sufficiently high energy states is usually low, and the probability for stimulated emission therefore low. The transitions are described using so-called Einstein coefficients, B_{12}, B_{21}, and A_{21}. If, in a certain radiation field of energy density $r(\nu)$ for the frequency (ν), the number of molecules in the lower energy state is N_1, in the upper state N_2, then the probability of upward transitions is $B_{12} \cdot \rho(\nu) \cdot N_1$, and the probability of downward stimulated transitions is $B_{21} \cdot \rho(\nu) \cdot N_2$,
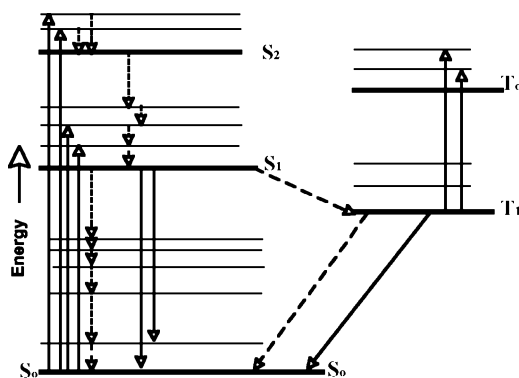
FIGURE 1.15. Jablonski diagram: the thick horizontal lines indicate electronic energy states, the thin horizontal lines above each thick line vibrational substates. Associated with each electronic state, and indicated by thinner lines above the thick lines, are several vibrational energy levels. The higher up in the diagram, the higher energy the lines indicate. Solid upward arrows represent absorption of photons (light energy), the downpointing solid lines emission of photons (either spontaneous or stimulated emission). The wider arrow to the far left indicates that energy increases upward in the diagram. To the left in the figure the system of singlet states (S_o, S_1, S_3, with only paired electrons), to the right the system of triplet states (T_1, T_2, containing unpaired electrons). Arrows with short dashes indicate radiationless transitions within each state system. Arrows with long dashes indicate intersystem transitions (intersystem crossing). In the singlet system radiative deexcitation (fluorescence) can take place only from the lowest excited state, since all other states are very short-lived. The transition from a triplet state to the ground level (S_o) does not take place easily, since an electron has to change spin. Thus the T_1 state (the lowest triplet state) is long-lived, and the radiative deexcitation from T_1 results in phosphorescence. This Jablonski diagram is not intended to depict energy relations in a particular molecule, but only general principles. A Jablonski diagram for the oxygen (O_2) molecule would, however, look radically different, since for this molecule the lowest-lying level represents a triplet state.

but there are also spontaneous downward transitions with a probability $A_{21} \cdot N_2$ Because of the spontaneous downward transitions, N_1 is generally much larger than N_2. When light intensity is increased more and more, N_2 gradually approaches N_1 but cannot be caused to exceed it by light absorption alone (see Fig. 1.16).

The most important applications of stimulated emission are the laser (acronym for **l**ight **a**mplification by **s**timulated **e**mission of **r**adiation) and some types of high-resolution optical microscopy, to be described later.

Apart from the changes in vibrational and rotational energy, there are other causes of the "broadening" of spectra mentioned above (from line spectra to band spectra). More complicated molecules are usually (and the biomolecules always) in a condensed phase (liquid or solid) rather than in a low-pressure gas.

Energy level 2
with N_2 molecules

$B_{12}\rho(\nu)N_1$ $B_{21}\rho(\nu)N_2$ $A_{21}N_1$

Energy level 1
with N_1 molecules
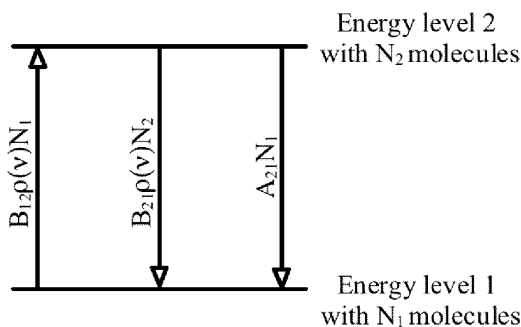
FIGURE 1.16. Simplified energy level diagram (Jablonski diagram) for a molecule to explain stimulated emission. The arrows symbolize transitions between the two levels, by (from left to right) absorption, stimulated emission, and spontaneous emission. The probability of a transition is proportional to the population (N_1 or N_2) of molecules from which the transition takes place. Absorption and stimulated emission are also proportional to the energy density, $\rho(\nu)$, at the frequency (ν), which corresponds to the energy difference ($\Delta E = h\nu$) bween the levels. (The energy density, in turn, is the product of the speed of light and the fluence rate.) For each one of these transition probabilities there is also a proportionality factor (called an Einstein coefficient), i.e., B_{12} for absorption, B_{21} for stimulated emission, and A_{21} for spontaneous emission. Einstein showed that $B_{12} = B_{21}$ and $A_{21} = B_{21} \cdot 8\pi \cdot h\nu^3/c^3$. In the steady state the upward and the total downward transition rates are the same, i.e., $B_{12} \cdot \rho(\nu) \cdot N_1 = B_{21}\ \rho(\nu) \cdot N_1 = B_{21} \cdot \rho(\nu) \cdot N_2 + A_{21} \cdot N_2$, from which follows $N_2/N_1 = \rho(\nu)/[\rho(\nu) + 8\pi \cdot h\nu^3/c^3]$. It follows from this that for low energy densities (weak light) N_2/N_1 and also N_2 increase proportionally to the light, but also that N_2/N_1 cannot exceed 1 even if the light is very strong. A so-called inverted population of molecules with $N_2/N_1 > 1$, which is necessary for laser action, can only be obtained in other ways than by simple light absorption from one energy state to another one.

The different molecules in the phase affect one another in complicated ways so that the energy levels of are not the same as those of its neighbors. Finally, the different molecules are not identical (as a collection of isolated atoms of the same kind are) since they, even if they correspond to a single chemical formula, may have different *conformations*, e.g., an extended or folded chain of atoms. This results in continuous absorption and emission spectra.

Because, at ordinary temperatures, transitions between different conformational states take place readily, we do not experience molecules with different conformations as different kinds of molecules. By greatly lowering the temperature we may prevent the transitions between different conformational states as well as between different vibrational and rotational states, and it becomes possible to selectively deplete one state by monochromatic light from a laser. In this way one may "burn holes" in an absorption spectrum and see which portion of a spectrum is associated with a particular state (Fig. 1.17).
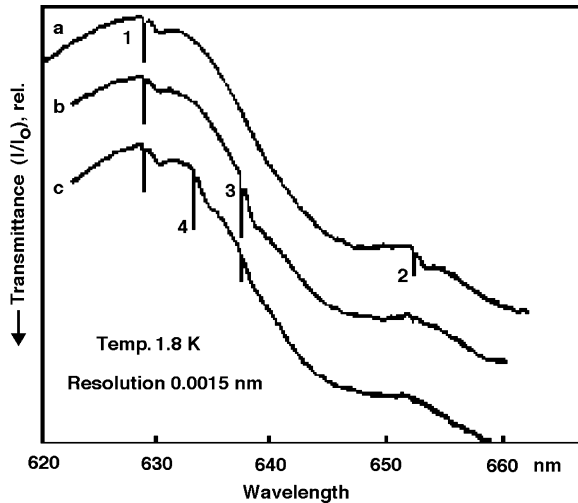
FIGURE 1.17. A solution of C-phycocyanin was irradiated with a strong laser beam. Various wavelengths were used in the order indicated by the numbers and the vertical lines on the curves. These lines are, in fact, narrow dips or "holes" in the absorption spectra caused by depopulation of specific molecular states by the laser light. Note that irradiation with light of shorter wavelength following one with light of longer wavelength causes a repopulation of the less energetic state (corresponding to the longer wavelength). For instance, irradiation 3 practically cancels the effect of irradiation 2 (but not that of irradiation 1 at an even shorter wavelength than 3). Similarly, irradiation 4 partly cancels the effect of irradiation 3. (From Friedrich et al. 1981, modified.)

Even at a temperature of absolute zero the oscillation continues, with all molecules in the lowest vibrational state, the zero state. In fact, even at room temperature the majority of the molecules are in this state, but a substantial fraction are in higher states.

Even at moderately lowered temperatures, absorption spectra (as well as fluorescence spectra) are sharpened (Fig. 1.18). This effect is often taken advantage of in spectroscopic investigations of biological samples containing several substances with similar spectra, such as cytochromes or chlorophyll proteins.

It should be understood that a molecule can appear in an electronically excited state for reasons other than having absorbed light or ultraviolet radiation. In rare cases the collisions with other molecules can give a molecule sufficient energy for transition to an excited state. Chemical reactions may also produce reactants in electronically excited states, which can lose their energy by emission of light. This is how chemiluminescence works, and bioluminescence, which will be described later, is biochemical chemiluminescence.
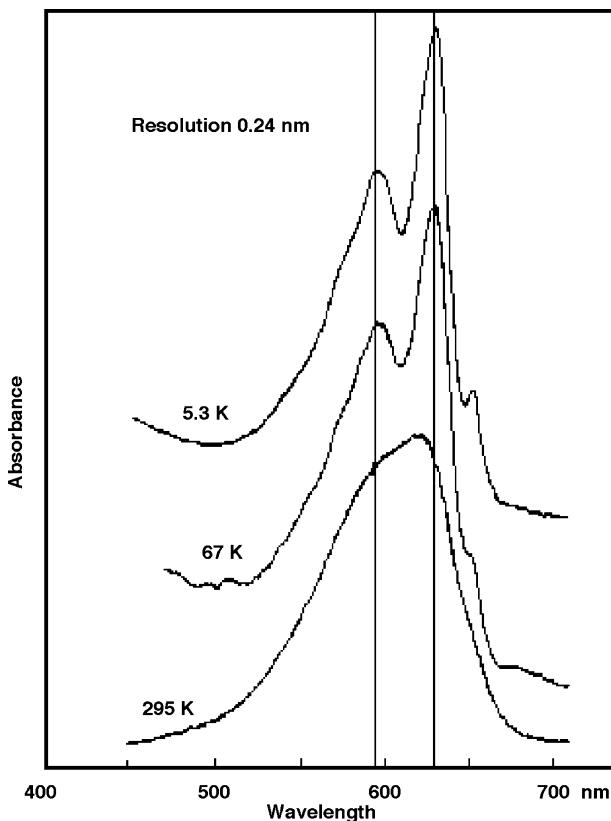
FIGURE 1.18. Absorption spectra of C-phycocyanin at various temperatures. (Redrawn from Friedrich et al. 1981.)

1.14. Quantum Yield of Fluorescence

It has been already mentioned that a molecule in the excited state may lose its energy in various ways it out as light radiative de-excitation. This process is called fluorescence if the transition is from a singlet excited state to a singlet ground state, and phosphorescence if the transition is from a triplet excited state to a singlet ground state or from a singlet excited state to a triplet ground state (the most important example of the latter is phosphorescence of singlet oxygen). It can also lose energy as vibrations to neighboring molecules (thermal de-excitation). Singlet excited states can disappear by "intersystem crossing" to produce triplet states; this happens, e.g., sometimes with chlorophyll molecules. And finally, energy may be lost through chemical reactions. Thus, the total rate of disappearance of singlet excitation can be described as the sum of the rates for the different de-excitation "pathways." In most cases each molecule "acts on its own," so the kinetics of disappearance of singlet excitate states is of first

order (in contrast, deexcitation of singlet oxygen is mixed first and second order at higher concentrations). It can thus be described by a first order rate constant k, which is a sum of the rate constants for the different pathways:

$$k = k_f + k_{th} + k_{ic} + k_{ch}$$

where f stands for radiative de-excitation (usually fluorescence), th for thermal de-excitation, ic for intersystem crossing, and ch for chemical de-excitation. Under steady illumination a steady state develops, so the rate of excitation by absorption of photons equals the total rate of de-excitation. Therefore, the ratio of the number of photons emitted as fluorescence to the number of photons absorbed will be

$$\phi_f = k_f/k = k_f/(k_f + k_{th} + t_{ic} + k_{ch})$$

The quantity ϕ_f is called the quantum yield of fluorescence. In the same way we have a quantum yield for each de-excitation path; for example, also for the chemical deactivation:

$$\phi_{ch} = k_{ch}/k = k_{ch}/(k_f + k_{th} + t_{ic} + k_{ch})$$

The different pathways compete with one another. Therefore, the chlorophyll fluorescence from a plant, which is usually weak and invisible, increases if we add a poison that stops photosynthesis, the main pathway for chemical de-excitation. The fluorescence from chlorophyll becomes even stronger and clearly visible if we extract the chlorophyll and illuminate it dissolved in an organic solvent as acetone. Then we have not only completely stopped chemical de-excitation, but also decreased thermal de-excitation.

Studying the changes of fluorescence from chlorophyll is an important way to investigate the functioning of the photosynthetic apparatus. In this context one often uses the terms photochemical quenching and nonphotochemical quenching, respectively, for the chemical and thermal de-excitations competing with fluorescence.

1.15. Relationship Between Absorption and Emission Spectra

A simple relationship between absorption and emission spectra of even very complicated molecules was first hinted at by E.H. Kennard and later elaborated upon mostly by B.I. Stepanov. The relationship is most commonly referred to as the Stepanov relationship. The basic idea is that it is of no consequence to the future behavior of a molecule in which way it reached a certain state. From

this it follows that any emission from an excited (energy-rich) electronic state of any kind of molecule in thermal and conformational equilibrium with its surroundings must have the same spectrum, whether the molecule reached the energy-rich state by collisions with its neighbors, or by absorbing a photon, or as a result of a chemical reaction. More specifically, the shape of the fluorescence spectrum (excited state reached by absorption of photons) is identical to the shape of the heat radiation spectrum from that kind of molecule. The heat radiation spectrum follows Planck's law for a blackbody, modified by the emissivity of the substance. But the emissivity, as was already mentioned, is the same as the absorptivity, which has the same spectral dependence as the experimentally measured absorption coefficient. Thus (fluorescence spectrum) = (absorption spectrum) × (blackbody spectrum). The multiplication sign here stands for *convolution*, i.e., multiplication of pairs of values throughout the spectrum. The fluorescence spectrum will then be expressed as photons per wavelength interval, energy per frequency interval, etc., depending on how the blackbody spectrum is entered into the equation.

The Stepanov relationship breaks down when heat energy cannot easily diffuse away from the emitting molecule. This happens in solid media or liquids of high viscosity and is always the case at low temperatures. Conversely, by comparing a fluorescence and an absorption spectrum, it can be found out whether or not the molecules in the excited state are in thermal and conformational equilibrium with the surroundings at the time of photon emission. An example of the application of these ideas to a biological system is provided by Björn and Björn (1986).

1.16. Molecular Geometry of the Absorption Process

In a molecule the center of positive charge (associated with the nuclei) may, or may not, coincide with the center of negative charge (associated with the electrons). If the center of positive charge does not coincide with the center of negative charge, the molecule is a dipole. Unless molecules are symmetrical, as are CCl_4 or CH_4, they are more or less strong dipoles.

A dipole is characterized by a dipole moment. This is a vector, having direction and magnitude. The magnitude is the distance between positive and negative charge centers times the amount of charge. The direction of the dipole moment is from the negative to the positive charge center. Like other vectors, the dipole moment is often symbolized by an arrow (Fig. 1.19).

When a molecule is electronically excited, the negative charge is generally displaced in relation to the positive charge, i.e., there is a change in dipole moment. This change in dipole moment is called the transition moment, and often symbolized by **M**. Like the dipole moment it is a vector; in fact it is the dipole moment of the excited state (D_E) minus the dipole moment of the ground state (D_G). Symbolizing the vectors by arrows, we may describe the subtraction as shown in Fig. 1.19.
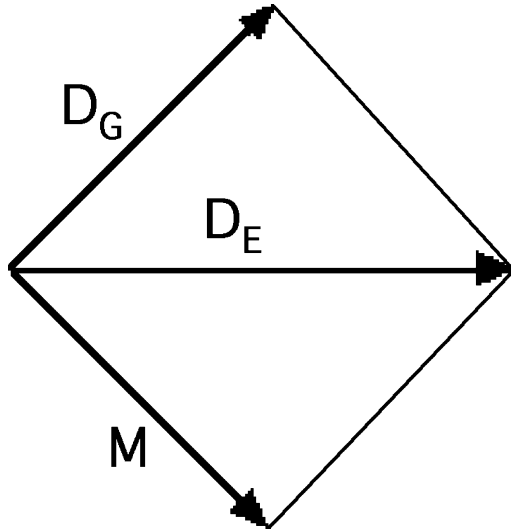
FIGURE 1.19. The transition moment **M** for a transition from the ground state to an excited state is the vectorial difference between the dipole moments of the molecule in the ground state (D_G) and in the excited state (D_E).

The magnitude of the transition moment can be estimated from the absorption spectrum of the compound in question. Denoting the molar absorption coefficient by ε and light velocity divided by wavelength (frequency, c/λ) by ν, the oscillator strength (the square of the magnitude of the transition moment), is approximately $4.32.10^{-9} \int \varepsilon d\nu$, where integration is carried out over the absorption band.

In most cases of excitation by light absorption, the probability of absorption is proportional to the square of the component of the transition moment in the direction of the electric field of the light. (There are cases of interaction between electrons and the magnetic field of the light rather than the electric field, but these cases are of little interest in photobiology.) Expressed in another way, the probability is proportional to $|M|^2 \cos^2 \alpha$, where α is the angle between the transition moment and the direction of the electric vector of the light wave, i.e., the direction in the plane of polarization which is perpendicular to the direction of light propagation.

To those of you who think this is hard to follow: remember that the probability of absorption depends on how the molecule is oriented in relation to the direction of the light and (for plane-polarized light) the plane of polarization. For absorption of light by molecules in ordinary solutions this is of no consequence, since the molecules (except in special cases) have random directions. For absorption of light by molecules in living cells it is sometimes very important, since these molecules may be very accurately aligned. In such cases light polarized in a direction parallel to the transition moment of the absorbing molecule is more strongly absorbed than light polarized in other directions. This phenomenon is called (absorption) dichroism.

In the same molecule there may be transition moments with different directions. For example, in the chlorophyll molecule, two transition moments are nearly at right angles to one another. The transition moment for emission of fluorescence may have a direction different from that for excitation of fluorescence. By measuring the polarization of fluorescence from molecules irradiated by polarized light, one can gain information about the angle between the transition moments.

1.17. Transfer of Electronic Excitation Energy Beween Molecules

Transfer of electronic excitation energy from compound A to compound B may be symbolized as A* + B → A + B*. The energy quantum to be transferred must have a size such that it can be given off by A, i.e., correspond to the enrgy of a photon within the fluorescence band of A. Furthermore, it must be of a size that can be taken up by B, i.e., correspond to the energy of a photon within the absorption band of B.

There are a few photobiological phenomena in which this energy transfer is actually mediated by a photon. As an example we may mention the transfer of energy from luciferin in the lantern of a firefly female to the rhodopsin in the eye of a firefly male. However, in the majority of cases, the radiation transfer is radiationless, a process that is much more efficient at short range. Very few of the photons emitted by firefly females happen to be absorbed in rhodopsin molecules of firefly males. The advantage of energy transfer by photons is that it can take place over distance. We also all depend on the energy transfer taking place directly between atoms in the sun and chlorophyll molecules in plants, but also this is a very wasteful process in the sense that a very small fraction of the photons emitted by the sun end up in chlorophyll molecules. On the other hand, once the quantum has been caught by a chlorophyll molecule (or a molecule of phycoerythrin or phycocyanin), it is channeled from molecule to molecule with an efficiency of practically 100% by radiationless energy transfer (Fig. 1.20).

There are two main mechanisms for radiationless energy transfer: *exciton coupling* and the *Förster mechanism*. Exciton coupling occurs in a pure form in the photosynthetic antennae of green photosynthetic bacteria like *Chloroflexus*. The so-called chlorosomes of these bacteria contain rods made up of bacterio-chlorophyll and carotenoid molecules. The pigment molecules are so tightly packed together that the whole rod behaves almost as a single pigment molecule; the energy is delocalized. This phenomenon, called *exciton coupling*, provides very fast transfer of the energy to the reaction center.

In other cases chromophores may just pairwise be close enough to share energy and form what is called *exciplexes*. When exciplexes are formed, the energy levels split up.

The other mechanism, the Förster mechanism or resonance transfer, or dipole–dipole interaction, is exemplified in a rather pure form in the phycobilisomes,
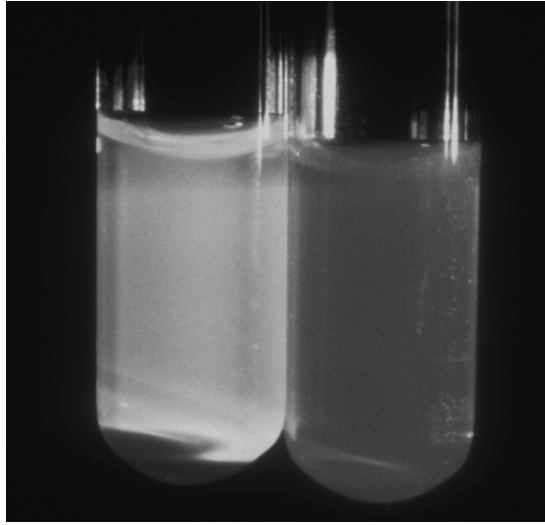
FIGURE 1.20. Demonstration of energy transfer in phycobilisomes prepared from a cyanobacterium. The chemical composition is exactly the same in the two test tubes, except for the concentration of the phosphate buffer in which the phycobilisomes are suspended. The test tubes are illuminated with green light (absorbed mainly by phyco-erythrin) and the yellow and red color is due to fluorescence of the phycobiliproteins. In the test tube to the left the phosphate concentration is low, the phycobilisomes are disso-ciated with large distances between the various phycobiliproteins, and the fluorescence is directly emitted by phycoerythrin. In the test tube to the right the phosphate concentration is high (0.15 M), the phycobiliproteins are close together in undissociated phycobilisomes, and energy is transferred from phycoerythrin, via phycocyanin, and finally emerges as red fluorescence from allophycocyanin. Such "fluorescence resonance energy transfer" (FRET) is nowadays exploited in a number of applications, such as a method for DNA sequencing. (Phycobilisome preparation by Dr. Gunvor Björn, photo by the author.) (*See* Color Plate).

pigment antennae of cyanobacteria and red algae composed of phycoerythrin, phycocyanin, allophycocyanin, and linker peptides holding the complex together (phycoerythrin is not always present, and in some cases there are also other phycobiliproteins, such as phycoerythrocyanin). Only a few of the chromophores in the phycobilisomes are close enough to form exciplexes. A special section will be devoted to the Förster mechanism because it is so important.

1.18. The Förster Mechanism for Energy Transfer

Thus, the transition of the molecule from one electronic energy state to another causes a change in the electrical field around it. Conversely, a change in the electric field can cause the transition from one energy state to another one. The

field change caused by the transition in one molecule can cause the opposite transition in a neighboring molecule. This is the essence of energy transfer by dipole–dipole interaction, the Förster mechanism for energy transfer.

Just as the field change from the transition taking place in one molecule (the donor) drops off with the third power of the distance, so the sensitivity of the other molecule (the acceptor) to a field change drops off with the third power of the distance. The combined effect is a sixth power relationship: the rate of dipole–dipole energy transfer between two molecules is inversely proportional to the sixth power of the distance.

We are now ready to have a look at a simplified Förster's formula:

$$\text{Energy transfer rate} = \text{factor} \cdot \phi \cdot (\text{overlap integral}) \cdot \cos^2 \alpha / (r^6).$$

Here ϕ is the fluorescence quantum yield in the absence of the acceptor (see Section 1.15), α the angle between the transition moments of the molecules, r is the distance, and the overlap integral is the convolution (pointwise product) of the donor fluorescence spectrum by the acceptor absorption spectrum, integrated over the whole spectral region in common.

1.19. Triplet States

Our description of molecular energy states so far has been aimed primarily at explaining the properties and processes associated with so-called singlet states. A molecule is said to be in a singlet state when all its electrons are grouped in pairs, so that the two electrons in each pair have opposite *spins*. Spin is a property of an electron or other charged particle that makes it act like a small magnet to produce a magnetic field. Positive charged particles such as atomic nuclei also have spin.

Because all electrons in a molecule in a singlet state occur in pairs, and the electrons in each pair have opposite spins, the electrons produce no net magnetic field. Most molecules like to be in a singlet state, so usually the ground state, the most stable state, having the lowest electronic energy, is a singlet state. A notable exception is the dioxygen molecule (making up ordinary oxygen in the air), which we shall come back to later.

However, it can occasionally happen that when a molecule has been excited from its ground (singlet) state to an excited singlet state, an electron "flips over," i.e., changes spin. Let us take a concrete and important example—the chlorophyll a molecule (Fig. 1.18). Like other chlorophyll forms, chlorophyll a has two prominent absorption bands corresponding to two electronic transitions with high probability. For chlorophyll a these absorption bands are in the blue and red parts of the spectrum. In a collection of chlorophyll a molecules, be it in the plant or in solution, most of the molecules are in the ground state. Absorption of a photon of red light transforms a ground-state molecule to the

first excited singlet state. Absorption of a photon of blue light transforms a molecule from the ground state to the second excited singlet state. A molecule in the second excited singlet state very rapidly transfers some of its electronic energy to vibrational energy (heat) and lands in the first excited singlet state. Then various things can happen. The most "exciting" (pardon the expression) of the possibilities is that an electron completely leaves the molecule. This is the key step in photosynthesis and the key step in the whole living world. Another possibility is that the molecule "shakes off" more energy, heats its environment even more, and returns to the ground state. A third possibility is that it emits a photon, which carries away the excess energy and also returns the molecule to the ground state. A fourth possibility, which is realized in only a small fraction of the cases, is that the molecule is transferred from the first excited singlet state to the first (excited) triplet state. Although this happens after only a small fraction of excitations, it is important, and if plants were not specially equipped to handle such events, they would not survive.

A change from a singlet to a triplet state, which involves a spin change, a "flip" of an electron, is sometimes referred to as "intersystem crossing," because singlet and triplet states can be considered to be two types of states. Intersystem crossings are still sometimes also called "forbidden transitions" because early theories did not include the rare occasions when they occur.

Also, the change from the excited triplet state to the (singlet) ground state is "forbidden." In fact, it does occur (as many forbidden things do in our society). In any case it does not take place quickly, or, in other words, the excited triplet state has a long lifetime. A triplet molecule does not easily react with a singlet molecule, but if it meets another triplet molecule things are different. The magnetic fields created by the unpaired electrons interact. Even if the triplet molecules should not react chemically, they can exchange energy and become two singlet molecules. But because creation of a triplet state is in most cases a rare event, most triplet molecules are in low concentration, and the chance that two will meet is not great. We shall now come to a very important exception to this rule, already mentioned above.

1.20. The Dioxygen Molecule

The molecules of ordinary oxygen that we breathe have very remarkable properties. The most remarkable, important, and unusual of them all is that dioxygen molecules have a triplet ground state. From what will follow, the reader might get the impression that this is very unfortunate, because it makes oxygen a bit difficult to handle for organisms and imposes many threats. We shall deal with some of these in the chapters on photoxicity and photsynthesis. But as is the case with many properties of the surprising and exciting world which we inhabit, if things were not exactly as they are, we would not be around. Just think for a moment that if the dioxygen in the air were in the singlet state, what would happen? We all know that oxygen under certain circumstances can react

with organic matter such as wood or our own bodies. Not only single houses or trees, but whole towns and forests have sometimes burned down. When oxygen oxidizes organic matter, large amounts of energy are released as heat. Processes that release energy usually take place quite easily. But for a house to catch fire, something has to get hot to start with. Once fire has started, other things get hot, and the fire is not easy to extinguish. Why is it that the fire does not start spontaneously?

The answer is that dioxygen consists of triplet molecules, and triplet molecules do not easily react with singlet molecules. Only after things get hot and some of the organic molecules get into states with lone electrons does a reaction with oxygen take place. When this happens, heat is released, more organic molecules acquire unpaired electrons and can react with oxygen, and so on.

Since we know that electrons like to join to pairs, one would expect that two oxygen atoms combine to a dioxygen molecule by joining two unpaired electrons to a pair. Instead, they combine to form a molecule with two lone electrons, a diradical.

1.21. Singlet Oxygen

Singlet dioxygen exists, but its lowest electronic state has more energy than the triplet ground state. Singlet oxygen can be produced by reaction of ordinary triplet oxygen with another compound in the triplet state, provided the energy of that other molecule is high enough. As we can see from Fig. 1.21, the energy of triplet chlorophyll (in relation to the singlet ground state of chlorophyll) is high enough to transfer oxygen from its triplet ground state to an excited singlet state called $^1\Delta g$, according to the following scheme:

$$\text{Chlorophyll(excited triplet)} + O_2(\text{ground state}) \rightarrow \text{chlorophyll (ground state)}$$
$$+ O_2(\text{singlet})$$

The singlet so created is very reactive and can attack various other singlet molecules in the cell. If the plant did not have special systems both for preventing as much as possible the formation of singlet oxygen (this is the role of carotene in the plant cell) and for ameliorating the effects of it if it is formed, the plant could not survive for long, as shown in mutants lacking these protective systems.

In addition to chlorophyll, many other pigments, when illuminated, can form triplet states and generate singlet oxygen. We shall deal with this further in the chapter on phototoxicity.

The electronic configurations of various O_2 molecules and O_2 ions are shown schematically in Fig. 1.22.
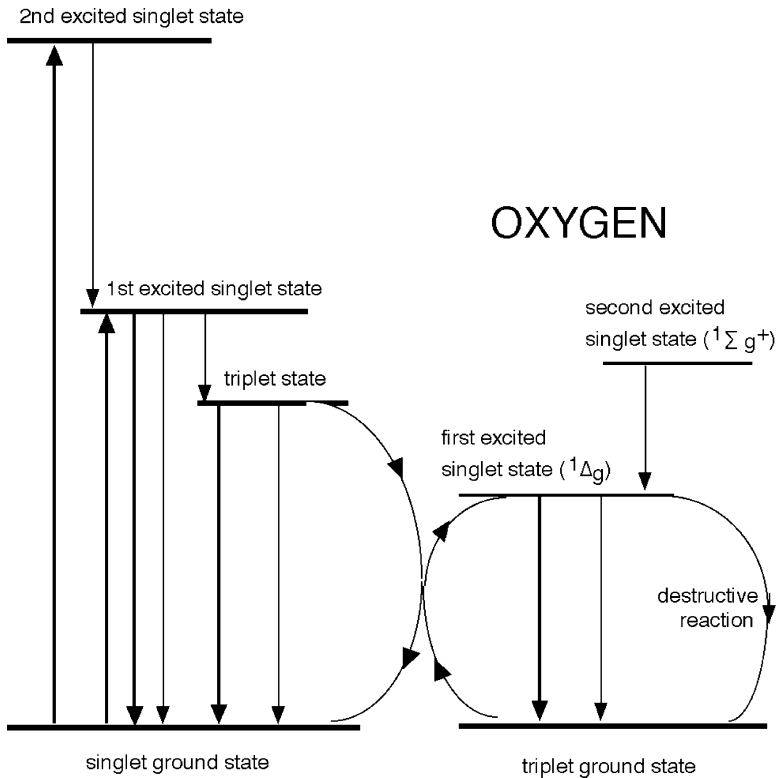
FIGURE 1.21. The various energy states (horisontal lines) of chlorophyll (left) and molecular oxygen (right) and their energy transitions (arrows). Energy is plotted upwards, i.e., a high horizontal line depicts a high energy state. Only the most important electronic levels are indicated, and the vibrational levels have been omitted. Thicker lines depict energy transitions associated with absorption (upward arrows) or emission (downward arrows) of light. The long upward arrow from the ground state of chlorophyll to the second excited state represents absorption of blue light; the shorter upward arrow from the ground state to the first excited state absorption of red light. Thin arrows represent radiationless transitions, in which energy is either transformed to heat (straight arrows) or reaction with another molecule (curved arrows) takes place. Emission of light can take place either as fluorescence (rapid light emission from singlet to singlet state) or as phosphorescence (slow light emission associated with change from singlet to triplet, as in chlorophyll at low temperature, or from triplet to singlet—in oxygen gas even at room temperature).
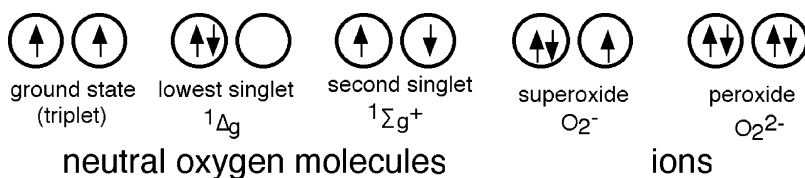
FIGURE 1.22. The electronic configurations in various forms of neutral dioxygen (left) and dioxygen ions of biological importance (right). Only the "antibonding" (π^*) electrons are shown, since all lower orbitals are similar (completely filled) for all the species. Arrows of opposite directions represent electrons of opposite spin.

References

Alonso, M. and Finn, E.J. 1967. *Fundamental university physics*, *Vol. II: Fields and waves*. Addison-Wesley, Reading, MA.

Björn, L.O. and Björn, G.S. (1986) Studies on energy dissipation in phycobilisomes using the Kennard-Stepanov relation between absorption and fluorescence emission spectra. Photochem. Photobiol. 44, 535–542.

Friedrich, J., Scheer, H., Zickendraht-Wendelstadt, B. and Haarer, D. (1981) High-resolution optical studies on C-phycocyanin via photochemical hole burning. J. Am. Chem. Soc. 103, 1030–1035.

Haupt, W. (1977) *Bewegungsphysiologie der Pflanzen*. Georg Thieme Verlag, Stuttgart.

Hecht, E. (1987). *Optics*. 2nd ed. Addison Wesley, Reading, MA.

Hecht, S., Shlaer, S. and Pirenne, M.H. (1942) Energy, quanta and vision. J. Gen. Physiol. 25, 819–840.

Hegemann, P. and Marwan, W. (1988) Single photons are sufficient to trigger movement responses in *Chlamydomonas reinhardtii*. Photochem. Photobiol. 48, 90–106.

Keijzer, M., Star, W.M. and Storchi, P.R.M. (1988) Optical diffusion in layered media. Appl. Optics 27, 1820–1824.

Kennard, E.H. (1918) On the thermodynamics of fluorescence. Phys. Rev. 11, 29–38.

Kubelka, P. and Munk, F. (1931) Ein Beitrag zur Optik der Farbanstriche. Phys. Rev. 11, 672–683.

Seyfried, M. and Fukshansky, L. (1983) Light gradients in plant tissue. Appl. Optics 22, 1402–1408.

Star, W.M., Marijnissen, J.P.A. and van Gemert, M.J.C. (1988) Light dosimetry in optical phantoms and in tissues: I. Multiple flux and transport theory. Phys. Med. Biol. 33, 437–454.

Stepanov, B.I. (1957) A universal relation between the absorption and luminescence spectra of complex molecules. Dokl. Akad. Nauk SSSR 112, 830-842 (Engl. transl. Soviet Phys. Doklady, 2, 81–84).

2
Principles and Nomenclature for the Quantification of Light

Lars Olof Björn

Abstract: This chapter does not deal with any practical aspects of light measurement, only with theoretical concepts. The following concepts are explained: energy fluence, energy fluence rate, photon fluence, photon fluence rate and radiance, mol, as well as the following superfluous or obsolete terms and synonyms: actinic flux, space irradiance, scalar irradiance, spherical irradiance, vectorial irradiance, and einstein. The chapter furthermore deals with spectral weighting of radiation and some psychophysical concepts, such as illuminance, lumen, lux, etc.

2.1. Introduction: Why This Chapter Is Necessary

This chapter will not deal with measuring equipment or measuring techniques, but with basic concepts of light quantification. This topic seems confusing, not only to the layman and the student, but also to the expert. Some reasons for this confusion are as follows:

1. The layman and beginning student erroneously regard the "amount" or "intensity" of light as something that can be completely described by a number. Such a view disregards the following:

    a) Light consists of components with different wavelengths. A full description of the light would thus give information about the "amount" of light of each wavelength.

    b) Light has direction. The simplest case is that all the light we are considering has the same direction, i.e., the light is collimated; the rays are all parallel. Another case is that light is isotropic, i.e., all directions are equally represented. Between these extremes there is an infinite number of possible distributions of directional components.

    c) Light may be polarized—either circularly polarized or plane polarized. In the rest of this chapter we shall disregard this complication, but one should always be aware of the fact that a device such as a photocell

may be differentially sensitive to components of different polarization, and polarization may be introduced by part of the experimental setup, such as a monochromator or a reflecting surface.

d) Light may be more or less coherent, with light waves "going in step." We will not address this complication in this chapter.

e) People often disregard or neglect or confuse the concept of time. We must decide whether we want to express an *instantaneous* or a *time-integrated* quantity, e.g., *fluence rate* or *fluence*, *power* or *energy*. Power means energy per time unit.

2. Light is of interest for people investigating or working with widely different parts of reality. Experts in different fields have used different concepts and different nomenclature, partially depending on what properties of light have been interesting for them, and partly due to the whims of historical development. Only rather recently have there been serious attempts to achieve a uniform nomenclature, and the process is not yet complete.

2.2. The Wavelength Problem

As we cannot always quantify light by giving the complete spectral distribution, we have to quantify it in some simpler way. From the purely physical viewpoint, there are two basic ways. Either we express a quantity related to the number of photons, or a quantity related to the energy of light. For a light of single wavelength, the energy of a photon is inversely proportional to the wavelength and the proportionality constant is Planck's constant multiplied by the velocity of light.

There is an ultimate way of calibration only for the energy of light. For this we can use a hollow heat radiator of known temperature, which will radiate in a way predictable by basic physics. Using such a radiator, a photothermal device, such as a thermopile or a bolometer (see Chapter 4), can be calibrated, and then any kind of light can be measured with it and expressed in energy or power units. We can use it for measuring a series of "monochromatic" (i.e., narrow-band) light beams, and they, in turn, can be used for calibrating other measuring devices in either energy or photon units.

Actinometers, i.e., photochemical devices, seem to count photons, but in this case the ability of photons to cause a response (the quantum yield) varies with wavelength.

We can also use photomultipliers as photon counters, but we should be aware that they do not, strictly speaking, count photons, but impulses caused by photons. Some impulses are not caused by incident photons, but by electrons knocked out from the photocathode by the heat vibration of the atoms in it. We try to minimize this by cooling the photocathode. Furthermore, all photons do not have the same ability to knock out electrons from the photocathode and cause pulses to be counted. This ability is wavelength-dependent. Therefore we cannot use photon counting as an independent calibration method.

The units for expressing light as photons are:

1. Photons (number of photons)
2. Moles of photons (the symbol is mol), which is $6.02217 \cdot 10^{23}$ photons, or a unit derived from this, such as micromole of photons ($6.02217 \cdot 10^{17}$ photons). The symbol for the latter is μmol.

Either of these can be expressed per time and/or per area or (rare in biological contexts) per volume.

The unit for energy is joule (J). Energy per time is power, and joule per second is watt (W). Both can be expressed per area (or, rarely in biological contexts, per volume, i.e., energy density or power density).

You should note that simply giving a value followed by "W/m^2" without further qualification is not defined, since one cannot be sure what kind of area you are expressing with m^2. Is it a flat area or a curved one? If it is flat, what is its direction? This brings us to the topic of the next section.

2.3. The Problem of Direction and Shape

Most light-measuring systems are calibrated using light of (approximately) a single direction, i.e., collimated light. However, light in nature, where most plants live, is not collimated. If the sky is cloudless and unobstructed, the rays coming directly from the sun are rather well collimated, but in addition there is skylight and light reflected from the ground and various objects. A plant physiologist who wants to understand how plants use and react to light has to take this into account.

Traditionally, most measuring devices can be regarded as having a flat sensitive surface, and when we calibrate the instrument we generally position this surface perpendicularly to a collimated calibration beam. A plant leaf is also flat, so in the first approximation we can measure light in single-leaf experiments with a flat device with the same direction as the leaf. But a whole plant is far from flat (except in very special cases). Different surfaces on the plant have different directions. Ideally we should know the detailed directional (and spectral) distribution of the light impinging on the plant, but this is not possible in practice. Since a plant is a three-dimensional object, it would in most cases be better to determine the light using a device having a spherical shape and equally sensitive to light from any direction. This brings us to the distinction between

1. Irradiance, i.e., radiation power incident on a flat surface of unit area, and
2. Energy fluence rate (or fluence rate for short), i.e., radiation power incident on a sphere of unit cross section. The term fluence rate was introduced by Rupert (1974).

Both these concepts have their correspondences in photon terms. For case 1 the nomenclature is not settled, but it would be logical to use the term photon irradiance. Many people, especially in the photosynthesis field, use the term
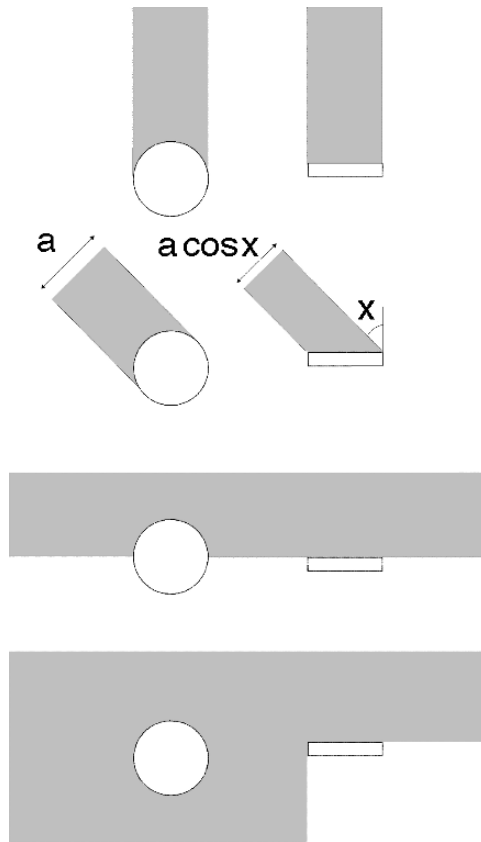
FIGURE 2.1. The concepts of irradiance and fluence rate. In the top diagram the incident light is perpendicular to the surface of the flat irradiance sensor. In this case fluence rate and irradiance are equal. In the next case the incidence angle is x. The irradiance sensor then intercepts only the fraction cos x of what the fluence rate sensor does. In the third case the light is diffuse, but incident only from above. Then the fluence rate is twice the irradiance. In the fourth case the sensors are immersed in diffuse radiation from all directions, but the irradiance sensor senses radiation only from above. In this case the fluence rate is four times the irradiance.

photon flux density and the abbreviation PFD (PPFD for photosynthetic flux density; see below). For case 2 the term photon fluence rate is well accepted among plant physiologists, but hardly among scientists in general.

Energy fluence is the energy fluence rate integrated over time. By fluence is meant as the same thing as energy fluence.

We shall now compare irradiance and energy fluence for different directional distributions of light (see Fig. 2.1).

1. Collimated light falling perpendicularly to the irradiance reference surface. In this case the flat surface of unit area and the sphere of unit cross sectional area will intercept the light equally, and irradiance will be the same as fluence rate.
2. Collimated light falling at an angle x to the normal of the irradiance reference plane. In this case the light intercepted by the flat surface of unit area will be less than that intercepted by the sphere of unit cross sectional area. The irradiance will be $\cos(x)$ times the fluence rate. Since $\cos(x)$ is less than unity, the irradiance in this case will be lower than the fluence rate.
3. Completely diffuse light falling from one side only. The ratio of irradiance to fluence in this case will be an average of $\cos(x)$ for all angles x from 0 to $+\pi/2$ weighted by $\sin(x)$, i.e., $\int \sin(x)\cdot\cos(x)\cdot dx / \int \sin(x)\cdot dx$ with the integral running from 0 to $+\pi/2$, and this is equal to 1/2. Thus the irradiance in this case is half the fluence rate. The reason we have to weight $\cos(x)$ by $\sin(x)$ is that all values of x are not equally "common" and do not have the same probability. The various directions may be thought of as corresponding to points on a big sphere, the center of which is the point of measurement. The sphere can be thought of as divided into a pile of rings, and each ring (corresponding to a value of x) has a radius, and hence a circumference proportional to $\sin(x)$.
4. Completely diffuse light from both sides, i.e., isotropic light. The sphere is then hit by light over its whole surface, but for the flat receiver we still count only one surface (irradiance is defined in this way), so irradiance is one quarter of the fluence rate in this case. We can easily remember this if we think that the area of a circle is one quarter of the area of a sphere with the same radius.

We may now make a table of various quantities associated with light measurements (Table 2.1).

In all the above cases we add the word "spectral" before the various terms if we wish to describe the spectral variation of the quantity. We may thus write, e.g., spectral fluence rate on the vertical axis of a spectrum of light received by a spherical sensor.

What we here have called fluence rate is termed *actinic flux* by atmospheric scientists. The term space irradiance was introduced by Grum and Becherer

TABLE 2.1. Various Quantities Associated with Light Measurements

	Flat receiver	Spherical receiver
Instantaneous values:		
Energy system	(energy) irradiance	(energy) fluence rate
	unit: $W\ m^{-2}$	unit: $W\ m^{-2}$
Photon system	photon irradiance	photon fluence rate
	(=photon flux density)	
	unit: $mol\ m^{-2}\ s^{-1}$	unit: $mol\ m^{-2}\ s^{-1}$
Time integrated values:		
Energy system	(energy density)	(energy) fluence
	unit: $J\ m^{-2}$	unit: $J\ m^{-2}$
Photon system	—	photon fluence
		unit: $mol\ m^{-2}$

(1979). Two more terms with the same meaning are *space irradiance* and *scalar irradiance*. The term *spherical irradiance* has been used in similar contexts, but means one quarter of the fluence rate. *Vectorial irradiance* is just the same as irradiance. The reader should use just one system of terms, preferably irradiance and fluence rate, but may encounter all these other terms in the literature.

Few instruments on the market, and very few spectroradiometers, are designed for direct measurement of fluence rate. Most of them are constructed for irradiance measurements and a few for measurement of radiance (see below). But Björn (1995) and Björn and Vogelmann (1996) have shown how irradiance meters can be used for estimation of fluence rate.

So far we have been dealing with light falling on a surface, either a flat or a spherical one. But we may need to express other quantities, for instance the total power (energy per time unit) output of a light source. The unit for this is, of course, W (watt). The power emission per unit area of the source is called the *radiant excitance* and is measured in W/m^2 (just like irradiance and fluence rate, so beware of confusing them). The power emission takes place in different directions; in total there is a solid angle of 4π steradians (sr) surrounding a source. Usually the emission is not equally distributed in all directions, so for a certain direction we might like to specify the power emission per steradian. This quantity is called the *radiant intensity* in that direction, and the unit is W/sr. (Note that the term intensity is often (erroneously) used in another and usually not well-defined sense). The radiant intensity per area unit on a plane perpendicular to the light is called *radiance*, and the unit is W/sr/m^2. The official definition of radiance (usually denoted by L) is as follows: radiant power (P), leaving or passing through a small transparent element of surface in a given direction from the source about the solid angle θ, divided by the solid angle and by the orthogonally projected area of the element in a plane normal to the given beam direction, dS cos θ. With mathematical symbols we write: L = d^{2}P/(dΩ dS cos θ)? for a divergent beam propagating in an elementary cone of the solid angle Ω containing the direction θ.

If we integrate the radiance over all 4π radians for both Ω and θ, we get back to the fluence rate that we are already familiar with.

Fortunately, the average photobiologist need not keep all these concepts in his or her head at all times. You can look them up when needed. However, you must be clear over the meaning of irradiance and fluence rate, and not confuse these two concepts. As a practical illustration of how the ratio of fluence rate to irradiance can vary under natural conditions see Fig. 2.2.

A comprehensive list of recommended units, concepts and symbols for photo-science is published by Braslavsky et al. (2007).

2.4. Biological Weighting Functions and Units

Section 2.3 concludes the physical quantification of light. However, there has been a need for additional concepts in connection with organisms and biological problems. Traditionally there has been a special system related to the human
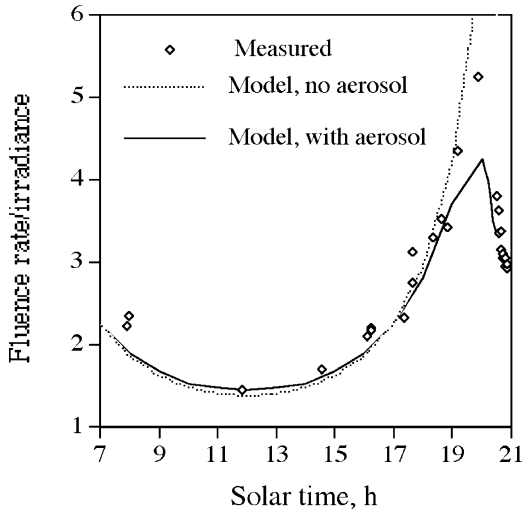
FIGURE 2.2. The variation of the ratio of fluence rate to irradiance over a clear summer day in southern Sweden. Presence of small particles in the air (aerosol) dampens the variation. The graph is for cloudless conditions and 400–700 nm ("PAR" spectral band, see Fig. 2.3). For ultraviolet radiation, especially for UV-B radiation, the variation is smaller, because even clean air scatters this radiation to make it to a large extent diffuse. For overcast conditions the variation is also smaller than for clear skies. (Measurements and calculations by the author.)

perception of light. We can here limit ourselves to *illuminance*, which is expressed in lux. Neglecting the historical development, we can say that lux is the integrated spectral irradiance weighted by a special weighting function. This weighting function is precisely described mathematically, but can be thought of as the average (photopic, i.e., related to strong light vision mediated by cones) eye spectral sensitivity for a large number of people. (Rarely we also see the expression "scotopic lux," which is the corresponding term using the scotopic visibility weighting function.) The photopic visibility function has its maximum at 555 nm, and for this wavelength 1 W/m^2 equals 683 lux. For all other wavelengths 1 W/m^2 is less than 683 lux. Illuminance integrated over a flat area is called *luminous flux*, and the unit is lumen. Thus lux is lumen per square meter. In older American literature the unit foot candle (f.c.) is used instead of lux. Foot-candle equals lumen per square foot, and since there are 3.2808399 feet in a meter, there are $3.2808399^2 = 10.763910$ square feet in a square meter, and also 10.763910 lux in a foot candle. There are also a number of other photometric concepts and units, which we seldom need in photobiology. Many of them are defined in the *Handbook of Chemistry and Physics* .

Similarly we may, for purposes other than vision (reading light, working light) weight the spectral irradiance by other functions. These functions approximate various photobiological action spectra (see Chapter 8). One special function is zero below 400 nm and above 700 nm, and unity from 400 to 700 nm. This describes by definition photosynthetically active radiation, or

PAR. Usually one uses the spectral photon irradiance to weight by this function, and this is the meaning of the often used term PPFD, photosynthetic photon flux density. To assume photosynthetic zero action outside the range 400–700 nm and the same action for all components within the range is, of course, physiologically speaking an approximation, but an approximation that people have agreed upon, just as the definition of lux involves an approximation that holds well only for scotopic (rod) vision.

   Other weighting functions are used for "sunburn" meters to yield "sunburn units," but in this field we have to watch out for various "units" used by various people. One kind of sunburn meter used much in the past is the Robinson-Berger meter, but recently a new agreement has been reached for using a weighting spectrum more closely resembling the true sunburn action spectrum (for Caucasian skin). One weighting function to determine safe working conditions shown in Fig. 2.3 is damaging UV. This particular function was agreed upon in 1991 by the International Radiation Protection Association (IRPA) and the International Commission on Nonionizing Radiation Protection (ICNIRP). Another, slightly different function for similar purposes was devised by the American Conference of Governmental Industrial Hygienists (ACGIH).
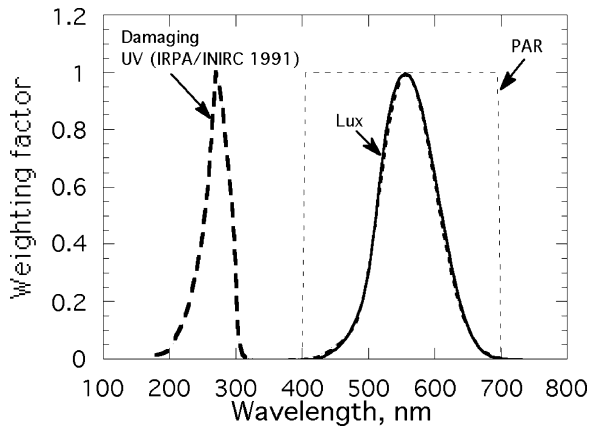
FIGURE 2.3. Examples of weighting functions. The damaging UV function is one devised by the International Radiation Protection Association (IRPA) and the International Commission on Nonionizing Radiation Protection (ICNIRP) and thus having a certain official status. PAR stands for photosynthetically active radiation, and this weighting factor is unity from 400 to 700 nm and zero outside this interval. This weighting function is applied more often to photon irradiance or photon fluence rate than to energy irradiance and energy fluence rate. The Lux function is that used for conversion of W/m^2 to lux (or W to lumen). The maximum is here made unity to allow plotting together with the other functions, but in absolute units it corresponds to 683 lux per W at 555 nm. The Lux graph in fact consists of two plots, so close that they hardly can be distiguished in the diagram—both the official values from a table and an analytical approximation consisting of the difference between two Gauss functions: weighting factor = $\exp[-(555-\lambda)/63.25]^2 - \exp[-(495-\lambda)/30]^2/6.8$, where λ stands for wavelength in nm.

In reality, of course, different kinds of damage, such as damage to the cornea and to the lens of the eye and to skin of persons with different pigmentation, have different action spectra. Also the standard PAR is an approximation to reality, since different plants, and even the same plant in different states, have different action spectra for photosynthesis.

There are numerous other weighting spectra in use for estimating radiation with other biological actions. We shall address some of them in the chapter on ultraviolet radiation effects.

Some meters, such as lux meters, sunburn meters, and meters for PAR, are constructed with spectral responses approximating the weighting functions and can therefore directly yield the values we want without spectral decomposition of the light. For more precise work, and in the case of, e.g., UV inhibition of plant growth, it is necessary to measure (using a spectroradiometer) each wavelength component separately and weight by the weighting function using arithmetics (usually computers are used).

References

Björn, L.O. (1995) Estimation of fluence rate from irradiance measurements with a cosine corrected sensor. J. Photochem. Photobiol. B. Biol. 29, 179–183.

Björn, L.O. and Vogelmann, T.C. (1996) Quantifying light and ultraviolet radiation in plant biology. Photochem. Photobiol. 64, 403–406.

Braslavsky, S.E. et al. (2007) *Glossary of terms used in photochemistry*. 3rd ed. (International Union of Pure and Applied Chemistry recommendations 2006). Pure Appl. Chem. 79, 293–465. Available at http://www.iupac.org/reports/III/2002-024-1-300_rec061012.pdf or http://www.iupac.org/reports/1993/homann/index.html.

Grum, F. and Becherer, R.J. (1979) *Optical radiation measurements*. Academic Press, New York, pp. 14–15.

Handbook of Chemistry and Physics (many editions). CRC Press, Cleveland, OH.

Rupert, C.S. (1974). Dosimetric concepts in photobiology. Photochem. Photobiol. 20, 203–212.

3
Generation and Control of Light

Lars Olof Björn

Abstract: This chapter describes various kinds of artificial light sources of interest to the photobiologist (natural light is described in separate chapters), starting with incandescent lamps and their properties, and continuing with gas discharge lamps, flashlamps, light-emitting diodes, and lasers. After a section on light filters, the chapter concludes with a treatment of monochromators, in which the mode of action of a grating is explained based on Young's double slit experiment (see Chapter 1).

3.1. Introduction

Any photobiological experimental setup consists of three main parts: a light source, a light path, and a target. The biological object under investigation may form the light source, part of the light path, or, as in the most common case, the target. In the following we shall treat the nonbiological components of the experimental setup.

3.2. Light Sources

3.2.1. The Sun

Almost all the natural light at the surface of the earth comes from the sun (this holds, of course, also for moonlight). The sun, on the whole, radiates as a glowing blackbody at a temperature of about 6000 K. We have already mentioned the absence of some wavelength components from sunlight due to absorption in the outer cooler layers of the sun. Sunlight is further modified by the earth's atmosphere before it reaches ground level. More about this and other natural light conditions will follow in Chapters 6 and 7.

3.2.2. Incandescent Lamps

The light from an incandescent lamp originates at the surface of a glowing filament, which nowadays is, almost invariably, made from tungsten. It is heated by an electric current flowing through it. In order not to be destroyed (oxidized) by the oxygen in the air, the filament is enclosed in an envelope made of glass or quartz. The envelope is either evacuated (most commonly for small lamps) or filled with an inert gas, or iodine vapor.

The spectral composition of the emitted light is strongly dependent on the temperature of the filament. As a first approximation the spectrum varies with temperature as does that of blackbody radiation (Planck's law). However, due to the wavelength dependence of the emissivity of tungsten, more short-wave radiation is emitted than from a blackbody of the same temperature. The filament is, in most cases, coiled, which makes it somewhat "blacker" (more like a glowing cavity) than a smooth tungsten surface would be.

In most cases it is desirable to obtain as much as possible of the radiation towards the short wavelength end of the spectrum, i.e., to operate the lamp with as high a filament temperature as possible (the temperature can be increased by increasing the voltage). However, this results in a shorter life of the lamp, because the tungsten evaporates more quickly (and condenses again on the envelope, which blackens it). As a rule of thumb, an increase of the voltage by 10% above the recommended voltage will decrease the lamp life to one third (i.e., by two thirds).

The lamp life at a certain filament temperature can be increased by making the filament thicker. Thereby a certain power (wattage) is reached at a lower voltage (using a higher current). A further advantage of low-voltage lamps is, in many cases, that the filament is shorter. Quite often a small ("point-like") light source is desirable in optical systems.

A gas-filled envelope permits a higher filament temperature than an envelope with vacuum. A mixture of argon and nitrogen is the most common choice (ordinary household bulbs). Addition of iodine ("halogen lamps" or "quartz-iodine lamps") permits an even higher temperature. This is because the iodine vapor combines with the tungsten vapor. The compound is decomposed again when the molecules hit the hot filament, which is thereby continuously regenerated. For the regeneration to work properly, the temperature of the envelope must be so high that the tungsten iodide cannot condense on it. Therefore such lamps are manufactured with a very small envelope made of quartz, which can withstand high temperature.

The advantages of incandescent lamps are their low cost, no requirement for complex electrical circuitry, and stability. The main disadvantage is that the emission at the short-wavelength end of the spectrum is low, and the spectrum is strongly dependent on the current through the lamp, and therefore difficult to keep absolutely constant. A method to estimate the spectrum of an incandescent lamp fed with direct current (within the spectral range where the glass or quartz envelope does not absorb appreciably) has been devised by Björn (1971). The principle is as follows: using a small current and measuring both the current
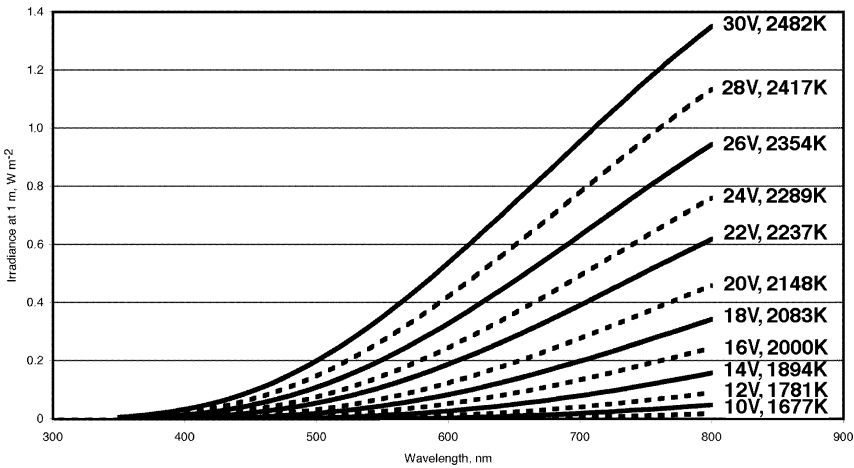
FIGURE 3.1. Emission spectra of an incandescent lamp with a nominal rating of 24 V run at different voltages, with computed filament temperatures indicated. The lowest dashed curve corresponds to 8 V and 1547 K.

through and the voltage across the lamp, the room temperature resistance of the lamp is measured (this is essentially the resistance of the tungsten filament). After the lamp has been powered up (with direct current), the current and voltage are measured again. From this the "hot" resistance is computed. The temperature of the glowing filament can be computed from the ratio between room temperature resistance and "hot" resistance, and from this (using the Planck formula for a blackbody radiator and the known temperature- and wavelength-dependent emissivity of tungsten) the spectrum can be computed.

Using these principles, emission spectra for a lamp with a 24 V rating operated at various voltages were computed (Fig. 3.1) according to Björn (1971).

3.2.3. Electric Discharges in Gases of Low Pressure

In a gas discharge lamp an electric current is flowing through a gas. The gas emits light, the spectral composition of which depends on the gas. When the gas has a low pressure it emits a line spectrum, i.e., only light of certain wavelengths is represented (in contrast to the continuous spectrum emitted by an incandescent lamp).

The basic parts of a gas discharge lamp are a gas enclosed in a transparent envelope and the two electrodes necessary for the conduction of current to and from the gas. In addition to this, it is often necessary with other parts, such as heating filaments, to release enough electrons to start the current through the gas or to vaporize, e.g., mercury or sodium when vapors of these metals are to be used as emitting gas.

The electric resistance of an incandescent lamp increases when the current through it increases, since tungsten has a higher resistivity the higher the

temperature. Thus an incandescent lamp is self-regulating and burns in a stable way as long as the voltage is constant. In a gas discharge lamp the reverse holds: its electric resistance decreases with increasing current. Therefore, such a lamp has to be connected to some kind of circuitry limiting the current. In the case of direct current a series resistor is often used, in the case of alternating current, a choke.

Gas discharge lamps containing mercury vapor of very low pressure emit most of energy as ultraviolet radiation of wavelength 253.7 nm. This wavelength is close to the absorption maximum of nucleic acids, and the radiation is also absorbed by the aromatic amino acids in proteins and many other biological molecules. The photons are also energetic enough to initiate many chemical reactions, and therefore this kind of radiation is very destructive for living matter. Low-pressure mercury lamps with quartz envelopes (which transmit this kind of radiation, in contrast to glass envelopes) are therefore used as sterilization (germicidal) lamps.

Fluorescent lamps are similar lamps, but with glass envelopes, which on the inner surfaces have a fluorescent layer converting the UV radiation to visible light (or, in certain cases, to UV radiation of longer wavelength than the original emission).

Glow lamps are a kind of low-pressure gas discharge lamp, usually containing neon. Lamps containing the element to be measured are used for atomic absorption spectroscopy. Low-pressure sodium lamps, emitting almost monochromatic light at 589 nm, have been used extensively as sources of outdoor working light, because they give more visible light per unit of energy input than any other type of lamp. To a large extent they have been abandoned, mostly because our color vision cannot be used with monochromatic light.

Microwave radiation is used for the energy input in some other gas-filled lamps, such as "electrodeless" high-pressure xenon lamps.

3.2.4. Medium- and High-Pressure Gas Discharge Lamps

If the vapor pressure in a mercury lamp is increased, more and more of the emission at 253.7 nm is reabsorbed, and finally very little of this radiation escapes from the vapor. Instead, spectral lines of longer wavelength emerge (medium-pressure mercury lamps). At even higher pressures the spectral lines are broadened to bands (high-pressure mercury lamps), and finally a continuous spectrum results (super-high-pressure mercury lamps).

Deuterium (heavy hydrogen) lamps of medium pressure are used as light sources for spectrophotometry in the ultraviolet region.

Lamps containing xenon of high pressure are used to obtain a strong continuous emission from 300 nm and into the infrared. Depending on the composition of the envelope, more or less of shorter wavelength ultraviolet also escapes. Xenon lamps come in a great variety of types. We use lamps running on about 24 V direct current (but ignited with about 2000 V = danger!!) and wattages (rated powers) from 150 to 900 W. Xenon lamps of higher wattage are

often water-cooled. Electrodeless xenon lamps are also manufactured. They are powered by microwave radiation.

Because xenon lamps with UV-transparent envelopes cause conversion of oxygen to ozone, such lamps must be provided with exhausts to transport the ozone out of the building. The same holds for high-pressure mercury lamps with UV-transparent envelopes.

All high-pressure lamps are dangerous because they can explode. They must therefore never be operated without protective housing. Even when cold they should be handled with care, using eye protection and other appropriate safety measures.

3.2.5. Flashlamps

Electronic flashes are xenon lamps through which a capacitor is discharged when a special triggering pulse has ionized the gas. The energy available is proportional to the capacitance of the capacitor and to the square of the voltage to which it has been charged. In many cases it is desirable to have a short flash duration. This requires that the impedance of the circuit is low (short leads) and the capacitance low (high voltage has to be applied to the capacitor to get enough energy with a low capacitance). It is also necessary to prevent the circuit from oscillating and causing multiple flashes. Ordinary photographic flashes have a flash duration of about 1 ms. If they are "automatic," i.e., combined with a light-sensing photodiode and appropriote circuitry, the flash will be cut off when a certain amount of light energy has been emitted.

3.2.6. Light-Emitting Diodes

Light-emitting diodes (LEDs) are used in applications where very strong light is not needed, for instance as indicator lights and displays. However, the maximum output power available from LEDs is increasing, and LEDs are the cheapest devices that can be modulated very rapidly: using an appropriate circuit they can be switched on and off in a few nanoseconds. For this reason they were used early as light sources for measuring variable fluorescence in plants. Initially the trouble with this was that only red-emitting diodes are intense enough, and their red light is not easy to efficiently separate from the chlorophyll fluorescence. Now suffiently intense blue-emitting diodes are also available.

LEDs of several spectral emission types are presently manufactured: ultraviolet A, B, and C, and blue, green, yellow, red, and infrared. It should be noted that they are not monochromatic light sources, and especially the short-wave rated LEDs have a broadband emission of longer wavelength than the nominal emission. For some types the emission spectrum changes with operating current. LEDs are powered by a low voltage source (e.g., a 1.5 V battery; some types need up to 5 V) in series with a resistor limiting the current to the rated value. Proper polarity should be observed.

TABLE 3.1. Examples of LEDs and Where to Obtain Them

Peak wavelength, nm	Semiconductor(s)	Company and URL
237–365 nm	AlGaN/GaN	Sensor ElectronicTechnology, Inc.www.s-et.com
370–390	GaN	Nichia America
460	GaN	www.nichia.com
470, 505, 525	SiC/GaP	Ledtronics
574, 595, 611	InGaAlP	www.ledtronics.com
630	GaAsP/GaP	
660	GaAlAs/G AlAs	
660, 700, 720	GaAlAsP	Roithner Lasertechnik
780, 810, 905	GaAlAsP	
375–1550	InGaN, AlGaAs/AlGaAs, InGaAsP	Epitex Incorporation http://www .epitex.com/global/catalog_mold.htm

Traditional LEDs contain inorganic semiconductors such as GaN, InGaN, SiC, and GaAsP (see Table 3.1). Very recently several laboratories and companies have started to develop organic light-emitting diodes (OLEDs), which will probably widen the range of spectral types available. Roithner also markets a range of infrared emitting diodes with emission peak wavelengths to greater then > 4.5 μm. A LED emitting at 210 nm has been constructed (Taniyasu, Kasu, and Makimoto 2006), but is of this writing not yet commercially available. An interesting new development is the construction of a LED that can generate a single photon at a time (Yuan et al. 2002).

3.2.7. Lasers

Laser is an acronym for light amplification by stimulated emission of radiation. Stimulated emission occurs when a photon causes a molecule in an excited state to emit a second photon. Stimulated emission as such requires no special equipment. It occurs regularly when photons of the proper energy encounter excited molecules. However, as a rule, excited molecules are very rare compared to molecules in the ground state (remember the equilibrium concentration formula, $N_y/N_x = \exp(E_x - E_y)/kT$). To get light amplification by stimulated emission we must have more stimulated emission than light absorption, which means that we must have more molecules in the proper excited state than in the ground state. This can be achieved in different ways, but never by "direct lift" from the ground state by absorption of light. Various lasers employ indirect "optical pumping" (sometimes by another laser), electrical energy, or chemical reactions. For a laser to work, photon losses must also be minimized by a suitable optical configuration, often involving mirrors.

Laser light has some unusual properties:

1. Laser light is coherent in the sense that the light constitutes very long wave trains, contrary to ordinary light, where each photon can be regarded as a limited wave packet independent of other photons.
2. Laser light can be made very collimated (all rays very parallel).
3. Laser light is usually very monochromatic (very narrow spectral bandwidth) or consists of a small number of such very narrow bands.
4. Laser light may be (but is not necessarily) plane polarized.
5. The light from some types of lasers is given off in extremely short pulses of extremely high power (energy per time unit). However, this does not hold for all lasers. Some lasers emit light continuously and have very feeble power.

Even lasers of low power, such as the helium–neon laser, should be handled with some caution. This is because the beam is so narrow, parallel, and monochromatic that if it hits your eye all its power will be focused onto a very small area of your retina and blind that particular spot.

One kind of laser that is in everyday use is the continuous helium–neon laser, emitting at 632.8 nm and a few infrared wavelengths. Dye lasers are advantageous in many cases because the wavelength can be selected over a wide range (within the fluorescence band of the dye used, and the dye can be changed if necessary). You may sometimes encounter a YAG laser. YAG is the acronym for yttrium aluminium garnet, containing trivalent neodymium ions in $Y_3Al_5O_{12}$. They are very powerful emitters of infrared radiation of 1060 nm wavelength. For photobiological purposes they are sometimes combined with frequency doublers made of potassium phosphate crystals, so that green light of 530 nm wavelength is obtained. The wavelength can be further changed either by letting the light undergo Raman scattering or using it as a power source for a dye laser. Diode lasers are photodiodes emitting coherent light. They are now the most common lasers, used in CD players and other optical readout devices and laser pointers. They are available from 370 nm in the UV-A band to the long-wavelength red.

3.3. Selection of Light

In many cases you do not want to use light as it comes from your light source. You may wish to remove some parts of the spectrum or select just a narrow spectral band, or select light with a certain polarization, or you might wish to modulate the light in time, for instance quickly change from darkness to light or obtain a series of light pulses. The first three sections below will deal with wavelength selection. A review of filters and mirrors of interest to biologists is provided by Stanley (2003).

3.3.1. Filters with Light-Absorbing Substances

The simplest devices for modifying the spectral composition of light are filters with light-absorbing substances that remove certain components from the spectrum. These color filters may be solid or liquid.

Cheap filters, which are quite useful for some purposes, consist of colored plastic (e.g., Plexiglas or cellulose acetate). Colored cellophane is not recommended as it is rather unstable, and cellulose acetate has to be used with great caution since it bleaches with time. It must also be realized that all these substances transmit far-red light and infrared radiation freely. Thus, a piece of green Plexiglas does not transmit just green light. It is very instructive to put one, two, three, etc. sheets of green Plexiglas on an overhead projector and watch the effect (or look through the sheets towards an incandescent lamp). One or two sheets look clearly green, after which the color becomes indescribably dirty and finally shifts to deep red. This is because far-red light is transmitted even more freely than green light, and when practically all the green light (to which our eyes are most sensitive) is gone, we see the remaining far-red, which is otherwise hidden by the green. Remember that plants, contrary to our eyes, are more sensitive to far-red light than to green!

Undyed cellulose acetate can be used as a cutoff filter to remove UV-C radiation but retain UV-A and UV-B. The exact absorption depends on the thickness and must be checked regularly because the filter changes, especially in front of a UV radiation lamp. A more stable alternative is a special type of uncolored Plexiglas, number FBL.2458 (from Röhm GmbH, ordinarily used in front of the UV radiators in solaria).

A great variety of gelatin filters for photographic use are manufactured by Ilford, Kodak, and other companies. They may also be very unstable in strong light and also freely transmit far-red light.

From an optical viewpoint, some solutions are much better filters than anything that can be made in solid form, but solutions are in many cases inconvenient to use. Thick layers may be required for the optical properties you want, and the liquid filters may therefore become bulky. Furthermore, some of the most useful colored substances are, unfortunately, carcinogenic or toxic in other ways.

One useful substance, which is not particularly dangerous, is water (see Figs. 3.2 and 3.3). It can be used for removing infrared radiation and thus avoid heating by light from incandescent and xenon lamps. Addition of copper sulfate increases the absorption of far-red. Copper sulfate should be used only with distilled water, and the solution should be acidified with sulfuric acid to avoid precipitation of cupric carbonate.

Solutions of potassium dichromate (carcinogenic!) are very good for removing light of wavelength shorter than about 500 nm, as one might want to do in, e.g., studies of fluorescence. For this purpose it is far superior to glass filters or any filters containing organic compounds because of the the total lack of fluorescence. We use it for filtering away the blue excitation light when we study the red chlorophyll fluorescence from plants.
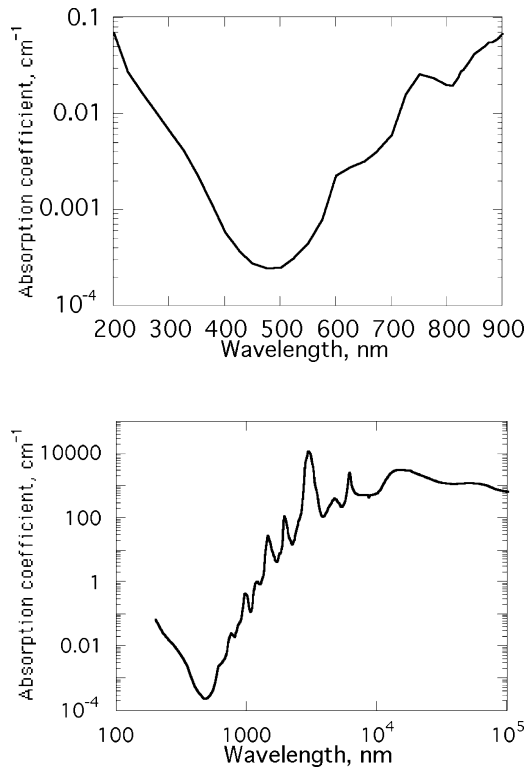
FIGURE 3.2. The absorption spectrum of pure water plotted in two different ways. (Data from Hale and Querry, 1973, replotted.)
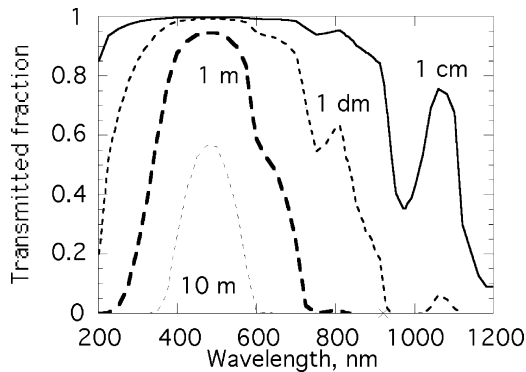
FIGURE 3.3. The fraction of light of various wavelengths absorbed by (pure) water layers of the thicknesses indicated. Ten-meter filters are not very practical in the laboratory, but 10 and even 100 m of water are natural light filters for many organisms. The transmission in natural waters differs from that in chemically pure water and will be dealt with in Chapter 7. (Calculated from data of Hale and Querry 1973.)

Containers (cuvettes) for solutions of copper sulfate or potassium dichromate can be made by gluing together pieces of ordinary clear Plexiglas. Be sure that the glue has dried thoroughly and throughout before you pour your solution into the cuvettes, or you will lose more time than you are trying to save. It is best to test for leaks using distilled water before you put your solutions in. Distilled water can be removed again from the leaks, but crystals cannot!

Cobalt chloride and nickel sulfate (nasty, carcinogenic, toxic, and in the case of nickel allergenic) dissolved in water or aqueous ethanol make very good broadband filters for the UV-B region, but because the substances are so dangerous I do not recommend them unless you really know what you are doing and are sure that your cuvettes will not leak. Detailed descriptions of solution filters, especially for isolationg lines of the mercury spectrum, can be found in Calvert and Pitts (1966), Rabek (1982), and Gahr, Seil, and Niessner (1995).

Colored glass filters are made by several companies. My personal experience is mainly with filters manufactured by Schott & Gen. (Mainz, Germany) and Corning (USA). A large assortment of such filters is available (Fig. 3.4), so a catalog should be consulted before ordering. Of the filters from Schott I have most often found BG12 and BG18 useful for isolating broadband blue light, and a series of cutoff filters, which cut off the short end of the spectrum (cutoff wavelengths from 250 to 780 nm) but transmit light of longer wavelength. For a particular kind of glass the cutoff point can be varied by having filters of different thickness or using several filters in tandem.
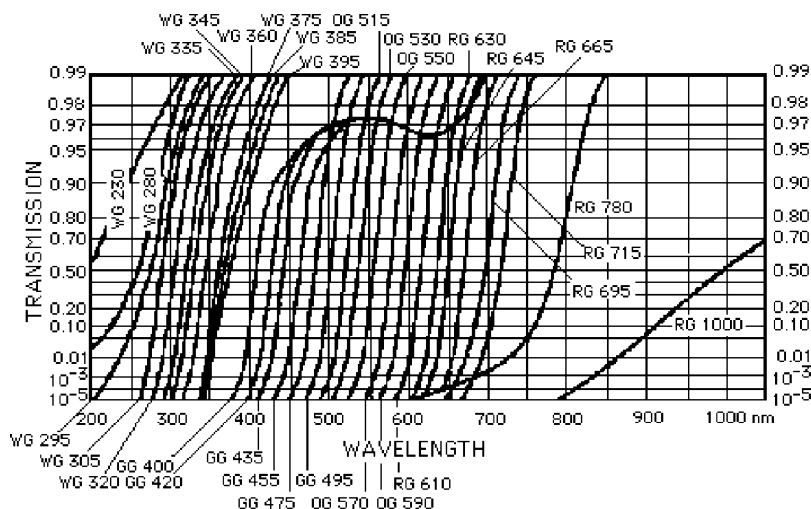
FIGURE 3.4. Cutoff filters made of glass, manufactured by Schott & Gen., Mainz. Note that the vertical transmission scale is not linear. The filters absorb short wavelength and transmit long wavelength light. The diagram, drawn for 1-mm (WG 230 to GG 395)- or 3-mm (GG 400 to RG 1000)-thick filters, does not take reflection (roughly 0.08 or 8%) into account.

All the filters absorbing the unwanted light convert the absorbed energy to heat. If the light to be filtered is strong, the filters may become overheated and be destroyed. Organic substances may be decomposed, plastic may melt or burn, solutions may boil, and glass may crack. The risk for these unwanted effects is considerably less in the case of interference filters.

3.3.2. Interference Filters

An interference filter removes the unwanted radiation from a beam not by absorption, but by reflection. It does not contain any colored substances, but instead a number of partially reflecting and partially transmitting interfaces. Some interference filters contain very thin metal films; others are made from alternating layers of transparent compounds of high and low refractive indices. The complete theory for interference filters is complicated. However, its essence is that when the spacing between the layers is a quarter of a wavelength, destructive interference will occur in the reflected beam, so no light is reflected for this particular wavelength. Instead, light of this wavelength is transmitted. Light with twice or three times (or any integer times) the basal wavelength will also be transmitted, since there will be layer distances corresponding to a quarter of these wavelengths. The reader is referred to Chapter 9, Section 9.10, which deals with a very similar topic.

Interference filters of the type just described will thus allow several narrow spectral bands to pass through, with wavelengths 4, 8, 12 … times the distance between interfaces. By combining interference and glass filters, one of the bands can be selected (Fig. 3.5). When using such combination filters, it is essential (at least if strong light is to be filtered) that the interference part of the filter faces the incident light. If the absorbing glass part is hit by the unfiltered light, the filter might become overheated.

For the filter to function properly, the light to be filtered must be nearly perpendicular to the filter, or the transmitted band will be broadened and shifted to longer wavelength. Thus, only collimated (parallel) light, not diffuse light or light from an extended light source (e.g., a fluorescent tube), can be efficiently filtered by an interference filter.

Even if interference filters do not heat up as easily as absorbing filters, care should be taken so that their temperature does not rise by conduction from other parts of your apparatus. They should also be protected from moisture. When not in use they should be kept in a desiccator with dry silica gel.

The half-band width of a spectral band is defined as the difference in wavelength (or frequency) between the two points in the spectrum where the band is half the maximum height. Photobiologists often use interference filters with half-band widths of about 15 nm. This gives a reasonable compromise between spectral purity and amount of light transmitted. For some purposes filters with half-band widths up to 50 nm are useful. There are also interference filters with half-band widths as small as a fraction of a nanometer. They are
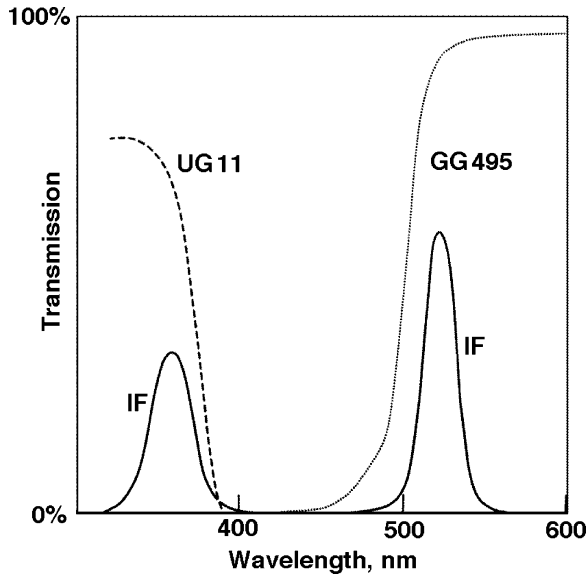
FIGURE 3.5. The transmission spectrum for an interference filter (IF) with two transmission peaks. The ratio betweeen the two peak wavelengths in this case is 3:2. Either one of the transmission bands can be selected by combining the interference filter with suitable glass filters: UG 11 for the short wavelength band or GG 495 for the long wavelength band.

used, e.g., by astronomers for photographing the sun using light emitted by a single kind of atom.

Continuous interference filters (also called spectral wedges) transmit light of different wavelengths at different points on the filter. They are usually oblong, with different wavelengths along their length. Also, circular spectral wedges have been manufactured.

There are interference filters other than the narrow band type. One useful type is Calflex (see http://www.linos.com/pages/no_cache/home/shop-optik/planoptik/filter/?sid = 12664&cHash = c8035311a6). One version of it transmits almost the full visible range and reflects ultraviolet and infrared (including far-red).

3.3.3. Monochromators

For high spectral purity of light, yet flexibility in the choice of wavelength, a monochromator is the device of choice. A very simple monochromator can be made from a continuous interference filter between two slits (Fig. 3.6). Light of different wavelength is obtained simply by sliding the interference filter. However, this arrangement is not suitable when a small half-band width (high purity light) is required.
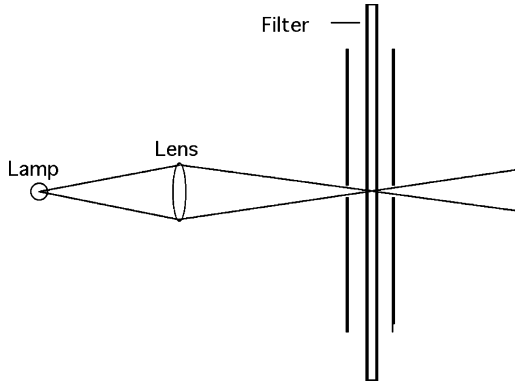
FIGURE 3.6. Simple monochromator consisting of an interference filter between two slits. It is here combined with a simple illuminator consisting of a lamp and a lens, providing light which is almost perpendicular to the filter, which is essential for proper function.

In earlier times, most monochromators contained a prism as the dispersing element (i.e., the component deflecting the light differently depending on wavelength). Gratings were too difficult to make, and hence expensive. New methods, however, allow the mass production of high-quality gratings, and nowadays practically all monochromators for the near infrared, visible, and ultraviolet regions use a reflection grating as the dispersing element.

The basic theory for a grating is best understood as an extension of Young's double slit experiment. Using a computer we can investigate the effect of increasing the number of slits more and more. An essential part of a program for this consists of the three equations relating wavelength (λl), deflection angle (θ) and relative fluence rate (I) to the width (b), number (n), and distance (a) of the slits:

$$\alpha = (a \cdot \pi / \lambda) \cdot \sin\theta$$

$$\beta = (b \cdot \pi / \lambda) \cdot \sin\theta$$

$$I = 4 \cdot [\sin\beta \cdot \sin(n \cdot \alpha) / (\alpha \cdot \beta)]$$

The highest central peak (nondeflected light) in Fig. 3.7a is called the first order light. With mixed input light this includes all wavelengths. The two peaks on each side of it is the first order light, and so on.

Comparing the last three printouts (Fig. 3.7b), we see that the deflection angles increase with wavelength. We can see that the second order light with wavelength 500 nm is deflected to the same angle as the first order light with wavelength 1000 nm. Likewise, fourth order light of 500 nm wavelength, second order light of 1000 nm wavelength, and first order light of 2000 nm wavelength are all deflected to the same angle. As will be explained later, this has important consequences for photobiological experimentation.
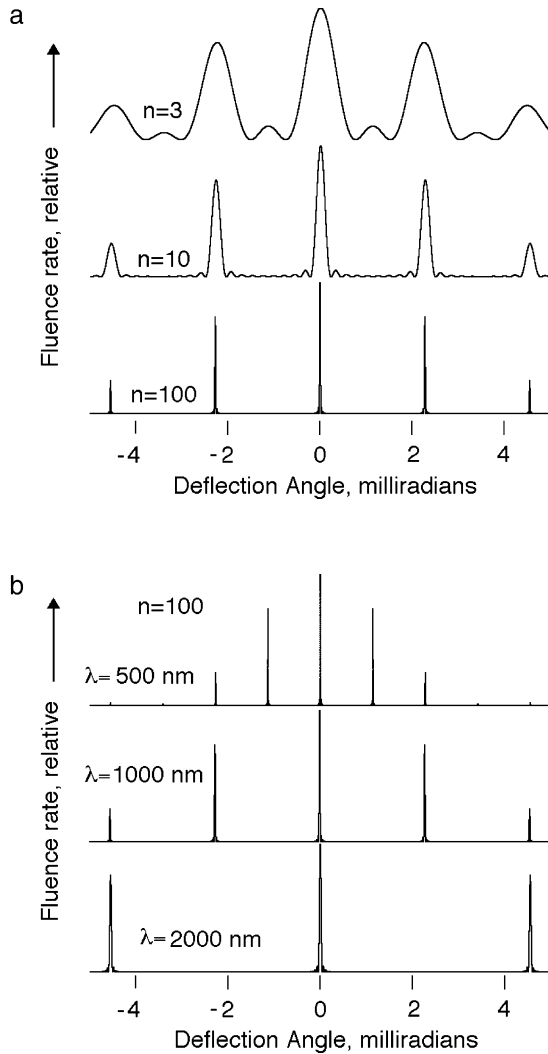
FIGURE 3.7. (a) Computed diffraction patterns from n slits (n = 1, 10, or 100). With increasing slit number the peaks become sharper. The slit width is 0.3 mm, the slit distance 1 mm, and the wavelength 1000 nm. (b) As in (a), but with slit number kept constant and the wavelength varied. With increasing wavelength the deflection angle increases.

Transmission gratings in the form of multiple slits are seldom used, except as here for teaching the theory of gratings. Instead, mirrors with grooves, called reflection gratings, are made in many variants, usually as replicas, i.e., copies molded in plastic from very expensive originals. The principle of operation is essentially the same, except that the light exits on the same side of the grating where it enters.

Modern reflection gratings have the added refinement of blaze. This means that the grooves are not symmetrical but shaped in such a way that the direction of specular reflection coincides with the diffraction direction for a certain wavelength—the blaze wavelength. That makes a grating particularly efficient for this wavelength. If you have a choice, you should select a grating with a blaze wavelength near the wavelength you are particularly interested in, or for which it is difficult to get sufficiently strong light. For a lamp–monochromator combination like the one shown in Fig. 3.8 it is usually preferred to have a low blaze wavelength to compensate for the lower lamp output in the UV and blue regions. On the other hand, in equipment for the analysis of light (monochromator–photomultiplier combinations in spectroradiometers or the emission units of spectrofluorometers) it may be advantageous to use a high blaze wavelength to compensate for the lower sensitivity of the photocell for long-wavelength light.

A grating monochromator, in addition to the grating, consists of an entrance slit, an exit slit, and optics, which forms an image of the entrance slit at the exit slit via reflection in the grating. In Fig. 3.8 we see a schematic diagram of one type of monochromator suitable for photobiological use. In this case a plane grating is combined with a concave mirror. Another solution is to use a concave grating, which focuses the light without any concave mirror. The wavelength of light leaving the exit slit is changed by rotating the grating. The monochromator is shown in combination with an illumination unit consisting of a lamp and a lens.

When using a grating monochromator, one should be aware of the fact that despite the name, with a certain setting, it transmits light of more than one wavelength:

First, we have the problem of light of various orders (first, second, etc.) mentioned above. The wavelength scale on the monochromator is valid for only a certain order, usually the first. When the dial is set at 300 nm, second order light of 150 nm wavelength may also be transmitted.

Second, the spectral composition of the light within one spectral transmission band depends on the size of the slits. A compromise has to be made in choosing the slits: The wider they are, the more light is transmitted (Fig. 3.9), but the narrower they are, the higher the spectral purity (which is, in many cases,
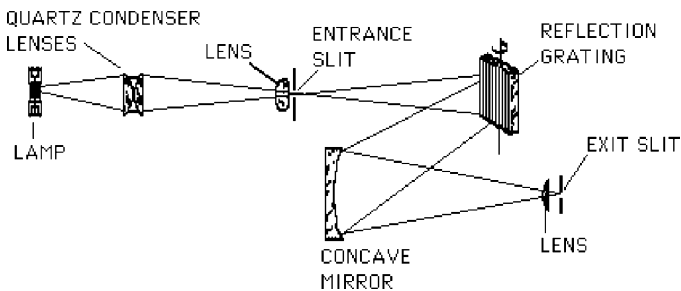
FIGURE 3.8. Schematic diagram for a monochromator used for photobiology experiments.
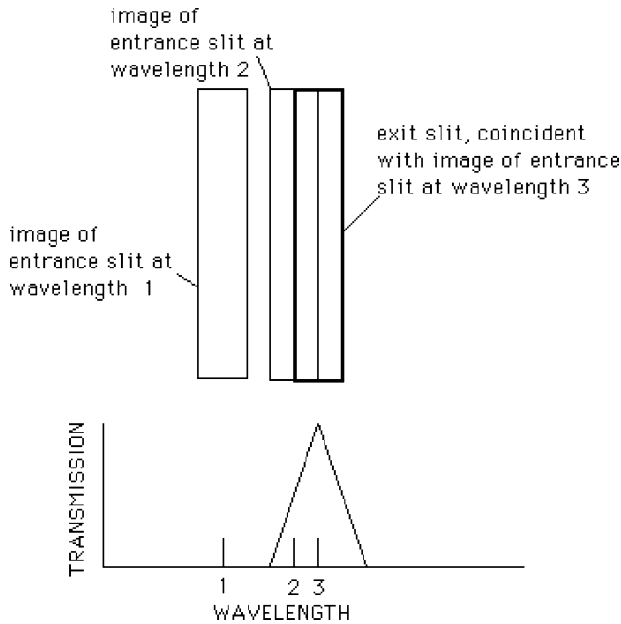
FIGURE 3.9. Images of the entrance slit for different wavelengths in relation to the exit slit (above), and the ideal transmission function, neglecting diffraction in entrance and exit slits.

important). The best compromises are found when the image of the entrance slit (in monochromatic light) just covers the exit slit. In this case, the spectral transmission band shape would be triangular were it not for diffraction at the slits and imperfections in the construction. In reality, the spectral band transmitted will be of a somewhat rounded triangular shape (see Chapter 4).

An interesting new development is the construction of acousto-optic tunable interference filters (see Tran 1997 for a review). Such a filter is in a way intermediate between an interference filter and a grating. The basic principle is that a sound wave in a crystal creates regions of alternating low and high refractive index, which causes diffraction of a light beam. In this way the unit functions as a grating. But unlike a grating it need not be rotated for changing the wavelength of light exiting in a certain direction. This can be done by changing the frequency of the sound wave, which is generated piezoelectrically. This makes possible very rapid scanning over a spectral range by changing the frequency of the driving voltage.

References

Calvert, J.G. and Pitts, J.N., Jr. (1966) *Photochemistry*. New York: Wiley.

Gahr, A., Weil, L. and Niessner, R. (1995) Polychromatic actinometry with filter solutions. Wat. Res. 29, 2125–2137.

Hale, G.M. and Querry, M.R. (1973) Optical constants of water in the 200 nm to 200 μm wavelength region. Appl. Opt. 12, 555–563.

Rabek, J.F. (1982) *Experimental methods in photochemistry and photophysics*, part 2. John Wiley, Chichester.

Stanley, C.M. (2003) Filters and mirrors for applications in fluorescence microscopy. Methods Enzymol. 360, 394–415.

Taniyasu, Y., Kasu, M. and Makimoto, T. (2006) An aluminium nitride light-emitting diode with a wavelength of 210 nm. Nature 441, 325–328.

Tran, C.D. (1997) Principles and analytical applications of acousto-optic tunable filters, an overview. Talanta 45, 237–248.

Yuan, Z.L., Kardynal, B.E., Stevenson, R.M., Shields, A.J., Lobo, C.J., Cooper, K., Beattie, N.S., Ritchie, D.A. and Pepper, M. (2002) Electrically driven single-photon source. Science 295, 102–105.

4
The Measurement of Light

Lars Olof Björn

Abstract: In this chapter various thermal, electronic, and chemical devices are described, as well as the construction and calibration of a spectroradiometer. A separate section is devoted to the measurement of very weak light, such as the ultraweak luminescence from living cells.

4.1. Introduction

There are three principal types of light-sensitive devices in common use, based upon three different effects of light on matter: photothermal, photoelectric, and photochemical devices. We shall describe these and their uses, and then go on to describe a more complex device, the spectroradiometer.

4.2. Photothermal Devices

Photothermal devices have slow response and low sensitivity. Their great advantage is that, unlike photoelectric and photochemical devices, they have the same response per energy unit throughout a very wide spectral range. Their principle of operation is that the light to be measured is allowed to be absorbed by a target. The temperature of the target is raised by the absorbed energy and the temperature rise is taken as a measure of the amount of energy absorbed.

4.2.1. The Bolometer

In a bolometer the target is a temperature-dependent resistor. The resistivity of all materials is temperature dependent. In the first bolometers thin platinum foils, blackened with colloidal platinum for efficient absorption of light, were used. The resistivity of platinum rises with temperature. The platinum foils were freely suspended in the air, and these bolometers were very sensitive to air currents.

In the bolometers commonly used in photobiology laboratories today, the targets are thermistors, i.e., semiconductor resistors with a large negative temperature coefficient. They are protected by a window made from sapphire, lithium fluoride, or other materials with a wide spectral transmittance range. The light target is part of a Wheatstone bridge, so that small changes in resistance can be recorded.

The setup is schematically depicted in Fig. 4.1. Of the four resistor arms of the bridge, one is variable, so that the bridge can be balanced (same potential at the top as at the bottom, and no current flowing through the meter) with the target resistor shielded from light. In general the potential difference between the top (R_1/R_2 junction) and bottom (R_3/R_4 junction) will be $U[R_2/(R_1+R_2) - R_3/(R_3+R_4)]$, so that when the bridge is balanced $R_2/(R_1+R_2) = R_3/(R_3+R_4)$. We now remove the light shield and allow the light to be measured to fall on R_2. This resistor now heats up and changes its resistance by the amount ΔR_2. The concomitant change in potential between "up" and "down" will be $U \cdot \Delta R_2/(R_1+R_2)$, and change in current flowing trough the meter will be proportional to the resistance change of the target.

Disregarding heating by the current flowing through it, the energy taken up by the target consists of the light to be measured plus heat radiation from the surroundings, assumed to be at absolute temperature T_a. The heat radiation received is proportional to T_a^4 (Stefan-Boltzmann's law). The radiation energy
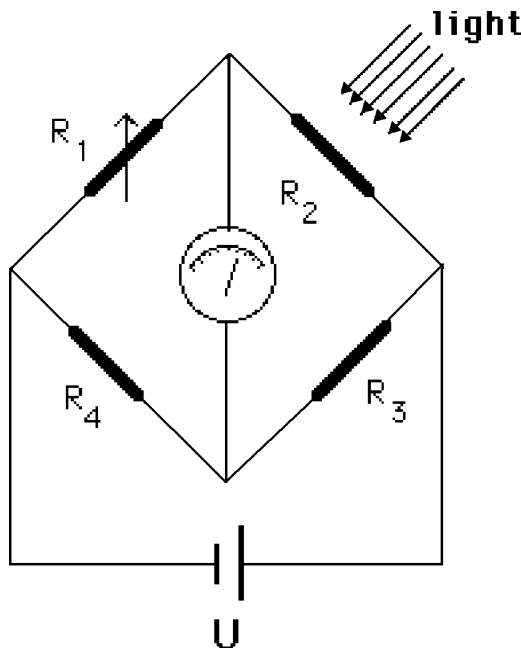
FIGURE 4.1. Schematic diagram of a bolometer. It is connected to a voltage source with voltage U.

given off by the target (at absolute temperature T_t) is proportional to T_t^4. When equilibrium has been reached, we thus have the relationship for the irradiance of the light to be measured (k_1 and k_2 are constants):

$$\text{Irradiance} = k_1.T_a^4 = k_1.T_t^4$$

or

$$\text{Irradiance} = k_1 \cdot (T_t^4 - T_a^4) = k_1 \cdot (T_t^2 + T_a^2) \cdot (T_t + T_a) \cdot (T_t - T_a) \approx k_2 \cdot (T_t - T_a)$$
$$= k_2 \cdot \Delta T$$

Thus, the irradiance is proportional to the temperature change of the target resistor and, thus, as shown previously, proportional to the current flowing through the meter.

Irradiances down to about 1 W/m^2 can be measured with a standard bolometer. At lower irradiances the drift problems become serious. When a low irradiance is to be measured, it is best to connect the bolometer to a strip-chart recorder or computer to keep track of the drift of the baseline. A suitable procedure is to expose the bolometer to the light for 30 seconds, then shield it for the same period for recording of the base line, then expose it again, etc. Prolonged exposure decreases the reading, because the balancing resistors (not directly exposed to the light) heat up by heat conduction.

The calibration of a bolometer can be easily checked as described by Björn (1971). For highest accuracy a special standard lamp should be used in the way specified in the directions supplied with it. For information regarding standard lamps, see the section on spectroradiometers.

4.2.2. The Thermopile

A thermocouple is a couple of junctions between two metals. Wherever two metals are in contact, a temperature-dependent potential difference exists. A thermopile consists of several thermocouples (each one with two junctions) connected in series, as shown in Fig. 4.2. Of each couple of junctions, one is shielded from and the other one exposed to the light to be measured. The sensitivity and speed of response are increased by attaching small light-absorbing (and heat-radiating) shields to the junctions, and these shields should be blackened for efficient absorption (and reradiation).

For optimal results the input resistance of the current measuring meter should be matched to the resistance of the thermopile, which is of the order of 10–100 ohm. A thermopile is usable down to about the same irradiance as a bolometer. As for the bolometer, the output current is proportional to the irradiance.
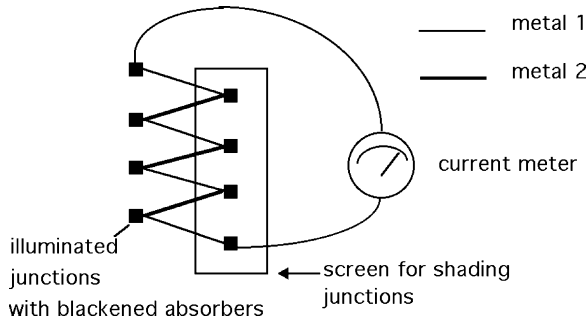
FIGURE 4.2. Schematic diagram of thermopile with current meter.

4.2.3. Thermopneumatic Devices

The principle of pneumatic thermal radiation detectors is that the radiation heats a gas. The resulting expansion can be detected by the movement of an enclosing membrane. In one of the early devices, the Golay detector, the movement was detected optically. Sensors based on this principle, used principally for infrared radiation, are still being refined, and very small movements of the membrane can be detected interferometrically. Pneumatic detectors are often used in connection with chopped or pulsating light. In this case the periodic expansion of the gas can be detected by a microphone. Many biologists have come in contact with this principle when measuring carbon dioxide, for instance, in the measurement of photosynthesis and respiration. An infrared gas analyzer (IRGA; Fig. 4.3) for such measurements often works in a differential mode.

External air passes through an optical cell ("reference cell"), then through the cell with the biological sample ("sample cell"), and finally through a second optical cell. A beam of infrared radiation passes alternatingly through one or
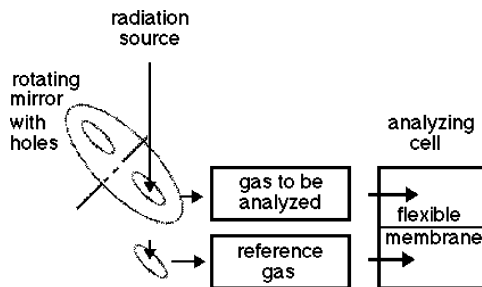
FIGURE 4.3. Principle for an infrared gas analyzer (IRGA), very schematic. Infrared radiation passes alternatingly through a cell with reference gas, for instance, ambient air, and alternatingly through a cell with gas to be analyzed, for instance, air that has passed a compartment with plants taking up carbon dioxide. Depending on how much radiation remains to be absorbed in the two halves of the analyzing cell, the flexible membrane separating the two halves is deflected to a greater or lesser extent.

the other of the cells. From there the radiation continues into an analyzing cell, partitioned by a flexible membrane. This cell contains the same kind of gas as the one being measured. Depending on how much radiation there remains after absorption in the reference cell and the sample cell, the gas in the two halves of the analyzing cell is heated more or less and temporarily expands in a corresponding way. Usually the heating and expansion is different in the two halves, which causes the membrane to vibrate in relation to how the radiation is deflected through the reference cell and the sample cell. By making the membrane form one plate in an electrical capacitor, this vibration can give rise to an electrical signal proportional to the difference in gas concentration in the sample cell and the reference cell.

Evans (2005) has suggested that some beetles use the thermopneumatic principle for detecting infrared radiation.

4.3. Photoelectric Devices

A great number of photoelectric devices exist. They can be divided into two main categories, depending on whether they exploit an outer photoeffect (at a metal surface in vacuum or gas) or an inner photoeffect inside a solid semiconductor.

4.3.1. A Device Based on the Outer Photoelectric Effect: The Photomultiplier

Although many kinds of photocells (as well as television camera tubes, image intensifiers, etc.) utilize the outer photoeffect, we shall limit ourselves here to a description of the photomultiplier, a device extensively used by photobiologists. Figure 4.4 shows the basic principle. Inside an evacuated envelope of glass or quartz there are a number of metal plates. The one marked C is the photocathode. It is held at a large negative potential relative to ground (wires connected to electrical circuitry not shown). The surface of the photocathode exposed to the light to be measured is covered with a layer of special metals. Usually a mixture of several metals, some of which are alkali metals, is used. Depending on the particular metal alloy, photomultipliers have different spectral responses.

When a photon hits the photocathode, an electron is released from the metal (as is known from chemistry, alkali metals are especially prone to losing electrons; they have a low *work function*). Because the photocathode is at a low electric potential, the electron does not return to the surface. Instead, it is accelerated towards another metal plate nearby, which is held at a higher potential, dynode 1 (D1). In flight the electron acquires such a velocity that when it hits the dynode it releases two or three electrons from it. They travel on to dynode 2 (at an even higher potential) where further electrons are released. Photomultipliers are constructed with up to 12 dynodes in series, and at each dynode more electrons are added. Finally, the electron swarm is collected at the final plate, the anode (A in Fig. 4.4). This is usually maintained close to ground potential. The
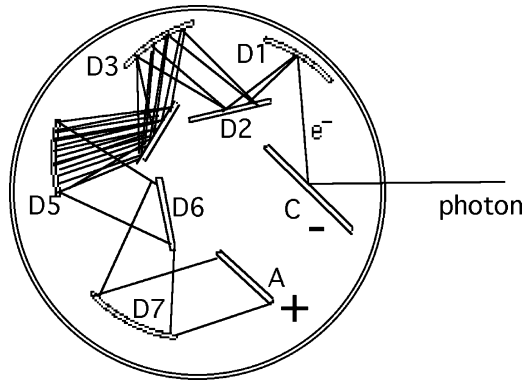
FIGURE 4.4. Diagram of (side-on) photomultiplier.

electrons flowing to the anode represent an electrical current, which also flows through the wire connected to the anode (not shown), and this can be recorded and used as a measure of the light incident on the photocathode.

Contrary to the thermoelectric devices described in the previous section, photomultipliers have different sensitivities to different kinds of light. Furthermore, they are rather unstable. Their great advantage lies in the high light sensitivity: even individual photons can be recorded by some photomultipliers under suitable conditions. Provided the electronic circuitry to which they are connected has a low time constant, photomultipliers also have a short response time (although different photomultipliers differ in this respect).

The diagram shows a so-called side-on photomultipler. There are also other designs. A common one is the end-on photomultiplier, where the photocathode consists of a thin, semitransparent metal film on the inside of the flat end of the cylindrical envelope. In this type the spectral response is also dependent on the thickness of the film, which usually varies somewhat over the surface. Photomultipliers require an operating voltage of 500–5000 V; in many cases about 1000 V is used. The different electrodes are given their proper voltages by a chain of resistors between the negative high voltage lead and ground. The output current is very strongly dependent on the operating voltage, which must therefore be held very constant (with N dynodes and operating voltage U, the output current is roughly proportional to U^N).

The output is not always measured as a current. As the incident irradiance is lowered, the discontinuous nature (quantization) of light becomes more and more apparent. At very low light levels it becomes advantageous to record individual photons by counting the pulses of current flowing to the anode. The measurement of very weak light is further dealt with in Section 4.7

Photomultipliers are made with different cathode layers for different spectral ranges from the ultraviolet to the near infrared (to about 900 nm). Photomultipliers sensitive to light of long wavelength generally have a higher dark current (dark noise) than others. The noise level can be decreased (to achieve a better

signal-to-noise [S/N] ratio) by lowering the temperature. Liquid nitrogen, dry ice, or Peltier coolers are generally used for this. Cooling must be combined with precautions to avoid dew on the optical components.

4.3.2. Devices Based on Semiconductors (Inner Photoelectric Effect)

In the inner photoelectric effect, absorption of a photon inside a solid semiconductor results in the separation of a positive charge from a negative one.

Photoconductive cells with a semiconductor as the light-sensitive element have been used extensively in the past. Among these can be mentioned lead sulfide cells for measurements in the near infrared, for which no photomultipliers or other suitable photocells were available, and cadmium sulfide cells for photographic exposure meters. Photoconductive cells are variable resistors and require an external source of voltage for creation of a current that can be measured. They have a slow response and are not used much for scientific measurements.

Photodiodes and phototransistors, on the other hand, can be made to have a very rapid response. For very long wavelengths (>1000 nm) they also compete with photomultipliers in terms of sensitivity. The so-called avalanche photodiode can be regarded as a semiconductor equivalent to the photomultiplier. Photodiodes are often preferred in applications where photomultipliers could also be used, because photodiodes are small, cheap, rugged and do not require high voltages. In combination with special electronics it is nowadays possible to detect single photons of 1550 nm wavelength using an avalanche photodiode (Namekata, Sasamori, and Inoue 2006), and this is possible also with special, cooled photomultipliers (Skovsen, Snyder, and Ogilby 2006). Photodiode arrays have become popular for recording a whole spectrum at one time (each diode in the array measures one spectral band).

Two main types of barrier layer cells are in current use: the selenium cell and the silicon cell. They are similar in principle, but differ in their spectral response: the selenium cell is most sensitive to green and blue light, the silicon cell to red and far-red light. The general principle is shown in Fig. 4.5.

Because selenium barrier layer cells have a spectral sensitivity somewhat resembling that of the human eye, they are used in photometers (lux meters)
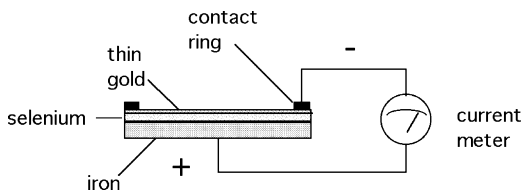
FIGURE 4.5. Selenium barrier layer cell with required circuitry. Note that the device generates its own operating voltage and does not require any battery or other external voltage source.

for measurement of visible light at, for example, working places. By combination with suitable filters, the spectral sensitivity curve can be made to almost completely match the curve for scotopic vision (which defines illuminance). In earlier days such cells were also used for photographic exposure meters, where they have now been replaced by cadmium sulfide photoconductive cells and, more recently, by photodiodes.

4.4. Photochemical Devices: Actinometers and Dosimeters

Chemical systems for measurement of light and ultraviolet radiation are called actinometers. (The best known photochemical device for recording light is photographic film. This has also been used for quantitative measurements, but it will not be further discussed here. Other chemical systems are usually better suited for quantitative measurements of radiation.)

Actinometers have the advantage of not having a need for calibration by the user, and thus do not require the purchase of an expensive standard lamp with an expensive power supply. Standardization has usually been taken care of by those who have designed the actinometer. Another advantage is that the geometry can more easily be adjusted to the measurement problem. The shape of a liquid actinometer can easily be made to correspond to the overall shape of the irradiated object under study. In many cases it is of interest to study a suspension or solution that can be put in an ordinary cuvette for spectrophotometry or fluorimetry, and the actinometer solution can be put into a similar cuvette.

A large number of actinometers have been devised. Kuhn et al. (1989) list and briefly describe and give references to 67 different systems involving gaseous, liquid, and solid phases. Of these they recommend five. In general actinomters are sensitive to short-wave radiation and insensitive to long-wave radiation. Insensitivity to long-wave radiation can be both a drawback and an advantage, but by choosing the best actinometer for the purpose one can avoid the disadvantages. One advantage of using an actinometer insensitive to long-wave radiation is that one can work under illumination visible to the human eye, without disturbing the measurement. We shall give an introduction below to a few different actinometers, not all of which are mentioned by Kuhn et al. (1989), and then go on to describe more in detail the most popular one for ultraviolet radiation—the potassium ferrioxalate or potassium iron(III) oxalate actinometer.

1. The potassium iodide actinometer (Rahn 1997) is sensitive primarily to UV-C radiation (wavelength <280 nm), and with slight sensitivity also for short-wave UV-A. It is suitable for determining the 253.7 nm radiation from low-pressure mercury lamps (bactericidal lamps), since the contribution from other spectral lines of the lamp will be negligible (but the ferrioxalate actinometer works almost as well for this purpose). It can be handled in ordinary incandescent light (not light from unshielded quartz-iodine lamps). The reaction on which this actinometer is based is the oxidation of iodide ion by iodate ion to form iodine, or rather triiodine ion (I_3^-).

2. An actinometer sensitive to visible light (photosynthetically active radiation) has been described by Wegner and Adamson (1966). It works up to above 700 nm and is based on potassium tetrathiocyanatodiamminechromate (III), $K[Cr(NH_3)_2(SCN)_4]$. The latter can rather easily be prepared from the commercially available Reinecke's salt, i.e, $NH_4[Cr(NH_3)_2(SCN)_4]$. Irradiation causes the uptake of water and release of thiocyanate, which can be measured spectrophotometrically after addition of an Fe(III) salt.
3. Two more actinometers that have recently been used in biological contexts are the 2-nitrobenzaldehyde actinometer (Allen et al. 2000) and the oxalic acid/uranyl sulfate actinometer (Mirón et al. 2000). A different version of the latter one preferable for small radiation doses is among those recommended by Kuhn et al. (1989).
4. As already mentioned, the most popular actinometer for ultraviolet radiation (and for violet and blue radiation as well) is the ferrioxalate actinometer. The description below will be sufficient for the experimenter starting in the field. For more detailed information one should consult Parker (1953), Hatchard and Parker (1956), Lee and Seliger (1964), and Goldstein and Rabani (2007). Complete recipies have also been published by, e.g., Seliger and McElroy (1965) and Jagger (1967).

In the ferrioxalate actinometer the following photochemical reaction is exploited:

$$\tfrac{1}{2}(COO^-)_2 + Fe^{3+} + photon \longrightarrow CO_2 + Fe^{2+}$$

or

$$\text{Oxalate ion} + Fe(III)\text{ion} + light \longrightarrow \text{carbon dioxide} + Fe(II)\text{ion}$$
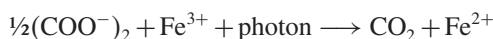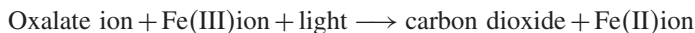
The quantum yield for this reaction (i.e., the number of iron ions reduced per photon absorbed) is slightly wavelength dependent but close to 1 in the spectral region, 250–500 nm, where the ferrioxalate actinometer is used. Usually a 1-cm layer of 0.006 M ferrioxalate solution is used. Quantum yield and the fraction of the radiation (perpendicular to the 1 cm layer) absorbed are shown in Table 4.1.

TABLE 4.1. Quantum Yield and the Fraction of Radiation (perpendicular to 1-cm layer) Absorbed

Wavelength	Quantum yield	Fraction absorbed	Quantum yield × fraction absorbed
253.7	1.26	1	1.260
300.0	1.26	1	1.260
313.3	1.26	1	1.260
334.1	1.26	1	1.260
365.6	1.26	1	1.260
404.7	1.16	0.92	1.067
435.0	1.11	0.49	0.544
509.0	0.85	0.02	0.017

The quantum yields for 0.15 M actinometer solution are 0.952 of the above values. Irradiation of the side walls of the cuvette should be avoided, i.e., the beam should be smaller than the cross section of the cuvette.

The amount of Fe(II) formed can be measured spectrophotometrically after addition of phenanthroline, which gives a strongly absorbing yellow complex with Fe(II) ions.

The ferrioxalate for the actinometer is prepared by mixing 3 volumes of 1.5 M $(COOK)_2$ with 1 volume of 1.5 M $FeCl_3$ and stirring vigorously. This step and all the following involving ferrioxalate should be carried out under red light (red fluorescent tubes). The precipitated $K_3Fe(C_2O_4)_3 \cdot 3H_2O$ should be dissolved in a minimal amount of hot water and the solution allowed to cool for crystallization (this crystallization should be repeated twice more).

Following is a recipe for the three solutions required for carrying out actinometry (see Goldstein and Rabani 2007 for a different procedure and other quantum yields):

Solution A: Dissolve 2.947 g of the purified and dried Fe(III) oxalate in 800 ml distilled water, add 100 ml 0.5 M sulfuric acid, and dilute the solution to 1 liter. This gives 0.006 M actinometer solution, which is suitable for measurement of ultraviolet radiation. For visible light, which is only partially absorbed, it may be advantageous to use 0.15 M Fe(III) oxalate instead, i.e., 73.68 g per liter solution.

Solution B: The phenanthroline solution to be used for developing the color with Fe(II) ions should be 0.1% w/v 1:10 phenanthroline monohydrate in distilled water.

Solution C: Prepare an acetate buffer by mixing 600 ml of 0.5 M sodium acetate with 360 ml of solution B.

Solution A is irradiated with the light to be measured. The geometries of the container and of the light are important and must be taken into account when evaluating the result. The simplest case is when the light is collimated, the container a flat spectrophotometer cell, the light strikes one face of the cell perpendicularly, and no light is transmitted. Even in this case one has to distinguish whether the cell or the beam has the greater cross section, and correct for reflection in the cell surfaces. The irradiation time should be adjusted so that no more than 20% of the iron is reduced.

After the irradiation two volumes of the irradiated solution are mixed with two volumes of solution B and one volume of solution C, and then diluted to 10 volumes with distilled water. After 30 minutes the absorbance at 510 nm is measured against a blank made up in the same way with unirradiated solution A.

Example of calculation: Four milliliters of 0.006 M actinometer solution are irradiated in a flat quartz container by parallel rays of UV-B impinging at right angles to one surface (and not able to enter any other surface). The radiation cross section intercepted by the solution is 2 cm^2. Five minutes of irradiation produces 0.6 μmol Fe(II).

Throughout the UV-B region the quantum yield is 1.26. Reflection from the surface is estimated to be 7% (by application of Snell's law). None of the

radiation penetrates the solution to the rear surface, since the solution thickness is well over 1 cm. Therefore 0.6 mmol corresponds to $0.6/(1.26 \cdot 0.93)$ μmol = 0.512 μmol radiation incident on 2 cm^2 in 5 minutes, and the photon irradiance (quantum flux density, in this case equal to the photon fluence rate, since the rays are parallel and at right angles to the surface) is $0.510/(2 \cdot 5)$ μmol/cm^2/min^1 = 5.10 nmol/cm^2/min^1 or $5.10 \cdot 10^4/60$ nmol/m^2/s^1 = 850 nm/m^2/s^1.

The great limitation of the ferrioxalate actinometer is that it is not sensitive to long-wavelength light (in many cases this is also an advantage; one reason being that red working light can be used without interference with the measurements). Several actinometers sensitive to longer wavelengths have been designed. Warburg, for instance, used one based on chlorophyll. A modern, red-sensitive actinometer has been described by Adick et al. (1989).

Chemical or biological systems, mostly in the solid state, for recording light, and ultraviolet radiation in particular, are widely employed for estimating exposure of people, leaves in a plant canopy, and other objects which for various reasons are not easily amenable to measurements with electronic devices. These chemical devices are generally referred to as *dosimeters* rather than actinometers, even if there is no defined delimitation between these categories. As the construction, calibration, and use of chemical and other dosimeters have been the subject of frequent reviewing (Bérces et al. 1999, Horneck et al. 1996, Marijnissen and Star 1987), I shall not dwell on them here, only stress that their radiation-sensitive components can be either chemical substances (natural like DNA or provitamin D, or artificial) or living cells (e.g., various spores and bacteria).

4.5. Fluorescent Wavelength Converters ("Quantum Counters")

As stated earlier, photomultipliers have the advantage of being very sensitive as well as the disadvantage of having wavelength-dependent sensitivity. Fluorescent wavelength converters or "quantum counters" are solids or solutions, usually used in conjunction with photomultipliers, to obtain devices which are sensitive, yet have a sensitivity per photon that is independent of wavelength over a certain interval. The idea is to use a solution that has an absorbance high enough that all photons (except those reflected) will be absorbed and that has a high fluorescence yield. Incident light of any wavelength distribution within certain limits is then converted, photon for photon, to light of a fixed wavelength distribution (the fluorescence spectrum of the "quantum counter"), to which the photomultiplier has a fixed sensitivity. One of the major uses of "quantum counters" is calibration of excitation units of spectrofluorimeters. The "quantum counter" most widely used consists of a concentrated solution of rhodamine B in ethylene glycol. It is useful for wavelengths up to 600 nm.

4.6. Spectroradiometry

4.6.1. General

A spectroradiometer is an apparatus with which you can measure the spectrum of light, i.e., either the spectral irradiance, the spectral fluence rate, or the spectral radiance as a function of wavelength (or frequency, which is equivalent, but less commonly used by biologists). It consists of three main parts: (1) input optics, different for spectral irradiance, spectral fluence rate, or spectral radiance, (2) a monochromator or, preferably, a double monochromator, and (3) a trans-ducer for converting the light signal to an electrical signal. The latter may be, in some cases, a photodiode, but is usually a photomultiplier. In some spectro-radiometers instead of a monochromator there is a spectrograph that projects a whole spectrum, and the transducer is a diode array, charge coupled device (CCD, see Section 4.8.), complementary metal oxide semiconductor (CMOS) or a multichannel plate, which samples the whole spectrum at once. The latter arrangement has the advantage of speed and synchronous sampling of all spectral channels, but is not always suitable. In particular, it is very unsuitable for measuring ultraviolet radiation in daylight, in which case straylight problems must be minimized by use of a double monochromator.

   A complete spectroradiometer system also requires some facility for frequent recalibration, as especially photomultipliers have very bad long-term stability.

4.6.2. Input Optics

Before deciding on input optics, we need to decide what quantity we wish to measure. For spectral radiance we need input optics with which we can sample a very narrow solid angle. This can be some kind of telescope, but for most purposes it is sufficient to have a tube with a terminal stop that determines the sampling angle and a few internal baffles and an inner matte black surface to avoid reflections inside the tube to reach the monochromator entrance slit Fig 4.6.

   For spectral fluence rate we need a device that samples all directions with equal sensitivity. This is an ideal that cannot really be fulfilled, but it can be approached. Using input optics for irradiance, it is possible to combine several measurements to obtain the fluence rate (Björn 1995, Björn and Vogelmann 1996).
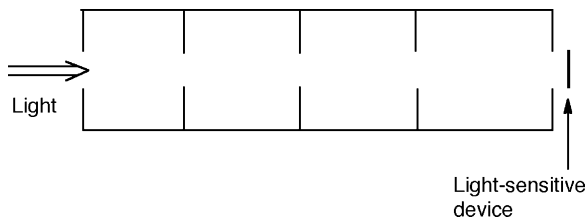
FIGURE 4.6. Input optics for radiance (narrow angle) measurements, consisting of a tube with stops and internal baffles, and inside painted dull black to prevent internal reflections.

For spectral irradiance measurements we need input optics, which has a "cosine response," meaning that the sensitivity, or the efficiency of sampling, for a certain direction should be proportional to the cosine of the angle between that direction and the optical axis. The concept of "cosine response" is graphically explained in Fig 4.7

As a first crude device to reach this situation one could let the light to be measured strike a strongly scattering but translucent plate above the entrance slit of the monochromator. Suitable materials for this include ground quartz or fused silica or teflon, depending on the spectral range. A flat plate is, however, not very satisfactory, especially for large deviations from the optical axis. For measuring irradiance of light from an extended light source, for instance, an overcast sky, light at these large angles is very important, since the "amount of sky" corresponding to a certain angular deviation from the optical axis is proportional to the sine of the angle. Somewhat better results are obtained using a hemispherical scattering dome over the slit. The only device that works well is an integrating sphere (Fig. 4.8), and to work well it must be well designed. Details on this subject are provided by Optronics Laboratories (1995, 2001).

In some cases we are more interested in the shape of a spectrum than in the absolute light level, and then the angular sensitivity function is less important. We may also be interested in measuring light in places where it is not easy to put the spectroradiometer itself (such as underwater or inside the mouth). In that case the best choice may be to use fiberoptics at the input end of the spectroradiometer. Even then one may add, for instance, a small scattering device at the tip of the fiberoptic conductor to collect light from different directions. Single light-conducting fibers may even be used to measure light inside plant or animal tissues (Vogelmann and Björn 1984).
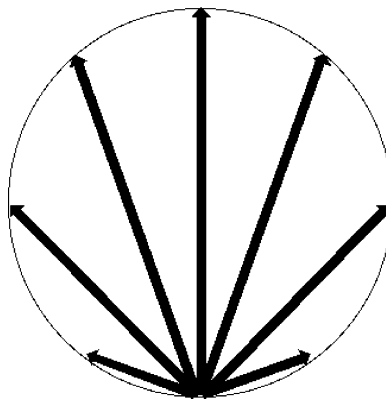
FIGURE 4.7. Cosine sensitivity of a receiver. The sensitivity is greatest straight up in this case and decreases proportionally to the cosine of the angle to the vertical. In the horizontal direction the sensitivity is zero.
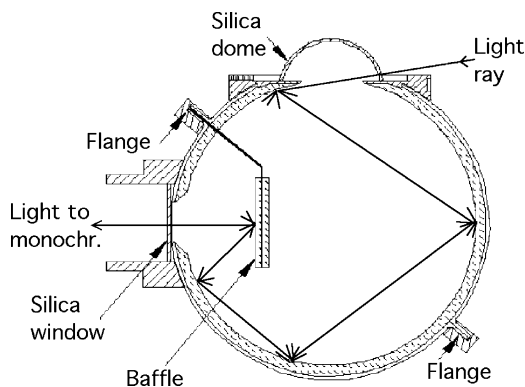
FIGURE 4.8. Integrating sphere used as input optics for spectroradiometric irradiance measurements. On top is a silica dome, which can be omitted if the instrument is to be used only indoors or in good weather conditions. Below that is the opening in the sphere that defines the area over which the irradiance measurement is taken and the direction of the reference surface. A light ray has been drawn that strikes this at a low angle. It is important that the walls of the sphere taper off to an edge to allow rays at such low angles to enter the sphere. The ray strikes the inner diffusely reflecting wall. From the point where it strikes, light is scattered in all directions. We have followed one possible path through the sphere, but the little "brushes" at each scattering point are meant to indicate that there are many possibilities. Eventually the light strikes the back side of the baffle, which serves as the direct light source for the monochromator (see Fig. 4.9).

4.6.3. Example of a Spectroradiometer

We show here (Fig. 4.9), as an example of a spectroradiometer often used by biologists, the construction of Model 754 from Optronic Laboratories.

Spectroradiometers for measurement of UV-B radiation in daylight do not work well with a single monochromator, mainly because spectral irradiance in the UV-B region changes very rapidly with wavelength. Very small amounts of radiation outside the intended band can therefore ruin the measurement. When two monochromators are used in tandem, it is of course very important that their wavelength settings agree throughout the scan. The only way to achieve this is to have both built on a single base plate and be driven by a single wavelength drive mechanism.

Because biological chromophores have rather broad spectra, the fine structure of the daylight spectrum or the spectrum of any other light is not of great importance. Still, it is important that the bandwidth of the measuring system is not too great, i.e., that the slits in the monochromator are not wide when daylight UV-B radiation is to be measured. This is because the spectrum is so steep in this region. Figure 4.10 illustrates this: when the bandwidth is increased above 1 nm, values in the short-wavelength part of the UV-B band start being too high. Errors are also introduced in the calibration (see below) if the bandwidth is too great.
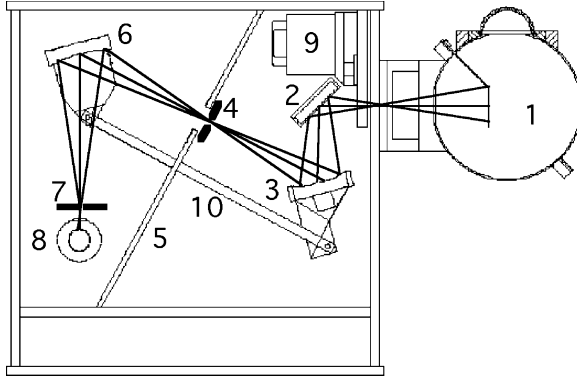
FIGURE 4.9. Diagram of spectroradiometer (Optronic Laboratories model 754), simplified to enhance the important optical parts. Light from the integrating sphere (1, see Fig. 4.8) enters the light-tight box through a slit (entrance slit for the first monochromator, not specifically shown) and is deflected by the mirror (2) to the first grating (3). The chosen wavelength band leaves this first monochromator unit through the exit slit (4) in the wall (5) separating the two monochromators. This slit (4) is also the entrance slit for the second monochromator. The second grating (6) again disperses the light and deflects the chosen wavelength band onto a slit (7) in front of the photomultiplier (8). A stepper motor (9) turns the grating to change the wavelength. The rotating grating supports are connected by a bar (10), thus assuring that they follow one another with high fidelity.
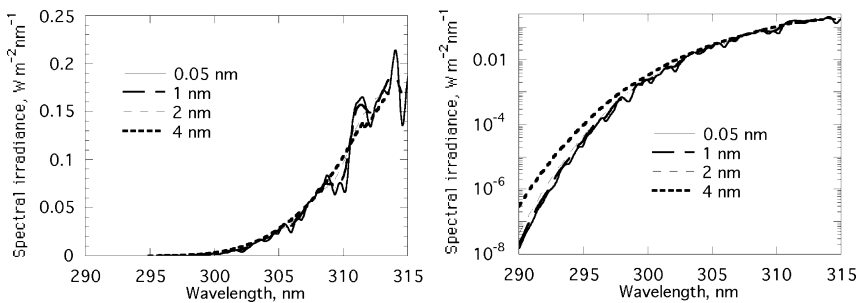
FIGURE 4.10. A portion of the ultraviolet daylight spectrum in Lund at noon on June 15, plotted with three different half-bandwidths (modeled values). Left frame with linear, right frame logarithmic spectral irradiance scale. In the linear plot we can see how the fine-structure is gradually smoothed out, while the semilogarithmic plot shows more clearly how systematic positive errors develop in the short-wavelength part. With 4-nm bandwidth the error is more than an order of magnitude for part of the spectrum.

4.6.4. *Calibration of Spectroradiometers*

4.6.4.1. Wavelength Calibration with Lamps

This is the simple part, but important. If the wavelength is not correct, then everything else will be wrong, too. The wavelength error should be less than 1 nm; for measurements of daylight UV-B radiation it should preferably be much less.

For such calibration any medium pressure mercury lamp works well, even an ordinary fluorescent lamp. Easily recognizable spectral lines occur at 253.7, 265.2, 312.6 + 313.2, 334.1, 365.0, 365.4, 366.3, 404.7, 435.8, 491.6, 496.0, 546.1, 577.0, 579.1, 623.4, and 690.7 nm. The short-wavelength bands do not penetrate the envelopes of most fluorescent lamps.

4.6.4.2. Irradiance Calibration with Standard Lamps

Usually a spectroradiometer is calibrated using a lamp with a known output at different wavelengths. The most commonly used lamp is a 1 kW tubular quartz–iodine incandescent lamp. The reason to use such a powerful lamp is to obtain sufficient output in the ultraviolet region, and a lamp of this power can be used down to 250 nm. (For shorter wavelengths usually deuterium standard lamps are used.)

Using transfer standards, these standard lamps are ultimately calibrated against cavity radiators held at a well-determined temperature and designed so they follow as closely as possible the theoretical Planck blackbody radiation formula (see Chapter 1). When you purchase such a lamp you will obtain a table of the spectral irradiance obtainable at certain wavelengths at certain distance using a specific geometry, and also information about the accuracy. You will be surprised at (1) the wide uncertainty limits compared to most other kinds of physical measurements (typically 3.5% at 250 nm) and (2) the high price of the lamp. After all, it looks almost like the lamp you have in the overhead projector in your lecture hall. What you should consider at this moment of surprise is that the lamp has been preburned and selected to be particularly stable and the effort and cost involved in calibrating it as accurately as possible. You should buy a second similar but uncalibrated lamp at a much lower cost, calibrate this as a working standard against your expensive lamp, and only occasionally use your expensive lamp to check your working standard.

The disadvantage of using a 1 kW lamp (apart from the heat it produces in your usually small calibration room) is that it requires a direct current of 8 A to run at 125 V, and quite a big power supply is needed to produce this with good accuracy. It is very important that you really run it at the specified current at which it was calibrated. An error of 0.1% in the current produces a 1.2% error in the spectral irradiance at 250 nm and a 0.6% error at 400 nm. It is important that the current is as ripple-free (has as little ac component) as possible. The best way of measuring the current is to measure the voltage across a precision resistor of, say, 0.1 ohm in the lamp circuit with a good digital voltmeter.

Calibration of a spectroradiometer is a tricky thing. When you calibrate it with your standard lamp you usually put the standard lamp on the optical axis. Suppose that you calibrate two spectroradiometers in this way with the same standard lamp in the same setup, so that they show the same result when you measure light from a lamp in the laboratory. Then you take the spectroradiometers outdoors and measure the daylight. You will then likely find that the two spectroradiometers show different results. This can have different causes, but the two major ones are probably that (1) the temperature is different and the two spectroradiometers have different temperature dependencies and (2) they have different off-axis sensitivities, and you are now measuring a very extended light source rather than an almost point-like standard source.

It is recommended that you recalibrate a spectroradiometer about once a month. This interval can be modified according to the experience you obtain over time with your particular instrument under your particular working conditions. If you move your instrument around, you should perform a rather easy wavelength check at each new location.

4.6.4.3. Irradiance Calibration with an Improvised Standard Lamp

Björn (1971) devised a method to use an ordinary tubular incandescent lamp as a standard lamp without prior optical calibration of the lamp, just relying on electrical measurements. The basic idea is that the temperature of the lamp filament is calculated from the increase in electrical resistance when it heats up from room temperature; calculate the spectrum of the glowing filament from its temperature using Planck's radiation formula with appropriate corrections for the (temperature and wavelength dependent) emissivity of tungsten. This method is not recommended if calibrated standard lamps are obtainable for the experimenter.

4.6.4.4. Calibration Without a Standard Lamp

Considering the cost of standard lamps, their instability, and the difficulty of ensuring the same standard everywhere in the world, it would be good if a radiation source were available free of charge so that everyone could use the same radiation source. There is such a radiation source: the sun.

4.6.4.5. Wavelength Calibration Using Daylight

The sun is essentially a heat radiator, thus radiating an essentially continuous spectrum, while a line spectrum is more suitable for wavelength calibration. However, some of the outer layers of the sun have a temperature that is low enough to reabsorb light from the inner layers, and still hot enough to contain single atoms, not united to molecules. They produce the so-called Fraunhofer lines in daylight, which are absorption spectral lines of these free atoms. The wavelengths of these Fraunhofer lines can be looked up in various sources. Here we just mention the two due to hydrogen, which are most suitable for

wavelength calibration in the visible region: 486.1344 nm (Fraunhofer F line) and 686.9955 nm (Fraunhofer C line).

4.6.4.6. Irradiance Calibration Using the Sun

Surprisingly, the sun can also be used for irradiance calibration. This is surprising because we have the variable terrestrial atmosphere between ourselves and the sun, and this atmosphere is not the same everywhere. If we are on a mountain there is less atmosphere between us and the sun than at sea level, and other factors also contribute to different attenuation of the sunlight at different places and times. However, these difficulties can be circumvented, provided the atmosphere is reasonably clear and stable over a day.

Consider first two (unrealistically) simple cases (Fig. 4.11). We have no clouds in the sky. In the first case the sun is direcly overhead, and the light is attenuated by, as the jargon in the field goes, one air mass. At a certain wavelength the spectral irradiance from the direct sunlight can be written as $I_1 = I_e \cdot e^{-a}$, where I_e is the corresponding extraterrestrial spectral irradiance, i.e., the spectral irradiance just outside the terrestrial atmosphere. The spectral irradiances we consider here are in the direction of the sun (light falling on a plane perpendicular to the direction to the sun). We consider only the direct sunlight, i.e., not that scattered in the atmosphere or reflected from the ground. In the second case the sun is at an angle of 60° to the vertical, i.e., the zenith angle of the sun is 60°. In this case the light path through the atmosphere is twice as long as in the first case. The irradiance then must be (provided the Lambert-Beer law is valid) $I_2 = I_e \cdot e^{-2a}$, since the light is now attenuated by two air masses. Only when the scattered light is excluded by a narrow-angle input does the Lambert-Beer law hold (see Chapter 1, Section 1.11.). The ratio between the two irradiances below the atmosphere is then $I_2/I_1 = e^{-a}$, and this ratio we should be able to determine without absolute calibration of the spectroradiometer. But knowing e^{-a} we can now calibrate the spectroradiometer against the extraterrestrial irradiance using the relationship $I_1 = I_e \cdot e^{-a}$.
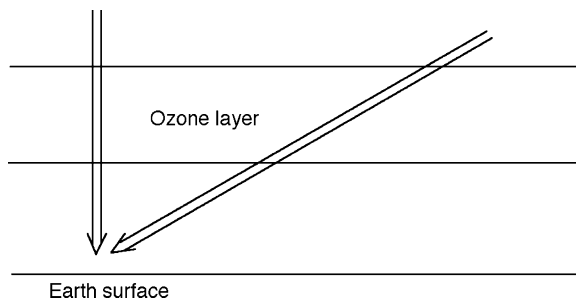
FIGURE 4.11. Effect of atmosphere on sunlight from different directions. If scattered light is excluded so only the direct beam is considered, the length of the path of light through the atmosphere is longer for obliquely incident light, in proportion to the cosine of the incidence angle.

This is the principle of the Langley calibration method. In practice it is a bit more complicated than described here. One has to take spectra of the sun over at least one day, and preferable over several days when the weather is stable and the sky without clouds. For the Lambert-Beer law to be valid, one has to measure the *direct* sunlight and exclude skylight as well as possible. One way of doing this is to measure the sunlight through a narrow baffled tube (Fig. 4.6) following the sun. Another way is to take a difference reading, i.e., the difference between the total daylight and the daylight when shadowing the sun. One then plots the logarithm of the reading against the air mass (the air mass is proportional to one over the cosine of the zenith angle). This gives a nearly straight-line relationship, which can be extrapolated to zero air mass, corresponding to the reading that would have been obtained outside the atmosphere. For high accuracy one must apply various corrections (especially for large zenith angles), for instance, for the refraction (bending) of the light rays in the atmosphere and for the curvature of the earth, and for the fact that different attenuators in the atmosphere do not have the same height distribution (especially for the fact that ozone, absorbing at short wavelengths, is higher than most attenuators). One must also take into account the variation of the sun–earth distance over the year, but this is easy. With decreasing wavelength the difficulties increase (e.g., due to the rapidly changing ozone attenuation, the strong wavelength dependence of ozone absorption, less constant output of the sun at short wavelengths, and the smaller signal in relation to instrument noise). Below 300 nm this method cannot be used at all.

4.7. Special Methods for Measurement of Very Weak Light

4.7.1. Introduction

Only methods based on photomultipliers will be reviewed here, but photomultipliers can be used in different ways. We shall not touch upon imaging of very weak light, which is important in many contexts from astronomy to biology. Photomultipliers can be used in the following main ways.

4.7.2. Direct Current Mode

This is the "classical way" described in Section 4.3.1. The dc component of the anode current is measured. If the light is steady or varies only slowly, an amplifier with a long time constant can be used to obtain a "smoothed" or averaged value of the current; alternatively, this averaging can, of course, be achieved using a computer. Then the light is shut off and the dark current is measured in the same way. With the photomultiplier connected to suitable electronic circuitry the difference between "light" and "dark" currents is proportional to the light to be measured.

If the light is very weak this does not work well. This is because the difference between "light" and "dark" currents will be a small difference between two larger terms, and a small relative error in any of them will result in a larger relative error in the difference. Furthermore, for weak light a long time will be required to get a reliable value of the light current, and in the meantime the dark current might drift.

4.7.3. *Chopping of Light and Use of Lock-In Amplifier*

In this mode, for instance, a rotating shutter or mirror is used to cut the light into short pulses separated by darkness of similar duration. A special amplifier amplifies the current during the light and dark periods separately, and the difference is continuously computed, or electric charges from the two sets of periods are stored for integration of the difference over time. In this way the effect of drift with time of the dark current is minimized. In this way much weaker light can be measured than is possible in the direct current mode. It is, for example, easy to measure the light emitted from a plant leaf (as a reversal of the photosynthetic process; see Chapter 16) for tens of minutes after the leaf has been placed in "darkness." However, "ultraweak luminescence" (Chapter 23), Section 23.9) can hardly be measured with this method.

4.7.4. *Measurement of Shot Noise*

Shot noise is the "noise" of the dc signal from the photomultiplier arising from the quantized nature of light, i.e., the current pulses generated by the single photons. Yoh-Han Pao et al. (1966) suggested that the shot noise, treated as an ac signal, could be used as a measure of the light. Later experiments indicate that the signal-to-noise ratio for this method is somewhat better than for the lock-in method. However, because of the advantages of the method to be described below, this method has not been used much.

4.7.5. *Pulse Counting*

The dominating technique today for measuring very weak light is to count the current pulses generated in a photomultiplier by single photons. All pulses of the anode current, however, are not due to photons. Electrons are also released both from the photocathode and from the dynode surfaces by thermal energy. This is what gives the dark current in the dc mode. One great advantage of the pulse-counting method is that pulses due to thermal emission from the dynodes can be filtered off, because they are smaller than those coming from the photocathode, since they have gone through fewer amplification steps. To achieve this the pulses from the anode go to a pulse discriminator, which allows only pulses above a certain amplitude to pass. The pulses passing through are then shaped to a uniform amplitude and pulse shape, so they can be more accurately counted.

However, this cannot be done in a perfect way. Some photon-induced pulses are discarded, and some spurious pulses are passed. Some photons do not give rise to any pulses at all, because the quantum efficiency of the photocathode is lower than one (even in the spectral region where it is highest). And there is no way by which thermal pulses arising in the photocathode can be distinguished from light-induced pulses. Therefore a photomultiplier can never be used as an absolute photon-counting device. To estimate the true number of photons arriving at the photocathode the photomultiplier has to be calibrated, and a correction has to be made for "dark pulses."

Just as in a Geiger counter there is a certain minimum time necessary for two pulses to be counted separately. Since the pulses are Poisson distributed in time, the counting efficiency starts to decline gradually when the photon absorption rate increases over a certain limit. The absolute standard error of the number of pulses recorded, according to Poisson statistics, is proportional to the square root of the number of pulses counted and the relative error proportional to one over this square root. With absolute standard errors of e_l for the light count and e_d for the dark count, the standard error of the difference between light and dark counts is the square root of $(e_l{}^2 + e_d{}^2)$.

4.8. A Sensor for Catching Images: The Charge-Coupled Device

There are different kinds of electronic sensors for recording images, but only the most commonly used one will be described here: the charge-coupled device (CCD). Most readers have probably used a CCD already as part of a digital camera. But a CCD is useful everywhere when you wish to record light in one or two dimensions. In Chapter 25 we show how it can be used for recording spectra. The principle for a CCD is shown in Fig. 4.12.
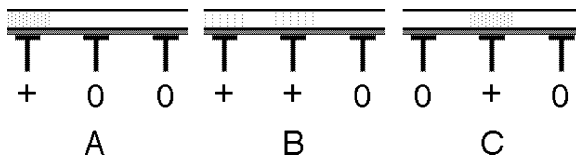
FIGURE 4.12. The principle for a charge-coupled device (CCD). A small part of the CCD is shown at three different times (A, B, and C). Electrodes are shown as **T**. In A, light has released electrons (shown as dots) in a doped silicon plate near the leftmost electrode. A wave of positive electrical potential (shown with the plus signs) is passed along the electrodes from left to right, and the electrons follow this positive wave through the silicon and can finally be collected sequentially from each location at a collection electrode at the right end (or edge, if it is a two-dimensional CCD).

References and Literature for Further Reading

Adick, H.-J., Schmidt, R. and Brauer, H.-D. (1989) A chemical actinometer for the wavelength range 610-670 nm. J. Photochem. Photobiol. 49A, 311–316.

Alfano, R.R. and Ockman, N. (1968) Methods for detecting weak light signals. J. Optical Soc. Am. 58, 90–95.

Allen, J.M., Allen, S.K. and Baertschi, W.W. (2000) 2-Nitrobensaldehyde: a convenient UV-A and UV-B chemical actinometer for drug photostability testing. J. Pharmaceut. Biomed. Anal. 24, 167–178.

Bérces, A., Fekete, A., Gáspár, P., Grof, P., Rettberg, P., Hornedk, G. and Rontó, G. (1999) Biological UV dosimeters in the assessment of biological hazards from environmental radiation. J. Photochem. Photobiol. B Biol. 53, 36–43.

Björn, L.O. (1971) Simple methods for the calibration of light measuring equipment. Physiol. Plant. 25, 300–307.

Björn, L.O. (1995) Estimation of fluence rate from irradiance measurements with a cosine corrected sensor. J. Photochem. Photobiol. B Biol. 29, 179–183.

Björn, L.O. and Vogelmann, T.C. (1996) Quantifying light and ultraviolet radiation in plant biology. Photochem. Photobiol. 64, 403–406.

Evans, W.G. (2005) Infrared radiation sensors of *Melanophila acuminata* (Coleoptera: Buprestidae): a thermopneumatic model. Ann. Entomol. Soc. Am. 98, 738–746.

Goldstein, S. and Rabani, J. (2007) The ferrioalate and iodide-idodate actinometers in the UV region. J. Photochem. Photobiol. A: Chemistry, doi: 10.10/6/jjphotochem.2007.06.006.

Hale, G.M. and Querry, M.R. (1973) Optical constants of water in the 200 nm to 200 μm wavelength region. Appl. Opt. 12, 555–563.

Hatchard, C.G. and Parker, C.A. (1956) A new sensitive actinometer. II. Potassium ferrioxalate as a standard chemical actinometer. Proc. Roy. Soc. A235, 518–536.

Jagger, J. (1967) *Introduction to research in ultraviolet photobiology*. Prentice-Hall, Englewood Cliffs, NJ.

Kuhn, H.J., Braslavsky, S.E. and Schmidt, R. (1989) Chemical actinometry. Pure Appl. Chem. 61, 187–210

Lee, J. and Seliger, H.H. (1964) Quantum yield of the ferrioxalate actinometer. J. Chem. Phys. 40, 519–523.

Marijnissen, J.P.A. and Star, W.M. (1987) Quantitative light dosimetry in vitro and in vivo. Lasers Med. Sci. 2, 235–242.

Mirón, A.S., Grima, E.M., Sevilla, J.M.F., Chisti, Y. and Camacho, F.G. (2000) Assessment of the photosynthetically active incident radiation on outdoor photobioreactors using oxalic acid/uranyl sulfate chemical actinometer. J. Appl. Phycol. 12, 385–394.

Namekata, N., Sasamori, S. and Inoue, S. (2006) 800 MHz Single-photon detection at 1550-nm using an InGaAs/InP avalanche photodiode operated with a sine wave gating. Optics Express 14, 10043–10049.

Optronics Laboratories (1995) *Improving integrating sphere design for near-perfect cosine response*. Application Note (A9). Downloadable from http://www.olinet.com

Optronic Laboratories (2001) *Standard spheres and sphere standards*. Application Note (A15). Downloadable from http://www.olinet.com

Rahn, R.O. (1997) Potassium iodide as a chemical actinometer for 254 nm radiation: Use of iodate as an electron scavenger. Photochem. Photobiol. 66, 450.

Rolfe, J. and Moore, S.E. (1970) The efficient use of photomultiplier tubes for recording spectra. Appl. Optics *9*, 63–71.

Ryer, A.D. (1997) *Light measurement handbook*. Newburyport: International Light, Inc., Technical Publications Dept. ISBN 0-9658356. Downloadable from http://www. intl-light.com/handbook/

Schmid, B. and Wehrli, C. (1995) Comparison of sun photometer calibration by use of the Langley technique and the standard lamp. Appl. Optics 34, 4500–4512.

Schmid, B., Spyak, P.R., Biggar, S.F., Wehrli, C., Sekler, J., Ingold, T., Mätzler, C. and Kämpfer, N. (1998) Evaluation of the applicability of solar and lamp radiometric calibrations of a precision sun photometer operating between 300 and 1025 nm. Appl. Optics 37, 3923–3941.

Schneider, W.E. and Young, R. *Spectroradiometry methods*. Application Note (A14), pp. 49. Orlando, FL: Optronics Laboratories. Downloadable from http://www. olinet.com

Seliger, H.H. and McElroy, W. (1965) *Light: Physical and biological action*. Academic Press, New York.

Skovsen, E., Snyder, J.W. and Ogilby, P.R. (2006) Two-photon singlet oxygen microscopy: The challenges working with single cells. Photochem. Photobiol. 82, 1187–1197.

Vogelmann, T.C. and Björn, L.O. (1984) Measurement of light gradients and spectral regime in plant tissue with a fiber optic probe. Physiol. Plant. 60, 361–368.

Wilson, S.R. and Forgan, B.W. (1995) *In situ* calibration technique for UV spectral measurements. Appl. Optics 34, 5475–5484.

Wegner, E.E. and Adamson, W.W. (1966) Photochemistry of complexions. III. Absolute quantum yields for the photolysis of some aqueous chromium (III) complexes. Chemical actinometry in the long wavelength visible region. J. Am. Chem. Soc. 88, 394–404.

5
Light as a Tool for Biologists: Recent Developments

Lars Olof Björn

Abstract: After a brief introduction this chapter covers optical tweezers and related techniques, uses of lasers for ablation, desorption, ionization, and dissection, fluorescent labeling, Abbe's diffraction limit to spatial resolution in microscopy, two-photon excitation fluorescence microscopy, stimulated emission depletion (STED), near-field microscopy, quantum dots and their uses in biology, photochemical internalization and caged compounds, photogating of membrane channels, and photo-crosslinking and photolabeling.

5.1. Introduction

Light has, of course, been exploited by scientists as far back as there has been any science. Until recently, almost everything we knew about the universe beyond the lower terrestrial atmosphere was information carried by light. Since Bunsen's time, optical spectroscopy has provided information about things as small as atoms and as large as galaxies. Spectrometry (absorption or fluorescence) or optical microscopy, or both, have been important for most biologists. The following account will therefore not attempt to be comprehensive but will focus on a few recent developments of interest for biologists. A good guide to much of the pre-2003 literature is provided by Methods in Enzymology, Vol. 360 and 361 (2003).

5.2. Optical Tweezers and Related Techniques

When we hear the word tool, we probably first see in our minds something we can hold in the hand, like a hammer, pliers, or tweezers. We use tweezers to handle things that are too small for our fingers to manipulate. But mechanical tweezers, and even traditional micromanipulators, are too large for particles smaller than single cells. Such objects can be handled with optical tweezers, invented by Ashkin (1970).

The description in Fig. 5.1 applies to light beams that are most intense in the center and with irradiance tapering off towards the periphery approximately as a Gauss function (as may be recalled from elementary statistical theory) does. But another type of beam has also been tried for optical forceps, a so-called Bessel beam. This beam has a complicated cross section. True Bessel beams cannot be produced, but an approximation can be made by focusing an ordinary beam from a laser (approximate Gauss beam), not with an ordinary lens, but with a conical lens. A Bessel beam has the advantage that the irradiance is kept high over a longer distance, not only in a focal spot. Therefore, it can be used to manipulate particles in directions perpendicular to the beam, while they can move freely along the beam.

In another method, instead of "clamping" particles in a spot (as with Gaussian beams) or along a Bessel beam, a kind of "optical washboard" or "corrugated surface" is produced, and this can be "shaken" so that particles move along the
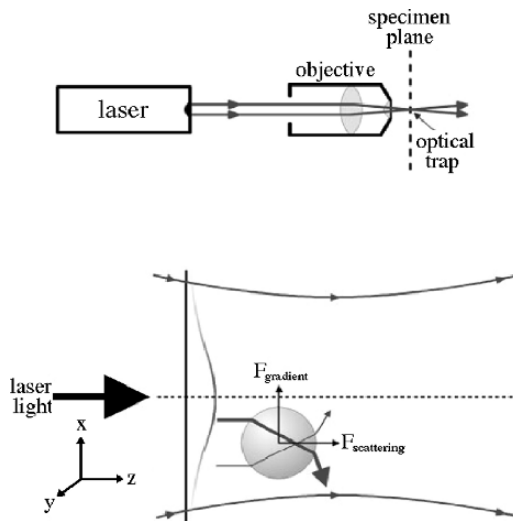
FIGURE 5.1. A simple form of optical tweezers. A particle is trapped in the focus of a laser beam. The picture shows how a strong ray of light is bent downwards by a transparent (or at least semitransparant, as all sufficiently small biological objects are) sphere. This gives an upward force acting on the sphere. If the sphere from the beginning is a little off-center in the beam, the corresponding ray giving a downward force is weaker, and the resulting force will be towards the beam center. Bending of both rays will also produce a force on the sphere towards the right, since they both decrease the rightward momentum of the light and this must be compensated for by the sphere's momentum. Light absorption as well as back-reflection will give a force in the direction of the light, but for small objects this will be a small effect. Light refraction will be more important for the forces along the light beam. There is a gradient in light refraction, and if the particle starts to move past the focus, a restoring force is created (see Fig. 5.2). (Slightly modified from Stanford University's URL http://www.stanford.edu/group/blocklab/Optical%20Tweezers%20Introduction.htm)
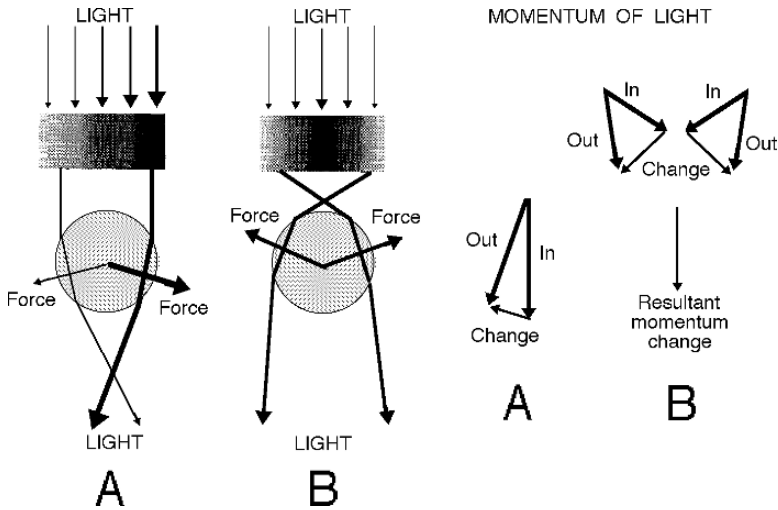
FIGURE 5.2. Diagrams showing the refraction of light in a transparent sphere (left), and the resulting change in momentum of the light (right). The forces on and movements of the sphere are such that they compensate for the change in momentum of the photons. Surprisingly, the amount of momentum transfer has even recently been a matter of much discussion among physicists (e.g., Loudon and Barnett 2006). The diagrams to the right show how the momentum change can be computed graphically by subtraction and addition of vectors.

surface, with different speeds depending on size (Paterson et al. 2005). For this a Bessel beam is used.

Using holograms, any light distribution can be created and used for manipulating objects (Grier and Roichman 2006), and light in combination with sheets of certain polymers can be used to transport materials over microscopic distances (Stiller et al. 2004). Dorman (2007) exemplifies the use of optical tweezers in biology.

5.3. Use of Lasers for Ablation, Desorption, Ionization, and Dissection

The reader has probably already heard or read about the "light scalpel" that doctors use for some kinds of surgery. Laser beams can be used for killing cancer cells, for fixing retinae that have come loose, and for several other medical purposes.

Lasers also have many uses related to this in nonmedical biology. One of the most important applications is to make large molecules, such as protein molecules, available for mass spectrometry, for determination of molecular mass and content of, e.g., phosphate groups (Krüger et al. 2006, Marshall et al. 2002).

The methods of evaporating the samples are referred to as laser ablation (any removal of material from a solid or liquid surface) and laser desorption (Peterson 2007). In addition, molecules and molecular fragments can be ionized by the laser beam, and the resulting electric charge is, of course, an important factor in mass spectrometry. A new method combining the use of laser and electro-spray ionization (ESI) is electrospray-assisted laser desorption ionization (ELDI) (Huang et al. 2006).

Laser beams can also be used for microdissection of biological specimens (Nelson et al. 2006). There are two main methods for this: "laser capture microdissection" (LCM) and "laser cutting." Several commercial instruments are marketed for each of these. In the former method a film of ethyl–vinyl–acetate is locally heated by an infrared laser beam, melted, and glued to the structure one wishes to pull away from the rest of the sample. In laser cutting, an ultraviolet laser beam (a 337-nm nitrogen laser is suitable) is used to cut out the desired structure.

5.4. Fluorescent Labeling

In classical light microscopy biological structures in most cases had to be stained with various pigments to become clearly visible. Gradually methods became more sophisticated, so that it became possible to determine the chemical makeup of various cell structures by staining them with specific colored compounds ("cytochemistry"). A great leap forward was taken when pigments were combined with antibodies, which make very specific associations with cell structures, and particularly with proteins. In the microscopy methods to be described in the following sections, labeling with fluorescent pigments play an important role, and these pigments are commonly combined with antibodies to make the labeling of cell constituents specific.

Many fluorescent compounds have been used in this way. One particular compound has become particularly important—the so-called "green fluorescent protein" (GFP). It is produced by the jellyfish *Aequorea victoria* (see Chapter 23). It has a major excitation peak at 395 nm and a minor excitation peak at 475 nm. The emission peak is in the green region at 509 nm, which makes it very suitable for visual detection of fluorescence. Another somewhat similar protein is produced by the sea pansy *Renilla reniformis*.

The advantage with a protein is that it can be used as a reporter for gene expression. For this purpose the gene for GFP is fused with a regulator gene to be studied and inserted into the genome of the organism under study. The first publication (Chalfie et al. 1994) introducing this technique has, at the time of this writing, been cited 2532 times. Tsien (1998) has written an early review of the subject, which is also well cited.

Fluorescent proteins with other emission spectra can be obtained in different ways: (1) by extracting and cloning proteins from other organisms, such as the red-emitting pigment from the railroad worm (Viviani 1999) or various proteins

from corals (Verkhusha and Lukyanov 2004); (2) by changing amino acids in the protein by genetic engineering, or chemically modifying the chromophore (Heim 1994, Shkrob et al. 2005); (3) by photoactivation or phototransformation, i.e., by various photochemical reactions of the protein (see below), and (4) by combining two proteins with different fluorescence properties so that energy absorbed by one can be transferred to the other one. By labeling a sample simultaneously with proteins having different fluorescence properties, regulation of different genes can be studied in the same sample (e.g., Jiang et al. 2006).

Proteins can also be made to change their fluorescence spectra by light treatment (e.g., Ando 2002, Elowitz et al. 1997, Habuchi et al. 2005, Lukyanov et al. 2005). The exact mechanism for this color change varies from case to case. It can be due to a conformational change of the protein or to photochemical change of an amino acid in the protein.

The fluorescence quantum yield of GFP is so high that single molecules can be registered (e.g., Cotlet et al. 2006, Peterman et al. 1999).

A recent comprehensive review (Fricker, Runions, and Moore 2006) describes a number of special methods in quantitative fluorescence microscopy which we shall not recount here. They include quantitative imaging of gene expression, in vivo imaging of mRNA localization and dynamics, methods for protein localization, level and turnover, and protein–protein interactions. One method for judging the proximity of two protein molecules is to study the resonance energy transfer between chromophores attached to them (see Chapter 1). Still another novel microscopy method using fluorescence is "fluorescent speckle microscopy" (Danuser and Waterman-Storer 2006) for the study of macromolecule dynamics (such as cytoskeleton assembly/disassembly) in living cells.

5.5. Abbe's Diffraction Limit to Spatial Resolution in Microscopy

We have seen in Chapter 1 that light is diffracted when passing through an opening. This diffraction limits the resolution of conventional light microscopy. A bright point will not be imaged as a point, but as a diffraction pattern, somewhat similar to what we have encountered in the section on diffraction in slits, but with a circular shape, a so-called Airy disk (Fig. 5.3).

More than 130 years ago Ernst Abbe showed that that the smallest distance between two points (Fig. 5.4) that can be resolved by a conventional light microscope is $s = 1.22 \cdot \lambda / (2 \cdot n \cdot \sin \alpha)$, where λ is the wavelength of the light used, n the refractive index of the medium between the objective lens and the object, and α the half-angle of the objective lens subtended at the object plane. The so-called numerical aperture, $n \cdot \sin \alpha$, is often stated on the objective of a microscope, so it is easy to estimate s. With immersion oil as the medium between the objective and the object and a high-quality immersion objective, the numerical aperture can be made as high as 1.4.
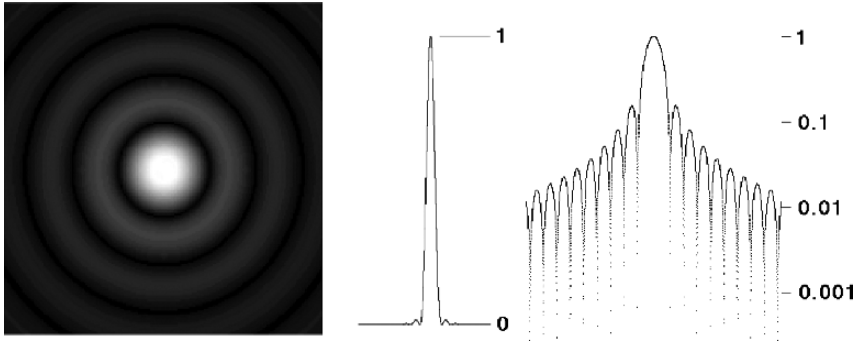
FIGURE 5.3. The Airy disk: the real appearance and graphs of the radiance distribution on logarithmic and linear scales.

With light for which the human eye has a high sensitivity and resolution, 500 nm, we get s = 1.22·500/(2·1.4) nm = 218 nm = 0.218 μm. The brightness distribution for this case, which is considered to be the limit for resolution of two points, is shown in Fig. 5.4.

Using a longer wavelength, while diminishing the resolution, has the advantage of better penetration and less scattering in most biological specimens.

The resolution can be further improved by using ultraviolet radiation instead of visible light (since the Airy disk will be smaller with a lower wavelength), and still further by using electrons instead of photons (electron microscopes use wavelengths in the nanometer range, but the numerical aperture is less favorable).

An improvement in factual resolution for biological specimens was achieved with the invention of the confocal microscope, but this is merely a way
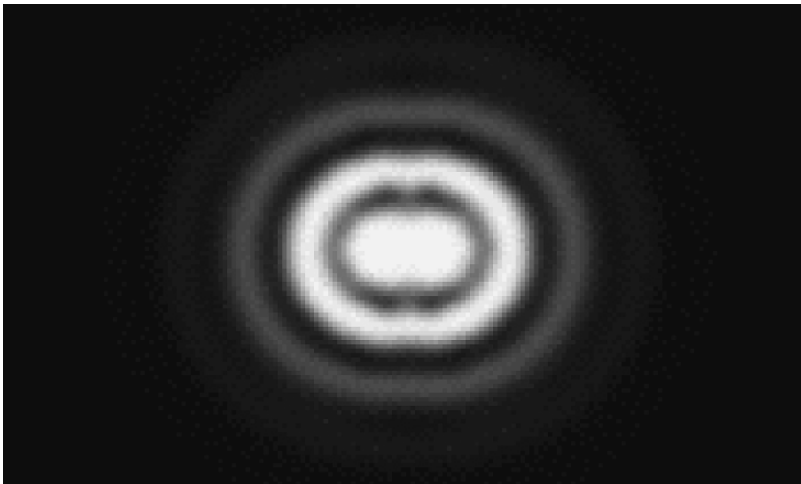
FIGURE 5.4. Image of two bright spots at the minimum resolvable distance.

of improving focusing and reducing disturbing scattered light. The ultimate resolution is still set by Abbe's criterion.

More recently, however, Abbe's diffraction limit has been broken through, in more than one way, and resolutions of only a few tens of nanometers achieved using visible light (see below).

5.6. Two-Photon Excitation Fluorescence Microscopy

In this technique the biological specimen is stained with antibodies to which a fluorescent pigment has been attached. The antibodies attach to the structures that one wishes to study, such as a specific protein. The method utilizes the fact that fluorescence can be induced not only by light of a wavelength corresponding to an absorption band of the fluorescent pigment, but also by light of twice that wavelength (photons with half the energy of the energy gap in the Jablonski diagram), provided the concentration of photons is high enough that two of them will be absorbed by the same molecule within a short enough time. If the equipment is suitably adjusted, this happens only in the center of the laser beam with which fluorescence is excited. The specimen must be examined point by point by a scanning laser beam. In two-photon microscopy, in order to use the same absorption band of the fluorescent pigment as in one-photon
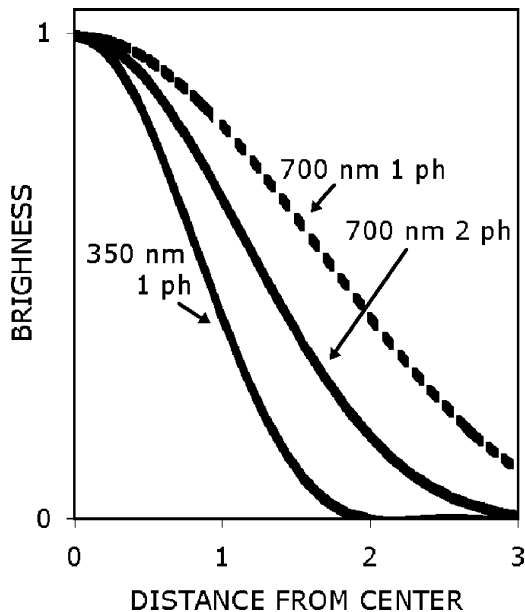
FIGURE 5.5. Brightness of a small fluorescing spot as imaged with one-photon fluorescence (350 and 700 nm) and two-photon fluorescence (700 nm).

microscopy, the wavelength must be doubled. Doubling of the wavelength alone would worsen the resolution by a factor of two. Since for two-photon excitation, the fluorescence brightness is proportional to the square rather than the first power of the fluence rate of the exciting light, this disadvantage is only partly compensated for, as shown in Fig. 5.5.

An important advantage with two-photon excitation is that less bleaching occurs than with one-photon excitation.

5.7. Stimulated Emission Depletion

Another method, stimulated emission depletion microscopy (STED microscopy or STEM), also uses fluorescent labeling of the specimen in the same way, but a different method for exciting the fluorescence. In this method, too, the specimen is scanned spot by spot by a laser beam, which excites fluorescence (Fig. 5.6). Diffraction of the beam causes the illuminated spot to have a minimum diameter of about 200 nm if blue light of 470-nm wavelength is used. Immediately after the pulse of blue light, and before any appreciable amount of fluorescence light has had time to be emitted, a second pulse, now of a higher wavelength, hits the sample. The time between the pulses is long enough for the excited pigment to decay to the lowest vibrational level of the first excited singlet state. The wavelength of the second pulse is such that it causes the pigment to return to the ground level via stimulated emission (the same phenomenon that takes place in
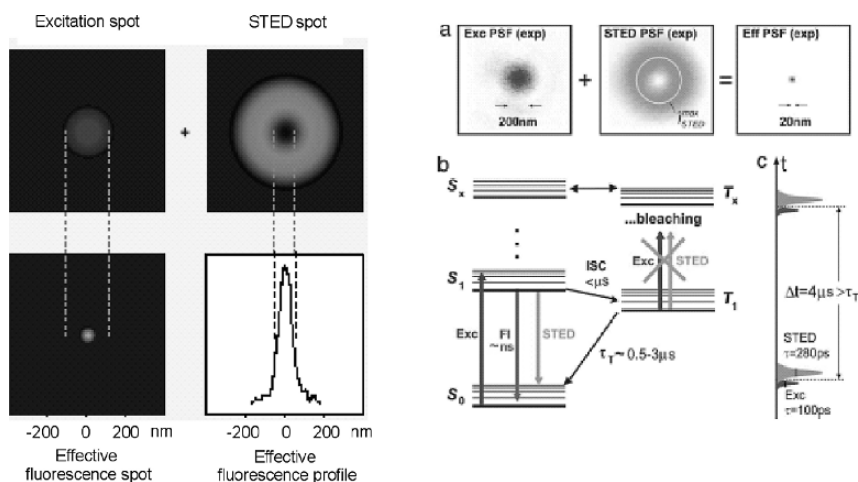
FIGURE 5.6. The principle for STED. (Left picture reprinted by permission from Macmillan Publishers Ltd: Nature 440, 879–880 (Simpson, G. J.), Copyright 2006. Right picture reprinted, with permission, from Donnert, G. et al. (2006) Macromolecular-scale resolution in biological fluorescence microscopy. Proc. Natl Acad. Sci. USA 103, 11440–11445.)

a laser). The second pulse has a ring-shaped cross section, i.e., the intensity in the center is almost zero. Thus the depletion of the excited state will take place around the circumference of the excited spot, and fluorescence will be emitted only from the most central part.

A problem with this method is that, since very strong light has to be used, and thus a high concentration of excited state, a triplet state is easily formed, resulting in chemical reactions that destroy the pigment (bleaching). This problem can be circumvented by suitable choice of pigment and irradiation protocol.

5.8. Near-Field Microscopy

A completely different approach for breaking the diffraction limit in microscopy was suggested long ago (Synge 1928), but was first implemented in a practically useful way by Betzig and Chichester (1992). The principle is to either collect or deliver the viewing light so close to the specimen that the light has had no space to spread by diffraction (Figs 5.7 and 5.8).

Betzig and Chichester (1992) introduced the use of a very thin light-conducting fiber for this purpose. The light aperture at the end of the fiber is much less than the wavelength of light, about 25–100 nm in diameter, and the distance between the fiber tip and the sample often even less, 5–50 nm. Also, in this method the specimen has to be probed point by point, and an image is obtained by scanning (Fig. 5.9). The method is sometimes referred to as near-field scanning optical
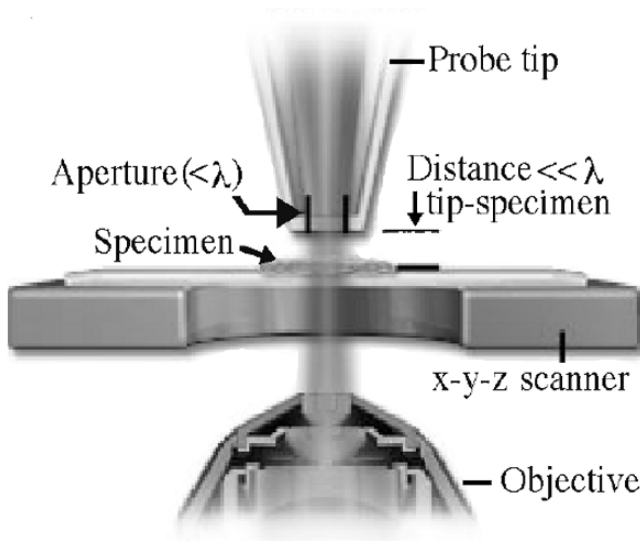
FIGURE 5.7. Near-field microscopy. (Slightly modified from http://www. olympus-micro.com/primer/tecniques/nearfieldintro.html. Courtesy Dr Michael W. Davidson.)
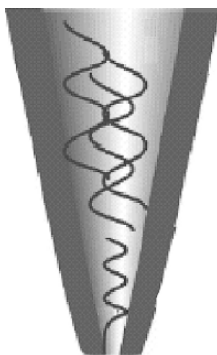
FIGURE 5.8. Tapered and aluminum-coated glass fiber for near-field microscopy, schematic. Light waves are squeezed together until there is no room for them to propagate further. But a so-called evanescent electromagnetic field still protrudes a short distance beyond the tip of the fiber, and if a scattering medium is brought into this region, the light energy can propagate into the "far field" and be registered with a photomultiplier. The same device can work in the opposite direction, and sample photons from the evanescent field of the sample if this is illuminated. (Modified from http:// www.azonano. com/details. asp?ArticleID = 1205.)
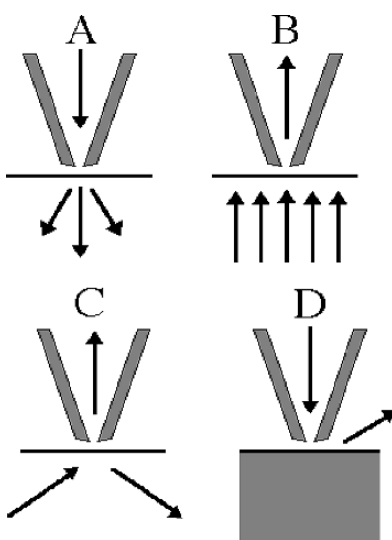
FIGURE 5.9. Four methods for scanning near-field microscopy. (A, B) Light is either delivered (A) from the tapered fiber or collected (B) by it. (C) How "frustrated" total reflection is used. All light coming from below undergoes total reflection except where the evanescent field from structures in the sample come sufficiently close to the fiber. (D) Light delivered from the fiber is scattered from structures in the sample only if they come within reach of the evanescent field, and then the scattered light can be picked up by a photomultiplier or photodiode.

microscopy (NSOM). Because the probe is so close to the sample, with a few modifications the setup can also be used for atomic (shear) force microscopy.

5.9. Quantum Dots

"Quantum dots" is a rapidly expanding field. A search for this term on the Web of Science by the end of 2006 gave 24,720 hits, the first two from 1986. Although the term quantum dot had not yet been coined, a few earlier publications, such as Brus (1984) and Rosetti, Nakahara, and Brus (1982), do in fact deal with them. During the past decade, each year an average of 274 more papers on the subject have been published than in the preceding year. The main application in biology is for fluorescent labeling of cell constituents. Overviews of biological applications are provided by Michalet et al. (2005), Du et al. (2006), Klostranec and Chan (2006), and Xu et al. (2006). Before going further into biological applications, it is necessary to begin with a general introduction to quantum dots.

A quantum dot is a semiconductor (or sometimes a metal) nanostructure that confines mobile charges, negative electrons, and/or positive holes, in all directions. In this respect the concept resembles the somewhat older ones, quantum well and quantum wire. However, a quantum well confines the charges in just one dimension and allows them to move freely in the other two, while a quantum wire allows the charges to move freely in one direction. The restriction can have various causes, such as electric potential gradients or interfaces between different materials. Quantum dots usually consist of 100–100,000 atoms. The smallest ones are slightly less than 2 nm across, and the largest ones of interest to biologists about 15 nm. Some of them share many properties with atoms, such as having discrete energy levels. Because the charges are spatially confined, quantum dots have optical properties which differ from the properties of larger objects of the same materials. The same principles apply here as for the double bond systems with π electrons described in the chapter on spectral tuning in biology. Thus smaller size corresponds to a smaller optical wavelength, and just by choosing size a quantum dot can be tuned, so it absorbs or emits light of a certain wavelength, without adjustment of chemical composition.

Although many scientists regard quantum dots to be semiconductors by definition, structures that behave in much the same way may also be constructed of some metals (Zheng, Nicovich, and Dickson 2007), and therefore it may also be acceptable to speak about metal quantum dots.

The most popular quantum dot material so far for basic and applied work has been cadmium selenide, CdSe. In biological contexts the main disadvantage of this material is its toxicity due to release of cadmium ions, but with appropriate coating (cladding) this disadvantage can be decreased (Bakalova et al. 2005, Derfus, Chan, and Bhatia 2004, Hardman 2006). There are also other reasons to provide the quantum dot core with a cladding. It increases the quantum yield for emission, and may modify the wavelength. Quantum dots with CdSe cores are usually coated with ZnS and outside this a shell of something else.

The outermost layer can be configured with ligands to biological structures, for instance, polynucleotides or antibodies.

The photon energy ($E = h\nu$) and thus the wavelength ($\lambda = c/\nu$) of the light emitted from a quantum dot depends mainly on two quantities, the energy gap E_{bulk} in the bulk material of which the (core of) the quantum dot is made and the extra energy arising from confinement of the mobile charge, E_{conf}: $hc/\lambda = E = E_{bulk} + E_{conf}$.

A somewhat simplified derivation from the time-independent Schrödinger equation of a formula for the emission wavelength of a spherical quantum dot with mobile electrons and holes, as for instance one made of CdSe, leads to $E_{conf} = h^2/(6.513 \bullet 8m_e R^2)$, where m_e is the electron mass and R the radius of the quantum dot. The value of E_{bulk} varies, of course, with the material, and for CdSe it is $3.85 \cdot 10^{-19}$ J. Using this relationship we can produce the solid curve in Fig. 5.10.

As seen in Fig. 5.10, with increasing quantum dot size the emission wavelength approaches a limiting value. Emission wavelengths up to 700 nm can be obtained with CdSe as core material (Wang and Seo 2006), and other types of quantum dots can be produced that emit above 1000 nm (see Michalet et al. 2005 for examples). Because, in practice, all quantum dots in a preparation do not have exactly the same dimensions, the emission is spread out over a spectral band of finite width. However, quantum dots have emission bands more narrow than most fluorescent molecules. The absorption spectrum is, on the other hand, quite
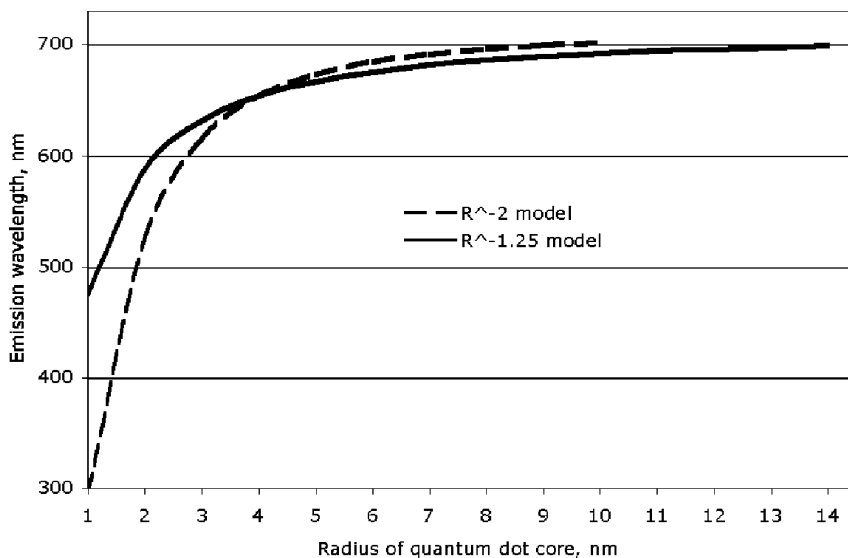
FIGURE 5.10. Emission wavelength versus quantum dot radius for spherical CdSe quantum dots without cladding, computed as described in the text. The solid line is for the empirical model with exponent –1.25, the dashed line for the theoretical model with exponent –2. An E_{bulk} value of $2.78781 \cdot 10^{-19}$ J is used here.

wide (Fig 5.11), so different types of quantum dots can be excited with the same kind of light, which is an advantage when one wishes to image quantum dots emitting different colors at the same time in the same sample.

The power dependence with the quantum dot radius raised to –2 based on the simplified theory is not universal, and Brus (1984) and more recently Wang and Seo (2006) and Cademartiri et al. (2006) derived more accurate relationships. One of these (more relevant for CdSe quantum dots) is shown in Fig. 5.10 (dashed curve).

The main advantages of using quantum dots rather than molecular fluorescent labels are (1) greater stability against bleaching, (2) higher fluorescence quantum yield, and therefore stronger fluorescence, (3) more narrow emission bands, and (4) the possibility of continuously tuning of the emission wavelength and choosing any desired value. The two first properties make it possible to follow single labeled macromolecules as they move around in a cell, are taken up, or are excreted. The second two properties make it possible to label several different kinds of molecule in different colors in the same preparation.
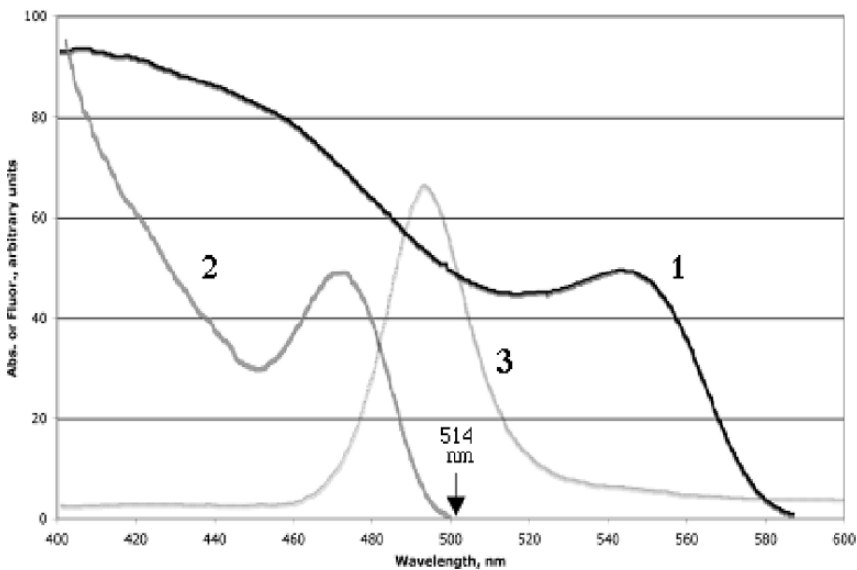
FIGURE 5.11. Phototuning of CdSe quantum dots with SiO_2 shells. (1) Absorption spectrum of the original quantum dots. The vertical axis does not show absorbance in this diagram, but absorbtion coefficient divided by scattering coefficient, but this does not make much difference in shape of the spectrum.These original quantum dots have an absorption maximum at 553 nm and an emission maximum at about 572 nm. After photoetching for 20 h with 514 nm light the absorption spectrum changes to curve 2 and the emission spectrum to curve 3. Quantum dots with other emission maxima can be obtained by photoetching with light of other wavelengths. In every case the absorption spectrum changes so that absorption becomes practically zero at the etching wavelength. (Redrawn and simplified, after Torimoto et al. 2006.)

The fluorescence yield of small CdSe quantum dots can be increased to > 0.5 by careful control of temperature, Cd/Se ratio, and other factors during production (Donega et al. 2003), and following treatment with ultraviolet radiation (Bakalova et al. 2005). McBride et al. (2006) show that structural relations between the CdSe core and the ZnS shell are important. The quantum yields decrease with increasing quantum dot size (increasing wavelength), which is attributed to decreasing overlap between the wave functions for electrons and holes. Larger quantum dots, on the other hand, absorb more excitation light. Quantum dot size and thus emission wavelength can be varied by varying the duration of crystal growth time at high temperature, and also by adjusting the temperature (190–270 °C) for crystal growth (Wang and Seo 2006). A particularly elegant method to tune cadmium selenide quantum dots with SiO_2 shells has been devised by Torimoto et al. (2006), who use monochromatic light of selected wavelengths to etch the quantum dots (by photochemical oxidation of the selenium) until they stop absorbing the etching light. The peak emission will then be at about 20 nm lower wavelength than the etching light. This procedure should also help to decrease the size variation between the particles and thus result in a narrower emission spectrum. The SiO_2 shell serves to prevent the particles from coalescing.

Because of the extremely low detection limits of quantum dot fluorescence labels, they can be employed for various forensic purposes, such as detection of anthrax spores (Park et al. 2006), specific DNA traces (Raymond et al. 2005), or fingerprints (Bouldin et al. 2000, Menzel et al. 2000). Specificity and suppression of background fluorescence interference can be improved by monitoring the fluorescence lifetime (Bouldin et al. 2000).

Among applications on the medical side, early cancer detection (Nida et al. 2005, Chu et al. 2006, Hu et al. 2006, Li et al. 2006) deserves special mention.

One of the most interesting properties discovered during the study of single quantum dots is that even if they are steadily illuminated they usually do not fluoresce continuously, but intermittently. In other words they "turn on and off," a phenomenon known as blinking. Although of great theoretical interest, we shall not expand on the reasons for blinking here. In some cases blinking may be a disadvantage, for instance, if quantum dots are used for tracking molecules which move rapidly in unpredictable ways, but in most cases it is not a problem because of the high speed of on and off switching. In other cases blinking can be taken advantage of. For instance, blinking makes it possible to determine whether light comes from a single or two quantum dots (by determining whether the blinks have just one light level or two) and to determine the distance between two quantum dots, even if they are too close to be resolved in the microscope (Lagerholm et al. 2006). Blinking can be suppressed by covering the quantum dots in a special way (Hammer et al. 2006).

For some applications it may be of advantage to make the quantum dots emit light without being themselves illuminated, and this is possible to achieve by supplying energy in some other way (So et al. 2006). If the quantum dots are tuned to emit very long-wavelength radiation, they may be visible (by

instruments) even if buried deep in the body, something that may be of great value for tracing cancers.

Because of the possibility of seeing individual quantum dots, many different molecules have been individually tagged with them, for instance, DNA (Crut et al. 2005) and RNA (Chan, Yuen, Ruf et al. 2005) molecules and ion channels (O'Connell et al. 2006, Nechyporuk-Zloy et al. 2006). Since quantum dots can be counted, they have also been used for counting molecules. For such a count to be reliable, however, one has to be able to ascertain that all molecules become labeled, and O'Connell et al. (2006) have worked out a procedure to check if this is the case, using two labels with different colors, and seeing how many two-color labeled points there are in relation to those labeled with one color only. In their particular case they determined that a membrane channel protein could be labeled with a maximum of two quantum dots.

By conjugating quantum dots to signal peptides (used by cells to target proteins to correct organelles), the quantum dots can be directed to specific organelles (Hoshino et al. 2004). Many other examples of adaptations of quantum dot surfaces for different cellular targets are described by Medintz et al. (2005). Mutations in DNA can be detected with a method employing quantum dots (Yeh et al. 2006).

Many different types of quantum dots are now commercially available. Some of them are so easy to make that several student experiments for this have been worked out, both for CdS and for CdSe quantum dots (Fig 5.12) (Kippeny, Swafford, and Rosenthal 2002, Boatman, Lisensy, and Nordell 2005,
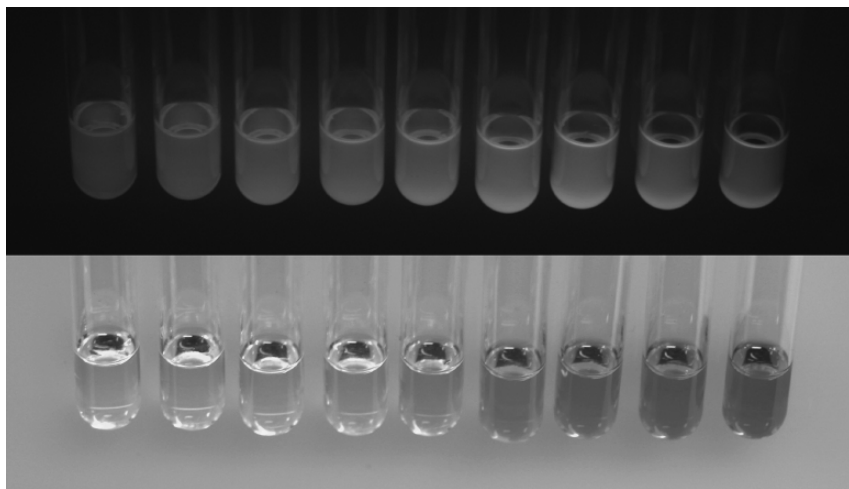
FIGURE 5.12. CdSe quantum dots prepared in a student experiment. The top picture shows fluorescent colors with UV-A excitation, the bottom one the absorptive colors under white light. CdSe quantum dots can be prepared emitting fluorescence at longer wavelength, up to 700 nm. (From Boatman et al. 2005 with permission from J. Chem. Educ. Vol. 82, No. 11, pp. 1697–1699; copyright ©2005, Division of Chemical Education, Inc.) (*See* Color Plate).

Winkler et al. 2005). Traditionally CdSe quantum dots have been manufactured at high temperature using poisonous organic solvents, but Deng, Yu, and Pan (2006) show that it is also possible to work below 100°C and use water as solvent. In addition to production by these "wet" methods, there exists a "dry" method for manufacture of another kind of quantum dots for the electronics industry.

5.10. Photochemical Internalization

Photochemical internalization is a technique for delivering macromolecules or other particles to the cytoplasm of cells. Molecules that would otherwise be excluded from the cell can be made to pass through the cell by being combined with a suitable molecule or atom group that causes it to be taken up into a vesicle by endocytosis. A problem with this is that the material taken up in a cell remains in membrane vesicles and may eventually end up in lysosomes and be broken down there. The enclosing membrane can, however, be punctured by photochemical production of singlet oxygen (Berg et al. 1999). Singlet oxygen is very short-lived in vivo (Moan and Berg 1991) and therefore does not diffuse more than a few nanometers (20 nm at most) before being destroyed. Therefore, the photodynamic attack on the vesicle membrane is most efficient if the sensitizing pigment is incorporated into the vesicle membrane. Some photosensitizers have, in fact, been found which after uptake in cells become specifically localized to lysosome membranes (Fig. 5.13). The photosensitizer may be administered together with the substance to be taken up. Alternatively, as shown in Fig. 5.14, the cell may be preloaded with the sensitizer and lysosomes punctured with light.
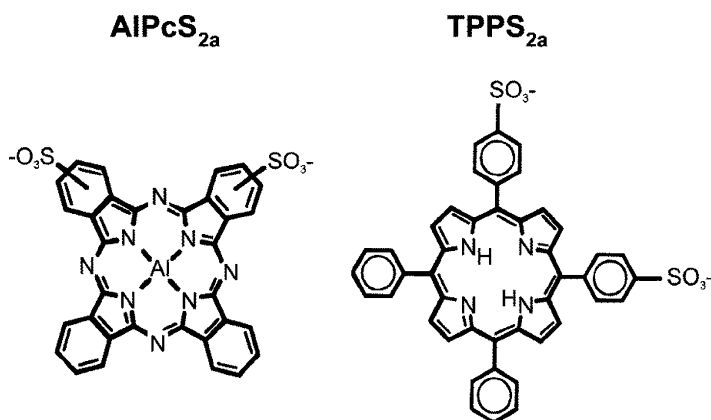
FIGURE 5.13. Two photosensitizers that become specifically localized to endocytic vesicle membranes after being taken up into cells. TPPS2a is *meso*-tetraphenylporphine with two sulfonate groups on adjacent phenyl rings and AlPcS2a is aluminum phthalocyanine with two sulfonate groups on adjacent rings. (From Høgset et al. 2004.)
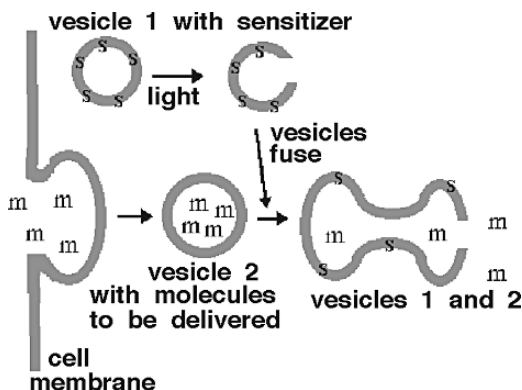
FIGURE 5.14. Photochemical internalization using preloaded sensitizer. The cell is first treated with sensitizer (s) and the vesicles containing sensitizer punctured with light. When then the molecules (m) to be delivered to the cytosol are taken up by endocytosis, the endocytosis vesicles fuse with the already punctured vesicles, and the molecules are released to the cytosol. (Redrawn and modified from Høgset et al. 2004.)

When afterwards the substance is taken up by endocytosis, the endocytic vesicles fuse with the punctured lysosomes and the substance is released to the cytosol.

An alternative to generation of singlet oxygen for puncturing liposomes is to use photocleavable lipids for constructing vesicle membranes (Chandra, Subramaniam, Mallik, and Srivastava 2006).

Many different kinds of molecule and molecular aggregates can be delivered to cells with liposomes in this way, and there are several variants of the method. One is to combine the molecule to be delivered in a liposome with a cationic peptide or cationic polyethyleneimine–amino acid combination. In this way a faulty (mutated) gene can be replaced with a correct one and find its proper place in the nucleus (Ndoye et al. 2006).

An advantage of photochemical internalization is that it can be very specifically applied to individual cells or groups of cells, for instance, cancers, while a drug remains membrane-enclosed and inactive in surrounding cells. Such specificity is achieved both by directing the membrane-puncturing light and by choosing sensitizers which are targeted to, for instance, cancer cells.

The other method for getting molecules where you want to have them in the cell is to attach them to a suitable carrier molecule. We have already mentioned the cell membrane–penetrating cationic peptides , but other ligands can be used for specific purposes. This so-called caged compound can then be set free by breaking the bond to the carrier molecule with light. An example is the delivery of oligonucleotide to the cell nucleus described by Ghosn, Haselton, Gee, and Monroe (2005). They attached the olignucleotide to 1-(4,5-dimethoxy-2-nitrophenyl) ethyl ester (DMNPE). The DMNPE alters the charge and makes the molecule more lipophilic, so it can pass the membranes into the nucleus. As long as the oligonucleotide is attached to DMNPE, repliction
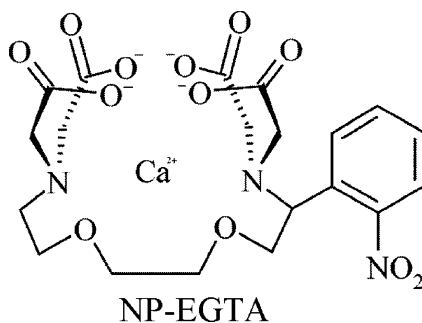
FIGURE 5.15. Nitrophenyl ethyleneglycol-bis(2-aminoethyl) *N,N,N´,N´*-tetraacetic acid, an example of a substance that can be used to deliver caged calcium ions.

is blocked, but after breaking the attachment by irradiation with 365 nm UV-A radiation, the oligonucleotide becomes integrated into the genome. The authors used an optical technique (a so-called molecular beacon) to check whether hybridization took place or not. Alternatives to DMNPE have been investigated by Kim and Diamond (2006). Marriott, Roy, and Jacobson (2003) describe how proteins can be caged by use of bromomethyl-3,4-dimethoxy-2-nitrobenzene (BMDNB) attached to cysteine residues in the protein. An alternative approach for caging proteins is the introduction of unnatural amino acids through mutagenesis (Petersson et al. 2003).

Calcium ion is an important cellular messenger. The Ca^{2+} concentration in the cytosol is usually near 0.1 mmol. When it is caused to rise, a number of processes, dependent on the type of cell, are initiated. The Ca^{2+} is released from organelles, the endoplasmic reticulum, or, in plants, the cell wall. To study these signaling pathways, it is desirable to be able to initiate experimentally a rise in cytosolic calcium concentration without having to activate the initial part of the signaling pathway. This can be done by supplying the cell with caged calcium ions, i.e., calcium ions in a cage of a chelator, which can be photochemically decomposed. Bacchi et al. (2003) describe a number of chelators that can be used in this way, nitrophenyl ethyleneglycol-bis(2-aminoethyl) *N,N,N´,N´*-tetraacetic acid (NP-EGTA) being one example (Fig. 5.15).

5.11. Photogating of Membrane Channels

For a long time investigators of the nervous system have used electrodes to stimulate nerve cells and find out what kind of signals they conduct and what the result of their activity is. To this new methods have now been added: photostimulation or photoinhibition.

There are basically three ways of making it possible for light to affect nerves:

1. Photodelivery of caged neurotransmitters. An example of this was provided by Callaway and Katz (1993). They bathed brain slices in a solution containing L-glutamic acid a-(4,5-dimethoxy-2-nitrobenzyl)ester. This compound in itself

is inactive. When a brief (1 ms) pulse of ultraviolet radiation is delivered to the preparation, the neurotransmitter L-glutamic acid is released and a spike of invard current can be recorded. The procedure can be repeated at least 30 times. Photorelease of caged compounds is treated more generally in the previous section.

2. Use of rhodopsins. Natural photogating of membrane channels takes place in our eyes with the help of rhodopsin in the membranes of outer segments of rods and cones. Also, in some microorganisms similar events occur, mediated by chromoproteins similar to our rhodopsins. Both vertebrate rhodopsin and so-called channelrhodopsin from a green alga have been used for artificial gating of other channels than their natural ones (Boyden et al. 2005, Li et al. 2005, Zhang et al. 2006). Genetic engineering is used to express the proteins in the desired tissues and couple them to the signaling pathways for the desired membrane channels.

3. Use of artificial pigments to regulate the channel. These methods can, in turn, be divided into two categories. A molecule that changes conformation upon illumination can be attached directly to the channel protein so that a part of it either blocks the channel or not, depending on the shape of the pigment molecule, or the pigment can be incorporated into the lipid of the membrane and change its conformation. The first method was pioneered by Lester et al. (1980), who chemically modified the nicotinic acetyl choline receptor to make it light sensitive. Banghart et al. (2004) used the method to regulate a potassium channel. They used a compound consisting of maleimide–azo group–quaternary amine. The maleimide reacted chemically with a cysteine sulfhydryl group in the channel protein, the azo group undergoes *cis-trans* isomerization upon absorption of light, and the nitrogen in the amine carries a positive charge, which, in the correct position, can prevent potassium ions from passing the channel. The arrangement is shown in Fig. 5.16. The *cis-trans* isomerization of the compound is photoreversible, and the photoequilibrium spectra (of same shape as action spectra) are shown in Fig. 5.17.

Membrane channel proteins can be stimulated electrically and in many cases also chemically. So what are the advantages and disadvantages of photoregulation? A particular cell can be probed with either an electrode or a light beam, while you can only use light to choose a particular kind of (modified) channel. The disadvantage with light is that you must modify the channel to make it light sensitive. With chemical stimulation you can reach a particular channel type, but both spatial and temporal resolution is extremely bad, especially compared to what can be achieved with light. As shown in Fig. 5.18, the switching of a channel on and off with light can be done very rapidly—within milliseconds.

Many of the experiments with photoregulation of membrane channels have been performed on nerve cells, and the results can be quite dramatic. Schroll et al. (2006) show how the behavior of fly larvae, in which neural cation channels have been amended with channel rhodopsin, can be altered just by illuminating the animals with blue light. Depending on what particular channel type has been
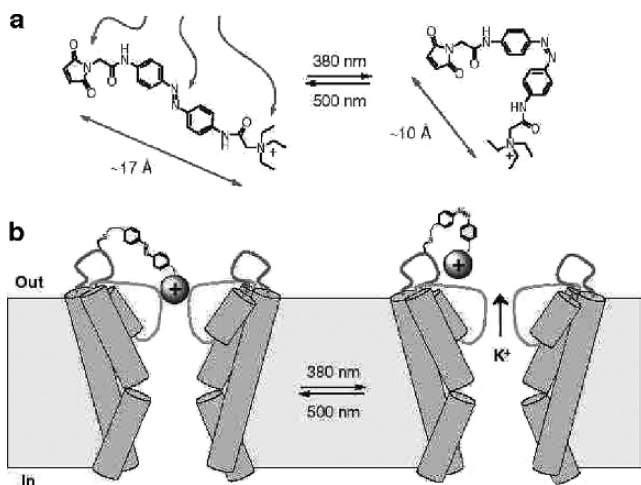
FIGURE 5.16. (a) The reversibly photochromic chromophore consisting of a maleimide group (MAL), an azo group (AZO), and a quaternary ammonium nitrogen (QA). The latter is, in turn, attached to the potassium channel protein. When the chromophore absorbs 380 nm radiation, the distance between its ends decreases by 0.7 nm (7 Å). (b) The potassium channel is reversibly blocked by the positive charge on the chromophore by 500 nm light, and opened again by 380 nm UV-A radiation. (Reprinted by permission from Macmillan Publishers Ltd: Nature Neurosci. 12, 1381-1386 (Banghart et al. 2004), Copyright 2004.)

modified, different behavioral changes result. Here we see another advantage of light stimulation over electrical stimulation: the animals can be completely unattached and free-moving, and all the channels of a particular type can be immediately activated at once.
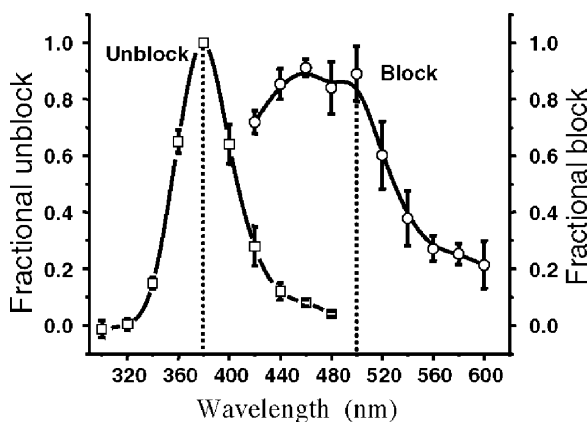
FIGURE 5.17. Steady-state spectra for open and closed states of the potassium channel in Fig. 5.16. Steady-state spectra are action spectra normalized so that the sum of the ordinates of the curves is unity for all wavelengths. (From Banghart et al. 2004.)
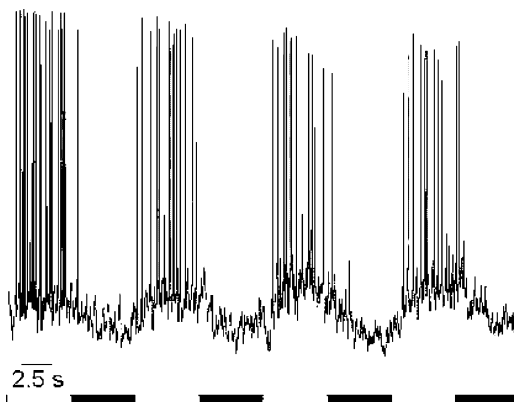
FIGURE 5.18. The action potentials in a nerve cell are rapidly switched on by 390-nm radiation (white bars) acting on a modified membrane channel and equally rapidly switched off by 505-nm light (black bars). (From Chambers et al. 2006.)

Folgering et al. (2004) show how a mechanosensitive channel can be regulated by light by incorporating a *cis-trans* photoreversible phospholipid-mimicking molecule into the lipid bilayer, so that the membrane can be photoreversibly distorted. So far this has only been done in vitro in patch-clamp experiments, but it does not appear impossible to use a similar procedure with living organisms. Koçer et al. (2005) also made a mechanosensitive channel light-switchable, but by a quite different method. By genetic engineering they replaced a glycine residue in the channel protein by a cysteine residue. The sulfhydryl group of this cysteine, which was the only one in the protein, could then be reacted with a photochromic compound, by which the channel could be reversibly blocked by irradiation with visible light ($\lambda > 460$ nm) and opened again by irradiation with UV radiation (366 nm).

Eisenman et al. (2007) have constructed a photoactivable neurosteroid by which $GABA_A$ receptor function can be light-regulated. It can be used for blocking neuron firing by 480-nm light.

5.12. Photocrosslinking and Photolabeling

It is of interest to know which molecules make contact with one another in the cells without forming strong and stable bonds. The three kinds of problem most often encountered are elucidation of protein–protein contacts, protein–DNA contacts, and hormone–receptor contacts. Photocrosslinking and photolabeling are methods that have been used for this purpose for four decades. The older literature is reviewed by Brunner (1993), and emphasis here will be placed on a specific recent developments.

For a couple of decades it has been possible to incorporate unnatural amino acids into proteins in a site-specific way in vitro (Bain et al. 1989). A great

leap was taken when Wang et al. (2001) designed a method for doing this in vivo. Soon thereafter (Chin et al. 2002) the method started to be used for incorporating photoreactive amino acids, which upon exposure to ultraviolet radiation form bonds to nearby protein molecules. In this way the in vivo contact points between proteins can be determined. It would carry too far to describe the details of the method here, but up-to-date accounts are given by Xie and Schultz (2005, 2006). In brief, the function of the "amber" codon (UAG) is modified and its natural function suppressed and, using molecular components from Archaea, a translation system is engineered, which uses this codon to insert the desired amino acid. Later the "opal" codon (UGA) was used for the same purpose. The first experiments dealt with insertion of the engineered systems into bacteria, but by now researchers have succeeded in doing the same also with eukaryotic (including mammalian) cells. The types of unnatural amino acids that have been inserted now number over 30, and among them are three photoreactive ones, *p*-azidophenylalanine, *p*-benzoylphenylalanine (pBpa) (Fig. 5.19), and *p*-(3-trifluoromethyl-3H-diazirin-3-yl)-phenylalanine. Among these derivatives pBpa is particularly useful, because it reacts to UV-A radiation (about 360-nm wavelength), which is not very destructive to cellular components and also gives greater penetration depth than the shorter-wavelength radiation necessary for the other photoreactive amino acids. A slight disadvantage to pBpa is that it has a preference for reacting with methionine. Therefore, it does not necessarily indicate the closest neighbor in an adjacent protein, but one up to 8 amino acid units away from it (Wittelsberger et al. 2006).

Results obtained by this method include elucidation of the contact between ATPase and a transport protein (Mori and Ito 2006), contacts between the
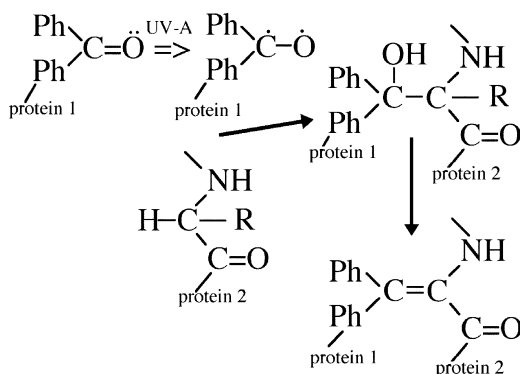
FIGURE 5.19. Photocrosslinking two proteins using a protein (protein 1 in the figure) in which *p*-benzoylphenylalanine (pBpa) has been inserted. Ph stands for the phenyl group. Under irradiation with UV-A the pBpa is converted to a diradical, which crosslinks to an amino acid in protein 2. If R in this amino acid is hydrogen, dehydratation takes place, resulting in the structure at lower right. A more detailed diagram, showing intermediates and alternative reactions, is provided by Dormán and Prestwich (1994).

components in dimeric enzymes (Blanck and Mehl 2006), and contacts between proteins in a signaling pathway (Hino et al. 2005).

When cells are irradiated with UV-C radiation crosslinks can develop between nucleic acids and adjacent proteins without any prior modification of either. These crosslinks, however, are not very informative since they do not necessarily reflect closest-neighbor relations. The use of UV-C also has drawbacks because of its destructive action and poor penetration in living matter. Therefore Geyer, Geyer, and Pingoud (2004) and others have developed more specific methods, which involve the addition of specific photoreactive groups that respond to UV-A radiation.

Also, some hormones can be photocrosslinked to their receptors without artificial photoreactants. Thus, the first photocrosslinking of a plant hormone, abscisic acid, was performed without prior modification (Hornberg and Weiler 1984). Also, steroid hormones containing unsaturated ketone groups can be photocrosslinked in the natural state (e.g., Gronemeyer and Pongs 1980, Schaltmann and Pongs 1982). If the hormone carries a label, such as a radioactive carbon atom, the hormone receptor is said to be *photoaffinity labeled*. But such experiments have later been complemented using hormones linked to artificial photocrosslinking groups (e.g., Todoroki et al. 2001), and for many other hormones artificial photocrosslinkers are required (e.g., Beale et al. 1992, Swamy, Addo, and Ray 2000). To determine how RNA molecules contact ribosomal proteins, Demeshkina et al. (2003) used mRNA analogs containing a perfluoroarylazido group. Arylazido derivatives are highly reactive and can therefore be expected to react with and indicate close neighbors (not only amino acids in proteins, but also bases in nucleic acids). The perfluoro group increases the lifetime of the excited singlet state and therefore also the reaction quantum yield.

5.13. Fluorescence-Aided DNA Sequencing

The Sanger method for DNA sequencing has enjoyed a remarkably long life in the rapidly developing field of molecular biology. However, the strong interest in DNA sequencing for phylogenetic research, forensic investigations, and other purposes has stimulated the search for cheaper and faster methods, and methods allowing sequencing of single molecules. In the past few years several methods using fluorescence techniques have been invented (Metzker 2005). Most of them are based either on the capillary electrophoresis introduced by Jorgenson and Lukacs (1981), or on immobilizing DNA molecules on a substrate (Seo et al. 2005, Krieg 2006), or on immobilizing an enzyme. Some of them can be used for sequencing single DNA molecules (Werner et al. 2003, Ramanathan et al. 2004, Bayley 2006). There are methods for labeling the bases in DNA with fluorophores with either absorption or emission spectra sufficiently different so that the bases can be distinguished by fluorescence (e.g., Lewis et al. 2005, Seo et al. 2005).

Another fluorescence method important in genomic research is fluorescence in situ hybridization (FISH) (see Jiang and Gill 2006 for a review on the application of the method to plants and references to other literature). In this method a sequence-specific probe that is made to fluoresce is attached directly to DNA while it is still in the chromosome.

References

Ando, R. (2002) An optical marker based on the UV-induced green-to-red photoconversion of a fluorescent protein. Proc. Natl. Acad. Sci. USA 99, 12651–12656.

Ashkin, A. (1970) Acceleration and trapping of particles by radiation pressure. Phys. Rev. Lett. 24, 156–159.

Bacchi, A., Carcelli, M., Pelizzi, C., Pelizzi, G., Pelagatti, P., Rogolino, D., Tegoni, M. and Viappiani, C. (2003) Synthesis and spectroscopic and structural characterization of two novel photoactivatable Ca2+ compounds. Inorg. Chem. 42, 5871–5879.

Bakalova, R., Zhelev, Z., Jose, R., Nagase, T., Ohba, H., Ishikawa, M. and Baba, Y. (2005) Role of free cadmium and selenium ions in the potential mechanism for the enhancement of photoluminescence of CdSe quantum dots under ultraviolet irradiation. J. Nanosci. Nanotechnol. 5, 887–894.

Bakalova, R. Zhelev, Z., Aoki, I., Ohba, H., Imai, Y. and Kanno, I. (2006) Silica-shelled single quantum dot micelles as imaging probes with dual or multimodality, Anal. Chem, 78, 5925–5932.

Bain, J.D., Glabe, C.G., Dix, T.A., Chamberlin, A.R. and Diala, E.S. (1989) Biosynthetic site-specific incorporation of a non-natural amino acid into a polypeptide. J. Am. Chem. Soc. 111, 8013–8014.

Banghart, M., Borges, K., Isacoff, E., Trauner, D. and Kramer, R.H. (2004) Light-activated ion channesl for remote control of neuronal firing. Nature Neurosci. 12, 1381–1386.

Bayley, H. (2006) Sequencing single molecules of DNA. Curr. Opinion Chem. Biol. 10, 628–637.

Beale, H., Hooley, R., Smith, S.J and Walker, R.P. (1992) Photoaffinity probes for gibberellin-binding proteins. Phytochemistry 31, 1459–1464.

Berg, K., Selbo, K., Prasmickaite, L., Tjelle, T.E., Sandvig, K., Moan, J., Gaudernack, G., Fodstad, Ø., Kjølsrud, S., Anholt, H., Rodal, G.H., Rodal, S.K. and Høgset, A. (1999) Photochemical internalization: A novel technology for delivery of macromolecules into cytosol. Cancer Res. 59, 1180–1183.

Betzig, E., and R. J. Chichester. (1992) Near-field optics: microscopy, spectroscopy, and surface modification beyond the diffraction limit. Science 257:189–195.

Blanck, S.M. and Mehl, R.A. (2006) Systematic study of protein interfaces with genetically incorporated photocrosslinking amino acid, p-benzoylphenylalanine. Abstr. Papers Am. Chem. Soc. 231.

Boatman, E.M., Lisensky, G.C. and Nordell, K.J. (2005) A safer, easier, faster synthesis for CdSe quantum dot nanocrystals. J. Chem. Educ. 82, 1697–1699.

Bouldin, K.K., Menzel, E.R., Takatsu, M. and Murdock, R.H. (2000) Diimide-enhanced fingerprint detection with photoluminescent CdS/dendrimer nanocomposites. J. Forensic Sci. 45, 1239–1242.

Boyden, E.S., Zhang, F., Bamberg, E. Nagel, G. and Deisseroth, K. (2005) Millisecond time-scale, genetically targeted optical control of neural activity. Nature Neurosci. 8, 1263–1268.

Brunner, J. (1993) New photolabeling and crosslinking methods. Annu. Rev. Biochem. 62, 483–514.

Brus, L.E. (1984) Electron-electron and electron-hole interactions in small semiconductor crystallites: The size dependence of the lowest excited electronic state. J. Chem. Phys. 80, 4403–4409.

Cademartiri, L., Montanari, E., Calestani, G., Migliori, A., Guagliardi, A. and Ozin, G.A. (2006) Size-dependent extinction coefficients of PbS quantum dots. J. Am. Chem.Soc. 128, 10337–10346.

Callaway, E.M. and Katz, L.C. (1993) Photostimulation using caged glutamate reveals functional circuitry in living brain cells. Proc. Natl. Acad. Sci. USA 90, 7661–7665.

Chalfie, M. (1994) Green fluorescent protein as a marker for gene-expression. Science 263, 802–805.

Chambers, J.J., Banghart, M.R., Trauner, D. and Kramer, R.H. (2006) Light-induced depolarization of neurons using a modified shaker K^+ channel and a molecular photoswitch. J. Neurophysiol. 96, 2792–2796.

Chan, P.M., Yuen, T., Ruf, F., Gonzalez-Maeso, J. and Sealfon, S.C. (2005) Method for multiplex cellular detection of mRNAs using quantum dot fluorescent in situ hybridization. Nucleic Acids Res. 33, E161.

Chandra, B., Subramaniam, R., Mallik, S. and Srivastava, D.K. (2006) Formulation of photocleavable liposomes and the mechanism of their content release. Org. Biomol. Chem. 4, 1730–1740.

Chin, J.W., Martin, A.B., King, D.S., Wang, L. and Schultz, P.G. (2002) Addition of a photocrosslinking amino acid to the genetic code of *Escherichia coli* . Proc. Natl Acad. Sci. USA 99, 11020–11024.

Chu, M.Q., Song, X., Cheng, D., Liu, S.P. and Zhu, J. (2006) Preparation of quantum dot-coated magnetic polystyrene nanospheres for cancer cell labelling and separation. Nanotechnology 17, 3268–3273.

Cotlet, M., Goodwin, P.M., Waldo, G.S. and Werner, J.H. (2006) A comparison of the fluorescence dynamics of single molecules of a green fluorescent protein: One- versus two-photon excitation. Chem. Phys. Chem. 7, 250–260.

Crut, A., Géron-Landre, B., Bonnet, I., Bonneau, S., Desbiolles, P. and Escude, C. (2005) Detection of single DNA molecules by multicolor quantum-dot end-labeling. Nucleic Acids Res. 33, e98.

Danuser, G. and Waterman-Storer, C.M. (2006) Quantitative fluorescent speckle microscopy of cytoskeleton dynamics. Annu. Rev. Biophys. Biomol. Struct. 35, 361–387.

Demeshkina, N.A., Laletina, E.S., Meschaninova, M.I., Repkova, M.N., Ven'yaminova, A.G., Graifer, D.M. and Karpova, G.G. (2003) The mRNA codon environment at the P and E Sites of human ribosomes deduced from photocrosslinking with pUUUGUU Derivatives. Mol. Biol. 37, 132-139. [Transl. from Molekulyarnaya Biologiya, Vol. 37, 147–155.]

Deng, D.-W., Yu, J.-S., and Pan, Y. (2006) Water-soluble CdSe and CdSe/CdS nanocrystals: A greener synthetic route. J. Colloid Interface Sci. 299, 225–232.

Derfus, A.M., Chan, W. C.W. and Bhatia, S.N. (2004) Probing the cytotoxicity of semiconductor quantum dots. Nano Lett., 4, 11–18.

Donega, C. D., Hickey, S. G., Wuister, S. F., Vanmaekelbergh, D. and Meijerink, A. J. (2003) Single-step synthesis to control the photoluminescence quantum yield and size dispersion of CdSe nanocrystals. Phys. Chem. B, 2003, 107, 489–496.

Donnert, G., Keller, K., Medda, R., Andrei, M.A., Rizzoli, S.O., Lührmann, R., Jahn, R., Eggeling, C. and Hell, S.W. (2006) Macromolecular-scale resolution in biological fluorescence microscopy. Proc. Natl Acad. Sci. USA 103, 11440–11445.

Dorman, C.J. (2007) Probing bacterial nucleoid structure with optical tweezers. BioEssays 29, 212–216.

Dormán, G. and Prestwich, G.D. (1994) Benzophenone photophores in biochemistry. Biochemistry 33, 5561–5673.

Du, W., Wang, Y., Qingming Luo, Q. and Liu, B.-F. (2006) Optical molecular imaging for systems biology: from molecule to organism. Anal. Bioanal. Chem. 386, 444–457.

Eisenman, L.N., Shu, H.-J., Akk, G., Wang, C., Manion, B.D., Kress, G.J., Evers, A.S., Steinbach, J.H., Covey, D.F., Zorumski, C.F. and Mennerick, S. (2007) Anticonvulsant and anaesthetic effects of a fluorescent neurosteroid analog activated by visible light. Nature Neurosci. 10, 523–530.

Elowitz, M.B., Surette, M.G., Wolf, P.E., Stock, J. and Leibler, S. (1997) Photoactivation turns green fluorescent protein red. Curr. Biol. 7, 809–812.

Folgering, J.H.A., Kuiper, J.M., de Vries, A.H., Engberts, J.B.F.N. and Poolman, B. (2004) Lipid-mediated light activation of a mechanosensitive channel of large conductance. Langmuir 20, 6985–6987.

Fricker, M., Runions, J. and Moore, I. (2006) Quantitative fluorescence microscopy: From art to science. Annu. Rev. Plant Biol. 57, 79–107.

Ghosn, B., Haselton, F.R., Gee, K.R. and Monroe, W.T. (2005) Control of DNA hybridization with photocleavable adducts. Photochem. Photobiol. 81, 953–959.

Geyer, H., Geyer, R. and Pingoud, V. (2004) A novel strategy for the identification of protein–DNA contacts by photocrosslinking and mass spectrometry. Nucleic Acids Res. 32, e132.

Grier, D.G. and Roichman, Y. (2006) Holographic optical trapping. Appl. Optics 45, 880–887.

Gronemeyer, H. and Pongs, O. (1980) Localization of ecdysterone on polytene chromosomes of *Drosophila melanogaster*. Proc. Natl Acad. Sci. USA 77, 2108–2112.

Habuchi, S., Cotlet, M., Gensch, T., Bednarz, T., Haber-Pohlmeier, S., Rozenski, J., Dirix, G., Michiels, J., Vanderleyden, J., Heberle, J., De Schryver, F.C. and Hofkens, J. (2005) Evidence for the isomerization and decarboxylation in the photoconversion of the red fluorescent protein DsRed. J. Am Chem. Soc. 127, 8977–8984.

Hammer, N.I., Early, K.T., Sill, K., Odoi, M.Y., Emrick, T. and Barnes, M.D. (2006) Coverage-mediated suppression of blinking in solid state quantum dot conjugated organic composite nanostructures. J. Phys. Chem. B 2006, 110, 14167–14171.

Hardman R (2006) A toxicologic review of quantum dots: Toxicity depends on physicochemical and environmental factors. Environ. Health Perspect. 114, 165–172.

Heim, R. (1994) Wavelength mutations and posttranslational autooxidation of green fluorescent protein. Proc. Natl Acad. Sci. USA 91, 12501–12504.

Hino, M., Okazaki, Y., Kobayashi, T., Hayashi, A., Sakamoto, K. and Yokoyama, S. (2005) Protein photo-crosslinking in mammalian cells by site-specific incorporation of a photo-active amino acid. Nature Methods 2, 201–206.

Høgset, A., Prasmickaite, L., Selbob, P-K., Hellumb, M., Engesæter, B.Ø., Bonsted, A, and Berg, K. (2004) Photochemical internalisation in drug and gene delivery. Adv. Drug Deliv. Rev. 56, 95–115.

Hornberg, C. and Weiler, E. W. (1984) High-affinity binding-sites for abs*cis*ic acid on the plasmalemma of *Vicia faba* guard cells. Nature 310, 321–324.

Hoshino, A., Fujioka, K., Oku, T., Nakamura, S., Suga, M., Yamaguchi, Y., Suzuki, K., Yashara, M. and Yamamoto, K. (2004) Quantum dots targeted to the assigned organelle in living cells. Micobiol. Immunol. 48, 985–994.

Hu, F.Q., Ran, Y.L., Zhou, Z.A., and Gao, M.Y. (2006) Preparation of bioconjugates of CdTe nanocrystals for cancer marker detection. Nanotechnology 17, 2972–2977.

Huang, J., Xudong Wang, X. and Wang, Z.L. (2006) Controlled replication of butterfly wings for achieving tunable photonic properties. Nano Lett. 6, 2325–2331.

Jiang, J. and Gill, B.S. (2006) Current status and the future of fluorescence in situ hybridization (FISH) in plant genome research. Genome 49, 1057–1068.

Jiang, P., Yamauchi, K., Yang, M., Tsuji, K., Xu, M.X., Maitra, A., Bouvet, M. and Hoffman, R.M. (2006) Tumor cells genetically labeled with GFP in the nucleus and RFP in the cytoplasm for imaging cellular dynamics. Cell Cycle 5, 1198–1201.

Jorgenson, J.W. and Lukacs, K.D. (1981) Zone electrophoresis in open-tubular glass capillaries. Anal. Chem. 53, 1298–1302.

Kippeny, T., Swafford, L.A., and Rosenthal, S.J. (2002) Semiconductor nanocrystals: A powerful visual aid for introducing the particle in a box. J. Chem. Edu. 79, 1094–1100.

Kim, M.S. and Diamond, S.L. (2006) Photocleavage of o-nitrobenzyl ether derivatives for rapid biomedical release applications. Bioorg. Medicinal Chem. Lett. 16, 4007–4010.

Klostranec, J.M. and Chan, C.W. (2006) Quantum dots in biological and biomedical research: recent progress and present challenges. Adv. Mater. 2006, 18, 1953–1964.

Koçer, A., Walko, M., Meijberg, W. and Feringa, B.L. (2005) A light-actuated nanovalve derived from a channel protein. Science 309, 755–758.

Krieg, A., Ruckstuhl, T. and Seeger, S. (2006) Towards single-molecule DNA sequencing: Assays with low nonspecific adsorption. Anal. Biochem. 349, 181–185.

Krüger, R., Kübler, D., Pallissé, R. , Burkovski, A.and Lehmann, W.D. (2006) Protein and proteome phosphorylation stoichiometry analysis by element mass spectrometry. Anal. Chem. 78, 1987–1994.

Lagerholm, B.C., Averett, L., Weinreb, G.E., Jacobson, K. and Thompson, N.L. (2006) Analysis method for measuring submicroscopic distances with blinking quantum dots. Biophys. J. 91, 3050—3060.

Lester, H.A., Krouse, M.E., Nass, M.M., Wassermann, N.H. and Erlanger, B.F. (1980) A covalently bound photoisomerizable agonist. Comparison with reversibly bound agonists at electrophorus electroplaques. J. Gen. Physiol. 75, 207–232.

Lewis, E.K., Haaland, W.C., Nguyen, F., Heller, D.A., Allen, M.J., MacGregor, R.R., C. Berger, S., Willingham, B., Burns, L.A., Scott, G.B.I., Kittrell, C., Johnson, B.R., Curl, R.F. and Metzker, M.L. (2005) Color-blind fluorescence detection for four-color DNA sequencing. Proc. Natl Acad. Sci. USA 102, 5346–5351.

Li, X., Gutierrez, D.V., Hanson, M.G., Han, J., Mark, M.D., Chiel, H., Hegemann, P., Landmesser, L.T. and Herlitze, S. (2005) Fast noninvasive activation and inhibition of neural and network activity by vertebrate rhodopsin and green algae channelrhodopsin. Proc. Natl Acad. Sci. USA 102, 17816–17821.

Li, Z.H., Wang, K.M., Tan, W.H., Li, J., Fu, Z.Y., Ma, C.B., Li, H.M., He, X.X. and Liu, J.B. (2006) Immunofluorescent labeling of cancer cells with quantum dots synthesized in aqueous solution. Anal. Biochem. 354, 169–174.

Loudon, R. and Barnett, S.M. (2006) Theory of the radiation pressure on dielectric slabs, prisms and single surfaces. Optics Express 14, 11855–11869.

Lukyanov KA, Chudakov DM, Lukyanov S. and Verkhusha, V.V. (2005) Photoactivable fluorescent proteins. Nat. Rev. Mol. Cell Biol. 6, 885–891.

Marriott, G., Roy, P. and Jacobson, K. (2003) Preparation and light-directed activation of caged proteins. Meth. Enzymol. 360, 274–288.

McBride, J., Treadway, J., Feldman, L.C., Pennycook, S.J. and Rosenthal, S.J. (2006) Structural basis for near unity quantum yield core/shell nanostructures. Nano Lett. 6, 1496–1501.1

Medintz, I.L., Uyeda, H.T., Goldman, E.R. and Mattoussi, H. (2005) Quantum dot bioconjugates for imaging, labelling and sensing. Nature Materials 4, 435–446.

Menzel ER, Savoy SM, Ulvick SJ, Cheng KH, Murdock RH, Suddeth MR (2000) Photoluminescent semiconductor nanocrystals for fingerprint detection. J. Forens. Sci. 45, 545–551.

Metzker, M.L. (2005) Emerging technologies in DNA sequencing. Genome Res. 15, 1767–1776.

Michalet, X., Pinaud, F.F., Bentolila, L.A., Tsay, J.M., Doose, S., Li, J.J., Sundaresan, G., Wu, A.M., Gambhir, S.S. and Weiss, S. (2005) Quantum dots for live cells, in vivo imaging, and diagnostics. Science 307, 538–544.

Moan, J. and Berg, K. (1991) The photodegradation of porphrins in cells can be used to estimate the lifetime of singlet oxygen. Photochem. Photobiol. 53, 549–553.

Moon Suk Kim, M.S. and Diamond, S.L. (2006) Photocleavage of o-nitrobenzyl ether derivatives for rapid biomedical release applications. Bioorg. Med. Chem. Lett.16, 4007—4010

Mori, H. and Ito, K. (2006) Different modes of SecY–SecA interactions revealed by site-directed photo-crosslinking in vivo. Proc. Natl. Acad. Sci. USA 103, 16159–16164.

Ndoye, A. Dolivet, G., Høgset, A., Leroux, A., Fifre, A., Erbacher, P., Berg, K., Behró, J.-P., Guillemin, F. and Merlin, J.-L. (2006) Eradication of p53-mutated head and neck squamous cell carcinoma xenografts using nonviral p53 gene therapy and photochemical internalization. Mol. Ther 13, 1156–1162.

Nechyporuk-Zloy, V., Stock, C., Schillers, H., Oberleithner, H. and Schwab, A. (2006) Single plasma membrane K^+channel detection by using dual-color quantum dot labeling. Am. J. Physiol. Cell Physiol. 291, 266–269.

Nelson, T., Tausta, S.L., Gandotra, N. and Liu, T. (2006) Laser dissection of plant tissue: What you see is what you get. Annu. Rev. Plant Biol. 57,181–201.

Nida, D.L., Rahman, M.S., Carlson, K.D., Richards-Kortum, R. and Follen, M. (2005) Fluorescent nanocrystals for use in early cervical cancer detection. Gynecol. Oncol. 99(Suppl. 1), S89–S94.

O'Connell, K.M.S., Rolig, A.S., Whitesell, J.D. and Tamkun, M.M. (2006) Kv2.1 Potassium channels are retained within dynamic cell surface microdomains that are defined by a perimeter fence. J. Neurosci. 26, 9609–9618.

Park, T.J., Park, J.P., Seo, G.M., Chai, Y.G. and Lee, S.Y. (2006) Rapid and accurate detection of Bacillus anthracis spores using peptide-quantum dot conjugates. J. Microbiol. Biotechnol. 16, 1713–1719.

Paterson, L., Papagiakoumou, E., Milne, G., Garcés-Chávez, V., Tatarkova, S.A., Sibbett, W., Gunn-Moore, F.J., Bryant, P.E., Riches, A.C. and Dholakia, K. (2005) Light-induced cell separation in a tailored optical landscape. Appl. Phys. Lett. 87, 123901.

Peterman, E.J.G., Brasselet, S. and Moerner, W.E. (1999) The fluorescence dynamics of single molecules of green fluorescent protein. J. Phys. Chem. A 103, 10553–10560.

Peterson, D.S. (2007) Matrix-free methods for laser desorption/ionization mass spectrometry. Mass Spectrom. Rev. 26, 19–34.

Petersson, E.J., Brandt, G.S., Zacharias, N.M., Dougherty, D.A., and Lester, H.A. (2003) Caging proteins through unnatural amino acid mutagenesis. Meth. Enzymol. 360, 258–273.

Ramanathan, A., Huff, E.J., Lamers, C.C., Potamousis, K.D., Forrest, D.K. and Schwartz, D.C. (2004) An integrative approach for the optical sequencing of single DNA molecules. Anal. Biochem. 330, 227–241.

Raymond, F.R., Ho, H.A., Peytavi, R., Bissonnette, L., Boissinot, M., Picard, F.J., Leclerc, M. and Bergeron, M.G. (2005) Detection of target DNA using fluorescent cationic polymer and peptide nucleic acid probes on solid support. BMC Biotechn. 5, Art. No. 10.

Rosetti, R., Nakahara, S. and Brus, L.E. (1982) Quantum size effects in the redox potentials, resonance Raman spectra, and electronic spectra of CdS crystallites in aqueous solution. J. Chem. Phys. 79, 1086–1088.

Schaltmann, K. and Pongs, O. (1982) Identification and characterization of the ecdysterone receptor in *Drosophila melanogaster* by photoaffinity labeling. Proc. Natl Acad. Sci. USA 79, 6–10.

Schroll, C., Riemensperger, T., Bucher, D., Ehmer, J., Völler, T., Erbguth, K., Berber, G., Hendel, T., Nagel, G., Buchner, E. and Fiala, A. (2006) Light-induced activation of distinct modulatory neurons triggers appetitive or aversive learning in *Drosophila* larvae. Curr. Biol. 16, 1741–1747.

Seo, T.S., Bai, X., Kim, D.H., Meng, Q., Shi, S., Ruparel, H., Li, Z., Turro, N.J. and Ju, J. (2005) Four-color DNA sequencing by synthesis on a chip using photocleavable fluorescent nucleotides. Proc. Natl. Acad. Sci. USA 102, 5926–5931.

Shkrob, M.A., Yanushevich, Y.G., Chudakov, D.M., Gurskaya, N.G., Labas, Y.A., Poponov, S.Y., Mudrik, N.N., Lukyanov, S. and Lukyanov, K.A. (2005) Far-red fluorescent proteins evolved from a blue chromoprotein from *Actinia equina*. Biochem. J. 392, 649–654.

So, M.-K., Xu, C., Loening, A.M., Gambhir, S.S. and Rao, J. (2006) Self-illuminating quantum dot conjugates for *in vivo* imaging. Nature Biotechnol. 24, 339–343.

Stiller, B., Karageirgiev, P., Geue, T., Morawetz, K., Saphiannikova, M., Mechau, N., Neher, D. (2004) Optically induced mass transport studied by scanning near-field optical- and atomic force microscopy. Physics Low-Dimensional Struct. 1–2, 129–137.

Swamy, N., Addo, J.K. and Ray, R. (2000) Development of an affininity-driven crosslinker: Isolation of a vitamin D receptor associated factor. Bioorg. Med. Chem. Lett. 10, 361–364.

Synge, E.H. (1928) A suggested method for extending microscopic resolution into the ultra-microscopic region. Phil. Mag. 6, 356–362.

Todoroki, Y., Tanaka, T., Kisamori, M. and Hirai, N. (2001) 3-Azidoabscissic acid as a photoaffinity reagent for abs*cis*ic acid binding proteins. Bioorg. Med. Chem. Lett. 11, 2381—2384.

Torimoto, T., Murakami, S., Sakuraoka, M., Iwasaki, K., Okazaki. K., Shibayama, T. and Ohtani, B. (2006) Photochemical fine-tuning of luminescent color of cadmium selenide nanoparticles: Fabricating a single-source mulitcolor luminiphore. J. Phys. Chem. 110, 13314–13318.

Tsien, R.Y. (1998) The green fluorescent protein. Annu. Rev. Biochem. 67: 509–544.

Verkhusha, V. V. and Lukyanov, K. A. (2004) The molecular properties and applications of *Anthozoa* fluorescent proteins and chromoproteins. Nature Biotechnol. 22, 289–296.

Viviani, V.R. (1999) Cloning, sequence analysis, and expression of active *Phrixothrix* railroad-worms luciferases: Relationship between bioluminescence spectra and primary structures. Biochemistry 38, 8271–8279.

Wang, L., Brock, A., Herberich, B. and Schultz, P.G. (2001) Expanding the genetic code of *Escherichia coli*. Science 292, 498–500.

Wang, Q.B. and Seo, D.K. (2006) Synthesis of deep-red-emitting CdSe quantum dots and general non-inverse-square behavior of quantum confinement in CdSe quantum dots. Chem. Mater. 18, 5764–5767.

Werner, J.H., Cai, H., Jett, J.H., Reha-Krantz, L., R.A. Keller, R.A. and Goodwin, P.M. (2003) Progress towards single-molecule DNA sequencing: a one color demonstration. J. Biotechnol. 102, 1–14.

Winkler, L.D., Arceo, J.F., Hughes, W.C., DeGraff, B.A. and Augustine, B.H. (2005) Quantum dots: An experiment for physical or materials chemistry. J. Chem. Educ. 82, 1700–1702.

Wittelsberger, A., Thomas, B.E., Mierke, D.F. and Rosenblatt, M. (2006) Methionine acts as a "magnet" in photoaffinity crosslinking experiments. FEBS Lett. 580, 1872–1876.

Xie, J. and Schultz. P.G. (2005) Adding amino acids to the genetic repertoire. Curr. Opin. Chem. Biol. 9, 548–554.

Xie, J. and Schultz. P.G. (2006) A chemical toolkit for proteins an expanded genetic code. Nature Rev. Mol. Cell Biol. 7, 775–782.

Xu, W.B., Wang, Y.X., Xu, R.H. and Yin, D.Z. (2006) Synthesis, modification and application in biology of quantum dots (in Chinese). J. Inorg. Mater. 21, 1031–1037.

Yeh, H.-C., Ho, Y.-P., Shih, I.-M. and Wang, T.-H. (2006) Homogeneous point mutation detection by quantum dot-mediated two-color fluorescence coincidence analysis. Nucleic Acids Res. 34, e35.

Zhang, F., Wang, L.P, Boyden, E.S. and Deisseroth, K. (2006) Channelrhodopsin-2 and optical control of excitable cells. Nature Methods 3, 785–792.

Zheng, J., Nicovich, P.R. and Dickson, R.M. (2007) Highly fluorescent noble-metal quantum dots. Annu. Rev. Phys. Chem. 58, 409–31.

6
Terrestrial Daylight

Lars Olof Björn

Abstract: Practically all natural daytime light at the earth's surface originates in the sun. The fluence rate, as well as spectral and directional distributions, is modified by the gases, clouds, and aerosols in the atmosphere in a way that depends on time and place, as well as by vegetation, snow, and other ground cover. A special section in this chapter is devoted to ultraviolet radiation.

6.1. Introduction

Natural light at the surface of the earth is almost synonymous with light from the sun. Light from other stars has, as far as is known, photobiological importance only for navigation by night-migrating birds.

Moonlight, which originates in the sun, is important for the setting of some biological rhythms. A full moon may perturb the photoperiodism of some short-day plants and also synchronize rhythms in some marine animals.

However, the majority of photobiological phenomena are ruled by daylight, and we shall devote the remainder of this chapter to this topic. We shall treat the shortest wavelength components of daylight, UV-B radiation, at the end of the chapter, as special problems are involved with this waveband.

6.2. Principles for the Modification of Sunlight by the Earth's Atmosphere

As mentioned earlier, the radiation from the sun (Fig. 6.1) is spectrally very similar to blackbody radiation of 6000 K (above 700 nm 5777 K). There are, however, deviations both in the basic shape and due to reabsorption (Fraunhofer lines) of some light by gases in the higher, cooler layers of the sun.

The earth's atmosphere reflects, refracts, scatters, and partially absorbs the radiation from the sun, and thereby changes its spectral composition considerably. Part of the absorption and Rayleigh scattering is due to the main gases in the atmosphere, the concentration of which can be regarded as constant. Another

Extraterrestrial solar spectrum
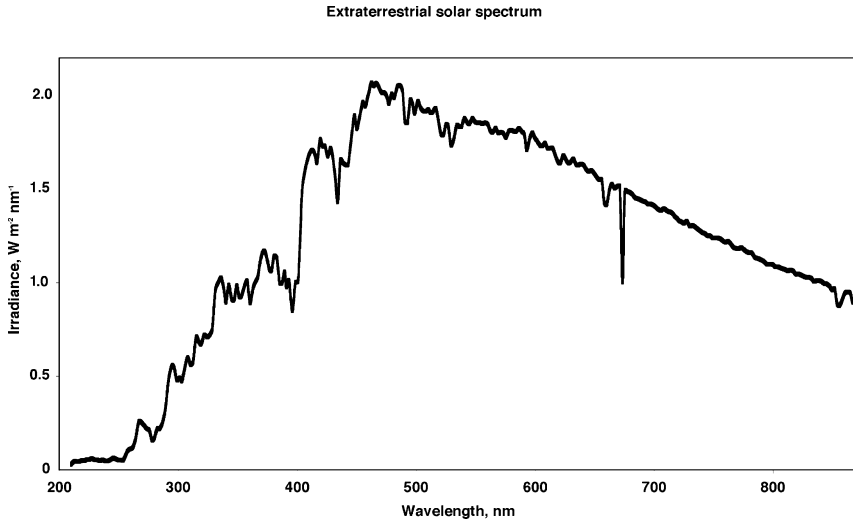
FIGURE 6.1. The spectrum of sunlight on a plane perpendicular to the direction to the sun, outside the earth's atmosphere.

part is due to ozone and water vapor (see Stomp et al. 2007), which occur in highly variable amounts. A third part is due to aerosol, which is also highly variable. The absorption causes loss of light, while scattering causes some light to be lost to space, while another part appears as diffuse light (skylight). Light is also reflected by clouds, and thereby mostly lost to space, but this will not be considered in detail here. Light reflected from the ground is partly scattered downward or reflected from clouds, and again appears at the surface as diffuse light, and for this reason the ground reflectivity has some effect on skylight.

Daylight is also strongly dependent on the elevation of the sun above the horizon (90° minus the solar elevation is called the zenith angle of the sun, and often symbolized by the Greek letter theta, θ), because the lower the sun, the more air the rays must pass before they reach the ground. Daylight can be considered as composed of two components—direct sunlight and scattered light. The scattered light is in most cases dominated by skylight, while some may reach the observer as scattered from the ground, trees, etc.

6.3. The UV-A, Visible, and Infrared Components of Daylight in the Open Terrestrial Environment Under Clear Skies

Accurate methods for computational modeling of daylight depart from the radiative transfer theory described by Chandrasekhar (1950, 1960). However, the fundamental formulas usually cannot be used directly; different approximations

have to be used for various cases, and this is nothing for the average biologist to work with. However, as long as we are dealing with clear skies (no clouds), relatively long wavelengths (near infrared, visible and UV-A radiations), and as long as we stay above water and vegetation, daylight can be well described by methods that are more easily handled.

A simple and for most purposes adequate procedure for this has been published by Bird and Riordan (1986). Their model has become very popular, and their paper had been cited nearly two hundred times when this book was being written. An alternative approach for this part of the spectrum is that of Green and Chai (1988). We shall use the approach of Bird and Riordan (1986) here to show how the direct component (sunlight) and the component scattered by the atmosphere (skylight) vary with the solar elevation (i.e., with the zenith angle). The same algorithm can be used also for visualizing how other factors, such as air pressure, air humidity, aerosol, ozone column, and ground albedo, affect daylight. We show the result only from 300 to 800 nm, but the paper by Bird and Riordan (1986) can be used to model radiation up to 4 µm, i.e., 4000 nm.

Figure 6.2 shows three spectra, representing the direct sunlight, the skylight (diffuse radiation), and their sum, the so-called global radiation (the total daylight). Note that the skylight has its maximum moved towards shorter wavelengths compared to the direct sunlight. This corresponds to the fact that the sky appears blue in color and also to the fact that Rayleigh scattering is inversely proportional to the fourth power of the wavelength.

Figure 6.3 shows the irradiance on a horizontal plane and the one for the irradiance on a vertical plane in the compass direction (azimuth) toward the sun. These spectra are rather different. The sunset sunlight is of course much stronger in the horizontal direction (on a vertical plane). The scattered light is now not only skylight, but also light scattered from the ground, and therefore it contains
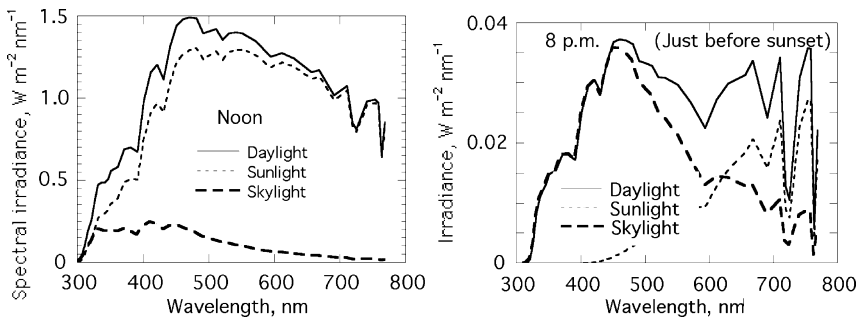
FIGURE 6.2. Irradiance at noon (left) and just before sunset (right) from above on a horizontal plane in Lund (south Sweden, 55.7°N, 13.4°E) on July 15, 2002, as computed using the algorithm of Bird and Riordan (1986). The ozone column was assumed to be 300 dobson units and the ground albedo 0.2, aerosol 0, and air pressure 1000 millibar.
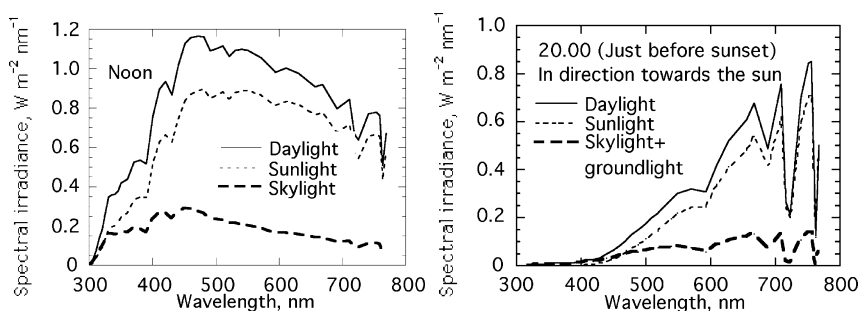
FIGURE 6.3. Same as Fig. 6.2, except that the plane is vertical and pointed in the compass direction of the sun.

much more long-wave components. Note also how deep the absorption bands for water vapor and oxygen have become, because the light must pass so much air when the sun is so low in the horizon. We can see from this that the concept "daylight spectrum" has no meaning if the geometry of measurement is not specified. We would get a third set of spectra for the fluence rate. The fluence rate can also be readily calculated using the algorithm of Bird and Riordan (1986), slightly modified: The diffuse component should be doubled, and the factor cosinus of incidence angle should be dropped in the expression for the direct component (sunlight).

The algorithm of Bird and Riordan (1986) assumes the skylight to come equally from all over the sky, or, in other words, the sky *radiance* is uniform. This is an approximation, and other more accurate descriptions exist. A model based on radiative transfer theory has been published by Liang and Lewis (1996), while the group of R.H. Grant (Grant and Heisler 1997, Grant et al. 1996a,b, 1997), based on measurements, has developed a set of very simple models for various cloud conditions.

The paper by Bird and Riordan (1986), as stated in its title, deals only with clear skies. In modeling the diffuse skylight it assumes the sky to have uniform (isotropic) radiance. This latter approximation works very well as long as we are interested only in the irradiance on a horizontal or nearly horizontal plane. For some other purposes it may be of interest to model more exactly the variations in sky radiance, and how this can be done (in a relative sense also for cloudy conditions and for UV-B radiation) in a simple way has been described by Grant et al. (1996a,b, 1997) and Grant and Heisler (1997) in a series of papers, with a summary presently available at http://shadow.agry.purdue.edu/research.model.skyrad.html.

Sky light is elliptically polarized (i.e., partly plane polarized), which is important for some animals who are able to determine the direction of polarisation and use it for orientation (see, e.g., Labhart 1999). The degree of polarization can be approximated by $p = p_o \cdot \sin\mu/(1+\cos^2\mu)$, where μ is the angular

distance from the sun. The value of p_o is never more than 94%, usually lower, depending on aerosol in the air, reflection from the ground, etc. The direction of the major electrical vector is approximately along the circumference of "circles" on the sky with the sun in the center (e.g., Schwind and Horváth 1993). A few comments should be added to this simplified description (again, a more exact mathematical description can be obtained using the radiative transfer theory). Thus, the polarization is increased in the spectral bands where the terrestrial atmosphere absorbs strongly (Aben et al. 1999). When the sun is higher than about 20° above the horizon, there are two points within 20° of the sun, one above and one below, where polarization is zero. When the sun is less than about 20° above the horizon, one such point is located about 20° above the antisolar point (Bohren 1995, 2004).

6.4. Cloud Effects

Clouds usually decrease both the irradiance and the degree of polarization of daylight. However, under some circumstances clouds can cause the irradiance above the values it would have had without clouds. This effect is particularly pronounced when most of the sky is overcast but the sun is not in clouds and when the ground is snow-covered or otherwise highly reflecting.

6.5. Effects of Ground and Vegetation

Reflection from the ground is particularly important in the ultraviolet, since ultraviolet light reflected upward by the ground is partially scattered downward again by the atmosphere, and the ground cover thus affects also downwelling radiation. The effect of reflection from the ground is greatest when it is covered by snow. Reflection from the ground can be quite important for the visible spectrum and for plant growth, as shown by Hunt et al. (1985) and Kasperbauer and Hunt (1987).

Penetration of light into the ground is important for the germination of seeds. Soil transmission generally increases with increasing wavelength, thus giving buried seeds a far-red–biased environment (Kasperbauer and Hunt 1988).

Plant canopies absorb visible light and ultraviolet radiation, but reflect and transmit far-red light and near-infrared radiation. Light in or under green vegetation is therefore strongly biased towards the longer wavelengths, a fact that is of paramount importance to the plants subjected to this regime. The plant-filtered light forces the phytochrome system to the Pr (inactive) state (Holmes and Smith 1977, Kasperbauer 1971, light *inside* plants and animals (Marijnissen and Smith 1977, Kasperbauer 1971, 1987, Smith 1986). This will be further dealt with in Chapters 9 and 16.

It is now possible to measure light *inside* plants and animals (Marijnissen and Star 1987, Star et al. 1987, Vogelmann 1986).

6.6. The UV-B Daylight Spectrum and Biological Action of UV-B

At the short-wavelength end of the daylight spectrum is the UV-B spectral band, 280–315 nm. This band is of particular interest because it is highly biologically active (mostly inhibitory). It is more difficult to measure than visible light and UV-A radiation because irradiance and fluence rate is lower. It is also more difficult to model than other daylight, because the spectral irradiance at ground surface is highly variable and dependent on other factors in addition to those influencing the longer wavelength components. The main factors influencing UV-B spectral irradiance at ground level are the elevation of the sun above the horizon and the amount of ozone in the atmosphere (Fig. 6.4).

A computer program to study the effects of these and other factors on the UV-B spectral irradiance and estimate the biological action was designed by Björn and Murphy (1985) based on Green (1983), and is further described by Björn (1989) and Björn and Teramura (1993). A more accurate code that can also be used for visible light and is based on radiative transfer theory is that of S. Madronich, presently available on the Internet (http://cprm.acd.ucar.edu/Models/TUV/).

UV-B is more highly scattered than longer daylight components, and even under clear skies much of it reaches the ground as skylight rather than direct sunlight. Thus the fluence rate can be appreciable even in shadow. If the ground is snow covered, and especially if the snow is fresh, much radiation can reach the observer from snow. Snow also increases the ultraviolet component of skylight, because radiation reflected from the ground is to an appreciable extent scattered down again by the atmosphere.
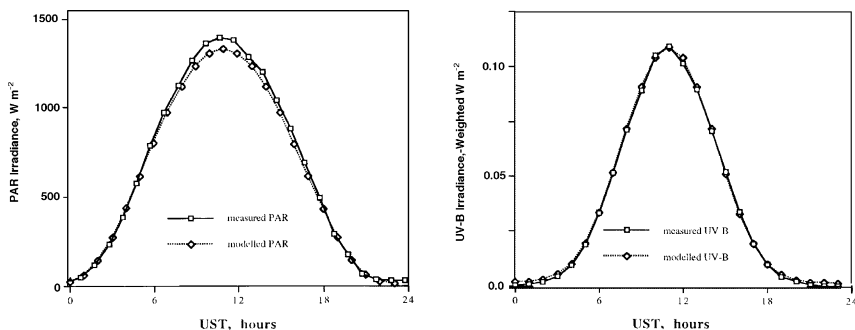
FIGURE 6.4. The variation of daylight during a cloud-free day (July 5, 1994) at Abisko in northern Sweden (68.35°N, 18.82°E). The left panel shows photosynthetically active radiation (PAR, 400–700 nm), the right panel UV-B radiation. The UV-B radiation was weighted with a mathematical function to enhance the biologically more active shorter wavelength components. The horizontal axis shows Universal Standard Time. Note that the UV-B is more concentrated toward the middle of the day than is PAR. (From Björn and Holmgren 1996.)

Also, underwater ultraviolet radiation has its special measuring and modeling problems. In freshwater bodies and coastal water the amount of UV-B–absorbing dissolved substances is usually so high that UV-B radiation does not penetrate very far. Exceptions are some Alpine lakes. But in clear ocean water, such as that in the Southern Ocean, UV-B radiation can be measured down to 60 m, and biological effects can be recorded at a depth of 20 m.

We shall return to UV-B radiation in Chapters 19–22.

References

Aben, I., Helderman, F., Stam, D.M. and Stamnes, P. (1999) Spectral fine-structure in the polarisation of skylight. Geophys. Res. Lett. 26, 591–594.

Bird, R.E. and Riordan, C. (1986) Simple solar spectral model for direct and diffuse irradiance on horizontal and tilted planes at the earth's surface for cloudless atmospheres. J. Climate Appl. Meteorol. 25, 87–97.

Björn, L.O. (1989) Computer programs for estimating ultraviolet radiation in daylight. In: B.L. Diffey (Ed.). *Radiation measurement in photobiology*, pp. 161–169. Academic Press, London.

Björn, L.O. and Murphy T.M. (1985) Computer calculation of solar ultraviolet radiation at ground level. Physiol. Vég. 23, 555–561.

Björn. L.O. and Teramura, A.H. (1993) Simulation of daylight ultraviolet radiation and effects of ozone depletion. In A.R. Young, L.O. Björn, J. Moan, and W. Nultsch, (Eds) *UV Photobiology,* pp. 41–71, Plenum Press, New York.

Bohren, C.F. (1995) Optics, atmospheric. In: G.L. Trigg (Ed.) *Encyclopedia of applied physics*, vol. 12, pp. 405–434.VCH Publishers, New York.

Bohren, C.F. (2004) Atmospheric optics. In: T.G. Brown et al. (Eds) *The optics encyclopedia: Basic foundations and practical applications*, vol. 1, pp. 53–91. Wiley, Hoboken, N.J.

Chandrasekhar, S. (1950) *Radiative transfer theory*. Oxford University Press. Reprinted (1960) by Dover Publications, New York.

Grant. R.H. and Heisler, G.M. (1997) Obscured overcast sky radiance distributions for UV and PAR wavebands. J. Appl. Meteor. 36, 1336–1345.

Grant, R.H., Gao, W. and Heisler, G.M. (1996a) Photosynthetically active radiation: sky radiance distributions under clear and overcast conditions. Agric. Forest Meteorol. 82, 267–292.

Grant, R.H., Heisler, G.M. and Gao, W. (1996b) Clear sky radiance distributions in ultraviolet wavelength bands. Theor. Appl. Climatol. 56, 123–135.

Grant, R.H., Gao, W. and Heisler, G.M. (1997) Ultraviolet sky radiance distributions of translucent overcast skies. Theor. Appl. Climatol 3–4, 129–139.

Green, A.E.S. (1983) The penetration of ultraviolet radiation to the ground. Physiol. Plant. 58, 351–359.

Green, A.E.S. and Chai, S.-T. (1988) Solar spectral irradiance in the visible and infrared regions. Photochem. Photobiol. 48, 477–486.

Green, A.S. and Chai, S.-T. (1988) Solar spectral irradiance in the visible and infrared regions. Photochem. Photobiol. 48, 477–486.

Holmes, M.G. and Smith, H. (1977) Spectral distribution of light within plant canopies. In: H. Smith (Ed.). *Plants and the daylight spectrum*, pp. 147–158.Academic Press, New York.

Hunt, P.G., Kasperbauer, M.J. and Matheny, T.A. (1985) Effect of soil surface color and *Rhizobium japonicum* strain on soybeen seeling growth and nodulation. Agronomy Abstr. 85, 157.

Kasperbauer, M.J. (1971) Spectral distribution of light in a tobacco canopy and effects of end-of-day light quality on growth and development. Plant Physiol. 47, 775–778.

Kasperbauer, M.J. (1987) Far red light reflection from green leaves and effects on phytochrome-mediated assimilate partitioning under field conditions. Plant Physiol. 85, 350–354.

Kasperbauer, M.J. and Hunt, P.G. (1987) Soil color and surface residue effects on seedling light environment. Plant Soil 97, 295–298.

Kasperbauer, M.J. and Hunt, P.G. (1988) Biological and photometric measurement of light transmission through soils of various colors. Bot. Gaz. 149, 361–364.

Labhart, T. (1999) How polarization-sensitive interneurones of crickets see the polarization pattern of the sky: A field study with an optoelectronic model neurone. J. Exp. biol. 202, 757–770.

Liang, S.L. and Lewis, P. (1996) A parametric radiative transfer model for sky radiance distribution. J. Quant. Spectroscopy Radiative Transfer 55, 181–189.

Marijnissen, J.P.A. and Star, W.M. (1987) Quantitative light dosimetry *in vitro* and *in vivo*. Lasers Med. Sci. 2, 235–242.

Schwind, R. and Horváth, G. (1993) Reflection-polarization pattern at water surfaces and correction of a common representation of the polarization pattern of the sky. Naturwissenschaft 80, 82–83.

Smith, H. (1986) The perception of light quality. In: R.E. Kendrick and G.M.H. Kronenberg (Eds.). *Photomorphogenesis in plants* , pp. 187–217. Martinus Nijhoff Publishers, Dordrecht, the Netherlands.

Star, W.M., Marijnissen, H.P.A., Jansen, H., Keijzer, M and van Gemert, M.J.C. (1987) Light dosimetry for photodynamic therapy by whole bladder wall irradiation. Photochem. Photobiol. 46, 619–624.

Stomp, M., Huisman, J., Stal, L.J., and Matthijs, H.C.P. (2007) Colorful niches of phototrophic microorganisms shaped by vibrations in the water molecule. ISME J. 1, 271–282.

Vogelmann, T.C. (1986) Light within the plant. In: R.E. Kendrick and G.M.H. Kronenberg (Eds.). *Photomorphogenesis in plants*, pp. 307–337. Martinus Nijhoff Publishers, Dordrecht, the Netherlands.

7
Underwater Light

Raymond C. Smith and Curtis D. Mobley

Abstract: The penetration of solar radiation into natural waters is dependent on a wide range of variables, both in the atmosphere and in water, and we do not have space to demonstrate all situations. We have selected only one fixed set of environmental input parameters, and the choice of inherent optical properties has been limited to only pure water and a range of chlorophyll concentrations. However, these few simulations display a wide range of variability found in solar radiation penetrating to depth underwater. In general, as the absorption increases, the wavelength of maximum penetration shifts from the blue to the green part of the spectrum and attenuation increases.

7.1. Introduction

The penetration of the sun's energy into natural waters (oceans, lakes, rivers, etc.) is dependent upon the incident solar radiation, the state of the wind-blown surface, bottom reflectance in shallower waters, and the inherent optical properties of the water body. In turn, the optical properties are dependent upon the absorption coefficient and the volume scattering function of the dissolved and suspended material within the water. Given the inherent optical properties and an appropriate radiative transfer model, other important optical characteristics of the water column can be estimated. These characteristics include the photosynthetically available radiation (PAR) as a function of depth, the quantity of potentially harmful UV-B penetrating to depth, the spectral water leaving radiance observable by satellite sensors, and the in-water radiance field available for visibility. Fundamental terms describing the transfer of radiative energy in natural waters and relevant optical properties of this medium can be found in Morel and Smith (1982), and complete texts providing information on photobiology in aquatic ecosystems and radiative transfer in natural waters can be found in Kirk (1994) and Mobley (1994), respectively.

7.2. Inherent Optical Properties

Aquatic photochemical and photobiological processes depend upon both the amount of solar radiation penetrating to depths in natural waters as well as its spectral composition. Preisendorfer (see Gordon, Brown and Jacobs 1975) demonstrated that optical properties can conveniently be divided into two classes: inherent and apparent. Inherent optical properties (IOPs) are those properties that depend only on the medium. The two fundamental IOPs are the total spectral absorption coefficient, $a(\lambda)$, and the volume scattering function $\beta(\Psi,\lambda)$. Both these properties are independent of the geometry of the ambient light field within the medium.

The total spectral absorption coefficient, $a(\lambda)$, is the spectral absorptance per unit distance within the medium with units of 1/length, normally expressed as reciprocal meters (m^{-1}). The total spectral scattering coefficient, $b(\lambda)$, is found by integrating the spectral volume scattering function, over all directions (solid angles):

$$b(\lambda) = \int_{4\pi} \beta(\Psi, \lambda) d\Omega \tag{1}$$

where Ψ is the direction of the scattered bean into the solid angle $d\alpha$. Other important IOPs include the index of refraction of the water body and products derived from the fundamental IOP's such as the total attenuation coefficient, $c(\lambda)$, and the single-scattering albedo, $\omega_o(\lambda)$, where

$$c(\lambda) = a(\lambda) + b(\lambda) \tag{2}$$

$$\omega_o(\lambda) = b(\lambda)/c(\lambda) \tag{3}$$

The total attenuation coefficient, $c(\lambda)$, provides a measure of the amount of radiant flux diminished along a path. The single-scattering albedo plays an important role in radiative transfer modeling within water bodies and is near one when the beam attenuation is primarily due to scattering and near zero when $c(\lambda)$ is primarily due to absorption. Preisendorfer has shown that the fundamental IOPs (c, β) are a sufficient and complete set for describing the in-water optical properties under any circumstances. That is, knowing the IOPs and an input radiance distribution illuminating the water, one can, in principle, deduce the resulting radiant flux distribution (Mobley 1994).

The total absorption and scattering coefficients are the sums of contributions from various components (e.g., pure water, phytoplankton, dissolved organic material, detritus, etc.) within the water body. For example,

$$a_{total}(z, \lambda) = \Sigma a_i(z, \lambda) \tag{4}$$

where $a_i(z, \lambda)$ is the absorption coefficient of the ith component of the water body and Σ indicates summation over all these components. A total scattering coefficient can be similarly derived.

7.3. Apparent Optical Properties

In the field, in-water optical observations are often made using a flat plate cosine collector designed to measure spectral downward plane irradiance, $E_d(z, \lambda)$ ($W \cdot m^{-2}/nm$). Downwelling plane irradiance is defined as the integral of the downwelling radiance distribution, weighted by the cosine of the incidence angle, over all solid angles in the upper hemisphere (Mobley 1994). Although radiometric variables such as irradiance provide information about the instantaneous light field within a water body, they can change quickly (e.g., if the sun goes behind a cloud) and thus are not useful descriptors of the water body itself. However, ratios and normalized depth derivatives of radiometric variables are independent of fluctuations in the magnitude of the incident irradiance onto the sea surface and are thus relatively stable. Such quantities are called apparent optical properties (AOPs). (e.g., see Mobley 1994, Fig. 3.27, which emphasizes the difference in radiometric variables and AOPs.)

AOPs depend on both properties of the medium (IOPs) and the geometric, or directional, structure of the ambient light field, but they display enough stability and regularity to be useful descriptors of the water body. Examples of AOPs are the irradiance reflectance, which is the ratio of upwelling to downwelling plane irradiance, and the diffuse attenuation coefficient

$$K_d(z, \lambda) = -(1/E_d(z, \lambda))dE_d(z, \lambda)/dz = -d(\ln E_d(z, \lambda))/dz \qquad (5)$$

AOPs are linked via radiative transfer theory to the IOPs.

The penetration of solar radiation into natural waters is then described in terms of the diffuse attenuation coefficient for irradiance, $K_d(z, \lambda)$, which describes how the downward irradiance diminishes in an approximate exponential manner with depth,

$$E_d(z, \lambda) = E_d(0, \lambda)e^{-Kd(z,\lambda) \cdot z} \qquad (6)$$

Here $E_d(0, \lambda)$ is the downwelling spectral irradiance just below the air/water interface and $E_d(z, \lambda)$ is the irradiance at depth z within the water column.

For applications in photobiology, it is often preferable to make use of scalar irradiance, $E_o(z, \lambda)$, defined as the integral of the radiance distribution at depth z over all solid angles, again with units of $W \cdot m^{-2}/nm$. Typically, in photobiology, the spectral energy units ($W \cdot m^{-2}/nm$) are converted to broadband quantum units (mol photons $\cdot s^{-1} \cdot m^{-2}$). In aquatic photobiology a valuable measure of the in-water light field is the photosynthetically available radiation, PAR or E_{PAR}, defined as the integral of the scalar irradiance from 400 to 700 nm at depth z,

$$E_{PAR}(z) = \int_{400}^{700} E_o(z, \lambda)(\lambda/hc) \cdot d\lambda \qquad (7)$$

In Eq. (7), the factor of λ/hc (h is Planck's constant and c is the speed of light) converts energy units into quantum units. PAR is thus a broadband quantity measuring the number of photons available for photochemical or photobiological reactions (Kirk 1994).

For studies concerned with the influence of ultraviolet radiation (UVR) on aquatic organisms, other broadband quantities are of interest. UV-A is the electromagnetic radiation of wavelengths in the 315- to 400-nm range and UV-B the radiation in the 280- to 315-nm range. Thus, for example, the solar scalar irradiance penetrating to depth within the UV-B region of the spectrum, $E_{UV-B}(z)$, is computed as

$$E_{UV-B}(z) = \int_{280}^{315} E_o(z, \lambda) \cdot d\lambda \tag{8}$$

An analogous equation holds for $E_{UV-A}(z)$.

7.4. Estimation of In-Water Radiant Energy

A wide range of bio-optical models has been used to relate various constituents of the water column to ocean optical properties. In turn, these optical properties, both IOPs and AOPs, have been used in various models to estimate the desired in-water radiant energy quantities. Modeling in hydrologic optics has often been discussed in terms of the "direct" problem of radiative transfer, estimating the radiometric variables and AOPs given the IOPs, and the "indirect problem," estimating the IOPs from measurements of the radiometric variables or AOPs. The latter has been discussed in an extensive review by Gordon (2002). With respect to the direct problem, Mobley et al. (1993) provide a comparison of several numerical models for computing underwater light fields. As an example of a direct radiative transfer model, HydroLight solves the radiative transfer equation, with input of IOPs, to compute the spectral radiance distribution as a function of depth, direction, and wavelength within the water. From the radiance distribution, various derived output quantities of interest in photobiology, including E_d, E_o, E_{PAR}, and E_{UV-B}, can be estimated.

Input to HydroLight includes the IOPs, the nature of the wind-blown sea surface, reflectance characteristics of the bottom boundary of the water column, and the radiance distribution of the sun and sky light. IOPs can either be measured directly, modeled in terms of contributions by the various components contributing to the attenuation (e.g., Eq. [4]), or a combination of both. The nature of the wind-blown sea surface is modeled using Cox-Munk (Cox and Munk 1954) wave slope statistics. Bottom characteristics and sky radiance can be measured directly or input from various models.

Natural waters vary widely in both optical properties and the geometry of solar input. As examples, we provide several HydroLight simulations. These simulations include the clearest natural waters (providing an estimate of the maximum

penetration of solar radiation) and waters displaying various chlorophyll concentrations to illustrate a range of typical situations. Figure 7.1 is a plot of absorption coefficient versus wavelength for clear water and clear water plus chlorophyll concentrations ranging from 0.01 to 3.0 mg/m^3. Here the first absorption component (Eq. [4]) is water, a_i, and the second component, a_2, is particulate absorption modeled from a range of chlorophyll concentrations. Other components, which may co-vary with chlorophyll or represent other in-water constituents, are not considered. These absorption coefficients, along with a fixed set of arbitrarily selected environmental inputs, are used in the following simulations.

Figure 7.2 shows plots of scalar irradiance, E_o [W m^{-2} nm^{-1}] vs wavelength [nm] for a range of depths (m). The upper left plot shows E_o vs. λ for clear water only and provides an estimate of the maximum penetration of solar radiation underwater. The other plots show E_o vs. λ for waters with increasing chlorophyll concentrations and provides estimations of the penetration of solar radiation into waters covering a range of phytoplankton concentrations. Noteworthy, when comparing these figures, is the wavelength of maximum penetration: roughly 410 nm in the clearest waters and shifting increasingly toward the green with increasing chlorophyll concentration. Also, with increasing particulate absorption, the penetration to depth decreases.

Figure 7.3 is a plot of E_{PAR} (z) vs. depth for the various examples given in the preceding two figures. In the clearest waters, PAR is reduced only by a factor of 34 at a depth of 200 m whereas with a chlorophyll concentration of 1.0 mgChl m^{-3} PAR is reduced by over eight orders of magnitude. These simulations dramatically illustrate the wide variability of the penetration of solar radiation into natural waters due to changes in the dissolved and suspended material within

Absorption coefficient [m^{-1}]
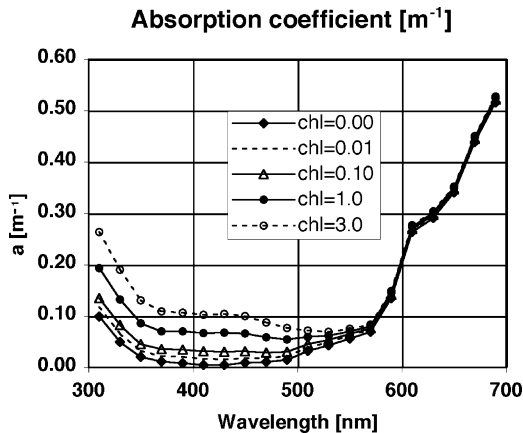
FIGURE 7.1. Absorption (m^{-1}) vs wavelength (nm) for clear water (Pope and Fry, 1997) and for water with various Chl concentrations (0.01, 0.03, 0.10, 0.30, 1.0 and 3.0 mg m^{-3}). In these examples the IOPs are constant with depth and a phase function for scattering is determined by the selected Chl value based on recent work by Morel, Antoine, and Gentili (2002).
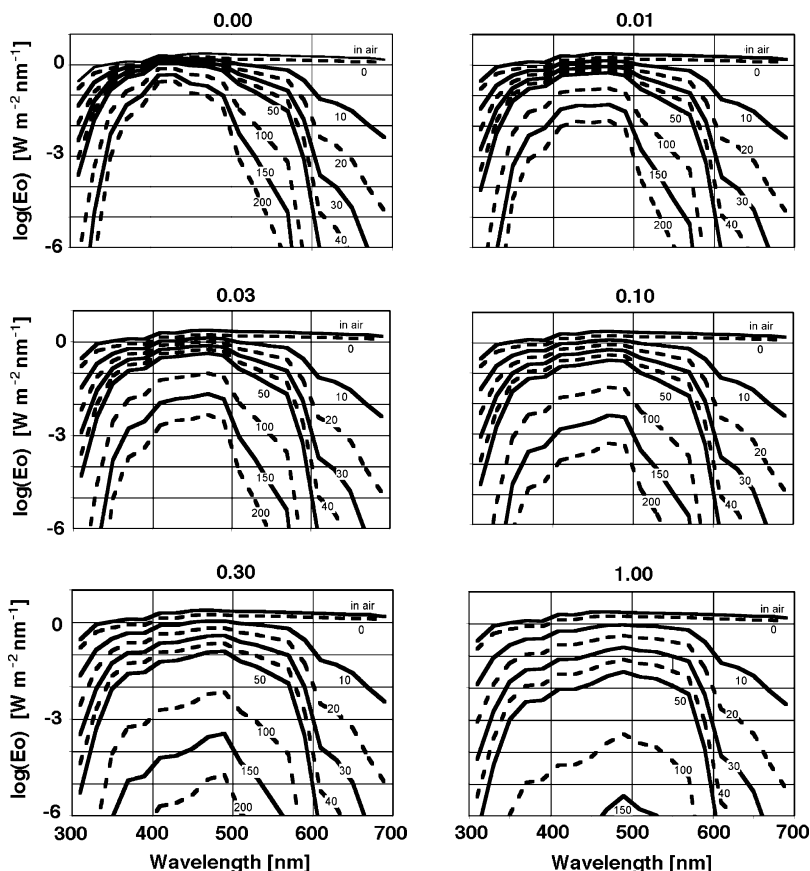
FIGURE 7.2. E_o (z, λ) (W/m²/nm) vs. wavelength (nm) for selected depths for various chlorophyll concentrations (absorption coefficients given in Fig. 7.1). Environmental conditions are held constant for each simulation: wind speed 1 m/s, no inelastic scattering, clear sky with solar zenith angle of 30°, and a water column that is considered infinitely deep. Spectra are for waters with chlorophyll concentrations of 0.00, 0.01, 0.03, 0.10, 0.30, and 1.0 mg Chl/m³, respectively.

the water column. They also demonstrate that with increasing depth the effective attenuation coefficient for PAR approaches that of the wavelength of minimum absorption (Fig. 7.1).

Figure 7.4 illustrates the relatively rapid attenuation of UV-B as compared to PAR. $E_{UV-B}(z)$ is reduced by two orders of magnitude at a depth of 40 m in the clearest waters and by more than four orders of magnitude at 40 m when the chlorophyll concentration is 1.0 mg Chl/m³. These examples may be considered an upper limit for the penetration of UV-B since dissolved organic material, which is known to significantly attenuate UV radiation, and other possible absorbing components have not been considered in these simulations.

PAR *vs* Depth
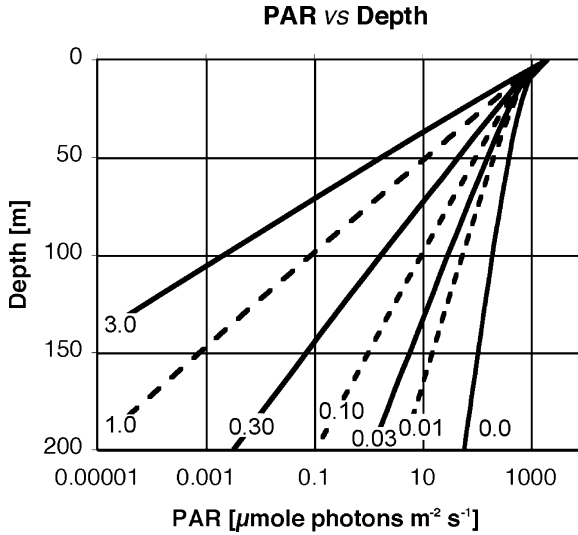
FIGURE 7.3. E_{PAR} (µmol photons/m²/s) vs. depth (m) for the examples in Fig. 7.1.

UV-B *vs* Depth
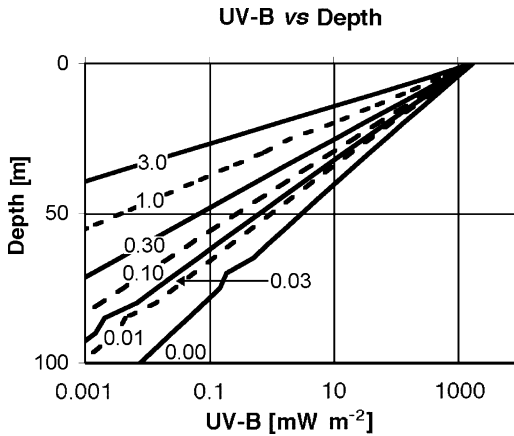
FIGURE 7.4. E_{UV-B} (W/m²) vs. depth (m) for same examples.

References

Cox, C. and Munk, W. (1954) Statistics of the sea surface derived from sun glitter. J. Marine Res. 13, 198–227.

Gordon, H.R. (2002) Inverse methods in hydrologic optics. Oceanologia 44, 9–58.

Gordon, H.R., Brown, O.B., and Jacobs, M.M. (1975) Computed relationships between inherent and apparent optical properties of a flat homogenous ocean. Appl. Optics 14, 417–427.

Kirk, J.T.O. (1994) *Light and photosynthesis in aquatic ecosystems.* Cambridge University Press, Cambridge.

Mobley, C.D. (1994) *Light and water*, *radiative transfer in natural waters*. Academic Press, New York (now out of print, but available on CD or at www.curtismobley.com/lightandwater.zip)

Mobley, C.D., Gentili, G., Gordon, H.R., Jin, Z., Kattawar, G.W., Morel, A., Reinersman, P., Stamnes, K. and Stavn, R.H. (1993) Comparison of numerical models for computing underwater light fields. Appl. Optics 32, 7484–7504.

Morel, A., Antoine A. and Gentili B. (2002) Bidirectional reflectance of oceanic waters: accounting for Raman emission and varying particle scattering phase function. Appl. Optics 41, 6289–6306.

Morel, A. and Smith R.C. (1982) Terminology and units in optical oceanography. Marine Geodesy 5, 335–349.

Pope, R.M. and Fry E.S. (1997) Absorption spectrum (380-700 nm) of pure water. II. Integrating cavity measurements. Appl. Optics 36, 8710–8723.

8
Action Spectroscopy in Biology

Lars Olof Björn

Abstract: Action spectroscopy is a method for identifying the light-absorbing chromophore in a photobiological or biochemical process by comparing the efficiency of radiation of different wavelengths in driving the process. This chapter explains the principle and gives several examples from the history of biology of what has been achieved using this technique.

8.1. Introduction

Action spectroscopy is a method for finding out what the initial step is in a photobiological or photochemical process. More exactly, the method serves to identify the kind of molecule absorbing the active light.

The basic principle of the method is the following: The more light that is absorbed, the greater its effect on the material systems under study. By comparing the effects of light having different wavelengths, a measure is obtained of the relative absorption at different wavelengths by the molecule directly affected by the light. This can then be compared to absorption spectra of various compounds. If everything works out, one can identify the compound absorbing the active light in the photoprocess under study.

A hypothetical example: molecule A, which is present in an organism, has the absorption spectrum shown in Fig. 8.1. Absorption of light by A causes a certain effect, say formation of anthocyanin in a plant. If a certain anthocyanin synthesis is obtained by irradiating for t minutes with N photons per m^2 and second of wavelength λ_1 (or λ_3), it ought to suffice with half as many photons of wavelength λ_2, since such light is absorbed twice as strongly. Or, conversely: if it is experimentally found that the two lights have the action described, this is an indication that molecule A is mediating the light effect. With only two wavelengths investigated the conclusion is still very uncertain. If the agreement between efficiency of the light and the absorptive power of A is extended over a wider spectral region, the conclusion will be more firmly founded.

Figure 8.2 shows the result of a fictive experiment involving the pigment with the absorption spectrum in Fig. 8.1. The effect of various exposures to light of
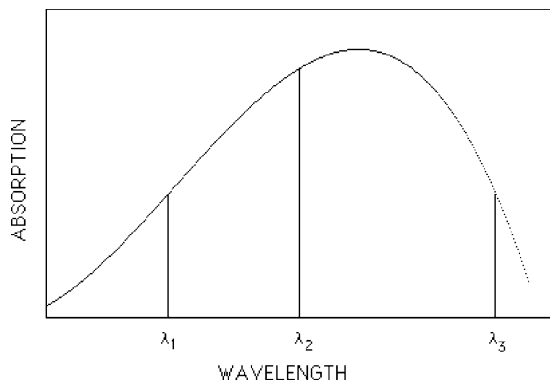
FIGURE 8.1. The concept of action spectrum (see text).

wavelengths l_1 and l_2 has been measured. The effect of the irradiation is plotted along the vertical axis versus some quantification of light on the horizontal axis (this can be either photon fluence or photon fluence rate or irradiance, depending on what is being studied).

Note that if we compare the effects of a certain amount of light or a certain irradiance (such as that indicated by 1 or 2 in Fig. 8.2) for the two wavelengths, these effects do not (except in very special cases) have the same ratio (2) as the corresponding absorption coefficients in Fig. 8.1. Thus, we cannot construct an action spectrum just by comparing effects of a fixed exposure or irradiance. We
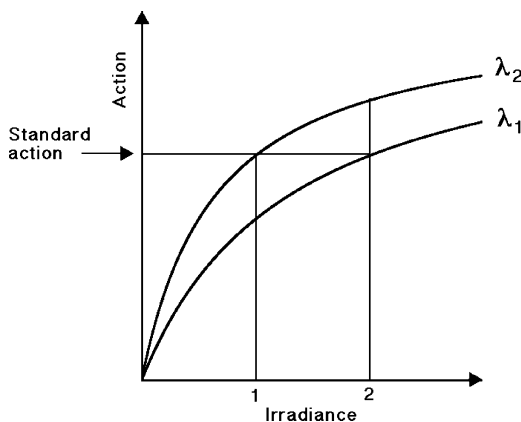
FIGURE 8.2. The effect of different exposures of a sample (same system as in Fig. 8.1) on light of wavelengths λ_1 and λ_2. The effect or action of the light is plotted on the vertical axis. We compare in particular how much light is needed to achieve a certain action, which we choose as a standard action. We can see that twice as much is needed at wavelength λ_1 as at λ_2. From this we can deduce that light of wavelength λ_1 is absorbed by the active pigment only half as efficiently as light of wavelength λ_2.

must construct curves such as those in Fig. 8.2, so we can see how much light is needed for a specific effect to follow, which we choose as standard action.

The rest of this chapter will be more historical in character than other chapters. My experience is that action spectroscopy is better understood by studying several real examples of its use than theory alone. In addition, the papers cited here include some that can stand as good examples for young scientists. In some cases they reflect real scientific ingenuity, and despite the rapid development of science they have withstood the ravages of time remarkably well.

8.2. The Oldest History: Investigation of Photosynthesis by Means of Action Spectroscopy

Action spectroscopy may have its roots in Young's and von Helmholtz's theories about color vision. The first one, to my knowledge, to directly use action spectroscopy was T.W. Engelmann (1882a,b, 1884). He projected, under the microscope, spectra onto different algae and assayed the amounts of oxygen formed as a consequence of photosynthesis taking place in the algae. He estimated the relative amounts of oxygen by watching the accumulation of oxygen-loving (aerotactic) bacteria (Fig. 8.3).

Engelmann compared the oxygen-forming efficiency of different lights by reducing the light until the swimming movements of the algae stopped due to oxygen deficiency. In this way he could ascertain that in green algae it is chlorophyll that absorbs the light active in photosynthesis, while other pigments also participate in other kinds of algae. Figure 8.4 shows some of his comparisons between absorption spectra and action spectra. The chlorophyll present in red algae (as evident from their absorption spectra) does not show up in the action
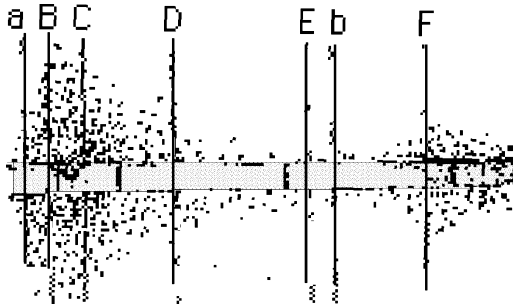
FIGURE 8.3. A piece of a filamentous green alga (*Cladophora*, of which two whole cells and parts of two more cells are seen) with swimming bacteria in the sunlight spectrum projected in a microscope. The letters indicate the Fraunhofer lines in the solar spectrum, which are used for wavelength calibration: a = 718 nm, B = 687 nm, C = 656 nm, D = 589 nm, E = 527 nm, b = 518 nm, F = 486 nm. The accumulation of bacteria is greatest in the red region around 680 nm, and in the blue region below 486 nm. These regions correspond to the main absorption bands of chlorophyll. (From Engelmann 1882a.)
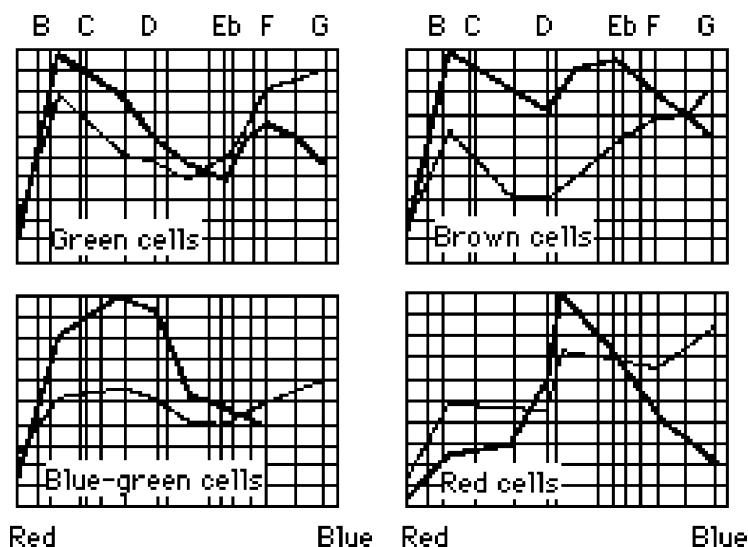
FIGURE 8.4. Absorption spectra for algal cells (percent of incident light not penetrating the cells, thin lines) and action spectra for photosynthesis (thick lines). The high efficiency of light around 520 nm for photosynthesis by brown algae is due to light capture by the carotenoid fucoxanthol, the high efficiency around 620 nm in blue green algae to light capture by phycocyanin, and the high activity around 560 nm in red algae to light capture by phycoerythrin. (From Engelmann 1884.)

spectrum for their oxygen production. The cause of this surprising fact was not revealed until after World War II when Duysens, Emerson, and others discovered that two different photochemical systems cooperate in plant photosynthesis.

In addition to being an important step in the development of action spectroscopy and also in the history of photosynthesis research, Engelmann's experiments are important as early examples of a very sensitive "bioassay" of a chemical compound. The method of measuring oxygen by means of bacteria was so unconventional and the stated sensitivity in relation to other methods available at the time so remarkable that Engelmann was challenging the scientific authorities of his time. The algologist Pringsheim (1886) in Berlin as well as the Russian photosynthesis expert Timiriazeff (1885) found reason to criticize him using very harsh words.

Engelmann drew the correct conclusion that, in addition to chlorophyll, other pigments (colored substances) are able to absorb light and make it available to the photosynthesis process. He also understood (Engelmann 1882b) that there are other pigments in plant cells, which do not participate in photosynthesis but, on the contrary, "shadow" or "screen" the photosynthetically active pigments.

Engelmann's student Gaudikov studied chromatic adaptation (a designation in today's language, more consistent with the usual meanings of adaptation and acclimation, would be chromatic acclimation) in red algae and cyanobacteria, i.e. their acclimation to light of different colors. However, action spectra for this process were not determined until the 1960s by the Japanese Fujita and Hattori
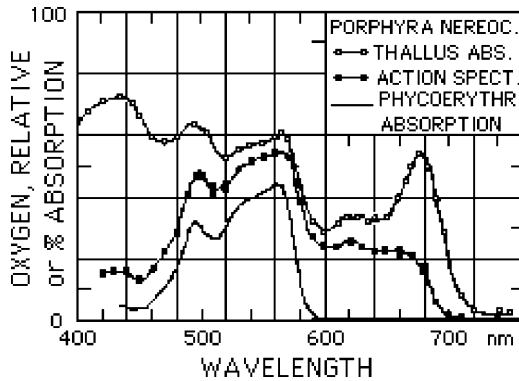
FIGURE 8.5. The action spectrum for photosynthetic oxygen production in the red alga *Porphyra nereocystis* compared to the absorption spectrum of the same alga (Thallus abs.) and to the absorption spectrum of extracted phycoerythrin. (From Haxo and Blinks 1950.)

(1962) and, in the 1970s, with greater precision, by the Americans J. Scheibe, S. Diakoff, and T.C. Vogelmann (see Diakoff and Scheibe 1973, Vogelmann and Scheibe 1978).

As for action spectra of photosynthesis, a few investigations were carried out during the intervening years, but real progress beyond Engelmann's results did not take place until the 1940s. For details of this development the reader is referred to Haxo (1960). An early attempt was made also by Levring (1947) in Sweden to determine action spectra for photosynthesis in various algae, but he used wide spectral regions isolated with filters.

In this connection it is interesting to see how different scientists emphasized different aspects: Engelmann discussed in detail his method, spectral bandwidth, etc., but lumped the algae together under the headings "green cells," "red cells," etc. Levring was less critical with regard to method but careful to state the species used, and published separate spectra for closely related species.

It was above all the spectra measured by the Americans Haxo and Blinks (1950) by a polarographic method for oxygen measurement that was to yield results valid to this day (Fig. 8.5). Because of them it became possible to do very careful comparisons between action spectra for photosynthesis and absorption spectra for various pigments in plants. Per Halldal brought this method to Sweden and improved it further (see Björn, Sundqvist and Öquist 2007).

8.3. Investigation of Respiration Using Action Spectroscopy

The great Otto Warburg and his constant coworker Erwin Negelein (who, by the way, also determined action spectra for photosynthesis) over many years studied how the respiration of yeast cells is inhibited by carbon monoxide and
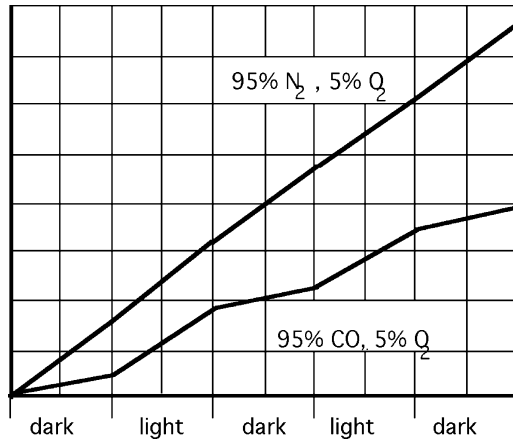
FIGURE 8.6. The effect of light on oxygen uptake (respiration, vertical axis) in yeast in an atmosphere of 95% nitrogen and 5% oxygen (straight line) and in a mixture of 95% carbon monoxide and 5% oxygen. The horizontal coordinate is time, with alternating light and dark periods. (From Warburg 1926.)

how this inhibition can be removed by light (Fig. 8.6). They developed action spectroscopy to an accurate quantitative method. As explicitly stated in one of their many papers, although they carried out the experiments together, it was Warburg who was the ingenious theoretician.

   Their investigation led to the conclusion that the *Atmungsferment* (which we now call cytochrome *c* oxidase) is a protein to which iron-containing heme is bound and that the inactive complex formed with carbon monoxide is dissociated by light. The conclusion rests on the observation that the action spectrum for removing the inhibition of respiration by carbon monoxide agrees very well with the absorption spectrum for a complex between carbon monoxide and heme (Fig. 8.7). There is only a small shift in wavelength, which is explained by the binding to protein.

8.4. The DNA That Was Forgotten

At the beginning of the last century Hertel (1905) in Jena had begun to study how microorganisms are affected by ultraviolet radiation. He managed to isolate nine different spectral lines from 210 to 558 nm and quantify the radiation using a thermopile. Considering the time, this was no small feat. Unfortunately, the evaluation of the biological effect was only semiquantitative. For constructing action spectra, he determined the irradiance that gave a just noticeable effect on the organism observable under the microscope. This effect could be stimulation of movement in *Paramecium* or contraction in rotifers. Unfortunately, he had no spectral line between 232 and 280 nm, and he therefore missed that region,
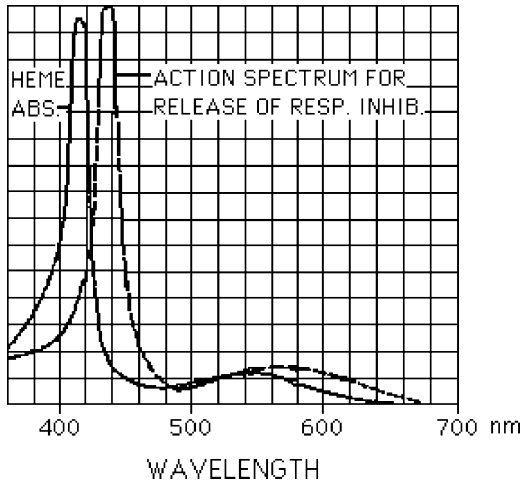
FIGURE 8.7. Comparison between the absorption spectrum for heme and the action spectrum for release from CO inhibition of yeast respiration. (From Warburg and Negelein 1929b; see also Warburg and Negelein 1929a.)

which would later prove to be particularly interesting. Hertel's action spectra for ultraviolet damage to microorganisms are shown in Fig. 8.8. His experiments gave rise to a long-lived opinion that the deleterious action of ultraviolet radiation rises at an even rate toward shorter wavelength.

In the late 1920s, however, Gates (1928, 1930) found that the ability of ultraviolet radiation to kill bacteria varies with wavelength in the same way as does the ability of nucleic acid to absorb radiation (Fig. 8.9). This was the
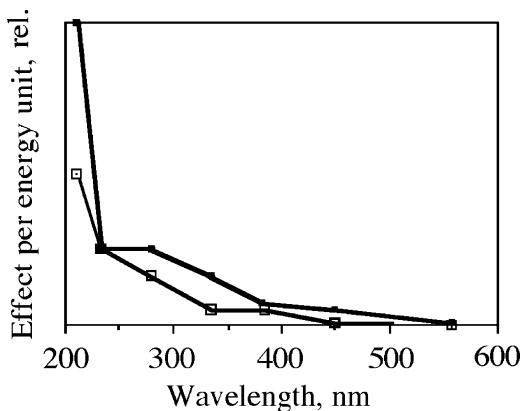
FIGURE 8.8. Action spectra for induction of swimming movements in *Paramecium* (top curve) and for contraction in Rotaria (curve with squares). (Redrawn after Hertel 1905.)
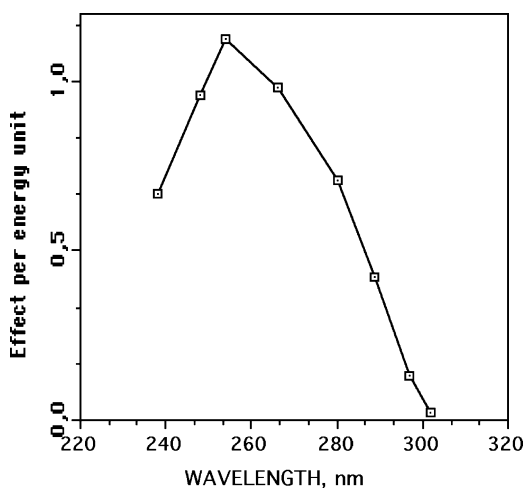
FIGURE 8.9. Action spectrum for "killing" (inactivation of cell division) in the bacterium *Staphylococcus aureus*. The graph is similar to the absorption spectrum for DNA. (Redrawn after Gates 1930.)

first indication of the fundamental importance of nucleic acid to life and a key experiment at the entrance to molecular biology.

At the same time as Gates's first report, another one was published, which was also on the road leading to the great revolution—Griffith's (1928) discovery of bacterial transformation. But it was not until after 1944 that the biological role of DNA became generally accepted by the demonstration of bacterial transformation by DNA (Avery, MacLeod, and MacCarty 1944).

One may wonder why Gates's experiments did not lead to a quicker development of DNA research. His work was in no way inferior to the transformation work. Perhaps an important reason was his way of publishing. In his first paper (1928) he does not show any convincing data. Despite this he clearly spelled out (although as we may think in retrospect, in a very cautious way) what was later proven to be essentially correct: "The close reciprocal correspondance between the curves of absorption of ultraviolet energy by these nuclear derivatives not only promotes the possibility that a single reaction is involved in the lethal action of ultra-violet light, but has a wider significance in pointing to these substances as essential elements in growth and reproduction." After discussing some experiments done by others, which strengthened his views, he wrote: "Thus, while the relation of thymonucleic acid [i.e., DNA] to cell growth and reproduction remains a matter of conjecture, nevertheless the high concentration in the thymus gland and the coincidence of the evidence from these three independent series of experiments seem worthy of note, without further comment at present."

In the next paper Gates (1929) includes data for a bacterium, but the diagram is not drawn in such a way that it is easy to see the similarity to the DNA absorption spectrum, and DNA is mentioned neither in the discussion nor in

the summary. In one more paper from 1930 the deleterious action of ultraviolet radiation is treated from another point of view. In one of his last publications, from 1931, Gates compares the action spectra for two bacterial species to the absorption spectra of the bacteria. About the critical substance, the destruction of which causes the death of the bacterial cells, Gates writes: "An examination of the evidence for its concentration in the cell nucleus, and the further search for evidence of its chemical character are reserved for the final paper of this series." Gates never got the opportunity to publish this final paper. He died on June 17, 1933. Although one paper was published posthumously, his followers obviously did not consider his ideas about DNA important, or even correct.

Contributing reasons to the fact that Gates's ideas never got the attention that their importance deserved were (1) that he was wrongly cited by later scientists (Hollaender and Claus 1936; e.g., "the maximum at 2499 A as reported by Gates"); (2), later scientists like Giese and Leighton (1935) went over to studying phenomena, e.g., swimming movements in *Paramecium*, which were very protein-dependent. Action spectra for such processes have maxima around 280 nm. This diverted the interest from nucleic acids to protein.

8.5. Plant Vision

One of the greatest triumphs of biological action spectroscopy is the discovery of the "vision pigment" of plants, phytochrome. However, at this point of the story action spectroscopy is getting more complicated.

When the phytochrome saga opened, it was known that some effects of red light on plants could be canceled by exposing the plants to far-red light after the red. For instance, some lettuce seeds do not germinate unless they are exposed to light after they have been allowed to take up water. Red light was found to be most efficient for this effect. Germination could be prevented by exposing the seeds to far-red light (720–740 nm) after the red.

Another example of red/far-red antagonism was the mode of growth of bean seedlings developing in darkness. The tip of such a seedling is curved to a "plumular hook," but if the seedling receives just a minute of red light, the hook straightens out during subsequent growth (Fig. 8.10). Withrow, Klein, and Elstad (1957) tackled the problem of quantifying the straightening effect of different kinds of light. For each of various fluences of light of different wavelengths, they measured by how many degrees the hooks of the bean plants were straightened out (Fig. 8.11).

They also quantified how efficient different kinds of light were in counteracting the straightening effect of a previously administered saturating fluence of red light (Fig. 8.11). Based on the results, they were able to postulate the existense of a light-sensitive growth regulator, phytochrome. Phytochrome is formed in the plant in an inactive form (called P_r), which is transformable into the active form (P_{fr}) by red light.
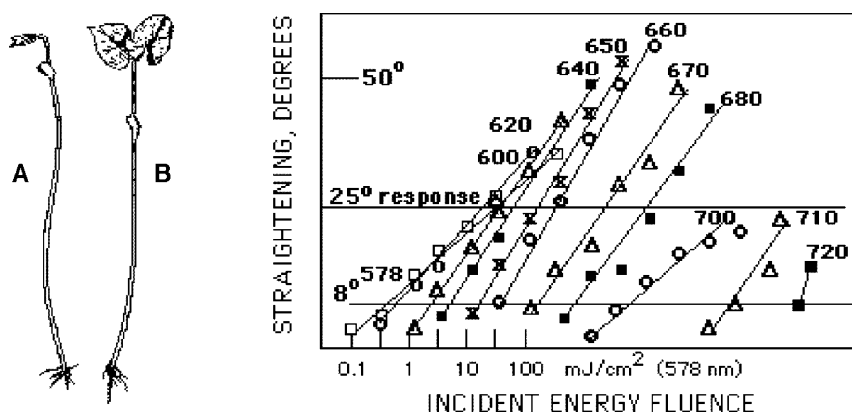
FIGURE 8.10. Left: Bean plants grown (A) in darkness and (B) in darkness except for a few minutes of red light. Right: The straightening effect on bean hooks of light of various wavelengths as a function of the energy fluence. The scale on the horizontal axis is for the wavelength 578 nm, as an example to show that this scale is logarithmic. The scales for the other wavelengths have been moved in factor steps of 0.3 to make all the data points and regression lines visible. In the original publication there is one more data panel like this for the spectral range 385–578 nm. (Redrawn from Withrow, Klein, and Elstad 1957.)
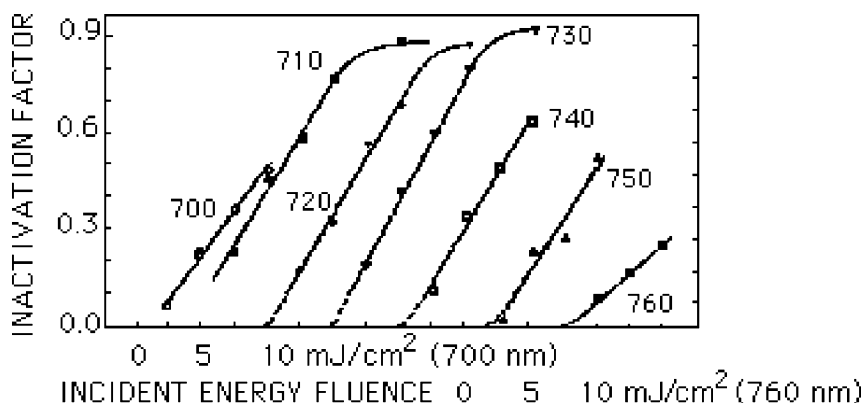
FIGURE 8.11. Inactivation of red-induced hook straightening in bean plants by light of different wavelength as a function of fluence. In this case a linear fluence scale was found to give better linearity of regression than the logarithmic scale in the previous graph. To make all data points and regression lines distinguishable, the fluence scales were given different zero points for different wavelengths; only the extremes are shown here. (Redrawn from Withrow, Klein, and Elstad 1957.)
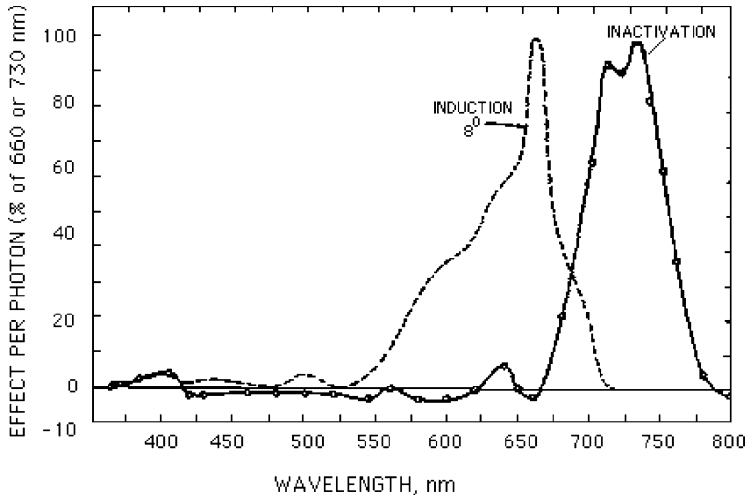
FIGURE 8.12. Action spectra for straightening and for the inhibition of red-light–induced straightening of the bean hook, constructed from regression lines of the kind shown in Figs. 8.10 and 8.11. (Redrawn from Withrow, Klein, and Elstad 1957.)

The spectral curves that were obtained for the "straightening" and "bending" effects (Fig. 8.12) were postulated to correspond to absorption spectra for P_r and P_{fr}, respectively. It would never have been possible to isolate the phytochrome had not its "spectral signature" been determined beforehand in this way.

In Figs. 8.10 and 8.11 the lines for different wavelengths are not parallel. This means that the shape of the action spectra that are constructed from these lines will depend on the chosen level of action. That the curves are not parallel has to do with the fact that two photochemical reactions are involved to varying extents in all cases, i.e., the transformation of P_r to P_{fr} and the transformation of P_{fr} to P_r. The "most correct" shapes, i.e., those most closely corresponding to the absorption spectra of P_r and P_{fr} (Fig. 8.13), are obtained by investigating the effects of very small fluences, resulting in small effects.

The complications of this light-sensitive system are well demonstrated by the action spectrum determined by Hartmann (1967) for the inhibiting effect of prolonged and relatively strong illumination on the extension growth of lettuce hypocotyls (Fig. 8.14). At first glance it does not seem to have anything to do with the shapes of the absorption spectra of the two phytochrome forms. But Hartmann showed that this phenomenon could be explained by phytochrome being the mediator of the light action. However, in this case one has to take into account not only the photochemical reactions, but also the fact that the physiologically active form of phytochrome, P_{fr}, is unstable and disappears if there is no Pr present from which P_{fr} can be continually reformed. For this reason that light gives the greatest physiological effect, which causes only a small part of the phytochrome to be continuously converted to P_{fr}. Light of longer wavelength has no effect because too little P_{fr} is formed. Light of too short a
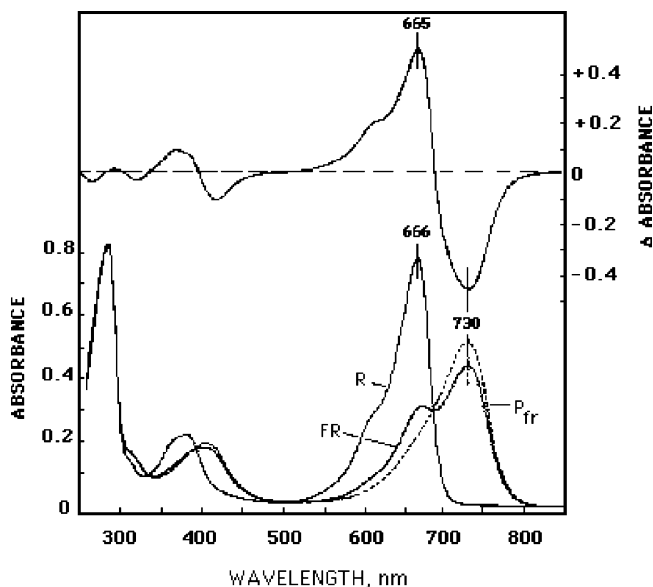
FIGURE 8.13. Absorption spectra of purified phytochrome from oats. The curve marked R is the measured absorption of far-red irradiated solution, containing almost only P_r. The curve marked FR is the measured absorption of red irradiated solution, containing mostly P_{fr} and some P_r. The dotted curve marked P_{fr} is the estimated spectrum of pure P_{fr}, which cannot be measured directly, since red light only partially converts P_r to P_{fr}. The top curve is a so-called difference spectrum showing the difference in absorption between far-red irradiated and red irradiated solutions. Since only the change due to irradiation shows up in this, almost the same difference spectrum can be obtained from plant tissue. (After Vierstra and Quail 1983a,b.)
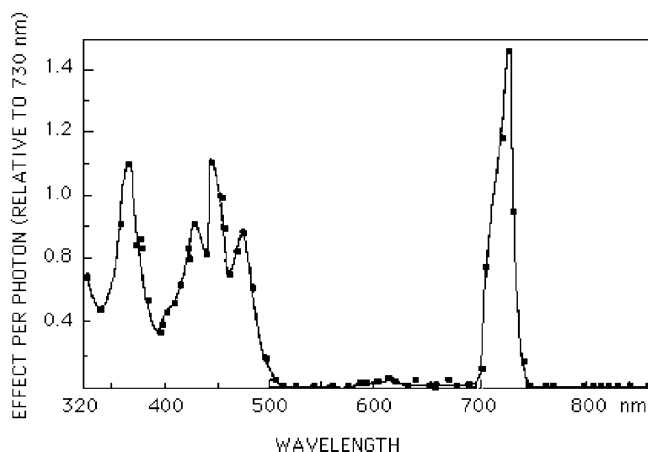
wavelength has no effect because P_{fr} is formed too quickly and all phytochrome disappears before it can act for a sufficient amount of time. The inhibition of the growth of the lettuce hypocotyls is an example of a so-called high intensity reaction (HIR).

8.6. Protochlorophyllide Photoreduction to Chlorophyllide *a*

The present author and many other researchers have studied the action spectra for synthesis of chlorophyll and formation of chlorophyll. Important early contributions were made by J.H.C. Smith at the Carnegie Institution, T.N. Godnev and A.A. Shlyk in Belorussia, and H. Virgin in Sweden. Virgin's former students have continued this line of research in Göteborg (see Sundqvist and Björn 2007).

Chlorophyll formation is governed by several light-sensitive processes: conversion of protochlorophyllide to chlorophyllide with enzyme-bound protochlorophyllide as the light absorber, conversion of phytochrome, and action on the so-called blue light receptor.

One specific question in this context was whether radiation absorbed in the aromatic amino acids of the enzyme NADPH–protochlorophyllide photooxidoreductase would be able to cause the conversion of protochlorophyllide to chlorophyllide in the same way as does radiation absorbed in the protochlorophyllide itself. In Fig. 8.15 the absorption of the NADPH–protochlorophyllide photoreductase complex with its substrates NADPH and protochlorophyllide is shown by the solid curve. In the visible region the absorption is due to the protochlorophyllide. The hight peak at 280 nm, on the other hand, is due to aromatic amino acids in the protein. The action spectrum for protochlorophyllide photoreduction, shown by dots, has essentially the same features in the visible region, but lacks the high peak at 280 nm. The conclusion is that energy absorbed in the aromatic aminoacids cannot be used for photoreduction. There is also a small difference between absorption and action spectrum in the blue region (the so-called Soret peak of the spectra). This is probably because there are two fractions of protochlorophyll with slightly different spectra, of which only one can be converted by light (there may be no reductant, NADPH bound to the "inactive" complexes). There is also some blue-absorbing carotenoid contributing to the absorption spectrum.

FIGURE 8.14. Action spectrum for the inhibition of extension growth of lettuce hypocotyls by prolonged irradiation with strong light (high intensity reaction). (After Hartmann 1967.)
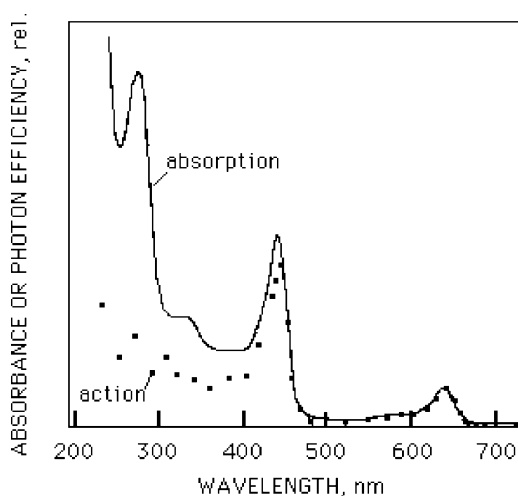
FIGURE 8.15. The absorption spectrum of purified "protochlorophyll holochrome" (complex between protochlorophyllide, NADPH and NADPH–protochlorophyllide photooxidoreductase) extracted from etiolated bean plants (Schopfer and Siegelman 1969) and the action spectrum for protochlorophyllide photoreduction to chlorophyllide *a* (Björn 1969a). (Redrawn from Björn 1969b.)

8.7. Limitations of Action Spectroscopy: The Elusive Blue Light Receptor

Numerous "blue light phenomena" have been studied in plants and fungi: phototropism, chloroplast rearrangements, plastid differentiation, and nastic movements, to mention a few. The discussion about the possible nature of the molecule absorbing the active light in these processes has centered mainly on carotenoids and flavoproteins, because the action spectra are similar to absorption spectra of these compounds (which are so similar to each other and so variable with conditions and molecular details that a conclusion on action spectra alone seems impossible). As described in Chapter 10, it has been found that most blue light phenomena are mediated by flavoproteins, but that some, e.g., stomatal movements, may be carotenoid mediated. Because of the similarity of the absorption spectra for these two groups of compounds, action spectroscopy has not been able to distinguish between them. The questions have now mostly been solved, mainly by methods of molecular biology. However, action spectroscopy, after more than a hundred years, is a method still in use (e.g., Ziv, Tovin, Strasser, and Gothilf 2007).

8.8. Another Use for Action Spectra

So far we have only discussed the use of action spectroscopy for identifying the molecules absorbing the light driving the various photoprocesses. I would like to point out one more important reason for determining action spectra. For this

we shall go back to near the beginning of this chapter, to the damaging effect of ultraviolet radiation, but look at it from another angle.

Over the past thirty years there has been concern about the depletion of the stratospheric ozone layer (see Chapter 19). Such depletion results in increased levels of ultraviolet radiation at the surface of the earth (unless other changes in the atmosphere were to compensate for the depletion in stratospheric ozone). Experiments have been carried out to forecast the biological effects of such changes in radiation. Ozone depletion has been simulated by exposing the organisms to be studied to artificial ultraviolet radiation. One problem has been that the artificial radiation cannot be given the same spectral composition as the additional solar radiation that would leak through a depleted ozone layer. Therefore, weighting functions have been needed to calculate how much artificial ultraviolet radiation that has to be administered to simulate a certain ozone depletion, and for this one has to determine action spectra for different ultraviolet effects. Initially one relied on ordinary, "monochromatic" action spectra, determined as the other spectra in this chapter. However, since so many different ultraviolet effects with different action spectra are involved, it has turned out to be more realistic to determine "polychromatic action spectra." For this, one starts with a full spectrum, and for different samples cuts away more and more of the short-wavelength part.

References

Avery, O.T., MacLeod, C.M. and McCarty, M. (1944) Studies on the chemical nature of the substance inducing transformation of pneumococcal types. J. Exp. Med. 79, 137–157.

Björn, L.O. (1969a) Action spectra for transformation and fluorescence of protochlorophyll holochrome from bean leaves. Physiol. Plant. 22, 1–17.

Björn, L.O. (1969b) Studies on the phototransformation and fluorescence of protochlorophyll holochrome in vitro. In H. Metzner (Ed.), *Progress in photosynthesis research*, Vol. II, pp. 618–629. H. Laupp Jr., Tübingen, Germany.

Björn, L.O., Sundqvist, C., and Öquist, G. (2007) A tribute to Per Halldal (1922–1986), a Norwegian photobiologist in Sweden. Photosynthesis Res. 92, 7–11.

Diakoff, S. and Scheibe, J. (1973) Action spectra for chromatic adaptation in *Tolypothrix tenuis*. Plant Physiol. 51, 382–385.

Engelmann, Th. W. (1882a) Ueber Sauerstoffausscheidung von Pflanzenzellen im Mikrospektrum. Bot. Ztg. 40, 419–426.

Engelmann, Th. W. (1882b) Ueber Assimilation von *Haematococcus*. Bot. Ztg. 40, 663–669.

Engelmann, Th. W. (1884) Untersuchungen über die quantitativen Beziehungen zwischen Absorption des Lichtes und Assimilation in Pflanzenzellen. Bot. Ztg. 42, 81–94, 97–106 and Tafel II.

Fujita, Y. and Hattori, A. (1962) Photochemical interconversion between precursors of phycobilin chromoproteids in *Tolypothrix tenuis*. Plant Cell Physiol. 3, 209–220.

Gates, F.L. (1928) On nuclear derivatives and the lethal action of ultra-violet light. Science 68, 479–480.

Gates, F.L. (1929) A study of the bactericidal action of ultra violet light. I. The reaction to monochromatic radiations. J. Gen. Physiol. 14, 31–42.

Gates, F.L. (1930). A study of the action of ultra violet light III. The absorption of ultra violet light by bacteria. J. Gen. Physiol. 14, 31–42.

Giese, A.C. and Leighton, P.A. (1935) Quantitative studies on the photolethal effects of quartz ultra-violet radiation upon *Paramecium*. J. Gen. Physiol. 18, 557–571.

Griffith, F. (1928) The significance of pneumococcal types. J. Hygiene 27, 113–159.

Hartmann, K.M. (1967) Ein Wirkungsspektrum der Photomorphogenese unter Hochenergiebedingungen und seine Interpretation auf der Basis des Phytochroms (Hypokotylwachstumshemmung bei *Lactuca sativa* L.). Z. Naturforsch. 22b, 266–275.

Haxo, F.T. (1960) The wavelength dependence of photosynthesis and the role of accessory pigments. In: M.B. Allen (Ed.), *Comparative biochemistry of photoreactive systems*, pp. 339–376. Academic Press, New York.

Haxo, F.T. and Blinks, L.R. (1950) Photosynthetic action spectra of marine algae. J. Gen. Physiol. 33, 389–422.

Hertel, E. (1905) Ueber physiologische Wirkung von Strahlen verschiedener Wellenlänge. Zschr. Allgem. Physiol. 5, 95–122.

Hollaender, A. and Claus, W.D. (1936) The bactericidal effect of ultraviolet radiation on *Escherichia coli* in liquid suspensions. J. Gen. Physiol. 19, 753–765.

Levring, T. (1947) *Submarine daylight and the photosynthesis of marine algae*. Göteborgs Kgl. Vetenskaps- och Vitterhets-samhälles Handl., 6:e följden, ser. B, band 5, nr 6. 90 s.

Pringsheim, N. (1886) Zur Beurtheilung der Engelmann'schen Bakterienmethode in ihrer Brauchbarkeit zur quantitativen Bestimmung der Sauerstoffabgabe im Spektrum. Berl. Deutsch. Bot. Ges. 4, 40–46.

Schopfer, P. and Siegelman, H.W. (1969) Purification of protochlorophyllide holochrome. In H. Metzner (Ed.), *Progress in photosynthesis research,* vol. II, pp. 612–618. H. Laupp Jr., Tübingen.

Sundqvist, C. and Björn, L.O. (2007) A tribute to Hemming Virgin, a Swedish pioneer in plant photobiology. Photosynth. Res. 92, 13–16.

Timiriazeff, C. (1885) État actuel de nos conaissances sur la fonction chlorophyllienne. Ann. des Sc. Nat. Botanique (3) Tome II.

Vierstra, R.D. and Quail, P.H. (1983a) Purification and initial characterization of 124-kilodalton phytochrome from *Avena*. Biochemistry 22, 2498–2505.

Vierstra, R.D. and Quail, P.H. (1983b) Photochemistry of 124-kilodalton *Avena* phytochrome *in vitro*. Plant Physiol. 72, 264–267.

Vogelmann, T.C. and Scheibe, J. (1978) Action spectra for chromatic adaptation in the blue-green alga *Fremyella diplosiphon*. Planta 143, 233–239.

Warburg, O. (1926) Über die Wirkung des Kohlenoxyds auf den Stoffwechsel der Hefe. Biochem. Z. 177, 471–486.

Warburg, O. and Negelein, E. (1929a) Über die photochemische Dissoziation bei intermittierender Belichtung und das absolute Absorptionsspektrum des Atmungsferments. Biochem. Z. 202, 202–228.

Warburg, O. and Negelein, E. (1929b) Absolutes Absorptionsspektrum des Atmungsferments. Biochem. Z. 204, 495–499.

Withrow, R.B., Klein, W.H. and Elstad, V. (1957) Action spectra of photomorphogenetic induction and its inactivation. Plant Physiol. 32, 453–462.

Ziv, L., Tovin, A., Strasser, D. and Gothilf, Y. (2007) Spectral sensitivity of melatonin suppression in the zebrafish pineal gland. Exp. Eye Res. 84, 92–99.

9
Spectral Tuning in Biology

Lars Olof Björn and Helen Ghiradella

Abstract: Spectral tuning is a diverse topic, both with regard to mechanism and with regard to biological significance. We have touched upon a related topic already when dealing with quantum dots in Chapter 5. In organisms, spectral tuning can be achieved both by chemical means (choice of pigment) and by physical means. The latter aspect is treated towards the end of the chapter in a section on structural color. As for the functional aspect, spectral tuning has significance for photosynthesis, vision, bioluminescence, and coloration both for protection and signalling in various contexts.

9.1. Introduction

The justification for a book about photobiology rests partly on combination of various specialities for interdisciplinary comparisons. One topic suitable for comparisons is "spectral tuning." By this we mean the principles for how spectra of pigments, and factors that can modify their spectral responses, are adjusted to the needs of the organisms that produce them. A number of examples will be found in this chapter.

To pigments, substances that produce color by absorbing light of some wavelengths and reflecting or transmitting the rest, we must add a second class of color mechanism, *structural* colors. These are produced by the interaction of light with the detailed architecture of the material or structure on which it falls. We will begin with a discussion of biological pigments and then move on to biological structural colors. Finally, we will discuss some additional mechanisms by which organisms control their spectral presentation to the world.

Spectral tuning is relevant for vision (not only for color vision), photosynthesis, bioluminescence, flower colors, and adaptive coloration of animals, and especially for animals that move around among green plants, to increase contrast of edges. These processes are not independent. Flower colors are adapted to the vision of pollinators and as a contrast to photosynthetic pigments. Bioluminescence and vision have evolved together. Phytochrome has evolved to discriminate between direct daylight and light modified by chlorophyll absorption. The basis is the spectrum of the sun. To begin with, let us see what the relation is between

the spectrum of the most important of all pigments, chlorophyll *a*, and the spectrum of the sun.

9.2. Why Are Plants Green?

Many people have discussed the spectrum of chlorophyll in relation to daylight. Some have come to the conclusion that they do not match well, as absorption "in the middle of the spectrum," i.e., the green band, is weak. A common idea is that an ideal pigment for photosynthetic energy conversion ought to be either black, absorbing all available radiation, or absorb most efficiently at the "peak" of daylight.

But what is the "peak" wavelength for daylight? The maximum of the daylight spectrum depends on how we plot it. For the present purpose, to simplify comparisons and calculations, we may represent the daylight spectrum by that of a 6000 K blackbody radiator, and thus apply Planck's radiation law (Chapter 1). We can then calculate that if we plot the spectrum as energy per uniform wavelength interval the maximum is at 480 nm. But if we instead plot it as photons per uniform wavelength interval, the maximum is at 600 nm, and if we, following the habits of physicists, plot the spectrum as energy per uniform frequency interval, or photons per uniform frequency interval, the peak will be seen at frequencies corresponding to 800 nm and 1200 nm, respectively.

Thus the "maximum of the daylight spectrum" is an ambiguous concept, and we have to find another way of optimizing our pigment. As for the idea that an ideal pigment should absorb everything, we should remember that the better a substance absorbs, the better it emits, and the transformation of radiant energy into other energy forms is just the balance between absorption and re-radiation. That total absorption is not an ideal is even more apparent in the case of color vision. Vertebrate cones, which are cells receiving light signals for color vision, are shorter than the rods involved in "noncolor night vision" (scotopic vision), and therefore absorb a smaller portion of the light and discriminate between wavelength bands better than they would if they were as long as rods.

Photosynthesis depends on photochemistry, and photochemistry works particle to particle, photon to molecule. The useful energy storage can be regarded as the product of the number of reacting photons and the free energy that each converted photon contributes. Björn (1976) following this principle comes to the conclusion that the long-wave absorption band of a pigment giving maximum energy conversion in direct sunlight should be rather narrow and have a maximum at 707 nm. Furthermore the pigment should be highly fluorescent (when not quenched by photochemistry). The maximum chemical potential difference that can be created by a one-step system is $\mu_o = kT \ln[\Phi r^2/4R^2)] + h\nu_o(1 - T/T_S) - b^2[h^2/(2k)]T(1/T^2 - 1/T_s^2)$, where k = Boltzmann's constant, Φ Planck's constant, T ambient temperature, T_S the temperature of the radiating surface of the Sun, μ the fluorescence yield, r the radius of the Sun, R the Earth-Sun distance, ν_o

the frequency of the spectral peak of the absorption band, and b a parameter determining the width of the absorption band such that the half-band width is $2b\sqrt{(2\ln2)} = 2.35b$. With numerical values inserted, this becomes $\mu_o = -0.342$ eV$+(19/20)$ h$\nu_o - 6.6.10^{-28}b^2$ eV s^2 (eV stands for electron volts). The effective chemical potential difference under conditions of maximum energy conversion is 0.13 eV lower than that (just as the voltage of an electrical battery is lowered when power is drawn from it).

All this is for full sunlight. The optimum position of the absorption peak is lowered by 12 nm for every 10-fold decrease of fluence rate, even if the spectrum of the daylight is not changed. Thus it appears that the long-wavelength band of chlorophyll *a* in vivo is rather well matched to the conditions of our planet. The "blue" absorption band of chlorophyll (the Soret band) does not contribute to chemical potential, but leads to increased photon absorption and thus increased energy conversion, as do various accessory pigments.

Mauzerall (1976) has speculated on how chlorophylls can have evolved from porphyrins along a path of increasing lipophilicity, making them suitable for incorporation into membranes.

Various types of bacterial chlorophylls have absorption bands at longer wavelengths. They are not adapted to direct daylight, but to the light that penetrates down to the places (such as anoxic sediments below algae absorbing shorter wavelength light) where these bacteria live. The record in long wavelengths is held by bacteriochlorophyll *b*. Its spectrum peaks at 1020 nm, beyond two infrared absorption bands of water.

Kiang et al. (2007) and Stomp et al. (2007) have detailed how various photosynthetic pigments are adapted for various environments on earth.

9.3. What Determines Spectra of Pigments?

Generally speaking, the absorption spectrum of a pigment is determined by (1) the structure of the chromophore(s) and (2) the environment of the chromophore.

The most important feature in chromophore structure is the arrangement of conjugated double bonds (alternating single and double bonds), i.e., the π electron clouds. The environment of the chromophore in many cases consists of, or is at least dominated by, a protein to which the chromophore is bound, but there are also important cases, such as vacuolar flower pigments, where the chromophore is not protein bound, and other factors are the main concern.

In general, the absorption peak with longest wavelength for a molecule with conjugated bonds increases with the length of the conjugated bond system. It depends, as we shall see, also very much on the shape of the conjugated system, whether it is straight or not and, in the case of macrocycles as in chlorophylls, on its symmetry. If conjugation is broken by single bonds and thus divided into two conjugated systems, the absorption spectrum is similar to the sum of the contributions from the two systems.

As a simple example of the effect of conjugated system length, let us consider a series of polyene hydrocarbons, $CH_2 = CH - (CH = CH)_{n-2} - CH = CH_2$, with n conjugated double bonds. Such a simple and regular system is fairly well understood. Energy levels for the ground state and the first excited state can be computed, and the wavelength of the long-wavelength absorption maximum corresponding to their difference determined. Two common approaches are the free electron (FE) theory and the linear combination of atomic orbitals (LCAO) method. In the former the Schrödinger equation is applied to a "gas" of π-electrons in a "box potential," i.e., a potential which is constant over an interval corresponding to the length of the conjugated system and zero outside of it. In the simplest version of this the wavelength of the maximum would vary linearly with the length of the conjugated system, i.e., with n. However, one must consider that the length of the bonds between carbon atoms is not constant (every second bond is longer, and there are "edge effects"), and therefore the potential is not constant in the "box"; and Kuhn has developed a method to allow for this, the result of which is shown in Fig. 9.1 (another complication, as we shall see later, is that the chain is not straight and may be folded in various ways). In the LCAO method one starts by computing the orbitals of the individual atoms, and then sums up their wave functions. In a refined version due to Hückel one allows for the variation in bond length. Both methods give quite good results for low values of n, but underestimate the wavelength for large values of n. The reader interested in more information on these computational methods is referred to a textbook on electron spectra of organic molecules, such as that by Jensen and Bunker (2000) or the still very readable one by Murrell (1963).

The carotenoids, and the retinals of visual pigments, are biologically important molecules resembling polyenes. The principle of spectral tuning by variation of
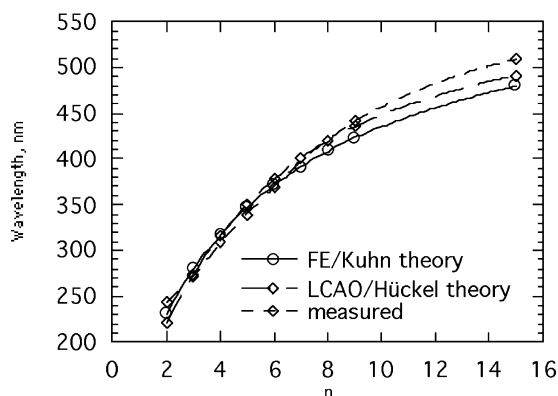
FIGURE 9.1. The wavelength of the absorption maximum with longest wavelength for a series of polyenes with formula $CH_2 = CH - (CH = CH)_{n-2} - CH = CH_2$. The graph shows experimental values, as well as values calculated by two different methods, the Kuhn version of the free electron theory, and the Hückel version of the linear combination of atomic orbitals theory.

the conjugated bond system is beautifully exploited by plants in the regulation by the xanthophyll cycle of energy intake for photosynthesis (see Chapter 13). Also, the phycobiliproteins show a change in wavelength position related to the length of the conjugated system, but we shall see also that other factors are important for the tuning. A complication with simple polyenes and carotenoids is that the first excited state is "optically forbidden" or "dipole forbidden," i.e., cannot be reached from the ground state by light absorption (Schulten and Karplus 1972; see also Chapter 13). The absorption spectrum in the daylight region is due to transition to the second excited state (or, for carotenoids, the third excited state). The first excited state can still, for some carotenoids, participate in energy transfer to chlorophyll and make this very efficient (Thrash et al. 1979, Ritz et al. 2000), while for other carotenoids it is too low (Polívka et al. 1999, but see Frank et al. 2000).

9.4. Relation Between the Absorption and Molecular Structure of Chlorophylls

Chlorophylls can be classified into three main groups, depending on whether the nucleus is that of porphin with 11 conjugated double bonds, dihydroporphin with 10, or tetrahydroporphin with 9 conjugated double bonds. In Fig. 9.2 it is shown which chlorophylls belong to each group, as well as the positions in organic solvent (in most cases ethyl ether) of their main absorption bands.

As is evident from Fig. 9.2 the long-wavelength transition, called Q_y, corresponds to a smaller energy change in the tetrahydroporphin type bacteriochlorophylls than in the dihydroporphin type pigments, and to a smaller energy change in the dihydroporphin pigments than in the porphin pigments. Even in the porphin pigments there is a certain asymmetry (not shown in Fig. 9.2) due to the side chains, so even in these one can distinguish between Q_x and Q_y transitions. Q_x and Q_y transitions can be distinguished through measurements of polarisation of fluorescence excited by plane polarised light. Another way is to align the molecules in some way, for instance in thin films, and study the absorption dichroism.

But the effects due to the chromophore environment are sometimes even larger than the effects of the differences in the conjugated double bond system. Thus the in vivo environment (mainly the bonding to protein) changes the Q_y band as shown in Table 9.1

Those chlorophylls having the smallest energy gaps and the absorption bands at longest wavelengths are the reaction center special pairs (for exceptions, see Section 9.5). Their special absorption properties are due to formation of exciton complexes (see Chapter 1).

The reader who wishes to understand chlorophyll absorption spectra in more detail is referred to Linanto and Korppi-Tommola (2000). The theory of electronic spectra of organic molecules and the computational methods used to understand the spectra are treated in many books, e.g., Murrell (1963).

		Band maximum, nm		
		Qy	Qx	Soret
Porphin nucleus	Protochlorophyll	623	571	432
	Chlorophyll $c1$	637	585	441
	Chlorophyll $c2$	628	579	448
	Chlorophyll $c3$	626	586	452
Dihydroporphin nucleus	Chlorophyll a	662	578	430
	Chlorophyll b	642	550	453
	Chlorophyll d	688	-	447
	Chlorobium	650	575	
	chlorophylls	660	622	432
	(bacterioviridins)			
Tetrahydroporphin nucleus	Bacteriochl. a	773	577	358 & 391
	Bacteriochl. b	795	582	368 & 407

FIGURE 9.2. The ring systems for the three main classes of chlorophylls. These ring systems are flat. The conjugated double bond systems are indicated by heavy lines. While the conjugated system is rather isodiametric (approximating circular form) for the porphins, it is more elongated for the other two groups. The long axis of this elongated system is often referred to as the y axis, and the transition moment for the so-called Q_y transition lies along this axis. The x axis, and the direction of the Q_x transition, is almost perpendicular to this, but also in the plane of the ring. The short-wavelength "Soret" band is complex with transitions along both axes. For instance, for bacteriochlorophyll a the 358 Soret component is in the y direction and the 391 component in the x direction.

TABLE 9.1. Comparison of Absorption Spectra of Chlorophyll Pigments Position of Long-Wavelength (Q_y) Band (nm)

Pigment	In ethyl ether	In vivo
Protochlorophyll	624	630–650
Chlorophyll a	662	670–700
Chlorophyll b	644	650
Chlorophylls c	626-637	
Bacteriochlorophyll a	773	800–890
Bacteriochlorophyll b	795	1020
Bacteriochlorophyll c		725–750

9.5. Tuning of Chlorophyll *a* and *b* Absorption Peaks by the Molecular Environment

Chlorophyll *a* is the key pigment in almost all organisms with oxygenic photosynthesis, i.e., cyanobacteria, algae, and plants. It functions in both reaction centers I and II, and as antenna pigment in both photosystems. A great number of spectral forms can be distinguished in vivo and in thylakoid preparations.

In organic solvents the long-wavelength absorption peak of chlorophyll *a* lies at 662 nm (ethyl ether) to 663 nm (acetone), when the solution is dilute and the chlorophyll in a monomeric state. In vivo all chlorophyll a fractions are "red-shifted," i.e., shifted to longer wavelengths compared to this. Some of the antenna chlorophylls in photosystem II (PSII) have the smallest shift, while a few molecules in photosystem I have the largest shift and, perhaps surprisingly, have peaks at even longer wavelength than photosystem I (PSI) reaction center chlorophyll (P700).

Cinque et al. (2000) were able to specify the spectra of two particular antenna chlorophyll chromophores in maize by comparing recombinant chlorophyll proteins which lacked them in the wild type. They found that the long-wavelength (Q_y) peak of CP29 chlorophyll a is at 680 nm, and that of LHC II chlorophyll b at 652 nm. Thus the redshifts (bathochromic shifts) compared to solution in, e.g., ethyl ether are very different. However, the overall shapes of the two spectra are very similar in organic solution and protein environments.

Some chlorophyll species are extremely red-shifted in vivo. Halldal (1968) discovered that the green alga *Ostreobium*, growing inside a coral on the Great Barrier Reef, contained unusually large amounts of such long-wavelength chlorophyll, "$C_a 720$." It seemed to be an adaptation to the unusual environment of this organism. Other algae growing outside *Ostreobium* filtered away much of the daylight and left mostly far-red light for *Ostreobium* to use. Halldal asked his student Öquist to find out whether a more "ordinary" alga, *Chlorella*, would also be able to adapt to far-red light by forming more long-wavelength chlorophyll, and to some extent it could (Öquist 1969). But some species of *Ostreobium* are exceptional, and are still attracting the interest of scientists. Although most of the long-wavelength chlorophyll is associated to photosystem I, there seems also to be long-wavelength chlorophyll in photosystem II (Fuad et al. 1983, Zucchelli et al. 1990, Koehne et al. 1999). Investigators are puzzled by the fact that these pigment forms seem to be able to deliver energy to the reaction centers, which have absorption spectra peaking at shorter wavelengths, and were thought to require higher energy quanta. The explanation may be, as in the case of dragonfish vision, that thermal quanta deliver the extra energy needed. This need not violate the second law of thermodynamics if the whole photosynthetic system is considered.

Some of the recent and detailed investigations have been done on cyanobacteria. It has been shown that also in this case the long-wavelength forms, at physiological temperatures (but not at very low temperature), can transfer absorbed energy to P700 (Pålsson et al. 1998). The main long-wavelength absorption peaks

of these long-wavelength forms are variously given as 708 and 719 nm (Pålsson et al. 1998), and 705, 714, and 723 nm (Kochubey and Samokhval 2000), both for *Synechococcus elongatus*. For *Synechocystis* sp. PCC 6803 only a single long-wavelength form peaking at 710 nm was identified (Gill and Wittmershaus 1999), possibly due to methodological differences. The 719-nm form seems to arise from the 708-form when monomers of PSI are combined to the trimers present in vivo (Pålsson et al. 1998, Jordan et al. 2001). In a structural model (Jordan et al. 2001) for PSI the 710/719-nm chlorophyll is tentatively identified with the aC-A32/aC-B7 molecule pair, which seems to connect the monomers energetically. Thus the long-wavelength band may arise by excimer splitting, just as in a long-wavelength spectral form of phycocyanobilin. However, Koehne et al. (1999) have obtained evidence that at least some long-wavelength forms in the eukaryotic alga *Oestrobium* have another origin.

To date the long-wavelength record for chlorophyll *a* tuning is held by the cyanobacterium *Spirulina platensis*, which has a form peaking at 738 nm (Shubin et al. 1991, Koehne and Trissl 1998, Karapetyan et al. 1997).

P700 of photosystem I as well as P680 of photosystem II are both dimers (within the photosystem monomer), with the tetrapyrrols closely stacked in a parallel manner and with tightly overlapping π orbitals, forming excimers. It is thus not difficult to understand that there is a large red-shift from the absorption peak of chlorophyll *a* in dilute organic solution.

Carotenoids may be important for the spectral fine-tuning of some other chlorophyll forms. Several of the carotenoids in PSI show extended overlap of their π orbitals with those of chlorophyll molecules (Jordan et al. 2001).

For cyanobacterial PSII a structural model has been published by Zouni et al. (2001). According to this model, $Chlz_{D1}$ and $Chlz_{D2}$ are identified with chlorophyll *a* bound to histidine in polypeptides D1 and D2. These chlorophylls have absorption peaks at 675 nm (Schelvis et al. 1994).

9.6. Phycobiliproteins and Phycobilisomes

In hardly any case is spectral tuning more important and critical than in photosynthetic antenna pigments. Light is absorbed by one chromophore and transferred over a series of other chromophores to photosynthetic reaction centers. The most common method for energy transfer is the Förster mechanism. For this to be efficient, the emission spectrum of the energy donor must in each step match the absorption spectrum of the receiver.

There are many kinds of antenna pigments in various organisms: chlorophylls, carotenoids, pteridines, and phycobiliproteins. We shall concentrate here on phycobiliproteins, which occur in cyanobacteria and several groups of algae, most important of which are the red algae. The description below will primarily reflect the conditions in cyanobacteria.

Cyanobacteria use several principles for spectral tuning, the first of which is variation of the structure of the chromophores (bilins). Different lengths of

TABLE 9.2. Number of Conjugated Double Bonds and Absorption Maxima for the Phycobilins

Phycobilin	Number of conjugated double bonds	Absorption maximum in free form, nm	Absorption maximum in phycobiliprotein
Phycourobilin (PUB)	5		495
Phycoerythrobilin (PEB)	6	530	545–565
Phycoviolobilin (PVB)	7		510–570
Phycocyanobilin (PCB)	8	600	610–671

the conjugated bond system results in different transition energies: the greater the length, the lower the energy. The types of chromophores known are shown in Table 9.2 and their distribution among proteins in Table 9.3.

When the chromophores attach to proteins (which takes place via sulfur bridges at one or two points) two changes are immediately apparent: The absorption bands become sharper, and the intensity of the long-wavelength band increases in comparison to those at lower wavelengths. The sharpening of the bands takes place because the conformation of the chromophore, which in the free form is very flexible and therefore distributed over a large number of conformational states, becomes restricted. The relative intensification of the long-wavelength band takes place because the chromophore becomes more straight, while in the free state it is, on average, more circular, as one turn of a helix (Scheer and Kufer 1977, Knipp et al. 1998), with overlapping ends. The spectrum therefore is in this case more "porphyrin-like," with a pronounced Soret-type band. Another effect of the binding to protein is that the position of the long-wavelength band is shifted, to very different extents in different cases which will be described below.

TABLE 9.3. Occurrence of Phycobilin Chromophores Among Cyano-bacterial Phycobiliproteins and Their *a* and *b* Peptides

	On *a* peptide	On *b* peptide
Allophycocyanin	1 PCB	1 PCB
C-Phycocyanin	1 PCB	2 PCB
Phycoerythrocyanin	1 PVB	2 PCB
R-Phycocyanin II	1 PEB	2 PCB
Phycocyanin WH8501	1 PUB	2 PCB
C-Phycoerythrin	2 PEB	2 PEB
CU-Phycoerythrin (1)	3 PUB	1 PEB + 1 PUB
CU-Phycoerythrin (2)	1 PEB + 2 PUB	2 PEB
CU-Phycoerythrin (3)	3 PUB	2 PEB
CU-Phycoerythrin (4)	2 PEB + 1 PUB	2 PEB + 1 PUB

Source: After MacColl (1998), slightly simplified. For corresponding information for rhodophycean phycobiliproteins, see Table 1 of Holzwarth (1991), and for cryptophycean (cryptomonad) phycobiliproteins Glazer and Wedemayer (1995).

The chromophore is not fixed in the protein with complete rigidity. Of particular interest are cases in which the conformation of the chromophore can change under the influence of light, causing photochromicity of the chromoprotein, analogous to the behavior of phytochrome. The behaviour was first noticed by Scheibe (1972) in an extract containing phycocyanin. The phenomenon was further examined in a number of papers by G.S. Björn, summarized by G.S. Björn (1980), L.O. Björn (1979), and Björn and Björn (1980). The experiments were mostly carried out on extracts, but in one case (G.S. Björn 1979) photoreversible photochromism was shown to occur also in vivo. In this case irradiation with light of 505 nm results in a decrease of absorption at this wavelength and an increase at 570 nm, while irradiation with 570 nm light reverses this effect, and the reaction can be repeated over and over again.

This particular case has been further explored by other researchers, in particular the group around H. Scheer in Germany (Zhao et al. 1995, Zhao and Scheer 1995; see also Ohad et al. 1979 and Scharnagl and Fischer 1993). It has been found that the change in absorption spectrum is primarily due to rotation around a double bond beween carbon atoms 15 and 16 in a phycoviolobilin chromophore in the a subunit of phycoerythrocyanin.

How rigidly the chromophore is held by the protein depends partly on the covalent (thioether) bonds between chromophore and protein. The bonds may go from either the A ring or the D ring, or both, and this affects the spectral properties. The extent to which the chromophore is stretched and kept rigid also affects another property of great importance for the function, namely the excited state lifetime. A phycobilin chromophore which is not fixed in a protein has great flexibility, which gives greater possibilities for thermal relaxation, i.e., shorter lifetime and less efficient energy transfer and photochemical efficiency. This is in contrast to what is the case with chlorophylls, which are already in the free state rigid structures. The attachment to protein also favors a protonated state, which also lengthens the excited state life.

The ordered arrangement of chromophores in a protein matrix affects the chromophore spectrum by one more mechanism. It keeps certain chromophores in the close vicinity of one another, which results in the formation of exciplexes. As described before, this splits the energy levels of the isolated chromophores in a higher and a lower level, in turn splitting the absorption bands in a corresponding manner.

Thus, even though cyanobacterial phycocyanins and allophycocyanins all contain only a single type of chromophore, namely phycocyanobilin, they exhibit a wide range of absorption bands, peaking from 620 nm in C-phycocyanin to 671 nm in allophycocyanin B and also in the "terminal linker polypeptide" in the center of the phycobilisomes, close to the chlorophyll in the thylakoid membranes.

Phytochromes constitute a quite different type of phycobiliproteins, which have a light-sensing function (Chapters 14–17). Plant phytochromes, which are those studied in most detail and that contain phytochromobilin (closely related to phycocyanobilin) as chromophore, are interconvertible between two forms,

of which one has evolved to absorb maximally near the absorption maximum of chlorophyll, while the other one absorbs maximally just outside the chlorophyll absorption. Therefore they are well suited for detecting the change in light spectrum caused by the presence of competing plants. Phytochromes of nonphotosynthetic bacteria, on the other hand (whose exact biological function is yet to be explored), contain a different type of phycobilin chromophore and absorb at longer wavelengths (Bhoo et al. 2001).

9.7. Chromatic Adaptation of Cyanobacterial Phycobilisomes

Although also other photosynthetic organisms have some ability acclimatize to different spectral regimes, cyanobacteria are the real experts. Most of the so-called "chromatic adaptation" of cyanobacteria depends on their ability to change the amounts of phycoerythrin and phycocyanin depending on the balance between green and red light in their environment. "Chromatic adaptation" (or "complementary chromatic adaptation") is a long- established term, although "chromatic acclimation" would be more in line with the common use of "acclimation" for phenotypic adjustment of the individual, and "adaptation" for genotypic adjustment through evolution.

In direct daylight, or in red light, some cyanobacteria do not build any phycoerythrin into their phycobilisomes. These cyanobacteria sometimes form thick mats or grow under other chlorophyll-containing organisms which filter out the red light but let some green light through. In the deeper layers of the mats, as well as under other organisms, the cyanobacteria are able to utilize the green light efficiently by equipping the phycobilisomes with phycoerythrin at the same time as they decrease the amount of phycocyanin. Some phycocyanin must always be present to allow for energy transfer from phycocyanin to allophycocyanin and on to chlorophyll in the thylakoids.

Long ago it was found that a short pulse of light of particular wavelength suffices to link the phycobilisome construction onto a phycoerythrin-rich or phycoerythrin-deficient path. The change in pigmentation itself can take place during a subsequent dark period. And just as with phytochrome responses of plants, in a series of alternate pulses of red or green light it is just the wavelength composition of the final pulse that matters. From this it could be concluded that the regulation is mediated by a photochromic pigment of some kind, in analogy with phytochrome (Ohki and Fujita 1978).

It was also established through action spectroscopy that this photochromic regulator must be a phycobiliprotein (Fujita and Hattori 1962, Diakoff and Scheibe 1973, Vogelmann and Scheibe 1978). Similar action spectra were also obtained for regulation of some other developmental processes in cyanobacteria (Lazaroff and Schiff 1962, Robinson and Miller 1970). Furthermore, the action spectra were also similar to those for conversions of "phycochrome b" (G.S. Björn 1979), later identified as the β-subunit of phycoerythrocyanin.

Phycochrome b itself could not, however, be the regulator, since chromatic adaptation takes place also in cyanobacteria lacking phycoerythrocyanin. Nevertheless, the spectral similarity with the photochromic β-subunit of phycoerythrocyanin made it plausible that the chromophore of the regulator is very similar to phycourobilin, the chromophore of the β-subunit.

Phytochrome in plants could be identified and characterized largely because plants lack other phycobiliproteins. In cyanobacteria, where phycobiliproteins make up a large part of the total protein, the situation is much less favorable, and the mechanism of chromatic adaptation remained elusive until recently.

Recent developments in the field are described by Grossman et al. (2001). As in some of the older investigations, *Fremyella diplosiphon* was used as experimental organism. It appears that the chromoprotein involved as photoreceptor is the product of a gene called rcaE. This is a 74 kDa polypeptide (Kehoe and Grossman 1997, 1998). The C-terminal region has motifs typical of bacterial sensor kinases. The N-terminal half binds a linear tetrapyrrole covalently at a cysteine within a phytochrome-like domain. The central part of the polypeptide contains a PAS domain (Kehoe and Grossman 1996, 1997, 1998, Kehoe and Gutu 2006).

Grossman et al. (2001) outline the events during chromatic adaptation under red light as follows: Red light causes RcaE to undergo an autophosphorylation followed by transfer of the phosphate groups to the response regulator RcaF. The phosphate group is then transferred to still one polypeptide, RcaC, which acts on genes cpcB2A2 and cpeBA to repress the synthesis of phycoerythrin and stimulate that of phycocyanin. In green light the phosphorylation is prevented, and the effect on the genes is reversed.

9.8. Visual Tuning

Visual pigments of animals span a spectral range of 300–700 nm (Marshall and Oberwinkler 1999) i.e. more than an octave of the electromagnetic spectrum. They are proteins with, in most cases, either 11-*cis*-retinal or 11-*cis*-3-dehydroretinal (Fig. 9.3: Makino et al. 1999) as chromophores. Proteins with 11-*cis*-retinal alone cover a range of absorption spectra with maxima from 360 to 635 nm (Kleinschmidt and Harosi 1992, Kochendoerfer et al. 1999). The term rhodopsin is somewhat ambiguous and sometimes covers all chromoproteins related to the human visual pigments, including light-sensitive proteins in algae and archaebacteria, but sometimes visual pigments containing 11-*cis*-dehydroretinal (which are then termed porphyropsins) are excluded. The spectra of visual pigments to some extent depends on which chromophore they contain; dehydroretinal (also called *retinal₂*) with its longer conjugated double bond system giving a red-shift of 10–50 nm compared to 11-*cis*-retinal. Two other "primary chromophores" involved in animal vision are also known: 11-*cis*-4-hydroxyretinal has been found (as well as retinal and 3-dehydroretinal) in the eyes of the bioluminescent squid *Watasenia scintillans* (Matsui et al. 1988) and give s blue-shift compared to retinal. 3-Hydroxyretinal occurs in several insect
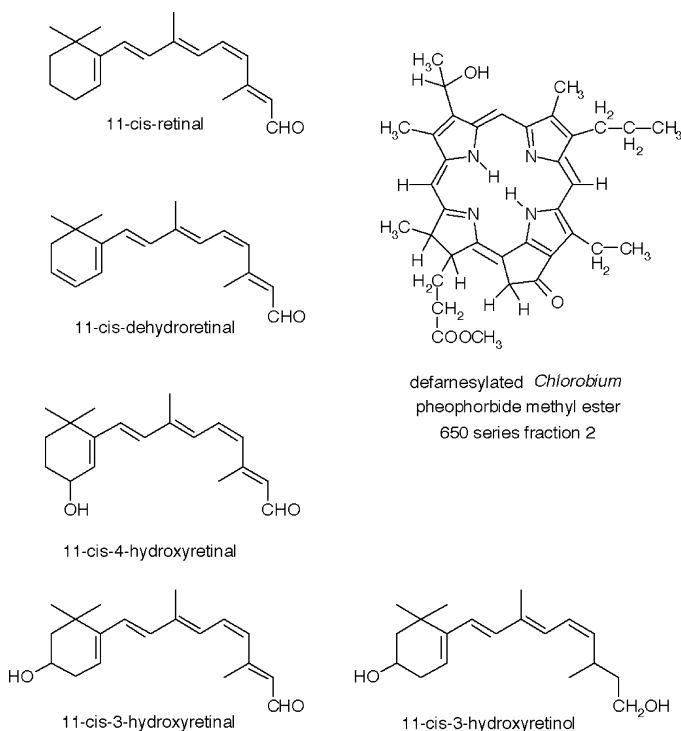
FIGURE 9.3. Structures of five chromophores known from animal visual pigments. Several compounds related to the *Chlorobium* pheophorbide derivative also occur in dragonfish eyes. 11-*cis*-3-Hydroxyretinal occurs as two different enantiomers, with different phylogenetic distributions.

orders (Vogt 1983, Vogt and Kirschfeld 1984, Tanimura et al. 1986, Seki and Vogt 1998), and different stereoisomers (3R and 3S enantiomers) of it occur, with different phylogenetic distributions (Seki and Vogt 1998). Many vertebrates, including humans, have a differentiation of light-sensitive cells in the retina between rods, specialized for "black-and-white vision" in weak light, and cones, specialized for color vision in stronger light.

In addition to these "primary chromophores," there are, in certain cases, "sensitizing chromophores" attached to the same proteins. These chromophores act in analogy to photosynthetic antenna pigments: they absorb light and transfer the energy to the primary chromophores. Only three such sensitizing chromophores have been detected so far: 11-*cis*-3-hydroxyretinol in Diptera (Vogt and Kirschfeld 1984) and defarnesylated *Chlorobium* pheophorbide methyl ester in bioluminescent dragonfish (Douglas et al.1998, 1999) and chlorin e6 in salamander (Isayama et al. 2006). More about the dragonfish can be found in Chapter 23.

In addition to visual pigment structure, spectral filters in the form of colored oil drops contribute to spectral tuning of photoreceptor sensitivity in some animals, especially birds (Maier and Bowmaker 1993, Bowmaker et al. 1997, Vorobyev et al. 1998, Hart et al. 2000) and reptiles (Schneeweis and Green 1995). We also have filters in our own eyes, namely in the yellow spot of the retina, macula lutea. This is the spot of highest visual acuity, devoid of blue-sensitive cones. Here the yellow pigment serves to prevent blue light to reach the green- and red-sensitive cones, for which it would degrade acuity by chromatic aberration.

However, most of the spectral tuning is achieved by variation of a few of the amino acids in the protein to which the chromophores are attached (Britt et al. 1993).

Humans use exclusively the 11-*cis*-retinal chromophore. In free form in methanol solution 11-*cis*-retinal absorbs maximally at 380 nm (in protonated Schiff's base form it absorbs maximally at 440 nm). Human rhodopsin, the protein–chromophore complex of rods, used in twilight vision, peaks at 493 nm (Wald and Brown 1958). The three human cone pigments, used in color vision, peak at 426, 530, and 552 nm (or 557 nm; all persons do not have exactly the same type). The human cone pigments are often referred to as SW (for short wavelength), MW, and LW pigments, respectively.

The effect of protein primary structure on spectral properties of visual pigments is studied (1) by comparing various naturally occurring pigments and (2) by site-directed mutagenesis experiments in which certain amino acids are changed.

An important determinant of the spectrum seems to be the negative charges on amino acids in proximity to the chromophore. We shall give two interesting examples of how this can works:

1. Ultraviolet vision has been demonstrated in many vertebrate (fish, amphibian, reptilian, avian, and mammal) species (Jacobs 1992). Yokoyama et al. (2000) have convincingly shown that ultraviolet-sensitive pigment in birds evolved from violet-sensitive pigments by a single amino acid substitution, namely by a change of serine to C at position 84. This shifts the absorption spectrum of the wild-type pigeon pigment with a maximum at 393 nm to one peaking at 358 nm. For the corresponding chicken pigment the shift was from 415 nm to 369 nm. Conversely, the zebrafinch UV pigment peaking at 359 nm could be shifted to 397 nm by a change at position 84 from C to serine. It should be noted, however, that ultraviolet-absorbing pigments in other vertebrate groups have arisen independently, and by other substitutions.

2. Human trichromatic color vision has arisen recently during evolution; most mammals have only dichromatic color vision and some, such as whales, do not have more than one type of cone pigment. Some New World monkeys also possess trichromatic color vision, but that has arisen independently. The human type of trichromacy has arisen by gene duplication of a long-wavelength pigment, and mutation of one of the gene copies to produce a middle-wavelength (MW) pigment. According to Neitz et al. (1991) the spectral differences between these pigments depend on three amino acid differences, and in addition there are several differences without spectral effect. Effects

TABLE 9.4. Spectral Effects of Amino Acid (aa) Substitutions in Human Cone Pigments

Position	aa in MWP	aa in LWP	$\Delta\lambda$ on change
180	Alanine	Serine	+6
277	Phenylalanine	Tyrosine	+9
285	Alanine	Threonine	+15

are detailed in Table 9.4 (values vary somewhat between investigators using different methods). In each case the change from a nonhydroxyl to a hydroxyl amino acid results in a "red-shift," i.e., absorption at longer wavelengths.

Those people who possess a 557-nm LW pigment have serine at position 180, while those with a 552-nm pigment have alanine. This position is also variable in the MW pigment, but seems to produce a smaller spectral shift there, and investigations are not as thorough as for the LW pigment (see Sharpe et al. 1999 for details). The same person may, in fact, possess more than three different cone pigments (Neitz et al. 1993).

Fujimoto, Hasegawa, Hayashi et al. (2005) have studied the spectral tuning of retinal proteins by quantum mechanical methods, while Nathans (1992) has discussed it in more general terms, easier to understand for the nonspecialist. Retinal undergoes a large decrease in dipole moment in going from the ground state to the photoexcited state: In the ground state a positive charge is localised mainly to the Schiff's base nitrogen, and this charge is distributed more evenly throughout the π-electron system upon photoexcitation (Nathans 1990). A negative charge, such as from glutamate or aspartate, along the polyene chain of retinal would favor charge delocalization in the ground state and thus a smaller energy gap, i.e., a red shift. Polar groups along the polyene chain would favor or disfavor charge delocalization depending on orientation. Polarizable groups along the polyene chain would stabilize the excited state (produce a red-shift) through compensatory charge movement. Twisting around single or double bonds would respectively decrease or increase charge delocalization. Moving the Schiff's base counterion further from the chromophore would decrease the effect of the ground state dipole moment and produce a red-shift. A record shift for a single amino acid change (which has not been found in nature), from 500 to 380 nm, was produced experimentally by changing glutamic acid to glutamine at position 113 (references in Yokoyama 1997).

Returning to the human MW and LW pigments, one may wonder why their absorption spectra are not more different. Color vision would appear to be more efficient if they were. The difference between the LW (552 or 557 nm) absorption peak and that of the MW (530 nm) pigment is much smaller than between MW and SW (426 nm) pigment maxima. The difference between the human LW and MW pigments is much smaller than the difference between corresponding pigments in, e.g., the fruitfly *Drosophila* (in this animal the two pigments absorbing at longest wavelengths peak at 420 nm and 480 nm, respectively; in addition the fly has two pigments peaking in the ultraviolet). One explanation

that has been proposed is that the image-forming optics of the human eye has a large chromatic aberration and the effect of this is minimized if the spectra are not too different. The perception of shapes and position depends mainly on the LW and MW cones, and the focusing of an image on the retina is adjusted for the average of their wavelengths. The blue color is mentally "painted" into the outlines formed by these receptors. In the part of the retina used for the sharpest vision, the luteum, has very few SW receptors, and contains a yellow pigment which absorbs blue light. The similarity of LW and MW spectra makes good focusing possible. On the other hand, the small difference in the human pigments may be just a consequence of the fact that the gene duplication has occurred so recently, and evolution has not had time to result in a bigger difference yet.

The fruitfly has a completely different system for image generation, without the chromatic aberration problems, but the visual acuity of the fruitfly eye is much lower than that of the human eye.

What are the evolutionary pressures causing visual pigment spectra to be tuned? Generally speaking, of course, color vision provides more information than monochromic vision. We prefer color television to black and white. According to Osorio and Vorobyev (1996) and Regan et al. (1998) the main importance of the differentiation into LW and MW pigments in primates has been to aid our forefathers in detecting fruits against a green background and judging the ripeness of fruits. This view has been questioned by Lucas et al. (1998) and Dominy and Lucas (2001), who provide evidence that trichromatic vision is important for the selection of leaves at an optimal developmental stage for consumption. As for ultraviolet vision in birds, one well-documented advantage for birds of prey is that UV vision allows them to see urine of rodents and thus to locate their whereabouts. Ultraviolet vision in birds is also important for recognition of plumage coloration of conspecifics and for detection and identification of edible berries (Siitari et al. 1999).

For insects depositing eggs on leaves, it is important to find the leaves and to judge their age and health status. It turns out that for this task a *red-light* receptor can be very important. Most insects do not have red-sensitive receptors, but both sawflies (Peitsch *et al.* 1992) and moths (Kelber 1999) that oviposit (lay eggs) on leaves do. Excitation of green-sensitive photoreceptors give an attractive signal, and the red-sensitive receptors provide a contrasting, repelling signal. In the case of moths, their ultraviolet-, violet-, and blue-sensitive receptors probably play a role in their orientation and choice of leaves (young leaves are preferred). On the other hand, in selecting green leaves, vision probably does not play an important role in the discrimination between plant species; for this, chemical cues are more important.

The daylight penetrating deepest into the ocean is in the blue-violet region, and consequently the vision of deep-water fish is tuned to this wavelength band (Lythgoe 1984), while surface-living fish and fish in shallow freshwater have a visual sensitivity peaking, like ours, in the green spectral region (although the span of pigments in fish is much wider than ours, with pigment absorption peaks spanning from the ultraviolet to the red). Although also several bioluminescent

deep sea fishes have maximum sensitivity in the blue-violet region (Fernandez 1978), others, who use their bioluminescence for environmental illumination, show remarkable deviations from this rule (Douglas et al. 1998, 1999). Other aspects of the connection between bioluminescence and the vision of deep sea fishes have been treated by Warrant (2000).

Deep-diving whales have rod pigments peaking at 485 nm, while rod pigments of aquatic animals foraging closer to the surface (seals, manatees) peak near 500 nm. To the surprise of some investigators none of six whale species and seven seal species possess SW cones (nor any LW cones), only MW cones (Peichl *et al.* 2001), with a pigment absorbing maximally around 524 nm (Fasick et al. 1998). It has been claimed that this means that they do not possess color vision (Peichl et al. 2001), but this may be jumping to a conclusion. Although color discrimination in whales has not been established, rods are saturated in strong light and cones useless in weak light; there may be intermediate depth and light levels where signals are obtained from both rods and cones and give whales and seals a dichromatic color vision (Fasick 1998, Fasick and Robinson 2000). A corresponding phenomenon in humans was demonstrated many years ago through a very interesting experiment by John J. McCann and Jeanne L. Benton, described by Land (1964). They first illuminated a multicolored display with "monochromatic" (narrowband) light of 550 nm (500 nm would probably have worked as well), which was so weak that only the rods of a human observer were stimulated. Of course no colors could be discriminated under such circumstances. They then added a second narrowband beam of 656-nm wavelength. The irradiance of this second light was adjusted so that only the LW cones were stimulated. Thus only the rods and the LW cones were operative. Nevertheless the observer was able to give names to colors in the display almost as if it was illuminated by natural daylight and all three types of cones had been stimulated.

Color vision is not restricted to di-, tri-, and tetrachromatic versions. The mantis shrimp (Osorio et al. 1997, Marshall and Oberwinkler 1999, Cronin et al. 2001) may have up to 16 types of visual pigment, although this does not mean that it has a corresponding number of color channels. It also has the ability to further tune the sensitivity spectra of their receptors by color filters as required by the light environment they inhabit. These animals may live close to the water surface (in full daylight spectrum) or as deep as 30 m (in a restricted blue-light environment). All 16 types of light-sensitive pigments may not correspond to separate sensory input channels, but no doubt they provide polychromatic vision.

9.9. Tuning of Anthocyanins

Anthocyanins are the most common vacuolar pigments, giving color to many flowers, fruits, and autumn leaves. We may think of the cell sap of plant vacuoles as structureless, and of interactions between anthocyanins and their environment as a dull subject, but if we do so we are in error.

The great pioneer in the elucidation of chemical structures of plant compounds, Richard Willstätter, got a surprise when he compared the structures of the blue pigment of the cornflower (*Centaurea cyanus*) with that of the red pigment of a rose. He found that the pigments were chemically identical (he was not completely right, but that does not destroy the story). He thought that the difference in color came about from a difference in pH of the cell sap of the two plants. He was not right there either, but he got the main point—that anthocyanins can produce very different colors with practically identical chromophores.

The basic structure of an anthocyanin is shown in Fig. 9.4. The molecule consists of two fused six-membered rings connected to a third six-membered ring. A system of conjugated double bonds extends over all rings. The fused rings carry three hydroxy groups, one or two of which form glycoside bonds with sugar molecules, often glucose. The sugar-free compound (the aglycon) is called anthocyanidin. The anthocyanidin of red rose flowers is cyanidin and that of cornflower succinyl-cyanidin (so they are indeed closely related, and the little difference does not explain the color difference). Pure cyanin (the glycosylated cyanidin) is red in acid solution, and if it is made alkaline the color changes towards blue, so it is understandable that Willstätter ascribed the color difference between roses and cornflowers to a pH difference of the cell sap. However, the blue color aquired upon alkalinization does not last long, the color fades away completely. This is because the molecule, already when the pH exceeds about 5, takes up water (Fig. 9.5). Furthermore, no plants are known with an alkaline cell sap, so the cornflower's blue color must be explained in another way.

The R-groups in Fig. 9.5 are numbered according to the conventional numbering of the carbon atoms to which they are bound. The groups can all be hydroxyl. R_3' and R_5' can also be hydrogen, methoxyl, a chelated metal ion, such as Fe^{3+} or Al^{3+}, a sugar or sugar derivative, while R_3 and R_5 can be a sugar or an acylated sugar. The equilibria between different forms depend on many things, such as the chelation with metal ions. In at least one case it is also light dependent (Figueiredo et al. 1994).

The reason for the blue color of the cornflower rests in the phenomena of copigmentation and self-association. Copigmentation means that the color of the anthocyanin is influenced by other molecules in its environment. Self-association means that the anthocyanin molecule can associate with other anthocyanin
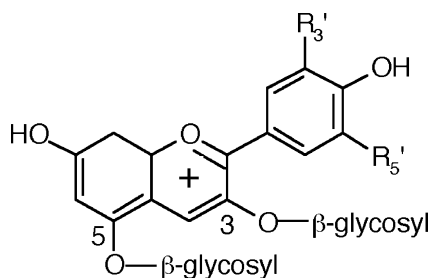
FIGURE 9.4. The general structure of an anthocyanin in the flavylium cation form.
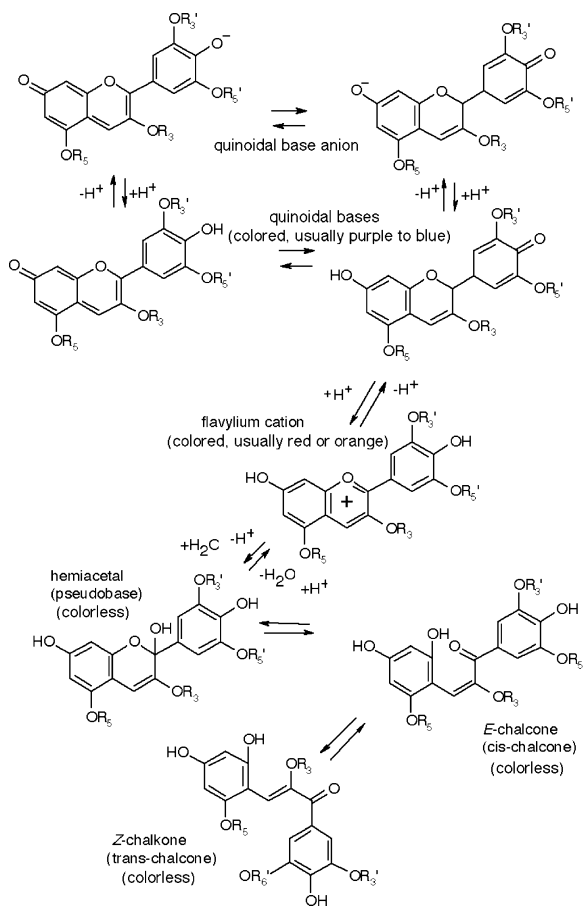
FIGURE 9.5. An anthocyanin can exist in many different interconvertible molecular forms, as shown in this diagram: as different quinoidal bases anions or unionized quinonoidal bases, as flavylium cation, as hemiacetal (pseudobase), or as chalcone (E or Z form). Although hemiacetals and chalcones are colorless, they absorb ultraviolet radiation, and can therefore appear colored to some animals. Their presence can also modify the hue of the colored forms.

molecules, and this also affects its color. Both self-association and associations between anthocyanins and uncolored phenolic compounds cause overlaps between the π-electron clouds of the individual molecules, and hence changes in the electron levels. The concentration of anthocyanin in cell sap can exceed 20 mM, and this is more than sufficient for the molecules to associate to one another and sometimes form helical stacks through a combination of hydrophobic bonds between the rings and hydrophilic bonds between the sugar residues. These associations also prevent the formation of pseudo-base, hence the bleaching of color that would otherwise take place at the pH prevalent in the cell sap.
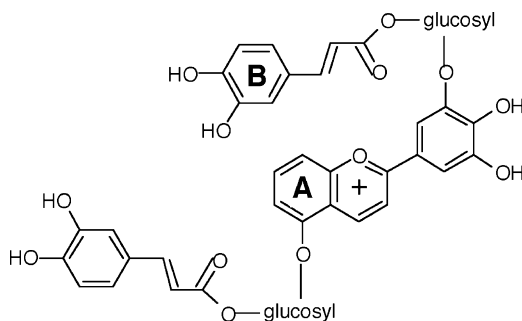
FIGURE 9.6. The structure of gentiodelphin, schematic. In reality the molecule is more bent, so ring B closely overlaps the double ring A, and the π orbitals of the ring systems fuse.

Many different kinds of (uncolored) molecules and ions produce copigmentation effects with anthocyanins. The most important ones are some metal ions and colorless flavonoids (absorbing in the ultraviolet spectral region) and other phenolic compounds. In the case of the blue cornflower pigment (Fig. 9.7), Fe^{3+} and Mg^{2+} have been reported as copigmenting ions, and a flavone as copigmenting phenol. Anthocyanins having two *ortho*-hydroxy groups at the B-ring (the leftmost ring in Fig. 9.6) form blue chelate complexes with trivalent metal ions such as iron(III) and aluminum(III), but not with magnesium. This latter ion is, however, very important in some other cases.

Goto and Kondo (1991) have written a very readable account of copigmentation, illustrated with color pictures. They describe structures of several more complex anthocyanins, with aromatic groups attached to the sugar residues, and a particularly interesting case of pigment complex, commelinin (rendering the blue
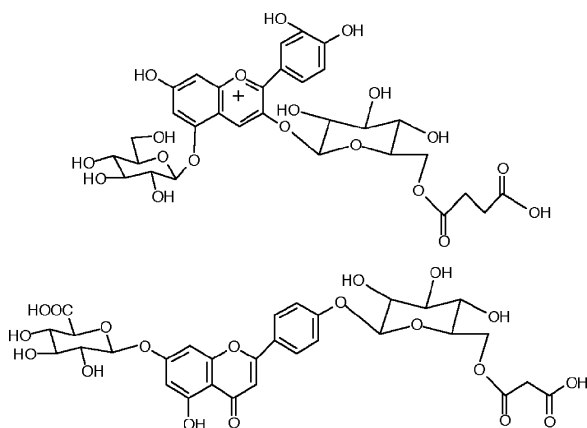
FIGURE 9.7. According to Goto and Kondo (1991) the blue pigment of cornflower, protocyanin, is built up of six molecules each of the succinylcyanin cation (top) and the malonylflavone shown in the figure, plus one Fe and one Mg ion.

color to *Commelina communis*). This consists of six molecules each of malony-lawobanin (a complex anthocyanin) and flavocommelinin (a flavone glycoside) arranged around two magnesium ions. The intense blue color is partly due to exciton coupling between adjacent anthocyanin units. The molecular mass of this complex is nearly 1000. Also chiral stacking (Fig. 9.8) can affect color.

The importance of the sugar groups in anthocyanins lies not in a direct effect on light absorption, but in their contribution to the folding and ordering of the chromophoric groups such that overlaps of π-electron clouds can take place.

The color of anthocyanins is affected not only by their chemical environment, but also by physical factors: temperature and light. One summer day when one of the authors and his wife were having tea in their garden, she remarked that she had noticed how some flowers of a variety of *Phlox paniculata* had shifted color when they were reached by sunlight. She was delivered a lecture on the psychology of color perception and the mistakes we can make, but she insisted. So we took the flowers to the lab and measured the reflection spectra after dark adaptation and after exposure to strong light for an hour (Björn, Braune and Björn 1985). And indeed, the reflectance spectrum did change with light conditions. Color photos of the phenomenon have been published in Swedish journals (Björn 1985 a,b). At the time we hypothesized that the color shift was caused by a light-activated proton pump in the tonoplast (the membrane surrounding the vacuole) which would change the pH of the cell sap. We attempted to show such a pH change using a white *Phlox* variety and artificial pH indicator dyes, but did not succeed. About a decade later Figueiredo et al. (1994) demonstrated that the absorption spectrum of an artificial anthocyanin-like compound, 4′,7-dihydroxyflavylium chloride, could be reversibly affected,
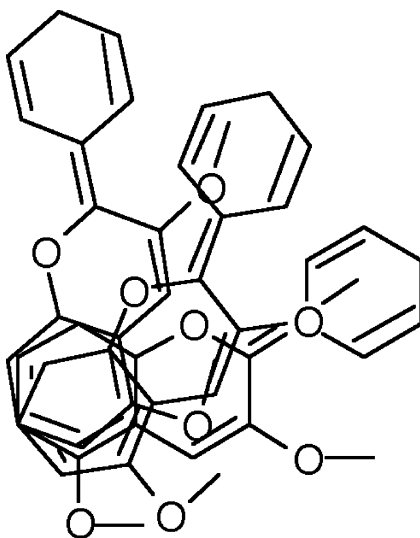
FIGURE 9.8. An attempt to show the chiral stacking of delphin molecules. The sugar groups are omitted for clarity.

due to Z/E photoisomerization, by ultraviolet radiation (changing under irradiation from pale yellow to intense yellow), so it is possible that the color shift of our *Phlox* is due to an analogous phenomenon.

Thus a number of factors can affect the color of anthocyanin-containing flower petals. Obviously the reason that plants have evolved colored flowers is that they attract pollinators. The pollinators also benefit from this, so a question naturally arises: To what extent have flowers adapted to pollinator vision, and to what extent has pollinator vision (and mental capacity, such as long-term and short-term memory) adapted to flower colors?

Chittka and coworkers (Chittka and Menzel 1992, Chittka 1996, Chittka et al. 1999, Chittka and Dornhous 1999) have studied this question. By comparison of color vision in various arthropod groups they claim to be able to follow the evolution of color vision in insect pollinators. Photoreceptors among most Crustacea and Insecta fall into three rather distinct spectral classes: ultraviolet receptors with maxima around 350 nm, blue receptors with maxima at 400–460 nm, and green receptors with maxima from 470 to 550 nm. All these types seem to be very ancient. In addition, a few groups have red receptors with maxima around 600 nm. Chittka and coworkers see little evidence of insect adaptation to flower colors and believe that the main adjustment has been of flower colors to insect vision.

Only a minority of pollinators, such as hummingbirds and some butterflies, have red-sensitive photoreceptors. However, it must be borne in mind that pollinators without such receptors can see red flowers and distinguish them from other flowers and from green leaves.

The flowers of many plants vary in color with stage of development (Lunau 1996) and in this way signal to pollinators when a visit will be rewarded. Of particular interest are flowers that change color during the year in synchronization with the availability of different pollinators.

FIGURE 9.9. A flower of creeping tormentil, *Potentilla reptans* photographed in visible light (left) and in UV-A radiation (right). (Photo by L.O. Björn.)

What has been described here for flower colors has, to some extent, a counterpart in the coloration of fruits of plants which depend on animals for seed dispersal.

The ultraviolet receptors of insects make it possible for them to see patterns invisible to us. Figure 9.9 shows an example of such a flower pattern due to ultraviolet-absorbing flavonoids.

9.10. Living Mirrors and the Tuning of Structural Color

9.10.1. Introduction

We now turn to the topic of structural colors. Let us begin with a discussion of *iridescence*, the display of brilliant, often metallic, colors characteristic of many birds, insects, fish, and marine annelids and other invertebrates. Pioneering work on the subject was done by Mason (1926, 1927a,b); since then there has been an explosion of interest in these systems. Recent reviews include Fox (1976), Ghiradella (1991, 1998), Herring (1994, 2002), Kinoshita and Yoshioka (2005), Parker (1998, 1999, 2000), Srinivasarao (1999), and Vukusic et al. (2000a).

Let us start by focussing on a particular iridescent form, the biological mirror. As those readers who have driven a car on a country road at night know, many night-active wild animals have efficient reflectors in their eyes, as do our favorite pets, dogs and cats. These reflectors, located in the back of the eye behind the retina, double the sensitivity of eyes to light. They do this by throwing photons, which have escaped absorption by the light-sensitive pigments at their first passage through the retina, back through the retina again to give it a second chance to absorb them.

There are even eyes that have having mirrors as image-forming optical elements (Land and Nilsson 2002) as do astronomical telescopes. Some light-emitting organs of marine animals have reflectors like the headlights of a car, which throw the light in a certain direction. Mirrors reflecting the daylight from the surface make it easier for many fish to avoid detection.

These mirrors are built up of alternating layers of high and low refractive index, forming a structure we call a "multilayer thin-film stack.." We have previously (Chapter 1) treated reflection at a single boundary between phases of different refractive index. When several such boundaries are stacked upon one another, we *cannot* simply compute the reflectivity at each of them using Fresnel's formulas (Section 1.9. in Chapter 1) and add them (or compute the transmittivities and take their product), for two reasons: (1) there will be multiple reflections of photons bouncing back and forth between the boundaries, and (2) there will be interference effects.

To understand how such complex mirrors function, we have to consider the phases of electromagnetic oscillations, which was not necessary for a single boundary. Phase and phase difference are usually expressed in angular measure (radians), where 2π radians correspond to a whole period (a whole wave) of the electromagnetic oscillation. Reflection of light traveling from a medium of

lower refractive index differs from reflection of light travelling from a medium of higher refractive index towards one with lower refractive index in one important respect (Fig. 9.10): During reflection towards a denser medium the oscillation may undergo a phase change by π radians (180°). The detailed general treatment of reflection in dielectric multilayers is complicated. We shall therefore focus here on some special cases, which are more easily understood and nevertheless demonstrate more general principles.

9.10.2. Reflection in a Single Thin Layer

Everyone is familiar with the reflections from soap films and knows that a range of colors can be produced by such reflection. In this case we have a thin film of higher refractive index (approximately that of water) with the same medium (air) on both sides of the film. We can generalize this to have a bulk medium of one refractive index, $n0$, on one side, a thin film with a different refractive index, $n1$, and on the other side a bulk medium with a third refractive index, $n2$ (Fig. 9.11). For the soap film case $n0 = n3 < n1$. A well-known example in which $n0 < n1 < n2$ is a camera lens with an antireflective coating. As we shall see, we can treat these and similar cases with the same set of equations.

We denote the incidence angle by $a0$. The angle that the light forms with the normal to the film within the film is $a1$, and Snell's law gives the relationship $n0 * \sin a0 = n1 * \sin a1$, or $\sin a1 = \sin a0 * n0/n1$.

The ordinary Fresnel reflection factors for a single surface (Chapter 1) are

$$[(n1 * \cos a0 - n0 * \cos a1)/(n1 * \cos a0 + n0 * \cos a1)]^2$$
$$[(n0 * \cos a0 - n1 * \cos a1)/(n0 * \cos a0 + n1 * \cos a1)]^2$$

low refractive index

high refractive index
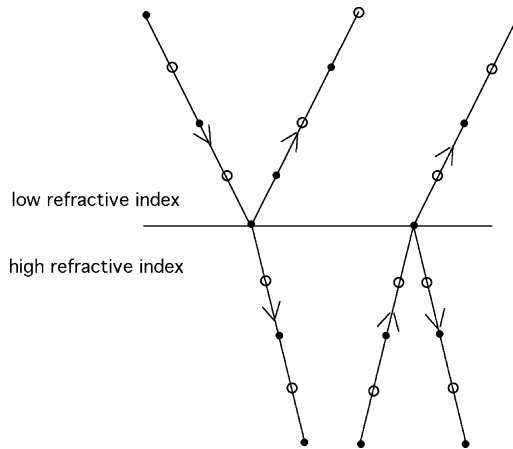
FIGURE 9.10. Reflections at an interface between a medium of higher and one of lower refractive index. Filled and empty circles denote opposite phases (i.e., phases differing by π radians) of the electromagnetic waves.

for light having the electric vector parallel to the plane of incidence (p-polarization), and perpendicular to it (s-polarization), respectively. These are the reflection coefficients for power or intensity, and of course they are always represented by positive real numbers.

It turns out that for a thin film, due to the interference effects, not only these angle-dependent factors, but also another angle-dependent factor, has to be taken into account. This is a function also of the layer thickness (d), the vacuum wavelength (λ), and the refraction index (n1) of the layer. To compute this, we first calculate the phase difference between the rays reflected from the first and from the second surface (Fig. 9.11). This phase difference can be thought of as composed of three components. The first component is π, due to the phase reversal at the first surface (if n1 > n0 as with the soap film and the camera lens, otherwise 0). The second component is due to the longer distance (AB+BC) traveled in the denser medium by the ray reflected from the second surface, while traveling through the film with refraction index n1, and therefore amounts to $2*n1*d*(2*\pi/\lambda)\cos$ a1 radians. The factor 2 in the second term stems from the fact that the ray reflected from the second surface traverses the layer twice, and $n1*d$ is the "optical thickness" of the layer, i.e., the geometrical thickness corrected for the shortening of the wavelength of light in proportion to the refraction index.
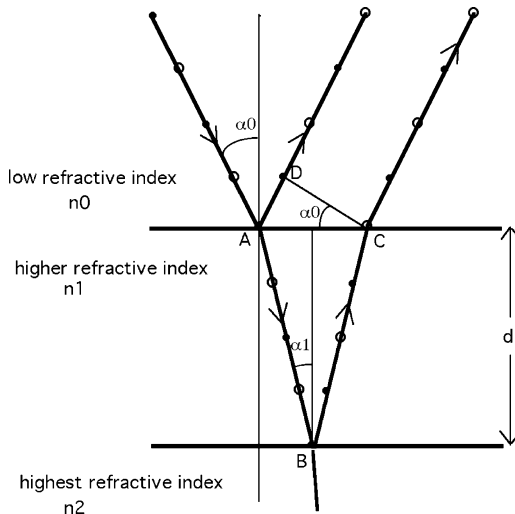
FIGURE 9.11. Phase relations during reflection at two consecutive phase boundaries. The drawing is for the case n0 < n1 < n2, corresponding to, e.g., the antireflection layer on a camera lens. In this case phase reversal takes place at both reflective surfaces, while with a soap film reversal takes place only at the first surface.

The third component of the phase difference is due to possible phase reversal during reflection at the second surface. It is 0 in the soap film case, because n1 > n2, and π in the camera lens case, because then n1 < n2.

The fourth component of the phase difference is due to the shorter distance, AD in Fig. 9.11, traveled in the n0 medium by the ray going through the film medium. The phase difference due to this is:

$$-AD * n0 * (2 * \pi/\lambda) =$$

$$-AC * \sin a0 * n0 * (2 * \pi/\lambda) =$$

$$-2 * d * \tan a1 * \sin a0 * n0 * (2 * \pi/\lambda) =$$

$$-2 * d * n1 * (\sin a1/\cos a1) * n1 * \sin a1 * (2 * \pi/\lambda) =$$

$$-2 * d * n1 * \sin^2 a1 * (2 * \pi/\lambda/\cos a1) \text{radians}$$

If we combine this with the second component we get:

$$2 * n1 * d * (2 * \pi/\lambda)/\cos a1 - 2 * d * n1 * \sin^2 a1 * (2 * \pi/\lambda)/\cos a1 =$$

$$2 * n1 * d * (1 - \sin^2 a1) * (2 * \pi/\lambda)/\cos a1 =$$

$$2 * n1 * d * \cos^2 a1 * (2 * \pi/\lambda)/\cos a1 =$$

$$2 * n1 * d * (2 * \pi/\lambda)/\cos \alpha$$

The Fresnel formulas given above, with expressions in squared brackets, as already mentioned, represent intensity reflection coefficients. For many computations, however, it is advantageous to work with the corresponding unsquared expressions, the so-called amplitude reflection coefficients, describing the change in amplitude of the electric wave motion upon reflection (the energy of the wavemotion is proportional to the square of the amplitude). These coefficients, in contrast to the intensity reflection coefficients, can be either positive or negative (if light-absorbing materials are involved, the intensity reflection coefficient is represented by a complex number, but we shall not consider this case here). A negative amplitude reflection coefficient means that the electric field changes direction during reflection, in other words, that we have a phase change of π radians. When we do calculations based upon the amplitude reflection coefficients, we do not have to worry about the phase changes of π radians during reflection that were mentioned above, since they will come automatically with the sign of the amplitude reflection coefficient used.

The following QuickBasic program will compute the reflectance over the range 0.3–1 mm for a thin film with refractive index n1 between media with refractive indices n0 (incidence side) and n2, respectively. In reality the refractive indices will vary with wavelength, but this has not been taken into account. If run on a Macintosh computer, the result will appear in the clipboard and can be transferred to other programs from there. If you wish to have the

output in another form, line 200 should be modified accordingly, and for other computers and Basic dialects, modifications may have to be made.

INPUT "incidence angle in degrees", a0:pi = 3.14159: a0 = a0 * pi/180

INPUT "thickness of thin layer in micrometres", d

sina1 = n0 * SIN(a0)/n1: a1 = ATN(sina1/SQR(1-sina1 * sina1))

sina2 = n1 * sina1/n2: a2 = ATN(sina2/SQR(1-sina2 * sina2))

50 :PRINT "Enter p for parallel (p) polarisation, s for perpendicular (s) polarisation."

PRINT "Polarisation directions are of electric vector relative to incidence plane."

INPUT "electric vector direction", polarisation$

IF polarisation$ = "p" THEN 150

IF polarisation$ = "s" THEN 100

PRINT "Mistake! Try again!": GOTO 50

100 : r1 = (n0 * COS(a0)-n1 * COS(a1))/(n0 * COS(a0)+n1 * COS(a1))

r2 = (n1 * COS(a1)-n2 * COS(a2))/(n1 * COS(a1)+n2 * COS(a2)):GOTO 170

150 :r1 = (n1 * COS(a0)-n0 * COS(a1))/(n0 * COS(a1)+n1 * COS(a0))

r2 = (n2 * COS(a1)-n1 * COS(a2))/(n1 * COS(a2)+n2 * COS(a1)):GOTO 170

170 :OPEN "O",1,"clip:"

FOR L = .3 TO 1 STEP .01

delta = 4 * pi * n1 * d/L * COS(a1)

I = (r1 * r1+r2 * r2+2 * r1 * r2 * COS(delta))

I = I/(1+r1 * r1 * r2 * r2+2 * r1 * r2 * COS(delta))

200: PRINT#1, I: NEXT L: CLOSE 1: END

We show in Fig. 9.12 the output of this program for a soap film ($n = 1.33$) of 0.33-mm thickness, both for normal incidence (a0 = 0) and for 45° incidence angle; in the latter case for both polarizations. This film would look yellow in a perpendicular direction, bluish green in a 45° direction. Note that the reflection spectrum shifts to shorter wavelength with increasing incidence angle, that there are several peaks in each spectrum corresponding to phase shifts of integer multiples of 2π, and that for oblique angles the s-polarized light is reflected better than the p-polarized light.

The angles of maximum and minimum reflectance vary according to

$$\lambda \max = [(4 * n1 * d)/(2m + 1)] * SQR[(1 - (n1/n2) * sin2a0]$$

$$\lambda \min = [(4 * n1 * d)/(2m)] * SQR[(1 - (n1/n2) * sin2a0]$$
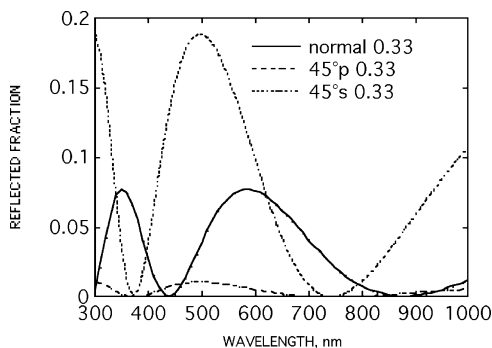
FIGURE 9.12. Reflection in a soap film of 0.33-mm thickness.

where m denotes any positive integer and SQR square root.

   Next we run the program for a typical camera lens antireflection coating with
n0 = 1, n1 = 1.38 (corresponding to magnesium fluoride) and n2 = 1.89 (heaviest
flintglass). The optical thickness (thickness × refractive index) of the layer is
adjusted to correspond to one quarter wavelength of yellow light (589 nm) in
the layer, i.e., (0.589/4)/1.38 mm (Fig. 9.13).

   To obtain zero reflection with an antireflective coating on a lens, two condi-
tions must be fulfilled: (1) the optical thickness of the coating must be equal
to one quarter of the wavelength of the light (or this plus an integer multiple
of the wavelength), which can be achieved only for a certain wavelengths; (2)
the coating material must have a refraction index which is the square root of
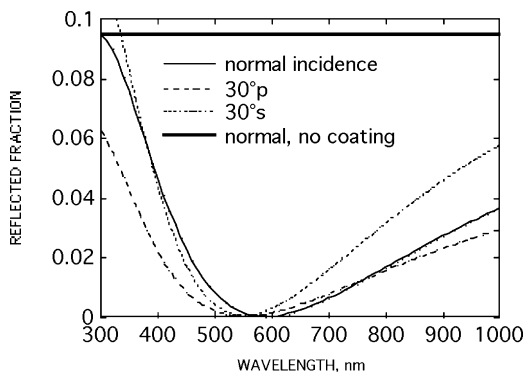
FIGURE 9.13. Reflectance of a lens of heaviest flint glass (n2 = 1.89) coated with a quarter-
wave thickness (0.107 mm) of magnesium fluoride (MgF$_2$, n1 = 1.38). Reflected fraction
of the incident light is shown for normal incidence and for 30° incidence angle with
different polarizations. For comparison the reflected ratio at normal incidence without
coating is also shown. For oblique angles even higher reflectance would be obtained
without coating. The mixture of violet-blue and red reflected light gives such a lens a
purple tint.

the refractive index of the lens material (i.e., $n1^2 = n2$). In practice compromises have to be made.

The reader might wonder what the construction of antireflection coatings on camera lenses has to do with photobiology. The fact is that even some eyes, notably in the insect orders Lepidoptera and Diptera, have antireflective surfaces (Miller et al. 1966, Parker 1998, 1999, Yoshida 2002). In this case, however, the antireflective surface is not obtained by addition of a layer of material of a different refractive index, but by finishing off the bulk material not with a smooth surface, but with tapering "nipples" smaller than the wavelength of light, which gives the same effect as if the refraction index were to decrease gradually. The main biological advantage might be to make the bearer of the eyes less conspicuous by avoiding a shiny surface (Stavenga, Foletti, Palasantzas and Arikawa 2006) and to some extent to improve vision. This "biological antireflection coating" is more efficient than the man-made one and has not yet been achieved technically on the same scale, but can be exploited on the microwave scale for military purposes to make surfaces invisible to radar.

9.10.3. Reflection by Multilayer Stacks

We shall now come to the more complicated case of multilayer stacks forming efficient biological mirrors with nearly 100% reflectivity. The most important case is that of normal incidence. Eyes, for instance, are constructed such that the light hits the retina almost perpendicularly, and therefore also the reflective backing of the retina. However, using the computer program at the end of the section, oblique incidence and both s and p polarization can be handled. The stacks have alternating layers of lower refractive index (n0) of thickness d0 and layers of higher refraction index (n1) and thickness d1. This computer program is based on the treatise by Huxley (1968) and is in agreement with the example treated by Land (1966). Figure 9.14 shows examples of the output of this computer program.

Within a certain wavelength range, about 100 nm, the reflectance reaches nearly 100% for only 20 high-index layers, i.e., 40 interfaces, while it is lower around this region, and oscillates with wavelength. The number of these oscillations increases with increasing number of layers. In reality this results in shiny reflectance only within a certain wavelength range, which gives the surface a colored appearance, as can be seen in, for instance green and blue beetles. The hue of this metallic shine also changes with incidence and viewing angles (Fig. 9.15; see Fig. 9.13). Common examples in Europe where this effect can be seen is the head of the male mallard, which changes between green and blue depending on from where it is seen, and in the rock dove, which changes between green and purple (Yoshioka et al. 2007). However, all such angle-dependent colors do not result from the multilayer construction described here; there are also many examples where gratings (Chapter 3) produce the colorful effects (Pfaff and Reynders 1999, Srinivasarao 1999). Very complicated structures, in which both mulitlayer and grating effects contribute to colors, have
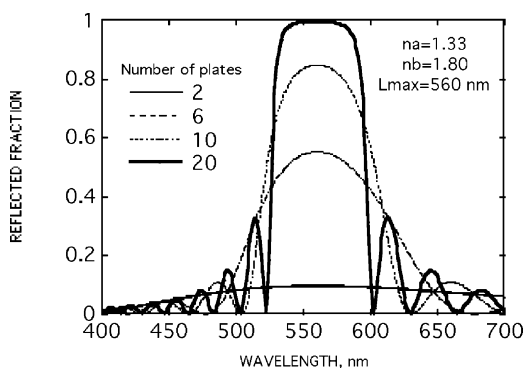
FIGURE 9.14. Reflectance at normal incidence of a stack of guanine plates (n = 1.80) with spaces between the plates having refractive index as seawater (n = 1.34). The thickness of both plates and spaces was chosen such that thickness times refraction index (optical pathlength) amounts to 140 nm. This leads to high reflection at 4 × 140 nm = 560 nm.

been described, especially for the scales of butterfly wings (Ghiradella 1998, Srinivasarao 1999, et al. Vukusic et al. 1999, 2000b, Kinoshita et al. 2002); for such cases mathematical models have been constructed (Gralak et al. 2001).

In those cases when high reflectance takes place over a wider wavelength range, such as often from the tapetum of eyes, this can be achieved in a number of ways. One mirror with high reflectance in one wavelength band (i.e., with one spacing and thickness of high-index plates) can be positioned behind one mirror with another spectral tuning. Or the dimensions of the layers can be continuously varied from wide to narrow ("chirped layers"), or have "chaotically" varying dimensions. An example of an animal in which layer thickness is varied in a way referred to as "doubly chirped" (thickest layers in the center) is the silverfish
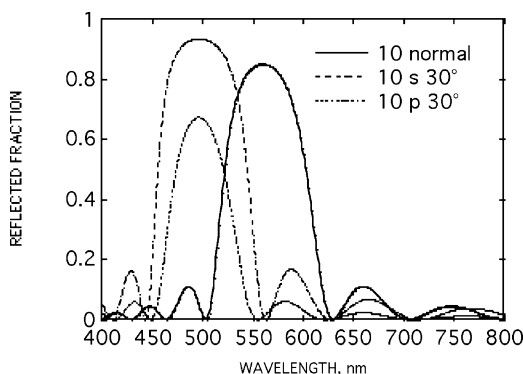
FIGURE 9.15. Reflectance of a stack of 10 plates similar to those in Fig. 9.14 and with the same medium in between. Reflectance was computed for normal incidence, and for an incidence angle of 30° and both polarizations.

(Large et al. 2001). In the herring, a neutral, silvery reflectance is obtained by a combination of different scales reflecting red, green, and blue wavebands (Denton and Land 1971).

Chemical compounds used by organisms for the layers of high refractive index include guanine (in eyes), chitin (in insect wings) and cellulose (in plants). The low refractive index layers are mostly aqueous solutions or air.

The computer program used for computations for Fig. 9.15 is:

```
pi = 3.14159
INPUT "refraction index of medium and spaces", na
INPUT "thickness of spaces, micrometres", da
INPUT "number of plates = ", p
INPUT "thickness of plates, micrometres", db
INPUT "refraction index of plates", nb
INPUT "incidence angle, degrees", aa:IF aa = 0 THEN aa = .001:aa = pi * aa/180
sinab = na * SIN(aa)/nb:ab = ATN(sinab/SQR(1-sinab * sinab))
27 : INPUT "choose polarisation, p for parallel, s for perpendicular", pol$
IF pol$ = "s" THEN 29
IF pol$ = "p" THEN 30
PRINT "MISTAKE! Try again!"
28 : GOTO 27
29 :r = SIN(aa-ab)/SIN(aa+ab):GOTO 31
30 : r = -TAN(aa-ab)/TAN(aa+ab)
31 :OPEN "O",1,"clip:"
FOR L =  .4 TO .85 STEP .001
fia = (2 * pi/L) * da * na * COS(aa):fib = (2 * pi/L) * db * nb * SQR(1-sinab * sinab)
kprim = -(COS(fia+fib)-r * r * COS(fia-fib))/(1-r * r)
k = (SIN(fia+fib)-r * r * SIN(fia-fib))/r/SIN(fib)/2
IF kprim * kprim<1 GOTO 100
REM In the following case mu is real
mu1 = kprim+SQR(kprim * kprim-1)
mu2 = kprim-SQR(kprim * kprim-1)
90 :murat = mu1/mu2:IF murat>1 THEN murat = 1/murat
95 :m2 = (murat)^p
RR = 1/(1+4 * m2 * (1-k * k)/(1-m2)/(1-m2)):GOTO 200
```

```
100 :REM In the following case mu is complex
costheta = (COS(fia+fib)-r * r * COS(fia-fib))/(1-r * r)
theta = ATN(SQR(1-costheta * costheta)/costheta)
RR = 1/(1+(k * k-1)/SIN(p * theta)/SIN(p * theta))
200 :PSET(1000 * (L-.39),310-300 * RR):PRINT# 1,RR
300 :NEXT L:CLOSE 1
400 :FOR L = .4 TO .85 STEP .05
CALL MOVETO(1000 * (L-.39),310):CALL LINETO(1000 * (L-.39),320)
IF 10 * L<>INT(10 * L) THEN 500
CALL MOVETO(1000 * (L-.41),330): PRINT 1000 * L;"nm"
500 :NEXT L
END
```

We have been reviewing so far structural colors as more or less traditionally described: multilayer stacks, diffraction, and scattering, but in the 1980s there appeared in the literature a new phrase, "photonic crystal," to describe many of the materials displaying such effects. As the concept developed, these materials were classified as one, two, and three dimensional (1D, 2D, and 3D); the multilayer thin film stacks qualify as 1D photonic crystals, and despite the complexity of our optical treatment above, these are considered the optically simple ones.

2D and 3D photonic crystals may selectively trap light of some wavelengths ("band gap" wavelengths) while reflecting and transmitting others. Were one to punch a regular array of minute holes in a film, one would have a 2D photonic crystal. If stretched into the third dimension, it may produce an iridescent hair or fiber. Biological examples of such iridescent 2D photonic crystals include the bristles of *Aphrodite*, a marine polychaete (Parker et al. 2001), barbules of bird feathers (Prum 2006) and the hairs of the comb rows of certain ctenophores (Welch et al. 2005). The ctenophores are especially interesting in that the comb bases rest above the light organs of the animals, and the hairs are apparently simultaneously producing reflected color and transmitting the bioluminescence out into the environment.

3D photonic crystals abound in nature. The mineral opal consists of silica spheres that pack into 3D face-centered cubic lattices; their band gap structure produces their iridescent colors. Analogous structures show up in insect scales, notably in those of certain butterflies (Morris 1975, Ghiradella 1984, 1985, 1989, 1998) and beetles (Ghiradella (1984, 1998; Parker et al. 2003).

The band gap characteristics of 2D and 3D photonic crystals are of current interest to the communications industry, which seeks to develop hollow core versions for more effective optical transmission fibers. In such designs the crystal cladding controls light leakage, while the air-filled core ($n = 1$) will transmit light faster than is now possible with glass fibers. Interestingly enough, two such hollow-core fibers are known from butterflies (Ghiradella 1994, 1998); in this

case the structure probably has a developmental rather than functional basis (but in the biological world, one never knows).

There exists in nature yet another class of structural color mechanism. Chemists have long known that certain liquid crystal (lc) molecules may orient themselves in so-called "helicoid" fashion and that if these are tuned properly they produce structural colors that are analogs of thin-film colors. Many lc thermometers are on the market; these work by reversably expanding (and thereby changing their optical geometry) when the temperature rises. A similar phenomenon occurs on the level just above the molecular; if collagen, chitin, or other biological fibrils are arranged in a regular helicoid fashion, the system can be tuned to produce color; this is the basis for the iridescent cuticles of many beetles, flies, and other insects (for reviews, see Neville 1993 and Srinivasarao 1999). The light reflected from these helicoid arrays is circularly polarized, and at least one beetle has found a way to simultaneously reflect both left and right circularly polarized light (Caveney 1971).

Let us bring the pigments back into play by noting that many organisms combine structural and pigmentary colors to get special effects. In birds, green plumage is often achieved by combining a structural blue color with a pigment yellow. In many, but not all, blue *Morpho* butterfles, a pigmentary "backing" intensifies the structural blue color by absorbing light entering the reflecting structures from the "wrong" direction. Such light would be out of phase with that from the mirror and would dilute the purity of the interference color. A particularly intriguing case is described in *Papilio* (Vukusic and Hooper 2005); the reflective scales have on their obverse surfaces a 2D photonic crystal which collimates the light so that it reaches and is reflected by a mirror lining the reverse surface. At the same time, a fluorescent pigment in the crystal re-emits entering light (420 nm) as light of 505 nm, which is right in the center of the animal's green visual pigment. What to our eyes appears as a dull blue must be striking indeed to the conspecifics. Other "combination effects" include simultaneous production of multilayer interference and diffraction reflectance in certain scales (Yoshioka et al. 2007, Vukusic et al. 1999, 2000a,b).

The biological world has a few additional ways of handling light. Some beetles can change color quickly by shifting between air and liquid in the cuticle (Hinton and Jarman 1972, 1973). Scattering produces brilliant whites (Vukusic, Hallam and Noyes 2007) and may yield more complex effects, especially if the combined optical behavior of all scales in a wing transect is taken into effect (Stavenga, Giraldo and Hoenders 2006) or if structures and pigments interact to produce "emergent" optical effects (Morehouse et al. 2007, Rutkowski et al. 2005). And of course there is transparency, a highly effective technique for evading predators. We have already mentioned antifreflective coatings, in particular the nipples that allow clearwing moths to become essentially invisible against any background. But invisibility is best understood in the open seas (see Herring 2002 for review), where there is no place to hide. Coelenterates and ctenophores may build bodies largely of transparent jelly, but arthropods and vertebrates must have muscles and skeletons.

To some degree these can be rendered transparent by arranging fibrous proteins so that they produce destructive interference in the predominantly blue light in their environment(s). But eyes must have pigment and gut contents quickly become opaque, even if they don't start that way. This may be a reason why so many fishes have instead evolved silvery mirrored sides to render themselves unseeable.

9.11. The Interplay of Spectra in the Living World

This chapter may seem very diverse to the reader, without a really common theme. However, spectral tuning in one pigment group is not independent of that in another one; in fact, they all depend on one another. As mentioned already, it all starts with the spectrum of the sun, and how that has determined the spectrum of the main photosynthetic pigment, chlorophyll *a*. The shielding effect of chlorophyll has led to the evolution of accessory pigments, like the phycobiliproteins, which can pick up light not absorbed by chlorophyll and make it available to photosynthesis. Also the long-wavelength bacterial chlorophylls of photosynthetic bacteria deep in sediments save the light energy that has been wasted by chlorophyll *a* containing organisms above them.

The daylight available from the sun, and that reflected from green plants, has also determined the spectral properties of visual pigments. The spectra of daylight, of chlorophyll, and of visual pigments, in turn, have tuned the floral pigments so that pollinators could easily detect flowers against a background of photosynthesizing leaves and also discriminate one kind of flower from another and judge the stage of development of the flower.

Likewise, the colors of fruits have evolved to make the fruits conspicuous to seed dispersers and make it possible for them to determine the degree of ripeness.

Flavonoids, pigments produced by plants and having many functions in plant life (such as shown in Fig. 9.9) are used "secondhand" by some insects. Butterflies that ingest them with their food use them to enhance their wing patterns and make themselves more attractive to the opposite sex (Knuttel and Fiedler 2001).

For plants, it was important to see their competitors for light and adapt their mode of growth thereafter. In phytochrome, first appearing among prokaryotes, they got an excellent tool for detecting the modification of the daylight spectrum by chlorophyll. The short-wave form of phytochrome, Pr, has an absorption peak near 660 nm, near the center of absorption of the combination of chlorophylls *a* and *b*. Its long-wavelength form, Pfr, has an absorption peak near 730 nm, just beyond the chlorophyll absorption bands. The balance between the two phytochrome forms is sensitively dependent on the presence of chlorophyll in the environment. Also for some insects, a red-light receptor plays an important role in the recognition of plant leaves, but in this case the green spectral region is used for contrast.

Bioluminescent systems have often evolved as substitutes for or complements to pigments. "Counterilluminating" fish with glowing bellies evade detection by mimicking the downwelling daylight. The dragonfish, in contrast, has evolved a bioluminescence that is undetectable for other animals, but visible to itself; it is able to detect prey which can see neither the searchlight nor the predator producing it. Fireflies that are active in late-night darkness send out green light, in the region of the spectrum where their eyes are most sensitive. Those flying at dusk, in contrast, use yellow light, which makes them more visible against green leaves.

It all fits together.

References

Bhoo, S.-H., Davis, S.D., Walker, J., Karniol, B. and Vierstra, R.D. (2001) Bacteriophytochromes are photochromic histidine kinasis using a biliverdin chromophore. Nature 414, 776–779.

Björn, G.S. (1979) Action spectra for conversions of phycochrome b, a reversibly photochromic pigment in a blue-green alga, and its separation from other pigments. Physiol. Plant. 46, 281–286.

Björn, G.S. (1980) *Photoreversibly photochromic pigments from blue-green algae (cyanobacteria).* Diss. Lund University, CODEN LUNBDS/(NBFB-1009)/1–28/(1980).

Björn, L.O. (1976) Why are plants green? Relationships between pigment absorption and photosynthetic efficiency.Photosynthetica 19, 121–129.

Björn, L.O. (1979) Photoreversibly photochromic pigments in organisms: properties and roles in biological light perception. Quart. Revs. Biophys. 12, 1–23.

Björn, L.O. (1985a) Varför håller växterna inte färgen? Forskning Framsteg, 85 (6), 40–46.

Björn, L.O. (1985b) Växternas ljusperception. Svensk Bot. Tidskr. 79, 249–264.

Björn, L.O. and Björn, G.S. (1980) Yearly review: Photochromic pigments and photoregulation in blue-green algae. Photochem. Photobiol. 32, 849–852.

Björn, G.S., Braune, W. and Björn, L.O. (1985) Light-induced, dark reversible colour shift in petals of *Phlox*. Physiol. Plant. 64, 445–448.

Bowmaker, J.K., Heath, L.A., Wilkie, S.E. and Hunt, D.M. (1997) Visual pigments and oil droplets from six classes of photoreceptor in the retinas of birds. Vision Res. 37, 2183–2194.

Britt, S.G., Feiler, R., Kirschfeld, K. and Zuker, C.S. (1993) Spectral tuning of rhodopsin and metarhodopsin in vivo. Neuron 11, 29–39.

Caveney, S. (1971) Cuticle reflectivity and optical activity in scarab beetles: The rôle of uric acid. Proc. R. Soc. London B 178, 205–225.

Chittka, L. 1996. Does bee color vision predate the evolution of flower color? Naturwissenschaft 83, 136–138.

Chittka, L. and Menzel, R. (1992) The evolutionary adaptation of flower colors and the insect pollinators's color vision. J. Comp. Physiol. A. 171, 171–181.

Chittka, L. and Dornhaus, A. (1999), Comparisons in physiology and evolution, and why bees can do the things they do. http://www.ciencia.cl/CienciaAlDia/volumen2/numero2/articulos/articulo5-eng.html.

Chittka, L., Thomson, J.D. and Waser, N.M. (1999) Flower constancy, insect psychology, and plant evolution. Naturwiss. 86, 361–377.

Cinque, G, Croce, R. and Bassi, R. (2000) Absorption spectra of chlorophyll *a* and *b* in Lhcb protein environment. Photosynthesis Res. 64, 233–242.

Cronin, T.W., Caldwell, R.L. and Marshall, J. (2001) Sensory adaptation—tunable colour vision in a mantis shrimp. Nature 411, 547–548.

Denton, E.J. and Land, M.F. (1971) Mechanism of reflection in silvery layers of fish and cephalopods. Proc. Roy. Soc. Lond. A 178, 43–61.

Diakoff, S. and Scheibe, J. (1973) Action spectra for chromatic adaptation in *Tolypothrix tenuis*. Plant Physiol. 51, 382–385.

Dominy, N.J. and Lucas, P.W. (2001) Ecological importance of trichromatic vision to primates. Nature 410, 363–367.

Douglas, R.H., Partridge, J.C., Dulai, K., Hunt, D., Mullineaux, C.W., Tauber, A.Y. and Hynninen, P.H. (1998) Science 393, 423–424.

Douglas, R.H., Partridge, J.C., Dulai, K.S., Hunt, D.M, Mullineaux, C.W. and Hynninen, P.H. (1999) Enhanced retinal longwave sensitivity using a chlorophyll-derived photosensitiser in *Malacoseus niger*, a deep-sea dragon fish with far red bioluminescence. Vision Res. 39, 2817–2832.

Fasick, J.I. and Robinson, P.R. (1998) Mechanism of spectral tuning in the dolphin visual pigments. Biochemistry 37, 433–438.

Fasick, J.I. and Robinson, P.R. (2000) Spectral-tuning mechanisms of marine mammal rhodopsins and correlations with foraging depth. Visual Neurosci. 17, 781–788.

Fasick, J.I., Cronin, T.W., Hunt, D.M. and Robinson, P.R. (1998) The visual pigments of the bottlenose dolphin (*Tursiops truncatus*). Visual Neurosci. 15, 643–651.

Fernandez, H.R.C. (1978) Visual pigments of bioluminescent and nonbioluminescent deep-sea fishes. Vision Sci. 19, 589–592.

Figueiredo, P., Lima, J.C., Santos, H., Wigand, M.-C., Brouillard, M., Macanita, A.L and Pina, F. (1994) Photochromism of the synthetic 4′,7-dihydroxyflavylium chloride. J. Am. Chem. Soc. 116, 1249–1254.

Fox, D.L. (1976) *Animal biochromes and structural colors.* University of California Press, Berkeley.

Frank, H.A., Bautista, J.A,, Josue, J.S. and Young, A.J. (2000) Mechanism of nonphotochemical quenching in green plants: Energies of the lowest excited singlet states of violaxanthin and zeaxanthin. Biochemistry 39, 2831–2837.

Fuad, N., Day, D.A., Ryrie, I.J. and Thorne, S.W. (1983) Photobiochem. Photobiophys. 5, 255–262.

Fujimoto, K., Hasegawa, J., Hayashi, S., Kato, S. and Nakatsuji, H. (2005) Mechanism of color tuning in retinal protein: SAC-CI and QM/MM study. Chem. Phys. Lett. 414, 239–242.

Fujita, Y. and Hattori, A. (1962) Photochemical interconversion between precursors of phycobilin chromoprotein in *Tolypothrix tenuis*. Plant Cell Physiol. 3, 209–220.

Ghiradella, H. (1984) Structure of iridescent lepidopteran scales: Variations on several themes. Ann. Entomol. Soc. Am. 77, 637–645.

Ghiradella, H. (1985) Structure and development of iridescent lepidopteeran scales: The Papilionidae as a showcase family. Ann. Entomol. Soc. Am. 78, 252–264.

Ghiradella, H. (1989) Structure and development of iridescent butterfly scales: Lattices and laminae. J. Morph. 202, 69–88.

Ghiradella, H. (1991) Light and color on the wing: Structural colors in butterflies and moths. Appl. Optics 30, 3492–3500.

Ghiradella, H. (1994) Structure of butterfly scales: Patterning in an insect cuticle. Micr. Res. Tech. 27, 429–438.

Ghiradella, H. (1998) Hairs, bristles and scales. In: Harrison, F.W. and Locke, M. (eds) *Microscopic anatomy of invertebrates*, Vol. 11A *Insecta*. Wiley-Liss, New York, pp. 257–287.

Gill, E.M. and Wittmershaus, B.P. (1999) Spectral resolution of low-energy chlorophylls in Photosystem I of *Synechocystis* sp. PCC 6803 through direct excitation. Photosynthesis Res. 61, 53–64.

Glazer, A.N. and Wedemayer, G.J. 1995. Cryptomonad biliproteins—an evolutionary perspective. Photosynthesis Res. 46, 93–105.

Goto, T. and Kondo, T. (1991) Structure and molecular stacking of anthocyanins—flower color variation. Angew. Chem. Int. Engl. 30, 17–33.

Gralak, B., Tayeb, G. and Enoch, S. (2001) Morpho butterfly wings color modelled with lamellar grating theory. Optics Express 9, 567–578.

Grossman, A.R., Bhaya, D. and He, Q. (2001) Tracking the ligh environment by cyanobacteria and the dynamic nature of light harvesting. J. Biol. Chem. 276, 11449–11452.

Halldal. P. (1968) Photosyntheic capacities and photosynthetic action spectra of endozoic algae of the massive coral. *Favia*. Biol. Bull. 134, 411–424.

Hart, N.S., Partridge, J.C., Bennett, A.T.D. and Cuthill, I.C. (2000) Visual pigments, cone oil droplets and ocular media in four species of estrildid finch. J. Comp. Physiol. A, 186, 681–694.

Herring (1994) Reflective systems in aquatic animals. Comp. Biochem. Physiol. 109A, 513–546.

Herring, P. (2002) *The biology of the deep ocean*. Oxford University Press, Oxford.

Hinton, H.E. and Jarman, G.M. (1972) Physiological color change in the Hercules beetle. Nature 238, 160–161.

Hinton, H.E. and Jarman, G.M. (1973) Physilogical color change in the elytra of the Hercules beetle, *Dynastes hercules.* J. Insect Physiol. 19, 533–549.

Holzwarth, A.R. (1991) Structure-function relationships and energy transfer in phycobiliprotein antennae. Physiol. Plant. 83, 518–528.

Huxley (1968) A theoretical treatment of the reflexion of light by multilayer structures. J. Exp. Biol., 48, 227–245.

Isayama, T., Alexeev, D., Makino, C.L., Washington, I., Nakanishi, K., and Turro, N.J. (2006) An accessory chromophore in red vision. Nature 443, 649.

Jacobs, G.H. 1992. Ultraviolet vision in vertebrates. Am. Zool., 32, 544–554.

Jensen, P. and Bunker, P.R. (2000) *Computational molecular spectroscopy*. John Wiley and Sons, Hoboken, NJ.

Jordan, P., Fromme, P., Witt, H.T., Klukas, O., Saenger, W. and Krauß, N. (2001) Three-dimensional structure of cyanobacterial photosystem I at 2.5 nm resolution. Nature 411, 909–917.

Karapetyan, N.V., Dorra, D., Schweitzer, G., Beszmertnaya, I.N. and Holzwarth, A.R. (1997) Fluorescence spectroscopy of the longwave chlorophylls in trimeric and monomeric photosystem I core complexes from the cyanobacterium *Spirulina platensis*. Biochemistry 36, 13830–13837.

Kehoe, D.M. and Grossman, A.R. (1996) Similarity of a chromatic adaptation sensor to phytochrome and to ethylene receptors. Science 273, 1409–1412.

Kehoe, D.M. and Grossman, A.R. (1997) New classes of mutants in complementary chromatic adaptation provide evidence for a novel four-step phosphorelay system. J. Bacteriol. 179, 3914–3921.

Kehoe, D.M. and Grossman, A.R. (1998) Use of molecular genetics to investigate comple-
    mentary chromatic adaptation: advances in transformation and complementation. Meth.
    Enzymol. 297, 279–290.

Kehoe, D.M. and Gutu, A. (2006) Responding to color: the regulation of complementary
    chromatic adaptation. Annu. Rev. Plant Biol. 57, 127–150.

Kelber, A. (1999) Ovipositing butterflies use a red receptor to see green. J. Exp. Biol.
    202, 2619–2630.

Kiang, N.Y., Siefert, J., Govindjee and Blankenship, R.E. (2007) Spectral signatures of
    photosynthesis. I. Review of Earth organisms. Astrobiology 7, 252–274.

Kinoshita, S, Yoshioka, S, Fujii, Y, and Okamoto, N. (2002) Photophysics of structural
    color in the *Morpho* butterflies. Forma 17, 103–121.

Kinoshita, S., and Yoshioka, S. (Eds.) (2005) *Structural colors in biological systems.*
    Osaka University Press, Osaka.

Kleinschmidt, J. and Harosi, F. (1992) Proc. Natl. Acad. Sci USA, 89, 9181–9185.

Knipp, B., Müller, M., Metzler-Nolte, N., Balaban, T.S., Braslavsky, S.E. and Schaffner,
    K. (1998) NMR verification of helical conformations of phycocyanobilin in organic
    solvents. Helv. Chim. Acta 81, 881–888.

Knuttel, H. and Fiedler, K. (2001) Host-plant derived variation in ultraviolet wing-patterns
    influences mate selection by male butterflies. J. Exp. Biol. 204, 2447–2459.

Kochendoerfer, G.G., Lin, S.W., Sakmar, T.P. and Mathies, R.A. (1999) How color visual
    pigments are tuned. Trends Biochem. Sci. 24, 300–305.

Kochubey, S.M. and Samokhval, E.G. (2000) Long-wavelength chlorophyll forms in
    Photosystem I from pea thylakoids. Photosynthesis Res. 63, 281–290.

Koehne, B., and Trissl, H.W. (1998) The cyanobacterium Spirulina platensis contains
    a long wavelength-absorbing pigment C-738 (F-760(77K)) at room temperature.
    Biochemistry 37, 5494–5500.

Koehne, B., Elli, G., Jennings, R.C., Wilhelm, C. and Trissl, H.-W. (1999) Spectroscopic
    and molecular characterization of a long wavelength absorbing antenna of *Ostreobium
    sp.* Biochim.Biophys. Acta 1412, 94–107.

Land, E. (1964) The retinex theory of color vision. Sci. Am. 108–128.

Land, M.F. (1966) A multilayer interference reflector in the eye of the scallop, *Pecten
    maximus.* J. Exp. Biol. 45, 433–447.

Land, M.F. and Nilsson D.-E. (2002) *Animal eyes.* Oxford University Press, Oxford.

Large, M.C.J., McKenzie, D.R., Parker, A.R., Steel, B.C., Ho, K., Bosi, S.G.,
    Nicorovici, N. and McPhedran, R.C. (2001) The mechanism of light reflectance in
    silverfish. Proc. R. Soc. Lond. A 457, 511–518.

Lazaroff, N. and Schiff (1962) Action spectrum for developmental photoinduction of the
    blue-green alga *Nostoc muscorum.* Science 137, 603–604.

Linanto, J. and Korppi-Tommola, J. (2000) Spectroscopic properties of Mg-chlorin, Mg-
    porphin and chlorophylls a,b,c(1), c(2), c(3) and d studied by semi-empirical and ab
    initio MO/CI methods. Phys. Chem. Chemical Phys. 2, 4962–4970.

Lucas, P.W., Darvell, B., Lee. P.K.D., Yuen, T.D.B. and Choong, M.F. (1998) Colour
    cues for leaf food selection by long-tailed macaques (*Macaca fascicularis*) with a
    new suggestion for the evolution of trichomatic colour vision. Folia Primatol. 69,
    139–152.

Lunau, K. (1996) Unidirectionality of floral colour changes. Plant Systematics Evol. 200,
    125–140.

Lunau, K. (2004) Adaptive radiation and coevolution - pollination biology case studies.
    Organisms Diversity Evol. 4, 207–224.

Lythgoe, J.N. (1984) Visual pigments and environmental light. Vision Sci. 24, 1539–1550.

MacColl, R. (1998) Cyanobacterial phycobilisomes. J. Struct. Biol. 124, 311–334.

Maier, EJ. and Bowmaker, J.K. (1993) Color-vision in the passeriform bird, Leiothrix lutea—correlation of visual pigment absorbancy and oil droplet transmission with spectral sensitivity. J. Comp. Physiol. A 172, 295–301.

Makino, C.L., Groesbeek, M., Lugtenburg, J. and Baylor, D.A. (1999) Spectral tuning in salamander visual pigments studied with dehydroretinal chromophores. Biophys. J. 77, 1024–1035.

Marshall, J. and Oberwinkler, J. (1999) The colourful world of the mantis shrimp. Nature 401, 873–874.

Mason, CW (1926) Structural colors in insects. I. J. Phys. Chem. 30, 383–395.

Mason, CW (1927a) Structural colors in insects. II. J. Phys. Chem. 31, 321–354.

Mason, CW (1927b) Structural colors in insects. III. J. Phys. Chem. 31, 1856–1872.

Matsui, S., Seidou, M., Uchiyama, I., Sekiya, N., Hiraki, K., Yoshihara, K. and Kito, Y. (1988) 4-hydroxyretinal, a new visual pigment chromophore found in the biolumi-nescent squid, Watasenia scintillans. Biochim. Biophys. Acta, 966, 370–374.

Mauzerall, D. (1976) Chlorophyll and photosynthesis. Pil. Trans. Roy. Soc. Lond. B 273, 287–294.

Miller, W.H., Møller, A.R. and Bernhard, C.G. (1966) The corneal nipple array. In: C.G. Bernhard (Ed.), The functional organgization of the compound eye. Pergamon Press, Oxford, pp. 21–33.

Morehouse, N.I., Vukusic, P, and Rutkowski, R. (2007) Pterin pigment granules are responsible for both broadband light scattering and wavelength selective absorption in the wing scales of pierid butterflies. Proc. Roy. Soc. London B 274, 359–366.

Morris, R.B. (1975) Iridescence from diffraction structures in the wing scales of Callophrys rubi, the Green Hairstreak. Proc. R. Soc. Entomology A 48, 149–154.

Murrell, J.N. (1963) The theory of the electronic spectra of organic molecules. Methuen, London. (German edition Elektronenspektren organischer Moleküle, Bibliographisches Institut Mannheim 1967).

Nathans, J. (1990) Determinants of visual pigment absorbance: Identification of the retinylidene Schiff's base counterion in bovine rhodopsin. Biochemistry 29, 9746–9752.

Nathans, J. (1992) Rhodopsin: Structure, function, and genetics. Biochemistry 31, 4923–4931.

Neitz, M., Neitz, J. and Jacobs, G.H. (1991) Spectral tuning of pigments underlying red-green color vision. Science 252, 971–974.

Neitz. J., Neitz, M. and Jacobs, G.H. (1993) More than three different cone pigments among people with normal color vision. Vision Res. 33, 117–122.

Neville, A.C. (1993) Biology of the Fibrous Composites. Cambridge University Press, Cambridge.

Ohad, I., Clayton, R.K. and Bogorad, L. (1979) Photoreversible absorption changes in solutions of allophycocyanin purified from Fremyella diplosiphon: Temperature dependence and quantum efficiency. Proc. Natl. Acad. Sci. USA 76, 5655–5659.

Ohki, K. and Fujita, Y. (1978) Photocontrol of phycoerythrin formation in the blue-green alga Tolypothrix tenuis growing in the dark. Plant Cell Physiol. 19, 7–15.

Öquist, G. (1969) Adaptations in pigment composition and photosynthesis by far red radiation in Chlorella pyrenoidosa. Physiol. Plant. 22, 516–528.

Osorio, D. and Vorobyev, M. (1996) Colour vision as an adaptation to frugivory in primates. Proc. R. Soc. Lond. B 263, 593–599.

Osorio, D., Marshall, N.J. and Cronine, T.W. (1997) Stomatopod photoreceptor spectral tuning as an adaptation for colour constancy in water. Vision Res. 37, 3299–3309.

Pålsson, L.O., Flemming, C., Gobels, B., van Grondelle, R., Dekker, J.P. and Schlodder, E. (1998) Energy transfer and charge separation in photosystem I: P700 oxidation upon selective excitation of the long-wavelength antenna chlorophylls of *Synechococcus elongatus*. Biophys. J. 74, 2611-2622.

Parker, A.R. (1998) The diversity and implications of animal structural colours. J. Exp. Biol. 201, 2343–2347.

Parker, A.R. (1999) Light-reflection strategies. Am. Sci. 87, 248–255.

Parker, A.R. (2000) 515 million years of structural color. J. Opt. A: Pure Appl. Opt. 2, R15-R28.

Parker, A.R., McPhedran, R.C., McKenzie, D.R., Botten, L.C., and Nicorovici, N.-A. P. (2001) *Aphrodite*'s iridescence. Nature 409, 36–37.

Parker, A.R., Welch, V.L., Driver, D., and Martini, N. (2003) An opal analogue discovered in a weevil. Nature 426, 786–787.

Peichl. L., Behrmann, G. and Kröger, H.H. (2001) For whales and seals the ocean is not blue: a visual pigment loss in marine mammals. Eur. J. Neurosci. 13, 1520–1528.

Peitsch, D., Fietz, A., Hertel, H., Desouza, J., Ventura, D.F. and Menzel, R. (1992) The spectral input systems of hymenopteran insects and their receptor-based color-vision. J. Comp. Physiol. A Sensory Neural Behav. Physiol. 170, 23–40.

Pfaff, G. and Reynders, P. (1999) Angle-dependent optical effects from submicron structures of films and pigments. Chem. Rev. 99, 1963–1981.

Polívka, T., Herek, J.L., Zigmantas, D., Åkerlund, H.E. and Sundström, V. (1999) Direct observation of the (forbidden) S-1 state in carotenoids. Proc. Natl Acad. Sci. USA 96, 4914–4917.

Prum, R.O. (2006) Anatomy, physics and evolution of structural colors In: G.E. Hill and K.J. McGraw (Eds.), *Bird coloration*, Vol. 1, *Mechanisms and measurements*. Harvard University Press, Cambridge, MA, pp. 295–353.

Regan, B.C., Julliot, C., Simmen, B., Viénot, F., Charles-Dominique, P. and Mollon, P. (1998) Frugivory and colour vision in *Alouatta seniculus*, a trichromatic platyrrhine monkey. Vision Res. 38, 3321–3327.

Ritz, T., Damjanovic´, A., Schulten, K, Zhang, J.P. and Koyama, Y. (2000) Efficient light harvesting through carotenoids. Photosynthesis Res. 66, 125–144.

Robinson, B.L. and Miller, J.N. (1970) Photomorphogenesis in the blue-green alga *Nostoc commune*. Physiol. Plantarum 23, 461–472.

Rutkowski, R.L., Macedonia, J.M., Morehouse, N., and Taylor-Taft, L. (2005) Pterin pigments amplify iridescent ultraviolet signal in males of the orange sulphur butterfly, *Colias eurytheme*. Proc. R. Soc. London B 272, 2329–2335.

Scharnagl, C. and Fischer, S.F. (1993) Reversible photochemistry in the a-subunit of phycoerythrocyanin: Characterisation of chromophore and protein by molecular dynamics and quantum chemical calculations. Photochem. Photobiol. 57, 63–70.

Scheer, H. and Kufer, W. (1977) Studies on plant bile pigments, IV: Conformational studies on C-phycocyanin from *Spirulina platensis*. Z. Naturforsch. 32c, 513–519.

Scheibe, J. (1972) Photoreversible pigment: occurrence in a blue-green alga. Science 1976, 1037–1039.

Schelvis, J.P.M, van Noort, P.I., Aartsma, P.I. and van Gorkom, H.J. (1994) Energy transfer, charge separation and pigment arrangement in the reaction center of photosystem II. Biochim. Biophys. Acta 1184, 242–250.

Schneeweis, D.M. and Green, D.G. (1995) Spectral properties of turtle cones. Visual Neurosci. 12, 333–344.

Schulten, K. and Karplus, M. (1972) On the origin of a low-lying forbidden transition in polyenes and related molecules. Chem. Phys. Lett. 14, 305–309.

Seki, T. and Vogt, K. (1998) Evolutionary aspects of the diversity of visual pigment chromophores in the class Insecta. Comp. Biochem. Physiol. B 119, 53–64.

Sharpe, L.T., Stockman, A., Jägle, H. and Nathans, J. (1999) Opsin genes, cone photopigments, color vision, and color blindness. In: K.Gegenfurtner, and L.T. Sharpe (Eds.), *Color vision: from genes to perception*. Cambridge University Press, New York.

Shubin, V.V., Murthy, S.D.S, Karapetyan, N.V. and Mohanty, P.S. (1991) Origin of the 77-K variable fluorescence at 758 nm in the cyanobacterium *Spirulina platensis*. Biochim. Biophys. Acta, 1060, 28–36.

Siitari, H., Honkavaara, J. and Viitala, J. (1999) Ultraviolet reflection of berries attracts foraging birds. A laboratory study with redwings (*Turdus iliacus*) and bilberries (*Vaccinium myrtillus*). Proc. R. Soc. Lond. B 266, 2125–2129.

Srinivasarao, M. (1999) Nano-optics in the biological world: Beetles, butterflies, birds, and moths. Chem. Rev. 99, 1935–1961.

Stavenga, D.G., Foletti, S., Palasantzas, G., and Arikawa, K. (2006) Light on the moth-eye corneal nipple array of butterflies. Proc. R. Soc. London B 273, 661–667.

Stavenga, D.G., Giraldo, M.A. and Hoenders, B.J. (2006) Reflectance and transmittance of light scattering scales stacked on the wings of pierid butterflies. Opt. Expr. 14, 4880–4890.

Stomp, M., Huisman, J., Stal, L.J., and Matthijs, H.C.P. (2007) Colorful niches of phototrophic microorganisms shaped by vibrations of the water molecule. ISME J. 1, 271–282.

Tanimura, T., Isono, K. and Tsukahara, Y. (1986) 3-hydroxyretinal as a chromophore of *Drosophila melanogaster* visual pigment analyzed by high-pressure liquid-chromatography. Photochem. Photobiol. 43, 225–228.

Thrash, R.J., Fang, H.L.-B. and Leroi, G.E. (1979) On the role of forbidden low-lying excited states of light-harvesting carotenoids in energy transfer in photosynthesis. Photochem. Photobiol. 29, 1049–1050.

Vogelmann, T.C. and Scheibe, J. 1978. Action spectra for chromatic adaptation in the blue-green alga *Fremyella diplosiphon*. Planta 143, 233–239.

Vogt, K. (1983) Is the fly visual pigment a rhodopsin? Zschr Naturforsch. C, 38, 329–333.

Vogt, K. and Kirschfeld, K. (1984) Chemical identity of the chromophores of fly visual pigment. Naturwiss. 71, 211–213.

Vorobyev, M., Osorio, D., Bennet, A.T.D., Marshall, N.J. and Cuthill, I.C. (1998) Tetrachromacy, oil droplets and bird plumage colours. J. Comp. Physiol. A Sensory Neural Behav. Physiol. 183, 621–633.

Vukusic, P., Sambles, J.R., Lawrence, C.R. and Wootton, R.J. (1999) Quantified interference and diffraction in single *Morpho* butterfly scales. Proc. R. Soc. Lond. B 266, 1403–1411.

Vukusic, P., Sambles, J.R., and Ghiradella, H. (2000a) Optical classification of microstructure in butterfly wing scales. Photonics Sci. News 6, 61–66.

Vukusic, P., Sambles, J.R. and Lawrence, C.R. (2000b) Colour mixing in wing scales of a butterfly. Nature 404, 457.

Vukusic, P., and Hooper, I. (2005) Directionally controlled fluorescence emission in butterflies. Science 310, 1151.

Vukusic, P., Hallam, B., and Noyes, J. (2007) Brilliant whiteness in ultrathin beetle scales, Science 315, 348.

Wald, G. and Brown, P.K. (1958) Human rhodopsin. Science 127, 222–226.

Warrant, E. (2000) The eyes of deep-sea fishes and the changing nature of visual scenes with depth. Phil. Trans. R. Soc. Lond. 355, 1155–1159.

Weiss, C., Jr. (1972) The pi electron structure and absorption spectra of chlorophylls in solution. J. Mol. Spectrosc. 44, 37–80.

Welch, V.L., Vigneron, J.P. and Parker, A.R. (2005) The cause of colouration in the ctenophore, *Beroë cucumis*. Curr. Biol. 15, R985-R986.

Yokoyama, S. (1997) Molecular genetic basis of adaptive selection: Examples from color vision in vertebrates. Annu. Rev. Genet. 31, 315-336.

Yokoyama, S., Radlwimmer, F.B. and Blow, N.S. (2000) Ultraviolet pigments in birds evolved from violet pigments by a single amino acid change. Proc. Natl Acad. Sci. USA 97, 7366-7371.

Yoshida, A. (2002) Antireflection of butterfly and moth wings through microstructure. Forma, 17, 75–89.

Yoshioka, S., Nakamura, E, and Kinoshita, S. (2007) Origin of two-color iridescence in rock dove's feather. J. Phys. Soc. Japan 76, 013801-1–013801-4.

Zhao, K.H. and Scheer, H. (1995) Type-I and Type-II reversible photochemistry of phycoerythrocyanobilin alpha-subunit from *Mastigocladus laminosus* both involve Z-isomerisation, E-isomerisation of phycoviolobilin chromophore and are controlled by sulphydryls in apoprotein. Biochim. Biophys. Acta 1228, 244–253.

Zhao, K.H., Haessner, R., Cmiel, E. and Scheer, H. (1995) Type I reversible photo-chemistry of phycoerythrocyanin involves Z/E-isomerisation of a-84 phycoviolobilin chromophore. Biochim. Biophys. Acta 1228, 235–243.

Zouni, A., Witt, H.T., Kern, J, Fromme, P, Krauß, N., Saenger, W. and Orth, P. (2001) Crystal structure of photosystem II from *Synechococcus elongatus* at 3.8 Å resolution. Nature 409, 739–743.

Zucchelli, G., Jennings, R.C. and Garlaschi, F.M. (1990) The presence of long-wavelength chlorophyll a spectral forms in the light-harvesting chlorophyll a/b protein complex II. J. Photochem. Photobiol. B, Biol. 6, 381–394.

10
Photochemical Reactions in Biological Light Perception and Regulation

Lars Olof Björn

Abstract: Many photochemical reactions involved in the sensing of and regulation by light and ultraviolet radiation by organisms consist of *cis-trans* (and *trans-cis*) isomerizations. This chapter starts with a description of these, and then goes on to the blue-light receptors cryptochrome and phototropin, which use other chemical mechanisms, and concludes with a discussion of ultraviolet-B receptors.

10.1. Introduction

Many photochemical reactions involved in the sensing of and regulation by light and ultraviolet radiation by organisms consist of *cis-trans* (and *trans-cis*) isomerizations. We shall start with this class of photosensors, and then go on to other mechanisms. There are many more known and unknown light-sensing molecular systems than those briefly described below, but (except for the first one) I have tried to concentrate on those more widespread. As examples of light-sensing pigments with a very limited distribution, one can mention stentorin and blepharismin of certain ciliates (Lenci et al. 2001).

The term "photoreceptor" means different things to different people. In zoology it means a cell which responds to light, such as rods and cones of our eyes, but to plant scientists it means a pigment molecule, such as rhodopsin or phytochrome, which absorbs light at the start of a chain of events leading to light perception or regulation of a physiological process by light. We shall use the term here in this latter sense.

"Photoreceptor" in this sense is a concept related to "photoenzyme," i.e., an enzyme active only in light. A class of photoreceptors, the cryptochromes, are thought to have evolved from certain photolyases. Another photoenzyme, NADPH-protochlorophyllide oxidoreductase, can also be regarded as a photoreceptor, helping the plant to regulate chlorophyll synthesis and chloroplast development (Beale 1999). An example of a flavine enzyme whose activity is

stimulated by blue light is glycine oxidase of *Chlorella* (Schmid and Schwarze 1969, Schmid 1970).

10.2. *Cis-Trans* and *Trans-Cis* Isomerization

Double bonds and conjugated double bond systems provide molecules with a certain rigidity. Molecular groups cannot rotate freely around double bonds or around single bonds in a continuous conjugation suite, as they can around isolated single bonds provided there is room enough. When a double bond is involved, there are two opposite torsion angles for which the energy has a minimum value, and which thus represent stable conformations. Often the carbon atoms at the double bonds carry one hydrogen atom and one larger atomic group. These atoms then lie in the same plane, which is the same plane as the corresponding groups on the carbon atom at the other end of the double bond (in Fig. 10.1 this is the plane of the paper).

   If the larger atomic groups are on the same side of the line through the double bond and the carbon atoms at its ends, the molecule is said to be in *cis*-configuration; if they are on opposite sides the molecule has a *trans*-configuration. However, for larger molecules this designation may be difficult to apply, and another nomenclature has been introduced, i.e. Z- (for German *zusammen*, together) and E- (for German *entgegen*, opposite) configurations. In this system a priority is assigned for the atoms immediately attached to the double bond, such that higher priority is assigned to atoms of higher atomic number. Thus carbon atoms in the example in Fig. 10.1 have first priority, hydrogen atoms second priority. When atoms of same priority are on the same side we have a Z-configuration, otherwise an E-configuration.

   By a very rough consideration we can appreciate why *cis-trans* (E-Z) isomer-izations are suitable for light sensing. A typical carbon–carbon single bond has a bond energy of 387 kJ per mole, while the typical double bond has a strength of about 610 kJ per mole. The difference is 263 kJ per mole. We can think of a rotation around a double bond to consist of the breaking of one of the bonds in the double bond, rotation around the remaining (single) bond, and reformation of a double bond. Thus one would need to add 263 kJ per mole (or $263,000/6.02 \cdot 10^{23}$ J per molecule) to achieve the rotation. The energy of a photon is $h \cdot c / \lambda$ (see Chapter 1), and by equating the two energies one obtains a typical wavelength for rotation of 455 nm, in the middle of the optical part of the electromagnetic
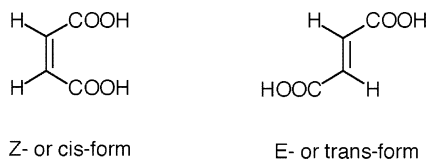

FIGURE 10.1. A simple example of *cis-trans* isomerism.

spectrum to which the atmosphere is transparent. In rhodopsin of our rods the actual energy barrier for isomerization is 238 kJ/mol (Okada et al. 2001), but in different other photoreceptors based on *cis-trans* (or *trans-cis*) isomerization, the wavelength varies from the UV-B region (for urocanic acid) to the near-infrared (for phytochrome). Some of the principles for this "tuning" are described in Chapter 9.

10.2.1. Urocanic Acid

Urocanic acid is present in human skin, and photoisomerization from the *trans* to the *cis* form causes downregulation of the immune system (Chapter 21). This radiation-sensing reaction appears at first glance to be a very simple one: The pigment is structurally simple, of low molecular weight, and not protein bound. The isomerization seems to be a very simple reaction (Fig. 10.2).

But the simplicity is only apparent. The first indication of this is the fact that the action spectrum for photoisomerization is very different from the absorption spectrum of *trans*-urocanic acid. The absorption spectrum has a broad band peaking at about 280 nm, but radiation of this wavelength does not produce any photoisomerization, i.e., the quantum yield is zero at this wavelength. The quantum yield is maximal, 0.5, at 310 nm, where absorption is much weaker (also for the *cis* to *trans* isomerization the quantum yield is about 0.5 at long wavelengths). Various theoretical explantations have been given for this strange behavior (Li et al. 1997, Hansson et al. 1997, Page et al. 2000, Ryan and Levy 2001), and the discussion is still going on. Urocanic acid is not the only substance which behaves in this way: cinnamic acid and related compounds have a quantum yield for *cis-trans* isomerization which is wavelength dependent (see the section on yellow protein below).
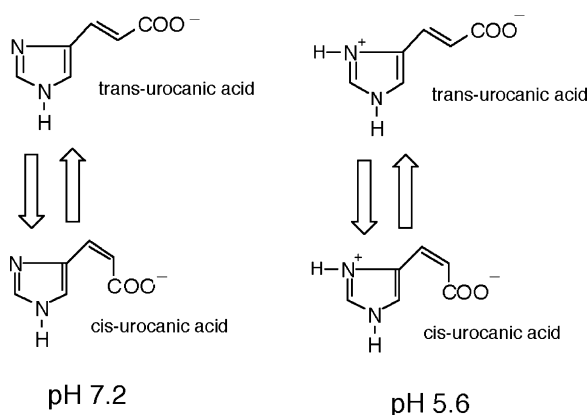

FIGURE 10.2. Photoisomerizations of anionic and zwitterionic forms of urocanic acid. The *trans* form is also called E-urocanic acid, the *cis* form Z-urocanic acid.
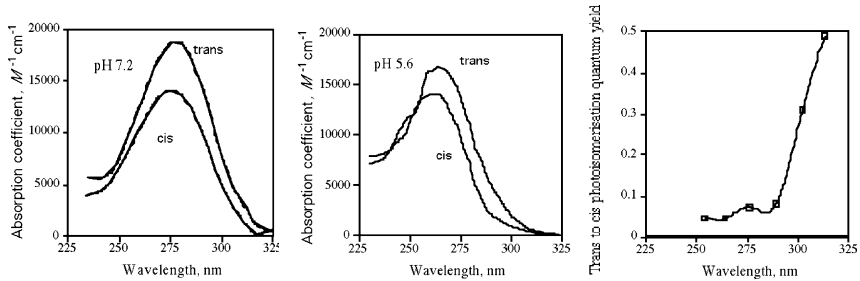
FIGURE 10.3. Absorption spectra for *trans*- and *cis*-urocanic acid at pH 7.2 (redrawn after Hanson et al. 1997) and at pH 5.6 (redrawn after Morrison et al. 1980), as well as the quantum yield for *trans* to *cis* photoisomerization (from data of Morrison et al. 1984).

Urocanic acid exists in several ionic forms depending on pH: at a low pH as a cation, at the slightly acidic pH in skin as a zwitterion, and at neutral or higher pH as an anion. Spectra for both *trans* and *cis* forms peak near 280 nm in neutral solution, but near 270 nm at ph 5.6 (Morrison et al. 1980, Hansson et al. 1997, Li et al. 1997; Fig. 10.3).

Trans-urocanic acid is formed from histidine in the outermost layer of the skin, and after photoisomerization the *cis*-urocanic acid diffuses inwards and acts on cells in deeper layers. The mechanism is uncertain. One view is that it interacts with a serotonin receptor (Walterscheid et al. 2006), a view that has been opposed by others (Prêle Finlay-Jone and Hart 2006).

10.2.2. Eukaryotic Rhodopsin

When we see the word rhodopsin our thoughts first go to the light-sensitive pigment of the rods in our own eyes. Very similar pigments, however, are present also in our cones and in the eyes of various insects, molluscs, and other animals. Recently it has been discovered that essentially the same type of pigment also occurs in various algae (Foster et al. 1984, Hegemann and Deininger 2001, Gualtieri 2001). Several types of archaea (archaebacteria) contain a kind of rhodopsins, but the latter are sufficiently different, both with respect to the chromophore and the protein structure, to warrant treatment in a separate section (Section 10.2.3.). Both eukaryotic and archaean rhodopsins, however, are membrane bound and have seven membrane-spanning helices in the molecule. It should also be noted that there are eukaryotes which have proteins more similar to the archaean than to typically eukaryotic rhodopsin.

The chromophore of rhodopsin is retinal (in some animals dehydroretinal; see Chapter 9). We show it first in isolated form (Fig. 10.4) to display in a simple way the phototransformation from the 11-*cis* form to the all-*trans* form, corresponding to the primary process of vision. The side chain changes from a bent to a straight form. In rhodopsin the terminal carbon atom of retinal polyene chain is covalently tethetered to a lysine side chain (lysine 296) of the protein

FIGURE 10.4. Photoisomerization of the isolated retinal chromophore.

(Fig. 10.5), forming a "Schiff base" in its protonated form. The counterion for the positive charge is formed by glutamine 113. The protein forms an antiparallel β-sheet in the vicinity of the chromophore, bringing the side chain of another amino acid (position 181) in close contact to the polyene chain of retinal. In our rod rhodopsin this aminoacid is glutamine, in the red- and green-sensitive pigments of our cones it is histidine.

When light isomerizes the rhodopsin-bound retinal from 11-*cis* to all-*trans*, the polyene chain cannot at once straighten out completely, because the straight chain does not fit in the protein pocket (see Okada et al. 2001 for a more detailed review of the events than the one given here). This restraint makes the retinal store energy, like a cocked spring. About two thirds of the photon energy is

FIGURE 10.5. The binding of retinal to a lysine side chain in the rhodopsin protein, forming a protonated Schiff base. Rectangles symbolize aminoacids of the opsin.

thus stored in the initial phase. Probably it is mainly the proximity of serine 186 that prevents the retinal from immediately reaching its *trans* equilibrium position. This intermediate stage is termed bathorhodopsin. Within microseconds the proton on the Schiff base is translocated to glutamine 113, whereby the attractive force between the two parts of the protein disappears, and the protein helices can adjust their relative postitions to allow the retinal to straighten out completely. This brings the rhodopsin to a low energy state called metarhodopsin I. From this the rhodopsin, within a millisecond, changes to metarhodopsin II. This has higher energy than metarhodopsin I, and the transformation is made possible by a simultaneous increase in entropy: the forces between different parts of the protein are decreased, and the different parts can move more freely with respect to each other. The process has some similarities to the melting of ice, and we may recall that the free energy change (ΔG) of a system consists of the change in total energy (enthalphy, ΔH) minus an entropy term, $T\Delta S$. In the transformation from metarhodopsin I to metarhodopsin II the free energy is thus decreased even though the total energy increases. In this respect eukaryotic rhodopsin resembles photoactive yellow proteins (Section 2.4), but differs from archaean rhodopsins (Section 2.3.). The transition also involves uptake of a proton.

Metarhodopsin II is the "signaling state" of rhodopsin. By its formation groups are exposed which can interact with a protein called transducin, a so-called G protein, and thus make the *trans*ition from a biophysical to a biochemical phase of the signal transduction. The activated *trans*ducin activates phophodiesterase which hydrolyzes cyclic guanosine-monophosphate (cGMP). When the concentrtion of cGMP has fallen sufficiently, sodium ion channels in the membrane close, the electric membrane potential increases, and an electrical impulse is sent on to the nervous system.

Recently a new light-sensitive system has been discovered in vertebrates (Provencio et al. 1998, Barinaga 2002, Berson et al. 2002, Hattar et al. 2002). The start in this new development came with the study of how frogs can adjust their skin colour by changing the size, shape and position of the pigment-containing cells in their skin, the melanophores (Provencio et al. 1998). It turned out that the skin cells contained a light-sensitive pigment which was named melanopsin. The same pigment was found also in the frog's retina, as well as in mouse retinas. However, it is not in the rods (or cones), but in cells, retinal ganglion cells, inside (in front of) the visual receptors. Some of these cells have nerve connections, not to the brain areas involved in vision, but to the suprachiasmic nuclei where the main clock of the body (see Chapter 14, Section 14.9.1) is thought to reside. The logical conclusion is that melanopsin is involved in the resetting of the biological clock by light. However, some of the melanopsin-containing retinal ganglion cells have connections to the part of the brain regulating pupil size in response to light. Melanopsin-containing cells, in contrast to rods and cones, do not adjust their sensitivity in response to light level. They are therefore suited to record the light level, which is important, e.g., in photoperiodism and pupil size regulation. Although the melanopsins studied so far occur in vertebrates, their
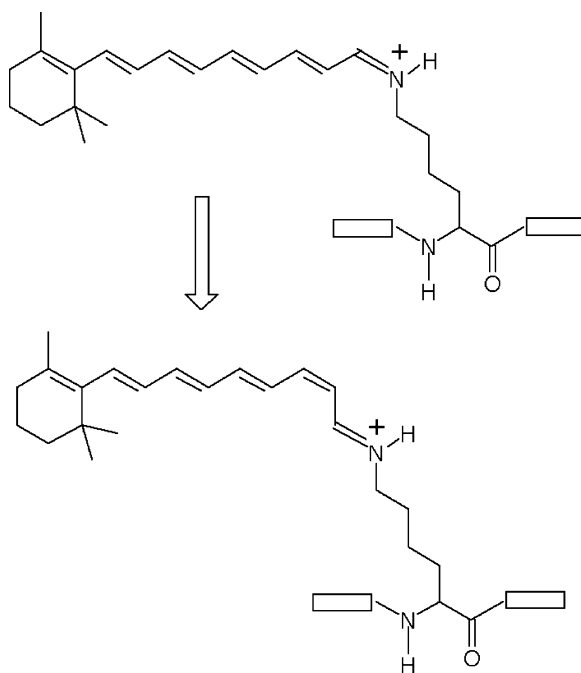
FIGURE 10.6. The *trans-cis* isomerization of the chromophore in bacteriorhodopsin. As in Fig. 10.5 the rectangles symbolize aminoacids of the opsin. The rapid *trans-cis* photoiso-merization is followed by slower rearrangements of the opsin structure and movements of protons (see Fig. 10.7).

protein structure is more closely related to that of invertebrate opsins than to the vertebrate opsins of rods and cones. Their photochemical reactions have so far not been studied in detail, but are thought to be similar to those of rhodopsins.

10.2.3. Archaean Rhodopsins

Four types of archaean rhodopsins are known. In contrast to the eukarytic rhodopsins, they all contain all-*trans*-retinal as the chromophore, and the photo-chemical step consists of its isomerization to 13-*cis* retinal. In some cases also the reverse reaction has some importance.

Many species within the Haloarchaea (the subdivision of Archaea formerly referred to as halobacteria) have been investigated, but only four distinct types have been found, which are all present in species of the best investi-gated genus, *Halobacterium*. One of these rhodopsins, called bacteriorhodopsin (BR, Fig. 10.6), uses light energy to pump hydrogen ions out of the cells, and another one, called halorhodopsin (HR) pumps chloride ions into the cells. Both reactions contribute to making the inside of the cells negative, thus allowing the cells to accumulate cations at the expense of light energy. The light-driven export
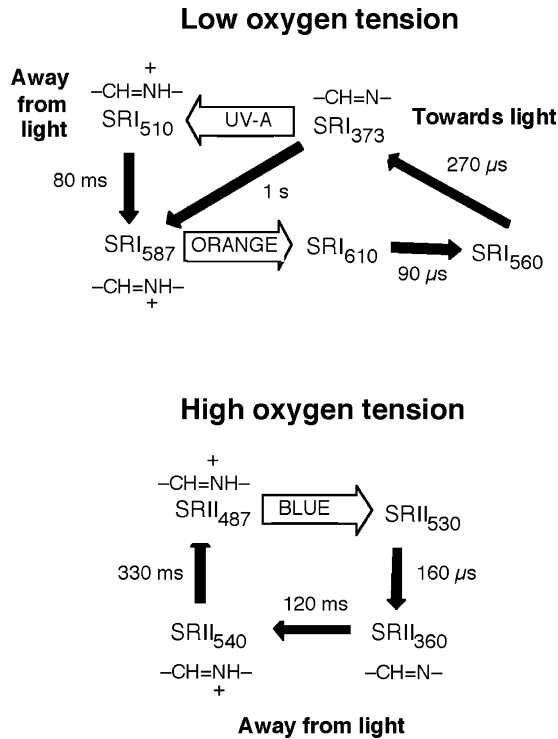
Low oxygen tension

High oxygen tension

FIGURE 10.7. The photocycles of sensory archaeal rhodopsins. Under low oxygen tension (top) *Halobacterium* and related organisms form bacteriorhodopsin and halorhodopsin, which pump ions, and sensory rhodopsin I (SRI). The latter is used to find a suitable light environment. As long as light is not very strong, the orange light–sensing reaction causes accumulation of the long-lived intermediate SRI373, which is a signaling state causing the organisms to move towards stronger light. If the UV-A light becomes too strong, the UV-A–sensing reaction causes conversion to SRI510, a signaling state which causes movement away from the strong light. In the presence of a high concentration of oxygen (bottom), only SRII is induced. The blue-light–sensitive reaction causes movement away from light. Like other nonoxygenic pigmented organisms, these are probably much more light sensitive in the presence of oxygen due to the possibility of formation of reactive oxygen species under illumination. As indicated in the figure, in some pigment forms the Schiff base is protonated, in other forms not. (After Hoff et al. 1997, modified.)

of protons also creates the proton motive force necessary for ATP synthesis and, indirectly, the free energy necessary for swimming and biochemical syntheses. BR and HR are induced only under low oxygen tension, while under high oxygen tension the organisms can utilize oxygen for creation of the necessary free energy.

The two remaining archaerhodopsins, designated SRI and SRII (SR for sensory rhodopsin, Fig. 10.7) are used by the halobacteria to orient with respect to light. SRI is induced only under low oxygen conditions, SRII only under high.

SRI, formed under low oxygen conditions, has two signaling states. One, SRI_{373}, formed by the orange component of weak daylight, causes the cells to move towards stronger light. This is not due to direct sensing of light direction as in the topophototaxis of eukaryotic flagellates, but by modulation of the frequencies of spontaneous reversals of swimming direction. If the light becomes very strong, another signaling state, SRI_{510}, is formed under the action of the UV-A component of daylight. This causes the cells to move towards weaker light.

Under high oxygen tension SRII, but not SRI (neither HR nor BR), is induced. SRI mediates only a light-avoiding signal.

SRI and SRII do not engage a signal-transmitting protein during only part of the photocycle (as eukaryotic rhodopsin engages transducin). Instead each one of them is permanently attached to its signal-transmitting protein, HtrI or HtrII, respectively. Obviously the conformational change in the rhodopsins caused by the photoisomerization of the chromophore is somehow transmitted to the signal-transmitting protein, but the details of this are not known.

10.2.4. Photoactive Yellow Proteins (PYPs, Xanthopsins)

Photoactive yellow proteins (PYPs) function as photoreceptors in purple bacteria, mediating negative phototaxis. One might think that this is too humble a function to warrant treatment in a book like this one, but PYP happens to be one of the best-known photoreceptor pigments, and we can learn some more general principles from it. PYPs are also referred to as xanthopsins, although this term is misleading, since the proteins are not opsins. Three photoreactions shuttles the pigment between several forms, as shown in Fig. 10.8.

The PYP chromophore is *trans*-4-hydroxy cinnamic acid, and light causes photoisomerization to the *cis* form (Fig. 10.9). This initial reaction is followed by rotation of one half of the molecule with respect to the other around a single bond. Genick et al. (1997, 1998) have succeeded in following in detail the changes in the protein structure associated with these changes (Fig. 10.10). They managed to crystallize the protein, and by time-resolved x-ray crystallography at low temperature capture the structure of the otherwise extremely short-lived (nanoseconds) intermediate.

By conversion to the signaling state forces between different parts of the protein are weakened. It becomes more flexible, and the conversion can be likened to "melting," just as in the case of animal rhodopsin.

PYP is interesting also because it contains the prototype for a "PAS domain" (Pellequer et al. 1998). By this we mean a protein structure that occurs in many other signaling proteins (Taylor and Zhulin 1999), including some other photoreceptor proteins: phytochrome, phototropin (Salomon et al. 2000, Christie and Briggs 2001), and a blue-light receptor in the fungus *Neurospora* (Ballario and Macino 1997). PAS domains have been identified in proteins from all types of organisms: Archea, Bacteria, and Eucarya. It comprises a region of 100–120 amino acids. They seem to occur almost exclusively in sensors of
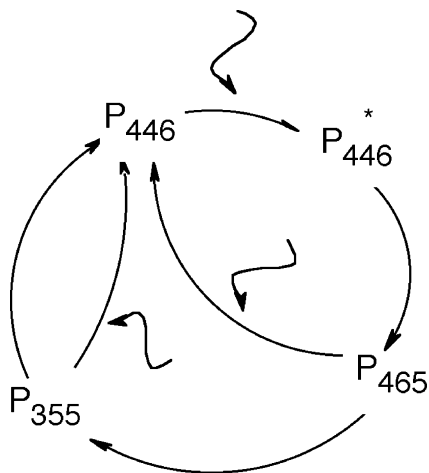
FIGURE 10.8. As shown in the diagram above, PYP is returned to the original P446 form either by dark conversion of the signaling state, P355, or by photochemical conversions from the intermediate or from the signaling state. (From Hoff et al. 1977.)
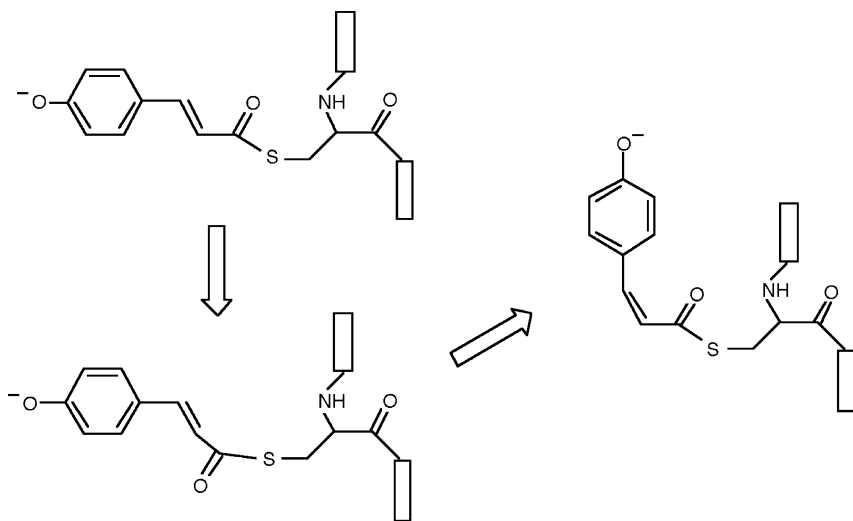

FIGURE 10.9. A sketch of change of the PYP chromophore structure in two steps. The rectangles symbolize part of the protein. The cystein residue which forms a thioester linkage with the cinnamic acid is outlined. Only the first step requires photon absorption and at physiological temperature is complete in a few nanoseconds. The second step takes several milliseconds.
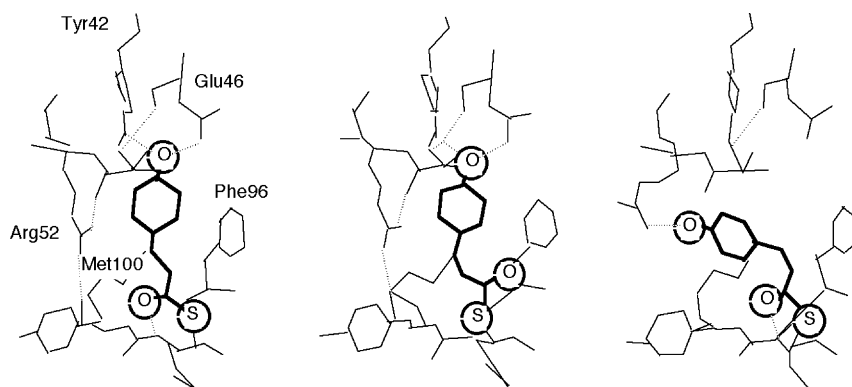
FIGURE 10.10. Changes in PYP induced by light. Shown to the left is the region around the chromophore before light absorption. The chromophore skeleton is outlined in bold, with oxygen and sulfur atoms indicated. Amino acid skeletons are outlined with thin lines. Dotted lines stand for noncovalent interactions (hydrogen bonds). In the center is the intermediate structure a few nanoseconds after light absorption. The *trans-cis* isomerization of the chromophore has taken place and its tail has flipped over, but the ring is still in its original position, with hydrogen bonds to the upper oxygen still intact. To the right is the "signaling state" reached after several milliseconds. The chromophore is still in its *cis*-state, but the whole chromophore has changed position, broken the original hydrogen bonds to the ring-attached oxygen atom, and formed a new hydrogen bond. By these rearrangements both the chromophore and the PAS domain of the protein become accessible from the outside. (Based on Genick et al. 1998.)

two-component "phosphorelay" regulatory systems. The activation of a PAS protein, by either the photoconversion of a chromophore, binding of an external activator, or voltage sensing (as in some proteins regulating voltage-sensitive ion channeling) seems to involve the exposure of the PAS domain and initiation of protein kinase activity (either histidine kinase or, as in the case of phytochrome, serine/threonine kinase).

10.2.5. Phytochrome

The discovery of phytochrome is one of the classical detective stories of plant science (Butler 1980, Björn 1980, Sage 1992). It started with the discovery that some effects of red light, such as the germination of seeds, photomorphogenesis of etiolated plants, and the inhibition of flowering in short-day plants, could be reversed by irradiation with light of longer wavelength, so called far-red light (700–740 nm). By accurate action spectroscopy (see Chapter 8) the spectral properties of two different pigment forms were defined, and this made possible the detection in plants by absorption spectrophotometry and the subsequent purification of phytochrome.

It is now known that plants contain several phytochromes with different properties and regulatory roles. This is not the place to describe this in detail, and the reader is referred to chapters in this volume on photomorphogenesis and photoperiodism in plants (Chapter 16) and on the biological clock and its resetting by light (Chapter 14).

Phytochrome or phytochrome-like proteins have also been found in various algae, a myxomycete, cyanobacteria, and other photosynthetic and nonphotosynthetic bacteria (Schneider-Poetsch et al. 1998, Davis et al. 1999, Jiang et al. 1999, Herdman et al. 2000, Lamparter and Marwan 2001, Hubschmann et al. 2001, Bhoo et al. 2001).

Phytochrome is synthesized by the plant in the red-absorbing form, called Pr, and can be converted, via several intermediates, to the far-red–absorbing form by red light or direct daylight. It is the far-red–absorbing form that is considered to be the active (signaling) state, but in some cases one or several intermediates may be active. The reverse conversion (via another set of intermediate states) can take place under far-red light, daylight filtered through vegetation or soil, or (with some phytochrome types and more slowly) in darkness. A pigment that changes its absorption spectrum in light (without being destroyed) is called photochromic; phytochrome is said to be photoreversibly photochromic, since the original state can be restored by another kind of light.

The chromophore in phytochrome has generally been believed to be an open chain tetrapyrrole (see Fankhauser 2001), phytochromobilin Fig. 10.11. Hanzawa et al. (2002) discuss other possibilities, such as the related phycocyanobilin, the same chromophore as is present in the photosynthetic antenna pigments phycocyanin and allophycocyanin of cyanobacteria and red algae. Phycocyanobilin is also the chromophore in cyanobacterial phytochrome, while those phytochromes of nonphotosynthetic bacteria that have been investigated so far have biliverdin as chromophore (Bhoo et al. 2001).

An interesting optical property of phytochrome is that conversion from Pr to Pfr or vice versa results in rotation of the transition moment corresponding to the long-wavelength absorption band with respect to the bulk of the protein. This was first shown by Etzold (1965) and Haupt (1970) by in vivo linear action dichroism, and later confirmed by various methods (Sarkar and Song 1981, Kadota et al. 1982, Sundquist and Björn 1983a,b, Tokutomi and Mimuro 1989). At first it was believed that the rotation amounts to 90°, but the newer experiments and reinterpretation of the old in vivo experiments (Björn 1984) point to a smaller angle. Based on this and other evidence, Rospendowski et al. (1989) produced a drawing of how the chromophore moves in the protein during conversion.

Phytochrome in solution is a dimer (Jones and Quail 1986), and there is evidence that it is also dimeric in vivo. Like many other sensors it has a PAS domain (see Section 2.4.) and is an autophosphorylating protein kinase (Boylan and Quail 1996, Watson 2000).
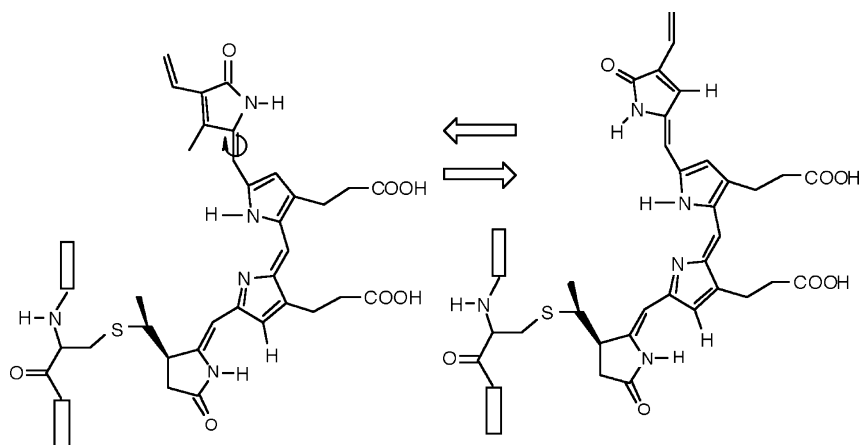
FIGURE 10.11. The chromophore of higher plant phytochrome A (phytochromobilin) in the Pr (left) and Pfr (right) forms. The rectangles symbolize amino acid residues in the protein. The circular arrow indicates the double bond at which the pyrrol group to the right rotates during photoisomerization. Phytochrome B may contain the very similar phycocyanobilin as chromophore, in which the double bond and CH_2 group pointing straight up on top of the right-hand formula is replaced by a single bond and a CH_3 group, and phytochromes in nonphotosynthetic bacteria contain biliverdin.

10.2.6. Photosensor for Chromatic Adaptation of Cyanobacteria

Many cyanobacteria have the ability to adjust the amounts of the photosynthetic antenna pigments phycocyanin (red-absorbing) and phycoeythrin (green-absorbing) according to the spectrum of ambient light. This regulation process is known as chromatic adaptation, although with present-day definitions it would more appropriately be called chromatic acclimation. Long ago action spectroscopy revealed that the photoreceptor for chromatic adaptation in cyanobacteria must be a phycobiliprotein (Fujita and Hattori 1962, Diakoff and Scheibe 1973, Vogelmann and Scheibe 1978), just like phytochrome. It was also found (reviewed by Björn 1979) that a similar system regulates also other processes in cyanobacteria. Scheibe (1962) was the first to show that a photoreversibly photochromic pigment could be obtained from a cyanobacterium, and this was further explored in a series of investigations by G.S. Björn (1980). A photoreversibly photochromic preparation, phycochrome c, with properties similar to those postulated for the regulator of chromatic adaptation, could be obtained from C-phycocyanin (Fig. 10.12).

A new start on an old problem has been made from the other end at the Department of Plant Biology of the Carnegie Institution of Washington. The recent work has been reviewed by Grossman et al. (2001). Kehoe and Grossman (1996) found a gene, rcaE, coding for the protein RcaE, which is necessary for chromatic adaptation. RcaE binds a tetrapyrrole chromophore covalently in a
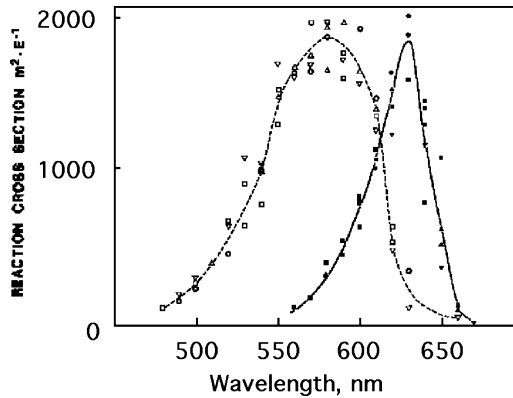
FIGURE 10.12. Action spectra for conversions of phycochrome *c* to the short-wavelength form (solid line and filled symbols) and to the long-wavelength form (dashed line, empty symbols). (From Björn and Björn 1978.) Somewhat similar action spectra were also obtained for phycochrome *a*, another polypeptide from phycocyanin (G.S. Björn 1980).

domain similar to that of phytochromes and also has a PAS domain typical for signal sensing proteins. It is believed that the chromophore is phycocyanobilin, which would fit well with the old spectral observations. According to the theory proposed by Grossman et al. (2001), there are, in addition to RcaE, two other proteins, RcaF and RcaC, involved in the signaling for chromatic adaptation. Under red light, RcaE autophosphorylates and transfers a phosphate group via RcaF to RcaC. In RcaC there are two sites that can be phosphorylated, and the one active in this context is near the N-terminal (the role of the other site is unclear). This chain of events results in increased phycocyanin production. Green light, on the other hand, causes RcaE to change to the nonphosphorylating conformation, resulting in phycoerythrin synthesis. Kehoe and Gutu (2006) and Montgomery (2007) point out that chromatic adaptation in cyanobacteria is more complex than formerly believed and involves at least three signaling pathways: in addition to the phytochrome-type Rca system with separate effects of red and of green light, the Cgi ("controlled-by-green-light") system.

10.2.7. *Violaxanthin as a Blue-light Sensor in Stomatal Regulation*

Stomata are adjustable valves in the outer layer (epidermis) of leaves and other photosynthetic plant organs. They are designed to let suffient carbon dioxide in from the external air without causing the plant to dry out due to outward diffusion of water vapour. Their regulatory system senses the water status, both directly in the leaves and indirectly in the rest of the plant body via the hormone abscisic acid. It also senses the internal carbon dioxide concentration. It senses light in several ways. One indirect way is via photosynthesis, since this causes the internal carbon dioxide concentration to fall. But the fastest and most dramatic

light effect is blue-light specific, and there seems to be another light-sensing molecule involved than the cryptochromes and phototropins dealt with in the next section: the xanthophyll zeaxanthin (see Zeiger 2000 and Assman and Wang 2001 for reviews).

The strongest evidence for participation of zeaxanthin as a blue-light sensor of stomata is the fact that stomata of an *Arabidopsis* mutant, npq1, which lacks a functional violaxanthin deepoxidase and therefore cannot accumulate zeaxanthin, does not show a blue-light–specific response (Frechilla et al. 1999). On the other hand, mutants defective in cryptochromes 1 or 2 or phototropin 1 have a normal response. However, there is also evidence of several independent blue-light channels for stomatal regulation (Lasceve et al. 1999) and that violaxanthin is only one of the sensors.

Violaxanthin has nine double bonds, so there are many possibilities for *cis-trans* isomerizations. Such a photoisomerization has not been directly shown, but postulated from kinetic experiments and the fact that the blue-light effect can be reversed by green light (Iino et al. 1985, Frechilla et al. 2000). The reversal spectrum has peaks at 490, 540, and 580 nm, similar to a wavelength-shifted zeaxanthin spectrum. We would like in this context to mention several experiments in the 1960s and 1970s in which blue-light effects in algae were reversed by light of longer wavelength (see Björn 1979 for a review).

10.3. Other Types of Photosensors

10.3.1. *Cryptochromes*

The term cryptochrome has been in use for a long time in plant physiology, as a name for the unknown blue-light photoreceptor. The name derives from the fact that it was hiding for such a long time. Now it is known that there are at least two quite different types of blue-light receptors in plants, called cryptochromes (cry1 and cry2) and phototropin. Thus the term has acquired a more restricted meaning than it used to have. On the other hand it has recently been discovered that chromoproteins similar to the plant cryptochromes are present also in other organisms than plants, including humans. These proteins are also called cryptochromes, but may have arisen independently during evolution (Todo et al. 1996). Recent reviews covering both cryptochromes and phototropins are provided by Lin (2000) and Christie and Briggs (2001). Regarding the effect of magnetic fields on cryptochromes, see Chapter 17 and Ahmad et al. (2007).

In plants cry2 represses phytochrome B action and plays a role in photoperiodism. cry1 regulates the period of the biological clock and is involved in the entrainment of the circadian oscillator (see Christie and Briggs 2001 for references).

Cryptochromes have two chromophores: 5,10-methenyltetrahydrofolic acid (Fig. 10.13) and flavin adenine dinucleotide (FAD). The latter is noncovalently bound to the protein. The role of the former is not known; probably it acts as an antenna pigment (in analogy with antenna pigments in photosynthesis)
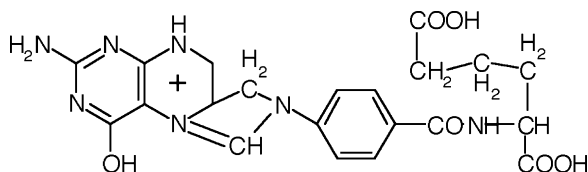
FIGURE 10.13. N5, N10-methenyl-5,6,7,8-tetrahydrofolic acid, one of the chromophores in cryptochrome, probably acting as an antenna pigment for the other chromophore, FAD (see Fig. 10.14).

and transfers absorbed light energy to FAD, as is the case is for the related photolyases.

The FAD part undergoes at least partial reduction upon illumination. The semiquinone formed by light action on cry1 has a long lifetime and seems to be able to act as a chromophore, too, giving the cryptochrome a sensitivity to green light under some circumstances. It has long been known that various blue-light effects in plants and fungi, in experiments designed to determine action spectra are not parallel in log fluence vs. effect diagrams (see, e.g., Shropshire and Withrow (1958). The explanation may be this light sensitivity of the semiquinone, or the participation of several photoreceptors (such as the two cryptochromes, phototropin, and phytochrome) in the effects studied.

The signal transduction chains associated with cryptochromes have been difficult to elucidate, not only because more than one cryptochrome probably act in different ways, but because plants have another blue-light receptor (phototropin), and because there are interactions with phytochrome. However, recently one signaling pathway proved surprisingly simple (Wang et al. 2001). In the dark, a protein called COP1 present in the nucleus prevents the activity of several genes by preventing the action of their transcription factors. After photoactivation of cryptochromes, their conformation is changed so they can bind to COP1 and prevent its action, thereby activating the genes.

Apart from their roles in the cell nucleus related to rhytmicity and gene regulation, cryptochromes seem to have direct effects on membranes. Thus cry1 activates an anion channel in the cell membrane, and thereby influences the membrane potential. As for the mechanism of action, there is so far hardly more than speculation. Flavins are known to mediate light-driven electron transfer in other cases, but this has not been shown for cryptochromes. One indication for a role of electron transfer is the similarity between cryptochromes and photolyases. Merrow and Roenneberg (2001) speculate about relations between redox potential, cryptochromes, and the mechanism of the circadian oscillator.

10.3.2. Phototropin

Phototropin is the photoreceptor primarily involved in plant phototropism, the phenomenon which, beginning with Darwin, has meant so much for stimulating interest research in plant photobiology and about plant hormones.

However, cryptochromes and phytochrome are also involved in the very complex phenomenon of phototropism (Galland 2001, Iino 2001). On the other hand, phototropin is involved in other blue-light reactions, such as high- and low-light–induced chloroplast movements (Sakai et al. 2001, Jarillo et al. 2001, Kagawa et al. 2001) and inhibition of hypocotyl extension growth (Folta and Spalding 2001). So far two main types of phototropin, phot1 and phot2 (Briggs et al. 2001), have been identified, of which phot1 acts primarily in phototropism, phot2 primarily in chloroplast photomovement.

Phototropin, like the cryptochromes, is a flavoprotein, and it also has two chromophores per molecule. In the phototropin, however, both chromophores consist of covalently bound flavine mononucleotide (FMN, Fig. 10.14). The protein part is quite different from that of the cryptochromes. The chromophore-binding regions are so-called PAS domains, designated LOV1 and LOV2 (Salomon et al. 2000, Christie and Briggs 2001). (LOV stands for Light, Oxygen, or Voltage regulated.) The properties of these two domains can be investigated separately using molecular biology techniques. The absorption

R= ribose-phosphate (FMN)
R=ribose-phosphate-phosphate-ribose-adenine (FAD)
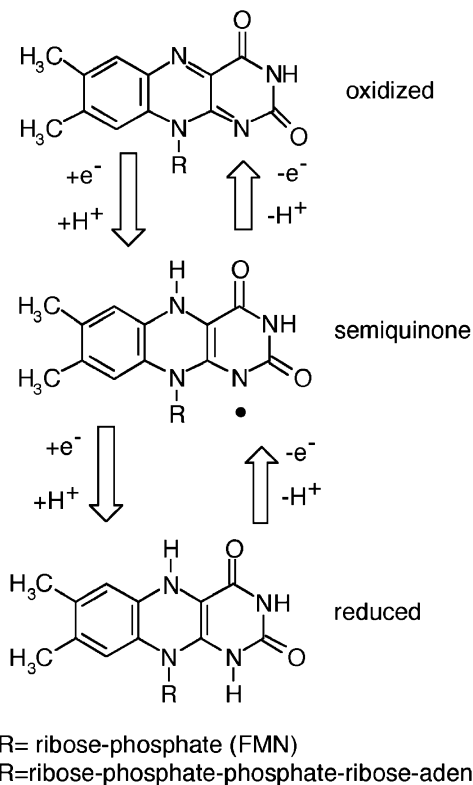
FIGURE 10.14. The structures of FMN and FAD in oxidized and reduced forms and in the half-reduced (semiquinone) form .

spectra of both show a striking (and expected) similarity to the action spectra for phototropism determined long ago (Fig. 10.15).

Upon illumination the chromophores, in both the LOV1 and LOV2 domains, undergo a spectral shift (Fig. 10.16); the absorbance in the blue region decreases, while that in the UV-A part of the spectrum changes only little. Illumination also causes quenching of the fluorescence. In darkness both LOV1 and LOV2 return to the original state with half-times at room temperature of 11.5 and 27 s, respectively. By amino acid substitution it has been made likely that the spectral change is caused by the formation of a bond between cystein (Cys39) and the FMN chromophore, with simultaneous reduction of the flavin (Fig. 10.17). This was confirmed by other methods (Crosson and Moffat 2001). The C-terminal end of phototropin is a serine-threonine kinase, which supposedly is activated by a conformational change resulting from the light-induced change in the chromophore region. The detailed structure of the LOV2 domain has now been determined and compared to other PAS domains (Crosson and Moffat 2001).

Red-light effects and blue-light effects in plants have traditionally been investigated by different sets of researchers, and there have been red-light meetings and blue-light meetings. It has become more and more difficult to uphold such a segregation as more and more interactions between the signaling channels have been discovered (Mohr 1994, Neff and Chory 1998, Parks et al. 2001). Nozue et al. (1998) even found a protein in a fern that possesses both phytochrome and phototropin properties.

10.3.3. The Plant UV-B Receptor

Ultraviolet-B radiation (280–315 nm) affects plants and other organisms in many destructive and inhibitory ways (Chapter 19). Plants, however, exhibit also
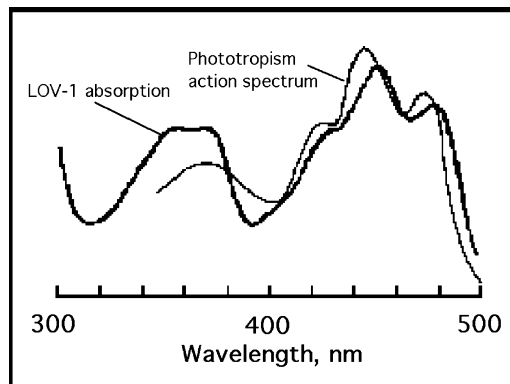
FIGURE 10.15. Comparison of the action spectrum for phototropism of oat coleoptiles determined by Thimann and Curry (1961) with the absorption spectrum of the LOV-1 protein domain of phototropin of an oat mutant determined by Salomon et al. (2000). The spectra for both LOV1 and LOV2 of the native oat are very similar, although not identical.
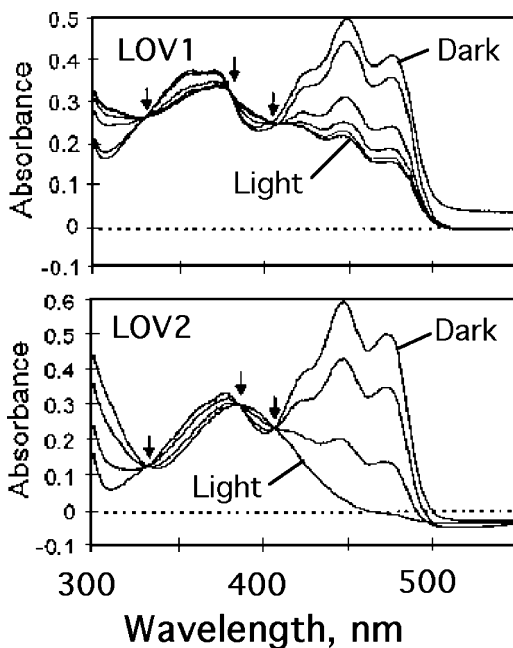
FIGURE 10.16. Light-induced spectral changes taking place in the LOV1 and LOV2 domains of phototropin upon illumination. The arrows point to isosbestic points (wavelength positions with unchanged absorbance). (Reprinted, slightly modified, with permission from Salomon et al. 2000.)

regulatory effects of UV-B. The most studied effect is the stimulation of UV-B–protecting pigments, or processes that are related to this stimulation. In many cases this stimulation (or induction) is specifically achieved by UV-B radiation, and radiation of longer wavelength is ineffective. This indicates an ability of plants to perceive and react to UV-B radiation. The topic has been reviewed recently by Björn (1999), Brosché (2001), and Kalbin (2001).
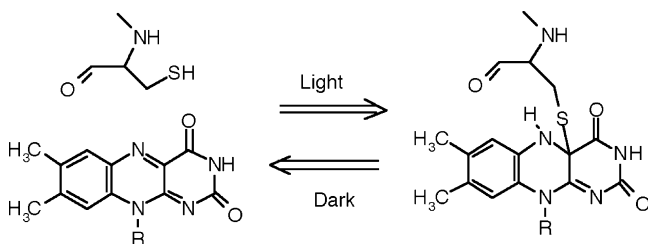
FIGURE 10.17. The proposed light-induced, dark-reversible bonding between FMN and the cysteinyl residue in phototropin. (Redrawn and simplified from Crosson and Moffat 2001.)

Although pigment induction is the most thoroughly studied aspect, there are also UV-B–specific photomorphogenetic effects, in particular inhibition of extension growth. Action spectroscopy reveals that the various ultraviolet effects on plants fall into two main categories. Either the efficiency per photon of the radiation increases monotonically towards shorter wavelength, into the UV-C region, or the effectiveness peaks at about 295 nm. It is the latter type of effect that is ascribed to a specific UV-B receptor. The effects increasing into the UV-C region, on the other hand, are regarded as stress effects caused by damage to DNA and other cell components.

Figure 10.18 shows examples of action spectra for regulatory UV-B effects, including pigment formation, gene activation, and inhibition of extension growth.

Although much effort has been expended, the nature of the UV-B receptor is not yet known. Flavoproteins and phytochrome have been suggested, but in those cases when the effects are strictly UV specific, these pigments can hardly be active. Another proposition is pterins, and certainly pterins can be found having absorption spectra fitting the UV-B action spectra well (Björn 1999). A fact increasing the plausibility of a pterin as UV-B receptor chromophore is the fact that they occur in cryptochromes, and also in the related photolyases (Chapter 19). But here they do not have a photochemical role of their own; they act only as antenna pigments absorbing light and transferring the energy to another chromophore. In any case, there is no hard evidence for the participation of pterins as UV-B receptor chromophores.

Another proposition is that an aromatic amino acid residue in a protein gives the spectral signature typical of UV-B regulatory effects. Several amino acids (tyrosine, phenylalanine, tryptophane, histidine) have absorption bands close
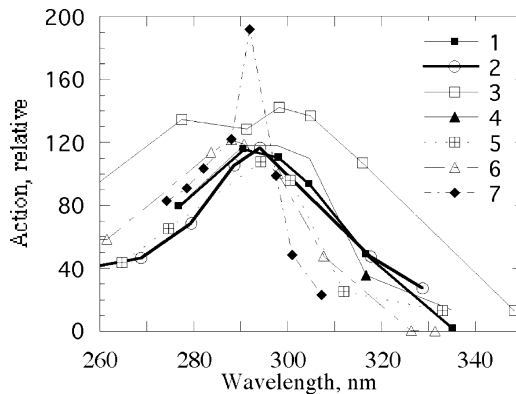
FIGURE 10.18. Action spectra for various processes thought to be mediated by a special UV-B receptor: (1) Induction of synthesis of flavonoid glycosides in cell cultures of parsley (Wellmann 1975 as cited by Wellmann 1983). (2) The same as 1 but according to Wellmann Beggs and (1994). (3) Induction of anthocyanin synthesis in maize coleoptiles (Beggs and Wellmann 1985). (4) The same as 3 but according to Wellmann (1983). (5) Inhibition of hypocotyl elongation in tomato (Ballaré et al. 1995). (6) Induction of anthocyanin formation in *Sorghum bicolor* in a background of red light (Yatsuhashi et al. 1982).

enough that one can not exclude that spectral tuning (Chapter 9) could bring the peak to 295 nm.

A third possible type of UV-B receptor chromophore is provitamin D (D_2 or D_3) or a related compound. These compounds have absorption peaks at the right position, but also at shorter wavelength. It is possible that in vivo the short-wavelength absorption bands are hidden by other absorbing compounds, as is the case for the conversion of provitamin D_3 to previtamin D_3 in human skin (Fig. 20.4). It should also be noted that other compounds with the same ring and π-electron structure and the same absorption spectra and photochemical properties are present as intermediates in plants, for instance, in the biosynthetic pathway leading to the brassinosteroid group of plant hormones.

Since it is known that the UV-B receptor regulates genes, there have been attempts to trace UV-B reception from this end. The UV-B signaling pathway seems to depend on species and on what gene or other endpoint is studied (see references in Brosché 2001, Frohnmeyer et al. 1997, 1998, 1999). For upregulation of the gene for chalcone synthase in *Arabidopsis* and parsley the following are components of the signal transduction chain: increase in cytosolic calcium ion concentration, calmodulin, serine/threonine kinase activity (as for phytochrome), and synthesis of new protein. A single millisecond flash of UV-B is sufficient to increase calcium ion concentration in the cytosol (Frohnmeyer et al. 1999). In soybean there is no indication of serine/threonine kinase involvement. For regulation of another gene (for "early light inducible protein") by UV-B, none of the above seem to be involved.

References

Ahmad, M., Galland, P., Ritz, T., Wiltschko, R. and Wiltschko, W. (2007) Magnetic intensity affects cryptochrome-dependent responses in *Arabidopsis thaliana*. Planta 225, 615–624.

Assmann, S.M. and Wang, X.-Q. (2001) From milliseconds to millions of years: guard cells and environmental responses. Curr. Opinion Plant Biol. 4, 421–428.

Ballaré, C.L., Barnes, P.W. and Flint, S.D. (1995) Inhibition of hypocotyl elongation by ultraviolet-B radiation in de-etiolating tomato seedlings. I. The photoreceptor. Physiol. Plant. 93, 584–592.

Ballario, P. and Macino, G. (1997) White-collar proteins: PASsing the light signal in *Neurospora crassa*. Trends Microbiol. *5*, 458–462.

Barinaga, M. (2002) How the brain's clock gets daily enlightenment. Science 295, 955–957.

Beale, S.I. (1999) Enzymes of chlorophyll biosynthesis. Photosynthesis Res. 60, 43–73.

Beggs, C.J. and Wellmann, E. (1985) Analysis of light-controlled anthocyanin formation in coleoptiles of *Zea mays* L.: The role of UV-B, blue, red and far-red light. Photochem. Photobiol. 41, 481–486.

Beggs, C.J. and Wellmann, E. (1994) Photocontrol of flavonoid synthesis. In: R.-E. Kendrick and G.H.M Kronenberg (eds.), *Photomorphogenesis in plants*, 2nd ed. Kluwer Academic Publishers, Dordrecht, pp. 733–751.

Berson, D.M., Dunn, F.A. and Takao, M. (2002) Phototransduction by retinal ganglion cells that set the circadian clock. Science 295, 1070–1073.

Bhoo, S.-H., Davis, S.D., Walker, J., Karniol, B. and Vierstra, R.D. (2001) Bacteriophytochromes are photochromic histidine kinasis using a biliverdin chromophore. Nature 414, 776–779.

Björn, G.S. (1980) *Photoreversibly photochromic pigments from blue-green algae*. Diss. Lund University. LUNBDS/(NBFB-1009/1-28/(1980).

Björn, G.S. and Björn, L.O. (1978) Action spectra for conversions of phytochrome c from *Nostoc muscorum*. Physiol. Plant. 43, 195–200.

Björn, L.O. (1979) Photoreversibly photochromic pigments in organisms: properties and role in biological light perception. Quart. Revs Biophys. 12, 1–23.

Björn, L.O. (1980) The history of phyto-photo-science (not to be left in skoto toto and silence). In: J. De Greef (Ed.), *Photoreceptors and plant development*. Proc. Annu. Europ. Photomorphogenesis Symp. pp. 9-13. Antwerp Univ. Press, Antwerp.

Björn, L.O. (1984) Light-induced linear dichroism in photoreversibly photochromic sensor pigments. V. Reinterpretation of the experiments on *in vivo* action dichroism of phytochrome. Physiol. Plant. 60, 369–372.

Björn, L.O. (1999) UV-B effects: Receptors and targets. In: G.S. Singhal, G. Renger, S.K. Sopory, K.-D. Irrgang, and Govindjee (Eds) *Concepts in photobiology: Photosynthesis and photomorphogenesis*. Narosa Publishing House, New Delhi, pp. 821–832.

Boylan, M.T. and Quail, P. H. (1996) Are the phytochromes protein kinases? Protoplasma 195, 12–17.

Briggs, W.R., Beck, C.F., Cashmore, A.R. et al . (17 authors) (2001) The phototropin family of photoreceptors. Plant Cell 13, 993–997.

Brosché, M. 2001. *Deconstruction of a plant UV-B stress response*. Diss. Göteborg University. ISBN 91-628-4606-X.

Butler, W.L. (1980) Remembrances of phytochrome twenty years ago. In: J. De Greef (Ed.), *Photoreceptors and plant development*. Proc. Annu. Europ. Photomorphogenesis Symp. pp. 3-7. Antwerp Univ. Press, Antwerp.

Christie, J.M. and Briggs, W.R. (2001) Blue light sensing in higher plants. J. Biol. Chem. 276, 11457–11460.

Crosson, S. and Moffat, K. (2001) structure of a flavin-binding plant photoreceptor domain: Insights into light mediated signal transduction. Proc. Natl Acad. Sci. USA 98, 2995-3000.

Davis, S.J., Vener, A.V. and Vierstra, R.D. (1999) Bacteriophytochromes: Photochrome-like photoreceptors from nonphotosynthetic eubacteria. *Science 286*, 2517–2520.

Diakoff, S. and Scheibe, J. (1973) Action spectra for chromatic adaptation in *Tolypothrix tenuis*. Plant Physiol. 51, 382–385.

Etzold, H. (1965) Der Polarotropismus und Phototropismus der Chloronemen von *Dryopteris filix-mas* (L.) Schott. Planta 64, 254–280.

Fankhauser, C. (2001) The phytochromes, a family of Red/Far-red absorbing photoreceptors. J. Biol. Chem. 276, 11453–11456.

Folta, K.M. and Spalding, E.P. (2001) Unexpected roles for cryptochrome2 and phototropin revealed by high-resolution analysis of blue ligh-mediated hypocotyl growth inhibition. Plant J. 26, 471–478.

Foster, K.W., Saranak, J., Patel, N., Zarilli, G., Okabe, M., Kline, T. and Nakashini, K. (1984) A rhodopsin is the functioning photoreceptor for phototaxis in the unicellular eukaryote *Chlamydomonas*. Nature 311, 756–759.

Frechilla, S., Zhu, J.X., Talbott, L.D. and Zeiger, E. (1999) Stomata from npq1, a zeaxanthin-less *Arabidopsis* mutant lacking a specific response to blue light. Plant Cell Physiol. 40, 949–954.

Frechilla, S., Talbott, L.D., Bogomolni, R.A. and Zeiger, E. (2000) Reversal of a blue-light stimulated stomatal opening by green light. Plant Cell Physiol. 41, 171–176.

Frohnmeyer, H., Bowler, C. and Schäfer, E. (1997) Evidence for some signal transduction elements involved in UV-light-dependent responses in parsley protoplasts. J. Exp. Bot. 48, 739–750.

Frohnmeyer, H., Bowler, C., Zhu, J.-K., Yamagata, H., Schäfer, E. and Chua, N.-H. (1998) different roles for calcium and calmodulin in phytochrome- and UV-regulated expression of chalcone synthase. Plant J. 13, 763–77.

Frohnmeyer, H., Loyall, L., Blatt, M.R. and Grabov, A. (1999) Millisecond UV-B irradiation evokes prolonged elevation of cytosolic-free Ca^{2+} and stimulates gene expression in trans*g*enic parsley cell cultures. Plant J. 20, 109–117.

Fujita, Y. and Hattori, A. (1962) Photochemical interconversion between precursors of phycobilin chromoprotein in *Tolypothrix tenuis*. Plant Cell Physiol. 3, 209–220.

Galland, P. (2001) Phototropism in *Phycomyces*. In: D.-P. Häder and M. Lebert (eds.), *Photomovement*. Elsevier, Amsterdam, pp. 621–657.

Genick, U.K., Borgstrahl, G.E.O., Kingman, N., Ren, Z., Pradervand, C., Burke, P.M., Srajer, V., Teng, T.-Y., Schildkamp, W., McRee, D.E., Moffat, K. and Getzoff, E.D. (1997) Structure of a protein cycle intermediate by millisecond time-resolved crystallography. Science 275, 1471–1475.

Genick, U.K., Soltis, S.M., Kuhn, P., Canestrelli, I.L. and Getzoff, E.D. (1998) Structure at 0.85 Å resolution of an early protein photocycle intermediate. Nature 392, 206–209.

Gilroy, S. and Trewavas, A. (2001) Signal processing and transduction in plant cells: The end of a beginning? Nature Rev. Mol. Cell. Biol. 2, 307–314.

Grossman, A.R., Bhaya, D. 6 He, Q. (2001) Tracking the light environment by cyanobacteria and the dynamic nature of light harvesting. J. Biol. Chem. 276, 11449–11452.

Gualtieri, P. 2001. Rhodopsin-like proteins: Light detection pigments in *Leptolyngbya*, *Euglena*, *Ochromonas*, *Pelvetia*. In: D.-P. Häder and M. Lebert (eds.) *Photomovement*. Elsevier, Amsterdam, pp. 281–295.

Hansson, K.M., Li, B. and Simon, J.D. (1997) A spectroscopic study of the epidermal ultraviolet chromophore *trans*-urocanic acid. J. Am. Chem. Soc. 119, 2715–2721.

Hanzawa, H., Shinomura, T., Inomata, K., Kakiuchi, T., Kinoshita, H., Wada, K., and Furuya, M. (2002) Structural requirements of bilin chromophore for the photosensory specificity of phytochromes A and B. Proc. Natl Acad. Sci. USA 99, 4725–4729.

Hartmann, U., Valentine, W.J., Christie, J.M., Hays, J., Jenkins, G.I. and Weisshaar, B. (1998) Identification of UV/blue light-responsive elements in the *Arabidopsis thaliana* chalcone synthasepromoter using a homologous protoplast *transi*ent expression system. Plant Molecul. Biol. 36, 741–754.

Hattar, S., Liao, H.-W., Takao, M., Berson, D.M. and Yau, K.-W. (2002) Melanopsin-containing retinal ganglion cells: Architecture, projections, and intrinsic photosensitivity. Science 295, 1065–1070.

Haupt, W. (1970) Localization of phytochrome in the cell. Physiol. Vég. 8, 551–563.

Hegemann, P. and Deininger, W. (2001) Algal eyes and their rhodopsin photoreceptors. In: D.-P. Häder and M. Lebert (eds.), *Photomovement*. Elsevier, Amsterdam, pp. 475–503.

Herdman, M., Coursin, T., Rippka, R., Houmard, J. and Tandeau de Marsac, N. (2000) A new appraisal of the prokaryotic origin on eukaryotic phytochromes. J. Mol. Evol. 51, 205–213.

Hoff, W.D., Jung, K.-H. and Spudich (1997. Molecular mechanism of photosignaling by archaeal sensory rhodopsins. Annu. Rev. Biophys. Biomol. Struct. 26, 223–258.

Hubschmann, T., Borner, T., Hartmann, E. and Lamparter, T. (2001) Characterization of the Cph1 holo-phytochrome from *Synechocystis sp*. PCC 6803. Eur. J. Biochem. 268, 2055–2063.

Iino, M., Ogawa, T., and Zeiger, E. (1985) Kinetic properties of the blue-light response of stomata. Proc. Natl Acad. Sci. USA 82, 8019–8023.

Iino, M. (2001) Phototropism in higher plants. In: D.-P. Häder and M. Lebert (eds.), *Photomovement*. Elsevier, Amsterdam, pp. 659–812.

Jarillo, J.A., Gabrys, H., Capel, J., Alonso, J.M., Ecker, J.R., and Cashmore, A.R. (2001) Phototropin-related NPL1 controls chloroplast relocation induced by blue light. Nature 410, 952–954.

Jiang, Z.Y., Swem, L.R., Rushing, B.G., Devanathan, S., Tollin, G. and Bauer, C.E. (1999) Bacterial photoreceptor with similarity to photoactive yellow protein and plant phytochromes. Science 285, 406–409.

Jones, A.M. and Quail, P. (1986) Quaternary structure of 124-kilodalton phytochrome from *Avena sativa* L. Biochemistry 25, 2987–2995.

Kadota, A., Wada, M., and Furuya, M. (1982) Phytochrome-mediated phototropism and different dichroic orientation of Pr and Pfr in protonemata of the fern Adiantum capillus-veneris. Photochem. Photobiol. 35, 533–536.

Kagawa, T., Sakai, T., Suetsugu, N., Oikawa, K., Ishiguru, S., Kato, T., Tabata, S., Okada, K. and Wada, M. (2001) *Arabidopsis* NPL1: A phototropin homolog controlling the chloroplast high-light avoidance response. Science 291, 2138–2141.

Kalbin, G. (2001) *Towards the understanding of biochemical plant responses to UV-B*. Diss. Göteborg University. ISBN 91-628-4627-2.

Kehoe, D.M. and Grossman, A.R. (1996) Similarity of a chromatic adaptation sensor to phytochrome and ethylene receptors. Science 273, 1409–1412.

Kehoe, D.M. and Gutu, A. (2006) responding to color: The regulation of complementary chromatic adaptation. Annu. Rev. Plant Biol. 57, 127–150.

Lamparter, T. and Marwan, W. (2001) Spectroscopic detection of a phytochrome-like photoreceptor in the myxomycete *Physarum polycephalum* and the kinetic mechanism for the photocontrol of sporulation by Pfr. Photochem. Photobiol. 73, 697–702.

Laudet, V. (1997) Evolution of the nuclear receptor superfamily: early diversification from an ancestral orphan receptor. J. Mol. Biol. 19, 207–226.

Lazaroff, N. (1973) Photomorphogenesis and Nostocacean development. In: N.G. Carr and B.A. Whitton (eds.), *Biology of blue-green algae* (Botanical Monographs, vol. 9). Blackwell Scientific Publications, Oxford.

Lazaroff, N. and Schiff, J. (1962) Action spectrum for developmental photoinduction of the blue-green alga *Nostoc muscorum*. Science 137, 603–604.

Lenci, F. Ghetti, F. and Song, P.-S. (2001) Photomovement in ciliates. In: D.-P. Häder and M. Lebert (eds.) *Photomovement.* Elsevier, Amsterdam, pp. 281–295.

Li, B., Hanson, K.M. and Simon, J.D. (1997) Primary processes of the electronic excited states of *trans*-urocanic acid. Phys. Chem. A. 101, 969–972.

Lin, C., Robertson, D.E., Ahmad, M., Raibekas, A.A., Schuman Jorns, M., Dutton, P.L. and Cashmore, A.R. (1995) Association of flavin adenine dinucleotide with the *Arabidopsis* blue light receptor CRY1. Science 269, 968–970.

Lin, C. (2000) Plant blue-light receptors. Trends Plant Sci. 5, 337–342.

Merrow. M. and Roenneberg, T. (2001) Circadian clocks: Running on redox. *Cell*, *106*, 141–143.

Mohr, H. (1994) Coaction between pigment systems. In: R.-E. Kendrick and G.H.M. Kronenberg (Eds.) *Photomorphogenesis in plants*, 2nd ed. Kluwer Acad. Publ., Dordrecht, pp. 545–564.

Montgomery, B.L. (2007) Sensing the light: photoreceptive systems and signal transduction in cyanobacteria. Molec. Microbiol. 64, 16–27.

Morrison, H., Avnir, D., Bernasconi, C. and Fagan, G. (1980) Z/E photoisomerization of urocanic acid. Photochem. Photobiol. 32, 711–714.

Morrison, H., Bernasconi, C. and Pandey, G. (1984) A wavelength effect on urocanic acid E/Z photoisomerization. Photochem. Photobiol. 40, 549–550.

Neff, M.M. and Chory, J. (1998) Genetic interactions between phytochrome A, phytochrome B, and cryptochrome 1 during *Arabidopsis* development. Plant Physiol. 118, 27–35.

Nozue, K., Kanegae, T., Imaizumi, T., Fukuda, S., Okamoto, H., Yeah, K.-C., Lagarias, J.C. and Wada, M. (1998) A phytochrome from the fern *Adiantum* with features of the putative photoreceptor NPH1. Proc. Natl Acad. Sci. USA, *95,* 15826–15830.

Okada, T., Ernst, O.P., Palczewski, K. and Hofmann, K.P. (2001) Activation of rhodopsin: new insights from structural and biochemical studies. Trends Bioch. Sci. 26, 318–324.

Page, C.S., Merchán, M. and Serrano-Andrés, L. (1999) A theoretical study of the low-lying excited states of *trans*- and *cis*-urocanic acid. J. Phys. Chem. A 103, 9864–9871.

Parks, B.M., Folta, K.M. 6 Spalding, E.P. (2001) Photocontrol of stem growth. *Curr. Opinion Plant Biol. 2001*, 436–440.

Pellequeler, J.-L., Wagner-Smith, K.A., Kay, S.A. and Getzoff, E.D. (1998) Photoactive yellow protein: A structural prototype for the three-dimensional fold o the PAS domain superfamily. Proc. Natl. Acad. Sci. USA 95, 5884–5890.

Portwich, A. and Garcia-Pichel, F. (2000) A novel prokaryotic UVB photoreceptor in the cyanobacterium *Chlorogloeopsis* PCC 6912. *Photochem. Photobiol. 71*, 493–498.

Prêle, C.M., Finlay-Jones, J.J. and Hart, P.H. (2006) The receptor for *cis*-urocanic acid remains elusive. J.Investig. Dermatol. 126, 1191–1193.

Provencio, I., Jiang, G., De Grip, W.J., Hayes, W.P. and Rollag, M.D. (1998) Melanopsin: An opsin in melanophores, brain, and eye. Proc. Natl. Acad. Sci. USA 95, 340–345.

Rospendowski, B.N., Farrens, D.L., Cotton, T.M. and Song, P.-S. (1989) Surface enhanced resonance Raman scattering (SERRS) as a probe of the structural differences between the Pr and Pfr forms of phytochrome. FEBS Lett. 258, 1–4.

Ryan, W. and Levy, D.H. (2001) Electronic spectroscopy and photoisomerization of *trans*-urocanic acid in a supersonic jet. J. Am. Chem. Soc. 123, 961–966.

Sage, L.C. (1992) *Pigment of the imagination: A history of phytochrome research.* Academic Press, San Diego.

Salomon, M., Christie, J.M., Knieb, E., Lempert, U. and Briggs, W.R. (2000) Photochemical and mutational analysis of the FMN-binding domains of the plant blue light receptor, phototropin. Biochemistry 39, 9401–9410.

Sakai, T., Kagawa, T., Kasahara, M., Swartz, T.E., Christie, J.M., Briggs, W.R., Wada, M., and Okada, K. (2001) Arabidopsis nph1 and npl1: Blue-light receptors that mediate both phototropism and chloroplast relocation. Proc. Natl Acad. Sci. USA 98, 6969–6974.

Sarkar, H.K. and Song, P.S. Nature of phototransformation of phytochrome as probed by intrinsic tryptophan residues. Biochemistry 21, 1967–1972.

Scheibe, J. (1962) Photoreversible pigment: occurence in a blue-green alga. Science 176, 1037–1039.

Schmid, G.H. (1970) The effect of blue light on some flavine enzymes. Hoppe Seylers Z. Physiol. Chem. 351, 575–578.

Schmid, G.H. and Schwarze, P. (1969) Blue light enhanced respiration in a colorless *Chlorella* mutant. Hoppe Seylers Z. Physiol. Chem. 350, 1513–1520.

Schneider-Poetsch, H.A.W., Kolukisaoglu, U., Clapham, D.H., Hughes, J. and Lamparter, T. (1998) Non-angiosperm phytochromes and the evolution of vascular plants. Physiol. Plant. 102, 612–622.

Shropshire, W. and Withrow, R.B. (1958) Action spectrum of phototropic tip-curvature of *Avena*. Plant Physiol. 33, 360–366.

Sineshchekov, V.A. (1995) Photobiophysics and photobiochemistry of the heterogeneous phytochrome system. Biochim. Biophys. Acta 1228, 125–164.

Spudich, J.L. (2001) Color-sensitive vision by halobacteria. In: D.-P. Häder and M. Lebert (eds.), *Photomovement* . Elsevier, Amsterdam, pp. 151–178.

Sundqvist, D. and Björn, L.O. (1983a) Light-induced linear dichroism in photoreversibly photochromic sensor pigments. II. Chromophore rotation in immobilized phytochrome. Photochem. Photobiol. 37, 69–75.

Sundqvist, D. and Björn, L.O. (1983b) Light-induced linear dichroism in photoreversibly photochromic sensor pigments. III. Chromophore rotation estimated by polarized light reversal of dichroism. Physiol. Plant. 59, 263–269.

Takeda, J., Ozeki, Y. and Yoshida, K. (1997) An action spectrum for induction of promoter activity of phenylammonia lyase gene by UV in carrot suspension cells. Photochem. Photobiol. 66, 464–470.

Taylor, R.R. and Zhulin, I.B. (1999) PAS domains: Internal sensors of oxygen, redox potential, and light. Microbiol. Mol. Biol. Revs. 63, 479–506.

Thimann, K.V. and Curry, G.M. (1961) Phototropism. In: W.D. McElroy and B. Glass (eds.), *Light and life*. Johns Hopkins Press, Baltimore, pp. 646–672.

Todo, T., Ryo, H., Yamamoto, K., Toh, H., Inui, T., Ayaki, H., Nomura, T. and Ikenaga, M. (1996) *Drosophila* (6-4)photolyase, a human photolyase homolog, and the blue-light photoreceptor family. Science 272, 109–112.

Tokutomi, S. and Mimuro, M. (1989) Orientation of the chromophore *transi*tion moment in the 4-leaved shape model for pea phytochrome molecule in red-light absorbing form and its rotation induced by the phototranstransformation to the far-red-light absorbing form. FEBS Lett. 255, 350–353.

Vogelmann, T.C. and Scheibe, J. (1978) Action spectra for chromatic adaptation in blue-green *Fremyella diplosiphon*. Planta 143, 233–239.

Walterscheid, J.P., Nghiem, D.X., Kazimi, N., Nutt, L.K., McConkey, D.J., Norval, M. and Ullrich, S.E. (2006) *Cis*-urocanic acid, a sunlight-induced immunosuppressive factor, activates immune supression via the 2A 5-HT receptor. Proc. Natl. Acad. Sci. USA 103, 17420–17425.

Wade, H.K., Bibikova, T.N., Valentine, W.J. and Jenkins, G.I. (2001) Interactions within a network of phytochrome, cryptochrome and UV-B transduction pathways regulate chalcone synthase gene expression in *Arabidopsis* leaf tissue. Plant. J. 25, 675–685.

Wang, H., Ma, L.G., Li, J.M., Zhao, H.Y. and Deng, W.W. (2001) Direct interaction of *Arabidopsis* cryptochromes with COP1 in mediation of photomorphogenic development. Science 294, 154–158.

Watson, J.C. (2000) Light and protein kinases. Adv. Botanical Res. Incorporating Adv. Plant Pathol. 32, 149–184.

Wellmann, E. (1975) Der Einfluss physiologischer UV-Dosen auf Wachstum und Pigmentierung von Umbelliferenkeimlingen. In: E. Bacher (ed.), *Industrieller Pflanzenbau*.Tech. Univ. Wien Selbstverlag, pp. 229–239

Wellmann, E. (1983) UV radiation in Photomorphogenesis. In: W. Shropshire Jr. and H. Mohr (eds.), *Enc. Plant Physiol.*, *New Series 16B*. Springer Verlag, Berlin, pp. 745–756.

Yatsuhashi, H., Hashimoto, T. and Shimizu, S. (1982) Ultraviolet action spectrum for anthocyanin formation in broom *Sorghum* first internodes. Plant Physiol. 70, 735–741.

Zeiger, E. (2000) Sensory transduction of blue light in guard cells. Trends Plant Sci. 5, 183–185.

11
The Diversity of Eye Optics

Lars Olof Björn

Abstract: This chapter starts with a description of the optics of camera-type eyes, in which an image is projected upon a retina with cornea and lens as refracting elements. Ray tracing is explained with the human eye as an example of a terrestrial vertebrate's eye. Then the comparison is made to camera eyes of aquatic and amphibious animals, with an explanation of different kinds of aberrations, difficulties in accommodation to air and water as external media, and different solutions to these problems. A brief section deals with feedback regulation of eye development, and another one with eyes of particularly high light sensitivity. A section on compound eyes explains the difference between apposition and superposition eyes. It is pointed out that geometric optics (ray optics) is not adequate for analyzing the function of the small components of these eyes, and an introduction is given to waveguide and mode theory. This is followed by sections on antireflective nipple arrays, eyes with reflective optics, scanning eyes, and the chapter concludes with a treatise of the evolution of eyes.

11.1. Introduction

In this review of the different solutions of the optical problems of eye designs encountered in the animal kingdom, we shall not follow the course of evolution. Instead we shall start with our own eyes, as this is what the readers in general are likely to be most familiar with. The emphasis will thus first be on "camera-type" eyes, and later we will deal with compound and other types of eyes.

11.2. The Human Eye

We assume that the reader has a basic knowledge of the structure of the human eye. It is probably a common misconception that the refraction of light necessary for the projection of an image on the retina is mainly due to the lens. In fact, 80% of the refractive power is due to the curved external surface of the eye, at the outer surface of the cornea, because the difference in refractive index between
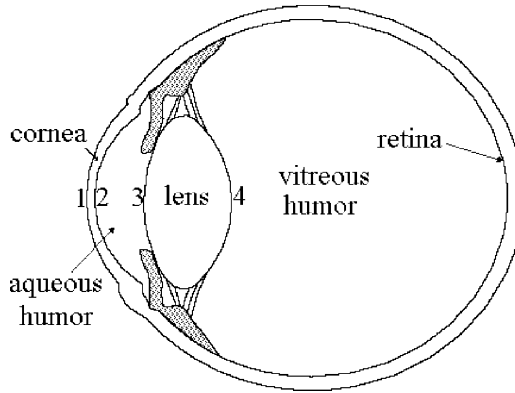
FIGURE 11.1. Longitudinal section of a human eye (schematic). The numbers indicate the numbering of interfaces used in the calculations in the text.

cornea and air is much greater than that between the lens and its surrounding media (aqueous humor in front, vitreous humor behind) (Fig. 11.1).

To understand how the optical components of the eye function, and why evolution of eye design in different environments has given the results it has, we shall start with how light is refracted in spherical interface.

From the formula derived in the legend of Fig. 11.2, we can see that:

1. For fixed n_1, n_2, and R, the smaller is a, the larger is b
2. For fixed a, n_1 and n_2, the smaller is R, the smaller is b
3. For fixed a and R, the larger is the difference between n_2 and n_1, the smaller is b.
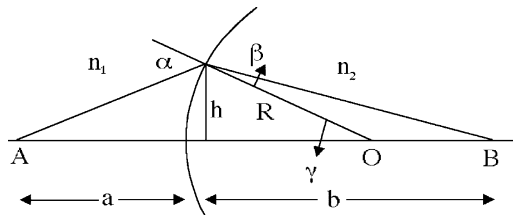
FIGURE 11.2. Refraction of light at a spherical interface between media with different refractive indices, n_1 and n_2. The radius of curvature is R, the center of the sphere O. A ray from A to B is refracted in the surface at a distance h from the line from A to B. The angle of incidence is α, the angle of refraction β. The shortest distance of A from the interface is a, that of B is b. For small values of h we have the following relations: $h/r = \tan(\gamma) \approx \gamma$; $h/a = \tan(\alpha - \gamma) \approx \alpha - \gamma$; $h/b = \tan(\gamma - \beta) \approx \gamma - \beta$. From this follows that $h/R + h/a \approx \alpha \approx \sin(\alpha)$ and $h/R + h/b \approx \beta \approx \sin(\beta)$. Since, according to Snell's law (see Chapter 1), $n_1 sin(\alpha) = n_2 sin(\beta)$, it follows that $n_1(h/R + h/a) = n_2(h/R + h/b)$, i.e., $n_1(1/R + 1/a) = n_2(1/R + 1/b)$ (independently of h as long as h is small compared to R), or $n_1/a + n_2/b = (n_2 - n_1)/R$.

4. For infinitely large a, i.e., point A at infinite distance, $n_2/b = (n_2 - n_1)/R$, or $b = R \cdot n_2/(n_2 - n_1)$. In this case b is the focal distance of the refracting interface. The inverse value of b is called the refractive power or dioptric power of the interface. With b expressed in m the refractive power will be expressed in diopters ($= m^{-1}$). Since the radius of the outer surface of the cornea is over 7 mm and the radius of the pupil less than 4 mm (in bright light much less), we can use the formula from Fig. 11.2 as a first approximation to judge the refractive power P_1 of the outer external surface of the eye using the dimensions in Table 11.1: $P_1 = (n_2 - n_1)/(n_2 R) = (1.3777 - 1)/0.00777 \ m^{-1} = 48.52 \ m^{-1}$ (or 48.52 diopters, or 48.52 D). As we can see in Fig. 11.1, the inner surface of the cornea is slightly more curved than the external surface, and the medium inside the cornea has a slightly lower refractive index, giving a negative contribution to the refractive power. Using the same formula again, we can calculate that the contribution from this interface is $P_2 = -6.34 \ m^{-1}$.

To get the total refractive power from these two interfaces, we would make no big error by just adding them: $48.52 - 6.34 \ m^{-1} = 42.18 \ m^{-1}$. But a more correct calculation is to take the distance between them, $d_{1,2} = 0.5 \ mm = 0.0005 \ m$, into account using the formula $P_{1,2} = P_1 + P_2 - P_1 \cdot P_2 \cdot d_{1,2}/n_{1,2} = 48.52 - 6.34 + 48.52 \cdot 6.34 \cdot 0.0005/1.3777 m^{-1} = 42.29 \ m^{-1}$. Here $d_{1,2}$ stands for the distance between the interfaces and $n_{1,2}$ for the refractive index of the medium between them. When we come to the lens below, the correction term is more important, because the thickness of the lens is greater than that of the cornea.

In analogy with the above, we can calculate the refractive power of the front surface of the lens to be $P_3 = (1.4000 - 1.3371)/(12.40 \cdot 0.001) \ m^{-1} = 5.31 \ m^{-1}$ and that of the back surface $P_4 = (1.3377 - 1.4000)/(-8.10 \cdot 0.001) \ m^{-1} = 7.69 \ m^{-1}$. Note that in the latter case we use a negative value for the radius, since the center of the curvature is now in the direction from which the light is coming. The total refracting power of the lens is $P_{3,4} = 5.31 + 7.69 - 5.31 \cdot 7.69 \cdot 4.02 \cdot 0.001/1.4000 \ m^{-1} = 12.88 \ m^{-1}$. We see that the refracting power of the lens is only about one quarter of that of the cornea. This is for an eye adjusted for vision at a distance. It is, as we shall see, different for an eye adjusted (accommodated) for vision at short distance, and even more so for eyes of aquatic animals.

TABLE 11.1. Properties of Eye Components

Eye component	Distal R	Proximal R	Thickness	Refr. ind.
1. Cornea	7.77	6.40	0.50	1.3777
2. Aqueous humor	3.16			1.3371
3. Lens	12.40	−8.10	4.02	1.4000
4. Vitreous humor	16.4			1.3377

The refractive index is for green light (center of visible range.) The refractive index for the lens is for a portion near the center of the lens. Sources: Liou and Brennan 1997, Liu, Wang, Song, and Mu 2005, Navarro, Santamaria, and Bescós 1985.

We can also make an estimate of the total refractive power of the eye: $P_{eye} = P_{1,2} + P_{3,4} - P_{1,2} \cdot P_{3,4} \cdot 16.4 \cdot 0.001/1.3371$ m^{-1} = 48.49. This is just enough to focus light from a distant object on the retina in the back of the eye.

We must remember that all these calculations are a bit approximative, since they all depend on the approximations $\tan(\alpha) \approx \alpha \approx \sin(\alpha)$. The further we go from the optical axis, the less valid are these approximations. Furthermore, the refractive index of the lens is not constant, it is higher in the center than in the perifery, it varies with wavelength, and the interfaces where refractions occur are not perfectly spherical.

In Section 11.3. we shall come to a case where we cannot use the approximations used here, and have to explore the function of an eye in another way.

The lens is elastic and has a tendency to contract radially and extend along the optical axis of the eye, i.e., increase the curvature of its refractive interfaces. This tendency is counteracted by the fibers in which it is suspended, which are stretched by the elasticity of the outer tissue of the eye. This in turn can be counteracted by contraction of the ciliary muscle. So by contraction of the ciliary muscle the refractive power of the lens is increased. This regulation is called accommodation. In Fig. 11.3 we see a comparison of the shape of the lens when it is adjusted for distance vision and for near vision. Birds and reptiles also accommodate by changing the shape of the lens, although with different mechanical systems (Ott 2006). Amphibians and fishes accommodate in an entirely different way by moving the lens, and we shall soon understand why.
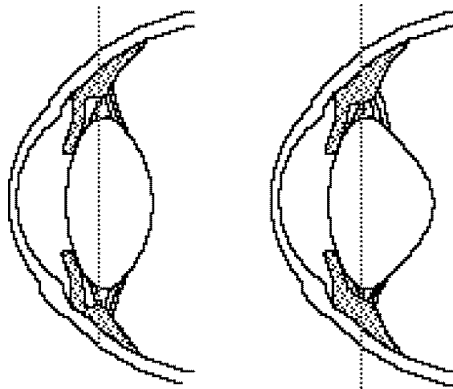
FIGURE 11.3. The shape of the human lens in an eye adjusted for vision at a distance (left) and on a nearby object (right).

11.3. An Eye in Water: The Problem

For a fish living in water the refractive index of the water in front of the cornea is about 1.33, i.e., close to that of the optical elements in the eye in Fig. 11.1, with the exception of the lens. The materials of which a fish eye is built do not differ much from the corresponding materials of a human eye. This means that the outer surface of the cornea has almost no refractive power, and the demands on the lens are much greater than for a terrestrial animal. Lens surfaces must be much more curved, and in general the lens of a fish eye has a spherical shape. This accentuates another problem: spherical aberration. To understand this, let us study the behavior of light passing through a sphere; we can take a glass sphere in air as example (Fig. 11.4).

In Fig. 11.4 we see a ray of light entering from a medium with refractive index n_1 into a sphere of refractive index n_2 and exiting on the other side into the medium of refractive index n_1. We have drawn the incident ray as parallel to to the horizontal optical axis, but this is not a special case. Because of the spherical symmetry any direction can be chosen for the optic axis. We have also drawn the two radii of the sphere and continued their directions outside the sphere to show the incidence and refraction angles α and β. For the first refraction the angle of incidence is α and the angle of refraction β, since the radius is perpendicular to the sphere's surface at the point of intersection. The relation between α and β, according to Snell's law, is $n_1\sin(\alpha) = n_2\sin(\beta)$. Because two sides of the triangle between the center of the sphere are equal ($= R$), it is clear that the angle of incidence at the other refraction is β, and so the angle of refraction there must be α, again according to Snell's law. Since the sum of angles in a triangle is π, the third angle in the isosceles triangle just referred to is $\pi - 2\beta$, and the angle γ is $\pi - \alpha - (\pi - 2\beta) = 2\beta - \alpha$. We express angles in radians here and in the following calculations. The angle δ is $\pi - \gamma - $(the top angle in the triangle containing γ and δ). This angle, as can easily be seen in Fig. 11.3, is $2\pi - \alpha - \beta$, and it follows that $\delta = \pi - \gamma - (2\pi - \pi - \beta) = \pi - (2\beta - \alpha) - (2\pi - \alpha - \beta) = 2\alpha - \beta - \pi$.

We can now calculate the distance between the focal point and the center of the sphere as $R \cdot \cos(\gamma) + R \cdot \sin(\gamma)/\tan(\delta)$. Using the other relationships we have derived, this can be expressed in terms of R, α, n_1, and n_2. If the glass sphere
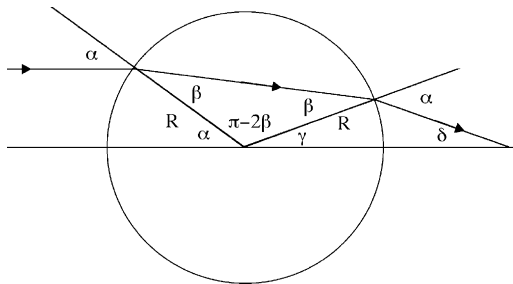
FIGURE 11.4. Refraction of light in a homogeneous sphere.
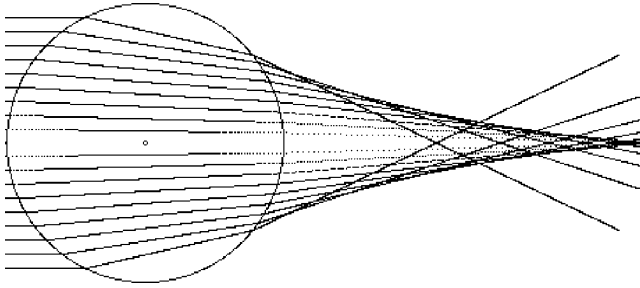
FIGURE 11.5. Propagation of light through a glass sphere with refractive index 1.538 immersed in water with refractive index 1.336. The inability of such a lens to focus sharply is a phenomenon known as spherical aberration.

were to act as a good lens, this distance should be independent of the distance of the incident rays from the optical axis, but it turns out that this is not at all the case. In Fig. 11.5 we have traced the rays through a glass sphere of refractive index 1.538 immersed in water of refractive index 1.336. The further from the optical axis the rays impinge on the sphere, the shorter is the distance at which the rays intersect the optical axis. It is this deviation from good focusing that is called spherical aberration.

11.4. An Eye in Water: The Solution

The solution to this problem used by most fishes and many other aquatic animals is to develop a lens with a variable refractive index. We have seen that in a sphere with a uniform refractive index, the rays far from the optical axis are deflected too much to be focused at the same point as the more central rays. Thus we can understand that to correct this we have to have a lens which has a lower refractive index in the perifery.

It turns out that it is possible to have a good lens with this property and still retain spherical symmetry. The pattern of refractive index decrease from center to perifery in the eye lens has now been measured for a number of aquatic animals. If we know the refractive index as a function of the distance from the sphere center, to trace the ray through the sphere we need to keep track of how far we are from the center, and of course of the ray's direction, to be able to compute how the light progresses from one point to another.

This is easiest to do if we use polar coordinates (Fig. 11.6), with the center of the sphere as origin and the angle θ between the optic axis and the point as one variable and the distance r from the point and the center of the sphere as the other variable.

The position of the tip of the advancing ray at any time is therefore described with the coordinates θ, r. We further use the following variables: n0, ncort, and ncore = the refractive index of the external medium, that of the of the
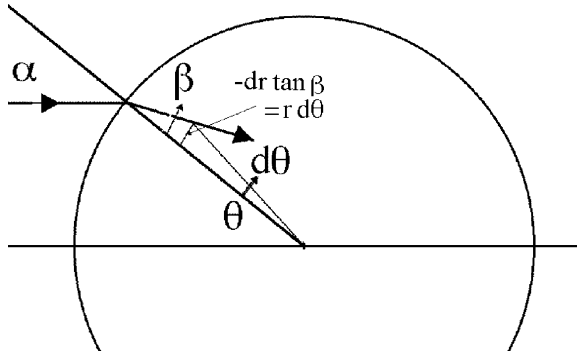
FIGURE 11.6. Tracing of a light ray through a sphere with variable refractive index.

periferal part of the sphere, and that of the center of the sphere. The angle of incidence at the external surface of the sphere is α, and the refraction angle at this refraction is β. The relation between them is the usual Snell's formula: $n_0 \cdot \sin(\alpha) = n_{cort} \cdot \sin(\beta)$. We can then see from Fig. 11.6 that, as we follow the ray a short bit into the sphere and θ is *increased* by a small amount, $d\theta$ (much smaller than in the drawing), then r *decreases* by the amount $dr = r \cdot d\theta/\tan(\beta)$. When we know the decrease in r we can compute the increase in refractive index, dn_r, and then we know how much the light is refracted and can compute a new direction of the ray. In this way we can can continue to trace the course of the light through the sphere. This has been done in Fig. 11.7.

The refractive index data for Fig. 11.7 is for a rainbow trout and have been taken from Jagger and Sands (1996). In this paper the refractive index n_r is given as the following function of the refractive index n_{core} in the center of the lens and n_{cort} in the perifery, radial distance r from the center of the lens
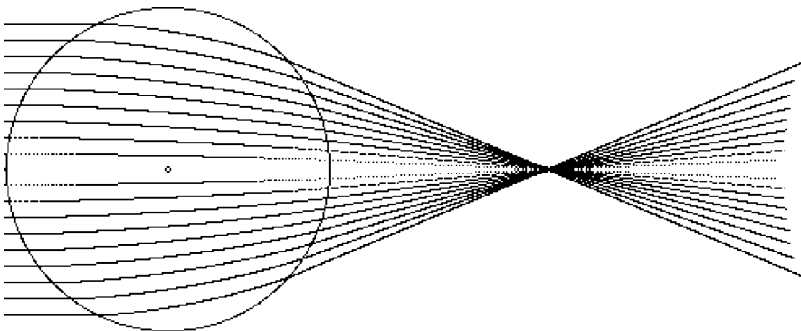
FIGURE 11.7. Light traversing a sphere with variable refractive index, highest in the center.

and $K = (n_{cort}/n_{core})-1$, the latter of course not being an independent variable, but introduced as an abbreviation:

$$n_r = n_{core} \cdot (1 + 0.78 \cdot K \cdot r^2 + 0.21 \cdot K \cdot r^6 - 0.01 \cdot K \cdot r^8 + 0.02 \cdot K \cdot r^{10})$$

To use this formula in a convenient way in a computer program, to know how much we have to change the refractive index for each small change dr in radial position, we differentiate the expression:

$$dn_r = n_{core} \cdot K \cdot (2 \cdot 0.78 \cdot r + 6 \cdot 0.021 \cdot r^5 - 8 \cdot 0.01 \cdot r^7 + 10 \cdot 0.02 \cdot r^9) \cdot dr$$

Note that this expression is negative, because K is negative, but we get an increase in n_r as we proceed inwards in the lens, because then also dr is negative. Eventually both dr and dn_r will turn positive, as the light starts to approach the surface of the sphere again.

Those readers who are interested in computing should now be able to implement a program for plotting figures such as Fig. 11.7 on their own computers. For other eyes there are various formulas like the one for n_r above. See, for instance, one for the *Octopus* lens in Jagger and Sands (1999) or a number of lenses in Jagger (1992). The cephalopod eyes and lenses, like that of *Octopus*, although evolved along a different path, are in principle very similar to fish eyes and lenses (Jagger and Sands 1996), and are often referred to as an example of convergent evolution. Convergent evolution is a phenomenon encountered over and over in the study of eyes.

As we shall learn in the next section, the sphere is only an approximation of the lens shape in fishes. Nature is more sophisticated than that.

11.5. Another Problem: Chromatic Aberration

The refractive index of all substances varies with wavelength (a phenomenon known as dispersion), and except in the vicinity of absorption bands it increases with decreasing wavelength. The refractive powers of cornea and lens can therefore not be optimal for all wavelengths at the same time. For some wavelength regions we get imaging errors collectively known as chromatic aberration. We distinguish between longitudinal chromatic aberration, which means that the image is projected at the wrong distance in relation to the retina, and lateral (or transverse) chromatic aberration, meaning that the projected image has different size for different wavelength regions. We humans overcome this problem by having sharp vision over a wide wavelength range only in the fovea, a small area of the retina close to the optic axis of the eye, where the chromatic abberration has minimal effect. We also have no ultraviolet-sensitive cells as fishes (and many other animals) do; we even have few blue-sensitive cones in the area for sharpest vision, and the yellow pigment there decreases blur from blue and violet light. Finally, we have small pupils when the things we are

looking at are well illuminated, so then we use only the central parts of cornea and lens, further limiting chromatic aberration.

For fishes the chromatic aberration constitutes a more severe problem. Generally they cannot restrict the pupil, so it is large even in strong light. A spherical shape of the lens is much worse from the viewpoint of chromatic aberration than our "lens-shaped" lens, and many fishes have ultraviolet vision (some are also sensitive to light of longer wavelength than we are). But fishes have their tricks, too. Kröger and Campbell (1996) found that the longitudinal chromatic aberration was less than predicted from lens dispersion in several fishes. The reason for this was found (Jagger 1997, Kröger, Campbell, Fernald and Wagner 1999) to be that, for a fixed wavelength, different zones of the lens have different refractive powers, by having slightly different radii of curvature. This makes light from at least one zone produce a sharp image for each spectral band (although some blurring will be produced from the other zones). Another structural finesse which counteracts (longitudinal) chromatic aberration is that the light-sensitive outer segments of retinal cells tuned to different wavelengths are positioned at different depths in the retina, corresponding to the depths where the spectral bands to which they are tuned are focused.

The trick to have the lens divided into zones with different refractive power would not work well for us, since our eyes are equipped with an iris that contracts in strong light. Thus, in strong light we use only the central part of the lens. But if you look into the eyes of a cat you will see that it has a pupil which is not circular like ours, but forming a vertical slit, which even when it closes lets the eye use periferal parts of the lens. A goat, on the other hand, has pupils which are horizontal slits, with the same consequence.

Nautilus, the mollusc with beautiful spiral shells, has a pinhole camera–type eye that has problems with neither spherical nor chromatic aberration, since its eye lacks lens as well as cornea. On the other hand, the visual acuity is low, especially in dim light when the pinhole in the iris has to open up to let more light in.

11.6. Problems and Solutions for Amphibious Animals

Terrestrial as well as aquatic animals each have their specific optical problems to solve in adaptation of their eyes to their environments. What then about animals who live both in air and water? There are many such animals: penguins and wingborne sea birds, such marine mammals as whales and seals, as well as many reptiles and even fishes. One can imagine that their problems must be much greater than those of animals who have to adapt to a single external medium. We can just think of how blurred our own vision is when we go underwater without goggles.

For birds diving for fish it can be assumed that it would be of great advantage to be able to see the fish clearly both from the air and immediately after the dive through the water surface. Can they do this? The question has been tested

for some birds. Katzir and Howland (2003) found that cormorants accommodate within 40–80 ms upon immersion in water. The cormorant has relatively low visual acuity in air relative to birds of the same body and eye size adapted to air vision only, and underwater its acuity is comparable to the higher values reported for fishes and marine mammals (Strod et al. 2004). On the other hand, cormorants are able to fish in darkness during the long arctic night (Grémillet et al. 2005), so perhaps there has been no strong evolutionary pressure for sharp air vision in their case. Martin, Rojas, Ramírez, and McNeil (2004) studied the eyes of albatross, which forage only in light. Albatross eyes have a flat cornea, which minimizes the change in refractive power of the eye upon immersion in water.

The bottlenose dolphin has a completely different eye, with a curved cornea and a spherical lens without accommodation capability (Litwiler and Cronin 2001), but a special shape of the pupil makes it possible for the dolphin to have almost the same visual acuity in air as in water (Herman et al. 1975). Herman et al. (1975) cite older literature about visual acuity for many other marine mammals. The harbor seal (Hanke et al. 2006) also has a largely curved cornea, but this has a central vertical strip that is flat, and a pupil which closes to a vertical slit, so in sufficiently strong light the seal has the same visual acuity in air and water.

Crocodiles, which have good distance focus in air (Fleishman, Howland, Howland, Rand, and Davenport 1988), as well some semiaquatic snakes (Schaeffel and Mathis 1991) surprisingly do not focus underwater, although they hunt underwater. On the contrary, some other snakes, even from the same genus (*Natrix*), possess an enormous accommodation ability. They can change the refractive power of the lens by over 100 diopters when they go from air to water, compared to some 15 diopters of accommodation in a human infant and a mere 1–2 diopters for the author at the age of 71.

The Atlantic flying fish seems to be able to select a suitable landing site among seaweed by means of vision. Instead of a smoothly curved cornea like those of most fishes, it has a pyramid shaped one with three flat "windows". Measurements show that this allows it to see reasonably well at a distance during its flight (Baylor 1967; Fig. 11.8).

A somewhat similar arrangement, but with two flat windows, is present in another fish, *Mnierpes macrocephalus*, living in the intertidal region (Graham and Rosenblatt 1970), and also in *Coryephoblennius galerita*, a fish living on rocky shores, which frequently makes excursions out of the water (Jermann and Senn 1992). The latter has one flat corna window pointing up and a curved one pointing down. Most interesting is the "four-eyed fish." *Anableps anableps* (Fig. 11.9). It is a minnow living in freshwater pools in Central and South America and catching prey both in the water and above it. It swims with the eye exactly at the water surface. The eye has separate retinae for looking in the water and looking in the air, but uses the same oblong lens for both retinae.
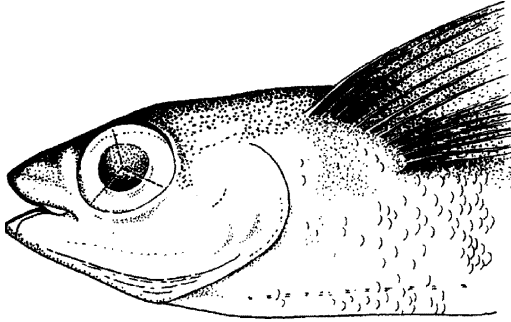
FIGURE 11.8. The Atlantic flying fish has a pyramid-shaped cornea with three flat "windows." (From Baylor 1967.)
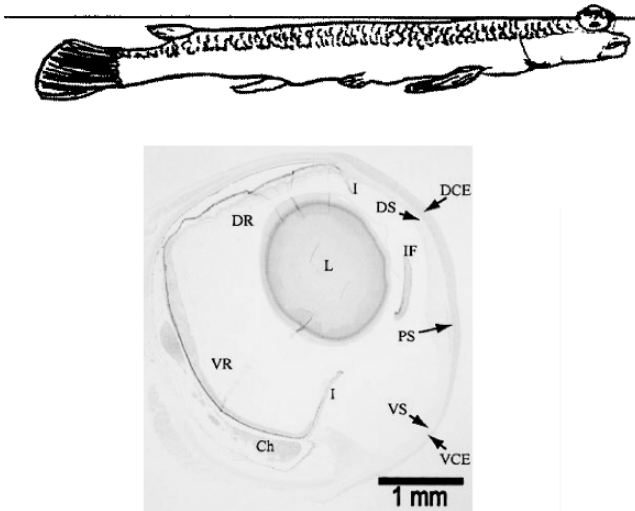
FIGURE 11.9. (Top) *Anableps* swimming at the water surface. (After Saidel and Fabiane 1998.) (Bottom) Light micrograph of longitudinal section through eye of *Anableps*. DR, dorsal retina, for looking down into the water; VS and VCE, layers of the corresponding ventral cornea; VR, ventral retina for looking into the air; DS and DCE, layers of the corresponding dorsal cornea. Note that the lens is flatter in the direction for looking in the air than in the direction for looking in the water. (From Swamynathan, Crawford, Robison, Kanungo, and Platigorsky 2003.)

Some crustaceans, and at least one mollusc (Land 2000), also have separate optical systems for different purposes, but in most cases both systems are then below the water's surface.

11.7. Feedback Regulation During Eye Development

How come everything fits together so well in an eye? The cones (or rhabdomeres in the arthropod eyes to be described later) with different spectral sensitivities must be properly connected to the correct brain cells, otherwise the animal could not distinguish blue from green. The lens must focus the image sharply on the retina. We have seen that eyes can accommodate by moving the lens or changing its shape, but that can only be done to a degree. And what causes the lens to have the proper refraction index gradient? A fish can grow from almost microscopic size to become bigger than a human, and throughout this development the eye must be able to produce sharp images to remain useful.

The answer can to a large extent be summarized in one word: feedback. The eye sends signals to the brain, and if the brain finds that the image is not good enough, it sends signals back to the eye to correct the situation. Accommodation is, of course, one result of such feedback, but the brain feeds back also to developmental processes. The refractive index gradient can be affected (Kröger, Campbell, and Fernald 2001), as well as the size of the eye (Kröger and Wagner 1996).

If animals are reared in red light, the kind of visible light refracted least by the eye, the eye will develop in such a way that if the animals are transferred to blue light, the image will be projected in front of the retina. Conversely, if they are reared in blue light and then transferred to red light, the red light will be too weakly refracted, and the image will be projected behind the retina (Kröger and Fernald 1994).

The most dramatic experiments have been carried out with chicks supplied with eyeglasses with positive or negative lenses. In such experiments it has been shown that the growth rate of the eye components is affected in a matter of hours by the distorted vision (Zhu, Park, Winawer, and Wallman 2005).

11.8. Eyes with Extreme Light Sensitivity

We have probably all noticed how night-active animals reflect the light from the car's headlights with their eyes. They have a reflective *tapetum*, a mirror, behind the light-sensitive cells, which directs any light that has escaped being caught in the first pass back through the light-sensitive layer.

The oilbird, *Steatornis caripensis,* lives in caves in Venezuela and Trinidad and flies out only at night to pick fruits in the forests in Venezuela. Thus it never experiences light stronger than full moonlight. In the cave, it also echolocates like bats, but vision is an important sense, as one can see from the construction of
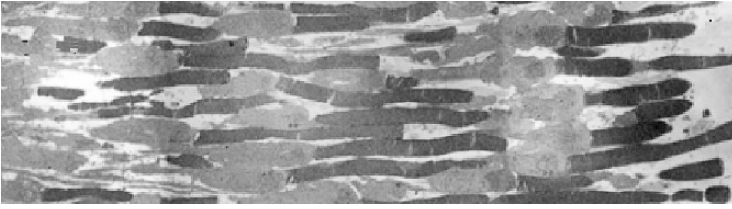
FIGURE 11.10. Part of the retina of an oil bird with multiple layers of rods. (From Martin et al. 2004.)

its retina (Martin, Rojas, Ramírez, and McNeil 2004; Fig. 11.10). In the human eye the ratio between the diameter of the fully dilated pupil and the length of the eye is approximately 0.3. In the oilbird eye it is 0.56, which means that the irradiance of the retina can be made 3.5 times that of the human eye for the same ambient lighting. The retina is packed with rods (the most light-sensitive kind of cell in vertebrates) and has only few cones. There are a million rods per mm^2 of retinal surface, as compared to a maximum of about 160,000 in the human retina. The high density of rods is possible in part because the rods are thin, but in addition they are packed three tiers thick. Light that penetrates the first layer may therefore be absorbed in the second or third. Surprisingly, though, the oil bird seems to lack a reflective tapetum. Also many deep-sea fishes have a tiered, or as the term of the trade goes, a "multibank" retina (Wagner et al. 1998).

11.9. Compound Eyes

As far as we know, the first sophisticated eyes to evolve were compound eyes. Of these early eyes, those of trilobites (Fig. 11.11) are best preserved (some for
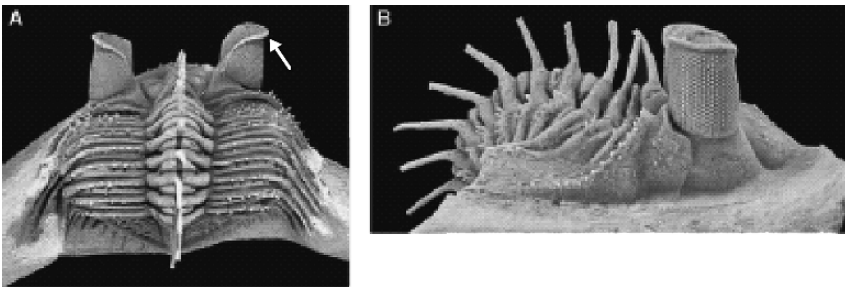
FIGURE 11.11. The Devonian trilobite *Erbenochile erbeni* (see Fortey and Chatterton 2003) from the back (A) and side (B). This animal could watch in all horizontal directions at once, and had an eyshade (arrow) above each eye to protect from light from the water surface. In the Devonian there were no birds in the sky to worry about. (Copyright the Natural History Museum, London. Reproduced with permission.)

more than half a billion years), partly because they had lenses made of calcite. Some of them are thought to have had bifocal lenses, so they could be used to see both nearby and more distant objects (Gál, Horváth, Clarkson, and Haiman 2000). A survey of different types of trilobite eyes is given by Thomas (2005).

Compound eyes in extant animals are known mainly from crustaceans and insects, but are present also in some other animals, such as horseshoe crabs. They can be broadly classified into apposition and superposition eyes (Fig. 11.12), and both these categories are present in both crustaceans and insects. Excellent reviews have been published by Horridge (2002) and by Land and Nilsson (2002), and compound eyes are treated also by Horridge (2005) and in a recent book edited by Warrant and Nilsson (2006). Here only a brief introduction will be given.

The optical system of a superposition eye is so constructed that an erect image is formed on the array of rhabdoms (the retina), not an inverted image as in our eyes. In general, animals adapted to strong light have apposition eyes, those adapted to dim light superposition eyes, but some dim-light adapted animals have rather light-sensitive apposition eyes. Acclimation to different light conditions can be achieved by movement of pigment grains.

A compound eye in a small animal cannot attain the resolutions provided by good camera type eyes. As one of the pioneers (Mallock 1894) in the study of this subject put it: "The best of the [compound] eyes … would give a picture about as good as if executed in rather coarse wool-work and viewed at a distance of a foot." But recent research has revealed that some eyes are a little better than previously thought (see below). Spatial or angular resolution of eyes can be
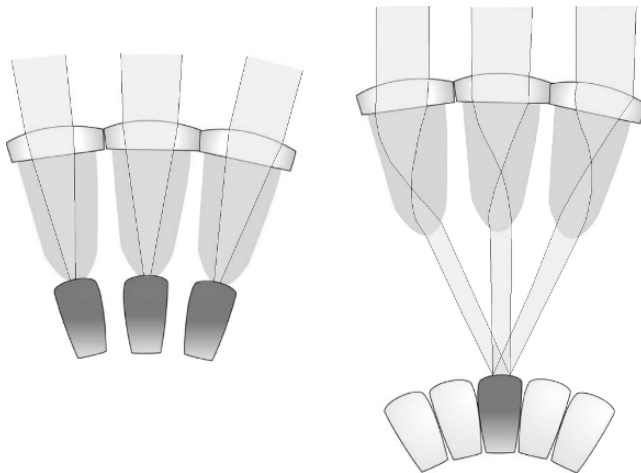
FIGURE 11.12. In an apposition eye (left) composed of several ommatidia, each ommatidium separately receives light from one direction. In an superposition eye (right), light from one direction is, via the lenses of several ommatidia, focused on the light-sensitive part (rhabdom) of one ommatidium.

measured and expressed in different ways, and distinguishing two bright points from one another is not the same as being able to resolve a pattern of equally sized parallel white and black lines. Applying the latter, most commonly used, criterion, we can say that even the best complex eyes seldom resolve better than 1–2 degrees. Only the largest eyes of dragonflies and praying mantis are about four times better than that, while we can resolve about one second of arc, and raptors such as eagles can do even better (see Gaffney and Hodos 2003 for a table of visual acuity for different birds).

Because of the small dimensions of the components of compound eyes, their function cannot be analyzed with the kind of optics ("ray optics" or "geometrical optics"; Fig. 11.13), which we used for camera-type eyes above. Instead one must use "physical optics," in which the electromagnetic wave nature of light is taken into account. To fully appreciate the following treatise, the reader is advised to first read Section 1.2 in Chapter 1.

One aspect of physical optics often encountered when dealing with the function of compound eyes is "propagation mode theory." This is a very complicated topic, and is easily misunderstood. For one thing, the term "mode" has several meanings, which are often confused. The propagation mode we shall be dealing with here is different from cavity mode or some other terms used when dealing with laser technology, but we shall just call it "mode" in the following. Considerable simplification of the full mode theory can be used when variations of refractive index are as small as in complex eyes (Snyder 1969), but even the simplified theory is something for the real experts (as can be understood from just reading the title of Snyder's treatment in the reference list below), and here I shall give only a nonquantitative account, with only very simple mathematics, to give the reader a feeling for what mode theory is about.

In an object ("light conductor") consisting of a light-transmitting medium for which some dimensions are of about the same size as the wavelength of light, light cannot propagate in as many ways as in a larger space. Such a light conductor can be a thin fiber used to transmit telephone signals, but it can also be an ommatidium in a complex eye (actually the rods and cones in our own eyes also behave in such a way, and an accurate treatment of their optics also requires physical optics and mode theory). A mode is a set of guided electromagnetic waves in the light conductor. We shall assume in the following that the light conductor is approximately cylindrical, and that the radius of the cylinder is not larger than the wavelength of the light it conducts. (Some light-conducting structures in real eyes are, it is true, far from cylindrical, but the
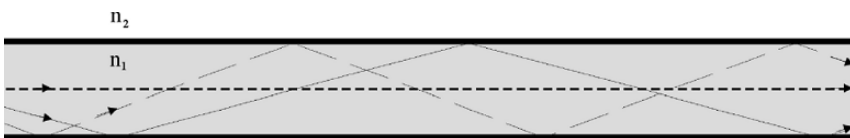
FIGURE 11.13. Light propagating along an internally reflecting cylinder according to ray optics.

cylinder approximation will be enough to get a qualitative understanding.) The cylindrical space itself has a higher refractive index than the surrounding, so the cylinder is delimited by the boundary between two media with different refractive indices.

Taking only ray optics into account, light rays can be described as bouncing in any way between the walls of the cylinder, as long as angles of incidence exceed the critical angle (Fig. 11.13) and equal the angles of reflection. But according to mode optics only certain modes can travel along the conductor, namely those for which the wavelength has a certain relation to the diameter of the light conductor (Fig. 11.14).

In geometrical optics we treat light as if it is exactly restricted to a certain space, as there exists, for instance, in front of a mirror, but not at all inside a mirror. But as we have already seen in the treatment of near-field microscopy in Chapter 5, this no longer holds exactly when we go to very great detail and small dimensions. We have something called the "near-field," a part of the electromagnetic field which goes a little bit outside the limits set by geometrical optics. Therefore we shall not be surprised that the waves representing the modes in Fig. 11.14 extend a little beyond the boundary between regions of different refractive index. The higher the mode order, the further outside the border does the mode penetrate, and the higher is the probability that light will escape to the external medium.

To compute how many modes that can propagate in a light conductor, it is convenient to introduce the concept of normalized frequency, V (also referred to as the waveguide parameter or V-number). This is a dimensionless number: $V = 2\pi(a/\lambda) \cdot (n_1^2 - n_2^2)^{1/2}$. Here a is the diameter of the conductor. If V is below 4.810, only one mode can propagate. From this it can be understood that in animal body structures, where the differences in refractive indices are small, not many modes can propagate. The number of modes is dependent on the refractive
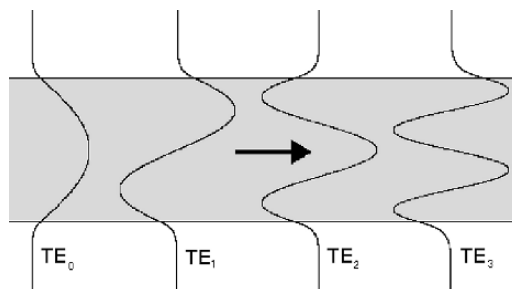
FIGURE 11.14. Electric fields of modes propagating in a cylindrical light guide. The arrow shows the direction of light propagation, and also the direction in which field strength is plotted. Note that with increasing mode number, more and more of the electrical field, and thus the electromagnetic energy (which is proportional to the square of the field strength), appears outside the fiber.

indices, so for a proper analysis these must be very accurately determined. Note that $(n_1^2 - n_2^2) = (n_1 - n_2) \cdot (n_1 + n_2)$.

We can use the formula to make a quick estimate of how light (we assume a wavelength of 500 nm) propagates in the ommatidium of a compound eye of a honeybee. The rhabdom, the light-sensitive structure to the right in Fig. 11.15, has a diameter of 4000 nm and a refractive index (n_1) of 1.347, as compared to the refractive index of the surrounding substance (n_2), 1.339.

Thus, $V = 2\pi(4000/500) \cdot (1.347^2 - 1.339^2)^{1/2} = 2\pi \cdot 8 \cdot (0.008 \cdot 2.686)^{1/2} = 0.92$, and in this structure only one mode can propagate. The crystalline cone (to the left of it in the diagram), as the name implies, has a conical shape rather than a cylindrical one, but since most of it has a diameter much larger than the rhabdom, and the refractive index difference at the boundary to neighboring cells is 3.7 times larger, we can guess that more than one mode can propagate in it. As we shall see below, interesting things can happen in the junction between crystalline cone and rhabdom. Different modes are associated with different energy distribution in the cross section of the conductor (and in the near field outside it). The total energy distribution of all the modes is not obtained by adding the energy distributions, but by adding the electromagnetic fields of the modes and squaring the sum, provided that the modes are coherent (in step with one another, in analogy with the famous Young's double slit experiment).

As an example of where the mode theory can lead us, I shall try to explain a discovery which also illustrates what was said above: "recent research has revealed that some eyes are a little better than previously thought." Nilsson, Land, and Howard (1984) and van Hateren and Nilsson (1987) found that the vision of certain butterflies with apposition eyes is sharper than what could be explained with simple-minded optics. The lens projects a bright point in the environment as an Airy disk into the crystalline cone. This Airy disk is wider than the rhabdom in that particular ommatidium, and consequently one might think that the neighboring rhabdoms would be affected by light from the bright point.
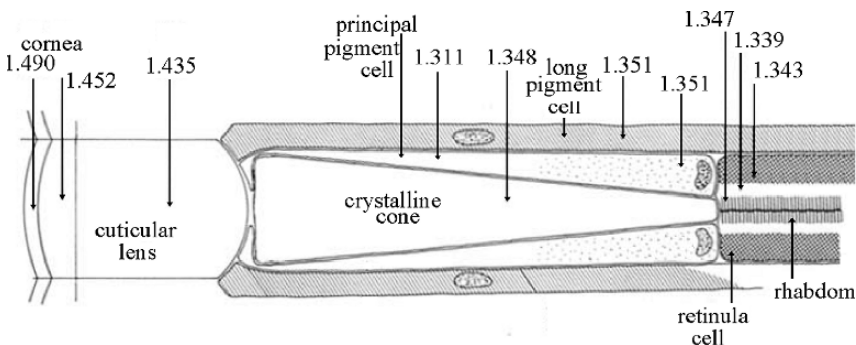
FIGURE 11.15. Outer part of an ommatidium in the apposition eye of the honeybee, *Apis mellifera*. To the right is the outermost part of the light-sensitive structure, the rhabdom (all of the rhabdom not shown). It has a cross section of 4 mm (4000 nm). (Adapted from Varela and Wiitanen 1970.)

However, in this case the dimensions of the rhabdom are such that two modes can propagate in it (can "be excited," as the jargon goes). The cross-sectional pattern of the electromagnetic field of the sum of these modes corresponds very well to the pattern of the Airy disk, with the consequence that the light from the bright point is conducted into only one rhabdom, and the image in the butterfly brain will be sharper than it would otherwise be.

11.10. Nipple Arrays on Insect Eyes

As was briefly mentioned in Chapter 1, some insect eyes carry tiny structures on their lenses that decrease reflection of light from them (Fig. 11.16). The biological advantage is probably not primarily to gain more light for vision, but to decrease the risk of being spotted by enemies.
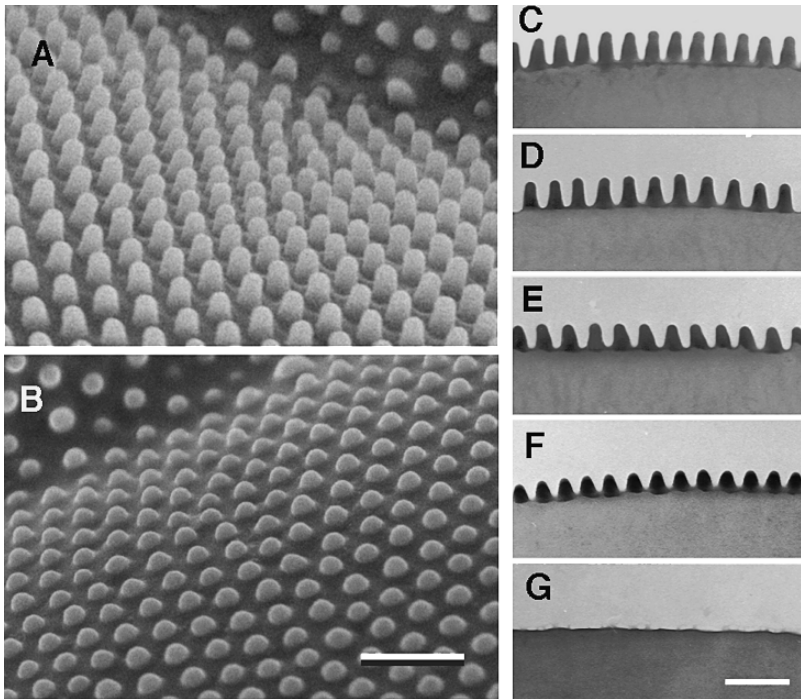
FIGURE 11.16. Left, in surface view: Corneal nipple arrays in the nymphalid *Polygonia c-aureum* (A) and the lycaenid *Pseudozizeeria maha* (B), showing differences in nipple height and shape. The bar is 500 nm. Right, in longitudinal section: Corneal nipple arrays in the nymphalids *Bicyclus anynana* and *Polygonia c-aureum* (C, D), the pierid *Pieris rapae* (E), the lycaenid *Pseudozizeeria maha* (F), and the papilionid *Papilio xuthus* (G). Bars are 500 nm. (From Stavenga, Foletti, Palasantzas, and Arikawa 2006.)

During an electron microscopic work on photoreceptor structures in a night moth, Bernhard and Miller (1962) discovered that the corneal surface carried cone-shaped protuberances termed nipples, about 200 nm in height and arranged in a hexagonal array. The antireflective effect of the nipple array was shown in microwave experiments on lens models scaled to the frequency of the microwaves (Bernhard, Miller, and Møller 1963, Bernhard, Møller, and Miller 1965) as well as in comparative spectrophotometric measurements on corneal fragments from insects with nippled and noninippled facets (Miller, Møller, and Bernhard, 1966).

Recently interest in and study of these structures has increased, partly due to the possibility of technical applications. A detailed analysis of the corneal nipple arrays of several moth and butterfly species has been carried out by Stavenga and coworkers (Stavenga, Foletti, Palasantzas, and Arikawa 2006). They modeled the reflectance from dimensions and optical theory. It was found that reflectance of the eyes decreases with increasing nipple height. Nipples with a paraboloid shape and height 250 nm, touching each other at the base, almost completely eliminates the reflectance for normally incident light.

Nipples and similar antireflective structures do not occur only in the order Lepidoptera, but also in Trichoptera and, although with smaller height, in some Diptera (Bernhard, Gemne, and Sällström 1969). In a very small moth with tiny eyes, instead of nipples, the cornea has a system of regular, radial ridges, spaced about 250 nm apart. For such eyes, operating near the diffraction limit, this was judged to be a better arrangement (Meyer-Rochow and Stringer 1993).

11.11. Eyes with Mirror Optics

The eyes treated so far have refraction optics, but (as is the case with telescopes and some other man-build instruments) eyes can also have mirror (reflection) optics or a combination of refraction and reflection optics. How biological mirrors themselves are constructed and function is described in Chapter 9, Section 9.10, so we will skip this subject here. One place for reflectors in eyes has already been touched upon, namely, those in the tapetum behind the light-sensitive cells, which let light pass a second time through them and thus increase the light sensitivity.

Only a couple of examples of reflection optics will be described here, and the reader is referred to Land (2000) for details and further examples.

One eye that combines refractive and reflective elements for projecting an image on the retina is that of a scallop. It has a lens like a normal camera-type eye, but the lens alone has not enough refracting power to produce a sharp image at the retina; it would fall far inside the eye. But the curved surface of the eye bottom reflects the rays back to converge on the retina in front of it from behind (Fig. 11.17).

For some time it was unknown how decapod crustaceans like crayfish, lobsters, shrimp, and prawns can see, when Vogt (1975, 1977) discovered that their
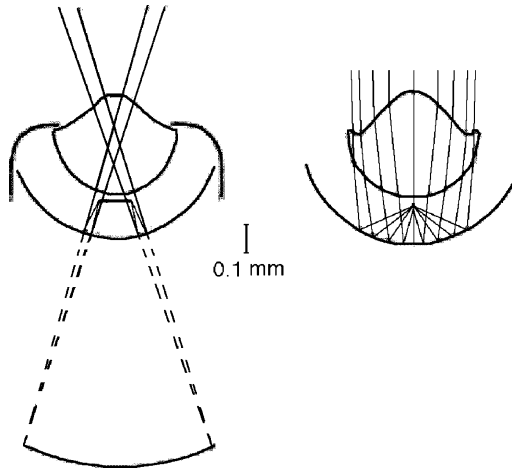
FIGURE 11.17. Scallop eye, schematic, modified after Land (2000). The sketch to the left shows where the image would fall if formed by the lens alone (dash-dot rays) and where it actually is projected after reflection at the bottom of the eye (solid line rays). The sketch to the right shows more in detail how a beam of light parallel to the optical axis is focused.

compound superposition eyes have reflection optics. The principle is shown in Fig. 11.18. Note that the corneas are flat. The material below them does not have a refractive index so that it can produce an image. It is instead the reflective walls of the ommatidia that direct the light to the rhabdoms. The diagram shows the ommatidia in a light-adapted state, where pigment grains (gray) separate the ommatidia optically from one another. In a dark-adapted eye the pigments grains are positioned in such a way that they do not separate the rhabdoms. In the upper center is a tangential section of the eye near the surface, and it can be seen that the ommatidia are square in cross section, not hexagonal as most ommatidia in insects.

It is interesting that a description of the reflection optics in compound eyes in a popular science magazine (Land 1978) inspired a design of an x-ray telescope for astronomy (Angel 1979, Lee, and Szema 2005). X-rays cannot be deflected by ordinary lenses, and one must use either reflecting optics or so-called zone-plates, based on diffraction, somewhat resembling transmission gratings, but with circular geometry.

11.12. Scanning Eyes

Both camera-type eyes, like ours, and compound eyes view a large solid angle "in one bite." This is different from a television camera, which scans the visual field point by point. We have examples of this way of imaging in the animal
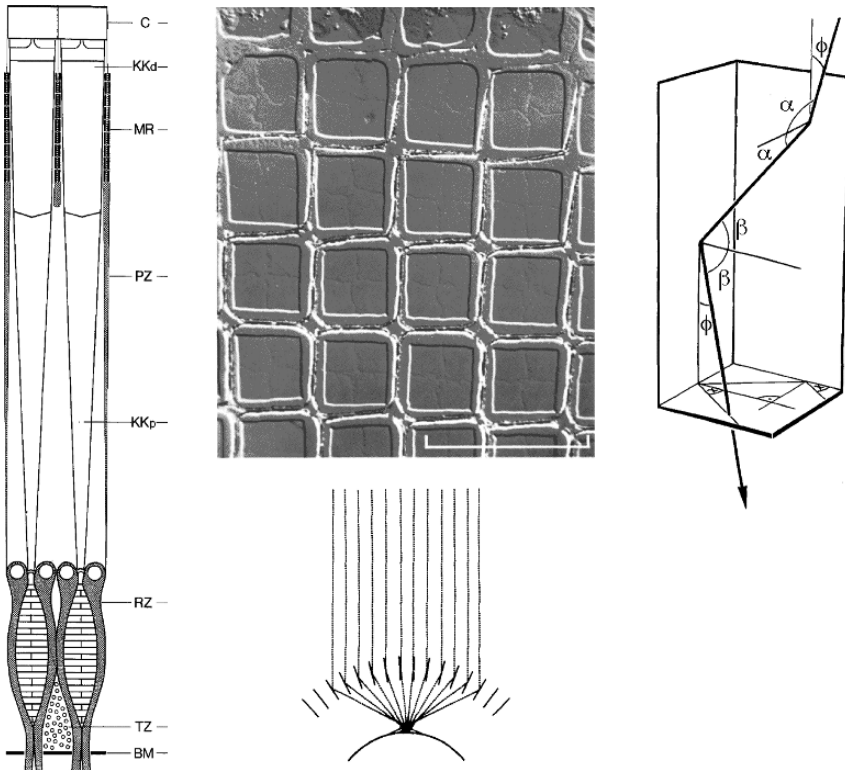
FIGURE 11.18. Crayfish eye, from Vogt (1980). To the left are two ommatidia from the compound superposition eye. To the right is a diagram showing how a light ray is reflected against the walls of an ommatidium on its way to the rhabdom, and at lower center one which shows the ray tracing in the whole eye for light from a distant point. The upper center is a surface view of the eye showing the square facets.

world, most pronounced in small crustaceans belonging to the copepods. The best studied genera are *Copilia* (Figs. 11.19 and 11.20) and *Sappherina*. These animals have two eyes, each with a very large (in relation to the body size) lens in front of the body, and deep in the body a smaller lens and a very tiny retina. The retina is so small that almost only one point at a time can be projected upon it. But the retinae of the two eyes oscillate sideways at a rate of up to 5 s^{-1}, getting alternatingly closer and further apart. In this way they scan a thin strip of the visual field.

    Copilia and *Sappherina* can be regarded as extreme cases of a common theme. They can image only two points at a time (one with each eye) and over a short time almost only a line. But scanning eye movements are common, not only in other crustaceans like *Daphnia* (Frost 1975) and crabs (Sandeman 1978), but
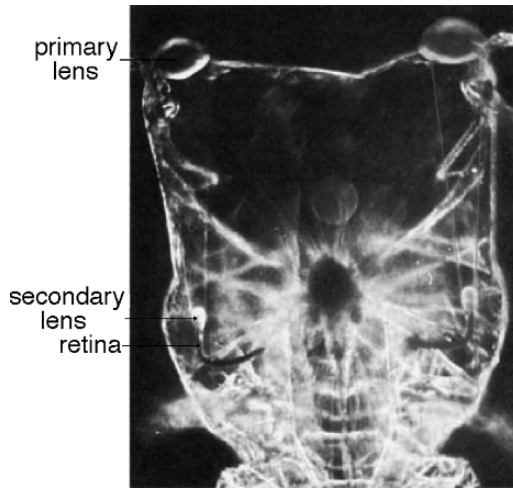
FIGURE 11.19. The front part of the body of *Copilia quadrata*. The width is about 1 mm. The approximately 2-mm-long tail is not visible. (From Gregory, Ross, and Moray 1964.)

also in spiders, molluscs (Land 1982), and other animals. In these cases the retina is not quite as small as in *Copilia* and *Sappherina*, but nevertheless the eye movements expand the visual field. Even unicellular organisms like *Euglena* or dinoflagellates, which rotate during their swim and thereby let a shadow from a pigment spot intermittently fall on the light sensor, and thereby determine the light direction, can be said to use a related principle.

In fact, we ourselves carry out small unconscious eye movements called saccades all the time, but these have a different function. In our case it is thought that these eye movements counteract a shutdown of the signals from the retina, which would be the case if the same stimulus were maintained on the same spot over a long time. It is thought that the jerky flight of some insects with fixed eyes serve the same purpose.

The tiny eyes of arthropods and other invertebrates have fascinated and inspired people from ancient times, over the years when magnifying glasses and primitive microscopes (Fig. 11.21) opened a new world, to our days. It has already been mentioned how the elucidation of the function of crayfish and lobster eyes helped astronomers to improved x-ray telescopes. The nipple arrays have been copied in solar energy collectors to help light get in, but also in light-emitting diodes to help light get out (Iwaya, Kasugai, Kawashima, Iida, Honshio, Miyake, Kamiyama, Amano, and Akasaki, I. 2006). There are many more examples of how eyes have inspired technology (Lee and Szema 2005, Duparré and Wippermann 2006).

This shows the importance of interdisciplinary communication, something which is also an aim of the present book.
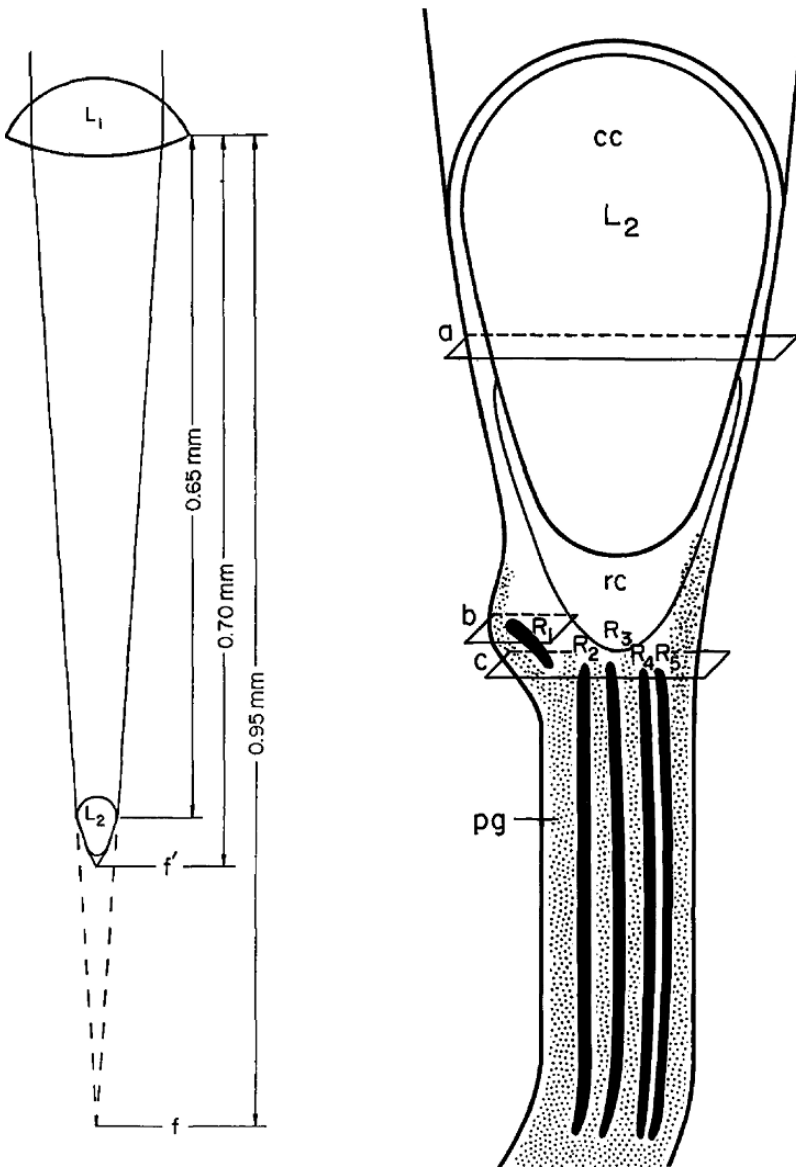
FIGURE 11.20. Sketch of a *Copilia* eye (left) and detail of the inner part (right). (From Wolken and Florida 1969.)
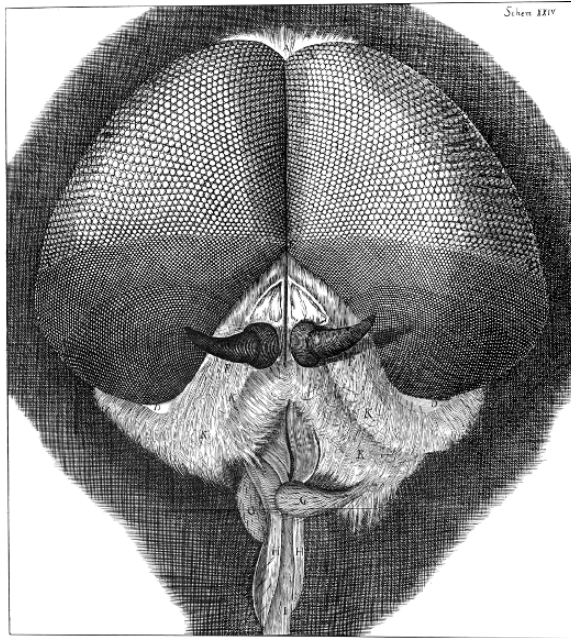
FIGURE 11.21. Robert Hooke's (1665) drawing of the head of grey drone fly.

11.13. Evolution of Eyes

Most organisms have some way to sense the light, and many can also sense the direction of light. But we shall restrict the term eye to a structure which can sense the direction of light rather well and produce a kind of "picture" of the external world, but not necessarily as a projection on a retina. Although many pigments are employed as light sensors (see Chapter 10), only a group of chromoproteins collectively known as rhodopsins are used as sensors in eyes. The chromophores, which together with the protein moities, the opsins, form the rhodopsins, are all closely related terpenoids known as retinals, although it has recently been found that in special cases chlorophyll derivatives are also involved in vision (Douglas, Partridge, Dulai, Hunt, Mullineaux, Tauber, and Hynninen 1998, Douglas, Partridge, Dulai, Hunt, Mullineaux, and Hynninen 1999, Isayama, Alexeev, Makino, Washington, Nakanishi, and Turro 2006), and archaean rhodopsin can have a carotenoid as antenna chromophore (Balashov, Imasheva, Boichenko, Antón, Wang, and Lanyi 2005).

   Rhodopsins occur throughout the three domains of life: Archaea, Bacteria, and Eukarya. The rhodopsins in Archaea are of a type, also occuring in Bacteria and Eukarya, which seems not to be involved in imaging vision and in eyes, although they may act in light sensing (while some use light to pump ions in or out of cells). The type of rhodopsin involved in vision, having amino acid sequences quite different form those of "archaeal" or "type 1" rhodopsins, occur only within

Bacteria and Eukarya. Both main types of rhodopsin may occur in the same bacterium, in which case the type 1 rhodopsins have probably been aquired by gene transfer from archaeans (Mongodin, Nelson, Daugherty, DeBoy, Wister, Khouri, Weidman, Walsh, Papke, Perez, Sharma, Nesbø, MacLeod, Bapteste, Doolittle, Charlebois, Legault, and Rodriguez-Valera 2005). Both main types of rhodopsin may have a distant common evolutionary relationship despite differences in amino acid sequence, since they share a seven-helix transmembrane structure (although some helices have been lost in some of them). There are also opsins which do not combine with retinal and are not used for vision (Terakita 2005).

From this it seems likely that all eyes have evolved from a common light-sensing structure. Opinions about the later evolution differ among experts. Some believe that imaging eyes have evolved independently more than 40 (or even more than 60) times in different animal groups (von Salvini-Plawen and Mayr 1961, as cited by Gehring 2005), while Gehring (2005) argues strongly for monophyly, and Fernald (2000) can be said to take an intermediate position. Nilsson (2006) says that there is a deep evolutionary split between ciliary photoreceptors (as the rods and cones in our eyes) and rhabdomeric photo-receptors (as the ones in simple and compound eyes of arthropods). But Arendt, Tessmar-Raible, Snyman, Dorresteijn, and Wittbrodt (2004) found both ciliary and rhabdomeric photoreceptors in the same animal species, a ragworm.

At least in part the differences between "monophylogenists" and advocates of convergent evolution are to some extent due to terminology confusion. "A has evolved from B" or "A is homologous with B" were clear as long as scientists had only visible morphological characters to consider. When molecular phylogeny emerged the terminology for a while became blurred, but is now beginning to clear up again. As Nielsen and Martinez (2002) point out, "homologous structures in two or more taxa are structures derived from the same structure in their latest common ancestor." In that sense all parts of all eyes are certainly not homologous. On the other hand, it has been clearly demonstrated that several of the genes and signaling systems for development of eyes are related between animals as different as insects and vertebrates. Most dramatic has been the demonstration (Gehring 2005) that eyes can be induced on the antenna of a fruitfly by transfer from a mouse of a gene (Pax6) which induces eye formation in that animal, or a similar gene from a fruitfly that induces eye formation in a toad. It should be pointed out that Pax6 has other functions, too, and perhaps this and related genes are more generally involved in organization of sense organs and nerve systems rather than specific eye organizers. A single Pax-type gene is present in the box jellies (cubozoans), where it is expressed both in parts of the eyes (retina and lens) and in the balance organs (Kozmik and Daube 2003). Oakley (2003 a,b) contemplates the question of monophyly or polyphyly specifically for compound eyes. He presents evidence that the compound eyes of insects and crustaceans are homologous. But the group among crustaceans with compound eyes that he has particularly studied, myococopid ostracods, seems to have no close relatives or ancestors with compound eyes, so it seems that

compound eyes have evolved again on that line. Oakley (2003b) suggests the possibility that "complex structures like eyes might not evolve *de novo* every time and many of the steps toward origin need not be repeated … genes or even whole developmental pathways may be retained during evolution, even in the absence of the morphological features where those genes were once expressed." As a classic example, the existence of a latent developmental program was proposed to explain the experimental induction of teeth in chickens (Kollar and Fisher 1980; Gould 1983; Chen, Zhang, Jiang, Barlow, St Amand, Hu, Heaney, Francis-West, Chuong, and Maas 2000). In a more recent example, Whiting, Bradler, and Maxwell (2003) suggested, based on phylogenetic distribution, that insect wings may be evolving by "switchback evolution." This appears to me to be a very reasonable standpoint, and Harris, Hasso, Ferguson, and Fallon (2006) can now be added to the list of citations as an even more striking illustration.

Although the opsin part of rhodopsins are all related (with the exception of the archaeal type), and the chromophores are also related, there are differences in the details, not only in the opsin proteins, but also in the chromophores (Chapter 9) and in their biosynthesis. In eukaryotes retinal is formed by the oxygenation of β-carotene, but in the cyanobacterium *Synechocystis* by oxygenation of a β-apocarotenal (Ruch et al. 2005). For formation of 3-hydroxyretinal and 3-hydroxyretinol from retinal in insects, one or, respectively, two more oxygenation steps are required, each using specific enzymes (Seki et al. 1998; Ahmad et al. 2006). All these oxygenations require molecular oxygen, and the pathways could not have evolved prior to the oxygenation of the environment. As in eukaryotes, retinal in halobacteria is formed by oxygenation of β-carotene (Peck et al. 2001). Since the split between eukaryotes and archaeans is thought to be older than environmental oxygen, this indicates either parallel evolution or horizontal gene transfer, a question that could perhaps be solved by comparison of the sequences of the various oxygenases.

The materials of the lenses have no common origin. The main proteins in vertebrate lenses, the crystallins (see Piatigorsky 2006), have nothing in common with the lens material in arthropods or molluscs, and lenses in some animals like trilobites (Thomas 2005) and brittlestars (Aizenberg et al. 2001) were or are made, wholly or in part, from an inorganic material, calcite.

One cannot but marvel when realizing how sophisticated the eyes or other light-recording structures are in some at first glance very "simple" animals, like the brittlestars (Aizenberg et al. 2001) or box jellies (Martin 2004; Nilsson et al. 2006), or even some unicellular organisms. Gehring (2005) shows pictures of various dinoflagellates having eye-like structures with lenses, light-sensitive regions, and pigmented areas within a single cell. Francis (1967) estimated the refractive index of the presumed lens of such an organism to be around 1.5, i.e., much higher than that of a human lens, which makes it even more likely that it really has an optical function. However, it is to go too far to speculate, as Gehring (2005) does, that a dinoflagellate structure could be an eye precursor, since the rather advanced eyes of trilobites probably evolved before dinoflagellates.

The lenses of brittlestars (Aizenberg et al. 2001) and of box jellies (Nilsson et al. 2006) have a surprisingly advanced construction, being able to produce images supposedly too sharp for the nervous systems of these animals to take full advantage of. In both cases they have refractive index gradients of the same type as described above for the lenses in fish and octopus eyes.

References

Ahmad, S.T., Joyce, M.V., Boggess, B. and O'Tousa, J.E. (2006) The role of *Drosophila* ninaG oxidoreductase in visual pigment chromophore biogenesis. J. Biol. Chem. 281, 9205–9209.

Aizenberg, J., Tkachenko, A., Weiner, S., Addadi, L., and Hendler, G. (2001) Calcitic microlenses as part of the photoreceptor system in brittlestars. Nature 412, 819–822.

Angel, J.R.P. (1979) Lobster eyes as x-ray telescopes. Astrophys. J. 233, 364–73.

Arendt, D., Tessmar-Raible, K. Snyman, H., Dorresteijn, A.W. and Wittbrodt, J. (2004) Ciliary photoreceptors with a vertebrate-type opsin in an invertebrate brain. Science 306, 869–871.

Balashov, S.P., Imasheva, E.S., Boichenko, V.A., Antón, J. Wang, J.M, and Lanyi, J.K. (2005) Xanthorhodopsin: A proton pump with a light-harvesting carotenoid antenna. Science 309, 2061–2064.

Baylor, E.R. (1967) Air and water vision of the Atlantic flying fish, *Cypselurus heterusus*. Nature 214, 307–308.

Bernhard, C.G. and Miller, W.H. (1962) A corneal nipple pattern in insect compound eyes. Acta Physiol. Scand. 56, 385–386.

Bernhard, C.G., Møller, A.R. and Miller, W.H. (1963) Function of corneal nipples in compound eyes of insects. Acta Physiol. Scand. 58, 381–382.

Bernhard, C.G., Miller, W.H. and Møller, A.R. (1965) Insect corneal nipple array—a biological broad-band impedance transformer that acts as an antireflection coating. Acta Physiol. Scand. S 63: 5- Suppl. 243.

Bernhard, C.G., Gemne, G. and Sällström, J. (1970) Comparative ultrastructure of corneal surface topography in insects with aspects on phylogenesis and function. Z. Vergl. Physiologie 67, 1–25.

Chen, Y., Zhang, Y., Jiang, T.X., Barlow, A.J., St Amand, T.R., Hu, Y., Heaney, S., Francis-West, P., Chuong, C.M. and Maas. R. (2000) Conservation of early odontogenic signaling pathways in Aves. Proc. Natl. Acad. Sci. USA 97, 10044–10049.

Douglas, R.H., Partridge, J.C., Dulai, K., Hunt, D., Mullineaux, C.W., Tauber, A.Y., and Hynninen, P.H. (1998) Dragon fish see using chlorophyll. Nature 393 (6684): 423–424.

Douglas, R.H., Partridge, J.C., Dulai, K.S., Hunt, D.M., Mullineaux, C.W., and Hynninen, P.H. (1999) Enhanced retinal longwave sensitivity using a chlorophyll-derived photosensitiser in *Malacosteus niger*, a deep-sea dragon fish with far red bioluminescence. Vision Res. 39, 2817–2832.

Duparré, J.W. and Wippermann, F.C. (2006) Micro-optical artificial compound eyes. Bioinsp. Biomim. 1 (2006) R1–R16

Fernald, R.D. (2000) Evolution of eyes. Curr. Opin. Neurobiol. 10, 444–450.

Fleishman, L.J., Howland, H.C., Howland, M.J., Rand, R.S., and M.L. Davenport. M.L. (1988) Crocodiles don't focus underwater. J. Comp. Physiol. A 163:441–443.

Fortey, R. and Chatterton, B. (2003) A Devonian trilobite with an eyeshade. Science 301, 1689.

Francis, D. (1967) On the eyespot of the dinoflagellate *Nematodinium*. J. Exp. Biol. 47, 495–501.

Frost, B.J. (1975) Eye movements in *Daphnia pulex* (De Geer). J. Exp. Biol. 62, 175–187.

Gaffney, M.F. and Hodos, W. (2003) The visual acuity and refractive state of the American kestrel (*Falco sparvensis*). Vision Res. 43, 2053–2093.

Gál, J., Horváth, G., Clarkson, E.N.K. and Haiman, O. (2000) Image formation by bifocal lenses in a trilobite eye? Vision Res. 40, 843–853.

Gehring, W.J. (2005) New perspectives on eye development and the dvolution of dyes and photoreceptors J. Heredity 96, 171–184.

Gould, S.J. (1983) *Hen's Teeth and Horse's Toes.* W.W. Norton, New York.

Graham, J.B. and Rosenblatt, R.H. (1970) Aerial vision: Unique adaptation in an intertidal fish. Science 168, 586–588.

Gregory, R.L., Ross, H.E. and Moray, N. (1964) The curious eye of *Copilia*. Nature 201, 1166–1168.

Grémillet, D., Kuntz, G., Gilbert, C., Woakes, A.J., Butler, P.J. and le Maho, Y. (2005) Cormorants dive through the Polar night. Biol. Lett. 1, 469–471.

Harris, M.P., Hasso, S.M, Ferguson, M.W.J. and Fallon, J.F. (2006) The development of archosaurian first-generation teeth in a chicken mutant. Curr. Biol. 16, 371–377.

Hanke, F.D., Dehnhardt, G., Schaeffel, F. and Hanke, W. (2006) Corneal topography, refractive state, and accomodation in harbor seals (*Phoca vitulina*). Vision Res. 46, 837–847.

Herman, L.M., Peacock, M.F., Ynkeer, M.P. and Madsen, C.J. (1975) Bottlenosed dolphin: Double-slit pupil yields equivalent aerial and underwater diurnal acuity. Science 189, 650–652.

Hooke, R. (1665) *Micrographia: or, some physiological descriptions of minute bodies made by magnifying glasses with observations and inquiries thereupon*. J. Martyn and J. Allestry, London.

Horridge, G.A. (2002) The design of the compound eye depends on the physics of light. In: L.O. Björn (Ed.), *Photobiology: The science of light and life.* Kluwer Academic Publishers, Dordrecht, pp. 181–218.

Horridge, G.A. (2005) The spatial resolutions of the apposition compound eye and its neurosensory feature detectors: observation versus theory. J. Insect Physiol. 51, 243–266.

Isayama, T., Alexeev, D., Makino, C.L., Washington, I., Nakanishi, K. and Turro, N.J. (2006) An accessory chromophore in red vision. Nature 443, 649.

Iwaya, M., Kasugai, H., Kawashima, T., Iida, K., Honshio, A., Miyake, Y., Kamiyama, S., Amano, H. and Akasaki, I. (2006) Improvement in light extraction efficiency in group III nitride-based light-emitting diodes using moth-eye structure. Thin Solid Films 515, 768–770.

Jagger, W.S. (1992) The optics of the spherical fish lens. Vision Res. 32, 1271–1284.

Jagger, W.S. (1997) Chromatic and monochromatic optical resolution in the rainbow trout. Vision Res. 37, 1249–1254.

Jagger, W.S. and Sands, P.J. (1996) A wide-angle gradient index optical model of the crystalline lens and eye of the rainbow trout. Vision Res. 36, 2623–2639.

Jagger, W.S. and Sands, P.J. (1999) A wide-angle gradient index optical model of the crystalline lens and eye of the octopus. Vision Res. 39, 2841–2853.

Jermann, T. and Senn, D.G. (1992) Amphibious vision in *Coryphoblennius galerita* L. (Perciformes). Experientia 48, 217–218.

Katzir, G. and Howland, H.C. (2003) Corneal power and underwater accomodation in great cormorants (*Phalacrocorax carbo sinensis*). J. Exp. Biol. 206, 833–841.

Kollar, E.J. and Fisher, C. 1980. Tooth induction in chick epithelium: Expression of quiescent genes for enamel synthesis. Science 207, 993–995.

Kozmik, Z., Daube, M., Frei, E., Kos, L., Dishaw, L.J., Noll, M., and Piatigorsky, J. (2003) Role of Pax genes in eye evolution: A cnidarian PaxB gene uniting Pax2 and Pax6 functions. Developmental Cell 5, 773–785.

Kröger, R.H.H. and Campbell, M.C.W. (1996) Dispersion and longitudinal chromatic aberration of the crystalline lens of the African cichlid fish *Haplochromis burtoni.* J. Opt. Soc. Am. A 13, 2341–2347.

Kröger, R.H.H., Campbell, M.C.W., Fernald, R.D. and Wagner, H.J. (1999) Multifocal lenses compensate for chromatic defocus in vertebrate eyes. J. Comp. Physiol. A 184, 361–369.

Kröger, R.H.H., Campbell, M.C.W. and Fernald, R.D. (2001) The development of the crystalline lens is sensitive to visual input in the African cichlid fish, *Haplochromis burtoni.* Vision Res. 41, 549–559.

Kröger, R.H.H. and Fernald, R.D. (1994) Regulation of eye growth in the African cichlid fish *Haplochromis burtoni.* Vision Res. 34, 1807–1814.

Kröger, R.H.H. and Wagner, H.J. (1996) The eye of the blue acara (*Aequidens pulcher*, Cichlidae) grows to compensate for defocus due to chromatic aberration. J. Comp. Physiol. A. 179, 837–842.

Land , M.F. (1978) Animal eyes with mirror optics. Sci. Am. 239, 126–34.

Land, M.F. (1982) Scanning eye movements in a heteropod mollusc. J. Exp. Biol. 96, 427–430.

Land, M.F. (2000) Eyes with mirror optics. J. Opt. A: Pure Appl. Opt. 2, R44–R50.

Land, M.F. and Nilsson, D.-E. (2002) *Animal eyes*. Oxford University Press, New York.

Lee, L.P. and Szema, R. (2005) Inspirations from biological optics for advanced photonic systems science 18, 1148–1150.

Liou, H.-L. and Brennan, N.A. (1997) Anatomically accurate, finite model eye for optical modeling. J. Opt. Soc. Am. A, 14, 1684–1695.

Litwiler, T.L. and Cronin, T.W. (2001) No evidence of accomodation in the eyes of the bottlenose dolphin, *Tursiops truncatus*. Marine Mammal Sci. 17, 508–525.

Liu, Y.-J., Wang, Z.-Q., Song, L.-P., and Mu, G.-G. (2005) An anatomically accurate eye model with a shell-structure lens. Optik 116, 241–246.

Mallock A. 1894. Insect sight and the defining power of compound eyes. Proc. R. Soc. London B 55, 85–90.

Martin, G.R. (1998) Eye structure and amphibious foraging in albatrosses. Proc. Roy. Soc. Lond. B.265, 665–671.

Martin, G., Rojas, L.M., Ramírez, Y. and McNeil, R. (2004) The eyes of oilbirds (*Steatornis caripensis*): pushing at the limits of sensitivity. Naturwiss. 91, 26–29.

Martin, V.J. (2004) Photoreceptors of cubozoan jellyfish. Hydrobiologia 530-531, 135–144.

Meyer-Rochow, V.B. and Stringer, I.A. (1993) A system of regular ridges instead of nipples on a compound eye that has to operate near the diffraction limit. Vision Res. 33, 2645-2647.

Miller, W.H., Møller, A. R. and Bernhard, C.G. (1966) The corneal nipple array. In: C. G. Bernhard, (Ed.), *The functional organization of the compound eye*. Pergamon Press, London, pp. 21–33.

Mongodin, E.F., Nelson, K.E., Daugherty, S., DeBoy, R.T., Wister, J., Khouri, J.H., Weidman, J., Walsh, D.A., Papke, R.T., Sanchez Perez, G., Sharma, A.K., Nesbø, C.L., MacLeod, D., Bapteste, E., Doolittle, W.F., Charlebois, R.L., Legault, B. and

Rodriguez-Valera, F. (2005) The genome of *Salinibacter ruber*: Convergence and gene exchange among hyperhalophilic bacteria and archaea. Proc. Natl Acad. Sci. USA 102, 18147–18152.

Navarro, R., Santamaría, J. and Bescós. J. (1985) Accommodation-dependent model of the human eye with aspherics. J. Opt. Soc. Am. A 8, 1273–1281.

Nielsen, C. and Martinez, P. (2003) Patterns of gene expression: homology or homocrazy? Development Genes Evol. 213, 149–154.

Nilsson, D.-E., Land, M.F. and Howard, J. (1984) Afocal apposition optics in butterfly eyes. Nature 312, 561–563.

Nilsson, D.E., Gislen, L., Coates, M.M., Skogh, C. and Garm, A. (2005) Advanced optics in a jellyfish eye, Nature 435, 201–205.

Oakley, T.H. (2003a) The eye as a replicating and diverging, modular developmental unit. Trends Ecology Evol. 18, 623–627.

Oakley, T.H. (2003b) On homology of arthropod compound eyes. Integr. Comp. Biol. 43, 522–530.

Onuma, Y., Takahashi, S., Asashima, M., Kurata, S. and Gehring, W.J. (2002). Conservation of Pax-6 function and upstream activation by Notch signaling in eye development of frogs and flies. Proc. Natl. Acad. Sci. USA 99, 2020–2025.

Ott, M. (2006) Visual accommodation in vertebrates: mechanisms, physiological response, and stimuli. J. Comp. Physiol. A. 192, 97–111.

Peck, R.F., Echavarri-Erasun, C., Eric A. Johnson, E.A., Wailap Victor Ngi, W.V., Kennedy, S.P., Hoodi, L., DasSarma, S. and Krebs, M.P. (2001) brp and blh are required for synthesis of the retinal cofactor of bacteriorhodopsin in *Halobacterium salinarum*. J. Biol. Chem. 23, 5739–5744.

Piatigorsky, J. (2006) Seeing the light: the role of inherited developmental cascades in the origins of vertebrate lenses and their crystallins. Heredity 96, 275–277.

Ruch, S., Beyer, P., Ernst, H. and Al-Babili, S. (2005) Retinal biosynthesis in Eubacteria: *in vitro* characterization of a novel carotenoid oxygenase from *Synechocystis* sp. PCC6803. Mol. Microbiol. 55, 1015–1024.

Saidel, W.M. and Fabiane, R.S. (1998) Optomotor response of *Anableps anableps* depends on the field of view. Vision Res. 38, 2001–2006.

Sandeman, D.C. (1978) Eye-scanning during walking in the crab *Leptograpsus variegans*. J. Comp. Physiol. 124, 249–257.

Schaeffel, F. and Mathis, U. (1991) Underwater vision in semi-aquatic European snakes. Naturwissenschaft 78, 373–375.

Seki, T., Isono, K, Ozaki, K., Tsukahara, Y., Shibata-Katsuta, Y., Ito, M., Irie, T. and Katagir, M. (1998) The metabolic pathway of visual pigment chromophore formation in *Drosophila melanogaster*. All-trans (3S)-3-hydroxyretinal is formed from all-trans retinal via (3R)-3-hydroxyretinal in the dark. Eur. J. Biochem. 257, 522–527.

Snyder, A.W. (1969) Asymptotic expressions for eigenfunctions and eigenvalues of a dielelectric or optical waveguide. IEEE Trans. Microw. Theory Techn. MIT-17, 1130–1138.

Stavenga, D.G., Foletti, S., Palasantzas, G. and Arikawa, K. (2006) Light on the mothe-eye corneal nipple array of butterflies. Proc. Roy. Soc. B 273, 661–667.

Strod, T., Arnd, Z., Izhaki, I. and Katzir, G. (2004) Cormorants keep their power: visual resolution in a pursuit-diving bird under amphibious and turbid conditions. Curr. Biol. 14, R376-R-377.

Swamynathan, S.K., Crawford, M.A., Robison, W.G., Kanungo, J. and Platigorsky, J. (2003). Adaptive differences in the structure and macromolecular compositions of the air and water corneas of the "four-eyed" fish (*Anableps anableps*). FASEB J. 17, 1996–2005.

Terakita, A. (2005) The opsins. Genome Biol. 6, 213.

Thomas, A.T. (2005) Developmental palaeobiology of trilobite eyes and its evolutionary significance. Earth-Science Rev. 71, 77–93.

Varela, F.G. and Wiitanen, W. (1970) The optics of the compound eye of the honeybee. J. Gen. Physiol. 55, 336–358.

Vogt, K. (1975) Zur Optik des Flusskrebsauges. Z. Naturforsch. 30, 691–691.

Vogt, K. (1977) Ray path and reflection mechanisms in crayfish eyes. Z. Naturforsch. 32, 466–468.

Vogt, K. (1980) Die Spiegeloptik des Flusskrebsauges. (The optical system of the crayfish eye.) J. Comp. Physiol. A 135, 1–19.

van Hateren, J.H. and Nilsson, D.-E. (1987) Butterfly optics exceed the theoretical limits of conventional apposition eyes. Biol. Cybernetics 57, 159–168.

von Salvini-Plawen, L.V and Mayr, E. (1977) On the evolution of photoreceptors and eyes. In: M. K. Hecht, W.C. Steere, and B. Wallace (Eds.) *Evolutionary Biology* 10. Plenum, New York, pp. 207–263.

Wagner, H.-J., Fröhlich, E., Negishi, K. and Collin, S.P. (1998) The eyes of deep-sea fish II. Functional morphology of the retina. Progr. Retinal Eye Res. 17, 637–685.

Warrant, E. and Nilsson, D.-E., Eds. (2006) *Invertebrate vision*. Cambridge University Press, Cambridge, UK.

Whiting, M. F., Bradler, S. and Maxwell, T. (2003) Loss and recovery of wings in stick insects. Nature 421, 264–267.

Wolken, J.J. and Florida, R.G. (1969) The eye structure and the optical system in the crustacean copepod *Copilia*. J. Cell Biology 40, 279–286.

Zhu, X.Y., Park, T.W., Winawer, J. and Wallman, J. (2005) In a matter of minutes, the eye can know which way to grow. Invest. Ophthalmol. Visual Sci. 46, 2238–2241.

12
The Evolution of Photosynthesis and Its Environmental Impact

Lars Olof Björn and Govindjee

Abstract: Photosynthesis in plants is a very complicated process, utilizing two photosystems in series to carry out the very energy-demanding process of oxidizing water to molecular oxygen and reducing carbon dioxide to organic compounds. The first photosynthetic organisms, living more than 3.4, perhaps even 3.8 Ga, i.e., American billion (10^9), years ago, carried out a simpler process, without oxygen production and with only one photosystem. A great variety of such one-photosystem photosynthesizers are living even today, and by comparing them, and from chemical fossils, researchers are trying to piece together a picture of the course of the earliest evolution of photosynthesis. Chlorophyll *a* probably preceded bacteriochlorophyll *a* as a main pigment for conversion of light into life energy. The process of carbon dioxide assimilation, today taking place mainly in conjunction with photosynthesis, is even older than photosynthesis itself. Oxygenic photosynthesis, i.e., photosynthetic production of molecular oxygen, first appeared in ancestors of present-day cyanobacteria more than 2.7, perhaps already 3.7 Ga ago. Cyanobacteria entered into close association with other organisms more than 1.2 Ga ago, and chloroplasts in green algae and green plants as well as those in algae on the "red" line of evolution (red algae, cryptophytes, diatoms, brown algae, yellow-green algae, and others) stem from a single early event of endosymbiotic uptake of a cyanobacterium into a heterotrophic organism. Only ecologically unimportant exceptions to this rule have been found. The chloroplasts on the "red line," except those of red algae, stem from a single event of secondary endosymbiosis, in which a red alga was taken up into another organism. There are also examples of tertiary (third level) endosymbiotic events. Thylakoids in land plants are partially appressed and form grana, while those of, e.g., red algae do not have this structure, and this difference can be explained by the different spectra of ambient light. At the end of the chapter a brief review is given of the evolution of the assimilation of carbon dioxide, the adaptation to terrestrial life, and the impact of photosynthesis on the terrestrial environment.

12.1. Introduction

The earth began to form about 4.6 Ga (gigayears, billion years) ago. Thirty million years later a core had formed (Yin, Jacobsen, Yamashita, Blicher-Toft, et al. 2002; Kleine, Münker, Mezger, and Palmer 2002), and 4.4 Ga ago there was a continental crust and an ocean (Wilde, Valley, Peck, et al. 2001). Between 4.2 and 3.7 Ga ago the earth was subjected to "the late heavy bombardment" (Gomes, Levison, Tsiganis, and Morbidelli, 2005), which is by many thought to have wiped out any life that might have existed at that time. The first organisms emerging after that cataclysm were not able to carry out photosynthesis. Probably they got their metabolic energy by reducing carbon dioxide to methane, using hydrogen as reductant. But photosynthetic life is also very ancient, probably at least 3.4 Ga (Blankenship 1992, Tice and Lowe 2004, 2006). The first photosynthesis differed from the process taking place in plants now, but there are some common features and a direct line evolution from these first forms.
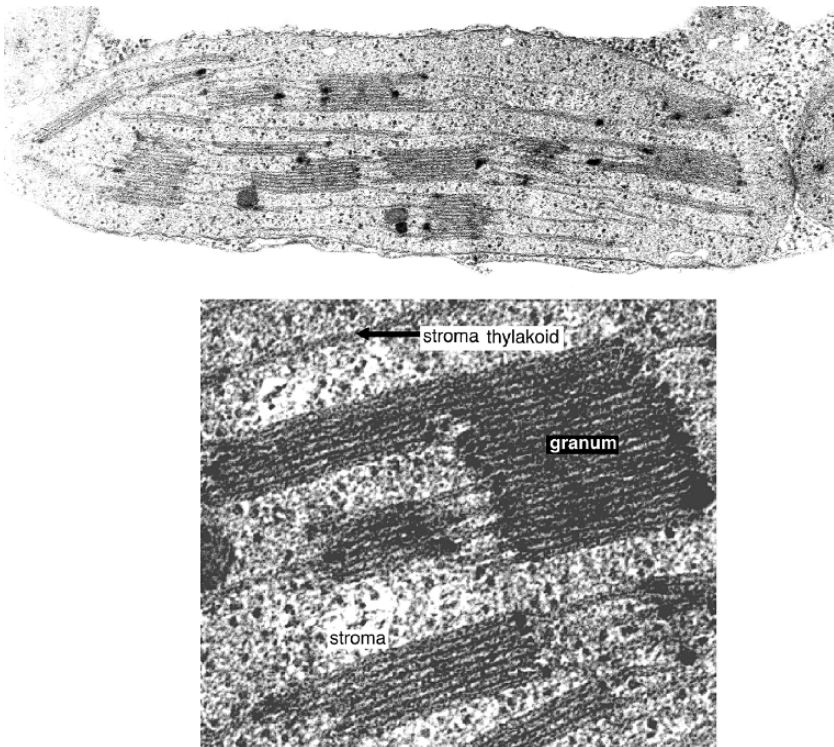
Figure 12.1. Chloroplast from tobacco plant (top), and at higher magnification (below) showing details of grana and thylakoids. The stroma thylakoids (stroma lamellae) run through the stroma between the grana. (Courtesy Professor Claes Weibull, Lund University.)

12.2. A Short Review of Plant Photosynthesis

Plant photosynthesis consists mainly of an oxidation of water to molecular oxygen and a reduction of carbon dioxide to organic matter, primarily carbohydrate. It takes place in the chloroplasts, with one set of reactions in the pigment-rich thylakoid membranes, and another set of reactions in the stroma, a solution of enzymes between the membranes (Figs. 12.1 and 12.2).

In the thylakoid membranes the following takes place: The light is absorbed in chlorophyll *a* and in other pigment molecules. The absorbed energy is transferred to a reaction center. Among other prosthetic groups, this contains chlorophyll *a*. There are two kinds of reaction center–containing pigment–protein complexes, called photosystem I (PSI) and photosystem II (PSII) (see Figs. 12.2 and 12.3). They can be regarded as light-powered "electron pumps" connected in series by
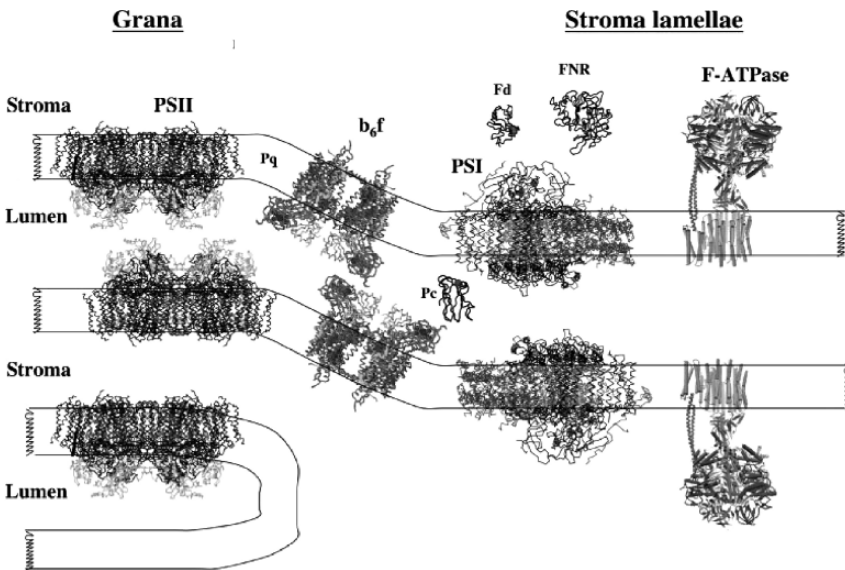
FIGURE 12.2. The arrangement of molecules participating in photosynthesis in a green plant. Of the large protein complexes, photosystem II (PSII) is located predominantly in the grana lamellae (the parts of the thylakoid memebranes forming grana) and photosystem I (PSI) and F-ATPase mainly in the stroma lamellae, but the photosystems are mobile. Electrons taken from water by PSII are transferred to the cytochrome b6f complex via plastoquinone (Pq), and from there to PSI via plastocyanin (Pc). Electrons from PSI go via ferredoxin (Fd) and ferredoxin-NADP reductase (FNR) to NADP. The resulting NADPH is used as a reductant in carbon dioxide assimilation, which takes place in the stroma. Coupled to the electron transport is a translocation of protons from the stroma to the lumen. Protons flowing back to the stroma via the F-ATPase drive the synthesis of ATP, which is also used in carbon dioxide assimilation. Variations of this scheme occur, and algae on the red line of evolution differ in several respects (see Sections 12.7 and 12.8). (From Nelson and Ben-Shem 2002.)
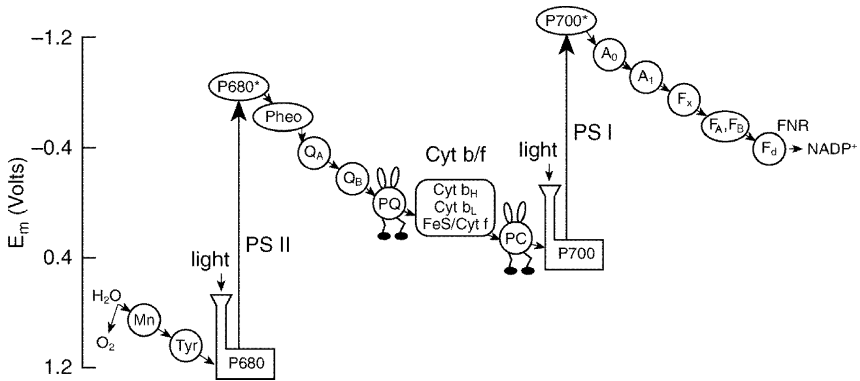
FIGURE 12.3. Drawing of electron transport in plant photosynthesis, the so-called Z-scheme. Light is collected by antenna pigments, symbolized as funnels and conducted to the reaction center pigments (P680 in PS II and P700 in PS I, in both cases chlorophyll *a*). Electrons are "sucked" from water via manganese atoms in the water-splitting enzyme and tyrosine residues in a PS II peptide. The photosystems "lift" the electrons to a higher energy (more negative redox potential). They leave the reaction center chlorophylls, which temporarely become positively charged, and flow over a chain of electron carriers. Of these Pheo (pheophytin), Q_A and Q_B (quinones), as well as A_0, A_1, F_X and F_A, F_B (iron-sulfur centers) are membrane bound, while PQ is plastoquinone diffusing in the membrane lipid, PC a small protein (plastocyanin) diffusing in the aqueous lumen space, and F_d (ferredoxin) and $NADP^+$ diffuse in the stroma. FNR stands for the enzyme ferredoxin-$NADP^+$ reductase. The feet and rabbit ears on PQ and PC symbolize their mobility. Between them is the large cytochrom b_6/f complex with several electron carriers. When $NADP^+$ takes up two electrons and one proton it becomes NADPH, which is used for carbon dioxide reduction. (From Govindjee 2000.)

another protein complex (the cytochrome b/f complex) and two smaller, mobile molecules, plastoquinone and plastocyanin. The "electron pumps" lift electrons from an energy-poor state in water to an energy-rich state in a substance called ferredoxin. What remains of the water from which electrons have been removed is free oxygen (molecular oxygen, O_2) and hydrogen ions (protons). The protons also gain energy by being pumped into the interior of the thylakoids, where they attain a higher concentration than they had before. This energy is then used to produce energy-rich phosphate, ATP. In the stroma, reduced ferredoxin and ATP and protons are used to reduce carbon dioxide to carbohydrate. This is a very short description of the essential steps of photosynthesis. For details the reader is referred to Ke (2001), Blankenship (2002), Golbeck (2006, for PS I), and Wydrzynski and Satoh (2005, for PS II).

12.3. The Domains of Life

The living world is nowadays subdivided into three "domains" or main organismal groups, i.e., Archaea (formerly called archaebacteria), Bacteria (eubacteria, or just bacteria), and Eukarya (eukaryotes, which comprise all organisms known
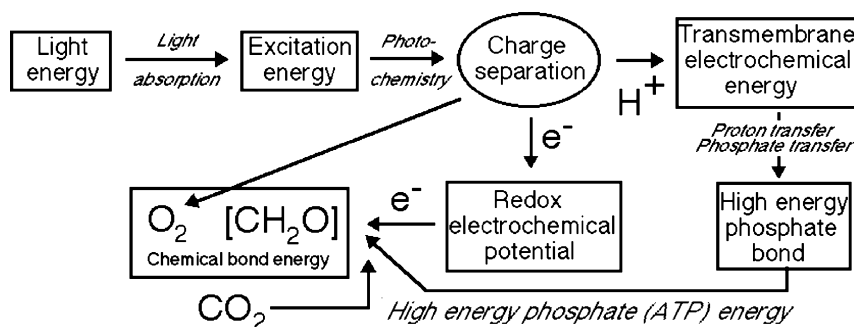
FIGURE 12.4. Energy transformations in photosynthesis. Light energy absorbed by antenna pigments is transferred to reaction centers where charge separation takes place. The positive charges are transferred to water, which splits into hydrogen ions (H^+) and molecular oxygen (O_2). The nonequilibrium distribution of hydrogen ion results in energy trapped in ATP, while the energy gained by electrons make it possible for them to act as reductants for carbon dioxide, aided by the energy from ATP.

200 years ago, and many others, plants, fungi, animals, and people). Photosynthesis has arisen only in the domain Bacteria. That plants, too, can carry out photosynthesis is because the precursors of plant cells have combined with bacteria. For the story of the discovery of Archaea, see Woese (2005) (Fig. 12.4).

12.4. Predecessors of the First Photosynthetic Organisms

As already mentioned, plant photosynthesis can be divided into two processes: (1) oxidation of water and transport of electrons and protons in the thylakoids, with ensuing synthesis of ATP, and (2) the reduction of carbon dioxide, taking place in the stroma. Of these, the reduction of carbon dioxide is a much more ancient process than the oxidation of water. We have already mentioned one type of light-independent carbon dioxide reduction, namely the reduction to methane with hydrogen as reductant. Also other light-independent forms of carbon dioxide reduction are more ancient than that driven by the thylakoids. The reduction taking place in the stroma of plant chloroplasts has evolved from one of these early light-independent processes. Plants use the enzyme rubisco (ribulose-1,5-bisphosphate carboxylase/oxygenase) to bind carbon dioxide, and some nonphotosynthetic bacteria also use this enzyme. One type of bacteria that has recently received much attention lives at deep sea hydrothermal vents, where hydrogen sulfide emerges. It gets its energy by oxidizing hydrogen sulfide with molecular oxygen, O_2. The first chemoautotrophs could not do that, since there was no free oxygen present. But they could get energy by reducing carbon dioxide with hydrogen, and later there emerged many other kinds of chemoautotrophs.

Rubisco has similarities to other enzymes with other functions in bacteria which do not fix carbon dioxide, such as 2,3-diketo-5-methylthiopentyl-1-phosphate enolase in *Bacillus subtilis* (Ashida, Saito, Kojima, et al. 2003; Ashida, Danchin, Yokota, et al. 2005), and may have evolved from a protein involved in sulfur metabolism.

When the first photosynthetic organisms appeared, they inherit many useful biochemical components from predecessors. This does not hold only for those soluble components present in the stroma in plant chloroplasts, but also many of the electron transporters in the thylakoid membranes. Such components are the iron-sulfur proteins (of which there are several kinds in the thylakoids; in addition the soluble ferredoxin belongs to the iron-sulfur proteins). Iron-sulfur proteins are thought to have ancestry back to life's beginning, and their active center is derived from inorganic iron sulfide. Eck and Dayhoff (1966) thought that the protein part of ferredoxin had evolved from a peptide with only four amino acids. Other types of electron transporters in the thylakoids with very ancient orgins are quinones and cytochromes. The most important of the thylakoid pigments, chlorophyll, is derived from the same biosynthetic pathway that leads to heme, the central part of cytochromes. Complex porphyrin-like molecules having a ring composed of four smaller, five-membered rings, similar to those forming parts of heme and chlorophyll, are thought to have arisen before the emergence of life and could have been one of the raw materials for life.

Cytochromes can be traced back to the last common ancestor of all extant organisms. This organism lived before there was any photosynthesis, and PSI and PSII are possibly descendents of cytochrome *b* (Xiong and Bauer 2002). There are similarities in structure between the cytochrome b6/f-containing complex that mediates electron transfer between the photosystems and the photosystems themselves. The cytochrome complex also contains one molecule of chlorophyll *a* per monomer (Bald, Kruip, Boekema, and Rögner 1992; Huang, Everly, Cheng, et al. 1994; Pierre et al. 1997; Stroebel et al. 2003; Kurisu et al. 2003; Dashdori et al. 2005). Cytochromes *b* from various sources, as well as other heme compounds, can be photoreduced (Pierre, Bazin, Debey, and Santus 1982; Asard, Saito, Kojima, et al. 1989; Gu, Li, Sage, and Champion 1993; Rubinstein 1993, Zhang et al. 2005).

12.5. The First Photosynthesis

The first photosynthetic organisms did not have two photosystems in series, as plants do, but only one. They could not oxidize water to molecular oxygen. Thus far the researchers agree, but no further. Extant photosynthesizing bacteria can, with regard to photosystems, be divided into three main groups. One is cyanobacteria (formerly referred to as blue-green algae), which have two photosystems (PSI and PSII) connected in series and are able to evolve oxygen; we shall return to them. Another group consists of green sulfur bacteria plus heliobacteria, which have a photosystem resembling PSI in plants and cyanobacteria. The third group consists of purple bacteria plus green nonsulfur bacteria, which have a photosystem resembling PSII in plants and cyanobacteria, but it has no water-oxidizing part. All photosystems, PSI-like as well as PSII-like, have important similarities so that there is no doubt that they all derive from the same ancestral photosystem.

Where is the origin of this first photosynthesizer? Some years ago Nisbet, Cann, and VanDover (1995) suggested that the ability to photosynthesize would have evolved from an orientation (phototaxis) system in bacteria living deep in the sea near hydrothermal vents, which were able to perceive the heat radiation from the vents. Björn (1995) showed that it would not have been possible to drive photosynthesis by the heat radiation from those vents. Since then White, Chave, Reynolds, et al. (2000, 2002a,b) have shown that the vents radiate not only heat radiation, but also another kind of light which probably originates from oxidation of sulfide (Tapley et al. 1999). Although White, Chave, and Reynolds (2002a) arrived at the conclusion that the light is too weak to sustain autotrophy, Beatty, Overmann, Lince, et al. (2005) later showed that photoautotrophic bacteria are present in the vicinity of the vents. The hypothesis of Nisbet, Cann, and VanDover (1995) is therefore worth pursuing further. One has to remember that chemiluminescence from sulfide oxidation probably has a prerequisite of molecular oxygen, but it is possible that also other kinds of light emission could have resulted in such an environment with steep temperature and chemical gradients.

Hirabayashi, Ishii, Takaichi, et al. (2004) have cultivated a photosynthetic bacterium, *Chlorobium phaeobacteroides*, in very weak light (less than 3 µmol photons/m^2/s[1] of photosynthetically active radiation). Raven, Kübler, and Beardall (2000) arrived by theoretical considerations at the opinion that a photosynthetic organism might be able to live from as little as 4 nmol photons/m^2/s[1] (0.004 µmol photons m^{-2} s^{-1}) as a daily average.

The most ancient type of photosynthesis of which we have undisputable preserved traces is a 3.416 Ga old chert in South Africa (Tice and Lowe 2004, 2006), but the carbon istotope composition in 3.8 Ga old graphite in Greenland has been attributed to photosynthesis (Olson 2006). These organisms seem to have used molecular hydrogen as a reductant. Later other forms developed, which used other reductants, such as divalent iron or hydrogen sulfide. Old morphological fossils attributed to photosynthetic organisms have been described by Awramik (1992) and others.

Green sulfur bacteria and heliobacteria, which have the same type of PSI-like photosystem reaction center, are not closely related in other respects. Nor are all the bacteria having PSII-like photosystems are closely related. *Chloroflexus auranticus* with a photosystem of type II has about the same pigment complement as *Chlorobium tepidum* with a photosystem of type I, and both bacteria are regarded as being rather closely related. These "inconsistencies" are explainable by "horizontal" or "lateral" gene transfer, meaning that a gene can be transferred from one unrelated organism to another (Raymond and Blankenship 2003; Raymond, Siefert, Staples, and Blankenship 2003; Raymond, Zhaxybayeva, Gogarten, and Blankenship 2003). During the enormous time spans of bacterial evolution, there have been sufficient occasions for transfer of all the genes required for construction of a photosystem. But it could also be that the group to which *Chloroflexus* and *Chlorobium* belong is the group in which the differentiation between photosystems of type I and type II has taken place during evolution.

12.6. Appearance of Oxygenic Photosynthesis

With the exception of cyanobacteria with PSII, bacteria lack the water-oxidizing (oxygen-evolving) part, even if they otherwise possess a photosystem of type II. The type II photosystems of these bacteria differ in some other respects from PSII of plants. A plant PSII reaction center has six losely interacting pigment molecules in place of the arrangement with a tightly coupled "special pair" of (bacterio)chlorophyll molecules in the bacteria. The arrangement with a tightly coupled pair of (bacterio) chlorophyll molecules gives a lower-lying first excited state than a single molecule would have. As long as the energy quanta for the electron transport need not be very great, this is an advantage in that it provides an efficient sink for the excitations in the pigment antenna. For the oxidation of water there is a need for larger quanta, and this is probably the reason there is a different pigment arrangement in the reaction center of oxygenic PSII (Rutherford and Faller 2002). It is well known that dimerization causes a shift to longer wavelength for the long-wavelength peak in the absorption spectrum, i.e., a lowering of the energy for the lowest-lying excited state.

Dismukes et al. (2001) have come up with an apparently well-founded theory for how the water-oxidizing system could have evolved via a bicarbonate-oxidizing and oxygen-evolving intermediate stage. The interesting finding of Warburg, Krippahl, and Jetschma (1965) that oxygen evolution is stimulated by carbon dioxide was the first indication of this. Clausen, Junge, Dau, and Haumann (2005) and Clausen, Beckmann, Junge, and Messinger (2005) have shown that *free* carbon dioxide is not an intermediate in the oxygen evolution of plants. Bicarbonate has been shown to function on both the electron acceptor and donor sides of PS II (review by van Rensen, Xu, and Govindjee 1999). Further, in the crystal structure of PS II, Ferreira, Iverson, Maghlaoui, et al. (2004) have modeled one bicarbonate anion near the nonheme iron on the acceptor side, and another on the electron donor side.

There are different opinions about how the evolution of organisms took place with only one photosystem to cyanobacteria, algae, and terrestrial plants with two photosystems in series. One can imagine that, from the first photosynthetic organism there has taken place an evolution along two lines, in both cases still with a single photosystem. One line has led to bacteria having photosystems of type I, the other one to bacteria with photosystems of type II. The two kinds of bacteria then entered into a symbiosis which has become more and more intimate, until the result was an integrated organism, which evolved into the first cyanobacterium. Another possibility is that gene transfer took place from one organism to another without complete fusion of the two lines of evolution. A third possibility is suggested by Allen (2005) and will be further described below.

Much of the views of how the early evolution of photosynthesis took place is based on comparisons between extant organisms. But there is also geological evidence to rely on. The morphological fossils do not give much guidance, except that the occurrence of heterocyst-like structures strengthen the view that

both cyanobacteria and an oxygen-containing atmosphere are of great antiquity (Tomitani, Knoll, Cavanaugh, and Ohno, 2006). But there are also chemical and physical fossils, even if their interpretation is often debated. The substance 2-α-methyl hopane is regarded as a reliable signature of the presence of cyanobacteria (Summons et al. 1999), and it has been found in 2.7 Ga old rocks (Brocks et al. 2003). However, similar compounds have also been traced to anaerobic bacteria. The ratio between the amounts of the carbon isotopes ^{13}C and ^{12}C in organic compounds has also played a part in the discussions. Sometimes a certain ratio has been seen as a sign that the carbon has been assimilated by the enzyme rubisco or been seen as a signature of a certain kind of assimilating organism. Banded iron formations (BIFs) have been interpreted in different ways (Krapež et al. 2003). It is thought that the formation of at least some of them has been mediated by photosynthetic bacteria, which have oxidized divalent to trivalent iron, instead of oxidizing water as plants do (Kappler et al. 2005).

The type of photosynthesis carried out by cyanobacteria requires very compli-cated machinery with cooperation between two photosystems in series and an enzyme which manages to collect four oxidation equivalents for the very difficult oxidation of water. Most researchers think that this required a very long evolution, during a vast expanse of time, from the first primitive bacterial photosynthesis. Contrary to this view, Rosing and Frei (2004) have arrived at the conclusion that such photosynthesis took place 3.7 Ga ago. This opinion rests on the ratio between thorium and uranium in old sediments. Under reducing conditions both elements are insoluble, and therefore the ratio between their concentra-tions should not change during sedimentation. But in fact, the ratio between the concentrations has changed, so some kind of fractionation must have taken place. This can happen in the presence of oxygen, when uranium is oxidized to soluble uranyl complexes. Thorium, on the contrary, remains insoluble under such conditions. More recently there have been several objections to regarding deposits of such age as showing traces of any kind of life (e.g., Brasier, Green, Lindsay, et al. 2005; Moorbath 2005), and other explanations have been offered for the thorium/uranium fractionation.

Small amounts of hydrogen peroxide could have formed abiotically in the Archaean age by action of ultraviolet radiation on pyrite, and there have been speculations that oxygenic photosynthesis evolved as a protective decompo-sition of hydrogen peroxide (Borda, Elsetinow, Schoonen, and Strongin 2001). However, the structure of the oxygen-evolving complex, which has no similarity to other manganese hydrogen peroxide, does not support such a theory.

The structure of the oxygen-evolving complex (Yano, Kern, Sauer, et al. 2006) has similarities to some manganese minerals and probably inherited its structure from these (Sauer and Yachandra 2002). Photochemical oxidation of manganese driven by ultraviolet radiation may have taken place early in the earth's history, and could have been the starting point for the evolution of the oxygen-evolving mechanism in oxygenic photosynthesis (Anbar and Holland 1992; Allen and Martin 2007). Related to this is the finding that UV inhibition of PSII in present-day organisms is partly caused by UV absorption

by manganese (Hakala, Tuominen, Keränen, et al. 2005; Hakala, Rantamäki, Puputti, et al. 2006).

According to a theory presented by Allen (2005) and further elaborated by Allen and Martin (2007) organisms having two photosystems are older than oxygenic photosynthesis. The ancestral photosystem was probably more similar to PSI than to PSII (Baymann, Brugna, Mühlenhoff, and Nitschke 2001; Mulkidjanian, Koonin, Makarova, et al. 2006). After gene duplication a PSII-like photosystem evolved within the same organism, but still without oxygen evolution (Fig. 12.5). The evolution pressure for the change in properties of the new photosystem could have been changing environmental conditions, in particular changing redox conditions. Because of the variability of the environment it would have been adventageous for the organism to keep both photosystems, and a regulatory switch evolved which made it possible for the organism to transcribe the gene most appropriate for the moment. With increasing scarcity of other electron donors, the PSII-like system evolved toward a state where it could connect to a manganese compound that was already able to be photooxidized by ultraviolet radiation, but could from now on be oxidized through PSII by light of longer wavelength. The mechanism for switching between transcription of one or the other photosystem gene then became superfluous and disappeared. The first cyanobacterium had evolved.
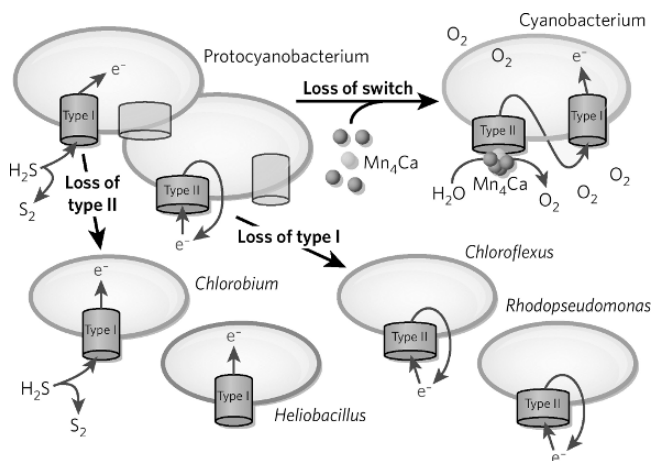
FIGURE 12.5. An early photosynthesizer having two photosystems and a switch to select expression of the gene for one or the other (upper left) could, during evolution, lose one or the other of the genes and turn into one of several types of nonoxygenic photosynthetic bacteria (either as *Chlorobium* or *Heliobacillus* with a type I photosystem or as *Chloroflexus* or *Rhodopseudomonas* with a type II photosystem). Alternatively it could, under appropriate environmental conditions, lose the switch and evolve into an organism constitutively equipped with two photosystems, and then evolve into a cyanobacterium with oxygenic photosynthesis. (From Allen and Martin 2007. Reprinted by permission from Macmillan Publishers Ltd: Nature 445, 610-612, copyright 2007.)

Once the cyanobacteria emerged and started to produce free oxygen, several hundred million years elapsed before oxygen started to accumulate in the atmosphere. The reason for this was that there were so many reducing substances (divalent iron, reduced sulfur, probably also methane) had to be oxidized first, and reproduction of cyanobacteria might also have been hampered by ultraviolet radiation and other environmental conditions. It took an even longer time before the deep strata of the ocean became oxidized, and this led to chemical problems which delayed full oxygenation (see below). But once the oxygen started to accumulate, many life forms were poisoned by the oxygen. Never before or after has any other form of life dominated the planet so completely for such a long time as cyanobacteria did— about a billion years. In some ways the cyanobacteria are still very important, not least in an altered form, as the chloroplasts in plants and algae.

12.7. From Cyanobacteria to Chloroplasts

"Let us imagine a palm tree, growing peacefully near a spring, and a lion hiding in the bush nearby, all of its muscles taut, with blood thirsty eyes, prepared to jump upon an antelope and to strangle it. The symbiotic theory, and it alone, lays bare the deepest mysteries of this scene, unravels and illuminates the fundamental principle that could bring forth two such utterly different entities as a palm tree and a lion. The palm behaves so peacefully, so passively, because it is a symbiosis, because it contains a plethora of little workers, green slaves (chromatophores) that work for it and nourish it. The lion must nourish itself. Let us imagine each cell of the lion filled with chromatophores, and I have no doubt that it would immediately lie down peacefully next to the palm, feeling full, or needing at most some water with mineral salts."

Constantin Sergeevich Mereschkowsky (1905) in Über Natur und Ursprung der Chromatophoren im Pflanzenreiche. Biol. Centralbl. 25, 593–604. Annotated English translation by W. Martin and K.V. Kowallik (1999) Eur. J. Phycol. 34, 287–295

The theory that chloroplasts are derived from cyanobacteria, which were long ago taken up by nonphotosynthetic organisms, is more than 100 years old. Complete proof that it is correct has been obtained from molecular biology. By comparisons of DNA sequences, the cyanobacterial ancestry of chloroplasts has been established, just as it is now certain that mitochondria are descendents of another bacterial clade.

Among chloroplasts there are two developmental lines, the "green line" (in green algae and plants) and the "red line" (in red algae and most other algae). Even if some researchers still believe that these two lines start with two separate endosymbiotic events, the contrary view prevails. This means that all chloroplasts are derived from one original chloroplast, which has appeared when a cyanobacterium entered another cell. It is a little surprising that it is so, since we have so many other examples of very intimate symbiotic relationships between a number of algae and a number of other organisms. A very recent appearance of a new type of chloroplast has also been observed: Marin, Nowack, and Melkonian

(2005) have found an ameba containing a plastid with a different cyanobacterial origin. This does not detract from the fact that the chloroplasts of all major organismal groups derive from a single endosymbiotic event. The chloroplasts of green algae, glaucophytes, land plants, and red algae are directly derived in such a way, while other chloroplasts on the red line are derived by secondary endosymbiosis, in which red algae were taken up by nonphotosynthetic organisms. The chloroplasts of some groups, especially some dinoflagellates, have an even more complicated evolutionary history (e.g., Stoebe and Maier 2002, Bhattcharaya et al. 2003).

Many cyanobacteria have red phycoerythrin and blue phycocyanin (and a small amount of another blue protein, allophycocyanin) as light-collecting pigments. They are assembled into complexes known as phycobilisomes, which are located on the external side of the thylakoid membranes which house the photosystems (PSI and PSII). (The most primitive cyanobacteria do not have any thylakoids, but carry out photosynthesis by their outer cell membrane, but they do have phycobilisomes [Gutiérrez-Cirlos et al. 2006].) Red algae have the same pigment arrangement. One type of cyanobacterium, sometimes referred to as prochlorophytes (after *Prochloron*, the genus first discovered), have, instead of phycocyanin and phycoerythrin, chlorophyll *a* and chlorophyll *b*, as green algae and plants do. It was once thought that the green and the red evolutionary lines each stemmed from two different types of cyanobacteria. Later a cyanobacterium (*Prochlorococcus marinus*) was discovered which is equipped with both sets of light-collecting pigments (Hess et al. 1996). Most researchers therefore now believe that the first chloroplast was derived from a cyanobacterium having both phycobilisomes and chlorophyll *b*. In each of the developmental lines, one of the pigment sets would have been lost later. The common origin of the chloroplasts on both lines is strengthened by the fact that the protein import machinery is of the same kind. These import systems must have evolved in connection with the genesis of chloroplasts, or later, because they would not be required as long as the cyanobacteria were independent with all required proteins made by themselves. The nuclear genes on both developmental lines are in general so similar that there cannot have occured endosymbiosis in quite different organisms.

Fossils of red algae have been found which date back 1.2 Ga (Butterfield 2000; Fig. 12.6). These are the oldest organisms for which one has been able to infer sexuality. Other algae on the red line, for instance cryptophytes, diatoms, brown algae, and yellow-green algae, have evolved by uptake of red algae into a nonphotosynthetic organism, and also this event is thought to have taken place only once (Petersen, Teich, Brinkmann, and Cerff, 2006). One reason to believe that these different algal chloroplasts have resulted from a single secondary endosymbiotic event is the surprising fact that they all have the same type of phosphoribulokinase (an enzyme of the Calvin–Benson–Bassham cycle) as organisms on the green line of chloroplast evolution, a type very different from the type present in red algae. The most probable interpretation of this is that soon after the secondary endosymbiotic event a lateral gene transfer from the green line took place, and the phosphoribulokinase from the red alga was lost.
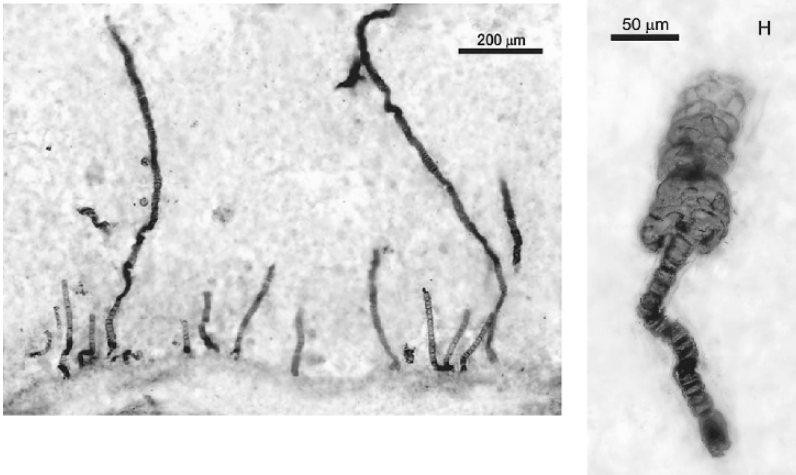
FIGURE 12.6. 1200-Ma-old fossils of the red alga *Bangiomorpha pubescens*. (From Butterfield 2000.)

Another indication that the secondary plastids on the red line are monophyletic is that they all share a type of glyceraldehyde-3-phosphate dehydrogenase (another enzyme in the Calvin–Benson–Bassham cycle), which does not occur in any other organisms (not in cyanobacteria, not in red algae, and not in organisms on the green evolutionary line) (reviewed by Petersen, Teich, Brinkmann, and Cerff 2006). In contrast, secondary plastids have evolved several times on the green line (e.g., Rogers, Gilson, Su et al. 2007).

The copper protein plastocyanin is lacking in chloroplasts on the whole red line of evolution (and also in some cyanobacteria). The electrons from the cytochrome b6/f complex are instead carried to PSI by a small soluble cytochrome, cytochrome c_6 (Raven et al. 1999). Many green algae and cyanobacteria can switch to using cytochrome c_6 when deficient in copper. An analog cytochrome (cytochrome c_6) is used by photosynthetic purple bacteria (Hu et al. 2002). Plastocyanin has probably evolved long after the emergence of oxygenic photosynthesis, as copper was tied up in insoluble sulfide during a period of the earth's history (see below). On the other hand, iron is less accessible now than it was before the oxygenation of the atmosphere.

12.8. Evolution of Photosynthetic Pigments and Chloroplast Structure

Forms of chlorophyll typical for extant photosynthetic bacteria, which do not evolve oxygen, are collectively referred to as bacteriochlorophyll. Chlorophyll *a* is a biochemical precursor to these chlorophyll forms. For this reason,

Granick (1957) postulated that bacteria with bacteriochlorophyll as photosynthetic pigment have evolved from those who have chlorophyll *a*. But those present-day bacteria which have bacteriochlorophyll (and only one photosystem) seem to be more primitive and carrying out a simpler kind of photosynthesis than cyanobacteria, which are the only extant bacteria with chlorophyll *a*. The solution to this apparent paradox could be that there had existed now extinct nonoxygenic organisms having only one photosystem, with chlorophyll *a*.

The reasons that chlorophyll is a suitable pigment for photosynthesis are discussed in Chapter 9, Section 9.2, by Kiang et al. (2007) from a spectral perspective, and by Mauzerall (1976) from a chemical perspective.

When two different photosystems started to evolve in the same organism (a primitive predecessor of present-day cyanobacteria), the spectra of the pigment molecules in their reaction center of PSI began to differ from the spectra of the pigment molecules in the PSII reaction center. This has to do with the different functions of the two photosystems. In PSII the difficult oxidation of water requires big energy quanta, and this sets an upper wavelength limit for the chlorophyll molecules involved. The reduction of ferredoxin by PSI does not require so big energy quanta, and in order to best make use also of longer wavelength light, the chlorophyll in PSI acquired a longer wavelength spectrum than that in PSII. The molecules are in both cases molecules of chlorophyll *a* (except in some cyanobacteria, such as *Acaryochloris*, where it is chlorophyll *d*), but the spectra differ due to different environments around the molecules.

When the cyanobacteria had turned into chloroplasts, the further evolution along the "green" path (green algae and plants) began to differ from that along the "red" path (red algae, diatoms, brown algae etc.). The cyanobacteria were equipped with very sophisticated light-collecting antennae in the form of phycobilisomes. These can be regarded as a kind of energy transformer, which collect all kinds of light and adapt the size of the energy quanta so they fit the energy levels of chlorophyll. The red algae inherited these structures rather unchanged. Cryptophytes have the same kinds of red and blue pigments arranged in a slightly different way. But why have these equisite light transformers disappeared from the rest of the "red" line, and never appeared on the line leading to land plants?

We probably have a good explanation for this now, but it is a bit involved and not easy to understand. We shall recount here in essence the explanation given by Anderson (1999). This has to do with the different light environments to which the organisms have adapted. In order not to make it too complicated, we shall limit ourselves to a comparison between red algae and land plants. Red algae live in water, often deeper than other algae. The light reaching them has been filtered through water, which absorbs long-wavelength light more strongly than other visible (and photosynthetically active) light. Therefore an energy deficiency in PSI relative to PSII could easily develop, if extra energy could not be added in addition to the light energy absorbed by PSI. This extra energy comes by "spillover" from PSII. Spillover of energy is possible, because the energy quanta collected in PSII are larger than is needed to "lift" electrons in PSI, and because the two photosystems are intermingled among one another in

red algae (as in cyanobacteria). Contrary to this, PSI cannot lose energy to PSII, because it cannot take up the small energy quanta from PSI. Red algae collect energy mainly via their phycobilisomes, and this energy can be used both by PS II and by PS I, so they can go "in step."

For land plants the situation is different. The first land plants were small beech organisms living without competition from larger plants, exposed to full sunlight; their forerunners, the green algae, lived in very exposed habitats. Their problem was not lack of light energy, and thus they did not have much use for phycobilisomes. With time plants grew larger and more numerous. The average chloroplast became more and more shaded, filtered by other chloroplasts. From the perspective of an individual chloroplast it did not matter much whether the chloroplasts shading it were located in other plants, in other leaves on the same plant, or even in the same leaf. The light hitting the chloroplast became, during the evolution of plants and ecosystems, more and more depleted in short-wave light, while the long-wave light, on the long-wave edge of the chlorophyll absorption spectrum, was not attenuated to the same extent. The spectral situation was opposite that for chloroplasts in red algae. Now the imbalance between the photosystems could not be adjusted by spillover, since the energy quanta of the most exposed photosystem (PSI) were too small. Therefore PSI and PSII had to be separated to prevent spillover, otherwise PSII would be even more depleted. Evolution has succeeded in this by development of grana in the chloroplasts of land plants (see Figs 12.1 and 12.2). Grana are regions in the chloroplasts where the thylakoid membranes are closely stacked on top of one another and are enriched in PSII. The stacking of membranes and absence of PSI give room for larger pigment antennae, not in the form of phycobilisomes, but in the form of protein bound chlorophyll *a* and chlorophyll *b*. PSI is located in the more sparsely distributed membranes between the grana. There it is in contact with stroma between the membranes, and this is advantageous because PSI delivers reduction equivalents via ferredoxin to NADP, which are then used for the reduction of carbon dioxide in the stroma.

The structure of the chloroplasts, and in particular the proximity of membranes to one other, is not static, but constantly adjusted to available light. During evolution more and more sophisticated regulation systems have appeared, as have various mechanisms for protection against too strong light. One of the most important of these mechanisms is the so-called xanthophyll cycle, giving protection against strong light while allowing efficient use of weak light. Remarkably, it exists in essentially the same form, while exploiting different kinds of xanthophylls, both in the "red" and the "green" line of evolution. It is left for future researchers to find out whether this is an example of convergent evolution or due to common descent. The reader is referred to Demmig-Adams, Adams III, and Mattoo (2006) for details about the topic of photoprotection.

Yoshi (2006) has traced the evolution of carotenoids on the "green line." The most primitive living algae on this line have carotenoids which absorb maximally in the violet part of the spectrum, while more modern types have carotenoids with absorption peaks at longer wavelengths. Yoshi speculates that this may

reflect the ultraviolet radiation conditions under which the algae have evolved. Those algae living long ago, before a protecting ozone layer had developed (and preserved as "living fossils" today), would have had to live at a depth where they were protected from ultraviolet radiation, and where only short-wave photosynthetically active radiation would penetrate. The modern types would have evolved near the surface in a light regime containing light between the chlorophyll absorption peaks, where long-wave absorbing carotenoids are efficient antenna pigments. A difficulty with Yoshi's interpretation is that an ozone layer most likely evolved long before the appearance of eukaryotic algae.

12.9. Many Systems for the Assimilation of Carbon Dioxide Have Been Tried in the Course of Evolution

Assimilation of carbon dioxide is not necessarily coupled to photosynthesis. The ability to take up carbon dioxide and assimilate the carbon to organic substance is older than the ability to photosynthesize. It takes place in both archaea and bacteria. The ability has either evolved before the two domains separated in evolution, or one of the organismal groups has acquired it from the other one by horizontal (lateral) gene transfer. Since many enzymes are involved the former possibility is the most likely one.

Apart from the first two, the enzymes in Table 12.1 and their assimilation pathways (Fig. 12.7) are present only in bacteria and archaea. But the typical carbon-binding enzyme of plants, rubisco, occurs also in some archaea, even though the whole Calvin–Benson–Bassham cycle has not been demonstrated in them.

The first alternative to the Calvin–Benson–Bassham cycle detected was a cycle discovered by Evans, Buchanan, and Arnon (1966) (see also Buchanan and Arnon 1990). The acetyl-CoA pathway is present in some acetate-forming bacteria, some sulfate-reducing bacteria, and some hydrogen-oxidizing archaea.

TABLE 12.1. Pathways and Enzymes for CO_2 Assimilation

CO_2-binding enzyme	Pathway for CO_2 assimilation
Ribulose-1,5-bisphosphate-carboxylase-oxygenase (RuBisCO, rubisco)	Calvin-Benson-Bassham cycle
Phosphoenol pyruvate carboxylase (PEPC)	C4- and CAM cycles
Formate dehydrogenase	Acetyl-CoA pathway
Carbon monoxide dehydrogenase	Acetyl-CoA pathway
Pyruvate:ferredoxin oxidoreductase	Arnon-Buchanan cycle (reductive TCA cycle)
2-Oxoglutarate: ferredoxin oxidoreductase	Arnon-Buchanan cycle
Isocitrate dehydrogenase	Arnon-Buchanan cycle
Pyruvate carboxylase	Arnon-Buchanan cycle
Acetyl-CoA carboxylase	3-Hydroxypropionate cycle
Propionyl-CoA carboxylase	3-Hydroxypropionate cycle

CoA, Coenzyme A.
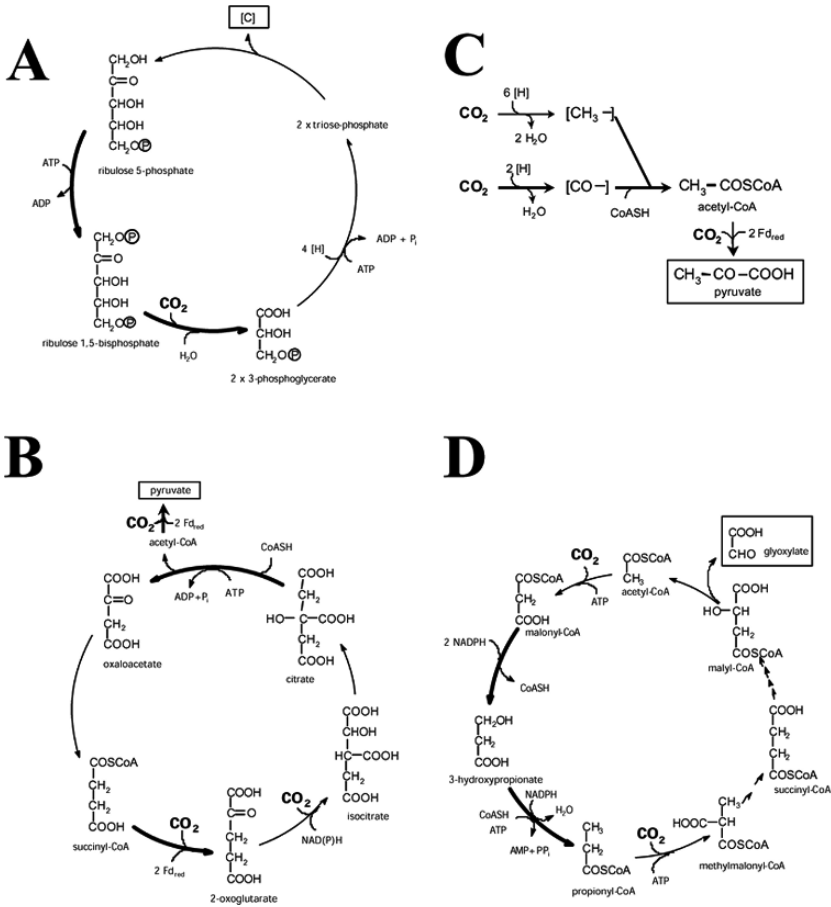
FIGURE 12.7. Metabolic cycles for assimilation of carbon dioxide present in various prokaryotes: (A) the Calvin–Benson–Bassham cycle; (B) the reductive TCA cycle (Arnon-Buchanan cycle); (C) the reductive acetyl-CoA pathway; and (D) the 3-hydroxpropionate cycle. Of these only the Calvin–Benson–Bassham cycle is present in photosynthetic eukaryotes (cyanobacteria, algae, and plants). C, assimilated carbon; H, reduction equivalents; Fd_{red}, reduced ferredoxin; P or P in a circle, phosphate groups; CH^{3-}, enzyme-bound methyl group; CO^-, enzyme-bound carbon monoxide. (From Hügler et al. 2003.)

The 3-hydroxypropionate pathway is present in green nonsulfur bacteria and some hydrogen-oxidizing bacteria and some sulfur-reducing archaea. Thus every type of carbon dioxide assimilation occurs in taxonomically quite different types of microorganisms. Selesi et al. (2005) has detected a large set of rubisco types in soil microorganisms, of which only a minor part is derived from photosynthetic organisms.

It is clear that rubisco is a very ancient enzyme, which was "designed" under conditions quite different from the present ones. The most important

differences are that oxygen was absent from the primordial environment, and the concentration of carbon dioxide was much higher than in the contemporary environment. Therefore the properties of rubisco are not optimal for the present environment. It works slowly. It binds carbon dioxide only weakly (has a low affinity and a high Michaelis constant for carbon dioxide). This was not a problem as long as the concentration of carbon dioxide was very high. It can react with oxygen instead of carbon dioxide, and when this happens a product, phosphoglycolic acid, is formed, which the organism has no real use for, and which can even act as a poison if not taken care of in a proper way. This substance was not formed when oxygen was absent from the environment. When it is formed in algae living in water it can be excreted to the environment, but for land plants it is an expensive affair to take care of it, and for this a special metabolic cycle had to be invented: the photorespiratory cycle.

To compensate for the bad properties of rubisco, different photosynthesizers have evolved different strategies. A common one is to produce large amounts of the enzyme to compensate for its slowness, and this has made it the most ubiquitous protein molecule on earth. Various systems for concentrating carbon dioxide at the enzyme surface have also evolved, so carbon dioxide can compete efficiently with oxygen for the common binding site. The methods used by cyanobacteria and algae have been described by Badger and Price (2003), Giordano, Beardall, and Raven (2006), and Keeley and Rundel (2003). Here we shall limit ourselves to the so-called C4-metabolism and to CAM.

12.10. C4 Metabolism

About half of this planet's photosynthetic production takes place on land, and the other half in water. According to Sage (2004) the mere 3% of the terrestrial plants having C4 metabolism carry out about half of the production on land. C4 photosynthesis has evolved at least 45 times (Sage 2004). From this we can understand that there has been a very strong evolution pressure towards this kind of metabolism. An important component in this evolution pressure has been the decrease in carbon dioxide pressure that took place between 30 and 40 Ma ago. Another component has been the drying of the environment that was an even more recent event (Osborne and Beerling 2006). C4 metabolism (Fig. 12.8) became a significant component of the carbon cycle as recently as 10 Ma ago.

In C4 metabolism carbon dioxide is not initially bound to rubisco, as is the case in C3 plants. Instead bicarbonate ions (formed from carbon dioxide and water with the aid of the enzyme carbonic anhydrase) are bound by the enzyme phosphoenolpyruvate carboxylase (PEPC; see Table 12.1) and united with phosphoenolpyruvate (PEP) to form malate. Malate has four carbon atoms, hence the designation C4 metabolism. In C3 metabolism the first formed assimilate product is 3-phosphoglyceric acid, which has three carbon atoms. C4 metabolism is more efficient at a low concentration of carbon dioxide, because PEPC binds bicarbonate very tightly, and because oxygen cannot compete with this. It is
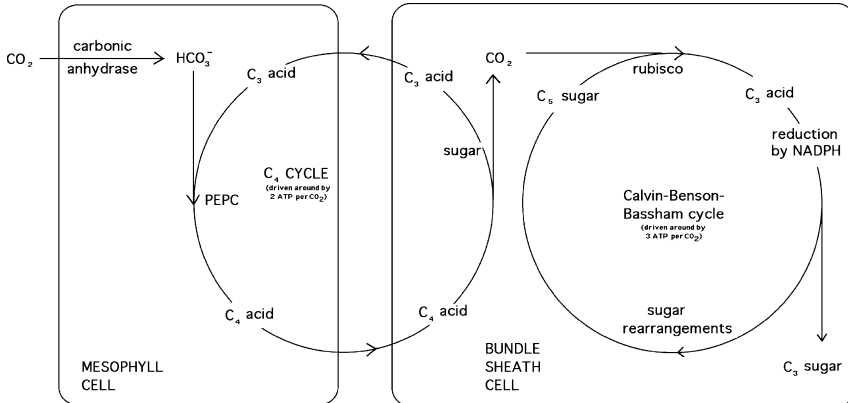
FIGURE 12.8. Carbon dioxide assimilation in C4 plants. The first cycle concentrates carbon dioxide at the rubisco, and the assimilation itself proceeds as in C3 plants.

also more efficient under dry conditions, since plants then can conserve water by keeping their stomata only slightly open. This causes a lowering of the inner carbon dioxide concentration in the plants, but this does not interfere with its uptake in C4 plants. It is also more efficient than C3 metabolism at high temperatures. In C3 plants photorespiration, caused by oxygen competition for rubisco binding, makes carbon dioxide uptake inefficient at high temperatures. Under other conditions, C4 metabolism is less efficient than C3 metabolism, because it uses up more ATP (5 molecules per molecule of CO_2 assimilated, compared to 3 for C3 plants).

One fascinating fact about C4 metabolism is that it has evolved within a relatively short time and independently within many groups of plants. C4 metabolism occurs primarily among seed plants, but has been found also elsewhere, even among diatoms (Reinfelder, Kraepiel, and Morel 2000; Reinfelder, Milligan, and Morel 2004).

Since oxygen concentration during the Carboniferous (370-300 Ma ago) was even higher, and the carbon dioxide concentration even lower than today (Fig. 12.9), one would have expected the C4 metabolism to have evolved by then. But the plant fossils from that time for which the isotopic composition of the carbon has been investigated all carry a C3-like signature, $\partial^{13}C \approx -20‰$ (Beerling, Lake, Berner, et al. 2002; Bocherens, Friis, Mariotti, and Pedersen 2002).

One enigmatic circumstance is that CAM plants were present earlier; why do we then have only C3-type discrimination? Perhaps CAM plants did not contribute much to biomass production? The corresponding value for C4 plants is about –13‰. There is some suspicion that some C4 plants could have evolved then, but not become very common (Osborne et al. 2006). A possible reason that more C4 plants did not evolve during this period is that the temperature was low.
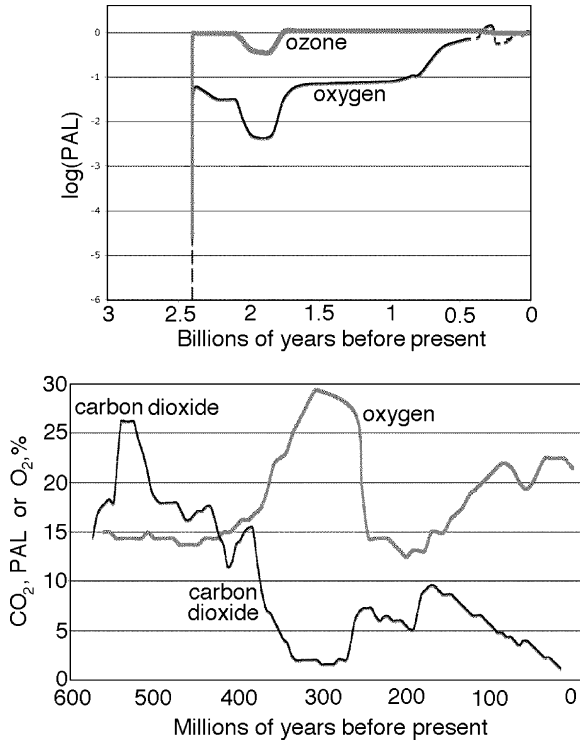
FIGURE 12.9. The evolution of the earth's atmosphere. (Top panel) Ozone and oxygen, on a logarithmic scale, as fraction of present atmospheric level, during the past 3 billion years. (Bottom panel) Oxygen (%) and carbon dioxide (in relation to present atmospheric level) on a linear scale during the last 570 million years. (Based on Beerling, Lake, Berner, et al. 2002, Berner 2006, Canfield 2005, Falkowski, Katz, Milligan et al. 2005, Huey and Ward 2005, Segura, Krelove, Kasting et al. 2003, and other sources.)

C4 plants have evolved at least 45 times in 19 families of higher plants. It is now present in about 7500 species of seed plants (3% of the species of terrestrial plants), of which 4500 are grasses, 1500 sedges, and 1200 dicots (Sage 2005). C4 plants occur primarily in warm and dry countries and among epiphytes, and a number of evolution centers for C4 metabolism can be distinguished.

We refer to Andrew Benson (pp. 793–813) and James A. Bassham (pp. 815–832) for the stories behind the discovery of the Calvin–Benson–Bassham pathway and to M. D. Hatch (pp. 875–880) for C4 metabolism (Govindjee et al. 2005).

12.11. Crassulacean Acid Metabolism

Another way of using PEPC to complement the assimilation by rubisco is shown by plants possessing crassulacean acid metabolism (CAM). As the name implies, this kind of metabolism was first found in the family Crassulaceae. CAM plants

have the ability to take up carbon dioxide during the night when the stomata are open, and bind it to PEP with the help of PEPC. The photosynthesis proper, using light to process the assimilate in the Calvin–Benson–Bassham cycle, is carried out during the day, when the stomata are closed. By keeping stomata open only during the night, the plants conserve water.

CAM is more ancient than is C4 metabolism, and it has been driven by water stress (Keeley and Rundel 2003). It is known only to exist in vascular plants, and it is present in species of clubmosses, ferns, the strange gymnosperm *Welwitschia mirabilis*, the cycad *Dioon edule*, monocots, and dicots. Among the latter the following families deserve to be mentioned: Aizoaceae, Cactaceae, Portulaceae, Crassulaceae, Euphorbiaceae, Asclepiadaceae, and Asteraceae, and among monocots Bromeliaceae and Orchidaceae. Like C4 metabolism, CAM has evolved several times within various plant groups when need has arisen due to water deficiency, mainly among desert plants and plants living on stones or as epiphytes (on other plants, see Keeley and Rundel 2003). However, there are also aquatic CAM plants, and the reason for this is not clear. Among the aquatic plants the large and primitive genus *Isoëtes* deserves special mention. All of its members seem to be CAM plants (although only about one third of the approximate 125 species have been investigated). Since this genus existed already during the early Triassic, more than 200 million years ago, it must be assumed that CAM existed then (Keeley and Rundel 2003). Dekker and de Wit (2006) give further evidence for the early evolution of CAM. See Black and Barry Osmond (pp. 881–893) in Govindjee, Beatty, Gest, and Allen (2005) for descriptions of the discovery of CAM.

12.12. Evolution of ATP-Synthesizing Enzymes

The use of proton gradients for synthesis of ATP occurs in all three domains of life—Archaea, Bacteria, and Eukarya—and the last common ancestor of all organisms must have made use of this. The ancestry of the ATP-synthesizing enzyme of chloroplasts, F-ATPase, has been described by Zhaxybayeva, Lapierre, and Gogarten (2005). This enzyme consists of several subunits, and corresponding subunits show similarities across the domain borders.

12.13. The Journey onto Land

Some kind of photosynthetic organisms are thought to have been present on land as early as 1.2 Ga ago, based on carbon isotope ratios, i.e., ^{13}C depletion (literature cited by Horodyski and Knauth 1994). These organisms were probably cyanobacteria forming crusts as can still be found in deserts. The oldest lichen-like fossils containing what has been interpreted as cyanobacteria are about 600 Ma old (Yuan et al. 2005). Stronger evidence, both morphological (Taylor et al. 2004) and chemical (Jahren 2003) for lichens, is found from the early

Devonian, approximately 400 Ma ago. However, based on the "molecular clock," Heckman, Geiser, Eidell, et al. (2001) estimate that terrestrial fungi existed prior to 900 Ma ago, and these first terrestrial fungi might well have been living in lichen-like associations. While land plants now account for about half of the planet's photosynthesis, the contribution of these early pioneers was likely almost negligible compared to that of the ocean.

The great change came with the evolution of the embryophytes. Their closest relatives are the Charales (stoneworts), a kind of green algae (Karol, McCourt, Cimino, and Delwiche 2001). Spores that are suspected to stem from liverwort-like plants have been found that are from the mid-Ordovician, 475 Ma ago (Wellman et al. 2003), but bryophyte fossils that can be identified with more certainty are younger, from late Silurian, 425 Ma ago. "Molecular clock" evidence points to a much earlier separation of the terrestrial-plant line from the algal line of evolution (Heckman, Geiser, Eidell, et al. 2001). In the early Devonian (approximately 410 Ma ago) plants had evolved that had leaves and roots (*Eophyllophyton bellum* [Hao, Beck, and Wang 2003]). The leaves seem to have been adapted to a dry climate and high carbon dioxide concentration. In the late Devonian (370 million years ago), as the atmospheric concentration of carbon dioxide fell (Fig. 12.9), larger leaves evolved, which were more efficient in collecting both carbon dioxide and light (Beerling, Lake, Berner, et al. 2001).

In the terrestrial environment, the weight of the plant body cannot be supported by buoyancy as in the water. To be able to stretch toward the light among competitors, plants had to improve their rigidity. An important means for this was to strengthen the cell walls with lignin. Such strengthening was also required for the water conduits to withstand the pressure difference. Lignin synthesis requires molecular oxygen, and could thus not commence until the oxygen concentration had risen to a sufficient level. Lignin synthesis builds on the phenylpropanoid pathway, which can be traced back to the characeans: Flavonoids have been found in *Nitella* (Markham and Porter 1969). The "molecular clock" indicates that the line leading to terrestrial plants diverged from the charophytes about 1 Ga ago (Heckman et al. 2001), so this pathway can be assumed to have at least this age.

Throughout their evolution land plants maintained a close association with fungi. A majority of extant plants have mycorrhiza, and many have endophytic fungi also in the shoots and, of course, fungi on the leaf surfaces. The combination of rooted plants and mycorhizal fungi increased the weathering of the continental rocks enormously. This, in turn, meant a postive feedback on photosynthesis by providing more nutrients, also for marine organisms.

Aquatic organisms need not be protected against desiccating evaporation, but when plants colonized land it was necessary for them to conserve water, and they developed cuticle and cutinized external cell walls, and sometimes wax coatings. All this is an obstacle to gas exchange, and so the sophisticated gas valves evolved which go under the name stomata. Stomata are adjustable openings which are regulated in a very complicated way for the optimal balance between loss of water and access to carbon dioxide. Water and carbon dioxide

conditions are sensed directly in the leaf for short-term regulation, but water availability is sensed also in the roots and hormonal signals (in the form of abscisic acid) sent to the stomata for long-term regulation. In addition, several light-sensing systems affect the stomatal aperture. But in addition to regulation of the individual stomata, there is also a developmental regulation to achieve an optimal number and size of stomata. The higher the atmospheric concentration of carbon dioxide, the more sparsely do stomata develop on the leaf surface. This provides a method for estimating past carbon dioxide concentrations by studying the stomatal density on fossilized leaves (McElwain 1998; McElwain et al. 1995, 2002; Haworth et al. 2005).

After having adapted to the terrestrial environment some plants returned to the water and had to cope with new problems (Rascio 2002). It was not simply a reversal of the adaptation to dry land (some researchers think that our modern charophytes have also made a transient visit to terra firma). On land, plants had become larger and needed to develop aerenchyma (air-conducting tissue) to provide all parts with sufficient oxygen. If roots or rhizomes were to be maintained in anoxic muddy bottoms, their oxygen requirement was of special importance, and in some cases diffusive oxygen transport did not suffice. Also the provision with carbon dioxide could be a problem, and this explains the evolution of various mechanisms for its concentration, including a kind of C4 metabolism.

12.14. Impact of Photosynthesis on the Biospheric Environment

When we think about how photosynthesis has affected our environment, we may first remember that it has produced the oxygen we breathe and (directly or indirectly) the food we eat. But the impact of photosynthesis is much wider. The oxygen produced by photosynthesis has also given rise to the ozone layer, which protects the biosphere from the UV-B radiation from the sun (Chapter 19). Fossil fuel, which we have now become too dependent on, has been produced by photosynthesis in times past. The sequestration of carbon from the atmosphere has given us a human-friendly climate, which unfortunately we are now destroying. But perhaps the process of photosynthesis, as an environmental-friendly way of energy transformation, can help us to draw up a blueprint for a solution to the conflict between our hunger for energy and the necessity to maintain an environment that can sustain humanity.

But we must not fall into the trap of believing that photosynthesis has always resulted in a good environment for the inhabitants of our planet. Free oxygen is still a hazard for our own cells, and even for the chloroplasts producing oxygen.

Photosynthesis has not always had a friendly, Gaia-like influence on inhabitants of the earth. When oxygen first started to accumulate, it almost certainly killed off a large part of the terrestrial population by direct poisoning. It was even a hurdle to the producers themselves. Many of the cyanobacteria (as many

other bacteria as well as archaea) carry out nitrogen fixation by means of nitrogenase. Nitrogenase is extremely sensitive to oxygen and easily inhibited by it, and organisms had to invent various methods for protecting the nitrogen fixing enzyme from oxygen. Some of the filamentous forms developed special cells (heterocysts) for a special kind of photosynthesis, which fixes nitrogen using PSI only, and does not fix carbon dioxide or evolve oxygen. From morphological fossils it has been deduced that this arrangement is 1.5 Ga old. No convincing fossil of heterocysts themselves has been found, so this opinion (Golubic and Seong-Joo 1999) rests on the presence of akinetes, a kind of resting cell. In modern cyanobacteria there is a strict correlation between occurence of heterocysts and of akinetes.

Before cyanobacteria evolved, the oxygen content of the atmosphere was less than 10^{-5} the present value. The initial effects of photosynthetic oxygen production on climate were disastrous. Before the oxygenation of the atmosphere the earth was kept comfortably warm (too warm for the human taste) not only by a high atmospheric content of carbon dioxide, but also by another greenhouse gas, methane. When oxygen arrived, methane was first oxidized to carbon dioxide by an emerging new group of microorganisms. Then the concentration of carbon dioxide was drastically lowered by cyanobacterial assimilation. This led to a sharp temperature decrease and a glaciation, which lasted for about 70 million years, between 2.32 and 2.22 Ga ago. Since traces from this time of glaciation (the Makganyene glaciation) are found near the ancient equator, some scientists believe that the whole globe became covered with ice and snow during at least part of this time. There was what has been called a "snowball earth" (Kirschvink et al. 2000). The ice cover prevented silicate weathering, a process that consumes carbon dioxide, and continuing volcanism increased the carbon dioxide content again and eventually put an end to the long ice age. In the meantime the hydrothermal vents at the bottom of the sea had spewed out nutrients at a rate which could not under the icy conditions be matched by consumption. Therefore, many cyanobacterial nutrients were abundant at the end of the glaciation, but probably not all.

Contributing to the severity of this glaciation may have been that the sun emitted less energy than it does today (e.g., Gough 1981; Fig. 12.10), but not all scientists today believe in this "faint young sun" theory. Neither is the "snowball" scenario unquestionable. An alternative explanation for glaciation in the equatorial region is that the "tilt" (the inclination) of the earth's axis was greater in the past (Williams, Kasting, and Frakes 1998; but see Levrard and Laskar 2003).

One way of constraining the timing of the oxygenation of the atmosphere comes from studies of the isotopic sulfur composition of pyrite. Most chemical and physical processes lead to a fractionation of isotopes of elements, which depends on atomic weight. Photochemical processes can lead to deviations from this, i.e., to mass-independent fractionation. As long as the atmosphere remains reducing, hydrogen sulfide emitted from volcanoes remains in the atmosphere long enough for photochemical processes to imprint their special signature on
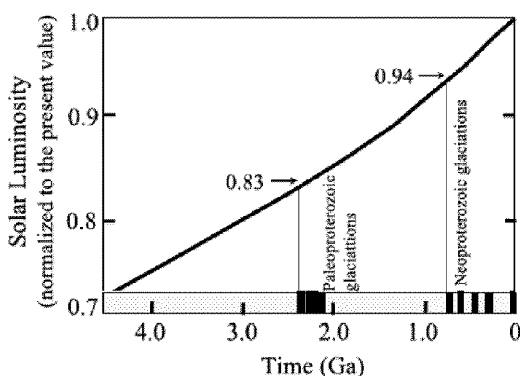
FIGURE 12.10. The relative power radiated by the sun during earth history, and the timing of glaciations. (From Tajika 2003, based on Gough 1981.) Not all scientists (see Sackmann and Boothroyd 2003) believe in this "faint young sun" scenario, the main argument being the documented presence of liquid water on Mars ≈ 3.8 Ga (gigayears) ago.

the pyrite that is eventually formed. In pyrites which, by use of osmium isotope ratios could be accurately dated to 2316 ± 7 Ma, the sulfur isotope ratio indicates an oxidizing atmosphere; thus this is taken as a minimum age for the oxic atmosphere (Hannah, Bekker, Stein, et al. 2005). The oxygen concentration at that time was, of course, much lower than today.

The protein complexes involved in the electron transport chain in the thylakoids contain several atoms of several metals. In addition to the magnesium atoms of chlorophyll, there are in PSI 12 Fe, in the cytochrome $b_{6/}$ f complex 6 Fe, and in PSII 2 Fe, 4 Mn, and one Ca. (The electron transfer chain in addition contains soluble metal proteins: iron containing ferredoxin and either copper containing plastocyanin or iron containing cytochrome c_6.) These metals can sometimes be difficult to obtain, depending on, for instance, redox potential and presence of hydrogen sulfide. PSI contains more iron than the other complexes, and Strzepek and Harrison (2004) have noted that diatoms adapted to coastal regions, where iron is more available, have a higher PSII/PSI ratio (around 9) compared to diatoms adapted to oceanic regions (around 3), where available iron is often a limiting factor for growth. Presumably the PSI of oceanic diatoms have larger light-collecting pigment antennae to compensate for the lower number of reaction centers. Furthermore, only the coastal diatoms have cytochrome c_6, another iron-containing protein. For historical accounts on the structure and function of PSI, see Petra Fromme and Paul Mathis (pp. 311–326) and Horst Witt (pp. 237–259) in Govindjee, Beatty, Gest, and Allen (2005).

During a period after the emergence of cyanobacteria and oxygen-evolving photosynthesis, the concentration of hydrogen sulfide rose in the depth of the ocean, and this made iron hard to get at (Canfield 1998). One can imagine that the cyanobacteria present at that time adapted their photosynthetic machinery to economize with iron. The closest present-day analog to this ancient ocean is the

Black Sea. According to Anbar and Knoll (2002) sulfidic conditions in the deep sea prevailed most of the time between 2500 and 543 Ma ago, although the ocean surface where photosynthesis could take place was oxygenated. Still, the sulfidic depth caused a deficiency of several important metals, such as iron and, even more so, molybdenum. This caused a pressure for evolution of molybdenum-free nitrogenases (using vanadium and iron, Berman-Frank et al. 2003). According to Canfield, Poulton, and Narbonne (2007) the increase of deep ocean oxygen over a critical point spurred the rapid evolution of animal life.

12.15. Conclusion

Photosynthesis is a very ancient process on our planet. It has had profound impact on the biosphere, the chemical composition of the earth's surface and the earth's atmosphere, and on climate, including the radiation climate. It is difficult to imagine what this planet would have been like had photosynthesis (and especially the oxygenic variant) not evolved. In any case we would not have been here to find out.

References

Allen, J.F. (2005) A redox switch hypothesis for the origin of two light reactions in photosynthesis. FEBS Lett. 579, 963–968.

Allen, J.F. and Martin W. (2007) Out of thin air. Nature 445, 61–612.

Anbar, A.D. and Holland, H.D. (1992) The photochemistry of manganese and the origin of banded iron formations. Geochim. Cosmochim. Acta 56, 2595–2603.

Anbar, A.D. and Knoll, A.H. (2002) Proterozoic ocean chemistry and evolution: a bioinorganic bridge. Science 297, 1137–1142.

Anderson, J.M. (1999) Insights into the consequences of grana stacking of thylakoid membranes in vascular plants: a personal perspective. Aust. J. Plant Physiol. 26, 625–639.

Asard, H., Venken, M., Caubergs, R., Reijnders, W., Oltmann, F.L. and De Greef, J.A. (1989) b-Type cytochromes in higher plant plasma membranes. Plant Physiol. 90, 1077–1083.

Ashida, H., Saito, Y., Kojima, C., Kobayashi, K., Ogasawara, N., and Yokota, A. (2003) A functional link between RuBisCO-like protein of *Bacillus* and photosynthetic RuBisCO. Science 302, 287–290.

Ashida, H., Danchin, A., and Yokota, A. (2005) Was photosynthetic RuBisCO recruited by acquisitive evolution from RuBisCO-like proteins involved in sulfur metabolism? Res. Microbiol. 156, 611–618.

Awramik, S. M. (1992) The oldest records of photosynthesis. Photosynthesis Res. 33, 75–89.

Badger, M.R. and Price, G.D. (2003) CO_2-concentrating mechanisms in cyanobacteria: molecular components, their diversity and evolution. J. Exp. Bot. 54, 609–622.

Bald, D., Kruip, J., Boekema, E.J. and Rögner, M. (1992) Structural investigations on cyt b_6 f complex and PS I complex from the cyanobacterium *Synechocystis* PCC6803. In:

N. Murata (Ed.), *Photosynthesis: from Light to Biosphere*, Part I. Kluwer Academic Publishers, Dordrecht, The Netherlands, pp. 629–633.

Baymann, F., M. Brugna, M., Muhlenhoff, U. and Nitschke, W. (2001) Daddy, where did (PS)I come from? Biochim. Biophys. Acta 1507, 291–310.

Bhattcharaya, D., Yoon, H.S. and Hackett, J.D. (2003) Photosynthetic eukaryotes unite: endosymbiosis connects dots. BioEssays 26, 50–60.

Beatty, J.T., Overmann, J., Lince, M.T., Manske, A.K., Lang, A.S., Blankenship, R.E., Van Dover, C.L., Martinson, T.A. and Plumley, G.F. (2005) An obligately photosynthetic bacterial anaerobe from a deep-sea hydrothermal vent. Proc. Natl. Acad. Sci. USA 102, 9306–9310.

Beerling, D.J. Lake, J.A., Berner, R.A., Hickey, J.J., Taylor, D.W. and Royer, D.L. (2002) Carbon isotope evidence implying high O_2/CO_2 ratios in the Permo-Carboniferous atmosphere. Geochim. Cosmochim. Acta, 66, 3757–3767.

Berman-Frank, I., Lundgren, P. and Falkowski, P. (2003) Nitrogen fixation and oxygen evolution in cyanobacteria. Res. Microbiol. 154, 157–164.

Berner, R.A. (2006) GEOCARBSULF: A combined model for Phanerozoic atmospheric O_2 and CO_2 . Geochim. Cosmochim. Acta 70, 5653–5664.

Björn, L.O. (1995) Origins of photosynthesis Nature 376, 25–26.

Björn, L.O., Ekelund, N.G.A. (2005) Dinoflagellater—hopplock från livets smörgåsbord. Svensk Bot. Tidskr. 99, 7–16.

Blankenship, R.E. (2002) *Molecular mechanisms of photosynthesi*s. Blackwell Science, Edinburgh.

Blankenship, R.E. and Hartman, H. (1998) The origin and evolution of oxygenic photosynthesis. Trends Biochem. Sci. 23, 94–97.

Bocherens, H., Friis, E.M., Mariotti, A. and Pedersen, K.R. (1993) Carbon isotopic abundances in Mesozoic and Cenozoic fossil plants—paleoecological implications. Lethaia 26, 347–358.

Borda, M.J., Elsetinow, A.R., Schoonen, M.A. and Strongin, D.R. (2001) Pyrite-induced hydrogen peroxide formation as a driving force in the evolution of photosynthetic organisms on an early Earth. Astrobiology 1, 283–288.

Brasier, M.D., Green, O.R., Lindsay, J.F., McLoughlin, N., Steele, A. and Stoakes, C. (2005) Precambrian Res. 140, 55–102.

Brocks, J.J., Buick, R., Summons, R.E. and Logan, G.A. (2003) A reconstruction of Archean biological diversity based on molecular fossils from the 2.78 to 2.45 billion-year-old Mount Bruce Supergroups, Hamersley Basin, Western Australia. Beochim. Cosmochim. Acta 67, 4321–4335.

Buchanan, B.B. and D.I. Arnon. (1990) A reverse Krebs cycle in photosynthesis: consensus at last. Photosynth. Res. 24,47–53.

Butterfield, N.J. (2000) *Bangiomorpha pubescens* n. gen., n. sp.: implications for the evolution of sex, multicellularity, and the Mesoproterozoic/Neoproterozoic radiation of eukaryotes. Paleobiology 26, 386–404.

Canfield, D.E. (1998) A new model for proterozoic ocean chemistry. Nature 396, 450-453.

Canfield, D.E. (2005) The early history of atmospheric oxygen: Homage to R.M. Garrels. Annu. Rev. Earth Planet. Sci. 33, 1–36.

Canfield, D.E., Poulton, S.W. and Narbonne, G.M. (2007) Late Neo-Proterozoic deep-ocean oxygenation and the rise of animal life. Science 315, 92–95.

Clausen, J., Beckmann, K., Junge, W. and Messinger, J. (2005) Evidence that bicarbonate is not the substrate in photosynthetic oxygen evolution. Plant Physiol. 139, 1444–1450.

Clausen. J., Junge. W., Dau H. and Haumann, M. (2005) Photosynthetic water oxidation at high O_2 backpressure monitored by delayed chlorophyll fluorescence. Biochemistry 44, 12775–12779.

Dashdori, N., Zhang, H., Kim, H., Yan, J., Cramer, W.A. and Savikhin, S. (2005) The single chlorophyll a molecule in the cytochrome b6 f complex, unusual optical properties protect the complex against singlet oxygen. Biophys. J. 88, 4178–4187.

Decker, J.E. and de Wit, M.J. (2006) Carbon isotope evidence for CAM photosynthesis in the Mesozoic. Terra Nova 18, 9–17.

Demmig-Adams, B., Adams III, W.W. and Mattoo, A. (eds.) (2006) *Photoprotection, photoinhibition, gene regulation, and environment*. Springer, New York.

Dismukes, G.C., Klimo, V.V. Baranov, S.V., Kozlov, Yu, N., DasGupta, J. and Tyryshkin, A. (2001) The origin of atmospheric oxygen on Earth: The innovation of oxygenic photosynthesis. Proc. Natl. Acad. Sci. USA 98, 2170–2175.

Eck, R.V. and Dayhoff, M.O. (1966) Evolution of the structure of ferredoxin based on living relics of primitive amino acid sequences. Science (N.S.) 152, 363–366.

Evans, M. C., Buchanan, B.B. and Arnon, D.I. (1966) A new ferredoxin dependent carbon reduction cycle in a photosynthetic bacterium. Proc. Natl. Acad. Sci. USA 55, 928–934.

Falkowski. P.G., Katz, M.E., Milligan, A.J., Fennel, K., Cramer, B.S., Aubry, M.P., Berner, R.A., Novacek, M.J. and Zapol, W.M. (2005) The rise of oxygen over the past 205 million years and the evolution of large placental mammals. Science 309, 2202–2204.

Fennel, K., Follows, M. and Falkowski, P.G. (2005) The co-evolution of the nitrogen, carbon and oxygen cycles in the Proterozoic ocean. Am. J. Sci. 305, 526–545.

Ferreira, K.N., Iverson, T.M., Maghlaoui, K., Barber, J. and Iwata, S. (2004) Architecture of the photosynthetic oxygen-evolving center. Nature 303, 1831–1837.

Giordano, M., Beardall, J. and Raven, J.A. (2005) CO concentrating mechanisms in algae: Mechanisms, environmental modulation, and evolution. Annu. Rev. Plant Physiol. 56, 99–131.

Golbeck, John H. (Ed.) (2006) *Photosystem I: The light-driven plastocyanin: Ferredoxin oxidoreductase*. Springer, New York.

Golubic, S. and Seong-Joo, L. (1999) Early cyanobacterial fossil record: preservation, palaeoenvironments and identification. Eur. J. Phycol. 34, 339–348.

Gomes, R., Levison, H.F., Tsiganis, K. and Morbidelli, A. (2005) Origin of the cataclysmic Late Heavy Bombardment period of the terrestrial planets. Nature 435, 466–469.

Gough, D.O. (1981) Solar interior structure and luminosity variations. Solar Physics 74, 21–34.

Govindjee (2000) Milestones in photosynthesis research. In: Yunus, M., Pathre, U. and Mohanty, P. (eds.), *Probing photosynthesis: Mechanisms, regulation and adaptation*. Taylor & Francis, London, pp. 9–39.

Govindjee, Beatty, J.T., Gest, H., Allen, J.F. (eds.) (2005) *Discoveries in photosynthesis*. Springer, Dordrecht.

Granick, S. (1957) Speculations on the origins and evolution of photosynthesis. Ann. NY Acad. Sci. 69, 292–308.

Gu, Y., Li, P., Sage, J.T. and Champion, P.M. (1993) Photoreduction of heme proteins: spectroscopic studies and cross-section measurements. J. Am. Chem. Soc. 115, 4993–5004.

Gutiérrez-Cirlos, E.B., Pérez-Gómez, B., Krogmann, D.W. and Gómez-Lojero, C. (2006) The phycocyanin-associated rod linker proteins of the phycobilisome of *Gloeobacter violaceus* PCC 7421 contain unusually located rod-capping domains. Biochim. Biophys. Acta 1757, 130–134.

Hakala, M., Tuominen, I., Keränen, M., Tyystjärvi, T. and Tyystjärvi, E. (2005) Evidence for the role of the oxygen-evolving manganese complex in photoinhibition of Photosystem II. Biochim. Biophys. Acta 1706, 68–80.

Hakala, M., Rantamäki, S., Puputti, E.-M., Tyystjärvi, T. and Tyystjärvi, E. (2006) Photoinhibition of manganese enzymes: insights into the mechanism of photosystem II photoinhibition. J. Exp. Bot. 57, 1809–1816.

Hannah, J.L., Bekker, A., Stein, H.J., Markey, R.J. and Holland, H.D. (2004) Primitive Os and 2316 Ma age for marine shale: implications for Paleoproterozoic glacial events and the rise of atmospheric oxygen. Earth Planetary Sci. Lett. 225, 43–52.

Hao, S.G., Beck, C.B. and Wang, D.M. (2003) Structure of the earliest leaves: Adaptations to high concentrations of atmospheric CO_2. Intern. J. Plant Sci. 164, 71–75.

Haworth, M., Hesselbo, S.P., McElwain, J.C., Robinson, S.A. and Brunt, J. (2005) Mid-Cretaceous pCO_2 based on stomata of the exinct conifer *Pseudofrenelopsis* (Cheirolepidiaceae). Geology 33, 749–752.

Heckman, D.S., Geiser, D.M., Eidell, B.R., Stauffer, R.L., Kardos, N.L. and Hedges, S.B. (2001) Molecular evidence for the early colonization of land by fungi and plants. Science 293, 1129–1133.

Hess, W.R., Partensky, F., van der Staay, G.W.M., Garcia Fernandez, J.M., Borner, T. and Vaulot, D. (1996) Coexistence of phycoerythrin and a chlorophyll a/b antenna in a marine prokaryote. Proc. Natl Acad. Sci. USA 93, 11126-11130.

Hirabayashi, H., Ishii, T., Takaichi, S., Inoue, K. and Uehara, K (2004) The role of carotenoids in the photoadaptation of the brown-colored sulfur bacterium *Chlorobium phaeobacteroides*. Photochem. Photobiol. 79, 280–285.

Horodyski, R.J. and Knauth, L.P. (1994) Life on land in the Precambrian. Science 263, 494–498.

Hu, X., Ritz, T., Damjanovic, A., Felix Autenrieth, F. and Schulten, K. (2002) Photosynthetic apparatus of purple bacteria. Quart. Revs Biophys. 35, 1–62.

Huang, D., Everly, R. M. Cheng, R.H., Heymann, J.B., Schagger, H., Sled, V., Ohnishi, T., Baker, T.S. and Cramer, W.A. (1994) Characterization of the chloroplast cytochrome b f complex as a structural and functional dimer. Biochemistry. 33, 4401–4409.

Huey, R.B. and Ward, P.D. (2005) Hypoxia, global warming, and terrestrial late Permian extinctions. Science 308, 398-401.

Hügler, M., Hüber, H., Stetter, K.O. and Fuchs, G. (2003) Autotrophic CO2 fixation pathways in archaea (Crenarchaeota). Arch. Microbiol. 179, 160–173.

Jahren, A.H., Porter, S. and Kuglitsch, J.J. (2003) Lichen metabolism identified in early Devonian terrestrial organisms. Geology 31,99–102.

Kappler, A., Pasquero, C., Konhauser, K.O. and Newman, D.K. (2005) Deposition of banded iron formtions by anoxygnic phototrophic Fe(II)-oxidizing bacteria. Geology 33, 865–868.

Karol, K.G., McCourt, R.M., Cimino, M.T. and Delwiche, C.F. (2001) The closest living relatives of land plants. Science 294, 2351–2353.

Ke, B. (2001) *Photosynthesis: Photobiochemistry and photobiophysics*. Springer, Dordrecht.

Keeley, J.E. and Rundel, P.W. (2003) Evolution of CAM and C4 carbon-concentrating mechanisms. Int. J. Plant Sci. 164 (3 Suppl.), S55–S77.

Kirschvink, J.L., Gaidos, E.J., Bertani, L.E., Beukes, N.J., Gutzmer, J., Maepa, L.N. and Steinberger, R.E. (2000) Paleoproterozoic snowball earth: Extreme climatic and geochemica global change and its biological consquences. Proc. Natl. Acad. Sci. USA 97, 1400–1405.

Kiang, N.Y., Siefert, J., Govindjee and Blankenship, R.E. (2007) Spectral signatures of photosynthesis. I. Review of earth organisms. Astrobiology 7, 252–274.

Kleine, T., Münker, C., Mezger, K. and Palmer, H. (2002) Rapid accretion and early core formation on asteroids and the terrestrial planets from Hf–W chronometry. *Nature* 952–955.

Kopp, R.E., Kirschwink, J-L., Hilburn, I.A. and Nash, C.Z. (2005) the Paleoproterozoic snowball Earth: A climate disaster triggered by the evolution of oxygenic photosynthesis. Proc. Natl. Acad. Sci. USA 102, 11131–11136.

Krapež, B., Barley, M.A. and Pickard, A.L. (2003) Hydrothermal and resedimented origins of the precursor sediments to banded iron formation: sedimentological evidence from the early Palaeoproterozoic Brockman supersequence of western Australia. Sedimentology 50, 979–1011.

Kurisu, G., Zhang, H., Smith, J.L. and Cramer, W.A. (2003) Structure of the cytochrome b f complex of oxygenic photosynthesis: tuning the cavity. Science 302, 1009–1014.

Lenton, T. (2001) The role of land plants, phosphorus weathering and fire in the rise and regulation of atmospheric oxygen. Global Change Biol. 7, 613–629.

Levrard, B. and Laskar, J. (2003) Climate friction and the earth's obliquity. Geophys. J. 154, 970–990.

Marin, B., Nowack, E.C.M. and Melkonian, M. (2005) A plastid in the making: evidence for a second primary endosymbiosis. Protist 156, 425–432.

Markham, K.R. and Porter, LJ. 1969. Flavonoids in the green algae (Chlorophyta). Phytochemistry 8, 1777–1781.

Mauzerall, D. (1976) Chlorophyll and photosynthesis. Phil. Trans. Roy. Soc. Lond. B 273, 287–294.

McElwain, J.C. (1998) Do fossil plants signal palaeatmospheric CO_2 concentration in teh geological past? Royal Soc. London Phil. Transact. B 353, 83–96.

McElwain, J.C., Mitchell, F.J.G. and Jones, M.B (1995) Relationship of stomatal density and index of *Salix cinerea* to atmospheric carbon dioxide concentrations in the Holocene. The Holocene 5, 539–570.

McElwain, J.C., Mayle, F.E. and Beerling, D.J. (2002) Stomatal evidence for a decline in atmospheric CO concentration during the Younger Dryas stadial: a comparison with Antarctic ice core records. J. Quaternary Sci. 17, 21–29.

Mercer-Smith, J.A. and Mauzerall, D. (1981) Molecular hydrogen production by uroporphyrin and coproporhyrin: A model for the origin of photosynthetic function. Photochem. Photobiol. 34, 407–10.

Moorbath, S. (2005) Palaebiology: Dating the earliest life. Nature 434, 155.

Mulkidjanian, A.Y., Koonin, E.V., Makarova, K.S., Mekhedov S.L., Sorokin, A., Wolf, Y.I, Dufresne, A., Partensky, F., Burd, H., Kaznadzey, D., Haselkorn, R. and Galperin, M.Y. (2006) The cyanobacterial genome core and the origin of photosynthesis. Proc. Natl Acad. Sci. USA 103, 13126–13131.

Nelson, N. and Ben-Shem, A. (2005) The structure of photosystem I and evolution of photosynthesis. BioEssays 27, 914–922.

Nisbet, E. G., Cann, J. R. and VanDover, C. L. (1995) Origins of photosynthesis. Nature (London) 373, 479–480.

Olson, J.M. (2006) Photosynthesis in the Archean era. Photosynthesis Res. 88, 109–117.

Osborne, C.P. and Beerling, D.J. (2006) Nature's green revolution: the remarkable evolutionary rise of C4 plants. Phil. Transact. Roy. Soc. B. – Biol. Sci. 361, 173–194.

Petersen, J., Teich, R., Brinkmann, H. and Cerff, R. (2006) A "green" phosphoribulokinase in complex algae with red plastids: Evidence fro a single secondary endosymbiosis

leading to haptophytes, cryptophytes, heterokonts, and dinoflagellates. J. Mol. Evol. 23, 1109–1118.

Pierre, J., Bazin, M., Debey, P. and Santus, R. (1982) One-electron photo-reduction of bacterial cytochrome P450 by ultraviolet light. 1. Steady-state measurements. Eur. J. Biochem. 124, 533–537.

Pierre, Y., Breyton, C., Lemoine, Y., Robert, B., Vernotte, C. and Popot, J.-L. (1997) On the presence and role of a molecule of chlorophyll a in the cytochrome b f complex. J. Biol. Chem. 272, 21901–21908.

Rascio, N. (2002) The underwater life of secondarily aquatic plants: Some problems and solutions. Critical Reviews in Plant Sciences, 21, 401–427.

Raven, J.A., Evans, M.C.W., and Korb, R.E. (1999) The role of trace metals in photosynthetic electron transport in O_2-evolving organisms. Photosynthesis Res. 60, 111–149.

Raven, J.A., Kübler, J.E. and Beardall, J. (2000) Put out the light and then put out the light. J. Mar. Biol. Ass. UK 80, 1–25.

Raymond, J. and Blankenship, R.E. (2003) Horizontal gene transfer in eukaryotic algal evolution. Proc. Natl Acad. Sci. USA 100, 7419-7420.

Raymond, J., Zhaxybayeva, O., Gogarten, J.P. and Blankenship, R.E. (2003) Evolution of photosynthetic prokaryotes: a maximum-likelihood mapping approach. Royal Soc. London Phil. Transact. B 358, 223–230.

Raymond, J., Siefert, J.L., Staples, C.R. and Blankenship, R.E. (2003) The natural history of nitrogen fixation. Mol. Biol. Evol. 21, 541–554.

Reinfelder, J.R., Kraepiel, A.M.L., and Morel, F.M.M. (2000) Unicellular C4 photosynthesis in a marine diatom. Nature 407, 996–99

Reinfelder, J.R., Milligan, A.J. and Morel F.M.M. (2004) The role of C4 photosynthesis in carbon accumulation and fixation in a marine diatom. Plant Physiol. 135, 2106–11.

Rogers, M.B., Gilson, P.R., Su, V., McFadden, G.I. and Keeling, P.J. (2007) The complete chloroplast genome of the chlorarachniophyte *Bigelowiella natan*s: Evidence for independent origins of Chlorarachniophyte and Euglenid secondary endosymbionts. Mol. Biol. Evol. 24, 54–62.

Rosing, M.T. and Frei, R. (2004) U-rich Archaean sea-floor sediments from Greenland—indications of >3700 Ma oxygenic photosynthesis. Earth Planet. Sci. Lett. 217, 237–244.

Rubinstein, B. (1993) Plasma membrane redox processes: components and role in plant processes. Annu. Rev. Plant Physiol. Plant Mol. Biol. 44, 131–55.

Rutherford, A.W. and Faller, P. (2003) Photosystem II: evolutionary perspectives. Phil. Trans. Roy. Soc. London B 358, 254–253.

Sage, R.F. (2004) The evolution of C4 photosynthesis. New Phytologist 161, 341–370.

Sauer, K and Yachandra, V.K. (2002) A possible evolutionary origin for the Mn-4 cluster of the photosynthetic water oxidation complex from natural MnO2 precipitates in the early ocean. Proc. Natl Acad. Sci. USA 99, 8631–8636.

Segura, A., Krelove, K., Kasting, JF., Sommerlatt, D., Meadows, V., Crisp, D., Cohen, M. and Mlawer, E. (2003) Ozone concentrations and ultraviolet fluxes on earth-like planets around other stars. Astrobiology 3, 689–708.

Selesi, D., Schmid, M. and Hartmann, A. (2005) Diversity of green-like and red-like ribulose-1,5-bisphosphate carboxylase/oxygenase large-subunit genes (*cbbL*) in differently managed agricultural soils. Appl. Environ. Microbiol. 71, 175–184.

Stoebe, B. and Maier, U.-G. (2002) One, two, three: nature's tool box for building plastids. Protoplasma 219, 123–130.

Stroebel, D., Choquet, Y., Popot, J.-L. and Picot, D. (2003) An atypical haem in the cytochrome b_6 f complex. Nature 426, 413–418.

Strzepek, R.F. and Harrison, P.J. (2004) Photosynthetic architecture differs in coastal and oceanic diatoms. Nature 431, 689–692.

Summons, R.E., Jahnke, L.L., Hope, J.M. and Logan, G.A. (1999) 2-Methylhopanoids as biomarkers for cyanobacterial oxygenic photosynthesis. Nature 400, 554–557.

Tajika, E. (2003) Faint young sun and the carbon cycle: implication for the Proterozoic global glaciations. Earth Planet. Sci. Lett. 214, 443–453.

Tapley, D.W., Buettner, G.R. and Shick, J.M. (1999) Free radicals and chemiluminescence as products of the spontaneous oxidation of sulfide in seawater, and their biological implications. Biol. Bull. 196, 52–56.

Taylor, W.A., Free, C., Boyce, C., Helgemo, R., and Ochoada, J. (2004) SEM analysis of *Spongiophyton* interpreted as a fossil lichen. Int. J. Plant Sci. 165, 875–881.

Tice, M.M. and Lowe, D.R. (2004) Photosynthetic microbial mats in the 3,416 Myr-old ocean. Nature 431, 549–552.

Tice, M.M. and Lowe, D.R. (2006) Hydrogen-based carbon fixation in the earlies known photosynthetic organisms. Geology 34, 37–40.

Tomitani. A., Knoll, A.H., Cavanaugh, C.M, and Ohno, T. (2006) The evolutionary diversification of cyanobacteria: Molecular-phylogenetic and paleontological perspectives. Proc. Natl Acad. Sci. USA 103, 5442–5447.

Van Rensen, J.J.S., Xu, C. and Govindjee (1999) Role of bicarbonate in Photosystem II, the water—plastoquinone oxido-reductase of plant photosynthesis. Physiol. Plant. 105, 585–592.

Warburg, O., Krippahl, G. and Jetschma, C. (1965) Widerlegung der Photolyse des Wassers und Beweis der Photolyse der Kohlensäure nach Versuchen mit lebender *Chlorella* und den Hill-Reagentien Nitrat und K Fe(Cn) . Z. Naturforsch. B B20, 993–996.

Wellman, C.H., Osterloff, P.L. and Mohiuddin, U. (2003) Fragments of the earliest land plants. Nature 425, 282–285.

White, S.N., Chave, A.D., Reynolds, G.T., Gaidos, E.J., Tyson, J.A. and Van Dover, C.L. (2000) Variations in ambient light emission from black smokers and flange pools on the Juan de Fuca Ridge. Geophys. Res. Lett. 27, 1151–1154.

White, S.N., Chave, A.D. and Reynolds, G.T. (2002) Investigations of ambient light emission at deep-sea hydrothermal vents. J. Geophys. Res. Solid Earth 107 (B1), Art. No. 2001.

White SN, Chave AD, Reynolds GT, Van Dover CL. (2002) Ambient light emission from hydrothermal vents on the. Mid-Atlantic Ridge. Geophys. Res. Lett. 29, Art. No. 1744.

Wilde, S.A., Valley, J.W., Peck, W.H. and Graham, C.M. (2001) Evidence from detrital zircons for the existence of continental crust and oceans on the earth 4.4 Gyr ago. Nature 409, 175–178.

Williams, D.M., Kasting, J.F. and Frakes LA (1998) Low-latitude glaciation and rapid changes in the Earth's obliquity explained by obliquity-oblateness feedback. Nature 396, 453–455.

Woese, C.R. (2005) The archaeal concept and the world it lives in: a retrospective. In: Govindjee, J.T. Beatty, H. Gest, and J.F. Allen (Eds.), *Discoveries in photosynthesi*s. Springer, Dordrecht, pp 1109–1120

Wydrzynski, T.J., Satoh, K. (Eds.) (2005) *Photosystem II — The light-driven water: Plastoquinone oxidoreductase* (Advances in photosynthesis and respiration, vol. 22). Springer, Dordrecht, The Netherlands.

Xiong, J. and Bauer, C.E. (2002) A cytochrome *b* origin of photosynthetic reaction centers: an evolutionary link betweeen respiration and photosynthesis. J. Mol. Biol. 322, 1025–1037.

Xiong, J. and Bauer, C.E. (2002) Complex evolution of photosynthesis. Annu. Rev. Plant Biol. 53, 503–521.

Yano, J., Kern, J,, Sauer, K., Latimer, M.J., Pushkar, Y., Biesiadka, J., Loll, B., Saenger, W., Messinger, J., Zouni, A. and Yachandra, V.K. (2006) Where water is oxidized to dioxygen: Structure of the photosynthetic Mn_4 Ca cluster. Science 314, 821–825.

Yin, Q., Jacobsen, S.B., Yamashita, K., Blichert-Toft, J., Télouk, P. and Albarède, F. (2002) A short timescale for terrestrial planet formation from Hf-W chronometry of meteorites. Nature 418, 949–952.

Yoshi, Y. (2006) Diversity and evolution of photosynthetic antenna systems in green plants. Phycol. Res. 54, 220–229.

Yuan, X., Xiao, S. and Taylor, T.N. (2005) Lichen-like symbiosis 600 million years ago. Science 308, 1017–1020.

Zhang, B.P., Janicke, M.T., Woodruff, W.H. and Bailey, J.A. (2005) Photoreduction of a heme peptide encapsulated in nanostructured materials. J. Phys. Chem. B. 109, 19547–19549.

Zhaxybayeva, O., Lapierre, P. and Gogarten, J.P. (2005) Ancient gene duplications and the root(s) of the tree of life. Protoplasma 227, 53–64.

13
Photosynthetic Light Harvesting, Charge Separation, and Photoprotection: The Primary Steps

Villy Sundström

Abstract: Photosynthesis is the process by which solar energy is converted into biomass at an overall efficiency of $\sim 1\%$. This conversion process starts with highly efficient energy- and electron transfer processes transforming the energy of light into excited states and trans-membrane potentials. Energy rich carbohydrates are then produced through a series of dark reactions. In this chapter we will review the processes and pigment systems by which light energy is collected and converted into chemical energy.

13.1. Introduction

As we have seen from the previous chapter a large variety of photosynthetic organisms is active today, ranging from very old photosynthetic bacteria containing only one photosystem to more recent cyanobacteria, algae, and green plants having two photosystems operating in series and capable of water oxidation and oxygen production. Despite large differences in composition and architecture of pigment-protein systems of various organisms, the overall function of most photosynthetic light energy–converting systems is surprisingly similar. Thus, it is generally seen that light is very efficiently collected by a light-harvesting antenna and within ~ 100 ps transferred to the photochemical reaction center (RC) where the light energy is converted to a stable charge separated state with almost 100% quantum efficiency creating a transmembrane potential, which is the source of energy for all subsequent processes in the organisms. This general pattern of overall time scale of the primary photosynthetic processes can easily be understood as a combined result of the high ($\sim 95\%$) overall quantum efficiency of light-to-charge conversion and the known nanosecond fluorescence lifetimes of many photosynthetic pigments (chlorophyll, bacteriochlorophyll, phycocyanin, etc.); to efficiently compete with fluorescence deactivation of the

excited states the functional energy and charge transfer processes have to be 10–100 times faster.

Some evolutionary and environmentally driven aspects of pigment differentiation in various organisms were discussed in the previous chapter. It is also interesting to view the spectral distribution of pigments used by photosynthetic organisms in relation to the solar spectrum. From Fig. 13.1 we can see that the useful parts of the solar spectrum from the blue (~ 400 nm) to the near-infrared (~ 1100 nm) is completely covered by various pigments without any gaps. Thus, nature has devised pigment systems and organisms have evolved to efficiently harvest all colors of the sunlight impinging on the earth. This large variety of pigmentation is integrated into a range of functional pigment–protein structures.

In Fig. 13.2 we show just a few examples to illustrate the great structural diversity of the photosynthetic pigment apparatus construction. In cyanobacteria (Fig. 13.2A) there is an extramembrane antenna, the phycobilisome, attached to the thylakoid membrane holding the core antenna and the photochemical reaction center. The chromophores of phycobilisomes are open chain tetrapyrrolles (phycoerythrin, phycocyanin, and allophycocyanin) arranged in such a way that downhill energy transfer (from high- to low-energy pigments) occurs towards the membrane and chlorophyll containing core antenna and reaction center. The overall construction of the photosynthetic pigment apparatus of green sulfur bacteria (Fig. 13.2B) is reminiscent of that of cyanobacteria. Here, a large
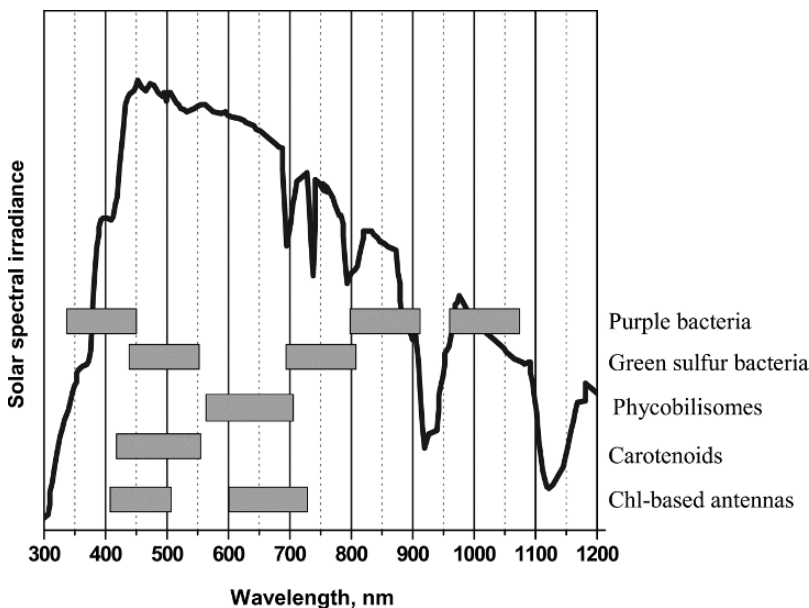
FIGURE 13.1. Solar radiation spectrum and wavelength distribution of absorption of various photosynthetic pigments. The grey bars indicate absorption bands for pigments shown at the same level.
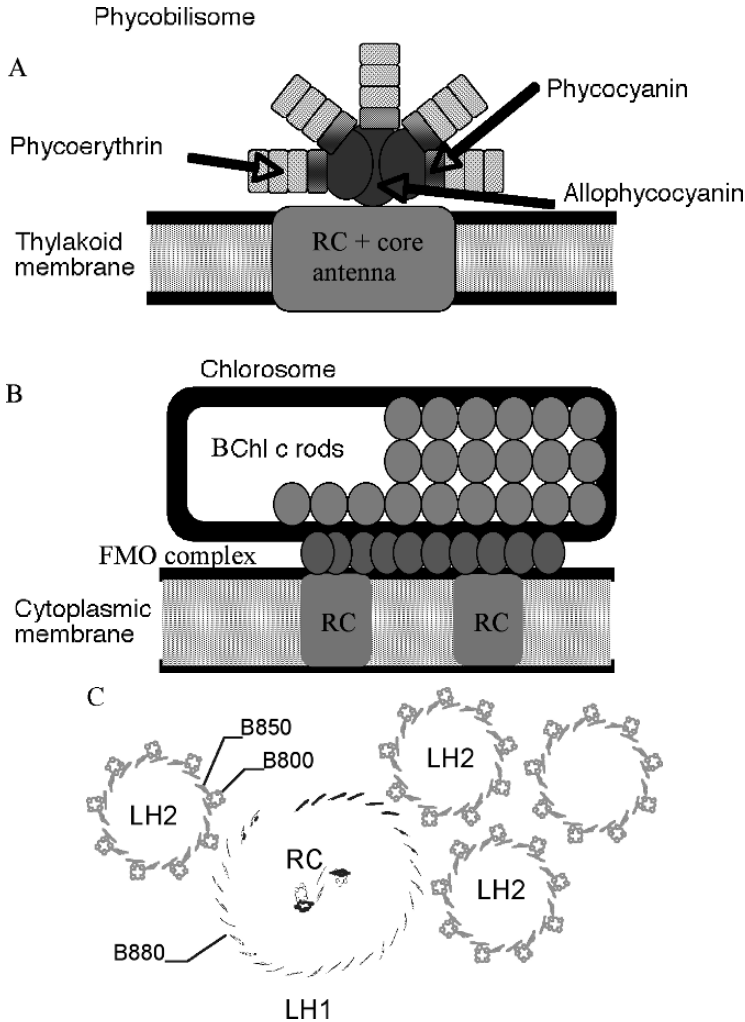
FIGURE 13.2. (**A**) Phycobilisome of blue-green bacteria. (**B**) Chlorosome and Fenna–Mathews–Olsen complex of green sulfur bacteria. (**C**) Photosynthetic unit of photosynthetic purple bacteria showing the ring-like antenna pigments LH1 and LH2. The reaction center is situated inside LH1. (*See* Color Plate).

antenna containing thousands of bacteriochlorophyll molecules arranged in rod-like structures and encapsulated in cigar-shaped structures (chlorosomes) are attached via a baseplate and a linking pigment–protein complex (the so-called Fenna–Mathews–Olsen, FMO, complex) to the membrane. One chlorosome can funnel energy to 10–15 reaction centers. The photosynthetic unit (PSU) of purple bacteria is structurally very different from those so far discussed. Here, both
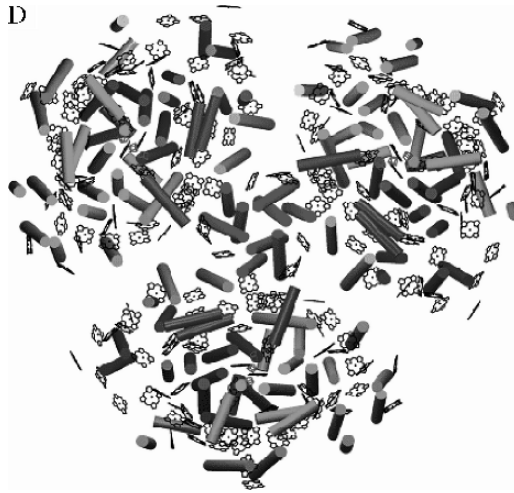
FIGURE 13.2. (Continued) **(D)** The PSI photosynthetic unit. (*See* Color Plate).

antenna and reaction centers are trans-membrane proteins fully integrated into the photosynthetic membrane (Fig. 13.2C).

The antenna consists of a circular core antenna LH1 surrounding the reaction center and a peripheral LH2 complex, also of circular shape. High-resolution crystal structures have been obtained for both LH1 and LH2. The pigments of these antennas have well-separated absorption and fluorescence spectra, and the high symmetry of the complexes makes them amenable for quantum chemistry calculations and computer simulations of energy and electron transfer processes. It also turns out that the antennas of purple bacteria constitute a representation of various energy transfer mechanisms (see below). Antennas and reaction centers of purple bacteria have therefore served as test grounds for studies of energy and electron transfer in photosynthesis; much of our knowledge today about these processes stems from studies of purple bacterial pigment–protein complexes. In this chapter we will therefore to a large extent use results obtained for purple bacterial antennas and reaction centers to illustrate in some detail the principles of photosynthetic light-harvesting and charge separation.

To conclude this survey of different photosynthetic units, we consider that of green plants consisting of the two photosystems PSI and PSII, operating in series. Here, chlorophyll *a* and chlorophyll *b* are the main chromophores of both antenna and reaction centers, and despite the presence of many different pigment–protein complexes the spectral properties are quite similar. This difficulty to spectroscopically distinguish different parts of the photosynthetic apparatus has delayed a detailed understanding of energy and electron transfer pathways and mechanisms. However, using the most powerful spectroscopic methods combined with theoretical modeling important progress has been made. Structurally, the PSI reaction center–core antenna complex and the PSII reaction center have been resolved to atomic resolution. Fig. 13.2D illustrates the PSI complex.

All photosynthetic organisms contain carotenoid molecules having important photoprotection and light-harvesting functions. In the last part of this chapter we will discuss the photophysics and excited state dynamics of carotenoid molecules underlying these functions.

13.2. Photosynthetic Antennas: Light-Harvesting and Energy Transfer

Time-resolved studies of energy transfer in light-harvesting antennas using picosecond pulses were initiated in the 1980s. Early experiments on purple bacterial LH1 and LH2 utilizing high-energy laser pulses made use of excitation annihilation effects (intensity-dependent excited state quenching) to obtain information about average energy transfer hopping times (vanGrondelle 1985). Low-intensity, high-repetition rate pulses were applied later and either the spontaneous emission or the time-resolved transmission was detected. These experiments provided information about the overall dynamics and gave upper limits for many of the essential steps (Sundström et al. 1986). Detailed studies of the most elementary ultrafast processes had to await experiments with shorter pulses.

A major breakthrough in our understanding of the organization of the bacterial antenna and consequently of the light-harvesting process itself came with the discovery of the structure of the LH2 complex of *Rps. acidophila* by Cogdell and coworkers in 1995 (Mcdermott et al. 1995), followed by the LH2 structure of *Rs. molischianum* by Michel and Schulten and coworkers in 1996 (Koepke et al. 1996). These structures revealed the 9- and 8-fold symmetrical rings of $\alpha\beta$-heterodimers for *Rps. acidophila* and *Rs. molischianum*, respectively. The corresponding structure of the LH1–RC complex from *Rhodopseudomonas (Rps.) palustris* reported in 2003 shows that the LH1 antenna does not form a full ring—one pair of BChls is missing, making it possible for the reduced ubiquinone to transport electrons out from the RC. Even if there are slight differences in structural details of various species, the PSUs from different purple bacteria are expected to be almost the same. In contrast, the long-range organization of LH2 and LH1 complexes within the photosynthetic membrane, on the hundreds of nanometer scale, appears to be quite different for different species of purple bacteria (Scheuring 2003, 2005).

Figure 13.3 shows the 2.5 Å LH2 structure of *Rps. acidophila* as obtained by Cogdell and coworkers (Mcdermott et al. 1995). The complex is a nonameric circular protein aggregate of $\alpha\beta$-heterodimers, with each subunit noncovalently binding three BChls and two carotenoid molecules. The chromophores are arranged in two concentric rings of BChl molecules named B800 and B850 according to their characteristic Q_y absorption maxima at 800 and 850 nm. The B850 ring is formed by the 9 pairs of BChls associated with conserved histidines and is sandwiched between the concentric rings of α- and β-polypeptides, and the inter- and intrasubunit BChl-BChl center-to-center distances are very similar, about 9 Å. The 9 B800s are in a plane approximately 1.7 nm shifted towards
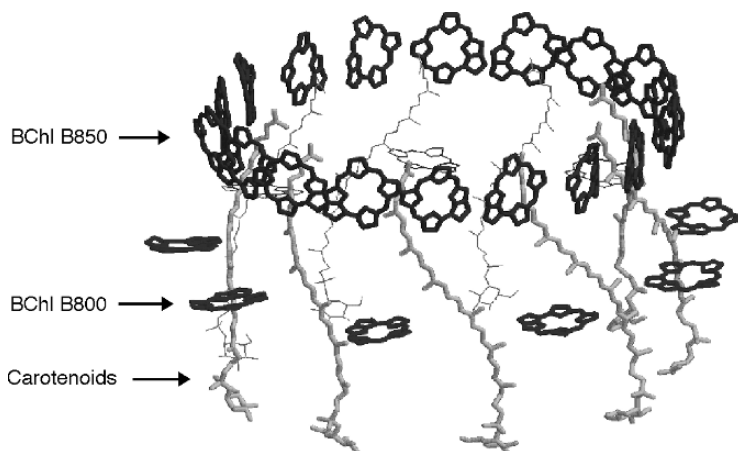
FIGURE 13.3. The LH2 antenna complex of purple bacteria. Only pigment molecules are shown.

the cytosolic side of the membrane and positioned between the β-helices. The B800–B800 center-to-center distance is about 21.2 Å.

13.2.1. Theoretical Considerations for Energy Transfer and Spectroscopy

Excitation transfer in photosynthetic antenna systems has usually been described as an incoherent Förster hopping (Förster 1946) in a two-dimensional antenna array of pigment molecules. It is hard to overestimate the physical insight obtained by this approach. At the same time, a number of experimental facts do not fit into this picture; for example, coherent nuclear motions in the antenna systems of photosynthetic purple bacteria or the highly structured spectra of so-called Fenna–Matthews–Olson complexes. The latter case in particular calls for a molecular exciton description where an excitation is coherently delocalized over a number of pigment molecules and the absorption spectrum exhibits a prominent exciton band structure. Time evolution in the exciton picture occurs via phonon-induced relaxation between exciton levels. These two descriptions, incoherent hopping and exciton relaxation, are the two qualitatively different limiting cases of the general process of excitation dynamics. What description should be chosen for a particular observation depends on the system properties and the experimental conditions (Pullerits and Sundström 1996; Sundström et al. 1999). It may happen that the real situation is somewhere in between these two limiting cases, in which case the analysis is particularly challenging. The important factor in deciding which process(es) occur is the ratio of the coupling between electronic transitions (V) and the disorder (Δ). The disorder may be either static (spectral inhomogeneity) or dynamic (electron–phonon interaction). If V/Δ is much less than unity, the interactions are considered very weak and energy transfer occurs

in the incoherent hopping limit. In the opposite case, if $V/\Delta > 1$, the interaction is very strong and the exciton picture is used. In both cases, the transfer rate can be calculated using first order perturbation theory leading to the Fermi Golden rule. In the hopping description, electronic coupling (V) acts as a perturbation; in the exciton picture, electron phonon coupling (dynamic disorder) is the perturbation. The real experimental situation determines which part of the Hamiltonian should be taken as a perturbation and in which basis (excitonic or molecular) to think and work. In the exciton picture, the excitation energy is delocalized over the interacting pigment molecules. However, the extent of delocalization is determined by the V/Δ ratio and in a real system exciton delocalization is generally smaller than the physical size of the molecular aggregate (the ring of BChl molecules in this case). The localization process may also have a dynamic part due to the dynamic contribution to the disorder Δ. The two processes, excitation hopping and exciton relaxation, coexist and are both accounted for in a density matrix formulation of the dynamics (Dahlbom et al. 2001; Kuhn and Sundström 1997a; Kuhn and Sundström 1997b; Meier et al. 1997).

The presence of both BChl and carotenoid pigment molecules in LH2, with different pigment–pigment distances giving rise to various types of interactions and strengths of interaction, has made LH2 a testing ground for studies of energy transfer mechanisms. The high symmetry of the complex implies that it is amenable to detailed calculations and simulations of the dynamics. The fact that the complex may be manipulated, practically at will, using molecular biology methods implies that couplings between pigment molecules or other parameters may be modified, a very useful approach in mechanistic studies. The light-harvesting processes of LH2 involve all pigments and energy transfer occurs between all molecules. In what follows we briefly describe two qualitatively different processes: (1) energy transfer among B800 BChls and from the B800 to the B850 BChl molecules, which occurs over relatively large distances ($\sim$ 17–21 Å) and at relatively weak coupling; (2) energy transfer among the densely spaced ($\sim$ 9 Å) and strongly coupled ($\sim$ 300 cm^{-1}) B850 molecules, which occurs in the delocalized exciton limit. Energy transfer from carotenoid to BChl molecules we describe in the section on carotenoids, where a more general discussion of photophysics and dynamics of carotenoid molecules is given. For a detailed account of all the processes in LH2 and similar light-harvesting complexes, we refer the reader to other recent reviews (Sundström et al. 1999).

13.2.2. Energy Transfer Between Weakly Dipole-Coupled Chromophores: B800–B800 and B800–B850 Transfer in LH2

The BChls of B800 are well separated from each other and from the B850s and thereby have mainly monomeric spectroscopic properties. Excitation absorbed in the B800 ring is first transferred among B800 BChls (Sundström et al. 1999). Calculations based on the Förster theory (Förster 1946) agree remarkably well with the measured pairwise transfer time of 300 fs, suggesting that for the

B800 ring the point-dipole approximation is applicable. Also low temperature transient absorption anisotropy kinetics measured at different wavelengths inside the B800 band were successfully simulated by a model of Förster hopping in a spectrally inhomogeneous ring of BChl molecules. B800 to B850 transfer occurs with a time constant of 0.7 ps at room temperature (Sundström et al. 1999) and it slows down upon lowering the temperature to 1.2 ps at 77 K and to 1.5 ps at 4 K. Both B800 and B850 can be spectrally tuned by selective mutations of key amino acids and the B800 BChls can be exchanged to other similar BChl and Chl pigments (Fraser et al. 1999, Sundström et al. 1999). A series of pigment–protein complexes where either the B800 or B850 band was spectrally shifted were studied and significant changes of the transfer time was observed (Herek et al. 2000, Sundström et al. 1999). The complex with the most blue-shifted B800 pigment, Chl at 670 nm, gave the transfer time of 8.3 ps, as compared to 0.7 ps for the wild-type complex. All the observed trends of the transfer time are in qualitative agreement with what one would expect based on Förster spectral overlap. However, quantitative Förster theory calculations of the transfer time based on the dipole–dipole interaction between B800 and nearby B850s failed to reproduce the observed lifetimes by almost an order of magnitude. Since the spectral overlap did describe the qualitative trend, it was suggested that the source of the discrepancy is the electronic coupling term (Herek et al. 2000). It has been pointed out that the carotenoid molecule may contribute to the electronic coupling between B800 and B850 (see (Sundström et al. 1999). Alternatively, the nondiagonal and/or diagonal (Sumi 1999) electron phonon coupling may facilitate efficient excitation transfer to optically forbidden exciton levels. In the spirit of the same ideas a modified Förster theory adapted for transfer to the collective exciton states with spectral inhomogeneity has been used for describing B800 to B850 transfer, apparently leading to quantitative agreement between theory and experiment (Scholes and Fleming 2000).

13.2.3. Energy Transfer Between Strongly Coupled Chromophores: B850 of LH2

The B850 ring forms a densely packed excitonically coupled aggregate. Shortly after the structure of the LH2 became available the question of the extent of exciton delocalization in B850 became a hot research subject. Different experimental techniques and theoretical methods led to diverging and sometimes even contradictory conclusions. Based on nonlinear absorption experiments (Leupold et al. 1996), it was concluded that the excitation is delocalised over almost the whole B850 ring, whereas analyses of the transient absorption spectra suggested quite limited exciton delocalisation on the picosecond timescale—about 4 BChl molecules (Pullerits et al. 1996). Many following studies supported one or the other point of view (Chachisvilis et al. 1997, Meier et al. 1997, Monshouwer et al. 1997). The apparent controversy was resolved by considering that the exciton, and thereby also exciton delocalization, is time-dependent (Dahlbom et al. 2001). Furthermore, different definitions of exciton delocalisation length led to rather

different numerical values for the quantity. We showed that at the moment of excitation certain measures of exciton delocalization indeed gave numerical values suggesting full-ring excitons. After a few hundred femtoseconds most of the measures gave the value ~ 4 BChls (Dahlbom et al. 2001). Figure 13.4 illustrates calculated time dependencies of exciton delolalization in B850 for several different definitions of the delocalisation. The calculated results are correlated to various types of measurements of exciton delocalisation.

At high light intensities it may happen that two or more excitations are simultaneously present in a set of molecules exchanging excitation, like B850. In this case excitation annihilation can take place (Denhollander et al. 1983, Mauzerall 1976). The annihilation process is usually described as excitation transfer to an already excited molecule, where it produces a higher (doubly) excited electronic state. By very fast internal conversion the molecule relaxes to the lowest excited molecular state and one excitation is lost. Simultaneous analysis of excitation annihilation dynamics and transient absorption anisotropy decay in well-separated rings of LH2 was recently used for obtaining detailed information
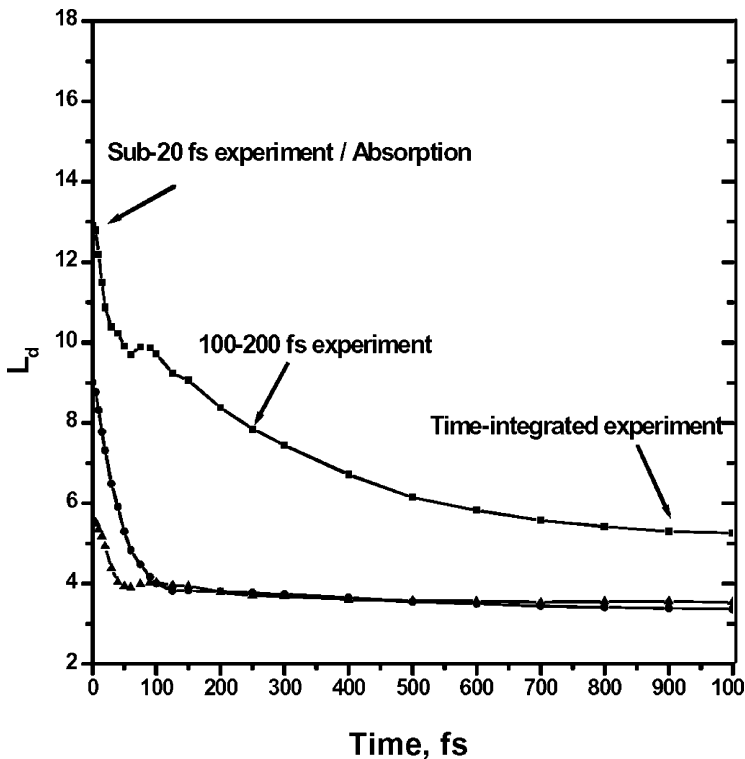
FIGURE 13.4. Calculated time dependencies of exciton delolalization, L_d, in B850 for several different definitions of the delocalization.

about excited state properties and dynamics in a B850 ring (Trinkunas et al. 2001). It was confirmed that excitons in B850 are delocalized over 3–4 BChls.

At low temperatures, transient absorption dynamics revealed a new significantly red-shifted stimulated emission band in B850 on a picosecond timescale (Polivka et al. 2000). It was suggested that the band appears due to polaron formation in B850. Later, a similar interpretation was given to strongly Stokes-shifted emission from B850 (Timpmann et al. 2001). In that work the process was called exciton self-trapping. Exciton self-trapping and polaron formation are two names of the same physical process where electron-phonon coupling leads to a significant change in the excited state nuclear configuration accompanied by lowering of the energy on the excited site and localization of the exciton.

13.2.4. The Photosynthetic Unit: Intercomplex Excitation Transfer

Study of long-range energy transfer between antenna complexes of a photosynthetic unit (PSU) and energy transfer between PSUs is important for the understanding of, e.g., adaptation processes triggered by various environmental stimuli. Energy transfer from an LH2 to an LH1 ring was studied in a membrane preparation of *Rb. sphaeroides* and concluded to be characterized by a ~ 5 ps transfer time, consistent with the estimated inter-ring distance. Transfer between aggregated B850 rings was studied using time-resolved excitation annihilation together with transmisson electron microscopy (Schubert et al. 2004). Figure 13.5 shows transient absorption kinetics of the B850 pigment for different degrees of aggregation and thus energy transfer over a varying number of B850 rings. In all curves a subpicosecond component is present reflecting the initial intra-ring annihilation for the B850 rings that have received more than one excitation from the laser pulse.

The slower dynamics contain two different components: the single-excitation decay (i.e., the fluorescence lifetime of the complex) and the inter-ring annihilation. These dynamics depend strongly on the aggregation state of LH2. In case of higher detergent concentration ($c_{CDAO} = 1.5$–15 mM), after the initial intra-ring annihilation, only the exponential single-excitation decay occurs with a time constant of ~ 750 ps corresponding well to the previously reported fluorescence lifetime of ~ 1 ns. This means that conditions are achieved where the LH2 complexes are well separated. For lower LDAO concentrations ($c_{CDAO} = 0.15$ mM and 0.5 mM) the decay of the signal is faster and nonexponential due to inter-ring annihilation, indicating aggregation of the LH2 protein complexes and long-range energy transfer. The population kinetics of the inter-ring annihilation process was modeled by a random walk of hopping excitations on a two-dimensional hexagonal lattice, each representing one B850-ring. Hexagonal coordination of the lattice is strongly suggested by TEM images of the aggregated B850 complex. The random-walk simulation by means of a Monte Carlo calculation showed that the ring-to-ring hopping time is ~ 30 ps and the number of B850 rings in an aggregate is ~ 15, in good agreement with the spot size observed in the TEM
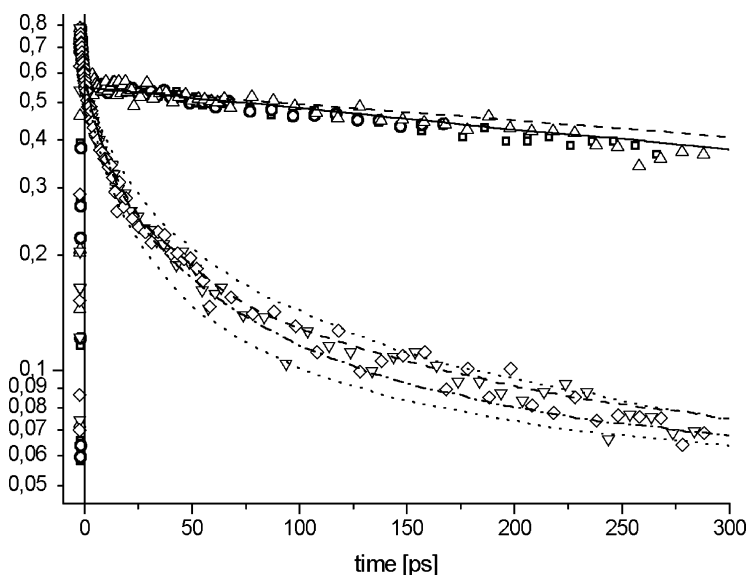
FIGURE 13.5. Annihilation kinetics of LH2 at different surfactant concentrations: c_{LDAO} = 15 mM (□), 5 mM (○), 1.5 mM (), 0.5 mM (∇), and 0.15 mM (◇). Simulations are shown for aggregate sizes N = 1 (solid line), 10 (dashed line), and 12 (dash-dotted line) both with a ring-to-ring hopping rate k = 30 ns^{-1}. For N = 12, simulations with k = 20 ns^{-1} (upper dotted line) and 40 ns^{-1} (lower dotted line) mark the confidence interval.

images (Schubert et al. 2004). The ring-to-ring hopping time of ∼ 30 ps implies that for a B850 ring surrounded by six neighboring rings the excitation residence time is ∼5 ps. This time is in good agreement with the 3–8 ps LH2-LH1 transfer time obtained for native membranes (Freiberg et al. 1989, Hess et al. 1995, Nagarajan and Parson 1997).

The last step in excitation transfer is trapping by the RC. Early studies indicated that the trapping by the RC is slow (Visscher et al. 1989). The rate of antenna to RC transfer was first determined by Timpmann et al. (1993) to be 30–40 ps. The trapping of excitation energy by the photosynthetic RC has often been discussed in terms of a trap-limited or diffusion-limited process. The new situation, after revealing the rates of all the energy transfer steps constituting the entire light-harvesting process, was termed transfer-to-trap limited, implying that it is the final energy transfer step into the reaction center that is the rate limiting step. The structure of the LH1-RC complex (Fig. 13.2C) explains the result—the distance between the RC and the LH1 BChls is the longest distance, which by virtue of the strong distance dependence (sixth power) of the energy transfer rate will be the slowest step. The functional importance of this large LH1-RC distance is that it prevents photooxidation of antenna BChls, and concomitant excited state quenching in the antenna, by the oxidized special pair of the reaction center.

An issue sometimes raised in literature is the role of collective excited states, excitons, in photosynthetic light-harvesting. Formation of collective excited

states through interchromophore interaction leads to increased dipole strength of the collective state as compared to the monomeric chromophore. Energy transfer involving collective excited states will therefore be faster than energy transfer involving monomeric pigments under otherwise identical conditions. Since the last energy transfer step to the RC is the slowest, this step is most influenced by collective excitations. Thus, the overall trapping and thereby efficiency of photosynthesis is significantly improved by exciton formation in LH1.

13.3. Photosynthetic Charge Separation: The Photosynthetic Reaction Center

From early picosecond studies of the photosynthetic reaction center it was rapidly realized that the primary charge separation occurs on a very fast time scale (<6 ps) (Kaufmann et al. 1975). Long before the crystal structure of the bacterial reaction center became available (Deisenhofer et al. 1985), spectroscopy and time-resolved methods had generated a picture of the reaction center that essentially had it all right. Only the double pigment branches, with an inactive set of pigments, turned out to be a real surprise. Nevertheless, the combination of known structure, possibilities to modify pigments and protein (via molecular biology) and ultrafast spectroscopy has turned out to be a successful approach, and today a very detailed picture of photosynthetic charge separation exists. The study of photosynthetic charge separation is in fact aimed at more than simply understanding this particular process. The well-defined structure and the possibilities to selectively modify pigments and proteins have made the bacterial reaction center a prototype system for evaluating electron transfer theory. Today, the primary electron transfer processes of all the different types of reaction centers (purple bacterial, photosystem I, photosystem II, etc.) have been extensively studied; to review all this work is not within the scope of this chapter. By giving a brief account of the most studied and best understood system, the purple bacterial reaction center (RC) we will highlight the important concepts. The main features of the function of other RCs are similar, but details may be different.

13.3.1. The Structure and Function of the Bacterial Reaction Center

The core of the RC is made up of two homologous membrane proteins, called L and M, while a third polypeptide, H, covers the cytosolic surface (Deisenhofer et al. 1985). Both L and M possess five membrane-crossing helices forming a cage around the four BChls, two bacteriopheophytins and two quinones noncovalently bound to the RC. With respect to both the proteins and the cofactors, the RC shows a remarkable C2 symmetry with the symmetry axis running through the middle of the centrally located "special pair" (P) of BChl molecules and

the nonheme iron. The pigments are arranged in two branches labeled A and B, but surprisingly, electron transfer occurs only along the A (or "active") branch. Following excitation of the special pair, charge separation occurs within a few picoseconds to yield the oxidized special pair, P^+, and a reduced bacteriopheo-phytin, H_A^-. The electron then hops to a quinone molecule, Q_A, in about 200 ps, and on to a second quinone Q_B in 100 μs. P^+ is restored to neutrality by electron transfer from a cytochrome. This sequence of reactions is repeated after the absorption of a second photon, and then the doubly reduced Q_B molecule leaves the RC as $Q_B H_B$ and an electrochemical gradient has been created across the photosynthetic membrane in which the RC is positioned.

13.3.2. The Mechanism of Primary Electron Transfer

The understanding that primary charge separation occurs within ~ 3 ps with the formation of P^+ and H_A^- was a result of subpicosecond absorption measurements in the mid-1980s. These results generated much discussion on the nature of the electron transfer between the special pair and the bacteriopheophytin. Taking into account that the edge-to-edge distance between P and H_A is 11 Å, a simple model predicted the time constant for direct electron transfer to be approximately 1 ns. From the crystal structure of the RC it was apparent that the monomeric BChl (B_A) is ideally situated to be an intermediate in the electron transfer pathway $P \rightarrow B_A \rightarrow H_A$. However, in the time-resolved measurements there were no known spectral changes that could be unambiguously interpreted as a transient population of a B^- species. To solve these difficulties, a mechanism was proposed that included B as a virtual intermediate. In this so-called superexchange mechanism it is assumed that the coupling between P and H_A is provided by B_A, but that the radical pair $P^+B_A^-$ is never significantly populated since it is far above the excited state of P (P^*) in free energy. Today, most workers in the field support the proposal originally made by Shuvalov and coworkers (Chekalin et al. 1987) and later verified by Zinth and coworkers (Arlt et al. 1993, Holzapfel et al. 1990) that B_A is transiently observable as an electron transfer intermediate, with the transfer time of the electron away from P^* (3–4 ps) almost three times slower than the transfer from B_A^- to H_A (about 1 ps). An important confirmation that $P^+B_A^-$ is indeed a detectable intermediate in charge separation came from the discovery of the B_A^- anion absorption band around 1020 nm.

In spite of the obvious symmetry of the RC, the electron transfer essentially occurs only along the A-branch. Estimates of the coupling strengths along both paths do indeed favor the active branch, but not in the experimentally observed 200:1 ratio. One conspicuous feature in the RC structure is a tyrosine residue (TyrM208 in *Rps. viridis*, TyrM210 in *Rb. sphaeroides*) strategically positioned between the cofactors in the active branch, while the symmetry-related residue in the inactive branch is a phenylalanine (PheL181). A variety of groups studied RCs with mutations introduced at these positions and they observed dramatic changes in the rate of charge separation (see, e.g., Jia et al. 1993; Visschers et al. 1999). For most mutations the rate slowed down, sometimes dramatically.

Surprisingly, for a mutation that restored the symmetry with tyrosines at positions L181 and M208 the rate increased slightly. These observations were explained within the framework of the Marcus theory (Marcus and Sutin 1985) for electron transfer and ascribed to changes in the free energy of the initial radical pair due to the mutation. The free energy dependence of the rate suggested that any change in the protein structure during electron transfer (the reorganization energy) is very small. Nevertheless, in none of the mutants was electron transfer observed along the inactive branch. Other types of mutants were also generated—mutants in which H-bonds of the protein were modified around P produced dramatic changes in its redox potential, again without affecting the asymmetry of electron transfer. In a double mutant with H_A replaced by a bacteriochlorophyll and $P^+B_A^-$ upshifted in free energy, Holten and coworkers detected a measurable amount of $P^+H_B^-$ (Kirmaier et al. 1991). This suggests that the free energy of the charge separated states controls the assymmetry of the electron transfer, rather than the differences in electronic coupling.

Following excitation of bacterial RCs with femtosecond excitation pulses, oscillatory patterns have been observed in the transient absorption changes (Vos et al. 1993) and spontaneous emission (Stanley and Boxer 1995). Typically these phenomena are explained by the generation of coherent wavepackets on the excited state surface due to the broad spectral bandwidth of the short excitation pulse. The Fourier transform spectrum of these oscillations indicated dominant modes at 15 cm^{-1} and 77 cm^{-1} and a smaller contribution from a mode at 90–100 cm^{-1}. The modes are consistent with the ground state resonance Raman spectrum of P and possibly result from the protein or are weak low-frequency modes from the BChls that are enhanced in the special pair configuration. Observation of these oscillatory signals questions the conventional assumption that vibrational dephasing and relaxation occur on a time scale that is much shorter than the electron transfer, and therefore challenges conventional theory used for describing the primary electron transfer steps in reaction centers.

The charge transfer processes described above account for the main function of the RC converting the light energy delivered to the special pair from the light-harvesting antenna into a stable charge separation across the photosynthetic membrane. All of the pigments of the RC can of course directly absorb light as well, but due to their relatively low concentration as compared to LH pigments, this contribution plays no practical role for the total light absorption of the photosynthetic unit. Nonetheless, for characterizing the various pathways of energy and electron flow within the RC it is of interest to study these processes. It is generally assumed that excitation of all other pigments than P results in ultrafast energy transfer to P (Breton et al. 1986), followed by the conventional charge separation to form the $P^+H_A^-$ radical pair. Indeed, a variety of ultrafast measurements in which B_A and B_B were selectively excited demonstrated that energy transfer to P occurs within a few hundred femtoseconds (Jonas et al. 1996). It has also been demonstrated that direct excitation of the accessory B_A pigment leads to a charge separation $P^+H_A^-$ within ~ 200 fs, without the involvement of P* (van Brederode et al. 1999). The reaction center contains

several chromophores, all at very short distances with strong interactions for energy and electron transfer. Under the natural conditions the majority of light is delivered to the RC via the special pair and these processes are therefore of little functional importance. However, their presence and properties can be exploited to elucidate the interactions of the involved pigment molecules.

In the PS2 reaction center of green plants, the charge separation starting at the accessory chlorophyll was shown to be functionally important. From the first purification work on the PS2 RC, showing strong homology between the bacterial and PS2 reaction centers, it was speculated that the operation of the two RCs would be similar. However, the spectroscopic similarity of all chromophores in the PS2 RC led to a proposal that charge separation in the PS2 RC follows the minor pathway of charge transfer demonstrated for bacterial RCs and starts at the accessory chlorophyll. Data from spectroscopic and time resolved measurements combined with theoretical modeling indeed now strongly suggest that the primary charge separation occurs between the accessory chlorophyll in the D_1 subunit and the pheophytin in the same subunit. Only by a secondary electron transfer step is the radical pair involving the special pair P680 and the pheophytin, $P680^+\text{-}H^-$, formed (Groot et al. 2005, Novoderezhkin et al. 2005).

13.4. Carotenoid Photophysics and Excited State Dynamics: The Basis of Carotenoid Light-Harvesting and Non-Photochemical Quenching

Carotenoids are, along with chlorophylls, the most abundant pigments found in nature. They are present in most organisms, including humans, but can be synthesized only by plants and microorganisms. While they are perhaps best known for their bright colors, they have well-documented multiple functions in nature: they serve as light-harvesting pigments in almost all photosynthetic organisms covering a region of the visible spectrum not accessible by (bacterio)chlorophylls and they protect against excessive light by quenching both singlet and triplet states of (B)Chls (Frank and Cogdell 1993, Frank and Cogdell 1996, Koyama et al. 1996, Ritz et al. 2000, van Amerongen and van Grondelle 2001).

Outside photosynthesis, they are known as efficient quenchers of dangerous singlet oxygen and various reactive radicals by intercepting the chain of oxidative reactions (Edge and Truscott 1999). There is accumulating evidence that this antioxidative function is a key mechanism of protection against various diseases including cancer, arteriosclerosis, and macular degeneration in humans (Landrum and Bone 2001, Nishino 1997). Yet, knowledge of the detailed molecular mechanism of such actions is so far very limited.

The diversity of carotenoid functions is unmatched by any other class of natural pigments. The functional variety is directly related to their unique spectroscopic properties resulting from the structure of the carotenoid molecule (Fig. 13.6).

The central pattern repeated in all carotenoids is a backbone consisting of alternating single and double carbon bonds that form a conjugated π-electron
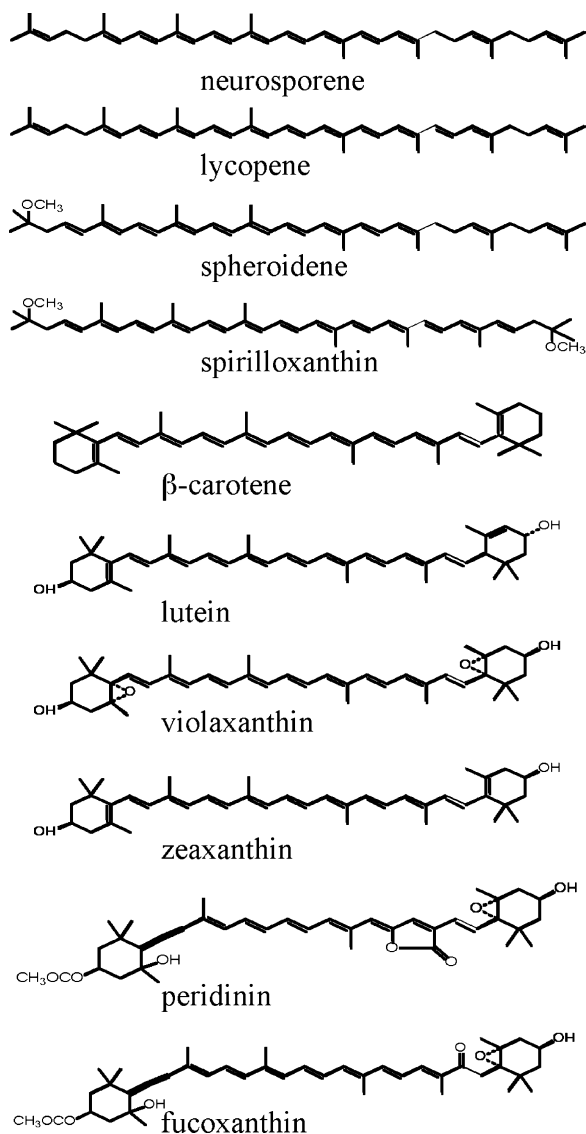
FIGURE 13.6. Molecular structures of carotenoids frequently used for studies of excited state dynamics.

system responsible for most of the spectroscopic properties of carotenoids. Until recently, most of our knowledge of properties of carotenoid excited states was largely based on spectroscopic studies of polyenes that belong to the same idealized C_{2h} point symmetry group as carotenoids. In terms of C_{2h} symmetry labels ((Atkins 1998a), the two low-lying singlet excited states denoted $2^1A_g^-$ and $1^1B_u^+$ are responsible for most of the spectroscopic properties of carotenoids.

Since the ground state of carotenoids is of A_g^- symmetry, the one-photon transition between ground state and the $2^1A_g^-$ state is symmetry forbidden, while that between ground state and the $1^1B_u^+$ state is allowed. In 1972, experiments on the polyene diphenyloctatetraene, supported by calculations established that the lowest excited state in this polyene is located below the strongly allowed $1^1B_u^+$ state, making the lowest energy transition symmetry forbidden. This discovery aroused a number of experimental and theoretical studies of polyenes, which established that the forbideness of the lowest energy transition is a common feature of all polyenes having conjugation length N>3. This reverse ordering of the excited states is also a central feature of all carotenoids occurring in nature, since most of them have a conjugation length between 7 and 13 (Fig. 13.6).

13.4.1. Excited States of Carotenoids

Knowledge of properties of excited states of carotenoids in solution is a necessary prerequisite for understanding their functions in more complex natural systems. Most of the features of the excited states that have been recognized as important for the functioning of carotenoids in more complex systems have been established by experiments performed in solution. An energy level scheme of a carotenoid molecule together with transitions that will be used to describe the dynamics of excited states in the following sections is depicted in Fig. 13.7.

The strong absorption of carotenoids (extinction coefficients of the order of 10^5) in the blue-green spectral region is caused by the strongly allowed S_0–S_2 transition. The S_0–S_2 transition of carotenoids usually exhibits a characteristic three-peak structure corresponding to the lowest three vibrational levels of the S_2 state. The energy gap between vibrational peaks of ~ 1350 cm^{-1} results from the combination of two symmetrical vibrational modes with energies of ~ 1150 cm^{-1} (C–C stretch) and ~ 1600 cm^{-1} (C=C stretch). While the resolution of vibrational structure is only little affected by the conjugation length, the energy of the S_0–S_2 transition decreases with the conjugation length. The dependence of the S_2 state energy on conjugation length (N) can be in the first approximation expressed as $E = A + B/N$, where the parameter A is the energy of the 0–0 vibrational band of the S_0–S_2 transition for an infinitely long carotenoid (see Polivka and Sundström 2004 and references therein). For both carotenoids and polyenes, A has been shown to be around 14000 cm^{-1} (700 nm); for naturally occurring carotenoids having conjugation lengths in the range 7–13, the 0–0 band of the S_0–S_2 transition is located between 475 and 525 nm (21200–19000 cm^{-1}), which gives the bright colors of carotenoids varying from yellow to red. Besides the number of conjugated double bonds, the 0–0 energy is also affected by the structure of the carotenoid. For example, the nonplanarity of the conjugated C=C bond located at the β-ionylidene ring leads to a decrease of the effective conjugation length. This results in higher S_2 energy of β-carotene and zeaxanthin than for their linear counterpart lycopene, which also possesses 11 conjugated double bonds.
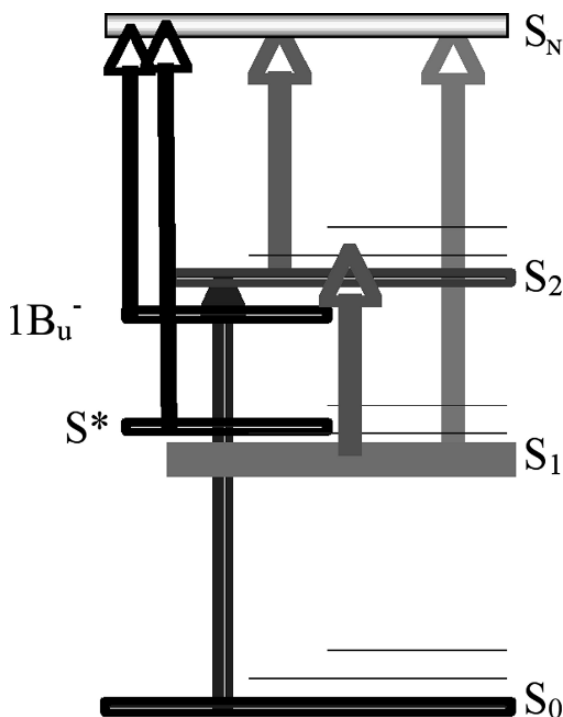
FIGURE 13.7. Carotenoid energy level diagram.

Longer carotenoids violate Kasha's rule as they exhibit emission from the S_2 state. The critical conjugation length for which the S_1 emission that dominates for shorter conjugation changes to S_2 emission is around 8 conjugated $C=C$ bonds. Studies of a series of open-chain carotenoids demonstrated that those with a conjugation length of 8 exhibit dual emission from both the S_1 and S_1 states (Frank et al. 2002). The S_2 emission constitutes almost a mirror image of the absorption spectrum with a Stokes shift of 150–300 cm^{-1}, almost independent on conjugation length for carotenoids with conjugation lengths 9–13 (Christensen et al. 1999, Fujii et al. 2001).

While the radiative lifetime of the S_2 state as calculated by the Strickler–Berg equation (Strickler and Berg 1962) is in the range of nanoseconds, measured quantum yields of the S_2 emission of the order of 10^{-5} showed that internal conversion on the subpicosecond time scale governs the S_2 dynamics. Thus, information about the dynamics of the S_2 state relies solely on ultrafast time resolved techniques. Application of such techniques to a number of carotenoids employed in photosynthesis established that the S_2 lifetime is in the range of 100–300 fs (Akimoto et al. 1999, 2002, Ricci et al. 1996) and dependent on both conjugation length and solvent parameters. The very short excited state lifetime of the carotenoid S_2 state implies that the properties of the S_1 state are crucial for understanding photophysics of carotenoids—in other words, much

of the functions of carotenoids involving excited states will originate from the S_1 state. Because of the forbidden nature of the S_0–S_1 transition, knowledge about energetics and dynamics of this key excited state was until recently very limited. Since the theoretical prediction in 1972 of the $2A_g^-$ state being the lowest excited state in longer polyenes and carotenoids, it took more than 20 years until the energy of this state could be determined experimentally for longer carotenoids.

Much effort has gone into determining the energy of the dark S_1 state of naturally occurring carotenoids having conjugation lengths in the range 7–13. An indirect approach that has been used is to determine the S_1 energy of short carotenoids from their S_1 fluorescence and extrapolate to longer carotenoids. Progress in very sensitive fluorescence detection during the 1990s enabled direct measurement of the very weak S_1 fluorescence even from photosynthetic carotenoids with conjugation lengths 9–13. Raman spectroscopy is another method that has been employed in carotenoid research. Under the conditions of resonance Raman when the excitation light is in resonance with an electronic transition of the studied molecule, the intensities of the Raman lines are greatly enhanced. Thus, tuning the detection to the frequency of either $C=C$ or $C-C$ stretching modes and scanning the excitation light over a broad spectral range, a resonance Raman profile can be obtained. The high sensitivity of Raman line intensities to the resonance conditions enables detection of even dark states with very low transition dipole moments. Using this technique the S_1 state energy of several carotenoids has been determined.

A different approach employing femtosecond time-resolved spectroscopy to locate the S_1 energy of carotenoids, based on the fact that the S_1–S_2 transition is symmetry allowed, emerged in 1999 (Polivka et al. 1999). A femtosecond excitation pulse populates the lowest vibrational band of the well-characterized S_2 state to avoid contribution from vibrational relaxation within this state. The excited molecule then relaxes to the S_1 state on the time scale of 50–300 fs as described above. By scanning the wavelength of the probe pulse within the time window dictated by the lifetime of the S_1 state, the S_1–S_2 resonance can be found. Given the known spectral profile of the S_2 state and lifetime of the S_1 state, the S_1–S_2 transition must (1) reflect the spacing between the S_2 vibrational bands and (2) decay with the S_1 lifetime. If these two conditions are fulfilled, the energies of the vibrational bands of the S_1–S_2 transition can be determined. The precise location of the carotenoid S_1 state can then be obtained, since its 0–0 spectral origin can be calculated from the spectral origins of the S_0–S_2 and S_1–S_2 transitions. Although this approach is quite straightforward, its application requires tunable femtosecond pulses in the 1–2 μm spectral range where the S_1–S_2 transition is expected. Along with availability of laser sources generating such pulses in the late 1990s, this method became a powerful tool to study the properties of the S_1 state of carotenoids. Typical S_1–S_2 profiles of two carotenoids with different conjugation lengths are shown in Fig. 13.8. The first application of this method was used to locate the S_1 energies of two carotenoids, violaxanthin and zeaxanthin, that participate in the xanthophyll cycle of higher
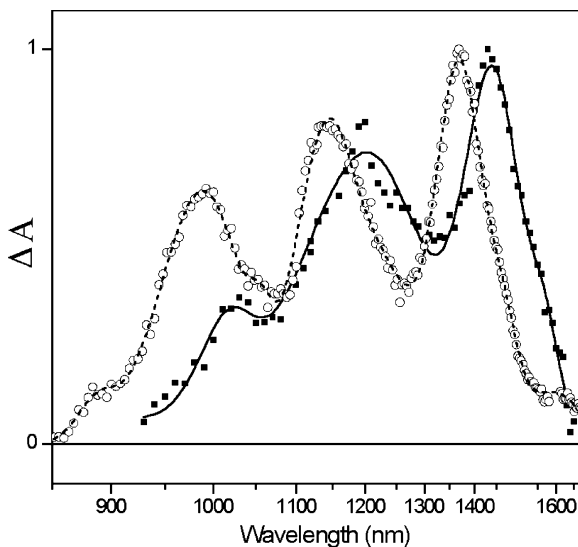
FIGURE 13.8. Transient absorption spectra of spheroidene in *n*-hexane (open circles) and violaxanthin in methanol (full squares) in the spectral region 850–1750 nm representing the spectral profile of the S_1–S_2 transition.

plants, to 14030 ± 90 cm^{-1} for zeaxanthin and 14470 ± 90 cm^{-1} for violaxanthin (Polivka et al. 1999).

Comparing the various methods used to locate the S_1 energy of carotenoids, it is clear that all of these methods have their own advantages and disadvantages, and success of their application depends on the studied system. While fluorescence and resonance Raman methods are useful tools for measurements of the S_1 energy of shorter carotenoids in solution, their use is rather limited for carotenoids having more than 10 C=C bonds, since the signals become extremely weak, putting severe constraints on a reliable data analysis. On the other hand, the S_1–S_2 spectra are more reliable for longer carotenoids, since the longer carotenoids exhibit a larger S_1–S_2 energy gap, shifting the S_1–S_2 profile towards higher energies, thus making the detection easier. For carotenoids with $N \leq 9$, the 0–0 band of the S_1–S_2 transition can extend below 5000 cm^{-1}, where vibrational overtones originating from solvent may occur. Although higher vibrational bands of the S_1–S_2 transition can be used to obtain the S_1 energy, the precision is certainly lower in such a case. Despite these complications, the S_1–S_2 method is the only one providing information about both energy and lifetime of the S_1 state, which makes it very useful in establishing excited state properties.

The S_1 lifetime strongly depends on the conjugation length of the carotenoid, ranging from several nanoseconds for $N = 5$ to a picosecond for $N = 19$ (Polivka and Sundström 2004). There is also 2004). There is also a weaker dependence of the S_1 lifetime on carotenoid structure and environment—the influence of structure can generally be correlated to variation of effective conjugation length

as a result of structural modifications and decrease in temperature increases the S_1 lifetime, while the S_1 lifetime of carotenoids without a conjugated carbonyl group is essentially independent of solvent (Polivka and Sundström 2004).

Carbonyl carotenoids, occurring in light-harvesting antennae of algae, have recently attracted substantial interest due to their unusual photophysical properties. The three most abundant, fucoxanthin, siphonaxanthin, and peridinin (Fig. 13.6), have been studied in some detail. Contrary to other, non–carbonyl containing carotenoids of similar conjugation length, these molecules exhibit a relatively strong S_1 fluorescence and the fluorescence lifetime is strongly solvent dependent. A systematic investigation of peridinin S_1 fluorescence showed that in nonpolar solvents the S_1 lifetime was about 160 ps and increase of solvent polarity in middle-polarity solvents such as tetrahydrofuran or propanol caused a shortening to 50–80 ps. In the polar solvents methanol and acetonitrile the S_1 lifetime was more than one order of magnitude shorter than in nonpolar solvents (12 and 7 ps, respectively). This behavior was explained to be a result of the presence of a new state with charge-transfer character in the excited state manifold—in polar solvents, the intramolecular charge transfer (ICT) state was suggested to lie below the S_1 state of peridinin resulting in quenching of the S_1 state and hence to a shorter S_1 lifetime. Initially, the ICT state was ascribed to the presence of a lactone ring, but more recent work showed that the carbonyl group is responsible for the polarity dependent S_1 lifetime. Thus, it is the interaction of the carbonyl group with the solvent that leads to a stabilization of the ICT state in a polar solvent.

Calculations on polyenes predicted additional states besides the S_1 and S_2 states. From extrapolations of state energies to longer polyenes it became apparent that two other excited states of $1B_u^-$ and $3A_g^-$ symmetry are of interest in carotenoids, since especially the $1B_u^-$ state approaches the S_2 state for $N \sim 9$ and it should be located in between the S_1 and S_2 states for $N > 10$ (Fig. 13.7). As a result, for most of naturally occurring carotenoids this state can be involved in the excited state dynamics. The $3A_g^-$ state was predicted to be in the vicinity of the S_2 state for $N \sim 13$, and thus above the S_2 state for most of carotenoids, but it could affect the dynamics of the longest carotenoids such as spirilloxanthin. Resonance Raman and femtosecond transient absorption spectroscopy have provided some insight into the properties of these and other (e.g., the so-called S* and S‡) excited states (Polivka and Sundström 2004), but their role in carotenoid function is not yet clear.

13.5. Energy Transfer from Carotenoids to (Bacterio)Chlorophyll

Most of the biological functions of carotenoids are carried out when carotenoids are bound to specific proteins. Although a number of carotenoid-binding proteins are known to date, excited state properties of carotenoids were studied in detail only in light-harvesting complexes. There are two main reasons for the lack of

knowledge about carotenoid excited states in other carotenoid-binding proteins. First, structures of a few light-harvesting complexes are known in great detail; the conformation of a carotenoid and its interaction with the protein environment deduced from the structure facilitates the studies of excited state properties. Second, in light-harvesting complexes, carotenoids serve as antenna pigments, making their excited states directly involved in the light-harvesting process, a vital function in all photosynthetic organisms.

The properties of excited states of carotenoids in pigment–protein complexes are best understood in light-harvesting complexes of purple bacteria, because the detailed structural knowledge provides an ideal platform for experimental and theoretical investigations of energy transfer processes between carotenoids and BChl. That carotenoids can transfer energy to BChls was known long before the x-ray structures were resolved. On the basis of fluorescence excitation spectra, carotenoid-BChl energy transfer efficiencies of 80–100% were reported for *Rb. sphaeroides* containing spheroidene (N = 10) (Angerhofer et al. 1986), while lower values between 35 and 70% were obtained for *Rps. acidophila* containing rhodopin glucoside (N = 11) (Polivka and Sundström 2004).

The carotenoid-BChl energy transfer yield drops to $\sim$30% for LH1 of *Rs. rubrum* containing spirilloxanthin (N = 13). Less than 25% efficiency was obtained for *Rps. palustris* accommodating rhodovibrin (N = 12) as the dominating carotenoid. Initial suggestions regarding mechanisms and pathways of carotenoid-BChl energy transfer in LH2 and LH1 complexes proposed energy transfer via the S_1 state, because of extremely fast deactivation of the S_2 state. The forbidden nature of the S_1 state led to a suggestion that the Dexter electron exchange mechanism (Dexter 1953) is active in this process (Cogdell and Frank 1987). However, the first time-resolved experiments performed in the early 1990s showed that following excitation of carotenoids, the B850 Q_y state was populated in less than 200 fs, signaling that both the S_1 and S_2 states may be efficient donors in the carotenoid-BChl energy transfer process (Trautman et al. 1990). Calculations of carotenoid-BChl energy transfer also led to the conclusion that both the S_1 and S_2 states can be active in energy transfer (Nagae et al. 1993). A large number of time-resolved studies on various LH1 and LH2 complexes later showed that energy transfer occurs from both the S_1 and S_2 states of carotenoids to the Q_y and Q_x excited states of BChl (for more details see Polivka and Sundström). All the documented energy transfer pathways of an LH2 complex are summarized in Fig. 13.9. Energy transfer from the optically excited carotenoid S_2 state was shown to occur in competition with the ultrafast S_2–S_1 internal conversion; transfer times varying between $\sim$50 and 150 fs, yielding energy transfer efficiencies for the S_2–Q_x channel of $\sim$50–60% have been reported. The mechanism of S_2 energy transfer was concluded to be of the Förster-type (Damjanovic et al. 1999), but contrary to the point dipole–point dipole interaction used in the Förster formula (Förster 1946), full Coulombic interaction is usually used to calculate couplings between carotenoids and BChl. The reason for this is that the point-dipole description of interacting chromophores inherent in the traditional Förster mechanism fails for extended molecules at interaction
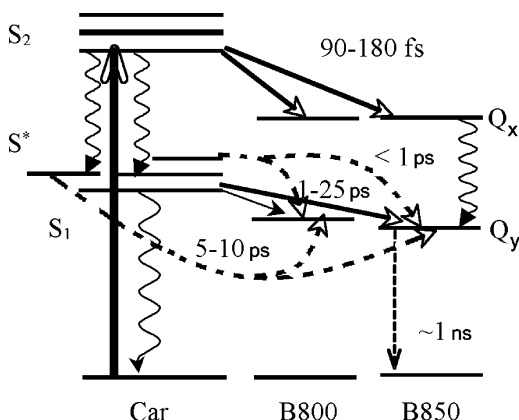
FIGURE 13.9. Schematic energy level scheme for energy transfer from carotenoids to BChls in LH2. Major pathways are indicated with full arrows, while minor paths are dotted.

distances comparable to or shorter than the size of the involved molecules. The contribution of the electron-exchange (Dexter) energy transfer mechanism (Dexter 1953) to S_2 energy transfer is negligible (Polivka and Sundström 2004).

The energy level scheme of Fig. 13.9 suggests that the carotenoid S_1 state must be higher in energy than the Q_y states of B800 and B850 BChls for efficient carotenoid–BChl transfer via the S_1 state. Before any carotenoid S_1 energy in a light-harvesting complex had been measured, estimates based on S_1 energies in solution indicated that carotenoids with $N \leq 10$ would have sufficiently high S_1 energies to efficiently transfer energy to both B800 and B850. By using several LH2 complexes having carotenoids of different conjugation lengths and comparing the S_1 lifetime of the carotenoids in solution and protein this expectation was confirmed—carotenoids with $N \geq 11$ were shown to have very little S_1 energy transfer to BChl, while shorter carotenoids exhibited transfer efficiencies of 80–95%. The energetic requirement for efficient S_1-mediated energy transfer was finally demonstrated by direct measurement of carotenoid S_1 energies in light-harvesting complexes through recording of S_1–S_2 spectra. Both B800 and B850 were shown to accept energy from carotenoids, although B800 appears to be a somewhat more efficient acceptor. Calculations of carotenoid S_1–BChl energy transfer for several LH2 complexes showed that the observed S_1 transfer rates can be explained in terms of the same energy transfer mechanism as for the S_2 route. Although the very small transition dipole moment of the S_0–S_1 transition led initially to a suggestion that the Dexter mechanism had to be invoked, more detailed calculations later showed that the Dexter contribution is negligible and that higher-order Coulombic and polarization interactions dominate the S_1-mediated energy transfer (Scholes et al. 1997).

The antenna complexes associated with PSII in green plants consist of a number of proteins belonging to the Lhcb gene family. A higher structural

complexity of these proteins, which usually bind more than one type of carotenoid in addition to Chl-*a* and Chl-*b* molecules, results in a more complicated network of possible energy transfer and internal conversion pathways. Nonetheless, the energy transfer between carotenoids and Chls was extensively studied in the recent few years, because in addition to the light-harvesting function, singlet excited states of carotenoids in these complexes were also suggested to play a photoprotective role, in which the back energy transfer from Chl to carotenoid was the central issue (see below).

The most abundant protein of the Lhcb family is LHCII, which is located at the periphery of PSII, while minor light-harvesting proteins called CP29, CP26, and CP24 are located close to the core of the PSII supercomplex. Structural knowledge of the Lhcb proteins is based on the crystal structure of LHCII (Liu et al. 2004, Standfuss et al. 2005) showing that the native form of LHCII has a trimeric organization, and each of the monomeric subunits binds 14 Chl molecules (8 Chl-*a* and 6 Chl-*b*) and 2 carotenoids. LHCII has a trimeric organization in the photosynthetic membrane and the Chl-*a* and Chl-*b* molecules are grouped in a few tightly packed clusters, each holding two to four Chl molecules. Theoretical modeling of the energy transfer with spectroscopy, time-resolved and structural data as input identified (van Grondelle and Novoderezhkin 2006) the pathways of energy transfer in the LHCII monomer. Thus, exciton relaxation occurs on the few hundred fs time scale within clusters of strongly coupled Chl-*a* and Chl-*b* molecules, followed by slower ∼ 1 ps transfer from Chl-*b* clusters to Chl-*a* clusters situated on the same side of the membrane. Slower ∼ 12 ps transfer occurs between Chl-*a* clusters on different sides of the membrane. Quite fast (∼ 0.5 ps) equilibration of energy occurs between Chl-*a* clusters situated on the same side of the membrane. The overall result of this complex transfer pattern is to within ∼ 20 ps concentrate energy collected by the entire LHCII complex to only a few low-energy Chl-*a* molecules on the lumenal side of the photosynthetic membrane.

Contrary to purple bacteria, in which the carotenoid content is species-dependent and more than 100 different carotenoids were detected in various species (Takaichi 1999), only five different carotenoids are accumulated in light-harvesting proteins of green plants: β-carotene, lutein, violaxanthin, neoxanthin, and zeaxanthin (DellaPenna 1999). Most of the studies of carotenoid–Chl energy transfer were performed on the LHCII and CP29 proteins. While LHCII is the only one whose structure is known to fine detail, the CP29 is favorable for studies of carotenoid–Chl energy transfer as it contains only two Chl-*b* molecules. This minimizes the overlap between the carotenoid S_2 state and the Chl-*b* Soret band peaking at around 475 nm. To overcome problems with the presence of a few different carotenoids with overlapping absorption spectra preventing selective excitation of only one carotenoid species, recombinant proteins that allow reconstitution with a single carotenoid species were also used (Croce et al. 2003). A number of studies established that the overall carotenoid–Chl energy transfer efficiency in the Lhcb family of proteins is in the range 70–90% (Polívka and

Sundström 2004) and that the majority of majority of the energy transfer occurs via the S_2 state.

13.6. Quenching of Chlorophyll Excited States by Carotenoids: Non-Photochemical Quenching

Quenching of various reactive excited states is probably the most important carotenoid function in photosynthesis. Carotenoids may quench both singlet and triplet (bacterio)chlorophyll excited states, as well as singlet oxygen. Here we will only consider the quenching of Chl excited singlet states. Under certain conditions one of the carotenoid-binding sites of LHCII can be occupied by zeaxanthin, and this was suggested to trigger a structural change of the protein leading to quenching of Chl fluorescence (Crimi et al. 2001), which is the origin of the photoprotective mechanism called non-photochemical quenching (NPQ). The early literature is reviewed by Demmig-Adams and Adams (1996), and aspects of the regulation mechanisms are described by Li et al. (2002) and Niyogi et al. (2005). This mechanism protects against damage caused by excessive photon flux by dissipating the energy thermally in PSII (Demmig-Adams and Adams 1996, Horton et al. 1996). It involves a cascade of processes triggered by high light conditions resulting in enzymatic conversion of violaxanthin to zeaxanthin by means of the xanthophyll cycle. Although a fundamental understanding of NPQ is still lacking, it is clear that one of the crucial components is a zeaxanthin-induced quenching of Chl-a excited state, as presence of this carotenoid reduces markedly the Chl-a fluorescence lifetime (Frank et al. 2001, Polivka et al. 2002, Richter et al. 1999). Several different mechanisms have been suggested for this quenching process. Frank et al. proposed the so-called molecular gear shift mechanism (Frank et al. 1994) as a mechanism for NPQ. In the initial proposal based on S_1 energies estimated from the energy gap law, violaxanthin was supposed to have its S_1 energy above the Q_y transition of Chl-a serving as energy acceptor, while zeaxanthin had an S_1 energy sufficiently low to act as quencher of excited Chl-a. Then, exchange of violaxanthin to zeaxanthin by means of the xanthophyll cycle would enable increase of quencher concentration, explaining the mechanism of NPQ. Later, direct measurements of the S_1 energies in both solution and LHCII (Polivka et al. 1999) challenged this mechanism, since the S_1 energies of both violaxanthin and zeaxanthin were shown to be below the Chl-a Q_y state. Nevertheless, although the initially proposed molecular gear shift would not work, the location of the zeaxanthin S_1 state below the Chl-a Q_y transition still allows direct quenching. Direct involvement of the zeaxanthin S_1 state in NPQ was also shown in a femtosecond transient absorption study of intact thylakoid membranes of *Arabidopsis thaliana* (Holt et al. 2005, Ma et al. 2003). After excitation of either Chl-b or Chl-a by ~ 100 fs pulses the zeaxanthin S_1 state was observed to be directly populated, signaling very fast energy transfer from Chl to zeaxanthin (and thus Chl excited state quenching). The formation of the zeaxanthin S_1 state was correlated to the presence of the PsbS protein that is

known to be an essential part of NPQ (Li et al. 2000), thus confirming the relation between population of the zeaxanthin S_1 state and NPQ. Further time resolved spectroscopy work (Holt et al. 2005) and calculations (Ma et al. 2003) indicated that the quenching mechanism could involve energy transfer from chlorophyll molecules to a chlorophyll–zeaxanthin heterodimer, which then undergoes charge separation and formation of a zeaxanthin$^+$–Chl$^-$ radical pair. Another hypothesis proposed that the essential function of zeaxanthin is to promote changes in structure and/or organization of the light-harvesting complexes that eventually lead to quenching conditions. One such mechanism involves a structural change facilitating a formation of Chl-*a* excitonic pairs, which than play a role of quenchers (Crofts and Yerkes 1994). Clearly, additional work is required before the mechanism of NPQ is fully clarified.

References

Akimoto, S., Yamazaki, I., Sakawa, T. and Mimuro, M. (2002) Temperature effects on excitation relaxation dynamics of the carotenoid beta-carotene and its analogue beta-apo-8 '-carotenal, probed by femtosecond fluorescence spectroscopy. J. Phys. Chem. A. 106, 2237–2243.

Akimoto, S., Yamazaki, I., Takaichi, S. and Mimuro, M. (1999) Excitation relaxation of carotenoids within the S-2 state probed by the femtosecond fluorescence up-conversion method. Chem. Physics Lett. 313, 63–68.

Angerhofer, A., Cogdell, R. J. and Hipkins, M. F. (1986) A spectral characterization of the light-harvesting pigment-protein complexes from *Rhodopseudomonas Acidophila*. Biochim. Biophys. Acta 848, 333–341.

Arlt, T., Schmidt, S., Kaiser, W., Lauterwasser, C., Meyer, M., Scheer, H. and Zinth, W. (1993) The accessory bacteriochlorophyll - a real electron carrier in primary photosynthesis. Proc. Natl Acad. Sci. USA 90, 11757–11761.

Atkins, P. W. (1998a) Molecular symmetry. In: *Physical chemistry,* pp. 427–451.Oxford University Press, Oxford.

Atkins, P. W. (1998b) Quantum theory:introduction and principles. In: *Physical chemistry*, pp. 285–312. Oxford University Press, Oxford.

Breton, J., Martin, J. L., Migus, A., Antonetti, A. and Orszag, A. (1986) Femtosecond Spectroscopy of excitation energy transfer and initial charge separation in the reaction center of the photosynthetic bacterium *Rhodopseudomonas viridis*. Proc. Natl Acad. Sci. USA 83, 5121–5125.

Chachisvilis, M., Kuhn, O., Pullerits, T. and Sundström, V. (1997) Excitons in photosynthetic purple bacteria: Wavelike motion or incoherent hopping? J. Phys. Chem. B, 101, 7275–7283.

Chekalin, S., Matveets, Y., Shkuropatova, A., Shuvalov, V. and Yartsev, A. (1987) Femtosecond spectroscopy of primary charge separation in modified reaction centers of *Rhodobacter sphaeroides* (R 26) FEBS Lett. 216, 245–248.

Christensen, R. L., Goyette, M., Gallagher, L., Duncan, J., DeCoster, B., Lugtenburg, J., Jansen, F. J. and van der Hoef, I. (1999) S-1 and S-2 states of apo- and diapocarotenes. J. Phys. Chem. A 103, 2399–2407.

Cogdell, R. J. and Frank, H. A. (1987) How Carotenoids function in photosynthetic Bacteria. Biochim. Biophys. Acta 895, 63–79.

Crimi, M., Dorra, D., Bosinger, C. S., Giuffra, E., Holzwarth, A. R. and Bassi, R. (2001) Time-resolved fluorescence analysis of the recombinant photosystem II antenna complex CP29 - Effects of zeaxanthin, pH and phosphorylation. Eur. J. Biochem.*268*, 260–267.

Croce, R., Muller, M. G., Caffarri, S., Bassi, R. and Holzwarth, A. R. (2003) Energy transfer pathways in the minor antenna complex CP29 of photosystem II: A femtosecond study of carotenoid to chlorophyll transfer on mutant and WT complexes. Biophys. J. 84, 2517–2532.

Crofts, A. R. and Yerkes, C. T. (1994) A Molecular Mechanism for Q(E)-Quenching. *FEBS Lett. 352*, 265–270.

Dahlbom, M., Pullerits, T., Mukamel, S. and Sandstrom, V. (2001) Exciton delocalization in the B850 light-harvesting complex: Comparison of different measures. J. Phys. Chem. B 105, 5515–5524.

Damjanovic, A., Ritz, T. and Schulten, K. (1999) Energy transfer between carotenoids and bacteriochlorophylls in light-harvesting complex II of purple bacteria. Physical Rev. 59, 3293–3311.

Deisenhofer, J., Epp, O., Miki, K., Huber, R. and Michel, H. (1985) Structure of the protein subunits in the photosynthetic reaction center of *Rhodopseudomonas viridis* at 3A resolution. Nature 318, 618–624.

DellaPenna, D. (1999) Carotenoid synthesis and function in plants: Insights from mutant studies in *Arabidopsis thaliana*. In: H. A. Frank, A. J. Young, G. Britton and R. J. Cogdell (eds.), *Photochemistry of carotenoid* . Kluwer Academic Publishers, Dordrecht, pp. 21–42.

Demmig-Adams, B. and Adams, W. W. III (1996) The role of xanthophyll cycle carotenoids in the protection of photosynthesis. Trends Plant Sci. 1, 21–26.

Denhollander, W. T. F., Bakker, J. G. C. and van Grondelle, R. (1983) Trapping, loss and annihilation of excitations in a photosynthetic system. 1. Theoretical aspects. Biochim. Biophys. Acta 725, 492–507.

Dexter, D. L. (1953) A theory of sensitized luminescence in solids. J. Chem. Physics 21, 836–850.

Edge, R. and Truscott, T. G. (1999) Carotenoid radicals and the interaction of carotenoids with active oxygen species. In: H. A. Frank, A. J. Young, G. Britton and R. J. Cogdell (eds.), *Photochemistry of carotenoids*. Kluwer Academic Publishers, Dordrecht, The Netherlands, pp. 223–237.

Förster, T. (1946) Energiewanderung und Fluoreszenz. Naturwissenschaft 33, 166–175.

Frank, H. A. and Cogdell, R. J. (1993) Photochemistry of carotenoids. In: A. J. Young (ed.) *Carotenoids in photosynthesis*. Chapman & Hall, Boca Raton, FL, pp. 252–270.

Frank, H. A. and Cogdell, R. J. (1996) Carotenoids in photosynthesis. Photochem. Photobiol. 63, 257-264.

Frank, H. A., Cua, A., Chynwat, V., Young, A., Gosztola, D. and Wasielewski, M. R. (1994) Photophysics of the carotenoids associated with the xanthophyll cycle in photosynthesis. Photosynthesis Res. 41, 389–395.

Frank, H. A., Das, S. K., Bautista, J. A., Bruce, D., Vasil'ev, S., Crimi, M., Croce, R. and Bassi, R. (2001) Photochemical behavior of xanthophylls in the recombinant photosystem II antenna complex, CP26. Biochemistry 40, 1220–1225.

Frank, H. A., Josue, J. S., Bautista, J. A., van der Hoef, I., Jansen, F. J., Lugtenburg, J., Wiederrecht, G. and Christensen, R. L. (2002) Spectroscopic and photochemical properties of open-chain carotenoids. J. Phys. Chem. B 106, 2083–2092.

Fraser, N. J., Dominy, P. J., Ucker, B., Simonin, I., Scheer, H. and Cogdell, R. J. (1999) Selective release, removal, and reconstitution of bacteriochlorophyll a molecules into the B800 sites of LH2 complexes from *Rhodopseudomonas acidophila* 10050. Biochemistry 38, 9684–9692.

Freiberg, A., Godik, V. I., Pullerits, T. and Timpman, K. (1989) Picosecond dynamics of directed excitation transfer in spectrally heterogeneous light-harvesting antenna of purple bacteria. Biochim. Biophys. Acta 973, 93–104.

Fujii, R., Ishikawa, T., Koyama, Y., Taguchi, M., Isobe, Y., Nagae, H. and Watanabe, Y. (2001) Fluorescence spectroscopy of all-trans-anhydrorhodovibrin and spirilloxanthin: Detection of the 1B(u)(-) fluorescence. J. Phys. Chem. A 105, 5348–5355.

Groot, M. L., Pawlowicz, N. P., van Wilderen, L. J. G. W., Breton, J., van Stokkum, I. H. M. and van Grondelle, R. (2005) Initial electron donor and acceptor in isolated Photosystem II reaction centers identified with femtosecond mid-IR spectroscopy. Proc. Natl Acad. Sci. USA 102, 13087–13092.

Herek, J. L., Fraser, N. J., Pullerits, T., Martinsson, P., Polivka, T., Scheer, H., Cogdell, R. J. and Sundström, V. (2000) B800 → B850 energy transfer mechanism in bacterial LH2 complexes investigated by B800 pigment exchange. Biophys. J. 78, 2590–2596.

Hess, S., Chachisvilis, M., Timpmann, K., Jones, M. R., Fowler, G. J. S., Hunter, C. N. and Sundström, V. (1995) Temporally and spectrally resolved subpicosecond energy transfer within the peripheral antenna complex (LH2) and from LH2 to the core antenna complex in photosynthetic purple bacteria. Proc. Natl Acad. Sci. USA 92, 12333–12337.

Holt, N. E., Zigmantas, D., Valkunas, L., Li, X. P., Niyogi, K. K. and Fleming, G. R. (2005) Carotenoid cation formation and the regulation of photosynthetic light harvesting. Science 307, 433–436.

Holzapfel, W., Finkele, U., Kaiser, W., Oesterhelt, D., Scheer, H., Stilz, H. U. and Zinth, W. (1990) Initial electron-transfer in the reaction center from *Rhodobacter sphaeroides*. Proc. Natl Acad. Sci. USA 87, 5168–5172.

Horton, P., Ruban, A. V. and Walters, R. G. (1996) Regulation of light harvesting in green plants. Annu. Rev. Plant Physiol. Plant Mol. Biol. 47, 655–684.

Jia, Y. W., Dimagno, T. J., Chan, C. K., Wang, Z. Y., Du, M., Hanson, D. K., Schiffer, M., Norris, J. R., Fleming, G. R. and Popov, M. S. (1993) primary charge separation in mutant reaction centers of *Rhodobacter capsulatus*. J. Phys. Chem. 97, 13180–13191.

Jonas, D. M., Lang, M. J., Nagasawa, Y., Joo, T. and Fleming, G. R. (1996) Pump-probe polarization anisotropy study of femtosecond energy transfer within the photosynthetic reaction center of *Rhodobacter sphaeroides* R26. J. Phys. Chem. 100, 12660–12673.

Kaufmann, K. J., Dutton, P. L., Netzel, T. L., Leigh, J. S. and Rentzepis, P. M. (1975) Picosecond kinetics of events leading to reaction center bacteriochlorophyll oxidation. Science 188, 1301–1304.

Kirmaier, C., Gaul, D., Debey, R., Holten, D. and Schenck, C. C. (1991) Charge separation in a reaction center incorporating bacteriochlorophyll for photoactive bacteriopheophytin. Science 251, 922–927.

Koepke, J., Hu, X. C., Muenke, C., Schulten, K. and Michel, H. (1996) The crystal structure of the light-harvesting complex II (B800-850) from *Rhodospirillum molischianum*. Structure 4, 581–597.

Koyama, Y., Kuki, M., Andersson, P. O. and Gillbro, T. (1996) Singlet excited states and the light-harvesting function of carotenoids in bacterial photosynthesis. Photochem. Photobiol. 63, 243–256.

Kuhn, O. and Sundström, V. (1997a) Energy transfer and relaxation dynamics in light-harvesting antenna complexes of photosynthetic bacteria. J. Phys. Chem. B 101, 3432–3440.

Kuhn, O. and Sundström, V. (1997b) Pump-probe spectroscopy of dissipative energy transfer dynamics in photosynthetic antenna complexes: A density matrix approach. J. Chem. Phys. 107, 4154–4164.

Landrum, J. T. and Bone, R. A. (2001) Lutein, zeaxanthin, and the macular pigment. Arch. Biochem. Biophys. 385, 28–40.

Leupold, D., Stiel, H., Teuchner, K., Nowak, F., Sandner, W., Ucker, B. and Scheer, H. (1996) Size enhancement of transition dipoles to one- and two-exciton bands in a photosynthetic antenna. Phys. Rev. Lett. 77, 4675–4678.

Li, X.-P., Bjorkman, O., Shih, C., Grossman, A. R., Rosenquist, M., Jansson, S. and Niyogi, K. K. (2000) A pigment-binding protein essential for regulation of photosynthetic light harvesting. Nature 403, 391–395.

Li, X.-P., Gilmore, A.M. and Niyogi, K.K. (2002) Molecular and global time-resolved analysis of a psbS gene dosage effect on pH- and xanthophyll cycle-dependent nonphotochemical quenching in photosystem II. J. Biol. Chem. 277, 33590–33597.

Liu, Z., Yan, H., Wang, K., Kuang, T., Zhang, J., Gui, L., An, X. and Chang, W. (2004) Crystal structure of spinach major lightharvesting complex at 2.72 A resolution. Nature 428, 287–292.

Ma, Y. Z., Holt, N. E., Li, X. P., Niyogi, K. K. and Fleming, G. R. (2003) Evidence for direct carotenoid involvement in the regulation of photosynthetic light harvesting. Proc. Natl Acad. Sci. USA 100, 4377–4382.

Marcus, R. A. and Sutin, N. (1985) Electron transfers in chemistry and biology. Proc. Natl Acad. Sci. USA 811, 265–322.

Mauzerall, D. (1976) Multiple excitations in photosynthetic systems. Biophys. J. 16, 87–91.

Mcdermott, G., Prince, S. M., Freer, A. A., Hawthornthwaitelawless, A. M., Papiz, M. Z., Cogdell, R. J. and Isaacs, N. W. (1995) Crystal-Structure of an integral membrane light-harvesting complex from photosynthetic bacteria. Nature 374, 517–521.

Meier, T., Chernyak, V. and Mukamel, S. (1997) Multiple exciton coherence sizes in photosynthetic antenna complexes viewed by pump-probe spectroscopy. J. Phys. Chem. B 101, 7332–7342.

Monshouwer, R., Abrahamsson, M., van Mourik, F. and van Grondelle, R. (1997) Superradiance and exciton delocalization in bacterial photosynthetic light-harvesting systems. J. Phys. Chem. B 101, 7241–7248.

Nagae, H., Kakitani, T., Katoh, T. and Mimuro, M. (1993) Calculation of the excitation transfer-matrix elements between the S(2) Or S(1) State of carotenoid and the S(2) Or S(1) state of bacteriochlorophyll. J. Chem. Phys. 98, 8012–8023.

Nagarajan, V. and Parson, W. W. (1997) Excitation energy transfer between the B850 and B875 antenna complexes of Rhodobacter sphaeroides. Biochemistry 36, 2300–2306.

Nishino, H. (1997) Cancer prevention by natural carotenoids. J. Cell. Biochem. 86–91.

Niyogi, K.K., Li, X.-P. Rosenberg, V. and Jung, H.-S. (2005) Is PsbS the site of nonphotochemical quenching in photosynthesis? J. Exp. Bot. 56, 375–382.

Novoderezhkin, V. I., Andrizhiyevskaya, E. G., Dekker, J. P. and van Grondelle, R. (2005) Pathways and timescales of primary charge separation in the photosystem II reaction center as revealed by a simultaneous fit of time-resolved fluorescence and transient absorption. Biophys. J. 89, 1464–1481.

Polivka, T., Herek, J. L., Zigmantas, D., Åkerlund, H. E. and Sundström, V. (1999) Direct observation of the (forbidden) S-1 state in carotenoids. Proc. Natl Acad. Sci. USA 96, 4914–4917.

Polivka, T., Pullerits, T., Herek, J. L. and Sundström, V. (2000) Exciton relaxation and polaron formation in LH2 at low temperature. J. Phys. Chem. B, 104, 1088–1096.

Polivka, T. and Sundström, V. (2004) Ultrafast dynamics of carotenoid excited states - From solution to natural and artificial systems. Chem. Revs 104, 2021–2071.

Polivka, T., Zigmantas, D., Sundström, V., Formaggio, E., Cinque, G. and Bassi, R. (2002) Carotenoid S-1 state in a recombinant light-harvesting complex of photosystem II. Biochemistry 41, 439–450.

Pullerits, T., Chachisvilis, M. and Sundström, V. (1996) Exciton delocalization length in the B850 antenna of *Rhodobacter sphaeroides*. J. Phys. Chem. 100, 10787–10792.

Pullerits, T. and Sundström, V. (1996) Photosynthetic light-harvesting pigment-protein complexes: Toward understanding how and why. Accounts Chem. Res. 29, 381–389.

Ricci, M., Bradforth, S. E., Jimenez, R. and Fleming, G. R. (1996) Internal conversion and energy transfer dynamics of spheroidene in solution and in the LH-1 and LH-2 light-harvesting complexes. Chem. Physics Lett. 259, 381–390.

Richter, M., Goss, R., Wagner, B. and Holzwarth, A. R. (1999) Characterization of the fast and slow reversible components of non-photochemical quenching in isolated pea thylakoids by picosecond time-resolved chlorophyll fluorescence analysis. Biochemistry 38, 12718–12726.

Ritz, T., Damjanovic, A., Schulten, K., Zhang, J. P. and Koyama, Y. (2000) Efficient light harvesting through carotenoids. Photosynthesis Res. 66, 125–144.

Scheuring, S., Levy, D. and Rigaud, J.-L. (2005) Watching the components of photosynthetic bacterial membranes and their in situ organisation by atomic force microscopy. Biochim. Biophys. Acta, 1712, 109–127.

Scheuring, S., Seguin, J., Marco, S., Livy, D., Robert, B. and Rigaud, J.-L. (2003) Nanodissection and high-resolution imaging of the *Rhodopseudomonas viridis*. Proc. Natl. Acad. Sci. USA 100, 1690–1693.

Scholes, G. D. and Fleming, G. R. (2000) On the mechanism of light harvesting in photosynthetic purple bacteria: B800 to B850 energy transfer. J. Phys. Chem. B, 104, 1854–1868.

Scholes, G. D., Harcourt, R. D. and Fleming, G. R. (1997) Electronic interactions in photosynthetic light-harvesting complexes: The role of carotenoids. J. Phys. Chem. B, 101, 7302–7312.

Schubert, A., Stenstam, A., Beenken, W. J. D., Herek, J. L., Cogdell, R., Pullerits, T. and Sundström, V. (2004) In vitro self-assembly of the light harvesting pigment-protein LH2 revealed by ultrafast spectroscopy and electron microscopy. Biophys. J. 86, 2363–2373.

Standfuss, R., van Scheltinga, A. C. T., Lamborghini, M. and Kuhlbrandt, W. (2005) Mechanisms of photoprotection and nonphotochemical quenching in pea light-harvesting complex at 2.5A resolution. EMBO J. 24, 919–928.

Stanley, R. J. and Boxer, S. G. (1995) Oscillations in the Spontaneous Fluorescence from Photosynthetic Reaction Centers. J. Phys. Chem. 99, 859–863.

Strickler, S. J. and Berg, R. A. (1962) Relationship Between Absorption Intensity and Fluorescence Lifetime of Molecules. J. Chem. Phys. 37, 814–825.

Sumi, H. (1999) Theory on rates of excitation-energy transfer between molecular aggregates through distributed transition dipoles with application to the antenna system in bacterial photosynthesis. J. Phys. Chem. B 103, 252–260.

Sundström, V., Pullerits, T. and van Grondelle, R. (1999) Photosynthetic light-harvesting: Reconciling dynamics and structure of purple bacterial LH2 reveals function of photosynthetic unit. J. Phys. Chem. B 103, 2327–2346.

Sundström, V., van Grondelle, R., Bergstrom, H., Åkesson, E. and Gillbro, T. (1986) Excitation-energy transport in the bacteriochlorophyll antenna systems of *Rhodospirillum rubrum* and *Rhodobacter sphaeroides*, studied by low-intensity picosecond absorption spectroscopy. Biochim. Biophy. Acta 851, 431–446.

Takaichi, S. (1999) Carotenoids and Carotenogenesis in Anoxygenic Photosynthetic Bacteria. In: H. A. Frank, A. J. Young, G. Britton and R. J. Cogdell (eds.), *Photochemistry of carotenoids*, pp. 39–54. Kluwer Academic Publishers, Dordrecht, The Netherlands.

Timpmann, K., Katiliene, Z., Woodbury, N. W. and Freiberg, A. (2001) Exciton self trapping in one-dimensional photosynthetic antennas. J. Phys. Chem. B 105, 12223–12225.

Timpmann, K., Zhang, F. G., Freiberg, A. and Sundström, V. (1993) Detrapping of excitation energy from the reaction center in the photosynthetic purple bacterium *Rhodospirillum Rubrum*. Biochim. Biophys. Acta 1183, 185–193.

Trautman, J. K., Shreve, A. P., Violette, C. A., Frank, H. A., Owens, T. G. and Albrecht, A. C. (1990) Femtosecond Dynamics of Energy-Transfer in B800-850 Light-Harvesting Complexes of *Rhodobacter sphaeroides*. Proc. Natl. Acad. Sci. USA 87, 215–219.

Trinkunas, G., Herek, J. L., Polivka, T., Sundström, V. and Pullerits, T. (2001) Exciton delocalization probed by excitation annihilation in the light-harvesting antenna LH2. Phys. Rev. Lett. 86, 4167–4170.

van Amerongen, H. and van Grondelle, R. (2001) Understanding the energy transfer function of LHCII, the major light-harvesting complex of green plants. J. Phys. Chem. B 105, 604–617.

van Brederode, M. E., van Stokkum, I. H. M., Katilius, E., van Mourik, F., Jones, M. R. and van Grondelle, R. (1999) Primary charge separation routes in the BChl: BPhe heterodimer reaction centers of *Rhodobacter sphaeroides*. Biochemistry 38, 7545–7555.

van Grondelle, R. and Novoderezhkin, V. I. (2006) Energy transfer in photosynthesis: experimental insights and quantitative models. Phys. Chem. Chem. Phys. 8, 793–807.

van Grondelle, R. (1985) Excitation energy transfer, trapping and annihilation in photosynthetic systems. Biochim. Biophys. Acta 811, 147–195.

Visscher, K. J., Bergström, H., Sundström, V., Hunter, C. N. and vanGrondelle, R. (1989) Temperature dependence of energy-transfer from the long wavelength antenna Bchl-896 to the reaction center in *Rhodospirillum rubrum* and *Rhodobacter sphaeroides* (Wt and M21 Mutant) from 77 to 177 K, studied by picosecond absorption spectroscopy. Photosynthesis Res. 22, 211–217.

Visschers, R. W., Vulto, S. I. E., Jones, M. R., van Grondelle, R. and Kraayenhof, R. (1999) Functional LH1 antenna complexes influence electron transfer in bacterial photosynthetic reaction centers. Photosynthesis Res. 59, 95–104.

Vos, M. H., Rappaport, F., Lambry, J. C., Breton, J. and Martin, J. L. (1993) Visualization of coherent nuclear motion in a membrane protein by femtosecond spectroscopy. Nature 363, 320–325.

14
The Biological Clock and Its Resetting by Light

Anders Johnsson and Wolfgang Engelmann

Abstract: Organisms use various clocks in order to adapt to the daily, tidal, monthly, and annual cycles of the environment. This chapter deals with circadian (daily) clocks and the role light plays in synchronizing them with the 24-hour cycles in the environment. We will first characterize these different clocks, their functions, and their properties (Section 14.1.). Then the effects of light on these clocks are presented (Section 14.2.). In the main part of the chapter the synchronization of the circadian system of several organisms by light is presented: *Synechococcus* and *Synechocystis* are chosen as representatives of cyanobacteria (Section 14.3.), the dinoflagellate *Lingulodinium* as a unicellular alga (Section 14.4.), *Arabidopsis* as a plant (Section 14.5.), the ascomycete *Neurospora* as a fungus (Section 14.6), *Drosophila* as an insect (Section 14.7.), and rodents (Section 14.8.) and humans (Section 14.9.) as mammals. In selecting these examples we want to show the general occurrence of circadian rhythms in almost all organisms and the similarities and differences in the effects of light and the mechanisms of the circadian clocks used by them. We furthermore mention models as important tools to deal with circadian clocks and their synchronization by light (Section 14.10.).

14.1. Biological Clocks

The daily revolutions of the earth around its axis are responsible for day and night and its annual orbit around the sun for the seasons with their fluctuations in daylength and temperature. Most organisms have adapted to these diurnal and annual cycles. The strategies and mechanisms used are partly quite delicate and complicated.

It came as a surprise that photosynthesis and many other processes are, however, *additionally controlled by internal clocks*. Thus, photosynthesis fluctuates not only during the daily light-dark cycle (=LD; LD 12:12 means 12 hours of light followed by 12 hours of darkness; see the List of Abbreviations that precedes the index), but also when the plants are kept under LL and constant temperature (Hennessey and Field 1991). The period length (period for

short) of this rhythmic event is typically not exactly 24 hours, but close to it and therefore called *circadian*. If in the absence of LD and temperature cycles other 24-hour time cues (also called Zeitgeber, German for time-giver) would control the rhythm, it should show an exact 24-hour rhythm. This is not the case, demonstrating the endogenous nature of a controlling clock that is sensitive to light signals.

14.1.1. Spectrum of Rhythms

Endogenous rhythms of organisms are not only tuned to the daily cycle of 24 hours. The range of rhythms found in organisms covers *ultradian* (with periods of several hours to very short ones), *circadian*, and *annual* (with periods of about a year) rhythms. Other rhythms, such as tidal, 14-day, and monthly ones, cope with influences of the moon on the earth, mainly on the water movements of the oceans, and they are therefore found in organisms at the coasts and in the sea. Annual rhythms interact with the day-length changes during the year. They are often synchronized by photoperiodic timing, which is the content of Chapters 15 and 16. There are furthermore rhythms with periods covering several years. The following discussion of the 'biological clock' is restricted to circadian rhythms. Even they are often not just composed of one clock type, but form a "circadian system" consisting of two or more clocks with different properties which are or are not coupled mutually (Panda and Hogenesch 2004).

14.1.2. Function of Clocks

The term "clock" usually implies a time-measuring device or function. For instance, the day length (or night length) can be determined by an organism. Since day length is a function of the time of the year (long days in summer, short days in winter), it can be used to time certain events such as tuber formation or flowering of a plant or breeding of birds and mammals during the most appropriate season (see Chapters 15 and 16). However, a clock can also be used to set a certain temporal order. For instance, the circadian control of our sleep–wake cycle ensures that we rise in the morning and fall asleep in the evening at a preferred time. Food intake and digestion are likewise controlled by this clock and gated to certain times of the day (Forsgren 1935). *The circadian clock will time these events under constant conditions*.

Furthermore, circadian clocks can serve as alarm clocks. They tell the organism important times of the day. For instance, the alarm clocks of insects such as bees allow them to visit the flowers of a plant at the time it offers nectar and/or pollen. From the standpoint of the plant, attracting certain insects is more efficient if timed to their active period. If flowers open at night pollination by moths or bats is facilitated. Evolution has worked on the plant and the pollinator to bring about this delicate interplay controlled by circadian clocks. Alarm clocks might also exist in humans. Some humans are able to wake up at a certain time of the night

without external help by relying on a 'head clock" (Clauser 1954). Although not tested yet, it is likely that this alarm device uses the circadian clock.

Circadian clocks can furthermore be used by insects, birds, fishes, and other animals for orientation using the direction of the sun. They have to take the changing position of the sun during the day into account, and the circadian clock is used as an internal time reference for this *sun compass orientation* (Schmidt-Koenig 1975; Able 1995; Zhu et al. 2005). Some birds fly at night and orient by using a *star compass*, which has to take into account the changing night sky.

14.1.3. Current Concepts and Caveats

In order to understand synchronization of the circadian clocks by light and other time cues, the mechanisms of circadian oscillators have to be known, as well as the photoreceptors and pigments involved in the *entrainment* (light *synchronizes* a clock, the clock is *entrained* by light). The clock mechanisms are currently intensively studied. (See Section 14.3.) The prevailing opinion is that *feedback loops between clock gene products acting on the promoters of their genes are at the heart of these clocks* (Hardin 2005). Transcription and translation are thus involved in modeling the clock.

However, the picture is probably more complicated, and cautions have been raised (Lakin-Thomas 2006b). For instance, these feedback loops might also be elements which are located before the clock mechanism proper (Merrow et al. 1999). There are other cases reported which make it difficult to accept the presently favored concept of a circadian clock mechanism involving nuclear genes. Enucleated *Acetabularia* still has a circadian rhythm of oxygen production (Karakashian and Schweiger 1976), dry seeds of bean plants have been reported to show circadian rhythms in respiration (Bryant 1972), and some enzymes of human erythrocytes fluctuate in a circadian way (Ashkenazi et al. 1975). What is common to the two last-mentioned systems is the complete lack of nucleic acid metabolism. This is an important issue, since several of the recently proposed models of circadian systems use feedback systems in transcriptional and translational events. It might therefore be wise to keep an open eye on alternative mechanisms underlying the circadian oscillators. Of course, there is no guarantee that all circadian clocks use the same mechanism, although their properties are often quite similar.

Proteins could, for instance, be involved in timing mechanisms. We refer to the circadian clock mechanism in *Synechococcus* in Section 14.3. and to a recent report of Meyer et al. (2006) on the *Drosophila* clock (see Section 14.7.3.). Another interesting case is the diapause of embryos in the eggs of silk moths (*Bombyx mori*), which is broken by exposure to low temperature. The duration of the chilling period is measured by esterase A4 complexing with another enzyme, PIN. After 14 days the esterase A4 dissociates from PIN, the conformation of the esterase A4 changes, and it becomes suddenly active. This enzyme is thus a kind of molecular timer (although here not on a 24-hour basis) (Kai et al. 1999).

14.1.4. Adaptive Significance and Evolutionary Aspects of Circadian Clocks

The different functions of circadian clocks just mentioned are surely not the only reasons why they evolved. Winfree (1986) and others have discussed that early in evolution circadian clocks might have served to protect organisms from adverse effects of light. *Circadian timing and light reception might have co-evolved* and even preceded the evolution of specialized photoreceptors. Homologies between pacemaking molecules and ancient photopigments from fungi to mammals suggest an evolutionary link between modern clock proteins and ancient light-sensing proteins (Crosthwait et al. 1997, Sharma 2003, Tauber et al. 2004). However, this is difficult to prove. It would be interesting to know whether primitive eyes contain circadian pacemaker cells. Among vertebrates, retinal clocks seem to be quite ancient (Lamprey et al. 1997).

The adaptive significance of possessing a circadian clock was demonstrated in cyanobacteria by using mutants with different periods in competition with each other and with the wild strain (Johnson et al. 1998, Ouyang et al. 1998), in *Arabidopsis* (Green et al. 2002, Michael et al. 2003), in *Drosophila* (Klarsfeld and Rouyer 1998, Fleury 2000, Beaver et al. 2002, Kumar et al. 2005), and in mammals (DeCoursey et al. 1997, DeCoursey and Krulas 1998). Vertebrates show a wide evolutionary variety in their circadian system. They possess a circadian axis (retina, pineal, suprachiasmatic nucleus) with circadian oscillators. In mammals the pineal as part of this axis does not contain a circadian oscillator. Mammals also lack extraretinal circadian photoreceptors (in the pineal) in contrast to other vertebrates (Bertolucci and Foà 2004). Menaker et al. (1997) discuss a "nocturnal bottleneck" that could have led to the evolution of mammals and their exceptional circadian system.

14.1.5. Properties and Formal Structures of the Circadian System

Besides being found in almost all living beings, from prokaryotes to higher organisms, circadian clocks possess a number of properties. The clocks

- have a period of roughly 24 hours (about 18 and 28 hours in extreme cases) under constant conditions
- are entrainable by time cues (mainly light and temperature changes) to 24 hours
- have a period that is only slightly dependent on temperature (if constant)
- function on the cellular level and are heritable
- are of advantage to the clock bearer

If, for instance, the plant *Kalanchoe blossfeldiana* is kept under constant weak green light conditions, the period of the opening and closing of the four petals of the flowers amounts to 22 hours at a temperature of 22°C. If exposed to an LD 12:12, the flowers open during the light period and close during the dark period. The period of the cycle is now exactly 24 h. Under constant conditions the free

run is 21.9 hours at 15°C, 22.3 hours at 20°C, and 21.3 hours at 25°C (Oltmanns 1960). The differences in period are quite small compared to the influence that temperature normally has on chemical and biochemical reactions.

Mutants of *Drosophila* and other organisms are known which differ in clock properties. For instance, the locomotor activity rhythm of the mutant per[s] has a period of 19.5 hours as compared to 24.4 hours for the wildtype, and the period of the mutant per[1] amounts to 28.6 h. Another mutant (per[0]) is arrhythmic. Any useful model of the circadian system has to take these properties into account and has to offer mechanisms which lead to the long circadian period of about 24 hours, to the low temperature dependence of period, to ways of synchronizing the rhythms to the 24-hour time cues (see Section 14.10.).

14.2. Synchronization of Clocks

A biological clock has to be *synchronized* to the environmental cycle, which amounts to 24 hours in the case of circadian clocks. This is necessary, since circadian clock periods typically deviate slightly from 24 hours. Time cues of the environment are effective for this synchronization. *The LD cycle is the most frequently used time cue*, but temperature rises or temperature drops can also be Zeitgeber. In animals, feeding, social cues, and other signals can synchronize (Mistlberger and Skene 2005, Satoh et al. 2006, Stephan 2002).

The dominant role of light in synchronizing might be due to the high reliability of this Zeitgeber, whereas temperature changes during day and night are less reliable. However, the onset of the light period and that of the dark period do not occur at the same time of the day during the course of the year. During the summer the light period is longer than during the winter, especially at higher latitudes. This fact has to be taken into account by the organisms if light is to be used for synchronization.

Photoreceptors are needed to perceive the light as an input signal for resetting the circadian clocks. Depending on the organism, these receptors can be quite diverse. In many unicellulars, such as yeast or most algae, e.g., the dinoflag-ellate *Lingulodinium*, no special receptor structures have been found. Pigment molecules in these unicellulars are changed by light and a transduction chain resets the clock. In animals the eyes are often used, but in other cases also, or only, extraretinal photoreceptors. For instance, in birds the pineal organ is light sensitive and synchronizes the circadian rhythm if the eyes are obscured or denervated or removed. In *Drosophila* flies, extraretinal structures in the brain (Hofbauer–Buchner eyelet, ventral and dorsal neurosecretory cells) have been shown to serve as additional devices for synchronization.

Photopigments like phytochrome (PHY), cryptochrome (CRY), opsins, and others synchronize circadian rhythms. Properties and functions of these pigments are described under the examples for organisms with circadian rhythms (Sections 14.3.–14.8.). The kind of light effective in clock resetting depends on the kind of pigment. Using varying fluence rates of colored light, action spectra can

be obtained (see Chapter 6) which tell us how many photons of the different wavelengths are needed in order to evoke identical biological effects (see Sections 14.3.–14.8.). The effect of light depends, however, not only on the *wavelength* and *fluence rate*, but *also on the phase of the circadian clock at which the light was given.*

Light or other Zeitgeber entrain the circadian clock of organisms, provided they are applied in a 24-hour cycle or in a cycle close to 24 hours. The *organism is synchronized* with the 24-hour day, and the *Zeitgeber has entrained the rhythm.* Organisms kept under constant conditions without synchronizing time cues of the environment show free run with a period of their circadian rhythm usually deviating from 24 hours. We should now look more closely at this entraining effect of light.

If an organism such as a *Kalanchoe* plant is kept for some days in an air-conditioned chamber with 12:12 hours LD and after the last 12 hours of light transferred to constant darkness, the circadian opening and closing of the flowers will continue to run with its characteristic period going through subjective day and night cycles (*subjective*, since the flowers behave as being in the day, respectively, night phase, in spite of constant conditions). A light pulse either shifts this rhythm or it does not, depending on the phase of the clock at which the pulse is applied. If given before the subjective midnight, the rhythm will be delayed; if given after this point, the rhythm will be advanced. During the subjective day period there is normally a dead zone where a light pulse is without effect on the rhythm. Phase shifts can be plotted in respect to magnitude and direction in a *phase response curve*. These are based on experiments with light pulses administered at different phases, and examples for the locomotor activity rhythm of a Syrian hamster are given in the upper part of Fig. 14.1. The phase response curve is shown in the lower left part. The lower right part is another example and gives a strong and a weak phase response curve of the eclosion rhythm of *Drosophila* flies to light pulses. Details are given in the figure. Photic phase response curves are similar in all mammals, nocturnal as well as diurnal, including humans. However, the amplitude and duration of the advance and delay portion might vary in different species (Rusak and Zucker 1979). This allows one to adjust the phase and period of the circadian clock to the 24-hour day. It is assumed that synchronization of circadian rhythms to an LD cycle is brought about by light effects similar to the light pulse actions, although under normal conditions light is impinging throughout the day phase.

If LD is applied not in a 24-hour pattern, but for instance in a 20- or 26-hour pattern (e.g., LD 10:10 or 13:13), most circadian clocks are still entrained. The *range of entrainment* in which the circadian rhythm of the organism can follow the LD pattern depends on the species and the fluence rate and duration of the light pulse. It usually is between 18 and 30 hours (Enright 1965; Daan 2000).

Circadian rhythms might damp out under certain environmental conditions such as LL and/or DD, at too high or too low temperatures, or after special pulse treatments (see Section 14.10.2.). There is apparently a permissive range allowing circadian rhythms to occur. However, arrhythmicity can also be induced
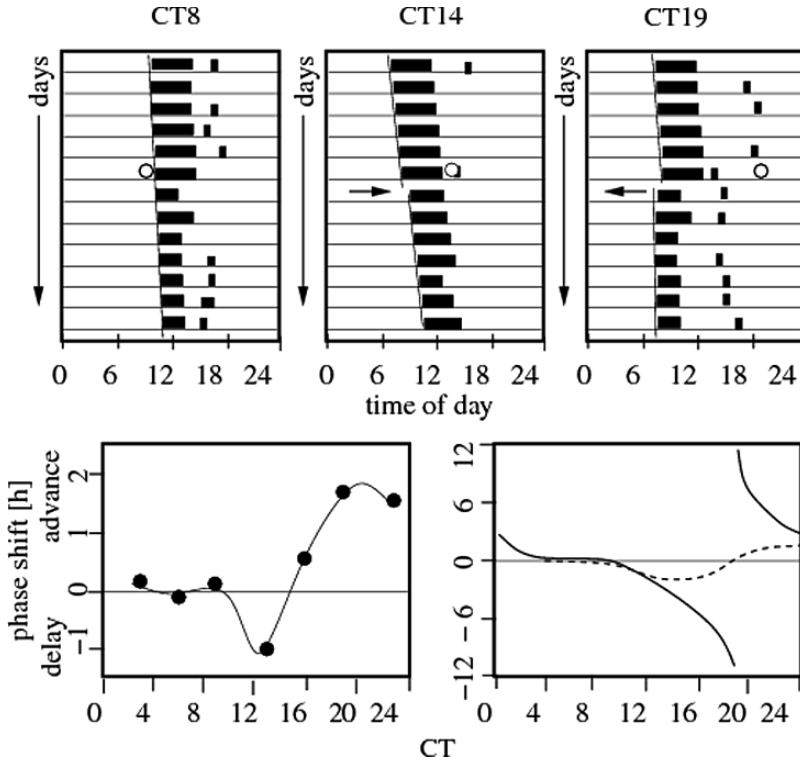
FIGURE 14.1. Phase shifting of the locomotor activity rhythm of a hamster and phase response curves. (Top) Phase shifting effect of brief light exposure at three different phases of rhythm is shown in actograms representing the locomotor activity rhythm of a Syrian hamster. The phases are marked by o on day 6 at CT 8, 14, and 19. No phase shift is observed with the light pulse at CT 8, the subjective day (hamsters are night active). A light pulse at CT 14 delays (→), but a light pulse at CT 19 advances (←) the rhythm. (Bottom left) Plotting these phase shifts results in a response curve which is of a weak type and typical for rodents. Only small phase shifts are then observed even with high fluence rate light pulses. The advance phase shifts (occurring at late night and early morning) are plotted upward, the delay phase shifts (occurring at early night) downward. (Bottom right) Phase shifting effect of light pulses on the eclosion rhythm of *Drosophila* flies (a population rhythm). Cultures of larvae were reared under LD 12:12 cycles and transferred after pupation into weak red light. Portions of the pupae were treated at different times with a short blue-light pulse (0.23 mW/cm^2). The resulting delay respectively advance phase shifts of the eclosion rhythm are depicted as a function of the phase at which the light pulse was administered. The dashed small amplitude curve is a weak phase response curve with phase shifts up to 2 hours only and obtained with short light pulses, the solid large amplitude curve a strong phase response curve with phase shifts up to 12 hours and obtained with longer light pulses. (Original illustration, actograms simplify an illustration by Rea 1998.)

by a special light pulse which is applied around a certain phase. The rhythm disappears after this pulse and the circadian system stays in arrhythmicity until a perturbation (e.g., a second light pulse) of sufficient strength starts the oscillation anew. Experiments on the eclosion rhythm of *Drosophila* (Winfree 1970), the petal movement rhythm of *Kalanchoe* (Engelmann et al. 1978), and the activity rhythm of the *Culex* mosquito (Peterson 1981b,a) revealed that the circadian system could be sent into a nonoscillating state by light pulses. The phase at which arrhythmicity can be induced in these experiments was fairly restricted (subjective midnight point; the strength of the pulse has to be such that it is just between evoking a strong or a weak phase response curve; but see also Section 14.10.2., third item in list).

14.3. Clocks and Light in Cyanobacteria

The simplest organisms known to possess a circadian clock are cyanobacteria. The first studies were by Stal and Krumbein 1985 and the results came as a surprise, because prokaryotes were not thought to be controlled by circadian clocks. Further research concentrated on *Synechococcus elongatus* and *Synechocystis* and was facilitated by using a bacterial luciferase luxAB gene set as a reporter, allowing continuous cooled CCD camera recording of the amount of emitted light from many clones on a solid medium in Petri dishes (Kondo et al. 1993). It allowed monitoring, by low-light-level microscopy, the rhythm and its strong temporal stability in single cells of *Synechococcus elongatus* (Mihalcescu et al. 2004). It turned out that almost every gene and thus the entire metabolism is under circadian control (Liu et al. 1995; see last paragraph of Section 14.3.2.). More than 100 mutants have been selected with altered properties of the clock (Kondo et al. 1994). The results are reviewed in several articles (e.g., Ditty et al. 2003; Iwasaki and Kondo 2004).

14.3.1. Photoreceptors and Zeitgeber

The circadian clock of *Synechocystis* is synchronized by LD cycles and light pulses (Aoki et al. 1997). The rhythm continues if the cultures are transferred to LL or DD conditions, but with different periods: 25 hours under DD, and 22.6 hours under LL. In *Synechococcus* temperature in addition to light entrains the circadian clock, but light has priority over temperature (Lin et al. 1999). An action spectrum of phase shifting light has been determined (Inouye et al. 1998).

Synchronization of this clock by light is thought to occur via the redox state of the metabolism (see Fig. 14.2). The redox state of the plastoquinone pool is sensed by *light-dependent period A* (LdpA): under low light conditions the plastoquinone (PQ) pool is oxidized and LdpA is active. Higher fluence rate inactivates LdpA. LdpA interacts with the clock protein KaiA (Ivleva et al. 2005). The PQ pool affects also the stability of CikA, a protein interacting with LdpA and the Kai clock mechanism; the output element *Synechococcus adaptive*

sensor A (SasA) serves as a primary transducer of temporal information for global gene expression. The current state of the cyanobacterial clock model and the changes of the Kai proteins during the circadian cycle are shown in Fig. 14.2.

The photo-transduction pathways leading to phase shifts and synchronization of the circadian rhythm by light are not yet fully clarified, but *Synechocystis* with its genome entirely sequenced will surely allow us to unravel it. Several candidates for photoreceptors are already known from the sequence of the genome, including the bacteriophytochrome CikA, which seems also to provide light
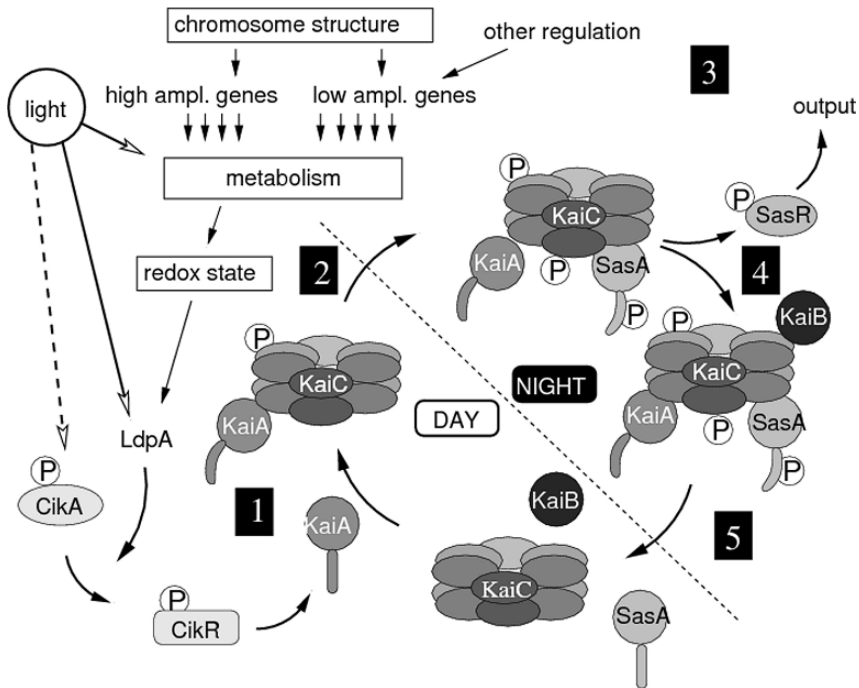
FIGURE 14.2. Model of the circadian clock of cyanobacteria. (1) Light affects metabolism and via plastoquinone the redox state (high light intensities: reduced; low intensities or darkness: oxidized). (Alternatively, light is received by LdpA directly and/or by CikA.) A signal cascade LdpA/CikA/CikR affects the receiver domain (straight tail) of KaiA, which interacts with KaiC, stimulating its autophosphorylation and hexamer formation. (2) In the early evening SasA joins the KaiA/KaiC complex and KaiC stimulates phosphorylation of SasA. Its phosphoryl group is transferred to the response regulator SasR. (3) SasR and other proteins in the output pathway transduce temporal information from the oscillator (the KaiA/KaiB/KaiC complex) to the genome by affecting the chromosome structure (top) and the metabolism via high- and low-amplitude expressing genes (and other regulations). (4) In the late evening KaiB binds to KaiC and dephosphorylates it. (5) Conformational changes of KaiA and SasA due to signal transduction are indicated by the straight or bend tails on the symbols. (Illustration based on several reports cited in the text and on personal information from T. Kondo, Nagoya University, Japan.)

input to the oscillator (Schmitz et al. 2000). Furthermore, a bacterial CRY has been found (Hitomi et al. 2000). Disrupting or overexpressing these genes will allow one to determine whether some of these candidates are involved in the transduction of the light signal to the circadian clock.

14.3.2. Molecular Clock Model and Temporal Orchestration of Gene Expression

The circadian system of cyanobacteria was supposed to consist of a negative feedback loop where the products of a gene cluster of three open reading frames—KaiA, KaiB, and KaiC—influence the transcription of their genes (Ishiura et al. 1998). It turned out, however, that these Kai proteins form a basic timing process of the circadian clock, which, in contrast to the circadian clock mechanisms in eukaryotic organisms, persist even *without transcription and translation* (Tomita et al. 2005). The properties of the circadian rhythm are not ascribed to the *kai promoters*, but to the Kai *proteins*. Specific regulation of the kaiBC promoter is not essential for the oscillation; even an *Escherichia coli*–derived promoter could do, provided the promoter supports sufficient RNA polymerase activity.

The clock mechanism consists of phosphorylation and dephosphorylation of KaiC (which occurs even in vitro with a 24-hour period without damping for at least three cycles autonomously in the presence of the Kai proteins and ATP [Nakajima et al. 2005]). KaiC phosphorylation is the molecular timer for the circadian rhythm in *Synechococcus*. It is proposed to control the expression of genes globally leading to circadian oscillation in metabolism and physiology. How this chemical clock could work was discussed by Naef 2005, and models were proposed by Kurosawa et al. 2006.

The period is mainly determined by the KaiC, since period mutations consist of single amino acid substitutions in the KaiC protein. The periods of the mutants range from 14to 60 hours (Kondo et al. 1994). Together with ATP, KaiC forms a homohexamer (observable under the electron microscope) (Mori et al. 2002; see also Fig. 14.2). KaiC contains two ATP/GTP-binding domains which play an important role in the rhythm generation (Nishiwaki et al. 2000). The histidine kinase SasA interacts with KaiC and is necessary for a robust circadian rhythm (Iwasaki et al. 2000). This simple proteinaceous clock explains also why and how a circadian timing mechanism can function in cyanobacteria with generation times of 8 hours or less (Kondo et al. 1997) and how division can still be gated by the circadian clock (Mori et al. 1996).

The circadian oscillator regulates or influences the whole metabolism, and the circadian oscillator is based on an integration of cellular metabolism (Nakahira et al. 2004). The extensive circadian control of gene expression in *Synechococcus* consists of at least two classes of clock-regulated genes: About 80% of the assayed promoters are active during the day with a maximum near the end of day. In the smaller group, expression has an opposite phase and is maximal at dawn and night when the chromosome is compacted and minimal at dusk. These

genes may encode, for instance, oxygen-sensitive enzymes, and they perform best at night, when photosynthesis is absent. No distinct phase element was found. Instead, chromosome dynamics or DNA topology may be phase determining (Min et al. 2004).

An important question is how this timing mechanism enables global circadian gene expression. The circadian clock seems to regulate the compaction (condensation or supercoiling status) of the chromosome (Nakahira et al. 2004) and controls in this way the access to promoter elements (Smith and Williams 2006).

14.4. Clocks in the Dinoflagellate *Lingulodinium*

Circadian rhythms are also found in unicellular organisms such as algae. *Euglena*, *Chlamydomonas*, and the giant cell alga *Acetabularia* could serve as examples (Roenneberg 1996). The synchronizing and phase-shifting effect of light has been studied particularly in *Chlamydomonas* (Kondo et al. 1991).

The marine dinoflagellate *Lingulodinium* has been used extensively to study the molecular mechanisms of the circadian rhythms and the processes controlled by it (Hastings 2001, Akimoto et al. 2004), but also with respect to light affecting the circadian rhythms (review Roenneberg and Foster 1997). In this alga a circadian rhythm of bioluminescence, of cell division, and of aggregation of the cells has been studied. The bioluminescence consists of two phenomena: a series of flashes caused by a mechanical or a chemical disturbance and a much weaker glow, which is observable in an undisturbed culture. The bioluminescence of the flash rhythm peaks during the middle of the dark period and lasts a few hours only each night. The glow rhythm peaks toward the end of the dark period. Circadian rhythms control other functions at the cellular and molecular level, such as photosynthesis, the tricarboxylic acid cycle (Akimoto et al. 2005), and mitosis.

Under conditions of constant light the bioluminescence rhythm continues in a circadian fashion. The period depends on the illuminance and amounts, under white light, to 24.4 hours at 1200 lux, and to 22.8 hours at 3800 lux with damping of the rhythm. Beyond 10,000 lux the bioluminescence rhythm disappears. In DD the period is 23.0–24.4 hours and the rhythm damps out. The period of the bioluminescence rhythm also depends on the light quality: Under continuous red light it is longer than 24 hours and will increase further in stronger light. Under continuous blue light it is shorter and will further shorten under higher fluence rates (further information and references in Roenneberg and Foster 1997).

As in most other organisms, light is the strongest time cue for synchronizing the *Lingulodinium* rhythms, but nutrients also act as Zeitgeber and interact with light. Light pulses given during weak LL at different phases of the cycle shift the rhythm. The phase response curve is asymmetrical with small delays and larger advances. For day-active organisms this makes sense and allows for a better adaptation to the varying light periods in the course of the year. The action spectrum shows maxima in the blue and red spectral regions: Light around

475 and 650 nm are the most effective wavelength components (Hastings and Sweeney 1960). This could indicate chlorophyll as the responsible photoreceptor. However, this was experimentally excluded for the bioluminescence rhythm. PHY also does not participate in synchronization.

Two photoreceptors influence the circadian system of *Lingulodinium*. One of them responds mainly to blue light and is highly sensitive, inducing strong phase responses and eliciting advance phase shifts during the subjective night (Morse et al. 1994). This receptor is furthermore under circadian control: It is activated after CT 15. The other photoreceptor is sensitive to blue *and* red light, delays the rhythm during subjective day (before CT 15), and does not lead to strong phase shifts even at higher fluence rates. There is furthermore an advance of the rhythm of the bioluminescence by UV, but in contrast to the visible light no delay shifts are induced (Sweeney 1963).

Lingulodinium furthermore exhibits a swimming activity rhythm which is synchronized by LD cycles and is circadian under constant conditions. The rhythm can be followed by measuring the aggregation of the cells. It is under the control of a circadian clock, the *A oscillator*, which is separate from the one controlling bioluminescence, the *B oscillator*. This can be shown under certain experimental conditions where the two rhythms dissociate from each other by exhibiting different periods. The phase shifts brought about by light pulses differ also for these two rhythms: The B oscillator is mainly blue light sensitive, whereas the A oscillator is sensitive to both blue and red light.

The core circadian clock mechanism of this marine alga is not yet understood, but type-1 phosphoprotein phosphatase is involved, as inhibitors of this enzyme and of protein kinases affect period-, phase-, and light-dependent regulation of the circadian rhythms (Comolli et al. 2003).

14.5. Light Effects on Circadian Clocks in Plants: *Arabidopsis*

Arabidopsis thaliana plants are well suited for studying circadian rhythms and their genetic and molecular background (Millar 1999b). Circadian rhythms have been described in leaf movement, elongation of the hypocotyl in seedlings (Dowson-Day and Millar 1999), and the inflorescence stem in mature plants (Jouve et al. 1998), in stomatal aperture (Webb 1998), coordination of metabolism (Kreps and Kay 1997) such as photosynthesis, activity of enzymes, in the expression of a wide variety of genes (overview Millar 1999a, Harmer et al. 2000), in posttranslational rhythms (overview in Màs 2005), in hormone production and responsiveness, and in photoperiodic control of flowering and other developmental steps (see Section 14.5.2. and articles in Lumsden and Millar 1998, Màs 2005, Engelmann 2007). Furthermore, numerous mutants are known, among them quite a number that affect the clock work, clock inputs, and clock outputs. Besides mutants in which the function of the photoreceptors is

affected, others are known in which the *transfer* of the light-induced signals is changed. Such mutants are known both for PHYs and for the blue light receptors.

For continuous recording it was of much advantage to use a construct of the firefly luciferase gene with a promoter of the *cab2* (chlorophyll A/B-binding) gene, which is under the control of the circadian clock (Millar et al. 1995a). The method allows us to monitor circadian rhythms in whole plants as well as in various tissues of the plant by recording the bioluminescence with a sensitive camera. It also makes screening of mutations in the clock easy by looking for aberrant temporal patterns of luciferase expression.

Light is the most important time cue for resetting the circadian clock of plants. Single light pulses delay or advance the clock, depending on the phase of application. Daily LD periods synchronize this clock to the 24 hours of the environment. In LL or DD the clock free runs with periods dependent on light intensity. In plants the molecular basis of circadian oscillations has been studied intensively in recent years and a model has emerged that consists of three interwoven feedback loops composing the clock work, the outputs to the driven processes and clock-controlled genes and the inputs from the entraining time cues, mainly light. Multiple photoreceptors are used by the plants to synchronize the circadian clock and the transduction pathways from light perception to the clock. They are apparently quite closely linked to the clock mechanism. Whereas in animals a hierarchy of clock units with pacemaker centers is the rule, in plants the different tissues and organs are equipped with cellular circadian clocks which are autonomously running and synchronized by the light/dark environment. Plant hormones might serve as coordinators of these local clocks. More details will be presented later.

14.5.1. *Light as the Most Important Zeitgeber*

Light is, as in most other organisms, the most important time cue for synchronizing the circadian rhythms of *Arabidopsis* with the environmental 24-hour day. How this is achieved can be found out by applying short light pulses at different phases of the circadian cycle in plants kept under constant conditions. The rhythm will be delayed by light applied in the first part of the subjective night and advanced by light in the second part of the subjective night. A phase response curve (see Section 14.5.2.) for *Arabidopsis* was published by Covington et al. (2001). Red and blue light shift the phase in a similar way, suggesting that PHY and CRY photoreceptors are involved.

In addition to resetting the phase, light modulates the period of the *Arabidopsis* clock. Period in LL depends on the quality and the fluence rate of the light (Somers et al. 1998). In DD the period is 30–35 hours (Millar et al. 1995b). In continuous white fluorescent light of 100 μmol/m^2/s the period is close to 24 h. With increasing fluence rates the period becomes shorter until at high fluence rates the rhythm is lost. The effect of LL on period has been used in mutants to determine which photoreceptors affect the clock under various light conditions (Devlin 2002).

Nonphotic time cues are also used by the plant. Temperature cycles entrain the clock. Imbibition of seeds sets a circadian clock which is insensitive to light during the first 60 h. From the 36th hour onward light initiates a second rhythm which runs independently of the imbibition rhythm (that is, the outputs, namely CAB2 and CAT2, show the two rhythms superimposed). Light applied after the 60th hour synchronizes the two rhythms (Kolar et al. 1998).

14.5.2. Photoreceptors

Many processes in plants are *directly* affected by light. Multiple photoreceptors measure the quality and quantity of light in the environment. PHYs (Schepens et al. 2004), CRYs (Banerjee and Batschauer 2005), phototropins (absorbing in the UV-A/blue), and an unknown UV-B photoreceptor are used by the plants (Millar 2003, Chen et al. 2004, Wada et al. 2005). This complex system of different photoreceptors with partially antagonistic functions and overlapping action spectra detects different wavelength bands over a wide spectral range.

Whereas photoreceptors and the light-regulated responses including gene expression have recently been intensively studied, the *signal transduction components* are much less known. A large number of signaling components exist, which are affected by external and internal factors. Both genetical and biochemical approaches are used to clarify these transduction pathways and modes (Larner 2005).

Light also affects processes which are *under circadian control* by entraining these rhythms (see Fig. 14.3). The immediate and circadian responses are genetically separable (Anderson et al. 1997). PHYB (PHYTOCHROME B), CRY2, and a UV-B photoreceptor entrain the circadian rhythms (reviews Fankhauser and Staiger 2002, Millar 2004). PHYB is a red-absorbing photoreceptor, and it interacts with the blue-light–absorbing CRY2 (Màs et al. 2000). While PHYA (PHYTOCHROME A) is used for low fluence rate red light and low fluence rate blue light to control the circadian clock, PHYB works at high fluence rates. At low fluence rates of blue light CRY1 controls the phase, and at high fluence rates it influences the period of the clock. A mutant lacking functional PHYs and CRYs is still entrainable by visible light (Yanovsky et al. 2000). This indicates that another photoreceptor besides the PHYs and CRYs is present in *Arabidopsis* and synchronizes the circadian clock to the LD cycle.

The light input pathways to the clock are indicated in Fig. 14.3, but not yet well understood (Fankhauser and Staiger 2002. Millar 2004). According to the PIF3 hypothesis (Nagy and Schäfer 2002), the light-activated (P_{fr}) form of PHYB interacts with PIF3, which leads to photo-entrainment. A further proposal for the pathway of light entrainment involves the ZTL- (ZEITLUPE), FKF- (FLAVIN-BINDING KELCH REPEAT F-BOX) and LOV (LIGHT OXYGEN VOLTAGE)-Kelch protein. They contain a specialized class of PAS domains and are involved in light, oxygen, and voltage sensing. This pathway represses the PHYB/CRY2 signaling to the clock by physically interacting with PHYB. Finally, the PRRs (PSEUDO-RESPONSE REGULATORs) and TOC1 (TIMING
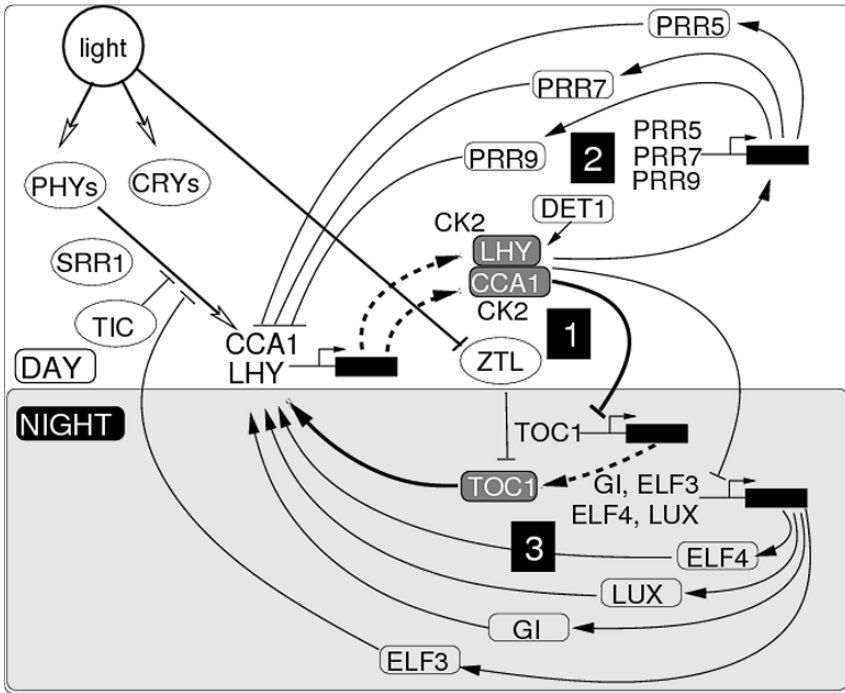
FIGURE 14.3. Molecular composition of the *Arabidopsis* clock and light resetting Genes are indicated by black bars. Three negative-feedback loops (1, 2, and 3 in dark boxes) are interlocked via the two transcription factors (grey boxes) CCA1 and LHY. In loop 1 CCA1 and LHY inhibit their expression (broken arrow) by binding to the promoters of *toc1*. *cca1* and *lhy* are induced by light (via PHYs) and expressed rhythmically. Their mRNA and protein abundance peak at dawn, whereas *toc1*-mRNA peaks at dusk. TOC1 regulates CCA1 and LHY positively (⟶). In loop 2 CCA1 and LHY regulate *prr5*, *prr7*, and *prr9* negatively. PRR5, PRR7, and PRR9 repress toc1. In loop 3 CCA1 and LHY regulate negatively *lux*, *elf4*, and *elf3*. ELF3 serves as a Zeitnehmer by inhibiting rhythmically the PHY inputs to the clock. In addition to transcriptional regulation, posttranscriptional events are involved in the clock work: CK2 phosphorylates CCA1, which is then degraded by proteasomes. ZTL affects the clock by recruiting TOC1 for proteasomal degradation. LHY is rapidly degraded via proteasomes. The upper part of the figure indicates high activities during the day, the gray lower part high activities during the night. (Illustration based on several reports cited in the text.)

OF CAB EXPRESSION) have been linked to light entrainment of the clock mechanism (Màs et al. 2003). But there seem to be additional routes where proteins without chromophores such as TIC (TIME FOR COFFEE) (Hall et al. 2003), ELF3 (EARLY FLOWERING 3), and SRR1 (SENSITIVITY TO RED LIGHT REDUCED 1) interact directly with photoreceptors. Whereas ELF3 functions as a light gate at night, TIC gates the clock at day. The double mutant *tic;elf* is arrhythmic.

The different PHY and CRY photoreceptors interact with each other and show complex responses at different expression levels, localizations, and accessibility to signaling intermediates. This communication between photoreceptors and transduction pathways allows a simultaneous response to two or more environmental parameters (Ahmad 1999, Franklin and Whitelam 2004). The situation is furthermore complicated by rhythmic regulation or *gating* (identical light signals affect the circadian system as a function of the phase at which it is seen) of light input: The clock affects the *phy* and *cry* photoreceptor genes at the level of transcription (Toth et al. 2001), but other types of rhythmic regulation are possible. This feature has been termed *Zeitnehmer* (German for time taker, in contrast to *Zeitgeber*, time giver or time cue).

For entrainment of the clock under natural conditions, the changing day length during the course of the year has to be taken into account. That is, neither dawn nor dusk drives the rhythm, but at least two signals must be used. (For more information see Millar 2003 and Màs 2005.)

14.5.3. Clock Mechanism and Clock-Controlled Genes

The *Arabidopsis* clock consists of autoregulatory feedback circuits which involve transcription and translation of clock genes. In a simplified version three negative feedback loops interlock with two transcription factors CCA1 (CIRCADIAN CLOCK ASSOCIATED) and LHY (LATE ELONGATED HYPOCOTYL). Figure 14.3 shows a current model of it (McClung 2006). Details and the inputs of light and outputs to overt rhythms are shown in the figure (for reviews see Salome and McClung 2005, Màs 2005). This regulated network integrates photoreceptor signals of the environmental light conditions to the clock, thus setting its phase. It further shows the output of the clock information to affect gene expressions. Light affects gene expressions directly and not only via the clock (immediate light effects). There is furthermore a developmental program involved which contributes information to the system. For more information see Màs (2005) and McClung (2006).

Transcription is in many cases controlled by the circadian clock (Piechulla 1999). At least 6% of the *Arabidopsis thaliana* genes are rhythmically expressed, as shown by microarray experiments (Harmer et al. 2000, Schaffer et al. 2001). Many of these genes are related to photosynthesis. They are expressed early in the subjective day, such as the *cab* gene (Millar and Kay 1996). The catalase gene *cat2* is also expressed in the morning (CAT2 is involved in the degradation of H_2O_2), but *cat3* in the late afternoon (CAT3 is probably scavenging H_2O_2 at night [Zhong and McClung 1996]). *cat* 1 does not cycle. This shows that even in one gene family the timing of expression may differ. Other gene expressions occur at the same circadian time such as chloroplastic (rubisco small subunit and rubisco activase), peroxisomal (catalase), and mitochondrial components of the photorespiratory pathway (McClung et al. 2000).

Seed germination (Hennig et al. 2002) and plant growth (Dowson-Day and Millar 1999) is also under circadian regulation. Other genes under circadian

control are related to environmental stress (Kreps et al. 2002). Genes involved in photoperiodic timing allow plants (and other organisms) to respond to the time of the year by using the day length as a key (Hayama and Coupland 2003).

14.5.4. Photoperiodism

Photoperiodic control of developmental steps such as flowering is widespread in plants (Lumsden and Millar 1998, Millar 1999a). Day length is sensed by the plants and, depending on the type—long day (photoperiodic effect occurs under long days), short day (photoperiodic effect occurs under short days), long-short day (photoperiodic effect needs first long-, then short days), short-long day— and on the time of the year, developmental switches such as from vegetative to reproductive are activated. The photoreceptors for perceiving day length (or length of night) for flower induction are PHYs, e.g., in peas (Weller et al. 1997). In Brassicaceae photoreceptors for blue light are involved. There are opposing roles of PHYA and PHYB on flowering by differentially regulating FT (FLOWERING LOCUS T) expression. The signaling occurs via a network of molecular interactions. It differs at short- and long-day conditions, and the environmental temperature can change the importance of the different photoreceptors (Halliday and Whitelam 2003).

Day length is measured in the leaves by a circadian clock. CO (CONSTANS) plays a central role (Putterill et al. 1995). It mediates between the environment, the clock, and the initiation of flowering (Hayama and Coupland 2003). CO-mRNA oscillates in a circadian manner. Under long-day conditions the peak is at the end of day and during the night; under short-day conditions during the night only. Since CO in a long-day plant such as *Arabidopsis thaliana* is stable only in the light and is degraded by proteasomes in darkness, it will accumulate in long days only. If sufficient CO has accumulated, FT-mRNA is produced. Thus, the coincidence of CO and the correct photoperiod (long day in long-day plants) is a key event in the photoperiodic control of flowering (Yanovsky and Kay 2003) and essentially what the external coincidence model requires (Suarez-Lopez et al. 2001).

FT-mRNA is transported from the leaves to the place of action in the apex. FT is a small protein and might also be transported to the apex (Imaizumi and Kay 2006). FT combines at the apex with FD (FLOWERING LOCUS D), which is present there, but inactive without FT. The FT-FD complex initiates reproductive development (flower evocation [Abe et al. 2005, Wigge et al. 2005]). Flower meristem identity genes such as *ap1 (apetala 1)*, *ap2 (apetala 2)*, *cal (cauliflower)*,and *lfy (leafy)* are activated, and flowers are induced according to the ABC (DE) model (Parcy 2005).

The CO-FT interaction is conserved among plants (Griffiths et al. 2003, Izawa et al. 2003). The photoperiodic responses are conferred by the same genetic pathway in the long-day plant *Arabidopsis thaliana* and the short-day plant rice *Oryza sativa*. But the functions differ (Hayama and Coupland 2003). In short-day plants CO is said to inhibit FT. Long dark periods would then promote FT

expression, because CO activity is low. It is not yet known how the switch at the biochemical level works which leads to flowering in long-day plants under long days and to flowering under short days in shortday plants (Cremer and Coupland 2003).

14.6. Fungal Clocks and Light Resetting: *Neurospora*

The ascomycete *Neurospora crassa*, originally thought to be a tropical fungus (see Section 14.6.4.), is nowadays found all over the world. It was used already since the 1950s (Pittendrigh et al. 1959) for studying circadian rhythms. The formation of aerial hyphae and asexual macroconidia (generation cycle in *Neurospora*; see Springer 1993) is under circadian control and can be measured easily by using the bands which are formed while the mycelium grows over the agar surface in "race tubes" (see: http://www.dartmouth.edu/~jdunlap/race_tube.html and http://www.dartmouth.edu/%7Ejdunlap/ for an animation). The period and phase shifts can be determined simply by using a ruler and time markings at the growth front, but more accurate and elaborate imaging methods were also applied (Morgan et al. 2003, Dunlap and Loros 2005).

The circadian rhythm is easily observed in conidiation, but manifested in many other functions. About 10% of the genes of *Neurospora* are clock controlled, allowing modulation of numerous biochemical and physiological processes in a circadian fashion. Pharmacological and genetical approaches have been used in order to unravel the circadian system which underlies overt rhythms such as conidiation (Lakin-Thomas et al. 1990). For an overview of modern molecular biological approaches used in *Neurospora* studies, see Dunlap and Loros (2005).

In the following the circadian system of *Neurospora* and its constituents will be described first (for reviews see Froehlich et al. 2003, Dunlap and Loros 2004, Lakin-Thomas and Brody 2004, Brunner and Schafmeier 2006). Thereafter it is shown how the circadian system is entrained by temperature and light (Liu 2003, Price-Lloyd et al. 2005, Merrow et al. 2006).

14.6.1. The Circadian System of Neurospora

The circadian system of *Neurospora* consists of interwoven negative- and positive-feedback loops made up by a complicated interplay of various factors which affect the expression and function of the core clock components transcriptionally and posttranscriptionally. Phosphorylations and dephosphorylations of clock components ensure the robustness, precision, and entrainment of the circadian system and account for the complexities in rhythmic behavior (Lakin-Thomas and Brody 2004, Bell-Pedersen et al. 2005).

A *transcription–translation oscillator* (TTO) has been proposed which possesses all the formal properties of a true circadian oscillator with light entrainment and temperature compensation. The molecular mechanism has been

studied intensively by several groups (reviews by Dunlap and Loros 2004, Brunner and Schafmeier 2006). The *frq* gene, its mRNA, and product FRQ are essential components and belong to a negative limb of a feedback loop. In this loop *frq* expression is inhibited by the transcription factor WCC (white color complex). Details are given in Fig. 14.4. Briefly, WC-1 (a flavoprotein) and WC-2 assemble to WCC, which binds to clock- and light-responsive elements in the *frq* promoter, thereby activating *frq* transcription. The gene product FRQ, with two kinds of FRQ expressed (Garceau et al. 1997), forms a homodimer (Cheng et al. 2001b). Having reached a certain level, FRQ inhibits WCC activity
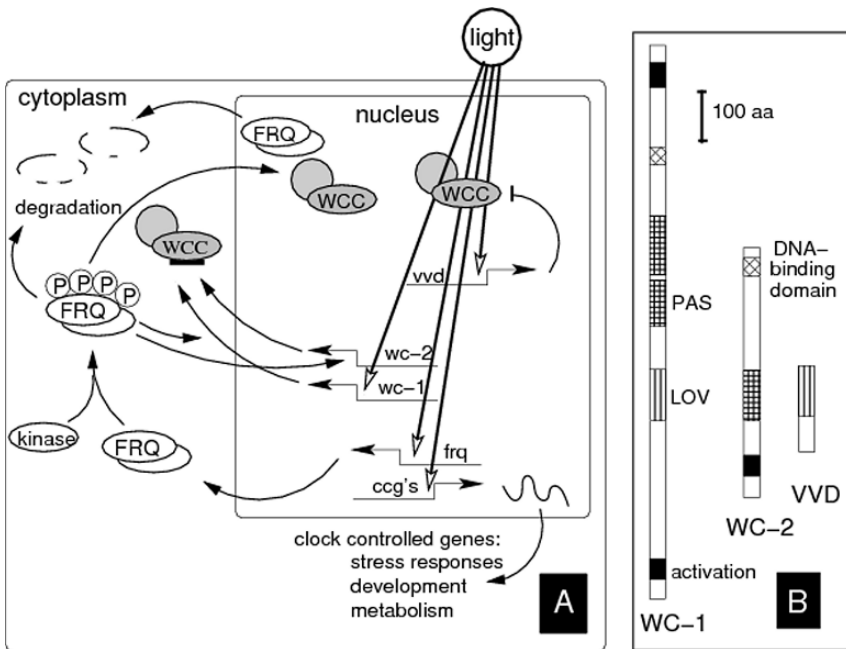
FIGURE 14.4. Circadian clock mechanism in *Neurospora*. (A) Molecular model of circadian oscillation in *Neurospora* and the effects of light upon it. FRQ is synthesized from mRNA and represses WCC in the nucleus. Low concentrations of hypophosphorylated FRQ^P promote phosphorylation and inactivation of WCC. Further accumulation of inactive WCC is supported by high levels of hypophosphorylated FRQ^{PP}. FRQ^{PPP} is progressively phosphorylated and degraded. With decreasing FRQ^{PPP} levels, phosphatases dephosphorylate WCC, which can now bind to the *frq*-promoter and activate transcription. Besides activating the expression of the *frq* in darkness WCC is the main blue light receptor for most light reactions including the entrainment and phase shifting of the circadian clock. It transfers light signals to light-responsive and clock-controlled genes (arrows to *frq* and *ccg*s). VVD modulates WCC. (B) Functional domains of *Neurospora* photoreceptors WC1 and WC2. VVD is another blue light receptor, which modulates WCC and contributes to photoadaptation. (Illustration based on several reports cited in the text.)

by modulating the phosphorylation status of the two subunits WC-1 and WC-2 (Schafmeier et al. 2005). As a result, *frq* transcription cannot be activated by WCC, and FRQ synthesis is inhibited. FRQ becomes, after its synthesis, progressively phosphorylated by kinases (Schafmeier et al. 2006). Phosphorylation destabilizes FRQ, and it is degraded (by proteasomes after ubiquination) during the night (upper part of Fig. 14.4; He and Liu 2005b). The slow phosphorylation of FRQ (several hours) could be due to a balanced activity of several kinases and phosphatases and in turn regulates the FRQ turnover and function on a circadian timescale. It might be independent of transcription/translation, in a similar manner as has been found in KaiC of cyanobacteria (Section 14.3.), but this is not yet known. Having dropped to a low level, FRQ no longer inhibits WCC and *frq* is transcribed again, thus initiating a new circadian cycle. However, the FRQ-WCC feedback loop is more complex. The negative limb as just described is connected with a positive limb, in which FRQ is progressively accumulated in the cytosol and posttranslationally modified by phosphorylation within its PEST-2 region. This supports the accumulation of high levels of WCC (Cheng et al. 2001a). How cytosolic FRQ regulates WCC levels is unknown, but might also change the phosphorylation status of the WCC subunits as it does in the nucleus.

Phosphorylation, ubiquination, and degradation of FRQ are major determinants of period. Distinct types of FRQ, distinguished by their phosphorylation status, mediate nuclear and cytoplasmic functions. Progressive phosphorylation triggers maturation of FRQ from a nuclear repressor towards a cytoplasmic activator (Schafmeier et al. 2006). By comparing the rhythmic behavior of the wild type with frq^0 or wc^0 mutants, this model of the circadian system of *Neurospora* had to be modified and further feedback loops introduced in view of findings where FRQ- and/or WC-deficient mutants could be restored to exhibit robust rhythmicity under certain conditions.

In addition to the FRQ-WCC oscillator there might be a *FRQ-less oscillator* (FLO) which is independent of FRQ and WCC (Lakin-Thomas and Brody 2000, Christensen et al. 2004) and coupled to the feedback loop shown in Fig. 14.4: strains lacking FRQ (e.g., the frq9 mutant) or lacking WC-1 (wc-1 knockout mutant) exhibit circadian rhythms in a choline-requiring strain depleted of choline (Lakin-Thomas and Brody 2000) or if grown on extra-long race tubes. Similar conclusions were drawn from experiments in which farnesol or geraniol was added to the growth medium (Granshaw et al. 2003) or in which the cultures were entrained to temperature cycles (for references see Lakin-Thomas 2006b). Rhythms in gene expression are present in these FLO cases (Bell-Pedersen et al. 2005, Correa et al. 2003). Finally, nitrate reductase induces FLO both under DD and LL conditions (Christensen et al. 2004).

Furthermore, a *FRQ-less oscillator which requires WC* (WFLO) but is independent of FRQ was proposed (Correa et al. 2003, de Paula et al. 2006). This oscillator requires WC-1 and WC-2 for activity. The WC-1 level is rhythmic in the absence of FRQ, indicating that this WC-FLO generates the rhythm of WC-1. The rhythm can be observed under DD and LL conditions. In contrast to

the FRQ-WCC oscillator, its rhythm is apparently not inhibited by high or low light levels. This oscillator and the FRQ-WCC oscillator may interact with each other through their common WC proteins.

A debate is going on about how to understand these oscillators in the context of circadian systems, and four positions were distinguished by Lakin-Thomas 2006a:

The FRQ- and WCC components of the TTO are important for the light input and stability of the rhythm, but the essential oscillator is not identical with it (Roenneberg and Merrow 1998).

The FLO and the TTO are equally important, interact and entrain mutually under normal conditions. In frq^0 only FLO is active and lacks some circadian properties (Granshaw et al. 2003, Morgan et al. 2003).

Several or many FLOs are normally coupled to the TTO, but they do not critically contribute to the circadian rhythm (Pregueiro et al. 2005, Bell-Pedersen et al. 2005).

The TTO is the only significant oscillator for the circadian rhythm; FLOs do not exist, and in frq^0 an unnatural oscillatory state occurs (Pregueiro et al. 2005).

Lakin-Thomas 2006b has discussed the increasing number of anomalous observations that do not fit the TTO mechanism. Rhythmic transcription may participate in input and output pathways and provide robustness to the oscillations. The frq^0 and wc^0 mutants in *Neurospora* are "conditionally rhythmic." She proposes to speak of FLOs in the sense of frequency-less oscillations instead of frequency-less oscillators, to emphasize that the underlying mechanism is not yet known (Lakin-Thomas 2006b). We have shown the TTO (case 4) in Fig. 14.4 but want to point out that the other cases are possible alternatives for the circadian system of *Neurospora*.

14.6.2. *Entrainment of the Circadian System*

Usually light is the strongest time cue for entraining circadian rhythms. However, *Neurospora* is an exception: moderate temperature changes can dominate LD cycles in phase shifting the rhythm (1–2°C are sufficient; Liu et al. 1998). The amount of FRQ depends on the phase of the oscillator and on the environmental temperature. Changing temperature corresponds to shifts in clock time, because the amount of FRQ is immediately changed within the clock mechanism. As is usual in circadian rhythms, the period is only slightly dependent on the environmental temperature. This temperature compensation is due to the ratio and abundance of a small and a large isoform of FRQ, which are expressed in a temperature-dependent fashion (Diernfellner et al. 2005).

Three types of light-induced circadian responses are observed in *Neurospora*: First, LL suppresses the circadian modulation of conidiation, and conidia are now formed all the time. In DD or dim red light, conidiation occurs in a circadian pattern. Second, a single brief pulse of light applied in DD phase shifts the conidiation rhythm either by advancing or by delaying it. An action spectrum

for phase shift of the rhythm shows maximal effects at 465 nm (Dharmananda 1980). A light pulse applied at late subjective day and early subjective night delays the rhythm; a light pulse at late subjective night and early subjective morning advances the rhythm. Third, LD cycles (or periodic light pulses) entrain the circadian clock. In Section 14.6.3. it will be shown how these effects of light—the rhythm annihilating one of LL, the phase shifting one of pulses, and the entraining one—are related in terms of molecular events. The light input pathways are also well understood.

14.6.3. *Photoreceptors of the Circadian System*

Besides the role that WC-1 and WC-2 play in the clock mechanism of *Neurospora* they are also essential for all known light responses. In contrast to plants, *Neurospora* is sensitive to the blue range only and is blind to light beyond 520 nm. The *wc-1* and *wc-2* genes encode the WCC subunits. WCC activates light-induced genes; at least 3% of the genes of *Neurospora* are light inducible, shown by micro-array analysis (Lewis et al. 2002), and they in turn mediate the light responses. In detail, light received by the FAD-associated LOV domain of WC-1 may induce a conformational change, allowing WCC to bind to LREs in promoters of immediate light-induced genes; i.e., induction begins in not more than 5 minutes (Lewis et al. 2002). In the WCC-LRE complex the capacity of WCC to activate transcription is enhanced. At the same time light induces phosphorylation of WCC by kinases, which, with a delay, reduces the affinity of WCC for LRE and thus WCC activity (He and Liu 2005a). This is a critical step for photoadaptation: WCC can only transiently bind to LREs. Once WCC has been photoactivated and inhibited by phosphorylation, it cannot be reused for photoactivation. It takes an hour before newly made WCC can photoactivate genes again, a result known already from experiments using a second light pulse after a first one (Schwerdtfeger and Linden 2001). Phosphorylation also inhibits the binding of the *dark* WCC to LRE and plays therefore an important role in the negative-feedback loop (He and Liu 2005a).

The light-induced activation of genes by WCC also applies for the *frq* gene (Lee et al. 2003): Blue light induces the circadian rhythm, but the double mutant white collar *wc-1* and *wc-2* is blind for it (Russo 1988). Both *wc-1* and *wc-2* are required for the light induction of *frq* (Lee et al. 2000): the WCC binds to the promoter of *frq* and activates its transcription. The promoter contains two LREs, which drive light-induced transcription. Both LREs bind two different WC-1/WC-2 complexes. The smaller complex binds to LREs in the dark and activates *frq* expression in the dark; light exposure reduces its binding. The larger complex replaces the smaller one after light exposure and is responsible for the light-induced activation of *frq* transcription. This light-induced LRE/WC binding corresponds to the light-induced clock resetting (Cheng et al. 2003).

The blue light photoreceptor that mediates binding of the large WCC to *frq* LREs is FAD (not FMN, as discussed in Liu 2003) as a chromophore. It is bound

to a LOV domain of WC-1. A mutant in which the LOV domain is removed does not show light responses (He et al. 2002) and is arrhythmic in LD cycles and in DD. Its circadian clock cannot be entrained by light, but temperature cycles do entrain it. Deleting the WC-1 LOV domain has thus separated the light and dark functions of WC-1.

VVD is another photoreceptor in *Neurospora*. It is not essential for clock function, but modulates all its light responses. In *vvd* mutants light-induced gene expression is elevated (leading, e.g., to higher carotenoid synthesis; the mutants have therefore a vivid orange color), the phase of the circadian clock altered, and light adaptation partially lost. Furthermore, circadian gating of light induction of gene expression is affected in *vvd* (induction is higher in the subjective morning). It turned out that *vvd* is an important negative regulator of light responses. VVD is a small protein composed essentially of a single FAD-binding LOV domain (Heintzen et al. 2001). Its expression is controlled by the circadian clock and an example for a *ccg* that regulates the input to the clock. Its gene is controlled by WCC, and light induces its expression. In the dark VVD expression is absent. In LL it is constitutively expressed at intermediate levels (Elvin et al. 2005). It mediates rapid light adaptation of WCC-dependent transcription. It is localized in the cytoplasm, while WCC is concentrated in the nucleus. VVD is not required for the clock to run in DD (Schwerdtfeger 2003).

There might be further photoreceptors, as suggested by the genome sequence of *Neurospora*. It indicates a putative *cry* gene, two *phy*-like genes, and two genes of the Archean rhodopsin. Their functions are unknown. The finding of Dragovic (2002) that under certain circumstances (high light intensities) the conidiation of *wc2* mutants is still driven by the LD cycle suggests the existence of a WC-independent photoreceptor.

14.6.4. Outputs of the Circadian System and Photoperiodism

The circadian clock–driven macroconidiation consists of a morphological change that needs many new gene products. Other known rhythmic outputs are growth rate, CO_2 production, several enzymatic activities, and lipid metabolism. Screens for *ccg*s were performed in *Neurospora crassa*, and so far over 180 (for functional categories see Table 1 in Dunlap and Loros 2004) have been found by using different methods (for review see Bell-Pedersen 2000).

The circadian system also seems to control photoperiodic propagation and reproduction (conidiation, protoperithecia formation) of *Neurospora crassa* (Tan et al. 2004). Without FRQ a photoperiod cannot be measured, indicating the role of the circadian system in the photoperiodic time measurement. The necessity of a photoperiodic reaction in a fungus isolated mainly from tropical areas can be doubted. However, Jacobson et al. (2004) found strains as far north as Alaska. Pandit and Maheshwari (1994) describe temporal segregation of asexual and sexual reproduction with conidiation in March and perithecia in July.

14.7. How Light Affects *Drosophila*'s Circadian System

The fruit fly *Drosophila* has many advantages as an experimental animal, such as easy rearing and a short generation time. It is well known genetically, and a large number of mutants is available. *Drosophila* is amenable to genetic and molecular methods. For these and other reasons this insect was and is used for studying circadian rhythms, especially *eclosion* of the flies out of the puparium (a case produced in the last larval stage, in which metamorphosis from the larva to the fly takes place) and *locomotor activity* of the adults. Many mutants affecting the circadian clock, the photoreceptors, and the photoreception are known. Therefore, the effects of light on the circadian system could be studied intensively and successfully.

General reviews on the circadian clocks of *Drosophila* (Hall 2002, Hardin 2005), their molecular mechanism (Stanewsky 2002, Hall 2003), and their location and neurobiology (Helfrich-Förster 2003, Helfrich-Förster 2005, Chang 2006) are available. Special reviews on the effect of light on the circadian rhythm and the pathways to the circadian system can be found in Helfrich-Förster and Engelmann (2002) and Ashmore and Sehgal (2003). Jackson et al. (2001) and Park (2002) review some of the output pathways of *Drosophila*'s circadian system.

14.7.1. Circadian Eclosion

After completing several larval stages *Drosophila* forms a puparium in which pupation and metamorphosis into the adult stage takes place. Eclosion from the puparium occurs under the daily LD cycles in a restricted gate only during the early morning hours. A fly which is not yet ready to eclose uses the next gate on the following day. If a culture of *Drosophila* flies is transferred into constant conditions of darkness and eclosion observed, it still occurs rhythmically. This shows that eclosion in a population of flies is not just the response to the onset of light, but under control of a circadian clock.

The eclosion rhythm can be entrained by an LD cycle and shifted by a single light pulse. Therefore light receptors must exist which transfer the light signal to the oscillator controlling eclosion. An action spectrum for phase shifting the eclosion rhythm with a single light pulse shows a broad maximum in the blue (457 nm) and further maxima at 375, 435, and 473 nm. Wavelengths beyond 540 nm are ineffective (Klemm and Ninnemann 1976). The photoreceptors responsible for eclosion are (1) the larval eyes (a pair of Bolwig organs close to the mouth hook, each consisting of 12 light-sensitive cells which are retained in the adult eyelet) using rhodopsin (Malpel et al. 2002) and (2) lateral neurons, LN cells, using CRY (Kaneko et al. 2000). Eclosion of mutants which lack extraretinal photoreception but possess functional larval eyes is still entrained. Mutants lacking CRY *and* the visual system cannot be entrained, but temperature cycles do entrain, demonstrating a functional oscillator system (Malpel et al. 2004).

Whereas the visual sensitivity of the compound eyes of flies reared on a carotenoid-free diet decreases by three orders of magnitude, the photosensitivity of the circadian eclosion rhythm is not affected. Furthermore, the eclosion rhythm of mutants lacking compound eyes is still synchronized by light. The compound eyes in the metamorphosed fly in the puparium are thus not needed to phase shift and entrain the eclosion rhythm. How the circadian signals which control eclosion arise and reach their targets is reviewed by Helfrich-Förster (2005).

14.7.2. *Locomotor Activity Controlled by Several Circadian Oscillators*

Drosophila flies, like other insects, possess a *multioscillatory system* to control different events in a circadian way (Stanewsky et al. 1997). Circadian oscillators seem to be widespread throughout the different tissues and cells: using a construct in which the luciferase gene *luc* is fused to *per* (which is under circadian control), the luminescence of the whole fly, of parts of the fly, and of cultured tissue could be monitored. In DD circadian fluctuations occur. The cultures are synchronized by LD cycles (Plautz et al. 1997), showing that these peripheral oscillators are cell autonomous and photoresponsive. Light entrains these oscillators directly, probably via Cry (see Section 14.7.4.).

However, behavior such as eclosion of the flies out of the puparium and locomotor activity is driven by circadian centers in the brain. In an LD cycle the flies are mainly active during the light period. The locomotor activity rhythm is usually bimodal, showing morning and evening peaks (Helfrich-Förster 2000). In constant darkness the bimodal activity pattern continues, but the period of the rhythm usually deviates from 24 hours, that is, it free runs. In LL the period lengthens with increasing fluence rate. At higher light intensities the flies become arrhythmic.

The clocks controlling locomotion reside in six neuron clusters in the brain consisting of discrete cells of three groups of lateral neurons (LNs, and of three groups of dorsal neurons (DNs) (see Fig. 14.5 and Helfrich-Förster 2002, Helfrich-Förster 2003, Rieger et al. 2006, Shafer et al. 2006). Based on cell-specific ablation (Stoleru et al. 2004), respectively, targeted expression of PER (Grima et al. 2004), it was suggested that the ventral subset of the small LN cells (s-LN$_v$) is responsible for the morning bout, and the dorsal set of LN cells (LN$_d$) for the evening bout, thus providing a neuronal basis for morning and evening oscillators. The two oscillators were thought to be functionally coupled. Two oscillators could allow the fly to adapt to the seasonal changes of day length. A model of Pittendrigh and Daan (1976) predicts that the morning oscillator (M) has a shorter, the evening oscillator (E) a longer free-run period in constant light (Daan et al. 2001).

This was indeed found (Yoshii et al. 2004). However, it is more complicated than expected: Under constant light the two rhythms dissociate from each other, and a long period component started from the E-activity bout. But a short period component originated not exclusively from the M-activity bout, but additionally
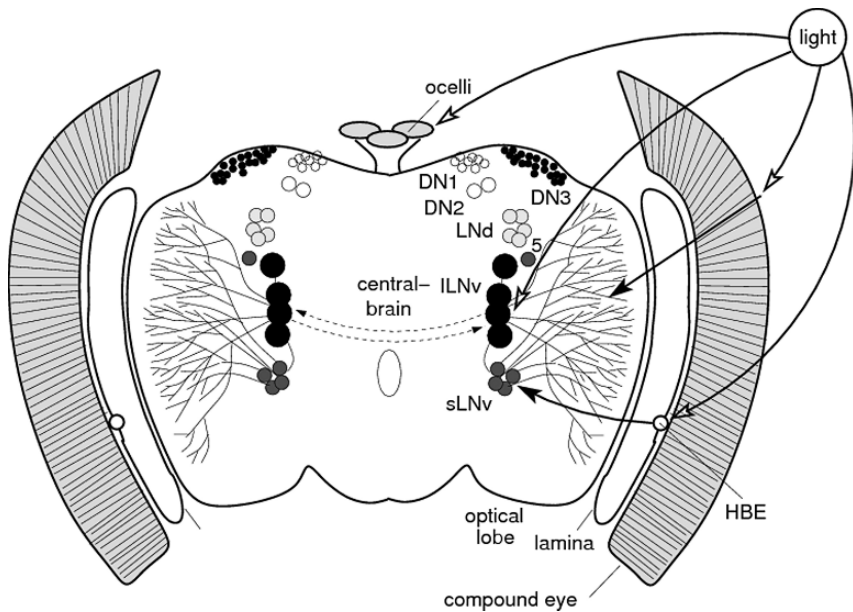
FIGURE 14.5. Photoreceptors and neuronal clockwork of *Drosophila*. Looking toward the front of the brain from the neck, rhythm-relevant neurons and photoreceptors are shown. Synchronizing light is received by the compound eyes, the Hofbauer–Buchner eyelets (HBE), ocelli, and ventrolateral neurons (LN$_v$). The LNs are deep brain cells and consist of the smaller sLN$_v$ (dark grey) and the larger lLN$_v$ (black). The smaller ones control adult circadian behavior: They project to dorsolateral neurons (LN$_d$, light grey) and to dorsal neurons (DN1, small circles, DN2, larger circles, DN3, small dark), which are other clock-gene expressing cells. The lLN$_v$ cells also project to the contralateral side across the midline of the brain in the posterior optical tract. And finally they project with highly ramified neurites to the optic lobes. The sLN$_v$ cells (except the fifth) and lLN$_v$ cells secrete the pigment dispersing factor PDF into the hemolymph in a circadian pattern. (Illustration based on teaching material kindly provided by C. Helfrich-Foerster.)

and even more prominently from the E-activity bout. Thus, there is not a pure M-oscillator, but a main-oscillator with an M and an Ecomponent (the period of both shortened by light) and an Eoscillator (the period lengthened by light). The oscillators responsible for the M bouts (*short* period) have been traced to four PDF (pigment-dispersing factor)-positive sLN$_v$ cells, the oscillators responsible for the E activity (*long* period) to the fifth PDF-negative sLN$_v$ and an extraordinary LN$_d$ cell. These two sets seem to desynchronize internally under the input from the compound eyes because the light signal shortens period in one set and lengthens it in the other set of cells (Rieger et al. 2006). The M-activity bout is more clearly expressed under LD cycles with moonlight (weak light of 0.25 μW/m^2) during the night. The photoreceptors in the compound eyes responsible for the lengthening respectively shortening of the period adequately time the E- and M-activity bouts in the changing day lengths during the seasons (Rieger

et al. 2003). M and Ecomponents are also involved in the circadian system of mammals (see Section 14.8.1.).

Adult activity rhythms can already be entrained by light applied in the first larval stage. The clock is apparently running at that time and throughout larval and pupal development and is resettable by light (Sehgal et al. 1992). It has been discussed whether two different clocks control eclosion and locomotion rhythm, since the periods differ (Engelmann and Mack 1978). The molecular mechanism is in both cases the same, but the downstream mechanisms differ. Some of the pacemaker cells exist in the larval stages, and others develop halfway through metamorphosis (Helfrich-Förster et al. 2006). It is known that the period depends on the group of neurons involved.

14.7.3. Mechanism of Circadian Clock

The circadian oscillators which control activity and eclosion are supposed to consist of a molecular feedback loop. It is generated by interactions of several *clock genes*, the products of which activate or repress transcription, alter the stability of proteins or degrade them and change subcellular localization. Transcription is *activated* by the transcription factors Clock (Clk), Cycle (Cyc), and PDP1 (PAR DOMAIN PROTEIN 1). Transcription is *repressed* by PER, TIM, and VRI. Protein *stability* and subcellular *localization* depends on the kinase Dbt, CK2 (CASEIN KINASE 2), Sgg, and PP2a. Slmb targets phosphorylated PER for degradation in the proteasome. Which role these components may play in each circadian oscillator cell of *Drosophila* is shown in Fig. 14.6.

Recent results (Meyer et al. 2006, Cyran et al. 2005) from experiments in which the FRET of PER and TIM (tagged with two different fluorescent proteins) was measured in single cells show that PER and TIM bind rapidly in the cytoplasm and accumulate in foci. After 6 hours the complexes abruptly dissociate, and PER and TIM move independently and rapidly into the nucleus. This speaks in favor of a timer in the foci, perhaps similar to the circadian timing in *Cyanophyceae* (Section 14.3.).

In this connection it should also be mentioned that in many insects PER is not found in the nucleus, and thus cycling of per mRNA might not always be necessary for PER cycling. Instead posttranscriptional mechanisms might be involved and the negative feedback of clock proteins on their own expression could be optional (Helfrich-Förster 2005).

14.7.4. Photoreceptors for the Entrainment of the Locomotion Clock

Drosophila uses several photoreceptors for entraining its circadian system. The rhythm of activity in adult flies can be entrained by (1) the compound eyes and (2) ocelli as *external photoreceptors* and by the (3) Hofbauer–Buchner eyelets behind the compound eyes (Helfrich-Förster et al. 2002, Veleri et al. 2006) and (4) LN_v and DN neurons in the brain as *internal photoreceptors* (see Fig. 14.5

FIGURE 14.6. Model of the circadian *Drosophila* clock. The model is based on a feedback loop involving transcriptional and translational events in the pacemaker cells. The feedback loop has the following structure: CLK and CYC are transcription factors. They form heterodimers and bind to an E-box in the promoters of the *per* and *tim* genes (and clock controlled genes *ccg*) in the nucleus activating the transcription of *per* and *tim*. mRNA levels increase to high levels early in the evening. The proteins PER and TIM reach with a lag maximal levels in late evening. Degradation of PER by PP2A is counteracted by rapid binding of PER and TIM in the cytoplasm and accumulation in foci. After 6 hours the complexes abruptly dissociate; PER and TIM move independently and rapidly into the nucleus. DBT and SGG in the cytoplasm interact with nuclear entrance or phosphorylate PER and destabilize it. In the nucleus PER and TIM repress their own transcription by directly interacting with CLK-CYC transcriptional activators. TIM and PER are phorphorylated and degraded. This stops transcriptional repression at the end of the circadian cycle. Due to the lag between mRNAs and proteins, and due to the 6-hour timer in the PER:TIM complex (see ! in figure), this negative feedback results in a stable cycling in per and tim mRNA and protein levels. Entrainment of the clock functions by light effects on the blue-sensitive CRY. It stimulates CRY:TIM interaction, which triggers TIM degradation and prevents PER:TIM binding. TIM is phosphorylated, ubiquinated, and degraded in proteasomes. Other photoreceptors (rhodopsin; see text) and their interaction with the molecular gears of the clock are not shown. (Illustration compiled from several reports cited in the text.)

and reviews by Helfrich-Förster et al. 1998, Rieger et al. 2003). Whereas in (1), (2), and (3) rhodopsins serve as the photopigment, in (4) and (5) it is CRY (Klarsfeld et al. 2004). However, flies with nonfunctional CRY can still be synchronized. The locomotor activity of mutants which lack compound eyes and ocelli can still be entrained by LD cycles. But compound eyes increase sensitivity of circadian photoreception (eyeless flies [*sine oculis*] are less sensitive to light by 2 orders of magnitude) and broaden spectral sensitivity (eyeless flies show a more narrow action spectrum as compared to the wild type and red light has no effect).

Why do *Drosophila* and other organisms use multiple photoreceptors for setting their circadian clocks? There are several reasons (Roenneberg and Foster 1997, Foster and Helfrich-Förster 2001):

Natural LD cycles do not simply consist of light steps. Instead, light is increasing and decreasing slowly during the twilight of the day. If organisms use certain light intensities during twilight, the day length can be measured accurately and reliably, and independently of daily weather conditions.

During twilight at dusk and dawn not only the intensity of light changes, but also its spectral composition. Different qualities of the environmental light can be used by a set of different photoreceptors.

Entraining by dawn and dusk is more effective than lights-on/off programs in all animals tested so far, including humans (Fleissner and Fleissner 2001). The signal-to-noise ratio is reduced if several inputs are used.

If the feedback loop described before is indeed the basis of the circadian rhythm, it must explain the following points:

attenuation of the rhythm by LL
phase shifting by light pulses
entrainment by LD cycles

According to the model (Fig. 14.6), all these effects are achieved through light-dependent degradation of TIM. LL keeps the TIM level permanently low. Because cytoplasmic PER is degraded if not protected by TIM, its level is low, too. *per* and *tim* mRNA remain at a medial level. Therefore, under LL the clock genes and proteins do not oscillate. This explains point 1.

Delaying and advancing phase shifts of the rhythm by light pulses are brought about in the following way: If a light pulse hits during phases of the rising TIM concentration, TIM is reduced before it enters the nucleus and builds up again after the end of the pulse. The following peaks in TIM concentration are thus delayed (see Fig. 14.5). If the light pulse hits at peak TIM concentrations or afterward, the degradation of TIM is enhanced and the subsequent buildup is earlier. Thus the following peaks in TIM are advanced. This explains point 2.

The entrainment by LD cycles is the result of advancing and delaying phase shifts. They will keep the circadian oscillation in a certain phase relationship to the LD cycle. This explains point 3.

Thus, the model can explain the three light effects mentioned. There is also experimental evidence: TIM degradation induced by light pulses can be measured

in the LN cells (see Fig. 14.5). It correlates well with the amount of phase shifts of the activity rhythm elicited by light pulses. Furthermore, the spectral response curves for TIM degradation and for phase shifts of the activity rhythm display a maximum between 400 and 450 nm (Suri et al. 1998). This shows that both events are causally related. TIM also degrades in the absence of PER (i.e., no functional clock). Finally, TIM degradation does not depend on functional compound eyes (even without functional CRY). This implies that the clock can be reset by an extraretinal pathway. All these results indicate that TIM degradation is crucial in circadian light perception.

TIM is not light sensitive by itself. The light signal must be transduced on its way to TIM. The blue- light–absorbing photo-pigment DCRY is one of the responsible factors. CRYs are flavoproteins (see review by Green 2004) and the absorption spectrum corresponds to the action spectra of the light effects on the *Drosophila* rhythm (Sancar 2000). Photochemical changes in the chromophore allow CRY to interact with TIM in the cytoplasm and the nucleus. Light changes the conformation of CRY, which allows it to enter the nucleus and to interact directly with the TIM/PER complex. From now on the complex is no longer able to participate in the negative-feedback loop (Ceriani et al. 1999). Degradation of TIM is thus a consequence of CRY blocking PER/TIM formation and not the first step in phototransduction.

Transcription of *cry* is clock-controlled, but the CRY protein level is controlled by light and independent of the clock molecules (Egan et al. 1999, Ishikawa et al. 1999). The gene dose correlates with the phase shifting of the activity rhythm by light: a low-dose phase shifts slightly, overexpression of *cry* shifts strongly (Emery et al. 1998). At higher light intensities the system is saturated, because CRY exceeds a certain level. The overexpression is more pronounced in the phase-delaying part of the cycle because the level of CRY is rather low and can be increased considerably by overexpression. At the phase-advancing part of the cycle, CRY is already close to its maximal level and almost saturated. Therefore, none or only small behavioral responses are found. In the delay zone the phase shifts with low light fluence rate pulses (high fluence rate pulses saturate!) should therefore be more pronounced than in the advance zone due to the different levels of available CRY. This was found experimentally in behavioral studies in the eclosion rhythm, but interpreted wrongly (Chandrashekaran and Engelmann 1973).

In both cases CRY leads to TIM degradation via tyrosine phosphorylation (Naidoo et al. 1999). CRY is thus an important player in circadian photoreception. The second kind of important players in circadian photoreception are the compound eyes. However, it is still unknown which intracellular transduction pathways lead to the degradation of TIM after the light signal has been transmitted to the circadian pacemaker neurons. The entrainment of the circadian clock is completely abolished in *glass/cry*[b] double mutants, which lack CRY and all external and internal eye structures. They free run in LD cycles because they are blind to it (Helfrich-Förster et al. 2001).

14.8. Light and Circadian Clocks in Mammals

Among vertebrates, mammals are the best studied class with respect to the circadian timing system. For experimental reasons rodents have been favored (easy rearing, small size, short generation time, simple recording of locomotion), and among these mice and rats are preferred because many mutants are available and genetic and molecular biological methods are applicable.

Locomotor activity is most frequently measured as a hand of the circadian clock by offering running wheels to the animals which activate a switch by turning the wheel. The contacts are used to construct *actograms* (e.g., Fig. 14.1 top), which allow easy determination of the period and phase shifting of the rhythm induced by different treatments. Body temperature can also be monitored with special implanted sensors. Recently more direct methods were used for following the course of the clock such as melatonin excretion (see Section 14.8.3.) or expression of clock genes or clock-driven genes. The photic entrainment of these rhythms is treated in Section 14.8.4. We should first have a look at the pacemaker center driving these rhythms.

14.8.1. SCN and Its Incoming and Outgoing Pathways

As in other vertebrates, a center of circadian control lies in the paired *suprachiasmatic nucleus* (SCN) of the anterior part of the hypothalamus at the ventral part of the third ventricle above the optic chiasma (Fig. 14.7). As a master oscillator it controls almost all aspects of physiology and behavior (Klein et al. 1991), including locomotor activity, the sleep–wake cycle, thermoregulation (Ruby et al. 2002; Kräuchi et al. 2006), torpor (Heller and Ruby 2004), hibernation (Ruby 2003; Heldmaier et al. 2004), functions of the circulatory and gastrointestinal system (Gachon et al. 2004), and many endocrine events (Vollrath 2002). The synthesis and secretion of melatonin are also controlled by the SCN (see Section 14.8.3. and Simonneaux and Ribelayga 2003). If these nuclei are destroyed, the circadian control of all these events disappears.

The SCN is not just a tissue that transfers information about the LD cycle from the eye to an oscillator. If this were the case, its destruction would have prevented *synchronization* of the various circadian rhythms, but the *rhythms* would not have disappeared: free run should have occurred instead. However, the animals become arrhythmic. There is further evidence for the SCN playing a master oscillator role shown by rhythmic metabolic, electrophysiological, and molecular assays in organotypic slice cultures (in which the dorsal/ventral architecture is preserved [Klein et al. 1991, Silver and Schwartz 2005]). A particular strong piece of evidence is that neural grafts of fetal SCN reestablish the circadian rhythms in SCN-lesioned arrhythmic recipients with the characteristic properties of the circadian pacemaker of the donor (Ralph et al. 1990, Silver and Moore 1998).

The structure and function of the mammalian SCN has been reviewed by Gachon et al. (2004), Silver and Schwartz (2005), and others. In the paired SCN
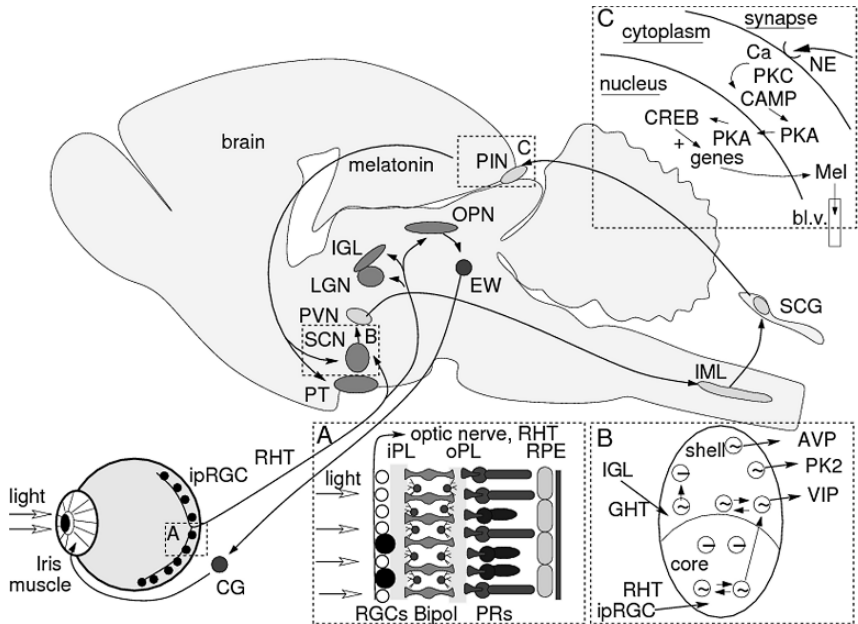
FIGURE 14.7. Circadian centers of mammals and important pathways. Light enters the circadian system in the brain via the eye (bottom left and insert A) and signals reach the SCN (main figure and insert B). The pineal (PIN) is depicted in the main figure and in insert C. The environmental L/D conditions are received by intrinsically photosensitive retinal ganglion cells (ipRGC, dark circles in inset A; light circles are nonphotosensitive RGC cells) and the information is sent to the SCN via the RHT. The signals are received by pacemaker cells (circles with ~) in the core of the SCN, which are entrained by these signals and by mutual interactions: right-left arrows). They synchronize pacemaker cells in the shell of the SCN, which interact with each other (right-left harpoons) and with nonpacemaker cells (circles with -). They communicate with target tissue/organs via substances like AVP (arginin vasopressin), PK2 (protein kinase 2), VIP (vasointesitnal protein), and others. Signals from the SCN reach the pineal (PIN) via sympathetic inner-vation with synapses in the PVN, IML, and SCG. Insert C shows part of one pinealocyte where the signals trigger, via norepinephrine (NE), the release of melatonin (Mel) into the blood vessels (bl.v.) of the brain. The signal cascade involves Ca^{2+} and PKC, which increase cAMP. PKA phosphorylates CREB in the nucleus, activating genes involved in melatonin synthesis. Melatonin reaches via the blood different targets, among them SCN cells and cells of the pars tuberalis (PT; main figure), both of which contain numerous melatonin receptors. The PT controls photoperiodic events. Another direct target of the ipRGC in the retina is the olivary pretectal nucleus (OPN) linking the papillary light reflex via EW (Edinger-Westphal nucleus), CG (Ciliary ganglion), and the iris muscles. (Illustration based on several reports cited in the text.)

of mammals about 8000–10,000 neurons are found. They form a heterogeneous cell population consisting of two parts—a core and a shell—which are charac-terized by their innervation and by the nature of the neurotransmitters of their

neurons (reviewed in Reuss 2003, Meijer and Schwartz 2003). However, the division of SCN in core and shell is debated (Morin and Allen 2006). A functional meaningful division seems to depend on the species, the criteria (e.g., neuro-transmitters), and the phenomena (e.g., resetting or morning-evening oscillators).

Using mutants and molecular biological methods, the genes composing the clock of mammals and their interactions have been studied. A molecular model was proposed consisting of four clock genes: *Cry1*, *Cry2*, *Per1*, and *Per2*. These encode repressors (negative components of the feedback loop), which are activated by the positive acting elements CLK and BMAL1 (see, however, DeBruyne et al. 2006). PER/CRY forms a hetero-polymeric complex. The repressors inhibit their transcription by feedback, time delay, and interactions with transcription factors. (For details see Gachon et al. 2004, Albrecht et al. 2004.)

The molecular oscillators in the SCN influence the membranes and ion channels of the neuronal cells by a second messenger system(s), which leads to circadian firing rates. In order to find out how this occurs, various electrophysiological techniques were applied to individual SCN neurons and to SCN *slices* (discussed in Schaap et al. 2003), which allows longer monitoring of a localized subpopulation of SCN neurons and testing of the effects of chemicals. Newer methods use organotypic slices (see above) from transgenic mice expressing a luciferase reporter driven by a clock gene promoter (Yamaguchi et al. 2003). Also, a short half-life green fluorescent protein reporter driven by a clock gene promoter can be monitored through time-lapse imaging (Quintero et al. 2003). These methods reveal the heterogeneity of the SCN. *Horizontally* cut slices showed two distinct oscillating components (Jagota et al. 2000), which might reflect the activity of *morning* and *evening oscillators* (Jagota et al. 2000, de la Iglesia et al. 2004) inferred earlier from behavioral studies (Pittendrigh and Daan 1976). Photoperiodic reactions are supposed to use such evening and morning oscillators, and a long and a short photoperiod do indeed affect the morning and evening peaks of the electrical recordings differently (Jagota et al. 2000; see Section 14.8.3.).

How the circadian oscillators in the SCN control the locomotor activity is unknown. Of the other outputs of the SCN, only the projections to the pineal organ are well known (see Section 14.8.3.). The synthesis and secretion of melatonin is also controlled by the SCN (see Section 14.8.3. and Simmoneaux 2003). If these nuclei are destroyed, the circadian control of events disappears. However, some rhythms are still maintained, such as the anticipatory food uptake behavior (Stephan et al. 1979, Mistlberger et al. 1996, Marchant and Mistlberger 1997). These must therefore be controlled by another pacemaker center. It is firmly established that the retina of the eye contains circadian pacemaker cells (see Section 14.8.4.).

14.8.2. Circadian Photoreceptors in the Retina

The circadian clock of mammals is synchronized mainly by the LD cycle of the environment. Light *pulses* can shift the phase of the circadian rhythms by inducing phase delays during the early night and phase advances during the late night.

Phosphorylation events are involved in delays as well as in advances (for details see Golombek et al. 2004). The synchronizing light is perceived via the eyes: Enucleated rodents cannot be synchronized by an LD cycle but show instead free run (Meijer et al. 1996). Rods and cones are not required (see, however, Dkhissi-Benyahya et al. 2006). Instead, a small subset of intrinsically photosensitive retinal ganglion cells (ipRGCs) in the inner nuclear layer of the retina function as autonomous photoreceptors (Warren et al. 2003, Husain 2005; for history, see Plachetzki et al. 2005) and are independent of the visual retinoid cycle (Tu et al. 2006). They use melanopsin (Brown and Robinson 2004, Isoldi et al. 2005, Kumbalasiri and Provencio 2005, Peirson and Foster 2006), found in all vertebrate classes, and with structural similarities and high sequential homologies to opsin (however, melanopsin uses its own regeneration mechanism, acting largely independently of the visual system). It seems to be a bistable pigment as used by invertebrates for vision with an intrinsic regeneration mechanism and resistant to bleaching (Lucas 2006). Whereas the opsin-containing rods and cones of the outer retina mediate vision, these ipRGCs are not involved in image formation, but responsible for the regulation of circadian rhythms for immediate melatonin suppression and for pupil reflexes to light. The ipRGCs are found within a large sampling area across the entire retina (Moore et al. 1995), form a network consisting of 0.2–0.8% of all ganglion cells in the human retina and arborize broadly throughout the entire inner retina layer (Hannibal et al. 2002). They are specialized to detect average illuminance of the day and integrate it over long intervals. Heterologous expression of human melanopsin in a mouse cell line (Neuro-2a) renders these cells photoresponsive (Melyan et al. 2005). Whereas mammals have just one melanopsin (Opn4m), fish, birds, and amphibians possess two—Opn4m, Opn4x (Bellingham et al. 2006).

The ipRGCs regulate not only circadian timing, but also masking behavior (Mrosowsky 1999), light-regulated melatonin secretion, and the pupillary light reflex. Mice in which the melanopsin gene has been ablated in the retinal ganglion cells lack the pupil reflex to light, do not phase shift the circadian rhythm when illuminated with light pulses, and period is not increased under LL conditions. Mice lacking rods and cones show an action spectrum for phase shifting the locomotor activity rhythm identical to that of the pupil light reflex and to that of ipRGCs. Mice lacking rods, cones, and the melanopsin gene, but with otherwise intact retina, do not show the pupil reflex, are not entrained by a LD cycle, and lack masking light responses. Thus, the rod–cone and melanopsin systems together provide all the light input for these accessory visual functions (Hattar et al. 2003).

The light information is transmitted from the ipRGCs through the monosynaptic retinohypothalamic tract (RHT, Fig. 14.7, and Berson 2003, Brainard and Hanifin 2005) to the clock cells, using the neurotransmitter pituitary adenylate cyclase-activating polypeptide (PACAP) and glutamate (Hannibal 2006). There are two further neuronal inputs to the SCN: the geniculo-hypothalamic tract (GHT) leading to the shell and other parts of the SCN (Hattar et al. 2006), and the midbrain raphe projection (anatomy and function; see Hannibal and Fahrenkrug 2006). Serotonin is an important regulator of circadian phase, probably by inhibiting the release of glutamate, and by modulating GABA-mediated chloride

channel activity (Bradbury et al. 1997): Light effects in the SCN are partly transmitted by GABA (an inhibiting neurotransmitter), and GABA pulses at different phases lead to phase shifts of the circadian firing which correspond to the one of light pulses (Albus et al. 2005). Some of the neuropeptides in the SCN serving as transmitters or modulators under LD and DD conditions (vasopressin, somatostatin) show marked circadian rhythms. They are restricted to the "core" of the SCN, which mediates the rhythm to other parts of the brain. Other neuropeptides show rhythms under LD, but not under constant conditions. They are found in the ventrolateral part ("shell") of the SCN and convey information on environmental light conditions to the pacemakers (Inouye 1993). Neurotransmitters of the core are VIP, those of the shell AVP. VIP is not only an important coupling agent in the SCN (similar to PDF in insects), but also seems to be important for maintaining the rhythms in clock genes (experiments with VIP and VIPreceptor knockout mice; e.g., Maywood et al. 2006, Aton et al. 2005, Michel et al. 2001). There is mounting evidence that the molecular machinery is not as self-sustained as it has been assumed, but that it requires some sort of feedback from the membrane. If one interferes with membrane excitabiltity (e.g., Nitabach et al. 2005) in *Drosophila* and/or manipulates calcium in rats (Lundkvist et al. 2005), the machinery can stop.

Intercellular communication in the SCN is dominantly by GABA, but additional nonsynaptic communication is found (e.g., glia, astrocytes, prokineticin). The ipRGCs project not only to the SCN, but also to other nonvisual nuclei such as the IGL, OPN, preoptic nuclei, and subparaventricular zones (Gooley et al. 2003).

Two distinct kinds of molecules synchronize the circadian rhythm in the SCN cells after light exposure of the retina (reviewed by Rea 1998): *immediate early genes* such as transcription regulator proteins and furthermore *nitrogen monoxide*. Both seem to play a role in the transfer of light-induced signals in the SCN. Nitrogen monoxide production is required for light-induced phase shifts of behavioral rhythms under circadian control.

Under conditions of constant darkness, the circadian rhythms are maintained by the pacemaker cells of the SCN. But the eyes, which also contain autonomous circadian pacemakers (see Section 14.8.4), can also modulate circadian rhythms in the SCN even in the absence of light. Removal of the eyes abolishes an endogenous circadian rhythm within cells of the SCN, suggesting that specific rhythms of the SCN are driven by input from the eyes. However, removal of the eyes can also amplify a normally dampened endogenous circadian rhythm within the SCN. Thus, the eyes can suppress the expression of specific rhythms within the SCN while promoting others (Beaule and Amir 2003).

14.8.3. Pineal Organ, Melatonin, and Photoperiodism

Reproduction of various mammals is controlled by day length (*photoperiodism*; Baker and Ranson 1932; see also Chapter 15) and the pineal plays a decisive role in it (for review see Lincoln et al. 2005). In contrast to other vertebrates the

pineal of mammals does not react directly to light and the cells of the pineal, the pinealocytes, do not possess circadian clocks. Instead, the photoperiodic signals of the environment are perceived by special cells in the retina of the eyes and transmitted via the retinohypothalamic tract to the SCN (see Section 14.8.1.). From the SCN neuronal signals are sent via sympathetic nerves to the pineal and synchronize it with the environmental LD cycles. Figure 14.C shows how a pinealocyte receives these signals; both cytoplasmic as well as nuclear reactions are involved.

During darkness the hormone melatonin is synthesized and transmitted via the blood stream to target tissue and organs. The duration and magnitude of the melatonin secretion is a function of the length of the daily dark period (review by Steinlechner and Niklowitz 1992) and used to inform the organism about the seasonal changes. This hormonal signal changes in photoperiodically responsive mammal reproduction (stimulating or inhibiting, depending on the species) (Hoffmann 1981, Stehle et al. 2001) and pelage color, among others.

The photoperiodic signal is encoded in the duration of melatonin production and affects clock genes in calendar cells of the *pars tuberalis* of the hypophysis (for localization see http://www.med.uiuc.edu/histo-/small/atlas/image/w78d/2a1.htm), which regulate prolactin release (studies on sheep: Lincoln et al. 2003, Johnston et al. 2006). These cells contain circadian clocks, and the phase relationship between the expression of the clock genes *Cry* and *Per1* is set by melatonin at dusk or, respectively dawn. Whereas the photoperiodic timing in the SCN for the melatonin secretion in the pineal can be described by an *external* coincidence model, the timing in the *pars tuberalis* seems to follow an *internal* coincidence model (see Section 14.10.). As a consequence the transcription of downstream genes (prolactin-releasing factor?) leads to either a long-day cell state or a short-day cell state (Lincoln et al. 2002).

Melatonin acts at the central level as well as at the periphery: It affects not only functions of the gonads and other centrally controlled processes, but also those of other tissues of the body and the brain (Pévet et al. 2006). Being a small molecule, melatonin can pass the placenta and convey circadian and seasonal information to the fetus. It modulates sleep propensity (Gillette and Abbott 2005), seasonal thermoregulation including torpor and hibernation (Saarela and Reiter 1994, Heldmaier and Steinlechner 1981, Chapter 12 in Heldmaier and Werner 2004), metabolism, energy balance (body weight regulation!), and immune responses (references in Barrenetxe et al. 2004). Orally or injected melatonin pulses advance or delay the circadian rhythm depending on the phase of application. The phase response curve to melatonin pulses is similar to that of light pulses, but displaced by 180°(Lewy et al. 1996). Therefore melatonin can be used in a similar way as light pulses—if properly phased—to shift the circadian system. Circadian phase disorders can be treated in this way (Lewy and Sack 1997). Melatonin has been used to cure sleep disturbances and insomnia (e.g., in elderly people), depression, jetlag, and shift work–related sleep cycle disorders

(see Section 14.9.). The antioxidant properties of melatonin (Reiter et al. 1999) might protect the skin against UV (Slominski et al. 2005).

Light affects melatonin synthesis by its resetting effect on the circadian system, but also has an immediate effect by reducing melatonin synthesis if applied during the night (Visser et al. 1999). Under optimal conditions a single light pulse of 200 lux is already sufficient.

Melatonin is produced not only in the pineal gland, but also in the Harderian gland, the gastrointestinal tract, the skin, and the retina, but is there only of local importance (see Section 14.8.4.).

14.8.4. Clocks Outside the SCN

There is growing evidence that peripheral oscillators in various tissues and organs have some capacity for maintaining a circadian rhythm independently from the SCN (for review see Schibler et al., Glossop and Hardin 2002), and the role of the SCN may be more likely to be a sort of conductor in an orchestra of circadian oscillators. After the ablation of the SCN other rhythms are still maintained, such as the anticipatory food uptake behavior (Stephan et al. 1979, Mistlberger et al. 1996, Marchant and Mistlberger 1997). They must therefore be controlled by another pacemaker center, which seems to involve dorsomedial hypothalamic neurons (Gooley et al. 2006, Landry et al. 2006).

Removal of the SCN or even photic resetting (jet lag) seems to lead to desynchrony between the central pacemaker and the periphery. These peripheral oscillators seem to play a functional role in olfactory bulbs (Herzog and Tosini 2001) and muscles (Takahashi 2004), but a discussion is beyond the scope of this chapter. The molecular components of these peripheral clocks are the same as the one in the SCN pacemaker cells (Yamazaki et al. 2000), and they possess the same properties (e.g., shorter periods of retinal rhythms in short period mutants). They affect, however, only the respective tissue or organ.

One of the better known and studied circadian clocks outside the SCN is the mammalian retina. The existence of a circadian clock in the mammalian eye was predicted by Reme et al. (1991). Such clocks have been found in the meantime in the retinas of all classes of vertebrates. The retina is a multilayered tissue consisting of various cell types (described, e.g., in Tosini and Fukuhara 2002) and contains besides the normal visual system an entire *circadian* system with receptors for synchronizing light and with multiple mutually coupled clocks (Ruan et al. 2006). Different aspects of retinal physiology such as sensitivity to light, neurohormone synthesis, and cellular events such as rod disk shedding, intracellular signaling, and gene expression are controlled by these clocks (Tosini and Menaker 1996; see reviews by Tosini and Fukuhara 2002, Green and Besharse 2004). The retinal pacemaker cells are responsible for a circadian output of melatonin in the eye. This changes the sensitivity of the retina to light (covering a range of more than 6 orders of magnitude). The genetic basis of this oscillator is the same as that of the SCN: Period mutants show altered periods

also in the output of the eye clock (Grace et al. 1996; see, however, for variations in molecular detail, e.g., Steenhard and Besharse 2000).

The peripheral oscillator allows one to study the relationships between the various cell types in the retinal tissue (which is well characterized). Many local clock-controlled rhythms are known and data are consistent with multiple or dual oscillators within the retina that control local physiology. An example is the antiphasic regulation of melatonin and dopamine in photoreceptors and in the inner retina. This might be driven by one or, more likely, two circadian clocks in the ganglion cells of the inner retina and a subset of the inner nuclear layer (Thompson et al. 2003) and/or by circadian clocks in the photoreceptor cells of the retina (Hattar et al. 2003). This demonstrates the tied connection between pacemakers and photoreceptors which are known also from invertebrates and *Neurospora*.

The similarities and differences in the molecular mechanisms of the retinal versus the SCN oscillators are discussed by Green and Besharse (2004). They also examined the interactions between the retinal clock(s) and the master clock in the SCN. Light and dopamine phase shift the retinal clock (Steenhard and Besharse 2000). The circadian release of melatonin in the eye is responsible for the rhythmic adaptation of phototransduction, for the recycling of biochemical components in the retina and for other aspects of the retinal physiology. Other rhythmic events in the eye such as visual resolution (Tassi et al. 2000), ERG, intraocular pressure (Nickla et al. 1998), choroid thickening, and eye growth might be or are also under circadian control. Furthermore, the shedding of outer segment tips and the phagocytosis of the shed membranes of rods and cones is under local circadian control (Young 1976, Grace et al. 1999). This *internal* renewal is important for the functional integrity of rods and cones, since they can not be replaced by new cells. Shedding of rod segments occurs in the morning, shedding of cones in the evening. In this way it does not interfere with the times the rods or cones are mainly used.

14.9. Light and the Human Circadian System

The effect of light on the circadian system of mammals has been discussed in Section 14.8. A few peculiarities of the human circadian system and its responses to light are mentioned in the following.

The circadian system governs not only the sleep–wake cycle, body temperature, alertness, and efficiency, but also many other physiological and metabolic events such as rapid eye movement (REM) sleep, hormonal secretion, enzymatic activities in organs such as the liver or in the red blood cells, and so on. There is a long list of circadian clock-driven events in humans (Minors and Waterhouse 1981).

Since the sleep–wake cycle (Dijk and von Schantz 2005), body temperature, and the amount of urine produced and its composition can be monitored easily, they have often been used as hands of the circadian system. Melatonin

concentration in the blood is a particularly useful measure because it is not greatly disturbed by activities (in contrast to the body temperature rhythm; light has, however, an immediate suppressing effect on melatonin concentration).

The circadian system shows up clearly under isolation from external time cues. In a cave or in an isolation facility, a person who has no information of the outside time will sleep and wake according to his or her internal circadian clock. In most cases it runs more slowly than the 24-hour day, as can be shown by continuously measuring the body temperature, the time of going to bed and rising up, and locomotor activities. The average free-run period of many such studies has been estimated to be about 25 hours (Wever 1979). However, this estimate was too high because of the design of the recording conditions: the subjects were living under artificial light, which influences period, because they were exposed to light during most of the *delay* portion of the phase response curve (see Section 14.5.2.) during wakefulness and to darkness during most of the phase *advance* portion. As a result of this pattern of light exposure and due to the light intensities used, the free-running periods were overestimated (Klerman et al. 1996, Honma et al. 2003).

Using other protocols such as forced desynchrony, period could be measured without the influence of self-selected sleep–wake and LD cycles (Duffy and Wright 2005) and turned out to be much closer to 24 hours, namely 24.2 hours on average. To entrain the circadian clock of a person with such a period to the 24-hour day, the rhythm has in principle to be advanced daily by about 0.2 hours (12 minutes). The period of about 25% of tested persons is less than 24.0 hours, requiring a daily *delay*, whereas in the remaining individuals the period is longer, thus requiring a daily *advance* of the rhythm.

14.9.1. Light Synchronizes the Human Circadian System

Which time cues synchronize the human circadian system? The free-running rhythm of humans can be synchronized to the 24-hour day by knowing the time of day or by external time cues such as light, temperature, noise, or social contact (for entrainment by nonphotic signals see Mistlberger and Skene 2005). Light plays a much more important role in humans than claimed in earlier studies (e.g., Wever 1979), and shorter exposures (Laakso et al. 1993) and lower intensities as previously assumed are able to entrain the human circadian system (Wright et al. 2001).

In humans, as in other mammals, the eyes seem to be the only places harboring photoreceptors, which are able to synchronize or phase shift the circadian rhythms in the SCN, the master clock in vertebrates (findings of Campbell and Murphy [1998] that extraretinal photoreception can phase shift the circadian rhythm of body temperature and melatonin concentration by illuminating the backside of the knees could not be verified in later experiments [Rüger et al. 2003]).

All humans with bilateral enucleation and 20% of the remaining blind people exhibit free-running circadian rhythms ("blind freerunners") (Emens et al. 2005;

see also Section 14.8.). In the rest either the blindness affects only normal vision of images, but not the *circadian* vision based on the intrinsically photosensitive retinal ganglion cells (ipRGCs), or other time cues are used for synchronization (Mistlberger and Skene 2005). Occasionally even in people with intact vision free run is observed, although they live in a normal environmental situation (Miles et al. 1977, Giedke et al. 1983). It is not known why light and other time cues are ineffective in these people.

As in other mammals, single light pulses are able to phase shift circadian rhythms in humans. The phase response curve is of the strong or weak type (see Section 14.2.), depending on the strength and length of the light exposure (Minors et al. 1991, Khalsa et al. 2003; a strong phase response in humans has, however, been questioned: Duffy and Wright 2005). The human circadian system is responsive to light throughout the day (and of course much more during the night, but under normal conditions the daytime light exposure synchronizes the human circadian system), and no "dead zone" exists (see Section 14.2. and Jewett et al. 1997).

In order to find out which wavelengths are effective in shifting the phase of the circadian rhythm in humans, action spectra (see Chapter 6) were determined by using the suppression of plasma melatonin. The results of those experiments are compiled and discussed by Brainard and Hanifin (2005). Light in the short wavelength range (459–484 nm) is most effective. This differs from the spectral sensitivity of the visual system and points to special circadian photoreceptors as discussed in Section 14.8.4. Spectral sensitivity of the retinal ganglion cells to light seems to change during the night (Figueiro et al. 2005).

Besides phase, the amplitude of the rhythm is an important parameter. A first light pulse suitably placed reduces the amplitude of the circadian rhythm in humans, and it becomes more sensitive toward the phase shifting effect of a second light pulse (Czeisler et al. 1989).

14.9.2. Significance of Light in Shift Work and Jetlag

The circadian system determines sleep propensity, timing of sleep, sleep structure, and consolidates sleep and wakefulness. Sleep homeostasis interacts with it according to the circadian principle: *The longer we are awake*, *the shorter we sleep*, and according to the homeostatic regulation of sleep: *The longer we are awake*, *the deeper our sleep*. The effects of light on sleep have been reviewed by Wright et al. (2005) and Ho et al. (2002).

The circadian rhythm of modern humans is often delayed with respect to the natural LD cycle. We use electric light and can therefore stay up during the winter much longer than natural daylight would otherwise permit (Cardinali 1998). This independence or even insulation from the natural light easily leads to permanent sleep deprivation. In addition, modern society expects full-range services throughout the 24 hours. Traffic, economy, health service, and security have to rely on shift work or night work by a considerable portion of workers (about 20% in the industrialized nations).

However, shift work clashes with our circadian clock. As a consequence, potential health (Knutsson 2003) and safety problems arise. Many accidents are due to ill-adapted circadian clocks (Folkard and Tucker 2003, Barger et al. 2005), and sleep disturbances (review by Akerstedt 2003) and other problems arise from it.

The synchronizing effect of light on the circadian system of humans is one of the problems of shift work (Monk 2000). For instance, the high fluence rate of outdoor light in the morning after a night shift prevents the phase shift of the circadian system of the night worker needed for optimal adjustment of his or her clock (Horowitz et al. 2001). Wearing dark goggles is advisable in this case (Eastman et al. 1994). On the other hand, light can also be used for adjusting the clock to the shift work schedule, if properly applied (Ho et al. 2002, Crowley et al. 2003, Turek 2005). Models are used successfully for constructing LD cycles which phase shift the rhythm in such a way that they align better with shift work and day sleep schedules (Jewett et al. 1999, Martin and Eastman 1998). More empirical data from shift work effects on the circadian rhythms are, however, needed for detailed simulations of this kind (Åkerstedt 1998). Other counteractions consist of light exposures at certain times of the circadian cycle (Eastman et al. 1995, Boivin and James 2005) and using chronobiotics such as melatonin (see Section 14.8.3. and Redfern et al. 1994, Arendt 2005). In using combinations of light and melatonin, it should be taken into account that the phase-shifting effect of light pulses and melatonin pulses are 180° out of phase (Boulos et al. 1995, Skene 2003).

Jetlag is another problem where the circadian clock is suddenly exposed to a new temporal environment and needs some time for adjustment (overviews by Boulos et al. 1995, Redfern et al. 1994; for practical considerations see Boivin and James 2002, Burgess et al. 2003, Revell and Eastman 2005). For a critical review of a potential beneficial effect of light on jetlag syndromes, see Samel and Wegmann (1997). The human phase response curve to light pulses tells us that we should after arrival avoid morning light after having flown westward and expose ourself to outdoor light in the evening. Faster adjustment after eastward flights demands exposure to light in the morning and avoiding evening light (however, flight time and duration also influence adaptation to the new time zone).

14.9.3. Light Treatment in Sleep Disorders

If the circadian system is abnormally entrained, sleep disorders might result (reviewed by Baker and Zee 2000, Reid and Burgess 2005, Manthena and Zee 2006).

In the delayed sleep phase syndrome, sleep onset in the evening and awakening in the morning are delayed (for review: Wyatt 2004). Cole et al. (2002) successfully treated this syndrome with a special facial bright light mask. It provides light through closed eyelids during sleep 4 hours before awakening in the morning. The phase of the circadian rhythm was advanced by the treatment.

In the advanced sleep phase syndrome, sleep onset in the evening and awakening in the morning are earlier than usual. Wolfson and Carskadon (2003) discuss the effects of this disorder on performance and schoolwork. This syndrome is associated with a mutation in *Per2*, a clock gene (Toh et al. 2001, Xu et al. 2005).

In the non–24-hour sleep–wake syndrome, individuals do not keep a 24-hour sleep–wake routine (Hashimoto et al. 1998). This syndrome might be caused by weakened or missing stimuli (e.g., light in the blind). Timed melatonin treatment and/or bright light treatment were successful in this syndrome (Watanabe et al. 2000, Hack et al. 2003).

14.9.4. Seasonal Affective Disorders and Endogenous Depressions

Clinical aspects of human circadian rhythms are discussed by Klerman (2005) and practical aspects of chronotherapeutics and chronopharmacology by Elliott (2001). One aspect, which relates to the effect of light on the circadian clock of humans, will be touched upon briefly here: in endogenous depression, abnormalities in the circadian system have been observed (Halaris 1987). Furthermore, treatments affecting the circadian rhythms and the sensitivity of the retina to light have a therapeutic effect (Terman and Terman 1999). Depressed patients might suffer under an anomalous phase of the rhythm of light sensitivity due to some defect in the retina (Steiner et al. 1987).

A special type of depression is seasonal affective disorder (SAD). It occurs during the winter as a response to the seasonal shortening of the light period (Graw et al. 1999) in adults as well as in children (Giedd et al. 1998) in the northern and southern hemispheres (Teng et al. 1995, Mersch et al. 1999). It has been discussed whether it might reflect some kind of photoperiodic reaction in humans. (For possible photoperiodic reactions in humans, see Roenneberg and Aschoff [1990], Wehr [2001], Bronson [2004]). Photoperiodism in primates is well known (Di Bitetti and Janson 2000, Cayetanot et al. 2005). Besides other abnormalities the circadian rhythms show abnormal amplitudes in this syndrome (Bunney and Bunney 2000, Koorengevel et al. 2002), and the phase response curve to light is increased (Thompson et al. 1997). SAD patients are more sensitive to variations in the length of the natural day (Guillemette et al. 1998). They are super-sensitive to light during the winter (Terman and Terman 1999), perhaps due to a phase delay of the circadian rhythm (Nathan et al. 1999). Light therapy in both seasonal and nonseasonal mood disorders was successful, as reviewed by Golden et al. (2005).

Many questions remain unanswered before the light/SAD/clock relations are settled (see Klerman 2005). Several types of SAD are known, some of which react poorly to light treatment (Terman et al. 1996). For general literature see Partonen and Magnusson (2001), and for special literature on SAD Lewy et al. (2006), two articles in Touitou (1998), and for practitioners Lam and Levitan (2000).

14.10. Models

In the preceding sections models have been used to illustrate complex situations. Models lie at the heart of natural science, and their usefulness should not be underestimated. They force us to systematize our knowledge and to quantify our predictions. They could give useful hints as to the interplay between light and circadian systems. One example is the discovery and the experiments around the concept of light-induced arrhythmicity of circadian systems, mentioned in Section 14.2. Other examples which illustrate the usefulness of models are found in applied fields. For humans, modern jet flights (Section 14.9.2.) imply rapid changes of time zones and accordingly changed light inputs to the circadian systems, as does shift work. Models are published which facilitate resynchronization to new light conditions. In the present section we would like to discuss and emphasize some formal aspects of models of circadian rhythms and of light effects on the rhythms.

14.10.1. Simple Model Description

Light Input to the Clock: The detailed way in which light affects the individual circadian systems is important for a model. The photoreceptors and receptor molecules have to be identified and might be specific for the system. Light signals from the environment are perceived in this photoreceptor organ or receptor system. After the light quanta are absorbed, the excitation energy gives rise to a signal chain to the clock. Models of this pathway for the light signals will differ widely between organisms. The details of the signal transduction pathways have to be known and the way in which the (transformed) light signal enters the circadian clock has to be determined. Again, the modeling might require specific knowledge for each circadian system, and much work remains to be done in this area.

The Circadian System—Feedback and Time Delay: The clockwork proper, or the circadian system, in a cell can often be modeled as a single unit model. In a multicellular organism, the concept of a multi-oscillator model might be appropriate (see Section 14.7.). Furthermore, a particular oscillating system should be modeled by the fewest possible variables that are relevant for the study in question.

In models for circadian systems, by necessity nonlinear ones, the concepts of positive and negative feedback and of time delay are frequently used. Control theory tells that feedback in a system leads to oscillations if the signal in the feedback loop is delayed in a suitable way and if it is fed back and reinforces an already existing signal. In several models of a circadian system such a negative feedback with suitable delays is introduced, often completed with a positive feedback. In order to increase the tendency to oscillate, the feedback system must also possess sufficient amplification and nonlinear elements. The time delays which exist in circadian clocks could be due to transcription, translation,

transport, and production or decomposition of clock-related components. Specific points have been discussed in Sections 14.3–14.8.

A simple description of a feedback oscillator can be given. Let $c(t)$ represent the concentration of an oscillating central variable in the clock (e.g., the protein FRQ). In a feedback model the signal $c(t)$ in the loop is delayed in a suitable way before feeding back to reinforce (amplify) an already existing signal and induce oscillations. If we assume that the substance is produced at time t according to the concentration of the same substance c(t) at a certain earlier time $(t - t_0)$, we have a simple feedback system with *delay t_0* . *The* situation can be expressed as

$$(\text{Production of substance c(t) at time t}) =$$
$$-K \cdot (\text{concentration of substance c at time } (t - t_0))$$

Here K is a positive constant and the negative sign indicates that production is decreased if the concentration was high t_0 hours earlier, while it is increased if concentration was low t_0 hours earlier (inhibition occurs if concentration was high, activation occurs if concentration was low at some time units earlier). Transformed into mathematical terms the expression shows sustained oscillations if the delay t_0 and the feedback signal have suitable magnitudes. Furthermore, the period of the oscillations will be about four times the delay time introduced. Circadian oscillations would thus need a delay of about 6 hours in the example in order to end up with a 24-hour period. Interestingly, experimental results pointing at an explicit delay of about 6 hours in a molecular feedback chain of the clock in *Drosophila* has recently been published (see Section 14.7.3. and Meyer et al. 2006).

Simple feedback models based on these concepts (but using nonlinearities that are always present in biological systems and which are needed to limit the maximal concentrations that can be reached) have been used to simulate features of circadian rhythms (*Kalanchoe* petal rhythm; Karlsson and Johnsson 1972, Johnsson et al. 1973), photoperiodic flowering in *Chenopodium* (Bollig et al. 1976), activity rhythm in the New Zealand Weta, (Lewis 1999), and a molecular model (Smolen et al. 2002).

As mentioned already, the photoreception can be clock-controlled by feedback links that change the properties of receptor systems (e.g., control of the iris muscle in mammals; Fig. 14.7). In addition, light adaptation and other changes of sensitivity to light might increase the level of complexity in modeling the light-induced effects on the circadian clock. The experimental investigations of the light perception and transduction must probably reach a new stage in order to allow detailed modeling of the light reactions of the circadian system.

Many models of the circadian clockwork have been published, emphasizing different aspects of the oscillating system. Not all of them focus on the light perception and the light reactions. We, therefore, do not try to mention all models here but would like to give references to some papers for readers who are interested in the modeling (Beersma 2005, Diez-Noguera 1994, Goldbeter 1995, Deacon and Arendt 1996, Leloup and Goldbeter 1998, Forger et al. 1999,

Lakin-Thomas and Johnson 1999, Leloup and Goldbeter 1999, Leloup et al. 1999, Ruoff and Rensing 2004, Rand et al. 2004, Zak et al. 2001).

Output Signals from the Clock: Reaction sequences downstream from the clock are also important to model. The period of the circadian system will be reflected in the reactions driven by the clock. Amplitude and phase of the driven reactions might change, but the final reactions that are observable—the hands of the clock—have the same period as the clock. This is stressed since environmental light signals might affect the downstream reactions directly, thereby changing for instance their amplitude. Such changes should not be mistakenly ascribed to light effects on the circadian system itself. We remind you that the clock output can also control the light perception and the light input signals to the clock.

14.10.2. Some Mathematical Properties of Circadian Models

As has been emphasized, light is the most important input signal to a circadian system, and there are several relevant features of a general nature that must be handled by models, such as:

Phase shifts and phase response curves: Any model of an oscillating, circadian system should react to external signals, for instance, light signals. One often assumes that light pulses given to the organism also enter the circadian system as pulses, affecting a model variable or a model parameter. Detailed modeling of the light signal pathway into the clock is certainly needed.

Entrainment: Repetitive light pulses given with a period T can, due to successive phase shifts, entrain the circadian rhythm (entrainment, synchonization, phase locking). The external light cycle will function as a synchronizer. This general property of circadian systems will also be simulated by models of circadian systems. The range of entrainment can be used to test models.

Stopping the clock by light pulses: In many models phase shifts and amplitude changes brought about by light pulses are concomitant features. One might ask if an external light pulse could cause a total amplitude reduction of the circadian system, i.e., lead to a stop of the oscillations. This was indeed found (see Section 14.2.). Several combinations of irradiance and pulse durations were still effective in *Drosophila* (Chandrashekaran and Engelmann 1973) and in *Kalanchoe* (Engelmann et al. 1978), indicating that a range of parameter choices could be used to reach this special state. This extended range of phases at which pulses can stop a circadian rhythm has been theoretically penetrated in a detailed model of the *Drosophila* rhythm (Leloup and Goldbeter 2001).

A mathematically and biologically interesting question arises: Will a circadian system start oscillating spontaneously again after having been sent into the nonoscillatory state or is it stable? The problems have attracted interest, and they focus on the mathematical structure of the circadian systems (on so-called singularities, limit cycles, etc.).

Besides light, temperature is also entraining circadian rhythms. At the same time, the speed of the circadian clock is only marginally affected by the environmental temperature (temperature compensated) and models should take care of both facts (see, e.g., Ruoff and Rensing 1996, Ruoff and Rensing 2004).

Light-On/Light-Off Effects: In several light pulse experiments circadian variations can be interpreted as if the light-on part of the pulse started one oscillation and the light-off part of the signal started another one. The resulting circadian variation should be the sum of the two oscillations (Engelmann 1966, Engelmann 1967). Models have been advanced to fit experimental data (Engelmann and Honegger 1967). They can be tested in several ways, e.g., by changing the slope of the light pulses to see if the derivative of the light pulse is determining the response, by investigating the action spectrum for the light-on effects as compared with the light-off effects (see references above) to see if two different oscillators are involved, etc.

Photoperiodic Induction: The Bünning hypothesis, stating that the circadian clock is used by organisms to measure day (night) length and to determine photoperiodic events accordingly (Bünning 1936), should be possible to describe by models for the circadian clock. Light/darkness conditions in combination with variations of the circadian clock could be used to predict, e.g., flower induction and hibernation. The modeling thus involves the proper treatment of the light perception for the induction of the photoperiodic events *and* the light perception for the phasing and entrainment of the clock. The two perception mechanisms can of course be unified—only experiments can verify the models proposed. Even simple approaches can in some cases model photoperiodic events fairly precisely (example: flower induction in *Chenopodium* as described by Bollig et al. 1976).

14.10.3. Single Versus Multioscillator Models—Outlook

Several important features of circadian systems are being modeled on the assumption that one single oscillator is controlling the clock. A one-oscillator model does not preclude the presence of many cellular oscillators—it only assumes that they are so strongly coupled to each other that they (in most cases) behave as one single unit (a "lumped" model). However, in multioscillator models the circadian system has new features that can not be explained under the assumption that the system consists of one single oscillator. The circadian system of humans is an example which is often modeled by two interacting oscillators. One of the oscillators is then assumed to have its strongest influence on (among other rhythms) the activity rhythm, and the other one on (among others) the temperature rhythm. Usually the two oscillators are coupled and oscillate in phase, but the dual nature of the system can show up in, for example, experiments in isolation where the rhythms might display different periods (Wever 1979, Kronauer et al. 1982, Oishi et al. 2001).

Modeling often starts with a simple one-oscillator assumption, an approach that eventually turns out to be too simple. But many circadian systems should be

modeled as multi-oscillatory systems, even on a single cell level (Roenneberg and Mittag 1996, Daan et al. 2001). In the case of *Drosophila*, several oscillators are nowadays implicated in more detailed modeling (see Section 14.7.3.).

As we have seen, published models of circadian systems have different structural features and emphasize different aspects of the circadian systems One form of models describes reactions in words and figures without deriving or attempting quantitative relations (see examples in Sections 14.3.–14.8.). Other models are purely mathematical ones, describing the dynamics of the variables in, usually, differential equations; others again are presented as block diagrams based on concepts from control theory. Usually numerical methods are used to simulate the circadian behavior. Ultimately all models should give precise qualitative and quantitative descriptions and predictions at the molecular, the cellular, and the organism level.

It is interesting that after a period of intensive studies of the molecular mechanisms which underlie circadian rhythms, formal modeling of circadian rhythms and their light reactions has gained impact.

Acknowledgments and Remark

References

Abe, M., Kobayashi, Y., Yamamoto, S., Daimon, Y., Yamaguchi, A., Ikeda, Y., Ichinoki, H., Notaguchi, M., Goto, K. and Araki, T. (2005) FD, a bZIP protein mediating signals from the floral pathway integrator FT at the shoot apex. Science 309, 1052–1056.

Able, K. P. (1995) Orientation and navigation: A perspective on fifty years of research. Condor 97, 592–604.

Ahmad, M. (1999) Seeing the world in red and blue: insight into plant vision and photoreceptors. Curr. Opin. Plant Biol. 2, 230–235.

Åkerstedt, T. Shift work and disturbed sleep/wakefulness. Occup. Med. 2003, 53, 89–94

Åkerstedt, T. Is there an optimal sleep–wake pattern in shift work? Scand. J. Work Environ. Health 1998, 24 (Suppl. 3), 18–27

Akimoto, H., Kinumi, T. and Ohmiya, Y. (2004) Biological rhythmicity in expressed proteins of the marine dino flagellate *Lingulodinium polyedrum* demonstrated by chronological proteomics. Biochem. Biophys. Res. Commun. 315, 306–312.

Akimoto, H., Kinumi, T. and Ohmiya, Y. (2005) Circadian rhythm of a TCA cycle enzyme is apparently regulated at the translational level in the dino flagellate *Lingulodinium polyedrum*. J. Biol. Rhythms 20, 479–489.

Albrecht, U., Sun, Z. S., Eichele, G. and Lee, C. C. (2004) A differential response of two putative mammalian circadian regulators mper1 and mper2 to light. Curr. Biol. 14, 975–980.

Albus, H., Vansteensel, M. J., Michel, S., Block, G. D. and Meijer, J. H. (2005) A gabaergic mechanism is necessary for coupling dissociable ventral and dorsal regional oscillators within the circadian clock. Curr. Biol. 15, 886–893.

Anderson, S., Somers, D., Millar, A., Hanson, K., Chory, J. and Kay, S. (1997) Attenuation of phytochrome A and B signaling pathways by the *Arabidopsis* circadian clock. Plant Cell 9, 1727–1743.

Aoki, S., Kondo, T., Wada, H. and Ishiura, M. (1997) Circadian rhythm of the cyanobacterium *Synechocystis* sp. strain PCC 6803 in the dark. J. Bacteriol. 179, 5751–5755.

Arendt, J. (2005) Melatonin: Characteristics, concerns, and prospects. J. Biol. Rhythms 20, 291–303.

Ashkenazi, I., Hartman, H., Strulovitz, B. and Dar, O. (1975) Activity rhythms of enzymes in human red blood cell suspension. J. interdisc. Cycle Res. 6, 291–301.

Ashmore, L. and Sehgal, A. (2003) A fly's eye view of circadian entrainment. J. Biol. Rhythms 18(3), 206–216.

Aton, S. J., Colwell, C. S., Harmar, A. J., Waschek, J. and Herzog, E. D. (2005) Vasoactive intestinal polypeptide mediates circadian rhythmicity and synchrony in mammalian clock neurons. Nature Neurosci. 8, 476–483.

Baker, J. and Ranson, R. (1932) Factors affecting the breeding of the field mouse (*Microtus agrestis*). I. Light. Proc. R. Soc. Lond. B 110, 113–332.

Baker, S. K. and Zee, P. C. (2000) Circadian disorders of the sleep–wake cycle. In: M. H. Kryger, T. Roth and W. C. Dement (Eds.), *Principles and practice of sleep medicine*, pp. 606–614. Saunders, Philadelphia.

Banerjee, R. and Batschauer, A. (2005) Plant blue-light receptors. Planta 220, 498–502.

Barger, L. K., Cade, B. E., Ayas, N. T., Cronin, J. W., Rosner, B., Speizer, F. E. and Czeisler, C. A. (2005) Extended work shifts and the risk of motor vehicle crashes among interns. N. Engl. J. Med. 352, 125–134.

Barrenetxe, J., Delagrange, P. and Martinez, J. A. (2004) Physiological and metabolic functions of melatonin. J. Physiol. Biochem 60, 61–72.

Beaule, C. and Amir, S. (2003) The eyes suppress a circadian rhythm of FOS expression in the suprachiasmatic nucleus in the absence of light. Neuroscience 121, 253–257.

Beaver, L. M., Gvakharia, B. O., Vollintine, T. S., Hege, D. M., Stanewsky, R. and Giebultowicz, J. M. (2002) Loss of circadian clock function decreases reproductive fitness in males of *Drosophila melanogaster*. Proc. Natl. Acad. Sci. USA 19, 2134–2139.

Beersma, D. G. (2005) Why and how do we model circadian rhythms? J. Biol. Rhythms 20, 304–313.

Bell-Pedersen, D. (2000) Understanding circadian rhythmicity in *Neurospora crassa*: from behavior to genes and back again. Fung. Genet. Biol. 29, 1–18.

Bell-Pedersen, D., Cassone, V., Earnest, D., Golden, S., Hardin, P., Thomas, T. and Zoran, M. (2005) Circadian rhythms from multiple oscillators: lessons from diverse organisms. Nature Rev. Genet. 6, 544–556.

Bellingham, J., Chaurasia, S., Melyan, Z., Liu, C., Cameron, M., Tarttelin, E., Iuvone, P., Hankins, M., Tosini, G. and Lucas, R. (2006) Evolution of melanopsin photoreceptors: Discovery and characterization of a new melanopsin in nonmammalian vertebrates. Public Library Sci. Biol. 4, e254.

Berson, D. M. (2003) Strange vision: ganglion cells as circadian photoreceptors. Trends Neurosci. 26, 314–320.

Bertolucci, C. and Foa, A. (2004) Extraocular photoreception and circadian entrainment in nonmammalian vertebrates. Chronobiol. Int. 21, 501–519.

Boivin, D. B. and James, F. O. (2002) Circadian adaptation to night-shift work by judicious light and darkness exposure. J. Biol. Rhythms 17, 556–567.

Boivin, D. B. and James, F. O. (2005) Light treatment and circadian adaptation to shift work. Ind. Health 43, 34–48.

Bollig, I., Chandrashekaran, M., Engelmann, W. and Johnsson, A. (1976) Photoperiodism in *Chenopodium rubrum* - an explicit version of the Bünning hypothesis. Int. J. Chronobiol 4, 83–96.

Boulos, Z., Campbell, S., Lewy, A., Terman, M., Dijk, D. and Eastman, C. (1995) Light treatment for sleep disorders: Consensus report. VII. Jet lag. J. Biol. Rhythms 10, 167–176.

Bradbury, M., Dement, W. and Edgar, D. (1997) Serotonin-containing fibers in the suprachiasmatic hypothalamus attenuate light-induced phase delays in mice. Brain Res. 768, 125–134.

Brainard, G. C. and Hanifin, J. P. (2005) Photons, clocks, and consciousness. J. Biol. Rhythms 20, 314–325.

Bronson, F. H. (2004) Are humans seasonally photoperiodic? J. Biol. Rhythms 19, 180–192.

Brown, R. and Robinson, P. (2004) Melanopsin -shedding light on the elusive circadian photopigment. Chronobiol. Int. 21, 189–204.

Brunner, M. and Schafmeier, T. (2006) Transcriptional and post-transcriptional regulation of the circadian clock of cyanobacteria and *Neurospora*. Genes Develop. 20, 1061–1074.

Bryant, T. (1972) Gas exchange in dry seeds: Circadian rhythmicity in the absence of DNA replication, transcription, and translation. Science 178, 634–636.

Bunney, W. and Bunney, B. (2000) Molecular clock genes in man and lower animals: Possible implications for circadian abnormalities in depression. Neuropsychopharmacol. 22, 335–345.

Burgess, H. J., Crowley, S. J., Gazda, C. J., Fogg, L. F. and Eastman, C. I. (2003) Preflight adjustment to eastward travel: 3 days of advancing sleep with and without morning bright light. J. Biol. Rhythms 18, 318–328.

Bünning, E. (1936) Die endonome Tagesrhythmik als Grundlage der photoperiodischen Reaktion. Ber. Deut. Bot. Ges. 54, 590–607.

Campbell, S. and Murphy, P. (1998) Extraocular circadian phototransduction in humans. Science 279, 396–399.

Cardinali, D. (1998) The human body circadian: How the biological clock influences sleep and emotion. Cienc. Cult. 50, 172–177.

Cayetanot, F., van Someren, E. J. W., Perret, M. and Aujard, F. (2005) Shortened seasonal photoperiodic cycles accelerate aging of the diurnal and circadian locomotor activity rhythms in a primate. J. Biol. Rhythms 20, 461–469.

Ceriani, M., Darlington, T., Staknis, D., Mas, P., Petti, A., Weitz, C. and Kay, S. (1999) Light-dependent sequestration of TIMELESS by CRYPTOCHROME. Science 285, 553–568.

Chandrashekaran, M. and Engelmann, W. (1973) Early and late subjective night phase of the *Drosophila* rhythm require different energies of blue light for phase shifting. Z. Naturforsch. 28c, 750–753.

Chang, D. C. (2006) Neural circuits underlying circadian behavior in *Drosophila melanogaster*. Behav. Process. 71, 211–225.

Chen, M., Chory, J. and Fankhauser, C. (2004) Light signal transduction in higher plants. Annu. Rev. Genet. 38, 87–117.

Cheng, H. Y. and Obrietan, K. (2006) Dexras1: Shaping the responsiveness of the circadian clock. Semin. Cell Dev. Biol. 43, 715–728.

Cheng, P., He, Q., Yang, Y., Wang, L. and Liu, Y. (2003) Functional conservation of light, oxygen, or voltage domains in light sensing. Proc. Natl. Acad. Sci. USA 100, 5938–5943.

Cheng, P., Yang, Y., Heintzen, C. and Liu, Y. (2001a) Coiled-coil domain-mediated FRQ/FRQ interaction is essential for its circadian clock function in *Neurospora*. EMBO J. 20, 101–108.

Cheng, P., Yang, Y. and Liu, Y. (2001b) Interlocked feedback loops contribute to the robustness of the *Neurospora* circadian clock. Proc. Natl. Acad. Sci. USA 98, 7408–7413.

Christensen, M., Falkeid, G., Loros, J., Dunlap, J., Lillo, C. and Ruoff, P. (2004) A nitrate-induced frq-less oscillator in *Neurospora crassa*. J. Biol. Rhythms 19, 280–286.

Clauser, C. (1954) *Die Kopfuhr*. Ferdinand Enke, Stuttgart.

Cole, R. J., Smith, J. S., Alcala, Y. C., Elliott, J. A. and Kripke, D. F. (2002) Bright-light mask treatment of delayed sleep phase syndrome. J. Biol. Rhythms 17, 89–101.

Comolli, J. C., Fagan, T. and Hastings, J. W. (2003) A type-1 phosphoprotein phosphatase from a dino flagellate as a possible component of the circadian mechanism. J. Biol. Rhythms 18, 367–376.

Correa, A., Lewis, Z. A., Greene, A. V., March, I. J., Gomer, R. H. and Bell-Pedersen, D. (2003) Multiple oscillators regulate circadian gene expression in *Neurospora*. Proc. Natl. Acad. Sci. USA 100, 13597–13602.

Covington, M. F., Pandab, S., Liu, X. L., Strayer, C. A., Wagner, D. R. and Kay, S. A. (2001) Elf3 modulates resetting of the circadian clock in *Arabidopsis*. Plant Cell 13, 1305–1316.

Cremer, F. and Coupland, G. (2003) Distinct photoperiodic responses are conferred by the same genetic pathway in *Arabidopsis* and in rice. Trends Plant Sci. 8, 405–407.

Crosthwait, S., Dunlap, J. and Loros, J. (1997) *Neurospora* wc-1 and wc-2: Transciption, photoresponses, and the origin of the circadian rhythmicity. Science 276, 763–769.

Crowley, S. J., Lee, C., Tseng, C. Y., Fogg, L. F. and Eastman, C. I. (2003) Combinations of bright light, scheduled dark, sunglasses, and melatonin to facilitate circadian entrainment to night shift work. J. Biol. Rhythms 18, 513–523.

Cyran, S., Yiannoulos, G., Buchsbaum, A., Saez, L., Young, M. and Blau, J. (2005) The double-time protein kinase regulates the subcellular localization of the *Drosophila* clock protein period. J. Neurosci. 25, 5430–5437.

Czeisler, C., Kronauer, R., Allan, J., Duffy, J., Jewett, M., Brown, E. and Ronda, J. (1989) Bright light induction of strong (type 0) resetting of the human circadian pacemaker. Science 244, 1328–1333.

Daan, S. (2000) Colin Pittendrigh, Jürgen Aschoff, and the natural entrainment of circadian systems. J. Biol. Rhythms 15, 195–207.

Daan, S., Albrecht, U., van der Horst, G. T. J., Illnerova, H., Roenneberg, T., Wehr, T. A. and Schwartz, W. J. (2001) Assembling a clock for all seasons: are there M and E oscillators in the genes? J. Biol. Rhythms 16, 105–116.

DeBruyne, J.P., Noton, E., Lambert, C.M., Maywood, E.S., Weaver, D.R. and Reppert, S.M. (2006) A clock shock: Mouse CLOCK is not required for circadian oscillator function. Neuron 50, 465–477.

de la Iglesia, H. O., Cambras, T., Schwartz, W. J. and Diez-Noguera, A. (2004) Forced desynchronization of dual circadian oscillators within the rat suprachiasmatic nucleus. Curr. Biol. 14, 796–800.

de Paula, R., Lewis, Z., Greene, A., Seo, K., Morgan, L., Vitalini, M., Bennett, L., Gomer, R. and Bell-Pedersen, D. (2006) Two circadian timing circuits in *Neurospora crassa* cells share components and regulate distinct rhythmic processes. J. Biol. Rhythms 21, 159–168.

Deacon, S. and Arendt, J. (1996) Adapting to phase shifts. I. An experimental model for jet lag and shift work. Physiol. Behav 59, 665–673.

DeCoursey, P. and Krulas, J. (1998) Behavior of SCN-lesioned chipmunks in a natural habitat: A pilot study. J. Biol. Rhythms 13, 229–244.

DeCoursey, P. J., Krulas, J. R., Mele, G. and Holley, D. C. (1997) Circadian performance of suprachiasmatic nuclei (SCN)-lesioned antelope ground squirrels in a desert enclosure. Physiol. Behav 62, 1099–1108.

Devlin, P. F. (2002) Signs of the time: environmental input to the circadian clock. J. Exp. Bot. 53, 1535–1550.

Dharmananda, S. (1980) *Studies on the circadian clock of* Neurospora crassa*: Light-induced phase shifting*. Ph.D. thesis, University of California, Santa Cruz.

Di Bitetti, M. S. and Janson, C. H. (2000) When will the stork arrive? Patterns of birth seasonality in neotropical primates. Am. J. Primatol. 50, 109–130.

Diernfellner, A. C., Schafmeier, T., Merrow, M. W. and Brunner, M. (2005) Molecular mechanism of temperature sensing by the circadian clock of *Neurospora crassa*. Genes Develop. 19, 1968–1973.

Diez-Noguera, A. (1994) A functional model of the circadian system based on the degree of intercommunication in a complex system. Am. J. Physiol. 267, 1118–1135.

Dijk, D.-J. and von Schantz, M. (2005) Timing and consolidation of human sleep, wakefullness, and performance by a symphony of oscillators. J. Biol. Rhythms 20, 279–290.

Ditty, J. L., Williams, S. B. and Golden, S. S. (2003) A cyanobacterial circadian timing mechanism. Annu. Rev. Genet. 37, 513–543.

Dkhissi-Benyahya, O., Rieux, C., Hut, R. and Cooper, H. (2006) Immunohistochemical evidence of a melanopsin cone in human retina. Invest. Ophthalmol. Vis. Sci. 47, 1636–1641.

Dowson-Day, M. and Millar, A. (1999) Circadian dysfunction causes aberrant hypocotyl elongation patterns in *Arabidopsis*. Plant J. 17, 63–71.

Dragovic, Z. (2002) Light reception and circadian behavior in 'blind' and 'clock-less' mutants of *Neurospora crassa*. EMBO J. 21, 3643–3651.

Duffy, J. F. and Wright, K. P. (2005) Entrainment of the human circadian system by light. J. Biol. Rhythms 20, 326–338.

Dunlap, J. and Loros, J. (2004) The *Neurospora* circadian system. J. Biol. Rhythms 19, 414–424.

Dunlap, J. C. and Loros, J. J. (2005) Analysis of circadian rhythms in *Neurospora*: Overview of assays and genetic and molecular biological manipulation. Methods Enzymol. 393, 3–22.

Eastman, C., Boulos, Z., Terman, M., Campbell, S., Dijk, D. and Lewy, A. (1995) Light treatment for sleep disorders: Consensus report. VI. Shift work. J. Biol. Rhythms 10, 157–164.

Eastman, C., Stewart, K., Mahoney, M., Liu, L. and Fogg, L. (1994) Dark goggles and bright light improve circadian rhythm adaptation to night-shift work. Sleep 17, 535–543.

Egan, E., Franklin, T., Hilderbrand-Chae, M., McNeil, G., Roberts, M., Schroeder, A., Zhang, X. and Jackson, F. (1999) An extraretinally expressed insect cryptochrome with similarity to the blue light photoreceptors of mammals and plants. J. Neurosci. 19, 3665–3673.

Elliott, W. J. (2001) Timing treatment to the rhythm of disease: A short course in chronotherapeutics. Postgrad. Med. 110, 119–129.

Elvin, M., Loros, J. J., Dunlap, J. C. and Heintzen, C. (2005) The PAS/LOV protein VIVID supports a rapidly dampened daytime oscillator that facilitates entrainment of the *Neurospora* circadian clock. Genes Develop. 19, 2593–2605.

Emens, J. S., Lewy, A. J., Lefler, B. J. and Sack, R. L. (2005) Relative coordination to unknown 'weak zeitgebers, in free-running blind individuals. J. Biol. Rhythms 20, 159–167.

Emery, P., So, W., Kaneko, M., Hall, J. and Rosbash, M. (1998) CRY, a *Drosophila* clock and light-regulated cryptochrome, is a major contributor to circadian rhythm resetting and photosensitivity. Cell 95, 669–679.

Engelmann, W. (1966) Effect of light and dark pulses on the emergence rhythm of *Drosophila pseudoobscura*. Experientia 22, 606–608.

Engelmann, W. (1967) Tagesrhythmisches Schlüpfen von *Drosophila pseudoobscura* und tagesperiodische Blütenblattbewegung von *Kalanchoe blossfeldiana* als Überlagerung von An- und Aus-Rhythmen. Nachr. Akad. Wiss. Göttingen II Math. Phys. Kl. 10, 141.

Engelmann, W. (2007) How plants identify the season by using a circadian clock. In: S. Mancuso and S. Shabala (Eds.), *Rhythms in plants: Phenomenology*, *mechanisms*, *and adaptive significance*. Springer, Heidelberg.

Engelmann, W. and Honegger, H. (1967) Versuche zur Phasenverschiebung endogener Rhythmen: Blütenblattbewegung von *Kalanchoe blossfeldiana*. Z Naturforsch. 22b, 200–204.

Engelmann, W., Johnsson, A., Kobler, H. and Schimmel, M. (1978) Attenuation of the petal movement rhythm of *Kalanchoe* with light pulses. Physiol. Behav 43, 68–76.

Engelmann, W. and Mack, J. (1978) Different oscillators control the circadian rhythm of eclosion and activity in *Drosophila*. J. Comp. Physiol. 127, 229–237.

Enright, J. (1965) Synchronization and ranges of entrainment. In: J. Ascho (Ed.), *Circadian clocks*. *Proceedings of the Feldafing summer school*, *7-18 September 1964*, pp. 112–124. North-Holland Publishing Co., Amsterdam.

Fankhauser, C. and Staiger, D. (2002) Photoreceptors in *Arabidopsis thaliana*: light perception, signal transduction and entrainment of the endogenous clock. Planta 216, 1–16.

Figueiro, M., Bullough, J., Parsons, R. and Rea, M. (2005) Preliminary evidence for a change in spectral sensitivity of the circadian system at night. J. Circadian Rhythms 3, 14.

Fleissner, G. and Fleissner, G. (2001) Perception of natural Zeitgeber signals. In: V. Kumar (Ed.), *Biological rhythms*. Narosa Publ. House, New Delhi.

Fleury, F. (2000) Adaptive significance of a circadian clock: temporal segregation of activities reduces intrinsic competitive inferiority in *Drosophila* parasitoids. Proc. Biol. Sci. 267, 1005–1010.

Folkard, S. and Tucker, P. (2003) Shift work, safety and productivity. Occup. Med. 53, 95–101.

Forger, D., Jewett, M. and Kronauer, R. (1999) A simpler model of the human circadian pacemaker. J. Biol. Rhythms 14, 532–537.

Forsgren, E. (1935) *Über die Rhythmik der Leberfunktion, des Stoffwechsels und des Schlafes*. Gumperts Bokhandel, Göteborg.

Foster, R. and Helfrich-Förster, C. (2001) Photoreceptors for circadian clocks in mice and fruit flies. Philos. Trans. R. Soc. London (Biol.) 356 B, 1779–1789.

Franklin, K. A. and Whitelam, G. C. (2004) Light signals, phytochromes and cross-talk with other environmental cues. J. Exp. Bot. 55, 271–276.

Froehlich, A., Pregueiro, A., Lee, K., Denault, D., Colot, H., Nowrousian, M., Loros, J. J. and Dunlap, J. C. (2003) The molecular workings of the *Neurospora* biological clock. Novartis Found. Symp. 253, 184–198.

Gachon, F., Nagoshi, E., Brown, S. A., Ripperger, J. and Schibler, U. (2004) The mammalian circadian timing system: from gene expression to physiology. Chromosoma 113, 103–112.

Garceau, N., Liu, Y., Loros, J. and Dunlap, J. (1997) Alternative initiation of translation and time-specific phosphorylation yield multiple forms of the essential clock protein frequency. Cell 89, 469–476.

Giedd, J. N., Swedo, S. E., Lowe, C. H. and Rosenthal, N. E. (1998) Case series: Pediatric seasonal affective disorder. A follow-up report. J. Am. Acad. Child Adolesc. Psychiatry 37, 218–220.

Giedke, H., Engelmann, W. and Reinhard, P. (1983) Free running circadian rest-activity cycle in normal environment. A case study. Sleep Res. 12, 365.

Gillette, M. and Abbott, S. (2005) Basic mechanisms of circadian rhythms and their relation to the sleep/wake cycle. In: D. P. Cardinali and S. R. Perumal (Eds.), *Neuroendocrine correlates of sleep/wakefulness*. Springer, New York.

Glossop, N. and Hardin, P. (2002) Central and peripheral circadian oscillator mechanisms in flies and mammals. J. Cell Sci. 115, 3369–3377.

Goldbeter, A. (1995) A model for circadian oscillations in the *Drosophila* period protein (PER). Proc. Biol. Sci. 261, 319–324.

Golden, R. N., Gaynes, B. N., Ekstrom, R. D., Hamer, R. M., Jacobsen, F. M., Suppes, T., Wisner, K. L. and Nemeroff, C. B. (2005) The efficacy of light therapy in the treatment of mood disorders: A review and meta-analysis of the evidence. Am. J. Psychiatry 162, 656–662.

Golombek, D. A., Agostino, P. V., Plano, S. A. and Ferreyra, G. A. (2004) Signaling in the mammalian circadian clock: the NO/cGMP pathway. Neurochem. Int. 45, 929–36.

Gooley, J. J., Fischer, D. and Saper, C. B. (2003) A broad role for melanopsin in nonvisual photoreception. J. Neurosci. 23, 7093–7106.

Grace, M., Chiba, A. and Menaker, M. (1999) Circadian control of photoreceptor outer segment membrane turnover in mice genetically incapable of melatonin synthesis. Visual Neurosci. 16, 909–918.

Grace, M. S., A., W. L., Pickard, G. E., Besharse, J. C. and Menaker, M. (1996) The tau mutation shortens the period of rhythmic photopreceptor outer segment disk shedding in the hamster. Brain Res. 735, 93–100.

Granshaw, T., Tsukamoto, M. and Brody, S. (2003) Circadian rhythms in *Neurospora crassa*: Farnesol or geraniol allow expression of rhythmicity in the otherwise arrhythmic strains frq 10, wc-1, and wc-2. J. Biol. Rhythms 18, 287–296.

Graw, P., Recker, S., Sand, L., Krauchi, K. and Wirz-Justice, A. (1999) Winter and summer outdoor light exposure in women with and without seasonal affective disorder. J. Affect. Disord. 56, 163–169.

Green, C. (2004) Cryptochromes: Tailored for distinct functions. Curr. Biol. 14, 847–849.

Green, C. B. and Besharse, J. C. (2004) Retinal circadian clocks and control of retinal physiology. J. Biol. Rhythms 19, 91–102.

Green, R. M., Tingay, S., Wang, Z. Y. and Tobin, E. M. (2002) Circadian rhythms confer a higher level of fitness to *Arabidopsis* plants. Plant Physiol. 129, 576–584.

Griffiths, S., Dunford, R. P., Coupland, G. and Laurie, D. A. (2003) The evolution of CONSTANS-like gene families in barley, rice, and *Arabidopsis*. Plant Physiol. 131, 1855–1867.

Grima, B., Chelot, E., Xia, R. and Rouyer, F. (2004) Morning and evening peaks of activity rely on different clock neurons of the *Drosophila* brain. Nature 431, 869–873.

Guillemette, J., Hebert, M., Paquet, J. and Dumont, M. (1998) Natural bright light exposure in the summer and winter in subjects with and without complaints of seasonal mood variations. Biol. Psychiatry 44, 622–628.

Hack, L. M., Lockley, S. W., Arendt, J. and Skene, D. J. (2003) The effects of low-dose 0.5-mg melatonin on the free-running circadian rhythms of blind subjects. J. Biol. Rhythms 18, 420–429.

Halaris, A. (1987) *Chronobiology and psychiatric disorders*. Elsevier, New York.

Hall, A., Bastow, R. M., Davis, S. J., Hanano, S., McWatters, H. G., Hibberd, V., Doyle, M. R., Sung, S. B., Halliday, K. J., Amasino, R. M. and Millar, A. J. (2003) The TIME FOR COFFEE gene maintains the amplitude and timing of *Arabidopsis* circadian clocks. Plant Cell 15, 2719–2729.

Hall, J. (2002) Genetics and molecular biology of insect rhythms. In: *Insect clocks*. Saunders, D. S.

Hall, J. C. (2003) Assembling a clock for all seasons: are there M and E oscillators in the genes? Adv. Genet. 48, 1–280.

Halliday, K. J. and Whitelam, G. C. (2003) Changes in photoperiod or temperature alter the functional relationships between phytochromes and reveal roles for PHYD and PHYE. Plant Physiol. 131, 1913–1920.

Hannibal, J. (2006) Roles of PACAP-containing retinal ganglion cells in circadian timing. Int. Rev. Cytol. 251, 1–39.

Hannibal, J. and Fahrenkrug, J. (2006) Neuronal input pathways to the brain's biological clock and their functional significance. Adv. Anat. Embryol. Cell Biol. 182, 1–71.

Hannibal, J., Hindersson, P., Knudsen, S. M., Geor, B. and Fahrenkrug, J. (2002) Melanopsin is expressed in PACAP-containing retinal ganglion cells of the human retinohypothalamic tract. Invest. Ophthalmol. Vis. Sci. 45, 4202–4209.

Hardin, P. E. (2005) The circadian timekeeping system of *Drosophila*. Curr. Biol. 15, R714–R722.

Harmer, S., Hogenesch, L., Straume, M., Chang, H., Han, B., Zhu, T., Wang, X., Kreps, J. and Kay, S. (2000) Orchestrated transcription of key pathways in *Arabidopsis* by the circadian clock. Science 290, 2110–2113.

Hashimoto, S., Nakamura, K., Honma, S. and Honma, K. I. (1998) Free-running of plasma-melatonin rhythm prior to full manifestation of a non-24 hour sleep–wake syndrome. Psychiat. Clin. Neurosci. 52, 264–265.

Hastings, J. and Sweeney, B. (1960) The action spectrum for shifting the phase of the rhythm of luminescence in *Gonyaulax polyedra*. J. Gen Physiol. 43, 697–706.

Hastings, J. W. (2001) Cellular and molecular mechanisms of circadian regulation in the unicellular dino flagellate *Gonyaulax polyedra*. In: J. Takahashi, F. Turek, and R. Y. Moore (Eds.), *Circadian clocks* pp. 321–334. Kluwer Academic/Plenum Publishers, New York.

Hattar, S., Kumar, M., Park, A., Tong, P., Tung, J., Yau, K. and Berson, D. (2006) Central projections of melanopsin-expressing retinal ganglion cells in the mouse. J. Comp. Neurol. 497, 326–349.

Hattar, S., Lucas, R. J., Mrosovsky, N., Thompson, S., Douglas, R. H., Hankins, M. W., Lem, J., Biel, M., Hofman, F. and Foster, R. G. (2003) Melanopsin and rod-cone photoreceptive systems account for all major accessory visual functions in mice. Nature 424, 75–81.

Hayama, R. and Coupland, G. (2003) Shedding light on the circadian clock and the photoperiodic control of flowering. Curr. Opin. Plant Biol. 6, 13–19.

He, Q., Cheng, P., Yang, Y., Wang, L., Gardner, K. and Liu, Y. (2002) White collar-1, a DNA binding transcription factor and a light sensor. Science 297, 840–843.

He, Q. and Liu, Y. (2005a) Degradation of the *Neurospora* circadian clock protein frequency through the ubiquitin–proteasome pathway. Biochem. Soc. Trans. 33, 953–956.

He, Q. and Liu, Y. (2005b) Molecular mechanism of light responses in *Neurospora*: from light-induced transcription to photoadaptation. Genes Develop. 19, 2888–2899.

Heintzen, C., Loros, J. J. and Dunlap, J. C. (2001) The PAS protein VIVID defines a clock-associated feedback loop that represses light input, modulates gating, and regulates clock resetting. Cell 104, 453–464.

Heldmaier, G., Ortmann, S. and Elvert, R. (2004) Natural hypometabolism during hibernation and daily torpor in mammals. Respir. Physiol. Neurobiol. 141, 317–329.

Heldmaier, G. and Steinlechner, S. (1981) Seasonal control of energy requirements for thermoregulation in the djungarian hamster (*Phodopus sungorus*), living in natural photoperiod. J. Comp. Physiol. B 142, 429–437.

Heldmaier, G. and Werner, D. (2004) *Environmental signal processing and adaptation*, Vol. 110. Blackwell Synergy.

Helfrich-Förster, C. (2000) Differential control of morning and evening components in the activity rhythm of *Drosophila melanogaster*—sex specific differences suggest a different quality of activity. J. Biol. Rhythms 15, 135–154.

Helfrich-Förster, C. (2002) The circadian system of *Drosophila melanogaster* and its light input pathways. Zoology 105, 297–312.

Helfrich-Förster, C. (2003) The neuroarchitecture of the circadian clock in the *Drosophila* brain. Micr. Res. Tech. 62, 94–102.

Helfrich-Förster, C. (2005) Neurobiology of the fruit fly's circadian clock. Genes Brain Behav. 4, 65–76.

Helfrich-Förster, C., Edwards, T., Yasuyama, K., Schneuwly, S., Meinertzhagen, I. and Hofbauer, A. (2002) The extraretinal eyelet of *Drosophila*: development, ultrastructure and putative circadian function. J. Neurosci. 22, 9255–9266.

Helfrich-Förster, C. and Engelmann, W. (2002) Photoreceptors for the circadian clock of the fruitfly. In: V. Kumar (Ed.), *Biological rhythms*, pp. 94–106. Narosa Publ. House, Pvt. Ltd., New Delhi.

Helfrich-Förster, C., Stengl, M. and Homberg, U. (1998) Organization of the circadian system in insects. Chronobiol. Int. 15, 567–594.

Helfrich-Förster, C., Winter, C., Hofbauer, A., Hall, J. and Stanewsky, R. (2001) The circadian clock of fruit flies is blind after elimination of all known photoreceptors. Neuron 30, 249–261.

Helfrich-Förster, C. (2005) Organization of endogenous clocks in insects. Biochem. Soc. Trans. 33, 957–961.

Helfrich-Förster, C., Shafer, O., Wülbeck, C., Grieshaber, E., Rieger, D. and Taghert, P. (2006) Development and morphology of the clock-gene-expressing lateral neurons of *Drosophila melanogaster*. J. Comp. Neurol. 500, 47–70.

Heller, H. and Ruby, N. (2004) Sleep and circadian rhythms in mammalian torpor. Annu. Rev. Physiol. 66, 275–289.

Hennessey, T. and Field, C. (1991) Circadian rhythms in photosynthesis. Plant Physiol. 96, 831–836.

Hennig, L., Stoddart, W. M., Dieterle, M., Whitelam, G. C. and Schäfer, E. (2002) Phytochrome E controls light-induced germination of *Arabidopsis*. Plant Physiol. 128, 194–200.

Herzog, E. and Tosini, G. (2001) The mammalian circadian clock shop. Semin. Cell Dev. Biol. 12, 295–303.

Hitomi, K., Okamoto, K., Daiyasu, H., Miyashita, H., Iwai, S., Toh, H., Ishiura, M. and Todo, T. (2000) Bacterial cryptochrome and photolyase: Characterization of two photolyase-like genes of *Synechocystis* sp. PCC6803. Nucleic Acids Res. 28, 2353–2362.

Ho, S. C., Wong, T. K., Tang, P. L. and Pang, S. M. (2002) Nonpharmacologic sleep promotion: bright light exposure. Complement Ther. Nurs. Midwifery 8, 130–135.

Hoffmann, K. (1981) The role of the pineal gland in the photoperiodic control of seasonal cycles in hamsters. In: B. Follett and D. Follett (Eds.), *Biological clocks in seasonal reproductive cycles*, pp. 237–250. Wright, Bristol.

Honma, S., Hashimoto, S., Nakao, M., Kato, Y. and Honma, K.-I. (2003) Period and phase adjustments of human circadian rhythms in the real world. J. Biol. Rhythms 18, 261–270.

Horowitz, T., Cade, B., Wolfe, J. and Czeisler, C. (2001) Efficacy of bright light and sleep/darkness scheduling in alleviating circadian maladaptation to night work. Am. J. Physiol. 281, 384–391.

Husain, M. (2005) The neural retina: Three channels of light detection. Adv. Clin. Neurosci. Rehabil. 5, 22–23.

Imaizumi, T. and Kay, S. (2006) Photoperiodic control of flowering: not only by coincidence. Trends Plant Sci. 11, 550–558.

Inouye, C. (1993) Circadian rhythms in peptides and their precursor messenger RNAs in the suprachiasmatic nucleus. In: H. Nakagawa, Y. Oomura, and K. Nagai (Eds.), *International Symposion Osaka: New functional aspects of the suprachiasmatic nucleus of the hypothalamus*, pp. 219–233. John Libbey and Co., London.

Inouye, C., Okamoto, K., Ishiura, M. and Kondo, T. (1998) The action spectrum of phase shift by light signal in the circadian rhythm in cyanobacterium. Plant Cell Physiol. 39 (Suppl.), S82.

Ishikawa, T., Matsumoto, A., Kato, T., Togashi, S., Ryo, H., Ikenaga, M., Todo, T., Ueda, R. and Tanimura, T. (1999) DCRY is a *Drosophila* photoreceptor protein implicated in light entrainment of circadian rhythm. Genes Cells 4, 57–65.

Ishiura, M., Kutsuna, S., Aoki, S., Iwasaki, H., Andersson, C., Tanabe, A., Golden, S., Johnson, C. and Kondo, T. (1998) Expression of a gene cluster kaiABC as a circadian feedback process in cyanobacteria. Science 281, 1519–1523.

Isoldi, M. C., Rollag, M. D., Castrucci, A. M. and Provencio, I. (2005) Rhabdomeric phototransduction initiated by the vertebrate photopigment melanopsin. Proc. Natl. Acad. Sci. USA 25, 1217–1221.

Ivleva, N. B., Bramlett, M. R., Lindahl, P. A. and Golden, S. S. (2005) LdpA: A component of the circadian clock senses redox state of the cell. Embo J. 24, 1202–1210.

Iwasaki, H. and Kondo, T. (2004) Circadian timing mechanism in the prokaryotic clock system of cyanobacteria. J. Biol. Rhythms 19, 436–444.

Iwasaki, H., Williams, S., Kitayama, Y., Ishiura, M., Golden, S. and Kondo, T. (2000) A kaiC-interacting sensory histidine kinase, SasA, necessary to sustain robust circadian oscillation in cyanobacteria. Cell 101, 223–233.

Izawa, T., Takahashi, Y. and Yano, M. (2003) Comparative biology comes into bloom: genomic and genetic comparison of flowering pathways in rice and *Arabidopsis*. Curr. Opin. Plant Biol. 6, 113–120.

Jackson, F., Schroeder, A., Roberts, M., McNeil, G., Kume, K. and Akten, B. (2001) Cellular and molecular mechanisms of circadian control in insects. J. Insect Physiol. 47, 822–842.

Jacobson, D., Powell, A., Dettman, J., Saenz, G., Barton, M., Hiltz, M., Dvorachek Jr, W., Glass, N., Taylor, J. and Natvig, D. (2004) *Neurospora* in temperate forests of western North America. Mycologia 96, 66–74.

Jagota, A., de la Iglesia, H. and Schwartz, W. (2000) Morning and evening circadian oscillations in the suprachiasmatic nucleus in vitro. Nature Neurosci. 3, 372–376.

Jewett, M., Kronauer, R. and Megan, E. (1999) Interactive mathematical models of subjective alertness and cognitive throughput in humans. J. Biol. Rhythms 14, 588–597.

Jewett, M., Rimmer, D., Duffy, J., Klerman, E., Kronauer, R. and Czeisler, C. (1997) Human circadian pacemaker is sensitive to light throughout subjective day without evidence of transients. Am. J. Physiol. 273, R1800–R1809.

Johnson, C., Golden, S. and Kondo, T. (1998) Adaptive significance of circadian programs in cyanobacteria. Trends Microbiol. 6, 407–410.

Johnsson, A., Karlsson, H. and Engelmann, W. (1973) Phase shifts in the *Kalanchoe* petal rhythm, caused by light pulses of different duration. A theoretical and experimental study. J. Chronobiol. 1, 147–156.

Johnston, J., Tournier, B., Andersson, H., Masson-Pevet, M., Lincoln, G. and Hazlerigg, D. (2006) Multiple effects of melatonin on rhythmic clock gene expression in the mammalian Pars tuberalis. Endocrinology 147, 959–965.

Jouve, L., Greppin, H. and Degli Agosti, R. (1998) *Arabidopsis thaliana* floral stem elongation: Evidence for an endogenous circadian rhythm. Plant Physiol. Bioch. 36, 469–472.

Kai, H., Arai, T. and Yasuda, F. (1999) Accomplishment of time-interval activation of esterase A4 by simple removal of pin fraction. Chronobiol. Int. 16, 51–58.

Kaneko, M., Hamblen, M. and Hall, J. (2000) Involvement of the period gene in developmental time-memory: Effect of the per short mutation on phase shifts induced by light pulses delivered to *Drosophila* larvae. J. Biol. Rhythms 15, 13–30.

Karakashian, M. and Schweiger, H. (1976) Circadian properties of the rhythmic system in individual nucleated and enucleated cells of *Acetabularia mediterranea*. Exp. Cell Res. 97, 366–377.

Karlsson, H. and Johnsson, A. (1972) A feedback model for biological rhythms. II. Comparisions with experimental results, especially on the petal rhythm of *Kalanchoe*. J. Theor Biol. 36, 175–194.

Khalsa, S., Jewett, M., Cajochen, C. and Czeisler, C. (2003) A phase response curve to single bright light pulses in human subjects. J. Physiol. 549, 945–952.

Klarsfeld, A., Malpel, S., Michard-Vanhee, C., Picot, M., Chelot, E. and Rouyer, F. (2004) Novel features of cryptochrome-mediated photoreception in the brain circadian clock of *Drosophila*. J. Neurosci. 24, 1468–1477.

Klarsfeld, A. and Rouyer, F. (1998) Effects of circadian mutations and LD periodicity on the life span of *Drosophila melanogaster*. J. Biol. Rhythms 13, 471–478.

Klein, D., Moore, R. and Reppert, S. (1991) *Suprachiasmatic nucleus: The mind's clock*. Oxford University Press, New York.

Klemm, E. and Ninnemann, H. (1976) Detailed action spectrum for the delay shift in pupae emergence of *Drosophila pseudoobscura*. Photochem. Photobiol. 24, 369–371.

Klerman, E. B. (2005) Clinical aspects of human circadian rhythms. J. Biol. Rhythms 20, 375–386.

Klerman, E. B., Dijk, D. J., Kronauer, R. E. and Czeisler, C. A. (1996) Simulations of light effects on the human circadian pacemeker: Implications for assessment of intrinsic period. Am. J. Physiol. 270, R271–R282.

Knutsson, A. (2003) Health disorders of shift workers. Occup. Med. 53, 103–108.

Kolar, C., Fejes, E., Adam, E., Schaefer, E., Kay, S. and Nagy, F. (1998) Transcription of *Arabidopsis* and wheat Cab genes in single tobacco transgenic seedlings exhibits independent rhythms in a developmentally regulated fashion. Plant J. 13, 563–569.

Kondo, T., Johnson, C. and Hastings, J. (1991) Action spectrum for resetting the circadian phototaxis rhythm in the CW15 strain I: Cells in darkness. Plant Physiol. 95, 197–205.

Kondo, T., Mori, T., Lebedeva, N. V., Aoki, S., Ishiura, M. and Golden, S. S. (1997) Circadian rhythms in rapidly dividing cyanobacteria. Science 275, 224–227.

Kondo, T., Strayer, C., Kulkarni, R., Taylor, W., Ishiura, M., Golden, S. and Johnson, C. (1993) Circadian rhythms in prokaryotes: Luciferase as a reporter of circadian gene expression in cyanobacteria. Proc. Natl. Acad. Sci. USA 90, 5672–5676.

Kondo, T., Tsinoremas, N., Golden, S., Johnson, C., Kutsuna, S. and Ishiura, M. (1994) Circadian clock mutants of cyanobacteria. Science 266, 1233–1236.

Koorengevel, K., Beersma, D., den Boer, J. and van den Hoofdakker, R. (2002) A forced desynchrony study of circadian pacemaker characteristics in seasonal affective disorder. J. Biol. Rhythms 17, 463–475.

Kräuchi, K., Cajochen, C., Pache, M., Flammer, J. and Wirz-Justice, A. (2006) Thermoregulatory effects of melatonin in relation to sleepiness. Chronobiol. Int. 23, 475–484.

Kreps, J. and Kay, S. (1997) Coordination of plant metabolism and development by the circadian clock. Plant Cell 9, 1235–1244.

Kreps, J. A., Wu, Y., Chang, H. S., Zhu, T., Wang, X. and Harper, J. F. (2002) Transcriptome changes for *Arabidopsis* in response to salt, osmotic, and cold stress. Plant Physiol. 130, 2129–2141.

Kronauer, R. E., Czeisler, C. A., Pilato, S. F., Moore-Ede, M. C. and Weitzman, E. D. (1982) Mathematical model of the human circadian system with two interacting oscillators. Am. J. Physiol. 242, 3–17.

Kumar, S., Mohan, A. and Sharma, V. (2005) Circadian dysfunction reduces lifespan in *Drosophila melanogaster*. Chronobiol. Int. 22, 641–653.

Kumbalasiri, T. and Provencio, I. (2005) Melanopsin and other novel mammalian opsins. Exp. Eye Res. 81, 368–375.

Kurosawa, G., Aihara, K. and Iwasa, Y. (2006) A model for circadian rhythm of cyanobacteria, which maintains oscillation without gene expression. Biophys. J. 91, 2015–2023.

Laakso, M.L., Hätönen, T., Stenberg, D., Alila, A. and Smith, S. (1993) The human circadian response to light – strong and weak resetting. J. Biol. Rhythms 8, 351–360.

Lakin-Thomas, P. (2006a) Circadian clock genes frequency and white collar-1 are not essential for entrainment to temperature cycles in *Neurospora crassa*. Proc. Natl. Acad. Sci. USA 103, 4469–4474.

Lakin-Thomas, P. and Brody, S. (2000) Circadian rhythms in *Neurospora crassa*: Lipid deficiencies restore robust rhythmicity to null frequency and white-collar mutants. Proc. Natl. Acad. Sci. USA 97, 256–261.

Lakin-Thomas, P. and Brody, S. (2004) Circadian rhythms in microorganisms: New complexities. Annu. Rev. Microbiol. 58, 489–519.

Lakin-Thomas, P., Cote, G. and Brody, S. (1990) Circadian rhythms in *Neurospora crassa*: biochemistry and genetics. Crit. Rev. Microbiol. 17, 365–416.

Lakin-Thomas, P. and Johnson, H. (1999) Commentary: Molecular and cellular models of circadian systems. J. Biol. Rhythms 14, 486–489.

Lakin-Thomas, P. L. (2006b) Transcriptional feedback oscillators: Maybe, maybe not. J. Biol. Rhythms 21, 83–92.

Lam, R. and Levitan, R. (2000) Pathophysiology of seasonal affective disorder: a review. J. Psychiat. Neurosci. 25, 469–480.

Larner, V. S. (2005) Photoreceptors and light signalling pathways in plants. In: A. J. W. Hall and H. McWaters (Eds.), *Endogenous plant rhythms*. Blackwell, Edinburgh.

Lee, H., Billings, H. and Lehman, M. (2003) The suprachiasmatic nucleus: A clock of multiple components. J. Biol. Rhythms 18, 435–449.

Lee, K., Loros, J. and Dunlap, J. (2000) Interconnected feedback loops in the *Neurospora* circadian system. Science 289, 107–110.

Leloup, J. and Goldbeter, A. (1998) A model for circadian rhythms in *Drosophila* incorporating the formation of a complex between the per and tim proteins. J. Biol. Rhythms 13, 70–87.

Leloup, J. and Goldbeter, A. (1999) Chaos and birhythmicity in a model for circadian oscillations of the PER and TIM proteins in *Drosophila*. J. Theor Biol. 198, 445–459.

Leloup, J. and Goldbeter, A. (2001) A molecular explanation for the long-term suppression of circadian rhythms by a single light pulse. Am. J. Physiol. 280, 1206–1212.

Leloup, J., Gonze, D. and Goldbeter, A. (1999) Limit cycle models for circadian rhythms based on transcriptional regulation in *Drosophila* and *Neurospora*. J. Biol. Rhythms 14, 433–448.

Lewis, R. (1999) Control system models for the circadian clock of the New Zealand Weta, *Hemideina thoracia* (Orthoptera: Stenopelmatidae). J. Biol. Rhythms 14, 480–485.

Lewis, Z. A., Correa, A., Schwerdtfeger, C., Link, K. L., Xie, X., Gomer, R. H., Thomas, T., Ebbole, D. J. and Bell-Pedersen, D. (2002) Overexpression of white collar-1(wc-1) activates circadian clock-associated genes, but is not sufficient to induce most light-regulated gene expression in *Neurospora crassa*. Mol. Microbiol. 45, 917–931.

Lewy, A., Ahmed, S. and Sack, R. (1996) Phase shifting the human circadian clock using melatonin. Behav. Brain Res. 73, 131–4.

Lewy, A. and Sack, R. (1997) Exogenous melatonin's phase-shifting effects on the endogenous melatonin profile in sighted humans: A brief review and critique of the literature. J. Biol. Rhythms 12, 588–594.

Lewy, A. J., Lefler, B. J., Emens, J. S. and Bauer, V. K. (2006) The circadian basis of winter depression. Proc. Natl. Acad. Sci. USA 103, 7414–7419.

Lin, R., Chou, H. and Huang, T. (1999) Priority of light/dark entrainment over temperature in setting the circadian rhythms of the prokaryote *Synechococcus* RF-1. Planta 209, 202–206.

Lincoln, G., Johnston, J., Andersson, H., Wagner, G. and Hazlerigg, D. (2005) Photore-fractoriness in mammals: Dissociating a seasonal timer from the circadian-based photoperiod response. Endocrinology 146, 3782–3790.

Lincoln, G., Messager, S., Andersson, H. and Hazlerigg, D. (2002) Temporal expression of seven clock genes in the suprachiasmatic nucleus and the pars tuberalis of the sheep: Evidence for an internal coincidence timer. Proc. Natl. Acad. Sci. USA 99, 13890–13895.

Lincoln, G. A., Andersson, H. and Loudon, A. (2003) Clock genes in calendar cells as the basis of annual timekeeping in mammals–a unifying hypothesis. J. Endocrinol. 179, 1–13.

Liu, Y. (2003) Molecular mechanisms of entrainment in the *Neurospora* circadian clock. J. Biol. Rhythms 18, 195–205.

Liu, Y., Golden, S., Kondo, T., Ishiura, M. and Johnson, C. (1995) Bacterial luciferase as a reporter of circadian gene expression in cyanobacteria. J. Bacteriol. 177, 2080–2086.

Liu, Y., Merrow, M., Loros, J. and Dunlap, J. (1998) How temperature changes reset a circadian oscillator. Science 281, 825–829.

Lucas, R. J. (2006) Chromophore regeneration: Melanopsin does its own thing. Proc. Natl. Acad. Sci. USA 103, 10153–10154.

Lumsden, P. and Millar, A. (1998) *Biological rhythms and photoperiodism in plants*. Environmental Plant Biology. Bios Scientific Publishers Oxford, Washington DC.

Lundkvist, G., Kwak, Y., Davis, E., Tei, H. and Block, G. (2005) A calcium flux is required for circadian rhythm generation in mammalian pacemaker neurons. J. Neurosci. 25, 7682–7686.

Malpel, S., Klarsfeld, A. and Rouyer, F. (2002) Larval optic nerve and adult extra-retinal photoreceptors sequentially associate with clock neurons during *Drosophila* brain development. Developm. 129, 1443–1453.

Malpel, S., Klarsfeld, A. and Rouyer, F. (2004) Circadian synchronization and rhythmicity in larval photoperception-defective mutants of *Drosophila*. J. Biol. Rhythms 19, 10–21.

Manthena, P. and Zee, P. C. (2006) Neurobiology of circadian rhythm sleep disorders. Curr. Neurol. Neurosci. Rep. 6, 163–168.

Marchant, E. and Mistlberger, R. (1997) Anticipation and entrainment to feeding time in intact and SCN-ablated C57BL/6j mice. Brain Res. 765, 273–282.

Martin, S. and Eastman, C. (1998) Medium-intensity light produces circadian rhythm adaptation to simulated night-shift work. Sleep 21, 154–165.

Más, P. (2005) Circadian clock signaling in *Arabidopsis thaliana*: from gene expression to physiology and development. Int. J. Dev. Biol. 49, 491–500.

Más, P., Devlin, P. F., Panda, S. and Kay, S. A. (2000) Functional interaction of PHYTOCHROME A and CRYPTOCHROME 2. Nature 408, 207–211.

Más, P., Kim, W. J., Somers, D. E. and Kay, S. A. (2003) Targeted degradation of TOC1 by ZTL modulates circadian function in *Arabidopsis*. Nature 426, 567–570.

Maywood, E., Reddy, A., Wong, G., O'Neill, J., O'Brien, J., McMahon, D., Harmar, A., Okamura, H. and Hastings, M. (2006) Synchronization and maintenance of timekeeping in suprachiasmatic circadian clock cells by neuropeptidergic signaling. Curr. Biol. 16, 599–605.

McClung, C., Hsu, M., Painter, J., Gagne, J., Karlsberg, S. and Salome, P. (2000) Integrated temporal regulation of the photorespiratory pathway. Circadian regulation of two *Arabidopsis* genes encoding serine hydroxymethyltransferase. Plant Physiol. 123, 381–391.

McClung, C. R. (2006) Plant circadian rhythms. Plant Cell 18, 792–803.

Meijer, J., Watanabe, K., Detari, L., deVries, M., Albus, H., Treep, J., Schaap, J. and Rietveld, W. (1996) Light entrainment of the mammalian biological clock. Prog. Brain Res. 111, 175–190.

Meijer, J. H. and Schwartz, W. J. (2003) In search of the pathways for light-induced pacemaker resetting in the suprachiasmatic nucleus. J. Biol. Rhythms 18, 235–249.

Melyan, Z., Tarttelin, E. E., Bellingham, J., Lucas, R. J. and Hankins, M. W. (2005) Addition of human melanopsin renders mammalian cells photosensitive. Nature 433, 741–744.

Menaker, M., Moreira, L. and Tosini, G. (1997) Evolution of circadian organization in vertebrates. Braz. J. Med. Biol. Res. 30, 305–313.

Merrow, M., Boesl, C., Ricken, J., Messerschmitt, M., Goedel, M. and Roenneberg, T. (2006) Entrainment of the *Neurospora* circadian clock. Chronobiol. Int. 23, 71–80.

Merrow, M., Brunner, M. and Roenneberg, T. (1999) Assignment of circadian function for the *Neurospora* clock gene frequency. Nature 399, 584–6.

Mersch, P. P., Middendorp, H. M., Bouhuys, A. L., Beersma, D. G. and van den Hoofdakker, R. H. (1999) Seasonal affective disorder and latitude: a review of the literature. J. Affect. Disord. 53, 35–48.

Meyer, P., Saez, L. and Young, M. (2006) PER-TIM interactions in living *Drosophila* cells: An interval timer for the circadian clock. Science 311, 226–229.

Michael, T. P., Salome, P. A., Yu, H. J., Spencer, T. R., Sharp, E. L., McPeek, M. A., Alonso, J. M., Exker, J. R. and McClung, C. R. (2003) Enhanced fitness conferred by naturally occurring variations in the circadian clock. Science 302, 1049–1053.

Michel, S., Colwell, C. and Colwell, C. (2001) Cellular communication and coupling within the suprachiasmatic nucleus. Chronobiol. Int. 18, 579–600.

Mihalcescu, I., Hsing, W. and Leibler, S. (2004) Resilient circadian oscillator revealed in individual cyanobacteria. Nature 430, 81–85.

Miles, L., Raynal, D. and Wilson, M. (1977) Blind man living in normal society has circadian rhythm of 24.9 hours. Science 198, 421–423.

Millar, A. J. (1999a) Biological clocks in *Arabidopsis thaliana*. New Phytol. 141,175–197.

Millar, A. J. (1999b) Tansley review no. 103—biological clocks in *Arabidopsis thaliana*. New Phytol. 141, 175–197.

Millar, A. J. (2003) A suite of photoreceptors entrains the plant circadian clock. J. Biol. Rhythms 18, 217–262.

Millar, A. J. (2004) Input signals to the plant circadian clock. J. Exp. Bot. 55, 277–283.

Millar, A. J., Carre, I. A., Strayer, C. A., Chua, N.-H. and A., K. S. (1995a) Circadian clock mutants in *Arabidopsis* identified by luciferase imaging. Science 267, 1161–1163.

Millar, A. J. and Kay, S. A. (1996) Integration of circadian and phototransduction pathways in the network controlling CAB gene transcription in *Arabidopsis*. Proc. Natl. Acad. Sci. USA 93, 15491–15496.

Millar, A. J., Straume, M., Chory, J., Chua, N.-H. and Kay, S. A. (1995b) The regulation of circadian period by phototransduction pathways in *Arabidopsis*. Science 267, 1163–1166.

Min, H., Johnson, C. H. and Golden, S. S. (2004) Phase determination of circadian gene expression in *Synechococcus elongatus* PCC 7942. J. Biol. Rhythms 19, 103–112.

Minors, D. and Waterhouse, J. (1981) *Circadian rhythms and the human*. Wright, London.

Minors, D., Waterhouse, J. and Wirz-Justice, A. (1991) A human phase response curve to light. Neurosci. Lett. 133, 36–40.

Mistlberger, R., de Groot, J. and Marchant, E. (1996) Discrimination of circadian phase in intact and suprachiasmatic nuclei ablated rats. Brain Res. 96, 12–18.

Mistlberger, R. E. and Skene, D. J. (2005) Nonphotic entrainment in humans? J. Biol. Rhythms 20, 339–352.

Monk, T. H. (2000) What can the chronobiologist do to help the shift worker? J. Biol. Rhythms 15, 86–94.

Moore, R., Speh, J. and Card, J. (1995) The rhd originates from a distinct subset of retinal ganglion cells. J. Comp. Neurol. 352, 351–366.

Morgan, L., Greene, A. and Bell-Pedersen, D. (2003) Circadian and light-induced expression of luciferase in *Neurospora crassa*. Fung. Genet. Biol. 38, 327–332.

Mori, T., Binder, B. and Johnson, C. (1996) Circadian gating of cell division in cyanobacteria growing with average doubling times of less than 24 hours. Proc. Natl. Acad. Sci. USA 93, 10183–10188.

Mori, T., Saveliev, S., Xu, Y., Stafford, W., Cox, M., Inman, R. and Johnson, C. (2002) Circadian clock protein KaiC forms ATP-dependent hexameric rings and binds DNA. Proc. Natl. Acad. Sci. USA 99, 17203–17208.

Morse, D., Hastings, J. and Roenneberg, T. (1994) Different phase responses of two circadian oscillators in *Gonyaulax*. J. Biol. Rhythms 9, 263–274.

Mrosovsky, N. (1999) Masking: history, definitions, and measurement. Chronobiol. Int. 16(4), 415–29.

Naef, F. (2005) Circadian clocks go in vitro: purely post-translational oscillators in cyanobacteria. Mol. Systems Biol. http://www.nature.com/msb/journal/v1/n1/full/msb4100027.html .

Nagy, F. and Schäfer, E. (2002) Phytochromes control photomorphogenesis by differentially regulated, interacting signaling pathways in higher plants. Annu. Rev. Plant Biol. 53, 329–355.

Naidoo, N., Song, W., Hunter-Ensor, M. and Seghal, A. (1999) A role for the proteasome in the light response of the timeless clock protein. Science 285, 1737–1741.

Nakahira, Y., Katayama, M., Miyashita, H., Kutsuna, S., Iwasaki, H., Oyama, T. and Kondo, T. (2004) Global gene repression by KaiC as a master process of prokaryotic circadian system. Proc. Natl. Acad. Sci. USA 101, 881–885.

Nakajima, M., Imai, K., Ito, H., Nishiwaki, T., Murayama, Y., Iwasaki, H. and Oyama, T., T. ans Kondo (2005) Reconstitution of circadian oscillation of cyanobacterial KaiC phosphorylation in vitro. Science 308, 414–415.

Nathan, P., Burrows, G. and Norman, T. (1999) Melatonin sensitivity to dim white light in affective disorders. Neuropsychopharmacology 21, 408–413.

Nickla, D., Wildsoet, C. and Wallman, J. (1998) Visual influences on diurnal rhythms in ocular length and choroidal thickness in chick eyes. Exp. Eye Res. 66, 163–181.

Nishiwaki, T., Iwasaki, H., Ishiura, M. and Kondo, T. (2000) Nucleotide binding and autophosphorylation of the clock protein KaiC as a circadian timing process of cyanobacteria. Proc. Natl. Acad. Sci. USA 97, 495–499.

Nitabach, M. N., Holmes, T. C. and Blau, J. (2005) Membranes, ions, and clocks: testing the Njus-Sulzman-Hastings model of the circadian oscillator. Methods Enzymol. 393, 682–93.

Oishi, T., Yamao, M., Kondo, C., Haida, Y., Masuda, A. and Tamotsu, S. (2001) Multi-photoreceptor and multioscillator system in avian circadian organization. Micr. Res. Tech. 53, 43–47.

Oltmanns, O. (1960) Über den Einfluss der Temperatur auf die endogene Tagesrhythmik und die Blühinduktion bei der Kurztagpflanze *Kalanchoe blossfeldiana*. Planta 54, 233–264.

Ouyang, Y., Andersson, C., Kondo, T., Golden, S. and Johnson, C. (1998) Resonating circadian clocks enhance fittness in cyanobacteria. Proc. Natl. Acad. Sci. USA 95, 8660–8664.

Panda, S. and Hogenesch, J. B. (2004) It's all in the timing: Many clocks, many outputs. J. Biol. Rhythms 19, 374–387.

Pandit, A. and Maheshwari, R. (1994) Sexual reproduction by *Neurospora* in nature. Fung. Genet. Newslett 41, 67–68.

Parcy, F. (2005) Flowering: a time for integration. Int. J. Dev. Biol. 49, 585–593.

Park, Y. (2002) Downloading central clock information in *Drosophila*. Neurobiol. 26, 217–233.

Partonen, T. and Magnusson, A. (2001) *Seasonal affective disorder: Practice and research*. Oxford University Press, New York.

Peirson, S. and Foster, R. (2006) Melanopsin: another way of signaling light. Neuron 49, 331–9.

Peterson, E. (1981a) Dynamic response of a circadian pacemaker. I. Recovery from extended light exposure. Biol. Cybern. 40, 171–179.

Peterson, E. (1981b) Dynamic response of a circadian pacemaker. II. Recovery from light pulse perturbations. Biol. Cybern. 40, 181–194.

Pévet, P., Agez, L., Bothorel, B., Saboureau, M., Gauer, F., Laurent, V. and Masson-Pévet, M. (2006) Melatonin in the multi-oscillatory mammalian circadian world. Chronobiol. Int. 23, 39–51.

Piechulla, B. (1999) Circadian expression of the light-harvesting complex protein genes in plants. Chronobiol. Int. 6, 115–128.

Pittendrigh, C. and Daan, S. (1976) A functional analysis of circadian pacemakers in nocturnal rodents. J. Comp. Physiol. A106, 333–355.

Pittendrigh, C. S., Bruce, B. G., Rosensweig, N. S. and Rubin, M. L. (1959) Growth patterns in *Neurospora*. Nature 184, 169–170.

Plachetzki, D., Serb, J. and Oakley, T. (2005) New insights into the evolutionary history of photoreceptor cells. Trends Ecol. Evol. 20, 465–467.

Plautz, J., Kaneko, M., Hall, J. and Kay, S. (1997) Independent photoreceptive circadian clocks throughout *Drosophila*. Science 278, 1632–1635.

Pregueiro, A., Price-Lloyd, N., Bell-Pedersen, D., Heintzen, C., Loros, J. and Dunlap, J. (2005) Assignment of an essential role for the *Neurospora* frequency gene in circadian entrainment to temperature cycles. Proc. Natl. Acad. Sci. USA 102, 2210–2215.

Price-Lloyd, N., Elvin, M. and Heintzen, C. (2005) Synchronizing the *Neurospora crassa* circadian clock with the rhythmic environment. Biochem. Soc. Trans. 33, 949–952.

Putterill, J., Robson, F., Lee, K., Simon, R. and Coupland, G. (1995) The CONSTANS gene of *Arabidopsis* promotes flowering and encodes a protein showing similarities to zinc finger transcription factors. Cell 80, 847–857.

Quintero, J., Kuhlman, S. and McMahon, D. (2003) The biological clock nucleus: A multiphasic oscillator network regulated by light. J. Neurosci. 23, 8070–8076.

Ralph, M. R., Foster, R. G., Davis, F. C. and Menaker, M. (1990) Transplanted suprachiasmatic nucleus determines circadian period. Science 247(4945), 975–978.

Rand, D. A., Shulgin, B. V., Salazar, D. and Millar, A. J. (2004) Design principles underlying circadian clocks. J. Royal Soc. Interface 1(1), 119–130.

Rea, M. (1998) Photic entrainment of circadian rhythms in rodents. Chronobiol. Int. 15, 395–423.

Redfern, P., Minors, D. and Waterhouse, J. (1994) Circadian rhythms, jet lag, and chronobiotics: An overview. Chronobiol. Int. 11, 253–265.

Reid, K. J. and Burgess, H. J. (2005) Circadian rhythm sleep disorders. Prim. Care 32, 449–473.

Reiter, R., Tan, D., Cabrera, J., D'Arpa, D., Sainz, R., Mayo, J. and Ramos, S. (1999) The oxidant/antioxidant network: role of melatonin. Biol. Signals Recept. 8, 56–63.

Reiter, R., Tan, D., Herman, T. and Thomas, C. (2004) Melatonin as a radioprotective agent: a review. Int. J. Rad. Oncol. Biol. Physics 59, 639–653.

Reme, C. E., Wirz-Justice, A. and Terman, M. (1991) The visual input stage of the mammalian circadian pacemaking system: I. Is there a clock in the mammalian eye? J. Biol. Rhythms 6, 5–29.

Reuss, S. (2003) *The clock in the brain: Anatomy of the mammalian circadian timing system*, pp. 1–40. University of Mainz, Germany.

Revell, V. L. and Eastman, C. I. (2005) How to trick mother nature into letting you fly around or stay up all night. J. Biol. Rhythms 20, 353–365.

Rieger, D., Shafer, O. T., Tomioka, K. and Helfrich-Förster, C. (2006) Functional analysis of circadian pacemaker neurons in *Drosophila melanogaster*. J. Neurosci. 26, 2531–2543.

Rieger, D., Stanewsky, R. and Helfrich-Förster, C. (2003) Cryptochrome, compound eyes, hofbauer-buchner eyelets, and ocelli play different roles in the entrainment and masking pathway of the locomotor activity rhythm in the fruit fly *Drosophila melanogaster*. J. Biol. Rhythms 18, 377–391.

Roenneberg, T. (1996) The complex circadian system of *Gonyaulax* polyedra. Plant Physiol. 96, 733–737.

Roenneberg, T. and Aschoff, J. (1990) Annual rhythm of human reproduction II: environmental correlations. J. Biol. Rhythms 5, 217–240.

Roenneberg, T. and Foster, R. (1997) Twilight times: light and the circadian system. Photochem. Photobiol. 66, 549–61.

Roenneberg, T. and Merrow, M. (1998) Molecular circadian oscillators: An alternative hypothesis. J. Biol. Rhythms 13, 167–179.

Roenneberg, T. and Mittag, M. (1996) The circadian program of algae. Semin. Cell Dev. Biol. 7, 753–763.

Ruan, G. X., Zhang, D. Q., Zhou, T., Yamazaki, S. and McMahon, D. G. (2006) Circadian organization of the mammalian retina. Proc. Natl. Acad. Sci. USA 20, 9703–9708.

Ruby, N. (2003) Hibernation: When good clocks go cold. J. Biol. Rhythms 18, 275–286.

Ruby, N., Dark, J., Burns, D., Heller, H. and Zucker, I. (2002) The suprachiasmatic nucleus is essential for circadian body temperature rhythms in hibernating ground squirrels. J. Neurosci. 22, 357–364.

Rüger, M., Gordijn, M. C. M., Beersma, D. G. M., de Vries, B. and Daan, S. (2003) Acute and phase-shifting effects of ocular and extraocular light in human circadian physiology. J. Biol. Rhythms 18, 409–419.

Ruoff, P. and Rensing, L. (1996) The temperature-compensated Goodwin model simulates many circadian clock properties. J. Theor. Biol. 179, 275–285.

Ruoff, P. and Rensing, L. (2004) Temperature effects on circadian clocks. J. Theor Biol. 29, 445–456.

Rusak, B. and Zucker, I. (1979) Neural regulation of circadian rhythms. Physiol. Rev 59, 449–526.

Russo, V. (1988) Blue light induces circadian rhythms in the bd mutant of *Neurospora*: double mutants bd,wc-1 and bd,wc-2 are blind. J. Photochem. Photobiol. B 2, 59–65.

Saarela, S. and Reiter, R. (1994) Function of melatonin in thermoregulatory processes. Life Sci. 54, 295–311.

Salome, P. A. and McClung, C. R. (2005) What makes the *Arabidopsis* clock tick on time? A review on entrainment. Plant Cell Environ. 28, 21–38.

Samel, A. and Wegmann, H. (1997) Bright light: A countermeasure for jet lag? Chronobiol. Int. 14, 173–183.

Sancar, A. (2000) Cryptochrome: The second photoactive pigment in the eye and its role in circadian photoreception. Annu. Rev. Biochem. 69, 31–67.

Satoh, Y., Kawai, H., Kudo, N., Kawashima, Y. and Mitsumoto, A. (2006) Time-restricted feeding entrains daily rhythms of energy metabolism in mice. Am. J. Physiol. 290, 1276–1283.

Schaap, J., Albus, H., vanderLeest, H., Eilers, P., Detari, L. and Meijer, J. (2003) Heterogeneity of rhythmic suprachiasmatic nucleus neurons: Implications for circadian waveform and photoperiodic encoding. Proc. Natl. Acad. Sci. USA 100, 15994–15999.

Schaffer, R., Landgraf, J., Accerbi, M., Simon, V., Larson, M. and Wisman, E. (2001) Microarray analysis of diurnal and circadian-regulated genes in *Arabidopsis*. Plant Cell 13, 113–123.

Schafmeier, T., Haase, A., Kaldi, K., Scholz, J., Fuchs, M. and Brunner, M. (2005) Transcriptional feedback of *Neurospora* circadian clock gene by phosphorylation-dependent inactivation of its transcription factor. Cell 122, 235–46.

Schafmeier, T., Kaldi, K., Diernfellner, A., Mohr, C. and Brunner, M. (2006) Phosphorylation-dependent maturation of *Neurospora* circadian clock protein from a nuclear repressor toward a cytoplasmic activator. Genes Develop. 20, 297–306.

Schepens, I., Duek, P. and Fankhauser, C. (2004) Phytochrome-mediated light signalling in *Arabidopsis*. Curr. Opin. Plant Biol. 7, 564–569.

Schibler, U., Ripperger, J. and Brown, S.A. (2003) Peripheral circadian oscillators in mammals: Time and food. J. Biol. Rhythms. 18, 250–260.

Schmidt-Koenig, K. (1975) *Migration and homing in animals*. Springer Berlin, Heidelberg, New York.

Schmitz, O., Katayama, M., Williams, S., Kondo, T. and Golden, S. (2000) CikA, a bacteriophytochrome that resets the cyanobacterial circadian clock. Science 289, 765–768.

Schwerdtfeger, C. (2003) Vivid is a flavoprotein and serves as a fungal blue light photoreceptor for photoadaptation. EMBO J. 22, 4846–4855.

Schwerdtfeger, C. and Linden, H. (2001) Blue light adaptation and desensitization of light signal transduction in *Neurospora crassa*. Mol. Microbiol. 39, 1080–1087.

Sehgal, A., Price, J. and Young, M. W. (1992) Ontogeny of a biological clock in *Drosophila melanogaster*. Proc. Natl. Acad. Sci. USA 89, 1423–1427.

Shafer, O., Helfrich-Förster, C., Renn, S. and Taghert, P. (2006) Re-evaluation of *Drosophila melanogaster*Fs neuronal circadian pacemakers reveals new neuronal classes and inter-class neurochemical interactions. J. Comp. Neurol. 498, 180–193.

Sharma, V. (2003) Adaptive significance of circadian clocks. Chronobiol. Int. 20, 901–919.

Silver, R. and Moore, R. (1998) Special issue on suprachiasmatic nucleus. Chronobiol. Int. 15, VII–X and 395 ff.

Silver, R. and Schwartz, W. (2005) The suprachiasmatic nucleus is a functionally heterogeneous timekeeping organ. Methods Enzymol. 393, 451–465.

Simonneaux, V. and Ribelayga, C. (2003) Generation of the melatonin endocrine message in mammals: A review of the complex regulation of melatonin synthesis by norepinephrine, peptides, and other pineal transmitters. Pharmacol. Rev. 55, 325–395.

Skene, D. J. (2003) Optimization of light and melatonin to phase-shift human circadian rhythms. J. Neuroendocrinol. 15, 438–441.

Slominski, A., Fischer, T. W., Zmijewski, M. A., Wortsman, J., Semak, I, Zbytek, B., Slominski, R. M. and Tobin, D. J. (2005) On the role of melatonin in skin physiology and pathology. Endocrine 27, 137–148.

Smith, R. M. and Williams, S. B. (2006) Circadian rhythms in gene transcription imparted by chromosome compaction in the cyanobacterium *Synechococcus eleongatus*. Proc. Natl. Acad. Sci. USA 103, 8564–8569.

Smolen, P., Baxter, D. A. and Byrne, J. H. (2002) A reduced model clarifies the role of feedback loops and time delays in the *Drosophila* circadian oscillator. Biophys. J. 83, 2349–2359.

Somers, D., Devlin, P. and Kay, S. (1998) Phytochromes and cryptochromes in the entrainment of the *Arabidopsis* circadian clock. Science 282, 1488–1490.

Springer, M. L. (1993) Genetic control of fungal differentiation: the three sporulation pathways of *Neurospora crassa*. BioEssays 15, 365–374.

Stal, L. and Krumbein, M. (1985) Oxygen protection of nitrogenase in the aerobically nitrogen fixing non-heterocystous cyanobacterium *Oscillatoria* sp. Arch. Microbiol. 143, 72–76.

Stanewsky, R. (2002) Clock mechanisms in *Drosophila*. Cell Tissue Res. 309, 11–26.

Stanewsky, R., Jamison, C., Plautz, J., Kay, S. and Hall, J. (1997) Multiple circadian-regulated elements contribute to cycling period gene expression in *Drosophila*. EMBO J. 16, 5006–5018.

Steenhard, B. M. and Besharse, J. C. (2000) Phase shifting the retinal circadian clock: xper2 mrna induction by light and dopamine. J. Neurosci. 20, 8572–8577.

Stehle, J., von Gall, C., Schomerus, C. and Korf, H. (2001) Of rodents and ungulates and melatonin: Creating a uniform code for darkness by different signaling mechanisms. J. Biol. Rhythms 16, 312–325.

Steiner, M., Werstiuk, E. and Seggie, J. (1987) Dysregulation of neuroendocrine cross-roads: depression, circadian rhythms and the retina—a hypothesis. Prog. Neuropsy-chopharmacol. Biol. Psych. 11, 267–278.

Steinlechner, S. and Niklowitz, P. (1992) Impact of photoperiod and melatonin on repro-duction in small mammals. Animal Reprod. Sci. 30, 1–28.

Stephan, F. (2002) The 'other' circadian system: Food as a zeitgeber. J. Biol. Rhythms 17, 284–292.

Stephan, F., Swann, J. and Sisk, C. (1979) Entrainment of circadian rhythms by feeding schedules in rats with suprachiasmatic lesions. Behav. Neural Biol. 25, 545–554.

Stoleru, D., Peng, Y., Agosto, J. and Rosbash, M. (2004) Coupled oscillators control morning and evening locomotor behaviour of *Drosophila*. Nature 431, 862–868.

Suarez-Lopez, P., Wheatley, K., Robson, F., Onouchi, H., Valverde, F. and Coupland, G. (2001) CONSTANS mediates between the circadian clock and the control of flowering in *Arabidopsis*. Nature 410, 1116–1120.

Suri, V., Qian, Z., Hall, J. and Rosbash, M. (1998) Evidence that the TIM light response is relevant to light-induced phase shifts in *Drosophila melanogaster*. Neuron 21, 225–234.

Sweeney, B. M. (1963) Resetting the biological clock in *Gonyaulax* with ultraviolet light. Plant Physiol. 38, 704–708.

Takahashi, J. (2004) Finding new clock components: Past and future. J. Biol. Rhythms 19, 339–347.

Tan, Y., Merrow, M. and Roenneberg, T. (2004) Photoperiodism in *Neurospora crassa*. J. Biol. Rhythms 19, 135–143.

Tassi, P., Pellerin, N., Moessinger, M., Hoeft, A. and Muzet, A. (2000) Visual resolution in humans fluctuates over the 24h period. Chronobiol. Int. 17, 187–195.

Tauber, E., Last, K., Olive, P. and Kyriacou, C. (2004) Clock gene evolution and functional divergence. J. Biol. Rhythms 19, 445–458.

Teng, C., Akerman, D., Cordas, T., Kasper, S. and Vieira, A. (1995) Seasonal affective disorder in a tropical country: A case report. Psychiat. Res. 56, 11–15.

Terman, J. and Terman, M. (1999) Photopic and scotopic light detection in patients with seasonal affective disorder and control subjects. Biol. Cybern. 46, 1642–1648.

Terman, M., Amira, L., Terman, J. and Ross, D. (1996) Predictors of response and nonresponse to light treatment for winter depression. Am. J. Psychiatry 153, 1423–1429.

Thompson, C., Childs, P., Martin, N., Rodin, I. and Smythe, P. (1997) Effects of morning phototherapy on circadian markers in seasonal affective disorder. Br. J. Psychiatry 170, 431–435.

Thompson, C. L., Rickman, C. B., Shaw, S. J., Ebright, J. N., Kelly, U., Sancar, A. and Rickman, D. W. (2003) Expression of the blue-light receptor cryptochrome in the human retina. Invest. Ophthalmol. Vis. Sci. 44, 4515–4521.

Toh, K. I., Jones, R., He, Y., Eide, E. J., Hinz, W. A., Virshup, D. M., Pt?cek, L. J. and Fu, Y. H. (2001) An hPer2 phosphorylation site mutation in familial advanced sleep phase syndrome. Science 291, 1040–1043.

Tomita, J., Nakajima, M., Kondo, T. and Iwasaki, H. (2005) No transcription-translation feedback in circadian rhythm of KaiC phosphorylation. Science 307, 251–254.

Tosini, G. and Fukuhara, C. (2002) The mammalian retina as a clock. Cell Tissue Res. 309, 119–126.

Tosini, G. and Menaker, M. (1996) Circadian rhythms in cultured mammalian retina. Science 272, 419–421.

Toth, R., Kevei, E., Hall, A., Millar, A. J., Nagy, F. and Kozma-Bognar, L. (2001) Circadian clock-regulated expression of phytochrome and cryptochrome genes in *Arabidopsis*. Plant Physiol. 127, 1607–1616.

Touitou, Y. (1998) *Biological clocks: Mechanisms and applications*. Proceedings of the International Congress on Chronobiology Paris 7 - 11 September 1997. Elsevier Amsterdam.

Tu, D., Owens, L., Anderson, L., Golczak, M., Doyle, S., McCall, M., Menaker, M., Palczewski, K. and Van Gelder, R. (2006) From the cover: Inner retinal photoreception independent of the visual retinoid cycle. Proc. Natl. Acad. Sci. USA 103, 10426–10431.

Turek, F. W. (2005) Role of light in circadian entrainment and treating sleep disorders— and more. Sleep 28, 548–549.

Veleri, S., Rieger, D., Helfrich-Förster, C. and Stanewsky, R. (2007) Hofbauer-Buchner eyelets affect circadian photosensitivity and coordinates TIM and PER expression in *Drosophila* clock neurons. J. Biol. Rhythms 22, 29–42.

Visser, E., Beersma, D. and Daan, S. (1999) Melatonin suppression by light in humans is maximal when the nasal part of the retina is illuminated. J. Biol. Rhythms 14, 116–121.

Vollrath, L. (2002) Chronoendokrinologia- quo vadis? Ann. Anatomy 184, 583–593.

Wada, M., Shimazaki, K. and Iino, M. (2005) *Light sensing in plants*. Springer, New York.

Warren, E., Allen, C., Brown, R. and Robinson, D. (2003) Intrinsic light responses of retinal ganglion cells projecting to the circadian system. Eur. J. Neurosci. 17, 1727–1735.

Watanabe, T., Kajimura, N., Kato, M., Sekimoto, M., Hori, T. and Takahashi, K. (2000) Case of non-24 h sleep–wake syndrome patient improved by phototherapy. Psychiatr. Clin. Neurosci. 54, 369–370.

Webb, A. (1998) Stomatal rhythms. In: P. Lumsden and A. Millar (Eds.), *Biological rhythms and photoperiodism in plants*, pp. 69–79. Bios Scientific Publishers, Abingdon.

Wehr, T. A. (2001) Photoperiodism in humans and other primates: Evidence and implications. J. Biol. Rhythms 16, 348–364.

Weller, J., Reid, J., Taylor, S. and Murfet, I. (1997) The genetic control of flowering in pea. Trends Plant Sci. 2, 412–418.

Wever, R. (1979) *The circadian system of man*. Springer, New York.

Wigge, P. A., Kim, M. C., Jaeger, K. E., Busch, W., Schmid, M., Lohmann, J. U. and Weigel, D. (2005) Integration of spatial and temporal information during floral induction in *Arabidopsis*. Science 309, 1056–1059.

Winfree, A. (1970) Integrated view of resetting a circadian clock. J. Comp. Physiol. A 28, 327–374.

Winfree, A. (1986) *The timing of biological clocks*. Scientific American Books, Inc., New York.

Wolfson, A. R. and Carskadon, M. A. (2003) Understanding adolescents, sleep patterns and school performance: A critical appraisal. Sleep Med. Rev. 7, 491–506.

Wright, K. P., Gronfier, C., Duffy, J. F. and Czeisler, C. A. (2005) Intrinsic period and light intensity determine the phase relationship between melatonin and sleep in humans. J. Biol. Rhythms 20, 168–177.

Wright, K. P., Hughes, R. J., kronauer, R. E., Dijk, D. J. and Czeisler, C. A. (2001) Intrinsic near-24-hour pacemaker period determines limits of circadian entrainment to a weak synchronizer in humans. Proc. Natl. Acad. Sci. USA 98, 14027–14032.

Wyatt, J. K. (2004) Delayed sleep phase syndrome: pathophysiology and treatment options. Sleep 27, 1195–1203.

Xu, Y., Padiath, Q. S., Shapiro, R. E., Jones, C. R., Wu, S. C., Saigoh, N., Saigoh, K., Ptacek, L. J. and Fu, Y. H. (2005) Functional consequences of a CKIdelta mutation causing familial advanced sleep phase syndrome. Nature 434, 640–644.

Yamaguchi, S., Isejima, H., Matsuo, T., Okura, R., Yagita, K., Kobayashi, M. and Okamura, H. (2003) Synchronization of cellular clocks in the suprachiasmatic nucleus. Science 302, 1408–1412.

Yamazaki, S., Numano, R., Abe, M., Hida, A., Takahashi, R., Ueda, M., Block, G. D., Sakaki, Y., Menaker, M. and Tei, H. (2000) Resetting central and peripheral circadian oscillators in transgenic rats. Science 288, 682–685.

Yanovsky, M., Mazzella, M. and Casal, J. (2000) A quadruple photoreceptor mutant still keeps track of time. Curr. Biol. 10, 1013–1015.

Yanovsky, M. J. and Kay, S. A. (2003) Living by the calendar: How plants know when to flower. Nature Rev. Mol. Biol. 4, 265–275.

Yoshii, T., Funada, Y., Ibuki-Ishibashi, T., Matsumoto, A., Tanimura, T. and Tomioka, K. (2004) *Drosophila cryb* mutation reveals two circadian clocks that drive locomotor rhythm and have different responsiveness to light. J. Insect Physiol. 50, 479–488.

Young, R. (1976) Visual cells and the concept of renewal. Invest. Ophthalmol. Vis. Sci. 15, 700–725.

Zak, D. E., Doyle, F. J., Vlachos, D. G. and Schwaber, J. S. (2001) Stochastic kinetic analysis of transcriptional feedback models for circadian rhythms. Proc. Second Int. Conf. Systems Biol. 1, 231–238.

Zhong, H. and McClung, C. (1996) The circadian clock gates expression of two *Arabidopsis* catalase genes to distinct and opposite circadian phases. Mol. General Genet. 251, 196–203.

Zhu, H., Yuan, Q., Froy, O., Casselman, A. and Reppert, S. M. (2005) The two crys of the butterfly. Curr. Biol. 15, R953–954.

15
Photoperiodism in Insects and Other Animals

David Saunders

Abstract: Many animals, particularly those living at higher latitudes, use information from day length (or night length) to regulate seasonally appropriate behavioral and developmental strategies. The most common of these are the onset of overwintering diapause in the insects, and seasonal breeding strategies in many animal groups. This chapter examines the role of light in these processes: the photoreceptive "input pathway" to the photoperiodic clock, whether that clock is a function of the circadian system, its relationship to overt behavioral circadian rhythms and, in insects, its endocrine output to diapause or continuous summer development. Major models for the photoperiodic clock are described and evaluated, particularly whether apparent hourglass-like responses represent a distinct non-circadian clock or merely a variant of a circadian-based mechanism in which constituent oscillators "damp" rather rapidly in extended periods of darkness. Finally, some recent developments in unraveling the molecular genetics of the photoperiodic response are described.

15.1. Introduction

Soon after Garner and Allard's (1920) seminal paper on plant photoperiodism, similar observations were made on animals. The first was by Marcovitch (1923, 1924), who observed that the appearance of seasonal morphs in several species of aphids was controlled by day length. The strawberry root aphid, *Aphis forbesi*, for example, produced sexual forms when natural summer days were restricted to seven hours. Conversely, long exposure to artificial light in September inhibited the sexual forms and induced viviparous reproduction typical of the summer. The first papers on the now enormous literature on the photoperiodic induction of insect dormancy (diapause) were those by Kogure (1933) and Sabrosky et al. (1933). Kogure's work on the commercial silkworm *Bombyx mori* was a pioneer in many ways, including observations on light intensity thresholds and spectral sensitivity of the response. Photoperiodic responses have also been

described for other arthropods such as crustacea (Stross and Hill 1968), ticks (Belozerov 1964) and mites (Lees 1953; Veerman 1977); also for other invertebrate phyla such as molluscs (Joosse 1984; Wayne 2001). Among the insects, photoperiodic induction of diapause has been demonstrated in over 500 species from 15 orders (Nishizuka et al. 1998) and must be considered widespread if not almost universal amongst those species living at higher latitudes (Saunders 2002).

Similar day length–dependent effects have been described in vertebrates. Rowan (1926) was the first to show that day length could have important effects on reproduction and behavior of birds (see Dawson et al. 2001). Many species of mammals, too, time their seasonal cycles of breeding by using a photoperiodic response (Baker and Ranson 1932; Bissonnette 1932; Goldman 2001). More limited information is available for "lower" vertebrates, such responses being known for fish, amphibia and reptiles (Underwood and Goldman 1987).

The selective advantages afforded by these photoperiodic responses are both clear and profound. Most animals restrict their physiologically "active" stages, such as growth and reproduction, to those times of the year when food supplies are abundant and climatic conditions are amenable for growth and development. At higher latitudes, therefore, most insects restrict such activities to the warmer months, and the winter is passed in a state of dormancy (diapause) induced, in most cases, by the shorter days of autumn. Among the vertebrates, birds build their nests and lay eggs as days increase in the spring so that the hatchlings are assured of a plentiful supply of food. For similar reasons, mammals also tend to give birth in the spring, those with a short gestation period such as rodents becoming sexually mature as the days lengthen, whereas those with a longer gestation, such as sheep or deer, become sexually active in the autumn. In all cases photoperiodic responses provide seasonally appropriate strategies ensuring maximum survival.

The literature on animal photoperiodism is now very large and cannot be covered adequately in a review of this length. For this reason emphasis will be on the insects, with reference to work on other taxa, particularly birds and mammals, given where appropriate. Particular attention will be paid to the photobiology of the response, and to the contentious question whether the time measurement inherent in insect photoperiodism is provided by components of the circadian system or by some form of nonoscillatory hourglass-like mechanism. Much of the work on insect photoperiodism is still at the stage of physiological experimentation and model building, with modern genetic and molecular investigations lagging behind those of closely related fields such as circadian rhythmicity (see Chapter 14). Here it should be noted that the "genetic" insect of choice—the fruitfly *Drosophila melanogaster*—presents only rudimentary photoperiodic responses (Saunders et al. 1989), unlike its robust daily rhythms of locomotor activity and pupal eclosion which have greatly facilitated analysis of the insect circadian "clock." Until a more congenial model for photoperiodism is forthcoming, analysis of the very complex processes involved in seasonal phenomena will be severely hampered.

15.2. Photoperiodic Regulation of Diapause and Seasonal Morphs in Insects

The enormous variety of photoperiodic responses seen in insects has been reviewed by Tauber et al. (1986), Danks (1987), and Saunders (2002). Very recently, the eco-physiological aspects of insect diapause have been described by Koštál (2006). In the present chapter we will be concerned almost entirely with photobiological aspects of facultative diapause induction in insects inhabiting higher latitudes, i.e., species that produce one or several nondiapause generations during the long days of summer, but divert their development along the diapause pathway in the autumn when days fall below a critical value.

Insects may enter diapause as larvae, pupae, adults, or as embryos within the egg, although the stage at which they do so is in most cases species-specific. For example, most species of *Drosophila* enter diapause as young adults showing a suspension of ovarian development (Lumme 1978), flesh flies (*Sarcophaga* spp.) enter diapause as pupae (Denlinger 1971) and *Aëdes* mosquitoes as embryos. In most cases the endocrinology of diapause is well understood (Denlinger 1985; Saunders 2000). Larval and pupal diapause results from a "block" to the release of the cerebral neuropeptide, prothoracicotropic hormone (PTTH), which, in turn, leads to lowered titers of hemolymph ecdysteroids and a cessation of further growth or moulting. Adult or reproductive diapause, on the other hand, is the result of a temporary "block" to the secretion of neuropeptides regulating the synthesis of juvenile hormones (JH) by the corpora allata, or of ecdysteroids (Richard et al. 1998), and a consequent cessation of vitellogenesis in the ovary. The pivotal event in diapause regulation is thus the control of neuropeptide secretion by neurons in the brain: neuropeptide release leading to non-diapause development, and retention to the diapause state.

Photoperiodic regulation of this pivotal event (Fig. 15.1) must occur at an earlier stage of development, during the so-called photoperiodic "sensitive period." In some insects, such as *Drosophila* adults, the sensitive period occurs in the newly emerged insect soon after eclosion and immediately before the onset of diapause (Lumme 1978). In many larval and pupal diapauses the sensitive period occurs at an even earlier stage; in *Sarcophaga* species, for example, maximum sensitivity to photoperiods regulating pupal diapause occurs in the intra-uterine embryos or during early larval development (Denlinger 1971). In even more extreme cases, diapause in one generation may be regulated by photoperiods experienced maternally. This, for example, is the case for the parasitic wasp *Nasonia vitripennis* (Saunders 1966) and the blowfly *Calliphora vicina* (Vinogradova and Zinovjeva 1972, Saunders 1987). Such delayed responses strongly suggest that the covert effects of photoperiod are stored, perhaps in the brain, or, in the case of maternal responses, transmitted from one generation to the next through the undifferentiated egg. During the sensitive period there is also evidence that inductive photoperiods are accumulated to a threshold above which diapause may be expressed: this phenomenon has been called the photoperiodic "counter" (Saunders 1981). In several species the accumulation of successive
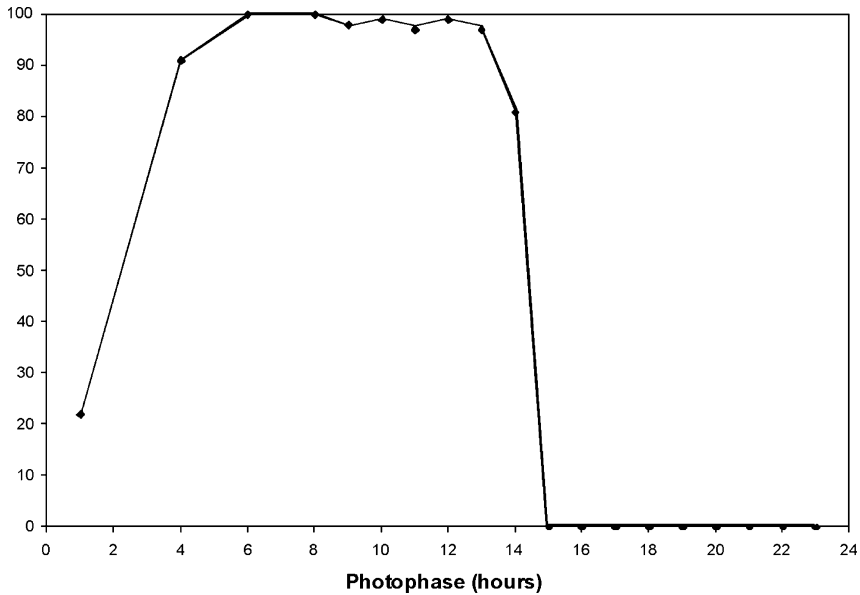
FIGURE 15.1. Photoperiodic induction of larval diapause in the blowfly, *Calliphora vicina*, by maternally operating light cycles. Adult flies were exposed to a range of photoperiods at 20°C; all larvae were raised in continuous darkness at 11–12°C. Note the sharp critical day length at about 14.5 hours light/24, and the fall in diapause incidence under ultra-short day lengths. (Data from Saunders 1987.)

short-day, diapause-inducing cycles is a temperature-compensated phenomenon, whereas the accumulation of long day, nondiapause-inducing cycles is not (Hardie 1990, Saunders 1992).

The effects of temperature on the photoperiodic response are many and varied (Saunders 2002) and will not be reviewed here; suffice it to say, however, that a general rise in diapause incidence occurs with a fall in temperature (see also Section 15.8.).

The diapause "syndrome" frequently includes a number of other physiological and behavioral changes including the deposition of fat and other reserves, the construction of a hibernaculum, and the acquisition of a degree of cold hardiness (Denlinger 1991, Saunders 2002). The whole process of diapause regulation thus comprises a long and often complex series of events, from photoreception through the expression of developmental and reproductive hormones to the behaviors regulated by them. If we regard photoperiodism as the expression of a biological "clock," then the whole of this concatenation must be included in this definition since, without photoreception, day length could not be registered and, without the endocrine effectors, the effects of these day lengths could not be observed.

15.3. Models for Photoperiodism

Formal models have underpinned research into photoperiodism since the earliest days mainly because of the complexity of the response. The first models clearly suggested some sort of "hourglass-like" process measuring either the light or the dark component of the daily cycle (see Saunders 2002). Versions of such models survive today, at least for insect photoperiodism, and will be returned to later.

Probably the greatest single advance in the modeling of this phenomenon was that by Erwin Bünning (1936, 1960, 1964), who suggested that photoperiodic time measurement (initially for plants, but later for insects) was a function of the circadian system. This suggestion has since become known as Bünning's hypothesis (Fig. 15.2).

This model suggested that:

Circadian rhythmicity may somehow provide the "clockwork" for photoperiodism (see Section 15.4.).

Light has a dual function: (1) entrainment of the constituent rhythms and (2) photoinduction of diapause or nondiapause development (Sections 15.4. and 15.7.).

Overt circadian rhythms may provide observable "hands of the clock" for the otherwise covert photoperiodic system (Section 15.5.).

The constituent circadian components may in some cases be damping oscillators (Section 15.6).

These four points will be addressed in the following account.

Experimental support for Bünning's hypothesis was first provided for plants, and then later for insects, birds, and mammals. In the 1960s Colin Pittendrigh became an enthusiastic and vociferous supporter of Bünning's hypothesis and proposed several ways (dubbed "coincidence" models) in which the circadian system could provide a "clock" for photoperiodic time measurement (Pittendrigh and Minis 1964, Pittendrigh 1966, 1972). These include the following:

1. *External coincidence* (Fig. 15.3) was a direct development of Bünning's original hypothesis using data from the entrainment of the pupal eclosion rhythm of *Drosophila pseudoobscura* to make it more relevant to the insects. Like Bünning's original it preserved the dual action of light. It proposed that the daily light cycle *entrained* the constituent oscillation(s) in such a way that a particular light-sensitive phase, which Pittendrigh called the *photo-inducible phase*, occurred toward the end of the dark component of the cycle. As with most insect circadian rhythms, the constituent oscillation(s) were phase-set by light phases longer than about 10 hours to circadian time (CT) 12 (the beginning of the "subjective night") so that the photo-inducible phase occurred about 9.5 hours (or the critical night-length) later. In short-day (or long-night) cycles the photo-inducible phase thus remained in the dark, whereas under long-day (or short-night) cycles it was illuminated by the "dawn" transition of the photophase. The insect photoperiodic "clock" thus "measured" night
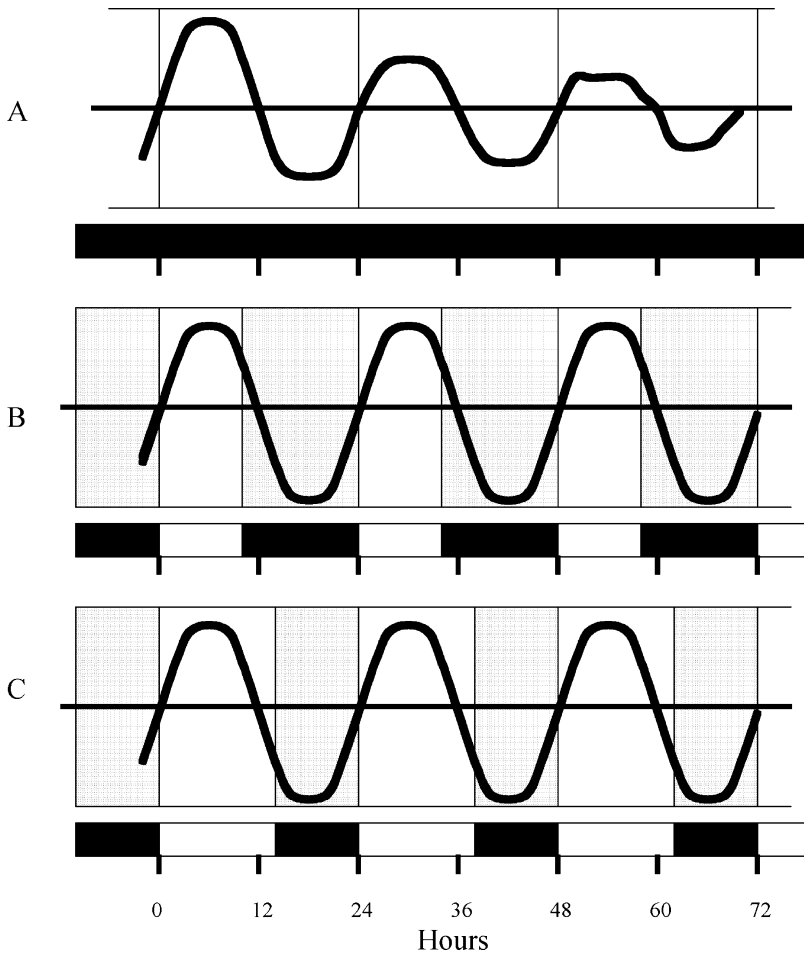
FIGURE 15.2. Bünning's (1936) model for the execution of photoperiodic time measurement by a circadian oscillation. (**A**) The free-running rhythm in continuous darkness (DD) showing slow oscillator damping. (**B**) Under short days (long nights) light does not extend into the second ("scotophil") half of the cycle, whereas in **C** (long days or short nights) it does. Illumination of the early part of the night was thought to activate the long-day or summer response. (After Bünning 1960.)

length rather than day length, and illumination or nonillumination of the photo-inducible phase became the pivotal event ultimately regulating the retention or release of the neurohormones controlling diapause or continuous development.

2. *Internal coincidence.* As an alternative to external coincidence, Pittendrigh (1972) proposed that the insect photoperiodic clock might comprise *two* oscillators, or groups of oscillators, one phase set primarily by the "dawn" transition of the daily photophase, the other by "dusk." Induction of the different physiological states was then controlled by the phase angle between these two
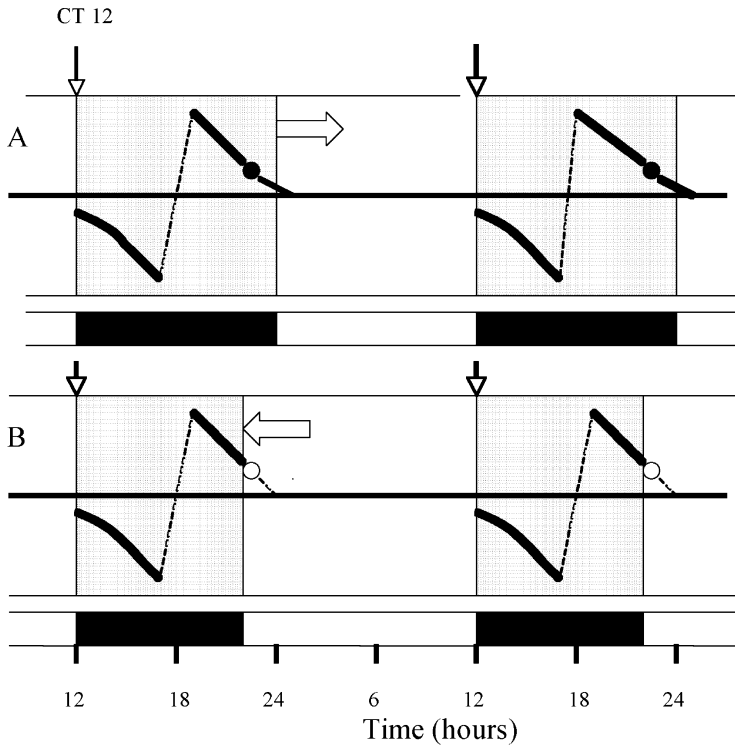
FIGURE 15.3. The external coincidence model for photoperiodic time measurement, a form of Bünning's hypothesis more appropriate for the insects. The oscillation is shown as a phase response curve (see Chapter 14) and the photo-inducible phase, occurring late in the subjective night, as a closed or open circle. In insects, the circadian oscillation is reset to a narrow range of phases close to circadian time (CT) 12 at the end of a protracted photophase (vertical arrows), before "release" into darkness. **(A)** Under short days or long nights, the photo-inducible phase (closed circle) then falls in the dark, leading to diapause induction. **(B)** Under long days or short nights, it is illuminated by the "dawn" transition of the daily photophase (open circle), leading to continuous or nondiapause (summer) development. The large open arrows show the seasonal direction of change of the "dawn" transition in relation to the "clock" oscillation, in **A** with an autumnal shortening of the day length, and in **B** with a springtime lengthening (After Pittendrigh 1966.)

oscillators as day length changed with the seasons. It should be noted here that, unlike external coincidence, this type of model proposes that light has a single role (entrainment) rather than two (entrainment and photoinduction). It should also be noted that external and internal coincidence are only two of a number of models, and are not mutually exclusive. Internal coincidence has been suggested for some species of insect such as the parasitic wasp *Nasonia vitripennis* (Saunders 1974), but external coincidence remains the favored model for many insects, as well as plants, birds (Dawson et al. 2001), and

some mammals (Elliott 1976). In birds, unlike insects, the photo-inducible phase seems to lie in the *early* subjective night.

Although external coincidence offers an attractive explanation for photoperiodic induction, the theoretical possibility of some sort of internal coincidence is provided by recent evidence for separate "morning" and "evening" oscillators in *D. melanogaster*, generated by different groups of neurons in the brain (Helfrich-Förster 2001, Stoleru et al. 2004, 2005), and together regulating overt rhythms of locomotor activity.

15.4. Evidence for the Involvement of the Circadian System in Photoperiodic Time Measurement

Evidence for the participation of the circadian system in photoperiodic time measurement is derived from experiments in which animals are subjected to light–dark cycles similar to those that have defined the properties of overt circadian rhythms and their entrainment by light (Fig. 15.4). The parallel peculiarities between photoperiodic responses and well-characterized behavioral rhythms often show very great similarities. These experiments have been reviewed on earlier occasions (Vaz Nunes and Saunders 1999, Saunders 2002, 2005, Saunders et al. 2004) and will not be dealt with here in detail. Broadly speaking, however, they fall into about four categories (Fig. 15.4; Sections 15.4.1.–15.4.3.).

15.4.1. Nanda-Hamner Experiments

In Nanda-Hamner or "resonance" experiments, insects (or other organisms) are exposed to a range of light cycles each containing a "main" photophase of, say, 6–12 hours coupled to a variable length of darkness to give overall cycles (T) ranging from about 20 to 72 hours or more. In these experiments, therefore, the light "comes on" at different circadian phases and should reveal any photo-inducible phase that might repeat itself with a circadian frequency in the periods of extended darkness. This experimental design was first employed for plants (see Chapter 17) and later for birds (Hamner 1963), mammals (Elliott 1976) and numerous insects. Results for plants, birds, and mammals usually show periodic maxima of induction when T is close to 24, 48, or 72 hours, but minima when T is close to 36 or 60 hours. Results for insects, however, are rather more complicated. "Positive" Nanda-Hamner responses, like those above, have been recorded in about 15 or more species from about six orders of insects and some mites. Examples are shown in Fig. 15.5A, in which alternate peaks and troughs in diapause incidence occur at roughly 24-hour intervals as the dark component of the cycle is increased. These peaks and troughs are interpreted as an expression of the circadian system in the inductive process. "Negative" Nanda-Hamner responses, however, fail to show such a periodic effect (Fig. 15.5B); their interpretation will be attempted later (see Section 15.7.).
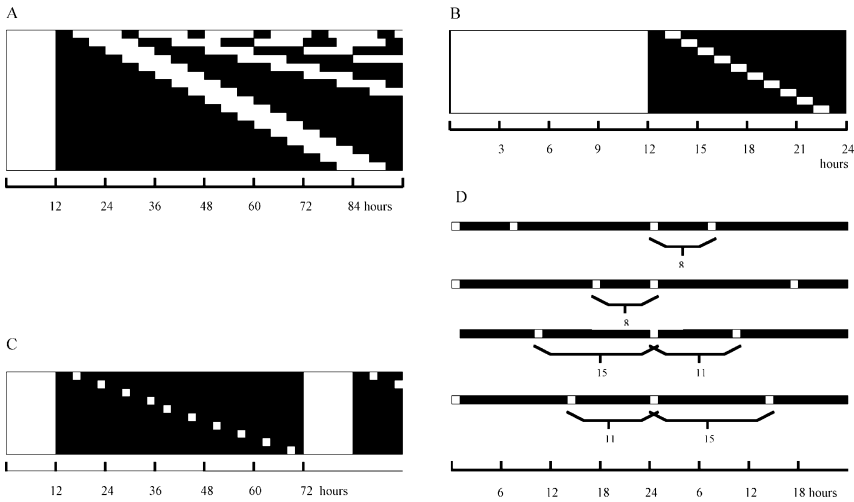
FIGURE 15.4. Illumination protocols used to uncover possible circadian participation in photoperiodic time measurement. **(A)** The Nanda-Hamner protocol in which different experimental subsets of the test organism are exposed to light–dark cycles (reading horizontally, left to right) consisting of a "short" photophase (in this case, 12 hours) coupled with a variable dark phase to give overall cycle lengths covering several circadian periods. **(B)** Night-interruption experiment in which the "long" night of an otherwise short-day regime is systematically interrupted by a short supplementary light pulse. **(C)** The Bünsow protocol in which the night-interruption technique is applied to light–dark cycles longer than 24 hours, in this case to LD 12:60. **(D)** "Skeleton" photoperiods and "zone of bistability." Top two panels: organisms are initially exposed to "skeletons" formed from two short (1-hour) pulses of light delimiting either an 8-hour photoperiod (1:6:1:16) or an 18-hour photoperiod (1:16:1:6). In both cases the constituent circadian oscillations accept the shorter "interpretation" (1:6:1) which simulates an 8-hour "complete" photoperiod, and results in a high incidence of the short-day response (diapause). Lower panels: organisms are initially exposed to 1:9:1:13 or 1:13:1:9, "skeletons" that lie within the "zone of bistability" (see text). Acceptance of the shorter "interpretation" (1:9:1:13) simulates a "complete" photoperiod of LD 11:13 and leads to a high incidence of diapause; acceptance of the longer "interpretation" (1:13:1:9) simulates a "complete" photoperiod of LD 15:9 and leads to a long-day response (nondiapause development). See text for further details.

15.4.2. Night Interruption Experiments and the Bünsow Protocol

In night-interruption experiments, the "long" night of an otherwise diapause-inducing 24-hour cycle is systematically interrupted, in different experimental subsets, by a short, supplementary, light pulse. In many insects such experiments produce two points of long-day (nondiapause) effect, one early in the night (called point A), the second later in the night (point B) (see Saunders 2002). The interpretation of such results by Pittendrigh and his associates (Pittendrigh and Minis 1964, Pittendrigh 1966) led directly to the "external coincidence" model.
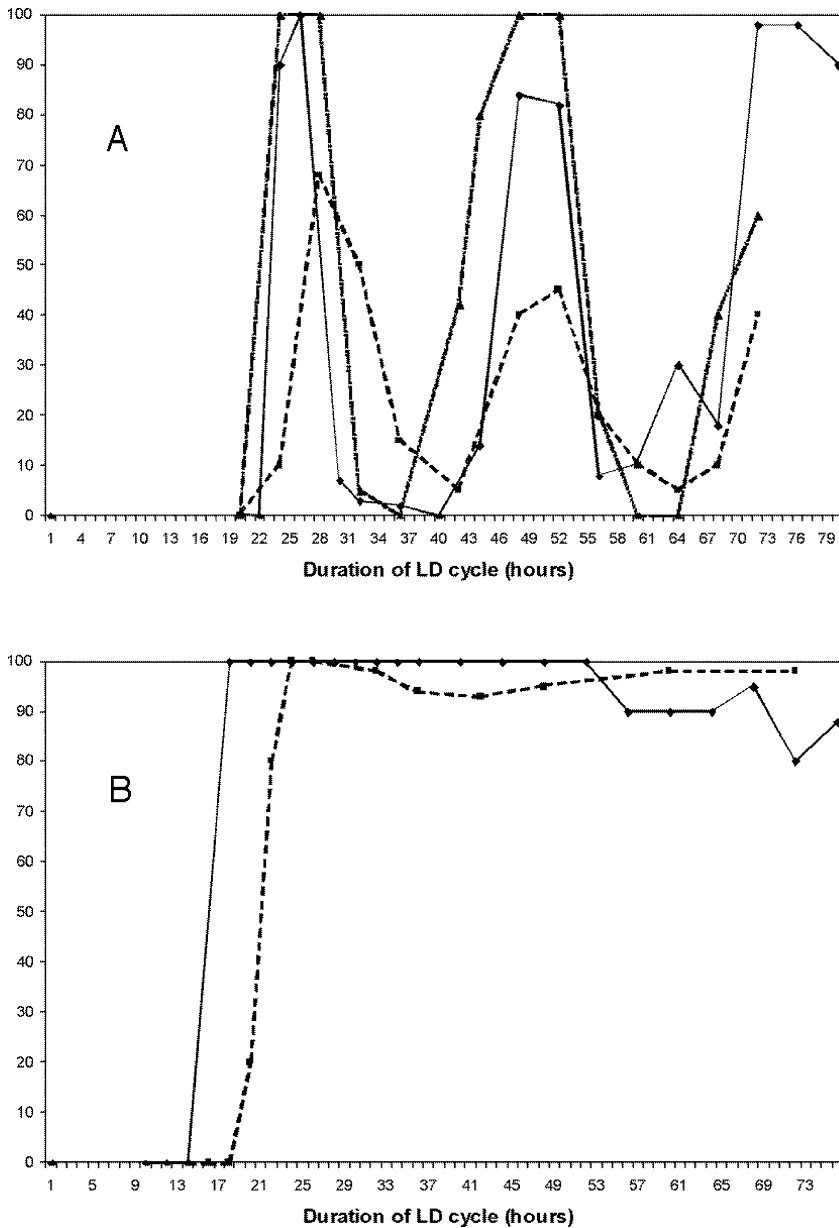
FIGURE 15.5. Results of Nanda-Hamner experiments with various insects. (**A**) "positive" responses showing alternate "peaks" and "troughs" of short-day effect (high diapause incidence) occurring with an increase in the duration of the LD cycle. Solid line: larval diapause induction in the blow fly *Calliphora vicina* with a 13-hour photophase at 23°C; dashed line: pupal diapause in the flesh fly *Sarcophaga argyrostoma* with a 14-hour photophase at 20°C; dotted line: larval diapause in the parasitic wasp *Nasonia vitripennis* with a 12-hour photophase at 17°C. (**B**) "negative" responses showing no peaks and

In short, the supplementary light pulses were seen to cause phase shifts (see Chapter 14) of the constituent circadian oscillator(s). Pulses falling early in the night caused phase *delay*s; those in the second part of the night caused phase *advance*s. The light pulse falling at point B *was thought to coincide directly with the photo-inducible phase*, that falling at point A merely causing a phase delay until the photo-inducible phase (at B) was delayed across the "dawn" transition of the "main" photophase. Such results clearly indicated the importance of the circadian system in photoperiodic time measurement, and drew attention to the probable dual function of light: entrainment and photo-induction.

In the so-called Bünsow protocol (Fig. 15.4C), first performed on plants (Bünsow 1953), the night-interruption technique was applied to non-24-hour light–dark cycles in which the dark component was greatly extended. In insects, as with Nanda-Hamner experiments, the results are complicated by both "positive" and "negative" responses (Saunders 2002). "Positive" responses revealing points of long-day effects (e.g., nondiapause development) at circadian intervals in the extended dark period have been recorded in about nine species from five insect orders and from some Acarina. "Negative" responses showing no such repeated long-day effects have been recorded in about five species from three insect orders. As with Nanda-Hamner responses, an interpretation of these "negative" responses will be attempted later (see Section 15.7.).

In another type of experiment (the so-called T experiment), different groups of insects were exposed to very short (e.g., 1-hour) pulses of light in cycles covering the primary range of entrainment, ranging from about T 21.5 hours to T 30.5 hours (i.e., from LD 1:20.5 to LD 1:29.5) (Saunders 1979). Entrainment theory (see Chapter 14) predicts that when T is *less* than the circadian period (about 24 hours) the light pulse must fall in the *late* subjective night to cause a *phase advance*, whereas when T is *greater* than the circadian period the pulse must fall in the *early* subjective night to cause a *phase delay*. Therefore, simply by changing the *period* of the light cycle (T) the pulse can be made to illuminate different phases of the oscillation when it reaches steady-state entrainment. With *S. argyrostoma* the results of such an experiment showed that long-day effects (nondiapause development) only occurred in a cycle of T 21.5 hours (LD 1:20.5), and calculations using the 1-hour phase response curve for eclosion rhythmicity (see Section 15.5.) indicated that, in this regime, the light pulse *coincided directly with the photo-inducible phase*. In all other cycles the photo-inducible phase fell in the dark and diapause incidence was high. The results of this particular experiment are important for three reasons, showing (1) that circadian entrainment is central to the phenomenon; (2) that a very short light pulse may operate the photoperiodic "switch" if it falls at the "correct" phase; and (3) therefore, the *timing* of that light pulse is crucial, rather than its duration.

FIGURE 15.5. (Continued) troughs in the response. Solid line: ovipara production in the vetch aphid *Megoura viciae* with an 8-hour photophase at 15°C; dashed line: pupal diapause in *S. argyrostoma* with a 12-hour photophase and reduced temperature (16°C).

15.4.3. Skeleton Photoperiods and Bistability Phenomenon

In plants (Hillman 1964) and in insects (Pittendrigh 1966; Saunders 2002), powerful evidence for photoperiodic time measurement being a function of the circadian system has also come from experiments using "symmetrical skeleton" photoperiods, particularly those within the *zone of bistability*. Symmetrical skeletons comprise *two* short (say 1-hour) pulses of light arranged *n* hours apart in each 24-hour cycle to give a pattern of LD $1:n_1:1:n_2$. When the interval defined by $1:n_1:1$ is less than about 10 hours a circadian oscillation entrains to the complex in almost the same way as it does to a "complete" photoperiod of that duration. On the other hand, when n_1 is greater than about 14 hours, the oscillation undergoes a phase-jump to accept $1:n_2:1$ as "day" because that is now the shorter interval. If insects are exposed to such cycles during their photoperiodically sensitive period, these "skeletons" lead to the induction of a high incidence of diapause unless the pulses are close to about 12 hours apart (Saunders 1975). Such experiments are of interest because they demonstrate once again that the short light pulses have a *timing* function rather than being important for their duration or energy input.

When the two dark intervals in a symmetrical skeleton are close to one-half of a circadian cycle (i.e., about 11–13 hours) the response becomes subject to "bistability" (Pittendrigh 1966) (Fig. 15.4D). Each skeleton photoperiod is now open to *two* "interpretations" depending on whether the longer or the shorter interval is taken as "day" when the system achieves steady state. Working with the pupal eclosion rhythm of *Drosophila pseudoobscura* it was shown that the phase relationship adopted was dependent on (1) the *phase* (circadian time) illuminated by the first pulse in the train and (2) the value of the first *interval* seen. For example, a skeleton of 11 hours assumed the phase characteristics of an 11-hour "complete" photoperiod when the first interval was 11 hours and the first pulse fell at circadian time (CT) 11 or 16. Conversely, the same skeleton assumed the characteristic phase of a 13-hour photoperiod when the first interval seen was 13 hours and the first pulse fell at CT 03 or 22 (Pittendrigh 1966). Similar responses were reported for the pink bollworm moth *Pectinophora gossypiella* using the egg-hatch rhythm as an indicator of phase (Pittendrigh and Minis 1971).

Working with the flesh fly *Sarcophaga argyrostoma,* larvae were exposed to symmetrical skeleton photoperiods (two 1-hour pulses of light per cycle) of either 11 hours (LD 1:9:1:13) or 15 hours (LD 1:13:1:9) with the first pulse in the train commencing at all circadian times (Saunders 1975). These skeletons were chosen because they were "mirror images" of each other and, if adopted by the circadian oscillator, would be "read" as short (diapause inductive) or long (nondiapause inductive) "complete" photoperiods, respectively. Results showed that when the 11-hour interval (1:9:1) was presented first, short-day responses (high diapause incidence) were observed when the first pulse started between CT 19 and 08, but long-day responses (low diapause incidence) when the first pulse started between CT 09 and 19. When the 15-hour interval (1:13:1) was presented first the results were a mirror image with a high incidence of diapause between
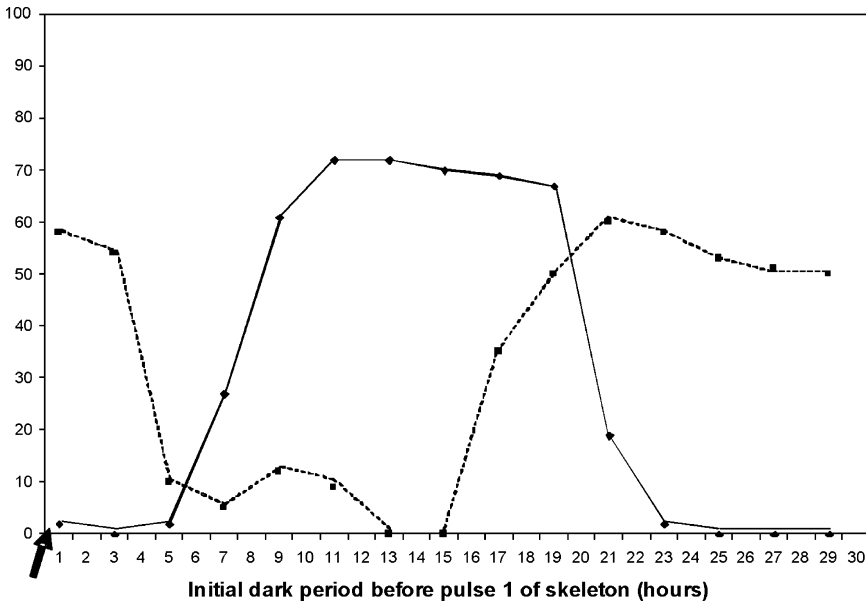
FIGURE 15.6. A "positive" bistability experiment on pupal diapause induction in the flesh fly *Sarcophaga argyrostoma*. Cultures of larvae were exposed, at 18°C, to "skeleton" photoperiods of LD 1:9:1:13 or LD 1:13:1:9 with the first 1-hour pulse of the "skeleton" starting at different times after transfer of the cultures from continuous light (LL) to darkness (equivalent to Circadian time, CT 12— arrow).Solid line: LD 1:9:1:13 given first. The 1:9:1 interval is interpreted as an 11–hour photophase (a high incidence of diapause) when the first pulse commences between 7 and 21 hours after the LL/DD transfer (i.e., between CT 19 and 08); in all other regimes the 1:13:1 interval is accepted as a 15-hour photophase (a low incidence of diapause).Dotted line: LD 1:13:1:9 given first. The 1:13:1 interval is interpreted as a 15-hour photophase (low diapause) when the first pulse commences between 5 and 15 hours after the LL/DD transfer (i.e., between CT 17 and 04); in all other regimes the 1:9:1 interval is accepted as an 11-hour photophase (high diapause). Data from Saunders (1975).

CT 04 and 17 and low incidence of diapause between CT 17 and 04 (Fig. 15.6). Other examples of a "positive" response to bistability have been recorded for the blowfly *Calliphora vicina* (Vaz Nunes et al. 1990) and the cabbage moth *Mamestra brassicae* (Kimura and Masaki 1993). In a number of other insects, however, results were "negative" (Saunders 2002) and were interpreted by some authors as evidence for a sort of nonoscillatory "hourglass" (see Section 15.6.).

15.4.4. The Effects of Transient or Non–Steady-State Entrainment on Diapause Induction

Short or "weak" light pulses cause small phase changes to a circadian oscillation and give rise to a low "amplitude" (Type 1) phase response curve (PRC) (see

Chapter 14). Conversely, longer or "stronger" light pulses cause larger phase shifts and produce a higher "amplitude" (Type 0) PRC. At the end of a long pulse of light the oscillation in many insects is also phase-set to a near constant phase of CT 12 (Pittendrigh 1966). Therefore when exposed to a train of "weak" light pulses, with the first pulse falling out of phase, the oscillation *goes through a greater number of transients* before steady-state entrainment that it does when exposed to a train of "strong" pulses. If circadian oscillations are involved in the photoperiodic input pathway, marked effects on diapause incidence would thus be expected between "weak" and "strong" pulses commencing at different initial phases and undergoing a different number of transients, probably because of effects on the summation of inductive cycles by the photoperiodic "counter."

Figure 15.7 shows the incidence of pupal diapause in cultures of *S. argyrostoma* exposed as larvae to trains of "weak" or "strong" pulses of light with the first pulses commencing at either CT 24/0 (initially out of phase) or CT 12 (initially in phase). With "strong" light pulses (10–13 hours) steady state was achieved rapidly with few transients, and diapause incidence was high in insects
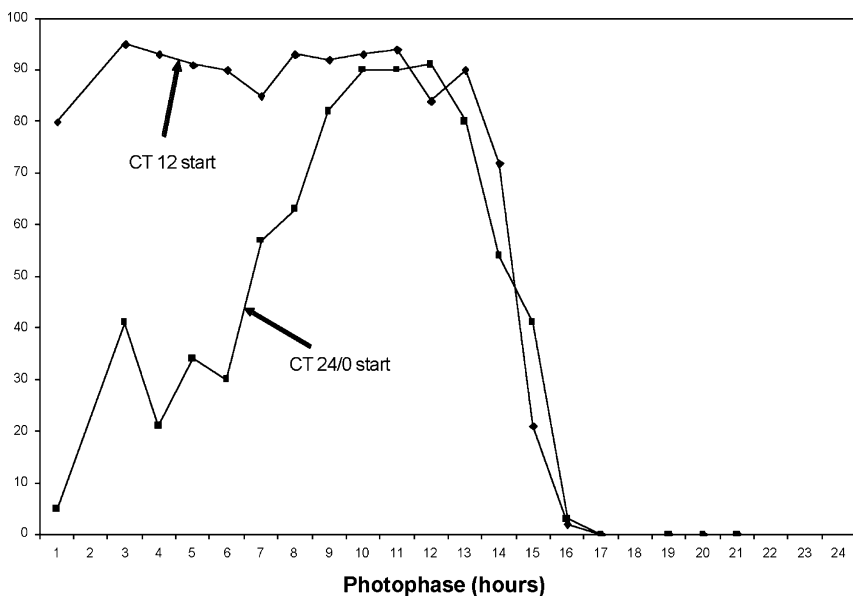
FIGURE 15.7. Pupal diapause induction in the flesh fly, *Sarcophaga argyrostoma*, with the first light pulse in the train of pulses commencing either at Circadian time (CT) 12 or at CT24/0. With a CT 12 start, all photophases shorter than about 13 hours induce a high incidence of diapause, whereas with an out-of-phase CT 24/0 start, photophases less than about 9 hours lead to a lower incidence of diapause. Computer modeling (e.g., Lewis 2002) has shown that cultures starting initially out of phase proceed to steady-state entrainment through a greater number of non–steady-state transient cycles; an increased number of such transients adversely affect the final incidence of diapause because inductive cycles are accumulated during the insect's "sensitive period." (Data from Saunders 2002.)

with both starting phases. On the other hand, with weaker pulses (1–8 hours), the resulting incidence of diapause was much lower, especially when the initial pulse occurred at an out-of-phase position (CT 24/0) and the oscillations went through a higher number of transient cycles before steady state was achieved (Saunders 2002).

15.5. Using Overt "Indicator" Rhythms as "Hands of the Clock"

The analysis of photoperiodic induction in *S. argyrostoma* described in the previous section was greatly facilitated by studying diapause incidence and the entrainment of an overt behavioral rhythm in the same or similar experiments, following Bünning's suggestion that such behavioral rhythms could be used as "hands of the clock." To do this, a "family" of phase response curves (PRCs) (see Chapter 14) for the pupal eclosion rhythm was established for pulse durations of between 1 and 20 hours of white light (240 $\mu W/cm^2$), and these were used to predict the phase relationship of the photo-inducible phase to the light cycle using a computer program to determine the steady states achieved after trains of pulses given during the insects' sensitive period. In all of the complex regimes described in Section 15.5. illumination of the supposed photo-inducible phase (at CT 21.5) led to nondiapause development, whereas if the photo-inducible phase fell in the dark, diapause supervened (Saunders 1975, 1978, 2002). In the flesh fly, therefore, an overt behavioral rhythm (pupal eclosion) served as the "hands of the photoperiodic clock" in a manner predicted by Bünning.

This approach, however, has also produced its problems. Even in *S. argyrostoma,* certain differences between the circadian oscillators involved in photoperiodic induction and eclosion soon became apparent: although both had an endogenous period close to 24 hours, the former showed evidence of oscillator damping whereas the latter was fully self-sustained (Saunders 1986). In other species, differences were more marked and a comparison consequently became more difficult. For example, in the blowfly *Calliphora vicina* the oscillator controlling the rhythm of adult locomotor activity showed a mean period of about 22.5 hours and was fully self-sustained, whereas the oscillator(s) involved in photoperiodic induction had a period (as judged from Nanda-Hamner interpeak intervals) of about 24 hours and showed marked evidence of damping (Saunders 1997) (see also Section 15.6.). In addition, artificial selection for a long critical day length in *C. vicina* had no effect on the period of the locomotor activity rhythm (Saunders and Cymborowski 2003), showing that they were physiologically separate components of the circadian system. Within geographical strains of *Drosophila littoralis,* eclosion rhythm period and critical day length showed rather similar latitudinal clines, but a clear cause-and-effect relationship between the two variables was not apparent (Lankinen 1986). This difference was underlined in a recent paper (Lankinen and Forsman 2006) in which 54 generations

of artificial selection led to a strain showing extreme "southern" character-
istics for diapause induction (i.e., a long critical night length), but extreme
"northern" characteristics for pupal eclosion (i.e., a short circadian period). The
"separate" nature of these two systems was therefore abundantly clear, and the
results indicated that the two processes (eclosion rhythmicity and photoperiodic
timing) were based, at least in part, on somewhat different genetic mechanisms.
In these and other examples, the "separate" nature of photoperiodic induction
from overt behavioral rhythmicity does not mean, however, that the former is
not controlled by components of the circadian system. Both processes may be
circadian based but may involve different light input pathways, different cellular
locations, different properties (of period, persistence, etc.) and different behav-
ioral or physiological outputs.

15.6. The "Hourglass" Alternative: Damping Oscillations

In a number of insects, the experiments described in Section 15.4. gave rise
to so-called "negative" responses, failing to indicate a clear circadian basis for
night length measurement (see Vaz Nunes and Saunders 1999, Saunders 2002).
To some authors this has suggested that photoperiodic time measurement might
be accomplished by an "hourglass type" of mechanism with little or no reference
to the circadian system. For the Nanda-Hamner protocol, the most widely used
experiment of this type, "negative" responses produced *short* night effects (i.e.,
a low incidence of diapause) until the duration of darkness exceeded the critical
night length, but then produced *long* night effects (i.e., a high incidence of
diapause) with a high "plateau" showing none of the peaks and troughs of
diapause induction seen in "positive" responses (Fig. 15.5). However, a signif-
icant complication was that "positive" and "negative" responses could sometimes
be observed *in the same species*, depending on conditions. For example, in
S. argyrostoma hourglass-like responses could be observed at lower temper-
ature (Fig. 15.5B) (Saunders 1973, 1982), in the beetle *Pterostichus nigrita* at
higher latitudes (Thiele 1977), and in the cabbage butterfly *Pieris brassicae*
merely with a change of diet (Dumortier and Brunnarius 1989). In other species,
such as the cricket *Pteronemobius nigrofasciatus* (Masaki 1984) and the spider
mite *Tetranychus urticae* (Veerman and Vaz Nunes 1980, 1987; Vaz Nunes
and Veerman 1982), "positive" responses were shown in some experiments but
"negative" responses in others. These complications have been reviewed in more
detail by Saunders et al. (2004) and Saunders (2005), to which papers the reader
is directed.

   It seems rather improbable that an insect could switch from one type of
photoperiodic "clock" (a circadian-based mechanism) to another (an "hourglass")
just with a change of temperature, latitude, or diet. An alternative explanation
for these diverse results might be that all photoperiodic responses are the product
of a single type of mechanism, but that its outcome (rhythmic or hourglass-
like) is merely the *expression* of this mechanism under different conditions. The

solution to this conundrum was supplied by Bünning himself, who suggested that so-called "hourglasses" might *be heavily damped circadian oscillators*; this possibility is illustrated in Fig. 15.2, taken from Bünning (1960, 1964) and showing such damping in protracted periods of darkness. In reality, however, the apparent damping of photoperiodic oscillators could be the result of a developing incoherence among a group of otherwise self-sustained oscillators, giving the outward *appearance* of damping.

The idea that apparent "hourglass" responses might be an expression of oscillator damping was further developed by Lewis and Saunders (1987) and Saunders and Lewis (1987a, b) using a computer model based on a feedback control system derived, in part, from an earlier model by Johnsson and Karlsson (1972). The damped oscillator model of Lewis and Saunders (1987) incorporated several simple components such as the rate of synthesis (of a protein), its degradation, the time delay between synthesis and degradation, and the effects of light and temperature, that were readily interpreted in terms of the physiology and behavior of potential molecular components of a "clock." A low synthesis rate (SR) gave rise to an oscillation that damped below a threshold, to a value below which the diapause inductive mechanism ceased to operate (Lewis and Saunders 1987, Saunders et al. 2004). Simulations using this model thus showed that a low value of SR could give rise to a damping oscillation and to many of the distinctive features of the insect photoperiodic response: (1) the fall in diapause incidence in darkness or ultra-short day lengths (Fig. 15.1), (2) the declining peaks of diapause incidence in Nanda-Hamner experiments as T increased (Fig. 15.5A), and (3) hourglass-like features arising from the inability of the oscillator to reset itself in protracted periods of darkness (Saunders and Lewis 1987a,b; Saunders et al. 2004; Saunders 2005). Very low values of SR gave rise to a rapidly dampening oscillator that fell below threshold after one or very few cycles; such simulations gave a good representation of the clear hourglass-like responses of insects such as the aphid *Megoura viciae* (Lees 1973).

15.7. Photoreception and Clock Location

Photobiological aspects of photoperiodic induction include the identification of the relevant photoreceptors, entrainment of the circadian oscillations (see also Chapter 14) in the light input pathway, and probably also the operation of the "pivotal" events occurring when the effects of light coincide (or not) with the photo-inducible phase.

In mammals, the sole photoreceptors for photoperiodism—as well as for the entrainment of behavioral rhythms—are the eyes, cutting the retinohypothalamic tracts between the eyes and the suprachiasmatic nuclei leading to free-running behavioral rhythms and an inability to distinguish short from long days (reviewed in Goldman 2001). In birds, however, the eyes are less important; their removal does not block the photoperiodic response. Light reception appears

to involve receptors deep in the septal-hypothalamic region of the brain (Dawson et al. 2001).

Multiple photoreceptors are probably important in insect photoperiodism (Saunders 2002). Early data suggested that "organized" photoreceptors such as the compound eyes and ocelli were not involved; this was the conclusion both for immature stages of the holometabola, which lack compound eyes (Shimizu 1982), as well as for adult insects, or the immature stages of hemimetabola, which do bear such eyes. For example, in the blowfly *Calliphora vicina*, an insect with a larval diapause induced by maternally perceived short days, complete bilateral removal of the optic lobes, an operation that effectively separates the compound eyes from the brain, left photoperiodic induction of diapause intact (Saunders and Cymborowski 1996). Lobectomized flies were found to differentiate short days from long days by producing diapause or nondiapause progeny accordingly, strongly suggesting that the compound eyes were *not essential* for photoreception. The brain was, therefore, a likely site both for both the clock mechanism and its photo-receptors. Brain-centered photoreception has also been demonstrated in numerous other species including the aphid *Megoura viciae* (Lees 1964, Gao et al. 1999), the cabbage white butterfly *Pieris brassicae* (Claret 1966), and the silk moth *Bombyx mori* (Shimizu and Hasegawa 1988).

Conclusive proof that the brain may contain the photoreceptors (and the entire clock mechanism) was afforded by the in vitro illumination of excised brain complexes (Bowen et al. 1984, Hasegawa and Shimizu 1987). Working with short-day (diapause-induced) larvae of the tobacco hornworm moth *Manduca sexta,* Bowen et al. (1984) showed that a brain, together with its corpus cardiacum (CC) and corpus allatum (CA), removed from such a larva and exposed to three long-day cycles in vitro, was capable, after implantation into a recipient short-day larva, of redirecting development along the nondiapause pathway. Similar results were later described by Hasegawa and Shimizu (1987) using larvae of *Bombyx mori*.

In contrast to the situation described above, some insects do use their compound eyes as photoperiodic photoreceptors (Ferenz 1975, Numata and Hidaka 1987, Shiga and Numata 1996). This is even the case for the black blow fly *Protophormia terraenovae* (Shiga and Numata 1997), a close relative of *Calliphora vicina* in which the eyes are apparently not essential. The conclusion must be that a range of different photoreceptors are used in the insects, perhaps with multiple photoreceptive inputs being used in a single species, as for the entrainment of behavioral rhythmicity in *D. melanogaster* (Rieger et al. 2003).

The spectral sensitivity of the photoperiodic response has been studied in a number of insects (see Saunders 2002). Most of these studies have indicated a maximum sensitivity to light between 400 and 500 nm with a sharp cutoff at longer wavelengths. Very few energy-compensated action spectra have been performed, however, the most notable exception being that of Lees (1966, 1971) with the green vetch aphid *Megoura viciae,* a species that produces parthenogenetic and viviparous daughters (*virginoparae*) under the long days of summer, but switches to the production of egg-laying *oviparae* as days shorten. Using

narrow-band filters in conjunction with neutral density filters, Lees exposed test virginoparae to 1-hour pulses of monochromatic light interrupting the dark phase of an otherwise ovipara-inducing cycle (LD 13.5:10.5), either *early* in the night (equivalent to point A) or *late* in the night (at point B), positions at which such interruptions cause long-day effects (see Section 15.4.2.). Results for early night interruptions showed a maximum sensitivity between 450 to 470 nm, with an intensity threshold at that wavelength of about 0.2 µW cm^{-2}. For late night interruptions, maximum effectiveness was again in the blue, but sensitivity extended some way into the red.

To many authors the pronounced blue sensitivity revealed by action spectra suggested that the photoperiodic photoreceptor might contain a carotenoid-based chromophore. In a number of elegant studies, Veerman and his colleagues (Veerman 1980, Veerman et al. 1983, 1985, Van Zon et al. 1981) then proceeded to demonstrate the importance of carotenoids and of vitamin A in the photoperiodic responses of several species of mites. Similar studies with insects reared on carotenoid-free diets, or diets deficient in vitamin A, have shown that lost photoperiodic responses may be restored following the addition of β-carotene or of vitamin A to the diet (Takeda 1978. Shimizu and Kato 1984. Claret 1989. Veerman et al. 1985).

Using immuno-cytochemical techniques, Gao et al. (1999) investigated the anatomical location and nature of the photoperiodic photoreceptor in the aphid *M. viciae*. Twenty antibodies raised against a range of invertebrate and vertebrate opsins and proteins in the phototransduction cascade were used. Seven of these, including *Drosophila* rhodopsin 1, vertebrate cone and rod opsins, vertebrate arrestin, vertebrate transducin. and vertebrate cellular retinoid binding protein, consistently labeled an area of the ventral neuropile close to the medial neurosecretory cells considered to be the photoperiodic (hormonal) effectors (Lees 1964, Steel and Lees 1977). Since then, Shimizu et al. (2001) have cloned a novel opsin (boceropsin) from the larval brain of the silk moth *Bombyx mori*. Immunohistochemical analyses have demonstrated that Boceropsin is localized bilaterally in defined cells of the larval brain, where it may function as the photoperiodic receptive pigment.

Given that the entrainment of circadian oscillations is important in the photoperiodic response, and that the most likely model for photoperiodic time measurement (external coincidence) strongly suggests a dual role for light, it seems possible that the two processes (entrainment and photo-induction) may use *different* photoreceptors. For example, light acting on the circadian input pathway to brain-centered receptors may use cryptochrome (or carotenoids if entrainment is through the eyes), whereas photo-induction may use a receptor with an opsin-based chromophore. Although speculative, this suggestion receives some support from two sources: (1) the somewhat different action spectra in night interruption experiments in *M. viciae* for points A (phase delay) and B (phase advance *and* illumination of the photo-inducible phase) (Lees 1964), and (2) work by Claret and Volkoff (1992) showing that vitamin A was essential for the full expression of point B in the cabbage butterfly *Pieris brassicae*.

For insects with multivoltine life cycles, and perhaps also for other animals, results from the experimental and theoretical analyses described in the foregoing sections have strongly indicated that:

Circadian oscillations and their entrainment by light are involved in photoperiodic induction, most probably in the input pathway.

The "external coincidence" model, derived from Bünning's original hypothesis, is a most likely type of mechanism. This model suggests that light has *two* functions: (1) entrainment, and (2) photo-induction, with light coinciding, or not, with a particular photo-inducible phase situated toward the end of the subjective night (in insects) or towards the beginning (in birds).

Entrainment of the photoperiodic oscillators, and photo-induction, may involve different photoreceptors and photopigments.

The circadian oscillator(s) involved in photoperiodism—in insects, but perhaps not in mammals—*are distinct from* those governing overt behavioral rhythms, having different properties (e.g., circadian period, persistence etc) and probably different cellular locations in the brain.

The circadian oscillator(s) involved in photoperiodism may *dampen* (or become mutually out of phase) in protracted periods of darkness to give clock mechanisms that resemble an "hourglass."

Further analysis of the phenomenon of photoperiodic time measurement must take account of these features of the response.

15.8. Diapause Induction in *Drosophila melanogaster* and the Potential Molecular Analysis of Photoperiodic Induction

The fruitfly *Drosophila melanogaster* is a species of tropical origin, extending its distribution northwards each summer. It has been reported as overwintering in sheltered places ("bake-houses and breweries") but rarely in the open at its northern extremes. Nevertheless, an ovarian diapause was observed in some strains— such as Canton-S (Saunders et al. 1989)—while being absent in others, such as Oregon-R, and in several strains from more tropical localities (Saunders and Gilbert 1990). Newly emerged females of Canton-S exposed to short days (<14 hours of light per day) at relatively low temperatures (<14°C) were found to enter a state of diapause lasting up to 6 weeks, during which time the corpora allata showed reduced production of juvenile hormone(s) and little yolk was deposited in the ovaries (Saunders et al. 1990). Flies exposed to long days at the same temperature underwent a slow cycle of egg development. The rather "shallow" developmental arrest under short days could be broken by a transfer to longer days, by an upshift in temperature, or by the topical application of natural or synthetic juvenile hormones. Although the response was weak, the diapause was similar to that recorded in a number of other drosophilids from northern latitudes (Lumme 1978).

The discovery of an ovarian diapause in *D. melanogaster* opened the possibility of using techniques in fly genetics to begin unraveling the molecular mechanisms of insect photoperiodism, particularly by ascertaining the role, if any, of known "clock" genes such as *period* (see Chapter 14) in the photoperiodic response. Results of exposing *period* mutants of *D. melanogaster* to a range of photoperiods showed that the critical day length (CDL) for diapause induction appeared to be identical in the short period (per^S), and long period (per^L) mutations, to the wild-type Canton-S (Saunders et al. 1989; Saunders 1990), but in the arrhythmic mutant (per^0) and a "double deletion" of *period* (per^-) the apparent CDL was shorter than the wild type by about 3 and 5 hours, respectively (Fig. 15.8).

Initially, these results suggested that the *period* gene played no role in photoperiodic time measurement (Saunders et al. 1989). This conclusion, however, may have been premature. In locomotor activity studies the circadian period (τ) in per^L is shortened towards wild-type values as the temperature is lowered (to 15°C) whereas that for per^S is lengthened (Konopka et al. 1989). It is thus conceivable that important phase relationships between the oscillators and the light (as in "external coincidence"; see Section 15.3) *may be almost identical* at the rather low temperatures (~12°C) required for diapause induction in *D. melanogaster*, thereby making this observation and its initial conclusion rather less compelling. In addition, since *phase response curves* (see Chapter 14) for these mutant flies suggest that the changes in period occur during the subjective day (Saunders et al. 1994), the duration of the subjective night—*which is the portion of the daily cycle that is "measured" by the photoperiodic clock*—may be the same in per^S, per^L, and wild-type. As far as the results for "clockless" mutants (per^0 and per^-) are concerned, the raised incidence of diapause observed in flies under the shortest days could be due to unavoidable effects of lower temperature on the overall incidence of diapause (Saunders 2002). These observations, therefore, provide no unequivocal evidence that the *period* gene is without a role in photoperiodic time measurement.

The few studies investigating the expression of the known "clock" genes in insect photoperiodism have been reviewed earlier (Saunders et al. 2004, Saunders 2005). As these progress, it is anticipated that the genetic and molecular analysis of photoperiodic induction will prove to be complicated, perhaps with recognized "clock" genes (including *period* and *timeless*) being involved in the input (entrainment) pathway, and with other genes and proteins involved at the pivotal events associated with light interacting with the photo-inducible phase and hormone release (or retention). It is also likely that different photoreceptors and different photoreceptive pigments are involved in the two aspects of photoperiodic induction: circadian entrainment and illumination of the photo-inducible phase.

Since *D. melanogaster,* with its "weak" photoperiodic response is not the ideal candidate for such a molecular analysis, an alternative genetic model organism should be sought. One such possibility is the parasitic wasp *Nasonia vitripennis,* whose photoperiodic responses are reviewed in this

A
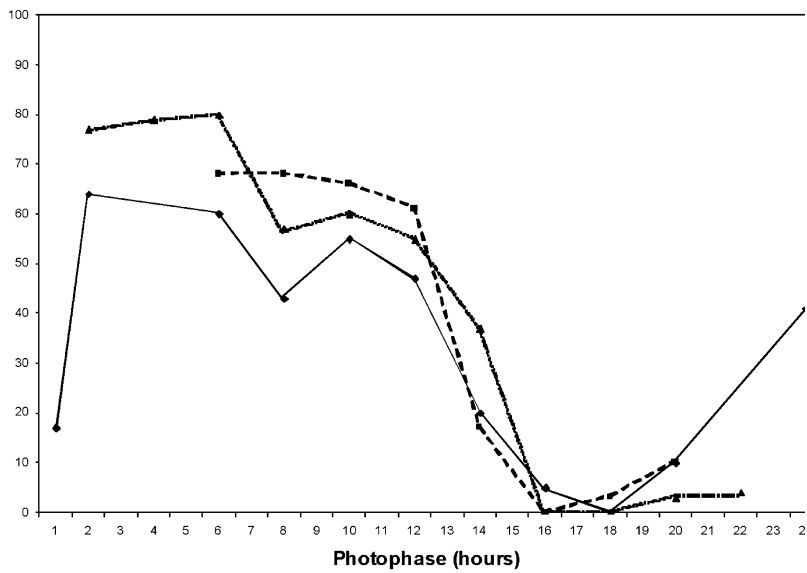
B
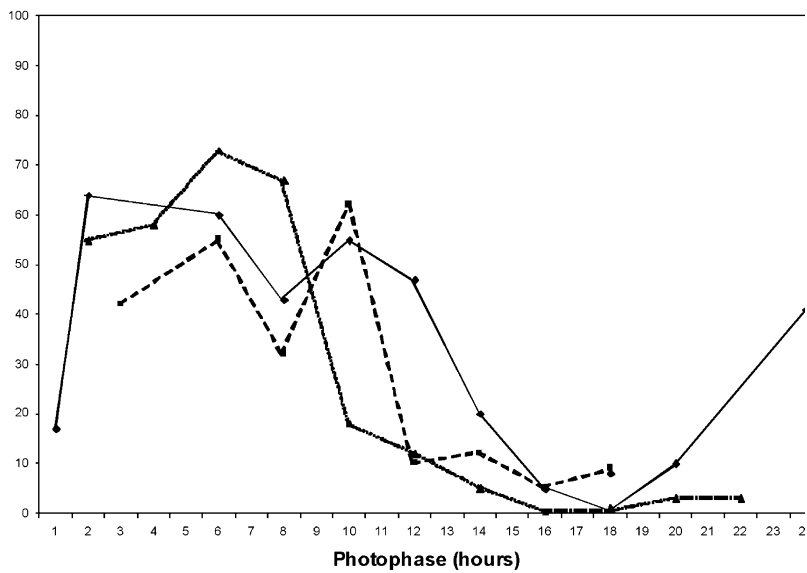
FIGURE 15.8. Photoperiodic induction of reproductive (ovarian) diapause in the fruitfly, *Drosophila melanogaster*, at 12°C. (**A**) Canton-S, wild type, solid line; short period mutant (per^S), dashed line; long period mutant (per^{L2}), dotted line. (**B**) Canton-S, solid line; behaviorally arrhythmic mutant (per^0), dashed line; a "double deletion" of period (per$^-$), dotted line. (Data from Saunders 1990.)

chapter, and whose genome is currently being unraveled (see J.H. Werren; http://www.hgsc.bcm.tmc.edu/projects/nasonia/).

Not only does this species present excellent evidence for the circadian involvement in photoperiodic time measurement, but its short life cycle, its ease of handling in the laboratory, its haplodiploid sex determination, and recent developments in mRNAi technology make *N. vitripennis* an attractive possibility.

References

Baker, J.R. and Ranson, R.M. (1932) Factors affecting the breeding of the field mouse (*Microtus agrestis*): I. Light. Proc. Roy. Soc. London B 110, 313–322.

Belozerov, V.N. (1964) Larval diapause in the tick *Ixodes ricinus* L., and its relation to external conditions. Zool. Zh. 43, 1626–1637 (In Russian).

Bissonnette, T.H. (1932) Modification of mammalian seasonal cycles. Reactions of ferrets (*Putorius vulgaris*) of both sexes to electric light added after dark in November and December. Proc. Roy. Soc. London B 110, 322–336.

Bowen, M.F., Saunders, D.S., Bollenbacher, W.E. and Gilbert, L.I. (1984) *In vitro* reprogramming of the photoperiodic clock in an insect brain-retrocerebral complex. Proc. Natl Acad. Sci. USA 81, 5881–5884.

Bünning, E. (1936) Die endogene Tagesrhythmik als Grundlage der photoperiodischen Reaktion. Ber. Dtsch. Bot. Ges. 54, 590–607.

Bünning, E. (1960) Circadian rhythms and time measurement in photoperiodism. Cold Spring Harbor Symp. Quant. Biol. 25, 249–256.

Bünning, E. (1964) *The physiological clock*. Springer-Verlag, Berlin.

Bünsow, R.C. (1953) Uber tages- und jahresrhythmische Anderungen der photoperiodischen Lichteropfindlichkeit bei *Kalanchoe blossfeldiana* und ihre Beziehungen zur endogonen Tagesrhythmik. Zschr. Botanik 41, 257-276.

Claret, J. (1966) Mise en evidence du role photorecepteur lors de l'induction de la diapause chez *Pieris brassicae* (Lepido.). Ann. d'Endocrinologie 27, 311–320.

Claret, J. (1989) Vitamine A et induction photoperiodique ou thermoperiodique de la diapause chez *Pieris brassicae*. C. R. Acad. Sci. Paris 308, 347–352.

Claret, J. and Volkoff, N. (1992) Vitamin A is essential for the two processes involved in the photoperiodic reaction in *Pieris brassicae*. J. Insect Physiol. 38, 569–574.

Danks, H.V. (1987) *Insect dormancy: An ecological perspective*. Biological Survey of Canada (Terrestrial Arthropods), Monograph Series 1, Ottawa.

Dawson, A., King, V.M., Bentley, G.E. and Ball, G.F. (2001) Photoperiodic control of seasonality in birds. J. Biol. Rhythms 16, 365–380.

Denlinger, D.L. (1971) Embryonic determination of pupal diapause in the flesh fly *Sarcophaga crassipalpis*. J. Insect Physiol. 17, 1815–1822.

Denlinger, D.L. (1985) Hormonal control of diapause. In: G.A. Kerkut and L.I. Gilbert (Eds.), *Comprehensive insect physiology*, *biochemistry and pharmacology,* vol. 8. Pergamon Press, Oxford, pp. 353–412.

Denlinger, D.L. (1991) Relationship between cold hardiness and diapause. In: *Insects at Low Temperature,* R.E. Lee Jr. and D.L. Denlinger (Eds.), Chapman & Hall, New York, pp. 174–198.

Dumortier, B. and Brunnarius, J. (1989) Diet-dependent switch from circadian to hourglass-like operation of an insect photoperiodic clock. J. Biol. Rhythms 4, 481–490.

Elliott, J.A. (1976) Circadian rhythms and photoperiodic time measurement in mammals. Federation Proc. 35, 2339–2346.

Ferenz, H.J. (1975) Photoperiodic and hormonal control of reproduction in male beetles, *Pterostichus nigrita.* J. Insect Physiol. 21, 331–341.

Gao, N., Von Schantz, M., Foster, R.G. and Hardie, J. (1999) The putative brain photoperiodic photoreceptors in the vetch aphid, *Megoura viciae.* J. Insect Physiol. 45, 1011–1019.

Garner, W.W. and Allard, H.A. (1920) Effect of the relative length of the day and night and other factors on growth and reproduction in plants. J. Agric. Res. 18, 553–606.

Goldman, B. D. (2001) Mammalian photoperiodic systems: Formal properties and neuroendocrine mechanisms of photoperiodic time measurement. J. Biol. Rhythms 16, 283–301.

Hamner, W.M. (1963) Diurnal rhythms and photoperiodism in testicular recrudescence of the house finch. Science 142, 1294–1295.

Hardie, J. (1990) The photoperiodic counter, quantitative day-length effects and scotophase timing in the vetch aphid *Megoura viciae.* J. Insect Physiol. 36, 939–949.

Hasegawa, K. and Shimizu, I. (1987) *In vivo* and *in vitro* photoperiodic induction of diapause using isolated brain-suboesophageal ganglion complexes of the silkworm, *Bombyx mori.* J. Insect Physiol. 33, 959–966.

Helfrich-Förster, C. (2001) The locomotor activity rhythm of *Drosophila melanogaster* is controlled by a dual oscillator system. J. Insect Physiol. 47, 877–887.

Hillman, W.S. (1964) Endogenous circadian rhythms and the response of *Lemna perpusilla* to skeleton photoperiods. Am. Naturalist 98, 323–328.

Johnsson, A. and Karlsson, H.G. (1972) A feedback model for biological rhythms. I—Mathematical description and basic properties of the model. J. Theor. Biol. 36, 153–174.

Joosse, J. (1984) Photoperiodicity, rhythmicity and endocrinology of reproduction in the snail *Lymnaea stagnalis.* In: *Photoperiodic regulation of insect and molluscan hormones.* Ciba Foundation Symposium 104, pp. 204–220.

Kimura, Y. and Masaki, S. (1993) Hourglass and oscillator expression of photoperiodic diapause response in the cabbage moth *Mamestra brassicae.* Physiol. Entomol. 18, 240–246.

Kogure, M. (1933) The influence of light and temperature on certain characters of the silk-worm, *Bombyx mori.* J. Dept Agriculture, Kyushu University 4, 1–93.

Konopka, R., Pittendrigh, C.S. and Orr, D. (1989) Reciprocal behaviour associated with altered homeostasis and photosensitivity of *Drosophila* clock mutants. J. Neurogenetics 6, 1–10.

Koštál, V. (2006) Eco-physiological phases of insect diapause. J. Insect Physiol. 52, 113–127.

Lankinen, P. (1986) Geographical variation in circadian eclosion rhythms and photo-periodic adult diapause in *Drosophila littoralis.* J. Comp. Physiol. A 159, 123–142.

Lankinen, P. and Forsman, P. (2006) Independence of genetic geographical variation between photoperiodic diapause, circadian eclosion rhythm, and Thr-Gly repeat region of the period gene in *Drosophila littoralis.* J. Biol. Rhythms 21, 1–10.

Lees, A.D. (1953) The significance of the light and dark phases in the photoperiodic control of diapause in *Metatetranychus ulmi* Koch. Ann. Appl. Biol. 40, 487–497.

Lees, A.D. (1964) The location of the photoperiodic receptors in the aphid *Megoura viciae.* J. Exp. Biol. 41, 119–133.

Lees, A.D. (1966) Photoperiodic timing mechanisms in insects. Nature 210, 986–989.

Lees, A.D. (1971) The relevance of action spectra in the study of insect photoperiodism. In: M. Menaker (Ed.), *Biochronometry.* National Academy of Science, Washington, DC, pp. 372–380.

Lees, A.D. (1973) Photoperiodic time measurement in the aphid *Megoura viciae*. J. Insect Physiol. 19, 2279–2316.

Lewis, R.D. (2002) Quantitative models for insect clocks. In: D.S. Saunders (Ed.), *Insect clocks,* 3rd ed. Elsevier, Amsterdam, pp. 213–243.

Lewis, R.D. and Saunders, D.S. (1987) A damped circadian oscillator model of an insect photoperiodic clock. I. Description of the model based on a feedback control system. J. Theor. Biol. 128, 47–59.

Lumme, J. (1978) Phenology and photoperiodic diapause in northern populations of *Drosophila.* In H. Dingle (Ed.) *Evolution of Insect Migration and Diapause*, pp. 145–170. Springer-Verlag, New York.

Marcovitch, S. (1923) Plant lice and light exposure. Science 58, 537–538.

Marcovitch, S. (1924) The migration of the Aphididae and the appearance of the sexual forms as affected by the relative length of daily light exposure. J. Agric. Res. 27, 513–522.

Masaki, S. (1984) Unity and diversity in insect photoperiodism. In: *Photoperiodic regulation of insect and molluscan hormones.* Ciba Foundation symposium 104, 7–25.

Nishizuka, M., Azuma, A. and Masaki, S. (1998) Diapause response to photoperiod and temperature in *Lepisma saccharina* Linnaeus (Thysanura: Lepismatidae). Entomol. Sci. 1, 7–14.

Numata, H. and Hidaka, T. (1987) Photoreceptors for photoperiodism in the bean bug, *Riptortus clavatus.* Rostria 38, 571–580.

Pittendrigh, C.S. (1966) The circadian oscillation in *Drosophila pseudoobscura* pupae: a model for the photoperiodic clock. Zschr. Pflanzenphysiol. 54, 275–307.

Pittendrigh, C.S. (1972) Circadian surfaces and the diversity of possible roles of circadian organization in photoperiodic induction. Proc.Natl Acad. Sci. USA 69, 2734–2737.

Pittendrigh, C.S. and Minis, D.H. (1964) The entrainment of circadian oscillations by light and their role as photoperiodic clocks. Am. Naturalist 98, 261–294.

Richard, D.S., Watkins, N.L., Serafin, R.B. and Gilbert, L.I. (1998) Ecdysteroids regulate yolk protein uptake by *Drosophila melanogaster* oocytes. J. Insect Physiol. 44, 637–644.

Rieger, D., Stanewsky, R. and Helfrich-Förster, C. (2003) Cryptochrome, compound eyes, Hofbauer-Buchner eyelets, and ocelli play different roles in the entrainment and masking pathway of the locomotor activity rhythm in the fruit fly *Drosophila melanogaster*. J. Biol. Rhythms 18, 377–391.

Rowan, W. (1926) On photoperiodism, reproductive periodicity and the annual migration of birds and certain fishes. Proc. Boston Soc. Natural History 38, 147–189.

Sabrosky, C.W., Larson, I. and Nabours, R.K. (1933) Experiments with light upon reproduction, growth and diapause in grouse locusts. Trans. Kansas Acad. Sci. 36, 298–300.

Saunders, D.S. (1966) Larval diapause of maternal origin—II. The effect of photoperiod and temperature on *Nasonia vitripennis*. J. Insect Physiol. 12, 569–581.

Saunders, D.S. (1973) The photoperiodic clock in the flesh-fly, *Sarcophaga argyrostoma*. J. Insect Physiol. 19, 1941–1954.

Saunders, D.S. (1974) Evidence for 'dawn' and 'dusk' oscillators in the *Nasonia* photoperiodic clock. J. Insect Physiol. 20, 77–88.

Saunders, D.S. (1975) 'Skeleton' photoperiods and the control of diapause and development in the flesh-fly, *Sarcophaga argyrostoma.* J. Comp. Physiol. 97, 97–112.

Saunders, D.S. (1978) An experimental and theoretical analysis of photoperiodic induction in the flesh-fly *Sarcophaga argyrostoma*. J. Comp. Physiol. 124, 75–95.

Saunders, D.S. (1979) External coincidence and the photoinducible phase in the *Sarcophaga* photoperiodic clock. J. Comp. Physiol. 132, 179–189.

Saunders, D.S. (1981) Insect photoperiodism: the clock and the counter. Physiol. Entomol. 6, 99–116.

Saunders, D.S. (1982) Photoperiodic induction of pupal diapause in *Sarcophaga argyrostoma:* temperature effects on circadian resonance. J. Insect Physiol. 28, 305–310.

Saunders, D.S. (1986) Many circadian oscillators regulate developmental and behavioural events in the flesh fly *Sarcophaga argyrostoma.* Chronobiol. Int. 3, 71–83.

Saunders, D.S. (1987) Maternal influence on the incidence and duration of larval diapause in *Calliphora vicina.* Physiol. Entomol. 12, 331–338.

Saunders, D.S. (1990) The circadian basis of ovarian diapause regulation in *Drosophila melanogaster:* is the *period* gene causally involved in photoperiodic time measurement? J. Biol. Rhythms 5, 315–331.

Saunders, D.S. (1992) The photoperiodic clock and "counter" in *Sarcophaga argyrostoma:* experimental evidence consistent with "external coincidence" in insect photoperiodism. J. Comp. Physiol. 170, 121–127.

Saunders, D.S. (1997) Insect circadian rhythms and photoperiodism. Invertebrate Neurosci. 3, 155–164.

Saunders, D.S. (2000) Arthropoda – Insecta: Diapause. In: A. Dorn (Ed.), *Reproductive biology of the invertebrates,* Vol. X, Part B. John Wiley & Sons Ltd, Chichester, pp. 145–184.

Saunders, D.S. (2002) *Insect clocks,* 3rd ed. Elsevier, Amsterdam.

Saunders, D.S. (2005) Erwin Bünning and Tony Lees, two giants of chronobiology, and the problem of time measurement in insect phtoperiodism. J. Insect Physiol. 51, 599–608.

Saunders, D.S. and Cymborowski, B. (1996) Removal of optic lobes of adult blow flies (*Calliphora vicina*) leaves photoperiodic induction of larval diapause intact. J. Insect Physiol. 42, 807–811.

Saunders, D.S. and Cymborowski, B. (2003) Selection for high diapause incidence in blow flies (*Calliphora vicina*) maintained under long days increases the maternal critical daylength: some consequences for the photoperiodic clock. J. Insect Physiol. 49, 777–784.

Saunders, D.S. and Gilbert, L.I. (1990) Regulation of ovarian diapause in the fruit fly *Drosophila melanogaster* by photoperiod at moderately low temperature. J. Insect Physiol. 36, 195–200.

Saunders, D.S. and Lewis, R.D. (1987a) A damped circadian oscillator model of an insect photoperiodic clock. II. Simulations of the shapes of the photoperiodic response curves. J. Theor. Biol. 128, 61–71.

Saunders, D.S. and Lewis, R.D. (1987b) A damped circadian oscillator model of an insect photoperiodic clock. III. Circadian and "hourglass" responses. J. Theor. Biol. 128, 73–85.

Saunders, D.S., Henrich, V.C. and Gilbert, L.I. (1989) Induction of diapause in *Drosophila melanogaster:* photoperiodic regulation and the impact of arrhythmic clock mutations on time measurement. Proc. Natl Acad. Sci. USA 86, 3748–3752.

Saunders, D.S., Gillanders, S.W. and Lewis, R.D. (1994) Light-pulse phase response curves for the locomotor activity rhythm in *period* mutants of *Drosophila melanogaster.* J. Insect Physiol. 40, 957–968.

Saunders, D.S., Lewis, R.D. and Warman, G.R. (2004) Photoperiodic induction of diapause: opening the black box. Physiol. Entomol. 29, 1–15.

Saunders, D.S., Richard, D.S., Applebaum, S.W., Ma, M. and Gilbert, L.I. (1990) Photoperiodic diapause in *Drosophila melanogaster* involves a block to the juvenile hormone regulation of ovarian maturation. Gen. Comp. Endocrin. 79, 174–184.

Shiga, S. and Numata, H. (1996) Effects of compound eye removal on the photoperiodic response of the band-legged ground cricket, *Pteronemobius nigrofasciatus*. J. Comp. Physiol. A 179, 625–633.

Shiga, S. and Numata, H. (1997) Induction of reproductive diapause via perception of photoperiod through the compound eyes of the adult blow fly, *Protophormia terraenovae*. J. Comp. Physiol. A 181, 35–40.

Shimizu, I. (1982) Photoperiodic induction in the silkworm, *Bombyx mori,* reared on artificial diet: evidence for extraretinal photoreception. J. Insect Physiol. 28, 841–846.

Shimizu, I. and Hasegawa, K. (1988) Photoperiodic induction of diapause in the silkworm, *Bombyx mori:* location of the photoreceptor using a chemiluminescent paint. Physiol. Entomol. 13, 81-88.

Shimizu, I. and Kato, M. (1984) Carotenoid functions in photoperiodic induction in the silkworm, *Bombyx mori.* Photobiochem. Photobiophys. 7, 47–52.

Shimizu, I., Yamakawa, Y., Shimazaki, Y. and Iwasa, T. (2001) Molecular cloning of *Bombyx* cerebral opsin (Boceropsin) and cellular localization of its expression in the silkworm brain. Biochem. Biophys. Res. Commun. 287, 27–34.

Steel, C.G.H. and Lees, A.D. (1977) The role of neurosecretion in the photoperiodic control of polymorphism in the aphid *Megoura viciae*. J. Exp. Biol. 67, 117–135.

Stoleru, D., Peng, Y., Agosto, J. and Rosbash, M. (2004) Coupled oscillators control morning and evening locomotor behaviour of *Drosophila.* Nature 431, 862–868.

Stoleru, D., Peng, Y., Nawathean, P. and Rosbash, M. (2005) A resetting signal between *Drosophila* pacemakers synchronizes morning and evening activity. Nature 438, 238–242.

Stross, R.G. and Hill, J.C. (1968) Photoperiod control of winter diapause in the fresh water crustacean, *Daphnia.* Biol. Bull. Marine Biological Lab., Woods Hole 134, 176–198.

Takeda, M. (1978) Photoperiodic time measurement and seasonal adaptation of the Southwestern corn borer, *Diatraea grandiosella* Dyar (Lepidoptera: Pyralidae). Ph.D. thesis, University of Missouri–Columbia.

Tauber, M.J., Tauber, C.A. and Masaki, S. (1986) *Seasonal adaptations of insects.* Oxford University Press, Oxford.

Thiele, H-U. (1977) Differences in measurement of daylength and photoperiodism in two stocks from sub-arctic and temperate climates in the carabid beetle, *Pterostichus nigrita* F. Oecologia (Berlin) 30, 349–365.

Underwood, H. and Goldman, B.D. (1987) Vertebrate circadian and photoperiodic systems: role of the pineal gland and melatonin. J. Biol. Rhythms 2, 279–315.

Van Zon, A.Q., Overmeer, W.P.J. and Veerman, A. (1981) Carotenoids are functionally involved in photoperiodic induction of diapause in a predacious mite. Science 213, 1131–1133.

Vaz Nunes, M. and Saunders, D.S. (1999) Photoperiodic time measurement in insects: a review of clock models. J. Biol. Rhythms 14, 84–104.

Vaz Nunes, M. and Veerman, A. (1982) Photoperiodic time measurement in the spider mite *Tetranychus urticae:* A novel concept. J. Insect Physiol. 28, 1041–1053.

Vaz Nunes, M., Kenny, N.A.P. and Saunders, D.S. (1990) The photoperiodic clock in the blowfly *Calliphora vicina.* J. Insect Physiol. 36, 61–67.

Veerman, A. (1977) Aspects of the induction of diapause in a laboratory strain of the mite *Tetranychus urticae*. J. Insect Physiol. 23, 703–711.

Veerman, A. (1980) Functional involvement of carotenoids in photoperiodic induction of diapause in the spider mite, *Tetranychus urticae*. Physiol. Entomol. 5, 291–300.

Veerman, A., Overmeer, W.P.J., Van Zon, A.Q., De Boer, J.M., De Waard, E.R. and Huisman, H.O. (1983) Vitamin A is essential for photoperiodic induction of diapause in an eyeless mite. Nature 302, 248–249.

Veerman, A., Slagt, M.E., Alderliest, M.F.J. and Veenendaal, R.L. (1985) Photoperiodic induction of diapause in an insect is vitamin A dependent. Experientia 41, 1194–1195.

Veerman, A. and Vaz Nunes, M. (1980) Circadian rhythmicity participates in the photoperiodic determination of diapause in spider mites. Nature 287, 140–141.

Veerman, A. and Vaz Nunes, M. (1987) Analysis of the operation of the photoperiodic counter provides evidence for hourglass time measurement in the spider mite *Tetranychus urticae*. J. Comp. Physiol. A 160, 421–430.

Vinogradova, E.B. and Zinovjeva, K.B. (1972) Maternal induction of larval diapause in the blowfly, *Calliphora vicina*. J. Insect Physiol. 18, 2401–2409.

Wayne, N. L. (2001) Regulation of seasonal reproduction in mollusks. Biol. Rhythms 16, 391–402.

16
Photomorphogenesis and Photoperiodism in Plants

James L. Weller and Richard E. Kendrick

Abstract: Plants depend on light as their main source of energy. However, light is also an important source of information for plants, and changes in the nature of the light reaching a plant can signal seasonal change, potential and actual competition by shading, proximity to the soil surface of roots and seeds, and potential photodamage. This chapter describes how plants detect and respond to their light environment. Plants possess several types of photoreceptors that collectively allow them to detect variation in a number of different light parameters including its spectral composition, irradiance, direction, and daily duration. Signaling pathways initiated by activation of these photoreceptors allow the plant to make adjustments to developmental processes such as germination, stem elongation, chloroplast development and orientation, stem and root bending, and the initiation of flowering. Recent molecular genetic analysis in the main higher plant model, *Arabidopsis thaliana*, has brought rapid progress to our understanding of the molecular nature and ecological significance of plant responses to light.

16.1. Introduction

It has long been observed that light affects the way plants grow. Effects of light can be observed on processes and phenomena throughout the plant life cycle, including seed germination, apical hook opening, stem elongation, leaf expansion, the synthesis of photosynthetic and protective pigments, lateral branching, bud dormancy, and flowering. The vast majority of these effects are unrelated to the use of light for photosynthesis and are mediated through a specialized system of photoreceptors that informs the plant about its surroundings and directs it to develop appropriately.

Photomorphogenesis is a general term encompassing all responses to light that affect plant form. Two specific classes of photomorphogenic response are sometimes distinguished. *Phototropic* responses involve the reorientation of plant organs with respect to an asymmetry in the incident light, as in the case of shoot

tips bending to grow towards the light. *Photoperiodic* responses are those in which various aspects of development are modified in response to changes in the daily light/dark cycle, and involve a circadian timing mechanism. Developmental features commonly subject to photoperiodic control include flowering, bud dormancy and leaf senescence.

This chapter will give an overview of our current knowledge about the way in which these different responses are achieved. We will discuss the discovery and nature of the photoreceptors involved in these phenomena, their physiological roles as determined in the laboratory, and their possible significance in the natural environment. We will also summarize what is known about transduction of the signals arising from photoreceptor activation. Although lower plants also show clear photomorphogenic responses, they have in general been less intensively studied, and we will restrict this discussion to higher plants.

16.2. Photomorphogenic Photoreceptors

As with other photobiological responses, an initial step in the investigation of photomorphogenic responses has been the determination of action spectra. Early measurements identified the blue (BL), red (R), and far-red (FR) regions of the spectrum as being particularly important for the control of plant growth (e.g., Went 1941, Parker et al. 1949), and formed the point of departure in the search for specific photoreceptor pigments for light in these wavebands (Fig. 16.1). Relatively rapid progress was made in biochemical characterization of the photoreceptor responsible for R and FR responses (Sage 1992). In contrast, progress towards identification of a specific BL photoreceptor was limited due to the large number of different BL-absorbing compounds in the plant with the potential to serve as a photoreceptor chromophore, and to the lack of a distinctive photophysiological assay.

However, the advent of a molecular genetic approach has brought rapid developments in our understanding of the nature, diversity, and functions of the photoreceptor pigments involved in informational light sensing. Three classes of higher plant photoreceptors have now been characterized in detail: the *phytochrome* family of R- and FR-absorbing photoreceptors, and two different photoreceptor families mediating responses in the BL and UV-A regions of the spectrum; the *cryptochrome* and *phototropin* families. We will discuss each of these in turn. We will also discuss evidence pointing to the existence of several additional photoreceptors.

16.2.1. Phytochromes

16.2.1.1. Isolation

The main impetus in the early search for photoreceptors came from observations that the inductive effects of R on several aspects of plant development could be
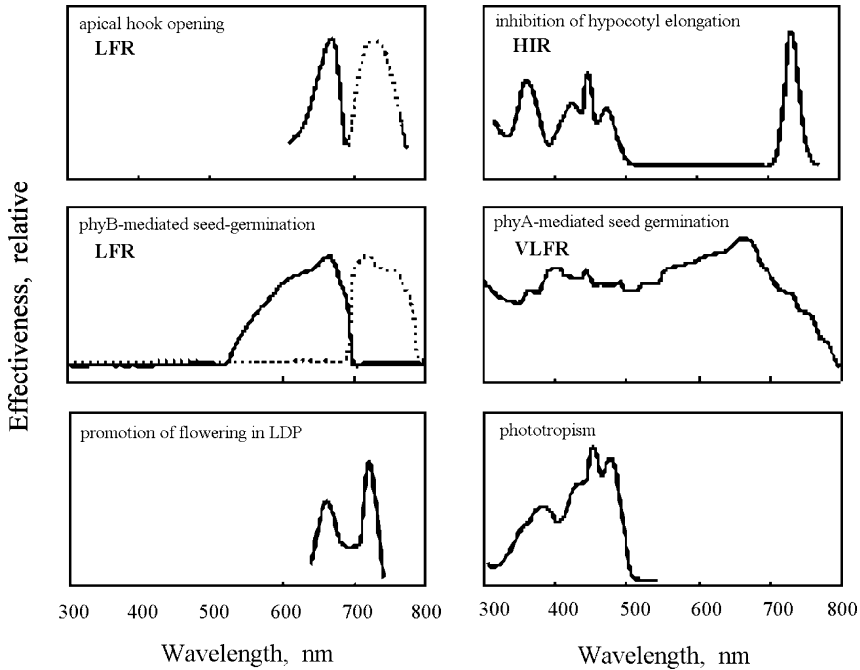
FIGURE 16.1. Action spectra for representative photomorphogenic responses. LFR, low-fluence response; HIR, high-irradiance response; VLFR, very-low-fluence response. Broken lines represent reversal of response. (Redrawn from Withrow et al. 1957, Hartmann 1967, Baskin and Iino 1987, Carr-Smith et al. 1989, and Shinomura et al. 1996.)

reversed by irradiation with FR (Fig. 16.1). The fact that this R/FR reversibility occurred for diverse responses suggested that it might be a property of a single photoreceptor (Withrow et al. 1957). This was proven by the purification of a protein that exhibited R/FR reversible absorption changes. The protein was named *phytochrome*, a name derived from the Greek words for *plant* and *color*. The two forms of phytochrome are characterized by absorption peaks at around 660 nm and 730 nm and are referred to as Pr and Pfr, respectively (Fig. 16.2). Both Pr and Pfr also have a minor absorption peak in the BL region of the spectrum. These two forms of phytochrome can be repeatedly interconverted by light pulses, and continuous light establishes a dynamic equilibrium between them that depends on the composition of the light.

16.2.1.2. Genes and Gene Surveys

The first phytochrome-encoding gene was identified from oat seedlings in 1984 by expression screening using antibodies raised against purified phytochrome (Hershey et al. 1984). Phytochrome genes were subsequently identified in other
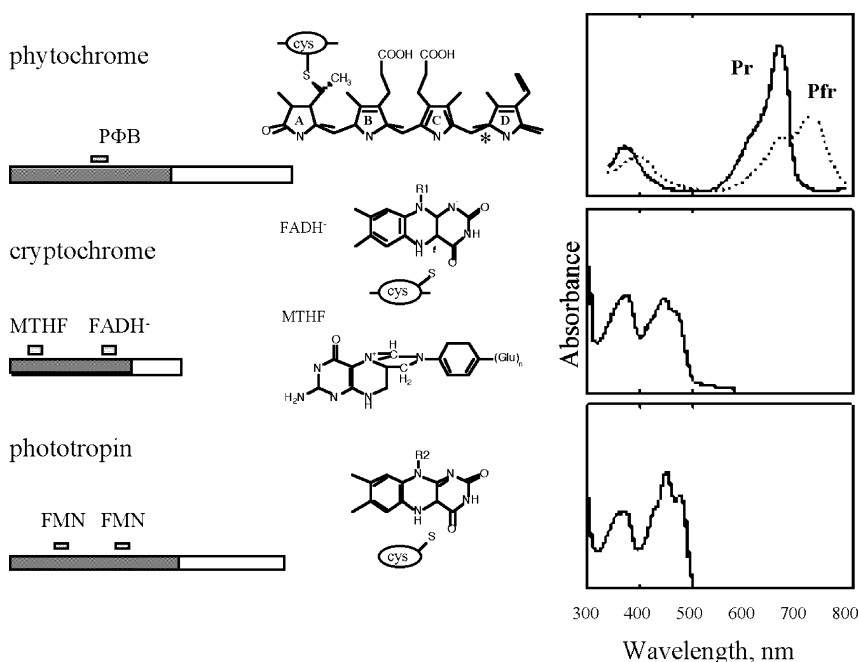
FIGURE 16.2. Diagram showing protein domain structures for generic phytochrome, cryptochrome, and phototropin photoreceptor proteins. The structures and approximate attachment sites of chromophores are shown for each protein. (Absorption spectra redrawn from Butler et al. 1964, Lin et al. 1995, and Christie et al.1999.) The asterix indicates the double bond involved in photoisomerization of the phytochrome chromophore.

flowering plants, as well as gymnosperms, ferns, mosses, and algae (Schneider-Poetsch et al. 1998). More recently, phytochrome-related sequences have also been found in cyanobacteria and even in nonphotosynthetic bacteria, suggesting a very ancient origin (Kehoe and Grossman 1996, Davis et al. 1999, Karniol et al. 2005). Many higher plants are now known to contain several different forms of phytochrome, which are encoded by a small gene family. *Arabidopsis* and tomato each have five expressed phytochrome genes, including two closely related phyB-type phytochromes (Clack et al. 1994, Hauser et al. 1995), whereas rice has only three. In vitro studies indicate that these phytochromes have rather similar absorption spectra and suggest that they may share a common chromophore. Phylogenetic studies suggest that an original phytochrome progenitor gene may have duplicated at around the time of origin of seed plants. Further duplications appear to have occurred soon after the origin of flowering plants, giving rise to four subfamilies corresponding to phyA, phyB/D, phyC, and phyE in *Arabidopsis*. More recent duplications within the phyA and phyB subfamilies have occurred independently within various taxa (Sharrock and Mathews 2006). It also appears that some major lineages may have lost one or more genes. For example, all monocotyledonous species examined lack representatives of the

phyE clade, and phyC has yet to be identified in legumes despite extensive PCR surveys (Sharrock and Mathews 2006). Interestingly, it appears that phyB-type phytochromes are capable of forming heterodimers (Sharrock and Clack 2004).

16.2.1.3. Gene/Protein Structure

The generic phytochrome apoprotein has a molecular mass of around 125 kDa and consists of two domains (Fig. 16.2): an N-terminal domain of 75 kDa that binds the chromophore and a C-terminal domain of 55 kDa that consists of two regions with homology to histidine kinases (Rockwell et al. 2006). The first of these C-terminal regions contains two PAS domains, which are implicated in protein-protein interactions. This region also contains a small domain that is essential for the regulatory activity of the molecule. Gene and protein structure are in general highly conserved across the phytochrome family, with the most notable difference being small poorly conserved N- and C-terminal extensions in phyB-type phytochromes (Sharrock and Mathews 2006). Phytochromes are synthesized in the cytosol in the red-light-absorbing (Pr) configuration, and form dimers in vivo. Deletion and point mutation studies have given some indication of areas of importance for determination of the absorption spectrum, photochromicity, dimerization and signal transduction (Rockwell et al. 2006).

16.2.1.4. Expression and Localization

Two features considered characteristic of phytochrome in early studies were its presence at much higher levels in dark-grown than in light-grown seedlings, and its rapid disappearance after exposure to light. It was clear that a major proportion of the phytochrome present in dark-grown seedlings was strongly regulated by light. However, physiological and spectrophotometric experiments also defined a small light-stable pool of phytochrome (Furuya 1989, Sharrock and Mathews 2006).

It is now known that the light lability of phytochrome mainly reflects the characteristics of phyA. The *PHYA* gene is expressed at a high level in darkness, and phyA accumulates as Pr in the cytosol. Conversion to Pfr after light exposure initiates both a rapid ubiquitin-mediated degradation of the protein, and a rapid down-regulation of *PHYA* transcription (Rockwell et al. 2006, Hennig 2006). In addition, a proportion of the Pfr pool appears to be able to revert spontaneously to Pr in darkness (Fig. 16.3).

In contrast to phyA, the message and protein levels of other phytochromes are much lower in darkness. Although they do not exhibit the strong and rapid downregulation in light shown by phyA, they are nevertheless regulated, by light and by the circadian clock (Hauser et al. 1998, Toth et al. 2001). Immuno-chemical detection of phyA apoprotein in dark-grown seedlings has shown that it is predominantly localized in the apical hook region, the root tip, and the epidermis of young leaves (Hisada et al. 2000). The distribution of other phytochromes has been investigated using promoter-GUS fusions and quantitation of native transcripts in various tissues of light-grown plants (Goosey et al.
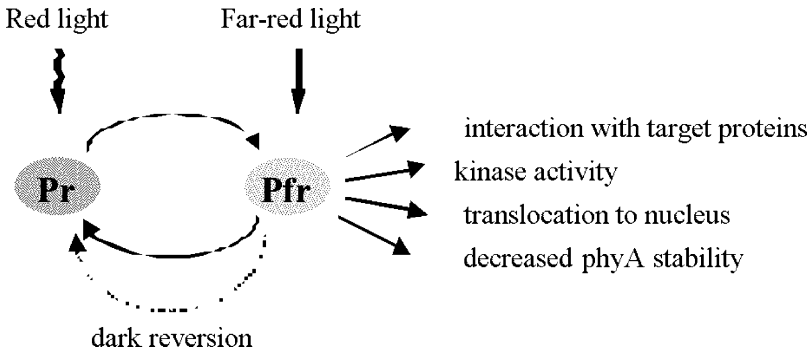
FIGURE 16.3. Summary of the activities and fates of phytochrome following photoconversion.

1997, Hauser et al. 1997). These studies have shown that phyA and phyB are generally more strongly expressed than the remaining phy, and that individual phytochrome genes are expressed at a generally similar level across different tissues. These and other studies have shown that different phytochromes show different diurnal expression rhythms at the transcript and/or protein level, are differentially responsive to light, and show specific expression in some tissues. The biological significance of these differences has yet to be fully explored.

The early fate of phytochrome within the cell after photoconversion has also been investigated, using promoter-GFP fusions and immunochemical techniques (Kircher et al. 1999, 2002, Hisada et al. 2000, Gil et al. 2000). Both phyA and phyB are synthesized in the cytosol in darkness and differentially translocated to the nucleus under specific irradiation regimes. Under R, phyA becomes rapidly localized in the cytosol before appearing in the nucleus within 10 minutes of exposure. FR is also effective for nuclear import of phyA. PhyB translocation is induced by R, but more slowly, and in a FR-reversible manner.

16.2.1.5. Chromophore

Early suggestions that the phytochrome chromophore might be a tetrapyrrole were confirmed after its release from purified phytochrome and chemical analysis. The chromophore phytochromobilin (PΦB) is an open-chain bilitriene (Fig. 16.3), similar to the chromophore for the photosynthetic pigment C-phycocyanin in cyanobacteria. Feeding studies combined with analysis of chromophore-deficient mutants have shown that phytochromobilin is formed in plastids by a pathway which branches from the pathway for chlorophyll synthesis with the chelation of Fe^{2+} rather than Mg^{2+} to protoporphyrin IX (Rockwell et al. 2006, Davis 2006). Heme is then oxygenized to biliverdin, resulting in the opening of the tetrapyrrole ring. This is followed by reduction of the A-ring to form PΦB. Free PΦB assembles autocatalytically to the phytochrome apoprotein and attaches at its C3 position to a cysteine residue in the middle of the N-terminal domain via a thioether linkage (Rockwell et al. 2006, Davis 2006).

Photoreversibility of the phytochrome holoprotein derives from isomerization of bound PΦB about the double bond between rings C and D. It is worth noting that the absorption peaks of the Pr and Pfr are red-shifted 35 and 100 nm, respectively, relative to that of free phytochromobilin conformers. This illustrates the importance of the protein environment for the light-absorbing properties of the chromophore and hence for the spectral characteristics of the photoreceptor. PΦB-deficient mutants have been isolated in a range of species and shown to carry mutations in structural genes for enzymes in PΦB biosynthesis (Muramoto et al. 1999, Kohchi et al. 2001). As a consequence of PΦB deficiency, they have reduced levels of spectrally active phytochrome and exhibit strong defects in responses to light attributable to reduced activity of multiple members of the phytochrome family (Parks and Quail 1991, Weller et al. 1997). All *Arabidopsis* phy apoproteins can assemble with PΦB in vitro (Eichenberg et al. 2000), and it is assumed that all phytochromes utilize PΦB as their sole chromophore in vivo, although this has not been demonstrated directly. Some lower plant phytochromes may use a related bilin phycocyanobilin (PCB) and microbial phy also utilize a wider range of chromophores including biliverdin (bacteria) and PCB (cyanobacteria) (Wu et al. 1997, Davis et al. 1999, Hübschmann et al. 2001, Bhoo et al. 2001).

16.2.2. Cryptochromes

The contribution of a BL-specific photoreceptor system to de-etiolation was first inferred from observations that BL could promote de-etiolation, even in plants grown under continuous red light (i.e., under conditions which are saturating for phytochrome activity). Detailed kinetic studies of growth inhibition also suggested that a photoreceptor other than phytochrome was responsible for a rapid component. In addition, mutants strongly deficient in phytochrome chromophore synthesis (and hence in the activities of all phytochromes) were shown to retain substantial responsiveness to BL (Briggs 2006). This unidentified pigment was often referred to as *cryptochrome*, from the Greek words for *hidden* and *color*, reflecting its elusive nature. The primary BL photoreceptor in de-etiolation was finally identified in 1994, after cloning of the defective gene in an *Arabidopsis* mutant showing impaired de-etiolation responses to BL (Ahmad and Cashmore 1994). This photoreceptor is now known as cryptochrome 1 (cry1). A second member of the cryptochrome family, cryptochrome 2 (cry2), was identified by its homology to cry1 (Lin et al. 1998). As in the case of the phytochromes, these two cryptochrome subfamilies have undergone independent duplication in certain taxa, e.g., cry1 in rice and tomato, cry2 in pea and Medicago (Perotta et al. 2000, Platten et al. 2005a, Hirose et al. 2006).

The cryptochrome apoproteins are around 75 kDa in molecular mass and have two distinct parts (Fig. 16.2). The N-terminal half shows similarity to enzymes called photolyases, which are activated by BL and UV light to repair certain kinds of damage to DNA. When expressed in *E. coli*, this part of the molecule binds the same two chromophores as photolyases: a flavin, (flavin adenine

dinucleotide) and a pterin (methenyltetrahydrofolate) (Lin et al. 1995, Malhotra et al. 1995), although it has yet to be confirmed that the latter chromophore is utilized *in planta*. It has been speculated that the pterin chromophore may serve as a kind of antenna, and may predominantly determine the UV-A/BL-absorbing properties of the molecule, while the flavin chromophore may be essential to the initial signaling reaction and may extend the absorption spectrum into the green region (Cashmore et al. 1999). The C-terminal halves of cry1 and cry2 show only a very low degree of similarity to each other and to other known proteins. One interesting feature of cry2 is its instability under high-irradiance BL (Lin et al. 1998). This is reminiscent of the rapid light-induced degradation of phyA. However, unlike phyA, light does not appear to affect *CRY2* transcription. Both cry1 and cry2 have been shown to localize to the nucleus (Kleiner et al. 1999), although studies of a number of BL-induced phenomena involving changes in ion fluxes across cell membranes (see below) suggest that cryptochromes could also be involved in light-driven redox reactions outside the nucleus.

16.2.3. Phototropins

Despite the substantial problems encountered in the biochemical search for a BL photoreceptor, this approach did prove successful in the identification of the photoreceptor for BL-induced phototropism. Work in the lab of Winslow Briggs identified a 120 kDa membrane protein that underwent autophosphorylation after irradiation with BL. The action spectrum and various kinetic aspects of this reaction showed a close correlation to those for phototropism, suggesting that the protein itself might function as a photoreceptor (Briggs 2006). The physiological significance of the protein was confirmed by its absence in aphototropic *nph1* mutants of *Arabidopsis* (Liscum and Briggs 1995), and cloning of the *NPH1* gene in 1997 subsequently revealed a protein with clear characteristics of BL receptor (Huala et al. 1997). This protein is now known as phototropin 1 (phot1). A second *NPH1*-like gene (*NPL1*) was subsequently identified, and analysis of null mutants for this gene showed that it also encodes an active phototropin photoreceptor (phot2) that functions together with phot1 in the BL regulation of phototropism, chloroplast movement, stomatal opening, and leaf expansion (Kagawa et al. 2001, Kinoshita et al. 2001, Sakai et al. 2001, Sakamoto and Briggs 2002).

The phot molecules consist of two distinct halves: a C-terminal domain with clear homology to classical serine/threonine kinases, and an N-terminal half containing two domains that each bind a flavin mononucleotide (FMN) chromophore (Fig. 16.2). These domains have been termed LOV domains for their presence in a range of proteins involved in the sensing of *l*ight, *o*xygen or *v*oltage (Christie et al. 1999). Both FMN chromophores undergo a photocycle in which BL absorbance is lost after light exposure and recovered in darkness. Both phot1 and phot2 are predominantly associated with the plasma membrane in dark-grown epidermal and subepidermal cells of the hypocotyl and in guard cells

(Sakamoto and Briggs 2002, Harada et al. 2003). Neither have obvious trans-membrane domains. Localization of phot2 to the Golgi apparatus has also been reported (Kang et al. 2006). *NPH1* gene expression shows circadian regulation in *Arabidopsis*, and expression of the closest *NPH1* homologue in rice is strongly downregulated in response to light (Kanegae et al. 2000).

16.2.4. Other Photoreceptors

Following the isolation of phototropins, sequence homologies identified three other LOV-domain proteins encoded in the *Arabidopsis* genome: LKP2, FKF1, and ZTL. However, outside the LOV domain these three related proteins show no similarity with the phototropins, instead incorporating an F-box domain (implicated in protein-protein interactions) and a kelch repeat domain. Light-related mutant phenotypes for *FKF1* and *ZTL* initially indicated a possible role for the encoded proteins in light sensing (Nelson et al. 2000, Somers et al. 2000, Schultz et al. 2001). It has subsequently been shown that LOV domains from all three proteins attach FMN chromophore and display spectral properties consistent with a role in photoperception (Imaizumi et al. 2003). *FKF1* contributes to photoperiodic response through light-dependent transcriptional regulation of the key flowering gene *CONSTANS* (see Section 16.5.2.1.). It seems likely that all three proteins may have a role as photoreceptors regulating light-dependent protein turnover.

In addition to the effects of BL and UV-A mediated by the phytochrome and cryptochrome families, shorter wavelength UV-B also affects plant growth. At high irradiances this is due to the effects of DNA damage, but at low irradiances photomorphogenic effects are also observed (Kim et al. 1998). In some cases phyA and phyB contribute to these low-irradiance effects. In other cases, they are independent of phytochrome and of cry1, suggesting the existence of a distinct photoreceptor for UV-B (Ulm 2006).

The existence of still other photoreceptors was proposed from various experiments examining photocontrol of stomatal opening, hypocotyl elongation, and gene expression. Interestingly two independent lines of evidence have identified green-light-specific responses, for reversal of BL-induced stomatal opening (Talbott et al. 2006) and the stimulation of hypocotyl elongation (Folta 2004) and regulation of gene expression (Dhingra et al. 2006) in etiolated seedlings. However, it remains to be thoroughly tested whether these responses can be attributed to any of the known photoreceptors.

16.3. Physiological Roles of Photoreceptors

Now that we have some idea of the number and nature of plant photoreceptors, it is easy to see how early attempts to interpret physiological observations of photomorphogenesis were hampered by the diversity and functional overlap of the photoreceptors involved. The identification of photoreceptor-specific mutants

has been essential for the characterization of the functions and interactions of the photoreceptors, and mutants continue to be an important tool in dissection of signaling pathways. Null mutants have now been identified for all of the eight known photoreceptors in *Arabidopsis*, and photoreceptor-specific mutants have also been identified in other higher plant species, notably tomato, rice, and pea. These have been useful in testing generalizations about photoreceptor function and in studying processes not easily studied in *Arabidopsis*. Sense and antisense transgenic lines expressing altered levels of specific photoreceptors have also been of use in exploring photoreceptor functions where no mutants have been available and in species not convenient for mutant analysis.

As the number of known plant photoreceptors has grown, it is becoming clear that many light-regulated processes are controlled by multiple photoreceptors, which may interact in different ways in different developmental contexts (Casal 2006). The following sections present an overview of what is known about the photocontrol of several of the better-studied processes in higher plants. The exception is flowering, which is dealt with in Section 16.5. (Photoperiodism).

16.3.1. Germination

In species that exhibit seed dormancy, germination can often be induced by a light treatment given to imbibed seed. In general, small-seeded species are more responsive than large-seeded ones. In studies of the effects of light on lettuce seed germination in the 1930s, Flint and MacAlister found that R was particularly effective at inducing germination, while FR and BL were inhibitory (Sage 1992). It was shown subsequently that the effect of R could be reversed by FR. In some highly sensitive seeds, including *Arabidopsis*, a distinct non-FR-reversible phase can be identified. Three hours after imbibition, germination of *Arabidopsis* seeds can be induced by R in a fully FR-reversible manner (Fig. 16.1), and this response is absent in the *phyB* mutant (Shinomura et al. 1996). After longer periods of imbibition, the sensitivity to light increases, and at 48 hours germination can be induced by very small amounts of light, including FR, and is therefore no longer FR-reversible (Fig. 16.1). This second phase is absent in the *phyA* mutant (Shinomura et al. 1996).

These two responses illustrate some more general features of phyA and phyB function. PhyB controls responses which can be induced by low-fluence R in the order of 1–1000 μmol/m^2 and which are reversible by FR (Fig. 16.1). These are called low-fluence responses (LFR) and are a function of the amount of phyB in the Pfr form. PhyA-mediated responses are much more sensitive to light, and have a range in threshold fluence approximately four orders of magnitude lower than LFR (0.1–100 nmol/m^2). These very-low-fluence responses (VLFR) require only a very small proportion of phyA ($<0.1\%$) to be converted to the Pfr form. They can therefore be induced by light of any wavelength from 300 to 750 nm and are not reversible by FR (Fig. 16.1). The molecular basis for the difference between these two forms of response is not yet understood.

16.3.2. Seedling Establishment

The development of the germinating seedling and its establishment as a fully autotrophic plant require the coordination of several different light-regulated processes. These include inhibition of stem or hypocotyl elongation, apical hook opening, opening and expansion of cotyledons and leaves, and the induction of accumulation of photosynthetic and protective pigments. The regulation of these processes by light, which is often termed "de-etiolation,' can be dramatically demonstrated by the exposure of dark-grown or "etiolated" seedlings to brief R pulses. Experiments of this kind show roles for phyA and phyB that are generally consistent with the LFR and VLFR response modes identified in the control of germination. These responses also manifest in coordinated changes in the expression of many different genes, both nuclear and plastidic (Tepperman et al. 2001, 2004). Prominent examples are the induction of genes involved in light harvesting (e.g., chlorophyll *a/b*-binding, *CAB*), carbon fixation (ribulose-1,5-bisphosphate carboxylase/oxygenase small subunit, *RBCS*), and anthocyanin biosynthesis (e.g., chalcone synthase, *CHS*). Other genes such as lipoxygenase and *PHYA* are repressed by light. Light responses during seedling establishment are also studied by growing plants under different irradiances of continuous monochromatic light (Fig. 16.4). The responses induced under these conditions

FIGURE 16.4. Diagram illustrating the phenotypes of phyA, phyB, and cry1 photoreceptor-deficient mutants under monochromatic blue, red, or far-red light. Grey shading of cotyledons indicates presence of chlorophyll.

are often stronger than those observed in response to a single light pulse and are termed high irradiance responses (HIR). HIRs to continuous BL, R, and FR have all been reported. The FR-HIR is in most cases controlled entirely by phyA, whereas the R-HIR is controlled mainly by the phyB-type phytochromes (phyB and phyD in *Arabidopsis*, phyB1 and phyB2 in tomato). The exception is in rice, where phyC also contributes to de-etiolation in response to continuous FR (Takano et al. 2005). PhyA can also act under continuous R, but its contribution can often only be seen at lower irradiances (Fig. 16.5), where the phyB-type phytochromes are not active (Kerckhoffs et al. 1997, Mazzella et al. 1997).

The HIRs can be considered as a series of responses to pulses of light, and the fundamental photoreactions have been explored by replacing the continuous irradiation with intermittent pulses. R-HIR can be effectively induced by an R pulse every 4 hours in a FR-reversible manner, suggesting that the R-HIR is effectively a continuous activation of LFR. In contrast, the FR-HIR can be replaced only by FR pulses given every 3 minutes. Under this regime, the effect of the FR pulses is reversible by R (Shinomura et al. 2000). The FR-HIR is therefore distinct from the phyA-mediated VLFR, and operates by a mechanism fundamentally different from phyB-mediated LFR. Once again, the molecular basis for these differences is not yet understood.

De-etiolation can also be induced by BL. Under high-irradiance continuous BL, cry1 is the predominant photoreceptor for de-etiolation responses in both *Arabidopsis* and tomato, with a threshold for activity of around 5 μmol/m^2/s. At lower irradiances, phyA becomes the predominant photoreceptor for BL (Fig. 16.5). PhyB-type phytochromes also make a minor contribution under high
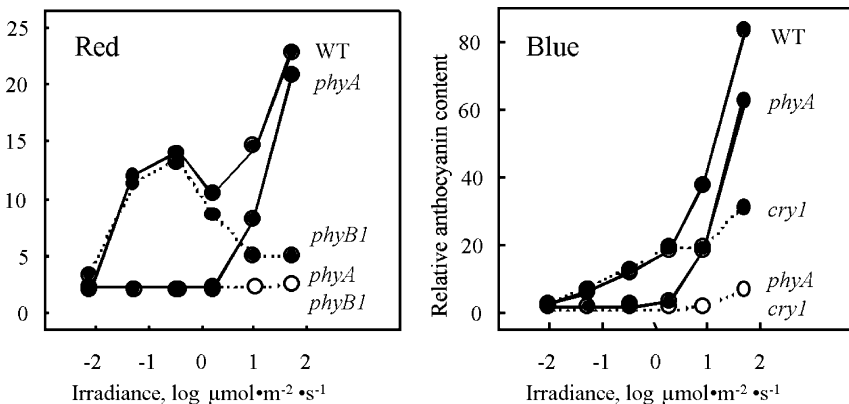
FIGURE 16.5. Irradiance dependence for anthocyanin accumulation in hypocotyls of dark-grown wild-type (WT) and photoreceptor-deficient mutant seedlings of tomato exposed for 24 hours to monochromatic red or blue light. (Redrawn from Kerckhoffs et al. 1997 and Weller et al. 2001b.)

irradiance BL that becomes more evident in the absence of phyA and cry1 (Poppe et al. 1998, Weller et al. 2001b, Platten et al. 2005b). In *Arabidopsis*, the second cryptochrome, cry2, is also reported to have a minor role in the control of seedling light responses under lower-irradiance BL (Lin et al. 1998).

Temporal differences in the action of different photoreceptors are also observed. Immediately following exposure of etiolated seedlings to R, phyA is the main photoreceptor controlling inhibition of hypocotyl elongation, and phyB only becomes predominant after several hours of exposure (Parks and Spalding 1999). This functional separation is similar to the temporal phases observed for phyA and phyB-mediated germination and may be due in part to phyA degradation. Similar analyses have shown that inhibition of elongation in response to blue light is mediated initially by phot1 for the first 30 minutes following exposure, and then subsequently by cry1 and cry2 (Folta and Spalding 2001).

16.3.3. Phototropism

Detailed action spectra indicated the photoreceptor responsible for seedling phototropism has an absorption peak in the UV-A and a three-component peak in the BL region of the spectrum (Fig. 16.1). Fluence-response curves for induction of phototropism by BL pulses resolved two components (Liscum and Stowe-Evans 2000). The "first-positive" component can be induced by fluences of 0.1–500 μmol/m^2 and shows reciprocity within a certain fluence range. The "second-positive" component has a similar fluence threshold, but is also time dependent, with a minimum time requirement of around 10 min. Phot1-deficient *nph1* mutants lack the first positive response, and are completely aphototropic under low irradiances of continuous BL, suggesting that they are also deficient in the second-positive response. However, under continuous BL of higher irradiance (<10 μmol/m$^{2/}$s) the *nph1* mutant shows a normal phototropic response (Sakai et al. 2000), implying the action of another photoreceptor, recently shown to be phot2 (*NPL1*) (Sakai et al. 2001) The function of phototropin in the control of hypocotyl elongation was initially thought to be restricted to the perception of unilateral B, because *nph1* plants exhibit grossly normal de-etiolation responses (Liscum and Briggs 1995). However, more detailed analyses have shown that phototropins can mediate a more general inhibition of elongation in response to B (Folta and Spalding 2001, Sakamoto and Briggs 2002).

Although phyA, phyB, cry1, and cry2 have all been proposed to contribute to the B phototropic response, it is now clear that these photoreceptors are neither necessary nor sufficient for directional light sensing, at least in *Arabidopsis* hypocotyls. Nevertheless, they can modulate expression of the phototropic response, by increasing its amplitude or speeding up its development. In addition, absorption of R by phytochrome can enhance the subsequent phototropin-mediated response to unilateral B (Parks et al. 1996). Recent evidence suggests that this may an indirect effect resulting from phytochrome suppression of gravitropism (Lariguet and Fankhauser 2004).

16.3.4. Shade Avoidance

Light responses in established, fully autotrophic seedlings are often referred to as shade-avoidance responses. In response to shading, stem elongation increases, development of lateral organs such as leaves and branches is suppressed, and flowering is accelerated (Franklin and Whitelam 2005). Vegetational shading involves changes in both irradiance and spectral quality of the light reaching the plant (Ballaré 1999). The main difference in spectral quality is an effective enrichment for FR, which is due to the fact that leaves transmit FR but absorb BL and R. The term shade avoidance as applied to laboratory experiments refers specifically to responses induced by manipulation of the FR content against a constant background of photosynthetically active radiation (Fig. 16.6).

Since shade-avoidance responses occur in fully green, de-etiolated plants, it was often assumed that phyA could not be important. Levels of phyA are very low in light-grown relative to dark-grown plants, and at least in *Arabidopsis* and rice, seedlings of phyA-deficient mutants show no substantial difference from WT seedlings when grown in white light. In contrast, *phyB* mutants have the appearance of strongly shade-avoiding plants, indicating an important role for phyB inactivation in the shade-avoidance response. In *Arabidopsis*, phyD and phyE also make an important contribution to perception of R:FR photon ratio (Devlin et al. 1998, 1999). These observations suggest that phyB, phyD, and phyE all have a similar mode of action, which can be understood in terms of LFR and phytochrome acting as a simple developmental switch. Light of high R:FR
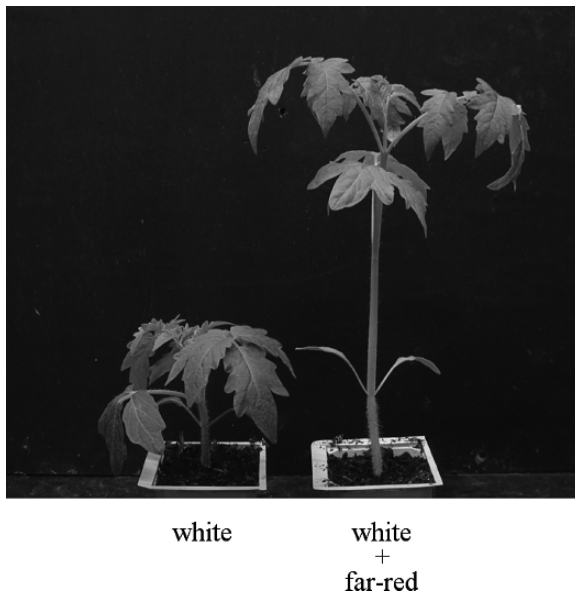
white   white
+
far-red

FIGURE 16.6. Shade-avoidance response of wild-type tomato seedlings simulated by addition of high irradiance far-red light to the white light source, lowering the ratio of red to far-red light from 6.3 to 0.1.

converts a large proportion of phytochrome into its Pfr form, which actively initiates photomorphogenic responses including leaf expansion and the inhibition of stem elongation. Increasing FR supplementation drives the photoequilibrium back towards the Pr form, reducing the level of the active Pfr form, and thus reducing the extent of the photomorphogenic response (Smith 2000).

More detailed investigations also show that phyA, although not able to perceive changes in R:FR in the manner of the phyB-type phytochromes, does influence the shade-avoidance response by promoting de-etiolation under light of low R:FR ratio (McCormac et al. 1992, Weller et al. 1997). This response opposes the reduction in activity of phyB under the same conditions, and it is clear that the balance of phyA to phyB is therefore important in determining the degree of responsiveness to changes in R:FR. Constitutive overexpression of phyA can enhance the photomorphogenic effect of FR-rich light to the extent that the normal shade-avoidance response acting through phyB is suppressed (Robson et al. 1996). Roles in the inhibition of internode and leaf elongation have also been identified for *Arabidopsis* phyA, but these appear to be independent of R:FR (Franklin et al. 2003)

16.4. Photoreceptor Signal Transduction

Most of the classical photomorphogenic responses listed above are whole-plant responses and occur on a scale of hours to days after first exposure to the light stimulus. Recent molecular and genetic dissections have begun to reveal some of the shorter-term cellular and molecular events underlying these responses. It is now clear that most responses require changes in gene expression, and the signaling pathways from photoreceptor to the transcriptional complexes that regulate gene expression are now the subject of intense interest. Other responses to light occur much more rapidly and do not seem to involve changes in gene expression, thus suggesting that some light signaling pathways may be located entirely in the cytoplasm.

Attempts to understand the transduction of signals from photoreceptor to responses have taken five main approaches. These have involved studies of the nature and primary reactions of photoreceptor, two-hybrid screens for inter-acting factors, mutant screens for downstream genes, transcriptional profiling, and pharmacological manipulations of putative signaling intermediates (Quecini and Liscum 2006, Fankhauser and Bowler 2006, Jenkins et al. 2001). These approaches clearly overlap and are converging, but it is perhaps still useful to distinguish them here.

16.4.1. Primary Reactions of Photoreceptors

16.4.1.1. Phytochrome

Early speculations about the initial reactions of phytochrome considered the possibility that it might possess enzymatic activity and, more specifically, that

it might function as a kinase (Sage 1992). Early studies reported a ser/thr kinase activity in purified phyA preparations, but these were considered inconclusive due to the possibility of a copurifying activity. Sequence comparisons show homology between a domain in the C-terminus of phytochrome and histidine kinases, and prokaryotic phytochromes have histidine kinase activity but this is unlikely for higher plant phy (Rockwell et al. 2006, Fankhauser and Bowler 2006). Instead, recombinant oat phytochrome does show light-dependent autophosphorylation characteristic of ser/thr kinase activity (Yeh and Lagarias 1998). Studies in vitro have identified several targets of phytochrome-regulated phosphorylation and in some cases the target proteins have also been shown to interact physically with phy (Ahmad et al. 1998, Fankhauser et al. 1999, Choi et al. 1999, Colon-Carmona et al. 2000). However, in most cases, evidence is still lacking about whether this phosphorylation is direct, and whether it is functionally significant. The exception may be PIF3, a transcription factor that associates with phytochrome in vivo at the promoters of light-regulated genes and undergoes phy-regulated changes in phosphorylation status, degradation, intranuclear localization, transcriptional activation activity, and degradation (Martinez-Garcia et al. 2000, Al-Sady et al. 2006).

16.4.1.2. Cryptochrome

To date, there is little known about the primary reactions of cryptochrome. As expected for a flavoprotein, electron transfer to the FMN chromophore from a series of externally-oriented tryptophans (Giovani et al. 2003). Cryptochromes also undergo light-dependent autophosphorylation (Shalitin et al. 2003) and bind ATP (Bouly et al. 2003) near the flavin-binding site (Brautigam et al. 2004).

The C-terminal domains of cry1 and cry2 each confer light-independent photomorphogenesis when constitutively expressed in transgenic plants (Yang et al. 2000). This suggests that activity of this domain in the full-length molecule is constrained in darkness by the N-terminal domain and that this constraint is somehow released following light absorption. Cryptochrome activation therefore appears to involve communication between two halves of the molecule, and the interaction of reaction partners with the C-terminal domain.

16.4.1.3. Phototropin

The primary structure of phototropin clearly identifies it as a classical ser/thr kinase. Although phototropin is autophosphorylated at multiple sites in response to BL (Huala et al. 1997, Salomon et al. 2003), no targets for transphosphorylation have yet been identified.

16.4.2. Mutants and Interacting Factors

A large number of genetic screens have been performed in *Arabidopsis* to identify genes that function downstream of photoreceptors in the mediation of light responses. Physiological and genetic studies with these mutants have

attempted to assign them to the signaling pathways of one or more photoreceptors (Fig. 16.7). Numerous putative signaling components have now been cloned, and their functions are currently being explored.

16.4.2.1. Phytochrome

Phytochrome was long thought to be a cytosolic protein, and it was therefore presumed that the initial steps in phytochrome signaling took place in the cytoplasm. The more recent demonstrations of rapid light-induced nuclear import of phytochrome have therefore been somewhat surprising and suggest that phytochrome might have a more direct role in the regulation of gene expression than previously considered. This has been confirmed by identification of PIF3, a phytochrome-interacting basic helix-loop-helix (bHLH) protein, which is nuclear localized and binds to specific light-responsive elements in the promoters of light-regulated genes. PhyB has been shown to bind to PIF3 in vivo and to control its ability to activate transcription in a light-dependent manner (Martinez-Garcia et al. 2000). PhyA can also bind to PIF3 but with much lower affinity (Zhu et al. 2000). Loss of a related bHLH protein, HFR1, specifically impairs de-etiolation under FR, indicating that it acts in a signaling pathway specific for phyA (Fairchild et al. 2000). Although transcriptional activation activity has not yet been demonstrated for HFR1, it can form a heterodimer with PIF3. This raises the possibility that the specificities of phyA and phyB may be partially determined by their differential affinities for different transcription factors. Loss of EID1, a nuclear F-box protein, specifically enhances phyA responses. EID1 participates
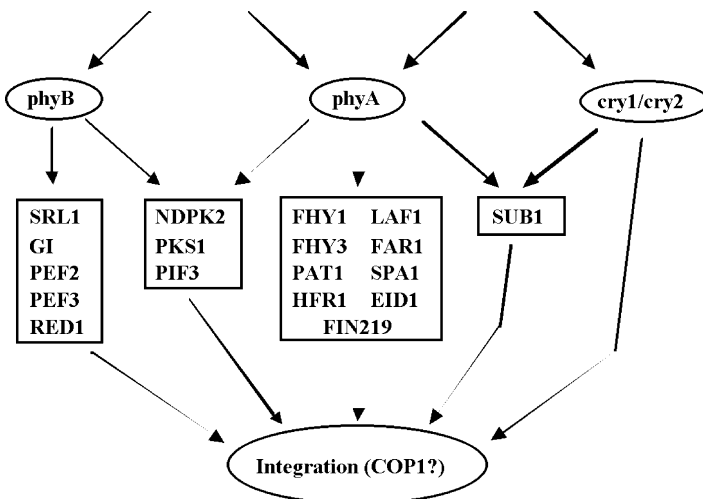
FIGURE 16.7. A number of proteins important in photoreceptor signal transduction have been identified from genetic and protein-protein interaction screens. These proteins can be classified according to their known interactions and the specificity of their null mutant phenotypes.

as a subunit of ubiquitin E3 ligase and may target activated components of the phyA signaling pathway for ubiquitin-dependent degradation (Dieterle et al. 2001). Recently, two related proteins FHY1 and FHL have been shown to bind directly to phyA and to act redundantly in control of phyA-mediated growth responses, phyA-regulated gene expression and nuclear import of phyA in both HIR and VLFR modes (Hiltbrunner et al. 2006). FAR1, FHY3, and SPA1 are other nuclear proteins for which mutant phenotypes indicate a role in phyA-specific signaling (Hudson et al. 1999, Hoecker et al. 1999, Hudson et al. 2003), and there is a growing list of nuclear proteins related to phyA function through mutant phenotypes and/or interaction studies. However, cytoplasmic proteins with specific role in phyA (PAT1, FIN219) and phyB (PKS1) signaling have also been identified (Fankhauser et al. 1999, Hsieh et al. 2000). This suggests that a separate pathway for phytochrome signaling may exist in the cytoplasm, or that certain cytoplasmic components are necessary to facilitate the movement of phytochromes to the nucleus after light exposure. Although the molecular roles of these phytochrome signaling components are not yet fully understood, they fall mainly into two categories representing functions in transcriptional regulation (e.g., PIF3, HFR1, FAR1, FHY3, LAF1) or posttranslational regulation of protein degradation (e.g., SPA1, EID1).

16.4.2.2. Cryptochrome

So far no genes have been identified which are specifically involved in BL signaling. Some screens have identified mutants with impaired BL responses (e.g., *hy5*, Koornneef et al. 1980; *sub1*, Guo et al. 2001) but these are also impaired in response to R and/or FR and may define signaling components common to phytochromes and cryptochromes (Fig. 16.7; see Section 16.4.2.4.). It is possible that the absence of specific cryptochrome signaling mutants may reflect a very close relationship between cryptochrome and the phytochrome signaling pathway. This explanation is supported by the demonstration that the C-terminal domains of both cry1 and cry2 interact directly with the key regulatory protein COP1 (Wang et al. 2001; see below).

16.4.2.3. Phototropin

Mutants impaired in phototropism have been identified by several groups, and define four distinct loci (*NPH2*, *NPH3*, *NPH4*, *RPT2*) in addition to *NPH1* (Liscum and Briggs 1996, Sakai et al. 2000). Three of these genes have now been cloned. *NPH3* encodes a protein that appears to interact physically with the phototropin photoreceptor. The NPH3 protein contains no motifs suggestive of a specific biochemical activity, but the presence of several protein-protein interaction domains has prompted the suggestion that it may function as a molecular scaffold, bringing together other components of phototropin signaling (Motchoulski and Liscum 1999). The RPT2 protein is also essential for normal phototropism of root and shoot and shows sequence similarity to NPH3, suggesting that it may function in a similar manner (Sakai et al. 2000). The

PKS1 protein initially isolated as a phytochrome-interacting protein (Fankhauser et al. 1999) has more recently been shown to also interact physically with the phot1 and NPH3 proteins and to play a role in the phototropic response (Lariguet et al. 2006). Mutants in the *NPH4* gene are aphototropic in low-fluence-rate BL and, unlike mutants at the other phototropism loci, also show impairment of gravitropic responses. *NPH4* encodes an auxin-regulated transcriptional activator, indicating that auxin-regulated changes in gene expression occur in response to phototropin activation and are necessary for normal tropic responses generally (Harper et al. 2000).

16.4.2.4. *Common Light-Signaling Components*

Several different screens have identified a number of mutants expressing constitutive photomorphogenic responses even when grown in darkness. The light-independent phenotype of these mutants has implied the existence of proteins that normally function to repress the de-etiolated state in darkness. It also suggests that photomorphogenesis can be viewed as the default pathway for seedling development and that the action of light is to overcome the active repression of this pathway.

One of the key proteins involved in this repression is COP1, a protein containing three domains recognized as important for protein-protein interaction (Strickland et al. 2006). COP1 accumulates in the nucleus in darkness, but is excluded from the nucleus in light. Both phytochrome and cryptochrome signaling can contribute to the nuclear exclusion of COP1 (Osterlund and Deng 1998). COP1 function in the nucleus involves physical interaction with HY5, a bZIP transcription factor which binds to LREs in promoters of light regulated genes and is necessary for normal de-etiolation responses. In darkness COP1 is enriched in the nucleus, where it binds HY5 and targets it for degradation (Fig. 16.8). This is suggested to be an important mechanism for the regulation of HY5-dependent gene expression (Osterlund et al. 2000). Recent evidence suggests that COP1 may have a similar role in degradation of a number of
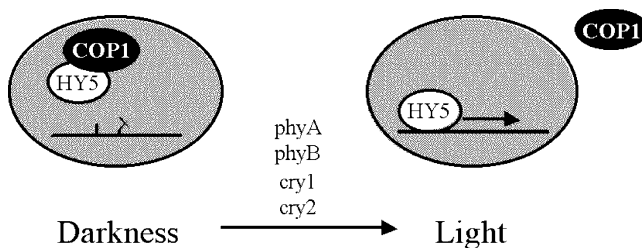
FIGURE 16.8. Proposed mechanism for the integration of light signals through the COP1 protein (Osterlund and Deng 2000). In darkness, COP1 accumulates in the nucleus where it interacts with the transcription factor HY5 and targets it for degradation. Photoreceptor activation by light results in the exclusion of COP1 from the nucleus, and the accumulation of HY5, which activates transcription of target genes.

different light-signaling components through an E3 ubiquitin ligase activity (Strickland et al. 2006).

Several proteins necessary for light regulation of COP1 activity have also been identified, and these may provide the first links between specific photoreceptors and COP1 activity. FIN219 is a cytoplasmic protein that is necessary for phyA activity and may contribute to the negative regulation of COP1 activity by phyA. *FIN219* expression is strongly upregulated by auxin, providing further evidence for the involvement of auxin in phytochrome responses (Hsieh et al. 2000). SUB1 functions downstream of cry1 and phyA to negatively regulate HY5 abundance, possibly through positive effects on COP1 (Guo et al. 2001). The identification of SUB1 as a Ca^{2+}-binding protein and its location in the nuclear envelope raise the intriguing possibility that it may be involved in the regulation of nuclear translocation by Ca^{2+}.

Other proteins with similar mutant phenotypes to COP1, such as COP9, COP8, FUS5, and FUS6, participate in a large multimeric complex referred to as the "COP9 complex." Subunits of the complex show a one-to-one correspondence with those making up the lid complex of the 26S proteasome, and interaction of the complex with ubiquitin E3 ligase has recently been demonstrated, suggesting a probable role in the regulation of protein degradation (Schweichheimer et al. 2001). In plants, the complex is necessary to maintain COP1 in the nucleus in darkness, an observation that may explain the COP1-like phenotype of mutants lacking individual complex components. Other proteins with similar mutant phenotypes, such as COP10 and DET1, are not part of the COP9 complex, but still seem to be involved in regulation of COP1 localization (Strickland et al. 2006).

In some other cases genes originally identified by light-dependent mutant phenotypes under a given set of monochromatic light conditions have subsequently been found to affect responses to other wavebands. Proteins encoded by such genes include transcription factors HRB1 (Kang et al. 2005), PIF4 (Kang et al. 2005) and OBP3 (Ward et al. 2005), the calcium-binding protein SUB1 (Guo et al. 2001) and SHB1, a protein of unknown biochemical function (Kang and Ni 2006). These genes all seem to be involved in the signaling from both phytochromes and cryptochromes, but in most cases the exact nature of this role has yet to be fully characterized. Several other genes studied initially as phyA-specific signaling components are now known to mediate signals from other photoreceptors (e.g., HFR1 and cryptochrome; Duek and Fankhauser 2003).

16.4.3. Expression Profiling

The availability of microarray systems for expression profiling has enabled a new, broader perspective on photoreceptor signaling. Comparisons between WT and photoreceptor mutants have been used to demonstrate the portion of the genome regulated by each individual photoreceptor (Tepperman et al. 2001, 2004, Ma et al. 2001, Wang et al. 2002). Use of signaling mutants and time series have then been used to further dissect these networks, identifying temporal/genetic

hierarchies of action. Somewhere around 20% of genes in the *Arabidopsis* genome are light-regulated, including genes in a broad range of functional categories. Sets of genes regulated by phyA and phyB show a large degree of overlap, suggesting that these two photoreceptors share a substantial proportion of their signaling network (Tepperman et al. 2004). Studies of this nature have been useful in identifying so-called primary-response genes that respond rapidly and directly to photoreceptor activation. Approximately 10% of phytochrome regulated genes are in this category, showing maximal response within 1 hour of initial light exposure (Tepperman et al. 2001, 2004). These genes include established transcriptional regulators and a wide range of other genes whose functions are not apparent. Interestingly, many of these early phytochrome-regulated genes have light-response elements (LREs) in promoters, suggesting that they themselves may be controlled by a smaller range of master regulators such as *PIF3* (Hudson and Quail 2003). Interestingly, only a small proportion of these early genes turn out to be necessary for expression of downstream de-etiolation responses (Khanna et al. 2006). Comparisons of expression profiles in different signaling mutants indicates FHY1, FAR1, and FHY3 act early, whereas HFR1 and SPA1 are likely to act later and regulate a smaller subset of downsteam genes (Wang et al. 2002).

16.4.4. *Pharmacological Approaches*

The involvement of putative signaling intermediates in light-signal transduction have been investigated in a number of different systems, including cell cultures and protoplasts, and by direct injection into hypocotyl cells of a phytochrome-deficient tomato mutant. Microinjection studies identified two distinct pathways involved in phytochrome regulation of gene expression in tomato hypocotyl cells (Fankhauser and Bowler 2006). Induction of *CHS* expression was found to require cGMP and his/tyr kinase activity, whereas induction of *CAB* expression was specifically blocked by Ca^{2+}/calmodulin (CaM) antagonists. G-protein inhibitors blocked both responses, and the full development of chloroplasts only occurred if both pathways were intact. Results using a soybean cell culture essentially confirmed these conclusions about signaling in plastid development. However, more recent reverse genetic analyses have failed to identify a substantial de-etiolation phenotype in mutants lacking G-protein subunits (Jones et al. 2003). In contrast, the induction of *CHS* by BL/UV-A and UV-B light in *Arabidopsis* cell cultures is not influenced by cGMP or his/tyr kinase antagonists, but uses a different signaling pathway involving redox reactions at the plasma membrane, specific Ca^{2+} channels, and ser/thr kinase activity (Jenkins et al. 2001). The UV-B effects are distinguished from the BL/UV-A effects by the involvement of CaM.

Another BL response that has been subjected to pharmacological dissection is the rapid membrane depolarization in hypocotyl cells and protoplasts. This response depends on the action of specific anion channels that are sensitive to the inhibitor 5-nitro-(3-phenylpropylamino)-benzoic acid (NPPB). BL-induced

membrane depolarization is dramatically reduced in *cry* mutants and is related to subsequent cry-mediated growth inhibition in intact *Arabidopsis* hypocotyls (Parks et al. 1998, Folta and Spalding 2001). Cry1-dependent anthocyanin accumulation is also inhibited by NPPB. These results indicate that ion fluxes at the plasma membrane may also play an important role in the early steps of cry1 signal transduction.

The involvement of calcium in BL responses has also been investigated in transgenic plants expressing the luminescent reporter protein aequorin (Baum et al. 1999). Targeting of aequorin to different cellular compartments has shown that BL pulses specifically induce Ca^{2+} transients in cytoplasm. The loss of cry1 or cry2 had no effect on this response, whereas it was somewhat impaired in the phototropin-deficient *nph1* mutant, suggesting a potential role for Ca^{2+} in phototropin signaling. This is strengthened by observations that the effects of R and BL pretreatment on phototropism in tobacco and *Arabidopsis* correlate well with their effects on the Ca^{2+} transient.

It is clear that although some promising progress has been made in identifying potential components of different light-signaling pathways, these have yet to be linked with transduction components identified by genetic means, and we are still far from understanding the complete sequence of events initiated by photoreceptor activation.

16.5. Photoperiodism

The importance of the duration of the daily photoperiod for plant development was first noted over 90 years ago. Using changes in daylength, plants can monitor the time of year and predict seasonal change in other environmental variables. A number of processes exhibit photoperiodic regulation, including the induction of flowering, the formation of storage organs such as bulbs and tubers, and the onset of bud dormancy. Of these, it is the induction of flowering that has been studied most intensively. Clear differences in photoperiodic responsiveness were first documented by Garner and Allard (1920), who classified plants according to whether flowering was preferentially induced under long days (long day plants or LDP) or short days (short-day plants or SDP) (Fig. 16.9). Other early observations indicated that flowering responses could be dramatically altered by low irradiances or short exposures to light. This suggested that the light served as a source of information rather than of energy and showed photoperiodism to be a truly photomorphogenic phenomenon.

16.5.1. Light and the Circadian Clock

Endogenous rhythms have been observed in plants for more than 200 years. However, the importance of an endogenous circadian rhythm for the timekeeping aspect of photoperiodism was first suggested in the 1930s by Erwin Bünning (Bünning 1964). In fact, photoperiodism can be thought of as the adaptation of
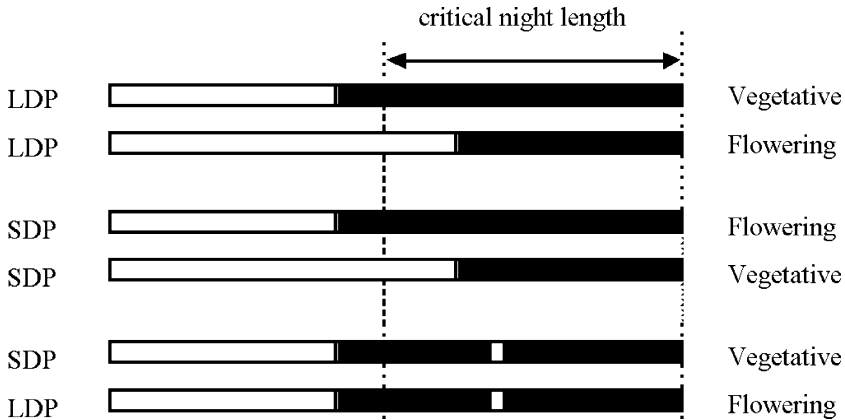
FIGURE 16.9. Summary of differences in flowering responses of short day plants (SDP) and long-day plants (LDP). Open and filled bars represent light and dark periods, respectively.

circadian timekeeping to the measurement of daylength. As such it must involve interaction of light signaling ("input") and specific flower induction ("output") pathways with a circadian oscillator or "clock." One characteristic feature of circadian rhythms is that they show a free-running period that is close to, but not exactly 24 hours. However, under daily light/dark (L/D) cycles, the rhythmic outputs become synchronized or *entrained* to a period of 24 hours exactly.

There are generally considered to be two basic models for the way in which light might interact with the clock (Thomas and Vince-Prue 1997). In the *internal coincidence* model, photoperiodic induction results from the increasing overlap in phase of two distinct circadian output rhythms. Light interacts with the induction process solely by controlling the phase and/or period (i.e., entrainment) of the two rhythms. In the *external coincidence* model, developed from ideas first proposed by Bünning, the circadian clock generates an output rhythm in light sensitivity and photoperiodic induction results from the coincidence of an inductive light signal with the light-sensitive phase of this rhythm. In this model, light has two roles: entrainment of the clock, and direct interaction with downstream components necessary for the response. A third effect of light in photoperiodism may be to influence output responses directly, without the involvement of a timing component. The challenge is to understand how the plant is able to integrate these signals and generate the appropriate response.

16.5.1.1. Physiological Approaches

Detailed physiological investigations of the relationship between light and the circadian clock have been performed across a wide variety of different species, both SDP and LDP (see Thomas and Vince-Prue, 1997). These studies have generated a large amount of complex and often contradictory literature. However, there is reasonable agreement on some of the more general conclusions, and these are summarised below.

Short-Day Plants. In a fixed daily cycle, it is clear that changes in day length could in theory be detected either as changes in length of the light period or of the dark period. It has been established that for many SDP it is mainly the length of the night that is measured, suggesting that processes necessary for floral induction can only take place if the night is longer than a certain *critical night length*. Interruption of an inductive long night with a short light treatment prevents its effect and delays flowering (Fig. 16.9). In many species this night-break (NB) response is relatively sensitive and has thus been amenable to pulse experiments and a detailed photobiological analysis (Thomas and Vince-Prue 1997).

NB responses in SDP show action spectra typical of phytochrome-mediated LFR, for which R is inhibitory to flowering and subsequent FR cancels this inhibition. In this response, phytochrome in its Pfr form is clearly acting to inhibit flowering. In addition to the light quality of the NB, its timing can also be important, and several different SDP species show circadian rhythmicity in the responsiveness to a NB (Fig. 16.10), consistent with the external coincidence model (Thomas and Vince-Prue 1997). Other light treatments can reset the phase of this rhythm. In some cases the phase-setting effects of light were shown to occur independently of effects on flower induction, and R was also the most effective wavelength for inducing phase shifts. Phase shifting has generally been found to require longer exposures to light than the NB response. With even longer periods of light exposure (<6 hours), the phase of the rhythm is no longer
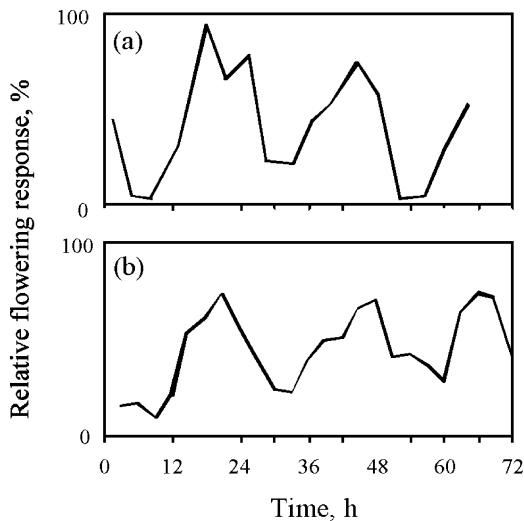
FIGURE 16.10. Circadian rhythms in flowering responses to light treatments in SDP and LDP. (a) Rhythmic response of the SDP Glycine max (soybean) to a 4-hour night-break with white light given at various times during an extended night following an 8-hour photoperiod (redrawn from Coulter and Hamner 1964). (b) Rhythmic response of the LDP Hordeum vulgare (barley) to 6 hours of far-red light added at various times during an extended photoperiod of continuous white light (redrawn from Deitzer et al. 1982).

shifted but suspended and only released approximately 9 hours after transfer to darkness (Thomas and Vince-Prue 1997).

Other studies have shown that in addition to the strong inhibitory effect of R shown in the NB response, FR is also effective for inhibition of flowering when given at the end of the day or early in the dark period. This clearly suggests the action of a second phytochrome, which promotes flowering in its Pfr form. This response does not affect the timing of NB sensitivity.

Long-Day Plants. Until recently, less was known about light requirements in LDP photoperiodism. As for SDP, light reactions governing flowering in LDP occur in both light and dark periods, although one or the other may predominate in any one species. The concept of a critical night length is again relevant, but for LDP nights must be shorter than the critical length for plants to flower. In some LDP, R NB are effective for promotion of flowering. Their effectiveness varies during the night, and the response can be partially reversed by FR. However, unlike in SDP, a clear rhythmicity in responsiveness is not observed, and in general, longer periods of light are required to elicit a response (Thomas and Vince-Prue 1997).

Light reactions during the photoperiod have also been demonstrated in LDP. For example, FR added to a photoperiod of R or white light (WL) can promote flowering, with rhythmic variation in effectiveness (Fig. 16.10). Although phase shifting experiments are much more difficult to perform in LDP and less conclusive, light-induced changes in phase of the rhythm of FR responsiveness have been reported (e.g., Deitzer et al. 1982).

Photoperiodic responses in LDP have more often been investigated using extensions of a short, noninductive photoperiod. Action spectra for the promotion of flowering by photoperiod extensions most commonly show peaks at around 710–720 nm, well above the absorbance peak of Pr and clearly below that of Pfr (Thomas and Vince-Prue 1997). This peak is similar to that seen for the FR-HIR in seedling de-etiolation, suggesting the involvement of phyA. However, in other species, action spectra with peaks in both R and FR have also been reported (Carr-Smith et al. 1989), indicating that a second phytochrome is probably involved (Fig. 16.1). In some species, notably crucifers, BL is also effective as a day-extension.

While it is not clear exactly how the light responses of LDP and SDP may be compared, it is clear that in each response type, two distinct types of reaction can be distinguished. One involves a promotive effect of FR (seen in end-of-day [EOD] responses of LDP and reversal of NB in SDP). The other involves a promotive effect of R (seen in day extensions and NB in LDP, and reversal of EOD-FR effects in SDP). These clearly suggest the opposing actions of two separate phytochromes (Fig. 16.11).

16.5.1.2. Genetic Approaches

Many of the species used in classical studies of photoperiodism have, for one reason or another, not proven suitable for genetic analyses. Thus, although
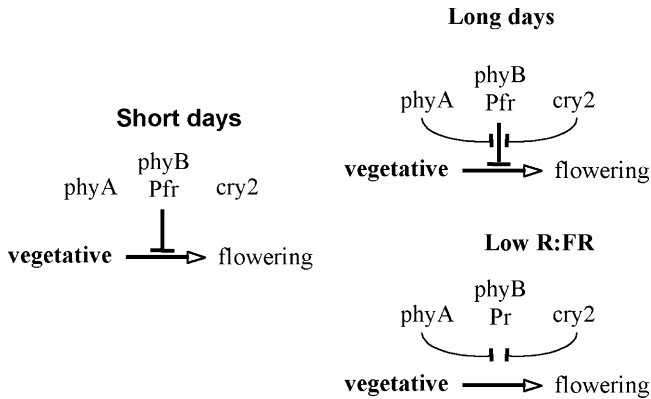
FIGURE 16.11. Photoreceptor interaction in the control of flowering in long-day plants. Under short days, phytochrome B in the Pfr form inhibits flowering. This inhibition is antagonized by phyA and cry2 under long days, resulting in early flowering. PhyB-mediated inhibition is reduced by light of low R:FR ratio given during the photoperiod or immediately before the dark period.

the physiology of photoperiodism has been most thoroughly characterized in SDP, the genetic dissection of photoperiodism has progressed most rapidly in LDP. This is of course due mainly to the prominence of the LDP *Arabidopsis*. Extensive mutational analysis of flowering in an SDP has yet to be performed, although the increasing prominence of rice as a model system for molecular genetics (including reverse genetics) and the recent cloning of several quantitative trait loci for flowering qualify it as the SDP system of choice for the foreseeable future (Yano et al. 2001). A number of flowering mutants or genetic variants have also been characterized in other photoperiodic species, including garden pea, wheat, barley (LDP), soybean, and tobacco (SDP).

Among mutants known to affect photoperiodic responses in *Arabidopsis* are mutants lacking various photoreceptors, in addition to those that affect light signaling to the circadian clock, maintenance of the circadian clock itself, or specific output pathways for photoperiodic flower induction (Fig. 16.12). Molecular and physiological analyses of these mutants are providing invaluable information about molecular components important for photoperiodic responsiveness.

Photoreceptor Mutants. In general, LDP flower early under low R:FR. By analogy with other shade-avoidance responses, this represents the switching off of a phytochrome necessary for inhibition of flowering under high R:FR (Fig. 16.11). Mutants for phyB-like genes in both SDP and LDP species show early flowering under both SD and LD, suggesting that phyB-like genes in both SPD and LPD show early flowering under both SD and LD, suggesting that phyD-type phy is not involved in photoperiod response as such but confers a general inhibition of flowering regardless of photoperiod conditions (Devlin et al. 1999, Weller et al. 2001a, Takano et al. 2005). A similar inhibitory role has also been
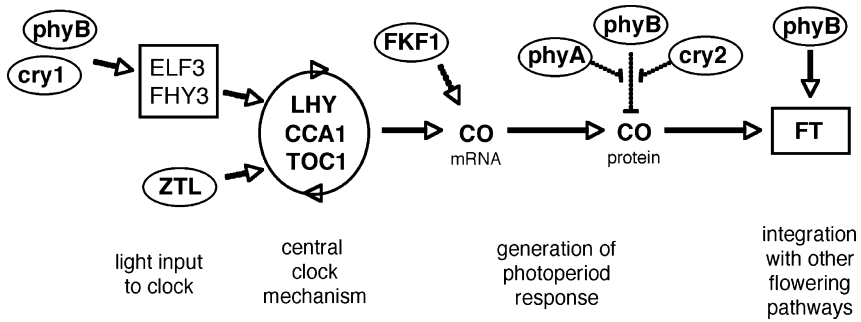
FIGURE 16.12. A proposed model for the genetic control of flowering by photoperiod in *Arabidopsis*. Light perceived by phyA and cry2 is thought to interact with a circadian timing mechanism to control the level and/or activity of the flower-promoting CONSTANS (CO) protein. CO is thought to be a specific regulator of the photoperiod response and induces the expression of downstream genes FT and SOC1, which are regulated by other environmental factors in addition to photoperiod.

described for *Arabidopsis* phyE (Devlin et al. 1998). PhyB is therefore unlikely to mediate the R NB effect in LDP, because this would require a promotive effect of Pfr. However, in the SDP rice, the R NB effect is solely mediated by phyB (Ishikawa et al. 2005). The promotion of flowering by EOD-FR treatments is also mediated by phyB, suggesting that after the light period, phyB is maintained in its inhibitory Pfr form during darkness. Inhibition may be directly related to length of time that phyB (and other phyB types) are present as Pfr, and not directly related to timing (Fig. 16.11).

The fact that relatively long periods of light are necessary for promotion of flowering in LDP, and the similarity of action spectra for this promotion to that seen for the FR-HIR in seedling de-etiolation, have for some time suggested that phyA might have a significant flower-promoting role in LDP. This has been confirmed in *phyA* mutants of *Arabidopsis* and pea. In *Arabidopsis*, phyA contributes to the promotive effect both of WL NB and FR-rich day extensions (Johnson et al. 1994, Mockler et al. 2003, Yanovsky and Kay 2002). In pea, phyA is also clearly needed for perception of LD and promotes flowering in response to day extensions of either high or low R:FR (Weller et al. 1997a). This promotion of flowering is dependent on the presence of phyB (Fig. 16.11). Pea *phyA* mutants also retain a strong response to low R:FR NB, but are completely deficient in response to high R:FR NB (Weller et al. 2001a) These results show that in pea, phyA is also active under white light and phyA effects on flowering cannot be explained solely as a classical FR-HIR.

Null mutations in the rice phyA gene have no apparent effect on flowering under LD or SD (Takano et al. 2005). This suggests that in SDP, unlike LDP, phyA does not contribute to the promotion of flowering under inductive conditions. The only clear evidence of a role for phyA in control of a photoperiodic response in SDP has come from studies of tuberization in potato. Potato plants expressing an antisense *PHYA* transgene and possessing reduced levels of

phyA tuberize early under noninductive LD, showing that phyA acts to inhibit tuberization (Yanovsky et al. 2000b). While it is difficult to relate this response to the photoperiodic flowering response, it is of interest that phyB in potato also acts to inhibit tuberization (Jackson et al. 1996). PhyA and phyB thus appear to act in the same direction to control tuberization, rather than antagonistically as in the control of LDP flowering.

In *Arabidopsis*, an important role in the photoperiodic control of flowering has also been demonstrated for the cryptochrome photoreceptor family. Cry2 in particular has a relatively minor effect on seedling photomorphogenic responses, but has a strong promotive effect on flowering under LD (Guo et al. 1998), which is dependent on the activation of phyB (Mockler et al. 2003) (Fig. 16.11). These findings suggest that the perception of daylength has become the dominant function of this photoreceptor in *Arabidopsis*. However, in general, relatively few species show strong control of flowering by BL, and the importance of cry2 in photoperiodism may not be widespread.

Photoreceptor Mutants and the Circadian Rhythm. The most thorough application of mutants in the exploration of phenomena related to photoperiodism has been the investigation of photoreceptor effects on clock period (Somers et al. 1998, Devlin and Kay 2000). In general, the period-shortening effects of continuous light are thought to represent a continuous entrainment response, and are thus expected to be relevant in plants grown under L/D cycles. Results from these studies show that photoreceptor roles in the regulation of circadian period closely parallel their roles in the control of de-etiolation. In *Arabidopsis*, phyB, phyD and phyE are responsible for period shortening under high-irradiance R, while phyA acts under low-irradiance R and BL. Cry1 and cry2 act redundantly to shorten the circadian period under BL across a wide irradiance range. PhyA has also been shown to mediate the phase-advancing effect of FR on leaf-movement rhythms in potato (Yanovsky et al. 2000b). These results suggest that all of these photoreceptors may have the ability to contribute to entrainment of the clock under certain circumstances. However, the significance of this for plants growing under high WL irradiances is unclear. Under such conditions, phyB and cry1 would be expected to be the predominant photoreceptors controlling clock period, although a quadruple mutant lacking phyA, phyB, cry1, and cry2 can entrain normally to WL/D cycles (Yanovsky et al. 2000a). It is interesting that phyA and cry2, which both have profound effects on flowering, are reported to have only minor effects on clock period, suggesting that their primary function may be interaction with an output rhythm.

Circadian Rhythm Mutants. Several genes essential for correct maintenance of circadian rhythms under light/dark cycles have now been identified in *Arabidopsis* (Salome and McClung 2004). Although they have been studied in slightly different ways, these genes have all been shown to affect rhythmic control of gene expression and leaf movement under some circumstances. In addition, they all have dramatic effects on the photoperiodic induction of flowering, emphasizing the importance of normal circadian regulation for photoperiodism.

The Arabidopsis circadian clock initially envisaged as a simple feedback loop involving two components; the closely-related myb transcription factors *LHY* and *CCA1* and the pseudo-response-regulator (PRR) homologue *TOC1* (Alabadi et al. 2002, Mizoguchi et al. 2002). Other genes have subsequently been identified that are also necessary for circadian rhythmicity under constant conditions: these include LUX (Hazen et al. 2005), GI (Park et al. 1999; Fowler et al. 1999), and other PRR genes (e.g., Farré et al. 2005; Nakamichi et al. 2005). Inclusion of these genes has necessitated a gradual shift to a more complex model involving two or even three interlocking feedback loops (Locke et al. 2006, Zeilinger et al. 2006).

As described above, light influences the clock in a number of different ways. Some of the mechanisms by which this occurs are now known. For example, the *LHY* and *CCA1* genes were both identified as early targets of phytochrome action in transcript profiling of seedling responses to R and FR (Martinez-Garcia et al. 2000). Both genes contain G-box LRE in their promoters and are transcriptionally activated by the binding of phytochrome and PIF3. In another example, the *ZTL* gene, thought to encode a novel class of blue-light receptor (see Section 16.2.4.), has been shown to regulate the stability of TOC1 by targeting it for proteasome-dependent degradation (Màs et al. 2003).

A number of other genes with defects in photoperiodic flowering and circadian rhythms have also been characterized. In contrast to mutants affecting core clock components, the conditional nature of the clock defects in these mutants have suggested that they play a role in light input to the clock. Mutants for the *ELF3* gene were originally identified on the basis of an extremely early-flowering, photoperiod-insensitive phenotype. Null mutants of *ELF3* have a relatively normal circadian rhythm in continuous darkness but show complete suppression of rhythmicity under continuous light (Hicks et al. 1996). Under L/D cycles, *elf3* plants have a relatively normal diurnal rhythm in SD, but show an increasingly aberrant rhythm in longer photoperiods. These observations suggest that *ELF3* may function in the pathway for input of light signals to the clock (Fig. 16.12), rather than in the central clock mechanism (McWatters et al. 2000). Other more recently identified genes with a role in light input include *TIC* (Hall et al. 2003) and *FHY3* (Allen et al. 2006).

16.5.2. Signaling in Photoperiodism

16.5.2.1. Genetic Analysis of Photoperiod-Specific Signaling

Signaling in photoperiodism has also been subject to genetic dissection. In *Arabidopsis*, several flowering mutants have been identified which have photoperiod-specific phenotypes and no apparent effect on clock or light signaling (Fig. 16.12). The best characterized of these is *CO*, which encodes a nuclear protein with motifs suggestive of a role in regulation of transcription or protein-protein interaction. CO is a potent promoter of flowering and its immediate and main regulatory target is the RAF-kinase-like inhibitor gene *FT* (Kardailsky et al. 1999, Samach et al. 2000, Wigge et al. 2005). CO transcription

is controlled by the circadian clock, with a peak around dusk in LD and early in the night in SD, and consistent with this, CO transcript levels and/or rhythms are altered in many of the clock mutants described above.

A series of studies have provided evidence that a high level of CO protein is necessary for activation of *FT* expression and that this in turn depends on the coincidence of light with high levels of *CO* expression. Initial studies demonstrated a correlation between *CO* expression levels, light, and *FT* expression (Suarez-Lopez et al. 2001), and the functional significance of this was subsequently tested using circadian clock mutants to shift peak CO expression relative to the light/dark transition (Roden et al. 2002, Yanovsky and Kay 2002). Other recent studies have shown that in addition to the clock, direct light input through the FKF1 photoreceptor is necessary to promote *CO* expression late in the day (Imaizumi et al. 2003). Another elegant study showed that post-transcriptional regulation of CO is also important for the photoperiod response (Valverde et al. 2004) In the middle of a LD photoperiod, a phyB-dependent mechanism promotes the proteasome-dependent degradation of CO protein, but in the evening this degradation is opposed by light through the action of phyA and cry2 (Valverde et al. 2004), stabilizing CO and allowing the activation of *FT*. The photoperiod response therefore depends on circadian regulation of CO expression and complex interactions between multiple photoreceptor inputs, which act to entrain the circadian clock (phyA, phyB, cry1, cry2), to otherwise regulate clock components (*ZTL*), to activate CO transcription (*FKF1*), and to regulate CO protein stability (phyA, phyB cry2).

This mechanism has been established entirely from studies in *Arabidopsis*, but it appears that at least the central elements are conserved in other species, and differences in their interactions may explain some of the differences in photoperiodic response. The main illustration of this comes from the SDP rice, in which CO and FT homologues have been identified as QTL controlling flowering time. Examination of their regulatory interactions showed that the FT homologue *Hd3a* is promoter of flowering upregulated in inductive (SD) conditions and that this upregulation requires the action of the CO homologue *Hd1* (Kojima et al. 2002). However, in contrast with *Arabidopsis CO*, rice *Hd1* appears to have a dual role, also acting to inhibit *Hd3a* expression under noninductive LD (Hayama et al. 2002). Consistent with the *Arabidopsis* model, phyB inhibits *Hd3a* expression to delay flowering, an interaction that is also the basis for the NB response (Ishikawa et al. 2005).

16.5.2.2. Long-Distance Signaling in Evocation of Photoperiod Responses

The sensitivity to flower-inducing light signals varies tremendously among different species. In many cases the site at which light is perceived can be separated from the eventual site of flower formation, indicating the existence of some form of long-distance communication. This has been studied in physiological experiments involving grafting, leaf-removal, and differential exposure of different parts of the plant. Experiments of this kind have provided evidence for both a promoter (sometimes referred to as "florigen") and an inhibitor of

flowering ("anti-florigen"). In general, the evidence for a promoter is clearer in SDP, whereas evidence for an inhibitor is clearer in LDP. However, in some species both influences have been shown to co-exist (Thomas and Vince-Prue 1997). In several SDP, the rate of transport of the floral stimulus out of an induced leaf is similar to the rate of phloem movement, suggesting that it may be transported via the phloem. Speculations about the nature of the floral regulators have considered known plant hormones (gibberellins, cytokinins), various metabolites (sugars, polyamines), and, more recently, specific RNA molecules (see below).

Evidence for a mobile floral stimulus in *Arabidopsis* has been demonstrated in leaf removal and grafting experiments (Corbesier et al. 1996, An et al. 2004), and some details have now emerged about the nature of this signal. Evidence from genetic studies with *CO* and *FT* suggested that the signal must lie between circadian events in leaf and activation of *FT* target genes *SOC1* and *AP1* in shoot apex. Experiments combining grafting and the use of tissue specific and inducible promoters have shown that *CO* expression is only required in leaf tissue, specifically in phloem companion cells, where it generates a mobile signal capable of inducing flowering (An et al. 2004). FT is required at the apex where it interacts with the bZIP transcription factor FD to induce expression of the inflorescence identity gene AP1 (Abe et al. 2005, Wigge et al. 2005). However, transgenic expression of *FT* in phloem alone is also sufficient to induce flowering (An et al. 2004), and recent reports suggest that it is the FT protein that may act as the phloem-borne mobile signal (Corbesier, Vincent, Jang et al. 2007, Lin, Belanger, Lee et al. 2007).

It is clear that powerful molecular genetic studies combined with careful physiological studies have enabled substantial recent progress in solving several of the long standing questions in higher plant photoperiodism: the molecular mechanisms underlying the photoperiod response, the basis for the difference between LDP and SDP response, and nature of mobile signaling in photoperiodism. We can look forward to continued rapid progress on all three fronts.

16.6. Photomorphogenesis and Photoperiodism in the Natural Environment

In discussing the significance of photomorphogenesis in the natural environment, several things must be kept in mind. We need to consider the changes that may occur in the properties of light reaching the plant, the kind of information plants may extract from these changes, and the way in which this information might be converted into an appropriate developmental response.

Most plants have adopted a sedentary habit and are therefore committed to adapt to changes in their environment by developmental plasticity. Natural selection is therefore likely to have favored modifications of development that

maximize energy capture or that improve the ability of the plant to resist detrimental effects of light. In addition, correlation between changes in light environment and other environmental variables such as cold or drought are also likely to have favored cross-talk between light signaling and other signaling pathways and the exploitation of light information as a predictive signal. Conditions of continuous selection would also result in pressure to extract increasing amounts of information from light, through an ability to monitor more subtle changes. This in turn could conceivably have supported the evolution of multiple photoreceptors with diverse light sensing properties. Speculations about the importance of photoreceptors in the natural environment have been largely based on studies of mutants and transgenic lines grown as single plants in controlled-environment conditions, combined with an intuitive appreciation for the developmental predicament of the plant. However, they have recently begun to receive solid support from experiments conducted under natural and/or competitive conditions (Ballaré 1999).

16.6.1. Improving Energy Capture

In general, higher plants have two strategies to increase their capture of energy. They can either gain access to more energy by extending their growth into areas of stronger light, or they can more efficiently capture the energy already reaching them.

Measurements of light quality in the natural environment have shown that changes in the amount of light due to cloud cover or the time of day are accompanied by relatively small changes in its spectral distribution (Franklin and Whitelam 2005). In contrast, chlorophyll-containing tissues absorb efficiently in the R and B region of the spectrum, but transmit and reflect a substantial proportion of light in the FR waveband. Thus the presence of plants affects the local light environment by causing a measurable decrease in the ratio of R to FR light energy. This may occur by the filtering out of R and/or by increased lateral reflection of FR. However, it is particularly significant that increases in lateral reflection of FR from neighboring plants occur prior to any reduction in the amount of photosynthetically active R and BL wavelengths (Ballaré et al. 1990). An increase in the amount of FR is thus an unambiguous signal to the plant that potential competitors are growing nearby. Where this signal is unidirectional, the appropriate response of the plant is obviously to redirect its growth away from the other plants. In a denser population, the gradient in FR will not be as great, and the response may also include an increase in overall growth rate. Although the horizontal and lateral components of the response to shading are often treated separately as phototropism and shade avoidance, it is more appropriate to consider both responses as aspects of a strategy in which the plant is actively "foraging" for light (Ballaré et al. 1997).

A negative phototropism in response to increases in lateral FR reflected from neighboring plants has been demonstrated in cucumber. This response is completely lacking in a phyB-deficient mutant, indicating that in addition

to its role in shade avoidance, phyB is also important for the detection of nonshading neighbors (Ballaré et al. 1992). The existence of additional phyB-type phytochromes with differing roles at different stages of development suggests that plants are still evolving to fine-tune their capacity for shade avoidance and neighbor detection, and emphasizes the importance of these responses for the plant.

As the canopy closes or population density increases, increases in the leaf area index also occur, and as a result the light energy in the R and BL wavebands decreases. Under such circumstances, a plant may also be exposed to a lateral gradient in BL and show a positive phototropic response. The phyB-deficient mutant of cucumber retains the ability to respond to such a gradient (Ballaré et al. 1991), implying the action of a BL photoreceptor, which is most probably phototropin. Under conditions of deep shade it is likely that the observed growth responses result from a reduction in activity of several photoreceptors, including the phyB-type phytochromes, cry1 and phototropin (Ballaré 1999). Without phyA, however, seedlings cannot sense the FR transmitted through the canopy and do not de-etiolate, indicating that phyA may be essential for maintaining a degree of de-etiolation in highly competitive situations (Yanovsky et al. 1995).

Under shade conditions many plants may also increase their efficiency of light capture by modifying various features of their photosynthetic organs. Depending on the species, this may include modification of light-harvesting complex composition, chloroplast organization, orientation or position, and leaf shape, size, or thickness (Terashima and Hikosaka 1995, Vogelmann et al. 1996, Mullineaux and Karpinski 2002). Acclimation to shade is therefore a complex phenomenon, but does at least in some cases involve responses that can be considered photomorphogenic. The phototropin photoreceptors have recently been shown to mediate BL control of chloroplast orientation and stomatal aperture (Sakai et al. 2001, Kinoshita et al. 2001), and may thus play an important role in the regulation of photosynthesis. However, in general the contribution of photomorphogenic photoreceptors to photosynthetic acclimation is not yet well understood.

16.6.2. Light and the Seed Habit

Other adaptive responses to light seem to have arisen with the development of the seed habit. Control of seed germination is important to allow seedlings to develop in favorable light environment. Particularly for small-seeded species germinating under the soil surface, seedlings must be able to emerge into full light before the seed energy reserves are exhausted. The extremely low fluences of light needed to induce germination of some species can be understood as a signal to the seed that it is near the soil surface before making the irreversible commitment to germinate. In other species, the higher light requirement and R/FR reversibility of germination may reflect a strategy to preferentially promote germination under gaps in the canopy (Casal and Sanchez 1998).

Investment of energy in the seed has allowed a period of time in which seedlings can develop independently of the need to photosynthesize. In effect

this provides a longer period of time over which the seedling can integrate information about its light environment and adjust its development appropriately. In combination with the seed habit, many species have developed a growth strategy of etiolation in which they are able to suppress normal light-regulated leaf development and elongate rapidly growing in darkness. This could conceivably have been favored in evolution because it increases the efficiency with which the plant uses stored seed reserves, but also because its rapid emergence into the light after germination will maximize competitive advantage. However, along with this strategy comes the need for anticipation of imminent emergence into the light environment and a rapid response immediately following emergence. PhyA does appear to serve this purpose under natural conditions, and it is conceivable that some of the distinct features of phyA could have arisen in response to this pressure (Mathews 2006).

16.6.3. Avoidance or Survival of Unfavorable Conditions

In addition to useful light for photosynthesis, sunlight also contains potentially damaging UV wavelengths. Various phenylpropanoid pigments, including sinapates and flavonoids, absorb UV and reduce its damaging effects on the plant (Bieza and Lois, 2001). The production of these pigments in many cases is strongly induced by light as a result of increased expression of certain genes in phenylpropanoid metabolism (Shirley 1996, Ryan et al. 2001). In many cases this induction is strongest in young seedlings and immature leaves, which are more susceptible to UV damage.

It is also possible that light can also serve as an indirect signal of other adverse aspects of the environment. For example, the fact that in some species light can act to inhibit germination can be understood in terms of the need for a damp environment and a correlation between reduced water availability near the soil surface and increased light levels. A similar association could explain the negative phototropism of some roots, and experimental evidence supporting this has recently been reported (Galen et al. 2007). The action of phot1 allows roots near the surface to reorient and grow downward into the soil, with consequences for the availability of water to those roots and performance under drought conditions (Galen et al. 2007).

A more complicated kind of correlative selection may underlie many seasonal responses. Factors such as temperature and water availability can clearly become limiting at certain times of year in some environments, and many plants are able to avoid the deleterious effects of these seasonal extremes through suppression of normal growth and the adoption of various survival strategies. These include seed and bud dormancy, formation of storage organs, and initiation of flowering, which can be timed so as to allow the reproductive cycle to be completed before unfavorable conditions return. Changes in limiting factors of temperature and water availability can act directly as triggers for these changes (as seen in cold-temperature requirements for germination or flowering). However, although seasonal, these factors are also subject to irregular short-term variation, whereas

change in daylength is a much more constant and reliable indicator of season from year to year. In general, the degree of photoperiod responsiveness is an important aspect of adaptation to growth at a given latitude (Thomas and Vince-Prue 1997).

As the molecular basis for light and photoperiod responses has become better understood, increasing numbers of studies are turning toward an investigation of the ecological significance of observed genetic variation or the genetic basis for natural variation in plant responses. Notable recent examples include demonstrations of the contribution of the phyC photoreceptor to natural variation in *Arabidopsis* flowering time (Balasubramanian et al. 2006), the role of *FT* homologues in latitudinal variation in seasonal dormancy in poplar (Böhlenius et al. 2006), and the fitness consequences of genetic variation in Arabidopsis circadian clock function (Michael et al. 2003).

16.7. Concluding Remarks

Considering that plants are fixed in one place and dependent on light as an energy source, it is not surprising that sophisticated mechanisms have evolved, enabling them to modify their development in response to light and thus to better compete with their neighbours. Persistent selective pressures for extracting more subtle information from the light environment have favored the evolution of several distinct photoreceptor systems. For the most part, these systems act synergistically, increasing the general sensitivity of the plant to light. However, some photoreceptors have developed discrete light-sensing abilities, which may be linked to specific physiological and ecological roles.

The past 25 years have seen major advances in our understanding of the photoreceptors involved in photomorphogenesis and the definitive identification of some of the molecular and cellular processes required for expression of light responses. We still do not understand the complexities of signal transduction, or the network of interactions between light, plant hormones, and other factors. Nevertheless, the genetic and molecular tools are now available to enable a thorough analysis of these aspects of photomorphogenesis over the coming years. Greater understanding of photomorphogenesis will bring an increased ability to manipulate plant light responses for practical purposes, such as in the control of density-dependent shading, flowering, and yield in horticultural and crop plants. It will also help us to better understand the origins and adaptive significance of natural variation in growth habit and flowering phenology.

References

Abe, M., Kobayashi, Y., Yamamoto, S., Daimon, Y., Yamaguchi, A., Ikeda, Y., Ichinoki, H., Notaguchi, M., Goto, K. and Araki, T. (2005) FD, a bZIP protein mediating signals from the floral pathway integrator FT at the shoot apex. Science 309, 1052–1056.

Ahmad, M. and Cashmore, A.R. (1994) *HY4* gene of *Arabidopsis thaliana* encodes a protein with characteristics of a blue-light photoreceptor. Nature 366, 162–166.

Ahmad, M., Jarillo, J.A., Smirnova, O. and Cashmore, A.R. (1998) The CRY1 blue light photoreceptor of *Arabidopsis* interacts with phytochrome A in vitro. Mol. Cell 1, 939–948.

Alabadí D., Yanovsky, M.J., Mas, P., Harmer, S.L. and Kay, S.A. (2002) Critical role for CCA1 and LHY in maintaining circadian rhythmicity in *Arabidopsis*. Curr. Biol. 12, 757–761

Allen, T., Koustenis, A., Theodorou, G., Somers, D.E., Kay, S.A., Whitelam, G.C. and Devlin PF (2006) *Arabidopsis* FHY3 specifically gates phytochrome signaling to the circadian clock. Plant Cell 18, 2506–2516

Al-Sady, B., Ni, W., Kircher, S., Schäfer, E. and Quail, P.H. (2006) Photoactivated phytochrome induces rapid PIF3 phosphorylation prior to proteasome-mediated degradation. Mol. Cell. 23, 439–446.

An, H., Roussot, C., Suarez-Lopez, P., Corbesier, L., Vincent, C., Pineiro, M., Hepworth, S., Mouradov, A., Justin, S., Turnbull, C. and Coupland, G. (2004) CONSTANS acts in the phloem to regulate a systemic signal that induces photoperiodic flowering of *Arabidopsis*. Development 131, 3615–3626.

Balasubramanian, S., Sureshkumar, S., Agrawal, M., Michael, T.P., Wessinger, C., Maloof, J.N., Clark, R., Warthmann, N., Chory, J. and Weigel, D. (2006) The PHYTOCHROME C photoreceptor gene mediates natural variation in flowering and growth responses of *Arabidopsis thaliana*. Nat. Genet. 38, 711–715.

Ballaré, C.L., Casal J.J., Kendrick R.E. (1991) Responses of light-grown wild-type and long-hypocotyl mutant cucumber seedlings to natural and simulated shade light. Photochem. Photobiol. 54, 819–826.

Ballaré, C.L. (1999) Keeping up with the neighbours: phytochrome sensing and other signaling mechanisms. Trends Plant Sci. 4, 97–102.

Ballaré, C.L., Scopel, A.L. and Sanchez, R.A. (1990) Far-red irradiation reflected from adjacent leaves: an early signal of competition in plant canopies. Science *247*, 329–332.

Ballaré, C.L., Scopel, A.L. and Sanchez, R.A. (1997) Foraging for light-photosensory ecology and agricultural implications. Plant Cell Environ. 20, 820–825.

Ballaré, C.L., Scopel, A.L., Radosevich, S.R. and Kendrick, R.E. (1992) Phytochrome-mediated phototropism in de-etiolated seedlings. Occurrence and ecological significance. Plant Physiol. 100, 170–177.

Baskin, T.I. and Iino, M. (1987) An action spectrum in the blue and ultraviolet for phototropism in alfalfa. Photochem. Photobiol 46, 127–136.

Baum, G., Long, J.C., Jenkins, G.I. and Trewavas, A.J. (1999) Stimulation of the blue light phototropic receptor NPH1 causes a transient increase in cytosolic Ca^{2+}. Proc. Natl Acad. Sci. USA 96, 13554–13559.

Bhoo, S.H., Davis, S.J., Walker, J., Karniol, B. and Vierstra, R.D. (2001) Bacteriophytochromes are photochromic histidine kinases using a biliverdin chromophore. Nature 414, 776–779.

Bieza, K. and Lois, R. (2001) An *Arabidopsis* mutant tolerant to lethal ultraviolet-B levels shows contsitutively elevated accumulation of flavonoids and other phenolics. Plant Physiol. 126, 1105–1115.

Böhlenius, H., Huang, T., Charbonnel-Campaa, L., Brunner, A.M., Jansson, S., Strauss, S.H. and Nilsson, O. (2006) CO/FT regulatory module controls timing of flowering and seasonal growth cessation in trees. Science 312, 1040–1043.

Bouly, J.P, Giovani, B., Djamei, A., Mueller, M., Zeugner, A., Dudkin, E.A., Batschauer, A., and Ahmad, M. (2003) Novel ATP-binding and autophosphorylation activity associated with *Arabidopsis* and human cryptochrome-1. Eur. J. Biochem. 270,

2921–2928.

Brautigam, C.A, Smith, B.S., Ma, Z., Palnitkar, M., Tomchick, D.R., Machius, M. and Deisenhofer, J. (2004) Structure of the photolyase-like domain of cryptochrome 1 from *Arabidopsis thaliana*. Proc. Natl. Acad. Sci. USA 101, 12142–12147.

Briggs W.R. (2006) Blue/UV-A receptors: Historical overview. In: E. Schäfer and F. Nagy (Eds.) *Photomorphogenesis in Plants and Bacteria, Third Edition, Function and Signal Transduction Mechanisms.* Springer, Dorcrecht. pp. 171–197.

Briggs, W.R. and Huala, E. (1999) Blue-light photoreceptors in higher plants. Annu. Rev. Cell Develop. Biol. 15, 33–62. (2006) Blue/UV-A photoreceptors: historical overview. In: E Schäfer and F Nagy (Eds.) *Photomorphogenesis in plants and bacteria*, 3rd ed. Springer, Dordrecht, pp. 171–198.

Bünning, E. (1964) *The physiological clock*. Springer Verlag, Berlin.

Butler, W.L., Hendricks, S.B. and Siegelman, H.W. (1964) Action spectra of phytochrome *in vitro*. Photochem. Photobiol. 3, 521–528.

Carr-Smith, H.D., Thomas, B. and Johnson, C.B. (1989) An action spectrum for the effect of continuous light on flowering in wheat. Planta 179, 428–432.

Casal, J.J. (2000) Phytochromes, cryptochromes, phototropin: photoreceptor interactions in plants. Photochem. Photobiol. 71, 1–11.

Casal, J.J. (2006) The photoreceptor interaction network. In: E. Schäfer and F. Nagy (Eds.), *Photomorphogenesis in plants and bacteria*, 3rd ed. Springer, Dordrecht, pp 407–438.

Casal, J.J. and Sanchez, R.A. (1998) Phytochromes and seed germination. Seed Sci. Res. 8, 317–329.

Cashmore, A.R., Jarillo, J.A., Wu, Y.J. and Liu, D.M. (1999) Cryptochromes: Blue light receptors for plants and animals. Science 284, 760–765.

Choi, G., Yi, H., Lee, J., Kwon, Y.K., Soh, M.S., Shin, B., Luka, Z., Hahn, T.R., and Song, P.S. (1999) Phytochrome signaling is mediated through nucleoside diphosphate kinase 2. Nature 401, 610–613.

Christie, J.M., Salomon, M., Nozue, K., Wada, M. and Briggs, W.R. (1999) LOV (light, oxygen, or voltage) domains of the blue-light photoreceptor phototropin (nph1): Binding sites for the chromophore flavin mononucleotide Proc. Natl Acad. Sci. USA 96, 8779–8783.

Clack, T., Mathews, S. and Sharrock, R.A. (1994) The phytochrome apoprotein family in *Arabidopsis* is encoded by five genes—the sequences and expression of *PHYD* and *PHYE*. Plant Mol. Biol. 25, 413–427.

Colon-Carmona, A., Chen, D.L., Yeh, K.C. Abel S. (2000) Aux/IAA proteins are phosphorylated by phytochrome in vitro. Plant Physiol. 124, 1728–1738.

Corbesier, L., Gadisseur, I., Silvestre, G., Jacqmard, A. and Bernier, G. (1996) Design in *Arabidopsis thaliana* of a synchronous system of floral induction by one long day. Plant J. 9, 947–952.

Corbesier, L., Vincent, C., Jang, S., Fornara, F., Fan, Q., Searle, I., Giakountis, A., Farrona, S., Gissot, L., Trunbull, C., and Coupland, G. (2007) FT protein movement contributes to long-distance signalling in floral induction in *Arabidopsis*. Science 316, 1030–1033.

Davis, S.J. (2006) The phytochrome chromophore. In: E. Schäfer and F. Nagy (Eds.), *Photomorphogenesis in plants and bacteria*, 3rd ed. Springer, Dordrecht, pp. 41–64.

Davis, S.J., Vener, A.V. and Vierstra, R.D. (1999) Bacteriophytochromes: phytochrome-like photoreceptors from nonphotosynthetic eubacteria. Science 286, 2517–2520.

Deitzer, G.F., Hayes, R. and Jabben, M. (1982) Phase shift in the circadian rhythm of floral promotion by far-red light in *Hordeum vulgare* L. Plant Physiol. 69, 597–601.

Devlin, P.F. and Kay, S.A. (2000) Cryptochromes are required for phytochrome signaling to the circadian clock but not for rhythmicity. Plant Cell 12, 2499–2509.

Devlin, P.F., Patel, S.R. and Whitelam, G.C. (1998) Phytochrome E influences internode elongation and flowering time in *Arabidopsis*. Plant Cell 10, 1479–1488.

Devlin, P.F., Robson, P.R.H., Patel, S.R., Goosey, L., Sharrock, R.A. and Whitelam, G.C. (1999) Phytochrome D acts in the shade-avoidance syndrome in *Arabidopsis* by controlling elongation growth and flowering time. Plant Physiol. 119, 909–915.

Dhingra, A., Bies, D.H., Lehner, K.R, and Folta, K.M. (2006) Green light adjusts the plastid transcriptome during early photomorphogenic development. Plant Physiol. 142, 1256–1266.

Dieterle, M., Zhou, Y.C., Schäfer, E., Funk, M. and Kretsch, T. (2001) EID1, an F-box protein involved in phytochrome A-specific light signaling. Genes Develop. 15, 939–944.

Duek, P.D. and Fankhauser, C. (2003) HFR1, a putative bHLH transcription factor, mediates both phytochrome A and cryptochrome signaling. Plant J. 34, 827–836.

Eichenberg, K., Baurle, I., Paulo, N., Sharrock, R.A., Rüdiger, W. and Schäfer, E. (2000) *Arabidopsis* phytochromes C and E have different spectral characteristics from those of phytochromes A and B. FEBS Lett. 470, 107–112.

Fairchild, C.D., Schumaker, M.A. and Quail, P.H. (2000) HFR1 encodes an atypical bHLH protein that acts in phytochrome A signal transduction. Genes Develop. 14, 2377–2391.

Fankhauser, C. and Bowler, C. (2006) Biochemical and molecular analysis of signaling components. In: E. Schäfer and F. Nagy (Eds.), *Photomorphogenesis in plants and bacteria*, 3rd ed.. Springer, Dordrecht, pp. 379–406.

Fankhauser, C., Yeh, K.C., Lagarias, J.C., Zhang, H., Elich, T.D. and Chory, J. (1999) PKS1, a substrate phosphorylated by phytochrome that modulates light signaling in *Arabidopsis*. Science 284, 1539–1541.

Farré, E.M., Harmer, S.L, Harmon, F.G., Yanovsky, M.J. and Kay SA (2005) Overlapping and distinct roles of PRR7 and PRR9 in the *Arabidopsis* circadian clock. Curr. Biol. 15, 47–54.

Folta, K.M. and Spalding, E.P. (2001) Unexpected roles for cryptochrome 2 and phototropin revealed by high-resolution analysis of blue light-mediated hypocotyl growth inhibition. Plant J. 26, 471–478.

Folta, K.M. (2004) Green light stimulates early stem elongation, antagonizing light-mediated growth inhibition. Plant Physiol. 135, 1407–1416.

Fowler, S., Lee. K., Onouchi, H., Samach, A., Richardson, K., Morris, B., Coupland, G. and Putterill, J. (1999) *GIGANTEA*: a circadian clock-controlled gene that regulates photoperiodic flowering in *Arabidopsis* and encodes a protein with several possible membrane-spanning domains. EMBO J. 18, 4679–4688.

Franklin, K.A., Praekelt, U., Stoddart, W.M., Billingham, O.E., Halliday, K.J. and Whitelam, G.C. (2003) Phytochromes B, D, and E act redundantly to control multiple physiological responses in *Arabidopsis*. Plant Physiol. 131, 1340–1346.

Franklin, K.A. and Whitelam, G.C. (2005) Phytochromes and shade-avoidance responses in plants. Ann Bot 96, 169–175.

Furuya, M. (1989) Molecular properties and biogenesis of phytochrome I and II. Adv. Biophys. 25, 133–167.

Galen, C., Rabenold, J.J, and Liscum, E. (2007) Functional ecology of a blue light photoreceptor: effects of phototropin-1 on root growth enhance drought tolerance in *Arabidopsis* thaliana. New Phytol. 173, 91–99.

Garner, W.W. and Allard, A.H. (1920) Effect of the relative length of day and night and other factors of the environment on growth and reproduction in plants. J. Agric. Res. 18, 553–606.

Gil P., Kircher S., Adam E., Bury E., Kozma-Bognar L., Schafer E., Nagy F. (2000) Photo-control of subcellular partitioning of phytochrome-B:GFP fusion protein in tobacco seedlings. Plant J. 22, 135–145.

Giovani, B., Byrdin, M., Ahmad, M. and Brettel K. (2003) Light-induced electron transfer in a cryptochrome blue-light photoreceptor. Nat. Struct. Biol. 10, 489–490.

Goosey, L., Palecanda, L. and Sharrock, R.A. (1997) Differential patterns of expression of the *Arabidopsis PHYB*, *PHYD*, and *PHYE* phytochrome genes. Plant Physiol. 115, 959–969.

Guo, H.W., Mockler, T., Duong, H. and Lin, C.T. (2001) SUB1, an *Arabidopsis* Ca^{2+}-binding protein involved in cryptochrome and phytochrome coaction. Science 291, 487–490.

Guo, H.W., Yang, W.Y., Mockler, T.C. and Lin, C.T. (1998) Regulation of flowering time by *Arabidopsis* photoreceptors. Science 279, 1360–1363.

Hall, A., Bastow, R.M., Davis, S.J., Hanano, S., McWatters, H.G., Hibberd, V., Doyle, M.R., Sung, S., Halliday, K.J., Amasino, R.M. and Millar, A.J. (2003) The *TIME FOR COFFEE* gene maintains the amplitude and timing of *Arabidopsis* circadian clocks. Plant Cell 15, 2719–2729.

Harada, A., Sakai, T. and Okada, K. (2003) Phot1 and phot2 mediate blue light-induced transient increases in cytosolic Ca^{2+} differently in *Arabidopsis* leaves. Proc. Natl Acad. Sci. USA 100, 8583–8588.

Harper, R.M., Stowe-Evans, E.L., Luesse, D.R., Muto, H., Tatematsu, K., Watahiki, M.K., Yamamoto, K. and Liscum, E. (2000) The *NPH4* locus encodes the auxin response factor ARF7, a conditional regulator of differential growth in aerial *Arabidopsis* tissue. Plant Cell 12, 757–770.

Hauser, B.A., Cordonnier-Pratt, M.M. and Pratt, L.H. (1998) Temporal and photoregulated expression of five tomato phytochrome genes. Plant J. 14, 431–439.

Hauser, B.A., Cordonnier-Pratt, M.M., Daniel-Vedele, F. and Pratt, L.H. (1995) The phytochrome gene family in tomato includes a novel subfamily. Plant Mol. Biol. 29, 1143–1155.

Hauser, B.A., Pratt, L.H. and Cordonnier-Pratt, M.M. (1997) Absolute quantification of five phytochrome transcripts in seedlings and mature plants of tomato (*Solanum lycopersicum* L.). Planta 201, 379–387.

Hauser, B.A., Cordonnier-Pratt, M.M., and Pratt, L.H. (1998) Temporal and photoregulated expression of five tomato phytochrome genes. Plant J. 14, 431–439.

Hayama, R., Yokoi, S., Tamaki, S., Yano, M. and Shimamoto, K. (2003) Adaptation of photoperiodic control pathways produces short-day flowering in rice. Nature 422, 719–722.

Hazen, S.P., Schultz, T.F., Pruneda-Paz, J.L., Borevitz, J.O., Ecker, J.R. and Kay, S.A. (2005) *LUX ARRHYTHMO* encodes a Myb domain protein essential for circadian rhythms. Proc. Natl Acad. Sci. USA 102, 10387–10392.

Hennig, L. (2006) Phytochrome degradation and dark reversion. In: E. Schäfer and F. Nagy (Eds.), *Photomorphogenesis in plants and bacteria*, 3rd ed. Springer, Dordrecht, pp. 131–154.

Hershey, H.P., Colbert, J.T., Lissemore, J.L., Barker, R.F. and Quail, P.H. (1984) Molecular cloning of cDNA for Avena phytochrome. Proc. Natl Acad. Sci. USA 81, 2332–2336.

Hicks, K.A., Millar, A.J., Carre, I.A., Somers, D.E., Straume, M., Meeks-Wagner, D.R. and Kay, S.A. (1996) Conditional circadian dysfunction of the *Arabidopsis early-flowering 3* mutant. Science 274, 790–792.

Hiltbrunner, A., Tscheuschler, A., Viczian, A., Kunkel, T., Kircher, S. and Schäfer, E. (2006) FHY1 and FHL act together to mediate nuclear accumulation of the phytochrome A photoreceptor. Plant Cell Physiol. 47, 1023–1034.

Hirose F., Shinomura T., Tanabata T., Shimada H., Takano M. (2006) Involvement of rice cryptochromes in de-etiolation responses and flowering. Plant Cell Physiol. 47, 915–925.

Hisada, A., Hanzawa, H., Weller, J.L., Nagatani, A., Reid, J.B. and Furuya, M. (2000) Light-induced nuclear translocation of endogenous pea phytochrome A visualized by immunocytochemical procedures. Plant Cell 12, 1063–1078.

Hoecker, U., Tepperman, J.M. and Quail, P.H. (1999) SPA1, a WD-repeat protein specific to phytochrome A signal transduction. Science 284, 496–499.

Hsieh, H.L., Okamoto, H., Wang, M.L., Ang, L.H., Matsui, M., Goodman, H. and Deng, X.W. (2000) *FIN219*, an auxin-regulated gene, defines a link between phytochrome A and the downstream regulator COP1 in light control of *Arabidopsis* development. Genes Develop. 14, 1958–1970.

Huala, E., Oeller, P.W., Liscum, E., Han, I.S., Larsen, E. and Briggs, W.R. (1997) *Arabidopsis* NPH1—a protein kinase with a putative redox-sensing domain. Science 278, 2120–2123.

Hübschmann, T., Borner, T., Hartmann, E. and Lamparter, T. (2001) Characterization of the Cph1 holo-phytochrome from *Synechocystis* sp. PCC 6803. Eur. J. Biochem. 268, 2055–2063.

Hudson, M,E, and Quail, P.H. (2003) Identification of promoter motifs involved in the network of phytochrome A-regulated gene expression by combined analysis of genomic sequence and microarray data. Plant Physiol. 133, 1605–1616.

Hudson, M.E., Lisch, D.R. and Quail, P.H. (2003) The *FHY3* and *FAR1* genes encode transposase-related proteins involved in regulation of gene expression by the phytochrome A-signaling pathway. Plant J. 34, 453–471.

Hudson, M., Ringli, C., Boylan, M.T. and Quail, P.H. (1999) The *FAR1* locus encodes a novel nuclear protein specific to phytochrome A signaling. Genes Develop. 13, 2017–2027.

Imaizumi, T., Tran, H.G, Swartz, T.E., Briggs, W.R. and Kay, S.A. (2003) FKF1 is essential for photoperiodic-specific light signaling in *Arabidopsis*. Nature 426, 302–306.

Ishikawa, R., Tamaki, S., Yokoi, S., Inagaki, N., Shinomura, T., Takano, M. and Shimamoto, K. (2005) Suppression of the floral activator Hd3a is the principal cause of the night break effect in rice. Plant Cell. 17, 3326–3336.

Jackson, S.D., Heyer, A., Dietze, J. and Prat S. (1996) Phytochrome B mediates the photoperiodic control of tuber formation in potato. Plant J. 9, 159–166.

Jenkins, G.I., Long, J.C., Wade, H.K., Shenton, M.R. and Bibikova, T.N. (2001) UV and blue light signaling: pathways regulating chalcone synthase gene expression in *Arabidopsis*. New Phytol. 151, 121–131.

Johnson, E., Bradley, M., Harberd, N.P. and Whitelam, G.C. (1994) Photoresponses of light-grown phyA mutants of *Arabidopsis*-phytochrome A is required for the perception of daylength extensions. Plant Physiol. 105, 141–149.

Jones, A.M., Ecker, J.R. and Chen, J.G. (2003) A reevaluation of the role of the heterotrimeric G protein in coupling light responses in *Arabidopsis*. Plant Physiol. 131, 1623–1627.

Kagawa, T., Sakai, T., Suetsugu, N., Oikawa, K., Ishiguro, S., Kato, T., Tabata, S., Okada, K. and Wada, M. (2001) *Arabidopsis* NPL1: A phototropin homolog controlling the chloroplast high-light avoidance response. Science 291, 2138–2141.

Kanegae, H., Tahir, M., Savazzini, F., Yamamoto, K., Yano, M., Sasaki, T., Kanegae, T., Wada, M. and Takano, M. (2000) Rice *NPH1* homologues, *OsNPN1a* and *OsNPN1b*, are differently photoregulated. Plant Cell Physiol. 41, 415–423.

Kang, X., Chong, J. and Ni, M. (2005) HYPERSENSITIVE TO RED AND BLUE 1, a ZZ-type zinc finger protein, regulates phytochrome B-mediated red and cryptochrome-mediated blue light responses. Plant Cell 17, 822–835.

Kang, X. and Ni, M. (2006) *Arabidopsis* SHORT HYPOCOTYL UNDER BLUE1 contains SPX and EXS domains and acts in cryptochrome signaling. Plant Cell. 18, 921–934.

Kardailsky, I., Shukla, V.K., Ahn, J.H., Dagenais, N., Christensen, S.K., Nguyen, J.T., Chory, J., Harrison, M.J. and Weigel, D. (1999) Activation tagging of the floral inducer FT. Science 286, 1962–1965.

Karniol, B., Wagner, J.R., Walker, J.M. and Vierstra, R.D. (2005) Phylogenetic analysis of the phytochrome superfamily reveals distinct microbial subfamilies of photoreceptors. Biochem J. 392, 103–116.

Kehoe, D.M. and Grossman, A.R. (1996) Similarity of a chromatic adaptation sensor to phytochrome and ethylene receptors. Science 273, 1409–1412.

Kerckhoffs, L.H.J., Schreuder, M.E.L., van Tuinen, A., Koornneef, M. and Kendrick, R.E. (1997) Phytochrome control of anthocyanin biosynthesis in tomato seedlings – analysis using photomorphogenic mutants. Photochem. Photobiol. 65, 374–381.

Khanna, R., Shen, Y., Toledo-Ortiz, G., Kikis, E.A., Johannesson, H., Hwang, Y.S. and Quail, P.H. (2006) Functional profiling reveals that only a small number of phytochrome-regulated early-response genes in *Arabidopsis* are necessary for optimal deetiolation. Plant Cell 18, 2157–2171.

Kim, B.C., Tennessen, D.J. and Last, R.L. (1998) UV-B-induced photomorphogenesis in *Arabidopsis thaliana*. Plant J. 15, 667–674.

Kinoshita, T., Doi, M., Suetsugu, N., Kagawa, T., Wada, M. and Shimazaki, K. (2001) phot1 and phot2 mediate blue light regulation of stomatal opening. Nature 414, 656–660.

Kircher, S., Gil, P., Kozma-Bognar, L., Fejes, E., Speth, V., Husselstein-Muller, T., Bauer, D., Adam, E., Schäfer, E. and Nagy, F. (2002) Nucleocytoplasmic partitioning of the plant photoreceptors phytochrome A, B, C, D, and E is regulated differentially by light and exhibits a diurnal rhythm. Plant Cell 14, 1541–1555.

Kircher, S., Kozma-Bognar, L., Kim, L., Adam, E., Harter, K., Schafer, E. and Nagy, F. (1999) Light quality-dependent nuclear import of the plant photoreceptors phytochrome A and B. Plant Cell 11, 1445–1456.

Kleiner, O., Kircher, S., Harter, K., Batschauer, A. (1999) Nuclear localization of the *Arabidopsis* blue light receptor cryptochrome 2. Plant J. 19, 289–296.

Kohchi, T., Mukougawa, K., Frankenberg, N., Masuda, M., Yokota, A. and Lagarias, J.C. (2001) The *Arabidopsis HY2* gene encodes phytochromobilin synthase, a ferredoxin-dependent biliverdin reductase. Plant Cell 13, 425–436.

Kojima, S., Takahashi, Y., Kobayashi, Y., Monna, L., Sasaki, T., Araki, T. and Yano M. (2002) *Hd3a*, a rice ortholog of the *Arabidopsis FT* gene, promotes transition to flowering downstream of *Hd1* under short-day conditions. Plant Cell Physiol. 43, 1096–1105.

Koornneef, M., Rolff, E. and Spruitt, C.J.P. (1980) Genetic control of light-inhibited hypocotyl elongation in *Arabidopsis thaliana* L. Heynh. Z. Pflanzenphysiol. 100, 147–160.

Lariguet, P. and Fankhauser, C. (2004) Hypocotyl growth orientation in blue light is determined by phytochrome A inhibition of gravitropism and phototropin promotion of phototropism. Plant J. 40, 826–834.

Lariguet, P., Schepens, I., Hodgson, D., Pedmale, U.V., Trevisan, M., Kami, C., de Carbonnel, M., Alonso, J.M., Ecker, J.R., Liscum, E. and Fankhauser, C. (2006) PHYTOCHROME KINASE SUBSTRATE 1 is a phototropin 1 binding protein required for phototropism. Proc. Natl Acad. Sci. USA 103, 10134–10139.

Lin, C., Robertson, D.E., Ahmad, M., Raibekas, A.A., Jorns, M.S., Dutton, P.L. and Cashmore, A.R. (1995) Association of flavin adenine dinucleotide with the *Arabidopsis* blue light receptor cry1. Science 269, 968–970.

Lin, C., Yang, H.Y., Guo, H.W., Mockler, T., Chen, J. and Cashmore, A.R. (1998) Enhancement of blue-light sensitivity of *Arabidopsis* seedlings by a blue light receptor cryptochrome 2. Proc. Natl Acad. Sci. USA 95, 2686–2690.

Lin, M., Belanger, H., Lee, Y., Varkonyi-Gasic, E., Taoka, K., Miura, E., Xoconostle-Cásares, B., Dendler, K., Jorgensen, R., Phinney, B., Lough, T.J., and Lucas, W.J. (2007) FLOWERING LOCUS T protein may act as the long-distance florigenic signal in curcubits. Plant Cell 19, 1488–1506.

Liscum, E. and Briggs, W.R. (1995) Mutations in the *nph1* locus of *Arabidopsis* disrupt the perception of phototropic stimuli. Plant Cell 7, 473–485.

Liscum, E. and Briggs, W.R. (1996) Mutations of *Arabidopsis* in potential transduction and response components of the phototropic signaling pathway. Plant Physiol. 112, 291–296.

Liscum, E. and Stowe-Ewans, E.L. (2000) Phototropism: A "simple" physiological response modulated by multiple interacting photosensory-response pathways. Photochem. Photobiol. 72, 273–282.

Locke, J.C., Kozma-Bognar, L., Gould, P.D., Feher, B., Kevei, E., Nagy, F., Turner, M.S., Hall, A., Millar, A.J. (2006) Experimental validation of a predicted feedback loop in the multi-oscillator clock of *Arabidopsis thaliana*. Mol. Syst. Biol. 2, 59.

Ma, L., Li, J., Qu, L., Hager, J., Chen, Z., Zhao, H. and Deng, X.W. (2001) Light control of *Arabidopsis* development entails coordinated regulation of genome expression and cellular pathways. Plant Cell 13, 2589–2607.

Malhotra, K., Kim, S.T., Batschauer, A., Dawut. L. and Sancar, A. (1995) Putative blue-light photoreceptors from *Arabidopsis thaliana* and *Sinapis alba* with a high degree of sequence homology to DNA photolyase contain the two photolyase cofactors but lack DNA repair activity. Biochemistry 34, 6892–6899.

Martinez-Garcia, J.F., Huq, E. and Quail, P.H. (2000) Direct targeting of light signals to a promoter element-bound transcription factor. Science 288, 859–863.

Màs, P., Kim, W.Y., Somers, D.E. and Kay, S.A. (2003) Targeted degradation of TOC1 by ZTL modulates circadian function in *Arabidopsis thaliana*. Nature 426, 567–570.

Mathews, S. (2006) Phytochrome-mediated development in land plants: red light sensing evolves to meet the challenges of changing light environments. Mol. Ecol. 15, 3483–3503

Mazzella, M.A., Magliano, T.M.A. and Casal, J.J. (1997) Dual effect of phytochrome A on hypocotyl growth under continuous red light. Plant Cell Environ. 20, 261–267.

McCormac, A.C., Whitelam, G.C., Boylan, M.T., Quail, P.H. and Smith, H. (1992) Contrasting responses of etiolated and light-adapted seedlings to red: far-red ratio: a comparison of wild type, mutant and transgenic plants has revealed differential functions of members of the phytochrome family. J. Plant Physiol. 140, 707–714.

McWatters, H.G., Bastow, R.M., Hall, A. and Millar, A.J. (2000) The ELF3 zeitnehmer regulates light signaling to the circadian clock. Nature 408, 716–720.

Michael, T.P., Salome, P.A., Yu, H.J., Spencer, T.R., Sharp, E.L., McPeek, M.A., Alonso, J.M., Ecker, J.R. and McClung, C.R. (2003) Enhanced fitness conferred by naturally occurring variation in the circadian clock. Science 302, 1049–1053.

Mizoguchi, T., Wheatley, K., Hanzawa, Y., Wright, L., Mizoguchi, M., Song, H.R., Carre, I.A. and Coupland, G. (2002) *LHY* and *CCA1* are partially redundant genes required to maintain circadian rhythms in *Arabidopsis*. Dev. Cell. 2, 629–641.

Mockler, T., Yang, H., Yu, X., Parikh, D., Cheng, Y.C., Dolan, S. and Lin, C. (2003) Regulation of photoperiodic flowering by *Arabidopsis* photoreceptors. Proc. Natl Acad. Sci. USA 100, 2140–2145.

Motchoulski, A. and Liscum, E. (1999) *Arabidopsis* NPH3: a NPH1 photoreceptor-interacting protein essential for phototropism. Science 286, 961–964.

Mullineaux, P. and Karpinski, S. (2002) Signal transduction in response to excess light: getting out of the chloroplast. Curr. Opin. Plant Biol. 5, 43–48.

Muramoto, T., Kohchi, T., Yokota, A., Hwang, I.H. and Goodman, H.M. (1999) The *Arabidopsis* photomorphogenic mutant *hy1* is deficient in phytochrome chromophore biosynthesis as a result of a mutation in a plastid heme oxygenase. Plant Cell 11, 335–347.

Nakamichi, N., Kita, M., Ito, S., Yamashino, T., Mizuno, T. (2005) PSEUDO-RESPONSE REGULATORS, PRR9, PRR7 and PRR5, together play essential roles close to the circadian clock of *Arabidopsis thaliana*. Plant Cell Physiol. 46, 686–698.

Nelson, D.C., Lasswell, J., Rogg, L.E., Cohen, M.A. and Bartel, B. (2000) *FKF1*, a clock-controlled gene that regulates the transition to flowering in *Arabidopsis*. Cell 101, 331–340.

Osterlund, M.T. and Deng, X.W. (1998) Multiple photoreceptors mediate the light-induced reduction of GUS-COP1 from *Arabidopsis* hypocotyl nuclei. Plant J. 16, 201–208.

Osterlund, M.T., Hardtke, C.S., Wei, N. and Deng, X.W. (2000) Targeted destabilization of HY5 during light-regulated development of *Arabidopsis*. Nature 405, 462–466.

Park, D.H., Somers, D.E., Kim, Y.S., Choy, Y.H., Lim, H.K., Soh, M.S., Kim, H.J., Kay, S.A. and Nam, H.G. (1999) Control of circadian rhythms and photoperiodic flowering by the *Arabidopsis GIGANTEA* gene. Science 285, 1579–1582.

Parker, M.W., Hendricks, S.B., Borthwick, H.A. and Went, F.W. (1949) Spectral sensitivities for stem and leaf growth of etiolated pea seedlings and their similarity to action spectra for photoperiodism. Am. J. Bot. 36, 194–204.

Parks, B.M. and Spalding, E.P. (1999) Sequential and coordinated action of phytochromes A and B during *Arabidopsis* stem growth revealed by kinetic analysis. Proc. Natl Acad. Sci. USA 96, 14142–14146.

Parks, B.M, and Quail, P.H. (1991) Phytochrome-deficient *hy1* and *hy2* long hypocotyl mutants of *Arabidopsis* are defective in phytochrome chromophore biosynthesis. Plant Cell 3, 1177–1186.

Parks, B.M., Cho, M.H. and Spalding, E.P. (1998) Two genetically separable phases of growth inhibition induced by blue light in *Arabidopsis* seedlings. Plant Physiol. 118, 609–615.

Parks, B.M., Quail, P.H. and Hangarter, R.P. (1996) Phytochrome A regulates red-light induction of phototropic enhancement in *Arabidopsis*. Plant Physiol. 110, 155–162.

Perrotta, G., Ninu, L., Flamma, F., Weller, J.L., Kendrick, R.E., Nebuloso, E. and Giuliano, G. (2000) Tomato contains homologues of *Arabidopsis* cryptochromes 1 and 2. Plant Mol. Biol. 42, 765–773.

Platten, J.D., Foo, E., Elliott, R.C., Hecht, V., Reid, J.B. and Weller, J.L. (2005b) Cryptochrome 1 contributes to blue-light sensing in pea. Plant Physiol. 139, 1472–1482.

Platten, J.D., Foo, E., Foucher, F., Hecht, V., Reid, J.B. and Weller, J.L. (2005a) The cryptochrome gene family in pea includes two differentially expressed *CRY2* genes. Plant Mol. Biol. 59, 683–696.

Poppe, C., Sweere, U., Drumm-Herrel, H. and Schäfer E. (1998) The blue light receptor cryptochrome 1 can act independently of phytochrome A and B in *Arabidopsis thaliana*. Plant J. 16, 465–471.

Quail, P.H. (1997) An emerging molecular map of the phytochromes. Plant Cell Environ. 20, 657–665.

Quail, P.H. (2006) Phytochrome signal transduction network. In: E. Schäfer and F. Nagy (Eds.) *Photomorphogenesis in plants and bacteria*, 3rd Ed., Springer, Dordrecht, The Netherlands, pp. 335–356.

Quecini, V. and Liscum, E. (2006) Signal transduction in blue light-mediated responses. In: E. Schäfer and F. Nagy (Eds.), *Photomorphogenesis in plants and bacteria*, 3rd ed. Springer, Dordrecht, pp. 305–327.

Robson, P.R.H., McCormac, A.C., Irvine, A.S. and Smith H. (1996) Genetic engineering of harvest index in tobacco through overexpression of a phytochrome gene. Nature Biotechnol. 14,995–998.

Rockwell, N.C., Su Y.S., Lagarias J.C. (2006) Phytochrome structure and signaling mechanisms. Annu. Rev. Plant. Biol. 57, 837–858.

Roden, L.C., Song, H.R., Jackson, S., Morris, K. and Carre, I.A. (2002) Floral responses to photoperiod are correlated with the timing of rhythmic expression relative to dawn and dusk in *Arabidopsis*. Proc. Natl Acad. Sci. USA 99, 13313–13318.

Ryan, K.G., Swinny, E.E., Winefield, C. and Markham, K.R. (2001) Flavonoids and UV photoprotection in *Arabidopsis* mutants. Z. Naturforsch. 56, 745–754.

Sage, L.C. (1992) *Pigment of the imagination: a history of phytochrome research.* Academic Press, New York.

Sakai, T., Wada, T., Ishiguro, S. and Okada, K. (2000) RPT2: A signal transducer of the phototropic response in *Arabidopsis*. Plant Cell 12, 225–236.

Sakai, T., Kagawa, T., Kasahara, M., Swartz, T.E., Christie, J.M., Briggs, W.R., Wada, M. and Okada, K. (2001) *Arabidopsis* nph1 and npl1: Blue light receptors that mediate both phototropism and chloroplast relocation Proc. Natl Acad. Sci. USA 98, 6969–6974.

Sakamoto, K. and Briggs, W.R. (2002) Cellular and subcellular localization of phototropin 1. Plant Cell. 14, 1723–1735.

Salome, P.A. and McClung, C.R. (2004) The *Arabidopsis thaliana* clock. J. Biol. Rhythms. 19, 425–435.

Salomon, M., Knieb, E., von Zeppelin, T. and Rüdiger, W. (2003) Mapping of low- and high-fluence autophosphorylation sites in phototropin 1. Biochemistry 42, 4217–4225.

Samach, A., Onouchi, H., Gold, S.E., Ditta, G.S., Schwarz-Sommer, Z., Yanofsky, M.F. and Coupland, G. (2000) Distinct roles of CONSTANS target genes in reproductive development of *Arabidopsis*. Science 288, 1613–1616.

Schneider-Poetsch, H.A.W., Kolukisaoglu, Ü., Clapham, D.H., Hughes, J. and Lamparter, T. (1998) Non-angiosperm phytochromes and the evolution of vascular plants. Physiol. Plant. 102, 612–622.

Schultz, T.F., Kiyosue, T., Yanovsky, M., Wada, M. and Kay, S.A. (2001) A role for LKP2 in the circadian clock of *Arabidopsis*. Plant Cell 13, 2659–2670.

Schwechheimer, C., Serino, G., Callis, J., Crosby, W.L., Lyapina, S., Deshaies, R.J., Gray, W.M., Estelle, M. and Deng, X.W. (2001) Interactions of the COP9 signalosome with the E3 ubiquitin ligase SCF/TIR1 in mediating auxin response. Science 292, 1379–1382.

Shalitin, D., Yu, X., Maymon, M., Mockler, T. and Lin, C. (2003) Blue light-dependent in vivo and in vitro phosphorylation of *Arabidopsis* cryptochrome 1. Plant Cell. 15, 2421–2429.

Sharrock, R.A. and Clack, T. (2004) Heterodimerization of type II phytochromes in *Arabidopsis*. Proc. Natl. Acad. Sci. USA 101, 11500–11505.

Sharrock, R.A. and Mathews, S. (2006) Phytochrome genes in higher plants. In: E. Schäfer and F. Nagy (Eds.), *Photomorphogenesis in plants and bacteria*, 3rd ed. Springer, Dordrecht, pp. 99–130.

Shinomura, T., Nagatani, A., Hanzawa, H., Kubota, M., Watanabe, M. and Furuya, M. (1996) Action spectra for phytochrome A- and B-specific photoinduction of seed germination in *Arabidopsis thaliana*. Proc. Natl Acad. Sci. USA 93, 8129–8133.

Shinomura, T., Uchida, K. and Furuya, M. (2000) Elementary processes of photoperception by phytochrome A for high-irradiance response of hypocotyl elongation in *Arabidopsis*. Plant Physiol.*122*, 147–156.

Shirley, B.W. (1996) Flavonoid biosynthesis—new functions for an old pathway. Trends Plant Sci. 1, 377–382.

Smith, Hm (1995) Physiological and ecological function within the phytochrome family. Annu. Rev. Plant Physiol. Plant Mol. Biol. 46, 289–315.

Smith, H. (2000) Phytochromes and light signal perception by plants – an emerging synthesis. Nature 407, 585–591.

Somers, D.E., Devlin, P.F. and Kay, S.A. (1998) Phytochromes and cryptochromes in the entrainment of the *Arabidopsis* circadian clock. Science 282,1488–1490.

Somers, D.E., Schultz, T.F., Milnamow, M. and Kay, S.A. (2000) *ZEITLUPE* encodes a novel clock-associated PAS protein from *Arabidopsis*. Cell 101, 319–329.

Strickland, E., Rubio, V. and Deng, X.W. (2006) The function of the COP/DET/FUS proteins in controlling photomorphogenesis: a role for regulated proteolysis. In: E. Schäfer and F. Nagy (Eds.), *Photomorphogenesis in plants and bacteria*, 3rd ed. Springer, Dordrecht, pp. 357–378.

Suarez-Lopez, P., Wheatley, K., Robson, F., Onouchi, H., Valverde, F. and Coupland, G. (2001) CONSTANS mediates between the circadian clock and the control of flowering in *Arabidopsis*. Nature 410, 1116–1120.

Takano, M., Inagaki, N., Xie, X., Yuzurihara, N., Hihara, F., Ishizuka, T., Yano, M., Nishimura, M., Miyao, A., Hirochika, H. and Shinomura, T. (2005) Distinct and cooperative functions of phytochromes A, B, and C in the control of deetiolation and flowering in rice. Plant Cell. 17, 3311–3325.

Talbott, L.D., Hammad, J.W., Harn, L.C., Nguyen, V.H., Patel, J. and Zeiger, E. (2006) Reversal by green light of blue light-stimulated stomatal opening in intact, attached leaves of *Arabidopsis* operates only in the potassium-dependent, morning phase of movement. Plant Cell Physiol. 47, 332–339.

Tepperman, J.M., Hudson, M.E., Khanna, R., Zhu, T., Chang, S.H., Wang, X. and Quail, P.H. (2004) Expression profiling of phyB mutant demonstrates substantial contribution of other phytochromes to red-light-regulated gene expression during seedling de-etiolation. Plant J. 38, 725–739.

Tepperman, J.M., Zhu, T., Chang, H.S., Wang, X. and Quail, P.H. (2001) Multiple transcription-factor genes are early targets of phytochrome A signaling. Proc. Natl Acad. Sci. USA 98, 9437–9342.

Terashima, I. and Hikosaka, K. (1995) Comparative ecophysiology of leaf and canopy photosynthesis. Plant Cell Environ. 18, 1111–1128.

Thomas, B. and Vince-Prue, D. (1997) *Photoperiodism in plants* (2nd ed.). Academic Press, London.

Toth, R., Kevei, E., Hall, A., Millar A.J., Nagy, F. and Kozma-Bognar, L. (2001) Circadian cloc-regulated expression of phytochrome and cryptochrome genes in *Arabidopsis*. Plant Physiol. 127, 1607–1616.

Ulm R. (2006) UV-B perception and signaling in higher plants. In: E. Schäfer and F. Nagy (Eds.), *Photomorphogenesis in plants and bacteria*, 3rd ed. Springer, Dordrecht, pp. 279–304.

Valverde, F., Mouradov, A., Soppe, W., Ravenscroft, D., Samach, A. and Coupland, G. (2004) Photoreceptor regulation of CONSTANS protein in photoperiodic flowering. Science 303, 1003–1006.

Vogelmann, T.C., Nishio, J.N. and Smith, W.K. (1996) Leaves and light capture-light propagation and gradients of carbon fixation within leaves. Trends Plant Sci. 1, 65–70.

Wang, H.Y., Ma, L.G., Li, J.M., Zhao, H.Y. and Deng, X.W. (2001) Direct interaction of *Arabidopsis* cryptochromes with COP1 in light control development. Science 294, 154–158.

Wang, H., Ma, L., Habashi, J., Li, J., Zhao, H. and Deng, X.W. (2002) Analysis of far-red light-regulated genome expression profiles of phytochrome A pathway mutants in *Arabidopsis*. Plant J. 32, 723–733.

Ward, J.M., Cufr, C.A., Denzel, M.A., Neff, M.M. (2005) The Dof transcription factor OBP3 modulates phytochrome and cryptochrome signaling in *Arabidopsis*. Plant Cell 17, 475–485.

Weller, J.L., Beauchamp, N., Kerckhoffs, L.H.J., Platten, J.D. and Reid, J.B. (2001) Interaction of phytochromes A and B in the control of de-etiolation and flowering in pea. Plant J. 26, 283–294.

Weller, J.L., Murfet, I.C. and Reid, J.B. (1997a) Pea mutants with reduced sensitivity to far-red light define an important role for phytochrome a in day-length detection. Plant Physiol. 114, 1225–1236.

Weller, J.L., Perrotta, G., Schreuder, M.E.L., van Tuinen, A., Koornneef, M., Giuliano, G. and Kendrick, R.E. (2001b) Genetic dissection of blue-light sensing in tomato using mutants deficient in cryptochrome 1 and phytochromes A, B1 and B2. Plant J. 25, 427–440.

Weller, J.L., Terry, M.J., Reid, J.B. and Kendrick, R.E. (1997c) The phytochrome-deficient *pcd2* mutant of pea is unable to convert biliverdin IX a to 3(*Z*)-phytochromobilin. Plant J. 11, 1177–1186.

Went, F.W. (1941) Effects of light on stem and leaf growth. Am. J. Bot. 28, 83–95.

Wigge, P.A., Kim, M.C., Jaeger, K.E., Busch, W., Schmid, M., Lohmann, J.U. and Weigel, D. (2005) Integration of spatial and temporal information during floral induction in *Arabidopsis*. Science 309, 1056–1059.

Withrow, R.B., Klein, W.H. and Elstad, V. (1957) Action spectra of photomorphogenic induction and its inactivation. Plant Physiol. 32, 453–462.

Wu, S.H., McDowell, M.T. and Lagarias, J.C. (1997) Phycocyanobilin is the natural precursor of the phytochrome chromophore in the green alga *Mesotaenium caldariorum*. J. Biol. Chem. 272, 25700–25705.

Yang, H.Q., Wu, Y.J., Tang, R.H., Liu, D.M., Liu, Y. and Cashmore, A.R. (2000) The C-termini of *Arabidopsis* cryptochromes mediate a constitutive light response. Cell. 103, 815–827.

Yano, M., Kojima, S., Takahashi, Y., Lin, H.X. and Sasaki, T. (2001) Genetic control of flowering time in rice, a short-day plant. Plant Physiol. 127, 1425–1429.

Yanovsky, M.J. and Kay, S.A. (2002) Molecular basis of seasonal time measurement in *Arabidopsis*. Nature 419, 308–312.

Yanovsky, M.J., Casal, J.J. and Whitelam, G.C. (1995) Phytochrome A, phytochrome B and HY4 are involved in hypocotyl growth responses to natural radiation in *Arabidopsis* – weak de-etiolation of the *phyA* mutant under dense canopies. Plant Cell Environ. 18, 788–794.

Yanovsky, M.J., Mazzella, M.A. and Casal, J.J. (2000a) A quadruple photoreceptor mutant still keeps track of time. Curr. Biol. 10, 1013–1015.

Yanovsky, M.J., Izaguirre, M., Wagmaister, J.A., Gatz, C., Jackson, S.D., Thomas, B. and Casal, J.J. (2000b) Phytochrome A resets the circadian clock and delays tuber formation under long days in potato. Plant J. 23, 223–232.

Yeh, K.C. and Lagarias, J.C. (1998) Eukaryotic phytochromes- light-regulated serine/threonine protein kinases with histidine kinase ancestry. Proc. Natl Acad. Sci. USA 95, 13976–13981.

Zeilinger, M.N., Farré, E.M., Taylor, S.R., Kay, S.A. and Doyle, F.J. 3rd. (2006) A novel computational model of the circadian clock in *Arabidopsis* that incorporates PRR7 and PRR9. Mol. Syst. Biol. 2, 1–13.

Zhu, Y.X., Tepperman, J.M., Fairchild, C.D. and Quail, P.H. (2000) Phytochrome B binds with greater apparent affinity than phytochrome A to the basic helix-loop-helix factor PIF3 in a reaction requiring the PAS domain of PIF3. Proc. Natl Acad. Sci. USA 97, 13419–13424.

17
The Light-Dependent Magnetic Compass

Rachel Muheim

Abstract: Animals can detect different parameters of the geomagnetic field by two principal independent magnetoreception mechanisms: (1) a light-dependent process detecting the axial course and the inclination angle of the geomagnetic field lines, providing the animals with magnetic compass information (inclination compass), and (2) a magnetite-mediated process, providing magnetic map information (map sense). In vertebrates like birds and newts, light-dependent magnetic compass orientation depends on both wavelength and intensity of light, and experimental evidence suggests that magnetic compass information is perceived by magneto-sensitive photoreceptors, possibly containing cryptochromes, in the retina or the pineal.

17.1. The Involvement of Light in the Magnetic Compass Orientation in Animals

The use of directional information from the earth's magnetic field for orientation has been demonstrated in a large variety of animals across different taxa (for reviews see Wiltschko and Wiltschko 1995, 2002, 2005). Light has been shown to be involved in the primary magnetoreception process in a growing number of species, including fruitfly (*Drosophila melanogaster*) (Phillips and Sayeed 1993, Dommer, Gazzolo, Painter and Phillips, in press), mealworm beetle (*Tenebrio* sp.) (Vacha and Soukopova 2004), bullfrog (*Rana catesbeiana*) (Freake and Phillips 2005), Eastern red-spotted newt (*Notophthalmus viridescens*) (e.g., Phillips 1986, Phillips and Borland 1992a), homing pigeon (*Columbia livia*) (Wiltschko and Wiltschko 1981, 1998), and several species of migratory bird (for reviews see Wiltschko and Wiltschko 2001, 2005, Muheim et al. 2002). In addition, there is strong evidence from behavioral experiments for a light-dependent magnetic compass in C57BL/6J mice (Muheim et al. 2006). Magnetic compass orientation independent of light has only been shown in a few exceptions, like the subterranean mole-rats (Marhold et al. 1997) and sea turtles (Lohmann and Lohmann 1993), possibly a result of an adaptation to the nonterrestrial lifestyle of these organisms. Thus, in general, animals need access to a specific range of wavelengths and intensities of light to perceive magnetic compass information.

Both behavioral and physiological studies suggest the presence of two principal independent magnetoreception mechanisms that detect different parameters of the geomagnetic field (for reviews see Wiltschko and Wiltschko 1995, 2002, Lohmann and Johnson 2000): (1) a light-dependent process detecting the axial course and the inclination angle of the geomagnetic field lines, providing the animals with magnetic compass information (inclination compass), and (2) a magnetite-mediated process, providing magnetic map information (map sense). This chapter summarizes the behavioral and physiological evidence for the involvement of light in the light-dependent magnetic compass and the proposed underlying biophysical processes. Since most research on magnetic compass orientation has been carried out with birds and newts, this chapter will mainly focus on these two groups of organism.

17.1.1. The Magnetic Inclination Compass

The light-dependent magnetic compass described in migratory birds and Eastern red-spotted newts is not sensitive to the polarity of the magnetic field, but instead uses the inclination of the magnetic field lines, i.e., is a so-called inclination compass (Wiltschko 1968, Wiltschko and Wiltschko 1972, Phillips 1986). The animals use information from the alignment of the magnetic field lines along the magnetic meridian to determine the magnetic north–south axis and the inclination of the geomagnetic field lines, presumably relative to gravity, to determine the correct side of this axis. The side of the axis where the magnetic field lines meet with the horizon always leads polewards, in both the northern and southern hemispheres, and the side where the field lines and the horizon diverge always leads towards the magnetic equator (Fig. 17.1) (reviewed by Wiltschko and Wiltschko 1995, 2005). Thus, migratory programs of long-distance migrants, like that of birds, are most likely coded similarly in both hemispheres, since species from both hemispheres migrate equatorwards in autumn after the breeding season when day length decreases, and polewards in spring when day length increases. An equator crossing, consequently, requires the animals to change their migratory program from "fly equatorwards" to "fly polewards." Experimental evidence suggests that exposure to the horizontal magnetic field at the magnetic equator (providing ambiguous inclination compass information because inclination cannot be used to determine the correct axis of the north–south meridian) may trigger this change in migratory program (Wiltschko and Wiltschko 1992).

An experimental tool to test the type of compass (inclination compass vs. polarity compass) is to artificially invert the vertical component of the magnetic field surrounding the testing apparatus with magnetic coils. Inverting the vertical component flips the magnetic field vector, i.e., reverses inclination, but leaves polarity unchanged. Consequently, animals responding to such a treatment use the inclination angle of the magnetic field to determine the correct side of the axis, while animals not responding to an inversion, but only to a shift in the horizontal component of the magnetic field, use the polarity of the magnetic field lines for orientation.
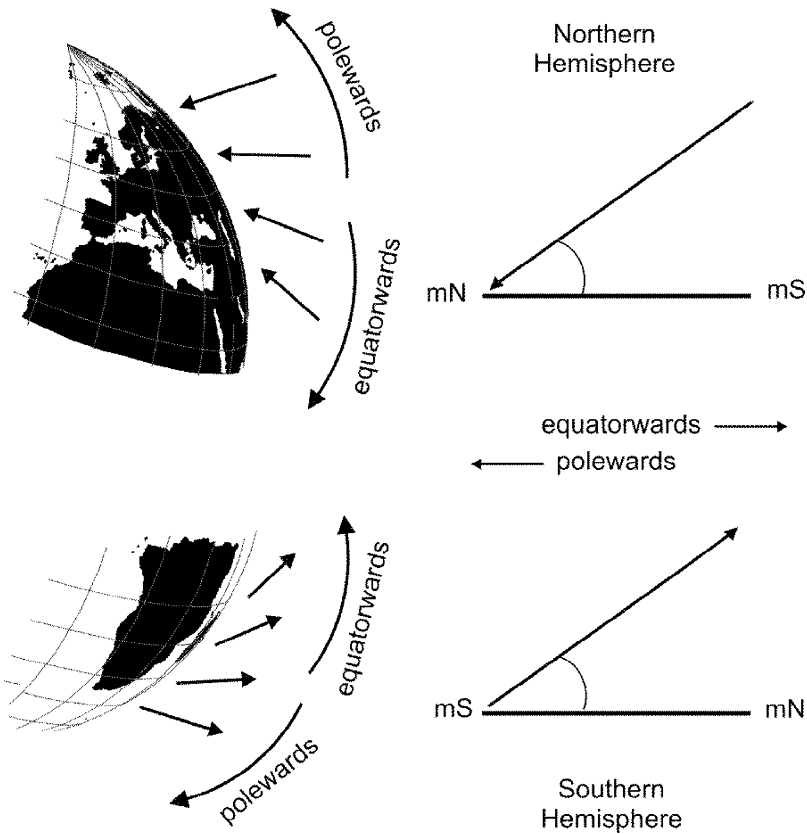
FIGURE 17.1. The magnetic inclination compass provides animals with information on the axial alignment of the magnetic field (direction along the magnetic north–south meridian). The inclination angle is used to distinguish the two ends of the axis: the direction towards the magnetic pole that lies closer coincides with the intersection of the magnetic field lines with the horizon; the magnetic equator lies towards the direction where the magnetic field lines and the horizon diverge. An inclination compass does not perceive the polarity of the magnetic field vector as human technical compasses do.

17.2. Light-Dependent Effects on Orientation at Different Wavelengths and Irradiances

17.2.1. Evidence for an Antagonistic Spectral Mechanism Mediating Magnetic Compass Orientation in Newts

In North American Eastern red-spotted newts two distinctive orientation behaviors can be studied in the lab (Phillips 1986): (1) shoreward orientation of newts trained to learn the magnetic alignment of an artificial shore, mediated by a light-dependent magnetic inclination compass, and (2) homing navigation to the site of capture (home pond), mediated by a magnetite-based map sense. John

Phillips and coworkers demonstrated that the light-dependent magnetic compass response of newts tested under long-wavelength light (>500 nm) is rotated by 90° from the trained shoreward directions shown under short-wavelength light (400–450 nm) (Phillips and Borland 1992a,c). Newts tested under the intermediate wavelength of 475 nm are disoriented. Since it is highly unlikely that this abrupt shift from oriented behavior to disorientation is caused by a decrease in sensitivity of one spectral mechanism alone, the involvement of two antagonistic spectral mechanisms was suggested (Phillips and Borland 1992a, Deutschlander et al. 1999b): a high-sensitive, short-wavelength mechanism mediating oriented behavior in the trained direction of shore and a low-irradiance, long-wavelength mechanism shifting orientation by 90° relative to shore; equal excitation of both mechanisms leads to disorientation. Complete elimination of compass orientation in newts tested under near-infrared light (>715 nm) adds additional support for the involvement of two discrete spectral mechanisms (Phillips and Borland 1992b).

17.2.2. Magnetic Compass Orientation of Birds Depends on Wavelength and Irradiance

Magnetic compass orientation in birds depends on the wavelength and intensity of light the birds are exposed to, similar to newts. Young, inexperienced homing pigeons were disoriented after displacement in complete darkness or under 660-nm red light, but oriented towards the home direction after transport to the release site under 565-nm green or full spectrum light (Wiltschko and Wiltschko 1981, 1998). Orientation experiments with passerine migrants in funnels illuminated with monochromatic lights give further support for the involvement of a light-sensitive magnetoreception process activated at specific wavelengths of light. European robins (*Erithacus rubecula*), Australian silvereyes (*Zosterops l. lateralis*), and garden warblers (*Sylvia borin*) tested under low-irradiance (0.57–21×10^{15} quanta/s/m^2) monochromatic lights of peak wavelengths between 424 nm (blue) and 565 nm (green) showed well-oriented behavior into the seasonally expected migratory directions, comparable to the responses shown under full-spectrum light (Rappl et al. 2000, Wiltschko and Wiltschko 2001, Muheim et al. 2002). However, when tested under 590-nm (yellow) or 630-nm (red) light the birds were disoriented (see below for exceptions) (Wiltschko et al. 1993, Wiltschko and Wiltschko 1999, Rappl et al. 2000). These results indicate that magnetoreception becomes critical under light of peak wavelengths longer than 565 nm. In a series of experiments with European robins tested under narrow-band (9- to 11-nm half bandwidth) green (560.5 nm) and green-yellow (567.5 nm) lights, Muheim et al. (2002) showed that the transition from oriented behavior under 560.5 nm to disorientation under 567.5 nm is very abrupt. However, they also showed that, under low-irradiance red light (617.0 nm), birds showed oriented behavior into an approximately 90° shifted direction (Muheim et al. 2002), comparable to the shift observed in newts under long-wavelength lights (see above). Experiments under similar light conditions confirmed this result and

added that this 90° shift can be observed during both spring and fall migration, though in the same geographic direction (W. Wiltschko and R. Wiltschko, unpublished results mentioned in Wiltschko et al. 2004b). Furthermore, birds preexposed to 635-nm red lights at higher irradiances and broader half bandwidth (∼30 nm) were oriented towards the expected migratory direction when subsequently tested for orientation under the same red spectrum (Wiltschko et al. 2004b). This implies that magnetoreception is not confined to wavelengths of less than 565 nm, but suggests the involvement of at least two magnetoreception mechanisms active at different wavelengths (see newts for comparison) (Muheim et al. 2002, Wiltschko et al. 2004a,b).

While there is consensus over the involvement of at least two magnetoreception mechanisms active at different wavelengths responsible for the observed effects, there is a vivid debate over the types and interaction of these receptors. The parallels between the findings in birds and newts, as well as additional reports of 90° shifts in orientation under longer wavelengths in fruitflies (Phillips and Sayeed 1993) and bullfrogs (Freake and Phillips 2005), suggest the presence of two antagonistically interacting spectral mechanisms, with a high-sensitive short-wavelength mechanism leading to oriented behavior and a low-sensitive long-wavelength mechanism leading to shifted orientation; the disorientation observed under the intermediate wavelengths can be explained by an equal excitation of both mechanisms (see Phillips and Borland 1992a, Deutschlander et al. 1999b, Ritz et al. 2002). Overexcitation of both mechanisms would make the pattern unrecognizable, and thus the birds would not be able to use the inclination compass any longer and would need to resort to a magnetite-based receptor. This theory is opposed by the view that the 90° shifts under red are not true shifts, but instead "fixed" orientations, and that the magnetoreception systems in birds and newts are not comparable (Wiltschko et al. 2004b). Instead, the responses observed under high light irradiances are suggested to be produced by an unspecified, novel type of light-dependent magnetoreceptor, not based on a radical pair mechanism (see below) or magnetite-based process, since the "fixed" orientation responses under such conditions differ between wavelengths and do not seem to be mediated by the inclination compass any longer (Wiltschko et al. 2005).

17.3. Localization of the Light-Dependent Magnetoreceptor

Light-dependent magnetoreception of the shoreward orientation of Eastern red-spotted newts takes place in photosensitive, extraocular photoreceptors in the pineal complex (Deutschlander et al. 1999a). Newts trained to learn the shoreward axis of a training tank with the top of their head, but not their eyes, covered with a red-light filter demonstrate the same 90° shifted response shown by newts tested completely illuminated by red light (Deutschlander et al. 1999a). In anuran amphibians and lizards, single photoreceptors with two antagonistic

photoreception mechanisms, like those proposed to underlie the light-dependent magnetic compass in newts, have been found in the pineal complex (Eldred and Nolte 1978, Solessio and Engbretson 1993).

In birds, extracellular recordings provided first evidence for the involvement of the visual center in light-dependent magnetoreception. Cells in the nucleus of the basal optic root (nBOR) and in the optic tectum showed magnetic responsiveness to changes in the direction of a magnetic field and to slow inversions of the vertical component of the magnetic field, with peak responses under wavelengths of 503 and 582 nm (Semm et al. 1984, Semm and Demaine 1986). Thus, there is strong evidence that light-dependent magnetoreception takes place at locations innervated by the optic nerve, with the eyes as likely candidates. Unlike in newts, an involvement of the pineal in magnetoreception is very unlikely, despite responsive cells in the avian pineal to magnetic field inversions (Semm 1983, Demaine and Semm 1985). Homing pigeons successfully homed after pinealectomy, while pinealectomized pied flycatchers (*Ficedula hypoleuca*) showed seasonally appropriate orientation as long as they received daily injections of melatonin, suggesting no involvement of the pineal in magnetoreception (Maffei et al. 1983, Schneider et al. 1994).

Lateralization experiments testing the magnetic orientation of birds with one eye covered with light-proof caps suggest that mainly the right eye is involved in magnetoreception: birds were well oriented and reacted to an inversion of the magnetic field when tested with the right eye open, but were disoriented when tested with the left eye open (Wiltschko et al. 2002, 2003).

17.4. Mechanisms of Light-Dependent Magnetoreception

The behavioral experiments imply that the information provided by the magnetoreceptor of the light-dependent inclination compass has to fulfill the following requirements: (1) the nature of the compass information has to be axial rather than polar, i.e., sensing the alignment of the magnetic field lines in space, but not the polarity of flux, and (2) the functional range of the magnetic compass has to be adaptable to different magnetic field intensities. This was shown in European robins that were disoriented when tested in artificial magnetic fields with field intensities weaker (16 and 34 μT) or stronger (60–105 μT) than the earth's magnetic field (Wiltschko 1968, 1978, Wiltschko et al. 2006). When the same birds, however, were preexposed to such unnatural magnetic fields for a minimum of 3 days, they were able to orient in the subsequent experiments. Birds thus are able to learn or adapt to changing properties of the ambient magnetic field, i.e., they can learn to orient under novel magnetic conditions, or the functional range of their magnetoreceptor is flexible and allows adjustment to previously not experienced magnetic conditions, allowing orientation as long as the magnetic field contains directional information.

17.4.1. Chemical Magnetoreception Based on a Radical Pair Mechanism

Different biophysical magnetoreception models have been proposed to explain the light dependence of the magnetic compass in animals. The currently most discussed model is based on the principle that an external magnetic field can influence photon-induced processes, which involve bimolecular reactions (Schulten 1982, Schulten and Windemuth 1986, Ritz et al. 2000). In this process, radical pairs are formed by photon excitation through light absorption similar to the photosynthetic reactions (it has to be noted, however, that such a process can also be chemically induced) (for reviews see Grissom 1995, Brocklehurst 2002, Woodward et al. 2002). The interconversion between the excited singlet and triplet products is modified by an external magnetic field, resulting in the formation of different yields of singlet and triplet products. Ritz et al. (2000) refined the model and proposed photoreceptor molecules like cryptochromes (see below) as likely organic reactants. Magneto-sensitive photoreceptors arranged in an ordered array, in, e.g., the retina or pineal, would respond differently, depending on their alignment relative to the magnetic field, and allow the animals to "see" the magnetic field lines (Fig. 17.2). In such a light-sensitive magnetoreception system the animals would perceive the magnetic field as a three-dimensional pattern of light irradiance or color variation in their visual field (Fig. 17.2).

   This radical-pair model meets the necessary criteria for being a likely candidate for the light-dependent magnetic compass receptor (Ritz et al. 2000, 2002): (1) the visual image perceived by the animal has axial properties (Fig. 17.2A), and thus does not allow determination of the polarity of the field lines; (2) the singlet-triplet yield and, consequently, the visual image perceived by the animal depends on the intensity of the magnetic field, and thus exposure to magnetic field intensities never experienced before can lead to disorientation, followed by a slow adaptation to the "new" pattern (see Wiltschko 1968, 1978, Wiltschko et al. 2006). Adaptation has also been suggested as explanation for the ability of birds to orient under monochromatic red light after preexposure to the same light for one hour before the start of the orientation experiments (Wiltschko et al. 2004b).

17.4.2. Involvement of Cryptochromes as Magneto-Sensitive Photoreceptors?

A photoreceptor molecule involved in the primary magnetoreception process mediated by a light-dependent radical pair mechanism as described above needs to meet a number of criteria, like the ability to form radical pairs that persist long enough so that the radical-pair yields can be modified by an earth-strength magnetic field and localization in a spatially fixed relationship relative to each other (Ritz et al. 2000, 2002, Mouritsen and Ritz 2005). The classical photopigments, like the opsins, are not known to form radical pairs, and thus are unlikely
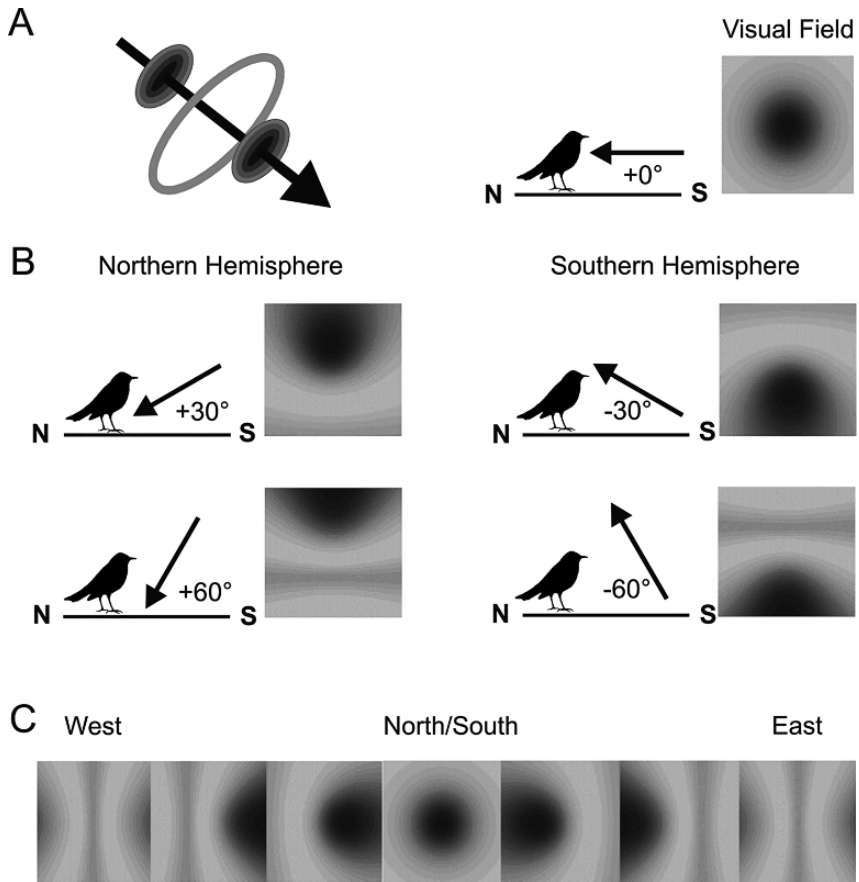
FIGURE 17.2. Illustration of light-dependent magnetic compass perception through magneto-sensitive photoreceptors (freely interpreted after Ritz et al. 2000) (A, left) Three-dimensional pattern of the magnetic field vector consisting of a dark area on each side of the magnetic field axis and a ring in the center. (A, right) Visual field pattern perceived by an animal (bird) looking parallel along the magnetic field vector (arrow). (B) Visual patterns at different latitudes (i.e., different magnetic field inclinations) in the northern and southern hemispheres. (C) Visual pattern perceived by animals facing different directions relative to the alignment of the magnetic field.

to be involved in magnetoreception. There are strong indications, however, that cryptochromes are candidates for the magnetoreception molecule (Ritz et al. 2000, 2002, Mouritsen and Ritz 2005). Cryptochromes are blue-green light photoreceptors, recently described to be involved in the animal circadian clock (e.g., Cashmore et al. 1999). They can form radical pairs upon excitation by light, and their ancestral form, the photolyases, can form radical pair intermediates that persist long enough for magnetic field effects to occur (Weber et al. 2002, Giovani et al. 2003).

Cryptochromes have been found in a large variety of organisms, including bacteria, plants, and animals, both invertebrates and vertebrates, including humans (for review see Cashmore et al. 1999, Sancar 2000, Partch and Sancar 2005). In species known to use a magnetic compass, cryptochromes have been reported for *Drosophila melanogaster* (Emery et al. 1998), bullfrogs (Eun and Kang 2003), laboratory mice (Van der Horst et al. 1999), and mole-rats (Avivi et al. 2004) and have also been found to be expressed in retinas of two migratory bird species, European robins and garden warblers (Möller et al. 2004, Mouritsen et al. 2004). In the garden warbler, cryptochrome expression in the displaced ganglion cells of the inner nuclear layer of the retina was found to colocalize with neuronal-activity markers during the night, when the birds expressed migratory restlessness and performed magnetic orientation (Mouritsen et al. 2004). In contrast, much lower or no cryptochrome expression was recorded during the day and in nonmigratory zebra finches (*Taeniopygia guttatta*), which further suggests the involvement of cryptochromes in magnetoreception (Mouritsen et al. 2004). However, more research is needed to unambiguously separate observations of cryptochrome expression as a result of circadian rhythmicity and magnetoreception (see below).

17.4.3. RF Fields as Diagnostic Tool for Testing the Radical Pair Mechanism

The use of low-intensity oscillating radiofrequency magnetic fields (RF fields) in the lower MHz range (0.1–100 MHz) has been proven a valuable tool to test whether a radical pair mechanism is involved in the primary magnetoreception process of an orientation response (Ritz et al. 2002; Henbest et al. 2004). RF fields of distinct frequencies, depending on the magnetoreceptor molecule involved, interfere with the interconversion between the singlet and triplet excited states, and consequently mask or alter the magnetic field effects produced by the earth's magnetic field. Such RF disturbances can lead to either disorientation or change in orientation, depending on the amount and type of change and how the animals integrate the information into a migratory direction. Magnetite-based magnetoreceptors, in contrast, are not affected by RF fields, since the rotation of magnetite particles as proposed in animal magnetoreceptors is too slow and the ferromagnetic resonance frequency is expected to be in the GHz rather than MHz range (Kirschvink 1996, Steiner and Ulbricht 1989). This makes the application of RF fields a unique diagnostic tool to study the involvement of a radical pair mechanism in magnetoreception.

Recently, this technique has been tested in migratory birds and mole-rats. European robins exposed to RF fields aligned nonparallel to the geomagnetic field vector became disoriented when tested under either a broadband RF field or distinct single frequencies of 1.375 or 7 MHz (Ritz et al. 2004, Thalau et al. 2005). The orientation of mole-rats, on the other hand, which is supposed to be mediated by a non–light-dependent magnetoreceptor, was not impaired by a RF field, supporting previous indications that their magnetic compass is magnetite based (Thalau et al. 2006).

17.5. Outlook

During the past few years, the involvement of biophysicists and the introduction of new techniques have led to significant advances in our understanding of the biophysical and molecular mechanisms of light-dependent magnetoreception. The use of inducible transcription factors to study neuronal activity during magnetoreception (Němec et al. 2005), the search for cryptochrome expression at potential sites of magnetoreception (Möller et al. 2004; Mouritsen et al. 2004), and the study of orientation behavior under RF fields all have provided valuable, but nevertheless indirect, evidence for the location, type, and biophysical and molecular mechanisms of the magnetoreceptor. With the development of reliable magnetic compass assays in two model organisms, *Drosophila melanogaster* (Dommer, Gazzolo, Painter and Phillips, in press) and laboratory mice (Muheim et al. 2006), access to cryptochrome knockout animals has opened up another new and promising avenue in magnetoreception research allowing direct tests of the involvement of cryptochromes or other molecules involved in the primary magnetoreception process.

Acknowledgments

References

Avivi, A., Oster, H., Joel, A., Beiles, A., Albrecht, U. and Nevo, E. (2004) Circadian genes in a blind subterranean mammal III: molecular cloning and circadian regulation of cryptochrome genes in the blind subterranean mole rat, *Spalax ehrenbergi*, superspecies. J. Biol. Rhythms, 19, 22–34.

Brocklehurst, B. (2002) Magnetic fields and radical reactions: recent developments and their role in nature. Chem. Soc. Rev. 31, 301–311.

Cashmore, A.R., Jarillo, J.A., Wu, Y.-J. and Liu, D. (1999) Cryptochromes: blue light receptors for plants and animals. Science 284, 760–765.

Demaine, C. and Semm, P. (1985) The avian pineal gland as an independent magnetic sensor. Neurosci. Lett. 62, 119–122.

Deutschlander, M.E., Borland, S.C. and Phillips, J.B. (1999a) Extraocular magnetic compass in newts. Nature 400, 324–325.

Deutschlander, M.E., Phillips, J.B. and Borland, S.C. (1999b) The case for light-dependent magnetic orientation in animals. J. Exp. Biol. 202, 891–908.

Dommer, D.H., Gazzolo, P.J., Painter, M.S., and Phillips, J.B. (in press) Magnetic compass orientation by larval *Drosophila melanogaster.* J. Insect Behav.

Eldred, W.D. and Nolte, J. (1978) Pineal photoreceptors: Evidence for a vertebrate visual pigment with two physiologically active states. Vision Res. 18, 29–32.

Emery, P., So, W.V., Kaneko, M., Hall, J.C. and Rosbash, M. (1998) CRY, a drosophila clock and light-regulated cryptochrome, is a major contributor to circadian rhythm resetting and photosensitivity. Cell 95, 669–679.

Eun, B.K. and Kang, H.M. (2003) Cloning and expression of cryptochrome2 in the bullfrog, *Rana catesbeiana*. Mol. Cells 16, 239–244.

Freake, M.J. and Phillips, J.B. (2005) Light-dependent shift in bullfrog tadpole magnetic compass orientation: evidence for a common magnetoreception mechanism in anuran and urodele amphibians. Ethology 111, 241–254.

Giovani, B., Byrdin, M., Ahmad, M. and Brettel, K. (2003) Light-induced electron-transfer in a cryptochrome blue-light photoreceptor. Nature Struct. Biol. 10, 489–490.

Grissom, C.B. (1995) Magnetic field effects in biology: a survey of possible mechanisms with emphasis on radical-pair recombination. Chem. Rev. 95, 3–24.

Henbest, K.B., Rodgers, C.T., Hore, P.J. and Timmel, C.R. (2004) Radio frequency magnetic field effects on a radical recombination reaction: a diagnostic test for the radical pair mechanism. J. Am. Chem. Soc. 126, 8102–8103.

Kirschvink, J. L. (1996) Microwave absorption by magnetite: a possible mechanism for coupling nonthermal levels of radiation to biological systems. Bioelectromagnetics 17, 187–194.

Lohmann, K.J. and Johnson, S. (2000) The neurobiology of magnetoreception in vertebrate animals. Trends Neurosci. 23, 153–159.

Lohmann, K.J. and Lohmann, C.M. (1993) A light-independent magnetic compass in the leatherback sea turtle. Biol. Bull. 185, 149–151.

Maffei, L., Meschini, E. and Papi, F. (1983) Pineal body and magnetic sensitivity: homing in pinealectomized pigeons under overcast skies. Z. Tierpsychol. 62, 151–156.

Marhold, S., Wiltschko, W. and Burda, H. (1997) A magnetic polarity compass for direction finding in a subterranean mammal. Naturwissenschaft 84, 421–423.

Möller, A., Sagasser, S., Schierwater, B. and Wiltschko, W. (2004) Retinal cryptochrome in a migratorybird: a possible transducer for the avian magnetic compass. Naturwissenschaft 91, 585–588.

Mouritsen, H., Janssen-Bienhold, U., Liedvogel, M., Feenders, G., Stalleicken, J., Dirks, P. and Weiler, R. (2004) Cryptochromes and neuronal-activity markers colocalize in the retina of migratory birds during magnetic orientation. Proc. Natl Acad. Sci. USA 101, 14294–14299.

Mouritsen, H. and Ritz, T. (2005) Magnetoreception and its use in bird navigation. Curr. Opin. Neurobiol. 15, 406–414.

Muheim, R., Bäckman, J. and Åkesson, S. (2002) Magnetic compass orientation in European robins is dependent on both wavelength and intensity of light. J. Exp. Biol. 205, 3845–3856.

Muheim, R., Edgar, N.M., Sloan, K.A. and Phillips, J.B. (2006) Magnetic compass orientation in C57BL/6J mice. Learn. Behav. 34, 366–373.

Němec, P., Burda, H. and Oelschläger, H.A. (2005) Towards the neural basis of magnetoreception: a neuroanatomical approach. Naturwissenschaft 92, 151–157.

Partch, C.L. and Sancar, A. (2005) Photochemistry and photobiology of cryptochrome blue-light photopigments: the search for a photocycle. Photochem. Photobiol. 81, 1291–1304.

Phillips, J.B. (1986) Two magnetoreception pathways in a migratory salamander. Science 233, 765–767.

Phillips, J.B. and Borland, S.C. (1992a) Behavioral evidence for use of light-dependent magnetoreception mechanism by a vertebrate. Nature 359, 142–144.

Phillips, J.B. and Borland, S.C. (1992b) Magnetic compass orientation is eliminated under near-infrared light in the Eastern red-spotted newt, *Notophthalmus viridescens*. Anim. Behav. 44, 796–797.

Phillips, J.B. and Borland, S.C. (1992c) Wavelength-specific effects of light on magnetic compass orientation of the Eastern red-spotted newt, *Notophthalmus viridescens*. Ethol. Ecol. Evol. 4, 33–42.

Phillips, J.B. and Sayeed, O. (1993) Wavelength-dependent effects of light on magnetic compass orientation in *Drosophila melanogaster*. J. Comp. Physiol. A *172*, 303–308.

Rappl, R., Wiltschko, R., Weindler, P., Berthold, P. and Wiltschko, W. (2000) Orientation behaviour of garden warblers, *Sylvia borin*, under monochromatic light of various wavelengths. Auk 117, 256–260.

Ritz, T., Adem, S. and Schulten, K. (2000) A model for photoreceptor-based magnetoreception in birds. Biophys. J. 78, 707–718.

Ritz, T., Dommer, D.H. and Phillips, J.B. (2002) Shedding light on vertebrate magnetoreception. Neuron 34, 503–506.

Ritz, T., Thalau, P., Phillips, J.B., Wiltschko, R. and Wiltschko, W. (2004) Resonance effects indicate a radical-pair mechanism for avian magnetic compass. Nature 429, 177–180.

Sancar, A. (2000) CRYPTOCHROME: The second photoactive pigment in the eye and its role in circadian photoreception. Annu. Rev. Biochem. 69, 31–67.

Schneider, T., Thalau, H.P., Semm, P. and Wiltschko, W. (1994) Melatonin is crucial for the migratory orientation of pied flycatchers, *Ficedula hypoleuca*. J. Exp. Biol. 194, 255–262.

Schulten, K. (1982) Magnetic field effects in chemistry and biology. Adv. Solid State Phys. 22, 61–83.

Schulten, K. and Windemuth, A. (1986) Model for a physiological magnetic compass. In: G. Maret, J. Kiepenheuer and N. Boccara (Eds.), *Biophysical effects steady magnetic fields*. Springer Verlag, New York, pp. 99–106.

Semm, P. (1983) Neurobiological investigations on the magnetic sensitivity of the pineal gland in rodents and pigeons. Comp. Biochem. Physiol. 76, 683–689.

Semm, P. and Demaine, C. (1986) Neurophysiological properties of magnetic cells in the pigeon's visual system. J. Comp. Physiol. A 159, 619–625.

Semm, P., Nohr, D., Demaine, C. and Wiltschko, W. (1984) Neural basis of the magnetic compass: interactions of visual, magnetic and vestibular inputs in the pigeon's brain. J. Comp. Physiol. A, 155, 283–288.

Solessio, E. and Engbretson, G.A. (1993) Antagonistic chromatic mechanisms in photoreceptors of the parietal eye of lizards. Nature 364, 442–445.

Steiner U.E. and Ulbricht T. (1989) Magnetic field effects in chemical kinetics and related phenomena. Chem. Rev. 89, 51–147.

Thalau, P., Ritz, T., Burda, H., Wegner, R. and Wiltschko, R. (2006) The magnetic compass mechanisms of birds and rodents are based on different physical principles. J. R. Soc. Interface 3, *583*–587.

Thalau, P., Ritz, T., Stapput, K., Wiltschko, R. and Wiltschko, W. (2005) Magnetic compass orientation of migratory birds in the presence of a 1.315 MHz oscillating field. Naturwissenschaft 92, 86–90.

Vacha, M. and Soukopova, H. (2004) Magnetic orientation in the mealworm beetle *Tenebrio* and the effect of light. J. Exp. Biol. 207, 1241–1248.

Van der Horst, G.T.J., Muijtjens, M., Kobayashi, K., Takano, R., Kanno, S., Takao, M., De Wit, R., Verkerk, A., Eker, A.P.M., Van Leenen, D., Buijs, R., Bootsma, D.,

Hoeijmakers, J.H.J. and Yasui, A. (1999) Mammalian Cry1 and Cry2 are essential for maintenance of circadian rhythms. Nature 398, 627–630.

Weber, S., Kay, C.W.M., Mogling, H., Mobius, K., Hitomi, K. and Todo, T. (2002) Photoactivation of the flavin cofactor in *Xenopus laevis* (6 – 4) photolyase: Observation of a transient tyrosyl radical by time-resolved electron paramagnetic resonance. Proc. Natl Acad. Sci. USA 99, 1319–1322.

Wiltschko, R., Ritz, T., Stapput, K., Thalau, P. and Wiltschko, W. (2005) Two different types of light-dependent responses to magnetic fields in birds. Curr. Biol. 15, 1518–1523.

Wiltschko, R. and Wiltschko, W. (1995) *Magnetic orientation in animals*. Berlin: Springer.

Wiltschko, R. and Wiltschko, W. (1998) Pigeon homing: effect of various wavelengths of light during displacement. Naturwiss. 85, 164–167.

Wiltschko, W. (1968) Über den Einfluss statischer Magnetfelder auf die Zugorientierung der Rotkehlchen, *Erithacus rubecula*. Z. Tierpsychol. *25*, 537–558.

Wiltschko, W. (1978) Further analysis of the magnetic compass of migratory birds. In: K. Schmidt-Koenig and W.T. Keeton (Eds.), *Animal migration*, *navigation and homing*. Springer, Berlin, pp. 301–310.

Wiltschko, W., Gesson, M., Stapput, K. and Wiltschko, R. (2004a) Light-dependent magnetoreception in birds: interaction of at least two different receptors. Naturwissenschaft 9*1*, 130–134.

Wiltschko, W., Möller, A., Gesson, M., Noll, C. and Wiltschko, R. (2004b) Light-dependent magnetoreception in birds: analysis of the behaviour under red light after pre-exposure to red light. J. Exp. Biol. 207, 1193–1202.

Wiltschko, W., Munro, U., Ford, H. and Wiltschko, R. (1993) Red light disrupts magnetic orientation of migratory birds. Nature 364, 525–527.

Wiltschko, W., Munro, U., Ford, H. and Wiltschko, R. (2003) Lateralization of magnetic compass orientation in silvereyes, *Zosterops l. lateralis*. Austral. J. Zool. 51, 597–602.

Wiltschko, W., Traudt, J., Güntürkün, O., Prior, H. and Wiltschko, R. (2002) Lateralization of magnetic compass orientation in a migratory bird. Nature 419, 467–470.

Wiltschko, W., Stapput, K., Thalau, P. and Wiltschko, R. (2006) Avian magnetic compass: fast adjustment to intensities outside the normal functional window. Naturwissenschaft 93, 300–304.

Wiltschko, W. and Wiltschko, R. (1972) Magnetic compass of European robins. Science 176, 62–64.

Wiltschko, W. and Wiltschko, R. (1981) Disorientation of inexperienced young pigeons after transportation in total darkness. Nature 291, 433–434.

Wiltschko, W. and Wiltschko, R. (1992) Migratory orientation: magnetic compass orientation of garden warblers, *Sylvia borin*, after a simulated crossing of the magnetic equator. Ethology 91, 70–74.

Wiltschko, W. and Wiltschko, R. (1999) The effect of yellow and blue light on magnetic compass orientation in European robins, *Erithacus rubecula*. J. Comp. Physiol. A, 184, 295–299.

Wiltschko, W. and Wiltschko, R. (2001) Light-dependent magnetoreception in birds: the behaviour of European robins, *Erithacus rubecula*, under monochromatic light of various wavelengths and intensities. J. Exp. Biol. 204, 3295–3302.

Wiltschko, W. and Wiltschko, R. (2002) Magnetic orientation in birds and its physiological basis. Naturwissenschaft 89, 445–452.

Wiltschko, W. and Wiltschko, R. (2005) Magnetic orientation and magnetoreception in birds and other animals. J. Comp. Physiol. A 191, 675–693.

Woodward, J.R., Timmel, C.R., Hore, P.J. and McLauchlan, K.A. (2002) Oscillating magnetic field effects on chemical reaction yields. RIKEN Review 44, 79–81.

18
Phototoxicity

Lars Olof Björn and Pirjo Huovinen

Abstract: Phototoxicity occurs when a substance is toxic only under the action of light and can, depending on the mechanism of toxic action, be divided into type I and type II phototoxicity. Other types are sometimes recongnized, and sometimes toxicity occurs through more than one mechanism. Plants often use phototoxins for their defense. They may be harmful to humans, but may also be exploited for medical treatments. On the other hand, drugs selected for other properties may show unwanted phototoxicity. Some fungi produce phototoxins. Due to other kinds of poisoning or to disease, even the human or animal body may produce phototoxins and be harmed by them. Polycyclic aromatic hydrocarbons (PAHs), widespread environmental contaminants, have a potential to become toxic or acquire increased toxicity when they interact with natural or simulated sunlight. Because of their chemical structure numerous PAHs absorb energy in the UV waveband. Phototoxicity of PAHs occurs mainly via photosensitization and/or photomodification reactions: photosensitization reactions of bioaccumulated PAHs in biological matrices are regarded as important mechanisms for phototoxicity, but PAHs may also be photomodified into more toxic form, e.g., via photooxidation. Phototoxicity of PAHs has been demonstrated in a variety of aquatic organisms, responses ranging from acute lethality to chronic effects. However, a variety of factors affecting the exposure of organisms to PAHs and to UV radiation, as well as interactions between multiple environmental factors and stressors present in natural conditions, complicate the risk assessment for phototoxicity.

18.1. Introduction

Phototoxicity means that something which is not toxic in itself is converted into a toxin or produces a toxin by the action of light. We can divide phototoxicity into several classes:

Type I phototoxicity arises when a pigment, after absorption of light and acquiring an excited state, either combines directly with an important cell constituent (Fig. 18.1), or transfers electrons or hydrogen atoms. The transfer may take place from or to another molecule, which then becomes a toxic radical
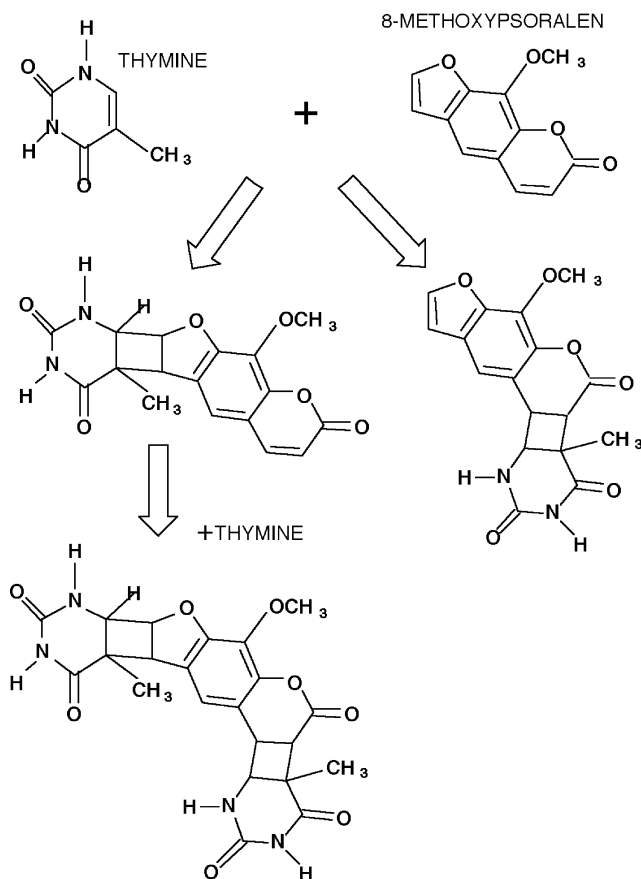
FIGURE 18.1. Formation of photoadduct between 8-methoxypsoralen and thymine residues in DNA. The thymine is shown for simplicity as free molecules, but is in reality part of a DNA molecule. One 8-methoxypsoralen molecule can combine with two thymine residues, and if they are bound to opposite DNA strands, cross-bridges can form between the strands. Although "phototoxicity" sounds dangerous, this and other similar reactions are also exploited in phototherapy of certain diseases.

or radical ion, or produces toxins in subsequent reactions. As an example of the action of a type I phototoxin, we show in Fig. 18.1 how 8-methoxypsoralen (MOPS in medical jargon) combines with thymine residues in DNA.

Type II phototoxicity arises when a pigment (photosensitizer) after absorption of light goes from the excited singlet state to a triplet state, and then reacts with molecular oxygen and produces singlet excited oxygen (see Chapter 1), which is highly toxic.

In some cases a pigment molecule excited by light absorption transfers an electron to molecular oxygen, thereby producing superoxide anion (see Fig. 18.1). According to the above definitions this is type I phototoxicity, but in the literature

it has also been designated type II phototoxicity, because in practice it is easier to distinguish between oxygen-independent and oxygen-dependent phototoxicity. The main cellular targets of both types I and II phototoxins are DNA, membrane lipids, and membrane proteins. A wide variety of organisms (except those having special protection systems) can be poisoned by most of the substances; i.e., they are rather unspecific with regard to poisoned organism.

As a third type of phototoxicity we can categorize those cases when a substance is converted into a toxin by a photochemical reaction which does not fall into any of the above categories.

As an example in which several mechanisms contribute to the photodestructive action, we show in Fig. 18.2 a schematic description of how membrane lipids are peroxidized by a photoexcited pigment (see Samadi et al. 2001).

An interesting consequence of lipid peroxidation is that a weak light (ultraweak luminescence) is emitted during the reaction. Lipid peroxidative chain reactions can be initiated also in ways other than through phototoxic action.

In our disposition of the topic "phototoxicity," we shall not follow the categorization into types I and II, but rather subdivide into the different contexts in which phototoxicity has been observed. We shall not include photoallergic reactions here, which, as they involve the immune system, are of a different character. Photoallergy will be treated in Chapter 21.
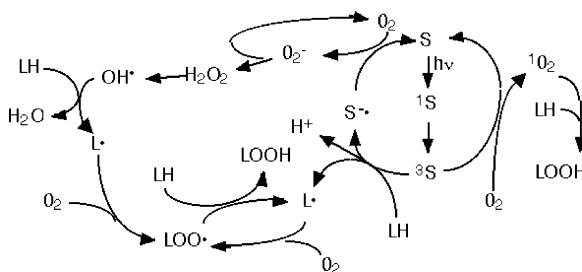
FIGURE 18.2. Diagram showing how a pigment (S), excited by light ($h\upsilon$) via an excited singlet state (^1S) to an excited triplet state (^3S) can damage a membrane lipid (LH) in several ways (note that the lipid molecules enter the reactions at four points in the diagram). (1) Type II reaction (right part of the diagram): the triplet pigment may react with triplet (ground state) oxygen (O_2) to form singlet oxygen ($^1O_2$), which can directly convert the lipid to a lipid peroxide (LOOH). (2) Classical type I reaction (lower part of the diagram): the triplet pigment abstracts a hydrogen atom from the lipid, creating a lipid radical (L•), which combines with triplet oxygen to form a lipid peroxy radical (LOO•). The latter abstracts a hydrogen atom from another lipid molecule to form a lipid peroxide. In this way a new lipid radical is formed, and a chain reaction is created. (3) Oxygen-dependent hydrogen abstraction (upper part of the diagram): an electron is donated to triplet oxygen, creating superoxide anion, which via formation of hydrogen peroxide and hydroxide radical abstracts hydrogen from the lipid. Also in this case the lipid is degraded to lipid peroxide and a chain reaction is initiated.

18.2. Phototoxicity in Plant Defense

The most important defenses of plants against parasites and grazers are of a chemical nature, and among chemical defenses phototoxicity plays an important role, especially among flowering plants. The phototoxic substances employed by plants can also affect people when they appear in food, perfumes and other cosmetic products, and even if we just touch certain plants.

Downum (1992) estimates that 75–100 different phototoxic molecules have been isolated from flowering plants. Phototoxins or phototoxic activity has been reported for about 40 of more than 100 angiosperm families, representing all subclasses except Alismatidae and Arecidae. Many plants have several phototoxic substances. From *Ammi majus* as well as from *Angelica archangelica* the following ones are reported: angelicin, bergapten, 8-methoxypsoralen, and pimpinellin—from the former one, in addition, furocoumarin and from the latter one psoralen. The plant family Apiace (former name Umbelliferae) dominates the cases of phototoxicity of most importance to humans.

The phototoxins affect bacteria, fungi, nematodes, insects, and other organisms. This wide spectrum is due to the fact that the toxins attack cellular constituents common to all cells. DNA is a major target for type I acting chemicals, such as acetophenones, coumarins, furanochromones, furanoquinolines, pterocarpans, and sesquiterpenes. Examples of type II acting compounds are isoquinolines and thiophenes.

Photosensitizers generally have many double bonds, i.e., many π-electrons, and most of them are polycyclic. The most common types in plants are acetylens and furanocoumarins, but many other types also occur.

Since absorption of ultraviolet radiation is a common feature of organic compounds, and absorption for polycyclic systems and acetylenes with conjugated triple bonds (compounds with many π-electrons) extends into the UV-A region, it is not surprising that UV-A (of which there is much more in daylight than of UV-B) in most cases is the most important spectral region for inflicting phototoxicity. However, there are exceptions, and hypericin (present in *Hypericum*, St John's wort) with its many fused phenyl rings absorbs and is excited to phototoxicity even by yellow and orange light, while some other substances require UV-B radiation. Detailed information on action spectra is still lacking in most cases. Guesses made based on absorption spectra are not reliable, since cases are known in which the phototoxic action takes place with radiation of longer wavelength than that absorbed by the pure substance. The reason for this is probably that the spectrum is shifted when the substance binds to cellular components.

The mode of action of hypericin has been debated, but it has now been established (Delaey, Vandenbougarde, Merlevede and de Witte 2000) that it required oxygen for phototoxicity. Like several other phototoxic compounds from plants (e.g., psoralen, 8-methoxypsoralen), it has been used in the phototherapy of diseases.

Specific plant species causing problems for humans and domestic animals naturally vary among countries, but the following are worth mentioning here:

Fig, *Ficus carica*. Fig can be troublesome only for those involved in picking and handling them professionally. One source speculates that fig could have caused trouble for Adam and Eve!

Angelica, *Angelica archangelica*. This and other *Angelica* species are used as traditional medicine from Korea to Lapland, and also in drinks. They have caused problems for growers and collectors.

Buckwheat, *Fagopyrum esculentum*. Causes trouble mainly in grazing cattle.

Celery, *Apium graveolens*. Has caused burns when ingested before visiting suntan parlor. Contains 5-methoxypsoralen, 8-methoxypsoralen (xanthotoxin), and 4,5',8-trimethylpsoralen. Of special interest is that this plant can contain 10-fold increased contents of psoralen derivatives after infection with a fungus, *Sclerotinia sclerotium* (pink rot disease). Persons handling celery professionally are at risk. Disease-resistant celery contains increased levels of furocoumarins (Fig. 18.3).

Hogweed (*Heracleum*), especially Russian hogweed (*Heracleum mantegazzianum*). Light produces severe blisters in skin that has been in touch with the plant. The plant has spread over large areas of Europe and North America. *Heracleum* species contain angelicin, bergapten, pimpinellin and 5-methoxypsoralen and other related substances.

Spring parsley (also erroneously called wild carrot), *Cymopteris watsonii*, growing in Oregon, Nevada, and western Utah. Problems with grazing sheep and cattle. Newborn lambs and calves die because mothers become so touch-sensitive that they refuse nursing. The plant contains furocoumarins, 8-methoxypsoralen (xanthotoxin), and bergapten.

Lei flowers, especially *Pelea anisata*. Leis are the greeting wreaths that visitors receive on their arrival to Hawaii.

Burning bush of Moses (also called gas plant), *Dictamnus albus*. The plant grows wild in Europe and Asia and is used as a garden plant also in other parts of the
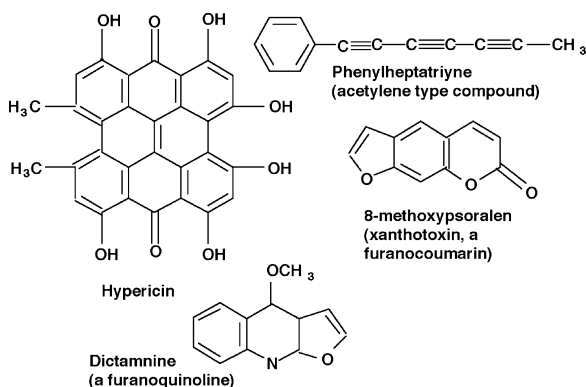
FIGURE 18.3. Examples of phototoxic substances from plants.

world. It belongs to the family Rutaceae, which harbors also other plants with some phototoxicity, among them *Citrus* species and *Ruta graveolens*, garden rue. St John's wort. *Hypericum* species contain hypericin and can cause trouble both to grazing animals and to persons who consume drinks based on *Hypericum* extracts and are exposed to light afterwards.

Some of the phytophototoxins are used for medical treatments. The most noteworthy example is treatment of vitiligo and psoriasis with 8-methoxypsoralen and related substances. In fact, the juice of the Egyptian plant *Ammi majus* has been used for this purpose since 2000 B.C. (Pathak and Fitzpatrick 1992). We can only give some examples of detailed mechanisms of action in phototox-icity. For further information on phototoxic plants and plant phototoxins, see Pathak (1986), Downum (1992), Lovell (1993), and the following Internet sites: (1) http://telemedicine.org/Botanica/Bot5.htm; (2) http://www.ars-grin.gov/cgi-bin/duke/chemical_activity.pl.

18.3. Phototoxins of Fungal Plant Parasites

Phototoxins are not used only for plant defense, but also for attack on plants by parasitic fungi. So far only one case has been thoroughly researched, but a number of plant pathogenic fungi produce photosensitizing substances. A review of the subject (Daub and Ehrenshaft 2000) has recently appeared.

The best known example of a plant parasite using a phototoxin to weaken its host is the genus *Cercospora*. About 500 parasitic *Cercospora* species are known and cause, e.g., leaf spot of sugar beet, grey leaf spot of corn, purple seed stain of soybean, frogeye leaf spot of tobacco, and brown eye spot of coffee. For sugar beet the active pigment, cercosporin (Fig. 18.4), has been isolated from 34 *Cercospora* species grown in culture, while other species do not produce cercosporin and still can parasitize plants.

Cercosporin is a type II phototoxin. After reaching its triplet state during illumination, it reacts with oxygen to form singlet oxygen. The singlet oxygen
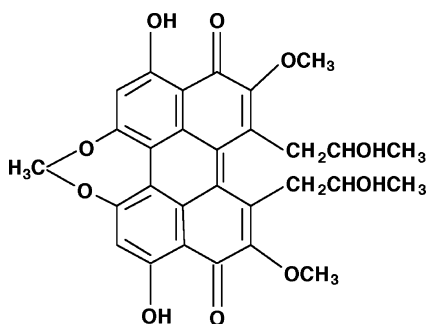
FIGURE 18.4. Cercosporin, the phototoxin of the parasitic fungus *Cercospora*.

destroys the cell membrane of host cells, which leads to leakage of nutrients to the fungus.

Of course, the fungus has cell membranes which could be damaged by cercosporin, so it must have some defense against its own toxin. In culture they can accumulate up to millimolar toxin in the medium without observable toxic effects. In fact, it defends itself in two ways:

1. As long as the cercosporin is inside the hyphae, it is kept in a reduced form, which in light produces only a small amount of singlet oxygen. After secretion to the environment it is oxidized to the highly active form. The two forms can be easily distinguished under the microscope, since the reduced form has a green, the oxidized one a red fluorescence.
2. In addition the fungus is extraordinarily well equipped with a set of triplet and singlet oxygen quenchers. That they are efficient is shown by the fact that *Cercospora* is resistant also to the effects of other singlet oxygen–producing phototoxins. Among the quenchers of singlet oxygen pyridoxine is thought to be particularly important for *Cercospora*.

Interestingly, *Cercospora* does not produce cercosporin in darkness (when it would be of no use); its synthesis is triggered by light.

Pigments having structures related to cercosporin (perylenequinones, see Fig. 18.4), and presumably having a corresponding function, are produced by a number of other fungi: by *Cladosporium* species, by the bamboo pathogens *Shiraia bambusicola* and *Hypocrella bambusae*, and by *Stempylium botryosum* and some *Alternaria* and *Elsinoe* species. Also, light-requiring fungal toxins of other types are known, produced by *Cercospora* species and *Dothistroma pini* (Jalal, Hossain, Robeson, and van der Helm 1992, Stoessl, Abramowski, Lester et al. 1990).

18.4. Phototoxic Drugs and Cosmetics

Many phototoxic drugs are either antibiotics or medications for blood pressure and heart disease, but there are also others. In combination with light they may cause extreme sunburn, vesicles, hives, and edema. Among antibiotics, photosensitivity reactions have more commonly been noted after administration of the following: Doxycycline ("Vibramycine" etc.), demeclocycline, tetracycline (Fig. 18.5), nalidixic acid, and lomefloxacin. For blood pressure and heart medications, a similar short list includes hydrochlorothiazide (occurs as an ingredient in a large number of formulations), chlorothiazide, furosemide, and amiodarone. Amiodarone is responsible for an unusually high number of cases. Among other drugs causing photosensitivity reactions, chlorpromazine and other phenothiazines and birth control pills containing estrogens may be mentioned.

Somewhat surprising is the fact that also sun lotions containing para-aminobenzoic acid (PABA) or esters of it, which are sold to protect one from the sun are also a common cause of photosensititivity. These substances were
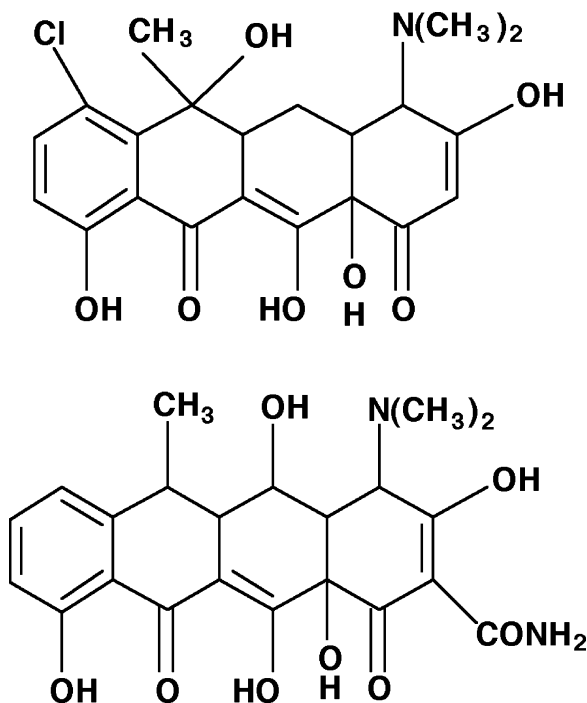
FIGURE 18.5. (Top) Chlortetracycline, the first tetracycline, introduced in 1948. Tetracycline itself (introduced in 1952) has the same structure, with hydrogen in place of chlorine. (Bottom) Doxycycline, introduced in 1968, is one of the most potent photosensitizers among the tetracyclines.

selected for their ability to absorb UV-B radiation (daylight with wavelength below 315 nm), since formerly this radiation was supposed to be the only threat from sunlight. At the long-wavelength edge of their absorption band they let radiation through to depths where they can cause the photosensitivity reactions.

It is well known that use of perfumes in combination with sunlight is unwise, because many perfumes are phototoxic or at least discolor the skin when exposed to sunlight. This is, of course, because many, if not most of them are based on plant extracts and often contain substances mentioned in the section on phototoxins in plant defense. Freund (1916) described skin discolorations, which he attributed to Eau de Cologne containing bergamot oil, although he did not clearly understand the role of sunlight. Bergamot orange, *Citrus bergamia*, like many other *Citrus* species, was later found to contain photosensitizing substances.

A book (Miranda 2001) has been assembled from 28 articles in the journal *Photochemistry and Photobiology* and is currently freely downloadable from the journal's homepage.

18.5. Metabolic Disturbances Leading to Phototoxic Effects of Porphyrins or Related Compounds

A number of different disturbances in both humans and animals lead to the appearance in the skin of phototoxic compounds such as uro- and coproporphyrinogens (porphyrin precursors), protoporphyrin IX (the immediate precursor of heme, Fig. 18.6), and phylloerythrin (a breakdown product of chlorophyll, Fig. 18.7). These substances are phototoxins of type II, generating singlet oxygen in light.

In human patients a variety of diseases have been described which go under the common designation of porphyria. With the exception of a type called acute intermittent porphyria, they lead to photosensitivity of the skin: variegate porphyria (Frank and Christiano 1998) and hereditary coproporphyria (acute porphyrias with increased levels of both porphyrin precursors and porphyrins) and porphyria cutanea tarda, erythropoietic protoporphyria and congenital porphyria (nonacute porphyrias with increased levels of porphyrins). Porphyria is due to a disturbance in either the liver (hepatic porphyria or protoporphyria) or the red blood cells (erythropoietic porphyria or protoporphyria). To complicate things further, an erythrohepatic porphyria has recently been described (Gauer, Goss and Riemann 1995), and erythropoietic porphyria may lead to secondary damage to the liver.

Porphyria may be inherited or acquired, and even in cases when it is caused by environment, lifestyle, alcohol (Doss, Kuhnel, Gross, and Sieg 1999), lead poisoning, liver transplantation (Sheth, Esterly, Rabinowitz et al. 1994), etc., inherited predisposition may play a role. Gross, Hoffmann, and Doss (2000) remarks in a recent review: "The molecular genetics of the porphyrias is very heterogenous. Nearly every family has its own mutation." Correct treatment of porphyria is therefore not easy and requires very careful examination. Porphyria
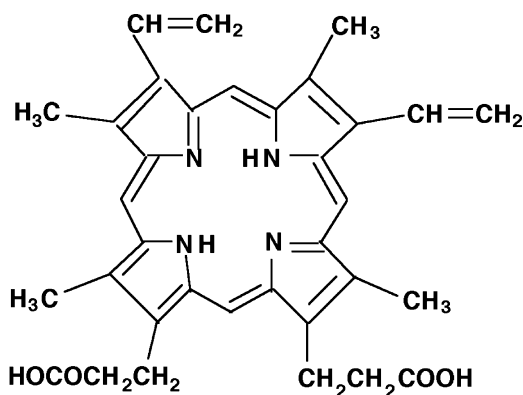
FIGURE 18.6. Protoporphyrin IX, the immediate precursor of heme, which accumulates in protoporphyria due to lack of ferrochelatase (or inhibition of the enzyme due to, e.g., lead poisoning).
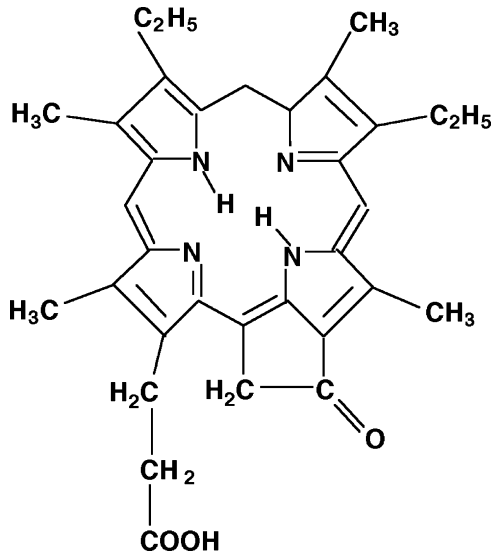
FIGURE 18.7. Phylloerythrin, which causes phototoxicity in animals due to malfunctioning of the liver. In healthy animals the substance is broken down in the liver.

cannot be cured, but symptoms can often be ameliorated in other ways than avoidance of light. There are prospects for a future cure of the erythropoietic protoporphyria. In this condition the enzyme ferrochelatase is lacking in the red blood cells, causing accumulation of protoporphyrin IX. It may become possible to cure this by retroviral mediated gene transfer to the bone marrow (Todd 1994). At present the symptoms can be alleviated using β-carotene; interestingly the same compound as used by plants to quench triplet chlorophyll.

In ruminants another group of diseases with names such as geeldikkop ("yellow head") and alveld is important. Geeldikkop, affecting sheep in South Africa, is the best studied of these. It is caused by saponins in the plant *Tribulus terrestris* (puncture vine or calthrops of the family Zygophyllacea) grazed upon by sheep (Miles, Wilkins, Erasmus et al. 1994, Wilkins, Miles, De Kock et al. 1996). Liver damage caused by these saponins prevents breakdown of phyllo-erythrin, a substance produced from chlorophyll by acid in the stomach and rumen bacteria. The phylloerythrin is circulated to skin capillaries, where it can be exposed to light. In other parts of the world *Panicum* species such as klein-grass or bambatsi grass, *P. coloratum* (Muchiri, Bridges, Ueckert et al. 1980, Bridges, Camp, Liningston, and Bailey 1987, Regnault 1990), and switchgrass, *P. virgatum* (Puoli, Reid, and Beletsky 1992), cause the same disease in sheep and in horses (Cornick, Carter, and Bridges 1988).

Similar symptoms were induced by *Myoporum laetum* in calves (Raposo, Mendez, de Adrade, and Riet-Correa 1998), and buttercup (*Ranunculus bulbosus*) has been suspected as a cause in cattle (Kelch, Kerr, Adair, and Boyd 1992). Mold fungi in hay and fungi in pasture can cause similar problems (Scruggs

and Blue 1994, Casteel, Rottinghaus, Hohson, and Wicklow 1995). Finally, it has been known for a long time that cyanobacterial toxins in drinking water can cause liver damage with associated photosensitivity in cattle. In the case of the fungus *Pithomyces cartarum* in lamb pasture (Hansen et al. 1994), it is not clear whether the photosensitivity is due to primary photosensitization or liver damage.

18.6. Polycyclic Aromatic Hydrocarbons as Phototoxic Contaminants in Aquatic Environments

18.6.1. Nature and Occurrence of PAHs

Some compounds have a potential to become toxic or acquire increased toxicity when they interact with natural or simulated sunlight. Such compounds with a possible environmental relevance include, e.g., photoactive insecticides, such as naturally occurring α-terthienyl (Kagan, Kagan, and Buhse 1984; Kagan, Bennett, Kagan, Maas, Sweeney, Kagan, Seigneurie, and Bindokas 1987) and some photodynamic dyes (Larson and Berenbaum 1988), a carbamate insecticide (Zaga, Little, Rabeni, and Ellersieck 1998), trinitrotoluene (TNT, an explosive), and some related compounds (Davenport, Johnson, Schaeffer, and Balbach 1994), and many polycyclic aromatic hydrocarbons (PAHs) (Newsted and Giesy 1987; Arfsten, Schaeffer, and Mulveny 1996). PAHs, composed of multiple aromatic rings (Fig. 18.8) and present in coal and petroleum products,
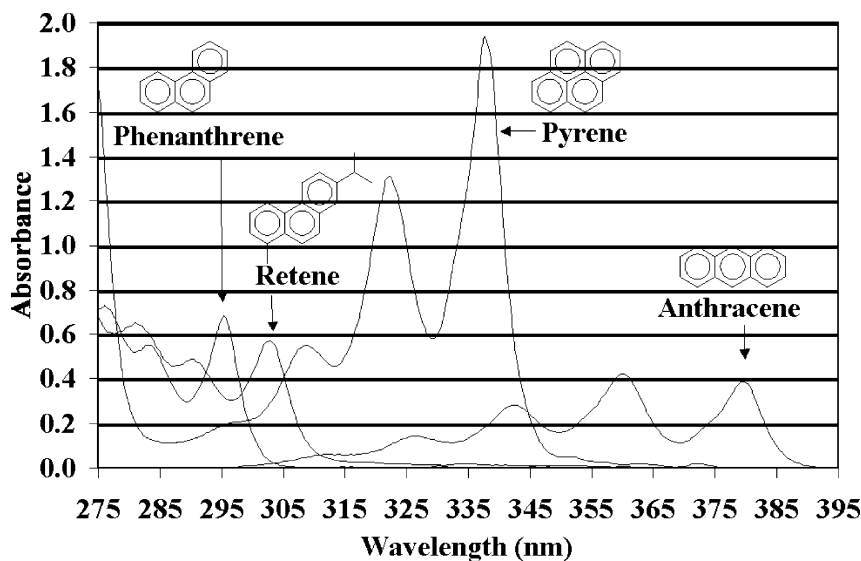
FIGURE 18.8. Absorption spectra of anthracene, pyrene, phenanthrene, and retene (7-isopropyl-1-methylphenanthrene) (10 mg^{-1} in dimethylsulfoxide). (Modified from Huovinen et al. 2001, with permission from Elsevier Science.)

are widespread organic environmental contaminants, some having carcinogenic potential (Neff 1979, 1985). PAHs can be introduced into the environment, e.g., through incomplete combustion of organic matter. In aquatic environments oil spills, surface runoff from land, and industrial and domestic wastewaters are among the possible sources of PAH contamination, as well as airborne PAHs entering aquatic systems through dry fallout and rainfall (Neff 1979, 1985). Photoenhanced toxicity of petroleum products (Pelletier, Burgess, Ho, Kuhn, McKinney, and Ryba 1997; Wernersson 2003) and creosote (Schirmer, Herbrick, Greenberg, Dixon, and Bols 1999) has been related to phototoxicity of PAHs present. Furthermore, liquid-phase elutriates of petroleum-containing sediments (Davenport and Spacie 1991), urban stormwater runoff (Ireland, Burton and Hess 1996), as well as PAH-contaminated sediments (Ankley, Collyard, Monson, and Kosian 1994; Monson, Ankley, and Kosian 1995) contain phototoxic components, suggesting the role of PAHs. Interaction with solar radiation has also been shown to increase the toxicity of weathered oil (Cleveland, Little, Calfee, and Barron 2000; Little, Cleveland, Calfee, and Barron 2000; Barron, Carls, Short, and Rice 2003).

Although generally considered relatively acutely nontoxic under normal laboratory lighting, numerous PAHs, such as anthracene, benzo[a]pyrene (3,4-benzopyrene, benzo[d,e,f]chrysene), fluoranthene, and pyrene have a potential to become highly toxic in the presence of UV radiation, and a risk that PAHs constitute through this photoenhanced toxicity, especially to aquatic organisms, has been recognized (reviewed by Landrum, Giesy, Oris, and Allred 1987; Arfsten et al. 1996; Schaeffer and Larson 1999; Pelletier, Sargian, and Demers 2006). Since bioassays used to test the toxicity of chemicals are commonly carried out in the laboratory under artificial lighting not including UV radiation, the risk related to photoactive compounds in natural conditions can be underestimated with traditional toxicity testing. On the other hand, the ecological relevance of PAH phototoxicity evaluations and their use in risk assessment has been criticized (McDonald and Chapman 2002) as often experimental approaches cannot be considered representative of natural environmental conditions where a suite of factors interact.

18.6.2. Mechanisms of PAH Phototoxicity

Because of their chemical structure, many PAHs absorb energy in the UV waveband (Newsted and Giesy 1987; Huang, Dixon, and Greenberg 1993; Diamond, Mount, Burkhard, Ankley, Makynen, and Leonard 2000; Huovinen, Soimasuo, and Oikari 2001) (Fig. 18.8). According to the quantitative structure/activity relationship (QSAR) model, the phototoxicity of PAHs can be related to the HOMO-LUMO gap (i.e., energy difference between the highest occupied molecular orbital and the lowest unoccupied molecular orbital), which

has been suggested as a suitable ground state index of the electronic structure relating to absorbed energy and molecular stability (Mekenyan, Ankley, Veith, and Call 1994). However, the comparison of the phototoxic potency of PAHs is complicated because it is also related to the bioaccumulation potential of each compound (Boese, Lamberson, Swartz, Ozretich, and Cole 1998). Contaminated environments generally contain a mixture of numerous PAHs, and phototoxicity of PAH mixtures is regarded as somewhat additive (Swartz, Ferraro, Lamberson, Cole, Ozretich, Boese, Schults, Behrenfeld, and Ankley 1997; Boese, Ozretich, Lamberson, Swartz, Cole, Pelletier, and Jones 1999; Erickson, Ankley, DeFoe, Kosian, and Makynen 1999). Also, substituted PAHs can contribute to phototoxicity (Boese et al. 1998; Kosian, Makynen, Monson, Mount, Spacie, Mekenyan, and Ankley 1998). With some exceptions, phototoxicity is likely in a substituted PAH only if the aromatic structure of its parent compound is phototoxic (Veith, Mekenyan, Ankley, and Call 1995).

Phototoxicity of PAHs is reported to occur mainly via photosensitization and/or photomodification reactions. The role of PAHs as active photosensitizers has been related to their capability of forming triplet states (Newsted and Giesy 1987; Larson and Berenbaum 1988) and transferring their triplet energy to oxygen, potentially resulting in the formation of biologically damaging singlet oxygen (Larson and Berenbaum 1988; see Chapter 1). Photosensitization reactions of bioaccumulated PAHs in biological matrices are regarded as important mechanisms for phototoxicity, which is supported by studies demonstrating enhanced toxicity when bioaccumulation of PAHs in aquatic organisms is followed by exposure to UV radiation in clean uncontaminated water (Bowling, Leversee, Landrum, and Giesy 1983; Allred and Giesy 1985; Ankley et al. 1994; Ankley, Erickson, Sheedy, Kosian, Mattson, and Cox, 1997; Boese, Lamberson, Swartz, and Ozretich 1997; Monson, Call, Cox, Liber, and Ankley 1999; Huovinen et al. 2001). Phototoxicity is considered a function of both PAH dose in tissue and UV intensity (Ankley, Erickson, Phipps, Mattson, Kosian, Sheedy, and Cox 1995).

In addition to photodegradation (Neff 1979, 1985), PAHs may be photomodified into more toxic form, e.g., via photooxidation (McConkey, Duxbury, Dixon, and Greenberg 1997; Mallakin, McConkey, Miao, McKibben, Snieckus, Dickson, and Greenberg, 1999; Lampi, Gurska, McDonald, Xie, Huang, Dixon, and Greenberg 2006). Photomodification of PAH can result in a complex mixture of products (Mallakin et al. 1999). The enhanced toxicity of many photoproducts can probably be attributed to increased aqueous solubility and thus potentially increased bioavailability, as well as increased bioactivity (Duxbury, Dixon, and Greenberg 1997; McConkey et al. 1997). Although many photomodified PAHs are toxic as such, they can be phototoxic as well (Huang et al. 1993; Mallakin et al. 1999). According to model predictions, photosensitization and photomodification contribute additively to phototoxicity (Huang, Krylov, Ren, McConkey, Dixon, and Greenberg 1997a; Krylov, Huang, Zeiler, Dixon, and Greenberg 1997; Mezey, Zimpel, Warburton, Walker, Irvine, Huang, Dixon, and Greenberg 1998; El-Alawi, Huang, Dixon, and Greenberg 2002).

18.6.3. Factors Affecting Exposure to Phototoxicity of PAHs in Aquatic Systems

Due to their hydrophobic nature, PAHs tend to accumulate in sediments and organic particles (Neff 1979, 1985), resulting in a decrease in their availability to organisms. However, disturbance of contaminated sediment, e.g., during a storm or dredging, may result in mobilization and resuspension of PAHs in the water, increasing the risk of phototoxicity (Davenport and Spacie 1991; Ireland et al. 1996). On the other hand, because of their lipophilic nature, PAHs also tend to bioaccumulate in organisms (Neff 1979, 1985). In addition to waterborne PAHs, a possible route of exposure to PAHs is their bioaccumulation from contaminated sediments (Ankley et al. 1994; Boese et al. 1998) and potentially also via the food chain.

The potential for UV exposure varies in different types of waters. UV-B penetration depths can range from a few centimeters in highly humic lakes (Kirk 1994; Lean 1998; Huovinen, Penttilä, and Soimasuo 2000) to dozens of meters in clear oceanic waters (Smith, Prézelin, Baker, Bidigare, Boucher, Coley, Karentz, MacIntyre, Matlick, Menzies, Ondrusek, Wan, and Waters 1992; Kirk 1994). The spectra of underwater UV irradiance change with depth, as penetration decreases with decreasing wavelength (Kirk 1994, Scully and Lean 1994; Lean 1998; Huovinen et al. 2000). This spectral change and variation among natural waters affect the potential for phototoxicity (Barron, Little, Calfee, and Diamond 2000), since the phototoxic response is related to the UV absorption characteristics of a compound (Newsted and Giesy 1987; Diamond et al. 2000; Huovinen et al. 2001; Lampi et al. 2006) (Fig. 18.8). Aquatic biota in PAH-contaminated areas (particularly in clear, shallow waters and littoral areas, which often provide habitats for various aquatic organisms during reproduction and early development) may be at risk. UV exposure and thus phototoxicity can also be increased, e.g., during low flow (Ireland et al. 1996), or when organisms move up in the water column. Other factors, such as increased turbidity, which reduce the penetration of UV radiation in the water column can attenuate phototoxicity as well (Ireland et al. 1996).

In addition to strongly contributing to attenuation of UV radiation (Kirk 1994; Scully and Lean 1994; Morris, Zagarese, Williamson, Balseiro, Hargreaves, Modenutti, Moeller, and Queimalinos 1995; Williamson, Stemberger, Morris, Frost, and Paulsen 1996; Lean 1998; Huovinen et al. 2000), humic substances have a complex role in aquatic systems in potentially affecting the phototoxicity of PAHs. Dissolved humic material may mitigate the potential for photoinduced toxicity (Gensemer, Dixon, and Greenberg 1998, 1999) by reducing the bioaccumulation of PAHs to organisms (Oris, Hall, and Tylka 1990; Weinstein and Oris 1999). However, UV radiation may also induce photochemical reactions, such as photochemical degradation in dissolved organic carbon, which may increase the UV transparency (Morris and Hargreaves 1997) and thus the risk for phototoxicity. Humic substances as potential photosensitizers (Larson and Berenbaum 1988) play a role in photodegradation of aquatic contaminants via formation of reactive oxygen species by UV radiation (Boule, Bolte, and Richard 1999).

In all, a variety of factors affecting the exposure of organisms to PAHs and to UV radiation, as well as interactions between multiple environmental factors and stressors present in natural conditions, complicate the risk assessment for phototoxicity. Actually, field mesocosm studies with natural plankton communities have demonstrated the complexicity in determining the impact of multiple stressors on aquatic ecosystems, and the enhancement of water-soluble crude oil toxicity in the presence of UV-B radiation could not be described as synergistic or additive (Sargian, Mostajir, Chatila, Ferreyra, Pelletier, and Demers 2005, Pelletier et al. 2006).

18.6.4. Phototoxicity of PAHs to Aquatic Biota

Phototoxicity of PAHs has been demonstrated in a variety of aquatic organisms, including bacteria, phytoplankton, aquatic higher plants, zooplankton, benthic invertebrates, and insect larvae, as well as in early life stages of amphibians, bivalves, and fish. Responses in biota to PAH phototoxicity range from acute lethality to chronic effects, such as reproductive impairment.

The major photooxidation product of phenanthrene was found to be more toxic to marine bacteria *Photobacterium phosphoreum* than phenanthrene (McConkey et al. 1997). Anthracene can inhibit algal growth and primary production (Gala and Giesy 1992) and reduce cell viability (Gala and Giesy 1994) in the green alga *Selenastrum capricornutum* in the presence of UV radiation. Growth inhibition due to photo-toxicity of benzo[a]pyrene has also been shown (Cody, Radike, and Warshawsky 1984). Xanthophyll cycling has been suggested as an energy dissipative response to photoinduced PAH toxicity in green microalga *Ankistrodesmus* sp. (Southerland and Lewitus 2004). Exposure of natural phytoplankton assemblages to intact or photomodified anthracene in sunlight diminished PSII photosynthetic efficiency, intact anthracene being more phototoxic than its photomodified product (Marwood, Smith, Solomon, Charlton, and Greenberg 1999). Photomodification of PAHs into more toxic form has been suggested as an important mechanism for phototoxicity to the aquatic higher plant the duckweed *Lemna gibba*, causing, e.g., inhibition of growth (Huang et al. 1993; Mallakin et al. 1999). Anthracene can inhibit photosynthesis after its photomodification, with the primary site of action possibly being the electron transport at or near PSI, followed by inhibition of PSII (Huang, McConkey, Babu, and Greenberg 1997b). Intact and photooxidized PAHs can accumulate in the thylakoids and microsomes of *L. gibba*, which possibly are the most susceptible subcellular compartments (Duxbury et al. 1997). Models using 16 different PAHs have indicated an additive role of photomodification and photosensitization in toxicity to *L. gibba* (Huang et al. 1997a; Krylov et al. 1997; Mezey et al. 1998).

Phototoxicity of several PAHs has been demonstrated in the aquatic crustacean *Daphnia magna* (Newsted and Giesy 1987; Wernersson 2003). Also, photo-products (oxy-PAHs) of numerous PAHs have been found to be highly toxic to *D. magna* (Lampi et al. 2006). Activation of anthracene on or within organisms caused acute phototoxicity in *D. pulex* in the presence of solar radiation (Allred

and Giesy 1985). Photosensitization of bioaccumulated anthracene and pyrene appeared to be the primary mechanism for acute photoinduced toxicity in *D. magna* (Huovinen et al. 2001). Also, sublethal effects, such as reduced feeding efficiency due to fluoranthene phototoxicity, have been shown in *D. magna* (Hatch and Burton 1999a). Chronic effects due to anthracene phototoxicity, like reduced fecundity, were reported by Holst and Giesy (1989). Genetic and ecological fitness were less severely impacted than clutch size and survivorship (Foran, Holst, and Giesy 1991).

Photoactivation of PAHs bioaccumulated in the benthic invertebrates *Lumbriculus variegatus* (an oligochaete) and *Hyalella azteca* (an amphipod) from contaminated field sediments can cause increased mortality (Ankley et al. 1994; Monson et al. 1995). UV exposure can increase the toxicity of PAH-contaminated sediments to the infaunal amphipods *Rhepoxynius abronius* and *Leptocheirus plumulosus*, decreasing survival and ability to rebury (Boese, Ozretich, Lamberson, Cole, Swartz, and Ferraro 2000). Exposure via water to fluoranthene and subsequently to UV radiation demonstrated increased mortality in *L. variegatus* as a function of both PAH dose in tissue and UV intensity (Ankley et al. 1995). Furthermore, the reported effects of fluoranthene photo-toxicity include reduced feeding efficiency of *H. azteca* (Hatch and Burton 1999a). The exposure to PAHs and UV radiation resulted in mortality of marine crab larvae (Peachey 2005). PAH phototoxicity can reduce survival and adult emergence in larvae of the mosquito *Aedes aegypti*, quite similar to phototoxic potency observed in highly carcinogenic benzo[a]pyrene and noncarcinogenic pyrene (Kagan and Kagan 1986).

Increased mortality due to phototoxicity of fluoranthene has been demonstrated in glochidial larvae of the freshwater mussel *Utterbackia imbecillis* exposed to waterborne PAH (Weinstein 2001) and in embryos of the marine bivalve *Mulinia lateralis* with body burden of PAH through maternal transfer from benthic adults (Pelletier, Burgess, Cantwell, Serbst, Ho, and Ryba 2000). In addition to fluoranthene, anthracene and pyrene as well as some petroleum products containing PAHs have displayed phototoxicity to larvae and juveniles of *M. lateralis* (Pelletier et al. 1997).

Juvenile bluegill sunfish (*Lepomis macrochirus*) kept in anthracene-contaminated water died upon exposure to sunlight in clean water, indicating photoactivation of PAH inside the organism rather than formation of toxic photo-products in the water (Bowling et al. 1983). Photo-enhaced toxicity of weathered crude oil was also observed in Pacific herring larvae only when oil was present in larval tissue, and it increased with increasing PAH tissue concentrations (Barron et al. 2003). Structural changes in gills and dorsal epidermis have been detected to result from anthracene phototoxicity (Oris and Giesy 1985), and the general disruption of cell membrane integrity and function including gills, blood, and other tissues, appears to be an important mode of acute phototoxicity in fish (Oris and Giesy 1985; McCloskey and Oris 1993). In juvenile fathead minnow (*Pimephales promelas*) respiratory stress has been indicated as the cause of death resulting from phototoxicity of fluoranthene, a disruption of mucosal cell

membrane function and integrity being the mode of phototoxic action (Weinstein, Oris, and Taylor 1997). Furthermore, studies using a cell line from fish gill indicated a specific action on lysosomes contributing to photocytotoxicity of PAHs (Schirmer, Chan, Greenberg, Dixon, and Bols 1998). Studies with fish liver microsomes (Choi and Oris 2000a) and fish hepatoma cell line (Choi and Oris 2000b) suggest that lipid peroxidation induced by reactive oxygen species is an important factor in the phototoxicity of anthracene to fish. Although reducing the reproductive output in fathead minnow as such, maternal transfer of anthracene in eggs with subsequent UV exposure can further decrease reproductive potential by decreasing hatching rate of eggs and causing teratogenic effects in fry (Hall and Oris 1991).

Phototoxicity of fluoranthene has been shown to reduce survival of the northern leopard frog larvae (*Rana pipiens*) (Monson et al. 1999), cause sublethal effects on locomotor behavior and signs of necrosis and structural alterations in the skin of the bullfrog larvae (*Rana catesbeiana*) (Walker, Taylor, and Oris 1998), and enhance teratogenic effects in the African clawed frog (*Xenopus laevis*) (Hatch and Burton 1998). Reduced survival of late embryonic stages of *R. pipiens* has been reported due to the phototoxicity of anthracene (Kagan et al. 1984).

Species vary in their sensitivity to the phototoxicity of PAHs (Boese et. al. 1997; Hatch and Burton 1998; Spehar, Poucher, Brooke, Hansen, Champlin, and Cox 1999), which could be related to behavioral (Hatch and Burton 1999b) and potentially to metabolic and morphological differences. Pigmentation in juvenile stages of some fish species has been related to lower risk to photoinduced toxicity as compared to species with translucent early life stages (Barron, Carls, Short, Rice, Heintz, Rau, and DiGiulio, 2005). Previous exposure of organisms to UV radiation can lead to development of protective mechanisms reducing their sensitivity (Boese et al. 1997). Photoprotective UV-absorbing compounds, such as mycosporine-like amino acids (MAAs) reported in various aquatic organisms (Karentz, McEuen, Land, and Dunlap 1991) might affect phototoxic potential by providing protection against UV exposure and possibly via antioxidant activity suggested for some MAA compounds (Dunlap and Yamamoto 1995). Carotenoid pigments may mitigate the effects of PAH phototoxicity by quenching singlet oxygen generated from PAH photosensitization (Gala and Giesy 1993). Furthermore, a possibility for repair of phototoxic effects has been demonstrated (Oris and Giesy 1986).

References

Allred, P.M. and Giesy, J.P. (1985) Solar radiation-induced toxicity of anthracene to *Daphnia pulex*. Environ. Toxicol. Chem. 4, 219–226.

Ankley, G.T., Collyard, S.A., Monson, P.D. and Kosian, P.A. (1994) Influence of ultraviolet light on the toxicity of sediments contaminated with polycyclic aromatic hydrocarbons. Environ. Toxicol. Chem. 13, 1791–1796.

Ankley, G.T., Erickson, R.J., Phipps, G.L., Mattson, V.R., Kosian, P.A., Sheedy, B.R. and Cox, J.S. (1995) Effects of light intensity on the phototoxicity of fluoranthene to a benthic macroinvertebrate. Environ. Sci. Technol. 29, 2828–2833.

Ankley, G.T., Erickson, R.J., Sheedy, B.R., Kosian, P.A., Mattson, V.R. and Cox, J.S. (1997) Evaluation of models for predicting the phototoxic potency of polycyclic aromatic hydrocarbons. Aquat. Toxicol. 37, 37–50.

Arfsten, D.P., Schaeffer, D.J. and Mulveny, D.C. (1996) The effects of near ultraviolet radiation on the toxic effects of polycyclic aromatic hydrocarbons in animals and plants: a review. Ecotox. Environ. Saf. 33, 1–24.

Barron, M.G., Little, E.E., Calfee, R. and Diamond, S. (2000) Quantifying solar spectral irradiance in aquatic habitats for the assessment of photoenhanced toxicity. Environ. Toxicol. Chem. 19, 920–925.

Barron, M.G., Carls, M.G., Short, J.W. and Rice, S.D. (2003) Photoenhanced toxicity of aqueous phase and chemically dispersed weathered Alaska North Slope crude oil to Pacific herring eggs and larvae. Environ. Toxicol. Chem. 22, 650–660.

Barron, M.C., Carls, M.G., Short, J.W., Rice, S.D., Heintz, R.A., Rau, M. and DiGiulio, R. (2005) Assessment of the phototoxicity of weathered Alaska North Slope crude oil to juvenile pink salmon. Chemosphere 60, 105–110.

Boese, B.L., Lamberson, J.O., Swartz, R.C. and Ozretich, R.J. (1997) Photoinduced toxicity of fluoranthene to seven marine benthic crustaceans. Arch. Environ. Contam. Toxicol. 32, 389–393.

Boese, B.L., Lamberson, J.O., Swartz, R.C., Ozretich, R. and Cole, F. (1998) Photoinduced toxicity of PAHs and alkylated PAHs to a marine infaunal amphipod (*Rhepoxynius abronius*). Arch. Environ. Contam. Toxicol. 34, 235–240.

Boese, B.L., Ozretich, R.J., Lamberson, J.O., Swartz, R.C., Cole, F.A., Pelletier, J. and Jones, J. (1999) Toxicity and phototoxicity of mixtures of highly lipophilic PAH compounds in marine sediment: Can the $\sum$PAH model be extrapolated? Arch. Environ. Contam. Toxicol. 36, 270–280.

Boese, B.L., Ozretich, R.J., Lamberson, J.O., Cole, F.A., Swartz, R.C. and Ferraro, S.P. (2000) Phototoxic evaluation of marine sediments collected from a PAH-contaminated site. Arch. Environ. Contam. Toxicol. 38, 274–282.

Boule, P., Bolte, M. and Richard, C. (1999) Phototransformations induced in aquatic media by NO_3^-/NO_2^-, Fe^{III} and humic substances. In: P. Boule (Ed.), *The handbook of environmental chemistry. Vol. 2 Part I. Environmental photochemistry*. Springer-Verlag, Berlin, pp. 181–215.

Bowling, J.W., Leversee, G.J., Landrum, P.F. and Giesy, J.P. (1983) Acute mortality of anthracene-contaminated fish exposed to sunlight. Aquat. Toxicol. 3, 79–90.

Bridges, D.H., Camp, B.J., Liningston, C.W., and Bailey, E.M. (1988) Kleingrass (*Panicum coloratum* L.) poisoning in sheep. Vet. Path. 24, 525–531.

Casteel, S.W., Rottinghaus, G.E., Hohson, G.C., and Wicklow, D.T. (1995) Liver disease in cattle induced by consumption of moldy hay. Vet. Hum. Toxicol. 37, 248–251.

Choi, J. and Oris, J.T. (2000a) Evidence of oxidative stress in bluegill sunfish (*Lepomis macrochirus*) liver microsomes simultaneously exposed to solar ultraviolet radiation and anthracene. Environ. Toxicol. Chem. 19, 1795–1799.

Choi, J. and Oris, J.T. (2000b) Anthracene photoinduced toxicity to PLHC-1 cell line (*Poeciliopsis lucida*) and the role of lipid peroxidation in toxicity. Environ. Toxicol. Chem. 19, 2699–2706.

Cleveland, L., Little, E.E., Calfee, R.D. and Barron, M.G. (2000) Photoenhanced toxicity of weathered oil to *Mysidopsis bahia*. Aquat. Toxicol. 49, 63–76.

Cody, T.E., Radike, M.J. and Warshawsky, D. (1984) The phototoxicity of benzo[a]pyrene in the green alga *Selenastrum capricornutum*. Environ. Res. 35, 122–132.

Cornick, J.L., Carter, G.K., and Bridges, C.H. (1988) Kleingrass-associated hepatoxicosis in horses. J. Am. Vet. Med. Assoc. 193, 932–935.

Davenport, R. and Spacie, A. (1991) Acute phototoxicity of harbor and tributary sediments from lower Lake Michigan. J. Great Lakes Res. 17, 51–56.

Daub, M.E. and Ehrenshaft, M. (2000) The photoactivated *Cercospora* toxin cercosporin: Contributions to plant disease and fundamental biology. Annu. Rev. Phytopathol. 38, 461–490.

Davenport, R., Johnson, L.R., Schaeffer, D.J. and Balbach, H. (1994) Phototoxicology. 1. Light-enhanced toxicity of TNT and some related compounds to *Daphnia magna* and *Lytechinus variagatus* embryos. Ecotoxicol. Environ. Saf. 27, 14–22.

Delaey, E., Vandenbougaerde, A., Merlevede, W., and de Witte, P. (2000) Photocyto-toxicity of hypericin in nomroxic and hypoxic conditions. J. Photochem. Photobiol. B: Biology 56, 19–24.

Diamond, S.A., Mount, D.R., Burkhard, L.P., Ankley, G.T., Makynen, E.A. and Leonard, E.N. (2000) Effect of irradiance spectra on the photoinduced toxicity of three polycyclic aromatic hydrocarbons. Environ. Toxicol. Chem. 19, 1389–1396.

Doss, M.O., Kuhnel, A., Gross, U., and Sieg, I. (1999) Hepatic porphyrias and alcohol. Medizinische Klinik 94, 314–328.

Downmum, K.R. (1992) Light-activated plant defence. New Phytol. 122, 401–420.

Dunlap, W.C. and Yamamoto, Y. (1995) Small-molecule antioxidants in marine organisms: antioxidant activity of mycosporine-glycine. Comp. Biochem. Physiol. 112B, 105–114.

Duxbury, C.L., Dixon, D.G. and Greenberg, B.M. (1997) Effects of simulated solar radiation on the bioaccumulation of polycyclic aromatic hydrocarbons by the duckweed *Lemna gibba*. Environ. Toxicol. Chem. 16, 1739–1748.

El-Alawi, Y.S., Huang, X.-D., Dixon, D.G. and Greenberg, B.M. (2002) Quantitative structure-activity relationship for the photoinduced toxicity of polycyclic aromatic hydrocarbons to the luminescent bacteria *Vibrio fischeri*. Environ. Toxicol. Chem. 21, 2225–2232.

Erickson, R.J., Ankley, G.T., DeFoe, D.L., Kosian, P.A. and Makynen, E.A. (1999) Additive toxicity of binary mixtures of phototoxic polycyclic aromatic hydrocarbons to the oligochaete *Lumbriculus variegatus*. Toxicol. Appl. Pharmacol. 154, 97–105.

Foran, J.A., Holst, L.L. and Giesy, J.P. (1991) Effects of photoenhanced toxicity of anthracene on ecological and genetic fitness of *Daphnia magna*: a reappraisal. Environ. Toxicol. Chem. 10, 425–427.

Frank, J. and Christiano, A.M. (1998) Variegate porphyria: past, present and future. Skin Pharmacol. Appl. Skin Physiol. 11, 310–320.

Freund, E. (1916) Über bisher noch nicht beschriebene kunstliche Hautverfarbungen. Dermatol. Wochenschrift 63, 931–933.

Gala, W.R. and Giesy, J.P. (1992) Photo-induced toxicity of anthracene to the green alga, *Selenastrum capricornutum*. Arch. Environ. Contam. Toxicol. 23, 316–323.

Gala, W.R. and Giesy, J.P. (1993) Using the carotenoid biosynthesis inhibiting herbicide, Fluridone, to investigate the ability of carotenoid pigments to protect algae from the photoinduced toxicity of anthracene. Aquat. Toxicol. 27, 61–70.

Gala, W.R. and Giesy, J.P. (1994) Flow cytometric determination of the photoinduced toxicity of anthracene to the green alga *Selenastrum capricornutum*. Environ. Toxicol. Chem. 13, 831–840.

Gauer, E.B., Doss, M.O., and Riemann, J.F. (1995) Erythrohepatic protoporphyria, a rare cause in the differential-diagnosis of parenchymatous jaundice. Deutsche Mediz. Wochenschr. 120, 713–717.

Gensemer, R.W., Dixon, D.G. and Greenberg, B.M. (1998) Amelioration of the photo-induced toxicity of polycyclic aromatic hydrocarbons by a commercial humic acid. Ecotoxicol. Environ. Saf. 39, 57–64.

Gensemer, R.W., Dixon, D.G. and Greenberg, B.M. (1999) Using chlorophyll *a* fluorescence to detect the onset of anthracene photoinduced toxicity in *Lemna gibba*, and the mitigating effects of a commercial humic acid. Limnol. Oceanogr. 44, 878–888.

Gross, U., Hoffmann, G.F., and Doss, M.O. (2000) Erythropoi9etic and hepatic porphyrias. J. Inherited Metabol. Dis. 23, 641–661.

Hansen, D.E., McCoy, R.D., Hedstrom, O.R., Snyder, S.P., and Ballerstedt, P.B. (1994) Photosensitization associated with exposure to *Pithomyces cartarum* in lambs. J. Vet. Med. Assoc. 204, 1668–1671.

Hall, A.T. and Oris, J.T. (1991) Anthracene reduces reproductive potential and is maternally transferred during long-term exposure in fathead minnows. Aquat. Toxicol. 19, 249–264.

Hatch, A.C. and Burton, G.A., Jr. (1998) Effects of photoinduced toxicity of fluoranthene on amphibian embryos and larvae. Environ. Toxicol. Chem. 17, 1777–1785.

Hatch, A.C. and Burton, G.A., Jr. (1999a) Phototoxicity of fluoranthene to two freshwater crustaceans, *Hyalella azteca* and *Daphnia magna*: measures of feeding inhibition as a toxicological endpoint. Hydrobiol. 400, 243–248.

Hatch, A.C. and Burton, G.A., Jr. (1999b) Photo-induced toxicity of PAHs to *Hyalella azteca* and *Chironomus tentans*: effects of mixtures and behavior. Environ. Pollut. 106, 157–167.

Holst, L.L. and Giesy, J.P. (1989) Chronic effects of photoenhanced toxicity of anthracene on *Daphnia magna* reproduction. Environ. Toxicol. Chem. 8, 933–942.

Huang, X.-D., Dixon, D.G. and Greenberg, B.M. (1993) Impacts of UV radiation and photomodification on the toxicity of PAHs to the higher plant *Lemna gibba* (duckweed). Environ. Toxicol. Chem. 12, 1067–1077.

Huang, X.-D., Krylov, S.N., Ren, L., McConkey, B.J., Dixon, D.G. and Greenberg, B.M. (1997a) Mechanistic quantitative structure-activity relationship model for the photoinduced toxicity of polycyclic aromatic hydrocarbons. II. An empirical model for the toxicity of 16 polycyclic aromatic hydrocarbons to the duckweed *Lemna gibba* L. G-3. Environ. Toxicol. Chem. 16, 2296–2303.

Huang, X.-D., McConkey, B.J., Babu, T.S. and Greenberg, B.M. (1997b) Mechanisms of photoinduced toxicity of photomodified anthracene to plants: inhibition of photosynthesis in the aquatic higher plant *Lemna gibba* (duckweed). Environ. Toxicol. Chem. 16, 1707–1715.

Huovinen, P.S., Penttilä, H. and Soimasuo, M.R. (2000) Penetration of UV radiation into Finnish lakes with different characteristics. Int. J. Circumpolar Health 59, 15–21.

Huovinen P.S., Soimasuo M.R. and Oikari, A.O.J. (2001) Photoinduced toxicity of retene to *Daphnia magna* under enhanced UV-B radiation. Chemosphere 45, 683–691.

Ireland, D.S., Burton, G.A., Jr. and Hess, G.G. (1996) *In situ* toxicity evaluations of turbidity and photoinduction of polycyclic aromatic hydrocarbons. Environ. Toxicol. Chem. 15, 574–581.

Jalal, M.A.F., Hossain, M.B., Robeson, D.I., and van der Helm, D. (1992) *Cercospora beticola* phytotoxins: cebetins that are photoactive, Mg^{2+}-binding, chlorinated anthraquinone-xanthone conjugates. J. Am. Chem.Soc. 114, 5967–5971.

Kagan, J. and Kagan, E.D. (1986) The toxicity of benzo[a]pyrene and pyrene in the mosquito *Aedes aegypti,* in the dark and in the presence of ultraviolet light. Chemosphere 15, 243–251.

Kagan, J., Kagan, P.A. and Buhse, H.E., Jr. (1984) Light-dependent toxicity of *α*-terthienyl and anthracene toward late embryonic stages of *Rana pipiens*. J. Chem. Ecol. 10, 1115–1122.

Kagan, J., Bennett, W.J., Kagan, E.D., Maas, J.L., Sweeney, S.A., Kagan, I.A., Seigneurie, E. and Bindokas, V. (1987) *α*-Terthienyl as a photoactive insecticide: toxic effects on nontarget organisms. In: J.R. Heitz and K.R. Downum (Eds.), *Light-activated pesticides*. ACS Symposium Series 339. Washington, D.C., American Chemical Society. pp. 176–191.

Karentz, D., McEuen, F.S., Land, M.C. and Dunlap, W.C. (1991) Survey of mycosporine-like amino acid compounds in Antarctic marine organisms: potential protection from ultraviolet exposure. Mar. Biol. 108, 157–166.

Kelch, W.R., Kerr, I.A., Adair, H.S., and Boyd, G.D. (1992) Suspected buttercup (*Ranunculus bulbosus*) toxicosis with secondary photosensitization in Charolais heifer. Vet. Hum.Toxicol. 34, 238–239.

Kirk J.T.O. (1994) Optics of UV-B radiation in natural waters. Arch. Hydrobiol. Beih. Ergebn. Limnol. 43, 1–16.

Kosian, P.A., Makynen, E.A., Monson, P.D., Mount, D.R., Spacie, A., Mekenyan, O.G. and Ankley, G.T. (1998) Application of toxicity-based fractionation techniques and structure-activity relationship models for the identification of phototoxic polycyclic aromatic hydrocarbons in sediment pore water. Environ. Toxicol. Chem. 17, 1021–1033.

Krylov, S.N., Huang, X.-D., Zeiler, L.F., Dixon, D.G. and Greenberg, B.M. (1997) Mechanistic quantitative structure-activity relationship model for the photoinduced toxicity of polycyclic aromatic hydrocarbons: I. Physical model based on chemical kinetics in a two-compartment system. Environ. Toxicol. Chem. 16, 2283–2295.

Lampi, M.A., Gurska, J., McDonald, K.I.C., Xie, F., Huang, X.-D., Dixon, D.G. and Greenberg, B.M. (2006) Photoinduced toxicity of polycyclic aromatic hydrocarbons to *Daphnia magna*: Ultraviolet-mediated effects and the toxicity of polycyclic aromatic hydrocarbon photoproducts. Environ. Toxicol. Chem. 25, 1079–1087.

Landrum, P.F., Giesy, J.P., Oris, J.T. and Allred, P.M. (1987) Photoinduced toxicity of polycyclic aromatic hydrocarbons to aquatic organisms. In: J.H. Vandermeulen and S.E. Hrudey (Eds.), *Oil in freshwater: chemistry*, *biology*, *countermeasure technology*. Proc. Symp. Oil Pollution in Freshwater, Edmonton, Alberta, Canada. Pergamon Press, New York, pp. 304–318.

Larson, R.A. and Berenbaum, M.R. (1988) Environmental phototoxicity. Solar ultraviolet radiation affects the toxicity of natural and man-made chemicals. Environ. Sci. Technol. 22, 354–360.

Lean, D. (1998) Attenuation of solar radiation in humic waters. In: D.O. Hessen and L.J. Tranvik (Eds.), *Aquatic humic substances. Ecology and biogeochemistry. Ecol. Studies 133*. Springer-Verlag, Berlin, pp.109–124.

Little, E.E., Cleveland, L., Calfee, R. and Barron, M.G. (2000) Assessment of the photoenhanced toxicity of a weathered oil to the tidewater silverside. Environ. Toxicol. Chem. 19, 926–932.

Lovell, C.R. (1993) Plants and the skin. Blackwell Scientific Publ., Oxford.

Mallakin, A., McConkey, B.J., Miao, G., McKibben, B., Snieckus, V., Dickson, D.G. and Greenberg, B.M. (1999) Impacts of structural photomodification on the toxicity of

environmental contaminants: anthracene photooxidation products. Ecotoxicol. Environ. Saf. 43, 204–212.

Marwood, C.A., Smith, R.E.H., Solomon, K.R., Charlton, M.N. and Greenberg, B.M. (1999) Intact and photomodified polycyclic aromatic hydrocarbons inhibit photosynthesis in natural assemblages of Lake Erie phytoplankton exposed to solar radiation. Ecotoxicol. Environ. Saf. 44, 322–327.

McCloskey, J.T. and Oris, J.T. (1993) Effect of anthracene and solar ultraviolet radiation exposure on gill ATPase and selected hematologic measurements in the bluegill sunfish (*Lepomis macrochirus*). Aquat. Toxicol. 24, 207–218.

McConkey, B.J., Duxbury, C.L., Dixon, D.G. and Greenberg, B.M. (1997) Toxicity of a PAH photooxidation product to the bacteria *Photobacterium phosphoreum* and the duckweed *Lemna gibba*: Effects of phenanthrene and its primary photoproduct, phenanthrenequinone. Environ. Toxicol. Chem. 16, 892–899.

McDonald, B.G. and Chapman, P.M. (2002) PAH phototoxicity—an ecologically irrelevant phenomenon? Mar. Poll. Bull. 44, 1321–1326.

Mekenyan, O.G., Ankley, G.T., Veith, G.D. and Call, D.J. (1994) QSARs for photoinduced toxicity: I. Acute lethality of polycyclic aromatic hydrocarbons to *Daphnia magna*. Chemosphere 28, 567–582.

Mezey, P.G., Zimpel, Z., Warburton, P., Walker, P.D., Irvine, D.G., Huang, X.-D., Dixon, D.G. and Greenberg, B.M. (1998) Use of quantitative shape-activity relationships to model the photoinduced toxicity of polycyclic aromatic hydrocarbons: Electron density shape features accurately predict toxicity. Environ. Toxicol. Chem. 17, 1207–1215.

Miles, C.O., Wilkins, A.L., Erasmus, G.L., Kellerman, T.S., and Coetzer, J. (1994) Photosensitivity in South Africa. 7. Chemical composition of biliary crystals from a sheep with experimentally induced geeldikkop. Onderstepoort J. Vet. Res. 61, 215–222.

Miranda, M.A. (ed.) (2001) Phototoxicity of drugs: A decade of non-steroidal anti-inflammatory 2-arylpropionic acids research. Downloadable from the Photochemistry and Photobiology homepage.

Monson, P.D., Ankley, G.T. and Kosian, P.A. (1995) Phototoxic response of *Lumbriculus variegatus* to sediments contaminated by polycyclic aromatic hydrocarbons. Environ. Toxicol. Chem. 14, 891–894.

Monson, P.D., Call, D.J., Cox, D.A., Liber, K. and Ankley, G.T. (1999) Photoinduced toxicity of fluoranthene to northern leopard frogs (*Rana pipiens*). Environ. Toxicol. Chem. 18, 308–312.

Morris, D.P., Zagarese, H., Williamson, C.E., Balseiro, E.G., Hargreaves, B.R., Modenutti, B., Moeller, R. and Queimalinos, C. (1995) The attenuation of solar UV radiation in lakes and the role of dissolved organic carbon. Limnol. Oceanogr. 40, 1381–1391.

Morris, D.P. and Hargreaves, B.R. (1997) The role of photochemical degradation of dissolved organic carbon in regulating the UV transparency of three lakes on the Pocono Plateau. Limnol. Oceanogr. 42, 239–249.

Muchiri, D.J., Bridges, C.H., Ueckert, D.N., and Bailey, E.M. (1980) Photosensitization of sheep on kleingrass pasture. J. Am. Vet. Sci. Assoc. 177, 353–354.

Neff, J.M. (1979) *Polycyclic aromatic hydrocarbons in the aquatic environment. Sources, fates and biological effects*. Applied Science Publishers Ltd., London.

Neff, J.M. (1985) Polycyclic aromatic hydrocarbons. In: G.M. Rand and S.R. Petrocelli (Eds.), *Fundamentals of aquatic toxicology. Methods and applications*. Hemisphere Publishing Corporation, New York. pp. 416–454.

Newsted, J.L. and Giesy, J.P. (1987) Predictive models for photoinduced acute toxicity of polycyclic aromatic hydrocarbons to *Daphnia magna*, Strauss (Cladocera, Crustacea). Environ. Toxicol. Chem. 6, 445–461.

Oris, J.T. and Giesy, J.P., Jr. (1985) The photoenhanced toxicity of anthracene to juvenile sunfish (*Lepomis* spp.). Aquat. Toxicol. 6, 133–146.

Oris, J.T. and Giesy, J.P., Jr. (1986) Photoinduced toxicity of anthracene to juvenile bluegill sunfish (*Lepomis macrochirus* Rafinesque): photoperiod effects and predictive hazard evaluation. Environ. Toxicol. Chem. 5, 761–768.

Oris, J.T., Hall, A.T. and Tylka, J.D. (1990) Humic acids reduce the photo-induced toxicity of anthracene to fish and daphnia. Environ. Toxicol. Chem. 9, 575–583.

Pathak, M.A. (1986) Phytodermatitis. Clin. Dermatol. 4, 102–121.

Pathak, M.A. and Fitzpatrick, T.B. (1992) The evolution of photochemotherapy with psoralens and UVA (PUVA): 2000 BC to 1992 AD. J. Photochem. Photobiol. B: Biolog 14, 3–22.

Peachey, R.B.J. (2005) The synergism between hydrocarbon pollutants and UV radiation: A potential link between coastal pollution and larval mortality. J. Exp. Mar. Biol. Ecol. 315, 103–114.

Pelletier, M.C., Burgess, R.M., Ho, K.T., Kuhn, A., McKinney, R.A. and Ryba, S.A. (1997) Phototoxicity of individual polycyclic aromatic hydrocarbons and petroleum to marine invertebrate larvae and juveniles. Environ. Toxicol. Chem. 16, 2190–2199.

Pelletier, M.C., Burgess, R.M., Cantwell, M.G., Serbst, J.R., Ho, K.T. and Ryba, S.A. (2000) Importance of maternal transfer of the photoreactive polycyclic aromatic hydro-carbon fluoranthene from benthic adult bivalves to their pelagic larvae. Environ. Toxicol. Chem. 19, 2691–2698.

Pelletier, E., Sargian, P. and Demers, S. (2006) Ecotoxicological effects of combined UVB and organic contaminants in costal waters: A review. Photochem. Photobiol. 82, 981–993.

Puoli, J.R., Reid, R.I., and Belesky, D.P. (1992) Photosensitization in lambs grazing switchgrass. Agron. J. 84, 1077–1080.

Raposo, J.B., Mendez, M.C., de Adrade, B.B., and Riet-Correa, F. (1998) Experimental intoxication by *Myoporum kaetyn* in cattle. Vet. Hum. Toxicol. 40, 275–277.

Regnault, T.R.H. (1990) Secondary photosensitization of sheep grazing bambatsi grass (Panicum coloratum var. makarikariense). Aust. Vet. J. 67, 419.

Samadi, A., Martinez, L.A., Miranda, M.A., and Morera, I.M. (2001) Mechanism of lipid peroxidation photosensitized by tiaprofenic acid: Product studies using linoleic acid and 1,4-cyclohexadienes as model substrates Photochem. Photobiol. 73, 359–365.

Sargian, P., Mostajir, B., Chatila, K., Ferreyra, G.A., Pelletier, E. and Demers, S. (2005) Non-synergistic effects of water-soluble crude oil and enhanced ultraviolet-B radiation on a natural plankton assemblage. Mar. Ecol. Progr. Ser. 294, 63–77.

Schaeffer, D.J. and Larson, R.A. (1999) Phototoxicology. The Chemist July-Aug., 18–24.

Schirmer, K., Chan, A.G.J., Greenberg, B.M., Dixon, D.G. and Bols, N.C. (1998) Ability of 16 priority PAHs to be photocytotoxic to a cell line from the rainbow trout gill. Toxicology 127, 143–155.

Schirmer, K., Herbrick, J.-A.S., Greenberg, B.M., Dixon, D.G. and Bols, N.C. (1999) Use of fish gill cells in culture to evaluate the cytotoxicity and photocytotoxicity of intact and photomodified creosote. Environ. Toxicol. Chem. 18, 1277–1288.

Scully, N.M. and Lean, D.R.S. (1994) The attenuation of ultraviolet radiation in temperate lake. Arch. Hydrobiol. Beih. Ergebn. Limnol. 43, 135–144.

Scruggs, D.W. and Blue, G.K. (1994) Toxic hepatopathy and photosensitization in cattle fed moldy alfalfa hay. J. Am. Vet. Med. Assoc. 204, 264–266.

Sheth, A.P, Esterly, N.B., Rabinowitz, I.G., and Poh-Fitzpatrick, M.B. (1994) Cutaneous porphyria-like photosensitivity after liver transplantation. Arch. Dermatol. 130, 614–617.

Smith, R.C., Prézelin, B.B., Baker, K.S., Bidigare, R.R., Boucher, N.P., Coley, T., Karentz, D., MacIntyre, S., Matlick, H.A., Menzies, D., Ondrusek, M., Wan, Z. and Waters, K.J. (1992) Ozone depletion: ultraviolet radiation and phytoplankton biology in Antarctic waters. Science 255, 952–959.

Southerland, H.A. and Lewitus, A.J. (2004) Physiological responses of estuarine phytoplankton to ultraviolet light-induced fluoranthene toxicity. J. Exp. Mar. Biol. Ecol. 298, 303–322.

Spehar, R.L., Poucher, S., Brooke, L.T., Hansen, D.J., Champlin, D. and Cox, D.A. (1999) Comparative toxicity of fluoranthene to freshwater and saltwater species under fluorescent and ultraviolet light. Arch. Environ. Contam. Toxicol. 37, 496–502.

Stoessl, A., Abramowski, Z., Lester, H.H., Rock, G.L., Towers, G.H.N. (1990) Further toxic properties of the fungal metabolite dothistromin. Mycopathologia 112, 179–186.

Swartz, R.C., Ferraro, S.P., Lamberson, J.O., Cole, F.A., Ozretich, R.J., Boese, B.L., Schults, D.W., Behrenfeld, M. and Ankley, G.T. (1997) Photoactivation and toxicity of mixtures of polycyclic aromatic hydrocarbon compounds in marine sediment. Environ. Toxicol. Chem. 16, 2151–2157.

Todd, D.J. (1994) Erythropoietic protoporphyria. Br. J. Dermatol. 131, 751–766.

Veith, G.D., Mekenyan, O.G., Ankley, G.T. and Call, D.J. (1995) A QSAR analysis of substituent effects on the photoinduced acute toxicity of PAHs. Chemosphere 30, 2129–2142.

Walker, S.E., Taylor, D.H. and Oris, J.T (1998) Behavioral and histopathological effects of fluoranthene on bullfrog larvae (*Rana catesbeiana*). Environ. Toxicol. Chem. 17, 734–739.

Weinstein, J.E. (2001) Characterization of the acute toxicity of photoactivated fluoranthene to glochidia of the freshwater mussel, *Utterbackia imbecillis*. Environ. Toxicol. Chem. 20, 412–419.

Weinstein, J.E. and Oris, J.T. (1999) Humic acids reduce the bioaccumulation and photoinduced toxicity of fluoranthene to fish. Environ. Toxicol. Chem. 18, 2087–2094.

Weinstein, J.E., Oris, J.T. and Taylor, D.H. (1997) An ultrastructural examination of the mode of UV-induced toxic action of fluoranthene in the fathead minnow, *Pimephales promelas*. Aquat. Toxicol. 39, 1–22.

Wernersson, A.-S. (2003) Predicting petroleum phototoxicity. Ecotoxicol. Environ. Saf. 54, 355–365.

Wilkins, A.L., Miles, C.O., DeKock, W.T., Erasmus, G.L., Basson, A.T., and Kellerman, T.S. (1996) Photosensitivity in South Africa. 9. Structure elucidation of a α-glucosidase-treated saponin from *Tribulus terrestris*, and the identification of saponin chemotypes of South African *T. terrestris*. Onderstepoort J. Vet. Res. 63, 327–334.

Williamson, C.E., Stemberger, R.S., Morris, D.P., Frost, T.M. and Paulsen, S.G. (1996) Ultraviolet radiation in North American lakes: Attenuation estimates from DOC measurements and implications for plankton communities. Limnol. Oceanogr. 41, 1024–1034.

Zaga, A., Little, E.E., Rabeni, C.F. and Ellersieck, M.R. (1998) Photoenhanced toxicity of a carbamate insecticide to early life stage anuran amphibians. Environ. Toxicol. Chem. 17, 2543–2553.

19
Ozone Depletion and the Effects of Ultraviolet Radiation

Lars Olof Björn and Richard L. McKenzie

Abstract: Because of the stratospheric ozone depletion that took place during the last decades of the past century, the effects of ultraviolet radiation on plants, animals, humans, and microorganisms became intensively studied. In this chapter we describe the role of the ozone layer as a radiation shield and various molecular and organismal effects of ultraviolet radiation, with an emphasis on the UV-B band (280–315 nm), which is strongly affected by the ozone content of the atmosphere. Also, physiological protection mechanisms and repair systems are briefly treated.

19.1. Introduction

The fear of increased ultraviolet radiation at the earth's surface in connection with depletion of stratospheric ozone caused by human activities has spurred not only diplomatic activity and political action, but also the investigation of ultraviolet radiation effects on biological systems, from cells to the biosphere as a whole. What has emerged is also a greatly increased understanding of daylight ultraviolet radiation as an ecological and health factor under natural conditions.

A great number of reviews and special volumes of books and journals on this subject have seen the light in recent years, such as Young et al. (1993), Lumsden (1997), Rozema (1999), and Rozema et al. (1997a, 2001). In fulfilment of the Montreal Protocol, the United Nations Environmental Protection Programme (UNEP) regularly evaluates the biological consequences of ozone depletion, and some of the reports from these evaluations are now available as special journal issues (van der Leun et al. 1995, 1999, 2003, 2007). Several popular-science books deal with the subject, e.g., Nilsson (1996). The field has even been considered interesting enough for scientists dealing with the sociology of the scientific process (Nolin 1995), and has resulted in an account of the negotiations involved in saving the ozone layer by one of the main actors (Benedick 1991, 1998). Velders et al. (2007) show that the Montreal Protocol has been important also for climate protection.

After a few words about ozone and ozone depletion and how it affects ultraviolet radiation, we shall start with a short account of some effects of ultraviolet radiation at the molecular level and go on to higher levels of biological organization.

19.2. The Ozone Layer

Ozone, O_3, is formed from oxygen, O_2, by the action of ultraviolet-C (UV-C) radiation in the 175- to 242-nm band in the stratosphere. The high-energy UV-C photons first split some of the oxygen molecules into free oxygen atoms, O, which then combine with oxygen to form ozone. Most of the ozone is present at an altitude of 20–30 km, but some of it extends down to ground level. The ozone molecules very efficiently absorb UV-B radiation (of much higher fluence rate than the UV-C) and are thereby split again into free oxygen molecules. The strong absorption of UV-B radiation in ozone molecules causes heating of the air, and layers higher up in the stratosphere, where the radiation is stronger, are heated more than the lower layers. This results in a lower density of the upper layers and is the reason that the stratosphere, in contrast to the lower atmosphere (troposphere), is stratified, with very little vertical movement of air.

The absorption maximum of ozone is at practically the same wavelength as that of DNA, and ozone protects DNA very efficiently from the radiation from the sun (Fig. 19.1).

It is only at the long-wavelength edge of the ozone absorption band that sufficient radiation leaks through to interact with the long-wavelength edge of the DNA absorption band, as well as with other cell constitutents. There is more ozone at high latitudes than near the equator (Fig. 19.2). The average solar zenith angle is also greater at high latitudes (i.e., the average solar elevation above the horizon during the day is lower), and both of these circumstances contribute to a much lower yearly UV-B exposure at high latitudes compared to the tropics (Fig. 19.3).

The ozone column (the total amount of ozone from ground level to space) varies over the year, and both amplitude and phase are latitude dependent. In the northern hemisphere the variation can be described by:

$$(\text{ozone column} - \text{yearly average}) = 0.07 \cdot (La + 10)/90 \cdot cos((Dn - 90 -$$
$$(44 - La) \cdot 3.1) \cdot 2 \cdot \pi/365.25)$$

dobson units (DU) for latitudes lower than 44°N, and

$$(\text{ozonecolumn} - \text{yearlyaverage}) =$$
$$0.07 \cdot (La + 10)/90 \cdot cos((Dn - 90) \cdot 2 \cdot \pi/365.25)$$
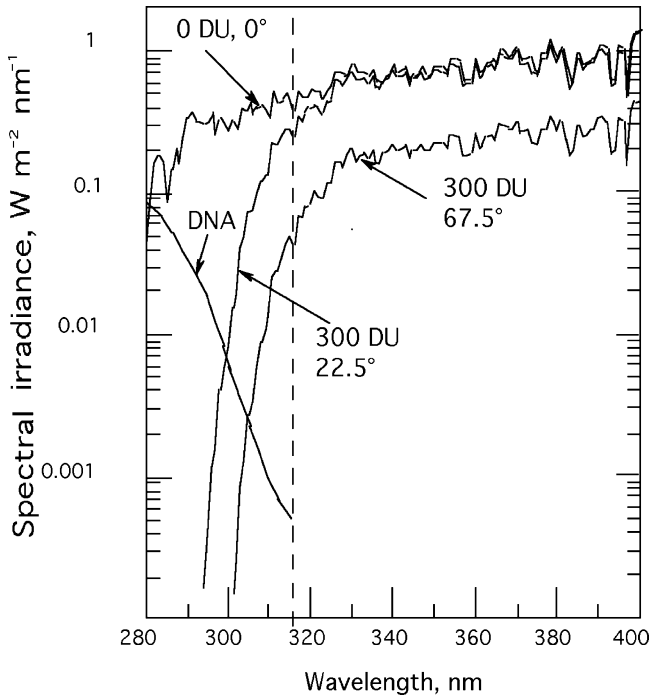
FIGURE 19.1. Spectrum of UV spectral irradiance for several observing conditions. Note the logarithmic scale. 300 DU (Dobson units) of ozone is an amount corresponding to a 3-mm-thick layer of pure ozone at a pressure of 1 bar and a temperature of 0°C. The dashed vertical line marks the limit between UV-A radiation (315–400 nm) and UV-B radiation (280–315 nm). Ozone has appreciable absorption in the UV-B band, but only a small effect on UV-A radiation. Therefore, the difference between the curves in the UV-A band corresponds mainly to the cos(solar zenith angle) factor.

DU for La >44°N, where La is the latitude in degrees and Dn the day number (January $1 = 1$). These equations can be used to estimate the expected column (total) ozone once you know the yearly average (Fig. 19.2), but does not take recent changes into account. For more recent values, go to NASA's website "Ozone over your house" http://toms.gsfc.nasa.gov/teacher/ozone_overhead_v8.html

The ozone colum is also affected by the rhythms of the sun. The changes due to the 11-year cycle are rather small, about 1.5–2% (Reid 1999). Although the sun radiates more ultraviolet radiation at a sunspot maximum than when the sun is "quiet," the change is much larger in the ozone-forming UV-C band than in the UV-B band, and therefore the net effect is to make the UV-B fluence rate at ground level slightly less at a "solar maximum." The effects due to changes in ozone transport are larger than the direct effect (Labitzke and van Loon 1997). Larger changes are likely to take place over longer solar cycles (Lean and Rind 1999). From the viewpoint of UV-B conditions at ground level,
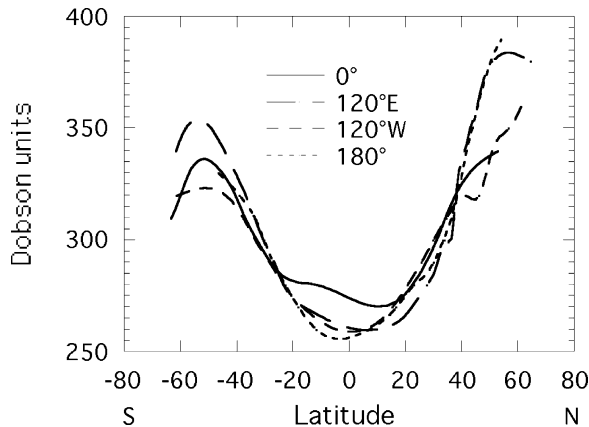
FIGURE 19.2. The latitudinal distribution of average ozone at three different longitudes (data from Labitzke and van Loon 1997). The values are averaged for all seasons over the years 1979–1993. Ozone formed near the equator is transported to higher latitudes, resulting in high values there, but at the highest latitudes anthropogenic depletion lowers the values. The ozone layer is subject to natural annual variations, as well as to anthropogenic and natural long-term changes.

the variations in cloudiness brought about by solar influence on the terrestrial magnetosphere and thus on cosmic ray flux are probably more important than the ozone variations in both 11-year and long-term perspectives, but as yet they are largely unexplored. Concerning the ozone layer and UV radiation in the past, see Björn and McKenzie (2007).

19.3. Ozone Depletion

Thus ozone is continuously formed by UV-C radiation and decomposed again by UV-B radiation. There are also other processes involved in the natural dynamics of the ozone layer. But this situation has been disturbed by emission of artificially generated substances, mainly organic halogen compounds and nitrogen oxides.

Many organic halogen compounds, such as the chlorofluorocarbons (CFCs), are very inert substances as long as they stay in the troposphere, but when they eventually reach sufficient altitude in the stratosphere they are decomposed by the UV-C radiation there and produce free halogen atoms. Of these, fluorine atoms are of minor interest, but both chlorine and bromine react with "odd oxygen" (O as well as O_3) and form monoxides: $Cl + O ==> ClO$ and $Cl + O_3 ==> ClO + O_2$. Nitrogen monoxide functions in an analogous way: $NO + O ==> NO_2$; $NO + O_3 ==> NO_2 + O_2$. These substances thus both destroy ozone already present and prevent formation of new ozone by sweeping up the free oxygen atoms. Still, this would not be catastrophic in itself if the ozone-depleting substances would themselves be depleted by the process. However, the following reactions also take place: $ClO + O ==> Cl + O_2$; $NO_2 + O ==> NO + O_2$. In other words, through
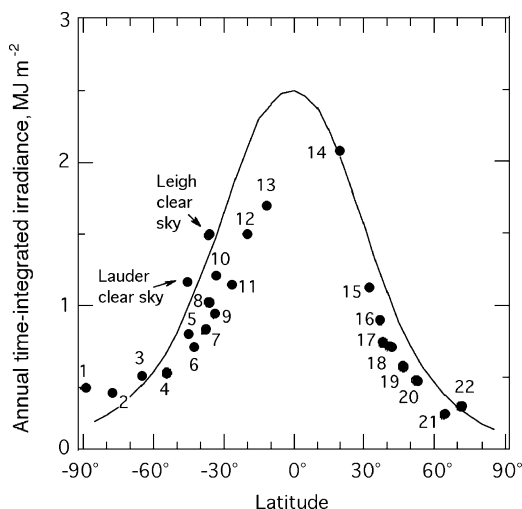
FIGURE 19.3. Latitude and cloud dependence of daylight UV-B radiation. The diagram shows (solid line) the annual erythemally active radiation (time-integrated irradiance) for various latitudes calculated for cloud free conditions and (numbered symbols) the actually measured values at different locations. The difference is mainly due to clouds. Note that clouds can increase the irradiance under certain conditions, which is particularly evident at high southern latitudes. For Lauder and Leigh clear sky values were also estimated from measurements on cloud-free days. The numbers represent the following locations: 1 South Pole, 2 McMurdo, 3 Palmer, 4 Ushuaia (Tierra del Fuego), 5 Lauder (New Zealand), 6 Hobart (Tasmania), 7 Melbourne, 8 Leigh (New Zealand), 9 Sydney, 10 Perth, 11 Brisbane, 12 Alice Springs, 13 Darwin, 14 Mauna Loa (Hawaii), 15 San Diego, 16 Kos (Greece), 17 Athens (Greece), 18 Thessaloniki, 19 Garmisch-Partenkirchen, 20 Oxford (England), 21 Reykjavik, 22 Barrow (Alaska).

reactions which further deplete the stratosphere of ozone-forming free oxygen, the ozone-destroying substances are regenerated; a chain reaction results. It has been estimated that a single halogen atom may destroy thousands of ozone molecules before it finally undergoes a chain-ending reaction of some kind. When we remember that the amount of ozone is so small, corresponding to about 3 mm of the whole atmosphere (or 6 g out of the 10 tons of air on a square meter), it is understandable that the effect is serious. The ozone hole over Antarctica, which started to develop in the early 1970s and appears every antarctic spring, is well-known, but it is less well known that depletion has taken place everywhere in the world except near the equator, and that it is quite significant even in some populated parts of the world (Fig, 19.4).

The ozone layer has, at least for the time being, ceased to thin. However, in some places (not everywhere), there is still an upward trend in UV-B radiation. In some places (such as mid-Sweden; Fig. 19.5) this seems to be due to changes in cloud cover associated with the global climate change. In other places it can be due to decreased aerosol or decreased tropospheric ozone due to better control of air pollution. A prediction of the future development of the ozone layer is

**Mean Summer Ozone and Estimated UV Index
Lauder, New Zealand**
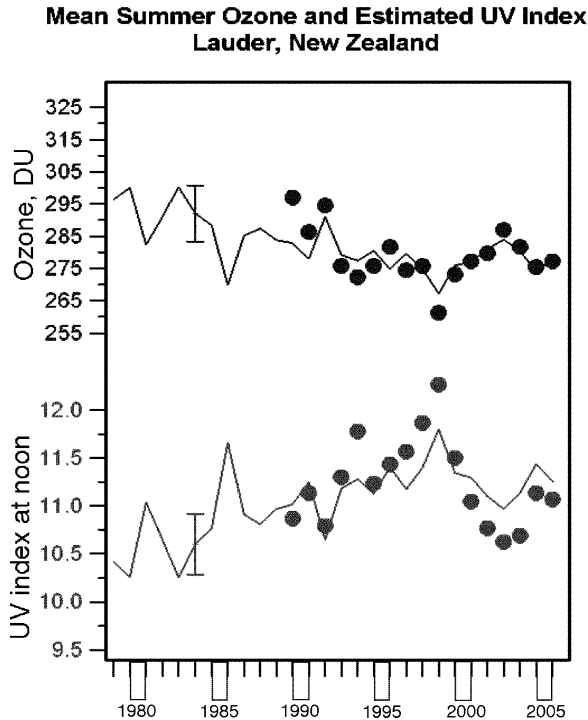
FIGURE 19.4. Changes in summertime ozone over the South Island of New Zealand since 1980 (upper panel) and the corresponding change in biologically active ultraviolet radiation over the same time period (lower panel). The lines show satellite-derived ozone and the calculated changes in UV that would result from those ozone changes. The symbols show results from spectrometer measurements averaged for the 5 peak UV days in the summer months (Dec+Jan+Feb). The decline in ozone that occurred during the 1980s and 1990s has not been sustained in more recent years.

shown in Fig. 19.6. However, in a long-term perspective the future of the ozone layer is uncertain, due to interactions between ozone and climate. Increases in greenhouse gases lead not only to increased surface temperatures, but also to decreased stratospheric temperatures, and this affects the ozone layer. In addition to forcasting the future of the ozone layer, attempts have been made to probe its distant past (Björn and McKenzie 2007).

19.4. Molecular Effects of UV-B Radiation

We shall describe the most important effects on the molecular level. As an example of the large number of effects, Fig. 19.7 gives an overview of UV-B effects on plants. Some of these effects are common to all organisms, while others are specific to plants. Some of the effects of special relevance to man are dealt with in Chapter 21.
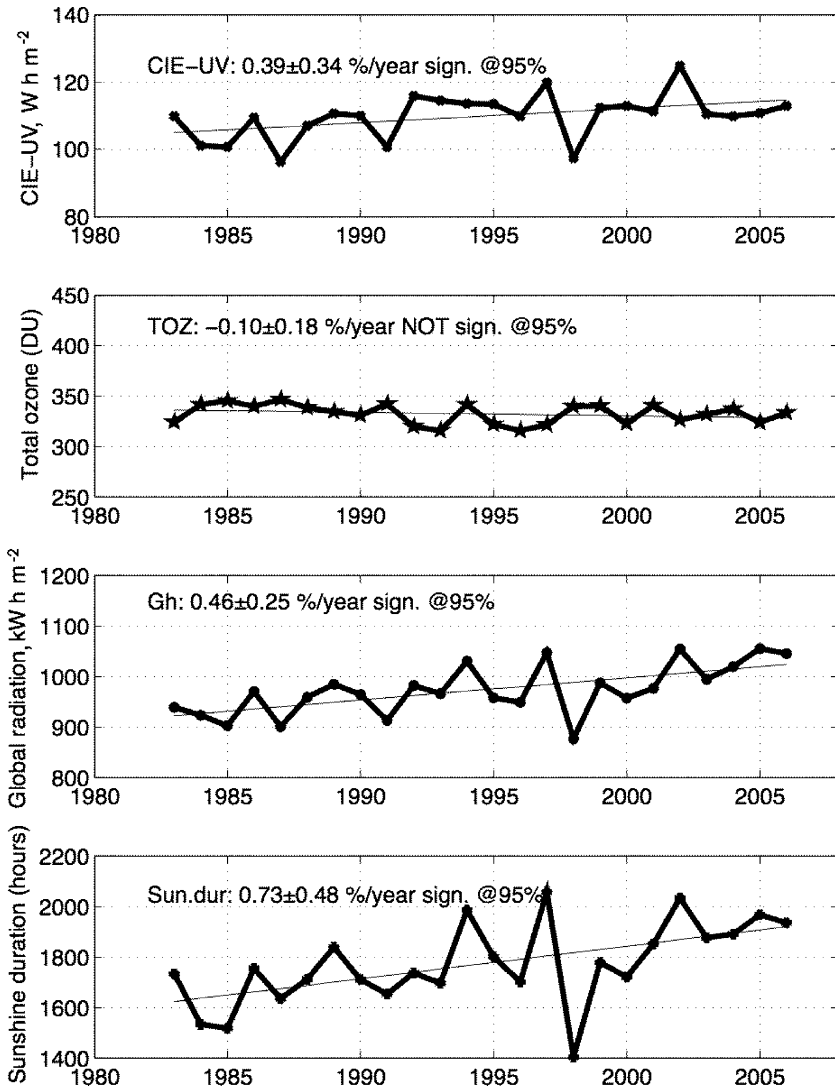
FIGURE 19.5. Measurements of various components of daylight, ozone, and sunshine duration over south Sweden (58.4°N) from 1980 to 2006. CIE refers to a weighting spectrum resembling the action spectrum for skin damage. The figure shows that the ozone layer does not decrease much during the period, and the ultraviolet radiation increases to about the same extent as other daylight components. The change is attributed mainly to changed cloudiness. (Courtesy Weine Josefsson and the Swedish Meteorological and Hydrological Institute [SMHI].)
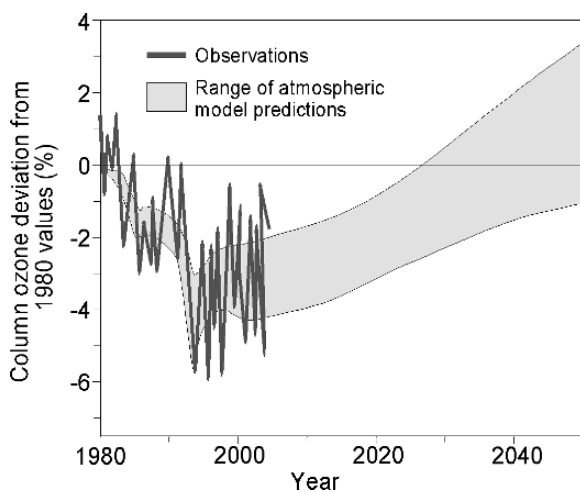
FIGURE 19.6. Projected future of the ozone layer. The future is uncertain, both because of uncertainty in the models and because it depends on political decisions. (From IPCC 2005.)
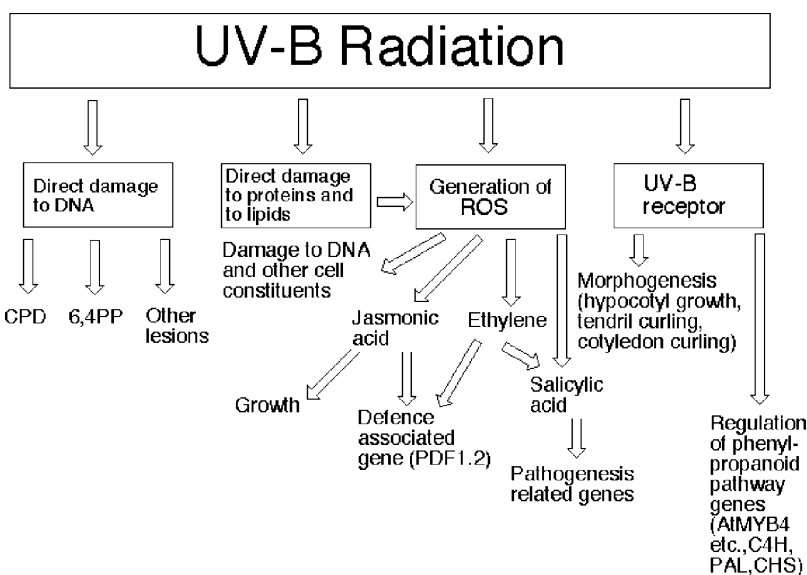
FIGURE 19.7. Overview of molecular effects of UV-B radiation on plants. ROS stands for reactive oxygen species (such as $HO^{\bullet}$, H_2O_2, O_2^{-}, and $^1O_2$).

19.4.1. Effects of Ultraviolet Radiation on DNA

Ultraviolet radiation directly absorbed by DNA (which may be UV-B under natural conditions, but also UV-C under experimental or otherwise artificial circumstances) can elicit a number of different lesions, but the great majority are either dimerisation or adduct formation affecting only adjacent pyrimidine bases (thymine and cytosine) on one DNA strand. The dimerization products are referred to as cyclobutane pyrimidine dimers (CPDs) and the adducts, properly termed 6-4[pyrimidine-2´-one] pyrimidines, are often called (6-4)photoproducts (Fig. 19.8).

Ultraviolet radiation transforms the (6-4)photoproducts to "Dewar photo-isomers". This transformation can take place with UV-A (Takeuchi et al. 1998), UV-B, or UV-C radiation (Ravanat et al. 2001). As shown in Figs. 19.8 and 19.9, several diastereoisomers of CPDs are theoretically possible, but only the *cis*-syn type is, in fact, formed in double-stranded DNA. In single-stranded or denatured DNA also the *trans*-syn form can be generated, but in low yield. Pyrimidine bases may react to form CPDs as well as (6-4)photoproducts in the combinations TT, TC, and CT; for CPDs also CC is possible. The biological effects are very variable. In some cases replication is stopped at a lesion, in other cases replication continues, resulting either in a mutation (e.g., a change from thymine to cytosine, Jiang et al. 1993) or a normal DNA strand. Only specialists in the field can keep track of this, since the same type of lesion may have different consequences in different organisms (e.g., Gibbs et al. 1993). The reader is referred to Ravanat et al. (2001) as an introduction to the literature.

CPDs are the most common UV-induced lesions in DNA. Under UV-C (254 nm) radiation 2–10 CPDs are formed per million bases per J/m^2. As UV-B is more

Unreacted pair of thymine residues in DNA

(6-4) TT photoproduct   Dewar TT photoisomer

Cis-syn TT dimer   Trans-syn TT dimer
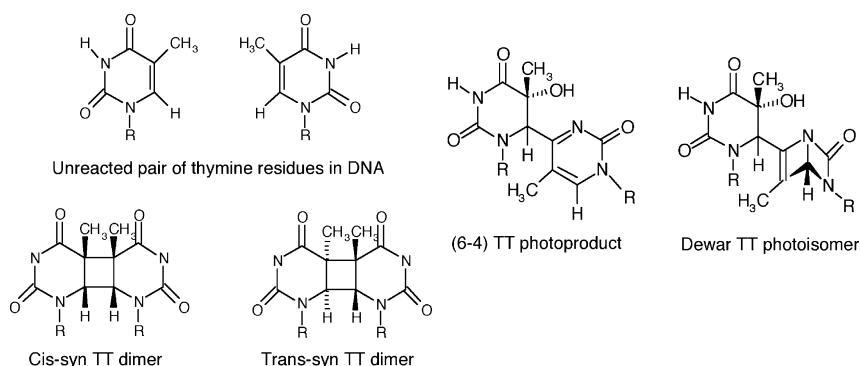
FIGURE 19.8. Thymine residues in DNA, and the most common types of lesion due to ultraviolet radiation. Dimers and (6-4)photoproducts arise from thymine by the action of UV-B or UV-C radiation, while Dewar photoisomers are formed from (6-4)photoproducts under the influence of UV-A radiation. Since cytosine (C) reacts in a similar way, and also can react with thymine, forming TT, TC, and CT dimers, there are in fact a multitude of possible lesion types, all with differently serious consequences for the organism.

cis-syn   cis-anti   trans-syn   trans-anti
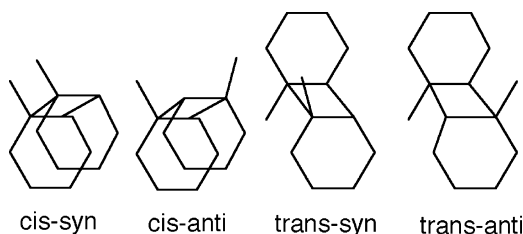
FIGURE 19.9. Perspective drawings of the four different diastereoisomers that are possible for a cyclobutane dimer. Due to steric constraints only the syn forms can be generated in DNA, and of these the *trans*-syn occurs only in single-stranded DNA. The lines indicate methyl groups. (Redrawn after Ravanat et al. 2001.)

weakly absorbed by DNA, it is not surprising that the same result requires about two orders of magnitude more UV-B. CPDs occur at higher frequencies than (6-4)photoproducts. Base order is important for UV susceptibility. Pyrimidine pairs with T (thymine) on the 5′-side, i.e., TT and TC, are about 10-fold more reactive than those with C (cytosine) on the 5′-side (CT and CC). C at the 3′-side favors (6-4) photoproduct formation. For more details see Ravanat et al. (2001) and Yoon et al. (2000). In diatoms the frequency of (6-4)photoproducts was, on average, 85% of that of CPDs (Karentz et al. 1991), but in most other organisms it seems to be lower. CPDs, (6-4)photoproducts, and Dewar photoisomers block DNA replication and are a main cause of UV-induced cancer.

Another kind of lesion affecting cytosine is photohydration followed by deamination to yield uracil hydrate.

Purine bases in DNA may also be altered by ultraviolet radiation. Thus, adenine may combine with either an adjacent adenine or with a thymine residue. This occurs with very low yield, but may be biologically important since it is not as easily repaired as the CPDs and (6-4)photoproducts. At least the adenine-thymine adduct is also highly mutagenic (Zhao and Taylor 1996).

DNA bases may also suffer photooxidative damage, and in this respect guanine is particularly sensitive. This photooxidation may take in various ways, and the frequency of various pathways has not yet been established. A direct photon hit in a base may expel an electron, and the electron hole can then migrate along the DNA chain until it encounters a guanine residue, via interaction with water, resulting in 2,6-diamino-4-hydroxy-5-formamidopyrimidine. Deprotonation instead of hydration may also occur, and gives another product. Another possibility is that a pyrimidine or purine base after photoexcitation enters a triplet excited state and reacts with oxygen, resulting in generation of singlet oxygen (see Chapter 1). The singlet oxygen then attacks a DNA base, preferably guanine. In this way 8-oxo-7,8-dihydro-2′-deoxyguanosine is formed. Finally, singlet oxygen and other reactive oxygen species (see Chapter 1 and below) formed after photoexcitation of other chromophores may also attack DNA in various ways. It is not known with certainty which cellular chromophores are most important for such processes, but flavines are among the likely canditates.

In any case UV-A is more important than UV-B, partly because its fluence rate in daylight is higher, and partly because it penetrates further into organisms and natural waters.

Lesions in addition to those mentioned can be induced by direct action of the radiation on DNA. They occur at lower frequency, but some of them may have some importance because they cannot be repaired by the rapid action of photolyases, only by the slower acting light-independent, "dark" repair systems.

19.4.2. Photolyases and Photoreactivation

Most prokaryotic and eukaryotic organisms are equipped with two kinds of photolyases, enzymes that under the influence of light repair these lesions. In older literature they are called photoreactivating enzymes. The physiological effects of photoreactivation were observed by Hausser and Oehmcke (1933) (see Fig. 19.10) long before the role of DNA was known. Other early publications on the subject include Dulbecco (1949) and Kelner (1949). Recent reviews have been written by Sancar (2003), Weber (2004), and Essen and Klar (2006). One main type of photolyase repairs the CPDs; the other type repairs (6-4)photoproducts. If a (6-4) photoproduct has been converted to a Dewar photoisomer, it can no longer be repaired by photolyase action.
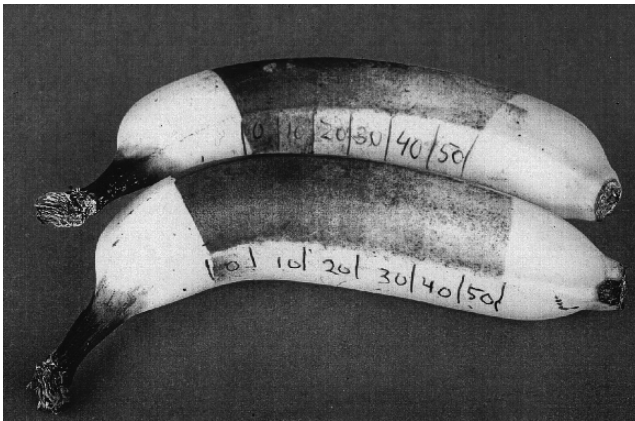
FIGURE 19.10. These bananas, while still unripe, were first irradiated for 2 minutes with UV-C radiation (254 nm, W/m^2), except for the ends, which were wrapped in aluminum foil during irradiation. They were then irradiated with white light for the number of minutes indicated on the different sections. Finally they were allowed to ripen in darkness. Where the epidermal cells have been damaged by ultraviolet radiation they have turned brown, while in other areas they have become yellow during ripening. White light after the ultraviolet has an ameliorating effect. This experiment, which is recommended as a student experiment (see Chapter 24), is in principle the same as that by which photoreactivation was discovered by Hausser and von Oehmcke (1933). (Photo L.O. Björn.)

The photolyases are of interest not only from the viewpoint of DNA repair, but also because they have played a role in the evolution of other photobiological systems (see Section 10.3.1. in Chapter 10). Since photolyases are so widespread among organisms and related types occur in distantly related organismal groups, and also because the need for DNA repair probably was very great before the emergence of the ozone layer, they are thought to have evolved very early. In addition to amino acid sequence and the specificity for different lesion types, photolyases differ also in the chromophore constitution, and therefore also in the action spectra (Figs. 19.11 and 19.12) for photorepair. All photolyases (except the recently discovered "deoxyribozyme photolyase"; see below) contain a flavin (FAD) as the main chromophore, but most of them also an accessory chromophore.

Based on amino acid sequences, the evolution of the photolyase/cryptochrome family of proteins is thought to have proceeded as follows (Todo 1999). An ancestral gene encoded a CPD photolyase and duplicated very early to form several copies. One of the copies evolved to become class II CPD photolyase gene, which now occurs only in eukaryotes. Another copy evolved to become class I CPD photolyase gene. One copy gave rise to several related genes coding for (6-4) photolyase and plant and animal cryptochromes.

CPD photolyase splits CPDs by transferring an electron from the flavin chromophore, which has either been directly excited by light or by energy transfer from the antenna chromophore. The negatively charged cyclobutane ring of the dimer then splits, after which the electron is returned to the flavin (Fig. 19.12). Yamada and Aoki (2006) have tried to study the reaction mechanism
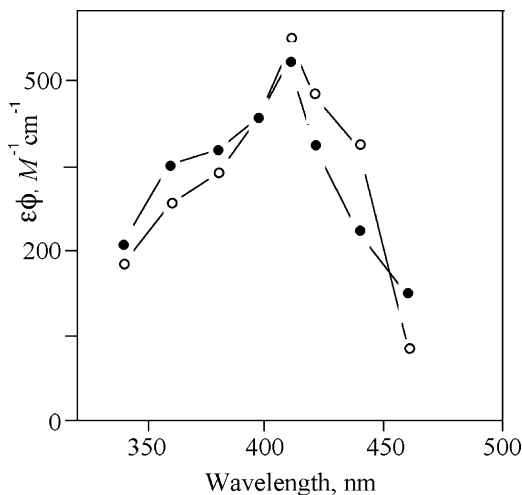
FIGURE 19.11. Absolute action spectrum for photoreactivation of (6-4)photoproducts by *Drosophila melanogaster* photolyase: filled circles, repair of T(6-4)T; empty circles, repair of T(6-4)C. The vertical axis shows the product of molecular absorption coefficient (e) and quantum yield (f). (Redrawn after Zhao et al. 1997.)
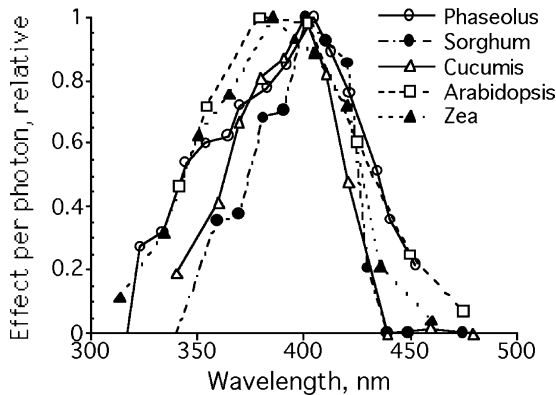
FIGURE 19.12. Collection of action spectra for photoreactivation of CPDs in plants by Class II photolyase to show the variability: *Phaseolus* (pinto bean) (Saito and Werbin 1969), *Sorghum* and *Cucumis* (cucumber) (Hada et al. 2000), *Arabidopsis* (Pang and Hays 1991), *Zea* (maize, Ikenaga et al. 1974).

in even greater detail in an artificial photolyase. A quite different kind of DNA photorepair by a "deoxyribozyme photolyase" activity has been described by Chinnapen and Sen (2004, 2007), without participation of protein, and Halldal (1961) has described photoreactivation in vivo (by direct photochemical splitting of lesions) by 223-nm radiation, a process without ecological significance under present-day conditions.

19.4.3. Formation and Effects of Reactive Oxygen Species

Under the common name of reactive oxygen species (ROS), we lump together a number of oxygen-containing chemical species which arise in organisms by a variety of reactions. Experts dealing with effects of ionizing radiation, such as radiation arising from radioactive decay of atomic nuclei, have been familiar with them for a long time. In photobiology, somewhat surprisingly, they are more important when we are dealing with effects of the less energetic UV-A photons than in the UV-B and UV-C fields, where direct radiation effects on DNA and other macromolecules dominate the picture. This is because the cell contains a number of chromophores which, when excited by UV-A photons can give rise to ROS. Murphy (1990) and Murphy and Huerta (1990) found that UV-C irradiation of plant cells can give rise to hydrogen peroxide, probably by another mechanism as that described below for UV-B (Fig. 19.13).

According to A.-H.Mackerness et al. (2001), the main mechanism by which ultraviolet radiation increases the generation of ROS is indirect, by increasing the activity of NADPH oxidase and peroxidases. The generation of ROS by NADPH oxidase is well known from the vertebrate defense against bacterial infection, and an "oxidative burst" similar to that generated in vertebrate neutrophils (a kind of blood corpuscles) takes place also in the plant's defense agains infection
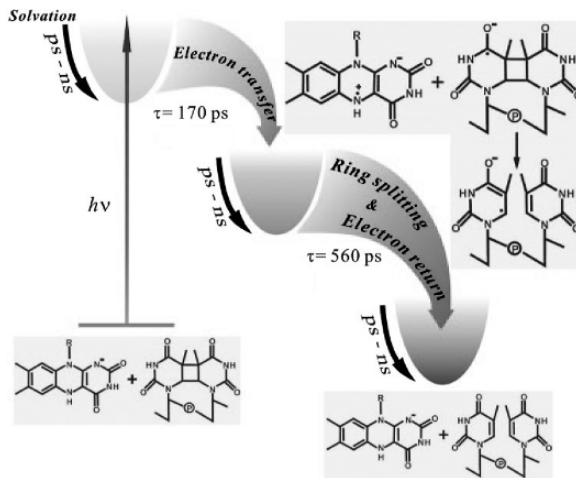
FIGURE 19.13. The reaction mechanism in dimer splitting by CPD photolyase. Reaction times (τ) are given in ns (10^{-9} s) and ps (10^{-12} s). (Slightly modified from Kao et al. 2005.)

(review by Lamb and Dixon 1997). NADPH oxidase functions according to the reaction formula $2O_2 + NADPH ==> 2O_2^- + NADP^+ + H^+$.

The superoxide anion, O_2^- so formed is very reactive, and may give rise to hydrogen peroxide:

$$H^+ + O_2^- ==> HO_2$$

$${}^\bullet HO_2 + {}^\bullet HO_2 ==> H_2O_2 + O_2$$

$${}^\bullet HO_2 + O_2^- + H_2O ==> H_2O_2 + O_2 + OH^-$$
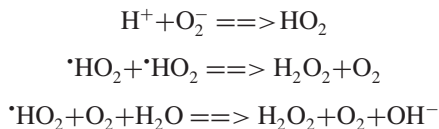
In the presence of iron as a catalyst, the most reactive of all ROS, the hydroxyl radical, $^\bullet OH$, may be generated from superoxide anion and hydrogen peroxide:

$$O_2^- + Fe^{3+} ==> O_2 + Fe^{2+}$$

$$Fe^{2+} + H_2O_2 ==> Fe^{3+} + OH^- + {}^\bullet OH$$
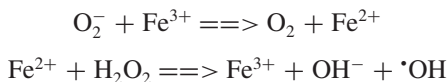
Peroxidase can contribute to the formation of O_2^- by first oxidizing NADH with H_2O_2 as an oxidant. This results in formation of a $^\bullet$NAD radical (2 mol per mol of hydrogen peroxide), which reduces O_2 to O_2^-, a reaction stimulated by monophenols and Mn^{2+}. If the superoxide, after protonation, dismutates to form hydrogen peroxide as shown above, more hydrogen peroxide is generated than was originally consumed.

Enzyme systems and antioxidants protecting against effects of ROS are often increased in response to ultraviolet irradiation.

19.4.4. Effects of Ultraviolet Radiation on Lipids

Lipids containing unsaturated fatty acids are particularly susceptible by photooxidation. Such attacks may be initiated in two different ways (see Girotti 2001 for a review).

Type I photooxidation is started by the formation of a radical when photon absorption in a sensitizer (S) results either in expulsion of an electron resulting in a radical (which can abstract an electron or a hydrogen atom from a lipid molecule) or in formation of a triplet excited state (^{3}S*). In the latter case the following reactions can take place (LH symbolizing a lipid molecule and RH another reductant such as ascorbate, glutathione, or a membrane component other than the lipid):

$$(1) \quad ^3S^* + RH ==> S^{-\bullet} + R^\bullet + H^+$$

$$(2) \quad S^{-\bullet} + O_2 ==> S + O_2^-$$

$$(3) \quad S^{-\bullet} + O_2^- + 2H^+ ==> H_2O_2$$

$$(4) \quad H_2O_2 + Fe^{2+} ==> OH^- + HO^\bullet + Fe^{3+}$$

$$(5) \quad LH + HO^\bullet ==> L^\bullet + H_2O$$

$$(6) \quad L^\bullet + O_2 ==> LOO^\bullet$$

$$(7) \quad LOO^\bullet + LH ==> LOOH + L^\bullet$$

Reaction (1) above results in two radicals: $S^{--\bullet}$ and $R^\bullet$. Either of these could initiate a peroxidative chain reaction (6–7) creating new radicals via a two-step reduction of oxygen (2–3) and a Fenton reaction (4) generating the highly reactive hydroxy radical ($HO^\bullet$) that readily attacks the lipid, eventually generating lipid peroxide (LOOH). A product also generated in such peroxidations is malonyl aldehyde, which is often used as an indicator to monitor peroxidative lipid breakdown. Another characteristic is generation of light ("ultraweak radiation"; see Chapter 16), which has been used to construct an action spectrum for lipid breakdown in plant leaves by ultraviolet radiation (Cen and Björn 1994). It should be pointed out that if suitable sensitizers are present in the appropriate compartments, this type of photooxidation can be mediated also by visible light. In addition to unsaturated fatty acids, other lipids, like cholesterol, can be broken down by essentially the same type of process.

The oxygen appearing in the above schemes is ordinary (triplet) oxygen. In a Type II photooxidation, singlet excited oxygen ($^1O_2$, see Chapter 1) is first generated by energy transfer from a sensitizer, which, after photoexitation to a singlet excited state, has reached the triplet state. The singlet oxygen then directly reacts with the double bond of an unsaturated fatty acid, and oxygen is added to form a peroxide: LH + $^1O_2$ ==> LOOH.

There are many experiments showing deleterious effects of ROS generated by ultraviolet radiation (mostly UV-A, but also UV-B), and in many cases hydrogen peroxide is blamed for the effect (e.g., Petersen, Gniadecki, Vicanova,

Thorn, and Wulf 2000). Not surprisingly the H_2O_2-degrading enzyme catalase has been shown to play a protective role. But it appears that catalase sometimes is to blame for the generation of ROS (Heck, Vetrano, Mariano, and Laskin 2003).

19.4.5. Photodestruction of Proteins

Proteins may be affected by ultraviolet radiation in various ways. Enzymes in which sulfhydryl groups are essential for the function are sensitive to photooxidative damage. One of the most sensitive proteins is photosystem II, a protein complex having a key role in oxygenic photosynthesis. In short-term experiments on photosynthesis this was frequently found to be the most ultraviolet-sensitive link. However, it seems that long-term, ecologically relevant inhibition of photosynthesis by UV-B radiation has other causes (see below).

Proteins can be photochemically cross-linked to adjacent nucleic acids, which is one more mechanism by which ultravilet radiation can affect DNA. Enzymes may be inactivated also by visible light if they absorb it (e.g., Björn 1969) or via sensitizers which absorb visible light.

19.4.6. UV Absorption Affecting Regulative Processes

Many organisms have special receptors for ultraviolet radiation, which enable them to regulate various processes in accordance with ambient radiation levels, or even to locate environments of higher or lower radiation, or to locate sources of radiation. Most of these, including receptor cells in the eyes of many animals, respond only to UV-A radiation. However, at least some plants and some algae possess receptors for UV-B, and in humans *trans*-urocanic acid (see Chapter 10) can probably be regarded as a molecular UV-B photoreceptor, even if we presently do not understand the significance. However, many processes are regulated by UV-B, seemingly without any photoreceptors specifically evolved for regulation. Thus, many genes are regulated in both plants and animals via photon absorption in DNA. It is too early to say whether this is, in general, to be regarded as a stress response to DNA damage inflicted by the radiation.

In other cases regulation proceeds via the formation of ROS (A.-H. Mackerness et al. 1999, 2000, and literature cited therein). This seems to be the case with the downregulation by increased UV-B of several genes of importance for photosynthesis. Reactive oxygen species also affect a number of hormone systems (Fig. 19.7).

The specific UV-B receptor in plants, with an action maximum at 295 nm, has not yet been identified. It regulates growth processes and the synthesis of flavonoids and other substances. Flavonoids serve as UV-B absorbing filters, and also have other functions in the plants.

It may be wrong, however, to regard the regulation by reactive oxygen species and regulation by an UV-B receptor as two different pathways. As described in

Section 4.3., a major way for generation of ROS may be the increase in activities of NAD oxidase and of peroxidase. This increase may be achieved via the UV-B receptor.

19.4.7. UV-Induced Apoptosis

Induction of apoptosis (programmed cell death), because of its medical importance, has been studied most thoroughly in mammals, but is known to occur in other eukaryotes as well. Apoptosis is a normal process in plant development, for instance, in xylem differentiation, and induction of apoptosis by UV-C has also been observed in plants (Danon and Gallois 1998). In the flagellate *Euglena* induction of an apoptosis-like process was observed by Scheuerlein et al. (1995).

   According to Godar (1999a,b) several mechanisms for apoptosis caused by UV-A radiation in the wavelength range 340–400 nm can be distinguished. Two of these depend on the generation of ROS. Formation of singlet oxygen results in "immediate pre-programmed cell death," which takes place in less than 20 minututes, does not require protein synthesis and depends on the opening of a "megapore" in the mitochondrial membrane, which releases chemical apoptosis signals into the cytosol. Another pathway for "immediate" apoptosis depends on the formation of superoxide anion, which probably is transformed to hydroxyl radical before interacting with another part of the mitochondrial megapore, which releases cytochrome *c*. The presence of cytochrome *c* in the cytosol then causes apoptosis. A third, slower ("intermediate") kind of apoptosis is caused by absorption of radiation in the plasma membrane, causing cross-links in the "Fas receptor" there, which via formation of "caspases" (apoptosis-signaling proteins) lead to opening of the mitochondrial megapore. Finally, there are several forms of "delayed" apoptosis, caused by lesions in DNA. At least some of these signaling channels also go via opening of the mitochondrial megapore. For UV-B–induced apoptosis, CPD formation in DNA can be involved, since Nishigaki et al. (1998) have shown that photorepair of CPDs can prevent UV-induced apoptosis.

19.5. Ultraviolet Effects on Inanimate Matter of Biological Relevance

We have already described how ultraviolet radiation affects the composition of the upper stratosphere. It also has effects on the troposphere. Among other processes it contributes to the formation of smog. Increased UV-B in the troposphere leads to increased concentration of hydroxyl radical, which in turn results in increased removal of organic compounds and oxides of sulfur and nitrogen. These effects are probably more beneficial than negative for life in general. On the other hand, concentrations of hydrogen peroxide, organic peroxides, and ozone in the troposphere increase when UV-B radiation increases. The overall effect on air quality is probably negative, and various organisms are affected to

very different degrees. Tropospheric ozone in particular is clearly a problem for vegetation in many parts of the world.

In the aquatic environment UV-B decomposes dissolved organic matter, thus making the water more transparent and increasing penetration of ultraviolet radiation, as well as making the organic substances more available for bacterial growth. Photochemical reduction of iron and manganese is an important process in some aquatic ecosystems (reviewed by Wu and Deng 2000). For this UV-A, and to some extent visible light, is more important than UV-B. UV-A and UV-B can also decrease availability of iron by chelating agents, which is a considerable problem in the use of artificial iron fertilization in some countries.

In the terrestrial environment ultraviolet radiation affects dead plant matter (litter) in a complex way. The chemical composition of the litter is affected already in the living state: More secondary substances are usually formed in plant parts under increased radiation, making the matter derived therefrom more resistant. After litter has formed, organic compounds in it are photochemically broken down by ultraviolet radiation, provided they are sufficiently exposed. The activity of some litter-decomposing fungi, on the other hand, is hampered by ultraviolet radiation. In some investigations the overall effect was that organic carbon as well as nitrogen disappeared more rapidly under increased UV-B radiation (Gehrke et al. 1995, Paul et al. 1999), while in other cases decomposition was decreased by UV-B radiation (Moody et al. 2001 and references therein). The rate of litter breakdown is very important in some environments, since it may be the most important process making plant nutrients available for new growth.

19.6. UV-B Radiation in an Ecological Context

As we have seen, UV-B radiation can act destructively on DNA and other cellular constituents, but it can also act in a regulating way, and it modifies the physical environment. In the early days of research regarding UV-B effects on organisms and ecosystems, there was an overemphasis on the direct, destructive effects of UV-B on organisms. Nowadays most researchers in the field are of the opinion that the important effects of UV-B change resulting from changes in the ozone layer and cloudiness will not be these effects, but modulations in the way organisms influence one another. The literature on this is voluminous. We shall here only briefly give some examples, and refer the interested reader to recent reviews, books, and special journal issues devoted to the subject (e.g., Björn 1996, Helbling et al. 2001a, Rozema et al. 1997a,b, 2001, 2002, Hessen 2002a).

19.6.1. Aquatic Life

Few biological effects of the increase in UV-B that has resulted from ozone depletion have been directly recorded, so most effects are inferred from experimental manipulation of the radiation level. Direct detection of ozone depletion

effects is hampered by the lack of baseline data, i.e., lack of information of the situation prior to ozone depletion. In the Southern Ocean one can clearly monitor how photosynthesis decreases when the ozone hole sweeps over the monitored area (Smith et al. 1992). Different phytoplankton species are affected to very different extents.

Even if the efects of ozone depletion are difficult to monitor in most water bodies, the impact of UV-B in situ can be inferred from the vertical distribution of photosynthesis, as photosynthesis is partly inhibited in the upper layers where the UV-B radition is strongest (e.g., Helbling and Villafañe 2002). The degree of vertical mixing of water, which varies with location and season, is important in this context. During the seasons most important for UV-B effects, the upper mixed layer is shallow in antarctic waters (mean depth 50 m), while in the Arctic it varies between 100 and 300 m. When arctic phytoplankton become exposed to UV-B, they are therefore to a higher degree "dark adapted" than antarctic phytoplankton and, therefore, on average, more sensitive (Helbling and Villafañe 2002).

In coastal waters, and in fresh water bodies in particular, UV-B does not penetrate as far as in the open sea, and therefore affects only a shallow layer. This can still be of importance, as larvae of many organisms important for the food web live near the surface in these waters. The food web in aquatic ecosystems is generally more complex than in terrestrial ecosystems, and organisms at each trophic level, with the possible exception of mammals and birds, can be affected by UV-B at some stage of development.

One might suspect that the smaller a unicellular organism is, the more susceptible it would be to UV-B radiation. A small organism has less possibility than a larger one to protect the most sensitive parts (especially its DNA) by shielding layers containing radiation-absorbing substances. Some evidence in this direction was presented by Karentz et al. (1991), who compared DNA damage and survival for a number of planktonic diatom species of different size exposed to UV-B radiation. Although the data were scattered, there was a clear tendency for fewer DNA lesions in species with a small surface area: volume ratio (as a large cell has in comparison with a small one, although there is also a shape factor involved). They also (but comparing only four species) showed a negative correlation between survival and frequency of DNA lesions. Such a size-selective effect of UV-B could have serious consequences for consumer organisms, who may simply find the surviving prey too big for consumption. In fact, van Donk et al. (2001) found UV-B irradiation to decrease the fraction of phytoplankton, which was considered "*Daphnia*-edible."

Several other authors have also mentioned a higher tolerance among larger species. But this relationship cannot be upheld when distantly related organisms are compared, and its generality is questionable even when organisms within the same group are compared. Thus Peletier et al. (1996) found no relationship between cell size and UV-B sensitivity among benthic diatoms. Laurion and Vincent (1998) conclude that cell size is not a good predictor of UV-B sensitivity and that, in particular, the cyanobacteria-dominated picophytoplankton is less sensitive than would be assumed on the basis of a size-sensitivity relation. Also,

Helbling et al. (2001b) find that picoplankton is more resistant than a cell size relationship would predict.

In the case of marine Prymnesiophyceae it was found (Mostajir et al. 1999b) that prolonged exposure to UV-B caused an increase in cell size, which possibly diminished the risk of genetic damage, but above all change the availability and quality of these organisms as food for grazers. Most organisms (including ourselves) have pigments which protect against ultraviolet radiation (the human skin pigment melanin protects in both optical and chemical ways, as do also some plant pigments). In cyanobacteria and many (but not all types of) algae so-called mycosporine-like amino acids (MAAs) constitute an important group of UV-protecting pigments. In general, however, they protect mainly against UV-A, rather than UV-B radiation (Sinha et al. 1998, 2001, Bishof et al. 2002). Although they are produced by cyanobacteria and some algae and fungi, they are taken up by grazing animals and used also by then as protecting pigments (Sinha et al. 1998). For many aquatic animals, carotenoids serve as important protectants (Hessen 2002b).

Despite the many negative effects of UV-B radiation, it is frequently found that concentrations of various aquatic organisms are increased when UV-B levels are increased. For both bacteria and phytoplankton species this can be due to a greater sensitivity of the predators, and therefore a decline in predation (Mostajir et al. 1999a). For bacteria it can also be due to increased availability of nutrients when dissolved organic matte is decomposed by the radiation (Herndl et al. 1997).

19.6.2. Terrestrial Life

As in the case of aquatic life, few biological effects of the increase in UV-B that has resulted from ozone depletion have been directly recorded, so the majority of effects are inferred from experimental manipulation of the radiation level. Only in Antarctica, and in Tierra del Fuego, where the ozone hole provides a great increase in radiation level, can a direct biological impact of ozone depletion be recorded. Thus Rousseaux et al. (1999) found that CPD frequency in DNA in plant leaves tracked variations in ambient UV-B in Tierra del Fuego. Several researchers have been inspired to do research on the two higher plant species in Antarctica. The 4-year study of Day et al. (2001) provides data to allow the conclusion that the ozone hole has had an impact on plant life there. These researchers compared plants under UV-B–transmitting and UV-B–excluding filters. Since the "natural" (prehole) UV-B level is so low, the plants under UV-B–excluding filters were probably developed in a way very similar to prehole plants. Many morphological differences between plants exposed to the two treatments were noted. There was some evidence that effects accumulated over the years.

Experiments with exclusion of ambient UV-B from natural ecosystems have also been conducted in Tierra del Fuego (Ballaré et al. 2001), and there are many exclusion studies carried out elsewhere showing that the ambient ultraviolet

radiation, even in regions of the world where the ozone depletion has not been severe, is an important environmental factor for many terrestrial (as for aquatic) organisms. In most cases there is little or no direct inhibition of photosynthesis and biomass production by plants. The important effects instead arise in the interaction between organisms. Thus morphological changes in plants can lead to changes in the interspecies competion for light (Barnes et al. 1988). Changes in UV-B often result in changes in herbivory. In most cases increased UV-B leads to decreased herbivory due to changes in chemical composition of the plants (Gwynn-Jones 1999 and reports cited therein). However, other cases are also known: Herbivory may be increased by increased UV-B (Lavola et al. 1998, Buck and Callaghan 1999), and it seems that some insects can perceive UV-B and react directly on changes (Buck and Callaghan 1999). Also, interactions between microorganisms and other organisms can be changed by changes in UV-B, although the conclusion of Paul (2000) is that it is not probable that ozone depletion will cause any substantial change in the incidence or severity of crop diseases.

19.7. Effects on Human Eyes

Most medical effects of ultraviolet radiation take place via the skin; such effects will be dealt with in Chapter 21. The only medical effects of ultraviolet radiation that shall concern us is the present chapter will therefore be those on the eyes.

According to Boottner and Welter (1962) different wavebands of ultraviolet radiation incident on the cornea are absorbed in the various tissues of the eye as shown in Table 19.1. The values in Table 19.1 should be regarded only as approximate values. Especially the lens transmission (Fig. 19.14) varies between individuals, and it is normal that it decreases with age (even if no cataract develops), and this decrease affects also the blue waveband, and thus decreases the eye's sensitivity to blue light. For further information on transmission of ocular media, see Polo et al. (1997).

Because it does not penetrate any further, UV-C radiation can directly affect only the cornea and conjunctiva, and the most common type of UV-C radiation (254-nm radiation from low-pressure mercury lamps) only the outermost part of the cornea.

TABLE 19.1. Percentage of Radiation Incident on the Cornea over the Pupil That Is Absorbed in Various Parts of the Eye

Wavelength, nm	Cornea	Aqueouslayer	Lens	Vitreousbody
280	100	0	0	0
300	92	6	2	0
320	45	16	36	1
340	37	48	48	1
360	34	52	52	2
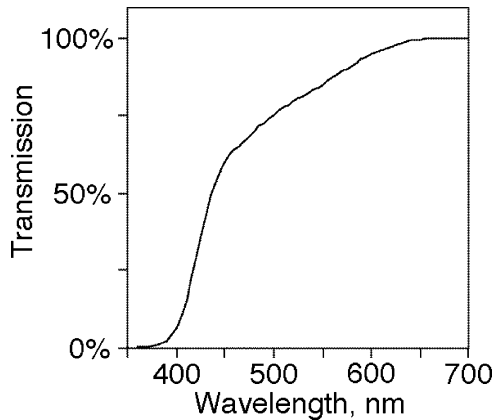
FIGURE 19.14. Typical spectral transmission of a human lens.

UV-C radiation is, in a way, the least dangerous kind of ultraviolet radiation as far as the eyes are concerned, since the person who has been exposed will very quickly be aware of it and will in the future avoid exposure. Within 2–3 hours after the radiation exposure very unpleasant symptoms will develop. It feels as if the eyelids are covered with sandpaper on the inside. If the exposure has not been very severe, the pain will disappear in a couple of days. The scientific name for this is photokeratitis, and it can also be caused by UV-B radiation in daylight. Well-known forms of photokeratitis are "snow-blindness" and "welder's flash." According to Podskochy et al. (2000) photokeratitis is caused by UV-induced apoptosis of cornea cells, resulting in a speeding up of the cell shedding, which normally takes place at a lower rate. This exposes subsurface nerve endings, which causes the gritty feeling and the pain. The action spectrum for ultraviolet damage to the cornea was determined by Pitts et al. (1977).

Cataract is a common and serious group of diseases, which lead to opacity of the lens, and ultimately to blindness. Cataracts are usually divided into cortical, nuclear, and posterior subcapsular cataracts. Of these, nuclear cataracts do not seem to be caused by UV exposure, while the two other forms are (Taylor 1994; see also Zigman 1995). In the United States the probability of cataract surgery increases by 3% for each degree decrease of latitude (Javitt and Taylor 1994). Such surgery involves removal of the lens, and often replacement of it with an artificial (acrylate) lens. Nowadays a lens material is chosen that absorbs ultraviolet radiation efficiently, so radiation exposure of the inner parts of the eye will not be increased after the operation.

Action spectra for cataract induction in lenses of rat and swine have been determined by Merriam et al. (2000) and Oriowo et al. (2001). The highest sensitivity occurs around 295–300 nm, i.e., in the middle of the UV-B band.

UV-related cancer forms, such as melanoma (Michalova et al. 2001) and squamous cell carcinoma, affect not only skin, but also the eye. Newton et al. (1996) estimate that the incidence of squamous cell carcinoma of the eye doubles

for a 50° increase in latitude (from the United Kingdom. to Uganda), but genetic factors have not been taken into account in this estimate.

Pterygium is an outgrowth of the conjunctiva over the cornea. It is strongly related to sun exposure (Threlfall and English 1999; see also literature cited by Longstreth et al. 1998), but the spectral dependence is not known.

Regarding the role of ultraviolet light (and visible sunlight) in eye disease, the reader is also referred to WHO (1994), Taylor (1994), Young (1994), Sliney (1997), Scott (1998) and Longstreth et al. (1998).

References

A.-H.-Mackerness, S., Jordan, B.R. and Thomas, B. (1999) Reactive oxygen species in the regulation of photosynthetic genes by ultraviolet-B radiation (UV-B: 280-320 nm) in green and etiolated buds of pea (*Pisum sativum* L.). J. Photochem. Photobiol. B: Biol. 148, 180–188.

A.-H. Mackerness, S., John, C.F., Jordan, B. and Thomas, B. (2001. Early singaling components in ultraviolet-B responses: distinct roles for different reactive oxygen species and nitric oxide. FEBS Lett. 489, 237–242.

Ballaré, C.L., Rousseaux, M.C., Searles, P.S., Zaller, J.G., Giordano, C.V., Robson, T.M., Caldwell, M.M., SDala, O.E., and Scopel, A.L. (2001) Impact of solar ultraviolet-B radiation on terrestrial ecosystems of Tierra del Fuego (southern Argentina) – An overview of recent progress. J. Photochem. Photobiol. B: Biology 62, 67–77.

Barnes, P.W., Jordan, P.W., Gold, W.G., Flint, S.D., Caldwell, M.M. (1988) Competition, morphology, and canopy structure in wheat (*Triticum aestivum* L.) and wild oats (*Avena fatua* L.) exposed to enhanced ultraviolet-B radiation. Functional Ecol. 2, 319–330.

Benedick, R.E. (1991) Ozone diplomacy: *New directions in safeguarding the planet* (enlarged edition 1998). Harvard University Press, Cambridge, MA.

Berrocal,-Tito, G., Saetz-Baron, L., Eichenberg, K., Horwitz, B.A. and Herrera-Estrella, A. (1999) Rapid blue light regulation of a *Trichoderma harzianum* photolyase gene. J. Biol. Chem. 274, 14288–14294.

Bischof, K., Hanelt, D. and Wiencke, C. (2002) UV radiation and arctic marine macroalgae. In: D.O. Hessen (Ed.), *UV radiation and arctic ecosystems*. Springer, Berlin, pp. 225–243.

Björn, L.O. (1969) Photoinactivation of catalases from mammal liver, plant leaves and bacteria. Comparison of inactivation cross sections and quantum yields at 406 nm. Photochem. Photobiol. 10, 125–129.

Björn, L.O. (1996) Effects of ozone depletion and increased UV-B on terrestrial ecosystems. Int. J. Environ. Stud. 51/3(A), 217–243.

Björn, L.O., Callaghan, T.V., Johnsen, I., Lee, J.A., Manetas, Y., PaJørgensen, H.S., Gehrke, C., Gwynn-Jones, D., Johanson, U., Kyparissos, A., ul, N.D., Sonesson, M., Wellburn, A., Coop, D., Heide-Lenzou, E., Nikolopoulos, D., Petropoulou, Y. and Stephanou, M. (1997) The effects of UV-B radiation on European heathland species. Plant Ecology 128, 252–264.

Björn, L.O. and McKenzie, R.L. (2007) Attempts to probe the ozone layer and the UV-B radiation levels of the past. Ambio 36, 366–371.

Boettner, E.K. and Wolter, J.R. (1962) Transmission of the ocular media. Investig. Ophthalmol. 1, 776-783.

Buck, N., Callaghan, T.V. (1999) The direct and indirect effects of enhanced UV-B on the moth caterpillar *Epirrita autumnata*. Ecol. Bull. 47, 68–76.

Cen, Y.-P. and Björn, L.O. (1994) Action spectra for enhancement of ultraweak luminescence by ultraviolet radiation (270–340 nm) in leaves of *Brassica napus*. J. Photochem. Photobiol. B: Biology 22, 125–129.

Chinnapen, D.J. and Sen, D. (2004) A deoxyribozyme that harnesses light to repair thymine dimers in DNA. Proc. Natl Acad. Sci. USA 101, 65–69.

Chinnapen, D.J. and Sen, D. (2007) Towards elucidation of the mechanism of UV1C, a deoxyribozyme with photolyase activity. J. Mol. Biol. 365, 1326–1336.

Danon, A. and Gallois, P. (1998) UV-C radiation induces apoptotic-like changes in *Arabidopsis thaliana* . FEBS Lett. 437, 131–136.

Day, T.A. (2001) Multiple trophic levels in UV-B assessments—completing the ecosystem. New Phytol. 152, 183–185.

Day, T.A., Ruhland, C.T. and Xiong, F.S. (2001) Influence of solar ultraviolet-B radiation on Antarctic terrestrial plants: results from a 4-year study. J. Photochem. Photobiol. B: Biology 62, 78–87.

Deisenhofer, J. (2000) DNA photolyases and cryptochromes. Mutat. Res, 460, 143–149.

Dulbecco, R. (1949) Reactivation of ultraviolet-inactivated bacteriophage by visible light. Nature 163, 949–950.

Essen, L.O. and Klar, T. (2006) Light-driven DNA repair by photolyases. Cell. Mol. Life Sci. 63, 1266–1277.

Gehrke, C., Johanson, U., Callaghan, T.V., Chadwick, D. and Robinson, C.H. (1995) The impact of enhanced ultraviolet-B radiation on litter quality and decomposition processes in Vaccinium leaves from the Subarctic. Oikos 72, 213–222.

Gibbs, P.E.M., Kilbey, B.J., Banerjee, S.K. and Lawrence, C.W. (1993) The frequency of and accuracy of replication past a thymine-thymine cyclobutane dimer are very different in *Saccharomyces cerevesiae* and *Escherichia coli*. J. Bacteriol. 175, 2607–2612.

Girotti, A. (2001) Photosensitized oxidation of membrane lipids: reaction pathways, cytotoxic effects, and cytoprotective mechanisms. J. Photochem. Photobiol. B: Biology 63, 103–113.

Godar, D.E. (1999a) Light and death: Photons and apoptosis. J. Invest. Dermatol. Symp. Proc. 4, 17–23.

Godar, D.E. (1999b) UVA1 radiation triggers two different final apoptotic pathways. J. Invest. Dermatol. 112, 3–12.

Gwynn-Jones, D. (1999) Enhanced UV-B radiation and herbivory. Ecol. Bull. 47, 77–83

Hada, M., Iida, Y. and Takeuchi, Y. (2000) Action spectra of DNA photolyases for photorepair of cyclobutane pyrimidine dimers in sorghum and cucumber. Plant Cell Physiol. 41, 644–648.

Halldal P (1961) Photoreactivation at 223 mµ in *Platymonas*. Physiol Plant 14, 890–895.

Hausser, K.W. and v. Oehmcke, H. (1933) Lichtbräunung an Fruchtschalen. Strahlentherapie 48, 223–229.

Heck, D.E., Vetrano, A.M., Mariano, T.M and Laskin, J.D. (2003) UVB Light stimulates production of reactive oxygen species. Unexpected role for catalase. J. Biol. Chem. 278, 22432–22436.

Helbling, W., Ballaré, C.L. and Villafañe, V.E. (2001a) Impact of ultraviolet rdiation on aquatic and terrestrial ecosystems, pp. ix+122. J. Photochem. Photobiol. B: Biology 62, 1–122.

Helbling, E.W., Buma, A.G.J., de Boer, M.K. and Villafañe, V.E. (2001b) In situ impact of solar ultraviolet radiation on photosynthesis and DNA in temperate marine phytoplankton. Mar. Ecol. Prog. Ser. 211, 43–49.

Helbling, E.W. and Willafañe, V.E. (2002) UV radiation effects on phytoplankton primary production: A comparison between Arctic and Antarctic marine ecosystems. In Hessen, D.O. (ed) (2002a) UV radiation and arctic ecosystems. Springer, Berlin, pp. 203–226.

Herndl, G.J., Brugger, A., Hager, S., Kaiser, E., Obernosterer, I., Reitner, B. and Slezak, D. (1997) Role of ultraviolet-B radiation on bacterioplankton and the availability of disolved organic matter. Plant Ecology 128, 42–51.

Hessen, D.O. (Ed.) (2002a) *UV radiation and arctic ecosystems*. Springer, Berlin.

Hessen, D.O. (2002b) UV radiation and arctic freshwater zooplankton. In: D.O. Hessen (Ed,), *UV radiation and arctic ecosystems*. Springer, Berlin, pp. 158–184.

Ikenaga, M., Kondo, S. and Fujii, T. (1974) Action spectrum for photoreactivation in maize. Photochem. Photobiol. 19, 109–113.

IPCC (2005) IPCC/TEAP Special report: Safeguarding the ozone layer and the global climate system: Issues related to hydrofluorocarbons and perflorocarbons. Summary for policymakers, IPCC, Geneva.

Javitt, J.C. and Taylor, H.R. (1994) Cataract and latitude. Documenta Ophthalmol. 88, 307–325.

Jiang, , N. and Taylor, J.-S. (1993) In vivo evidence that UV-induced C→T mutations at dipyrimidine sites could result from the replicative bypass of *cis-syn* cyclobutane dimers or their deamination products. Biochemistry 32, 472–481.

Karentz, D., Cleaver, J.E. and Mitchell, D.L. (1991) Cell-survival characteristics and molecular responses of antarctic phytoplankton to ultraviolet radiation. J. Phycol. 27, 326–341.

Kao, Y.-T., Saxena, C., Wang, L., Sancar, A. and Zhong, D. (2005) Direct observation of thymine dimer repair in DNA by photolyase. Proc. Natl Acad. Sci. USA 102, 16128–16132.

Kelner, A. (1949) Effect of visible light on the recovery of *Streptomyces griseus* conidia from ultraviolet-injury. Proc. Natl Acad. Sci. USA 35, 73–79.

Labitzke, K. and van Loon, H. (1997) Total ozone and the 11 yr-sunspot cycle. J. Atmospheric Solar-Terrestrial Phys. 59, 9–19.

Lamb, C. and Dixon, R.A. (1997) The oxidative burst in plant disease resistance. Annu. Rev. Plant Physiol. Plant Mol. Biol. 48, 251–275.

Laurion, I and Vincent, W.F. (1998) Cell size versus taxonomic composition as determinatnts of UV-sensitivity in natural phytoplankton communities. Limnol. Oceanogr. 43, 1774–1779.

Lavola, A., Julkunen-Tiitto, R., Roinenen, H., Aphalo, P. (1998) Host-plant preference of an insect herbivore mediated by UV-B and CO_2 in relation to plant secondary metabolites. Biochem. Syst. Ecol. 26, 1–12.

Lean, J. and Rind, D. (1999) Evaluating sun-climate relationships since the Little Ice Age. J. Solar-Terrestrial Physics 61, 25–36.

Longstreth, J., de Gruijl, F.R., Kripke, M.L., Abseck, S. Arnold, F., Slaper, H.I., Velders, G., Takizawa, Y. and van der Leun, J.C. (1998) Health risks. J. Photochem. Photobiol. B: Biology 46, 20–39.

Lumsden, P. (ed.) (1997) *Plants and UV-B: Responses to environmental change*. Society for Experimental Biology Seminar Series: 64. Cambridge University Press, Cambridge.

Merriam, J.C., Löfgren, S., Michael, R., Söderberg, P., Dillon, J., Zheng, L. and Ayala, M. (2000) An action spectrum for UV-B radiation and the rat lens. Investig. Ophthalmol. Visual Sci. 41, 2642–2647.

Michalova, K., Clemett, R., Dempster, A., Evans, J. and Allardyce, R.A. (2001) Iris melanomas: are they more frequent in New Zealand? Brit. J. Ophthalmol. 85, 4–5.

Moody, S.A., Paul, N.D., Björn, L.O., Callaghan, T.V., Lee, J.A., Manetas, Y., Rozema, J., Gwynn-Jones, D., Johanson, U., Kyparissis, A. and Oudejans, A.M.C. (2001) The direct effects of UV-B radiation on *Betula pubescens* litter decomposing at flur European sites. Plant Ecology 154, 29–36.

Mostajir, B., Sime-Ngando, T., Demers, S., Belzile, C., Roy, S., Gosselin, M., Chanut, J.P., de Mora, S., Fauchot, J., Vidussi, F. and Levasseur, M. (1999a) Ecological implications of changes in cell size and photosynthetic capacity of marine Prymnesiphyceae induced by ultraviolet-B radiation. Marine Ecol. Progr. Ser. 187, 89–100.

Mostajir, B., Demers, S., de Mora, S., Belzile, C., Chanut, J.P., Gosselin, M., Roy, S., Villegas, P.Z., Fauchot, J., Bouchard , J., Bird, D., Monfort , P. and Levasseur, M. (1999b) Experimental test of the effect of ultraviolet-B radiation in a planktonic community. Limnol. Oceanogr. 44, 586–596.

Murphy, T.M. (1990) Effect of broadband and visible radiation on hydrogen peroxide formation by cultured rose cells. Physiol. Plant. 80, 63–68.

Murphy, T.M. and Huerta, A.J. (1990) Hydrogen peroxide formation in cultured rose cells in response to UV–C radiation. Physiol. Plant. 78, 247–253.

Nilsson, A. (1996) *Ultraviolet reflections: Life under a thinning ozone layer*. Wiley, Chichester.

Nishigaki, R., Mitani, H., and Shima, A. 1998. Evasion of UVC-induced apoptosis by photorepair of cyclobutane pyrimidine dimers. Exp. Cell Res. 244, 43–53.

Nolin, J. (1995) *Ozonskiktet och vetenskapen*. Almqvist and Wiksell, Stockholm.

Oriowo, O.M., Cullen, A.P., Chou, B.R. and Sivak, J.G. (2001) Action spectrum and recovery for *in vitro* UV-induced cataract using whole lenses. Invest. Ophthalmol. Visual Sci. 42, 2596–2602.

Paul, D.D. (2000) Stratospheric ozone depletion, UV-B radiation and crop disease. Environ. Pollut. 108, 343–355.

Pang, Q.S. and Hays, J.B. (1991) UV-B inducible and temperature-sensitive photoreactivation of cyclobutane pyrimidine dimers in *Arabidopsis thaliana*. Plant Physiol. 95, 536–543.

Paul, N.D., Callaghan, T.V., Moody, S., Gwynn-Jones, D., Johanson, U. and Gehrke, C. (1999) UV-B impacts on decomposition and biogeochemical cycling. In: J. Rozema (Ed.), *Stratospheric ozone depletion: the effects of enhanced UV-B radiation on terrestrial ecosystems*, pp. 117–133. Backhaus, Leiden.

Peletier, H., Gieskes, W.W.C and Buma, A.G.J. (1996) Ultraviolet-B radiation resistance of benthic diatoms isolated from tidal flats in the Dutch Wadden Sea. Marine Ecol.-Progr. Series 135,163–168.

Petersen, A.B., Gniadecki, R., Vicanova, J., Thorn, T. and Wulf, H.C (2000) Hydrogen peroxide is responsible for UVA-induced DNA damage measured by alkaline comet assay in HaCaT keratinocytes. J. Photoch. Photobiol. B: Biology 59, 123–131.

Pitts, D.G., Cullen, A.P. and Hacker, P.D. (1977) Ocular effects of ultraviolet radiation from 295 to 365 nm. Investig. Ophthalmol. 16, 932–939.

Podskochy, A., Gan, L., Fagerholm, P. (2000) Apoptosis in UV-exposed rabbit corneas. Cornea 19, 99–103.

Polo, V., Pinilla, I., Abecia, E., Larrosa, J.M., Pablo, L.E. and Honrubia, F.M. (1997) Assessment of the ocular media absorption index. Int. Ophthalmol. 20, 1–3.

Ravanat, J.-L., Douki, T. and Cadet, J. (2001) Direct and indirect effects of UV radiation on DNA and its components. J. Photochem. Photobiol. B: Biology 63, 88–102.

Reid, G.C. (1999) Solar variability and its implications fo the human environment. J. Atmospheric Solar-Terrestrial Phys. 61, 3–14.

Ren, H.W. and Wilson, G. (1994) The effect of ultraviolet-B irradiation on the cell shedding rate of the corneal epithelium. Acta Ophthalmol. 72, 447–452.

Rozema J. (Ed.) (1999) *Stratospheric ozone depletion: the effects of enhanced UV-B radiation on terrestrial ecosystems*. Backhuys, Leiden.

Rozema, J., van de Staaij, J., Caldwell, M.M. and Björn, L.O. (1997a) UV-B as an environmental factor in plant life: stress and regulation. Trends Ecol. Evolution 12, 22–28.

Rozema, J., Gieskes, W.W.C., van de Geijn, S.C., Nolan, C. and de Boois, H. (Eds.) (1997b) *UV-B and biosphere*. Kluwer, Dordrecht.

Rozema, J., Manetas, Y. and Björn, L.O. (eds) (2001) *Responses of plants to UV-B radiation*. Kluwer Academic Publishers, Dordrecht.

Rozema, J. and Björn, L.O. (Eds.) (2002) Special issue: Evolution of UV-B absorbing compounds in aquatic and terrrestrial plants. J. Photochem. Photobiol. B: Biology 66, 1–87.

Rousseaux, J.C., Ballaré, C.L., Giordano, C.V., Scopel, A.L., Zima, A.M., Szwarccberg-Bracitta, M., Searles, P.S., Caldwell, M.M. and Diaz, S.B. (1999) Ozone depletion and UVB radiation: impact on plant DNA damage in southern South America. Proc. Natl Acad. Sci. USA 96, 15310–15315.

Saito, N. and Werbin, H. (1969) Action spectrum for a DNA-photoreactivating enzyme isolated from higher plants. Radiation Botany 9, 421–424.

Sancar, A. (2003) Structure and function of DNA photolyase and cryptochrome blue-light photoreceptors. Chem. Rev. 103, 2203–2237.

Scheuerlein, R., Treml, S., Thar, B., Tirlapur, U.K. and Häder, D.-P. (1995) Evidence for UV-B-induced DNA degradation in *Euglena gracilis* mediated by activation of metal-dependent nucleases. J. Photochem. Photobiol. B: Biol. 31, 113–123.

Scott, B.R. (1998) Ultraviolet radiation effects upon the eye: Problems of dosimetry. Radiation Prot. Dosim. 76, 277–277

Sinha, R.P., Klisch, M., Gröninger, A. and Häder, D.-P. (1998) Ultraviolet-absorbing Ultraviolet-absorbing/screening substances in cyanobacteria, phytoplankton and macroalgae. J. Photochem. Photobiol. B: Biol. 47, 83–94.

Sinha, R.P., Klisch, M., Gröniger, A. and Häder, D.-P. (2001) Responses of aquatic algae and cyanobacteria to solar UV-B. Plant Ecology 154, 221–236.

Sliney, D.H. (1997) Ultraviolet radiation effects upon the eye: Problems of dosimetry. Radiation Prot. Dosim. 72, 197–206.

Smith, C.C., Prézelin, B.B., Baker, K.S., Bidigare, R.R., Boucher, N.P., Coley, T.L., Karentz, D., MacIntyre, S., Matlick, H.A., Menzies, D., Ondrusek, M., Wan, Z., and Waters, K.J. (1992) Ozone depletion: ultraviolet radiation and phytoplankton biology in Antarctic waters. Science 255, 952–959.

Takeuchi, Y., Murakami, M., Nakajima, N., Kondo, N. and Nikaido, O. (1998) The photorepair and photoisomerization of DNA lesions in etiolated cucumber cotyledons after irradiation by UV-B depends on wavelength. Plant Cell Physiol. 39, 745–750.

Taylor, H.R. (1994) Ocular effects of UV-B exposure. Documenta Ophthalm. 88, 285–293.

Threlfall, T.J. and English, D.R. (1999) Sun exposure and pterygium of the eye: A dose-response curve. Am. J. Ophthalmol. 128, 280–287.

Todo, T. (1999) Functional diversity of the DNA photolyase/blue light receptor family. Mutat. Res. 434, 89–97.

van der Leun, J., Tang, X. and Tevini, M. et al. (1995) Environmental effects of ozone depletion: 1994 assessment. Ambio 24, 137–197.

van der Leun, J., Tang, X. and Tevini, M. et al. (1999) Environmental effects of ozone depletion: 1998 assessment. J. Photochem. Photobiol. B: Biology 46, 1–108.

van der Leun, J., Tang, X. and Tevini, M. et al. (2003) Environmental effects of ozone depletion and its interactions with climate change: 2002 assessment. Photochem. Photobiol. Sci. 2, i-xxiv and 1–72.

van der Leun, J., Bornman, J.F., Tang, X. et al. (2007) Environmental effects of ozone depletion and its interactions with climate change: 2006 assessment. Photochem. Photobiol. Sci. 6, 208–330.

van Donk, E., Faafeng, B.A., De Lange, H.J. and Hessen, D.O. (2001) Differential sensitivity to natural ultraviolet radiation among phytoplankton species in Arctic lakes (Spitsbergen, Norway). Plant Ecology 154, 213–223.

Velders, G.J.M , Andersen, S.O., Daniel, J.S., David W. Fahey, D.W. and Mack McFarland, M. 2007) The importance of the Montreal Protocol in protecting climate. Proc. Natl Acad. Sci. USA 104, 4814–4819.

Weber, S. (2004) Light-driven enzymatic catalysis of DNA repair: a review of recent biophysical studies on photolyases. Biochim. Biophys. Acta 1707, 1–23.

Wu, F. and Deng, N.S. (2000) Photochemistry of hydrolytic iron (III) species and photoinduced degradation of organic compounds. A minireview. Chemosphere 41, 1137–1147.

WHO (1994) Environmental health criteria 160: Ultraviolet radiation. World Health Organisation, Geneva.

Yamada, Y. and Aoki, S. (2006) Efficient cycloreversion of cis,syn-thymine photodimer by a Zn^{2+}-1,4,7,10-tetraazacyclododecane complex bearing a lumiflavin and tryptophan by chemical reduction and photoreduction of a lumiflavin unit. J. Biol. Inorg. Chem. 11, 1007–1023.

Yoon, J.-H., Lee, C.-S., O'Connor, T.R., Yasui, A. and Pfeifer, G.P. (2000) The DNA damage spectrum produced by simulated sunlight. J. Mol. Biol. 299, 681–693.

Young, A.R. Björn, L.O., Moan, J., and Nultsch, W. (Eds) (1993) Environmental UV Photobiology, pp. xxi+479. Plenum Press, New York.

Young, R.W. (1994) The family of sunlight-related eye diseases. Optometry Vision Sci. 71, 125–144.

Zhao, X. and Taylor, J-S. (1996) Mutation spectra of TA, the major photoproduct of thymidylyl-(3´5´)-deoxyadenosine, in Escherichia coli under SOS conditions. Nucleic Acids Res. 24, 1561–1565.

Zhao, X., Liu, J., Hsu, D.S., Zhao, S., Taylor, J.-S. and Sancar, A. (1997) Reaction mechanism of (6–4) photolyase. J. Biol. Chem. 272, 32580–32590.

Zigman, S. (1995) Environmental near-UV radiation and cataracts. Optometry Vision Sci., 72, 899–901.

20
Vitamin D: Photobiological and Ecological Aspects

Lars Olof Björn

Abstract: Abstract. Vitamin D was discovered as a result of its ability to cure rickets, but recently many other important functions for it in the human body have been discoverred, and it counteracts several other diseases, such as diabetes and some forms of cancer. The nuclear vitamin D receptor has been found throughout the vertebrate phylum down to jawless fishes, but not in invertebrates. Its role in those organisms that are repsonsible for the main input to the aquatic food web and to human nutrition, i.e., phytoplankton and zooplankton, is not understood.This chapter summarizes the discovery of vitamin D and the chemistry and photochemistry of its precursors, transformations, and metabolites. The physiological roles of 1,25-dihydroxyvitamin D are briefly described, as well as evolutionary aspects of the signaling in animals based on this compound. The chapter is concluded with an overview of what is known about the occurrence and role of vitamin D in the plant kingdom, biogeographical aspects of vitamin D, and the relatively recent discovery of nonphotochemical production of vitamin D.

20.1. Introduction

As a young boy I was forced to swallow a spoonful of cod liver oil every day. I was told that it contained vitamin D and that I had to eat it to get good bones in my body. I did not wonder why it was in the cod or how it got there. In fact, I did not start to ask such questions until a few years ago. For some of the questions I have so far found no good answers. I learned some surprising things, for instance, that vitamin D is not really a vitamin in the strict sense, and that the cod can hardly make any of it at all.

The early research history relating to vitamin D has been recounted many times, for instance, by DeLuca (1997), and only a short summary will be given here. Rickets was first described in England by Whistler (1645) and Glisson (1650). In the next century Sniadecki established a connection between skeleton
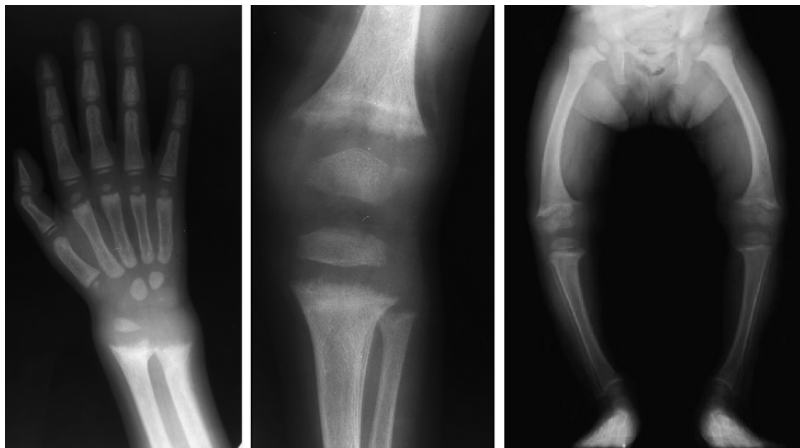
FIGURE 20.1. X-ray plates showing signs of vitamin D deficiency (rickets): incomplete bone-formation in wrist and knee, and malformed legs in a child. (Courtesy Dr. Michael L. Richardson, University of Washington Department of Radiology.)

malformation and lack of sunlight among children in Warszaw (Mozolowski 1939). The disease became known as the English disease in many countries. Mellanby (1918) demonstrated that rickets (Fig. 20.1) could be prevented in dogs by supplanting their diet with cod liver oil, and Hess and Unger (1921) showed that rickets could be cured by sunlight. Hess and Weinstock (1924) and Steenbock and Black (1924) showed that the exposure of lettuce and several other foodstuffs to UV-C radiation would render them antirachitic.

The present review will not treat medical aspects of vitamin D in any detail. Several treatises of this topic are available, e.g., Feldman and Glorieux (1997, 2005), Holick (1999), Bouillon et al. (2004), Lips (2006), and Norman (2006).

20.2. Chemistry and Photochemistry of Provitamin and Vitamin D

There are at least two kinds of vitamin D (also called calciferol), i.e., vitamin D_2 (ergocalciferol) and vitamin D_3 (cholecalciferol), with slightly different structures (Fig. 20.2). The reason that there is no vitamin D_1 is that the product first given this name turned out not to be a single compound, but a mixture containing vitamin D. There seem to be in some nonmammal vertebrates other compounds that act in a similar way as vitamins D_2 and D_3 (Holick 1989), but they have not been chemically defined. In most organisms the synthesis of vitamin D requires UV-B radiation. Exceptions to this rule will be described later. Vitamins D are formed from the provitamins (provitamin D_2, also called ergosterol, and provitamin D_3, also called 7-dehydrocholesterol). UV-B radiation can photoisomerize the provitamins to the corresponding previtamins, either in vivo without the
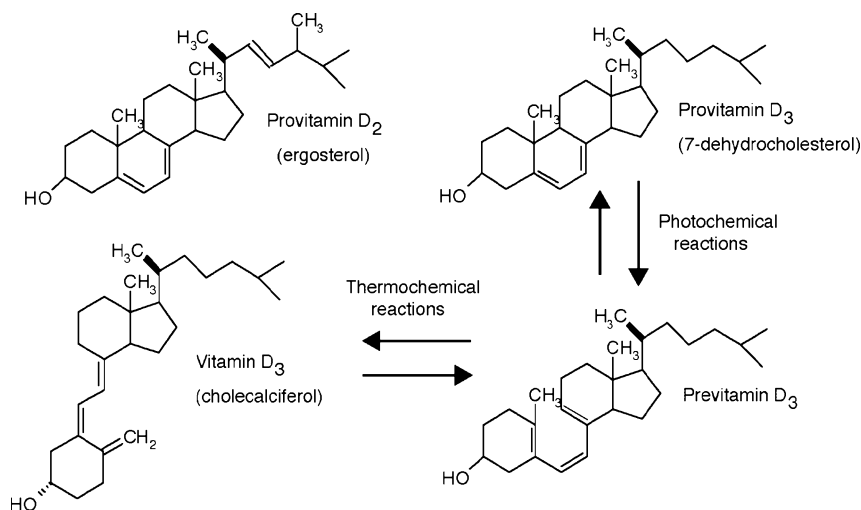
FIGURE 20.2. The structure of the two types of provitamin D: the reversible photoconversion of provitamin D_3 to previtamin D_3, and the reversible thermochemical conversion of previtamin D_3 to vitamin D_3.

mediation of any enzyme, or in solution. The previtamins are slowly converted by a nonenzymatic and nonphotochemical reaction to the vitamins (Fig. 20.2).

The curing of rickets by sunlight can be explained by the fact that provitamin D_3 is synthesized in human skin cells. Exposure to sunlight converts it to previtamin D_3, which is in turn converted to vitamin D_3. Since a vitamin is defined as a substance necessary for health which cannot be synthesized by the body and must be ingested with the food, vitamin D is, strictly speaking, not a vitamin. Since, however, exposure to sunlight is often insufficient for maintaining health, and deficiency can be prevented by vitamin D in the food, the vitamin status is defendable.

On the other hand, it should be noted that the commonly recommended daily vitamin D intake (200 international units [IU] per day) is insufficient for prevention of deficiency if exposure to UV-B radiation does not supplement the intake (Glerup et al. 2000). Attempts to avoid the need for ultraviolet exposure by high daily intake cannot be recommended, as this can lead to vitamin D poisoning. Exposure even to high daily fluence of UV-B radiation can never lead to vitamin D overdosage, as will soon be explained.

As mentioned, the vitamin D precursor previtamin D is formed from provitamin D by a photochemical reaction (Figs. 20.2 and 20.3) driven by ultraviolet radiation (UV-B in the natural condition, but UV-C can also be used artificially). But this is far from the only ultraviolet-driven reaction in the vitamin D context. The basic photochemistry of the vitamin D system was summarized by Havinga (1973). Previtamin D is also sensitive to ultraviolet radiation and can undergo three different photoreversible photochemical reactions. It can be either reconverted to provitamin D or converted to lumisterol or tachysterol and
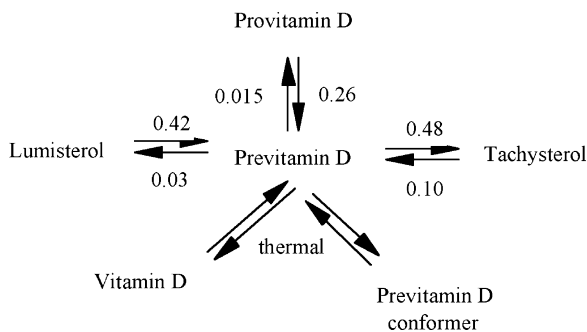
FIGURE 20.3. The reversible conversions of previtamin D with quantum yields of the photochemical reactions. Previtamin D can also be photochemically converted to various compounds termed toxisterols (not shown). (From Havinga 1973, modified.)

further irreversibly to products known under the common name of toxisterols (Boomsma et al. 1975). Vitamin D is sensitive to ultraviolet radiation and can be photoconverted to three compounds: 5,6-*trans*-vitamin D_3, suprasterol 1, and suprasterol 2 (Webb et al. 1989).

Havinga (1973) states that the quantum yields are independent of wavelength, or at least have the same values at 254 and 313 nm. There is, however, as will be detailed below, an important exception to this rule. Although some literature sources give values slightly different from those of Fig. 20.3, there is nothing pointing to differences in quantum yield between the D_2 and D_3 series.

Provitamin D_3 is present in mammalian skin not only in free form, but also esterified with fatty acids, and the esterified provitamin is tranformed to esterified vitamin D_3 upon exposure to ultraviolet radiation (Takada 1983). In fact, most of the provitamin and vitamin D in rat skin is in the esterified form.

A number of authors (reviewed by Dmitrenko et al. 2001) have found curious behavior for the quantum yield for photochemical ring closure of previtamin D (ring closure results in either conversion back to provitamin D, or to formation of lumisterol, which has the same structure as provitamin D except for the direction of a methyl group, which is up for previtamin D in Fig. 20.2, down for lumisterol). This quantum yield increases slowly with wavelength from 295 to 302 nm, but then doubles from 0.08 at 302 nm to 0.16 at 305 nm, and then increases steadily to 0.29 at 325 nm. The quantum yield of *cis-trans* isomerization to tachysterol decreases correspondingly over the same wavelength range. Various explanations for this behavior have been advanced (see Dmitrenko et al. 2001 for further literature).

There are more complications to this photochemical system, which at first glance looks rather simple. It was found that the thermochemical step forming vitamin D following the photochemical conversion of provitamin D takes place much faster in cells than in solution (Tian et al. 1993, Holick et al. 1995). The reason for this is the existence of the conformer of previtamin D (lower right, Fig. 20.3). In solution this is the preferred conformer, and it cannot

be converted directly to vitamin D. In membranes—both natural and artificial liposome membranes (Tian and Holick 1999), the previtamin is held in the active, vitamin-producing conformer (cf. Saltiel et al. 2003). The same effect can be achieved by complexing the previtamin with β-cyclodextrin (Tian and Holick 1995).

Provitamins, previtamins, and vitamins D occur not only in free form, but in plants as glycosides and in mammal skin also as fatty acid esters (Takada et al. 1983). In rat skin at least 80% of the provitamin D_3 was found to be esterified, and upon exposure of the skin to ultraviolet radiation the provitamin D_3 ester is converted to vitamin D_3 ester.

The action spectrum for conversion of provitamin D_3 to previtamin D_3 in human skin has been determined by MacLaughlin et al. (1982). It has a single peak at 295 nm. This roughly corresponds to the long-wavelength absorption band of provitamin D_3 dissolved in n-hexane (Fig. 20.4). The absorption spectrum for provitamin D_3 is three-peaked, but the two short-wave absorption bands are lacking in the action spectrum. Two circumstances could contribute to this lack: (1) the stratum corneum of the skin could filter off the shorter wavelength components, and (2) since at the shorter wavelengths both provitamin and previtamin absorb, but at the longer wavelengths (around 295 nm) only provitamin and tachysterol, the conversion of provitamin to previtamin is favored at long wavelengths, while at shorter wavelengths the back and sidereactions of previtamin are important competitors. Probably, under the conditions in which the action spectrum was determined, the first reason is the more important one.

Lehmann et al. (2001) measured the action spectra for formation of vitamin D_3 as well as $1\alpha,25(OH)_2D_3$ ($1\alpha,25$-dihydroxyvitamin D_3) from provitamin D_3 in "artificial skin" containing cultured human keratinocytes. Remarkably, this action spectrum is displaced about 7 nm toward longer wavelength (peaking
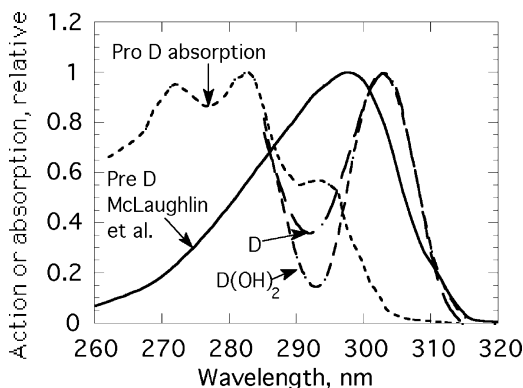
FIGURE 20.4. Absorption spectrum for provitamin D_3, action spectrum for photosynthesis of previtamin D_3 according to MacLaughlin et al. (1982), and action spectra for photosynthesis of vitamin D_3 and $1\alpha,25$-dihydroxyvitamin D_3 accoring to Lehmann et al. (2001).

at about 302 nm) compared to the spectrum determined by MacLaughlin et al. (1982). Although no wavelength below 285 nm was tested, the spectrum indicates a rise from 290 nm toward shorter wavelengths. The minimum at approximately 293 nm is deeper than would be expected from the provitamin D_3 absorption spectrum.

20.3. Transport and Transformation of Vitamin D in the Human Body

In the human body the endogenous provitamin D_3 is present in the cell membranes of cells in the skin. After conversion to vitamin D_3 the molecule no longer fits well into the membrane; one of the hydroxyl groups is sticking out on the outside. This hydroxyl group attaches itself to a carrier protein present in the intercellular liquid, which carries the vitamin into the bloodstream. In the liver it is hydroxylated at carbon atom 25, and after transport to the kidneys also at carbon atom 1. The resulting $1\alpha,25(OH)_2D_3$ is the main active form, an important hormone which travels to different target cells in the body. To some extent also the skin cells are able to transform the vitamin D formed in them to $1\alpha,25(OH)_2D_3$ (Lehmann et al. 2001).

20.4. Physiological Roles of 1,25-Dihydroxyvitamin D in Vertebrates

$1\alpha,25(OH)_2D_3$ (1,25-dihydroxyvitamin D) regulates calcium transport and metabolism at several levels. In our bodies it probably stimulates calcium uptake into enterocytes by keeping calcium channels open (this phase of the calcium uptake is passive). The movement of calcium ions through these cells may also be stimulated by $1\alpha,25(OH)_2D_3$ via vitamin $1\alpha,25(OH)_2D_3$ -dependent calbindin. We know for sure that the energy-requiring extrusion of calcium ions on the inside of the cells is stimulated by vitamin $1\alpha,25(OH)_2D_3$, probably by increasing expression of the calcium pump (Zelinski et al. 1991). $1\alpha,25(OH)_2D_3$ also regulates calcium excretion in the kidneys. It also regulates calcium fluxes to and from the skeleton and bone formation. But apart from its obviously calcium-related effects, it has many other functions (in some cases also related to calcium, but in a less obvious way). Of special interest in understanding the evolution (see below) of the vitamin D system may be the effects on the immune system. It can stimulate the differentiation of bone marrow cells into macrophages (Abe et al. 1981) and regulate T-cell proliferation (Nunn et al. 1986). Recently, however, the opinion has been voiced (Mathieu et al. 2001) that, although immune cells carry $1\alpha,25(OH)_2D_3$ receptors, and although calcium is involved in the functioning of the immune system, vitamin $1\alpha,25(OH)_2D_3$ is redundant in the context. At the same time others maintain a role for vitamin $1\alpha,25(OH)_2D_3$ in immune response (Panda et al. 2001, Griffin et al. 2001).

Vitamin D may protect from some forms of cancer (e.g., prostate cancer, colorectal cancer and non-Hodgkin's lymphoma), infectious diseases (Schauber et al. 2007), and type 1 diabetes. Grant (2006) has reviewed various effects of vitamin D insufficiency on disease risk. The fragility of the skeleton, very common in elderly people due to osteoporosis caused by low vitamin D status, is one cause of bone fracture. A contributing cause of bone fracture is that vitamin D deficiency also affects the muscles in such a way that the risk of falling increases (Bischoff et al. 2003).

20.5. Cellular Effects and the Vitamin D Receptor: Two Basic Modes of Action

$1\alpha,25$-Dihydroxy vitamin D, hereafter abbreviated $D(OH)_2$, is the main physiologically effective vitamin D metabolite, although some effects may be mediated by related derivatives of vitamin D. As far as is known, $D(OH)_2$ acts exclusively through its association with a protein called the vitamin D receptor (VDR). There are two main modes for $D(OH)_2$ to influence cells: the "classical" mode, which is transcription control of nuclear genes, and a "rapid pathway" or "membrane mode." The latter goes via changes in the cell membrane. For a time it was thought that the "rapid response pathway" was mediated by a separate membrane receptor. Interestingly, several other hormones and receptors have this dual action, too. Examples in plants that have been known for a long time are the hormone auxin and the light receptor phytochrome. While regulation of gene transcription takes hours to show up as a physiological effect, the "rapid" responses show up within minutes or even seconds if experiments are properly designed.

One of the reasons for a belief in two different receptor proteins for vitamin D was that compounds related to $D(OH)_2$ (usually referred to as $D(OH)_2$ analogues in the specialized literature) have differential effects via the "classical" and "rapid response" pathways, depending on whether their molecular shape resembles one or the other of two ways in which the flexible $D(OH)_2$ molecule can fold. In Fig. 20.2 the vitamin D molecule is shown stretched out (*trans*-configuration), but it can also have a *cis*-conformation, which is more similar to that shown in the same figure for previtamin D, i.e., more steroid-like. $D(OH)_2$ can exist in the same two conformations. In the conformation shown in Fig. 20.2 it acts preferably via the "classical" mode (controlling gene transcription in the nucleus), in the other conformation preferably via the "rapid" pathway (Norman 2006). But even within the same main pathway, different analogues have differential effects (e.g., DeLuca et al. 2007) due to the complexity of the VDR and its interaction with other proteins.

However, it has recently been found that it is the same receptor protein (VDR) that acts at the cell membrane and in the nucleus, and it appears to have two different binding sites for the two conformers of $D(OH)_2$ (Norman, Mizwicki, and Norman 2004, Norman 2006). At the membrane the VDR is located in caveolae regions. Caveolae are flask-shaped membrane invaginations enriched in sphingolipids and cholesterol.

20.6. Evolutionary Aspects

Why has nature chosen, for the hormonal regulation of calcium metabolism and other bodily functions, a substance requiring the uncertain exposure to ultraviolet radiation for its synthesis? Because the answer to this question is not obvious, we shall take a look into our past to search for it.

One explanation, proposed by Chevalier et al. (1997), is that the formation of 1,25-dihydroxyvitamin D_3 from 7-dehydrocholesterol was originally a catabolic pathway, which has later been taken over for regulatory purposes. Arguments for this are (1) that vitamin D and related substances are rather toxic, and (2) that P450-type enzymes are involved both in hydroxylations that lead to detoxification and solubilization of known toxins and in several hydroxylation steps of vitamin D and its analogs (see reviews of the vitamin D-related hydroxylations by Jones [1999] and Okuda and Ohyama [1999]).

One way of probing into the past is to compare amino acid sequences in proteins of living organisms. We believe that the vitamin D nuclear receptor (VDR) belongs to a class of nuclear receptors of very ancient origin. The nuclear receptor class can be divided into several subclasses, and the divergence into these subclasses occurred at least 600 million years ago (Bertrand et al. 2004). The closest known relative to the VDR is the ecdysone receptor in insects. One way of tracing the origin of the vitamin D regulation system is to track the evolution of the VDR more in detail. Until this has been done we can look for other cues.

In terrestrial vertebrates, i.e., birds, reptiles, and amphibians, the role of vitamin D seems to be in principle rather like that in mammals, although birds are not able to use vitamin D_2 efficiently and there may exist in lizards and frogs other provitamins and vitamins D than D_2 and D_3 (Holick 1989). In humans vitamin D_2 is claimed to be less efficient than D_3 (Armas, Hollis, and Heaney 2004). When we dig further back into our evolutionary past, the evidence starts to become, excuse the expression, more fishy.

Holick (1999) opens a book on vitamin D with the sentence: "Approximately 400 years ago, as vertebrates ventured from the ocean unto land, they were confronted with a significant crisis. As they had evolved in the calcium-rich ocean environment…. However, on land, the environment was deficient in calcium; as a result, early marine vertebrates that ventured onto land needed to develop a mechanism to utilize and process the scarce amounts of calcium in their environment…."

This view is supported by several investigations, which show that various fishes are doing well without vitamin D, and this is true also for at least one freshwater fish (Ashok et al. 1998, 1999). There are, however, an even larger number of investigations pointing to a function for vitamin D in other fish species (Barnett et al. 1979, Brown and Robinson 1992, Larsson 1999 and sources cited therein). It is also not clear why regulation would be unnecessary if calcium uptake does not require energy. There must be some mechanism then to avoid too high a calcium concentration in the cytosol.

The first vertebrates were the jawless Heterostraci and Osteostrachi, whose bodies were covered by bony plates. They were followed in evolution by the first true fishes, the sharklike Placodermi. These, belonging to the Elasmo-branchiomorphi (cartilagous fishes), had no bones inside their bodies, but they were also covered with a bony armor. Could it possibly be that early in evolution the deposition of calcium phosphate and calcium carbonate served as a protection against ultraviolet radiation, and that therefore it was reasonable that its deposition was regulated by radiation? The hypothesis may seem far-fetched, but it is at least in principle testable. One could try to find out whether the thickness of the armor varied with latitude (and thus with UV-B exposure), of course taking continental drift and polar migration into account.

Even the earliest vertebrates mentioned lived less than 550 million years ago, at a time when the protecting ozone shield is thought to have afforded almost the same protection as today (see Chapter 12). The nuclear vitamin D receptor has been found in a jawless fish (Whitfield, Dang, Schluter et al. 2003). But could the regulation of calcium metabolism by vitamin D be of even more ancient origin than the vertebrates? Several investigations point in this direction.

Coccolithophorids are microscopic organisms regarded as protozoans by zoologists and as a kind of golden algae by botanists. They are covered by plates of calcium carbonate, and it has been reported by several authors that they lose their ability to form plates when grown in indoor cultures. If the cultures were exposed to "fluorescent light," the ability to deposit calcium carbonate was restored (Dorigan and Wilbur 1973), but the spectral composition of the fluorescent light was not stated. Vitamin D_2 is reported to have, in combination with bacteria and other food, a beneficial effect on the growth of a copepod (Guerin et al. 2001). In a kind of coral (incidentally a relative of the kind of red coral used for gems) ultraviolet radiation favored the development of normal spicules, structures containing collagen and calcium carbonate. The animal was also shown to produce 1,25-dihydroxy vitamin D in a UV-dependent manner (Kingsley et al. 2001).

The most compelling evidence, however, for the ancient origin of vitamin D as a calcium regulator comes from experiments with snails (Kriajev and Edelstein 1994, 1995 Kriajev et al. 1994). In these animals certain vitamin D–like compounds elevate inracellular exchangable calcium and suppress alkaline phosphatase activity. The authors conclude in their latest paper that the snails adapt to light conditions via the vitamin D endocrine system. The evolutionary lines leading to molluscs and to vertebrates are estimated to have diverged about 720 million years ago (with great uncertainty, from information in Van de Peer et al. [2000] combined with the divergence time of 833 MbP for vertebrates and arthropodes in Nei et al. [2001]). If more compelling evidence of vitamin D regulation in copepods, corals, and coccolithophorids turns up, a much higher age for the regulation system would have credence. If we assume that the vitamin D–elicited induction of calmodulin in plant roots (see Section 20.7.) has an evolutionary origin common with the regulation of calcium metabolism in animals, then this origin lies more than a one and a half billion years back in time (Nei et al. 2001).

There remains the unlikely possibility of convergent evolution—that distantly related organism have independently chosen vitamin D as their calcium regulator. If this is the case, what is so special about vitamin D; why is it the best choice?

Calcium carbonate itself is a poor absorber for ultraviolet radiation and may appear to be a bad choice for production of a radiation shield. Even a cm-thick layer absorbs only half of the incident radiation at the DNA absorption maximum (260 nm) as calculated from data for clear calcite crystals (Washburn et al. 1929). However, to this should be added the scattering effect and, above all, the absorption by proteins and other substances always associated with calcium carbonate shells and other calcified structures.

If the reason for the choice of the ultraviolet-sensitive vitamin D system is not regulation of ultraviolet shielding, what could it be? In Chapter 21 is described how our immune defense is modulated by ultraviolet radiation, but the evolutionary pressure that has selected for this modulation is obscure. It is likely to be relevant, since it occurs through two different mechanisms: UV absorption in urocanic acid and absorption in DNA. Could it be that the original function of the vitamin D system was to modulate the immune defense, a function that to some extent seems still to exist?

That vitamin D (with provitamin D as radiation receptor) even in the human body has a role to play in the defense against ultraviolet radiation is indicated by the recent finding by Sigmundsdottir, Pan, Debes et al. (2007) that production of vitamin D in the skin may induce the migration of T cells to the epidermis, and also the fact that vitamin D counteracts UV-B–induced malignant melanoma (Berwick, Armstrong, Ben-Porat et al. 2005) and the importance of the vitamin D receptor for protection against melanoma (Halsall, Osborne, Potter, Pringle, and Hutchinson 2004; Santonocito, Capizzi, Concolino et al.; 2007). Vitamin D has also been reported to prevent formation of cyclobutane pyrimidine dimers in DNA (De Haes, Garmyn, Verstuyf et al. 2005). The explanatation for nature's choice of a UV-B–induced regulator may be found to be associated with these circumstances.

According to Dixon et al. (2007), the UV protective function of $D(OH)_2$ is mediated by the "rapid effects" (membrane associated) pathway. One can perhaps speculate that the present function of $D(OH)_2$ in vertebrates could have originated as a change in membrane properties caused by the conversion of provitamin D to vitamin D in some way improving the UV resistance without the help of the vertebrate VDR. Only later would rapid VDR-mediated effects have evolved, and finally $D(OH)_2$-mediated gene expression control via the VDR.

20.7. Distribution of Provitamin and Vitamin D in the Plant Kingdom

Among microalgae several (but not all) species of the green algae *Chlorella* (Patterson 1971) and *Chlamydomonas reinhardtii* (Patterson 1974) contain ergosterol. This provitamin has also been found in the diatom *Skeletonema menzelii*

and the coccolithophorid *Emaliana huxlei* (Holick 1989), and the chrysophycean *Ochromonas danica* (Gershengorn et al. 1968). In addition there are numerous investigations on phytoplankton of mixed composition. Of special interest is perhaps a case in which a correlation with the probable ultraviolet exposure has been established, using season as radiation exposure proxy (Takeuchi et al. 1991; see also Tables 1a and 1b in Björn and Wang 2001). Among macroalgae not only ergosterol, but also provitamin D_2 and vitamins D_2 and D_3 have been found in the brown alga *Fucus vesiculosus* grown under natural conditions with higher content of the vitamins at a lower (southern Sweden) than at a higher (northern Norway) latitude, and provitamin D_3 is reported present in the gameto-phyte of the red alga *Chondrus crispus*, while the sporophyte of the same species contained the isomer 22-dehydrocholesterol.

Higher plants generally contain provitamins and vitamins D_2 and D_3 in their leaves (Napoli et al. 1977, Rambeck et al. 1981, Horst et al. 1984, Prema and Raghuramulu 1996, Boland et al. 2003), and in general vitamins are present only after exposure to ultraviolet radiation (Hess and Weinstock 1924, Skliar et al. 2000, Björn and Wang 2001 and references cited therein), but there are exceptions (see Section 20.11). Some plants even form the hydroxylated forms of vitamin D (Napoli et al. 1977, Skliar et al. 2000, Gil, Dallorso and Horst 2007).

20.8. Physiological Effects of Provitamin and Vitamin D in Plants and Algae

Fries (1984) showed that growth of the green macroalga *Enteromorpha compressa*, the red alga *Nemalion helminthoides*, and the brown alga *Fucus spiralis* is stimulated by vitamins and provitamins D. Vitamin D_3 applied to herbaceous and woody plants stimulates initiation of adventitious roots (Buchala and Schmid 1979, Jarvis and Booth 1981, Moncousin and Gaspar 1983). Vitamin D at a nanomolar concentration inhibits root elongation in *Phaseolus vulgaris* and promotes germination of light-sensitive lettuce seed in darkness (Buchala and Pythoud 1988). Vitamin D_3 induces the synthesis of the calcium-binding signaling protein calmodulin in bean roots (Vega and Boland 1986).

20.9. Roles of Provitamin and Vitamin D in Plants

In most plant parts and in algae, ultraviolet radiation seems to be an obligatory requirement for vitamin D formation. It has been proposed (see Chapter 10) that provitamin D could function as a UV-B photoreceptor.

Solanum glaucophyllum forms such large amounts of the active vertebrate hormone form, $1\alpha,25(OH)_2D_3$, that grazing animals are poisoned (see Curino et al. 1998 and Boland et al. 2003 for literature). In this case one can assume a protective function.

There are some still rather uncertain indications that vitamin D and its hydroxy-lated forms can be involved in some way in calcium handling in plants. Thus

Aburjai et al. (1997) found that calcium deprivation increases the concentrations of vitamin D and 25-hydroxyvitamin D in cell cultures of *Solanum malacoxylon*, while results for $1\alpha,25(OH)_2D_3$ were not so clear due to analytical difficulties. Burlini, Bernasconi, and Manzocchi (2002) showed that also the concentration of $1\alpha,25(OH)_2D_3$ increases when calcium ions are removed from the medium. Conversely, Habib and Donelly (2005) claim that the calcium content of potato (*Solanum tuberosum*) plants is increased by either exposure to ultraviolet radiation or administration of vitamin D. This latter claim clearly needs confirmation by independent investigators. Vega and Boland (1988, 1989) and Milanesi and Boland (2006) have pointed to the similarity between the vertebrate vitamin D receptor and proteins present in *Phaseolus vulgaris* and *Solanum glaucophyllum*.

20.10. Biogeographical Aspects

Human complexion tends to be darker the higher the ultraviolet radiation in the environment. This is an inherited ("racial") trait that has evolved independently in Europe and Asia (Norton et al. 2007), but we are also able to acclimatize phenotypically to some extent (i.e., the skin of an individual forms pigment in response to ultraviolet radiation; see Chapter 21 and Cui et al. 2007). Ultraviolet radiation can cause skin cancer and other problems, and these effects are particularly frequent for people poorly adapted for the high environmental radiation they are exposed to, such as people of European origin living in South Africa and Australia. Thus, clearly, the pigment works as protection against high radiation. It has been proposed (Branda and Eaton 1978, Jablonski and Chaplin 2000) that pigmentation is important for photoprotection of folic acid, but in vivo this substance is photoprotected in another way (Vorobey et al. 2006). Although vitamin D is toxic at too high a concentration, it has been shown by Holick et al. (1981) that skin pigment is not necessary to prevent its overaccumulation; the photochemical system is self-regulating. The reason for this is the low rate of conversion of previtamin to vitamin, in combination with the photochemical side and back reactions of previtamin D. Thus, poisoning can occur only by excessive intake (e.g., Koutkia et al. 2001).

There is, however, another connection between complexion and vitamin D. All humans are thought to originate from Africa, and presumably we are all descendents of black people, although at a prehuman furred stage they may have had lighter skin, like chimpanzees (Jablonski and Chaplin 2000). But as our forefathers emigrated to higher and higher latitudes, they became paler (Fig. 20.5), and the selection pressure for this is clear: avoidance of vitamin D deficiency (Clemens et al. 1982). African people who have emigrated north in historic time are known to suffer from just such a deficiency (Shewakramani et al. 2001). Inuits may have more pigment than one would expect from their northern habitat, but their traditional food is from the sea and mostly rich in vitamin D (because the sea currents bring vitamin D from lower and more sunny
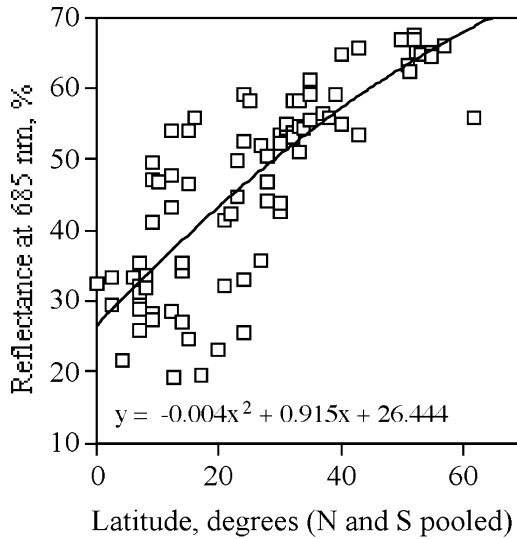
FIGURE 20.5. The relation between skin color (reflectance at 685 nm) and latitude for 85 samples of "indigenous populations" from different parts of the world. Darker skin color is lower in the diagram, and on the abscissa 0 stands for the equator. In the regression equation at the bottom of the graph y stands for reflectance in percent, and x for latitude in degrees. There is a clear trend of darker skin color toward the equator. The great variation around the regression curve has several causes. Even "indigenous populations" have migrated and settled in their present regions within a time span which is often too short to allow complete adaptation to the environment. The way of life also modulates the need for sunlight. Thus, the square at the highest latitude (a little above 60 degrees) lies far below the regression curve. It represents Inuits in southern Greenland. It is thought that they, due to their vitamin D–rich food from the sea, have a lesser need for vitamin D from photochemical conversion in the skin than most other populations. (Data adapted from those compiled by Jablonski and Chaplin 2000).

latitudes), so they have not been exposed to the same selection pressure as people with more terrestrial habits.

Jablonski and Chaplin (2000) found that in in all human populations where data were available, the complexion of women is lighter than that of men. It may be difficult to separate out the acclimation component due to different lifestyles, but the authors believe that it could be an adaptation to the greater need for calcium and vitamin D during pregnancy and lactation.

The question remains: How do nonhuman terrestrial vertebrates manage at high latitudes? As they are often covered with hair or plumage, or are "cold-blooded" (poikilothermic), they would have difficulties in producing their own vitamin D by having either inefficient photochemical conversion of pro- to previtamin or inefficient thermochemical conversion of previtamin to vitamin. In fact, amphibians, and reptiles in particular, decline in frequency with increasing latitude. The arctic dinosaurs may, in fact, have been homeothermic (thermoregulating).

According to an old and abandoned theory, birds produce provitamin D in their uropygial gland, distribute it over their plumage when preening, and thus expose it to sunlight and convert it to vitamin D and ingest it at the next preening. Later investigations with more modern methods of analysis have failed to establish with certainty provitamin D in the uropygial secretion. Disregarding very old and unreliable findings, there is a single paper (Uva et al. 1978) stating the presence of provitamin D_3 in the uropygial gland of domestic fowl (*Gallus*). The analytical methods used are good for their time. Nevertheless, the investigation should be repeated using high-performance liquid chromatography, nuclear magnetic resonance, and absorption spectroscopy, since the identification of provitamin D_3 among all the steroids present in uropygial secretion is no easy matter, and if its presence can be established the analysis should be extended to other kinds of birds. It should also be mentioned that Holick (1989; referring to unpublished observations by himself and M.A. St. Lezin) found no provitamin D_3 in chicken feathers. On the other hand, it is well established that fowl can use UV absorbed by the head and legs to improve their vitamin D and calcium status and egg production. It must be assumed that birds like arctic owls and ptarmigans are totally dependent on vitamin D in the food for covering their requirements. Birds cannot efficiently use vitamin D_2, only D_3.

For arctic mammals, like reindeer, the situation appears grim. Reindeer need a great deal of calcium, not only for the skeleton, but also for the yearly production of antlers. They are covered with fur and do not have a uropygial gland, so their only vitamin D source is food. The critical time is the dark winter, and the most important winter food is reindeer lichen. We (Wang, Bengtsson, Kärnefelt, and Björn 2001) investigated one species of reindeer lichen from different latitudes
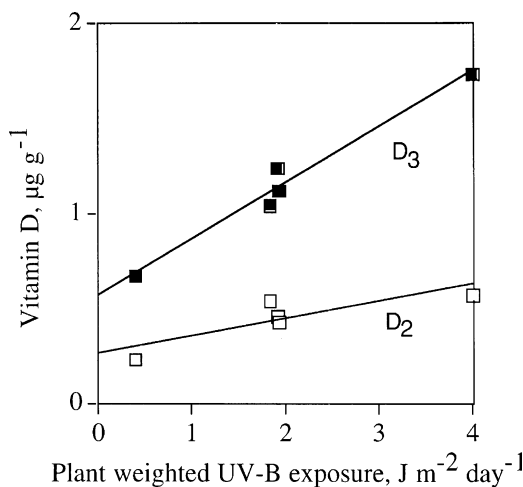
FIGURE 20.6. Vitamins D_2 and D_3 contents in the reindeer lichen *Cladina arbuscula* at different latitudes (northern Finland to Greece). (From Wang, Bengtsson, Kärnefelt, and Björn 2001.)

(Fig. 20.6) and found that it contains both vitamins D_2 and D_3 and in a strongly latitude-dependent manner, with the lowest values in northern Scandiavia even by the end of the summer. Still, 10 g of the lichen from northern Scandinavia would provide a human with the necessary daily amount. Wild reindeer survive, even on Spitsbergen island at 78°N, where the vitamin D content in their food must be lower than this. Could there be another source? It would perhaps be worth looking at what the rumen bacteria can produce.

20.11. The Bright and Dark Sides of Sunlight

Most scientists agree that sunlight has both good and bad effects on health, but opinions differ as to what one should emphasize and what recommendations to give. The positive effect of UV exposure is synthesis of vitamin D and a large number of benefits resulting from it. We Scandinavians and other palefaces also appreciate a "healthy" tan, even if it is clear that all tan (acquired pigmentation in contrast to the genetically determined, constitutive pigmentation) is due to DNA damage (Gilchrest and Eller 2005). The main negative effect is induction of various skin cancers, but there are also others, such as aging of the skin, immunosuppression (Chapter 21), and eye problems (see Chapter 19, Section 19.8.) such as cataracts.

It is not easy even for experts to resolve this dilemma. A number of factors have to be taken into account:

1. The UV-B content of sunlight varies with location and time. An aid for the nonexpert to get an idea of ambient UV exposure is the introduction of the ultraviolet index (UVI), which is in some countries reported in connection with weather forecasts.
2. People are not all equally sensitive, depending mainly on pigmentation, but also on other factors. Darker skin is up to 500 times (Wickelgren 2007) less prone to the negative effects of sunlight, but also less efficient in photosynthesizing vitamin D.
3. Optimal vitamin D synthesis can be achieved by a low but daily exposure to UV-B radiation. A large acute exposure does not result in more vitamin D than a moderate one, while skin cancer risk increases with exposure, perhaps after a threshold. Even so, at high latitudes, for a large part of the year the available radiation is not sufficient for optimal vitamin D synthesis even if people stay out all day, and the winter temperature does not encourage exposure of a large skin area.

In most countries a large part of the population has suboptimal vitamin D status. The best estimate of vitamin D status is the concentration of 25-hydroxyvitamin D_3, not $D(OH)_2$, in the blood serum. The level is Gaussian distributed among individuals with a standard deviation (Fig. 20.7A). When we compare this to Fig. 20.7B, we can see that although the "average person" has a
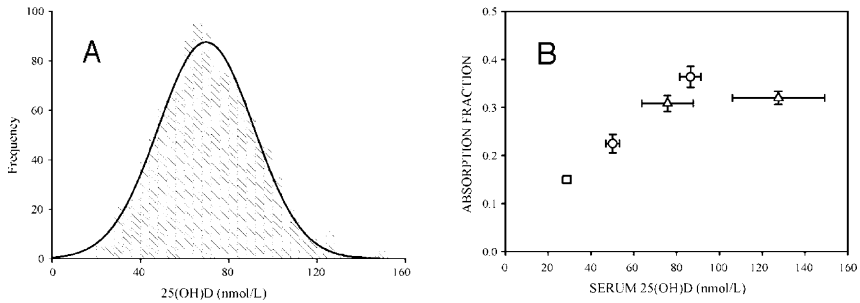
FIGURE 20.7. (**A**) Frequency distribution of seasonally adjusted serum concentrations of 25-hydroxyvitamin D in a semi-rural female population in eastern Nebraska, latitude about 42°N. The solid line is a Gaussian (normal) distribution with mean 71 nmol/L and standard deviation 20 nmol/L. (**B**) Relationship between serum concentration of 25-hydroxyvitamin D serum concentration and calcium absorption. (Copyright Robert P. Heaney, 2006. Used with permission [see Heaney 2007 for details].)

vitamin status that almost meets the need for calcium absorption, about half of the population has a concentration of 25-hydroxyvitamin D that is limiting. Such differences among individuals make it difficult to give proper advice about sun exposure without measuring the 25-hydroxyvitamin D level for each individual and give individual advice.

The graph in Fig. 20.7B is for one function of vitamin D, but Bischoff-Ferrari (2007), taking several criteria into account, arrived at the conclusion that 75 nmol/L of 25-hydroxyvitamin D in the serum represents the minimum level for sufficiency.

20.12. Non-Photochemical Production of Vitamin D

Can vitamin D be produced nonphotochemically? The answer is yes. Curino et al. (1998, 2001) have shown that cells of *Solanum glaucophyllum* grown in culture in darkness form $1\alpha,25(OH)_2D_3$, albeit at lower concentrations than the plant under sun-exposed field conditions. The mechanism is not known, but one has been proposed by Norman and Norman (1993). The mechanism was proposed to explain how animals like subterranean mole-rats, living in darkness from underground plant parts, can obtain their requirement. It is, however, (1) doubtful whether these animals need vitamin D (Pitcher and Buffenstein 1995 and literature cited there) and (2) unlikely that their diet is really completely vitamin D–free, as we have found small amounts of vitamins D_2 and D_3 in carrot roots not exposed to ultraviolet radiation (Wang and Björn, unpublished). The same holds for nocturnal animals (Oppermann and Ross 1990, Kwiecinski et al. 2001). Larsson (1999) has erroneously claimed that Oppermann and Ross (1990) found that the nocturnal fruit-eating bat *Rousettus aegyptiacus* can form 7-dehydrocholesterol from mevalonate.

References

Abe, E., Miyaura, C., Sakagami, H., Takeda, M., Konno, K., Yamazaki, T., Yoshiki, S. and Suda, T. (1981) Differentiation of mouse myeloid leukemia cells induced by 1,25-dihydroxyvitamin D$_3$. Proc. Acad. Sci. USA 78, 4990–4994.

Aburjai, T., Bernasconi, S., Manzocchi, L.A. and Pelizzoni, F. (1997) Effect of calcium and cell immobilization on the production of cholecalciferol and its derivatives by *Solanum malacoxylon* cell cultures. Phytochemistry 46, 1015–1018.

Armas, L.A.G., Hollis, B.W. and Heaney, R.P. (2004) Vitamin D$_2$ is much less effective than vitamin D$_3$ in humans. J. Clin. Endocrin. Metabol. 89, 5387–5391.

Ashok A., Rao, D.S. and Raghuramulu, N. (1998) Vitamin D is not an essential nutrient for rora (*Labeo rohita*) as a representative of freshwater fish. J. Nutrit. Sci. Vitaminol. 44, 195–205.

Ashok, A., Rao, D.S., Chennaiah, S. and Raghuramulu, N. (1999) Vitamin D$_2$ is not biologically active for rora (*Labeo rohita*) as vitamin D$_3$. J. Nutrit. Sci. Vitaminol. 45, 21–30.

Barnett, B.J., Cho, C.Y. and Slinger, S.J. (1979) The essentiality of cholecalciferol in the diets of rainbow trout (*Salmo gairdneri*). Comp. Biochem. Physiol. 63A, 291–297.

Bertrand, W., Brunet, F.G., Escriva, H., Parmentier, G., Laudet, V., and Robinson-Rechavi, M. (2004) Evolutionary genomics of nuclear receptors: From twenty-five ancestral genes to derived endocrine systems. Molec. Biol. Evol. 21, 1923–1937.

Berwick, M., Armstrong, B.K., Ben-Porat, L.J., Fine, J., Kricker, A., Eberle, C. and Barnhill, R. (2005) Sun exposure and mortality from melanoma, J. Natl Cancer Inst. 97, 195–199.

Bischoff-Ferrari, H.A. (2007) The 25-hydroxyvitamin D threshold for better health. J. Steroid Biochem. Mol. Biol. doi:10.1016/j.jsbmb.2006.12.016.

Björn, L.O. and Wang, T. (2001) Is provitamin D a UV-B receptor in plants? Plant Ecology 154, 3–8.

Boland, R., Skliar, M., Curino, A., and Milanesi, L. (2003) Vitamin D compounds in plants. Plant Sci. 164, 357–369.

Bouillon, R., Norman, A.W. and Pasqualini, J.R. (Eds.) (2004) *Vitamin D: Proceedings of the 12th Workshop on Vitamin D*, *July 6–10*, *2003*. Maastricht, the Netherlands. Elsevier, Amsterdam. (Reprinted from J. Steroid Biochem. Mol. Biol. 89–90.)

Boomsma, F., Jacobs, H.J.C., Havinga, E. and van der Gen, A. (1975) Studies of vitamin D and related compounds, part 24. New irradiation products of pre-vitamin D$_3$. Tetrahedron Lett. 7, 427–430.

Branda, R.F. and J.W. Eaton, J.W. (1978) Skin color and nutrient photolysis: an evolutionary hypothesis. Science 201, 625–626.

Brown, P.B. and Robinson, E.H. (1992) Vitamin D studies with channel catfish (*Ictalurus punctuatus*) reared in calcium-free water. Comp. Biochem. Physiol. 103A, 213–219.

Buchala, A.J. and Pythoud, F. (1988) Vitamin D and related compounds as plant growth substances. Physiol. Plantarum 74, 391–396.

Buchala, A.J. and Schmid, A. (1979) Vitamin D and its analogues as a new class of plant growth substances affecting rhizogenesis. Nature 280, 230–231.

Burlini, N., Bernasconi, S. and Manzocchi, L.A. (2002) Effects of elicitors and Ca^{2+} deprivation on the levels of sterols and 1,25-dihydroxy vitamin D-3 in cell cultures of *Solanum malacoxylon*. Functional Plant Biol. 29, 527–533.

Chevalier, G., Baudet, C., AvenelAudran, M., Furman, I. and Wion, D. (1997) Was the formtion of 1,25-dihydroxyvitamin D initially a catabolic pathway? Medical Hypotheses 48, 325–329.

Clemens, T.L., Henderson, S.L., Adams, J.S. and Holick, M.F. (1982) Increased skin pigment reduces the capacity of skin to produce vitamin D in response to ultraviolet irradiation. Lancet 9, 74–76.

Cui, R., Widlund, H.R., Feige, E. Lin, J.Y., Wilensky, D.L., Igras, V.E., D'Orazio, J., Fung, C.Y., Schanbacher, C.F., Granter, S.R. and Fisher, D.E. (2007) Central role of p53 in the suntan response and pathologic hyperpigmentation. Cell 128, 853–864.

Curino, A., Skliar, M. and Boland, R. (1998) Identification of 7-dehydrocholesterol, vitamin D_3, 25(OH)-vitamin D_3 and 1,25(OH)$_2$-vitamin D_3 in *Solanum glaucophyllum* cultures grown in absence of light. Biochim. Biophys. Acta 1425, 485–492.

Curino, A., Milanesi, L., Benassati, S., Skliar, M. and Boland, R. (2001) Effect of culture concitions on the synthesis of vitamin D_3 metabolites in *Solanum glaucophyllum* grown in vitro. Phytochemistry 58, 81–89.

De Haes, P., Garmyn, M., Verstuyf, A., De Clercq, P., Vandewalle, M., Degreef, H., Vantieghem, K., Bouillon, R. and Segaert, S. (2005) 1,25-Dihydroxyvitamin D_3 and analogues protect primary human keratinocytes against UVB-induced DNA damage. J. Photochem. Photobiol. B: Biology 78, 141–148.

DeLuca (1997) Historical overview. In: D. Feldman, F.H. Glorieux, and J.W. Pike (Eds): *Vitamin D*. Academic Press, New York, pp. 3–12.

DeLuca, H.F., Plum, L.A. and Clagett-Dame, M. (2007) Selective analogs of 1,25-dihydroxyvitamin D3 for the study of specific functions of vitamin D. J. Steroid Biochem. Mol. Biol. doi:10.1016/j.jsbmb.2006.12.005.

Dixon, K.M., Deo, S.S., Norman, A.W., Bishop, J.E., Halliday, G.M., Reeve, V.E., and Mason, R.S. (2007) In vivo relevance for photoprotection by the vitamin D rapid response pathway. J. Steroid Biochem. Molec. Biol. 103, 451–456.

Dmitrenko, O.G., Terenetskaya, I.P., and Reischl, W. (1997) Solvent effect on previtamin D conformational equilibrium and photoreactions. J. Photochem. Photobiol. A - Chemistry 104, 113–117.

Dorigan, J.L. and Wilbur, K.M. (1973) Calcification and its inhibition in coccolithophorids. J. Phycol. 9, 450–456.

Fries, L. (1984) D-vitamins and their precursors as growth regulators in axenically cultivated marine macroalgae. J. Phycol. 20, 62–66.

Feldman, D., Glorieux, F.H. and Pike J.W. (Eds.) (1997, 2nd ed. 2005) *Vitamin D*. Academic Press, New York.

Gershengorn. M.C., Smith, A.R.H., Goulston, G., Goad, L.J., Goodwon, T.W. and Haines, T.H. (1968) The sterols of *Ochromonas danica* and *Ochromonas malhamensis*. Biochemistry 7, 1698–1706.

Gil, S., Dallorso, M. and Horst, R. (2007) Screening of vitamin D activity (VDA) of *Solanum glaucophyllum* leaves measured by radioimmunoassay (RIA). J. Steroid Biochem. Mol. Biol. doi:10.1016/j.jsbmb.2006.11.008.

Gilchrest, B.A. and Eller, M.S. (2005) The tale of the telomere: Implications for prevention and treatment of skin cancers. J. Investig. Dermatol. Symp. Proc. 10, 124–130.

Glerup, H., Mikkelsen, K., Poulsen, L., Hass, E., Overbeck, S., Thomsen, J., Charles, P. and Eriksen, E.F. (2000) Commonly recommeded daily intake of vitamin D is not sufficient if sunlight exposure is limited. J. Internal Med. 247, 260–268.

Glisson, F. (1650) De Rachitide sive morbo puerili, qui vulgo The Rickets diceteur.

Grant, W.B. (2006) Epidemiology of disease risks in relation to vitamin D insufficiency. Progr. Biophys. Molec. Biol. 92, 65–79.

Griffin, M.D., Lutz, W., Phan, V.A., BAchman, L.A., McKean, D.J. and Kumar, R. (2001) Dendritic cell modulation by 1,25 dihydroxyvitamin D_3 and its analogs: A vitamin D

receptor-dependent pathway that promotes a persistent state of immaturity in vitro and in vivo. Proc. Natl. Acad. Sci. USA 98, 6800–6805.

Guerin, J.P., Kirchner, M. and Cubizolles, F. (2001) Effects of *Oxyrrhis marina* (Dinoflagellata), bacteria and vitamin D_2 on population dynamics of *Tisbe holothuris* (Copepoda). J. Exp. Marine Biol. Ecol. 261, 1–16.

Habib, A. and Donnelly, D.J. (2005) Stimulation of Ca^{2+} uptake into micropropagated potato plantlets by UV light and vitamin D3. Am. J. Potato Res. 82, 191–196.

Halsall, J.A., Osborne, J.E., Potter, L., Pringle, J.H. and Hutchinson, P.E. (2004) A novel polymorphism in the 1A promoter region of the vitamin D receptor is associated with altered susceptibilty and prognosis in malignant melanoma. Br. J. Cancer 91, 765–770.

Havinga, E. (1973) Vitamin D, example and challenge. Experientia 29, 1181–1193.

Heaney, R.P. (2007) The case for improving vitamin D status. J. Steroid Biochem. Molec. Biol. 103, 635–641.

Hess, A.F. and Unger, L.G. (1921) Cure of infantile rickets by sunlight. J. Am. Med. Assoc. 77, 39.

Hess, A.F. and Weinstock, M. (1924) Antirachitic properties imparted to inert fluids and green vegetables by ultraviolet irradiation. J. Biol. Chem. 62, 301–313.

Holick, M.F. (1989) Phylogenetic and evolutionary aspects of vitamin D from phytoplankton to humans. In: Pang, P.K.T. and Schreibman, M.P. (Eds.), *Vertebrate endocrinology: Fundamentals and biomedical implications*, vol. 3. Academic Press, Orlando, FL, pp. 7–43.

Holick, M.F., MacLaughlin, J.A. and Doppelt, S.H. (1981) Regulation of cutaneous previtamin D3 photosynthesis in man: skin pigment is not an essential regulator. Science 211, 590–592.

Holick, M.F., Tian, X.Q. and Allen, M. (1995) Evolutionary importance for the membrane enhancement of the production of vitamin D_3 in the skin of poikilothermic animals. Proc. Natl Acad. Sci. USA 98, 3124–3126.

Holick, M.F. (Ed.) (1999) *Vitamin D: Physiology*, *molecular biology*, *and clinical*. Humana Press, Totowa, NJ).

Horst, R.L., Reinhardt, T.A., Russell, J.R., and Napoli, J.L. (1984) The isolation and identification of vitamin D_2 and vitamin D_3 from *Medicago sativa* (alfalfa plant). Arch. Biochem. Biophys. 231, 67–71.

Jablonski, N.G. and Chaplin, G. (2000) The evolution of human skin coloration. J. Human Evol. 39, 57–106.

Jarvis, B.C. and Booth, A. (1981) Influence of indole-butyric acid, boron, *myo*-inositol, vitamin D_2 and seedling age on adventitious root developmant in cuttings of *Phaseolus aureus*. Physiol. Plantarum 53, 213–218.

Jones, G. (1999) Metabolism and catabolism of vitamin D, its metabolites and clinically relevant analogs. In: M.F. Holick (Ed.), *Vitamin D: Physiology*, *molecular biology*, *and clinical applications*. Humana Press, Totowa, NJ), pp. 57–84.

Kingsley, R.J., Corcoran, M.L., Krider, K.L. and Kriechbaum, K.L. (2001) Thyroxine and vitamin D in the gorgonian *Leptogorgia virgulata*. Comp. Biochem. Physiol. A 129, 897–907.

Kwiecinski, G.G., Lu, Z.R., Chen, T.C. and Holick, M.F. (2001) Observations on serum 25-hydroxyvitamin D and calcium concentrations form wild-caught and captive neotropical bats, *Artibeus jamaicensis*. Gen. Comp. Endocrinol. 122, 225–231.

Koutkia, P., Chen, T.C. and Holick, M.F. (2001) Vitamin D intoxication associated with an over-the-counter supplement. N. Engl. J. Med. 345, 66–67.

Kriajev, L. and Edelstein, S. (1994) Vitamin D metabolites and extracellular calcium currents in hemocytes of land snails. Biochem. Biophys. Res. Commun. 204, 1096–1101.

Kriajev, L. and Edelstein, S. (1995) Effect of light and nutrient restriction on the metabolism of calcium and vitamin D in land snails. J. Exp. Zool. 272, 153–158.

Kriajev, L., Otremski, I. and Edelstein, S. (1994) Calcium shells from snails: Response to vitamin D metabolites. Calcified Tissue Int. 55, 204–207.

Larsson, D. (1999) *Vitamin D in teleost fish: Non-genomic regulation of intestinal calcium transport*. Diss. Göteborg Univ., Dept of Zoophysiology. ISBN 91-628-3681-1.

Lehmann, B., Genehr, T., Pietzsch, J. and Meurer, M. (2001) UVB-induced conversion of 7-dehydrocholesterol to $1\alpha,25$-dihydroxyvitamin D_3 in an in vitro human skin equivalent model. J. Investig. Dermatol. 117, 1179–1185.

Lips, P. (2006) Vitamin D physiology. Progr. Biophys. Molecul. Biol. 92, 4–8.

Mathieu, C., Van Etten, E., Gysemans, C., Decallone, B., Kato, S., Laureys, J., Devovere, J., Valcx, D., Verstuyf, A. and Bouillon, R. (2001) *In vitro* and *in vivo* analysis of the immune system of vitamin D receptor knockout mice. J. Bone Mineral Res. 16, 2057–2065.

MacLaughlin, J.A., Anderson, R.R. and Holick, M.F. (1982) Spectral character of sunlight modulates photosynthesis of previtamin D_3 and its photoisomers in human skin. Science 216, 1001–1003.

Mellanby, E. (1918) The part played by an "accessory factor"in the production of experimental rickets. J. Physiol. (Lond.) 52, 11–14.

Milanesi, L. and Boland, R. (2006) Presence of vitamin D-3 receptor (VDR)-like proteins in *Solanum glaucophyllum*. Physiol. Plant. 128, 341–350.

Moncousin, C. and Gaspar, T. (1983) Peroxidase as a marker for rooting improvement of *Cynara scolymus* L. cultured in vitro. Biochem. Physiol. Pflanzen 178, 263–271.

Mozolowski, W. (1939) Jedrzej Sniadecki (1768–1838) on the cure of rickets. Nature 143, 121.

Napoli, J.L., Reeve, L.E., Eisman. J., Schnoes, H.K. and DeLuca, H.F. (1977) *Solanum glaucophyllum* as source of 1,25-dihydroxyvitamin D_3. J. Biol. Chem. 252, 2580–2583.

Nei, M., Xu, P., and Glazko, G. (2001) Estimation of divergence times from multiprotein sequences for a few mammalian species and several distantly related organisms. Proc. Natl Acad. Sci. USA 98, 2497–2502.

Norman, A.W. (2006) Minireview: Vitamin D receptor: New assignments for an already busy receptor. Endocrinology 147, 5542–5548.

Norman, A.W., Mizwicki, M.T. and Norman, D.P.G. (2004) Steroid hormone rapid actions, membrane receptors and a conformational ensemble model. Nature Rev. Drug Discov. 3, 27–41.

Norman, T.C. and Norman, A.W. (1993) Consideration of chemical mechanisms for the nonphotochemical production of vitamin D_3 in biological systems. Bioorg. Medical Chem. Lett. 3, 1785–1788.

Norton, H.L., Kittles, R.A., Parra, E., McKeigue, P., Mao, X., Cheng, K., Canfield, V.A., Bradley, D.G., McEvoy, B. and Shriver, M.D. (2007) Genetic evidence for the convergent evolution of light skin in Europeans and East Asians. Mol. Biol. Evol. 24, 710–722.

Nunn, J.D., Katz, D.R., Barker, S., Fraher, L.J., Hewison, M., Hendy, G.N. and O'Riordan, J.L.H. (1986) Regulation of human tonsillar T-cell proliferation by the active metabolite of vitamin D_3. Immunology 59, 479–484.

Okuda, K.-I. and Ohyama, Y. (1999) The enzymes responsible for metabolizing vitamin D. In: M.F. Holick (Ed.), *Vitamin D: Physiology*, *molecular biology*, *and clinical applications.* Humana Press, Totowa, NJ), pp. 85–107.

Opperman, L.A. and Ross, F.P. (1990) The adult fruit bat (Rousettus aegypticus) expresses only calbindin-D9K (vitamin D-dependent calcium-binding protein) in its kidney. Comp. Biochem. Physiol. B: Biochem. Mol. Biol. 97, 295–299.

Panda, D.K., Miao, D., Tremblay, M.L., Sirois, J., Faroohki, R., Hendy, G.N. 6 Goltzman, D. (2001) Targeted ablation of the 25-hydroxyvitamin D 1α-hydroxylase enzyme: evidence for skeletal, reproductive, and immune dysfunction. Proc. Natl Acad. Sci. USA 98, 7498–7503.

Patterson, G.W. (1971) The distribution of sterols in algae. Lipids 6, 120–127.

Patterson, G.W. (1974) Sterols of some green algae. Comp. Biochem. Physiol. B 47, 453–457.

Pitcher, T. and Buffenstein, R. (1995) Intestinal calcium-transport in mole rats (*Cryptomys damarensis* and *Heterocephalus glaber*) is independent of both genomic and non-genomic vitamin D mediation. Exp. Physiol. 80, 597–608.

Prema, T.P. and Raghuramulu, N. (1996) Vitamin D_3 and its metabolites in the tomato plant. Phytochemistry 42, 617–620.

Rambeck, W.A., Kreutzberg, O., Bruns-Droste, C. and Zucker, H. (1981) Vitamin D-like activity of *Trisetum flavescens*. Zschr. Pflanzenphysiol. 104, 9–16.

Saltiel, J., Cires, L., and Turek, A.M. (2003) Conformer-specific photoconversion of 25-hydroxytachysterol to 25-hydroxyprevitamin D_3: Role in production of vitamin Ds. J. Am. Cenm. Soc. 125, 2866–2867.

Santonocito, C., Capizzi,, R. Concolino, P., Lavieri,, M.M., Paradisi, A., Gentileschi, S., Torti, E., Rutella, S., Rocchetti, S., Di Carlo, A., Di Stasio, E., Ameglio, M., Zuppi, C. and Capoluongo, E. (2007) Association between cutaneous melanoma, Breslow thickness and vitamin D receptor BsmI polymorphism. Br. J. Dermatol. 156, 277–282.

Schauber, J., Dorschner, R.A., Coda, A.B., Büchau, A.S., Liu, P.T., Kiken, D., Helfrich, Y.R., Kang, S., Elalieh, H.Z., Steinmeyer, A., Zügel, U., Bikle, D.D., Modlin, R.L. and Gallo, R.L. (2007) Injury enhances TLR2 function and antimicrobial peptide expression through a vitamin D–dependent mechanism. J. Clin. Investig. 117, 803–811.

Skliar, M., Curino, A., Milanesi, E., Benassati, S., and Boland, R. (2000) *Nicotiana glauca*: another plant species containing vitamin D_3 metabolites. Plant Sci. 156, 193–199.

Schwartz, G.G. and Skinner, H.G. (2007) Vitamin D status and cancer: New insights. Curr. Opin. Clin. Nutr. Metab. Care. 10, 6–11.

Shewakramani, S., Rakita, D., Tangpricha, V. and Holick, M.F. (2001) Vitamin D insufficiency is common and under-diagnosed among African American patients. J. Bone Mineral Res. 16, S512.

Sigmundsdottir, H., Pan, J., Debes, G.F., Alt, C., Habtezion, A., Soler, D. and Butcher, E.C. (2007) DCs metabolize sunlight-induced vitamin D3 to "program" T cell attraction to the epidermal chemokine CCL27. Nature Immunol. 8, 283–292.

Steenbock, H. and Black, A. (1924) The induction of growth-promoting and calcifying properties in a ration by exposure to ultra-violet light. J. Biol.Chem. 64, 263–298.

Takada, K. (1983) Formation of fatty acid esterified vitamin D_3 in rat skin by exposure to ultraviolet radiation. J. Lipid Res. 24, 441–448.

Takeuchi, A., Okano, T., Tanda, M. and Kobayashi, T. (1991) Possible origin of extremely high contents of vitamin D_3 in some kinds of fish liver. Comp. Biochem. Physiol. 100A, 483–487.

Tasende, M.G. (2000) Fatty acid and sterol composition of gametophytes and sporophytes of *Chondrus crispus (*Gigartinaceae, Rhodophyta). Scientia Marina 64, 421–426.

Tian, W.Q. and Holick, M.F. (1995) Catalyzed thermal isomerization between previtamin D_3 and vitamin D_3 via β-cyclodextrin complexation. J. Biol. Chem. 270, 8706–8711.

Tian, W.Q. and Holick, M.F. (1999) A liposomal model that mimics the cutaneous production of vitamin D_3. J. Biol. Chem. 274, 4174–4179.

Tian, X.Q., Chen, T.C., Matsuoka, L.Y., Wortsman, J. and Holick, M.F. (1993) Kinetic and thermodynamic studies of the conversion of previtamin D_3 to vitamin D_3 in human skin. J. Biol. Chem. 268, 14888–14892.

Uva, B.M., Ghiani, P., Deplano, S., Madich, A., Vaccari, M. and Vallarino, M. (1978) Occurrence of 7-dehydrocholesterol in the uropygial gland of domestic fowls. Acta Histochem. 62, 237–243.

Van de Peer, Y., Baldauf, S.L., Doolittle, W.F., and Meyer, A. (2000) An updated and comprehensive rRNA phylogeny of (crown) eukaryotes based on rate-calibrated evolutionary distances. J. Molec. Evol. 51, 565–576.

Vega, M.A. and Boland, R.L. (1986)Vitamin D-3 induces the novo synthesis of calmodulin in *Phaseolus vulgaris* root segments in vitro. Biochim. Biophys. Acta 881, 364–374.

Vega, M.A. and Boland, R.L. (1988) Presence of sterol-binding sites in the cytosol of French-bean (*Phaseolus vulgaris*) roots. Biochem. J. 250, 565–569.

Vega, M.A. and Boland, R.L. (1989) Partial characterization of the sterol binding macro-molecule of *Phaseolus vulgaris* roots. Biochim. Biophys. Acta 1012, 10–15.

Vorobey, P., Steindal, A.E., Off, M.K., Vorobey, A. and Johan Moan, J. (2006) Influence of human serum albumin on photodegradation of folic acid in solution. Photochem. Photobiol. 82, 817–822.

Wang, T., Bengtsson, G., Kärnefelt, I. and Björn, L.O. (2001) Provitamins and vitamins D_2 and D_3 in *Cladina* spp. over a latitudinal gradient: possible correlation with UV levels. J. Photochem. Photobiol. B: Biology 62, 118–122.

Washburn, E.W. et al. (Eds.) (1929) *International critical tables of numerical data, physics chemistry and technology*, vol. V, p. 270.McGraw-Hill, New York.

Webb, A.R., de Costa, B. and Holick, M.F. (1989) Sunlight regulates the cutaneous production of vitamin D_3 by causing its photodegradation. J. Clin. Endocrin. Metab. 68, 882–887.

Whistler, D. (1645) Morbo puerili Anglorum, quem patrio idiomate indigenae vocant The Rickets. Lugduni Batavorum 1–13.

Whitfield, G.K., Dang, H.T.L., Schluter, S.F., Bernstein, R.M., Bnag, T., Manzon, L.A., Hsieh, G., Domnguez, C.E., Youson, J.H., Haussler, M.R. and Marchalonis, J.J. (2003) Cloning of a functional vitamin D receptor from the lamprey (*Petromyzon marinus*), an ancient vertebrate lacking a calcified skeleton and teeth. Endocrinology 144(6): 2704–2716.

Wickelgren, I. (2007) A healthy tan? Science 315, 1214–1216.

Zelinski, J.M., Sykes, D.E. and Weiser, M.M. (1991) The effect of vitamin D on rat intestinal plasma membrane Ca-pump mRNA. Biochem. Biophys. Res. Commun, 179, 749–755.

21
The Photobiology of Human Skin

Mary Norval

Abstract: The phenotypes and functions of the cells that comprise the layers of the skin and the skin immune system are described first. The changes occurring in the skin during the induction and elicitation phases of contact hypersensitivity and delayed-type hypersensitivity are summarized as examples of cutaneous immune responses. The exposure of human skin to solar UV radiation can result in a number of effects, many with adverse health outcomes, and the mechanisms involved in each are explained in turn. Pigmentation can develop (immediate pigment darkening and delayed tanning), depending on the phototype of the individual. If the exposure is greater than the minimal erythema dose, sunburn occurs. The features of photoageing are found in chronically sun-exposed skin. Skin cancer, the most common form of cancer in fair-skinned subjects, is also associated with sun exposure, either cumulative or intermittent but intense. The two forms of nonmelanoma skin cancer are squamous cell cancer and basal cell cancer, while the third type of skin cancer, malignant melanoma, is less frequent but more dangerous. Solar UV radiation causes suppression of cell-mediated immune responses, and the implication of this downregulation for the effective control of skin tumors and infectious diseases are considered. Finally, the photodermatoses, which represent a diverse group of conditions linked to abnormal skin responses to UV and/or visible radiation, are described in brief.

21.1. Introduction

The skin is the largest organ of the body and the one which is most exposed to external insults, such as chemicals, infecting microorganisms and mechanical trauma. These insults include UV radiation from the sun. The structure of skin is complex: it is composed of three basic layers—the epidermis, dermis, and subcutis—each comprising a variety of cell types. It has been recognized that the skin contains its own immune system, first called skin-associated lymphoid tissues (Streilein 1978), which generally acts very effectively to deal with any local disturbances. It is now termed the skin immune system. However, UV radiation poses two unique and potentially dangerous consequences for the skin. It induces genotoxic changes, mutations leading on some occasions to the development of skin cancers,

and it can also suppress cell-mediated immune responses to a variety of antigens. The reason for the latter change may be to prevent excessive inflammation in sun-exposed skin, but, if it occurs at the same time as, say, an infection or oncogenesis, then there may be disadvantages for the host. Solar UV radiation does not always cause harmful effects in the skin, and one case where it is beneficial is in promoting the synthesis of vitamin D, essential for calcium metabolism and a healthy skeleton. This aspect is covered in Chapter 20.

The following section outlines the structure of the skin and describes the skin immune system. Consideration is then given to UV radiation in the context of cutaneous pigmentation, sunburn, and photoageing. Sections on photocarcinogenesis and UV-induced immunomodulation follow, and the final part of the chapter outlines some photosensitivity disorders that can occur in human subjects.

21.2. The Structure of Skin and the Skin Immune System

21.2.1. Skin Structure

The outermost layer of the skin is the epidermis, which is separated from the dermis by a basement membrane, and the layer underlying the dermis is the subcutis. UV-B (280–315 nm) penetrates into the epidermis and UV-A (315–400 nm) deeper into the dermis. These layers are transversed vertically by the skin appendages, such as the sweat glands, hair follicles, and sebaceous glands. The appendages are rarely affected by UV radiation and are not considered in this chapter.

The epidermis is composed mainly of keratinocytes that are formed in the basal layer and migrate upward to terminally differentiate at the skin surface. It takes about 4 weeks to complete this process. The appearance of the keratinocytes at each stage divides the epidermis into four layers: (1) the basal layer where the cells divide intermittently, giving rise to one daughter cell remaining in the basal layer and one which begins to differentiate and move upwards, (2) the prickle cell layer, so-called as the keratinocytes have distinct interconnecting junctions, (3) the granular layer where the keratinocytes begin to flatten and contain keratohyalin granules and degenerating organelles, and (4) the stratum corneum where the keratinocytes die and are sloughed off. The thickness of each layer depends on the location in the body. Other important cell types contained within the epidermis are the melanocytes and the Langerhans cells. The former give the skin its color and are found mainly at the dermato-epidermal junction. The latter are dendritic cells whose processes form a network throughout the epidermis. There are also scattered lymphocytes. Figure 21.1 illustrates the cellular structure of the epidermis.

The dermis is very different from the epidermis, consisting of collagen fibers with fibroblasts and elastic tissue throughout. There are blood vessels, nerve fibers, and some smooth muscle, together with small numbers of dendritic cells
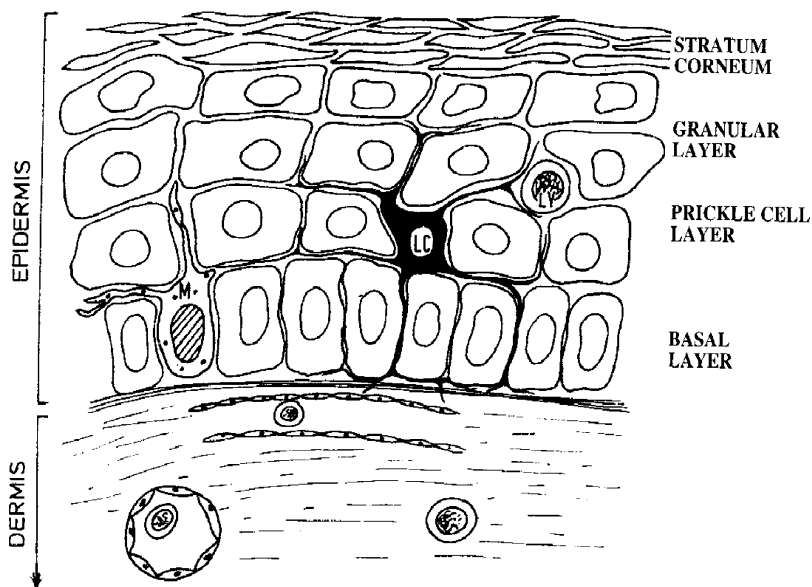
FIGURE 21.1. Diagram of the epidermis indicating the keratinocyte layers and a representative Langerhans cell (LC), melanocyte (M), and lymphocyte (LY). Part of the dermis is also shown illustrating collagen fibers and a small blood vessel.

and tissue macrophages. Mast cells are also present which contain histamine and other inflammatory mediators.

21.2.2. The Skin Immune System

The skin immune system consists of contributions from many skin types, some resident in the epidermis or dermis, and others highly mobile, frequently connecting the cutaneous environment with the blood or lymph (reviewed in Bos 2005). The major populations of resident cells are shown in Table 21.1. The

TABLE 21.1. Major Resident Cells of the Skin Immune System

Skinlayer	Cellcategory	Function(s)
Epidermis	Keratinocytes	Production of cytokines and hormones
	Langerhans cells	Processing and presentation of antigens
	Melanocytes	Production of α-melanocyte stimulating hormone
	T cells	Effector and regulatory functions
Dermis	Mast cells	Production of inflammatory mediators
	Endothelial cells	Regulation of cell migration
	Dendritic cells	Processing and presentation of antigens
	Nerve cells	Production of neuroendocrine hormones and neuropeptides
	T cells	Effector and regulatory functions

Langerhans cells are the initiators of the process, acting as the major antigen-presenting cells of the epidermis. On contact with an antigen, they internalize it, often by phagocytosis, and process it into smaller peptides for presentation on the cell surface. There are associated changes around the Langerhans cells due to a variety of cytokines expressed by the local keratinocytes, including tumor necrosis factor (TNF)-α and interleukin (IL)-1β. In response to these and other mediators, the Langerhans cells migrate from the epidermis. They move down the afferent lymph and enter into the draining lymph node. This process takes around 18 hours following cutaneous application of a contact sensitizer. During the migration, the Langerhans cells mature into dendritic cells, as indicated by the changed expression of various adhesion and co-stimulatory molecules on their surfaces. In the paracortical area of the lymph node, they then present the processed antigenic peptides to specific CD4-positive T cells. These T cells are stimulated to proliferate and to express a particular cytokine profile. The T cells can be divided into T helper 1 (Th1) and Th2 subsets on the basis of the cytokines they produce: the Th1 cells secrete cytokines such as IL-2 and interferon (IFN)-γ, while the Th2 cells secrete cytokines such as IL-4 and IL-10. In some instances the activated T cells home preferentially to the skin as they express particular surface markers. They leave the lymph node in the efferent lymph, enter the bloodstream through the thoracic duct, and migrate via the blood to the site of antigen application. They extravasate through the high endothelial venules and enter the dermis or epidermis to act as effector cells locally.

The cytokine profile of the T cells largely determines the type of immune response generated and its efficiency.

21.2.3. Contact and Delayed-Type Hypersensitivity

Contact hypersensitivity (CHS) is frequently used to assess immune responses in the skin under experimental conditions. In brief, it is divided into two phases: the first is induction/sensitization (afferent) and the second is elicitation/challenge (efferent). During sensitization small, structurally simple haptens are placed on the skin. Haptens on their own are incapable of generating immune responses, but they react with proteins locally in the skin to create immunologically relevant hapten-derivitized proteins. These are taken up by Langerhans cells in the epidermis, as described above, carried to the draining lymph nodes and presented there to specific T cells. In the elicitation phase, rechallenge with the same contact sensitizer occurs on topical application. Antigen-specific T cells are recruited or activated in situ, leading to the release of particular cytokines, infiltration of macrophages and neutrophils, and inflammation. This can be quantified at 24–72 hours postchallenge either by a color change, as is frequently used in human studies, or by swelling, such as of an ear, in the case of mice. The majority of contact sensitizers promote a Th1-like cytokine profile. Resolution of the inflammatory response is an active immune process mediated by specific T cells with regulatory activity. These T cells are thought to act in the lymph nodes draining the challenge site and locally in the skin. A summary of the sequence of events in CHS is given above, and the subject is reviewed in Vocanson et al. (2005) (Table 21.2):

TABLE 21.2. Induction/Sensitization (Afferent) and the Elicitation/Challenge (Efferent).

Induction/sensitization	Elicitation/challenge
First skin contact with antigen	Second skin contact with same antigen
Interaction of antigen with Langerhans cells	Cytokines induced locally
	Recruitment of T-helper 1 cells to skin
Local changes in cytokines in the epidermis	Interaction of T cells with antigen-presenting cells
Local changes in adhesion molecules	
Migration of Langerhans cells from the epidermis	Production of IFN-γ and other immune mediators
Arrival of Langerhans cells in the draining lymph nodes as dendritic cells	Mast cell degranulation
	Local inflammatory response
Interaction of dendritic cells with antigen-specific T cells	Resolution by antigen-specific T-regulatory cells in lymph nodes and skin
Proliferation of T cells polarized to type 1 cytokine production	
Release of T helper 1 cytokines	

Delayed-type hypersensitivity (DTH) has the same end-points but, in contrast to CHS, the antigens are complex. Under natural circumstances and in some animal models, these antigens are often derived from infectious microorganisms or developing tumors. Under experimental conditions, they are frequently injected subcutaneously or intradermally. They are therefore taken up, processed, and presented differently from the simple haptens applied epicutaneously, and the pathway by which UV radiation affects DTH is thought to be slightly different from that involved in CHS.

21.2.4. Effect of Solar UV Radiation on the Skin: Action Spectra

Exposure of human skin to solar UV radiation results in a number of effects which are outlined in Sections 21.3.–21.7. In some instances the wavelength of the radiation which promotes an individual effect with maximal efficiency has been derived from the action spectrum; these results are shown in summary form in Table 21.3, with more detail in the text.

21.3. Pigmentation and Sunburn

21.3.1. Pigmentation and Phototypes

Skin color is determined by cutaneous pigments, particularly melanin, by blood circulating through the skin, and by the thickness of the stratum corneum. Melanin is synthesized by the melanocytes and is released by exocytosis as granules (melanosomes), which are then taken up by the adjacent keratinocytes. Melanin is present in at least two forms: eumelanin, a brown polymer predominating in darkly pigmented skin, and pheomelanin, a reddish-yellow pigment

TABLE 21.3. Selected Skin Responses to UV Radiation

Process	Peak, nm	Ref.
Induction of nonmelanoma skin cancer (mouse)	293	de Gruijl et al.(1993)
Immediate pigment darkening (human)	350	Irwin et al. (1993)
Melanogenesis (human)	290	Parrish et al. (1982)
Erythema (human)	300	McKinley and Diffey 1987)
Decrease in epidermal Langerhans cell numbers (mouse)	270–290	Noonan et al. (1984)
Systemic suppression of contact hypersensitivity (mouse)	260–280	DeFabo and Noonan (1983)
Induction of cyclo-butane pyrimidine dimers (mouse)	290	Cooke and Johnson (1978)
Isomerisation from *trans-* to *cis-*urocanic acid (mouse)	300–315	Gibbs et al. (1993)
Isomerisation from *trans-* to *cis-*urocanic acid (human)	280–310	McLoone et al.(2005)
Formation of pre-vitamin D_3(human)	295–300	MacLaughlin et al. (1982)
T-cell apoptosis	290	Novak et al. (2004)

Note:The peak wavelength is the wavelength of maximum responsiveness.

found in lighter skin types. The production of melanin is influenced by genetic factors, hormones, and exposure to

UV radiation. Racial variation in skin color—black, brown, yellow, and white—is not determined by the absolute number of melanocytes but by their activity in producing melanosomes. As might be expected, the melanosomes are larger and more numerous in black-skinned people. On exposure of the skin to UV radiation, the melanocytes are stimulated to produce melanin, which gives the skin its tan. Individuals vary enormously in this response. Those with fair nonpigmented skin, who cannot or are hardly able to synthesize melanin in response to sun exposure, suffer more cutaneous damage than those who tan, mainly because more UV radiation reaches the dermis. Similarly the ability to tan correlates with less risk of burning after solar UV. There are six phototypes, originally recognized by Fitzpatrick (1988), as shown in Table 21.4.

21.3.2. Sunburn and Minimal Erythema Dose

Sunburn is recognized by erythema and blistering and is caused most effectively by radiation of wavelengths around 300 nm in the UV-B waveband. It is a delayed response, being maximal 8–24 hours after exposure, and it gradually resolves with subsequent skin dryness and peeling. Solar lentigines or freckles can be formed after only one or two episodes of acute solar burning and are often seen on the shoulders, particularly of men. Factors involved in the vasodilatation which characterizes sunburn include direct effects of UV on the vascular endothelium, especially endothelial cell enlargement, the loss of epidermal Langerhans cells, the release of epidermal inflammatory mediators

TABLE 21.4. Classification of Skin Phototypes (Fitzpatrick 1988)

Phototype/Ethnicity	UV-sensitivity	Sunburn/tan
I / White Caucasian	Extremely sensitive	Always burns, never tans
II/ White Caucasian	Very sensitive	Burns readily, tans slowly and with difficulty
III/ White Caucasian	Moderately sensitive	Can burn after highexposure, tans slowly
IV/White Caucasian, often southern Mediterranean	Relatively tolerant	Burns rarely, tans easily
V/Brown, Asian/middle Eastern	Variable	Can burn easily, difficult to assess as pigment is already present
VI/ Black, Afro-Caribbean	Relatively insensitive	Rarely burns

such as TNF-α, and the secretion of vasoactive substances from mast cells, for example, histamine and prostaglandins (Gilchrest et al. 1981).

In sun-burned skin, so-called sunburn cells are seen in the epidermis. They are thought to represent apoptotic keratinocytes and are characterized by a glassy eosinophilic cytoplasm and a pyknotic nucleus (Young 1986). They are induced in a UV-dose–dependent manner, most efficiently by radiation towards the lower end of the UV-B waveband, and are found maximally at 24 hours post-irradiation. They are removed either by desquamation or by keratinocyte-mediated phagocytosis.

It is sometimes necessary to ascertain the minimal erythema dose (MED) of an individual. This is defined as the smallest dose of radiation that results in just detectable reddening of the skin, usually assessed at 24 hours after exposure. It is determined by irradiating the normal, untanned skin, often on the back or the inner upper arm, with a graded series of UV doses. The MED for skin type I is about 150–300 effective J/m^2, while for skin type IV it is 450–600 J/m^2. A monochromatic source is frequently used so that the erythemal response can be investigated at several wavelengths, for example, 300, 320, 350, and 400 nm. Several methods can be used to determine erythema, such as visually, by reflectance spectrophotometry, or by scanning laser Doppler velocimetry. As the MED is a measure solely of each person's sensitivity to UV radiation, another term, the standard erythema dose (SID), has been proposed to refer to UV exposure from natural and artificial sources. One SID is equivalent to an erythemal effective radiant exposure of 100 J/m^2 (Diffey 2002).

21.4. Photoageing

Photoageing is associated with chronically exposed skin and can be distinguished from the more subtle changes which occur during intrinsic ageing due to the passage of time (Taylor et al. 1990). Animal models which have

been used to investigate photoageing and its possible repair include the micropig and the hairless mouse. The UV-B waveband induces the majority of the changes observed. Photoageing is found on the body sites most frequently exposed to sunlight, such as the face and the back of the hands and neck. The last site was first recognized over a hundred years ago, and the condition called "farmer's neck"—the heavily wrinkled nape of the neck—was seen in farmers and sailors who worked outdoors predominantly. The involvement of the endocrine system and other environmental factors, such as smoking, can act to accelerate photoageing (reviewed in Tsoureli-Nikita et al. 2006).

The characteristic features of photoageing include coarse and fine wrinkles, age spots (actinic lentigines containing increased numbers of dermal melanocytes), mottled hyperpigmentation and freckles, elastosis, leathery and thickened skin with surface roughness, and actinic keratoses, which are small scaly lesions, often multiple and persistent. In contrast unexposed skin or intrinsically aged skin is pale, smooth, and relatively unwrinkled.

The first stages of photoageing are inflammatory, where mast cells, monocytes, and neutrophils invade the dermis (Lavker et al. 1988). An increase in dermal elastin is found in the deep to mid-dermis where the fibers are not laid down in an orderly fashion but are amorphous and severely truncated (Sams et al. 1961). Glycosaminoglycans, such as hyaluronate, are deposited in the dermis. The dermal vasculature is reduced and more liable to damage from trauma. The epidermis is initially increased in thickness but then becomes atrophic. The melanin content varies from none to increased in different areas. Loss of collagen within the papillary dermis probably leads to the wrinkled appearance. Fibrillin, which connects the papillary dermal elastic fiber network to that of the deeper dermis, is not expressed. On each exposure to UV, collagen catabolism is induced, followed by repair, but the repair process is not absolute, and, over time, a net loss in collagen occurs, with the skin becoming more fragile as a result (Fisher et al. 1997). There is also impaired wound healing. The signaling pathways involved in photoageing are beginning to be identified and are reviewed in Tsoureli-Nikita et al. (2006).

One of the main concerns regarding photoageing is that it is related to the risk of developing basal cell carcinoma (BCC) and squamous cell carcinoma (SCC) (see next section). Solar elastosis of the back of the neck is one of the most accurate predictors for the risk of developing either of these cutaneous tumors.

21.5. Photocarcinogenesis

The three skin tumors associated with sun exposure are malignant melanoma (MM), arising from the melanocytes in the epidermis, and SCC and BCC, together called the nonmelanoma skin cancers (NMSCs). Both SCCs and BCCs arise from keratinocytes, also in the epidermis, the latter probably from a pluripotential epidermal stem cell. Skin cancer is the most common form of cancer in fair-skinned individuals.

21.5.1. *Nonmelanoma Skin Cancer*

SCCs are found as persistent red, crusted lesions on sun-exposed areas of the body, most frequently on the face and scalp (Fig. 21.2). They metastasize more readily than BCCs and are sometimes fatal. The incidence of SCCs is about 25% that of BCCs in immunocompetent subjects, but SCCs are 15 times more common than BCCs in immunosuppressed subjects, such as those receiving organ transplants. SCCs are found frequently in such patients, with the incidence rising in direct proportion to the time since transplantation and there is an association with papillomavirus infection (see Section 21.6.3.). For example, in a study of renal allograft recipients in Edinburgh, 20% had papillomas and 2% had SCCs by 5 years posttransplantation, while 77% had papillomas and 13% had SCCs by 22 years posttransplantation (Barr et al. 1989).

BCCs present as raised translucent nodules (Fig. 21.3) which develop slowly over a period of months or years. The central area of the face, often around the eyes, is the most likely site to be affected. BCCs are sometimes called rodent ulcers as they have the property of relentless local spread and destruction of large areas of skin, cartilage, and even bone, if left untreated. They can be cured by surgery or radiotherapy, and rarely recur.

Both BCCs and SCCs are very common. For example, NMSC accounted for 20% of registered malignancies in Scotland in 1997, which is probably a substantial underestimation, but for less than 0.5% of cancer deaths. The highest recorded incidences of NMSC are in Australia. One study in Western Australia in 1987–92 in people aged 40–64 recorded incidence rates of 7.1 per 100 per annum in men and 3.4 per 100 in women for BCC, and 0.8 and 0.5 per 100 per annum, respectively, for SCC (English et al. 1997). Although the numbers of cases of NMSC in a population are difficult to assess accurately, various reports indicate an increasing incidence of both BCC and SCC in whites in

FIGURE 21.2. Squamous cell carcinoma at the corner of the mouth shown as a crusted lesion with ulcerated center.
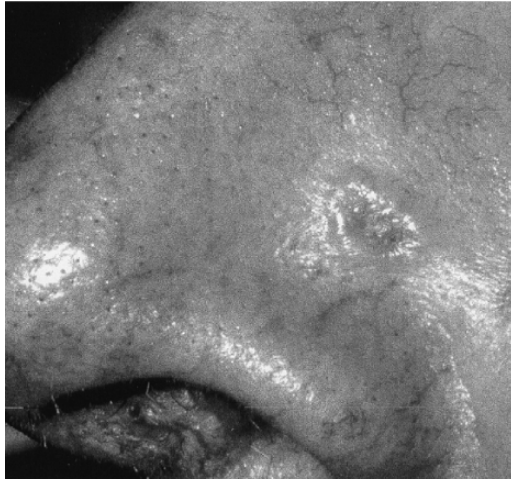
FIGURE 21.3. Basal cell carcinoma on the side of the nose showing a raised rolled edge and translucent appearance.

temperate countries and in places nearer to the equator. As one example, in Norway SCCs more than tripled in men and more than quadrupled in women between 1966/70 and 1991/95 (Iversen and Tretli 1999). As a second example, in southeast Netherlands there was a rapid and continuous increase in the incidence rate of BCC between 1973 and 2000, most marked in young females and on body sites intermittently exposed to sunlight, such as the trunk (de Vries et al. 2004). Forecast modeling of SCC and BCC in the Netherlands predicts that the rates of both cancers will double by 2015 compared with the rates in 2000 (de Vries et al. 2005).

NMSC has a much higher incidence in white than in nonwhite individuals, and those with skin type I are at particular risk. In people with evidence of long-term cutaneous sun damage, such as elastosis of the neck and a large number of solar keratoses, there is also a raised risk of both SCC and BCC. The involvement of DNA damage in the induction of NMSC is shown most clearly in patients with the rare genetic disorder xeroderma pigmentosum (XP), in which there is a defect in the ability to repair DNA following UV exposure and a clinical hypersensitivity to UV radiation. These individuals are at greatly increased risk (5000 times) of developing NMSC compared with normal people, and almost all of the tumors are on constantly exposed sites (Kraemer et al. 1987). A practical and important study indicates that application of a cream containing a DNA repair enzyme to sun-exposed areas of the body reduced the rates of actinic keratosis (a precursor lesion to NMSC) and skin cancer in patients with XP, compared with a placebo cream (Yarosh 2004).

The risk of NMSC in white populations of similar ethnicity increases with decreasing latitude. Positive correlations have been demonstrated between the incidence/mortality of NMSC and solar UV irradiation in the same location. In

most studies outdoor workers have a higher incidence of NMSC than indoors workers. In addition the body sites where the tumors most frequently occur, the face and neck, indicate the importance of sun exposure in their etiology.

The pattern of exposure for the two types of NMSC seems to be somewhat different: for SCC the risk increases with increasing cumulative lifetime dose of UV radiation (Kricker et al. 1994), but for BCC the relationship is more complex, and, although the cumulative dose of UV matters, exposure early in life or intermittent intense exposure such as may be experienced by sunbathing or outdoor recreational activities may be equally important (Kricker et al. 1995). A study in Queensland has revealed that sunscreens applied daily over a period of 4.5 years could prevent the development of SCC and that the dose of solar UV experienced as recently as in the past 5 years can affect the risk of developing SCC (Green et al. 1999). The incidence of BCC was not affected by the sunscreen use.

21.5.2. Malignant Melanoma

Although MM is much less common than BCC or SCC, it causes 80% of the deaths associated with skin cancer. The most frequent type is called superficial spreading, seen as small brown or black lesions characterized by irregular lateral edges (Fig. 21.4), and occurring predominantly on the legs of women and the trunk of men. Survival after surgical removal of a primary melanoma is directly related to the thickness of the tumor, which signals how far the melanocytes have invaded into the underlying dermis. In many areas of the world, the incidence of cutaneous melanoma increases as the latitude decreases, with the highest recorded incidence being in Queensland at 51/100,000 per year in men and 41/100,000 per year in women. However, in Europe the rates are higher in the
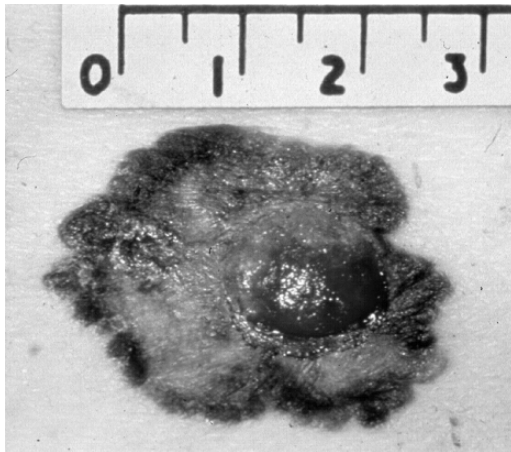
FIGURE 21.4. Superficial spreading malignant melanoma with irregular lateral edge and varying pigments within (size in cm).

north than in the south. This may reflect the propensity of northern Europeans to take holidays in more southern countries. In addition skin phototype may be an important factor as the risk of melanoma is highest in people who burn and do not tan in response to solar UV. The incidence of MM has risen in recent decades in whites, although not in blacks. For example, in the United Kingdom between 1975 and 2000, MM showed the largest increase in incidence rate for all the major tumors. Future forecasts predict that the rate will not decrease for about another 30 years, by which time it will be double that found in 2004 (Diffey 2004). In Australia, similar projections indicate that MM will account for 11% of all new cancer cases in men by 2011 and will be the third most common cancer in men of all ages (McDermid 2005). However, while the mortality rate of MM rose sharply in the second half of the last century, in the past 10 years or so deaths from MM have not risen in line with incidence and have even stabilized in some countries. This may be due to the predominance of thin melanomas (early stage) diagnosed in recent years that respond to treatment with high survival rates. Greater awareness in the population regarding the dangers of changes in the appearance of pigmented moles and subsequent self-referral may account at least in part for this situation.

The strongest risk factor for MM discovered to date is large numbers of atypical nevi (moles) (Swerdlow et al. 1986). It is possible that at least some MM arise from pre-existing benign melanocytic nevi, presumably by further genetic changes. There is an association between early childhood solar exposure and the development of nevi, particularly episodes of sunburn or intense sun exposure, and the number of nevi is also determined, in part, by genetic factors. Studies which attempt to correlate cumulative UV exposure in white populations with the rise in the number of cases of MM have not yielded consistent results. The consensus view at present is that intermittent recreational exposure to the sun may be critical (Elwood and Jopson 1997, Rosso et al. 1998). Certainly there are lifestyle trends in recent decades, such as the fashion to be tanned, many people holidaying in the sun, especially with the advent of cheap charter flights, and minimal clothing being socially acceptable, all of which could lead to intense solar radiation exposure of untanned skin. If this hypothesis is true, then tanning and skin thickening should protect, at least to some extent, against the mutagenic effects of solar UV radiation on melanocytes. The age at which acute solar exposure is experienced may be a factor, and, in general, as for the development of nevi, there is a greater risk in childhood compared with adult UV irradiation.

21.5.3. Animal Studies of Skin Cancer

Many animal studies have investigated the induction of SCC, BCC, and MM and their association with UV exposure. Mice, particularly hairless mice, have been used most frequently and protocols where irradiation is given daily for weeks or months. SCCs are most readily formed in rodents and BCCs very rarely. Quantitative experiments in hairless mice have revealed the action spectrum and

dose-dependence for the induction of SCC (de Gruijl et al. 1993). Radiation of wavelengths around 290 nm is the most effective, but there is also a second, lesser peak in the UV-A waveband at about 390 nm. Experiments in transgenic mice have revealed the type of UV-induced DNA damage that leads to SCC (Jans et al. 2005). Mutations in the tumor suppressor gene, *p53*, are implicated as early events in the etiology of SCC (Berg et al. 1996), and microscopic clusters of epidermal cells with strong expression of mutant p53 are thought to be potential precursors of SCC (Kramata et al. 2005, Rebel et al. 2005). For BCC, UV-induced mutations in the sonic hedgehog signaling pathway, particularly of the *patched* gene, are thought to be important in the initiation of the tumor (Daya-Grosjean and Sarasin 2000; Reifenberger et al. 2005). This pathway plays a role in embryonic development and is involved in oncogenic transformation. Melanin-like tumors can be induced in hybrid fish (Setlow et al. 1989) and in a marsupial (a South American opossum) (Ley 1997) following UV radiation, but not in rodents, unless given at the same time as a chemical carcinogen. However, some transgenic mouse melanoma models have become available recently, and these, together with models in which full thickness human skin is grafted onto immunocompromised mice, have enabled rapid progress to be made regarding the involvement of UV radiation in MM. For example, neonatal activation of the RAS pathways by UV in one transgenic model has been demonstrated to be an important initiating step (Noonan et al. 2001, Hacker et al. 2005). Furthermore, the induction was dependent on the UV-B waveband, with UV-A having no effect (de Fabo et al. 2004).

21.6. Immunosuppression

21.6.1. *UV-Induced Immunosuppression*

In addition to the mutagenic properties of UV, irradiation also leads to suppression of cell-mediated immune responses. Immunomodulation was first recognized three decades ago in a study of the induction of skin tumors in mice by chronic UV-B exposure when a decrease in immunosurveillance against the tumor cells was observed (Fisher and Kripke 1977). The suppression is considered local when the antigen is applied to a body site that has been directly exposed to the UV radiation. It is considered systemic if the antigen is applied to a distant site that has not been directly exposed to the UV radiation. A variety of antigens have been tested, including microorganisms and tumor cells.

It is envisaged that a complex cascade of reactions is initiated when the skin is exposed to UV radiation (reviewed in Duthie et al. 1999, Ullrich 2005, Schwarz 2005a). The major events are shown in (Fig. 21.5).

Exactly what happens may depend to some extent on the dose and wavelength of UV, the surface area irradiated, and the antigen in question and how it is administered. Due to the poorly penetrating power of UV, the initiating event is thought to be absorption at the body surface by chromophores, which change their structure as a result, leading to the production of various immune mediators

UV radiation
↓
Epidermal chromophores: DNA, *trans*-urocanic acid, membrane components
↓
Release of immune mediators: platelet activating factor, prostaglandins,
histamine, cytokines, neuropeptides, neuroendocrine hormones
↓
Changes in Langerhans cell numbers and function
↓
Impaired antigen presentation

Reduction in IL-12 and T helper 1 cytokine production
Induction of T regulatory cells
↓
Immunosuppression of cell-mediated immunity.

FIGURE 21.5. Steps leading to UV-induced immunosuppression.

locally. DNA and *trans*-urocanic acid (UCA), both major absorbers of photons in the epidermis, act as important chromophores. In addition membrane damage and induction of cytoplasmic transcription factors may play critical roles. Brief consideration is now given to each of these.

With UV irradiation of the skin, various types of DNA damage occur, the most common of which is the formation of cyclobutane pyrimidine dimers (CPDs). CPDs have been located in keratinocytes and Langerhans cells after UV exposure, and also in dendritic cells in lymph nodes draining irradiated sites. The CPDs can be repaired artificially using specific enzymes, and thus experiments can be performed in mice to demonstrate that repair leads to the restoration of the immune responses normally suppressed by the UV radiation (Vink et al. 1998). It is not known precisely how the DNA damage affects immunity, but one mechanism might be through activation of particular cytokine genes. It has been shown, for example, the CPD formation leads to the release from keratinocyte cultures of IL-6 and IL-10, both important immunoregulatory molecules. Recently it has been revealed that the cytokine IL-12, already known to abrogate UV-induced immunosuppression if administered following the irradiation (Schmitt et al. 1995), can stimulate repair of the CPDs (Schwarz et al. 2005), thus demonstrating a further link between DNA and cytokine production.

UCA is formed as the *trans*-isomer from histidine as the enzyme histidase is activated in the stratum corneum. It accumulates in that site as no urocanase is found there to catabolize it. On UV exposure of the skin, there is conversion from *trans*- to *cis*-UCA, a reaction which is dose-dependent until the photostationary state is reached with approximately equal quantities of the two isomers. UCA was first suggested in 1983 (De Fabo and Noonan 1983) to be an initiator of UV-induced immunosuppression as its absorption spectrum matched the action spectrum for the suppression of CHS. Since that time, a variety of approaches have confirmed this role (reviewed in Mohammad et al. 1999). For example,

if *cis*-UCA is applied to the skin of mice before infection with a microorganism, the subsequent DTH response to that microorganism is considerably reduced. Furthermore, treating mice with a monoclonal antibody with specificity for *cis*-UCA at the time of UV exposure followed by infection with a microorganism, then challenge with the microorganism, led to the restoration of the DTH response, normally suppressed by the UV radiation. The mechanism of action of *cis*-UCA is not clear at present, or, indeed, where it acts. There is some evidence that it may induce mast cells in the dermis to degranulate, thus releasing mediators such as histamine, or it may alter the function of antigen-presenting cells in the epidermis, or even interact with particular neuropeptides of the sensory nerve system in the skin.

UV-B radiation has been shown to alter the cellular redox equilibrium, which causes oxidative stress and membrane lipid peroxidation. There is activation of various enzymes at the cell surface, leading in turn to the phosphorylation and activation of important transcription factors such as NF-κB. These factors control the production of the immunoregulatory cytokines (reviewed in Schade et al. 2005).

As a result of the above events, there are changes in the cytokine profiles of several cell types, mainly in the epidermis, which have both pro-inflammatory and anti-inflammatory activities (reviewed in Takashima and Bergstresser 1996). For example, keratinocytes begin to produce IL-1α and IL-6. There are also changes in other mediators, such as histamine, neuropeptides, and prostanoids, which are equally important in determining the type of immune response generated. In addition to these mediators, expressed locally within irradiated skin, there are modulations in the function and phenotype of the antigen-presenting cells. One of the most striking effects is the decrease in the number of Langerhans cells in the epidermis with loss of the interdigitating network (Toews et al. 1980). Many migrate to the draining lymph node, while others may undergo apoptosis. If antigen is applied during this time, the dendritic cells, which arrive in the lymph node bearing antigen, cluster abnormally with the T cells due to modulation in the expression of adhesion and co-stimulatory molecules on their surface and perhaps additional changes in antigen internalization and processing. This is thought to lead to the preferential stimulation of Th2 cytokine release, with concomitant downregulation in Th1 cytokine production. For many infections and tumors, the Th1 cytokines are thought to be protective and to confer resistance, so a shift to a Th2 response may be adverse.

There is also generation of antigen-specific T cells that can act as regulatory cells to suppress the immune response. Such cells have been demonstrated in mouse models where they have been purified and transferred to naive mice, thereby downregulating the immune response to that antigen when tested. In one system involving CHS, the T regulatory cells released the immunosuppressive cytokine IL-10 on activation, and, in a different system involving tumor cells, they released IL-4 on activation (reviewed in Schwarz 2005b).

Finally, within 2–3 days of UV exposure, a new population of antigen-presenting cells enters the dermis. These are macrophage in nature, rather than

dendritic. They express high levels of particular cytokines such as IL-10 and different co-stimulatory molecules from Langerhans cells, thereby helping to promote immunosuppression in the skin.

21.6.2. UV-Induced Immunosuppression and Tumors

Skin cancers, induced by chronic UV exposure of mice, are highly antigenic, and the human equivalent is likely to be just as antigenic. It is hypothesized that a neoantigen is formed in the skin by UV at a time when the antigen-presenting cells are altered, resulting in the activation of T cells, which suppress the normal immune responses to the tumor antigens (Kripke 1981). Therefore, the interference in the normal host defense mechanisms by UV may be critical. This can be seen most clearly in immunosuppressed individuals who are at significantly increased risk of developing cutaneous malignancies, particularly SCC. Furthermore, the work on XP patients described in Section 21.5.1. provides compelling evidence to suggest that UV-induced immunosuppression is a crucial factor in the generation of NMSC. Such a conclusion has also been reached using various murine models. For example, preirradiation of mice at one site led to enhanced primary tumor growth at a second irradiated site, with the promotion phase of carcinogenesis being most affected (de Gruijl and van der Leun 1982). In addition, mice which had received T regulatory (suppressor) cells prepared from UV-irradiated animals during the course of chronic UV exposure developed skin tumors earlier than mice receiving T cells from control unirradiated mice. Skin phototype may be an important variable as it has been revealed that people with skin types I/II (see Section 21.3.1.) demonstrate an increased susceptibility to UV-induced immunosuppression compared to people with skin types III/IV (Kelly et al. 2000). This may help to explain why the former group is at higher risk of developing skin cancer than the latter group.

21.6.3. UV-Induced Immunosuppression and Microbial Infection Including Vaccination

Investigations into the impact of UV radiation on human infectious diseases are relatively few. However about 15 models of infection in rodents have been examined in terms of UV and immunity, with the organisms ranging from viruses through bacteria and yeasts to worms (reviewed in Halliday and Norval 1997). In practically all cases, suppression of immunity resulted, together with a decreased ability to clear the infectious agent and sometimes increased severity of symptoms or even death. Calculations have been made to relate the results obtained in the animal models to the human situation, and Garssen et al. (1996) concluded that people could receive sufficient solar UV in about 100 minutes or less at mid-latitudes around noon to suppress their immune responses by 50%. Therefore, on the basis of this study, sunlight irradiance is likely to be biologically relevant to the effectiveness of the human immune response against microbial agents. Questions then arise concerning many infectious diseases,

particularly persistent infections where the organisms are not cleared from the body following the primary infection: these can lead to severe symptoms on reactivation or to oncogenesis.

However, in reality, there are only two convincing examples studied to date where solar UV radiation adversely affects the pathogenesis of human infections. These are herpes simplex virus (HSV), which causes cold sores, and human papillomavirus (HPV), which causes a variety of warts: details are outlined below. In both cases the UV has dual effects–on the virus itself and on the immune response to the virus. The apparent inability of UV to affect other human infections might be because the organisms themselves do not contain any UV-response elements, or because the human immune system has multiple effector pathways so that if one is downregulated, another can compensate. Alternatively, a lack of investigation and awareness of common human infections may account for the apparent difference between the human and the rodent situations.

For HSV, exposure to solar UV radiation is recognized both anecdotally and in epidemiological surveys (for example, Ichihasi et al. 2004) as being one of the most common triggering factors for recrudescence from the latent state. This means that the virus is activated in the ganglia and travels down the nerve axon to the skin, where it can replicate to form the cold sore. UV-induced reactivation of the virus has also been shown experimentally in volunteers (for example, Spruance 1985). It is speculated that one mechanism could involve the delay in, or the downregulation of, the local HSV-specific cell-mediated immunity caused by the UV radiation, which would allow the virus in the cutaneous site time to replicate and to cause the cold sore before recovery of the immune system occurred. A second mechanism may be required to reactivate the virus in the ganglia and thus represents a more direct interaction between the UV radiation and HSV. It has been shown, for example, that UV-induced damage to nerve endings results in changes leading to the activation of HSV promoters; viral reactivation from latency and replication then follow (Loiacono et al. 2003).

For HPV, about 100 genotypes have been discovered that cause infections with variable clinical outcomes. Several years ago, a role for certain types of HPV in NMSC was first suggested in subjects who were immunosuppressed due either to drugs or to genetic disorders. It was noted that the skin tumors in these individuals develop almost entirely on areas of the body most exposed to sunlight (face and backs of the hands) (Hartevelt et al. 1990) and the prevalence is higher in sunny climates. More recently similar HPV types have been found in a significant proportion of NMSC in immunocompetent subjects (reviewed in Akgul et al. 2006). The interactions between UV radiation and HPV infection are complex, but, in brief, HPV is able to stimulate cell proliferation and to inhibit UV-induced apoptosis in the epidermis. These changes, together with the local immunosuppression and specific mutations, both caused by the UV exposure, are thought to lead to tumor progression. A causal role for solar UV radiation in the development of SCC in the conjunctiva of the eye is also proposed from

finding particular HPV types in the majority of such tumors and from the very high prevalence of typical UV-induced mutations in the *p53* gene in the SCCs (Ateenyi-Agaba et al. 2004).

If UV radiation downregulates the immune response to a microorganism, then the efficacy of vaccination could be significantly reduced by the exposure, resulting in a higher chance of symptomatic infection if the organism is encountered at a future date. Only one large-scale experimental study has been carried out thus far to evaluate this important question. Subjects were whole-body UV irradiated before vaccination with recombinant hepatitis surface antigen, and their immune responses compared with a group similarly vaccinated but unirradiated. No difference in antibody or T-cell responses to the vaccine was observed although other nonspecific immune responses were reduced (Sleijffers et al. 2001). However, when the two groups were subdivided on the basis of cytokine polymorphisms and epidermal UCA content, those irradiated individuals with a particular polymorphism in the cytokine IL-1β gene demonstrated suppressed antibody responses to the vaccine (Sleijffers et al. 2002), and other irradiated individuals with high *cis*-UCA content demonstrated suppressed T-cell responses to the vaccine (Sleijffers et al. 2003). Therefore, UV exposure in some people may indeed reduce vaccine effectiveness. Further studies are required to examine the situation for more common vaccines, particularly those such as measles vaccine, that are administered in tropical as well as in temperate climates, and that are designed to promote the Th1 cytokines—the immune response most likely to be suppressed by UV radiation.

21.7. Photodermatoses

The photodermatoses represent a diverse group of conditions associated with abnormal skin responses to UV and/or visible radiation. These diseases have differing aetiologies and symptoms and can be divided into four main categories, each of which is described briefly below.

21.7.1. Genodermatoses: Xeroderma Pigmentosum

The first photodermatos group contains the genodermatoses, which are usually inherited. One example of this group, already mentioned above, is XP, a rare autosomal recessive disorder where the repair of DNA after UV exposure is defective, most frequently because of a mutation in the nucleotide excision repair process (reviewed in Copeland et al. 1997). The subjects suffer from extreme photosensitivity, burning after even minimal sun exposure. They are at greatly increased risk of developing all forms of skin cancer, but especially SCC and BCC. In former times they died before the age of 30 from a metastatic malignancy, usually SCC or MM. More recently, better sun protection is offered and their life expectancy has increased.

21.7.2. *Idiopathic Photodermatoses: Polymorphic Light Eruption*

The second group is the idiopathic photodermatoses, comprising a variety of diseases that probably all have an immunological basis. One of the most common is polymorphic light eruption (PLE), estimated to affect 15% of the population in Britain, for example. PLE is thought to have a higher incidence in temperate climates than nearer the equator and is found in females three to nine times more frequently than in males. In some subjects, provocation occurs on exposure to sources emitting the UV-A waveband, while in others the UV-B waveband is effective. It has been demonstrated from family histories that PLE has a major genetic component with contributing environmental components, mainly sunlight exposure. PLE is manifest as an intermittent pruritic skin eruption which occurs several hours after sun exposure and takes the form of multiple small red papules, which resolve without scarring after a few days to weeks (Fig. 21.6).

Many years ago it was suggested that a photoallergen could be induced in the skin of PLE patients, which then stimulates a cell-mediated immune response, precipitating the development of the lesions. Such a "self" photoallergen has not been identified as yet, although an influx of first CD4-positive lymphocytes, then CD8-positive lymphocytes, is found in the exposed skin, a pattern that mimics a DTH response. In addition it has been shown that fewer neutrophils infiltrate the skin in PLE patients compared with normal subjects in response to erythemal UV doses, indicating a possible defect in neutrophil responsiveness. Because neutrophils represent a major source of immunosuppressive cytokines such as IL-4, the lack of such mediators may contribute to a less suppressed environment and thus to the pathogenesis of PLE (reviewed in Rhodes 2004).

21.7.3. *Cutaneous Porphyrias*

The third group comprises the cutaneous porphyrias, in which there are inherited enzymic defects in heme synthesis leading to the accumulation of photoreactive
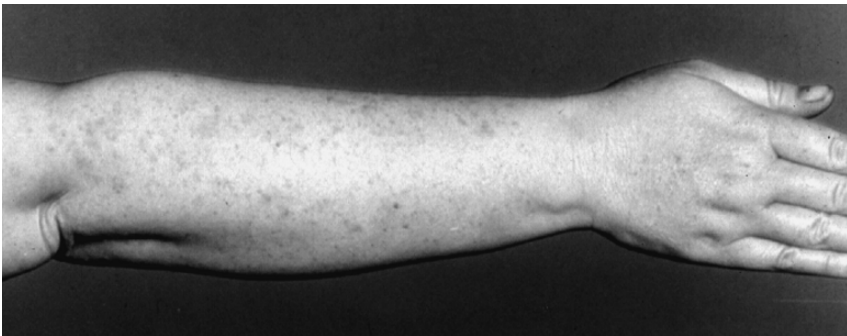
FIGURE 21.6. Polymorphic light eruption showing multiple small papules.

porphyrins, which then photosensitize the skin. However, the porphyrias are precipitated by visible light (around 410 nm) rather than UV and are not considered further here.

21.7.4. Photoallergic Contact Dermatitis

The fourth group comprises photosensitisation by systemic and tropical drugs and by chemicals. Compounds with such properties are increasing in number at the moment with the development of many novel pharmaceutical agents. When these substances get into the skin, they can act as chromophores to absorb UV, thus becoming either phototoxic or triggering a range of biochemical or immunological responses in a proportion of individuals. (Phototoxicity is considered in Chapter 19.) At low concentrations, some drugs and chemicals cause topical photoallergic contact dermatitis where an eczematous eruption occurs on UV-exposed skin sites, activated mainly by UV-A. The drug is converted to a photoproduct, which then binds to proteins or to cells in the skin, forming a novel antigen which then triggers a DTH response. More than one and frequently many exposures to the photoallergen in the presence of UV are required before this response is induced. As one example, 4-para-aminobenzoic acid has been implicated in photoallergic reactions, and its inclusion in sunscreen preparation has declined as a result. Photoallergic contact dermatitis can be diagnosed by duplicate photopatch testing of subjects, in which the substance is assessed with and without exposure to UVA. The structural features of some classes of chemicals which make them active as photoallergens have been identified as part of the European Phototoxicology Project (Barratt et al. 2000).

References

Akgul, B., Cooke, J.C. and Storey, A. (2006) HPV-associated skin disease. J. Pathol. 208, 165–175.

Ateenyi-Agaba, C., Weiderpass, E., Smet, A., Dong, W., Dai, M., Kahwa, B., Wabinga, H., Katongole-Nbidde, E., Franceschi, S. and Tommasino, M. (2004) Epidermodysplasia verruciformis human papillomavirus types and carcinoma of the conjunctiva: a pilot study. Br. J. Cancer 90, 1777–1779.

Barr, B.B., Benton, E.C., McLaren K., Bunney, H., Smith, I.W., Blessing, K. and Hunter, J.A.A. (1989) Human papillomavirus infection and skin cancer in renal allograft recipients. Lancet 1, 124–129.

Barratt, M.D., Castell, J.V., Miranda, M.A. and Langowski, J.J. (2000) Development of an expert system rulebase for the prospective identification of photoallergens. J. Photochem. Photobiol. B: Biol. 58, 54–61.

Berg, R.J., van Kranen, H.J., Rebel, H.G., de Vries, A., van Voten, W.A., van Kreijl, C.F., van der Leun, J.C. and de Gruijl, F.R. (1996) Early p53 alterations in mouse skin carcinogenesis by UVB radiation: immunohistochemical detection of mutant p53 protein in clusters of preneoplastic epidermal cells. Proc. Natl Acad. Sci. USA 93, 274–278.

Bos, J.D. (2005) Skin immune system (SIS), 3rd ed. CRC Press, New York.

Cooke, A. and Johnson, B.E. (1978) Dose response, wavelength dependence and rate of excision of ultraviolet radiation-induced pyrimidine dimers in mouse skin DNA. Biochim. Biophys. Acta 517, *24*–30.

Copeland, N.E., Hanke, C.W. and Michalak, J.A. (1997) The molecular basis of xeroderma pigmentosum. Dermatol. Surg. 23, 447–455.

Daya-Grosjean, L. and Sarasin, A. (2000) UV-specific mutations of the human *patched* gene in basal carcinomas from normal individuals and xeroderma pigmentosus patients. Mutat. Res. 450, 193–199.

De Fabo, E.C. and Noonan, F.P. (1983) Mechanism of immune suppression by ultraviolet irradiation in vivo. I. Evidence for the eistence of a unique photoreceptor in skin and its role in photoimmunology. J. Exp. Med. 157, 84–98.

De Fabo, E.C., Noonan, F.P., Fears, T. and Merlino, G. (2004) Ultraviolet B but not ultraviolet A radiation initiates melanoma. Cancer Res. 64, 6372–6376.

de Gruijl, F.R., Sterenborg, H.J., Forbes, P.D., Davies, R.E., Cole, C., Kelfkens, G., van Weelden, H., Slaper, H and van der Leun, J.C. (1993) Wavelength dependence of skin cancer induction by ultraviolet irradiation of albino hairless mice. Cancer Res. 53, 53–60.

de Gruijl, F.R. and van der Leun, J.C. (1982) Systemic influence of pre-irradiation of a limited area on UV-tumorigenesis. Photochem. Photobiol. *35*, 379–383.

De Vries, E., Louwman, M., Bastiaens, M., de Gruijl, F and Coebergh, J.W. (2004) Rapid and continuous increases in incidence rates of basal cell carcinoma in the southeast Netherlands since 1973. J. Invest. Dermatol. 123, 634–638.

De Vries, E., van de Poll-Franse, L.V., Louwman, W.J., de Gruijl, F.R. and Coebergh, J.W.W. (2005) Prediction of skin cancer incidence in the Netherlands up to 2015. Br. J. Dermatol. 152, 481–488.

Diffey, B.L. (2002) Sources and measurement of ultraviolet radiation. Methods 28, 4–13.

Diffey, B.L. (2004) The future incidence of cutaneous melanoma within the UK. Br. J. Dermatol. 151, 868–872.

Duthie, M.S., Kimber, I. and Norval M. (1999) The effects of ultraviolet radiation on the human immune system. Br. J. Dermatol. 140, 995–1009.

Elwood, J.M. and Jopson, J. (1997) Melanoma and sun exposure: an overview of published studies. Int. J. Cancer, 73, 198–203.

English, D.R., Kricker, A., Heenan, P.J., Randell, P.L., Winter, M.G. and Armstrong, B.K. (1997) Incidence of non-melanocytic skin cancer in Geraldton, Western Australia. Int. J. Cancer, 73, 629–633.

Fisher, M.S. and Kripke, M.L. (1977) Systemic alteration induced in mice by ultraviolet light irradiation and its relationship to ultraviolet carcinogenesis. Proc. Natl Acad. Sci USA 74, 1688–1692.

Fisher, G.J., Wang, Z.Q., Datta, S.C., Varani, J., Kang, S. and Vourhees, J.J. (1997) Pathophysiology of premature skin ageing induced by ultraviolet light. N. Engl. J. Med. 337, 1419–1428.

Fitzpatrick, T.B. (1988) The validity and practicality of sun-reactive skin types I through VI. Arch. Dermatol. 124, 869–871.

Garssen, J., Goettsch, W., de Gruijl, F., Slob, W and Van Loveren, H. (1996) Risk assessment of UVB effects on resistance to infectious diseases. Photochem. Photobiol. 64, 269–274.

Gibbs, N.K., Norval, M., Traynor, N.J., Wolf, M., Johnson, B.E. and Crosby, J. (1993) Action spectra for the *trans* to *cis* photoisomerisation of urocanic acid *in vitro* and in mouse skin. Photochem. Photobiol. 57, 584–590.

Gilchrest, B.A., Soter, N.A., Stoff, J.S. and Mihm, M.C. (1981) The human sunburn reaction: Histologic and biochemical studies. J. Am. Acad. Dermatol. 5, 411–422.

Green, A., Williams, G., Neale R., Hart, V., Leslie, D., Parsons, P., Marks, G.C., Gaffney, P., Battistutta, D., Frost, C., Lang, C. and Russell, A. (1999) Daily sunscreen application and betacarotene supplementation in prevention of basal-cell and squamous-cell carcinoma of the skin: a randomised controlled trial. Lancet 354, 723–729.

Hacker, E., Irwin, N., Muller, H.K., Powell, M.B., Kay, G., Hayward, N. and Walker, G. (2005) Neonatal ultraviolet radiation exposure is critical for malignant melanoma induction in pigmented Tpras transgenic mice. J. Invest. Dermatol. 125, 1074–1077.

Halliday, K.E. and Norval, M. (1997) The effects of ultraviolet radiation on infectious diseases. Rev. Med. Microbiol. 8, 179–188.

Hartevelt, M.M., Bouwes Bavinck, J.N., Kootte A.M., Vermeer, B-J. and Vanden-broucke, J.P. (1990) Incidence of skin cancer after renal transplantation in the Netherlands. Transplantation, 49, 506–509.

Ichihashi, M., Nagai, H. and Matsunaga, K. (2004) Sunlight is an important causative factor of recurrent herpes simplex. Cutis 74 (Suppl. 5), 14–18.

Irwin, C., Barnes, A., Veres, D. and Kaidbey, K. (1993) An ultraviolet action spectrum for immediate pigment darkening. Photochem. Photobiol. 57, 504–507.

Iversen, T. and Tretli, S. (1999) Trends for invasive squamous cell neoplasia of the skin in Norway. Br. J. Cancer, 81, 528–531.

Jans, J., Schul, W., Sert, Y.G., Rijksen, Y., Rebel, H., Eker, A.P., Nakajima, S., van Steeg, H., de Gruijl, F.R., Yasui, A., Hoeijmakers, J.H. and van der Horst, G.T. (2005) Powerful skin cancer protection by a CPD-photolyase transgene. Curr. Biol. 15, 105–115.

Kelly, D.A., Young, A.R., McGregor, J.M., Seed, P.T., Potten, C.S. and Walker, S.L. (2000) Sensitivity to sunburn is associated with susceptibility to ultraviolet radiation-induced suppression of cutaneous cell-mediated immunity. J. Exp. Med. 191, 561–566.

Kraemer, K.H. Lee, M.M. and Scotto, J. (1987) Xeroderma pigmentosum. Cutaneous, ocular, and neurologic abnormalities in 830 published cases. Arch. Dermatol. 123, 241–250.

Kramata, P., Lu, Y.P., Lou, Y.R., Singh, R.N., Kwon, S.M. and Conney, A.H. (2005) Patches of mutant p53-immunoreactive epidermal cells induced by chronic UVB irradiation harbor the same p53 mutations as squamous cell carcinomas in the skin of hairless SKH-1 mice. Cancer Res. 65, 3577–3585.

Kricker, A., Armstrong B.K. and English, D.R. (1994) Sun exposure and non-melanocytic skin cancer. Cancer Causes Control 5, 367–392.

Kricker, A., Armstrong, B.K., English, D.R. and Heenan, P.J. (1995) Does intermittent sun exposure cause basal cell carcinoma? A case-control study in Western Australia. Int. J. Cancer 60, 489–494.

Kripke, M.L. (1981) Immunologic mechanisms in UV radiation carcinogenesis. Adv. Cancer Res. 34, 69–106.

Lavker, R.M. and Kligman, A.M. (1988) Chronic heliodermatitis: a morphologic evaluation of chronic actinic dermal damage with emphasis on the role of mast cells. J. Invest. Dermatol. 90, 325–330.

Ley, R.D. (1997) Ultraviolet radiation A-induced precursors of cutaneous melanoma in Monodelphus domestica. Cancer Res. 57, 3682–3684.

Loiacono, C.M., Taus, N.S. and Mitchell, WJ. (2003) The herpes simplex type 1 ICP0 promoter is activated by viral reactivation stimuli in trigeminal ganglia neurons of transgenic mice. J. Neurovirol. 9, 336–345.

MacLaughlin, J.A., Anderson, R.R. and Holick, M.F. (1982) Spectral character of sunlight modulates photosynthesis of previtamin D3 and its photisomers in human skin. Science 216, 1001–1003.

McDermid, I. (2005) *Cancer incidence projections Australia 2002–2011*. Australian Institute of Health and Welfare, Australasian Association of Cancer Registries and the National Cancer Strategies Group, Report No. 30, Canberra, Australia, p. 166.

McKinlay, A.F. and Diffey, B.L. (1987) A reference action spectrum for ultraviolet induced erythema in humans skin. In: W.F. Passhier and B.F. Bosnjakovic (Eds.), *Human exposure to ultraviolet radiation: Risks and regulation*, pp. 45–52. Elsevier, Amsterdam.

McLoone, P., Simics, E., Barton, A., Norval, M. and Gibbs, N.K. (2005) An action spectrum for the production of *cis*-urocanic acid in human skin. J. Invest Dermatol. 125, 1071–1074.

Mohammad, T., Morrison, H. and HogenEsch, H. (1999) Urocanic acid photochemistry and photobiology. Photochem. Photobiol. 69, 115–135.

Noonan, F.P., Bucana, C., Sauder, D.N. and De Fabo, E.C. (1984) Mechanism of systemic immune suppression by UV radiation *in vivo*. II. The UV effects on number and morphology of epidermal Langerhans cells and the UV-induced suppression of contact hypersensitivity have different wavelength dependencies. J. Immunol. 132, 2408–2416.

Noonan, F.P., Recio, J.A., Takayama, H., Duray, P., Anver, M.R., Rish, W.L., De Fabo, E.C. and Merlino, G. (2001) Neonatal sunburn and melanoma in mice. Nature 413, 271–272.

Novak, Z., Berces, A., Ronto, G., Pallinger, E., Dobozy, A and Kemeny, L. (2004) Efficacy of different UV-emitting light sources in the induction of T-cell apoptosis. Photochem. Photobiol. 79, 434–439.

Parrish, J.A., Jaenicke, K.F. and Anderson, R.R. (1982) Erythemas and melanogenesis action spectra of normal human skin. Photochem. Photobiol. 36, 187–191.

Rebel, H., Kram, N., Westerman, A., Banus, S., van Kranedn, H.J. and de Gruijl, F.R. (2005) Relationship between UV-induced mutant p53 patches and skin tumors, analysed by mutation spectra and by induction kinetics in various DNA-repair-deficient mice. Carcinogenesis 26, 2123–2130.

Reifenberger, J., Wolter, M., Knobbe, C.B., Kohler, B., Schonicke, A., Scharwachter, C., Kumar, K., Blaschke, B., Ruzicka, T. and Reifenberger, G. (2005) Somatic mutations in the PTCH, SMOH, SUFUH and TP53 genes in sporadic basal cell carcinomas. Br. J. Dermatol. 152, 43–51.

Rhodes, L.E. (2004) Polymorphic light eruption: does a neutrophil defect contribute to the pathogenesis? J. Invest. Dermatol. 123, xiii–xv.

Rosso, S., Zanetti, R., Pippioni, M. and Sancho-Garnier, H. (1998) Parallel risk assessment of melanoma and basal cell carcinoma: skin characteristics and sun exposure. Melanoma Res. 8, 573–583.

Sams, W.M. and Smith, J.G. (1961) The histochemistry of chronically sun damaged skin. J. Invest. Dermatol. 37, 447–452.

Schade, N., Esser, C. and Krutmann, J. (2005) Ultraviolet B radiation-induced immuno-suppression: molecular mechanisms and cellular alteration. Photochem. Photobiol. Sci. 4, 699–708.

Schmitt, D.A., Owen-Schaub, L. and Ullrich, S.E. (1995) Effect of IL-12 on immune suppression and suppressor cell induction by ultraviolet light. J. Immunol. 154, 5114–5120.

Schwarz, T. (2005a) Mechanisms of UV-induced immunosuppression. Keino J. Med. 54, 165–171.

Schwarz, T. (2005b) Regulatory T cells induced by ultraviolet radiation. Int. Arch. Allergy Immunol. 137, 187–193.

Schwarz, A., Maeda, A., Kernbeck, K., van Steeg, H., Beissert, S. and Schwarz, T. (2005) Prevention of UV radiation-induced immunosuppression by IL-12. J. Exp. Med. 201, 173–179.

Setlow, R.B., Woodhead, A.D. and Grist, E. (1989) Animal model for ultraviolet radiation-induced malignant melanoma. Proc. Natl Acad. Sci. USA 86, 8922–8926.

Sleijffers, A., Garssen, J., de Gruijl, F.R., Boland, G.J., van Hattum, J., van Vloten and van Loveren, H. (2001) Influence of ultraviolet B exposure on immune responses following hepatitis B vaccination in human volunteers. J. Invest. Dermatol. 117, 1144–1150.

Sleijffers, A., Yucesoy, B., Kashon, M., Garssen, J., de Gruijl, F.R., Boland, G.J., van Hattum, J., Luster, M.I. and van Loveren, H. (2003) Cytokine polymorphisms play a role in susceptibility to ultraviolet B-induced modulation of immune responses after hepatitis B vaccination. J. Immunol. 170, 3423–3428.

Sleijffers, A., Kammeyer, A., de Gruijl, F.R., Boland, G.J., van Hattum, van Vloten W.A., van Loveren, H., Teunissen, M.B. and Garssen, J. (2003) Epidermal cis-urocanic acid levels correlate with lower specific cellular immune responses after hepatitis B vaccination of ultraviolet B-exposed humans. Photochem. Photobiol. 77, 271–275.

Spruance, S.L. (1985) Pathogenesis of herpes simplex labialis: experimental induction of lesions with UV light. J. Clin. Microbiol. 22, 366–368.

Streilein, J.W. (1978) Lymphocyte traffic, T cell malignancies and the skin. J. Invest. Dermatol. 71, 167–171.

Swerdlow, A.J., English, J., MacKie, R.M., O'Doherty, C.J., Hunter, J.A.A., Clark, J. and Hole, D. (1986) Benign melanocytic naevi as a risk factor for malignant melanoma. Br. Med. J. 292, 1555–1559.

Takashima, A and Bergstresser, P.R. (1996) Impact of UVB radiation on the epidermal cytokine network. Photochem. Photobiol. 63, 397–400.

Taylor, C.R., Stern, R., Leyden, J.J. and Gilchrest, B.A. (1990) Photoageing, photodamage and photoprotection. J. Am. Acad. Dermatol. 22, 1–15.

Toews, G.B., Bergstresser, P.R. and Streilein, J.W. (1980) Epidermal Langerhans density determines whether contact hypersensitivity or unresponsiveness follows skin painting with DNFB. J. Immunol. 124, 445–453.

Tsoureli-Nikita, E., Watson, R.E.B. and Griffiths, C.E.M. (2006) Photoageing: the darker side of the sun. Photochem. Photobiol. Sci. 5, 160–164.

Ullrich, S.E. (2005) Mechanisms underlying UV-induced immune suppression. Mutat. Res. 571, 185–205.

Vink, A.A., Schreedhar, V., Roza, L., Krutmann, J. and Kripke, M.L. (1998) Cellular target of UVB-induced DNA damage resulting in local suppression of contact hypersensitivity. J. Photochem. Photobiol. B: Biol. 44, 107–111.

Vocanson, M., Hennino, A., Chavagnac, C., Saint-Mezard, P., Dubois, B., Kaiserlian, D. and Nicolas, J.-F. (2005) Contribution of CD4^{+} and CD8^{+} T-cells in contact hypersensitivity and allergic contact hypersensitivity. Expert Rev. Dermatol. 1, 75–86.

Yarosh, D.B. (2004) DNA repair, immunosuppression, and skin cancer. Cutis, 74 (Suppl 5), 10–13.

Young, A.R. (1986) The sunburn cell. Photodermatology 4, 127–134.

22
Light Treatment in Medicine

Theresa Jurkowitsch and Robert Knobler

Abstract: The beneficial uses of light have been noted and observed since ancient times; it is only since the last century that these beneficial effects have also been studied and explored from a scientific point of view leading to more specific applications as well as a better understanding of the mechanisms of action, both chemical and biological, responsible for the observed effects. Among the fields of medicine that have taken it upon themselves to deal with the therapeutic effects of light, dermatology is considered to be a major representative. As examples for the medical uses of light we concentrate on the following: phototherapy (use of UV-A and UV-B radiation without added photosensitizer), photochemotherapy, extracorporeal photochemotherapy (both of which combine photosensitizers and ultraviolet radiation), and photodynamic therapy (using photosensitizers activated by light in the red or blue range). Some other very widespread medicinal uses of light are briefly covered.

22.1. Introduction

Sunlight has both beneficial and deleterious effects on the human body. As Paracelsus stated about 600 years ago, "dosis sola facit venenum" (the dose determines the poison). For the deleterious effects we refer the reader to Chapters 18, 19, and 21, and we shall concentrate here on how light can be used for medical treatment.

Light has been used as a therapeutic agent since ancient times. In ancient Egypt, more than 4000 years ago, the juice of *Ammi majus* (Apiaceae), False Bishop's Weed, which grows throughout the Nile River valley, was rubbed on patches of vitiligo (unpigmented patches of skin), after which patients were encouraged to lie in the sun. Corresponding treatments are known also from old India and China. The active substances in *Ammi majus* consist of a mixture of furocoumarins, a group of substances still used in phototheraphy. In the early nineteenth century Sniadecki found that rickets among children in Warsaw could be cured by sunlight (Mozolowski 1939; Chapter 20). Downes and Blunt (1877, 1878) showed that sunlight could kill bacteria. Niels Finsen discovered that lupus

vulgaris, a form of cutaneous tuberculosis common in the nineteenth century, could be cured by short-wavelength light, for which he received the 1903 Nobel Prize for Physiology or Medicine. (To avoid misunderstanding, we wish to mention here that the beneficial effect of sunlight on other forms of tuberculosis discovered more recently is due to a completely different mechanism.) For further information on the history of phototherapy the reader is referred to Ackroyd et al. (2001), Fitzpatrick and Pathak (1959), Hobday (1997), Kick et al. (1996), Moan and Peng (2003), Rauschmann et al. (2003), Roelandts (2002), and Urbach et al. (1976).

The effect of light on a human tissue can be *photochemical* or *thermal*. We shall limit ourselves here to the photochemical ones, and not even all of those will be covered. Thermal effects are briefly mentioned in Chapter 5, Section 3. We shall leave out depilation (hair removal) and so-called photomodulation (Karu and Kolyakov 2005) for pain relief and wound healing. For treatment of seasonal affective disorder (SAD), the reader is referred to Chapter 14, and for treatments related to vitamin D to Chapter 20.

When light treatment is performed without administration of chemicals the general term used is *phototherapy*, and when artificial photosensitizers are also used, the appropriate term is *photochemotherapy*. The mechanism of action of light can in either case be independent of oxygen or involve oxygen. In the chapter on phototoxicity we have introduced the terms type I (oxygen-independent) and type II (oxygen-dependent) mechanisms. In phototherapy the terminology is, unfortunately, completely confused and inconsistent (see Smith 2005) or quite different (e.g., Serrano-Perez, Serrano-Andrés and Merchán 2006). We recommend that the well-established photochemical–phototoxicological tradition with type I as oxygen-independent and type II as oxygen-dependent be continued, as it is also by some authors dealing with phototherapy. The effect of a type II (oxygen-dependent) process is often referred to as a photodynamic effect, and medical treatment in which this is utilized is called *photodynamic therapy* (PDT). PDT will be treated in a separate section.

22.2. Phototherapy (Use of Light Without Applied Photosensitizer)

We shall give three examples of diseases treatable with three different wavelength bands.

22.2.1. UV-B

We choose *psoriasis* as an example of a disease which is often treated with UV-B phototherapy, although other forms of therapy are also used. For a general review describing psoriasis we refer the reader to Schön and Boehncke (2005). Psoriatic patients have reddish spots in the skin covered by scales that are continuously shed, like dandruff. Psoriasis expresses itself in three ways:

22.2.1.1. T-Cell Inflammatory Reaction

Cytokines are a group of water-soluble low molecular weight (8–30 kDa) proteins and glycoproteins involved in intercell communication. Among cytokines are interleukins (IFs), interferons (IFNs), and tumor necrosis factors (TNFs). There are no sharp division lines between these categories. Some cytokines are pro-inflammatory, others anti-inflammatory. It is believed that an unknown (auto)antigen causes T-cell activation, implying the production of various pro-inflammatory cytokines (IL2, TNF-α, and IFN-γ), and thus inflammation of the skin.

   The concentrations of many interleukins are up- (Sigmundsdottir et al. 2005) or downregulated by UV-B radiation. Also, interferons are affected by UV-B. In the short term, the concentrations of IL-6 (Kuhn et al. 2006) and the anti-inflammatory IL-10 (Grewe et al. 1995) are increased by UV-B, while those of IL-2, IL-4, IFN-γ, and TFN-α are decreased, and T-cell activation suppressed (Li-Weber et al. 2005).

22.2.1.2. Hyperproliferation

Increased cell division causes a thickening of the epidermis, resulting in a visible raised plaque. This is counteracted by ultraviolet radiation (partly UV-A) via the creation of active oxygen species (see Chapter 19).

22.2.1.3. Dysfunction of Differentiation

This consists of defective layering of the skin, decreased stability, and formation of scales. ICAM1 (intercellular adhesion molecule 1) is a surface protein on keratinocytes and endothelial cells which is overproduced in psoriasis. UV-B inhibits the gene for ICAM 1 by formation of cyclobutane pyrimidine dimers (CPDs, see Chapter 19).

   It has long been noted that sunlight exerts a healing effect on psoriasis patients. Usually the condition improves during the summer months and worsens during winter. Since vitamin D has an alleviating effect and vitamin D insufficiency can occur, especially during winter, it is likely that some of the light effect is due to improvement of vitamin D status. However, it is clear that this is not the whole story. Although attempts to pinpoint the molecule mediating the light effect have been made by action spectroscopy (e.g., Parrish and Jaenicke 1981), nothing more can be said with certainty than that all radiation in the range 296–313 nm is effective (Farr and Diffey 2006). No effect was found with 290-nm radiation (Parrish and Jaenicke 1981), which makes an effect via vitamin D synthesis unlikely in this case, at least if the action spectrum by MacLaughlin et al. (1982) is correct (see Fig. 20.4 in Chapter 20). Fluorescent lamps, such as Philips TL01 or Arimed 311, emitting 310- to 313-nm radiation (in medical circles referred to as narrow-band UV-B) are often used. TL01 is described by the manufacturer as emitting with a peak at 311 nm and a half-bandwidth of 2 nm. For other brands of similar construction, some of the mercury emission (313 nm) from the

lamp interior may leak through. In order to irradiate small areas on the skin with similar kinds of radiation, xenon chloride eximer laser light (308 nm) has been employed (Goldinger et al. 2005).

Because of the short wavelength, this type of radiation hardly penetrates into the dermis, and the effect is mainly on the cells of the epidermis, especially on keratinocytes and Langerhans cells.

Psoriasis, especially if not responding to phototherapy, can also be treated with PUVA-photochemotherapy; see below).

22.2.2. Long-Wave (>340 nm) UV-A ("UV-A1")

Scleroderma (meaning "hard skin") is a rare, chronic, autoimmune disease characterized by excessive deposits of collagen. It can be successfully treated with long-wave UV-A radiation, but UV-B also has an effect. There are other diseases, e.g., *atopic eczema* (Grabbe et al. 1996), for which phototherapy with long-wave UV-A is used.

Sometimes the spectral range (340–400 nm) is referred to as UV-A1, but it is recommended not to use this term without further specification, as there is no official definition of it. In many cases radiation up to 500-nm wavelength is included in the treatment referred to as UV-A1 phototherapy, for instance, when a device called Photomed CL is used for irradiation.

On the molecular level, a main effect of long-wavelength UV-A radiation is production of reactive oxygen species (see Chapter 1, Section 1.21.), and this starts several other responses.

The long-wave UV-A penetrates deeper into the skin than shorter-wave UV radiation. It probably acts in different ways, but one important primary reaction seems to be the excitation of flavoproteins, which results in formation of singlet oxygen, which then can react with different molecules (e.g., Lubart et al. 2006), i.e., photodynamic action. Possibly as a consequence of photodynamic action, a peroxidation chain reaction may start in the unsaturated membrane lipids (see Chapter 21).

22.2.3. Visible Light

Neonatal jaundice is also known as icterus neonatorum and neonatal hyperbilirubinemia. In jaundice (from the French word for yellow, *jaune*) the skin is colored yellow because of a high concentration of bilirubin, a breakdown product of hemoglobin. Newborn babies ("neonates") usually are more yellow than adults because while in the womb, the fetus is exposed to a lower oxygen pressure than somebody breathing with his own lungs, and therefore needs a more efficient system for oxygen transport within the body. After birth the excess hemoglobin is broken down, and usually the breakdown product bilirubin normally starts to decrease in the skin about a week after birth. In several percent of babies, however, the clearance is delayed, especially in cases of premature birth and if the father has Rh-positive and the mother Rh-negative blood and no precautions

have been taken. Prolonged jaundice can also have a number of other causes, such as deficient kidney function. If not treated, the neonatal jaundice can lead to a kind of brain damage known as kernicterus.

The basis for phototherapy of neonatal jaundice is photochemical oxidation of bilirubin. This can be carried out with any radiation that penetrates sufficiently deep into the skin and is absorbed by bilirubin. It is desirable, in order to avoid thermal or photochemical damage to the skin, to use radiation which is preferentially absorbed by bilirubin. Recently blue light-emitting diodes (LEDs) with 465- to 470-nm emission, which is close to the absorption maximum of bilirubin, have been found to be suitable for this purpose (Vreman et al. 1998, Chang et al. 2005). For the photochemistry of bilirubin we refer the reader to Zietz (2006).

22.3. Photochemotherapy

22.3.1. PUVA (Photochemotherapy Mediated by UV-A Radiation with a Psoralen Derivative as Photosensitizer)

Plants produce, for protection, compounds that can act as photochemical sensitizers in animals. To this class of compounds belong psoralen and various related substances. The same principle is used in PUVA, and the most frequently used substances are 8-methoxypsoralen (8-MOP; formula in Fig. 20.3 of Chapter 20), 5-methoxypsoralen (5-MOP), and 4,5,8-trimethylpsoralen (TMP). These substances can be applied by bathing in a solution, by application of a cream on the skin, or by ingestion of tablets.

The action of psoralen derivatives is complex (Knobler et al. 1988, Averbeck 1999). The dominating mode is, under most circumstances, a photochemical attack on DNA, as indicated in Fig. 18.1 of Chapter 18, but some singlet oxygen (Knox et al. 1986, Seret et al. 1992, Redmond and Gamlin 1999) and other forms of reactive oxygen species are also formed, and membrane alteration can take place (Dall'Acqua and Martelli 1991).

The following conditions can be treated with PUVA:

Psoriasis is often clinically treated with PUVA as an alternative to photothereapy.

Cutaneous T-cell lymphoma (CTCL), a type of non-Hodgkin lymphoma.

Allergic and irritant contact dermatitis, a local inflammation of the skin. Symptoms of inflammation are itching, pain, redness, swelling, and the formation of small blisters or wheals (itchy, red circles with a white center) on the skin. The inflammation is caused by an allergy or irritation, often as a result of substances found in the workplace that come into direct contact with the skin.

Lichen planus (red, itching spots on the skin and similar lesions on mucous membranes, sometimes on the skin).

Granuloma annulare, a chronic skin disease consisting of a rash with reddish bumps arranged in a circle or ring; some forms can be associated with diabetes.

Graft-versus-host disease (GvHD), a common side effect of an allogeneic bone marrow or cord blood transplant. An allogeneic transplant uses blood-forming cells donated by a family member, unrelated donor or cord blood unit. In GvHD, the immune cells from the donated marrow or cord blood (the graft) attack the body of the transplant patient (the host). GvHD can affect many different parts of the body. The skin, eyes, stomach, liver, and intestines are affected most often. GvHD can range from mild to life-threatening.

Grover's disease (also called transient acantholytic dermatosis) hyperkeratotic brownish spots, often in older men, and often triggered by bed rest.

22.3.2. Implementation of Phototherapy and Photochemotherapy

Since ultraviolet radiation and light have both healing and destructive effects, phototherapy must be applied with caution. There are a number of diseases which preclude use of ultraviolet phototherapy. Examples of these are *xeroderma pigmentosum* and *Cockayne syndrome*. Both of these diseases are due to deficient DNA repair systems, and both make the skin very sensitive to ultraviolet radiation.

Also, people with normal repair systems differ in their sensitivity to ultraviolet radiation due to different skin pigmentation, thickness of stratum corneum, and other factors. There are, apart from these, other differences between ethnic skin types (Caucasian, Oriental, African, etc.) affecting ultraviolet sensitivity. For this reason the ultraviolet sensitivity should be tested before deciding on irradiation protocols. This is routinely done by determining the minimum erythemal dose (MED). In most cases treatments have to be repeated over extended periods (months to years).

22.3.3. Extracorporeal Photochemotherapy

22.3.3.1. Principle and Areas of Use

Extracorporal photochemotherapy (also called extracorporeal photoimmunotherapy or photopheresis) is a way to better reach the intended photochemotherapy target cells. These target cells are not only in the skin, but also consist of nucleated cells circulating in the blood, such as lymphocytes. In this way a number of T-cell–mediated diseases can be treated, which cannot be well treated with traditional PUVA. The method has been used for cutaneous T-cell lymphoma for two decades (Knobler and Girardi 2001, Duvic et al. 1996, Perrit 2006, Zic et al. 1996). Some diseases that are currently being explored for response and efficacy to ECP are:

Acute and chronic solid organ transplant rejection (lung, kidney, heart, liver)
Acute and chronic GvHD after allogeneic bone marrow transplantation

Progressive systemic sclerosis (Knobler et al. 2005)
Crohn's disease
Cutaneous T-cell lymphoma (Sezary syndrome variant)
Therapy refractory pemphigus vulgaris and atopic dermatitis
Therapy refractory rheumatoid arthritis

The procedure in our department is as follows: for obtaining blood for the pheresis procedure from a patient in a recumbent position, a large-gauge needle is placed in an appropriate arm vein (large lumen). A plastic tube system connects the patient with the photopheresis machine. This machine resembles one used for separating blood elements in a blood bank center. It has a pump system that draws the blood from the patient to a centrifuge, where the blood can be separated into its components (red blood cells, white blood cells, and plasma). The treatment is carried out on two consecutive days. Each time approximately 540 mL of blood is collected in six cycles. A heparin-containing solution is added continuously to the system in order to prevent clotting of the patients' blood in the machine (up to 15,000 IE heparin). The instrument is programmed in such a manner that each individual step follows the same pattern: first, the white blood cells will be collected in a plastic bag; then the red blood cells (erythrocytes) are returned to the patient before the next collection cycle begins. After six consecutive cycles a solution containing 8-MOP is added to the collected plasma/white blood cell fraction. Subsequently this 8-MOP–containing blood cell/plasma fraction is circulated in a special chamber exposed to UV-A radiation. Once a sufficient radiation dose has been delivered, the entire treated fraction is returned to the patient. The length of the radiation depends on the hematocrit of the collected fraction and the fluence rate from the lamp. On average the treatment takes between 2.5 and 3.5 hours.

The potential side effects are usually very limited: slight dizziness (when the blood is removed too fast and blood pressure is too low) or hematomas on the site of venipuncture.

Initially photopheresis is carried out once every 2 weeks and then the interval is increased in accordance to the patient's response. In general the treatment is coordinated with other medications. One of its objectives, besides to treat the specific disease, is to help reduce systemic immunosuppressive therapy, which often is associated with a very high rate of life-threatening side effects (Gottlieb et al. 1996). In some indications photopheresis is a good alternative for patients who have not responded to other treatments. Since this treatment is relatively time and cost intensive, the indications have to be carefully evaluated.

22.3.3.2. Mechanism of Action

A common denominator to the pathogenesis of the diseases that appear to respond to photopheresis is a dysregulation of the immune system.

Through selective irradiation of the 8-MOP plasma buffy coat fraction (all nucleated cells) apoptosis of the T-cells causing disease and a conversion of monocytes to functional dendritic antigen-presenting cells appears to be

achieved. Apoptosis (programmed cell death) results in release of cell-specific proteins (peptides) which can be picked up by antigen-presenting cells and presented to the immune system (Maeda et al. 2005). Similarly, cell-specific cytokines are released. The resulting reaction plays an important role in the control of the above-mentioned diseases, whereby it appears that more than one specific mechanism is associated with the beneficial effects of this therapy. Though much knowledge has been gained recently, including the possibility that photopheresis may be associated with the induction of regulatory T cells, its immuno(?)modulatory effects are not yet fully understood (Bladon et al. 2006; see also Peritt 2006).

22.3.4. Photodynamic Therapy (PDT) with Porphyrins or Chlorins as Photosensitizers

We shall concentrate here on use of porphyrins and the related chlorins (with a more reduced ring system, similar to that of chlorophyll) as photosensitizers for photodynamic therapy, but it should be understood that in principle also other sensitizers can be used for this purpose, for instance, methylene blue (Tardivo et al. 2005) and hypericin (Bublik et al. 2006). The *Propionibacterium* itself in the acne lesion synthesizes porphyrins, which can be utilized as photosensitizer for generation of singlet oxygen (photodynamic action), so treatment can be performed without addition of any exogenous chemical. However, in this case one increases the concentration of porphyrins by adding a porphyrin precursor, often 5-aminolevulinic acid (ALA) (Granick and Mauzerall 1957), or the methyl ester of ALA (the latter penetrates the skin more easily due to its lipophilicity). The method is thus a photochemotherapeutic method where the cellular machinery is used to produce, in a natural way, a higher sensitizer concentration in the area to be treated. Since porphyrins are, in the natural state, partly converted to heme (which does not act as a photodynamical sensitizer), sometimes steps are taken to limit this conversion, such as administration of an iron chelator.

The historical development and other aspects of PDT have been reviewed by, among many others, Dougherty, Gomer, Henderson, et al. (1998), Kalka, Merk, and Mukhtar (2000), and Moan and Peng (2003). The term photodynamic was coined by von Tappeiner and Jodlbauer (2004) to describe oxygen-consuming chemical reactions induced by photosensitization in biology. It became generally known by the work of Blum (1941).

The physiological mechanisms involved in PDT have recently been reviewed by Castano et al. (2005). Briefly, the singlet oxygen generated is thought to have two main effects: (1) induce apoptosis or actively kill cells and (2) induce an immune response, which will kill the malignant cells. The primary site of action is often the mitochondria and their membranes, but not necessarily so, as exemplified by the PDT effects on propionibacteria. Damage to the tumor vascular system, limiting the blood supply, is also a cause for the effect.

The oxygen level in the tumors (cells) must be high enough for PDT to be effective. If oxygen is scarce one might get enough supply if so-called fractionated light doses are given. This means that a certain light dose is divided into pulses—giving oxygen a possibility to be transported to the illuminated area between the pulses.

Various diseases can be treated with photodynamic therapy, but above all it is a therapy for a number of cancer forms. One reason for this is that cancer tumors accumulate porphyrins or precursors to a higher degree than normal tissue. Clinically, some forms of skin cancers are now often treated with PDT, often ALA-PDT. From the beginning, phototherapy and photochemotherapy were only applied to the skin and oral mucosa. We have seen in the previous section how extracorporeal photochemotherapy allows treatment also of circulating blood cells. There are two more ways to reach deeper into the human body, and both are used in conjunction with PDT. One is to use fiber optics to guide the light into inner organs such as the bladder. The other one is to use two-photon or multiphoton excitation (see below).

Internal sites which are either already being treated with PDT or for which possibilities seem hopeful (in most cases using fiber optics) include the esophagus (Mitton et al. 2004, Maunouri et al. 2005), bone (Bisland and Burch 2006), breast (Allison et al. 2006), trachea (Barber et al. 2004), lungs (Moghissi et al. 2004, Zeng et al. 2004), pleura (Pass et al. 1994, Moghissi and Dixon 2005), other sites in the thorax (Ris et al. 1996), pancreas (Ayaru et al. 2004), bladder (Dhallewin 1995, Stavropoulos et al. 2006), and even the brain (Eljamel 2004a,b).

Light sources for PDT have been reviewed by Juzeniene, Juzenas, Ma, Iani, and Moan (2004) and Juzeniene, Nielsen, and Moan (2006); the latter paper deals also with other physical factors. Mercury lamps, LEDs and quartz halogen lamps are often used. *Lasers* have advantages due to their high power output, their monochromatic light, and the easy coupling of the beam into optic fibers that are used in several forms of treatment (in body cavities or interstitially in tumors). Since the porphyrins absorb both blue and red light, both wavelength intervals are used. Red light penetrates better into tissue and is therefore often preferred.

Two-photon and multiphoton excitation is still at an early experimental stage. As described in Chapter 5, a pigment that has an absorption peak at wavelength λ can also be excited by radiation of wavelength 2λ or 3λ, if it can be made to absorb two or three photons within a very short time (of the order of 10^{-16} s as determined by the Heisenberg uncertainty principle and the period of molecular oscillations; see Fig. 22.1).

To achieve this, the photon concentration, i.e., the fluence rate, must be very high. To prevent too much energy from being deposited in the tissue, and also for technical reasons, this must be achieved with very short light flashes, in the picosecond (10^{-12} s) to femtosecond (10^{-15} s) range. Thus, for hematoporphyrin IX (a main component in the frequently used commercial photosensitizer Photofrin®) with an absorption band around 400 nm ("Soret band"), two-photon excitation can be achieved with 800- to 900-nm radiation
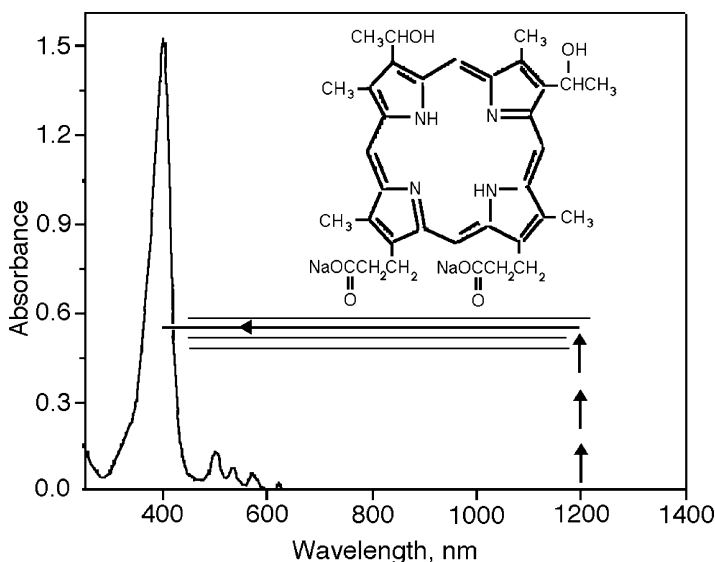
FIGURE 22.1. Chemical structure and absorption spectrum of a component of the photodynamic sensitizer Photofrin® (porfimer sodium), with an indication of how a molecule can be excited in the Soret band by either one photon of 400-nm wavelength or three photons with 1200-nm wavelength. Porfimer sodium is not a single compound but a mixture of porphyrin units similar to that shown above, linked together to oligoporphyrins by ether and ester linkages. The structure of another important photodynamic sensitizer is shown in Fig. 18.6

(Karotki et al. 2006) and tree-photon excitation with infrared radiation of 1200 nm wavelength (Cohanoschi et al. 2006). It should be noted that the peak wavelength for three-photon excitation is always at three times that for two-photon excitation, while that for two-photon excitation is not necessarily twice that for one-photon excitation. The absorption cross sections, which for one-photon processes have dimension of area (m^2 photon^{-1}), are in these cases 10×10^{-58} m^4 s photon^{-1} and 1.2×10^{-90} m^6 s^2 photon^{-2} for two- and three-photon excitation of hematoporphyrin IX at the absorption peak.

Two-, three-, and multiphoton excitation has several advantages. The infrared radiation is less absorbed and less scattered by the tissue, and therefore reaches deeper. One can also more precisely target it, since absorption by the photo-sensitizer occurs only where the radiation is sufficiently focused. Even further control of the spacial distribution of PDT action can be achieved by a special interference technique (Dela Cruz et al. 2004).

References

Ackroyd, A., Kelty, C., Brown, N. and Reed, M. (2001) The history of photodetection and photodynamic therapy. Photochem. Photobiol. 74, 656–669.

Allison, R.R., Sibata, C., Downiea, G.H. and Cuenca, R.E. (2006) Photodynamic therapy of the intact breast. Photodiagn. Photodynamic Ther. 3, 139–146.

Ayaru, L., Stephen G. Bown, S. and Pereira, S.P. (2004) Photodynamic therapy for pancreatic carcinoma: experimental and clinical studies. Photodiagn. Photodynamic Ther. 1, 145–155.

Averbeck, D. (1999) Recent advances in psoralen phototoxicity mechanism. Photochem, Photobiol. 50, 859–882.

Barber, P. Deiraniya, A.K. and Allen, E. (2004) Photodynamic therapy for tracheal thyroid metastasis. Photodiagn. Photodynamic Ther. 1, 99–102.

Bisland, S.K. and Burch, S. (2006) Photodynamic therapy of diseased bone. Photodiagn. Photodynamic Ther. 3, 147–155.

Bladon J., and Taylor P.C. (2006) Extracorporeal photopheresis: a focus on apoptosis and cytokines. J. Dermatol. Sci. 43, 85–94.

Blum, H.F. (1941) *Photodynamic action and diseases caused by light*. Reinhold, New York.

Bublik, M., Head, C., Benharash, P., Paiva, M., Eshraghi, A., Kim, T. and Saxton, R. (2006) Hypericin and pulsed laser therapy of squamous cell cancer *in vitro*. Photomed. Laser Surgery 24, 341–347.

Castano, A.P., Demidova, T.N. and Hamblin, M.R. (2005) Mechanisms in photodynamic therapy: part two—cellular signaling, cell metabolism and modes of cell death. Photodiagn. Photodynamic Ther. 2, 1–23.

Chang, Y.S., Hwang, J.H., Kwon, H. N., Choi, C.W., Ko, S.Y., Park, W.S., Shin., S.M and Lee, M. (2005) In vitro and in vivo efficacy of new blue light emitting diode phototherapy compared to conventional halogen quartz phototherapy for neonatal jaundice. J. Korean Med. Sci. 20, 61–64.

Cohanoschi, I., Lorenzo Echeverrí, L., Florencio E. and Hernández, F.E. (2006) Three-photon absorption measurements in hematoporphyrin IX: Ground-breaking opportunities in deep photodynamic therapy. Chem. Phys. Lett. 419, 33–36.

Dall'Acqua, F. and Martelli, P. (1991) Photosensitizing action of furocoumarins on membrane components and consequent intracellular events. J. Photochem. Photobiol. B: Biol. 8, 235–254.

Dela Cruz, J.M., Pastirk, I., Matthew Comstock, M. and Dantus, M. (2004) Multiphoton intrapulse interference 8. Coherent control through scattering tissue. Optics Express 12, 4144–4149.

Dhallevin, M.A. (1995) Long-term results of whole bladder wall photodynamic therapy for carcinoma in-situ of the bladder. Urology 45, 763.

Dougherty, T.J., Gomer, C.J., Henderson, B.W., Jori, G., Kessel, D., Korbelik, M., Moan, J., and Peng, Q. (1998) Photodynamic therapy. J. Natl Cancer Inst. 90, 889–905.

Downes, A. and Blunt, J.P. (1877) Researches on the effect of light on bacteria and other organisms. Proc. R. Soc. Lond. 26, 488–500.

Downes, A. and Blunt, T.P. (1878) On the influence of light upon protoplasm. Proc. Roy. Soc. Lond. 28, 199–212.

Duvic M., Hester J.P. and Lemark N.A. (1996) Photopheresis therapy for cutaneous T-cell lymphoma. J. Am. Acad. Dermatol. 35, 573–579.

Eljamel, S.J. (2004) Photodynamic assisted surgical resection and treatment of malignant brain tumours: technique, technology and clinical application. Photodiagn. Photodynamic Ther. 1, 93–98.

Eljamel, M.S. (2004) Brain PDD and PDT unlocking the mystery of malignant gliomas. Photodiagn. Photodynamic Ther. 1, 303–310.

Farr, P.M. and Diffey, B.L. (2006) Action spectrum for healing of psoriasis. Photodermatol. Photoimmunol. Photomed. 22, 52–52.

Fitzpatrick, T.B. and Pathak, M.A. (1959) Historical aspects of methoxsalen and other furocoumarins. J. Invest. Dermatol. 31, 229–231.

Goldinger, S.M., Dummer, R., Schmid, P., Prinz Vavricka, M., Burg, G. and Läuchli, S. (2005) Excimer laser versus narrow-band UVB (311 nm) in the treatment of psoriasis vulgaris. Dermatology 213, 134–139.

Grabbe J.,Welker P., Humke S., Grewe M., Schopf, E., Henz, B.M. and Krutmann, J. (1996) High-dose UVA-1 therapy, but not UVA/UVB therapy, decreases Ig E binding cells in lesional skin of patients with atopic eczema. J. Invest. Dermatol. 107, 419–423.

Granick, S. and Mauzerall, D. (1957) Porphyrin biosynthesis in erythrocytes ii: enzymes converting 5-aminolevulinic acid to coproporphyrinogen. J. Biol. Chem. 232, 1119–1140.

Grewe M., Gyufko K., and Krutmann J. (1995) Interleukin-10 production by cultured human keratinocytes: regulation by ultraviolet B and ultraviolet A1 radiation. J. Invest. Dermatol. 104, 3–6.

Gottlieb, S.L., Wolfe J.T., Fox, F.E.. DeNardo, B.J., Macey, W.H., Bromley, P.G., Stuart R. Lessin, S.R. and Rook, A.H. (1996) Treatment of cutaneous T-cell lymphoma with extracorporal photopheresis monotherapy and in combination with recombinant interferon alfa: A10-year experience at a single institution. J. Am. Acad. Dermatol. 35, 946–957.

Hobday, R.A. (1997) Sunlight therapy and solar architecture. Medical History 42, 455–472.

Juzeniene, A., Juzenas, P., Ma, L.W., Iani, V. and Moan, J. (2004) Effectiveness of different light sources for 5-aminolevulinic acid photodynamic therapy. Lasers Med. Sci. 19, 139–149.

Juzeniene, A., Nielsen, K.P. and Moan, J. (2006) Biophysical aspects of photodynamic therapy. J. Environm. Pathol. Toxicol. Oncol. 25, 7–28.

Kalka, K., Merk, H., and Mukhtar, H. (2000) Photodynamic therapy in dermatology. J. Am. Acad. Dermatol. 42, 389–413.

Karotki, A., Khurana, M., Lepock, J.R. and Wilson, B.C. (2006) Simultaneous two-photon excitation of Photofrin in relation to photodynamic therapy. Photochem. Photobiol. 82, 443–452.

Karu, T.I. and Kolyakov, S.F. (2005) Exact action spectra for cellular responses relevant to phototherapy. Photomed. Laser Surgery 23, 355–361.

Kick, G., Messer, G. and Plewig, G. (1996) Historische Entwicklung der photodynamischen Therapie. Hautarzt 8, 644–649.

Knobler, R.M., Hönigsmann, H. and Edelson, R.L. (1988) Psoralen phototherapies. In: F.P. Gasparro (Ed.), *Psoralen DNA photobiology,* Vol. II. CRC Press, Boca Raton, FL, pp. 117–143.

Knobler R. and Girardi M. (2001) Extracorporeal photochemoimmunotherapy in cutaneous T cell lymphomas. Ann. NY Acad. Sci. 941, 123–138.

Knobler R., French L., Kim Y., Bisaccia, E., Graninger, W., Nahavandi, H., Strobl, F.J., Keystone, E., Mehlmauer, M., Rook, A.H. and Braverman, I. (2005) A randomized, double blind, placebo- controlled trial of photopheresis in systemic sclerosis. J. Am. Dermatol. 54, 793–799.

Knox, C.N., Land, E.J. and Truscott, T.G. (1986) Singlet oxygen generation by furocoumarin triplet states. 1. Linear furocoumarins (psoralens). Photochem. Photobiol. 43, 359–363.

Kuhn, M., Wolber, R. and Kolbe, L., Schnorr, O. and Sies, H. (2006) Solar-simulated radiation induces secretion of IL-6 and production of isoprostanes in human skin in vivo. Arch. Dermatol. Res. 297, 477–479.

Li-Weber, M., Treiber, M.K., Giaisi, M., Palfi, K., Stephan, N., Parg, S., and Krammer, P.H. (2005) Ultraviolet irradiation suppresses T cell activation via blocking TCR-mediated ERK and NF-kappa B signaling pathways. J. Immunol. 175, 2132–2143.

Lubart, R., Lavi, I.R. and Friedmann, H. (2006) Photochemistry and photobiology of light absorption by living cells. Photomed. Laser Surgery 24, 179–185.

MacLaughlin, J.A., Anderson, R.R. and Holick, M.F. (1982) Spectral character of sunlight modulates photosynthesis of previtamin D3 and its photoisomers. Science 216, 1001–1003.

Maeda A., Schwarz A., Kernebeck K. and Schwarz, T. (2005) Intravenous infusion of apoptotic cells by photopheresis induces antigen-specific regulatory T cells. J. Immunol. 174, 5968–5976.

Maunoury, V., Mordon, S., Bulois, P., Mirabel, X., B. Hecquet, B, and Mariette, C. (2005) Photodynamic therapy for early oesophageal cancer. Digestive Liver Dis. 37, 491–495.

Mitton, D., Claydon, P. and Ackroyd, R. (2004) Photodynamic therapy and photodiagnosis for Barrett's oesophagus and early oesophageal carcinoma. Photodiagn. Photodynamic Ther. 1, 319–334.

Moan, J. and Peng, Q. (2003) An outline of the hundred-year history of PDT. Anticancer Res. 23, 3591–3600.

Moghissi, K., Dixon, K., Thorpea, J.A.C., Oxtoby, C. and Stringer, M.R. (2004) Photodynamic therapy (PDT) for lung cancer: the Yorkshire Laser Centre experience. Photodiagn. Photodyn. Therapy 1, 253–262.

Moghissi, K and Dixon, K. (2005) Photodynamic therapy in the management of malignant pleural mesothelioma: A review. Photodiagn. Photodynamic Therapy 2, 135–147.

Mozolowski, W. (1939) Jedrzej Sniadecki (1768-1838) on the cure of rickets. Nature 143, 121.

Parrish, J.A., Jaenicke, K.F. (1981) Action spectrum for phototherapy of psoriasis. J. Invest. Dermatol. 76, 359–362.

Pass, H.I., DeLaney, T.F., Tochner, Z., Smith, P.E., Temeck, B.K., Pogrebniak, H.W., Kranda, K.C., Russo, A. Friauf, W., Cole, J.W., Mitchell, J.B. and Thomas, G. (1994) Intrapleural photodynamic therapy — results of a phase-1 trial. Ann. Surgical Oncol. 1, 28–37.

Perrit, D. (2006) Potential mechanisms of photopheresis in hematopoietic stem cell transplantation. Biol. Blood Marrow Transplant.12, 7–12.

Rauschmann, M.A., Eberhardt, C., Patzel, U. and Thomann, K.-D. (2003) Das rachitische X-Bein im Kindesalter (Rachitic knock knees in children). Orthopäde 32, 101–109.

Redmond, R.W. and Gamlin, J.N. (1999) A compilation of singlet oxygen yields from biologically relevant molecules. Photochem. Photobiol. 70, 391–475.

Ris, H.-B., Altermatt, H.J., Nachbur, B., Stewart, C.M., Qiang Wang, Q., Chung K. Lim, C.K. Bonnett, R., and Ulrich Althaus, U. (1996) Intraoperative photodynamic therapy with m-tetrahydroxyphenylchlorin for chest malignancies. Lasers Surg. Med. 18, 39–45.

Roelandts, R. (2002) The history of phototherapy: Something new under the sun? J. Am. Acad. Dermatol. 46, 926–930.

Schön, M.P. and Boehncke, W.-H. (2005) Psoriasis. N. Engl. J. Med. 352, 1899–1912.

Seret, A., Piette, J., Jacobs, A. and Vandevorst, A. (1992) Singlet oxygen quantum yield of sulfur and selenium analogs of psoralen. Photochem. Photobiol. 56, 409–412.

Serrano-Pérez, J.J., Luis Serrano-Andrés, L. and Merchán, M. (2006) A theoretical insight into the photophysics of psoralen. J. Chem. Phys. 124, 124502 1–7.

Sigmundsdottir, H., Johnston, A., Gudjonsson, J.E., and Valdimarsson, H. (2005) Narrowband-UVB irradiation decreases the production of pro-inflammatory cytokines by stimulated T cells. Arch. Derm. Res. 297, 39–42.

Smith, K.C. (2005) Laser (and LED) therapy is phototherapy. Photomed- Laser Surg. 23, 78–80.

Stavropoulos, N.E., Kim, A., Nseyo, U.U., Tsimaris, I., Chung, T.D., Miller, T.A., Redlak, M., Nseyo, U.O. and Skalkos, D. (2006) Hypericum perforatum L. extract—Novel photosensitizer against human bladder cancer cells. J. Photochem. Photobiol. B: Biology 84, 64–69.

Tardivo, J.P., Del Giglio, A., Santos de Oliveira, C., Gabrielli, D.S., Couto Junqueira, H., Batista Tada, D., Severino, D., de Fátima Turchiello, R., Mauricio, S. and Baptista, M.S. (2005) Methylene blue in photodynamic therapy: From basic mechanisms to clinical applications. Photodiagn. Photodynamic Ther. 2, 175–191.

Urbach, F., Forbes, P.D., Davies, R.E. and Berger, D. (1976) Cutaneous photobiology: Past, present and future. J. Invest. Dermatol. 67, 209–224.

von Tappeiner, H. and Jodlbauer, A. (1994) Über die Wirkung der photodynamischen (fluorescierenden) Stoffe auf Protozoen und Enzyme. Dtsch Arch Klin Med 80, 427–87.

Vreman, H.J., Wong, R.J., Stevenson, D.K., Route, R.K., Reader, S.D., Fejer, M.M., Gale, R., and Seidman, D.S. (1998) Light-emitting diodes: A novel light-source for phototherapy. Pediatric Res. 44, 804–809.

Zeng, H., McWilliams, A. and Lam, S. (2004) Optical spectroscopy and imaging for early lung cancer detection: a review. Photodiagn. Photodynamic Ther. 1, 111–122.

Zic J., Stricklin G.P., Greer, J.P., Kinney, M.C., Shyr, Y., Wilson, D.C. and King, L.E. (1996) Long-term follow-up of patients with cutaneous T-cell lymphoma treated with extracorporal photochemotherapy. J. Am. Acad. Dermatol., 35, 935–945

Zietz, B. (2006) An Ultrafast Spectroscopic and Quantum-Chemical Study of the Photochemistry of Bilirubin. Doctoral Diss. Umeå University. ISBN 91-7264-010-3. Abstract available at http://www.diva-portal.org/umu/theses/abstract.xsql?dbid=672&lang=sv

23
Bioluminescence

Lars Olof Björn and Helen Ghiradella

Abstract: Three kinds of light emission from organisms take place: bioluminescence in a narrow sense from some animals, dinoflagellates, fungi, and bacteria; delayed light emission from photosynthetic cells; and ultraweak light emission from all kinds of cells. All these phenomena are treated in this chapter.

23.1. Introduction

Apart from the fluorescence and phosphorescence introduced in Chapter 1, three kinds of light emission that from a living organism may take place:

1. Photosynthetic *delayed light emission*, also called *delayed fluorescence* or *afterglow*. This is weak red light emitted by all green plants and algae. The intensity is so low, and the light of such long wavelength, that we cannot see it, but it is easily measured. It is due to reversion of the first steps of photosynthesis.
2. *Ultraweak light emission* takes place in all organisms. It is due to various processes, mostly (but not always) involving molecular oxygen. It is regarded as a byproduct of metabolic activity and has no biological function in itself. It is even weaker than the previous kind of light emission, and although it is often of shorter wavelength, it cannot be seen. Rather sophisticated equipment is needed for its measurement. It can be exploited for studying what is going on in cells in a noninvasive and nondestructive way.
3. *Bioluminescence* is the best-known of the biological luminescence phenomena, mostly because it can be observed using only one's eyes. We shall devote most of this chapter to bioluminescence. Although photosynthetic delayed light emission and ultraweak light emission in our terminology are not bioluminescence, sections at the end of the chapter will deal with these phenomena.

In addition to the more recent literature cited in this chapter, we would like to mention the book by Harvey (1952) as an excellent summary of the older bioluminescence literature. Extensive reviews of marine bioluminescence are provided by Tett and Kelly (1973) and Herring (1982, 2002, pp. 188–216).

23.2. Evolution and Occurrence Among Organisms

Although most species are nonbioluminescent, most phyla have bioluminescent representatives. Among the exceptions are true plants and higher vertebrates (i.e., amphibians, reptiles, birds, and mammals).

Comparison of the biochemical systems involved clearly shows that bioluminescence has evolved multiple times. About 30 independently evolved systems are still extant (Hastings 1983, Wilson and Hastings 1998). Still, most bioluminescence systems share some common features, as we shall see in the section on biochemistry.

Thus bioluminescence occurs among bacteria, fungi, dinoflagellates, protozoa, sponges, cnidaria, ctenophores (comb jellies), molluscs, annelids, crustaceans, insects, bryozoa, echinoderms, and fish. The majority of bioluminescent species live in the sea, although there are also many bioluminescent insects (all terrestrial), especially beetles. It has been estimated that 60–80% of the fish species in the deep sea are bioluminescent. Table 23.1 shows the distribution in more detail.

Since bioluminescent microorganisms exist, one must be careful not to confuse microbial luminescence with luminescence of the host. Many fish and mollusc species that have been regarded as bioluminescent organisms have been shown to glow by the light of symbiotic bacteria. There are, however, also cases of true fish and mollusc bioluminescence.

It is probable that bioluminescence first appeared during the "Cambrian explosion" when the evolution of eyes had made it meaningful. Molecular oxygen is required for all known bioluminescence mechanisms, but the required oxygen

TABLE 23.1. Systematic Distribution of Bioluminescence

Phylum	Approximate number of genera with bioluminescence
Bacteria	5
Pyrrophyta	11
Protozoa	9
Porifera	1
Cnidaria	66
Ctenophora	15
Rhyncocoela	1
Nematoda	1
Mollusca	74
Annelida	40
Arthropoda	207
Bryozoa	1
Echinodermata	47
Chordata	208

Source: Adapted from Campbell 1988.

partial pressure (or equivalent chemical activity) is much lower than that of the contemporary atmosphere.

23.3. Biological Roles: What Is Bioluminescence Good for?

In some cases the advantage to the organisms of bioluminescence is quite clear, in other cases quite obscure. An old hypothesis for explaining bioluminescence in cases where no other explanation could be found is that it takes care of big energy quanta, which could act destructively, and converts them to harmless photons (McElroy and Seliger 1962, Seliger and McElroy 1965). The energy in a bioluminescence photon is an order of magnitude greater than the energy bound in a high-energy phosphate bond in, e.g., ATP. The evolution of bioluminescence could have been triggered by the appearance of free oxygen, causing formation of dangerous peroxides. As we shall see, peroxides play a role in most bioluminescent systems. It has also been pointed out (Seliger and McElroy 1965) that bioluminescent reactions, although depending on the presence of oxygen, require only very low partial pressures, corresponding to conditions in the distant past when organisms would first have had to adapt to this dangerous triplet molecule. More recently (Rees et al. 1998) present evidence for antioxidant activity in coelenterazine, a common marine luciferin, and Lyzen and Wegrzyn (2005) demonstrate similar protective effects in bacterial luciferases. Barros and Bechara (2000) further discuss the protective effect of an insect luciferase with special regard to a beetle larva.

In those cases when we can clearly see a present-day biological role for bioluminescence, we can divide the advantages gained into five main categories: (1) reproduction, (2) protection from predation (defence, camouflage or aposematic signaling), (3) food acquisition, (4) protection from reactive oxygen species (ROS), and (5) DNA repair by means of activation of photolyase repair enzymes. We shall give examples of each of them.

23.3.1. Reproduction

The best known examples of bioluminescence having a role in the propagation of the species is found among the beetles of the family Lampyridae (true fireflies and glow worms), although bioluminescence also occurs in several other beetle families. In glow worms only the female glows brightly (with a steady light) and by this attracts the male, and the same is the case in some firefly species. In other fireflies a sophisticated "light conversation" between males and females has evolved, with a different "language" for each species. Males send out an "interrogation" flash, and females respond. Species specificities are obtained both by the time course of the flash on a half-second time scale and on the time delay between "interrogation" and "answer." Some details of this with references are given by Seliger and McElroy (1965).

The competitive value of various flashing abilities has been investigated by Branham and Greenfield (1996), Vencl, Blasko, and Carlson (1994), and Vencl and Carlson (1998). For one species Branham and Greenfield (1996) found that the flash rate, rather than the flash length or flash intensity, determined the female's preference.

An intriguing phenomenon is the synchronous flashing of the males of some fireflies. These males often collect in a tree, and the whole tree flashes "in step" (Buck and Buck 1976, Buck 1988). Species differences and various ideas about how this synchronized flashing comes about as well as how it aids the reproduction of the species are discussed with many references by Buck (1988). For newer investigations on the phenomenon, we refer the reader to Moiseff and Copeland (2000).

There is also a multitude of deep sea animals which use bioluminescence for finding a mate in the dark abyss, and here new discoveries are certainly going to be made for some time to come. Among the more interesting cases is the dragonfish, which uses light of a wavelength so long (maximum 702 nm) that it cannot be perceived by other organisms on which the dragonfish preys (Herring 2002).

There is no solid information on the role of bioluminescence in fungi. Bioluminescence has been reported in about 40 species of fungi, of which nearly two thirds belong to the genus *Mycena*. Other genera with luminescent members are *Panellus*, *Armilariella*, *Lampteromyces*, *Pleurotus*, *Omphalia*, and *Omphalotus*. *Panellus stypticus* is a brightly luminescent fungus common in North America, which has served as material for several investigations. It has been speculated that luminescent fungi attract insects which aid in dispersal of spores (O'Kane et al. 1990a, Bermudes et al. 1992, and many others). However, in many fungi only the mycelium, and not the fruiting bodies, luminesce.

23.3.2. Protection from Predation

One of the best-known examples of bioluminescence, described by Aristotle, is the "fire of the sea" caused by dinoflagellates such as *Noctiluca* and *Gonyaulax*. Its survival value remained obscure for a long time, but it has now been shown that it protects from grazing by copepods (Esaias and Curl 1972, Buskey and Swift 1983).

In different animal groups there are examples of how bioluminescence can protect by diverting the attacker's attention away from the prospective prey. Some squid, when attacked, give off a luminescent secretion which confuses the attacker, and luminescent secretion from a shrimp (Inouye et al. 2000) may serve a similar purpose. A kind of marine annelid called a scale worm is covered on the dorsal side by scales which first emit flashes when the animal is attacked and then are shed, still glowing (Herrera, Hastings, and Morin 1974). Its light-emitting protein may have use for detection of superoxide anions (Bassot and Nicolas 1995).

By aposematic coloration we mean easily recognized bright color patterns like the black-yellow banding of wasps, spots on ladybugs, and stripes on coral snakes, which warn a predator of nasty consequences of an attack (and frequently are mimicked by species which do not have any other protection). It was shown by Underwood et al. (1997) that bioluminescence of firefly larvae serves a similar purpose.

Somewhat surprisingly, bioluminescence can also be used for camouflage in two different ways. Fish can be either luminescent by themselves or can harbor luminescent bacteria. Some fish of both categories use bioluminescence for counterillumination and "disruptive illumination" (McFall-Ngai and Morin 1991), to avoid perception of their shape and size. Most fish are lighter on the ventral than on the dorsal side, and this can be regarded as minimizing their visibility: from above they look dark like the background depth, and from below they look bright like the sky above. This cannot give complete protection; they still look rather dark against a bright sky. But some fish, by bioluminescence, do match both the intensity and the angular distribution of the downwelling surface light (Denton et al. 1972). The spectral match is also very good (Denton et al. 1985), and the intensity is regulated according to ambient light (McFall and Morin (1991).

An intriguing function might be what is commonly called the "burglar alarm" hypothesis (Fleisher and Case 1995, Mensinger and Case 1992, and papers cited in these). Bioluminescent organisms such as the dinoflagellate, *Noctiluca*, respond to predation, or even movement, by flashing, thereby increasing the visibility of actual or potential predators to secondary predators, and thus protecting themselves.

23.3.3. Food Acquisition

The deep sea angler fish *Linophryne arborifera* uses a bait with luminescent bacteria. Female fireflies of the genus *Photuris* reply to the "interrogating flashes" from males of other fireflies, lure them to approach, and eat them (Lloyd 1984a). Most sly and cunning of them all are the females of *Photuris versicolor*, who know firefly languages sufficiently well to be able to prey on 11 different species (Lloyd 1984b). In other cases luminescent fireflies rely for their catch on the more unspecific attraction of insects to light.

In addition to beetles, among bioluminescent insects one finds fungus gnats, members of the order Diptera. About a dozen of more than 3000 species in the family have larvae which use bioluminescence in different ways to catch prey. Particularly famous are the larvae in the Te Ana-au caves on the South Island of New Zealand. The gnat larvae sit on the roof and deploy luminescent and sticky "fish lines," which attract other insects which are caught and devoured.

In many cases, marine animals are aided in their vision by their own luminescence, which functions mainly in the service of food acquisition. Several fish species, such as *Aristomonias scintillans* in the deep sea and *Photoblepharon palpebratus* and *Anomalops katoptron* in shallow waters, have luminescent

organs in proximity to their eyes. The dragonfish, which are so remarkable that we shall return to them later, also belong to those for which vision is aided by own bioluminescence, as are the shrimplike euphausiids.

23.3.4. Protection from Reactive Oxygen Species

Rees et al. (1998) investigated the properties of coelenterazine, a common marine luciferin and documented its strong antioxidant properties. They proposed that during the early stages of their evolution the primary function of these systems would have been detoxification of oxygen and other ROS at a time in which environmental oxygen levels were rising (modern surface waters are rich in superoxide [SO] and hydrogen peroxide). Along the way, these organisms would have developed effective ways of handling these potentially toxic and high-energy systems, and as they colonized the less oxidatively stressful deeper levels of the seas (less light, including UV, less oxygen, and slower metabolisms), their systems would be preadapted to produce light for other purposes (as these authors note, all bioluminescent reactions are high energy and require involvement of oxygen or its activated species)

Studies of luminescence in bacteria (Gonzales-Flecha and Demple 1994, Katsev et al. 2004, Lyzen and Wegrzyn 2005, Szpilewska et al. 2003) have reinforced and extended this view. There has long been speculation about the role of luminescence in bacterial life, besides its role in those symbionts, which presumably gain shelter, food, and possibilities of a future life.

Luminous bacteria occur in the genera *Vibrio*, *Photobacterium*, *Lucibacterium*, *Alteromonas*, and *Xenorhabdus*; most investigations deal with either the first or second of these. The cited studies demonstrate that wild-type (= luminescent) bacteria of *Vibrio harveyi* and other strains are able to survive UV irradiation or exposure to hydrogen peroxide better than nonluminescent *lux* mutants and, further, that this wild-type resistance can be conferred to *E. coli* via constructs between the *lux genes* and the promotor of a stress-response gene. Gonzales-Flecha and Demple found that in *E. coli* the bacterial luciferase was producing superoxide as a byproduct, and they urge caution in using this construct system to report oxidative stress in bacteria that normally do not produce such luciferase. It is highly probable, given the connection between ROS and bioluminescence, that other such systems will show similar effects.

23.3.5. DNA Repair

Many of the above luminescent bacteria display a behavior called "quorum sensing," in which the bioluminescent systems are not expressed until the colony reaches a certain density (Swift et al. 1998). A common interpretation is that this may deter predators from disturbing a colony that has gained a beachhead in a food item. But many luminescent bacteria luminesce at extremely low density, and in addition to possible detoxification of ROS, evidence now suggests strongly that this solo luminescence may function in activation of photolyase

enzymes in DNA repair (Czyz et al. 2000, Kosakiewicz et al. 2005). In *V. harveyi* (nonluminescent), *lux* mutants irradiated with UV light and then cultured in the dark did not survive as well as the (luminescent) wild type or as *lux* mutants returned to light after irradiation; this result has been generalized to other strains of bacteria as well. In short, bacteria living in relatively dark levels of the ocean may be achieving photoreactivated DNA repair by producing their own "photo." However, experiments by Walker, Bose, and Stabb (2006) do not support the theory that bioluminescence protects DNA. Given that bioluminescence in these organisms may be extremely expensive metabolically (requiring about 20% of cellular energy; Kozakiewicz et al. 2005), its use for protection against ROS and for DNA repair would certainly be a strong factor for its evolution and conservation. Indeed, cells are able to handle and manipulate many types of ROS. We will meet another such system later.

23.4. Mechanisms of Light Production

As mentioned earlier, bioluminescence has evolved several times, and it is not surprising therefore that there are many different mechanisms (Hastings and Tu 1995). The different mechanisms do, however, have in common that they all require oxygen at some stage. Many of them also involve a peroxide—either a hydroperoxide or a cyclic peroxide. They involve catalysis by an enzyme called luciferase, but luciferases from different organisms are different (the outcome of comparisons of luciferase sequences is the main reason for the statement that bioluminescence in extant taxa probably has evolved about 30 times). Luciferase action on a relatively low molecular organic compound called luciferin results in an excited state of a pigment, which either emits light directly or transfers excitation energy to another emitter.

Bacterial luminescence is based on peroxidation of flavin mononucleotide and oxidation of a long-chain aldehyde to carboxylic acid, so flavin mononucleotide can be said to be the luciferin in this case. The reaction scheme is shown in Fig. 23.1. The flavin molecule is here drawn isolated, but is, in fact, bound to the luciferase. The emission may be either the blue-green emission from FMN or be from an accessory chromoprotein to which the excitation is transferred. There are several such proteins known for different bacteria (Eckstein et al. 1990, Lee et al. 1991), but the mechanisms for light emission are not completely understood. Some bacteria can emit radiation with different spectra.

Fungal bioluminescence is relatively little explored, and in most investigations spectral analysis of the emitted light suffers from deficient methods and equipment. The most reliable spectrum so far was published by O'Kane et al. (1990b). They found an emission maximum (on a photons per wavelength interval basis) of about 525 nm. Shimomura (1980, 1989, 1992) favors the view that the emission is caused by a reaction between hydrogen peroxide, a low molecular amine, and panal (sesquiterpene aldehyde). However, as O'Kane et al. (1990b) point out, such a conclusion cannot be based on spectral data, since
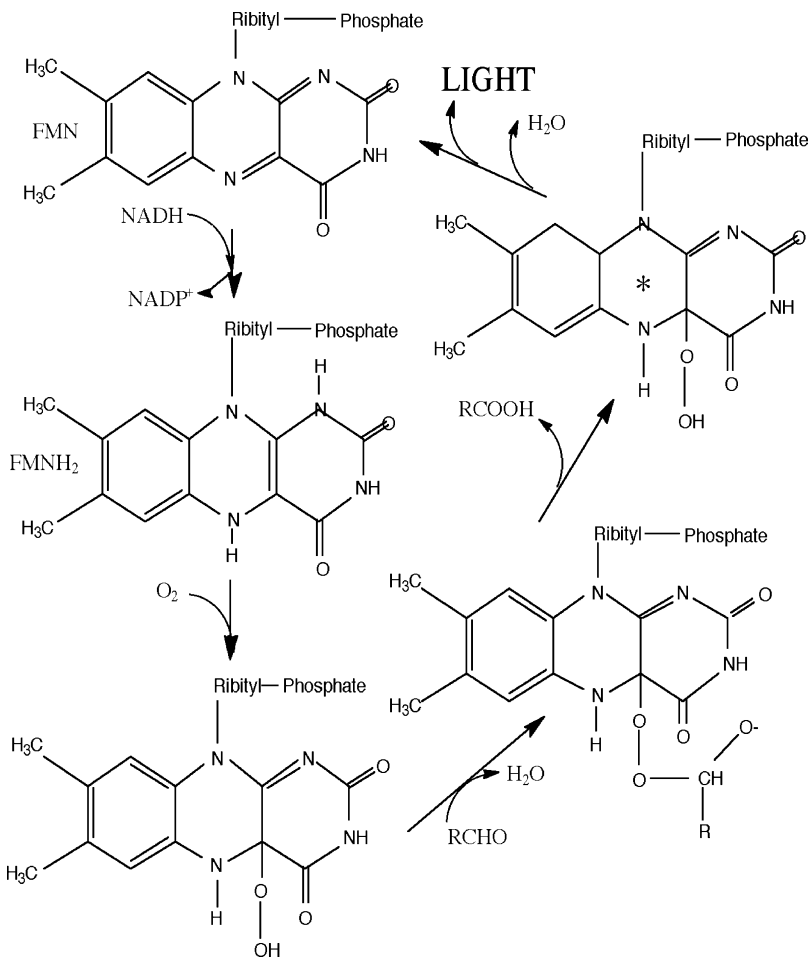
FIGURE 23.1. Reactions involved in bacterial bioluminescence.

chemiluminescence of the latter system in vitro has emission maxima ranging from 485 to 570 nm, depending on conditions. Several other emitters have been proposed in fungal bioluminescence; one of which is riboflavin (Isobe et al 1987).

Dinoflagellates have different luciferins depending on the species. In the most studied organism, *Gonyaulax polyedra*, it is a tetrapyrrol-like substance with an extra ring (Nakamura et al. 1989), clearly derived from chlorophyll (Fig. 23.2), but in another species, *Pyrocystis lunula*, it is quite different (Nakamura et al. 1989). The bioluminescence of *Gonyaulax* differs from that of most bioluminescent organisms in that no peroxide seems to be involved. Another remarkable thing is that the spectrum of luminescence agrees with the fluorescence spectrum of unreacted luciferin (Hastings 1978), while the postulated emitter is
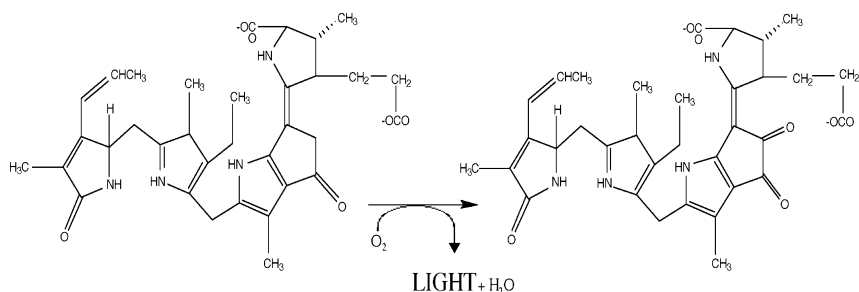
FIGURE 23.2. Bioluminescence reaction in the dinoflagellate *Gonyaulax*.

nonfluorescent. Therefore the mechanism sketched in Fig. 23.2 must be regarded as tentative.

For light emission by the firefly luciferin/luciferase reaction (Fig. 23.3) prior adenylation of the luciferin by reaction with ATP is required. Both luciferin and luciferase are located in the peroxisomes in one part of the cell, while another part of the cell is full of ATP-generating mitochondria.

Although different beetles can produce light with different colors from green to red, they all seem to possess the same kind of luciferin. The differences in wavelength distribution are probably due to differences in luciferase. Possibly there are two different molecular species involved as emitters, as sketched in Fig. 23.3.

As for color of emitted light, the most remarkable animal is the larva in the beetle family Phengodidae (*Phrixothrix vivianii* and *Euryopa* species), so-called
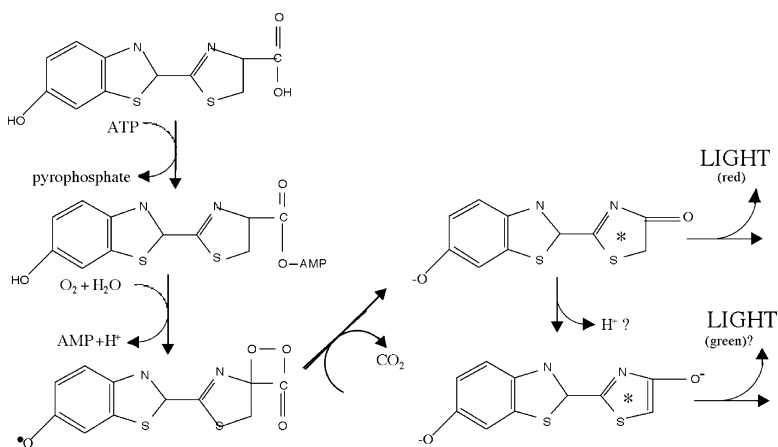
FIGURE 23.3. Reactions leading to luminescence in fireflies and other beetles. The luciferin and its derivatives remain bound to luciferase throughout the reaction sequence. The asterisk indicates an excited state. The diagram is essentially according to Wilson and Hastings (1998).

railroad worms (Viviani and Bechara 1997, Viviani and Ohmiya 2000). They carry both red (on the head) and yellow-green (on the sides) lanterns on the same individual. Color pictures of these magnificent animals are available at several Internet sites, e.g., http://www.lifesci.ucsb.edu/~biolum/forum/vviviani2.html.

The mechanism of bioluminescence in dipterans differs from that of beetles, but is as yet little explored.

In addition to *Vargula* (see below), among crustaceans the euphausiids are worth special mention because of their strong light and sophisticated lantern optics. They are shrimp-like animals, but distinct from true shrimps and not members or the group Decapoda. Like the dinoflagellate *Gonyaulax* they have a tetrapyrrole chlorophyll derivative as a light-emitting chromophor, but the macrocycle of the chlorophyll molecule is split open at another site. Their lanterns are equipped both with a reflective backing and a lens system to direct the light. Those lanterns which are located on the eye stalks just above the eyes certainly serve as an aid to vision.

The structure of the luciferin typical of the coelenterates, i.e. cnidaria and ctenophores, (coelenterazine) has great similarities to the prosthetic group of a light-generating chromoprotein, aequorin, of the jellyfish *Aequorea.* The luciferin of the squid *Watasenia* is coelenterazine with the hydroxy groups replaced by sulfate groups. The luciferin of the crustacean (ostracod) *Vargula* (formerly known as *Cypridina*) is also structurally related to these chromophores (Fig. 23.4).

The luciferins of coelenterates and of *Vargula* function together with luciferases and also require oxygen for the light-emitting reactions to take place. Earlier it was thought that the bioluminescence of *Aequorea* (Fig. 23.5) was something in principle different, since the chromoprotein aequorin extracted from it would glow in vitro when calcium ion was added, without the need for molecular oxygen. However, it is now realized that aequorin is an enzyme–substrate (luciferase–luciferin) complex which requires oxygen for formation and is stable in the absence of calcium ions.

Just like some bacteria, some animals also have accessory light-emitting chromoproteins, proteins different from the luciferin–luciferase complexes. This is the case with *Aequorea* (Fig. 23.6), and also the sea pansy *Renilla* (Pennatulacea, relatives of corals). Excitation energy is transferred by the Förster mechanism from the excited reaction product of the luciferin to the covalently bound chromophores of these accessory proteins.
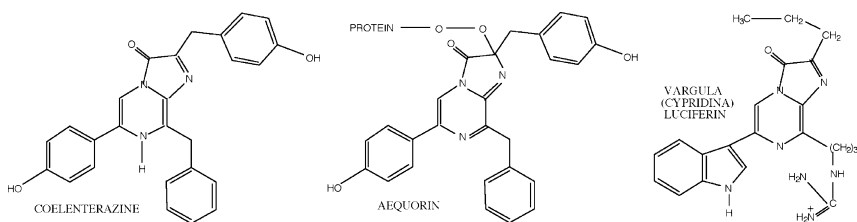
FIGURE 23.4. Coelenterazine and related chromophores.
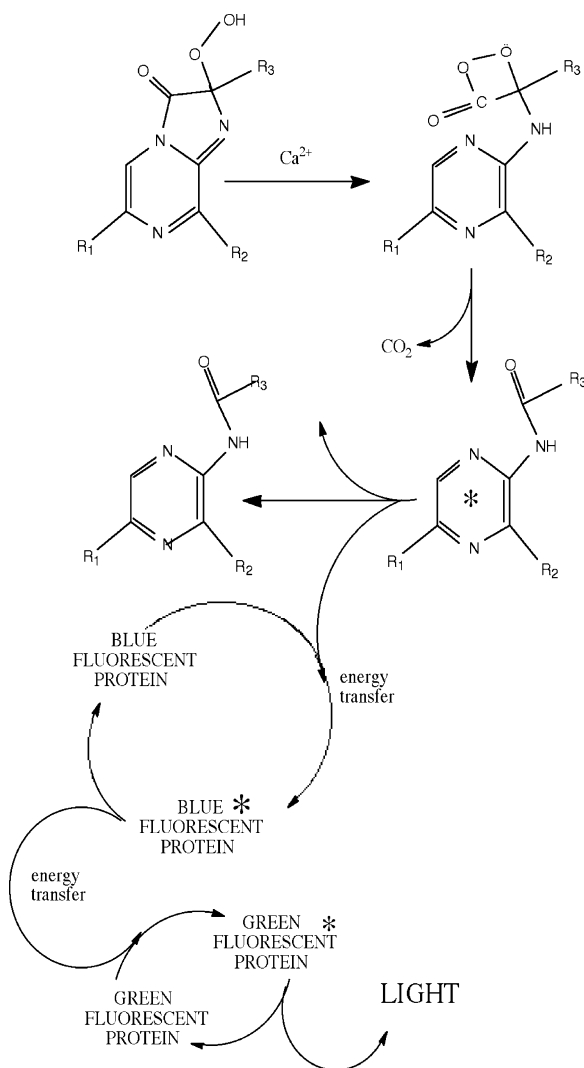
FIGURE 23.5. *Aequorea* bioluminescence. The asterisk indicates an excited state

23.5. Dragonfishes: Long-Wave Bioluminescence and Long-Wave Vision

Even the dark deep sea harbors creatures of great interest to photobiologists. Dragonfishes are worth our attention for two reasons: their bioluminescence and their vision. Both operate at the long-wavelength limit of our own perceptual abilities, at wavelengths of around 700 nm.
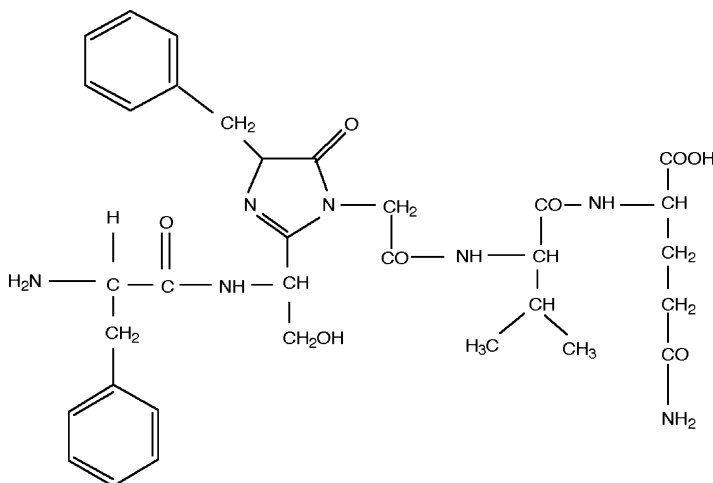
FIGURE 23.6. Structure of the chromophore of the green fluorescent protein from *Aequorea* according to Cody et al. (1993). A slightly different structure has been published by Shimomura (1979). The fluorescence spectrum has a narrow band peaking at 509 nm.

Three genera, *Aristomias*, *Malacosteus*, and *Pachystomias*, emit both blue light from organs behind the eyes and far-red light from organs below the eyes (Widder et al. 1984, Douglas et al. 2000). It is possible that the basic luminescence system is the same in both blue-emitting and far-red–emitting organs, and that the latter are equipped with secondary emitters to which excitation energy is transferred from the luciferin. If this is the case, probably also an intermediary pigment is required to span the spectrum from the 479-nm (*A. scintillans*) or 469-nm (*M. niger*) primary emitter to the final 703-nm (*A. scintillans*) or 660-nm (*M. niger*) emitter, to make possible sufficiently large overlap integrals for Förster energy transfer to take place. *M. niger* has a short-wavelength cutoff filter in front of the light emitter to shift the emission maximum from 660 nm to 702 nm (Widder et al. 1984, Denton et al. 1985).

What could the pressure be to drive evolution of emission maxima in both these fishes to such long wavelength, using different methods? This for a long time was an enigma. Water absorbs such radiation rather efficiently, so its range cannot be very large. And, above all, what could its use be? It was hard to believe that any visual pigment could exist to permit the fish to see such long-wave radiation.

But in the difficulty of constructing a retinal-based visual pigment with such long-wavelength absorption lies the explanation for the advantage. The dragonfish can use its far-red torch to watch its prey without being observed by other animals. But still, to have any use for the light, it must be able itself to perceive it. And how it manages to do that is the most remarkable fact about this fish.

The genera *Aristomias* and *Pachystomias* use a "conventional" method. They have managed to tune a rhodopsin by "protein engineering" to get an absorption band peaking at 588–595 nm (Bowmaker et al. 1988, Douglas et al. 1998, 2000). This is quite a feat, considering that essentially the same chromophore, in a different protein environment, is used by other animals for UV receptors with sensitivity peaks around 360 nm. The tail of the 588-nm pigment extends above 700 nm and would give some sensitivity overlapping the bioluminescence spectrum. However, in addition to rhodopsins (retinal-based visual pigments), fishes (and also dragonfishes) usually contain porphyropsins (3,4-dehydroretinal–based pigments) with the same opsin-type protein moiety. Although Douglas et al. (2000) were unable to find the porphyropsin analogue of the 588 nm rhodopsin, they speculate that *A. tittmanni* is equipped with it. They calculate the absorption peak to be at 669 nm and show that it would match the bioluminescence almost perfectly.

But *Malacosteus* has not succeeded with this "protein engineering." It has only two "conventional" visual pigments with peaks at 520 and 540 nm. But it has another trick up its sleeve.

Not only is it difficult to construct a retinal-based pigment with an absorption maximum above 650 nm, but there are, in fact, very few types of organic substances which absorb at such long wavelengths. One well-known type widespread in the biosphere is chlorophyll. Bacterial variants of this may have absorption peaks even above 1 µm.

And this type of pigment is just what *M. niger* uses for its vision. Chlorophyll from photosynthetic bacteria at the base of the food chain has been converted to a mixture of pheophorbides and deposited in the outer segments of the photoreceptor cells in close contact with the 520- and 540-nm pigments. It seems either that in some way energy can be transferred from pheophorbide to these pigments (Douglas et al. 1998, 1999 speculate that this could take place via the triplet state of the rhodopsin or porphyropsin) or that pheophorbide can act in place of ordinary visual pigments.

23.6. Control of Bioluminescence

Even in bacteria bioluminescence is regulated; bacteria do not glow unless the cell density is high, as it is for instance in the organs where some squids and fishes harbor luminescent bacteria.

A common feature for many bioluminescent systems is that the light intensity decreases when ambient light increases. This indicates both that the light has some function in itself (and not primarily serves to divert excess energy) and that bioluminescence is energetically and metabolically demanding and that an organism cannot afford to waste the resources. In a couple of cases action spectra have been constructed for the inhibition of luminescence (Esaias, Curt, Jr., and Seliger 1973, Li et al. 1996; Fig. 23.7), but the chromophore corresponding to this spectrum is unknown, as is the mechanism of inhibition.
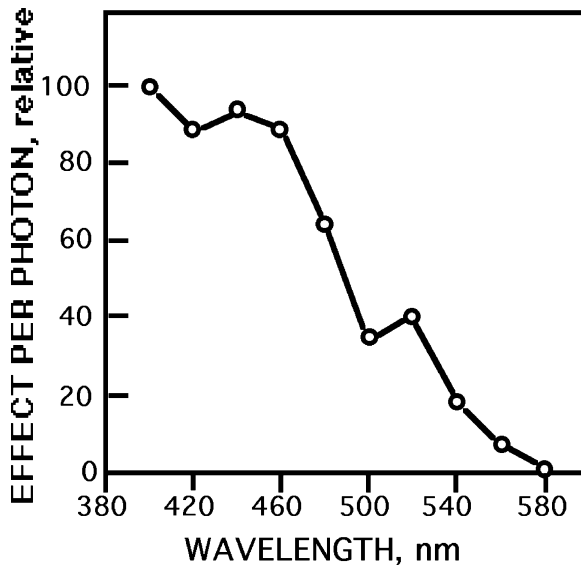
FIGURE 23.7. Action spectrum for the inhibition of bioluminescence of the dinoflagellate *Protoperidinium depressum*. (Redrawn from Li et al. 1996.)

There are many interesting findings regarding regulation of bioluminescence. These range from the rapid flashing of fireflies and dinoflagellates and the circadian rhythms to long-term effects of environment and nutrient status, and from the organismal to the subcellular levels. We must refrain from descriptions of most of this here, and the reader is referred to the treatises by Campbell (1988), Ulitzur and Dunlap (1995), Hosseini and Nealson (1995), and Wilson and Hastings (1998). A few words will be devoted to recent findings about one of the best investigated cases, firefly bioluminescence.

Most fireflies flash with precise timing in a species-specific way and rapidly respond to flashes from other fireflies. Obviously they must have very tight control of their so-called photocytes, the light-emitting cells. How this control is possible has been an enigma, since in some case they have no direct nerve connections. As we have seen, the light-emitting process requires oxygen, and the photocytes are located in close proximity to the the profusely branched tracheae (Figs. 23.8–23.10). Trimmer et al. (2001) suggest that the signaling takes place along the same path as the supply of oxygen, using the gaseous hormone nitrogen monoxide (NO). This hormone, coined "molecule of the year" by *Science* in 1992, is also important in human physiology, but in humans and most other animals it is transported in the dissolved state. According to this model, the fireflies take advantage of the fact that it is a small molecule diffusing very rapidly in the gaseous phase. The nitrogen monoxide is produced in the terminal cells of the tracheal system, where the nerve projections end, and in some of the peripheral (and mitochondria-rich) parts of the photocytes (Fig. 23.10).
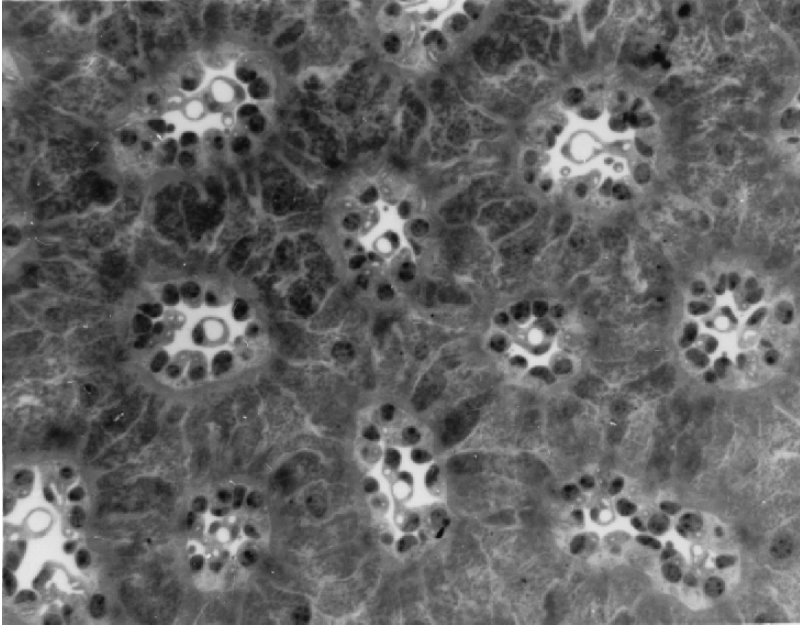
FIGURE 23.8. A section through the light-emitting organ of the firefly *Photuris* sp. showing tracheae surrounded by cylindrical tracheal end organs and photocytes. The photocytes stretch rosette-fashon from one cylinder to the next (see the following figures). (From Ghiradella 1998.)
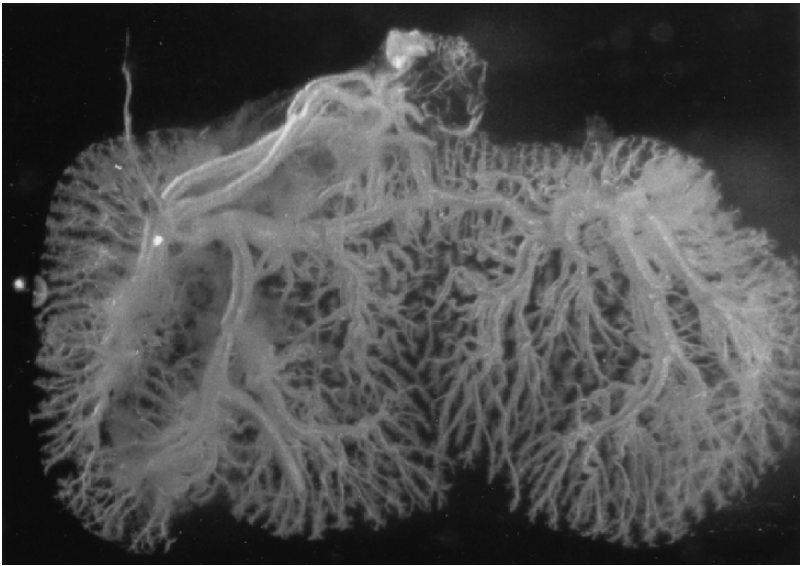
FIGURE 23.9. Preparation of isolated tracheae from a light-emitting organ of a firefly, showing the repeated ramification. (From Ghiradella 1998.)
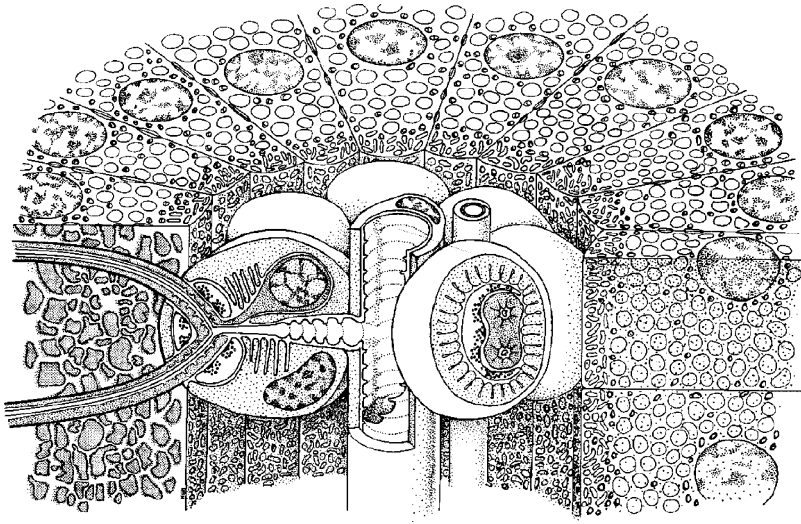
FIGURE 23.10. Diagrammatic view of part of a firefly lantern. At center the main trachea (parallel to a nerve) is connected to a cluster of tracheal end organs. At left is shown a longitudinally sectioned end organ with its tracheolar branches and the webbed intercellular border of an associated photocyte. To the right is shown a transversely sectioned end organ. In the upper part of the picture is a half-circle of cross sections of photocytes. (From Ghiradella 1998.)

This model, as many earlier ones, depends on oxygen as the controlling molecule and builds on earlier suggestions that the mitochondria that occupy the photocyte borders between the branches of the tracheal system and photocyte interiors (where the light is actually produced) may serve as "gate keepers," using up incoming oxygen before it can penetrate into the photocyte. NO reversibly shuts down mitochondrial action, which in this case would then "open the gate" and allow free passage of oxygen. However, the model does not account for important morphological and physiological features of the lantern, especially the presence in the photocyte interior of huge numbers of peroxisomes, organelles particularly adept at handling peroxides and other ROS.

Ghiradella and Schmidt (2004) propose that to complete the flash reaction (and thus control the flash) the photocyte is in fact using *hydrogen peroxide*, produced in its peroxisomes from incoming oxygen, rather than the oxygen itself. This new proposal has required reworking of the current chemical model, which was generated by superb scientists, but working at a time and in a climate in which it was not believed that cells can in fact control and manipulate these high-energy ROS compounds. We are learning that they can (Hoffman 2004) and our new knowledge of the capabilities of cells suggests that many models, these included, are ripe for reexamination and revision.

23.7. Human Exploitation of Bioluminescence

Warfare is perhaps not an application one would guess at for bioluminescence. Japanese soldiers are said to have used dried *Vargula* for reading maps during World War II. When moistened these dried animals emitted sufficient light for the purpose.

The cloned gene of the fluorescent accessory protein of *Aequorea* ("green fluorescent protein") has found wide application in molecular biology as a reporter gene. It has even been improved by genetic engineering (Blinks 1989, Cubitt et al. 1995a, Heim et al. 1995, Heath 2000, Deo and Daunert 2001).

The "arrested" luciferin–luciferase complex of *Aequorea* can be used for extremely sensitive assays of calcium ion. Using this protein it is even possible to map the concentration of calcium ions inside cells. The protein can be introduced into the cells under study by different methods. If the aqueorin gene is cloned into the organism under study, it ends up in the cytoplasm of that organism. The cytoplasm has a low calcium ion concentration most of the time, but one step in many signal transduction chains consists in a sudden elevation of the concentration, and this can be studied by this method (Knight et al. 1991, 1993, Cubitt et al. 1995b, Wood et al. 2000, 2001).

Various other luciferase genes, especially the firefly luciferase gene, are also used for the study of gene regulation. The luciferase gene is fused to the regulator gene under study. A disadvantage is that the organism has to be killed and treated in such a way that ATP and luciferin can be added. This can be circumvented by using instead bacterial luciferase, which can be activated by addition of the vapor of an aldehyde. However, as mentioned above, Gonzáles-Flecha and Demple (1994) warn of at least one case in which the results were ambiguous. In a study aimed at reporting concentrations of redox stress agents, specifically superoxide, they fused the *lux* luciferase genes to the promotor of *soxS*, part of the cell's response system to such agents, and discovered that the alien (to *E. coli*) bacterial luciferase was raising superoxide concentration, thereby complicating the measurements and the interpretation of the results.

The classic use of bioluminescence, however, is the use of a luciferin-luciferase mixture from fireflies as an assay for ATP. The sample to be analyzed is mixed with a luciferin–luciferase mixture or crude firefly lantern extract. Since the luciferase preparations usually also contain an enzyme capable of converting two molecules of ADP to one molecule of AMP and one of ATP (a slower reaction than the luciferase reaction), AMP in the sample will also produce light, but with much slower kinetics. Therefore the intensity of the initial flash upon mixing the sample with the reagents is taken as a measure of ATP.

The firefly assay for ATP has found very wide use, and kits for assay are commercially available. This application forms a natural bridge to the next section.

23.8. Photosynthetic Afterglow

In the 1950s many people were involved in the discovery and study of photosynthetic phosphorylation, and one of present authors had the privilege of working as an assistant to D.I. Arnon during this exciting time. Early in the decade Strehler and Arnold (1951) had attempted to demonstrate the formation of ATP in a preparation of isolated chlorplasts by mixing the chloroplast suspension with firefly extract. After a period of illumination to let the chloroplasts synthesize ATP, the experimenters shut off all external light and tried to measure bioluminescence from the mixture. They were pleased to find a clear light signal, which rapidly decayed with time (as they expected, because the tiny amount of ATP would soon be consumed by the luciferase reaction). Then they did a control experiment without firefly extract, and to their surprise found that the light was as strong as before. This was the discovery of a phenomenon to which several names have been given: afterglow, delayed light emission, delayed fluorescence. Briefly, it is due to the reversion of early steps in photosynthesis: light energy recently converted to chemical, electrical, and proton gradient energy is reconverted to light. Chlorophyll serves as the emitter.

The delayed light emission is due almost exclusively to emission by photosystem 2 (PSII), and consists of several kinetic components. The most rapidly decaying component is due to return of electrons from pheophytin and the quinone called Q_A to the chlorophyll ion in the reaction center, resulting in excited chlorophyll. The slowest component also involves PSI and is best excited using long-wavelength light preferentially absorbed by this system. It is also dependent on molecular oxygen (Björn 1971). Energy for this emission is stored as proton gradient and as ATP and is inhibited not only by such electron transport blockers as DCMU, but also by uncouplers. Even before the acceptance of the chemiosmotic theory of Mitchell, study of this long-lived component demonstrated that the membrane system in a chloroplast stores energy as a unit (Björn 1971). Several reviews have been written on delayed light emission; one of the best and most comprehensive is still that by Lavorel (1975). Apart from its use in studies of the mechanism of photosynthesis, delayed light emission has been used for study of plant damage by disease, frost, etc. A special technique for this is "phytoluminography," whereby pictures of plants are produced using only the delayed light (Sundbom and Björn 1977, Björn and Forsberg 1979, Pérez-Bueno et al. 2006; Figs. 23.11 and 23.12).

Photosynthetic cells also exhibit a phenomenon known as thermoluminescence (light emission caused by a temperature rise). It has, as has afterglow and chlorophyll fluorescence, been used for experiments aimed at understanding the mechanism of photosynthesis (DeVault, Govindjee, and Arnon 1983; Tyystjärvi and Vass 2004).

FIGURE 23.11. Part of a bean leaf imaged in different ways by its own emitted light: Left: Fluorescence light; center: fast luminescence (about 0.25 second after the cessation of light incident on the leaf); right: slow luminescence (integrated between 30 and 60 seconds after the cessation of incident light). The leaf veins were injected with DCMU, a substance that interrupts electron transfer between the photosystems, before the picture was taken. This makes photosystem 2 dissipate energy faster, so fluorescence and fast luminescence become stronger, but slow luminescence weaker than from unpoisoned cells further away from the veins. (From Björn and Forsberg 1979.)

23.9. Ultraweak Light Emission

So far we have treated special organisms, which emit bioluminescence, and photosynthetic organisms, which produce delayed light emission due to reversal of photosynthesis. But all other organisms and all cells with active metabolism which have been studied emit very weak light. This is called ultraweak light emission. The ultraweak light emission from green leaves can be studied when the delayed light emission has decayed for about 4 hours (at room temperature).

Ultraweak light emission probably has several components with different causes. The main emission from green leaves is of a wavelength exceeding 600 nm, and probably is emitted from chlorophyll. In most other cases the emission is of shorter wavelength. It is believed that a main component stems from peroxidation of unsaturated membrane lipids. However, most cells contain other components which can emit light. For instance, when hydrogen peroxide is decomposed by catalase in the presence of various organic compounds (the plant hormone auxin is one example, pyrogallol another), light is emitted. A number of other causes of ultraweak light emission are listed by Campbell (1988).

If plants are irradiated with UV-B or UV-C radiation, the intensity of ultraweak light emission increases after a long lag period (about 2 days). The reason is probably that the ultraviolet radiation initiates a chain reaction, leading to peroxidation of membrane lipids. An action spectrum for this ultraviolet effect has been determined (Cen and Björn 1994).

Various medical and other applications of measurements of ultraweak light emission are described by Campbell (1988) and Jezowska-Trzebiatowska et al. (1990).
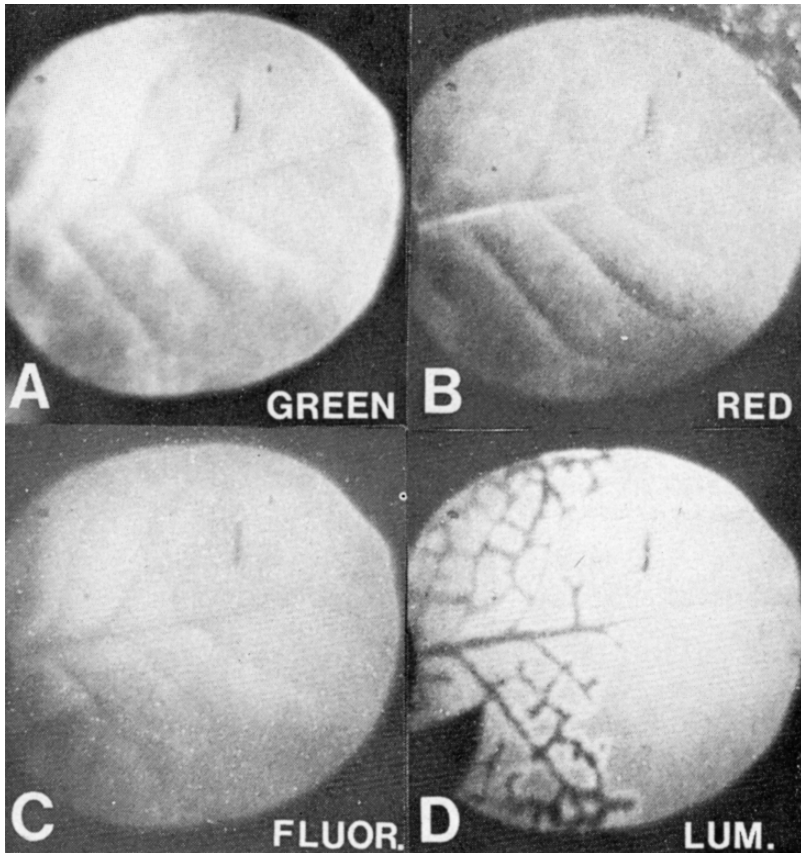
FIGURE 23.12. leaf on a tobacco plant on which another leaf was inoculated with tobacco mosaic virus 6 days before the picture was taken. The virus has spread through the veins to the depicted leaf. Pictures were taken using reflected green (A) and red (B) light, red fluorescence evoked by blue light (C), and light emitted by the leaf after cessation of external illumination (D). Only in the last case does the infection become visible at this early stage. (From Björn and Forsberg 1979.)

References

Barros, M.P. and Bechara, E.J.H. (2000) Luciferase and urate may act as antioxidant defenses in larval Pyrearinus termitilluminans (Elateridae: Coleoptera) during natural development and upon 20-hydroxyecdysone treatment. Photochem. Photobiol. 71, 648–654.

Bassot, J.M. and Nicolas, M.T. (1995) Bioluminescence in scale-worm photosomes: the photoprotein polyoidin is specific for the detection of superoxide radicals. Histochem. Cell Biol. 104, 199–210.

Bermudes, D., Petersen, R.H. and Nealson, K.H. (1992) Low-level bioluminescence detected in *Mycena haematopus* basidiocarps. Mycologia 84, 799–802.

Björn, L.O. (1971) Far-red induced, long-lived afterglow from photosynthetic cells. Size of afterglow unit and paths of energy accumulation and dissipation. Photochem. Photobiol. 13, 5–20.

Björn, L.O. and Forsberg, A.S. (1979) Imaging by delayed light emission (phytoluminography) as a method for detecting damage to the photosynthetic system. Physiol. Plant. 47, 215–222.

Blinks, J.R. (1989) Use of calcium-regulated photoproteins as intracellular Ca^{2+} indicators. Meth. Enzymol. 172, 164–203.

Bowmaker, J.K., Dartnall, H.J.A. and Herring, P.J. (1988) Longwave-sensitive visual pigments in some deep-sea fishes: Segregation of paired rhodopsins and porphyropsins. J. Comp. Physiol. A163, 685–698.

Branham, M.A. and Greenfield, M.D. (1996) Flashing males win mate success. Nature 381, 745–746.

Buck, J. and Buck, E. (1976) Synchronous fireflies. Sci. Am. 234, 74–85.

Buck, J. (1988) Synchronous rhythmic flashing of fireflies. II. Quart. Rev. Biol. 63, 265–289.

Buskey, E.J. and Swift, E. (1983) Behavioural responses of the coastal copepod Acartia hudsonica to simulated dinoflagellate bioluminescence. J. Exp. Biol. Ecol. 72, 43–58.

Campbell, A.K. (1988) *Chemiluminescence: Principles and applications in biology and medicine*, pp. 608. Ellis Horwood, Chichester. ISBN 3-527-26342-X

Cen, Y.-P. and Björn, L.O. (1994) Action spectra for enhancement of ultraweak luminescence by ultraviolet radiation (270-340 nm) in leaves of *Brassica napus*. J. Photochem. Photobiol. B: Biol. 22,125–129.

Cody, C.W., Prasher, D.C.. Westler, W.M., Prendergast, F.G. and Ward, W.W. (1993) Chemical structure of the hexapeptide chromophore of the *Aequorea* gfreen-fluorescent protein. Biochemistry 32, 1212–1218.

Cubitt, A.B., Heim, R., Adams, S.R., Boyd, A.E., Gross, L.A. and Tsien, R.Y. (1995a) Understanding, improving and using green fluorescent proteins. Trends Biochem. Sci. 20, 448–455.

Cubitt, A.B., Firtel, R.A., Fischer, G., Jaffe, L.F. and Miller, A.L. (1995b) Patterns of free calcium in multicellular stages of *Dictyostelium* expressing jellyfish apoaqeorin. Development 121, 2291–2301.

Czyz, A., Wrobel, B. and Wegrzyn, G. (2000) *Vibrio harveyi* bioluminescence plays a role in stimulation of DNA repair. Microbiology 146, 283–288.

Denton, E.J. Gilpin-Brown, J.B. and Wright, P.G. (1972) The angular distribution of the light produced by some mesopelagic fish in relation to their camouflage. Proc. R. Soc. Lond. B 182, 145–158.

Denton, E.J., Herring, P.J., Widder, E.A., Latz, M.F. and Case, J.F. (1985) The roles of filters in the photophores of oceanic animals and their relation to vision in the oceanic environment. Proc. R. Soc. Lond. B 225, 63–97.

Deo, S.K. and Daunert, S. (2001) Luminescent proteins from *Aequorea victoria*: applications in drug discovery and in hight throughput analysis. Fresenius J. Anal. Chem. 369, 258–266.

DeVault, D., Govindjee and Arnold, D. (1983) Energetics of photosynthetic glow peaks. Proc. Natl Acad. Sci. USA 80, 983–987.

Douglas, R.H., Partridge, J.C., Dulai, K.S., Hunt, D.M., Mullineaux, C.W Tauber, P.H. and Hynninen, P.H. (1998) Dragon fish see using chlorophyll. Nature 393, 425.

Douglas, R.H., Partridge, J.C., Dulai, K.S., Hunt, D.M., Mullineaux, C.W and Hynninen, P.H. (1999) Enhanced retinal longwave sensitivity using a chlorophyll-derived photosensitiser in *Malacosteus niger*, a deep-sea dragon fish with far red bioluminiscence. Vision Res. 39, 2817–2832.

Douglas, R.H., Mullineaux, C.W. and Partridge, J.C. 2000. Long-wave sensitivity in deep-sea stomiid dragonfish with far-red bioluminescence: evidence for a dietary origin of the chlorophyll-derived retinal photosensitizer of *Malacosteus niger*. Phil. Trans. R. Soc. Lond. B 355, 1269–1272.

Eckstein, J., Cho, K.W., Colepicolo, P., Ghisla, S., Hastings, J.W. and Wilson, T. 1990. A time-dependent bacterial luminescence emission spectrum in an in vitro singel turnover system: energy transfer alone cannot account for the yellow emission of *Vibrio fischeri* Y-1. Proc. Natl. Acad. Sci. USA 87, 1466–1470.

Esaias, W.E. and Curl, H.C. (1972) Effect of dinoflagellate bioluminescence on copepod ingestion rates. Limnol. Oceanogr. 17, 901–906.

Esaias, W.E., Curl, H.C., Jr and Seliger, H.H. (1973) Action spectrum for a low intensity rapid photoinhibition of mechanically stimulable bioluminescence in the marine dinoflagellates *Gonyaulax catenella*, *Gonyaulax acatenella* and *Gonyaulax tamarensis*. J. Cell Physiol. 82, 363–372.

Fleisher, K.J. and Case, J.F. (1995) Cephalopod predation facilitated by dinoflagellate luminescence. Biol. Bull. 189, 263–271.

Ghiradella, H. (1998) The anatomy of light production: The fine structure of the firefly lantern. In: F.W. Harrison and M. Locke (Eds.), *Microscopic anatomy of invertebrates*, vol. 5 *Insecta*, pp. 363–381. Wiley-Liss, New York.

Ghiradella, H. and Schmidt, J.T. (2004) Fireflies at one hundred plus: a new look at flash control. Integr. Comp. Biol. 44, 203–212.

Gonzales-Flecha, B. and Demple, B. (1994) Intracellular generation of superoxide as a by-product of *Vibrio harveyi* luciferase expressed in *Escherichia coli*. J. Bact. 176, 2293–2299.

Harvey, E.N. (1952) *Bioluminescence*. Academic Press, New York.

Hastings, J.W. (1978) Bacterial and dinoflagellate luminescent systems. In: P.J. Herring (Ed.), *Bioluminescence in Action*, pp. 129–170. Academic Press, London.

Hastings, J.W. (1983) Biological diversity, chemical mechanisms, and the evolutionary origins of bioluminescent systems. J. Mol. Evol. 19, 309–321.

Hastings, J.W. (1996) Chemistries and colors of bioluminescent reactions: a review. Gene, *173*, 5–11.

Hastings, J.W. and Tu, D. (eds) (1995) Symposium-in-print: Molecular mechanisms in bioluminescence. Photochem. Photobiol. 62, 597–673.

Heath, M.C. (2000) Advances in imaging the cell biology of plant-microbe interactions. Annu. Rev. Phytopath. 443–459.

Heim, R., Cubitt, A.B. and Tsien, R.Y. (1995) Improved green fluorescence. Nature 373, 663–664.

Herrera, A.A., Hastings, J.W. and Morin, J.G. (1974) Bioluminescence in cell-free extracts of scale-worm Hamrmothoe (Annelida: Polynoidae). Biol. Bull. 147, 480–481.

Herring, P.J. (1982) Aspects of the bioluminescence of fishes. Oceanogr. Mar. Biol. Ann. Rev. 20, 415–470.

Herring, P. (2002) *The biology of the deep ocean*. Oxford University Press, Oxford, UK.

Hosseini, P. and Nealson, K.H. (1995) Symbiotic luminous soil bacteria: Unusual regulations for an unusual niche. Photochem. Photobiol. 62, 633–640.

Inouye, S., Watanabe, K, Nakamura, H. and Shimomura, O. (2000) Secretional luciferase of the luminour shrimp *Opiophorus gracilirostris*: cDNA cloning of a novel imida-zopyrazinone luciferase. FEBS Lett. 481, 19–25.

Isobe, M., Uyakul, D. and Goto. T. (1987) *Lampteromyces* bioluminescence—1. Identification of riboflavin as the light emitter in the mushroom *L. japonicus*. J. Biolum. Chemilum. 1, 181–188.

Jezowska-Trzebiatowska, B., Kochel, B., Slawinski, J. and Strek, W. (Eds.) (1990) *Biological luminescence*. World Scientific, Singapore.

Katsev, A.M., Wegrzyn, G. and Sziplewska, H. (2004) Effects of hydrogen peroxide on light emission by various strains of marine luminescent bacteria. J. Basic Microbiol. 44, 178–184.

Knight, M.R., Campbell, A.K., Smith, S.M. and Trewavas, A.J. (1991) Transgenic plant aequorin reports the effects of touch and cold-schock and elicitors on cytoplasmic calcium. Nature 352, 524–526.

Knight, M.R., Read, N.D., Campbell, A.K. and Trewavas, A.J. (1993) Imaging dynamics in living plants using semisynthetic recombinandt aequorins. J. Cell Biol. 121, 83-90.

Kozakiewicz, J., Gajewska, M., Lyzen, R., Czyz A. and Wegrzyn, G. (2005) Bioluminescence-mediated stimulation of photoreactivation in bacteria. FEMS Microbiol. Lett. 250, 105–110

Lavorel, J. (1975) Luminescence. In: Govindjee (Ed.), *Bioenergetics of photosynthesis*, pp. 223–317. Academic Press, New York.

Lee, J., Matheson, I.B.C., Müller, F., O'Cane, D.J., Vervoort, J. and Visser, A.J.W.G. (1991) The mechanism of bacterial bioluminescence. In: F.Muller (Ed.), *Chemistry and biochemistry of rlavins and flavoenzymes*, pp. 109–151. CRC Press, Orlando, FL.

Li, Y., Swift, E. and Buskey, E.J. (1996) Photoinhibition of mechanically stimulable bioluminescence in the heterotrophic dinoflagellate *Protoperidinium depressum* (Pyrrophyta). J. Phycol. 32, 974–982.

Lloyd, J.E. (1980) Male *Photuris* mimic sexual signals of their females' prey. Science 210, 669–671.

Lloyd, J.E. (1984a) On deception, a way of all flesh, and firefly signaling and systematics. Oxford Surveys Evol. Biol. 1, 49–84.

Lloyd, J.E. (1984b) Evolution of a firefly flash code. Florida Entomologist 67, 368–376.

Lloyd, J.E. and Wing, S.R. (1993) Nocturnal aerial predation of fireflies by light-seeking firefles. Science 222, 634–635.

Lyzen, R. and Wegrzyn, G. (2005) Sensitivity of dark mutants of various strains of luminescent bacteria to reactive oxygen species. Arch. Microbiol. 183, 203–208.

McFall-Ngai, M. and Morin, J.G. (1991) Camouflage by disruptive illumination in leiognathids, a family of shallow-water, bioluminescent fishes. J. Exp. Biol. 158, 119–137.

McElroy, W.D. and Seliger, H.H. (1962) Origin and evolution of bioluminescence. In: M. Kasha and B. Pullman (Eds.), *Horizons in biochemistry,* pp. 91–101. Academic Press, New York.

Mensinger, A.F. and Case, J.F. (1992) Dinoflagellate luminescence increases the susceptibility of zooplankton to teleost predation. Mar. Biol. 112, 207–210.

Moiseff, A. and Copeland, J. (2000) A new type of synchronied flashing in a North American firefly. J. Insect Behav. 13, 597–612.

Nakamura, H., Kishi, Y., Shimomura, O., Morse, D. and Hastings, J.W. (1989) Structure of dinoflagellate luciferin and its enzymatic and non-enzymatic air-oxidation products. J. Am. Chem. Soc. 111, 7607–7611.

O'Kane, D.J., Lingle, W.L., Porter, D. and Wambler, J.E. (1990a) Localization of bioluminescent tissues during basidiocarp development in *Panellus stypticus*. Mycologia 82, 595–606

O'Kane, D.J., Lingle, W.L., Porter, D. and Wambler, J.E. (1990b) Spectral analysis of bioluminescence of Panellus stypticus. Mycologia 82, 607–616.

Partridge, J.C. and Douglas, R.H. (1995) Far-red sensitivity of dragon fish. Nature 375, 21–22.

Pérez-Bueno, M.L., Ciscato, M., vandeVen, M., García-Luque, I., Valcke, R. and Barón, M. (2006) Imaging viral infection: studies on Nicotiana benthamiana plants infected with the pepper mild mottle tobamovirus. Photosynthesis Res. 90, 111–123.

Rees, J.-F., De Wergifosse, B., Noiset, O., Dubuisson, M., Janssens, B. and Thompson, E.M. (1998) The origins of marine bioluminescence: Turning oxygen defence mechanisms into deep-sea communication tools. J. Exp. Biol. 201, 1211–1221.

Seliger, H.H. and McElroy, W.D. (1965) *Light: Physical and biological action*. Academic Press, New York.

Shimomura, O. (1979) Structure of the chromophore of *Aequorea* green fluorescent protein. FEBS Lett. 1054, 220–222.

Shimomura, O. (1980) Chlorophyll-derived bile pigment in bioluminescent euphausiids. FEBS Lett. 116, 203–206.

Shimomura, O. (1989) Chemiluminescence of panal (a sesquiterpene) isolated from the luminous fungus *Panellus stipticus*. Photochem. Photobiol. 49, 355–360.

Shimomura, O. (1992) The role of superoxide dismutase in regulating the light emission of luminescent fungi. J. Exp. Bot. 43, 1519–1525.

Strehler, B. and Arnold, W. (1951) Light production in green plants. J. Gen. Physiol. 34, 809–820.

Sundbom, E. and Björn, L.O. (1977) Phytoluminography: Imaging plants by delayed light emission. Physiol. Plant. 40, 39–41.

Swift, S., Throup, J., Bycroft, B., Williams, P. and Stewart, G. (1998) Quorum sensing: bacterial cell-cell signaling from bioluminescence to pathogenicity. In: S.J.W. Busby, C.M. Thomas, and N.L. Brown (Eds.), *Molecular microbiology*, pp. 185–207. Springer, Berlin.

Szpilewska, H., Czyz, A. and Wegrzyn, G. (2003) experimental evidence for the physiological role of bacterial luciferase in the protection of cells against oxidative stress. Curr. Microbiol. 47, 379–382.

Tett, P.B. and Kelly, M.G. (1973) Marine bioluminescence. Oceanogr. Mar. Ann. Rev. 11, 89–173.

Trimmer, B.A., Aprille, J.R., Dudzinski, D.M., Lagace, C.J., Lewis, S.M., Michel. T., Qazi, S. and Zayas, R.M. (2001) Nitric oxide and the control of firefly flashing. Science 292, 2486–2488.

Tyystjärvi, E. and Vass, I. (2004) Light emission as a probe of charge separation and recombination in the photosynthetic apparatus: relation of prompt fluorescence to delayed light emission and thermoluminescence. In: G.C. Papageorgiou and Govindjee (Eds.), *Chlorophyll a fluorescence: A signature of photosynthesis. Advances in photosynthesis and respiration* (Govindjee, series and vol. Ed.), vol. 19, pp. 363–388. Springer, Dordrecht.

Ulitzur, S. and Dunlap, P.V. (1995) Regulatory circuitry controlling luminescence autoinduction in *Vibrio fischeri*. Photochem. Photobiol. 62, 625–632.

Underwood, T.J., Tallamy, D.W., and Pesek, J.D. (1997) Bioluminescence in firefly larvae: A test of the aposematic display hypothesis (Coleoptera:Lampyridae). J. Insect Behavior 10, 365–370.

Vencl, F.V., Blasko, B.J. and Carlson, A.D. (1994) Flash behavior of female *Photuris versicolor* fireflies (Coleoptera: Lampyridae) in simulated courtship and preadatory dialogs. J. Insect Behav. 7, 843–858.

Vencl, F.V. and Carlson, A.D. (1998) Proximate mechanisms of sexual selection in the firefly *Photinus pyralis* (Coleoptera: Lampyridae). J. Insect Behav. 11, 191–207.

Viviani, V.R. and Bechara, E.J.H. (1997) Bioluminescence and biological aspects of Brazilian railroad worms (Coleoptera: Phengodidae). Ann. Entomol. Soc. Am. 90, 389–398.

Viviani, V.R. and Ohmiya, Y. (2000) Bioluminescence and color determinants of *Phrixothrix* railroad worm luciferases: Chimeric luciferases, site-directed mutagenesis of Arg 215 and guanidine effect. Photochem. Photobiol. 72, 267–271.

Walker, E., Bose, J.L. and Stabb, E.V. (2006) Photolyase confers resistance to UV light but does not contribute to the symbiotic benefit of bioluminescence in *Vibrio fischeri* ES114. Appl. Environm. Microbiol. 72, 6600–6606.

Widder, E.A., Latz, M.I., Herring, P.J. and Case, J.F. (1984) Far red bioluminescence from two deep-sea fishes. Science 225, 512–513.

Wilson, T. and Hastings, J.W. (1998) Bioluminescence. Annu. Rev. Cell Dev. Biol. 14, 197–230.

Wood, N.T., Allan, A.C., Haley, A., Viri-Moussaid, M. and Trewavas, A.J. (2000) The characteristics of differential calcium signalling in tobacco guard cells. Plant J. 24, 335–344.

Wood, N.T. Haley, A., Viri-Moussaid, M., Johnson, C.H., van der Luit, A.H. and Trewavas, A.J. (2001) The calcium rhythms of different cell types oscillate with different circadian phases. Plant Physiol. 125, 787–796

24
Hints for Teaching Experiments and Demonstrations

Lars Olof Björn

Abstract: Directions are given for demonstrating various topics from the other book chapters: the wave-nature of light, singlet oxygen, chromatic adaptation of cyanobacteria, the properties of the human visual system, photoconversion of rhodopsin, photosynthesis of previtamin D, spectral properties of chlorophyll, photoconversion of protochlorophyllide, separation of chloroplast pigments, photoadaptation of plant leaves, ultraviolet radiation damage, photoreactivation, phytochrome, plant photomorphogenesis, and bioluminescence. At the end a short list of further ideas is provided for the reader to work on. The references are listed separately for each topic.

24.1. Introduction

The following is not meant to represent a complete set of practicals for a photobiology course. I shall try to do just what the title says—give some hints. As a general reference book for photobiological teaching experiments, Valenzeno et al. (1991) merits special mention. Those planning a general photobiology course should consult that book also in addition to the present one. One disadvantage of several of the experiments in the book by Valenzeno et al. (1991) is that one needs advanced equipment which may not be available everywhere, and I have tried to concentrate below on less demanding experiments (although some do need special equipment).

Experiments and demonstrations must, of course, always be adapted to the audience. In the following you will find some which, with suitable adaptations, can be used from elementary school to graduate student levels. From some of them you may even learn something yourself.

I am grateful to former students, Drs. Björn Sigfridsson, Gunvor Björn, and Susanne Widell, for testing some of the descriptions below.

24.2. A Good Start

I shall start with my own pet demonstration, which I have used as an intro-
duction to many courses, which makes students start thinking, and which can be a
starting point for discussions on the interaction of light with matter, vision, photo-
synthesis, and phytochrome. It requires a lecture hall which can be efficiently
darkened, an overhead projector, a beaker, and an acetone extract of plant leaves.
You should also make a cover of cardboard or masonite for the projector, so
the light can emerge only from a hole slightly smaller than the bottom of the
beaker.

Before the demonstration you should prepare the leaf extract. It is essential
that it be very concentrated. The easiest way, if you have the time, is to put
leaves into a bottle together with the acetone and let it stand in the cold and dark.
A faster way is to grind the leaves with some sand and acetone in a mortar and
filter the slurry. You will require about 1 L of extract for a 2-L beaker. Make
sure that the extract is clear.

Ask your audience what color plant leaves have, and whether they know what
makes them have that color. They are likely to answer that plant leaves are green
and in most audiences at least somebody is likely to answer that it is chlorophyll
that makes them green. Explain that in your bottle (which should preferably be
brown or opaque so as not to show the color of the extract) you have an extract
with the pigments of plant leaves, and that you are now going to demonstrate
the color.

Switch on the overhead projector, put the cardboard mask on, and place the
beaker so that it covers the hole in the mask. Turn off the room light completely.
Pour a small amount of your extract into the beaker. As expected, a green color
will be projected onto the screen.

Pour more and more of the extract into the beaker and let the (usually very
surprised) audience see how the color on the screen goes through a dirty brown
to a clear red. Then point to the beaker to make them see the brilliant red
chlorophyll fluorescence and ask them again what the color of chlorophyll is,
and to think about what color really is: a property of an object, or a sensation in
our brains.

A few explanations follow:

1. The red color to be seen on the screen is something quite different from the
   red light radiating in all directions from the solution. The light on the screen,
   which appears red to us, is really far-red, i.e., light of very long wavelength
   which chlorophyll cannot absorb. This is the kind of light dominating at the
   bottom of a dense forest or inside a wheat canopy. It is the kind of light
   driving phytochrome (a light-sensitive pigment in plants; see Chapters 10 and
   16) from the Pfr form to the Pr form.
2. The red light radiating from the solution is energy that has been absorbed by
   and excited chlorophyll molecules and been reradiated as fluorescence when
   the chlorophyll molecules reverted to the ground state. Chlorophyll in solution

fluoresces much more intensely than chlorophyll in the plant, because the plant uses more of the absorbed energy for photosynthesis.

3. For us the color on the screen and the light radiated by the solution look the same, although the wavelength composition is different, because we do not have any light-sensitive pigment in our eyes absorbing at longer wavelength than the one that has an absorption maximum at 552 or 557 nm (depending on the person; see Chapter 9).

You can do a similar demonstration—except that there will be no fluorescence—using colored Perspex or Plexiglass instead of the chlorophyll solution. You start with one layer of green acrylate, showing a green color on the screen, and add additional layers of green acrylate until only far-red light goes through. The version with chlorophyll solution is no doubt best, but if you are traveling around or have to arrange a demonstration in a hurry, it may be good to have the colored plastic version available. You can also use blue acrylate; in fact any color will end up far-red if you add a sufficient amount of acrylate.

24.3. The Wave Nature of Light

The laser pointers now available on the marked make demonstrations of diffraction and interference much easier than they used to be. Pointers with laser diodes can be obtained very cheaply now. Even laser pointers of the same type emit light with slightly different wavelengths, but with the same indistinguishibly red color. If you have a couple of such pointers with different spectral tuning, you can therefore easily arrange one more demonstration of the fact that wavelength and color are not the same. It is possible to find some colored plastic, for instance, blue plexiglass, which transmits light from one pointer but not from the other, although both give light of the same red color.

More importantly, you can easily demonstrate both single slit diffraction and Young's famous double-slit experiment with using laser pointers. You may be able to cut out sufficiently thin slits in (not too thick) cardboard. Alternatively, you can use black adhesive tape that you stick either on a glass slide or over a hole in a piece of cardboard. Better precision can be obtained by drawing one black line (or for the double-slit experiment two parallel black lines with a small spacing in between) on white paper, photographing the paper with ordinary negative black-and-white film, and using the negative. A number of other items for optical experiments can be purchased from Edmund Scientific.

If you want to demonstrate how a grating works and have not got one from an instrument, you can use a recordable CD or a DVD. The latter has many more lines per mm, and thus deflects light more. The curvature of the grooves will not matter with the small spot from a laser pointer. If you have sufficient money for teaching your course, you may want to buy the (much more expensive) laser pointers with green light and UV-A radiation now available to show how the behavior of the beam depends on wavelength.

24.4. Singlet Oxygen

Singlet oxygen for demonstration purposes can be easily generated by mixing hydrogen peroxide (30%) with solid sodium hypochlorite. If you do this in a darkroom you will see a rapidly fading red glow. This is the so-called dimol emission of singlet oxygen, which has half the wavelength of emission from isolated singlet oxygen molecules. Dimol emission takes place when the concentration of singlet oxygen is sufficiently high, and the probability is high that two singlet oxygen molecules collide and the excitation energy of both are added to form one photon.

Concentrated hydrogen peroxide is extremely caustic, and mixing it with sodium hypochlorite will cause heating and gas production, so you have to take great care to avoid splashing, and especially to protect your eyes. Try it out in a lighted room before you do it in the dark. One good way is to use a Pasteur pipette with a rubber baloon for the hydrogen peroxide, fill it in the light, and put it in a test tube that you hold in one hand together with a test tube with the hypochlorite. To see the dimol emission well, you should first dark-adapt your eyes for 5 minutes.

24.5. Complementary Chromatic Adaptation of Cyanobacteria

Some cyanobacteria form no phycoerythrin when grown under red light, and then appear blue-green in color from chlorophyll, phycocyanin, and allophycocyanin. When grown under green light they change to almost black, because of the presence of phycoerythrin.

The most difficult part of this is to obtain a suitable culture of cyanobacteria. We recommend either *Tolypothrix tenuis* or *Fremyella diplosiphon*. The American Type Culture Collection (http://www.atcc.org) has *Tolypthrix tenuis* Kutzing 20335 and many other strains, but at high cost. From Carolina Science and Math (http://www.carolina.com/#) you can buy a set of fifteen cultures including a *Tolypothrix* sp. (not tested) for US$ 86.25 (Oct. 2007). Sammlung Algenkulturen at the University of Göttingen sells *Tolypothrix tenuis* (accession number 94.79) and *Fremyella diplosiphon* (accession number 1429-1b) to noncommercial customers for 12.50 Euro per culture (early 2007) plus postage. The most complete collection of chromatically adapting cyanobacteria is available at the Institut Pasteur in Paris, http://www.pasteur.fr/recherche/banques/PCC/help/htm. The following culture medium is suitable for *Tolypothrix tenuis* (concentrations in g/L): KNO_3 (3.0), $MgSO_4 7H_2O$ (0.5), Na_2HPO_4 (0.2, or $Na_2HPO_4 12H_2O$ 0.5), $CaCl_2$ (0.02, or $CaCl_2 2H_2O$ 0.027), $FeSO_4.7H_2O$ (0.02), and trace elements (B, Mn, Zn, Mo, Cu, Co). Trace element amounts and recipes for other suitable media are listed on the Internet at the above culture collection sites.

Light to adapt to is generated by green and red fluorescent lamps (e.g., Philips TLD 17 and TLD 15, respectively). The red lamps can be wrapped in red (or yellow) cellulose acetate foil to filter off small amounts of blue light given off (particularly at the ends), the green lamps with green (or yellow) foil. If colored fluorescent lamps are hard to obtain, white ones can be used if several layers of appropriate-colored cellulose acetate are wrapped around them. The cultures grow more rapidly if they are bubbled with 5% carbon dioxide in air, but ordinary air will also do. With added carbon dioxide 1 week should be allowed for sufficient growth—without added carbon dioxide 2 weeks.

For evaluation of the result you may be content just looking at the cyanobacteria with the naked eye and in the microscope. You can also do in vivo absorption spectra using a "Shibata plate." i.e, a scattering plate, just behind the cuvettes in the spectrophotometer, or use the apparatus described in Chapter 25. For quantitative estimation of the phycobiliprotein pigments, proceed as follows.

Separate the organisms from the culture medium by low-speed centrifugation and resuspend them in a small amount of 0.01 M phosphate buffer (pH 7.0) and sonicate them. Avoid overheating by precooling the suspension, keeping it in ice during treatment, and sonicating in several short pulses. If you have a French press or equivalent, you can disintegrate the cells more completely by using it. Only grinding in a mortar does not give a very good result. Centrifuge the slurry at 10,000xg for 5 minutes and then the supernatant for 1 hour at 80,000xg to obtain a clear phycobiliprotein extract.

Measure the absorbance of the extract (if necessary after dilution) at 565, 620, and 650 nm. The specific absorption coefficients of the phycobiliproteins, in g/L/cm, are as follows:

	Phycoerythrin	Phycocyanin	Allophycocyanin
565 nm	12.6	3.12	1.81
620 nm	0.22	6.77	4.39
650 nm	0.15	1.75	6.54

The absorbance you measure at each wavelength will be the sum of the products of concentration (c) and absorption coefficient (ε) for each of the three pigments times the pathlength (L), i.e., $A_\lambda = (c_E \cdot \varepsilon_E + c_C \cdot \varepsilon_C + c_A \cdot \varepsilon_A)L$, where subscripts E, C, and A stand for phycoerythrin, phycocyanin, and allophycocyanin, respectively. You will thus have an equation system with three equations and three unknowns, which can be solved for the pigment concentrations.

Instead of continuous light treatments, you can try inductive pulses according to descriptions in the literature. The colored polypeptides can be separated into very beautiful bands by isoelectric focusing.

24.6. What Is Color? The Benham Disk

The Benham disk (or Benham's disk or Benham top) was originally a toy, not even evented by Benham, but described by him in a paper in *Nature* (Anon. 1894). Since then many learned papers have been written about it. A review with 67 references was published by von Campenhausen and Schramme (1995), and publications continue on the subject until the present day (e.g., Le Rohellec and Vienot 2001). There is no real consensus about how it works, but in any case it affords a clear demonstration that color and spectral composition of light are not the same. It is a disk with a black-and white pattern. Surprisingly, you can change the apparent color in different sectors of it just by changing the direction of rotation.

A template for the disk is shown in Fig. 24.1. Copy it (double size) and glue the copy to cardboard, cut it out and attach it to an electric or hand-driven drill so you can rotate it around its center. An electric drill with variable speed and the ability to reverse the direction is ideal. The disk in Fig. 24.1 is an example; other versions can be found on the Internet, but one half of the disk should always be black. In my experience, the most vivid colors are obtained if the black sectors in the other half are narrow, like the one shown. It can be instructive to make a disk with stripes of various widths. It is very important that one is able to adjust the speed. If the rotation is too slow or too fast, you will see no color.

One of the first explanations for appearance of the color phenomena was that receptors in the eye for different spectra regions have different time constants. This explanation, however, is no longer regarded to be correct. The contrast between different parts of the image projected on the retina is regarded as an essential ingredient.
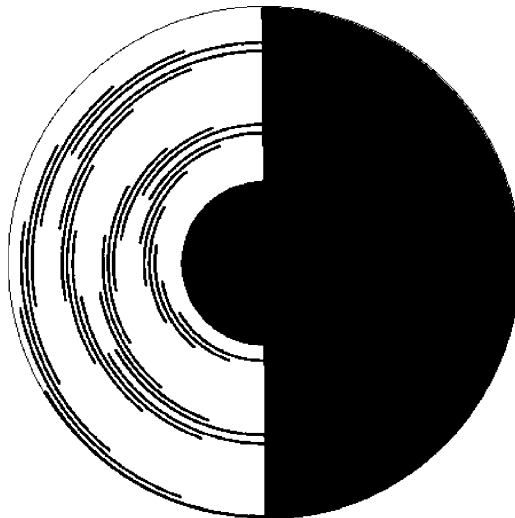
FIGURE 24.1. Template for a Benham disk.

24.7. Photoconversion of Rhodopsin

Background. Visual pigments in vertebrate eyes are concentrated in cells called rods and cones. The rods are active in "dusk vision," while cones are used for color vision in stronger light. The light-sensitive pigment in rods is rhodopsin, a protein with 11-*cis*-retinal as a chromophore (see Chapters 9 and 10). Absorption of light triggers a multistep isomerization process, resulting in the separation of protein and chromophore, and to bleaching of the initially red color. The first part of the rhodopsin conversion, from rhodopsin to metarhodopsin I, is photoreversible.

   Chemicals required for the experiment are as follows:

Sodium phosphate buffer (0.15 M, pH 6.5)
Sucrose solution (40% w/v dissolved in the phosphate buffer)
Potassium-aluminum sulfate ($KAl(SO_4)_2$ 4% w/v in water)
Hydroxylamine hydrochloride (NH_2OH HCl, 0.05 M in
phosphate buffer)
Digitonin (2% w/v dissolved in phosphate buffer in a heated water bath)

Biological Sample. Obtain several (at least eight) cattle eyes from a slaughter-house and leave them in the dark for an hour at room temperature. Dissect out the retinas under red light. The retinas can be frozen and preserved for use later.

Extraction of Rhodopsin. The preparation is carried out in a cold-room under red light. Avoid too much of the working light on the retinae. Put eight retinas in a cold mortar and grind very thoroughly for 20 min. Then add 5–10 ml of the sucrose solution (about three times the volume of the ground retinae). Mix well and transfer the suspension to a transparent centrifuge tube. Carefully layer phosphate buffer (about the same volume) on top, using, for instance, a syringe with a short tubing. Try to keep a sharp interface between the two liquids. Centrifuge at high speed for 30 min. The rod outer segments have about the same density as the sucrose solution and will be enriched at the interface between the liquids.

   Carefully suck the rod outer segments into a syringe. Transfer them to a new centrifuge tube and fill it halfway with buffer. Centrifuge at high speed for 10 minutes. Discard the supernatant and repeat the washing procedure. Then add three ml $KAl(SO4)_2$, which will fix the rhodopsin. Let stand for 10 minutes. Precipitate the segments again by 10-minute high-speed centrifugation and wash twice more, but now with water. Add 4 ml of the digitonin solution to the rod segments. Stir thoroughly, and let stand in the cold overnight. This procedure will solubilize the rhododpsin. Centrifuge just before the experiment, which is carried out on the clear supernatant.

Experiment 1. Low Fluence Rate Treatment. Under red working light, pipette 600 μL of rhodopsin solution and 150 μL of NH_2OH HCl into a 10-mm spectrophotometer cuvette. Prepare a reference cuvette with 600 μL of buffer

plus 150 μL of NH_2OH HCl. Determine the absorbance difference between the cuvettes throughout the range 500–600 nm.

Remove the sample cuvette from the spectrophotometer and put it about half a meter from a small incandescent lamp, such as a microscope lamp. Illuminate for 30 seconds and let stand for 2–3 minutes. In this time the retinal released from the opsin protein will react with the hydroxylamine, which results in a product with absorption maximum at much shorter wavelength than rhodopsin. Disappearance of intermediates will also be speeded up by the hydroxylamine. Again determine the difference absorption spectrum between sample and reference cuvettes. Repeat the procedure until 80–90% of the rhodopsin has been bleached. Then switch on normal room light and bleach the remaining rhodopsin.

Repeat the irradiation experiment with one quarter of the fluence rate. If you cannot measure the light and have not calibrated the filter, and provided you have a small light source (not a fluorescent tube) and a not too white or shiny lab bench, you can approximate this by doubling the distance between lamp and cuvette.

Compute the ratio $(A_i–A_t)/(A_i–A_e)$ as a measure of converted rhodopsin for each time point: A_i = initial absorbance difference, A_e = final absorbance difference, A_t absorbance difference for irradiation time t. Compare the result for the two fluence rates and figure out whether the process follows the Bunsen-Roscoe law ("reciprocity law"). What is the reaction order?

Experiment 2. High Fluence Rate Illumination. Repeat the same, but using a photoflash instead as light source. Does this alter the validity of the reciprocity law, and if so, why?

24.8. Photosynthesis of Previtamin D

An experiment to determine the quantum yield of provitamin D_3–to–previtamin D_3 conversion is described by Pottier and Russell (1991). Part of their description concerns the use of the ferrioxalate actinometer, which is already covered elswhere (Chapter 4) in the present book, as is the theoretical introduction. One difficulty in carrying out the experiment as described by Pottier and Russell (1991) is that the pure previtamin D_3 used for calibration in their experiment is not commercially available. The present description is modified with this in mind.

I shall also take the opportunity to show an unusual way of determining the quantum yield, which sometimes has advantages.

For determination of quantum yield of a photochemical reaction, one usually determines the number of molecules converted and the number of photons absorbed and takes the ratio between the two quantities. Björn (1969b), when faced by the problem of determining the quantum yield of inactivation of an enzyme, could not directly measure the amount of light absorbed by the enzyme, because the enzyme solution was dilute, and the amount of light absorbed by it very small. He showed, instead, that the quantum yield equals $^{10}\log(a_o/a_t)/(\varepsilon \cdot t \cdot I)$,

where a_o is the concentrations at the start and a_t that after irradiation time t, I the photon fluence rate, and ε the molar absorption coefficient.

In our present case, the photoconversion of provitamin D, we have to keep in mind that the primary product, previtamin D, can undergo a number of photochemical reactions which could disturb our measurement. We avoid them in two ways: by limiting the amount of radiation to keep the amount of product (previtamin D) much lower than the amount of substrate (provitamin D), and by choosing a wavelength at which the substrate absorbs much more strongly than the product, i.e., 294 nm. For an ethanol solution containing 5 μg provitamin D per ml (which is a suitable concentration for experimentation), the absorbance at 294 nm in a 1-cm layer is 0.088. The absorbance of a corresponding solution of previtamin D is only 0.034.

We choose the initial provitamin concentration with the following in mind: it should be high enough to allow accurate spectrophotometry, yet low enough to keep the fluence rate within the sample reasonably uniform. If the absorbance in a 1-cm cuvette is 0.088, then the irradiance at the exit side of the cuvette is $10^{-0.088} = 81.7\%$ of that on the illuminated side, i.e., transmission T = 0.817 for a thickness x = 1 cm. The average irradiance is $\int T^x dx = (T-1)^{10}\log e/^{10}\log T = -0.183/\ln 0.817 = 0.905$. Use of such an average irradiance in the calculations requires that the solution is stirred. For an unstirred solution it is better to mentally divide the solution into, say, 10 (or 100) layers, calculate for each layer separately how the chemical change (and the change in irradiance) takes place, and finally add up the chemical change for the layers. I leave this as an exercise for the reader.

The molecular weight for provitamin D_3 is 384.65 (for provitamin D_2 it is 400.70; this can be looked up in the Handbook of Chemistry and Physics, where the compounds are called $\Delta^{5,7}$-cholestadien-3β-ol and ergosterol, respectively). Thus the molar absorption coefficient ε (for the D_3 form) is $384.65 \cdot 10^6 \cdot 100/5/1000$ m^{-1} M^{-1} = $7.7 \cdot 10^4$ m^{-1} M^{-1} (the factor 10^6 is for converting μg to g, 100 for converting cm to m, and 1000 for converting ml to L). Thus the quantum yield in our special case is $^{10}\log(a_o/a_t)/(\varepsilon \cdot t \cdot I \cdot 0.905)$ = $^{10}\log(a_o/a_t)/(7.7 \cdot 10^4 \cdot t \cdot I \cdot 0.905)$, with t and I in SI units.

24.9. Photoconversion of Protochlorophyllide

Background. The synthesis of chlorophyll *a* proceeds via 5-aminolevulinic acid (ALA), protochlorophyllide, and chlorophyllide *a*. When angiosperms are grown in darkness, the synthesis is arrested at the protochlorophyllide stage. However, there is no major buildup of protochlorophyllide, because the synthesis of ALA is exposed to feedback inhibition by protochlorophyllide and is resumed only when protochlorophyllide is used up. This is the reason that plants do not become visibly green in darkness, even if protochlorophyllide in itself has a green color. When the plant is illuminated, protochlorophyllide is transformed to chlorophyllide by photoreduction, and it is the protochlorophyllide itself, bound

to NADPH:protochlorophyllide oxidoreductase (POR, EC 1.6.99.1) that absorbs the active light (Björn 1969a). The reductant is NADPH, which in darkness is bound to the enzyme together with protochlorophyllide.

The transformation of protochlorophyllide to chlorophyllide *a* can be monitored spectrophotometrically directly in living leaves, since the weak light beam in the spectrophotometer does not noticeably affect the process. A single flash from an electronic photoflash, on the other hand, transforms a large part of the protochlorophyllide present.

Spectrophotometer. You will need a good split-beam spectrophotometer (or a single-beam spectrophotometer with computer that can store a reference signal). For this you should make a special leaf holder. If you use bean leaves (see below) the leaf holder should consist of two glass plates and some kind of clamp holding the plates together, so you can position the leaves between the plates, covering the measuring beam. The details depend on the spectrophotometer. One of the glass plates should be scattering (ground surface, or milky glass), or you must add a special Shibata plate to scatter light after passage of the sample and reference.

If you use grass leaves, you can use the standard cuvette holder (except that you need to add a Shibata plate). Instead of a cuvette you use a square rod of Plexiglas or Perspex (1 cm × 1 cm × 4 cm) in which you have drilled nine holes (1.5 mm diameter) along the 4-cm direction. Five of the holes are in a row, with 1 mm in between. The remaining four holes are in another row, such that the holes are in between the holes in the first row. Figure 24.2 gives an idea of what the grass leaf holder looks like from above. You may need to adjust the dimension to the kind of grass you use; maize needs larger holes.

Experimental Procedure. You can use either bean or wheat plants (or some other grass). All steps in which you handle your plants or leaves after sowing should be carried out in dim green working light. Your eyes, fortunately, are most sensitive to this light, whereas the process you want to study has a sensitivity minimum in the green spectral region.

If you use bean plants, soak the beans in dilute hydrogen peroxide (initial concentration 1–2%) overnight and then remove the seed coats. The hydrogen peroxide serves both to kill some mold spores and to facilitate peeling by producing gas under the seed coats. Sow the beans directly in Vermiculite or sand that has been heated to kill microorganisms, or pregerminate on filter paper and then sow under green light. Let the plants grow (about 5–7 days) until the first true leaves (between the cotyledons) have become a little longer than the
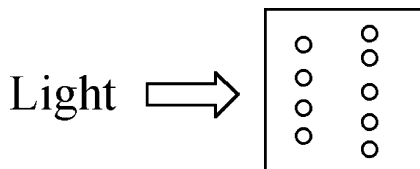
FIGURE 24.2. Sketch of holder for grass leaves in spectrophotometer.

cotyledons. If you wait until the plants have become much older, only part of the protochlorophyll(ide) will be immediately phototransformable.

If you use grass leaves, after sowing a few dozen caryopses allow the plants to grow in darkness until you (by inspection under green light) see that the leaves have just emerged from the coleoptiles. They will still remain tightly rolled together unless you have used too much of your inspection light (unrolling is a phytochrome-controlled reaction). Collect nine leaves, cut out 5 cm of the middle portion, and put them in the holes in your leaf holder. No matter what kind of leaf you use, it is important that the leaves completely cover the whole measuring beam in the spectrophotometer.

Record a spectrum for the unirradiated leaves from 500 to 720 nm. Do not worry about absolute absorbance; it is the shape of the spectrum that is of interest. To balance the split-beam spectrophotometer with the leaves on the sample side, you may need to put something "neutral" in the reference beam. One or a few pieces of filter paper serve well.

When you have recorded the "dark" spectrum, irradiate in a suitable way, for instance, with a photoflash. Record a new spectrum. If you want to produce a good-looking series of spectra, as in Fig. 24.3, it is important that you work fast, since the Shibata shift from the initial chlorophyllide *a*–enzyme complex starts at once (rate depending on age of leaves and other factors).

This experiment can be modified in a number of ways. The protochlorophyllide–enzyme complex ("protochlorophyllide holochrome") can be extracted and the conversion studied in solution, and fluorescence spectroscopy can be used in place of absorption spectroscopy (Björn 1969a).

In case you do not have access to an advanced research spectrophotometer, it should be possible to adapt this experiment for the home-built apparatus described in Chapter 25.

24.10. Separation of Chloroplast Pigments

There are many ways of carrying out this experiment, but I have my definite favorite. It is to use a cylindrical chromatography paper, as described below.

Pigment Extraction. Choose a plant species that does not have extremely acid cell sap, which will result in conversion of chlorophyll to pheophytin. We have used, among others, spinach, bean, and stinging nettle. Extract a leaf using a small amount of 100% acetone. We have usually done this in a mortar with sand, and then one has to filter or centrifuge to get a clear extract. I have read that other people, with good result, have just left the leaf with acetone in a bottle in the dark for a day or two, so if you do not want to do the whole experiment in one day this saves some work and dishwashing.

The acetone extract may be applied as it is to the chromatogram, but then you cannot put on very much of it without getting into trouble. It is better to mix it with a little (one-tenth the volume of the extract or so) light petroleum (or hexane) and add water (about the same volume as the original extract) to
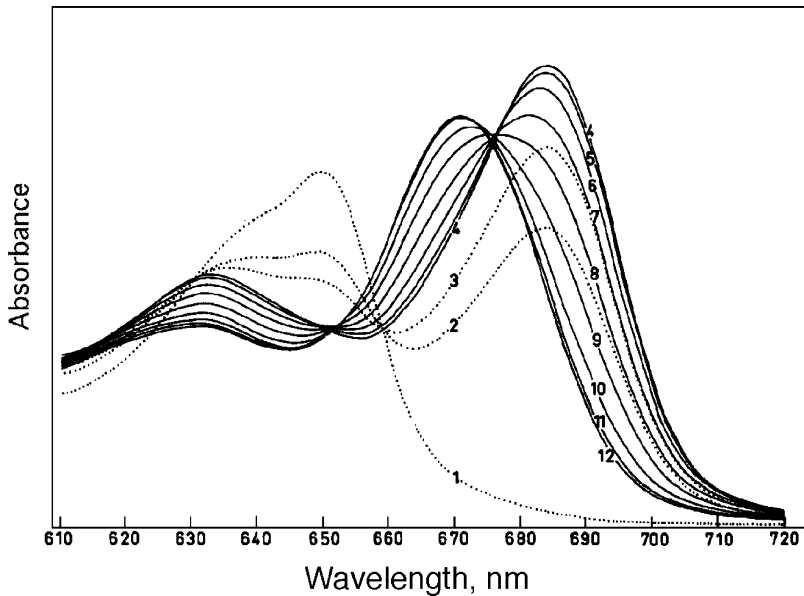
FIGURE 24.3. Absorption spectra for dark-grown bean leaves, before illumination (curve 1), after 1, 2, and 10 exposures to a photographic flash (curves 2–4), and after incubation for various times in darkness after the light exposures (curves 5–12). The first curve represents mainly the absorption of the protochlorophyllide–NADPH–enzyme complex, which is changed to a chlorophyllide a–NADP$^+$–enzyme complex by illumination. During the following dark incubation the chlorophyllide is released from the enzyme, attaches to another protein, and is esterified to chlorophyll a. More sophisticated experiments reveal several spectral shifts.

separate into two layers. Discard the lower (aqueous) layer (the most convenient way is to suck up the upper layer using a Pasteur pipette and transfer the liquid to a clean test tube), add water again, shake, and let separate. If you have difficulty getting a clean phase boundary, add some sodium chloride. Pipette the organic, dark green phase to a clean test tube.

Chromatography. Get a glass jar with a tightly fitting lid (it is very important that it fits tighly). You may find one in your home that has contained mayonnaise or some other food product. A suitable size is 150 mm high and 70 mm wide. Cut out a rectangular paper of a size that can produce a cylinder that fits inside the jar without touching the walls or the lid, but do not fold it into a cylinder yet. Avoid touching the paper with your fingers.

Pour into the jar a mixture of 90% (v/v) petroleum ether and 10% (v/v) acetone. You should have a layer about 10 mm deep at the bottom of the jar. Put on the lid.

Use a Pasteur pipette to apply your pigment extract along a line parallel to and 15–20 mm from a side of the paper that will form the base of your cylinder.

The paper edge should rest on a test tube or glass rod or stick out over the edge of the lab bench, so it is free in the air (or put the paper in a book, with the edge sticking out). With some practice you will be able to produce a nice green line. You should let the tip of the pipette move quickly across the paper to avoid big blobs. Try not to scratch the paper with the tip of the pipette. If the extract is in light petroleum or hexane it will dry quickly, and you can in a short time repeat the application until you have quite a lot of pigment on the line. But do not apply so much that you clog the pores in the paper.

Now shape the paper into a cylinder with the green line at the bottom. Staple it together along the edges perpendicular to the bottom edge in such a way that the edges do not touch (if they do, the liquid will rise in the paper in an irregular way). Open the jar briefly and put down your paper cylinder, green line down. Put on the lid immediately to avoid liquid evaporating from the paper. Do not move the jar until you finish the experiment. Wait and enjoy the result!

This chromatography is mainly a liquid/liquid distribution of substances according to lipophily/hydrophily between the moving hydrocarbon and stationary water molecules hydrogen-bonded to the OH groups in the cellulose.

Within a few minutes you can see the pigments separating into several bands: A yellow band almost at the rising liquid front indicates carotenes. They do not stick to the water adsorbed on the paper because they contain only carbon and hydrogen. Next comes another yellow band, the oxygen-containing xanthophylls. Lower down follow chlorophylls *a* and *b*, in that order because chlorophyll *a* has a lipophilic methyl group whereas chlorophyll *b* has an aldehyde group.

Spectrophotometry. When the liquid front has almost reached the top of the paper after half an hour or so, take it out and let it dry. This experiment is easily done as a demonstration during a lecture, in which case you can conclude it by cutting strips of the paper and sending them around in the audience for inspection. If it is done as a student experiment, it can be concluded by determining the absorption spectra of the various pigments. If you have a hand-held reflection spectrophotometer such as the Colortron (see next section), or the device described in Chapter 25 this can be done in a couple of minutes directly on the paper. Otherwise the, chromatogram can be eluated with acetone. Cut out the strips with the various pigments. If you dip an end into acetone, the acetone will rise and carry all of the pigment with the front, so you can easily concentrate the pigment and dissolve it in a small amount of acetone. You will easily get a concentration high enough and of sufficient volume for a standard spectrophotometer cuvette from a single chromatogram.

24.11. Light Acclimation of Leaves: The Xanthophyll Cycle

We have used a simple hand-held reflectance spectrophotometer (Colortron and a later model, Colortron II) for a number of biological experiments. It has already been mentioned in connection to photoreactivation (Section 24.6.) and spectrophotometry of paper chromatograms (Section 24.10.). These excellent and cheap

(about US\$ 1000) instruments (originally marketed by Light Source, Inc.) are, unfortunately, no longer available. Other companies sell other instruments of a similar type that should also work. Such instruments can certainly also be used to evaluate complementary chromatic adaptation (Section 24.5.), changes in skin color, changes in leaf color during senescence or nutrient deficiency, and a large number of other experiments. A very simple but interesting experiment, relating to the light acclimation of leaves and the xanthophyll cycle, can also be carried out.

24.11.1. Introduction to the Xanthophyll Cycle

We start with an introduction to the xanthophyll cycle (see also Chapter 13, Sections 13.4.1 and 13.6).

Daylight is highly variable, and the plant must be able to adjust to strong as well as weak light. When the rate of light absorption by the photosynthetic system exceeds the rate with which carbon dioxide can be assimilated, or other assimilatory reactions can be carried out, there is risk for damage to the plant. One thing that may happen when carbon dioxide cannot be reduced by the electrons transported through the electron transport chain is that *electrons* may end up on molecular oxygen and reduce it to superoxide anion. The plant has superoxide dismutase to take care of this. However, the electron transport chain itself may be overloaded, so that the excitations in the pigment system cannot be used up for electron transport at all. What may then happen is that the *energy* is transferred to oxygen molecules, resulting in a form of excited oxygen called singlet oxygen (actually there is more than one kind of singlet oxygen). Singlet oxygen is very reactive and may cause damage. The plant needs a way of disposing of excitation energy, but this should operate only when there is an excess. In weak light the plant needs all the energy it can collect.

One way for the plant to regulate the dissipation of excess energy absorbed by the photosynthetic system is by adjusting the amount of violaxanthin and zeaxanthin through the reactions of the xanthophyll cycle. In this cycle violax-anthin is converted to zeaxanthin via the intermediate antheraxanthin, a reaction (so-called deepoxidation) catalyzed by the enzyme violaxanthin de-oxidase. The reverse reaction (epoxidation of zeaxanthin to violaxanthin) can also take place (Fig. 24.4). De-epoxidation takes place in strong light, epoxidation in weak light or darkness.

Both zeaxanthin and violaxanthin have long conjugated double-bond systems. The important difference between them is that the zeaxanthin molecule has a longer conjugated system (11 double bonds vs. 9 for violaxanthin). This causes the lowest excited state in the zeaxanthin molecule to be at a lower level than the lowest excited state of violaxanthin. It so happens that the lowest energy levels of the chlorophyll *a* molecule are just between that of zeaxanthin and that of violaxanthin.

I must here introduce a small complication. If you do not understand this paragraph, do not worry, since it is not important for an understanding of the plant's physiology. Xanthophylls, like zeaxanthin and violaxanthin, are yellow because they have energy levels low enough for blue light photons to be absorbed
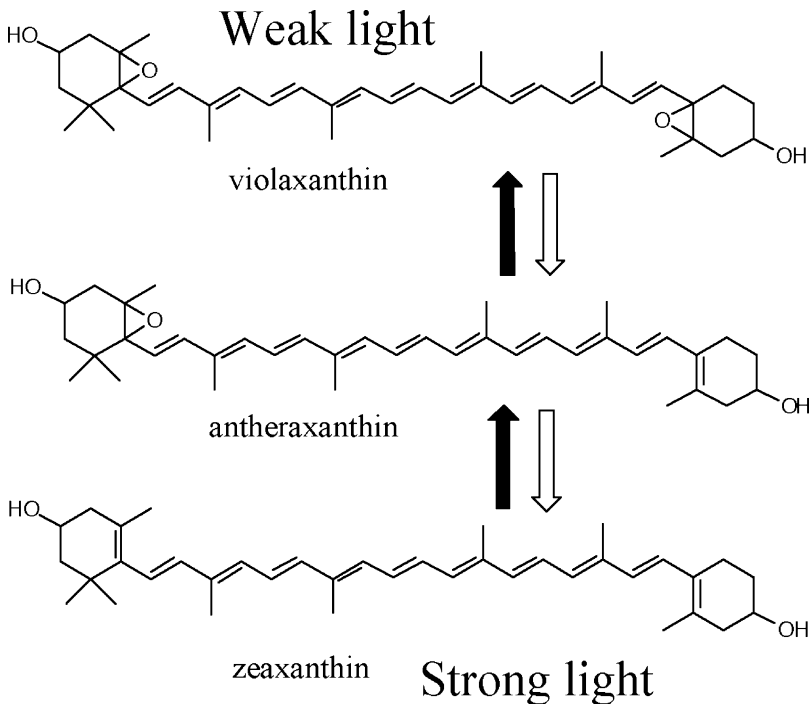
FIGURE 24.4. The xanthophyll cycle in higher plants (also called the violaxanthin cycle). In some algae an analogous cycle with other carotenoids takes place.

and excite them to an excited state. These energy levels cause the bands in the blue part of the absorption spectrum. Xanthophylls possess these energy levels because they have long conjugated bond systems. However, these are *not* the energy levels we are talking about in explaining the xanthophyll cycle. There are even lower energy levels, corresponding to red light. They do not, however, show up in the absorption spectra, because the transition to this state from the ground state is forbidden. Like most of quantum mechanics, we shall, as biologists specializing in another branch of science, just have to accept this.

Let's now return to the main line of thought. Since the lowest excited state of violaxanthin is slightly higher than the lowest excited state of chlorophyll *a*, energy from an excited violaxanthin molecule may be transferred to a chlorophyll *a* molecule, provided it is close enough. In other words, violaxanthin can act as an antenna pigment.

Zeaxanthin, on the other hand, cannot act as an antenna pigment for chlorophyll *a*, since its lowest energy level is lower than the lowest energy level of chlorophyll *a*. On the contrary, it can accept energy from an excited chlorophyll *a* molecule, provided it is close enough (Fig. 24.5).

We are more accustomed to describing the photosynthetic pigments in terms of the positions of their absorption maxima than in terms of energy levels. This is
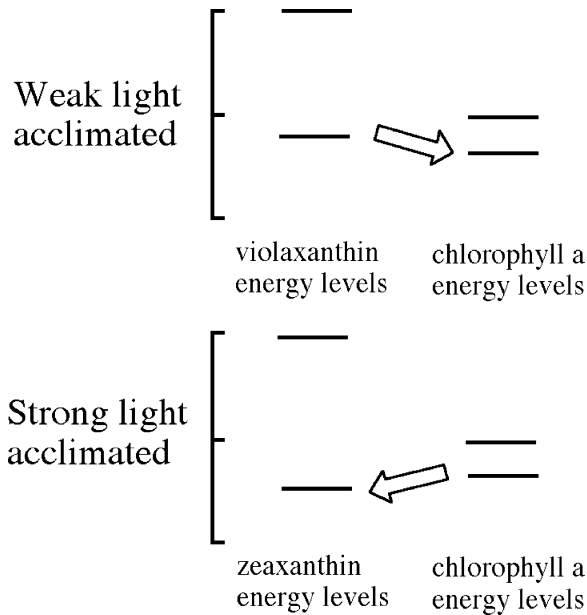
FIGURE 24.5. Energy levels in violaxanthin, chlorophyll *a*, and zeaxanthin. For violax-
anthin the lowest excited state is higher, for zeaxanthin lower than the lowest (singlet)
excited state in chlorophyll. The arrows show direction of energy transfer. (Simplified
from Frank et al. 1994.)

OK as long as we remember that energy is inversely proportional to wavelength.
The reaction center pigment in photosystem I is referred to as P700, because
its (long-wavelength) absorption peak is at 700 nm, and that of photosystem II
is called P680 for the corresponding reason. These wavelengths correspond to
energies of 1.77 and 1.82 eV, respectively. The antenna pigments have peaks
at shorter wavelength, corresponding to higher energy. This is the reason that
energy can flow from antenna pigments to reaction centers, while some of the
energy is degraded to heat, giving an overall positive entropy change.

   The lowest energy level (1.89 eV) of violaxanthin corresponds to 655 nm,
allowing this pigment to donate energy to any pigment with an absorption peak at
longer wavelength. This includes all forms of protein-bound chlorophyll *a*. The
lowest energy level (1.76 eV) of zeaxanthin corresponds to 704 nm. It allows it
to accept energy from any antenna chlorophyll *a*.

   For the intermediate xanthophyll, antheraxanthin with 10 conjugated double
bonds, the lowest energy level corresponds to 680 nm. It therefore can accept
energy from photosystem II antenna pigments on the same terms as the reaction
center, but donate energy to photosystem I.

   The xanthophyll cycle can thus function as a safety valve for the photosynthetic
system when it is overloaded with energy. The valve opens when zeaxanthin
is formed from violaxanthin. The energy received by zeaxanthin is degraded to

small quanta (heat), which is less dangerous than the large energy quanta that can break bonds and cause chemical reactions.

This is just half the truth, though. There are energy sinks other than zeaxanthin in the photosynthetic system. Violaxanthin has a third important function in addition to being an antenna pigment and a source of zeaxanthin. It is able to inactivate the other (not yet characterized) energy sinks. The xanthophyll cycle thus regulates the electron pumping by the photosystems in a threefold way.

Violaxanthin deepoxidase has a pH optimum of about 5, and it is likely that deepoxidation is activated by the proton uptake into the thylakoids that occurs in light, and the "trigger point" is the pH that is just a little bit lower than that required for ATP synthesis.

The acidification of the thylakoids and the conversion of violaxanthin to zeaxanthin that take place when the plant is subjected to excess light cause secondary changes in the antenna pigments. The structure is changed, which can be seen as increased light-scattering power. This is a contributing factor to the signals that we shall monitor in our experiment.

The xanthophyll cycle pigments are present both in photosystem I and photosystem II antennas (chlorophyll *a/b*–binding proteins), and also dissolved in the thylakoid membrane lipid. In addition, violaxanthin occurs in the envelope membrane. All violaxanthin in the plant is not available to the deepoxidase, and the available fraction seems to increase with increasing reduction of the plastoquinone pool. This may be an important point for us who are interested in effects of UV-B radiation on plants. UV-B inhibits photosystem II more than photosystem I and thus presumably leads to a more oxidized plastoquinone pool, resulting in less substrate for the xanthophyll cycle. UV-B may also inhibit the deepoxidase, and both these changes may lead to a decrease in the ability of the plant to protect the photosystem against overloading by excess light. One of the experiments we can carry out is to look just at how UV-B affects the deepoxidation.

The pool of xanthophylls that can participate in the xanthophyll cycle also increases when the plant prepares for the winter. There is a big need for safety valve function during the spring, when the plant may be subjected to strong light at the same time that the temperature is so low that carbon dioxide assimilation is impaired. The pool is larger in plants adapted or acclimated to strong light than in shade plants.

Finally, a different role has also been proposed for zeaxanthin and the xanthophyll cycle: as a blue light–sensing system in stomatal regulation and phototropism.

24.11.2. Experiment

Gamon et al. (1990) described a principle for sensing of the xanthophyll cycle state by monitoring reflectance at 530 nm. The method described here employs the same principle. The advantage with our variant is that it uses equipment that is cheap, battery-operated, and portable. Although leaves picked from plants
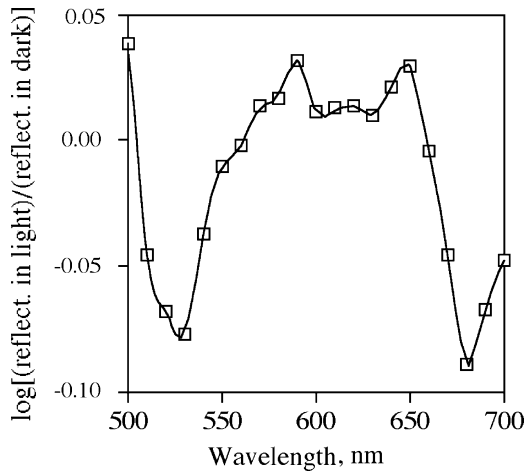
FIGURE 24.6. Light/dark difference reflectance spectrum of a *Prunus laurocerasus leaf* measured with Colortron. The dip at 530 nm signals the xanthophyll changes, the dip at 680 nm the quenching of chlorophyll fluorescence associated with it. CricketGraph was used for plotting the data.

were used for the examples shown here, the method has potential of being nondestructive, as there seems to be nothing preventing measurements to be made on attached leaves.

A leaf is kept in darkness for at least 10 minutes. The reflectance spectrum is then recorded. If a Colortron instrument is used, this simply means pressing the instrument, connected to a Macintosh or PC with the appropriate software running, against the leaf. In a few seconds the spectrum from 390 to 700 nm is then automatically stored in the computer, using the two lamps built into the instrument as light sources. We have built a simple leaf holder, so a leaf can be placed in front of the instrument in a repeatable way. After the first spectrum is stored, the leaf is exposed to strong light (PAR) for 0.5–7 minutes, and the spectrum again recorded. The spectra can be viewed with the original software, but in this case they are best transferred to another program (we have used CricketGraph III or KaleidaGraph for the purpose; see Figs. 24.6 and 24.7), in which the light–dark difference spectra can be computed and displayed; Excel can of course also be used. An alternative is to not follow the directions for calibrating the spectrophotometer using the "100% reflectance standard" supplied, but to use the dark-adapted leaf as reference, against which the illuminated leaf is compared. One can easily investigate the kinetics using a series of irradiations. Best (Figs. 24.6 and 24.7) is to plot the logarithm of the ratio of reflectances in order to have an analogue to the absorbance used in transmission measurements.

The result of this experiment is that the reflectance in the green region, especially near 530 nm, is decreased by the radiation. This change is caused by conversion of violaxanthin to zeaxanthin, which causes rearrangements in the
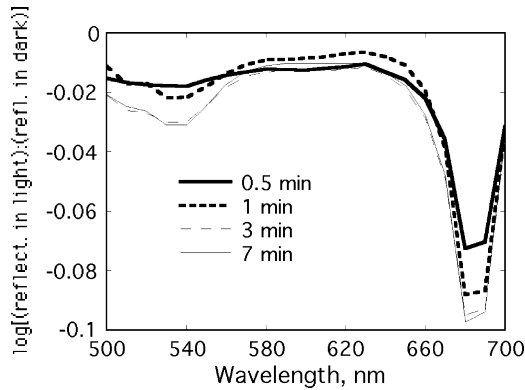
FIGURE 24.7. Experiment similar to that in Fig. 24.6, but with several irradiation times and with leaves of *Vaccinium vitis-idaea* as experimental material. As can be seen from a comparison of the two figures, the relation between the scattering and the fluorescence change varies among species. It can also be seen here that the change is complete after 3 minutes in strong light.

thylakoid membranes with cocomitant changes in light scattering. One can also see an apparent reflectance decrease in the red region. This, however, is not a true reflectance decrease, but signals the quenching of fluorescence associated with it.

This measurement is in principle similar to that explored by Gamon et al. (1990) as a method for remote sensing of photosynthetic efficiency of plants, and later in more detail by Gamon et al. (1992, 1997), Gamon and Surfus (1999), Penuelas et al. (1995, 1997), Filella et al. (1996), Nichol et al (2000), and Barton and North (2001).

I have also successfully used the home-built spectrophotometer (Chapter 25) for this experiment, using a green-light laser pointer as source for actinic and fluorescence excitation light and for reflectance measurement.

24.12. Ultraviolet Radiation Damage and Its Photoreactivation

This exercise can be carried out as a demonstration, but is recommended as a practical for students. In its simplest form it is a direct repeat of the classical first demonstration of photoreactivation by Hausser and Oehmcke (1933) and is evaluated visually. With relatively cheap equipment, also useful for other experiments, it can be evaluated quantitatively.

You will need a low-pressure (germicidal) mercury lamp, a strong lamp, preferably medium-pressure mercury with fluorescent coating (or other lamp with sufficient emission in the blue and UV-A) for photoreactivating light, a big jar or (preferably) small plastic aquarium, and a few unripe (green) bananas.

You should also have goggles for protecting your eyes from the UV-C radiation from the mercury lamp.

Mount the germicidal lamp so you can irradiate the bananas at a distance of about 20–30 cm (not critical, but suitable exposure times vary with distance). Mount the photoreactivation lamp with the aquarium below it, and some space below the aquarium. The bananas can be irradiated for photoreactivation in the space below the aquarium. The purpose of the aquarium (which should be filled with clear water) is to remove infrared radiation and avoid heating of the bananas by the strong lamp. If you find it more convenient, it is also possible to mount the bananas in the water in the aquarium, but there should be at least 10 cm of water above them.

If green bananas are exposed to the bactericidal radiation (mainly 253.7 nm) only (about 1–2 minutes, but depending on the lamp, the distance, and the bananas), and then left to ripen during a couple of days at room temperature, they will turn brown instead of yellow. If they are exposed to photoreactivating light (15–60 minutes required depending on lamp etc.) immediately after the ultraviolet radiation, the browning is prevented, and they will turn yellow during ripening. You can use, e.g., aluminum foil to shade different parts of the banana during exposure, and so expose different parts for different times and get many combinations of damaging and reactivating exposures on the same banana. The result can be evaluated visually or by reflectance spectrophotometry (Figs. 24.8 and 24.9), or photographically.

A simple spectrophotometer for reflectance measurements, such as Colortron (see Section 24.11.), can be used to evaluate "color changes" (or more correctly:
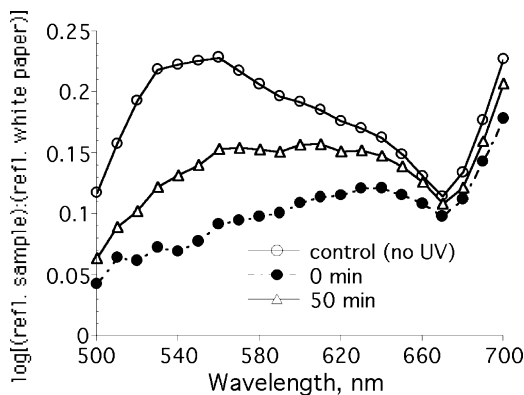
FIGURE 24.8. Reflectance spectra of bananas measured with Colortron. The top curve is an average spectrum for five bananas which were not exposed to ultraviolet radiation, the two others for bananas exposed to UV–C radiation for 2 minutes. The bananas for the middle curve, in addition, received 50 minutes of white light immediately after UV–C irradiation. In this case spectra were measured 2 days after irradiations, when the bananas were still green. If the UV–C irradiation is decreased, more complete approach to the control curve can be achieved by white light irradiation.
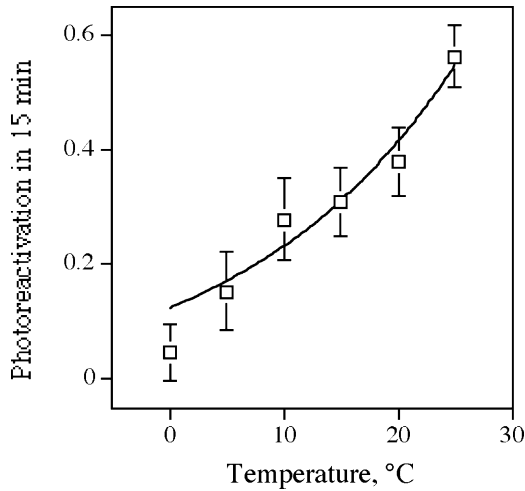
FIGURE 24.9. A study of the temperature dependence of photoreactivation of the UV-C–induced darkening of bananas. The experiment was carried out as in Fig. 24.8, except that the bananas were kept in water of different temperature during white light irradiation. The UV-C irradiation lasted 1 minute, and the reactivation time was only 15 minutes. The reflectance at 570 nm was monitored, and photoreactivation expressed as fractional approach to the control curve. The curve in the diagram here is an Arrhenius plot fitted to the data with the zero degree data omitted.

reflectance changes) quantitatively. You can also adapt a spectrophotometer intended for transmission measurements by attaching a Y-shaped light conductor to it. One arm of the conductor picks up light from the monochromator, the other arm delivers it to the photomultiplier, and the base of the Y is placed at a distance of about 5 mm from the banana. Light conductors of this kind can be obtained, e.g., from Oriel. It is best to plot the logarithm of the reflectance of the sample relative to a white standard (Figs. 24.8 and 24.9), but the easiest way is to photograph the banana with a digital camera under standardized illumination conditions and then evaluate the picture with a program for image analyzes such as ImageJ.

24.13. Ultraviolet Damage to Microorganisms

Any actively swimming microorganism can be used to repeat in a simplified form Hertel's (1905) classical experiment, using UV-C radiation (254 nm) from a germicidal lamp to stop the movement. Note that a visible effect takes time to develop, so it is in many cases sufficient to irradiate for a minute, and then wait. (Take care to protect your eyes!) We have used *Euglena gracilis* for the purpose. In addition to stopping the movement, the radiation causes this organism to change shape, and with sufficient radiation the color will also eventually

change from green to yellow. This is a very simple experiment to carry around if you are a "traveling teacher," as I have sometimes been. See also Delpech (2001) and either Valenzeno et al. (1991) or Smith (1977). Another educational photoreactivation experiment is described by Delpech (2001).

24.14. Photomorphogenesis in Plants and Related Topics

For those readers who know German I recommend the book by Schopfer (1970), in which a number of class experiments on plant photomorphogenesis are described in detail. I do myself have three favorite experiments, the first two of which are in principle similar to experiments in Schopfer's book. Many experiments, such as basic observations on phototropism, solar tracking leaves, phototaxis, etc., are so simple that they do not need to be described here. For those who feel they need some guidance, see Valenzeno et al. (1991) for phototropism and phototaxis and Vogelmann and Björn (1983) for sun-tracking.

24.14.1. Photomorphogenesis of Bean Plants

Prepare sources for red and far-red light as follows. For red light, wrap a red fluorescent lamp in red cellulose acetate film to remove traces of blue light. If you cannot obtain a red fluorescent lamp, use a white one with red acetate film. For far-red light, use an incandescent lamp (25–40 W) behind one layer (3 mm) of red and one layer (3 mm) of blue plexiglass (many other colored plastic filters will also work). You can use a standard photographic darkroom lamp in which you change the filter for the far-red irradiation, or you can build your own lamp and filter holder; just make sure that only far-red light escapes to your experimental darkroom or cabinet. Do not leave the incandescent lamp on when not in use, since it gives off heat which may damage the filter.

Soak red beans (*Phaseolus vulgaris*) overnight in water, peel off the seed coats and sow in (at least) five pots with soil (or sow seeds directly without soaking and peeling, although the result will be more variable then). Place one pot in a greenhouse or other suitable place where the plants can continue development under normal light conditions. Put the other pots in a completely dark place, where you can inspect them using dim green light from a green fluorescent lamp (preferably wrapped in green or yellow cellulose acetate film to remove traces of blue light), and water when necessary (not too much, which may result in mold development). Do not unnecessarily expose the plants even to the green safelight. It is not ideal to use an incandescent lamp with a green filter as safelight, since it will emit a lot of far-red light, to which the plants are sensitive, even if you do not see it yourself. When the seedlings have reached a few cm in height, expose one pot to red, one pot to far-red, one pot to red followed by far-red light, and keep one pot as dark control. Each exposure should be for 10 minutes. Let all bean plants continue their development in darkness, except that you repeat the light treatments on each of the two following days. After the three

days of light treatment, let the plants develop for two more days, after which they can be inspected in full (cf. Withrow et al. 1957) angle, and compare pigmentation visually. As a variant, you can do a similar experiment with peas (Björn and Virgin 1958).

24.14.2. Regulation of Seed Germination by Phytochrome

The red and far-red light sources for this experiment can be the same as in the bean plant experiment. As plant material most educators have used lettuce seeds of a variety called Grand Rapids, available from many sources (see the Web). However, even different lots of seeds obtained from a particular source do not react uniformly, depending on temperature prehistory and other factors. If you find that seeds germinate independently of light treatment, try one of the following pretreatments:

1. Hydrate the seeds in the dark, expose them for 10 minutes to far-red light, and dry them again for class use (recommendation by John Hoddinott, University of Alberta).
2. Try doing the experiment at a high temperature (25–28 °C) rather than normal room temperature (recommendation by Brad Goodner, University of Richmond). When you have got a good lot, keep it in a closed container in your freezer for future use, preferably in small portions, so you do not have to refreeze.

The above advice was found on an Internet chat site at http://www.clemson.edu/biolab/phyt.html. One participant (Jon Monroe), who points out that Grand Rapids is no longer as good for the experiment as it used to be, because suppliers treat the seeds to ensure complete germination, used seeds from the Harris Seed Company (http://commercial.harrisseeds.com/), while Ross Koning at Eastern Connecticut State University recommends "Salad Bowl" lettuce from Agway (http://www.seedway.com/catalog). Dan Tennessen at Cornell University suggests trying seeds of *Poa pratensis* (bluegrass) and *Lepidium virginianum* (peppergrass). For the experiment, cover the bottoms of 12 small petri dishes with a double layer of filter paper, cut to size so it is flat on the bottom. Pour distilled water into the dishes and pour it off again, so the paper is moist but no longer dripping. Place 50 seeds in rows in each dish. Cover the dishes with aluminum foil. After letting the seeds imbibe for 1–3 hours in the dark, irradiate with your red (R) and far-red (FR) as follows: each time for 5 minutes, or leave as dark control. Do duplicates of each treatment.

Irradiation sequences: R, FR, R+FR, R+FR+R, R+FR+R+FR.
Leave in complete darkness (wrapped in aluminium foil) for 2 days, then evaluate the result.

As an alternative to seeds, fern spores can be used for a red/far-red germination experiment. The procedure for preparing and sowing spores described in the next experiment can be used for this.

24.14.3. *Effects of Blue and Red Light on Development of Fern Prothallia*

Collection of Fern Spores. When fern spores are about to be released (late August in northern Europe), collect spore-bearing leaves and put them on a white paper, sporangia side down. We have used *Dryopteris filix-mas*, but some other species should also work. After a couple of days most spores have fallen out on the paper and form a beautiful imprint of the leaf. By holding the paper at a slight angle and gently tapping it, it is easy to separate spores from empty sporangia and other debris. This is easily done manually, but if you like gadgets you can use the handle of an electric toothbrush to vibrate the paper.

Nutrient Medium. (according to Etzold 1965, amounts in g/L). NH_4NO_3 (0.2), K_2HPO_4 (0.1), $MgSO_47H_2O$ (0.1), $CaCl_22H_2O$ (0.1); add a couple of drops of a solution of $FeCl_3$ (1% w/w) per liter. Adjust pH to 6.0–6.3 with HCl. Add 5 g of agar per liter and heat to dissolve the agar. Transfer the medium to Erlenmayer flasks, plug with cotton, and autoclave for 10 minutes at 1 atmosphere overpressure. Let cool to about 40 °C and pour the medium into sterile 9-cm plastic petri dishes. The dishes can be stored in the dark at 5°C until use.

Sterilization and Sowing of Spores. Pour a few (about 20) drops of dilute (5% w/v) sodium hypochlorite solution (or corresponding concentration of commercial bleach) into a small glass cup. Put a small amount of spores (as much as the outermost mm of the tip of a knife or spatula can hold) on the solution and stir with a glass rod until all spores are in the solution. After 3–4 minutes you can start to sow your petri plates with the suspension using a sterile inoculation loop. Put the loop under the spores and lift, so you get a drop with spores in the loop. Streak out the drop on a plate, and repeat with more plates (you need at least four plates). The spores can remain in the hypochlorite solution for some time without being damaged. After transfer to the agar the hypochlorite will be sufficiently diluted and need not be removed.

Irradiation and Development. Put two plates under blue light, and two under red light (best to use colored fluorescent lamps, but white fluorescent lamps with colored cellulose acetate film will probably also work well). After about 6 days the spores should have germinated. Study the development for 1 week. When you see that the protallia have started to grow, you can transfer one plate from red light to blue light, and one from blue light to red light. Under red light the prothallia will grow as filaments, under blue light as plates.

If you run a dark control you will find that the spores do not germinate. You can do red/far-red reversion experiments as on the seeds in the previous experiment.

24.15. Spectrophotometric Studies of Phytochrome In Vivo

Photobiology practicals in our own photobiology courses have included purification of phytochrome and in vitro experiments with the purified phytochrome,

but this may be too laborious to set up in a laboratory not doing research on phytochrome. The following is a simple experiment to carry through, but requires a good dual wavelength spectrophotometer such as Aminco DW-2. It may be possible to adapt the experiment for an ordinary double-beam single-wavelength computerized spectrophotometer of good quality, but I have not tried this.

The aim of the experiment is to demonstrate spectrophotometrically the in vivo transformations between the red-absorbing (P_r) and far-red–absorbing (P_{fr}) forms of phytochrome: $P_r ==> P_{fr}$ (under red light) and $P_{fr} ==> P_r$ (under far-red light).

Plant Material. Oats or wheat is sown in moist Vermiculite (mica) in plastic or metal trays (a total of 0.25 m^2 required). The trays are incubated in complete darkness at 20–25 °C for about 4 days. When the seedlings have emerged, and preferably before the leaves have broken through the coleoptiles, the shoots are harvested. Harvesting and the following manipulations should be carried out using dim green working light. About 50 plants are required for an experiment.

Sample Preparation. The coleoptiles are cut open so the leaves in them can be removed. This procedure is rather time-consuming and not absolutely necessary if you just want to demonstrate the presence of phytochrome. For quantitative experiments it is of advantage to get rid of the leaves, which are rich in protochlorophyllide. This is also photoconvertible, which obscures the phytochrome signal.

The coleoptiles are collected in a petri dish with water, so they do not dry out. When you have enough coleoptiles, arrange them in a bundle which you cut across with a razor or scalpel in the middle to get two bundles with a sharp delimitation. Join them with the cut ends in the same direction and press them into a water-filled spectrophotometer cuvette in such a way that you avoid air bubbles between the coleoptiles. There is no need to crush an expensive cuvette trying to squeeze in the coleoptiles; you might as well use a cheap plastic one. We have also with good results used small round glass test tubes, which fit the cuvette holder of the spectrophotometer.

Measurement. Switch the spectrophotometer to dual-wavelength mode, set the monochromators to measure the absorbance difference between 660 and 730 nm (or, preferably, between 660 and 800 nm in one series of measurement and 730 and 800 nm in another series of experiments). If you have not removed the leaves it is best to focus on measuring the P_{fr} changes only by recording the absorbance difference between 730 and 800 nm. Using the Aminco DW-2 and DW-2a spectrophotometers, we have set full scale to 0.01 absorbance units and the damping to medium.

After taking a reading, irradiate the sample with strong red light for one minute and take a new reading. Then do the same with far-red light and take a new reading. If this works you can continue the experiments in a variety of ways, studying reaction kinetics and action spectra, for instance. We have also let students take coleoptiles outside to different environments, above and below

tree canopies, etc., and then bring the coleoptiles back to the laboratory (on ice) for evaluation of the phytochrome state.

The phytochrome-transforming irradiation can either be carried out with the sample cuvette still in the spectrophotometer, using a xenon lamp–monochromator combination, or after removal from the spectrophotometer. In the former case the photomultiplier should be protected with a piece of sheet metal during irradiation, and if the spectrophotometer does not switch the photo-multiplier voltage off automatically, this should be done manually. In the latter case, we have used light sources similar to those used for photomorphogenesis and germination experiments. In this case it is important to handle the cuvette carefully so the coleoptiles or any air bubble present do not change position, so as not to touch the places where the measuring beam is to enter and exit, and to put the cuvette back with the original orientation.

As an alternative to coleoptiles, the epicotyls (internodes between cotyledons and first two leaves) of dark-grown pea plants serve very well. This circumvents the time-consuming task of removing leaves.

24.16. Bioluminescence

24.16.1. Fireflies

If you do not have bioluminescent insects where you live, or if the season is not the right one, you can buy dried fireflies from one of several suppliers, such as Sigma Chemical Co. (St. Louis, MO) or Worthington Chemical Corp. (Freehold, NJ). The simplest experiment you can do is to wet the abdomen of such a dead insect with ATP solution (dissolve 10 mg ATP in 10 ml 0.1 M phosphate buffer, pH 7.6, containing 1 mM $MgCl_2$) and watch it glow. If you remove oxygen by flushing with nitrogen, the glow disappears. Other experiments can be carried out with extracts of the fireflies containing luciferin and luciferase. For extraction of the fireflies in a mortar with sand, use a solution of 0.4 g glycine and 0.1 g ammonium bicarbonate in 100 ml distilled water. You can also buy ready-made, dried firefly extract, which only needs reconstitution with water. If you can get living bioluminescent insects, it would be interesting to try repeating the new observation of the role of nitrogen monoxide (Trimmer et al. 2001), but I have not done this myself.

24.16.2. Bacteria

A culture of luminescent *Photobacterium phosphoreum* can be purchased from a culture collection, such as the American Type Culture Collection (http://www.atcc.org), but the cost is considerable. It is, however, not very difficult to get luminescent bacteria to grow on old decaying fish (if you can stand the smell), preferably fish from the sea (Lee 1977, 1991).

24.17. Miscellaneous Teaching Experiments and Demonstrations

Here are a few ideas which I have not tried myself, but which appear worth exploring:

1. Gelatin optics. Many interactions between light and matter can be demonstrated using gelatin. Knotts (1996) has published a rather detailed description, and variations of this are availble from various Internet sites—search, for instance, for "gelatin optics" or "edible optics" or "optics fun with gelatin." The main thing to remember is that the gelatin gel should be prepared three times more concentrated as most cooking recipies require. From such gels you can prepare lenses, prisms, and fiberoptics. Demonstrations of refraction and reflection (including total reflection) can be carried out using a laser pointer as light source. The slight scattering in the gel makes the light rays visible. Knotts (1998) reviewed several books for elementary optics experimentation.
2. Optical tweezers for students are described by Smith et al. (1999).
3. Quantum dots. Several student experiments for production of quantum dots by the wet method have been worked out, both for CdS and for CdSe quantum dots (Kippeny et al. 2002, Boatman, Lisensky and Nordell 2005, Winkler et al. 2005). All of the methods involve dangerous chemicals, and a qualified chemist to lead the exercises is required, as well as proper disposal of chemicals. The method of Boatman, Lisensky, and Nordell for CdSe quantum dots is probably the safest.
4. An exercise about the ozone layer is found at NASA's site: "Ozone over your head," http://edmall.gsfc.nasa.gov/inv99Project.Site/Pages/trl/inv3-1.html

References

Anon. (1894) Artificial spectrum top. Nature 51, 113–114.

Barton, C.V.M. and North, P.R.J. (2001) Remote sensing of canopy light use efficiency using the photochemical reflectance index: Model and sensitivity analysis. Remote Sensing Environ. 78, 264–273.

Björn, L.O. (1969a) Action spectra for transformation and fluorescence of protochlorophyll holochrome from bean leaves. Physiol. Plant. 22, 1–17.

Björn, L.O. (1969b) Photoinacivation of catalases from mammal liver, plant leaves and bacteria. Comparison of inactivation cross sections and quantum yields at 406 nm. Photochem. Photobiol. 10, 125–129.

Björn, L.O. and Virgin, H.I. (1958) The influence of red light on the growth of pea seedlings. An attempt to localize the perception. Physiol. Plantarum 11, 363–373.

Boatman, E.M., Lisensky, G.C. and Nordell, K.J. (2005) A safer, easier, faster synthesis for CdSe quantum dot nanocrystals. J. Chem. Educ. 82, 1697–1699.

Cone, J.E. and Kendrick, R.E. (1986) Photocontrol of seed germination. In: R.E. Kendrick and G.H.M. Kronenberg (Eds.), *Photomorphogenesis in plants*, pp. 443–463. Martinus Nijhoff/Junk Publishers, Dordrecht.

Delpech, R. (2001) Using *Vibrio natriegens* for studying bacterial population growth, artificial selection, and the effects of UV radiation and photo-reactivation. J. Biol. Educ. 35, 93–97.

Diakoff, S. and Scheibe, J. (1973) Action spectra for chromatic adaptation in Tolypothrix tenuis. Plant Physiol. 51, 382–385.

Etzold, H. (1965) Der Polarotropismus und Phototropismus der Chloronemen von *Dryopteris filix-mas* (L.). Schott. Planta 64, 254–280.

Filella, I., Amaro, T., Araus, J.L. and Penuelas, J. (1996) Relationship between photosynthetic radiation-use efficiency of barley canopies and the photochemical reflectance index (PRI). Physiol. Plant. 96, 211–216.

Frank, H.A., Cua, A., Chynwat, V., Young, A., Gosztola, D. and Wasielewski, M.R. (1994). Photophysics of the carotenoids associated with the xanthophyll cycle in photosynthesis. Photosynthesis Res., 41, 389–395.

Frankland, B. and Taylorson, R.B. (1983) Light control of seed germination. In: W. Shropshire, Jr., and H. Mohr (Eds.), *Encycl. Plant Physiol.*, *New Series*, *16A*, pp. 428–456. Springer, Berlin.

Fujita, Y. and Hattori, A. (1960a) Formation of phycoerythrin in preilluminated cells of *Tolypothrix tenuis* with special reference to nitrogen metabolism. Plant Cell Physiol. 1, 281–292.

Fujita, Y. and Hattori, A. (1960b) Effect of chromatic lights on phycobilin formation in a blue-green alga, *Tolypothrix tenuis*. Plant Cell Physiol. 1, 293–220.

Gamon, J.A., Field, C.B., Bilger, W., Bjorkman, O., Fredeen, A.L., and Peñuelas, J. (1990) Remote-sensing of the xanthophyll cycle and chlorophyll fluorescence in sunflower leaves and canopies. Oecologia 85, 1–7.

Gamon, J.A. and Surfus, J.S. (1999) Assessing leaf pigment content and activity with a reflectometer. New Phytol. 143, 105–117.

Gamon, J.A., Peñuelas, J. and Field, C.B. (1992) A narrow-waveband specral index tht tracks diurnal changes in photosynthetic efficiency. Remote Sensing Envir. 41, 35–44.

Gamon, J.A., Serrano, L. and Surfus, J.S. (1997) The photochemical reflectance index: an optical indicator of photosynthetic radiation use efficiency across species, functional types, and nutrient levels. Oecologia 12, 492–501.

Haupt, W. and Björn, L.O. (1987) No action dichroism for light-controlled fern-spore germination. J. Plant Physiol. 129, 119–128.

Hausser, K.E. and v. Ohmcke, H.V. Lichtbräunung an Fruchtschalen. Strahlentherapie 48, 223–229.

Hertel, E. (1905) Ueber physiologische Wirkung von Strahlen verschiedener Wellenlänge. Zschr. Allgem. Physiologie 5, 95–122.

Johnson, R.H. and Williams, Th.P. (1970) Action of light upon the visual pigment rhodopsin. J. Chem. Edu. 47, 736–739.

Kippeny, T., Swafford, L.A., and Rosenthal, S.J. (2002) Semiconductor nanocrystals: A powerful visual aid for introducing the particle in a box. J. Chem. Edu. 79, 1094–1100.

Knotts, M.E. (1996) Optics fun with gelatin. Optics and Photonics News, April 1996, 50-51. Available from http://www.opticsforkids.org/resources/GO_3.pdf.

Knotts, M.E. (1998) Books for optics experimenters. Optics and Photonics News, January 1998, 50–51.

Lee, J. (1977) Bioluminescence. In: K.C. Smith (Ed.), *The science of photobiology*, Chapter 14. [Reprinted in D.P. Valenzeno et al. (Eds.) (1991) *Photobiological techniques*, pp. 359–360. Plenum, New York.]

Lee, J. (1991). Experiment 33: Bacterial bioluminescence. In: D.P. Valenzeno et al. (Eds.), *Photobiological Techniques*, pp. 317–320. Plenum, New York.

Le Rohellec, J. and Vienot, F. (2001) Interaction of luminance and spectral adaptation upon Benham subjective colors. Color Res. Appl. S174–S179.

Nichol, C.J., Hümmrich, K.F., Black, T.A., Jarvis, P.G., Walthall, C.L., Grace, J. and Hall, F.G. (2000) Remote sensing of photosynthetic light-use efficiency of boreal forest. Agric. Forest Meteorol. 101, 131–142.

Peñuelas, J., Filella, I. and Gamon, J.A. (1995) Assessment of photosynthetic radiation-use efficiency with spectral reflectance. New Phytol. 131, 291–296.

Peñuelas, J., Llusia, J., Pinol, J. and Finella, I. (1997) Photochemical reflectance index and leaf photosynthetic radiation-use efficiency assessments in Mediterranean trees. Int. J. Remote Sensing 18, 2863–2868.

Pottier, R.H. and Russell, D.A. (1991) Quantum yield of a photochemical reaction. In: D.P. Valenzeno, R.H. Pottier, P. Mathis, and R.H. Douglas (Eds.), *Photobiological techniques*, pp. 45–52. Plenum Publishing Corp., New York.

Scheibe, J. (1972) Photoreversible pigment in a blue-green alga. Science 176, 1037–1039.

Schopfer, P. (1970) *Experimente zur Pflanzenphysiologie*. Rombach Verlag, Freiburg.

Smith, K.C. (Ed.) (1977) *The science of photobiology*. Plenum, New York.

Smith, S.P., Bhalotra, S.R., Brody, A.L., Brown, B.L., Boyda, E.K. and Prentiss, M. (1999) Inexpensive optical tweezers for undergraduate laboratories. Am. J. Phys. 67, 26–35.

Trimmer, B.A., Aprille, J.R., Dudzinski, D.M., Lagace, C.J., Lewis, S.M., Michel. T., Qazi, S. and Zayas, R.M. (2001). Nitric oxide and the control of firefly flashing. Science 291, 2486–2488.

Valenzeno, D.P., Pottier, R.H., Mathis, P. and Douglas, R.H. (Eds.) (1991) *Photobiological techniques*. Plenum Publishing Corp., New York.

Vogelmann, T.C. and Björn, L.O. (1983) Response to directional light by leaves of a sun-tracking lupine (*Lupinus succulentus*). Physiol. Plant. 59, 533–538.

von Campenhausen, C. and Schramme, J. (1995) 100 years of Benham top in color science. Perception, 24, 695–717.

Winkler, L.D., Arceo, J.F., Hughes, W.C., DeGraff, B.A. and Augustine, B.H. (2005) Quantum dots: An experiment for physical or materials chemistry. J. Chem. Educ. 82, 1700–1702.

Withrow, R.B., Klein, W.H. and Elstad, V.B. (1957) Action spectra of photomorphogenetic induction and its inactivation. Plant Physiol. 32, 453–462.

25

The Amateur Scientist's Spectrophotometer

Lars Olof Björn

Abstract: This chapter describes the construction and performance of a spectrophotometer that is very easily constructed from a DVD, a digital camera, a lamp and some cardboard, wood, and sheet metal.

25.1. Introduction

A spectrophotometer is a very useful instrument for many types of chemical and biological measurements. The most common types are designed for measuring light absorption in solutions, but there are also spectrophotometers with which you can take measuremements on living tissues or even single cells, and there are reflectance spectrophotometers for measurements on surfaces, and many other special types. A common property is that they are expensive. Here we shall see that it is easy to build a low-cost spectrophotometer. It is not a precision instrument, but it is sufficient for many demonstrations and teaching experiments. It is an elaboration of a design for a spectroscope described by Wakabayashi and Hamada (2006).

A spectrophotometer has the following main parts: a lamp, a dispersing element (usually a reflecting grating; see Chapter 3) that divides the light into spectral components, a place to put the sample, a light detector, and some device for reading or recording the result. In addition there is usually a number of lenses and mirrors, The most expensive parts are the grating and the light detector; the recording system may also be expensive.

A reflecting grating is a mirror with many fine parallel grooves ruled into it. For our low-cost spectrophotometer we shall use a DVD as a grating. Perhaps you have an old one with a movie that you have seen enough of. It is all right if it is scratched and useless for watching your movie, if it is just OK in a small sector, because that is all we will use. Otherwise you will have to buy a movie DVD, and if so this may be your major investment in the project. Some of the DVDs (DVD-R or DVD-RW) that you buy for making your own recording are

not suitable because they have a laquer that will show up as a dark band in the red region of the spectrum. Some other types of DVDs are also unsuitable. Check that the reflection from the DVD does not look colored (except for the rainbow type reflection you see in some directions). CDs can be used with modifications of the present description, but give much lower resolution, since they have only 625 grooves per mm, as compared to 1350 grooves per mm for a DVD. A CD also has to be mounted in a slightly different way from a DVD.

You might already have the other expensive component of your spectrophotometer, the light detector, because for this we shall use a digital camera. It does not have to be a very fancy type. The one that I have used (Fujifilm F601 Zoom) has only 3 megapixels, which is considered little nowadays. I do not even use the highest resolution of 6 Mb per picture, but only half of that, to save computer memory. Even this gives me a nominal spectral resolution of 3.515 pixels per nm, which is much better than what the primitive optics allows me to take full advantage of anyway. But the camera should allow for manual exposure, so that it does not automatically set stop and/or exposure time.

A third component that could be expensive is the recording system, and for this we shall use a personal computer, which you probably already own or have access to.

25.2. Construction

Start by making a cardboard box according to Fig. 25.1. When the box is finished and the glue has dried, you can insert the DVD in the slot, ruled side up. Push it right into the corner of the box (part of it will stick out, and if you wish you can cut that part away). To reduce stray light, one potential problem, a mask of black paper should be put on top of the DVD to leave uncovered only that part which we wish to use optically. Figure 25.2 shows a template of the mask.

On a piece of plywood or other board, assemble the cardboard box, a suitable lamp (I use a quartz-iodine lamp with built-in "cold mirror," i.e., a mirror which lets infrared radiation through but reflects visible light), and your camera. To get the proper height relations between my lamp and the cardboard box I put two extra plywood pieces and an aluminum sheet between the box and the base board. I let a little of the aluminum sheet protrude in front of the plywood support and made a hole in it for a screw that fixed the camera. I also mounted a sheet of brass with a hole in it to screen out unwanted light from the lamp and covered the box, including the protruding part of the DVD with duct tape. The cardboard box and the completed assembly are shown in Fig. 25.3 and Fig. 25.4.

25.3. Calibration of Wavelength Scale

The most convenient way to calibrate the wavelength scale is to use a mercury lamp. Just remove the ordinary lamp and point the slit toward a mercury lamp; a streetlamp may do. (The first time I went outdoors and pointed my strange
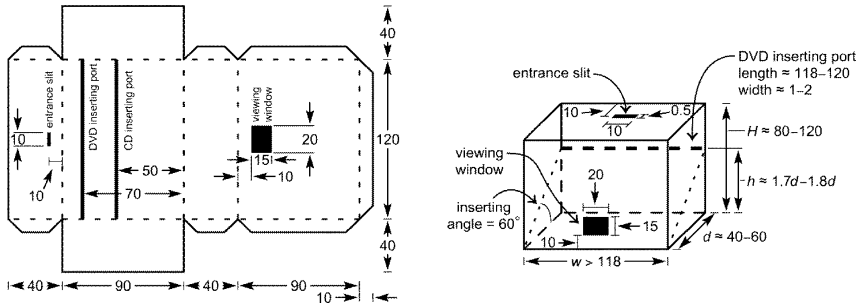
FIGURE 25.1. Construction of the light-dispersing unit box (spectroscope) of the spectrophotometer. Measures are given in mm. The best material to use is black cardboard. If you use other cardboard, paint the inside of the box with black paint that is as dull as possible. In one trial I used a black marker pen which worked, but this is not ideal since it results in a surface that is a little shiny. The rectangle marked "viewing window" should be cut out, as well as a slot for insertion of the DVD and a 10 mm by 0.5 mm entrance slit. In the figure a slot for a CD is also indicated, but if you are going to use only a DVD (recommended), do not cut out this slot since it may lead to stray-light problems. (From Wakabayashi and Hamada 2006, with permission.).

gadget towards a streetlamp, a lady passing by, worried about my mental health, asked whether I was all right or needed help.) Figure 25.5 shows to the left part of the picture obtained in this way. With more exposure it is also possible to show weaker emission lines, but then the closer lines, like 577 and 579 nm, can no longer be resolved.

For quantitative work with spectra, a computer program, ImageJ is available for download without charge from the Internet. To download it, go to http://rsb.info.nih.gov/ij/, where you can read some general information, then
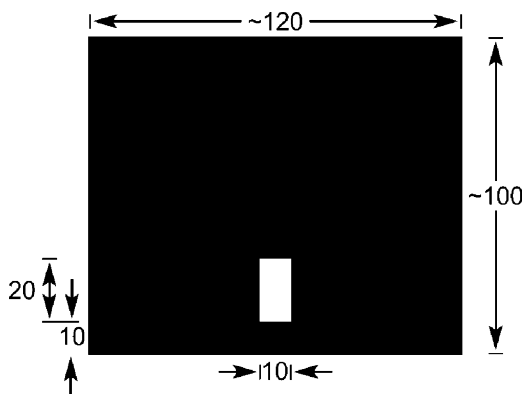
FIGURE 25.2. Dimensions of the black paper mask to cover the DVD. The whole paper is 120 mm by 100 mm, the hole 10 mm by 20 mm, at a distance of 10 mm from the edge of the paper.
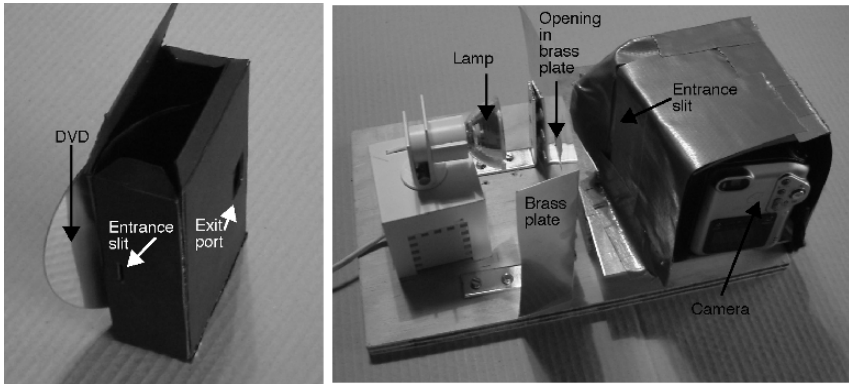
FIGURE 25.3. The finished cardboard box with DVD inserted, just before gluing on the lid (left), and the completed assembly (right).

click on "download" to get to http://rsb.info.nih.gov/ij/download.html, where you can download ImageJ for your particular computer platform. In the following I shall show how to use the Macintosh OS-X version, but it is probably no different with another computer. The program was written for another purpose, and I got the idea of using it for spectral analysis from Kohl, Landmark, and Stickle (2006).

The first thing I see when I load a picture from the camera into the ImageJ program is the color picture with the spectrum. In the example shown in Fig. 25.5 I used a UV-B lamp (Philips TL12 fluorescent lamp with merucury lines). In this case I also captured the violet mercury line (404.7 nm), but due to overexposure the two yellow lines (577 and 579 nm) are not separated. The red lines are not visible, probably because the mercury vapor in this lamp has a lower pressure than in the street lamp. That the violet line did not appear in the spectrum of the street lamp is probably due to absorption in the weatherproof cover of that lamp. The blue to the far right in the spectrum is the second order of the 404.7-nm line, with a position corresponding to 2×404.7 nm = 809 nm in the first-order spectrum. Also, this value can be used for the wavelength calibration.

Moving the cursor over the picture with the mouse button down you can select a rectangle in the picture delimiting the area you wish to analyze. In doing so, select a part of the spectrum which is central in a vertical direction, so you avoid including too much of the curvature of the lines. Also be careful to include everything in the horizontal direction, so you start with the leftmost line of pixels and end with the rightmost one. Otherwise it will not be possible to compare different spectra. The next thing to do is to pull down the menu under "Analyze" and select "Plot profile" (Figs. 25.5 and 25.6).Then the spectral plot of "gray value" versus "Distance (Pixels)" pops up.

When you move the cursor over this picture both the horizontal and vertical coordinates are displayed. If you position the cursor at the various peaks you see, you can read and note their horizontal pixel coordinates (x values). Since there
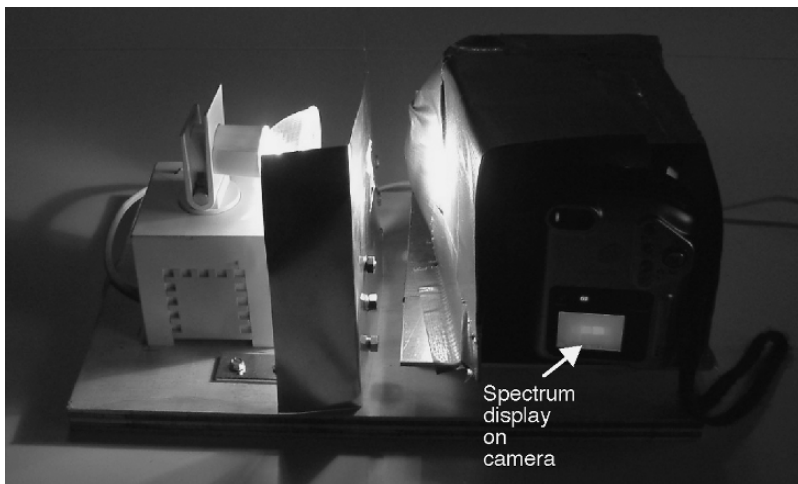
Figure 25.4. The almost completed spectrophotometer with lamp switched on. You can see the spectrum displayed on the camera screen. The only thing that is lacking now is a sample. This should be placed between the brass screen and the entrance slit on the box, according to the nature of the sample. A plant leaf could be attached with Scotch tape directly over the entrance slit, while a cuvette with solution has to stand on some support or placed in a holder. Using the kind of lamp shown here, which turned out to be unnecessarily strong (20 W rating), the light should not be switched on too long to avoid heating the box too much (fire risk).

are relatively few peaks in this spectrum, and you can see their colors in the color picture, it is not difficult to relate them to wavelength values for mercury found in a table. Enter the pixel numbers and their corresponding wavelengths in a table in Excel or a similar program. If you do not have one, you can download "Open Office" without charge from the Internet. To the right in Fig. 25.6 we have done this, produced a plot of the table in Excel, and added a linear trend line and a trend equation. It is this trend equation that you will use for calibrating the wavelength in other spectra.

As you can see, the wavelength calibration turns out to be surprisingly linear, considering the very simple optics used. The equation $y = 2864x + 233.72$, with x as the pixel number and y as the wavelength in nm, is what you use to convert pixel numbers in other spectra to wavelength in nm. The constant term in the right member depends on the position of the camera. Since you may wish to use the camera for other purposes between calibration and other measurements, you must either devise some way of repositioning the camera exactly or use a trick to be described below.

Before we lose Fig. 25.5 from sight, I should explain that the table in the panel to the right is only the beginning of a 2047-line table of the complete spectral plot that you obtain by selecting "List" below the spectral plot. It is not necessary for the wavelength calibration, but we will soon use this facility for computations on measured spectra.
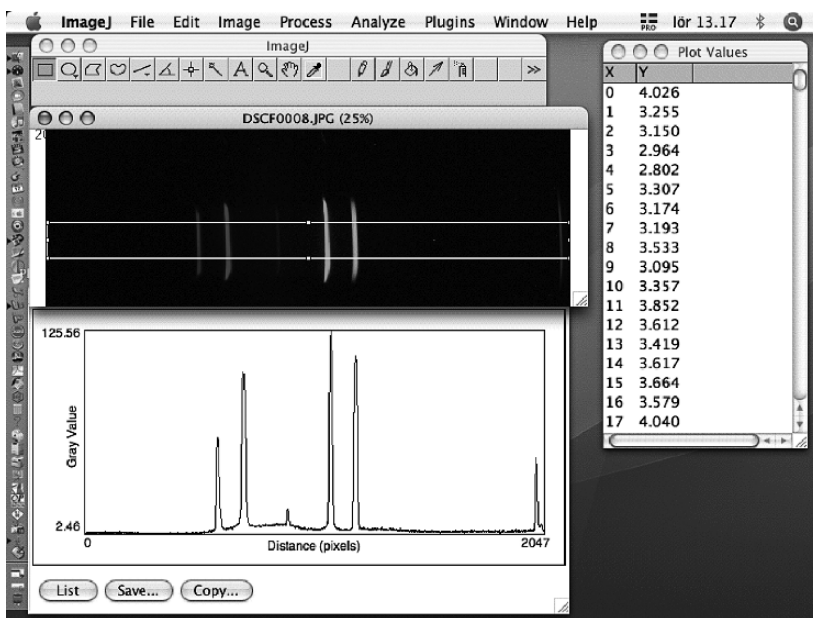
FIGURE 25.5. Appearance of Macintosh computer screen during work with ImageJ for wavelength calibration using a mercury spectrum. (*See* Color Plate).

25.4. Measurement and Manipulation of Spectra

We now come to the real measurements. Suppose we wish to measure the absorption spectrum of an acetone extract of a plant leaf. Before positioning the sample itself, we must take a reference spectrum of the lamp (the quartz-iodine lamp shown in Figs. 25.4 and 25.5, or whatever lamp we have chosen to use). If we wish to be careful, we can insert a cuvette with acetone in front of the
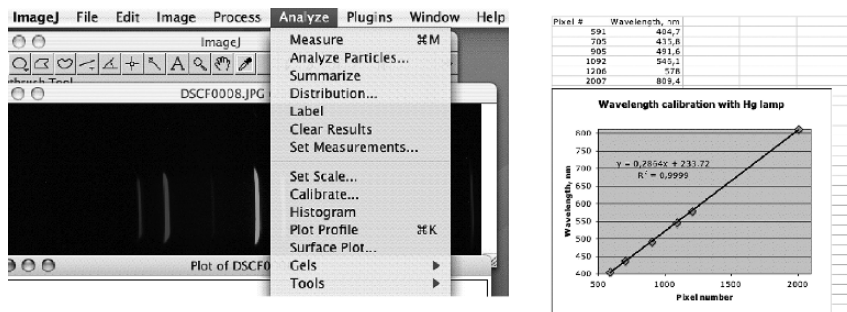
FIGURE 25.6. How to pull down the menu for selecting "Plot Profile" and make a wavelength calibration table and calibration plot in Excel. (*See* Color Plate).
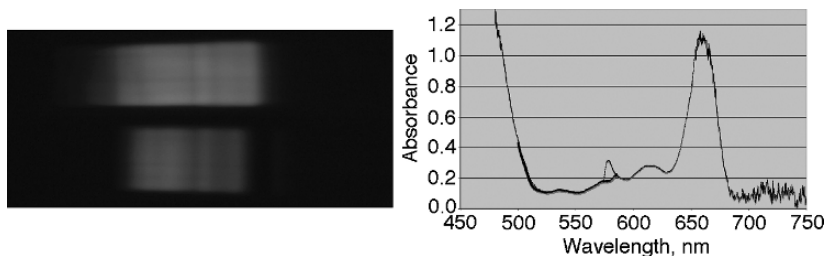
FIGURE 25.7. Reference spectrum without sample (upper left) and with plant leaf extract (lower left). To the right is shown the corresponding plot of the absorbance of a plant leaf extract in acetone. For the thin curve all three camera color channels (blue, green, and red) were used. The bump at 580 nm is an artefact. It coincides with the steepest portion of the reference spectrum (the segment from C to D in Fig. 25.12), where the red channel takes over from the green one. If only the green channel is used for this region (thick curve), the bump disappears. See inset for a color version of the spectra. (*See* Color Plate).

entrance slit to get just the absorption of the plant constituents in the end. We then get a spectrum like the upper one shown in Fig. 25.7. The lower spectrum is made with the plant extract in the cuvette.

Initially follow the same procedure as for the wavelength calibration: Open the picture in ImageJ, select the rectangular portion we wish to use, pull down the "Analyze" menu, and select "Plot Profile." Then choose "List" under the spectral plot and display all the pixel positions of the spectral plot. The first column in this is the horizontal pixel position, the second one the gray value, or more appropriately, the brightness of the corresponding portion of the spectrum. These values are then transferred to Excel or another spreadsheet program. Users of commas rather than periods in decimal numbers can easily change from one to the other by first copying the values into Word, using the "replace all" facility of this program, and then copying the values into Excel. Using Word as an intermediate for changing "." to "," seems more reliable than changing directly in Excel.

In Excel you can change the horizontal pixel positions to wavelength values using your calibration equation. Then you can divide the sample column by the reference column to get transmittance values, and you can take minus the logarithm of this to get the absorbance. We show the result of these manipulations in Fig. 25.11.

A few more remarks relating to this measurement: in cases such as these, when you compare the brightness of two spectra, it is important to use the same camera stop and exposure time values for the spectra to be compared. This means that you cannot use the camera's facility for automatic exposure. For the above measurement I used the least possible exposure, i.e., f/8 and 1/1600 second exposure time. In some cases, if you have very dense samples to compare to a bright control spectrum, it might be better to use different settings, but you must then take this into account to get the correct absorbance value.

In order to be able to remove the camera between wavelength calibration and measurement of a sample, and not have to reposition it very exactly, I used a special trick. It turned out that with my camera and the lamp I used, the reference spectrum without sample had several very easily recognizable and useful features, as shown in Fig. 25.8.

One more facility of the ImageJ program may be useful in some cases. The color picture of the spectrum can be divided into RGB (red-green-blue) components, and each of these three pictures can be evaluated separately. In some cases some parts of the spectrum can be over- or underexposed, and then it may still be possible to retrieve useful values by such a decomposition.

In Fig. 25.7 a case is shown where a single color channel (the green channel) seems to give a better result in a certain spectral region than the three channels combined. One can also expect that using only one channel at a time will decrease the effect of scattered light. Such scattered light is a problem in spectropho- tometry when measuring samples in spectral regions of high absorbance, when other regions have low absorbance. The left graph in Fig. 25.9 gives an example of how using all the color channels in such a case gives lower absorption peaks than a single channel; in such cases one should use only a single channel. With a more dilute solution and lower absorbance (more favorable measurement condi-
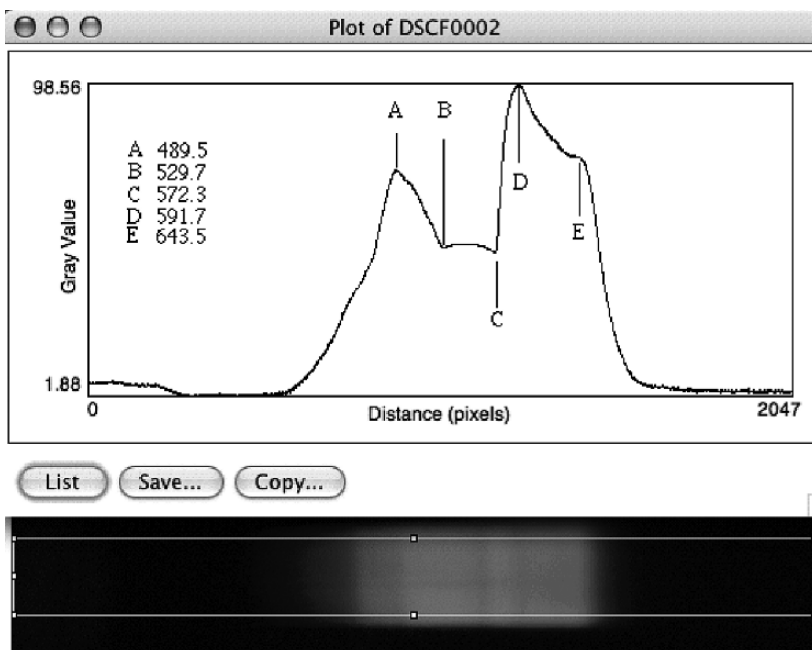
FIGURE 25.8. Appearance of my control spectrum without sample. Once the wavelengths for points A, B, C, D, and E have been determined, these points can be used to convert pixel positions to wavelength values without having to record a mercury spectrum every time. (*See* Color Plate).
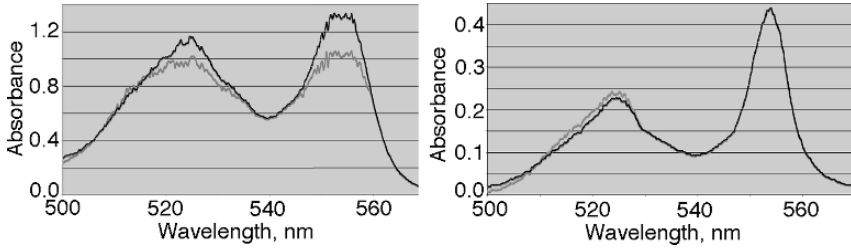
FIGURE 25.9. (Left) Absorption spectrum of the a and b band region of reduced cytochrome *c* (in phosphate buffer, pH 7, and reduced with dithionite) measured with all three color channels (grey curve) or the green channel only (black curve). The absorbance is too high for the spectrophotometer to cope with. (Right) The same, except more dilute solution of reduced cytochrome *c*. There is a wavelength error of about 4 nm (the literature value for the peak is 550 nm), which is about what one can expect.

tions) we do not have this effect (right graph). To perform a decomposition for selecting the correct channel, pull down the "Image" menue and choose "Color," and in the menu that pops up then choose "RGB Split."

It is also possible to use the same equipment for spectrofluorimetry, using a different light source. I used a blue light–emitting diode, with emission centered at 469 nm and the same acetone extract as used for the absorption spectrum. This light did not interfere with the fluorescence recording, but to get rid of the blue light signal completely one can use only the red light channel for plotting the fluorescence. This also improves the signal-to-noise ratio considerably (Fig. 25.10). My camera does not have a good sensitivity above 640 nm, so it is not particularly good for this purpose. The red and infrared sensitivity differs between camera models. To test a camera for infrared sensitivity, you
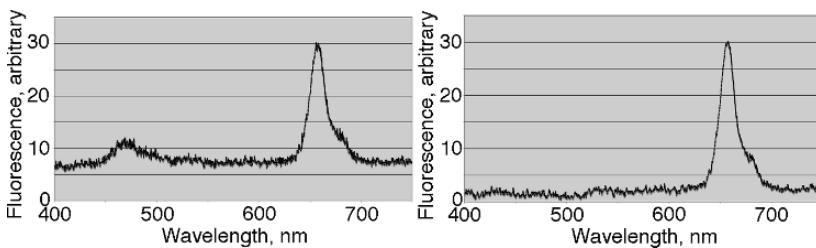
FIGURE 25.10. Fluorescence of an acetone extract of a plant leaf excited by light from a blue-light–emitting diode (469 nm). With such excitation most of the fluorescence comes from chlorophyll *b*. For the left panel all three color channels of the camera were used; for the right one the red channel only. The spectra are not corrected for wavelength dependence of the camera sensitivity, and because of rapid decline of sensitivity above 640 nm, only the short-wavelength portion of the spectrum is visible. The easiest way for an amateur to make an apporximative sensitivity calibration would be to use the sun when it is high in the sky.
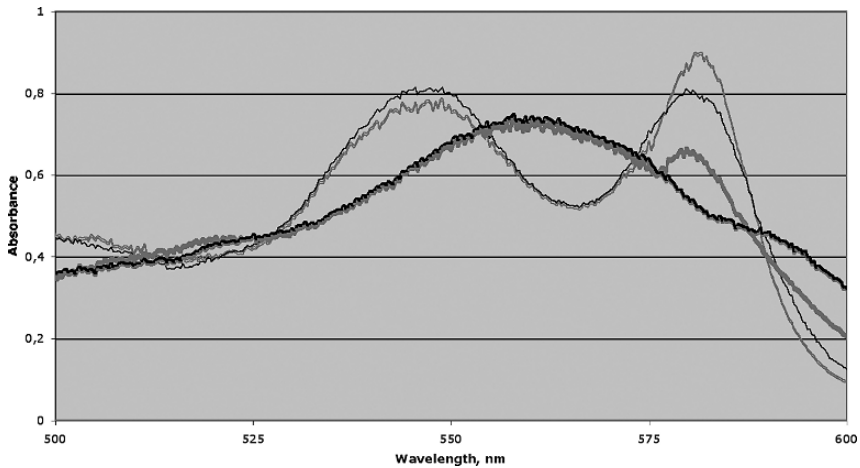
FIGURE 25.11. Blood diluted in oxygenated water (i.e., spectrum of oxyhemoglobin, thin lines), and after removal of oxygen with dithionite (i.e., spectrum of hemoglobin, thick lines). Either all three color channels were used (grey lines), or only the green channel (black lines), and we see here again the artifactual elevation at 585 nm when all channels are used (c.f. Fig. 25.7). With other digital cameras other similar artifacts may occur at other wavelengths.

can use an infrared remote control, for instance, one used for TV. You should use a filter to block short-wave radiation from the second-order spectrum if you are particularly interested in the long-wavelength region.

Best results were obtained with the sample very close to the slit. Since light-emitting diodes with a number of peak wavelengths are now available, it should also be possible to determine rough excitation spectra with this device and to analyze mixtures of fluorescent substances. Using 532 nm excitation light from a "green" laser pointer I have recorded light-induced fluorescence and reflectance changes in plant leaves.

25.5. Suggestions for Further Experimentation

There are many experiments that one can perform with this simple equipment or simple modifications of it. With the lamp I used, it is a bit difficult to get proper exposure in the blue part of the spectrum. A more appropriate spectrum would probably be obtained from a photographic flashlight, but my camera lacks the possibility to synchronize an external flash. Otherwise this could protect sensitive samples from excessive light, since the measurement light is required only for about a millisecond.

Many cameras can a series of pictures in rapid succession. Using this it should be possible to study rapid spectral changes, such as those that rhodopsin and phytochrome undergo upon illumination. If you wish to do such experiments,

you should equip your lamp (or sample compartment) with some kind of shutter, so that you start exposing your sample only when you start recording spectra. For showing spectra to a large auditorium you can use a video camera instead of an ordinary digital camera.

Recording such spectra of scattering samples as plant leaves or yeast suspensions is more difficult than clear samples, because light is scattered in unwanted directions. However, it should be possible to record also spectra of such samples if you insert light baffles of black paper or cardboard in the box, to prevent as much scattered light as possible from reaching the DVD surface. There should be no risk that the measurement light is too weak, since the exposure time of the camera can be increased. Figure 25.12 shows an example of what can be measured without extra light baffles. Note again the artefact near 580 nm appearing when the red channel is included. Note that this graph does not show all light that penetrates through the leaf, only that which propagates in the direction of the camera (via the DVD). A better approximation of the total transmitted light can perhaps be obtained if a piece of filter paper or similar scattering, nonabsorbing material, is inserted between the leaf and the slit and also used for the reference measurement.

Upon reduction, oxygenation, or pH changes, many substances, like cytochrome c and hemoglobin, undergo absorption changes that you should be able to observe (certainly in solution, and in some cases even in vivo). For a procedure for preparing a solution of cytochrome c from yeast see the original
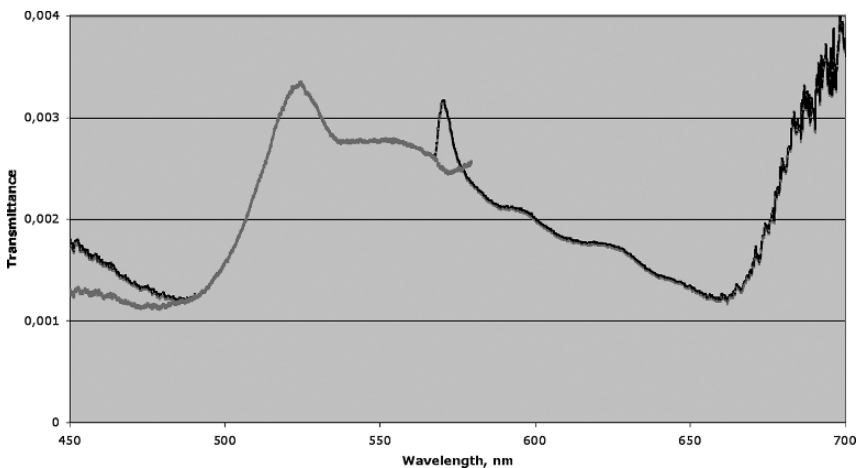
FIGURE 25.12. Transmission spectrum of a leaf of *Abutilon hybridum*. This leaf is neither very thin nor very thick. All three color channels were used for the range 450–700 nm (black line), and from 450 to 580 the spectrum was also recorded using blue and green channels only. The two methods deviate in the 450- to 470- nm and the 570- to 580-nm bands. An exposure time of 1/1600 second was used for the reference and ½ second for the sample, in both cases with stop 8. No extra light baffles were used.

paper by Keilin (1930), but you can scale it down at least 10 times (i.e., extract 100 g or less of yeast instead of 1 kg).

If you are interested in computer programming, it should be possible to modify the ImageJ program so that spectra can be immediately displayed on the computer screen when a sample is put in place. Many "plug ins" for ImageJ are already available in the public domain.

Some simple chemical experiments are suggested by Wakabahyashi, Hamada, and Sone (1998). Information about CDs and DVDs is provided by Birkett (2002).

If the slit of the apparatus is illuminated with sunlight or skylight, one can record some Fraunhofer absorption lines. I could catch lines for hydrogen (434, 486, and 656 nm), magnesium (517 nm), and sodium (589 nm) in the sun, and the molecular band of oxygen (688 nm) in the terrestrial atmosphere. A use of Fraunhofer lines in biological research is to measure chlorophyll fluorescence from plants at these wavelengths, where disturbing daylight is very weak (Liu et al. 2005, Corp et al. 2006). For satellite measurements only the lines from the solar atmosphere can be used.

References

Birkett, D. (2002) The chemistry of optical discs. J. Chem. Educ. 79, 1081–1087.

Corp, L.A., Middleton, E.M., McMurtrey, J.E., Entcheva Campbell, P.K., and L. Maryn Butcher, L.M. (2006) Fluorescence sensing techniques for vegetation assessment. Appl. Optics 45, 1023–1033.

Keilin, D. (1930) Cytochrome and intracellular oxidase. Proc. Roy. Soc. London B 106(749), 418–444.

Kohl, S.K., Landmark, J.D. and Stickle, D.F. (2006) Demonstration of absorbance using digital color image analysis and colored solutions. J. Chem. Educ. 83, 644–646.

Liu, L., Zhang, Y., Wang, J. and Zhao, C. (2005) Detecting solar-induced chlorophyll fluorescence from field radiance spectra based on the Fraunhofer line principle. IEEE Transact. Geosci. Remote Sensing 43, 827–832.

Wakabayashi, F. and Hamada, K. (2006) A DVD spectroscope: A simple, high-resolution classroom spectroscope. J. Chem. Educ. 83, 56–58.

Wakabayashi, F., Hamada. K and Sone, K. J. (1998) CD-ROM spectroscope: A simple and inexpensive tool for classroom demonstrations on chemical spectroscopy. J. Chem. Educ. 75, 1569–1570.

Index